EUROPEAN WATER RESOURCES ASSOCIATION

11th WORLD CONGRESS
on Water Resources and Environment
[EWRA 2019]

Managing Water Resources for a Sustainable Future

Madrid, 25-29 June 2019

PROCEEDINGS

Editors

Luis Garrote
George Tsakiris
Vassilios A. Tsihrintzis
Harris Vangelis
Dimitris Tigkas

2019

EUROPEAN WATER RESOURCES ASSOCIATION

11th WORLD CONGRESS

on Water Resources and Environment
[EWRA 2019]

Managing Water Resources for a Sustainable Future

25-29 June 2019
Madrid, Spain

PROCEEDINGS

Editors

Luis Garrote
George Tsakiris
Vassilios A. Tsihrintzis
Harris Vangelis
Dimitris Tigkas

2019

ISBN: 978-618-84419-0-3

Managing Water Resources for a Sustainable Future
Proceedings of the 11th World Congress of EWRA on Water Resources and Environment
[EWRA 2019]
25-29 June 2019, Madrid, Spain

Editors:
Luis Garrote, George Tsakiris, Vassilios A. Tsihrintzis, Harris Vangelis, Dimitris Tigkas

Disclaimer:
Although this book of proceedings has been compiled with utmost care, the Editors cannot be held responsible for any misprints and/or omissions. The options expressed by the authors are not necessarily endorsed by the Association.

EWRA Editorial Office:
Iroon Polytechniou 9, 157 80, Athens, Greece
e-mail: puboffice@ewra.net

Cite this publication as:
Garrote L., Tsakiris G., Tsihrintzis V.A., Vangelis H., Tigkas D., (eds.) 2019. Managing Water Resources for a Sustainable Future. Proceedings of the 11th World Congress of EWRA on Water Resources and Environment, 25-29 June 2019, Madrid, Spain.

Organising Bodies

Principal Organiser
Universidad Politécnica de Madrid
(Technical University of Madrid)

Sponsors

Prince Sultan Bin Abdulaziz
International Prize for Water

Organising and Scientific Committee

Garrote L. (chairman)	Technical University of Madrid
Iglesias A.	Technical University of Madrid
Rodríguez-Sinobas L.	Technical University of Madrid
Marchamalo M.	Technical University of Madrid
Cueto L.	Technical University of Madrid
Mediero L.	Technical University of Madrid
Sordo A.	Technical University of Madrid
Tigkas D.	National Technical University of Athens
Vangelis H.	National Technical University of Athens

International Scientific Committee

Batelaan O.	Flinders University, Australia
Cancelliere A.	University of Catania, Italy
Caporali E.	University of Florence, Italy
Chau K.W.	Hong Kong Polytechnic University, Hong Kong
Christodoulou S.	University of Cyprus, Cyprus
Ferreira T.	University of Lisbon, Portugal
Grafton R.Q	Australian National University, Australia
Harmancioglu N.B.	Dokuz Eylül University, Turkey
Iglesias A.	Technical University of Madrid, Spain
Karnib A.	Lebanese University, Lebanon
Khalili D.	Shiraz University, Iran
Kindler J.	Warsaw University of Technology, Poland
Koutsoyiannis D.	National Technical University of Athens, Greece
Loucks D.P.	Cornell University, USA
Loukas A.	University of Thessaly, Greece
Madani K.	Yale University, USA
Maia R.	University of Porto, Portugal
Noto L.V.	University of Palermo, Italy
Oel P. van	University of Wageningen, Netherlands
Pahl-Wostl C.	Osnabrück University, Germany
Reddy J.	Indian Institute of Technology Bombay, India
Rossi G.	University of Catania, Italy
Savic D.	University of Exeter, UK
Sechi G.	University of Cagliari, Italy

Schumann A.	RUHR – University of Bochum, Germany
Shatanawi M.	University of Jordan, Jordan
Shiau J.T.	Tamkang University, Taiwan
Simonović S.P.	Western University, Canada
Singh V.P.	Texas A & M University, USA
Spiliotis M.	Democritus University of Thrace, Greece
Srdjevic B.	University of Novi Sad, Serbia
Tanyimboh T.	University of the Witwatersrand, South Africa
Tayfur G.	Izmir Institute of Technology, Turkey
Tortajada C.	Institute of Water Policy, Singapore
Tsakiris G.	National Technical University of Athens, Greece
Tsihrintzis V.	National Technical University of Athens, Greece
Werner M.	Unesco IHE, Netherlands
Wu J.	Chinese Academy of Sciences

National Scientific Committee

García-Jalón D.	Technical University of Madrid
Roldán J.	University of Córdoba
Pulido M.	Technical University of Valencia
Llasat C.	University of Barcelona
Delgado F.	University of Granada
Expósito A.	University of Seville
López-Gómez D.	Hydrographic Studies Centre of CEDEX
Castro-Orgaz, O.	University of Córdoba
Santillán D.	Technical University of Madrid
Polo M.J.	University of Córdoba
Martín-Carrasco F.	Technical University of Madrid
Granados A.	Technical University of Madrid
Hernández-Mora N.	FNCA
Bejarano, D.	Geological and Mining Institute of Spain
Gómez-Valentín M.	Technical University of Catalunya
Frances F.	Technical University of Valencia
Tejero I.	University of Cantabria
Sanz, E.	Technical University of Madrid
Pulido, D.	Geological and Mining Institute of Spain
Castillo L.	Technical University of Cartagena
González J.	University of Castilla-La Mancha
López J.	Public University of Navarra

Editors' Preface

This volume of Proceedings includes the papers presented at the 11th World Congress of the European Water Resources Association (EWRA) on Water Resources and Environment. The Congress was held in Madrid, Spain, 24-29 June 2019, under the title "Managing Water Resources for a Sustainable Future".

EWRA was established in 1992 as an international non-profit association aiming at enhancing cooperation and exchanges in research and application in the field of water resources. Among its diverse activities, EWRA organises a bi-annual World Congress to provide a forum of discussions between scientists and professional engineers. The aim of the 11th Congress was to discuss innovation pathways in water resources management to address current and future challenges, such as: growing uncertainty, more frequent extremes, increasing demand, water scarcity, global change, water quality and environmental degradation. While traditional management practice is still effective, new technologies and approaches are emerging to better protect, regulate, allocate and recycle water resources. Sustainable management of water resources in the 21st Century requires a comprehensive understanding of the interaction of complex natural and social components in a changing context.

The Congress is an open forum where scientists and engineers from diverse cultures around the world promote environmentally sustainable water resources management and discuss their understanding of water resources systems at various scales. The Proceedings contain a compilation of extended abstracts describing the communications presented at the Congress. This volume is therefore a compendium of scientifically sound and economically-efficient solutions to current water management problems and is a valuable asset for scientists and practitioners.

These Proceedings are organised following the eleven specialised conferences of the Congress:

I. Hydroclimatic Extremes and Water Resources Management
II. Water Quality and Water Treatment
III. Hydrological Processes
IV. Urban Water Management
V. Agricultural Water Management
VI. Water-Energy-Food Nexus
VII. Ecosystems and Environmental Processes
VIII. Groundwater Hydrology, Contamination and Management
IX. Geoinformatics, Remote Sensing and Water Resources
X. Global Change and Water Resources
XI. Water Policy and Socioeconomic Issues

All the papers presented at the Congress will be assessed for possible invitation to be extended and enhanced, so as to be published as full articles after peer review process in the journals of EWRA (*Water Resources Management*, *Environmental Processes*, *European Water* and *Water Utility Journal*).

The editors would like to thank:

- The Universidad Politécnica de Madrid for hosting the Congress, providing the academic space to share ideas and interchange opinions
- The authors of the papers and the participants of the Congress, for their knowledge and contributions.
- The members of the Scientific and Organizing Committees for their efforts devoted to prepare the structure of the Congress, to supervise peer-review of the contributions and to conduct the sessions in an efficient way.
- The sponsors of the Congress for their financial support.

The Editors

TABLE OF CONTENTS

Keynote Speeches

I. Hydroclimatic Extremes and Water Resources Management

II. Water Quality and Water Treatment

III. Hydrological Processes

IV. Urban Water Management

V. Agricultural Water Management

VI. Water-Energy-Food Nexus

VII. Ecosystems and Environmental Processes

VIII. Groundwater Hydrology, Contamination and Management

IX. Geoinformatics, Remote Sensing and Water Resources

X. Global Change and Water Resources

XI. Water Policy and Socioeconomic Issues

Keynote Speeches

11th World Congress on Water Resources and Environment (EWRA 2019)
"Managing Water Resources for a Sustainable Future", 25-29 June 2019, Madrid, Spain

Challenges in flood risk management

A. Schumann
Faculty for Civil and Environmental Engineering, Ruhr-University Bochum, Germany
** e-mail: andreas.schumann@rub.de*

Introduction

Flood risk management moved into the focus of water policies in many European countries. The assessment of flood risk demands the combination of the probability of a flood event with the potential adverse consequences associated with it. Since more than 100 years, we apply the probabilistic concept of return period to specify the probabilities of floods by the exceedance probabilities of their peaks only. Less emphasis is given to the fact that the probability of the harmful event depends on the relationship between load and resistance capacities of the endangered elements. In this context, other criteria of floods, e.g. the flow velocity or the flood volume and the shape of hydrograph, become relevant. To consider the complex failure mechanisms of flood protection structures, multivariate probabilities of hydrological loads are needed. Our statistical tools were refined within the last two decades to provide multivariate statistical relationships. Unfortunately, these methods reached a state where it becomes more and more difficult to apply them in practice. Other problems of flood risk management result from spatial aspects. The local consequences of a flood vary with their event-specific spatial structure and the interplay with the existing structural and non-structural measures of flood protection. Resulting from these and other problems it is no longer sufficient to specify a single design flood at one side of interest. Flood risk management requires a holistic view on flood protection systems to take into account all potential interventions that may alter flood risk in its spatial dimension. The assessments of effectivity and efficiency of interventions in the flood regime depend strongly on the choice of flood characteristics, which are considered or neglected. To select these characteristics, we have to notice the variety of flood events, the different modes of failures of flood protection structures as well as expected and unexpected changes of flood risk in future. Often such a holistic view on flood risk management does not exist and if it would be provided, the decision makers are faced with the problem to make decisions under uncertainty.

Material and methods

The procedure to estimate flood risk is described in the EU Flood Directive. Flood hazard maps have to be set-up to characterise the geographical areas, which could be flooded according to scenarios of floods, specified by low, medium and high probabilities. However, these probabilities are very uncertain with regard to their specification and often the statistical approach to specify them is insufficient. To characterise flood risk in a more realistic way, three aspects have to be considered: - the large variety of floods by categorisation of flood events according to their origin, shapes of hydrographs and spatial characteristics, - the uncertain effectiveness of flood protection measures under consideration of this variety of hydrological loads and - the "known unknowns" of risk assessments, especially resulting from rare flood events with uncertain locations as e.g. flash floods (Schumann 2017). Based on analyses for German river basins, several ways to consider these uncertainties were applied. It was demonstrated how the flood characteristics have to be analysed to specify the most critical events by their relationships between flood peaks, volumes and shapes of hydrographs. In order to estimate these characteristics, long series of daily discharges were analyzed automatically. The flood events were categorized according to their drivers and hydrological characteristics. In this context, analyses of the seasonality of floods and their temporal variability but also estimations of the frequencies of different flood types (Fischer and Schumann 2019) are very important. The results were summarised within a statistical model (Figure 1) which can be applied to simulate a large variety of flood events. The model specifies flood types by their type-specific relationships between peaks and flood volumes. As flood types specify the shape of hydrographs also, only the flood volume derived from the total amount of precipitation and the runoff coefficients were

considered as random variables. It could be shown that this model is able to represent the distribution functions of flood peaks well with the exception of very rare events with high peaks (outliers).

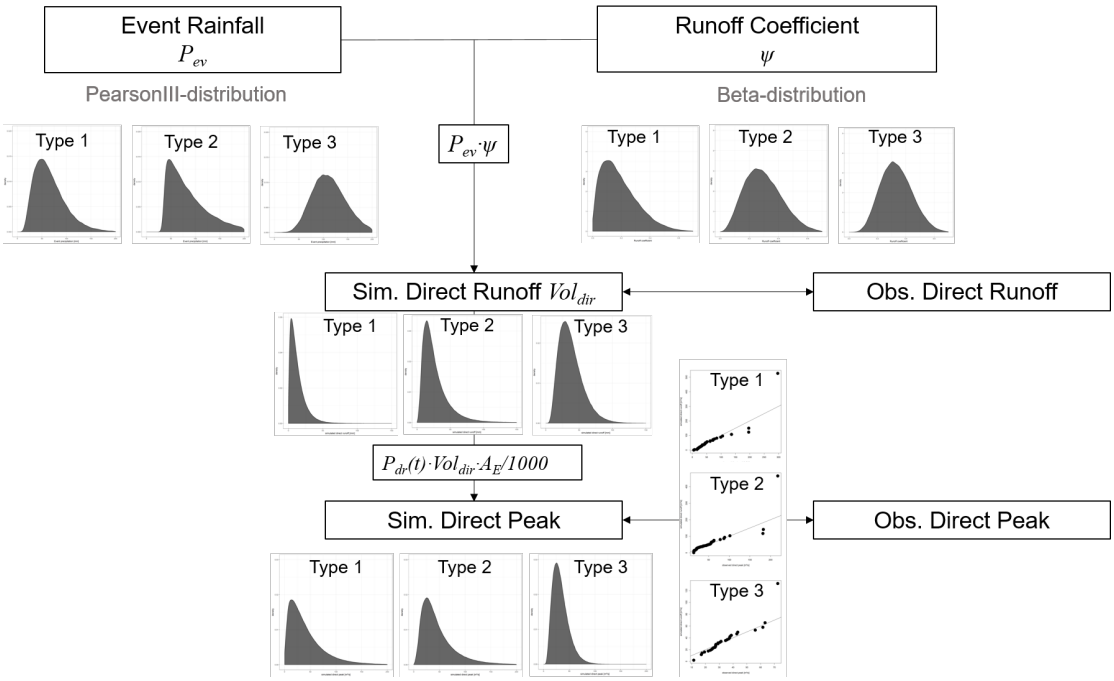

Figure 1. Schematic plot of a flood simulation procedure based on a detailed analyses of long discharge series.

A typing of floods is essential to estimate the efficiency of reservoir systems on flood risk management in river basins, depending on event characteristics. This is demonstrated with a flood protection system in Germany. Its efficiency depends strongly on the spatial structure of rain events causing floods. It is very difficult to estimate flood probabilities for such complex flood scenarios but it can be shown how worst and best case assumptions could be derived from a combination of statistical and deterministic models.

Results and discussion

As risk depends on many different factors, risk management requires either a regulatory framework, which describes one way to specify it or complex analyses to consider the many uncertainties of risk assessments. Unfortunately, the first approach is preferred in most countries. With a certain stage of flood protection, the interplay of loads and resistance becomes more and more important. To consider it, many additional flood characteristics are needed which are difficult to specify by their probabilities. A more holistic approach to specify flood risk demands a good knowledge of hydrological and water management systems as well as tools to describe their interactions. Here we have to leave the zone of statistical probabilities to consider possibilities instead. The assumption of these possibilities should be realistic and in accordance with the observed flood conditions.

Acknowledgments: I acknowledge the German Research Foundation and the Federal Ministry for Research and Education of Germany for funding.

References

Schumann AH (2017) Flood safety versus remaining risks - options and limitations of probabilistic concepts in flood management. Water Resources Management 31(10):3131–3145

Fischer S, Schumann A (2019) Spatio-temporal consideration of the impact of flood event types on flood statistic, Stochastic Environmental Research and Risk Assessment, https://doi.org/10.1007/s00477-019-01690-2

11th World Congress on Water Resources and Environment (EWRA 2019)
"Managing Water Resources for a Sustainable Future", 25-29 June 2019, Madrid, Spain

On the (f)utility of supporting water allocation policies with new data sources, models and forecasts

M. Werner[1,2]
[1] Department of Water Engineering, IHE Delft Institute for Water Education, Delft, The Netherlands
[2] Deltares, Delft, The Netherlands
e-mail: m.werner@un-ihe.org

Introduction

Allocation of water resources to contending water users is a complex task, particularly when available water resources are scarce. To water resources planners, the water allocation process will depend on the information they have at their disposal on the available water at the time of making a decision on the allocation, as well as the information available on the demand of water from the users. If the expected demands outstrip expected availability, then curtailments may be applied; limiting the amount of water allocated to users. Curtailments are often applied in order to maximise the probability of reaching the end of season with the available water resources. There are, however, many uncertainties that influence the water allocation process. The availability of water to the end of the season is often uncertain, as is in many cases the evolution of water demand over the season. Uncertainty in the water demand is exacerbated by feedbacks. Depending on how risk averse or risk acceptant users are, they will make plans according to their perception of the availability of water, and these plans will in turn determine the demands.

Materials and methods

In this paper we consider the potential of reducing uncertainties in the water allocation processes through new data sources; including information from remote sensing, hydrological models and (seasonal) forecasts. Over the last decades these data have increasingly become available at greater accuracy and resolution, and research and innovation is stimulated to build and deliver climate services at European and Global Scale (Street 2016). Such services can provide added information on expected water availability at the seasonal scale, helping planners better allocate resources across the season. Additionally, tailored information has the potential to provide more certainty to users on the water allocation they can expect across the year, allowing them to make better plans and reduce actual losses as well as opportunity costs.

However, these new sources of information are uncertain, and this will influence the utility of the data. There are, however, several other factors that also determine whether there is real utility in the information, and how these are used to inform decisions, either by those making the water allocation decisions, or by those making decisions on for example the crops to plant conditional on the water they expect to be allocated. We explore some of the factors that influence the utility of these new data sources in water allocation processes, including the uncertainty of the data itself, but also the degree of integration of new data-sources within the decision making processes and water allocation policies, the beliefs and behaviour of the users, and economic factors. We explore the use of new data sources in three water allocation processes in irrigated agriculture; the Ebro Basin in Spain, the Murrumbidgee Basin in Australia; and the West Rapti Basin in Nepal. In all three of these case studies, decision models were established to emulate decision making processes and water allocation policies. These decision models were then tested using the data that is currently used in decision making, as well as new data sources, including remote sensing data of snow cover, and seasonal (hydrological) forecasts.

Results and concluding remarks

In the Ebro basin, the water allocation process is currently informed primarily by the expected available water as observed in reservoirs, balanced with the expected demand by farmers, which in turn depends on

the crops farmers they decide to plant. The farmers' decision depends, however, on their perception of the expected water availability and any curtailments that may be imposed by the agency as the season progresses. Providing additional information on the snow cover (from remote sensing) in the headwaters as additional information on the available resource is shown to be beneficial, allowing farmers to make better informed decisions and obtaining better returns over the years tested. However, results also show the benefits of the information depends on the risk averseness of the farmers, and is very sensitive to the ratio of the investment cost to the market value of the crop (Linés et al. 2018). Similar results were found in the West Rapti basin in Nepal, where the crops that farmers' plant depends on their perception of possible water shortage. This perception can be informed seasonal forecasts of water availability (Ensemble Streamflow Prediction), and while this does lead to a benefit through better decisions made, these benefits may be quite different (and normally higher) to cash crop farmers when compared to the benefits to subsistence farmers. In the Australian basin, a complex water allocation policy is in used. At the start of the season a (often conservative) estimate of available water is made, and based on this farmers are allocated a percentage of their entitlement This allocation is re-assessed and may be reviewed (generally increased) as the season progresses. The benefit of using seasonal hydrological forecasts to inform the decision process is shown to be that a better estimate of the final allocation to farmers is established 1-2 months earlier, which is of benefit to how they plan the irrigation season (see Figure 1). However, while this works well in normal and wet years, in exceptionally dry years farmers may be faced with reductions to the allocation, which is highly undesirable. These downward revisions of allocated water may lead to losses as well as raise questions as to who should bear the risk of the initial overconfidence in available resource.

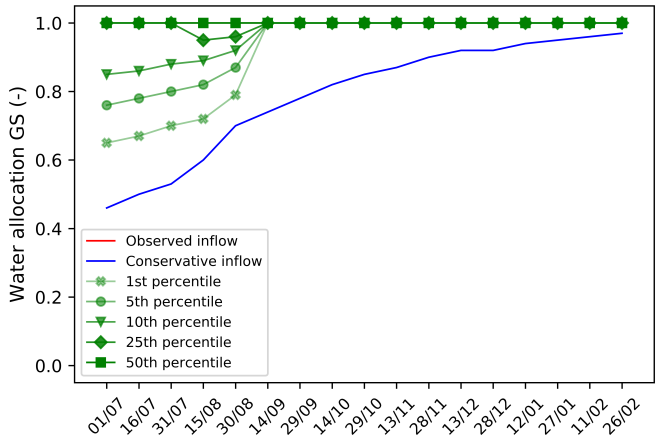

Figure 1. Water allocated to annual crops in the Murrumbidgee basin in 1998 as a ratio of their full entitlement. The blue line shows how the allocation is revised over the year using the current conservative approach, while the green lines show the allocation based on the seasonal hydrological forecast. The perfect decision using the observed flow would have resulted in a100% allocation of the entitlement.

The three cases presented show that there is real potential in using new data sources from remote sensing and seasonal forecasts to improve water allocation decisions. However, the utility of these datasets depends not only on how well the datasets themselves perform, but also to the extent these have real influence on the decision making process or in the water allocation policy. Several factors need to be considered that may affect the true utility of new and innovative data sources. We conclude that research and operational use of such new and increasingly available datasets should consider these factors, and argue that not doing so may render many improvements and innovations to the datasets themselves futile.

Acknowledgments: We would like to thank Clara Linés, Alka Subedi, Alexander Kaune Schmidt, and Mohamed Faysal Chowdhury who through their research have contributed the results presented.

References

Linés C, Iglesias A, Garrote L, Sotés V, Werner M (2018) Do users benefit from additional information in support of operational drought management decisions in the Ebro basin? Hydrol. Earth Syst. Sci. 22:5901-5917. https://doi.org/10.5194/hess-22-5901-2018

Street RB (2016) Towards a leading role on climate services in Europe: A research and innovation roadmap Climate Services 1:2-5. https://doi.org/10.1016/j.cliser.2015.12.001

11th World Congress on Water Resources and Environment (EWRA 2019)
"Managing Water Resources for a Sustainable Future", 25-29 June 2019, Madrid, Spain

Emerging water policy and economic challenges: Discovering the meaning of the world's trends

A. Garrido[1,2,3]
[1] Department of Agricultural Economics, Statistics and Business Management, ETSIAAB, and Vice-Rector for Quality and Efficiency, Universidad Politénica de Madrid (UPM), Spain
[2] CEIGRAM – UPM
[3] Water Observatory, Botin Foudation
* e-mail: alberto.garrido@upm.es

Introduction

The world is being transformed and evolving quickly in three main dimensions: population growth, coupled with growing disposable income and engrossing of the world's middle class; urbanisation and changing food habits. The three have relevant influence for world, national and regional water resources.

Middle-class inhabitants can virtually afford the same goods and services of the high-class world inhabitants in terms of food consumption and water services (access to drinking water and sanitation). Yet, both raise important challenges that stand in the way to promote some Sustainable Development Goals.

The goals of my presentation are:

(a) Show recent population, income and geographical data and facts and relate them to the main water challenges at world's and regional scale.
(b) Infer particular aspects from the previous point that will require economic and policy considerations from politicians as well as water resources scientists.
(c) Describe the challenges related to water and ecosystems conservation.
(d) In view of the above, show the importance of considering water scarcity in an economic context, complementing other indicators generally used in proposing water management strategies.
(e) Suggest science-relevant conclusions that may ease and facilitate the transformations required to meet world's water challenges.

Material and methods

I rely on various databases from the World's bank, FAO, European Commission, International Virtual water trade to construct and base my arguments. I rely also on recent literature about: virtual water trade, water foodprint, data on drinking and water sanitation around the world, changing food habits and demand, population growth and geographical distribution.

By connecting in a coherent and systems-view all these trends and findings, I will draw several economic and policy conclusions.

Results and discussion

1. Increasing food demand at world level will not be a problem for keeping and improving the ecological and physical status of the world's water bodies, provided:
   - Food diets change, both for environmental and health reasons
   - International trade is well managed and regulated, to ensure that food production is efficiently done socially, economically and environmentally
2. Wastewater treatment in cities and megacities is a primary and affordable environmental goal for the world's new middle class. It is also a moral obligation that requires proper governance, finance and smart engineering. The have-nots of the world cannot afford it, and deserve the support of the international community.
3. In many circumstances, water scarcity is an economic problem that can only be solved with the right economic principles. There are not free lunches. Vulnerable people must be protected. Unsolved

scarcity issues spill over to other people and the environment. Always.

4. Social, governance and technology innovation must be jointly innovation to avoid mistakes and missed opportunities.

Acknowledgments: I acknowledge the support of Universidad Politécnica de Madrid, the Botin Foundation and CEIGRAM's colleagues, co-authors and fellow researchers.

References

FAO (2019) The State of World's Biodiversity for Food and Agriculture. Food and Agriculture Organisation of the United Nations, Rome

Garrido A, Rabi A (2016) Managing Water in the 21st Century: Challenges and Opportunities. Proceedings of the 8th Rosenberg International Forum in Water Policy, University of California, Oakland

Rosling H (2018) Facfulness. Flatiron Books, New York

Villholth KG, Lopez-Gunn E, Conti KI, Garrido A, van der Gun J (eds) (2018) Advances in Groundwater Governance. CRC Press, Taylor and Francis, London, UK

Willaarts BA, Garrido A, Llamas MR (eds) (2014) Water for Food and Wellbeing in Latin America and the Caribbean. Social and Environmental Implications for a Globalized Economy. Routledge, Oxon and New York

11th World Congress on Water Resources and Environment (EWRA 2019)
"Managing Water Resources for a Sustainable Future", 25-29 June 2019, Madrid, Spain

Management of complex water resources systems under global change

J. Andreu*, A. Solera, S. Suarez, J. Madrigal, J. Paredes
IIAMA (Instituto Universitatrio de Ingenieria del Agua y Medio Ambiente), Universitat Politecnica de Valencia, Camino de Vera s/n, 46022, Valencia, Spain
** e-mail: ximoand@upvnet.upv.es*

Introduction

During the last decades, in many basins around the world, water resources systems (WRS) have been developed to provide water and food security, and to cope with water scarcity and water services vulnerability. Complex WRS generally include facilities for water storage, conveyance and distribution, as well as water and wastewater treatment plants. Also, in many instances, groundwater management is an essential feature of complex WRS. Planning and management of complex WRS in water stressed basins has become more difficult due to Global Change (GC) considerations. GC includes not only Climate Change (CC), but also other changes that act as stressors of WRS. Among them, we can find unprecedented population increase rates, changes in land use, urbanization, pollution, and also societal changes and socio-political factors. This study presents different methodologies and tools used in the Jucar River Basin (JRB), in Spain, in order to incorporate GC issues. The main objectives of the work are to analyze the suitability of the different approaches and to draw conclusions and recommendations for future planning and management studies aiming to find measures to be implemented for mitigation of GC. The main focus is on water scarcity, and multiannual droughts, as essential issues in JRB, altogether with environmental objectives.

Material and methods

Some obvious consequences of GC scenarios for the water sector can be expressed with general quantitative and qualitative statements that can serve as warning messages to the society. Also, pan-continental and/or national studies using general models can be conducted for first appraisals of the impacts of GC to inform policy makers. However, for practical planning and management of complex WRS, detailed assessments of the impacts of GC are needed for decision making in the search of adequate combinations of measures that have to be deployed to anticipate the problems, and to provide resiliency in front of future extremes, such as droughts. For this purpose, adequate methodologies and tools must be used. Nowadays, we can say that ample tools for the analysis of WRS are available, including models covering quantitative hydrological aspects, as well as water quality and environmental issues. Furthermore, Decision Support Systems (DSS) can be developed, providing integration of these issues and models (Andreu et al. 1996; Momblanch 2017), hence facilitating the knowledge transfer between scientists and practitioners, and also allowing a participatory development of the DSS with the stakeholders, which provides a common shared vision of the WRS (Andreu et al. 2009).

One of the key inputs for the analysis, and therefore for the results obtained, is the future climatic scenario that the WRS will confront, mainly in terms of temperature (T) and precipitation (P). Numerous ensembles of predictions of T and P for future CC scenarios have been generated by climatologists in the last years, and some of them have been selected for the analysis, showing different skills to render an adequate structure of spatial and temporal variability inherent to Spanish Mediterranean basins.

The use of some of the above mentioned CC inputs, approaches, and tools for assessment of impacts of GC in the JRB WRS is introduced, including mainly the approaches used in the drawing of the official River Basin Plans since 1998 to date (CHJ 2015), and the approaches used in multidisciplinary research projects where the JRB has been used as a case of study (Suarez et al. 2017).

Results and discussion

The main objective of this work was to introduce different approaches applied in the JRB to link GC

scenarios with decision-making in water resources planning and management under water scarcity. As shown in the study, different chains of models (GCM, RCM, hydrological model, stochastic models, WRS management and allocation models) produce different results, requiring an exhaustive and detailed analysis, since the decisions considered for them are influencing the final results. This uncertainty is added to the one inherent to CC. Hence, the results obtained by the different approaches and Climate Change scenarios are highly variable. The average change rates for each future period (2011-2040, 2041-2070 and 2071-2098) compared with the ensemble of the reference period (1980-2000) for the total JRB streamflow are +2%, -4% and -11%. Also, different variations of streamflows by zones are observed. While for the last future period, the headwaters streamflows are reduced up to 20%, in the middle-lower sub-basin they decrease only by 1%, with increases up to 12% in the first and second periods. With respect to the Operative Drought Indicator (ODI) used in the JRB for Drought monitoring, results show that the average probability of falling into Drought Scenario increases from 10% in the first future period to 25% in the second and 50% in the third. For both cases (Total JRB streamflows and ODI probabilities), and in general, the results are more pessimistic for RCP 8.5 and more optimistic for RCP 4.5. But also differences are realized for different chains of models within the same RCP.

Among the conclusions obtained from the study, we can highlight the following:

- GCM and RCM tend to underestimate space and time variability of precipitation in JRB, which are critical elements for drought risk assessment. Bias corrections are usually not enough to correct this problem in a coherent manner. More research is needed to improve this aspect.
- General models used at pan-continental or national scales do not capture the physical reality of the JRB, mainly due to the complexity provided by the groundwater component, and the high anthropic influence on the streamflows regime. Therefore, better results are obtained with models that have been specifically designed, calibrated and validated for the JRB. Nevertheless, the tool to build the model can be a generic tool, whenever it is able to capture specific features of the JRB.

It seems that there is room for research and improvement in the chain of models used for the assessment of GC impacts in complex WRS under stress and drought. Nevertheless, and based on the experiences in JRB, a recommendation is that river basin planning exercises must be conducted regularly, as required by European Water Framework Directive, adopting flexible measures for adaptation, and incorporating the improvements provided by observations, experience and research in every update.

Acknowledgments: The authors thank the Spanish Research Agency (MINECO) for the financial support to ERAS project (CTM2016-77804-P, including EU-FEDER funds). Additionally, we also value the support provided by the European Community's in financing the projects SWICCA (ECMRWF-Copernicus-FA 2015/ C3S_441-LOT1/SMHI), AGUAMOD (INTERREG-SUDOE Ref: SOE1/P5/F0026) and IMPREX (H2020-WATER-2014–2015, 641811).

References

Andreu J, Capilla J, Sanchís E (1996) AQUATOOL, a generalized decision-support system for water-resources planning and operational management. J. Hydrol. 177:269–291. http://dx.doi.org/10.1016/0022-1694(95)02963-X.

Andreu J, Pérez MA, Paredes J, Solera A (2009) Participatory analysis of the Jucar-Vinalopo (Spain) water conflict using a Decision Support System. In: R.S. Anderssen et al. (eds), 18th IMACS World Congress - MODSIM09 International Congress on Modelling and Simulation, pp 3230-3236

Confederación Hidrográfica del Júcar (2015) Plan Hidrológico de la Demarcación Hidrográfica del Júcar. Valencia, Spain

Momblanch A, Paredes-Arquiola J, Andreu J (2017) Improved modelling of the freshwater provisioning ecosystem service in water scarce river basins. Environmental Modelling & Software 94:87-99. http://dx.doi.org/10.1016/j.envsoft.2017.03.033

Suárez S, Pedro-Monzonis M, Paredes J, Andreu J, Solera A (2017) Linking Pan-European data to the local scale for decision making for global change and water scarcity within water resources planning and management. Science of the Total Environment 603-604:126-139. https://doi.org/10.1016/j.scitotenv.2017.05.259

I. Hydroclimatic Extremes and Water Resources Management

11th World Congress on Water Resources and Environment (EWRA 2019)
"Managing Water Resources for a Sustainable Future", 25-29 June 2019, Madrid, Spain

Genetic algorithm based optimization of multipurpose cascade reservoirs for sustainable economic growth

M. Usman Rashid[1*], M. Azmat[2], F. Raees[3]
[1] Department of Civil Engineering, University of Management and Technology, Lahore, Pakistan
[2] Institute of GIS, School of Civil and Environmental Engineering, NUST, Islamabad, Pakistan
[3] Cosmos Science Corporation, Lahore, Pakistan
* e-mail: usman.rashid@umt.edu.pk

Introduction

Reservoirs are major source of socio-economic development along with sustainable agriculture food and cheap energy around the world. Water resources are very precious and it is the need of era for their optimum management to achieve the United Nation's sustainable development goals of zero hunger, affordable and clean energy, economic growth and water availability. Initially the reservoirs were built primarily for single objective during the last century especially after 1950s and 1960s when number of feasible sites were available. Moreover, the most feasible sites have already been utilized by most of the countries and the major shift in focus on multiple objectives is observed for new and already built reservoirs. Rasanen et al. (2015) assessed the potential benefits of multipurpose cascade reservoirs with focus on irrigation and hydropower for Sesan River, the tributary of Mekong River Basin. The results depicted the irrigation potential of about 28350 ha and relatively less hydropower generation capacity. A multi-objective optimization model ResOOSE (Reservoirs Operation Optimization considering Sediment Evacuation) was used for optimizing the rule curves to minimize the irrigation deficits. The model was applied to Terbela and Diamer Basha Reservoirs on Indus River of Pakistan. The RESOOSE model reduced the irrigation deficits up to 16% from 6.9 Billion m^3 to 5.8 Billion m^3 yearly in comparison with existing rule curves. There is still a great potential of benefits available from existing reservoirs which needs to be capitalize using optimization of cascade reservoirs approach (Rashid et al. 2018).

The present study involved developing innovative optimized rule curves of cascade reservoirs in series to maximize the irrigation, hydropower and sediment evacuation benefits. The optimized rule curves' benefits were compared the results of existing rule curves of same cascade reservoirs. The multipurpose Diamer Basha and Terbela Reservoirs were selected for optimization of the benefits using RESOOSE model.

Materials and methods

The study focused genetic algorithm based optimization of rule curves for maximizing the hydro-power, irrigation and evacuation of sediment benefits of cascade reservoirs in the study. RESOOSE Model was applied on multipurpose Diamer Basha and Terbela Reservoirs of Indus River in Pakistan. Forty years (1976 to 2016) spatial and temporal data of the reservoirs including hydraulic, hydrologic and sediment parameters along with existing rule curves were utilized for modeling. Moreover, reservoir levels, water releases, spillways and power generating capacities, rainfall and evaporation data, tunnel capacities of dams, and reservoir operation rule curves were used for analysis. The Terbela dam, one of the largest earth/rock fill dams of Pakistan, was completed in 1976 whereas Diamer Basha's proposed completion is 2020. The Diamer Basha Dam's location is about 315 km upstream of Terbela Reservoir on Indus River. The live storage capacity of Terbela and Diamer Basha Reservoirs are 11.9 and 7.9 billion m^3, respectively, whereas the power capacities are 3478 and 4500 MW, respectively. RESOOSE Model is constructed of four interconnected modules of reservoir operation, hydropower, sediment evacuation and optimization. RESOOSE Model has been developed and programmed in MATLAB. Some of the benefits of the model are the multi-objective optimization capabilities to compute irrigation, power and sediment evacuation benefits, graphical user interface, robust back end engine and compiler, ease to use and availability of built-in engineering/mathematic functions library.

The objective function developed comprised of technical parameters and unit economic values on the

basis of 2016 prices of three major benefits i.e. irrigation, hydro-power and sediment removal. The selection of most suitable methods and values of genetic algorithm parameters were utmost important for optimum results which had been computed using sensitivity analysis in the study. The RESOOSE Model was successfully calibrated and validated and the results were within ±5% range for 80 years hydraulic simulations (Rashid et al. 2018; Suiadee 2000).

Results and concluding remarks

Hydraulic modeling has been carried out for three scenarios and the benefits of rule curves of each scenario were computed and compared. The three scenarios considered in the study are as follows:

- Scenario I: Terbela Reservoir only
- Scenario II: Both Terbela and Diamer Basha Reservoirs
- Scenario III: Multi-objective optimization of joint operation Terbela and Diamer Basha Reservoirs.

For scenarios I and II, the current rule curves published by Water and Power Developing Authority (WAPDA) of Pakistan were used to compute their irrigation, power and sediment evacuation benefits. The basis of current rule curves of both the reservoirs are fulfilling irrigation demands on priority and other benefits of power and sediment evacuation are acquired as secondary benefits. Both the reservoirs are large and Terbela has strategic importance in the water resources systems of Pakistan. An effort has been carried out that during modeling the constraints specified by the WAPDA has been used as such to enhance the credibility of the results. Some constraints of Terbela and Diamer Basha Reservoirs are the minimum operating water levels of 421.8 m and 1060 m respectively whereas maximum conservation levels of 472.5 m and 1160 m respectively. The maximum outflows more than 122 million m^3 to check floods and minimum releases have also been used during simulations. The net economic average irrigation, sediment and hydropower benefits were 444, 0.69 and 1119 million US$ yearly for rule curves of scenario I respectively, which enhanced to 585, 4.6 and 2277 million US$ respectively (83% enhancement) for scenario II. Moreover, due to multi-objective optimization through RESOOSE Model, the benefits of the cascade reservoirs were further raised to 718, 7.32 and 2492 million US$ annually respectively for scenario III (103% enhancement). The maximum total annual benefits of 3217 million US$ were computed for the optimized rule curves of scenario III, which was found 12.2% more as compared to scenario II and 106% more when compared with scenario I. Optimized rule curves of the cascade reservoirs have substantially enhanced all the three considered benefits i.e., hydropower, irrigation and sediment removal.

The most suitable methods and values of genetic algorithm parameters have been computed using sensitivity analysis in the study for optimum results. The best methods and values identified in the study are tournament selection method with 2 teams, population size 288, single point crossover method with crossover probability 0.8 and adapt feasible mutation method. The annual irrigation, power and sediment evacuation benefits of Terbela Reservoir due to existing rule curves are 444, 0.69 and 1119 million US$, which have been enhanced by its conjunctive operation with Diamer Basha Reservoir upto 4.6 and 2277 million US$, i.e. overall 87% enhancement. The optimized rule curves of Terbela and Diamer Basha have enhanced the irrigation, power and sediment evacuation benefits upto 4.6 and 2277 million US$, overall 3333 million US$, which are 12% more than their existing rule curves and 106% more than the rule curves as single reservoir. The article recommends revising the rule curves of Diamer Basha and Terbela Reservoirs for enhanced benefits and achieving the sustainable development goals. Moreover, the basis of upgrading the rule curves should also be economic benefits of hydropower and sediment evacuation in addition to fulfilling the irrigation demands.

References

Rasanen TA, Joffre OM, Someth P et al. (2015) Model-Based Assessment of Water, Food, and Energy Trade-Offs in a Cascade of Multipurpose Reservoirs: Case Study of the Sesan Tributary of the Mekong River. Journal of Water Resources Planning and Management 141(1):05014007. DOI: 10.1061/(ASCE)WR.1943-5452.0000459

Rashid MU, Latif A, Azmat M (2018) Optimizing Irrigation Deficit of Multipurpose Cascade Reservoirs. Water Resources Management 32(5):1675-1687. https://doi.org/10.1007/s11269-017-1897-x

Suiadee (2000) An integrated approach to real time optimal operation and irrigation water system: A case study of Nam Oon irrigation project. Dissertation no WM-05-02, Asian Institute of Technology, Thailand

11th World Congress on Water Resources and Environment (EWRA 2019)
"Managing Water Resources for a Sustainable Future", 25-29 June 2019, Madrid, Spain

A DSS tool for stochastic optimization of large-scale water resource systems

H. Macian-Sorribes*, M. Pulido-Velazquez
Research Institute of Water and Environmental Engineering (IIAMA), Universitat Politècnica de València, Spain
** e-mail: hecmasor@upv.es*

Introduction

Stochastic programming algorithms are able to explicitly incorporate inflow uncertainty in their formulation and avoid the "perfect foresight" in order to deliver more realistic optimization results (Labadie 2004). However, their real-life applicability is challenged by its mathematical complexity and the lack of generalized Decision Support System (DSS) shells implementing stochastic programming algorithms. Although the standard Stochastic Dynamic Programming (SDP) is hindered by the curse of dimensionality (Nandalal and Bogardi 2007), recent stochastic programming algorithms can adequately handle large-scale water resource systems with reasonable computational requirements. Among them, Stochastic Dual Dynamic Programming (SDDP) has proven to be applicable to large-scale water resource systems including hydropower production (Pereira and Pinto 1985), irrigated agriculture (Tilmant et al. 2008), and groundwater and stream-aquifer interactions (Macian-Sorribes et al. 2017).

This contribution presents a general-purpose DSS shell to implement stochastic programming algorithms in large-scale water resource systems, named Explicit Stochastic Programming Advanced Tool (ESPAT). Stochastic optimization is performed using SDP and SDDP algorithms. It uses a hydroeconomic approach in which optimization seeks maximizing the total economic benefits in the system (summation of individual benefits in economic activities). The code is written in the GAMS language and the DSS shell implements a GAMS-Excel link to execute the optimization process, so no knowledge of GAMS is needed to run it.

Materials and methods

The tool is divided into four modules according to the algorithm employed, coded separately in GAMS.

- ESPAT_R: solves stochastic programming problems using the SDDP algorithm considering neither aquifers nor stream-aquifer interaction.
- ESPAT_RA: solves stochastic programming problems using a modified version of SDDP, named CSG-SDDP, able to solve stochastic programming problems in large-scale water resource systems including aquifers and stream-aquifer interactions.
- ESPAT_SDP: uses a standard SDP approach to solve stochastic optimization problems in small water resource systems.
- ESPAT_DET: implements a deterministic optimization algorithm with the same applicability range of SDDP but subject to the perfect foresight of future hydrological conditions.

All modules share a common graphical user interface (GUI) that controls loading of the system features (topology, hydrology, infrastructure, demands and economics) into the code, runs it and presents results (storages, streamflows, deliveries, deficits, pumping rates, energy produced and monetary gains) in the form of Excel sheets. This common feature-loading interface allows an easy change between modules and enables the possibility to compare results from different algorithms (e.g. between SDDP and deterministic optimization). It also implements a simulation module to obtain the system performance in response to predefined operating rules.

Results and concluding remarks

The ESPAT tool application is illustrated using as example the Jucar River Basin (Spain). It consists of 8 reservoirs, 3 main groundwater bodies, 4 urban demands, 9 irrigation demands, 1 industrial demand, 9 hydropower plants. The analysis period covered 14 years, between 1998 and 2012. Results from ESPAT

simulation module (current operation), ESPAT_RA (stochastic programming) and ESPAT_DET (deterministic programming) are shown. The stored water distribution among the main reservoirs Alarcon, Contreras and Tous (Figure 1) shows significant variations according to the alternative. Both current operation and stochastic programming show a clear and similar pattern, although the former stores generally more water in Tous (downstream reservoir) while the latter keeps water upstream (Alarcon and Contreras). Furthermore, stochastic programming a flexible operation compared with current rules as shown in the span of the dotted areas (particularly in Alarcon). The messy scatterplot of deterministic programming, on the other hand, shows no clear pattern in storage distribution due to an (unrealistic) perfect foresight of future hydrology that drives decisions taken into account both the short and the long term.

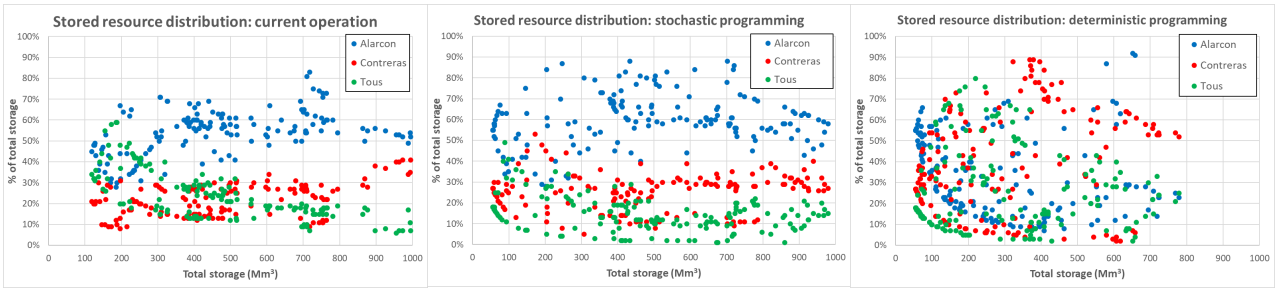

Figure 1. Stored resource distribution in the Jucar River Basin.

Benefit levels comparison (Table 1) show economic gains in both stochastic and deterministic programming. Stochastic programming overwhelms current operation by 5.31 M€/year. However, deterministic programming offers an (ideal) upper bound, improving stochastic programming by 5.91 M€/year. Agricultural revenues offered by stochastic programming are close to deterministic optimization.

Table 1. Average benefits (M€/year) per alternative for the analysis period (1998-2012)

Benefits (M€/year)	**Current operation**	**Stochastic programming**	**Deterministic programming**
Urban	289.04	289.14	288.98
Agricultural	193.91	196.38	197.74
Hydropower	22.26	25.00	29.71
Total	505.21	510.52	516.43

The ESPAT tool is able to perform stochastic optimization runs in large-scale water resource systems, with more realistic results than deterministic programing due to the removal of the perfect foresight. Furthermore, it eases comparing simulation, stochastic optimization and deterministic optimization.

Acknowledgments: The European Research Area for Climate Services programme (ER4CS) supports this study under the INNOVA project (grant agreement: 690462).

References

Labadie JW (2004) Optimal Operation of Multireservoir Systems: State-of-the-Art Review. Journal of Water Resources Planning and Management 130:93–111. https://doi.org/10.1061/(ASCE)0733-9496(2004)130:2(93)

Macian-Sorribes H, Tilmant A, Pulido-Velazquez M (2017) Improving operating policies of large-scale surface-groundwater systems through stochastic programming. Water Resources Research 53:1407–1423. https://doi.org/10.1002/2016WR019573

Nandalal KWD, Bogardi JJ (2007) Dynamic Programming Based Operation of Reservoirs. Cambridge University Press, Cambridge, United Kingdom.

Pereira MVF., Pinto LMVG (1985) Stochastic Optimization of a Multireservoir Hydroelectric System: A Decomposition Approach. Water Resources Research 21:779–792. https://doi.org/10.1029/WR021i006p00779

Tilmant A, Pinte D, Goor Q (2008) Assessing marginal water values in multipurpose multireservoir systems via stochastic programming. Water Resources Research 44(12):W12431. https://doi.org/10.1029/2008WR007024

11th World Congress on Water Resources and Environment (EWRA 2019)
"Managing Water Resources for a Sustainable Future", 25-29 June 2019, Madrid, Spain

New approaches toward efficient and robust uncertainty quantification in real-time flood forecasting

V. Ngoc Tran, J. Kim*
School of Civil and Environmental Engineering, University of Ulsan, South Korea
** e-mail: kjongho@ulsan.ac.kr*

Introduction

In the past decade, with three main problems in a rainfall-runoff model of real-time flood prediction including accuracy, predictability, and computational efficiency, many approaches have been developed. However, most of the prior studies concentrated on the objective of improving predictive accuracy without evaluating the effectiveness. Therefore, in this study, a new coupling unified framework is proposed, which can improve the predictive performance with three issues above. First, to increase the forecast accuracy and predictability, the sequential data assimilation is implemented to address the uncertainty sources such as model state and model parameter. Ensemble Kalman filter (EnKF) (Evensen 1994) is selected instead of the particle filter (PF) because this method is computationally cheaper than PF as it generally requires less ensemble members based on the sequential Monte Carlo method. In addition, in initialization of EnKF in prior studies the initial ensemble of model state and parameter are generated according to the uniform distributions in the corresponding ranges and the initial state values of zero are set (so-called Random method) while in this study, Generalized Likelihood Uncertainty Estimation (GLUE) (Beven and Binley 1992) method is suggested as an approach to initialize the ensemble member of states and parameters to robust increase the convergence in assimilation EnKF. The use of GLUE also improves the accuracy and predictability of the forecast. Finally, the EnKF method required a large of a number of models runs to obtain the ensemble results lead to very PCU intensive while time is important for timely flood warning and emergency responses. Therefore, the surrogate model based on Polynomial chaos expansion (PCE) (Ghanem and Spanos 1991; Wiener 1938) is considered to alternate the conceptual rainfall runoff (CRR) model, which can significantly increase the computational efficiency of the forecast.

In this work, we investigate and tackle and essential estimation problem that is the accuracy, predictability, and computational efficiency of the hydrological model on real-time flood forecasting depending on different approaches of coupling framework, the optimal unified framework to robust quantify and reduce uncertainties in hydrologic prediction is proposed. The results of 18 approaches will show that: (i) the efficiency of computation of proposed unified framework on real-time forecasting (ii) the effect of GLUE on initialization of real-time forecasting; (iii) the capable of PCE model on real-time forecasting; and (iv) the effect of EnKF on real-time forecasting.

Materials and methods

As described in the introduction, the methods used in the study included GLUE, PCE, and EnKF. First, building a PCE-based CRR model depends on the training of the CRR model with the input as parameters, state, and rainfall and the result is streamflow. In addition, there are two approaches to construct the PCE model depends on the method to select the parameter for training, one through random parameter sets, one through the behavior parameter sets after GLUE. In this study, both methods are implemented with the corresponding models are called PCE-I and PCE-II, respectively. Meanwhile, this study uses both EnKF only state update and Dual EnKF parameter-state update (Moradkhani et al. 2005), the results are compared with approaches that do not use data assimilation.

Depends on the components of the unified framework including state-parameter initialization method (Random, GLUE) – Model (hydrological model, PCE-I, PCE-II) – Data assimilation method (No DA, EnKF, Dual EnKF), eighteen approaches study are developed depending to demonstrate the simulation capabilities of the coupling framework. All of the approaches are employed to answer four questions in the introduction.

Regarding the construction of the PCE model and the comparison of the performance of the approaches, the conceptual rainfall-runoff model NAM model (Nedbør - Afstrømnings Model) is used in this study. The application of approaches was conducted with a flood in Vu Gia watershed in Central Vietnam, one of the areas frequently affected by severe flooding.

Results and concluding remarks

This study has focused on the developed coupling unified framework to improve the accuracy, predictability, and computational efficiency of streamflow forecast by considering the strengths of three aspects: GLUE – PCE – EnKF. The analysis was applied to the Vu Gia watershed in central Vietnam with 18 different approaches, the major findings from the results analysis are as follow:

- The calibration period with GLUE method has a major impact on the predictive performance of the hydrological model. The forecast results of GLUE approaches are better accuracy and predictability than the Random method, which has significant meaning for accurate forecasting and flood level determination to make decisions for the manager. Even the approaches coupling GLUE and EnKF also provide the results near-real-world than Random method.
- With two approaches of PCE construction, both PCE models are providing the good result as NAM model in calibration period although the time construction of PCE-II is much smaller than PCE-I (e.g., approximately 23.9 and 541.3 seconds). However, when applying both PCE model for the real-time forecast for a different flood event, the PCE-II does not provide good result even using GLUE or EnKF, while the result obtained from PCE-I is as well as NAM model. It can be seen that the approach using a behavioral set to build the PCE model is much faster than using the random set, but this approach is failing in predicting the different flood conditions. Besides, the computational efficiency of the surrogate PCE-I model is significantly increasing (e.g., approximately 20 times faster with the approaches using Random method and 80 times faster with the approaches using GLUE).
- The EnKF and Dual EnKF are a powerful technique in real-time forecasting, which major improve both accuracy and predictability of predicting results. Although Dual EnKF requires more computation time than EnKF, with the significant performance of PCE, the calculation time is not the main issue. The results illustrate that the Dual EnKF provides the predicting result more accurate and predictability than EnKF. Because there is no certain guarantee confirm that there is an optimal parameter set that can be suitable for every flood events, therefore, the approaches using updating the parameter-state will result in more accurate measurement than not using DA or state update only.

Finally, with the goal of improving accuracy, predictability, and computational efficiency, the result of 18 approaches demonstrate that the unified framework of coupling of GLUE – PCE – Dual EnKF is proposed as a good framework, which can be applied in real-time flood forecasting and provide predictive information high-precision and quickly in mitigating the flood risk.

Acknowledgment: This research was supported by the Water Management Research Program funded by Ministry of Environment of Korean government (127554), and by the Basic Science Research Program of the National Research Foundation of Korea funded by the Ministry of Education (2016R1D1A1B03931886).

References

Beven K, Binley A (1992) The future of distributed models: Model calibration and uncertainty prediction. Hydrological Processes 6:279-298. doi:10.1002/hyp.3360060305

Evensen G (1994) Sequential data assimilation with a nonlinear quasi-geostrophic model using Monte Carlo methods to forecast error statistics. Journal of Geophysical Research 99:10143. doi:10.1029/94jc00572

Ghanem RG, Spanos PD (1991) Stochastic Finite Elements: a Spectral Approach. Springer, Verlag New York. doi: 10.1007/978-1-4612-3094-6

Moradkhani H, Sorooshian S, Gupta HV, Houser PR (2005) Dual state–parameter estimation of hydrological models using ensemble Kalman filter. Advances in Water Resources 28:135-147

Wiener N (1938) The Homogeneous Chaos. American Journal of Mathematics 60:897. doi: 10.2307/2371268

11th World Congress on Water Resources and Environment (EWRA 2019)
"Managing Water Resources for a Sustainable Future", 25-29 June 2019, Madrid, Spain

The influence of land use change and urban growth on river flood hazard in Villahermosa (Mexico)

O.S. Areu-Rangel[1], L. Cea[2], R. Bonasia[3], V.J. Espinosa-Echavarria[1]
[1] Departamento de Ciencias de la Tierra/Tecnológico Nacional de México/Instituto Tecnológico de Pachuca, Pachuca Hidalgo, Mexico
[2] Universidade da Coruña/Environmental and Water Engineering Group, Department of Civil Engineering, Spain
[3] CONACYT – Instituto Politécnico Nacional, ESIA, UZ, Mexico City, Mexico
* e-mail: rosannabonasia017@gmail.com

Introduction

The state of Tabasco (Mexico) is recurrently facing inundation events through its territory. The lack of environmental planning has drastically modified the territory characteristics of this state during the last decades. The elimination of vegetable cover has led to a loss of soils and to a reduction of the infiltration capacity, causing higher volumes of surface runoff, silting and hillslope erosion. From 1940 to 1990, the state of Tabasco lost 97% of its forest resources, causing wind and water erosion to affect almost 50% of the territory. In October 2007, Tabasco was hit by an intense flooding event that affected about 70% of the state. The capital city, Villahermosa, was especially badly hit, suffering huge economic losses.

In the last 40 years, the construction of housing complexes and containment bridges within Villahermosa have not only modified the landscape but have also caused a phenomenon of irregular settlements on the margins of the embankments.

This work analyses two of the main causes that explains the increase on flood frequency and magnitude in Villahermosa: the change in land use on the hydrological basins located upstream the city and the increase of the urban area. First, we analyse the effect of change in land use of the catchments that drain to Villahermosa. Flood discharges for different return periods are calculated considering the oldest information on basin's land use (until 1992) and the most recent one (2013). The obtained scenarios are numerically simulated with the 2D flood inundation model IBER (Bladé et al. 2014). Secondly, the effect of the increase in the area occupied by buildings in the city was analysed by comparing the inundation depths for three possible future urbanization scenarios.

Materials and methods

The city of Villahermosa is located within the hydrological zone Grijalva-Usumacinta (INEGI 2011), which is divided into 83 basins, eight of which drain into the city. The rivers directly responsible for flood events in Villahermosa are: the Carrizal, the Viejo Mezcalapa, the Pichucalco and the de la Sierra rivers.

Flood discharges of each river for different return periods were estimated with the Chow's method (Chow et al. 1988), including two adjustment factors to account for the spatial and temporal variability of extreme rainfall in large catchments. The information on the land uses of the catchments under study over the last years has been provided by the National Institute of Statistics and Geography (INEGI 2011). In order to analyse the impact that the changes in land use have on the inundation levels, the flood discharges for the return period of 10, 25, 50 and 100 years were calculated using the curve numbers corresponding to the oldest land use series (Series I 1992) and the most recent one (Series V 2013).

The inundation scenarios were modelled with the software IBER, that solves the 2D shallow water equations to compute spatial distribution of the water depth and the two horizontal components of the depth-averaged velocity.

Three land uses were considered within the simulation domain in order to characterize the surface roughness: urban, agricultural and river channel. Given the dense and complex urbanization pattern of the city, the effect of the buildings on drag resistance was accounted for using and augmented Manning coefficient to characterize the surface roughness in the urban districts (Huang et al. 2014).

Results and concluding remarks

Water depth differences computed for the flood discharges obtained with the basin's land use of Series I and Series V show that, for lower return periods (10 and 25 years) the change in land use from mainly pasture soils (Series I) to agricultural soils (Series V), produced a significant increase on the flood depths, with maximum values between 1.0 and 1.6 m. These values are reduced to an increase between 0.6 and 1.2 m as the return period increases. To quantify the average difference in water depth over the whole study area, a flood Depth Index was computed for each return period. Values of DI indicate that the influence of land use changes in the inundation levels is very relevant. These results confirm what was analysed by Zuñiga and Magaña (2018), who studied the frequency of floods in Mexico comparing observed and modelled frequency for the period 1970-2010 and found that most of the flooding events in the Mexican territory occurred as a consequence of the rapid deforestation process that affected the basins of the main rivers in the country.

In order to analyse the impact on flood inundation of the urban expansion of Villahermosa, three urbanization scenarios have been proposed for 2050, taking into account the areas that are more prone to future urbanization. For each scenario, inundation depths were computed for the flood discharge corresponding to the return period of 100 years and the land use of Series V.

Results show that the extension of the flood is similar for the three urbanization scenarios and it seems not to have a considerable effect on the increase of flood levels, specially when compared to the effect of land use changes in the basins. However, it is important to consider that since 80s flooding events increased in Villahemrosa, as consequence of the uncontrolled demographic growth that lead to legal and illegal expansion of the urban area within the districts most prone to be flooded.

Results of this work indicate that one possible way to reduce river inundation in Villahermosa could be a sustainable management of land uses in the basins located upstream the city, in order to increase the infiltration capacity of soils. Moreover, this work provides indications about the increase of flood levels if the expansion of the urban area continues in an uncontrolled manner, and it can be considered as a useful tool for future territorial planning, as well as for the design of new embankments and retaining walls within the city.

References

Bladé E, Cea L, Cortesein G, Escolano E, Puertas J, Vázquez-Cendón J, Dolz J, Coll A (2014) IBER: herramienta de simulación numérica de flujo en ríos. Rev Int Métodos Num para Cálculo y Diseño en Ing 30(1):1-10

Chow VT, Maidment D, Mays L W (1988) Applied hydrology. New York: McGraw-Hill

Huang C, Hsu M, Teng W, Wang Y (2014) The impact of building coverage in the metropolitan area on the flow calculation. Water 6:2449-2466

Instituto Nacional de Estadística, Geografía e Informática (INEGI) (2011) Uso del suelo y vegetación Series 1 a 5. http://www.beta.inegi.org.mx

Zuñiga E, and Magaña V (2018) Vulnerability and risk to intense rainfall in Mexico: The effect of land use coverage change. Investigaciones Geográficas 95. doi: 10.14350/rig.59465

Development and validation of a flood forecasting system for 3 small catchments in the Northwest of Spain

I. Fraga[1*], L. Cea[2], O. García-Feal[3]
[1] CITIC, University of A Coruña, A Coruña, Spain.
[2] Environmental and Water Engineering Group, Department of Civil Engineering, Universidade da Coruña, Spain.
[2] Environmental Physics Laboratory (EPHYSLAB), University of Vigo,Spain.
* e-mail: ignacio.fraga@udc.es

Introduction

Flood events are becoming more frequent due to the urbanization of floodplains and to the impact of climate change. In addition, the increase of population has raised the anthropogenic pressure on water courses, triggering the negative impact of flood events. As a result of all these factors, floods have become the main type of natural disaster during the last decades. Against this background, several international organizations consider that increasing resilience is a more efficient approach towards flood damage reduction than building structural defences. However, this approach demands accurate and reliable flood forecasting systems.

In this context, we present a new flood early warning system implemented in 3 catchments located on the northwest of Spain (Figure 1), with sizes of 4.95 (Cee), 16.93 (Grova) and 83.9 (Mendo) km^2. The catchments are flood prone areas and have urbanized areas that have been declared as Areas with Potentially Significant Flood Risk (APSFR) by the regional water administration. The forecasting system proposed was tested during the 2018 spring and fall seasons, with a satisfactory performance.

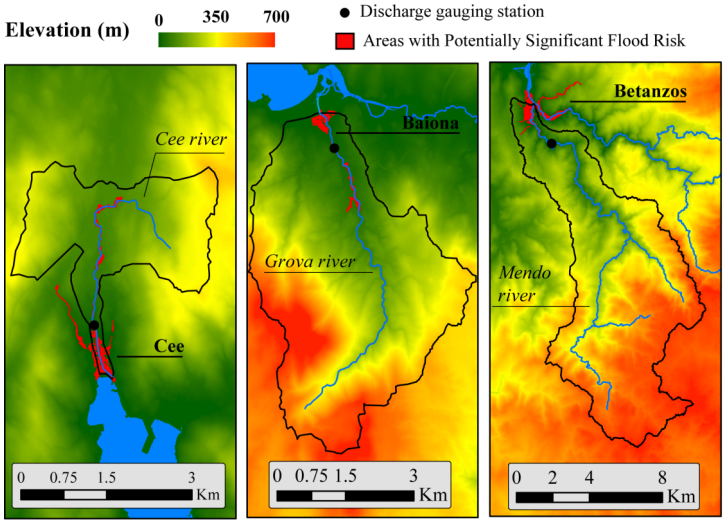

Figure 1. Study catchments.

Materials and methods

The flood early warning system operates in two steps, both of them performed on a daily basis within each catchment. In the first step, the rainfall fields in the catchment during the antecedent 30 days are estimated from observed data from the rain gauge and meteorological radar of MeteoGalicia. For this purpose, radar and rain gauge data are merged using the kriging with external drift technique. Also, temperature, humidity, wind speed and solar radiation are spatially interpolated from pointwise observations registered by the meteorological network of MeteoGalicia. These data are used as inputs of a semi-distributed HEC-HMS (Scharffenberg and Fleming 2006) hydrological model of the catchment. The

hydrological model uses the Soil Moisture Account Method to compute rainfall losses and the SCS Unit Hydrograph to determine the rainfall-runoff transformation. The input parameters of the model are calibrated against discharge data measured by the Augas de Galicia monitoring network during the antecedent 30 days.

In the second step, the outputs of a weather forecast model are used as inputs of the hydrological model calibrated in the first step. The weather forecast model corresponds to the WRF model operated by MeteoGalicia, which has temporal and spatial resolutions of 1 hour and 5 km respectively. The hydrological model computes the hydrographs upstream the APSFR area during the following 4 days. The computed hydrographs are used as boundary conditions of Iber+ (García-Feal et al. 2018) bidimensional inundation models of the APSFR areas. The outputs of the inundation models are flood maps with the spatial and temporal distribution of water depth and velocity in the APSFR. The flow model Iber+ is parallelized using GPU-based techniques, which allows computing the hydrodynamics of the APSFR area for the next 4 days in only a few minutes.

Results and concluding remarks

The validation with observed data of the peak discharges forecasted during several storm events shows an acceptable performance of the system (Figure 2). Results also show that the errors on the peak discharges are lower than those on the forecasted rainfall volume. The performance of the system is similar in the three catchments analysed, even if their size and topography is quite different. No comparison between observed and predicted water depths was performed since no flood event occurred during the validation of the model.

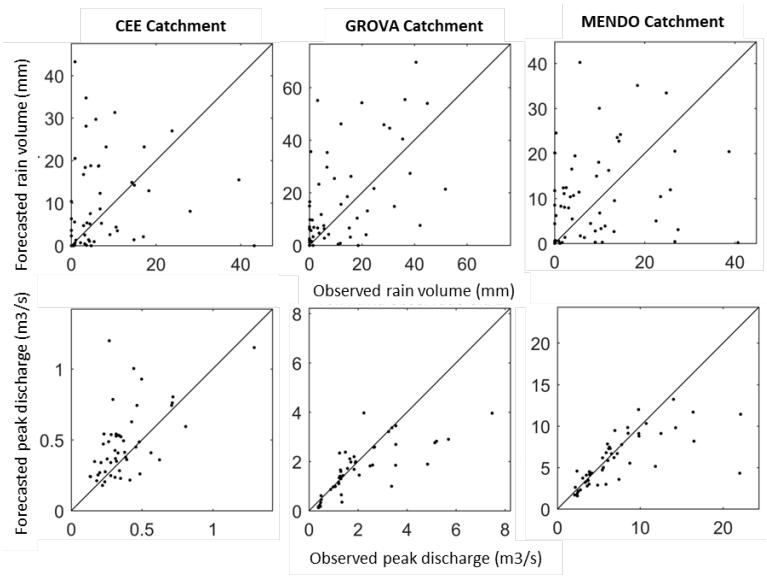

Figure 2. Observed and forecasted rain volumes and peak discharges in the three catchments.

Acknowledgments: Ignacio Fraga received financial support from the Xunta de Galicia (Centro Singular de Investigación, Galicia, accreditation 2016-2019) and the European Union (European Regional Development Fund-ERDF). The authors would also like to thank MeteoGalicia (Galician Regional Weather Service) for the rainfall data provided for this study.

References

García-Feal O, González-Cao J, Gómez-Gesteira M, Cea L, Domínguez J, Formella A (2018) An accelerated tool for flood modelling based on Iber. Water 10(10):1459. https://doi.org/10.3390/w10101459

Scharffenberg W, Fleming M (2006) Hydrologic modeling system HEC-HMS: User's manual. US Army Corps of Engineers, Hydrologic Engineering Center

Skamarock W, Klemp J, Dudhia J, Gill D, Barker D, Wang W, Powers (2005) A description of the advanced research WRF version 2 (No. NCAR/TN-468+ STR). National Center For Atmospheric Research, Boulder Colorado. Mesoscale and Microscale Meteorology Division

11th World Congress on Water Resources and Environment (EWRA 2019)
"Managing Water Resources for a Sustainable Future", 25-29 June 2019, Madrid, Spain

Application of the Humidity index in the Crati River basin (Italy)

E. Infusino[1], T. Caloiero[2*], F. Fusto[3]
[1] University of Calabria-DIATIC, Rende (CS), Italy
[2] CNR-ISAFOM, Rende (CS), Italy
[3] Multi-Risk Functional Centre of the Regional Agency for Environmental Protection of Calabria, Catanzaro, Italy
* e-mail: tommaso.caloiero@isafom.cnr.it

Introduction

According to the fifth IPCC report (2013), the forecasted climate changes and extreme events are expected to have a dramatic impact on natural ecosystems and economy in many parts of the world. In this context, the Mediterranean basin has been categorized as a global warming hotspot (Segnalini et al. 2013), in that the area is expected to face particularly high impacts from global warming and climate change and to be most vulnerable to their deleterious effects. Indeed, climate change could increase the risk of future meteorological extremes over large regional areas. For example, extreme heat events, which regularly lead to excess mortality, have been documented worldwide (Ho et al. 2016). An appropriate quantification of human heat exposure is a necessary foundation for studying the effect of heat on human health. Moreover, it is well known that the discomfort that is felt in hot weather depends to a significant degree on air humidity as well as the actual air temperature (Schoen 2005). Among the numerous attempts which have been made to quantify this effect, one of the most used is the application of the humidity index.

In this study, an analysis of the temperature and humidity data registered in the largest catchment of the Calabria region (southern Italy) has been performed.

Materials and methods

The humidity index (Humidex), first applied in Canada by Masterton and Richardson (1979), is defined as follows:

$$H = T + \frac{5}{9} \cdot (e - 10) \quad (1)$$

where T is the dry-bulb air temperature (in °C), e is the air vapour pressure (in hPa) measured with a psychrometer.

If the value of air vapour pressure is not available, it can be estimated through a function which combines relative humidity and temperature:

$$e = 6.112 \cdot 10^{\frac{7.5 \cdot T}{237.7 \cdot T}} \cdot \frac{R}{100} \quad (2)$$

where R is the air relative humidity (%).

The Humidex can be interpreted as the temperature actually perceived by the human body due to the combination of the dry-bulb air temperature and the relative humidity and it is measured in Celsius degrees. Different values of H identify different categories of discomfort, corresponding to the following levels of alert: Full comfort ($H < 27$), Subtle discomfort ($27 < H < 30$), Great discomfort ($30 < H < 40$), Danger ($40 < H < 55$) and Imminent heat stroke ($H > 55$).

The area under investigation is the valley of the Crati river, located in the NW sector of the Calabria region, which is the main basin in the region with a perimeter of about 320 km and an area of 2447.7 km^2. It presents high climatic variability due to its position in the Mediterranean area and its mountainous nature, denoting a subtropical Mediterranean climate (Coscarelli et al. 2004, Infusino et al 2004). The database used in this study consists of sub-daily temperature and humidity series registered at three stations in which the data are both available: S. Antonello, managed by the laboratory GICA of the University of Calabria, and Cosenza and Torano Scalo managed by the Multi-Risk Functional Centre of the Regional Agency for Environmental Protection. The observation period is 2001-2017.

Results and concluding remarks

First, a trend analysis on the temperature and humidity series has been performed. Results evidenced a clear increase in the temperature extreme values, thus confirming past studies which, in the Calabria region, showed a growing risk of extreme heat events (Caloiero et al. 2017). Then, the Humidex has been evaluated at hourly time scale. As a result, for all the stations, an increase in the Humidex values has been detected during the observation period, with the highest values occurring after 2008, when the maximum annual values always exceed the "Danger" threshold. In particular, in 2011, in 2015, and in 2017 more than 150, more than 200 and about 100 time intervals showed Humidex values higher than 40, respectively. Moreover, in these years, the "Imminent Heat Stroke" threshold has been exceeded, thus evidencing high human risks due to heat exposure. As an example, in Figure 1 the temporal evolution of the Humidex during the summer (from June to August) of 2017 is shown. In this period, in 21 days the index values exceed the "Danger" threshold, with the longest exceeding sequence identified between the end of July and the beginning of August (10 consecutive days). These results could help to improve our understanding of the changing climate and severe weather conditions, as well as to provide guidance to inhabitants in making informed decisions about future risks associated with weather hazards.

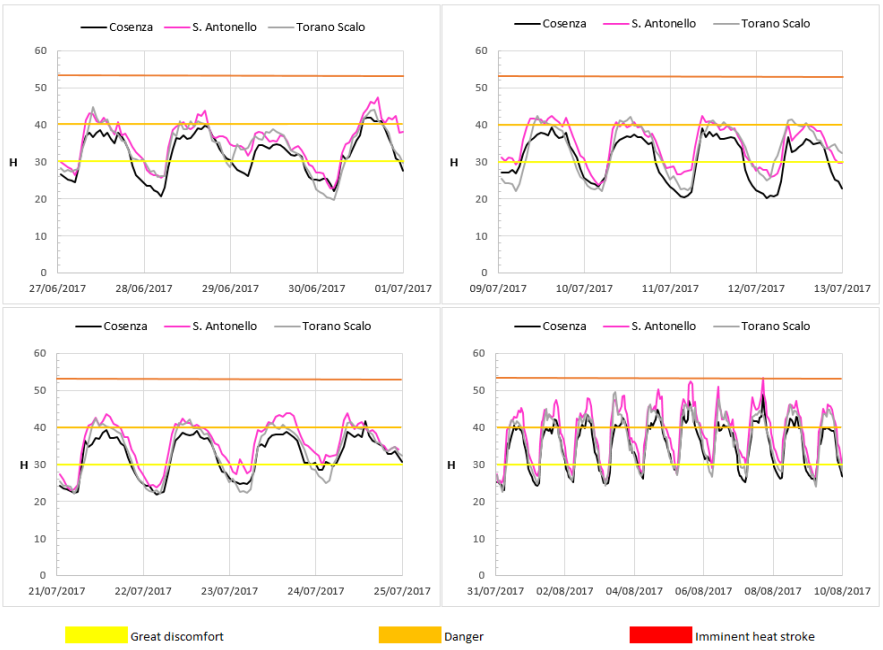

Figure 1. Temporal evolution of the Humidex during the summer of 2017.

References

Caloiero T, Coscarelli R, Ferrari E, Sirangelo B (2017) Trend analysis of monthly mean values and extreme indices of daily temperature in a region of southern Italy. International Journal of Climatology 37:284-297

Coscarelli R, Gaudio R, Caloiero T (2004) Climatic trends: an investigation for a Calabrian basin (southern Italy). IAHS Publications 286:255-266

Ho HC, Knudby A, Xu Y, Hodul M, Aminipouri M (2016) A comparison of urban heat islands mapped using skin temperature, air temperature, and apparent temperature (Humidex), for the greater Vancouver area. Science of the Total Environment 544:929-938

Infusino E, Callegari G, Frega G (2004) Problemi di stabilità atmosferica. Loro influenza sulle precipitazioni- un caso di studio nella valle del F. Crati. SIDISA Simposio Internazionale di Ingegneria sanitaria Ambientale, Taormina

IPCC (2013) Summary for Policymakers. Fifth Assessment Report of the Intergovernmental Panel on Climate Change. Cambridge University Press, Cambridge, UK

Masterton JM, Richardson FA (1979) Humidex, a method of quantifying human discomfort due to excessive heat and humidity, CLI 1-79. Environment Canada, Atmospheric Environment Service, Downsview, Ontario

Schoen C (2005) A New Empirical Model of the Temperature–Humidity Index. Journal of Applied Meteorology 44:1413-1420

Segnalini M, Bernabucci U, Vitali A, Nardone A, Lacetera N (2013) Temperature humidity index scenarios in the Mediterranean basin. International Journal of Biometeorology 57:451-458

11th World Congress on Water Resources and Environment (EWRA 2019)
"Managing Water Resources for a Sustainable Future", 25-29 June 2019, Madrid, Spain

Investigating trends in rainfall in a small island: The case of Madeira Island, Portugal

L.A. Espinosa[1,2*], M.M. Portela[1], R. Rodrigues[2]
[1] Civil Engineering Research and Innovation for Sustainability (CERIS), Instituto Superior Tecnico (IST), University of Lisbon (UL), Portugal
[2] National Laboratory for Civil Engineering (LNEC), Portugal
* e-mail: luis.espinosa@tecnico.ulisboa.pt

Introduction

Studying climate variability, hydrological extreme events, trends in hydrological variables, along with their prediction, from global to regional and local scales, are of primary importance for agricultural, forestry and water management activities. These activities are scheduled or designed mainly in accordance to rainfall seasonality and spatiotemporal distribution (Villafuerte II et al. 2014). However, assessing climate variability and the mechanisms that cause changes and their related impacts is rather difficult. In recent years, these non-evenly distributed changes have led to an increased temporal variability mostly of precipitation, streamflow and evaporation patterns. For the purpose of understanding the climate change effects, trend analysis and change-point detection in time series of climate variables, such as temperature and precipitation, have been the focus of research worldwide. Hence, precipitation trend analyses are crucial in water planning and management (Rao et al. 2015).

The features of the small islands, such as the reduced areas of their catchments and the limited, and often low, surface and groundwater storage capacity, make their hydrology and water resources development and management issues very distinct from those on larger islands or continental areas. Thus, in the former islands understanding the behaviour of the climate variables and being able of detecting their trends are fundamental issues (Falkland et al. 1991).

The aim of this paper is to provide a suitable understating about the variations in rainfall and of the recent dynamics of change in rainfall over a small island environment as is the case of Madeira Island – a Portuguese island which has suffered from sustained below-average rainfall conditions in recent years (Liberato et al. 2017), located in the North Atlantic (NA), in the European part of Macaronesia.

Materials and methods

Changes in the rainfall in Madeira Island (with an area of 741 km^2, a length of 57 km and a largest width of 22 km) were analyzed, based on complete time series of monthly, seasonal and annual maximum (from 1-day to 7-day) rainfall, from October 1937 to September 2017 (80 hydrological years). Some commonly used tools for detecting changes in climatic and hydrological variables, namely, the non-parametric Mann-Kendall (MK) statistical test to detect significant trends coupled with the Sen's slope approach to quantify such trends were applied to the 80 years of data at 41 rain gauges evenly distributed over the island. Additionally, change-point detection techniques were used in order to identify statistically significant abrupt changes in the data at different time-spans.

Results and concluding remarks

Figure 1 exemplifies (based on January, the first semester and year) the spatial distribution of the Sen's slope estimates. From the 41 rain gauges, the few ones with series denoting statistical significant trends (either negative or positive) for the confidence level of $\alpha = 0.05$ are identified. Although most of the results are not statistically significant, they are similar, regardless the period of the year, denoting a generalized decrease of the rainfall over the island, except for a very small area of the southern slope where a slight increase was detected.

The mountainous central region, where most of the groundwater recharge takes place, shows the

highest annual rainfall decrease (e.g. the rain gauge M01-Areeiro with - 9.30 mm year−1), also often with statistical significance at different time-spans, whereas for the lowland southern slope, with high population density, the annual decrease is much less pronounced and even slightly positive (e.g. M22-Ribeira Brava rain gauge with 2.30 mm year−1).

These results are in accordance to previous climatic studies about recent global rainfall changes in the European Macaronesia which have reported generalized decreasing trends in different periods of the year. Regarding Madeira Island, Miranda et al. (2006) investigated the presence of linear monotonic trends based on 135 years (1865–2000) of rainfall at Funchal meteorological station and Santos et al. (2004) utilized rainfall data from 14 rain gauges coupled with the atmosphere-ocean general circulation model HadCM3 (Hadley Centre Coupled Model Ver. 3) to produce scenarios of precipitation anomalies, with particular attention given to the winter and summer seasons in the late 21st century.

Different from the previous studies about rainfall trends, whose results were based on a very small number of rain gauges, this study utilized a considerable number of complete rainfall time series covering 80 years each – 41 series of daily rainfall from 1937/38 to 2016/17. It is, therefore, the first comprehensive and detailed study about rainfall trends in Madeira Island, thus providing new insights towards the understanding of the rainfall patterns in the island in recent decades.

Due to the specificity and diversity of climatic conditions of the small island, characterization methods, as those aiming at detecting rainfall trends, taken directly from continental territory applications may be crude, even irrelevant or inaccurate approaches. Therefore, specific methods should be developed or adapted, taking into account each island's peculiarities, as done in this study for Madeira Island.

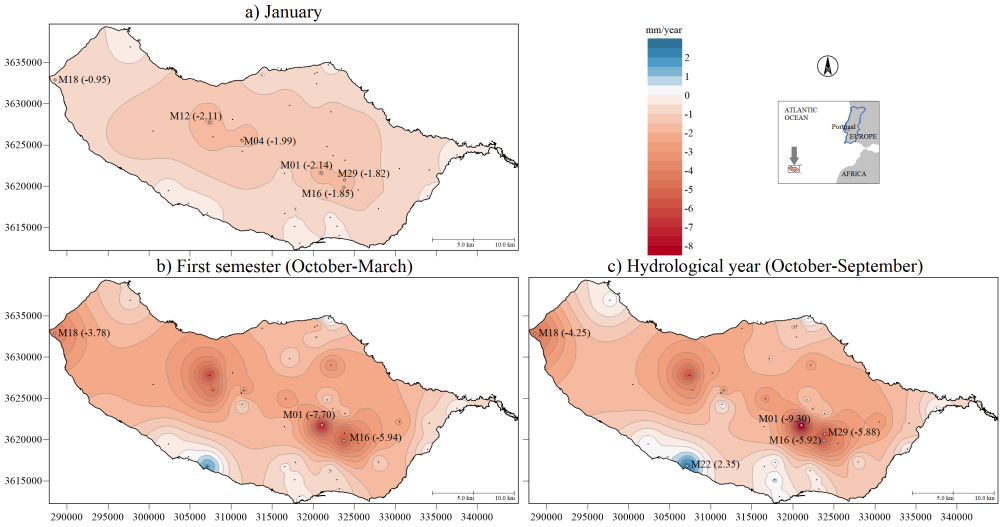

Figure 1. Rainfall trends (1937/38-2016/2017) at different time-spans.

Acknowledgments: The work of the first author is funded by The Portuguese Foundation for Science and Technology(FCT), grant No. PD/BD/128509/2017.

References

Falkland A, Custodio E, et al. (1991) Hydrology and water resources of small islands: A practical guide (No. 49). UNESCO

Liberato M, Ramos A, Gouveia C, Sousa P, Russo A, Trigo R, Santo F (2017) Exceptionally extreme drought in Madeira Archipelago in 2012: Vegetation impacts and driving conditions. Agricultural and Forest Meteorology 232:195–209

Miranda P, Valente M, Tomé A, Trigo R, Coelho M, Aguiar A, Azevedo E (2006) O clima de Portugal nos séculos XX e XXI. Alterações Climáticas em Portugal. Cenários, Impactos e Medidas de Adaptação, 45e113

Rao G, Uppala R, Singh V, Giridhar M (2015) Rainfall Trend Analysis: A Case Study of Godavari Sub Basin–Kadam Water Shed, Adilabad District, Telangana State. 3rd National Conference on Water, Environment and Society

Santos F, Valente M, Miranda P, Aguiar A, Azevedo E, Tomé A, Coelho F (2004) Climate change scenarios in the Azores and Madeira islands. World Resource Review 16(4):473–491

Villafuerte II M, Matsumoto J, Akasaka I, Takahashi HG, Kubota H, Cinco TA (2014) Long-term trends and variability of rainfall extremes in the Philippines. Atmospheric Research 137:1–13

11th World Congress on Water Resources and Environment (EWRA 2019)
"Managing Water Resources for a Sustainable Future", 25-29 June 2019, Madrid, Spain

Calibration procedure of regional flow-duration curves evaluating water resource withdrawal from diversion dam

E. Sassu*, R. Zucca, G.M. Sechi
Department of Civil and Environmental Engineering and Architecture, University of Cagliari, Cagliari, Italy
** e-mail: emanuelasassu@live.it*

Introduction

To face climatic changes and more frequent droughts in Mediterranean regions, an increase of water availability for supply systems is often required. Therefore, withdrawal volumes from diversion dams located along rivers can be used to increase the available water resources. Usually, diversion dams do not have a large storage volume: they are not able to comply with river flow regulation and only a partial incoming flow can be diverted to demand centres or to larger capacity reservoirs. Consequently, it is not easy to correctly quantify the achievement in increasing water resource in the supply system.

This study provides a modelling approach to correctly evaluate the water volumes withdrawal from diversion dams taking into account river flow estimation and design capacity of the diversion works.

The evaluation procedure has been calibrated using the regional flow-duration curves (FDCs) of the Sardinian Region (PSURI 2006). FDCs and their reliability for ungauged basins have been a frequent subject of interest in the research literature (Mimikou and Kaemaki 1985; Claps et al. 1996; Castellarin et al. 2004).

Herein, the effectiveness of a regional evaluation approach based on monthly time scale analysis has been investigated. The proposed methodology aims to find the optimal values of regional FDCs parameters to correctly evaluate the water volume withdrawal from diversion dams.

FDC parameters calibration procedure

Observed daily runoff of 36 gauging stations in Sardinia region (Italy) has been considered to perform the calibration procedure of FDC parameters. Regional hydrological database extends from 1922 to 2013. Stations with at least 5 years of daily flow records have been taken into account. Considering the 36 gauge stations, monthly water withdrawal volumes have been evaluated by two methods:

- *Method 1*: using a regional FDC given by the following exponential curve:

  $$q(t) = q_a(i)\,(\exp(-t/k)/k(1- \exp(-t/k)) \quad (1)$$

  where q_a is the average monthly discharge and k is the parameter with a log-normal distribution of probability (Saba and Deriu 1998);
- *Method 2*: evaluating the monthly diversion from observed data, calculated as the sum of minimum values between the maximum design withdrawal and the observed daily runoff.

In a first step, Method 1 has been used while considering a fixed value of the parameter k, given by Regional Water Plan (PSURI 2006), equal to 0.132 (corresponding to a non-exceedance probability of 7%). This k-value used in (PSURI 2006) brings to underestimate the withdrawal volumes and it could be extremely precautionary. Therefore, the optimal values of k-parameter have been evaluated by minimizing the average percent error in estimation of withdrawal volumes.

Using a planning approach, the design capacity of diversion withdrawals has been assumed varying between several values: we refer to values equal to 0.1, 0.3, 1.0, 3.0, and 10.0 times of the average monthly runoff. Correlation and regression analysis have been performed to estimate optimal k-parameters for ungauged basins. After considering several hydrological variables, the optimal k values estimation was obtained linking k-parameters to the coefficient of variation (CV) of the average monthly runoff.

Time-variability of the runoff data suggested the application of a regression models considering a "seasonally-adjusted" CV to estimate k-parameters. Particularly, for Sardinia region, CV of the dry season

was calculated by using runoffs from June to September, and the CV of the wet season using runoffs from October to May. In order to improve correlations, river basins have been analysed separately in two groups: firstly, by dividing them in relation to the extension of the basin (considering 100 km^2 as discriminating value); then by taking into account the geographical orientation (western and eastern basins).

Results and concluding remarks

The obtained results highlight that the k-parameter of regional FDCs decreases by increasing CV of observed runoff. Moreover, for lower design values of withdrawal capacities (equal to 0.1, 0.3 times of the average runoff) the goodness of obtained relations improves considering CV of dry season. Considering higher design withdrawal capacities (up to 10 times of the average runoff) models improve by using CV of the wet season. Considering intermediate capacities (equal to 1 and 3), the k parameter is better correlated to the annual CV.

Regarding the basin area, small basins with catchment area below 100 km^2 are better correlated considering high values of the aforementioned ratio, while basins with a larger surface show an opposite behaviour. Finally, the geographical orientation seems do not have a significant correlation.

In conclusion, the described analysis allows to optimize regional k-parameters of Sardinian FDCs in order to obtain a robust estimation of withdrawal volumes from diversion dams. The obtained results are currently in use to update the Sardinia Regional Water Plan using the WARGI simulation model (Sechi and Sulis 2009; Sechi and Zuddas 2000).

References

Castellarin A, Galeati G, Brandimarte L, Montanari A, Brath A (2004) Regional flow-duration curves: reliability for ungauged basins. Advances in Water Resources 27:953-965

Claps P, Fiorentino M, Silvagni G (1996) Curve probabilistiche di possibilità di derivazione dei deflussi. Proceedings of: XXV Convegno di Idraulica e Costruzioni Idrauliche, Vol. III, pp 95-106

Mimikou M, Kaemaki S (1985) Regionalization of flow duration characteristics. Journal of Hydrology 82:77-91

Regione Autonoma della Sardegna (2006) Piano Stralcio di Bacino Regionale per l'Utilizzo delle Risorse Idriche

Saba A, Deriu M (1998) Valutazione probabilistica del volume derivabile da una presa ad acqua fluente per i bacini della Sardegna. Proceedings of: XXVI Convegno di Idraulica e Costruzioni Idrauliche, pp 359-370

Sechi GM, Sulis A (2009) Water System Management Through a Mixed Optimization-Simulation Approach. Journal of Water Resources Planning and Management 135(3):160-170

Sechi GM, Zuddas P (2000) WARGI: Water Resources System Optimization Aided by Graphical Interface. In: Blain WR, Brebbia CA (eds) Hydraulic engineering software, WIT-PRESS, pp 109-120

Optimal operation of Bakhtiari and Roudbar dams using differential evolution algorithm

B. Moshedzadeh[1], R. Mansouri[1*], A. Karbakhsh[1], M. Zounemat-Kermani[2]
[1] Department of Civil Engineeing, Azad University,Sirjan Branch, Sirjan, Iran
[2] Water Engineering Department, Shahid Bahonar University of Kerman, Kerman, Iran
* e-mail: Ramin_Mansouri@yahoo.com

Introduction

These days water shortfall in the most countries has become a serious crisis. Therefore, the management of water resources is one of the most important actions to resolve challenges in the water crisis. Due to the contrast of rivers discharge regime with water demands, one of the best ways to use water resources is to regulate the natural flow of the rivers and supplying water needs to construct dams. Optimal utilization of reservoirs, consideration of multiple important goals together at the same is of very high importance. Optimization modeling in water resources in engineering and management has largely been addressed in the literature. Early mathematical optimization dates back to the work of Varlet in 1923 for the flood control and water supply (Varlet 1923), Massé in 1946 for hydropower operations (Massé 1946), and the numerical optimization methods Little (1955) for the application of stochastic dynamic programming to hydropower. Different optimization methods were used in the water system such as differential evolution algorithm for optimal design of water distribution networks (Suribabu 2010), optimization of the water distribution networks with differential evolution (Mansouri et al. 2015) and Simulation and Optimization of Integrated Hydraulic and Water Resources (Torabi et al. 2016).

Most multi-purpose dams have contradictions in the aims of operation which leads the issues of operation to be complicated and unrelated. For proper operation, the reservoir's volume should be managed every month. In this research, the differential evolution algorithm is used to find the optimal monthly operation of Bakhtiari and Roudbar dams by adopting an objective function to minimize the release and storage penalty. The historical inflow data of 116 months, formed the input data to the optimization model to find the (upper and lower) rule curves. the development of heuristic algorithms of utilization of particles in Bakhtiari and Roudbar dams was analyzed with the purpose of supplying agriculture water, drinking, environment, flood control and hydroelectric power generation.

Materials and methods

In this study, the target area is located in the west of Iran in the longitude of 49 ^{o} 41'E and the latitude of 32^{o} 54' N, which is part of Lorestan watershed, Iran. To study about analyzing this method, statistical data of Bakhtiari and Roudbar dam over 46 years (1955 until 2001) is used. In Figure 1, respectively, the time series of the inflow into reservoirs of Bakhtiari and Rudbar dams are considered as years.

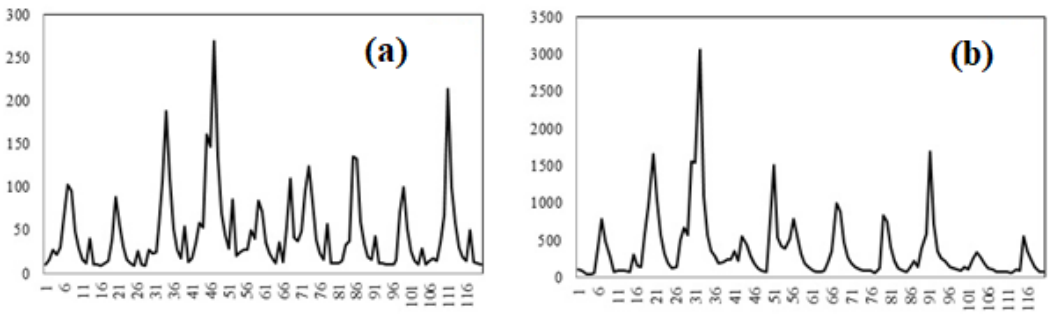

Figure 1. Time series of flow into the reservoir of the dam (a) Rudbar (b) Bakhtiari

Differential Evolution (DE) algorithm has used to find out the optimal release with maintaining all the

general constraints (such as- water balance, release bounds and storage constraints) of a reservoir system.

Initially an appropriate objective function was specified and using DE algorithm, the rule curve was developed. Differential Evolution (DE) algorithm is a branch of evolutionary programming developed by Storn and Price (1995) for optimization of continuous domains. In DE, each variable's is represented by a real number. The advantages of DE are its simple structure, ease of use, speed and robustness. DE is one of the best genetic type algorithms for solving problems with the real valued variables. There are three important operators involved in the application of the DE algorithm: a mutation operator, a crossover operator, and a selection operator.

The results from the model and the patterns of the release curves shows that, DE can be used as a useful and easily applicable tool to developed the release policy for optimal operation of Bakhtiari and Rudbar dams.

Results and concluding remarks

Operation policy using rule curves was compared to standard comparative operation policy. The proposed method distributed the lack to the whole year and lowest damage was inflicted to the system. Performance evaluation criteria of reservoirs in the single reservoir system of Rudbar dam (Table 1) and two reservoir system of Bakhtiari dam (Table 2) in both bases of exploitation were investigated.

Table 1. Performance evaluation criteria in Rudbar dam.

	Time reliability			**Amount reliability**			**Reversibility**			**Vulnerability**		
α	1	0.8	0.6	1	0.8	0.6	1	0.8	0.6	1	0.8	0.6
DE Algorithem	33.33	75	100	89.12	100	100	25	33	100	10.82	2.26	0
SOP	25	25	25	75	93	100	20	20	25	25	24.94	24.94

Table 2. Performance evaluation criteria in Bakhtiari dam.

	Time reliability			**Amount reliability**			**Reversibility**			**Vulnerability**		
α	1	0.8	0.6	1	0.8	0.6	1	0.8	0.6	1	0.8	0.6
DE Algorithem	75	91.66	100	94.40	100	100	75	91	100	5.61	1.06	0
SOP	66.66	66.66	66.66	73.79	92	100	66.66	66.66	66.66	0.26	0.25	0.25

The standard deviation of monthly shortfall of each year with the proposed algorithm was less deviated than the other two methods. Standard operation policy had better reversibility percentage, but inflicts severe vulnerability to the system. The results obtained in years of low rainfall had very good results compared to other comparative methods.

References

Little JDC (1955) The use of storage in a hydroelectric system. Operations Research 3:187-197

Mansouri R, Torabi H, Hoseini M, Morshedzadeh H (2015) Optimization of the Water Distribution Networks with Differential Evolution (DE) and Mixed Integer Linear Programming (MILP). Journal of Water Resource and Protection 7:715-729

Masse P (1946) Les Reserves et la Regulation de l'Avenir Dans La Vie. Economique Hermann, Paris

Storn R, Price K (1995) Differential Evolution—A Simple and Efficient Adaptive Scheme for Global Optimization over Continuous Spaces. Technical report, International Computer Science Institute, Berkeley, CA

Torabi H, Mansouri R, Haghiabi AH, Yonesi HA (2016) Optimization of Hydraulic-Hydrologic complex system of reservoirs and connecting tunnel. Water Resource Management 30:5177–5191. doi: 101007/s11269-016-1477-5

Varlet M (1923) Étude Graphique des Conditions d'Exploitation d'un Réservoir de Régularisation Annales des Ponts et Chaussées Partie. Technique 93e Année 11e Série-Time 64 Fasc 4 Tome 2 July-August

11th World Congress on Water Resources and Environment (EWRA 2019)
"Managing Water Resources for a Sustainable Future", 25-29 June 2019, Madrid, Spain

Non-stationary flood frequency analysis in Langat basin, Malaysia

V. Filipova
JBA Risk Management, Skipton, United Kingdom
e-mail: valeriya.filipova@jbarisk.com

Introduction

In the last few decades, there has been rapid urbanisation in the Langat basin. In addition, there has been an increase in the industrial zones in the basin as well as the infrastructure developments such as Kuala Lumpur International Airport, West Port at Klang, the Multimedia Super Corridor (MSC) and Putrajaya (Juahir et al 2010). As a result, the percent forest has decreased from 41.42% in 1981 to 24.11% in 2001, while the percentage of urban areas has increased from 2.6% in 1981 to 17.56% in 2001. These changes in land use have resulted in faster flood response and increase in the AMAX (Annual maxima) peak flows.

The objective of this study is to quantify the differences between using stationary and non-stationary flood frequency analysis using the GAMLSS method which has not yet been applied in the basin.

Materials and methods

In this study, we have selected the catchment Sg. Langat di Kajang, which is highly urbanised and has an area of 380 km^2. The gauge has hourly timestep and available data from 1978 to 2018. After extracting the AMAX events, we used the Mann-Kendall test to check for trends and the Petit test to test for changepoints.

Several different methods can be used in the presence of non-stationarity. We have selected the GAMLSS method (Stasinopoulos and Rigby 2007). In the GAMLSS method, the parameters of the distribution for the response variable can be modelled as additive functions of different covariates. For example, the GAMLSS method can be applied using time as covariate (Debele et al. 2017) but also using other covariates such as Reservoir Index and climate indices (Lopez and Frances 2013). Examples of additive functions include linear or non-linear (e.g. smooth splines) relation with the covariates. This flexibility is a strength of the method.

The GAMLSS method has been implemented in an R package for a large number of statistical distributions; however, only a few of those distributions are applicable to hydrological variables. From these, we have selected the lognormal distribution which is appropriate for modelling AMAX series.

As there was no available detailed information on the land use within the catchment, we have used time as the covariate. Fitting this model to the data we could then compare the resulting quantiles when calculated using an assumption of stationary or non-stationary conditions.

Results and concluding remarks

As discussed in the previous section, first the Mann-Kendall and the Petit test were applied. The results for both tests were statistically significant: the p value was 4.7×10^{-7} for the Mann-Kendall test and 1.5×10^{-4} for the Petit test. This strongly suggests that a non-stationary flood frequency analysis is required. Figure 1 shows a comparison of the flood frequency curves generated from the non-stationary and stationary analysis.

In Figure 1, we have compared the quantiles using stationary and non-stationary assumptions to demonstrate how the estimate of flood frequency for the current time period is heavily dependent on this assumption. We can also look at how the quantile estimates change with time at this site. For example, the 100-year quantile shows considerable variation in time, as shown in Figure 2.

The results strongly suggest that carrying out flood frequency estimation under the assumption that the catchment system is stationary can result in a significant underestimate of flood risk. In addition, it is evident that the flood risk is increasing, most likely due to increase in urbanisation. Therefore, it is

important to offset these changes by flood mitigation strategies such as increasing the amount of forested areas.

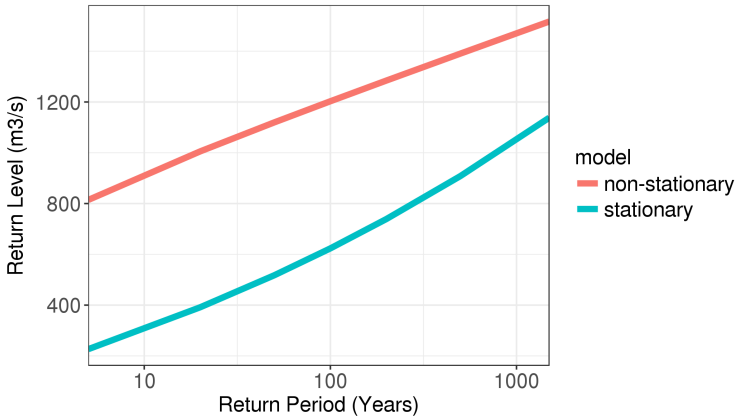

Figure 1. Lognormal distribution using stationary flood frequency analysis and lognormal distribution fitted using the GAMLSS method

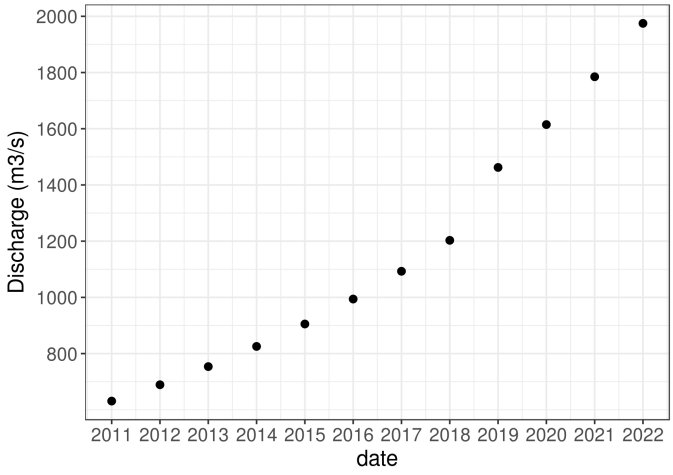

Figure 2. Difference in the 100-year return period estimate with time

Acknowledgments: This study was supported with funding from the Newton Ungku Omar Fund and Innovate UK for the project entitled 'Disaster Resilient Cities: Forecasting Local Level Climate Extremes and Physical Hazards for Kuala Lumpur'. In addition, the author would like to acknowledge Sisay Debele for sharing his R scripts that implement GAMLSS methodology.

References

Debele SE, Strupczewski W, Bogdanowicz E (2017) A comparison of three approaches to non-stationary flood frequency analysis, Acta Geophysica 65(4):863–883. doi: 10.1007/s11600-017-0071-4

Juahir H et al. (2010) Hydrological Trend Analysis Due to Land Use Changes at Langat River Basin Hafizan. Environment Asia 3:20–31. doi: 10.14456/ea.2010.61

López J, Francés F (2013) Non-stationary flood frequency analysis in continental Spanish rivers, using climate and reservoir indices as external covariates, Hydrology and Earth System Sciences 17(8):3189–3203. doi: 10.5194/hess-17-3189-2013

Stasinopoulos DM, Rigby RA (2007) Generalized Additive Models for Location Scale and Shape (GAMLSS) in R. Journal of Statistical Software 23(7). doi: 10.18637/jss.v023.i07

11th World Congress on Water Resources and Environment (EWRA 2019)
"Managing Water Resources for a Sustainable Future", 25-29 June 2019, Madrid, Spain

Reservoir operation under the uncertainties of rainfall-runoff models

R.V. Rocha*, F.A. Souza Filho, Á.B.S. Estácio, V.C. Porto, L.Z.R. Rolim
Department of Hydraulic and Environmental Engineering, Federal University of Ceará, Fortaleza, Brazil
** e-mail: renanvierocha@gmail.com*

Introduction

The operation of a multi-purpose pluriannual reservoir is intrinsically dependent of its inflow time series characteristics and therefore is affected by its spatio-temporal reliability and statistical significance. In data scarcity regions, reservoir operation may be entirely based on synthetic series derived from hydrological rainfall-runoff models, and thus, outflow results of such approach carry the uncertainty associated with hydrological modelling.

This present work proposes to quantify the parameter uncertainties associated with a rainfall-runoff modelling through a Bayesian approach and analyse its consequences on the outflow results of a reservoir operation, comparing the results with the uncertainty of natural climate. The area chosen for this study was the Orós reservoir basin, one of the main reservoirs of the Ceará state (Brazil). This region suffers with severe multiannual droughts and has historically used synthetic series to simulate the operation of its numerous reservoirs (Barros et al. 2013), that characteristic may also have affected its local water granting policy which is based in the Q90 outflow. The authors emphasize that despite the significant number of articles about uncertainty estimation in hydrological modelling its derived consequences are still not well documented or explored.

Materials and methods

The Ceará region currently more recent series of streamflows are a result of a partnership work between the local water management company (COGERH) and the Federal University of Ceará (UFC) (Barros et al. 2013). In order to estimate the uncertainties faced from using the resulting series this article employed the same hydrological model and used the same input data of the mentioned paper.

The rainfall-runoff modelling was performed using the conceptual model SMAP (*Soil Moisture Accounting Procedure*) with a monthly time step, the simulated period range from January 1912 to December of 2012.

For each of the model parameters a probability distribution was obtained using the DREAM (*Differential Evolution Adaptive Metropolis*) algorithm (Vrugt et al. 2009) through the R implementation of Guillaume and Andrews (2012). This algorithm uses a formal Bayesian approach and performs robust and efficient search in the sample space of the parameters through multiple simultaneous Markov Chains Monte Carlo simulations to obtain the posterior distributions from an imposed priori distribution, the stopping criteria of the algorithm is the convergence of the chains, verified by the R statistics of Gelman and Ruben. This work assumed a uniform distribution for all parameters. More information about the method and the SMAP model can be found in cited references.

From the converged chain it was sampled 10,000 groups of parameters, resulting in the corresponding number of synthetic series. The Nash Sutcliffe coefficient of efficiency was then calculated for each one for the whole period simulated with observed data, to measure the closeness between the series and data. In the previous work this coefficient was used to calibrate the parameters.

The Orós reservoir operation was then simulated to obtain the corresponding Q90 outflow for each series in four distinct scenarios: (I) using the complete series; using only the 30 years with the (II) lowest (III) average and (IV) highest precipitation. The results were fitted to a statistical distribution and the corresponding 95 % confidence interval was thus analysed.

Results and concluding remarks

The Nash coefficient implies minor differences between the synthetic series, with a minimum value of 0.737, a maximum of 0.763 and 95 % between 0.753 and 0.763.

The Figure 1 synthesizes the Q90 results for the four reservoir operation cases. The results for all cases shows a good fit to the normal distribution. The confidence interval of the case (I) has an amplitude of 5.65 m^3/s which corresponds to 27.6 % of its mean value, showing that despite the similar behaviour implied by the series Nash coefficients they impose significant different results in the reservoir operation, revealing a considerable uncertainty derived from the rainfall-runoff modelling.

The case II revealed very similar results of the case I, with a higher value of the coefficient of variation (CV) and amplitude of the confidence interval (6.1 m^3/s).

The simulation with just the 30 drought years (II) provided a mean value equivalent of one fourth of the case (I) whereas the 30 wettest years (IV) resulted in a mean value 2.5 times higher, thus, it is possible to conclude that the regions natural uncertainty is considerable higher than the imposed by the hydrological modelling. However, the hydrological modelling uncertainty of the case II is significantly higher than the others, as can been seen from its higher CV and higher proportional amplitude of variation (61.8 %). The case IV showed the smallest proportional amplitude of variation (20.2 %) and value of CV.

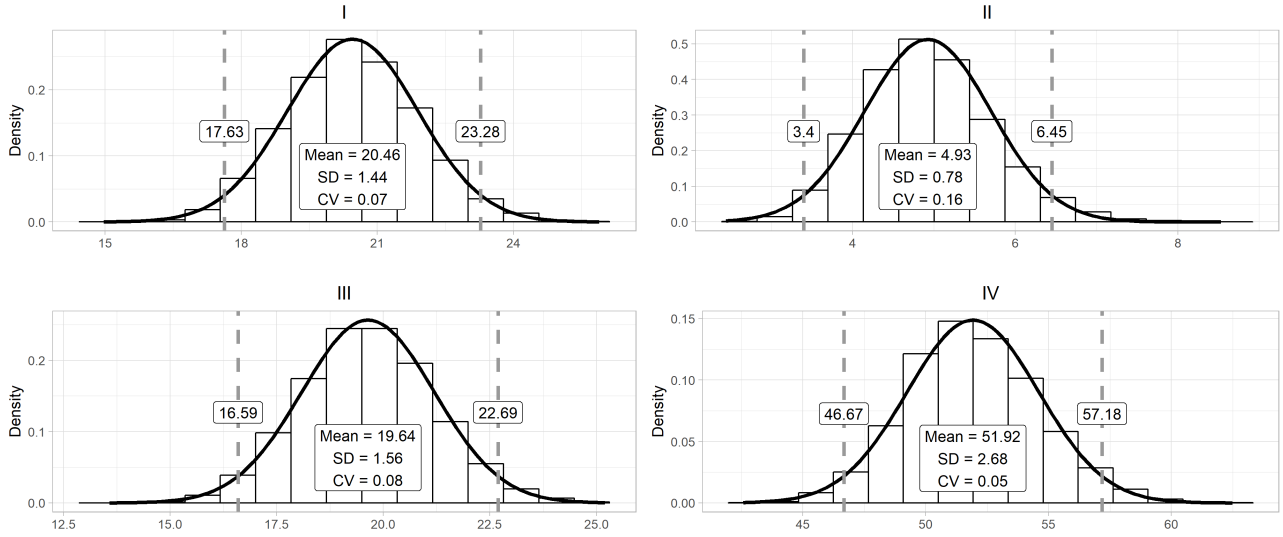

Figure 1. Histogram, normal density plot (black line) and 95 % confidence interval (dotted lines) of the Q90 results.

The results conclude that even in regions where the natural climate uncertainty is higher than the derived from rainfall-runoff modelling, its possible significant amplitude needs to be accounted for in the determination of the operational Q90 value. In the case studied the drought periods presented higher uncertainties than normal or wetter periods, revealing that each period has to be analysed carefully.

Acknowledgments: The authors thank National Council for the Improvement of Higher Education (CAPES) and National Council for Scientific and Technological Development (CNPq) for the financial support.

References

Barros F et al. (2013) Regionalização de parâmetros do modelo chuva-vazão SMAP das bacias hidrográficas do Ceará. In: Souza Filho FA et al. (eds) Gerenciamento de Recursos Hídricos no Semiárido, 1st ed, Expressão Gráfica e Editora, Fortaleza, pp 186-207

Guillaume J, Andrews F (2012) DiffeRentialEvolution Adaptive Metropolis. R package version 0.4-2. http://dream.r-forge.r-project.org/

Vrugt JA et al. (2009) Accelerating Markov Chain Monte Carlo Simulation by Differential Evolution with Self-Adaptive Randomized Subspace Sampling. International Journal of Nonlinear Sciences and Numerical Simulation 10(3). https://doi.org/10.1515/IJNSNS.2009.10.3.273

11th World Congress on Water Resources and Environment (EWRA 2019)
"Managing Water Resources for a Sustainable Future", 25-29 June 2019, Madrid, Spain

WEBFRIS: A web based flood information system for enhanced resilience through risk awareness

M.P. Mohanty[1], S. Karmakar[1,2,3*], S. Ghosh[2,3,4]
[1] Centre for Environmental Science and Engineering, Indian Institute of Technology Bombay, Mumbai-400076, India
[2] Interdisciplinary Program in Climate Studies, Indian Institute of Technology Bombay, Mumbai-400076, India
[3] Centre for Urban Science and Engineering, Indian Institute of Technology Bombay, Mumbai-400076, India
[4] Department of Civil Engineering, Indian Institute of Technology Bombay, Mumbai-400076, India
* e-mail: skarmakar@iitb.ac.in

Introduction

Flood risk management (FRM) is an emerging global hot-topic in climate research (Hartmann and Driessen 2017). With the emergence of numerous sophisticated flood models, difficulties associated with data handling and computational efforts, though not leading to an end, is declining substantially (Dottori et al. 2016). For FRM to be a success, it is important to give equal footing to information flow on various aspects of flood disaster at ground level. The knowledge on regions affected by different levels of flood hazard, vulnerability, and risk is vital not only for citizens but also to various government agencies, disaster managerial teams, and policy makers.

This paper presents an innovative Web-based Flood-Risk Information System (WEBFRIS) at a very fine scale of village level for the severely flood-prone Jagatsinghpur district (Orissa, India), accomplished through a unified flood risk mapping framework. The unique representation of the information system enhances its flexibility and modularity, allowing users gain priori knowledge on regions affected to different degrees of flood hazard, vulnerability, and risk.

Materials and methods

The concept of flood risk (R) stands on two pillars namely, Flood Hazard (H) and Vulnerability (V). To quantify the first component, we adopted a detailed 1-D-2D coupled flood modelling framework at a super high grid resolution of 10 m X 10 m by including all essential inputs: hydrological (design discharge and design storm-tide elevation), meteorological (regionalised design rainfall) (Mohanty et al. 2018), and geographical (land-use, built-up area etc.). The flood hazard from the model simulations was quantified in terms of depth (d) and a tuple of depth and velocity '(d,f)'. On the other hand, socioeconomic vulnerability is determined at the finest village level by considering a set of 21 relevant socioeconomic indicators in a multivariate data analysis framework involving principal component analysis (PCA), followed by data envelopment analysis (DEA) (Sherly at al. 2015). Instead of the conventional flood risk definition given as a product of hazard and vulnerability, we introduce a new concept, "Risk-Classifier", in the form of a 5×5 choropleth. This innovative representation portrays different degrees of risk from the individual and compound contribution of hazard and vulnerability components. The complete design architecture of the web-based interface is illustrated in Figure 1. This flood risk is quantified for return periods (RPs) of 25, 50, 100, and 200 years for two scenarios: (I) Scenario-I: 1970-2011 and (II) Scenario-II: 1970-2001. The entire flood related information is embedded into the web database.

Results and concluding remarks

Firstly, we analyse the decadal changes of flood risk in Scenarios I and II. These two time patterns were characterised by majority of the villages coming under H-dominated and V-dominated flood-risk, respectively.

At the same time, we observe a prominent increase in number of villages (in the NE and SW regions) affected with high and very high flood risk, respectively, contributed equally from H and V. We present this information in the WEBFRIS platform. The user-friendly and simple layout supports a swift access to flood

related information. By clicking on any village, the user can notice a pop-up that displays various geographical (e.g., location, area, perimeter etc.) and flood related (e.g., flood hazard, vulnerability, and risk values for all Scenarios) information.

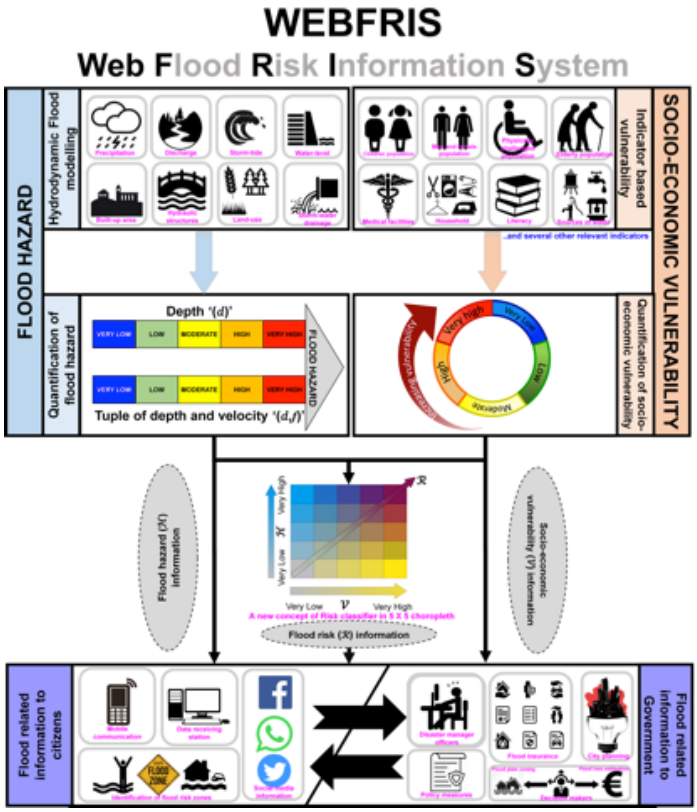

Figure 1. Design architecture of Web-based Flood-Risk Information System (WEBFRIS)

The huge stack of information embedded in the database aims to promptly gain information on the damage inflicted upon the dwellers along with potential future damage scenarios. In addition, it also draws attention of disaster managerial groups and government organisations for prioritizing flood mitigation actions. With the unique manifestation of flood-risk, it is now much easier to enhance the existing FRM by giving due weightage either to hazard, vulnerability or both aspects. For areas facing severe hazard in the upstream and coastal stretches, more attention should be exercised on improving flood plain zoning and constructing flood control structures. On the other hand, policy and upliftment schemes can be enforced in vulnerability-dominated areas. This structured approach shall plummet the ambiguous economic expenditure on FRM measures and provide substantial benefits to a broad community group on suitable adaptation and flood combating strategies.

Acknowledgments: The work presented here is supported financially by ISRO-IIT(B)-Space Technology Cell (STC) through a sponsored project (No. 14ISROC009).

References

Dottori F, Salamon P, Bianchi A, Alfieri L, Hirpa FA, Feyen L (2016) Development and evaluation of a framework for global flood hazard mapping. Advances in Water Resources 94:87-102. http://doi.org/10.1016/j.advwatres.2016.05.002

Hartmann T, Driessen P (2017) The flood risk management plan: towards spatial water governance. Journal of Flood Risk Management 10(2):145-154. http://doi.org/10.1111/jfr3.12077

Mohanty MP, Sherly MA, Karmakar S, Ghosh S (2018) Regionalized Design Rainfall Estimation: An Appraisal of Inundation Mapping for Flood Management Under Data-Scarce Situations. Water Resources Management 32(14): 4725-4746. http://doi.org/10.1007/s11269-018-2080-8

Sherly MA, Karmakar S, Parthasarathy D, Chan T, Rau C (2015) Disaster vulnerability mapping for a densely populated coastal urban area: An application to Mumbai, India. Annals of the Association of American Geographers 105(6): 1198-1220. http://doi.org/10.1080/00045608.2015.1072792

11th World Congress on Water Resources and Environment (EWRA 2019)
"Managing Water Resources for a Sustainable Future", 25-29 June 2019, Madrid, Spain

Quantification of expected changes in peak flow quantiles in climate change by combining hydrological modelling with the modified Curve Number method

E. Soriano*, L. Mediero, C. Garijo
Dept. of Civil Engineering Hydraulic, Energy and Environment, Universidad Politécnica de Madrid, Madrid, Spain
** e-mail: e.soriano@upm.es*

Introduction

Floods are the natural hazard that causes the largest material and human damage in Europe (IPCC 2007). In addition, floods will be affected by climate change. Consequently, new methodologies have to be developed for studying floods considering climate change. In Spain, there are two sources of climate change projections: AEMET ('Agencia Estatal de Meteorología', in Spanish) and CORDEX. AEMET projections have been proven to work well for water resource studies, as average values are well characterised. However, they do not supply a good characterisation of extremes, which are the events that usually generate floods in Spain (Garijo and Mediero 2018). Consequently, the data provided by the CORDEX programme have been used in this study.

Climate change projections usually present bias errors that must be corrected before its use. Soriano and Mediero (2018) developed a methodology to identify the best bias correction method, in terms of flood frequency curve fitting. In addition, it was found that the HBV rainfall-runoff model soften the behaviour of extreme events. However, the HBV model characterises adequately the temporal evolution of soil moisture content in the catchment that depends on both precipitation and temperature. In this study, expected changes in flood frequency curves driven by climate change in the future are assessed through an approach that combines rainfall-runoff modelling with the modified curve number (CN) method proposed by Michael and Andréassian (2005), in order to overcome the limitations identified previously.

Materials and methods

Four catchments have been selected as case studies. They are located in the Douro river catchment in northwest Spain. The four catchments have a dam in their outlet. Observations at the four dams were supplied by the Centre for Hydrographic studies of CEDEX, consisting of reservoir levels and discharges released downstream the dam. Inflow discharge time series were estimated from such data.

Observations of daily rainfall and temperature time series were provided by AEMET at a set of gauging stations. Such data was used to calibrate the HBV rainfall-runoff model, as well as to identify errors between climate projections and observations in the control period. Gaps in time series were filled by using observations at nearby gauging stations.

Climate projections used in the study are composed of daily rainfall and temperature time series supplied by 12 regional climate change models of the EURO-CORDEX programme. Climate projections consist of two periods, the control period (1971-2004, hydrological years) and the future period (2011-2094, hydrological years). In the future period, three periods were studied (2011-2040, 2041-2070 and 2071-2095). In addition, two different representative concentration pathways (RCP) were considered: RCP 4.5 and 8.5.

The four catchments were modelled by using the HBV rainfall runoff model (Seibert and Vis 2012), in order to obtain how soil moisture content in each catchment will change in the future. Specifically, the version HBV-light-GUI 4.0.07 has been used. The model parameters have been calibrated in each catchment by using Monte Carlo simulations and GAP optimization. The calibration was focused on improving the model fitting in extreme events and accounting for the parameters related to the soil moisture account.

After calibrating the four catchments, bias correction of both precipitation and temperature data

supplied by the regional climate change models was carried out using a variety of methodologies (Teutschbein and Seibert 2010). The best bias correction method was selected for each catchment, comparing flood frequency curves fitted to simulation and observation time series, by using a Generalized Extreme Value distribution with the L-moment method (Soriano and Mediero 2018), as this study has application to hydrological dam safety.

Daily soil moisture time series can be sued as input to the modified curve number method (Michael and Andréassian 2005), in order to improve the characterisation of expected floods in the future, in terms of both peak magnitudes and hydrograph volumes.

Expected delta changes in flood quantiles in the future are estimated by comparing the results in the future periods with the results in the control period.

Results and concluding remarks

By using the methodology described previously, the future delta changes in the four catchments for the three periods in the future selected previously were obtained. It has been found differing results, as in some cases peak flow values are expected to be higher in the future, and in other cases they are expected to decrease in the future. In most cases, the largest changes are expected to occur in the period 2071-2095.

The proposed methodology overcomes the softening of extreme flood events of the HBV model, improving the characterisation of flood behaviour. In addition, the HBV parameter that characterises the maximum soil moisture content in the catchment is essential in the method, as annual maximum flow magnitudes are high sensitive to such parameter.

In the future, it is expected to apply the same methodology to obtain delta changes in flood volumes, as hydrograph volumes are needed for conducting hydrological dam safety analysis.

Acknowledgments: The authors acknowledge funding from the Fundación Carlos González Cruz. On the other hand, the authors wish to thank AEMET and CEDEX for providing the data that made this study possible.

References

Garijo C, Mediero L, Garrote L (2018) Usefulness of AEMET generated climate projections for climate change impact studies on floods at national-scale (Spain). Ingeniería del agua 22(3):153-166

Garijo C, Mediero L (2018) Influence of climate change on flood magnitude and seasonality in the Arga River catchment in Spain. Acta Geophysica 66. doi: 10.1007/s11600-018-0143-0

IPCC (Intergovernmental Panel on Climate Change) (2007) Climate change 2007: impacts adaptation and vulnerability. Contribution of Working Group II to the Fourth Assessment Report of the Intergovernmental Panel on Climate Change. Cambridge University Press, Cambridge, UK, p 976

Michel C, Andréassian V, Perrin C (2005) Soil Conservation Service Curve Number Method: How to mend a wrong soil moisture accounting procedure? Water Resources Research 410. doi: 10.1029/2004WR003191

Seibert J, Vis M (2012) Teaching hydrological modelling with a user-friendly catchment-runoff-model software package. Hydrology and Earth System Sciences 16:3315-3325. doi: 10.5194/hess-16-3315-2012.

Soriano E, Mediero L, Garijo C (2018) Selection of bias correction methods to assess the impact of climate change on flood frequency curves. Proceedings of the 3rd International Electronic Conference on Water Sciences (ECWS-3). doi: 10.3390/ECWS-3-05809.

Teutschbein C, Seibert J (2010) Regional Climate Models for Hydrological Impact Studies at the Catchment Scale: A Review of Recent Modeling Strategies. Geography Compass 4:834 - 860. doi: 10.1111/j.1749-8198.2010.00357.x

11th World Congress on Water Resources and Environment (EWRA 2019)
"Managing Water Resources for a Sustainable Future", 25-29 June 2019, Madrid, Spain

Exploring the relationship between climate indices and hydrological time series using a machine learning approach

L.Z.R. Rolim*, F.A. Souza Filho, R.V. Rocha, G.A. Reis, T.M.N. Carvalho
Department of Hydraulic and Environmental Engineering, Federal University of Ceará, Fortaleza, Brazil
** e-mail: larissazairarr@gmail.com*

Introduction

Large-scale climate oscillations have been known to have a direct impact into the variability of hydrological systems and their relationship have been documented in different parts of the world. Those indices play an important role in the hydrological time series behaviour, thus identifying their relationship is an important tool for an accurate time series forecast, especially under uncertain hydrological time series and multiobjective demands from reservoirs.

This paper proposes to use random forests, a powerful ensemble learning technique, to evaluate the relative relationship of each climate index to the streamflow's time series. Such nonlinear machine learning methods have been successfully used in different areas of knowledge. Then, a regression decision tree is built aiming to extract useful information about dry and wet periods from streamflow data related to the climate oscillation and adjust the decision tree model to forecast future values of streamflow. The data used in this study belongs to the gauge station of Itaipu's hydropower plant located in the Paraná River (Brazil). The basin has an annual cycle of discharges with large-amplitude and high flows in the summer.

Materials and methods

Monthly mean discharges, ranging from January 1931 to December 2016, measured at a gauging station located along the Paraná River were acquired from the National System Operator (ONS). Time series of climate oscillation indices used such as El Nino (Nino 1+2, Nino 3, Nino 3+4 and Nino 4), Pacific Decadal Oscillation (PDO), Southern Oscillation Index (SOI), North Atlantic Oscillation (NAO) and Atlantic Multidecadal Oscillation (AMO) were acquired in the National Oceanic and Atmospheric Administration website (*https://www.esrl.noaa.gov/psd/gcos_wgsp/Timeseries/*).

A random forest (RF) (Breiman 2011), a type of regression model, was used to identify the most important climate indices related with the observed streamflow time series by comprising an ensemble of regression trees. Importance measures in a regression model regression is given by the average of outputs of the various trees. The RF introduces random variation when bootstrapping a sample of the variables to grow an ensemble of decision trees. We used default values for the number of predictors and a large number of trees (500). For random forest model development, the randomForest package within the statistical software R was used.

A regression decision tree was built based on the three most voted climate indices classified by the random forest model. The decision tree split a complex decision into a set of simple "rules" which lead to a flowchart-like structure that can lead to easy interpret solutions (Breiman et al. 1984). The values produced by the trees at the final nodes, also referred as the target variables, were adjust to a probabilistic distribution and analysed separately. For decision tree model development, the rpart package was used.

From the regression model adjust for the decision tree, predictions were made for an interval of one, tree and five years ahead and their respective mean absolute percentage error (MAPE) was calculated.

Results and concluding remarks

The random forest model implied that the most important variables for the streamflow data were the Nino 1+2, Nino 3 and Nino 4, the climate indices that indicate the El Nino and La Nina phenomena. This reflects the strong relation of hydrological time series linked to climate cycles like El Nino/Southern Oscillation documented in previous studies (Antico et al. 2014).

The decision tree was carried out using the chosen climate indices as predictor variables in the regression. In Figure 1, it can be observed each "rule" given by the decision tree and the respective thresholds for the streamflow data. Those values were used to classify the below/above average periods of streamflow given a certain value of the climate oscillation.

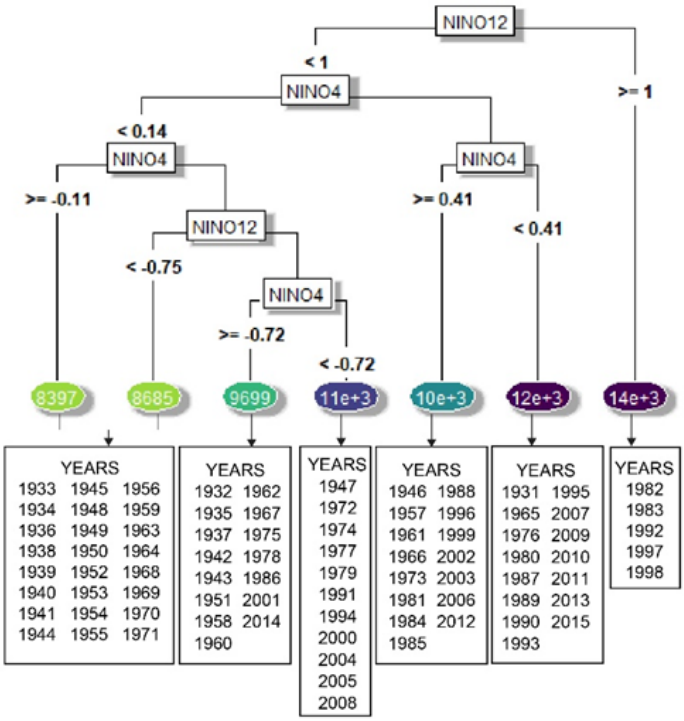

Figure 1. Decision tree and years classified from each final node of the tree.

For example, Nino 1+2 values above 1, gives us a streamflow value of 13,830 m^3/s. It was evaluated the years that presented a value of streamflow higher than that value and was observed that those same years were classified by the Center for Weather Forecasting and Climate Studies (CPTEC/INPE) as El Nino with high intensity, exhibiting that decisions tree can be a powerful to understanding streamflow behaviour.

The forecast model for the one year ahead prediction presented good results, having a MAPE of 0.002, but for the three and five years it worked poorly, presenting a MAPE value of 0.55 and 0.25, respectively.

It was investigated the ability to use this data-driven model to determine the climate oscillation that might have an impact on hydrological time series and used a regression model to make short-term forecasts which presented acceptable results, thus providing us with a powerful and easy to interpret tool to identify relation between hydrological and climate time series. Also, the prediction on this data-driven model can supply valuable information for reservoir system operations, being of great importance in water resources studies.

Acknowledgments: The authors thank National Council for the Improvement of Higher Education (CAPES), National Council for Scientific, Technological Development (CNPq) and Cearense Foundation of Meteorology and Water Resources (FUNCEME) for the financial support.

References

Antico A, Schlotthauer G, Torres ME (2014) Analysis of hydroclimatic variability and trends using a novel empirical mode decomposition: application to the Paraná River Basin. Journal of Geophysical Research: Atmospheres 119(3):1218-1233

Breiman L, Friedman JH, Olshen R, Stone CJ (1984) Classification and Regression Trees. Routledge, New York

Breiman L (2001) Random forests. Machine learning 45(1):5-32

11th World Congress on Water Resources and Environment (EWRA 2019)
"Managing Water Resources for a Sustainable Future", 25-29 June 2019, Madrid, Spain

Determination of hedging rule curves to mitigate water supply deficit for a single dam using dynamically dimensioned search method

Y. Jin, S. Lee*
Department of Civil Engineering, Pukyong National University, Busan, Republic of Korea
** e-mail: peterlee@pknu.ac.kr*

Introduction

Water supply deficit may be occurred in drought periods and it induces damage to societies. Reservoirs can be operated to reduce the damage applying the hedging rules. A hedging policy (Adeloye et al. 2016) still is a study subject on reservoir operation. Water supply from the discrete hedging rule suggested by Shih and Revelle (1995) is based on the available water and the phase in which the available water is. The available water of a reservoir is defined by the current storage plus the inflow volume of the future time period. Shih and Revelle (1995) determined the trigger volumes using the mixed integer programming. Determining decision variables using linear programming is not easy because it has to be constrained by the number of variables and constrain equations. A heuristic method can simply search a global optimum with an objective function and ranges of decision variables for a complex problem. We suggest a methodology for searching the hedging rule curves applying the heuristic method of dynamically dimensioned search (DDS) algorithm developed by Tolson and Shoemaker (2006). The contents of the research include the derivation of discrete hedging rule using DDS algorithm and reservoir simulations applying the derived hedging rule curves.

Materials and methods

Reservoir operations applying a hedging rule may be a useful method to cope with droughts. The Korean drought emergency phases consist of four stages. The rationing phases of the discrete hedging rule curves need to be matched with the above four stages. One rationing phase of the discrete hedging rule curve consists of twelve monthly trigger volumes. The decision variables are 48 trigger volumes that correspond to four sets of hedging rule curves. The DDS was used to search trigger volumes of available water for rationing. The objective function of the optimization model included a term to minimize the total water supply deficit for the whole period of reservoir simulation. We also added a penalty term to the objective function to let the trigger volume of the severer phase for a period be smaller than the trigger volume of the less severe phase. The optimization model deriving the discrete hedging rule was applied to Hapcheon dam in the Republic of Korea. The monthly inflow of Hapcheon dam has been recorded since 1990. The optimization period for searching the hedging rule curves is from 1990 to 2010. The derived hedging rule curves were validated for the period from 2011 to 2017.

Results and concluding remarks

Figure 1 shows the hedging rule curves of Hapcheon dam derived from the results of the optimization model. From August to November in Figure 1, the trigger volumes in alert and severe phases, respectively, are larger than those of March to July. That indicates that the water supply must be reduced proactively in order to mitigate the shortage of water supply in the next spring when the available water in the August and autumn period becomes smaller.

The results of reservoir simulation using derived hedging rule curves were compared with the Historical data in the optimization period (Figure 2). It can be seen from the simulation results that the hedging operation hindered releases for hydropower generation that exceeded the planned amounts of water supply. It also diminished the water supply deficit. On the other hand, the historical data can be seen to be more frequently rationed due to lots of releases for hydropower generation for the periods of larger storage amounts of the reservoir.

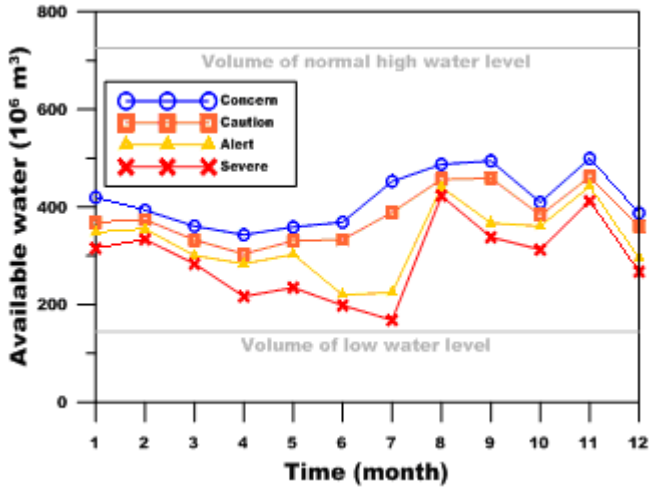

Figure 1. The derived Hedging rule curves of Hapcheon dam.

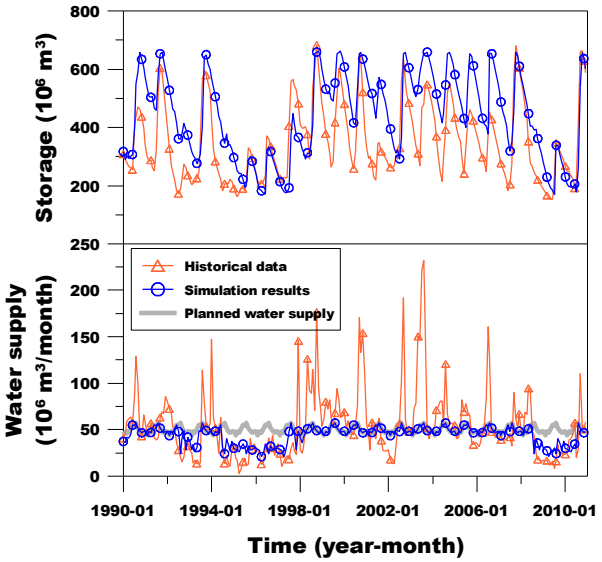

Figure 2. Comparison between observed data and simulated results in optimization period.

Table 1 compares historical and simulation operation results over the optimization and validation periods by the indices of the deficits of total water supply and maximum water supply. During the optimization period, the total water supply deficit was 46% less than the historical record, and the maximum water supply deficit was mitigated by 29%. During the validation period, the total water supply deficit was mitigated by 46% compared with the historical record, and the maximum water supply deficit was mitigated by 26%.

The derived hedging rule curves using DDS were believed to be effective to cope with drought. Further studies, however, are needed to evaluate total benefits including water supply and hydropower generation.

Table 1. Comparison of historical data and reservoir simulation results at the Hapcheon dam.

Index	Optimization period (1990 - 2010)		Validation period (2011 - 2017)	
	Historical data	Simulation result	Historical data	Simulation result
Total water supply deficit (million m^3)	2,761	1,498 (46 % reduction)	934	508 (46 % reduction)
Maximum water supply deficit (million m^3/month)	46.2	32.9 (29 % reduction)	44.5	32.9 (26 % reduction)

Acknowledgments: This work has also been supported by a grant (NRF-2017R1A2B2003715) from the National Research Foundation of Korea (NRF), funded by the Ministry of Education of the Korean government.

References

Shih JS, Revelle C (1995) Water supply operations during drought: a discrete hedging rule. European Journal of Operational Research 82(1):163-175. https://doi.org/10.1016/0377-2217(93)E0237-R

Tolson BA, Shoemaker CA (2007) Dynamically dimensioned search algorithm for computationally efficient watershed model calibration. Water Resources Research 43:W01413. https://doi.org/10.1029/2005WR004723

Adeloye AJ, Soundharajan BS, Ojha CSP, Remesan R (2016) Effect of hedging-integrated rule curves on the performance of the Pong Reservoir (India) during scenario-neutral climate change perturbations. Water Resources Management 30(2):445-470. https://doi.org/10.1007/s11269-015-1171-z

11th World Congress on Water Resources and Environment (EWRA 2019)
"Managing Water Resources for a Sustainable Future", 25-29 June 2019, Madrid, Spain

Impacts of changing precipitation patterns on hydrology and pollutant transport in a subsurface-drained watershed

M.W. Gitau[1*], S. Mehan[2]
[1] Department of Agricultural and Biological Engineering, Purdue University, West Lafayette, IN. U.S.A.
[2] Formation Environmental, LLC, Sacramento, CA. U.S.A.
* e-mail: mgitau@purdue.edu

Introduction

Water quality impairments due to pollutants from agricultural, rural, and urban lands continue to present environmental and health related challenges, attributable to a combination of climatic and anthropogenic factors. Changes in climate can potentially affect the movement of water and pollutants in our environment. This is particularly so in areas with subsurface drainage systems which, by design, provide rapid removal of water from landscapes but, inadvertently, provide accelerated conduits for associated pollutants. Subsurface drainage is particularly important in the U.S. Midwest region as it provides a viable means of growing crops in an otherwise waterlogged environment. In the Western Lake Erie Basin (WLEB), part of the aforementioned region, 70% of the land area is agricultural. It is generally unclear how much of the land area is in subsurface drainage (OLEPTF 2013) but best guess estimates can be derived based on the proportion of cultivated area with soils classified as poorly drained or very poorly drained (Sui and Frankenberger 2008). This basin has experienced increases in spring precipitation over the past 50 years (Sekaluvu et al. 2018) and one-day maximum precipitation is expected to increase going into the future, particularly during the spring and summer (Mehan 2018). The aim of this study was to assess the impact of changing precipitation patterns on hydrology and nutrient losses in subsurface-drained systems in the WLEB. The study site for this work was the Matson Ditch Watershed, a 46 km^2 (18 mi^2) agriculture-dominated subsurface-drained watershed that is a constituent of the WLEB. Consistent with the larger Basin, agricultural land comprises about 68 % of the watershed and is dominated by corn, soybeans, and winter wheat. This study was conducted using a modelling approach with the Soil and Water Assessment Tool (Arnold et al. 1998). Methodologies and approaches are applicable beyond the study region.

Materials and methods

Primary data used in this study were obtained from several different repositories including: U.S. Geological Survey (DEM, Hydrography); USDA-Natural Resources Conservation Service (soils); National Agricultural Statistical Service (crop data layer); National Climate Dataset (climate); and USDA Agricultural Research Service and county-level sources (climate, management, streamflow and water quality). So as not to exclude small but potentially hydrologically important areas, a 0-0-0 hydrologic response unit (HRU) threshold was used. A similar configuration has been used successfully with previous versions of SWAT (e.g. Gitau et al. 2006). Based on site soils and the afore-mentioned criterion, about 42% of the watershed was modelled as being in subsurface drainage systems. A combination of no-till and conventional tillage was simulated consistent with current practice in the study watershed. The model was calibrated for the period 01/01/2006-12/31/2009 and validated for the period 01/01/2010-12/31/2012. Overall, model performance ranged from satisfactory to very good based on performance measures including graphical plots and performance statistics, published criteria (e.g. Moriasi et al. 2015) and soft data (Seibert and McDonnell 2003) and the model was found suitable for further assessments. Watershed responses for the period 2006-2009 under two different emission scenarios (RCP 4.5 and RCP 8.5) were simulated using bias-corrected climate projections developed from nine GCMs (Mehan 2018). Results obtained for water quantity and quality were compared with those obtained from the baseline model to determine the impacts of a changing climate. Individual simulations (as opposed to ensembles) were analysed so as to capture the range of possible responses.

Results and concluding remarks

Anticipated changes in water quantity: It is expected that more of the precipitation will go to surface runoff under both emission scenarios, with an anticipated increase of up to 110% based on model results. This is attributable to the anticipated increases in precipitation and particularly in extreme precipitation events, which would result in higher runoff volumes. More water will also move through subsurface drains although the relative proportion with respect to precipitation is not expected to change much. Overall, an increase in streamflows of up to 80% is expected in the watershed attributable to the anticipated increases surface runoff and subsurface drainage flows.

Anticipated changes in water quality: The amount of soluble phosphorus being lost through subsurface drainage systems could decrease by up to 60% under both emission scenarios. This is attributable to the increase in surface runoff, which would then become the primary transport pathway for soluble phosphorus. This (surface runoff) is also an important transport pathway for sediment and sediment-bound phosphorus, hence increases in these two pollutants are also expected in response to a changing climate. Other pollutants that move primarily in their soluble form (such as nitrogen) would also increase overall, even while they are expected to decrease in subsurface drainage flows. Increases are also expected at the extremes, with values frequently exceeding the 95^{th} percentile value of the baseline scenario.

Other considerations: 1) To better inform decision-making and to facilitate the design of suitable pollutant control measures, there is the need to analyse responses over discrete periods—corresponding to periods were distinct changes in climate are expected—in addition to analysis over the continuous timeline. This can be accomplished using change point detection algorithms on climate projections to isolate distinct climate periods on which to base the analysis. 2) Pollutant control practices used in agricultural watersheds—such as no till and conservation tillage—slow down and reduce surface runoff, encourage infiltration, and trap soil particles. This mechanism of operation effectively reduces sediment loss and most of the nutrients attached to sediments (Gitau et al. 2005), but may inadvertently increase soluble phosphorus in subsurface soil layers. More studies are needed to determine suitable measures that will reduce pollutant movement through surface pathways without transferring the problem to the subsurface.

Concluding remarks: The aim of this study was to assess the impact of changing precipitation patterns on hydrology and pollutant losses in a subsurface-drained watershed. Surface runoff is expected to increase under medium and high emission scenarios (RCP 4.5 and RCP 8.5) in response to anticipated increases in precipitation amounts and one-day maximum precipitation, resulting in increases in pollutant losses through surface pathways. Responses are expected to be larger in the spring and summer, which is where changes in precipitation are expected to be more pronounced.

Acknowledgments: This work was supported in part by the USDA National Institute of Food and Agriculture, Hatch Project 1009404.

References

Arnold JG, Srinivasan R, Muttiah RS, Williams JR (1998) Large area hydrologic modeling and assessment. Part I: Model development. J Am Water Resour As 34(1):73-89

Gitau MW, Gburek WJ, Jarrett AR (2005) A tool for estimating best management practice effectiveness for phosphorus pollution control. J Soil Water Conserv 60(1):1-10

Gitau MW, Veith TL, Gburek WJ, Jarrett AR (2006) Watershed level best management practice selection and placement in the Town Brook Watershed, New York. J Am Water Resour As 42(6):1565-1581

Mehan S (2018) Impact of changing climate on water resources in the Western Lake Erie Basin using SWAT. PhD Dissertation, Purdue University

Moriasi DN, Gitau MW, Pai N, Daggupati P (2015) Hydrologic and water quality models: Performance measures and evaluation criteria. Transactions of the ASABE 58 (6):1763-1785

OLEPTF (2013) Ohio Lake Erie Phosphorus Task Force II Final Report. OH

Seibert J, McDonnell JJ (2003) The quest for an improved dialog between modeler and experimentalist. Advances in Calibration of Watershed Models, American Geophysical Union: Washington

Sekaluvu L, Zhang L, Gitau M (2018) Evaluation of constraints to water quality improvements in the Western Lake Erie Basin. J Environ Manage 205:85-98. https://doi.org/10.1016/j.jenvman.2017.09.063

Sui Y, Frankenberger JR (2008) Nitrate loss from subsurface drains in an agricultural watershed using SWAT2005. Transactions of the ASABE 51(4):1263-1272

11th World Congress on Water Resources and Environment (EWRA 2019)
"Managing Water Resources for a Sustainable Future", 25-29 June 2019, Madrid, Spain

Drought monitoring and early warning framework

G. Tsakiris*, H. Vangelis, D. Tigkas, V. Tsakiris
Centre for the Assessment of Natural Hazards and Proactive Planning, National Technical University of Athens, Greece
** e-mail: gtsakir@central.ntua.gr*

Introduction

Droughts are recurrent natural multidimensional phenomena affecting almost all regions of the world. Drought monitoring is a fundamental necessary process for assessing the severity of each drought episode, in order to initiate actions and measures for protecting the affected systems from droughts (Tsakiris 2017; Wilhite 1993). The monitoring of meteorological droughts should be based on a dense meteorological network including principally precipitation and temperature measurements. The data of the meteorological variables can then be transferred to the unit area of the study region (Tsakiris et al. 2016). Drought severity at each unit area is assessed through the calculation of some drought indices such as SPI (McKee et al. 1993) and RDI (Tsakiris and Vangelis 2005; Tsakiris et al. 2007a). Drought maps can be produced for each reference period starting from the first trimester of the year commencing in October (Tsakiris et al. 2007b).

The forecasting process starts with the severity level of the first trimester and through existing historical drought events, the transition probabilities to each severity level of the 12-month reference period are calculated. The forecasting uncertainty is reduced as we proceed from the 3-month reference period to greater reference periods (e.g. 6 or 9 months).

The forecasting process is the basis for establishing an early warning system in which apart from the technocratic aspects, the organisational / institutional dimension, the implementation process and the participation of stakeholders are also considered. For simplicity the last two aspects can be incorporated in the organisational / institutional dimension.

Materials and methods

The methodological steps in the decisional procedure on the measures and actions to be taken for each river basin (as proposed by the water resources management plans of the WFD) during a year with signs of drought can be divided into two broad categories:

a) Technocratic
b) Organizational / institutional

On the technocratic dimension the following basic steps should be followed:

1. The meteorological stations to be used are selected
2. The meteorological indices should be selected
3. The partition and integration of each basin regarding the drought indices selected should be devised
4. The potential consequences at each basin for each level of drought severity should be calculated
5. The levels alert and emergency should be established at each basin
6. Drought severity analysis should be performed leading to transition probabilities from 3 to 6, from 6 to 9 and from 9 to 12-month reference periods
7. Forecasts of drought severity and reports on possible actions should be made considering the initial conditions and the capacity of each system to cope with drought phenomena

On the organizational / institutional side the methodological steps to be followed are:

1. Establishment of the task force and supporting scientific team
2. Assignment of responsibilities, coordination, synergies and financial support
3. Decisional procedure for early warning announcements and actions (involving also key stakeholders)
4. Inventory of droughts and consequences (from the supporting scientific team)

5. Cooperation with local authorities and central government
6. Public awareness and mobilization of people
7. Detailed implementation process of measures and actions

Results and concluding remarks

A comprehensive preparedness planning for combating drought and drought consequences mainly contains technocratic and organizational / institutional aspects. The territorial units on which drought monitoring and warning framework is established are the river basins of WFD implementation plans.

A number of necessary steps both on the technocratic and organizational dimensions should be taken at times not affected by the intense / severe drought episodes.

The assignment of responsibilities, the establishment of a competent task force and the supporting scientific team, and the clear decisional process involving key stakeholders, are among the most important issues for a successful preparedness plan against droughts of each river basin.

References

McKee TB, Doeskin NJ, Kleist J (1993) The relationship of drought frequency and duration to time scales. In: Proceedings of the Eighth Conference on Applied Climatology, Anaheim, 17–23 January 1993. American Meteorological Society, Boston, pp 179-184

Tsakiris G (2017) Drought Risk Assessment and Management. Water Resources Management 31(10):3083-3095. https://doi.org/10.1007/s11269-017-1698-2

Tsakiris G, Kordalis N, Tigkas D, Tsakiris V, Vangelis H (2016) Analysing Drought Severity and Areal Extent by 2D Archimedean Copulas. Water Recourses Management 30:5723–5735. http://doi.org/10.1007/s11269-016-1543-z

Tsakiris G, Pangalou D, Vangelis H (2007a) Regional drought assessment based on the Reconnaissance drought index (RDI). Water Recourses Management 21(5): 821-833. https://doi.org/10.1007/s11269-006-9105-4

Tsakiris G, Tigkas D, Vangelis H, Pangalou D. (2007b) Regional Drought Identification and Assessment. Case Study in Crete. In: Rossi G, Vega T, Bonaccorso B (eds), Methods and Tools for Drought Analysis and Management, Water Science and Technology Library, vol 62, Springer, Dordrecht. https://doi.org/10.1007/978-1-4020-5924-7_9

Tsakiris G, Vangelis H (2005) Establishing a drought index incorporating evapotranspiration. European Water 9-10:3-11

Wilhite DA (1993) The Enigma of Drought. In: Wilhite DA et al. (eds) Drought Assessment, Management, and Planning: Theory and Case Studies. Natural Resource Management and Policy, vol 2, Springer, Boston, MA

11th World Congress on Water Resources and Environment (EWRA 2019)
"Managing Water Resources for a Sustainable Future", 25-29 June 2019, Madrid, Spain

Insuring water supply in irrigated agriculture: A proposal for hydrological drought index-based insurance in Spain

J.A. Gómez-Limón*, M.D. Guerrero-Baena
Department of Agricultural Economics, University of Cordoba, Cordoba, Spain
**e-mail: jglimon@uco.es*

Introduction

In recent years, the changing climate has generated growing concern among irrigators in Mediterranean-climate regions about irrigation water reliability. It is expected that hydrological drought episodes (not enough water available in reservoirs and instream flows) to be more recurrent and intense, motivating more frequent 'water supply gaps', when irrigators cannot fully meet all their crop water needs. The consequences of water supply gaps in irrigated agriculture are *economic* (decreasing farmers' income and agricultural production), *social* (declining agricultural employment generation) and *environmental* (leading to illegal extraction of groundwater resources to partially cover irrigators' water needs). Due to all these negative impacts, it is obvious that uncertainty about the availability of water for irrigation constitutes a major *production risk* for irrigators in Mediterranean-climate regions.

For the reasons explained above, there is an urgent need to design new risk management instruments that could be implemented by irrigators to minimize drought related negative impacts (OECD 2016). Of all the risk management tools suggested to date, insurance has been highlighted as a particularly efficient instrument to cope with this risk (Rey et al. 2018), but it has been the focus of very little analysis in the literature (Leiva and Skees 2008; Maestro et al. 2016). Moreover, there are virtually no reports of this kind of insurance scheme having been implemented in a real-life setting (only in USA, and under rather constraining circumstances, irrigators are able to insure against this risk). Within this context, the main objective of this paper is to contribute to the debate on how to support irrigators in managing hydrological drought risk, by proposing a new insurance scheme for irrigated agriculture capable of overcoming the problems that currently make this risk uninsurable. This scheme is tailored to Spain, as it provides an interesting case study, but the appeal of the developed proposal extends beyond this national scope.

Materials and methods

There are many factors that can explain why hydrological drought insurance for irrigators has not been implemented in a real-life setting worldwide. Some of these factors relate to information asymmetries between the insurer and the insured (the well-known *moral hazard* and *adverse selection* problems), which also affect other types of agricultural insurance schemes. In addition, there are specific problems, such as: i) hydrological drought is a systemic risk, which implies that water supply gaps affect a large number of irrigators at the same time; ii) there is a high degree of uncertainty about future changes in the probability distribution function characterizing the stochastic variable 'water allotments'; iii) the existence of different sources of water supply for irrigation could difficult the compliance with the indemnity principle; iv) as irrigators are commonly represented in river basin agencies and take part in the decision-making process regarding the setting of annual water allotments, they may influence the probability of loss occurrence.

In this paper, a hydrological drought index-based insurance scheme for irrigated agriculture is proposed as the most suitable insurance design for minimizing the abovementioned problems, where the *insurable interest* is the full annual water allotment, as established in the water right granted by the River Basin Agency (RBA). Regarding the *insured capital* (IC), it is equivalent to the difference between the annual gross margin of the insured farm with full water allotment and the estimated annual gross margin of the same farm under rainfed conditions. Other relevant material elements of the proposed insurance contract are the following:

- *Index:* We suggest using an estimate of the *'stock of water available in reservoirs'* (*SW*) of the water

system that supplies irrigation water to the insured farmer. It is proposed that this index should be calculated annually on 1st June (at the beginning of the irrigation season, when *SW* reaches it maximum annual values).

- *Loss*: The occurrence of loss is verified when the value of the *SW* index is lower than a previously determined threshold *T* of water stored (the minimum stock of water in reservoirs that would allow the RBA to approve full water allotments). This loss could be 'partial' (*SW* lower than *T*, but higher than *L*, with the latter parameter defined as the lowest limit of water stock that allows the RBA to approve non-zero irrigation allotments), or 'total' (*SW* lower or equal to *L*, which would mean zero annual water allotments for irrigation). The declaration of losses could be made at the beginning of the irrigation season, specifically on 1st June, once the value of the *SW* index has been calculated.
- *Indemnity* (*I*): As it is an index-based insurance scheme, the calculation of the indemnity would not require in-field damage assessment, as it is the case in traditional agricultural insurance. It would be calculated automatically, after determining the value of SW, as follows:

$$I = \begin{cases} 0 & \text{if} \quad SW \geq T \\ IC \times (1 - DED) \times f(SW) & \text{if} \quad T > SW > L \\ IC \times (1 - DED) & \text{if} \quad SW \leq L \end{cases} \tag{1}$$

  As can be seen, the indemnity depends on the deductible (*DED*), the percentage of the insured capital that the farmer is responsible for covering, and on the intensity of the loss, quantified by the function *f(SW)*, that could be assumed to be linear: *f(SW)=(T-SW)/(T-L)*.
- *Premium:* An annual policy with an annual premium is proposed.

Regarding the personal elements of the insurance contract, the following options are proposed:

- *Insured:* Individual policies (irrigators) and collective policies (irrigators' associations).
- *Insurer:* It is proposed that Agroseguro, S.A., the insurance company pooling all private insurance firms engaged in the Spanish Agricultural Insurance System, should be the only insurer.
- *Re-insurer:* We suggest that the proposed scheme be reinsured by the Insurance Compensation Consortium, a public non-profit reinsurance body, currently reinsuring all agricultural insurance schemes.

Results and concluding remarks

Due to climate change, the failure to guarantee water supply for irrigation is an increasingly pressing risk in Mediterranean-climate regions. The severe consequences that hydrological droughts may entail for irrigated agriculture are prompting policy and academic debates about how to effectively manage this type of risk. In this regard, hydrological drought insurance is a promising instrument for managing the risk of water supply gaps in irrigated agriculture.

In this paper, hydrological drought insurance indexed to the variable *'stock of water available in reservoirs'* has been proposed to cover the risk of water supply gaps in irrigated agriculture. The implementation of the proposed insurance in a real-life setting requires additional studies from a supply-side perspective, in order to calculate the commercial premium of the insurance scheme. Also, further studies from the demand perspective are needed to determine the potential acceptance of this risk management instrument by irrigators through their willingness to pay for such an insurance policy.

References

Leiva AJ, Skees JR (2008) Using irrigation insurance to improve water usage of the Rio Mayo Irrigation System in Northwestern Mexico. World Development 36(12):2663-2678. http://doi.org/10.1016/j.worlddev.2007.12.004

Maestro T, Barnett BJ, Coble KH, Garrido A, Bielza M (2016) Drought index insurance for the Central Valley Project in California. Applied Economic Perspectives and Policy 38(3):521-545. http://doi.org/10.1093/aepp/ppw013

OECD (Organisation for Economic Co-operation and Development) (2016) Mitigating Droughts and Floods in Agriculture. Policy Lessons and Approaches. OECD Publishing, Paris

Rey D, Pérez-Blanco CD, Escriva-Bou A, Girard C, Veldkamp TIE (2018) Role of economic instruments in water allocation reform: lessons from Europe. International Journal of Water Resources Development 35(2):206-239. http://doi.org/10.1080/07900627.2017.1422702

11th World Congress on Water Resources and Environment (EWRA 2019)
"Managing Water Resources for a Sustainable Future", 25-29 June 2019, Madrid, Spain

Nonstationary frequency analysis over a flood prone Indian catchment

M. Ghosh[1], J. Singh[2], S. Karmakar[1,2,3*], S. Ghosh[1,3,4]
[1] Interdisciplinary Program in Climate Studies, Indian Institute of Technology Bombay, Mumbai 400076, India
[2] Centre for Environmental Science and Engineering, Indian Institute of Technology Bombay, Mumbai 400076, India
[3] Centre for Urban Science and Engineering, Indian Institute of Technology Bombay, Mumbai 400076, India
[4] Department of Civil Engineering, Indian Institute of Technology Bombay, Mumbai 400076, India
*e-mail: skarmakar@iitb.ac.in

Introduction

In a monsoon prevalent country like India, which receives more than 80% of the total annual rainfall during June to September (Jain and Kumar 2012), modelling of hydroclimatic extremes is very necessary since it plays a decisive role in the estimation of design values. However, the conventional assumption of stationarity in hydrological time series may no longer be valid owing to perceivable impacts of climate change, urbanization and concurrent changes in land use pattern which has led to the rise in extreme events like floods and droughts. The recent Kerala floods of 2018, which had a return period of more than 500 years (Mishra et al. 2018) and the droughts of 2016, which hit almost 11 states, bear testimony to the rise in such events. The previous literature suggests significant nonstationarity in the characteristics of Indian monsoon extremes. Under such circumstances, the inclusion of the concept of nonstationary frequency analysis (FA) is imperative for policy and decision makers to have an accurate knowledge of occurrence and severity of extremes.

The currents study aims to quantify the changes in return period of precipitation extremes over Kosi river basin situated in the state of Bihar in India with a catchment area of 9200 km^2 under nonstationary scenario. While no detailed study for nonstationary FA has been performed over this highly flood-prone catchment for fine resolution rainfall data the observations may facilitate to provide reliable return periods. This will help us to understand the nature of precipitation over the region such as changes in the patterns of the extremes for proper planning and adaptation strategies.

Materials and methods

Being one of the developing states of India, Bihar has experienced rapid urbanization in the past few decades. These changes are likely to cause variability in local climate thus introducing nonstationarity in streamflow discharges which may lead to catastrophic flood events. In the current study, stationary and nonstationary frequency analyses have been performed with more focus towards nonstationary FA for which the major steps involved are enumerated in Figure 1. A cluster of 74 GAMLSS based models developed by Singh et al. (2016) has been utilised for nonstationary FA. This increases the accuracy of quantile estimates when the underlying distribution density function is changing with time (or hydro-climatic variables having nonstationary behaviour). The flexible platform of GAMLSS to model nonstationarity (Rigby and Stasinopoulos 2005) gives an edge over other additive models.

Results and concluding remarks

Figure 2 presents a summary of the comprehensive frequency analyses performed in the present study. The 10-year, 100-year and 500-year return levels were calculated for both stationary and nonstationary conditions, and the changes in the AM rainfall intensity between these scenarios were estimated. The return levels under nonstationary condition were obtained from the best-fit nonstationary model from a cluster of 74 models. The spatial pattern of the extreme events under the stationarity and nonstationary assumption has been represented. The results from this analysis indicate some intensification of rainfall, e.g., an increase up to ~ 100% in the 500-year events under the nonstationary scenario and a decrease up to ~-60%. It can also be observed that difference in rainfall extremes gets magnified with increase in return

period. Overall, majority of the grids indicate a decrease in the AM intensity under nonstationary condition, which may help to reduce the construction and operation cost of flood control structures by considering more accurate return levels. The influence of nonstationarity will be further investigated at the flood inundation level for different return periods and subsequently a comparison may be assessed over the hazard maps.

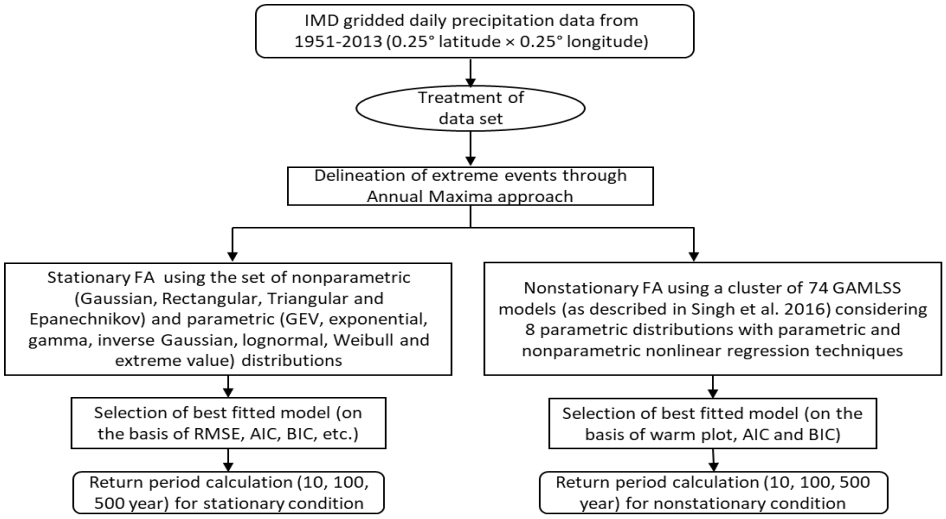

Figure 1. A proposed framework for stationary and nonstationary frequency analyses

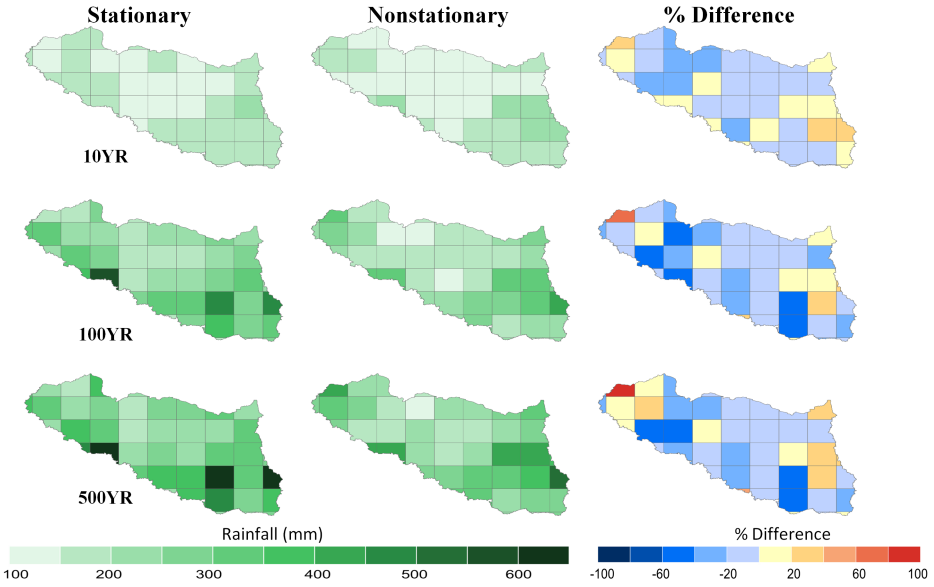

Figure 2. Spatial variability of 10-, 100- and 500-year AM events under stationary and nonstationary scenarios and their percentage change rainfall extremes under these scenarios. The percentage change has been calculated using [((nonstationary - stationary)/stationary)×100].

Acknowledgments: The work presented here is supported by Ministry of Earth Sciences, Govt. of India through a sponsored project no. 16MES003 (RD/0116-MES0000-010).

References

Jain SK, Kumar V (2012) Trend analysis of rainfall and temperature data for India. Current Science 102(1):37-49

Mishra V, Aaadhar S, Shah H, Kumar R, Pattanaik DR, Tiwari, AD (2018) The Kerala flood of 2018: combined impact of extreme rainfall and reservoir storage. Hydrology and Earth System Sciences Discussions: 1-13

Rigby RA, Stasinopoulos DM (2005) Generalized additive models for location, scale and shape. Journal of the Royal Statistical Society: Series C (Applied Statistics) 54(3):507-554

Singh J, Vittal H, Karmakar S, Ghosh S, Niyogi, D (2016) Urbanization causes nonstationarity in Indian summer monsoon rainfall extremes. Geophysical Research Letters 43(21):11,269-11,277. doi: 10.1002/2016GL071238

11th World Congress on Water Resources and Environment (EWRA 2019)
"Managing Water Resources for a Sustainable Future", 25-29 June 2019, Madrid, Spain

Drought analysis with Standardized Precipitation Evapotranspiration Index (SPEI) in Marmara region, Turkey

Ü. Güner Bacanlı[1*], G.N. Akşan[2]
Department of Civil Engineering, University of Pamukkale, Denizli, Turkey
** e-mail: ugbacanli@pau.edu.tr*

Introduction

Drought is a very scalar phenomenon due to time affected by many parameters (Potop et al. 2012). Drought indices have been proposed by many researchers for the calculation of drought. Examples include Standardized Precipitation Evapotranspiration Index (SPEI; Vicente-Serrano et al. 2010), the Palmer Drought Severity Index (PDSI; Palmer 1965) and the Reconnaissance Drought Index (RDI; Tsakiris and Vangelis 2005) (Potop et al. 2012; Bamimahd and Khalili 2013; Wang et al. 2014; Hou et al. 2017; Stagge et al. 2015). The purpose of all these indices is to detect drought and minimize the risks that may occur. In this study the advantage of SPEI compared to other indices used is that it combines temperature and precipitation with evapotranspiration capacity.

SPEI has been used to determine drought in more than one country (van der Schrier et al. 2013). In Turkey from the past and present has been used many drought indices. These are available in SPEI (Onusluel Gul and Kuzucu 2017). However, the SPEI calculation was applied for in Turkey's the Marmara Region for the first time in this study. The aim is to determine the drought disaster by achieving a more accurate result with SPEI and to minimize the risk by planning drought (Alam et al. 2017; Dai 2011).

Materials and methods

When calculating SPEI, a simple solution is applied using average rainfall and average temperature data (Bamimahd and Khalili 2013). Potential evapotranspiration (PET) is assisted when calculating this solution. The PET calculation can be calculated in more than one method. However, Thornthwaite method was used in this study.

SPEI values were estimated for the station at 1-, 3-, 6-, 9- and 12-month time scales. The equations obtained by Vicente-Serrano et al. (2010) are used for SPEI calculation. The SPEI data obtained are aimed at reaching a conclusion by looking at Table 1 (McKee et al. 1993; Abramowitz and Stegun 1965).

Table 1. Drought classification (McKee et al. 1993)

Categories	Index value
Exceptionally wet	≥+2
Severely wet	≥+1.5 to <+2
Slight wet	≥+1 to <+1.5
Close to Normal	>−1 to <+1
Slight dry	>−1.5 to ≤−1
Severely dry	>−2 to≤−1.5
Exceptionally dry	≤−2

Results and concluding remarks

SPEI values were estimated with 1-, 3-, 6-, 9- and 12-month time scale for all stations. All stations in the Marmara Region (11 stations) were used for this study. While 29-year data were used in Balıkesir and Istanbul stations, 48-year data was used in Kırıkkale station and 49-year data were used in other stations.

When the Marmara Region is examined in general, the percentage of dryness varies between 17.40% and 23.77%. The frequency at which the percentage of dryness is minimum is 1-month frequency, and the frequency at which it is maximum belongs to the frequency of 6 months. The percentage of wetness varies between 17.06% and 19.90%. The frequency with which the percentage of wetness is minimum is seen at a

frequency of 12 months and the frequency with the maximum frequency is seen at a 6-month frequency.

When the stations are examined one by one, the minimum dryness in all stations except Kırıkkale is at 1-month frequency. In Kırıkkale, this situation was observed at 9-month frequency. However, in the stations other than Bursa and Edirne, the maximum dryness was seen in 6-month frequency, while in these two stations this was seen in 3-month frequency. Canakkale station has the lowest value with 15.57% when the frequencies with which the installation is minimum are compared. Balikesir has the highest value with 26.44% when the frequencies with which the installation is maximum are compared.

When one looked at each station in the wetness, it was observed at a frequency of 12 months in a minimum of 6 stations and a frequency of 9 months in 3 stations. The maximum percentage was observed at 6-month frequency in 9 stations except Edirne and Kırıkkale, while it was observed in Edirne and Kırıkkale at 1-month frequency. Kırıkkale station has the lowest value with 15.33% compared to the frequencies where the wetness is minimum. When frequencies are maximum, İstanbul and Balikesir have the highest frequency with an equal percentage of 21.26%.

When the 11 stations are examined, the maximum percentage values are in the close to normal drought class in all frequencies of 1, 3, 6, 9 and 12 months. When the drought class close to normal is examined, the maximum percentage is 68.10% in Balikesir station, while the minimum percentage is 52.30% in Balikesir station again.

When the data were graphed, it was observed that the dryness and wetness periods increased from 1 month to 12 months.

At all stations, it can be said that the range of values is between -1 and +1. It can therefore be concluded that it belongs to the normal drought class. However, it can be said that drought values will increase as a result of imbalances in rainfall and temperature in the future.

References

Abramowitz M, Stegun IA (1965) Handbook of Mathematical Functions, with Formulas, Graphs, and Mathematical Tables. Dover Publications, USA

Alam NM, Sharma GC, Moreira E, Jana C, Mishra PK, Sharma NK, Mandal D (2017) Evaluation of drought using SPEI drought class transitions and log-linear models for different agro-ecological regions of India. Physics and Chemistry of the Earth 100:31-43

Bamimahd SM, Khalili D (2013) Factors Influencing Markov Chains Predictability Characteristics, Utilizing SPI, RDI, EDI and SPEI Drought Indices in Different Climatic Zones. Water Resources Management 27:3911-3928

Dai A (2011) Drought under global warming: a review. Wiley Interdisciplinary Reviews: Climate Change 2(1): 45–65

Hou M, Li H, Zou X, An W, Gao G, Zhao H (2017) Timescale differences between SC-PDSI and SPEI for drought monitoring in China. Physics and Chemistry of the Earth 102:48-58

McKee TB, Doesken NJ, Kleist J (1993) The relationship of drought relative frequency and duration to time scales. Eighth Conference on Applied Climatology, USA

Onusluel Gul G, Kuzucu A. (2017) Analysis of drought severity in Seyhan river basin. European Water 60:211-217

Palmer WC (1965) Meteorological drought. U.S. Weather Bureau Research Paper 45, 58 pp.

Potop V, Možný M, Soukup J (2012) Drought evolution at various time scales in the lowland regions and their impact on vegetable crops in the Czech Republic. Agricultural and Forest Meteorology 156:121-133

Stagge JH, Tallaksen LM, Gudmundsson L, Van Loon A, Stahl K (2015) Candidate Distributions for Climatological Drought Indices (SPI and SPEI). International Journal of Climatology 35(13):4027-4040

Tsakiris G, Vangelis H (2005) Establishing a drought index incorporating evapotranspiration. Eur. Water 9/10:3–11

van der Schrier G, Barichivich J, Briffa KR, Jones PD (2013) A scPDSI-based global data set of dry and wet spells for 1901–2009. Journal of Geophysical Research: Atmospheres 118(10):4025–4048

Vicente-Serrano SM,,Beguera,S, López-Moreno JI (2010) A multiscalar drought index sensitive to global warming: The standardized precipitation evapotranspiration index. J. Climate, 23:1696–1718

Wang W, Zhu Y, Xu R, Liu J (2014) Drought severity change in China during 1961–2012 indicated by SPI and SPEI. Natural Hazards 75(3):2437–2451

11th World Congress on Water Resources and Environment (EWRA 2019)
"Managing Water Resources for a Sustainable Future", 25-29 June 2019, Madrid, Spain

Integrated model of capacity expansion and operation of water supply systems including non-conventional water sources

T.M.N. Carvalho*, F.A. Souza Filho, V.C. Porto, G.A. Reis, L.Z.R. Rolim
Department of Hydraulic and Environmental Engineering, Federal University of Ceará, Fortaleza, Brazil
** e-mail: taismarianc@gmail.com*

Introduction

Planning for the capacity expansion of water supply systems requires efficient operation of available water resources and the expansion of existing infrastructure. The need to attend water demand is associated with climate, social and economic uncertainties, increasing the supply costs. Besides, most water supply systems are no longer able to meet increasing demands, resulting in the need to include non-conventional water sources.

Previous work applied simulation and optimization techniques through Dynamic Programming (Fraga et al. 2017), Mixed-Integer Programming (Beh et al. 2014) and Genetic Algorithms (Zhang and Babovic 2012) for expansion of urban water systems. This paper proposes a multistage modelling approach to define operation and expansion strategies that reduce the supply costs under risks of water shortage, incorporating reservoir operation and alternative sources. Besides, the impact of climate uncertainty on the system expansion costs will be assessed as well as the efficiency of incorporating alternative sources.

The method is applied in Fortaleza Metropolitan Region (FMR), Brazil. FMR consists of eight storage reservoirs and transmission canals that transfer water from the Jaguaribe basin, where is located the largest reservoir of the state (6.2 billion m³). Rainfall variability and recurrent droughts reduce the reliability on the system, that is in a stage of insufficient adaptation to urban and industrial activity growth.

Materials and methods

The optimization model aggregates monthly operational and annual expansion decisions in a 30 years planning horizon. Thus, short-term operational decisions are limited by prior expansion decisions. Except for superficial reservoirs, all sources considered in the model have expansion capacity. The reservoir system that supplies the FMR was modelled as two simplified equivalent reservoirs.

Future water demand was calculated as a function of the population growth projections and per capita consumption. An annual population growth rate of 0.83% was assumed, resulting in 4.6 million habitants in 2040. The estimation of industrial demand was based on the development plan of Pecém harbour, main industrial area of the state. Water demand on Jaguaribe area is primarily agricultural and was calculated from the expected increase of irrigated areas (about 28% during the planning horizon).

In order to evaluate the cost of reducing the water supply risk of incorporating alternative water sources, three different infrastructure configurations were analysed, considering: (1) existing reservoir system, (2) surface water sources and desalination plants and (3) superficial reservoir, desalination and non-conventional water sources.

In the first scenario, the objective function corresponds to the minimization of demand shortage. In the other two scenarios the objective is to minimize supply costs of meeting different percentages (95, 99 and 100%) of total water demand. The alternative sources included rainwater tanks, wastewater reuse and greywater recycling. Water from wastewater reuse was designated exclusively to industrial purposes. The model chooses the water source to be used and the timing of the expansion to minimize the following objective function, where y, x and T are the decision variables:

$$\sum_{i=1}^{q}\sum_{m=2}^{f} CI_{m,i} y_{m,i} + \sum_{j=1}^{n}\sum_{m=1}^{f} CO_{m,j} x_{m,j} + \sum_{j=1}^{n}\sum_{k=1}^{t} CT_{k,j} T_{k,j} + \sum_{i=1}^{q}\sum_{m=1}^{f} CM_{m,i} Cap_{m,i} \quad (1)$$

where $CI_{m,i}$, $CO_{m,j}$, $CT_{k,j}$ and $CM_{m,i}$ correspond to investment, operational, water transfer and maintenance

costs coefficients, respectively; $x_{m,j}$ is the withdrawal from source m in month j; $y_{m,j}$ is the expansion of source m in year j; $Cap_{m,i}$ is the maximum capacity of source m during year j; f is the number of water supply alternatives; q is the number of years; n the number of months in the planning horizon; t is the number of interbasin transfer pipes and $T_{k,j}$ is the water transfer between basins in pipe k in month j.

The supply costs coefficients were estimated from the local Water Company capacity expansion projects. In order to evaluate the impact of climate uncertainty in the optimization solution, 10000 synthetic annual rainfall series were generated and disaggregated to a monthly scale. Then, the rainfall-runoff model Soil Moisture Accounting Procedure (SMAP) was used to convert them into streamflow series. The rainfall series were needed to simulate the rainwater tanks. The capacity expansion model was optimized for each of the generated series and the algorithm used was the Particle Swarm Optimization.

Results and concluding remarks

In the first scenario, the current infrastructure was analysed to verify the water supply failure for future water demand. Optimization results varied with the streamflow series, but for most of them less than 95% of water demand was met, which means failure during months and an imminent collapse of the system risk. Hence, the current supply system would not be able to attend water use increase in the next 30 years, implying in the need for expansion and inclusion of alternative sources.

The second scenario included water from desalination, that does not have its availability dependent on climate variability. Reducing the shortage risk and ensuring higher percentages of the total demand means higher supply costs. There was a significant increase in the installation cost from meeting 99 and 100% of total demand, since the available volume of water was greater than needed for some periods due to the fixed size of desalination plants expansion. However, in a long-term perspective, investments in desalination pay off, since once the plant is installed, the water volume is available during its entire lifetime, supplying water even during eventual drought periods. Operation costs were sensible to the climate variation in the streamflow series, especially in dry periods where reservoirs capacity was not enough to attend the demand and a greater volume of desalinated water was needed.

At last, the same demand supply levels were taken into consideration in the third configuration, now including alternative sources that are less expensive, but have uncertain availability (rainwater tanks, wastewater reuse and greywater recycling). Incorporating non-traditional sources reduced the costs of the water system in about 11% when compared with the exclusive use of superficial and seawater. This reduction varied with the demand supply level and the precipitation and streamflow series. These results demonstrated that the cost reduction effectiveness of the alternative sources was higher for high supply levels by avoiding the installation of large desalination plants and was lower for the dryer series due their dependence on climate variability. The variability of the results due to climate uncertainty make it hard to define the best configuration for the water system expansion. The model solution could be improved by applying stochastic optimization techniques.

Acknowledgments: The authors thank the National Council for the Improvement of Higher Education (CAPES) and National Council for Scientific and Technological Development (CNPq) for the financial support.

References

Beh EHY et al. (2014) Optimal sequencing of water supply options at the regional scale incorporating alternative water supply sources and multiple objectives. Environmental Modelling and Software 53:137–153. http://doi.org/10.1016/j.envsoft.2013.11.004

Fraga CCS et al. (2017) Planning for infrastructure capacity expansion of urban water supply portfolios with an integrated simulation-optimization approach. Sustainable Cities and Society 29:247–256. http://doi.org/10.1016/j.scs.2016.11.003

Zhang SX, Babovic VA (2012) A real options approach to the design and architecture of water supply systems using innovative water technologies under uncertainty. Journal of Hydroinformatics 14(1):13-29. http://doi.org/10.2166/hydro.2011.078

11th World Congress on Water Resources and Environment (EWRA 2019)
"Managing Water Resources for a Sustainable Future", 25-29 June 2019, Madrid, Spain

Application of stochastic dual dynamic programming in operation optimization of the Jaguaribe-Metropolitano reservoirs system

V.C. Porto*, F.A. Souza Filho, T.M.N. Carvalho, R.V. Rocha , R.L. Frota
Department of Hydraulic and Environmental Engineering, Federal University of Ceará, Fortaleza, Brazil
** e-mail: victorcporto@gmail.com*

Introduction

The application of mathematical optimization techniques to reservoir system operation, besides allowing a more rational use of water, can also help to justify allocation decisions and solve conflicts. However, this application is not a simple task since it must deal with the inherent uncertainties, nonlinearities and multiobjectivity of the hydrosystems (Rani and Moreira 2009). In the literature, reservoir systems operation optimization is often modelled as a multistage stochastic programming problem and solved with a Stochastic Dynamic Programming (SDP) algorithm. However, the application of SDP is limited to systems with few reservoirs due to its curse of dimensionality. Pereira and Pinto (1991) developed the Stochastic Dual Dynamic Programming (SDDP), an extension of SDP that attenuates the curse of dimensionality by avoiding the variables discretization. The SDDP was first developed for the optimization of large hydropower generation systems (Pereira and Pinto 1991; Scott and Read 1996; Mo et al. 2001) and today its application to multipurpose reservoir systems is becoming more usual (Tilmant et al. 2008; Marques and Tilmant 2013; Raso et al. 2017).

The present work seeks to apply and evaluate the performance of the SDDP algorithm in the optimization of the joint operation of two multipurpose reservoir systems. The hydrossystem chosen for this study is the Jaguaribe-Metropolitano wich supplies water for most of the Ceará state (Brazil). The hydrosystem is composed by the Jaguaribe and Metropolitan basins reservoir systems. Jaguaribe comprises the greatest reservoirs of the State, presenting a predominant demand for irrigation and Metropolitan includes five smaller reservoirs that supply urban and industrial water demands. The two systems are artificially integrated.

Materials and methods

The approach was developed for a 5-year operating horizon with monthly decisions where optimization is performed annually. The Jaguaribe-Metropolitano hydrosystem is modeled as two equivalent reservoirs (one for each system) with linear evaporation losses due to the linearity constraint of the SDDP algorithm convergence.

The model is formulated with withdrawals and the transfers between the basins as decision variables. The state variables are the reservoir stocks that are updated through the water balance equation. The optimization aims to minimize the deficit in meeting demands and the losses due to spills, both are standardized to have the same weight in the objective function.

10,000 synthetic annual series were generated and monthly disaggregated for the probabilistic modeling of the streamflow. They were considered in the model with same occurrence probability in the composition of the 5-year operation horizon. The SDDP is then applied to find the optimal operating decisions through the Julia language package StochDynamicProgramming.

The optimal operating rule obtained from the SDDP model was compared with the current operation of the hydrosystem by simulating the years 2013-2017, a dry period in which there was a collapse risk of the supply system. The efficiency of the model was also verified for other three scenarios of specific inflows, one dry, one medium and one wet, that were defined from the 5-years series generated. These simulations aim to evaluate the sensitivity of the model to avoid spillages during the wet periods and emptying the reservoirs during the dry periods.

Results and concluding remarks

The SDDP algorithm has proved to be appropriate for the optimization of the Jaguaribe-Metropolitano system operation. This suitability was evaluated through the low processing speed required (less than three minutes), the convergence of the algorithm and the good performance of the optimal operation found. The optimal solution was defined even for the extreme scenarios.

The results also showed the importance of the integration of the two basins to maintain the efficiency of the Metropolitan system during the dry season, even in years with inflows close to the average of the historical series. Also, the required transfer between the two basins results in a decrease of Jaguaribe reservoirs stocks. Thus, guaranteeing better efficiency in the Metropolitan system is a consequence of increasing risk in Jaguaribe basin for the next horizon of operation (risk transfer between the two systems). This shows the need to discuss compensation mechanisms between the two basins.

The explicitly stochastic approach showed better performance than the current operation rules for the 2013-2017 period. Furthermore, this approach allows the incorporation of a seasonal forecasting system of inflows. This should increase the performance through a better definition of the probabilities of the inflow series sample space based on climate observations. The proposed methodology can be used for the system real-time operation with a monthly inflow and stocks updates and the estimated inflow for the next month as an alternative to the actual operation rules. This approach can bring significant gains by directly incorporating the streamflow uncertainty.

Acknowledgments: The authors thank National Council for the Improvement of Higher Education (CAPES) and National Council for Scientific and Technological Development (CNPq) for the financial support.

References

Pereira MVF, Pinto LMVG (1991) Multi-stage stochastic optimization applied to energy planning. Mathematical Programming 52(1–3):359–375

Marques GF, Tilmant A (2013) The economic value of coordination in large-scale multireservoir systems: The Parana River case. Water Resour. Res. 49(11):7546–7557

Mo B et al. (2001) Integrated risk management of hydropower scheduling and contract management. IEEE Trans. Power Syst. 16:216–221

Rani D, Mmoreira MM (2009) Simulation-optimization modeling: A survey and potential application in reservoir systems operation. Water Resources Management 24(6):1107–1138

Raso L et al. (2017) Effective streamflow process modeling for optimal reservoir operation using stochastic dual dynamic programming, J. Water Resour. Plann. Manag. 4017003

Scott T, Read E (1996) Modelling hydro reservoir operation in a deregulated electricity market. Int. Trans. Oper. Res. 3:243–253

Tilmant A et al. (2008) Assessing marginal watervalues in multipurpose multireservoir systems via stochastic programming. Water Resources Research 44(12):W12431

11th World Congress on Water Resources and Environment (EWRA 2019)
"Managing Water Resources for a Sustainable Future", 25-29 June 2019, Madrid, Spain

Drought and scarcity joint indicators for transboundary Iberian river districts: The case of Minho and Lima river basins

R. Maia*, M. Costa, J. Mendes
FEUP – Faculty of Engineering of the University of Porto / Department of Civil Engineering / Hydraulics, Water Resources and Envirnment Division
** e-mail: rmaia@fe.up.pt*

Introduction

Drought is one of the most damaging natural hazards in the Iberian Peninsula (IP), causing varied socioeconomic and environmental impacts (Maia and Serrano 2017). To prevent these impacts, there must be a close cooperation between Portugal (PT) and Spain (SP), namely regarding drought planning and management in the IP, as the two countries share five river basins, to which correspond four international River Basin Districts (Minho and Lima river basins on a same RBD, both in Portugal and in Spain). Unlike Portugal, which only approved a national drought plan in 2017, Spain has already approved (in 2007) and implemented drought plans in all the RBDs, and those have been revised in 2017. In the Spanish plans, two types of indicators are defined: prolonged drought indicators and scarcity indicators. In this context, the main objective of the present work was the definition of indicators in the Portuguese part of Minho and Lima river basins, corresponding to those that have been established in the drought plan of the Spanish part of both basins (CHMS 2017). A comparison was made between the Portuguese and Spanish parts of the two basins regarding the values and evolution of the indicators. This work is aimed to be a prototype for the definition of new and similar drought indicators to be applied in common by Portugal and Spain, in the shared river basins, and was developed in close collaboration with the Portuguese Minho and Lima RBD and the corresponding Spanish RBD authorities (respectively APA - Agência Portuguesa do Ambiente and CMS - Confederación del Miño-Sil) under the scope of the RISC-ML project (RISC_ML 2018).

Materials and methods

The definition of the prolonged drought and scarcity indicators for the Portuguese part of Minho and Lima river basins was carried out according to the methodology defined in the review of the "*Plan Especial de Actuación en Situaciones de Alerta y Eventual Sequía de la parte Española de la Demarcación del Miño-Sil"* (CHMS 2017).

The prolonged drought indicator is defined as to allow identifying temporally and spatially the temporal and spatial circumstantial reduction of runoff due to natural causes, independent of the management of resources by human action. The scarcity indicator is based on the relationship between the availability of resources and the demands, and should reflect the impossibility of meeting the demands, serving, at the same time, as an instrument of assistance in the decision making related to the management of water resources (CHMS 2017).

The general methodology defined for the calculation of each of the two indicators is very similar and starts by the selection of the hydrometeorological variables. After the selection of the variables, those are rescaled into dimensionless variables with values varying between 0 and 1. Afterwards, the dimensionless variables are aggregated, in a weighted way, resulting in a single indicator.

In the definition of prolonged drought indicators two variables were used: cumulative 12 month records of (i) precipitation (weighted over the river basin) and of (ii) the natural runoff (at a chosen point of the river basin network). Due to the scarce flow data on unregulated Portuguese sub-basins, it was necessary to perform, in both river basins on study, hydrological modelling in one sub-basin with natural runoff. Pontilhão de Celeiros, in the Lima river basin, and Segude, in the Minho River basin, were the chosen sub-basins. For the hydrological modelling, the HEC-HMS software was used in a continuous simulation mode, based on daily precipitation recorded in rainfall stations in the region.

These two variables were then standardized into SPI_{12} (precipitation) and SRI_{12} (runoff), then rescaled and aggregated in a weighted way, resulting in a single prolonged drought indicator, in which the value 0.3 corresponds to prolonged drought threshold (established based on historical drought events' records).

The scarcity indicator is defined based on hydrological variables: stored dam volumes, input flows to reservoirs, river flow in gauging stations and aquifer water levels. The first step is to choose, for each river basin, the variables that are the most representative of the evolution of the resource availability to meet the demands for water supply. In the Spanish part of Minho and Lima river basins, the variables chosen were of two types: stored dam volumes and river flows in gauging stations.

For each of the selected variables the thresholds corresponding to the different categories were established: normality (absence of scarcity), pre-alert (moderate scarcity), alert (severe scarcity) and emergency (serious scarcity). Prior to this step, the procedure is similar to the one mentioned before for the prolonged drought indicator, resulting in a single dimensionless scarcity indicator, in which the value 0.5 corresponds to the pre-alert threshold, 0.3 to the alert threshold and 0.15 to the emergency threshold.

In correspondence to the Spanish drought plan, both the prolonged drought indicator and the scarcity indicator, in the Portuguese parts of Minho and Lima river basins, were defined for the period between 1980/1981 – 2016/2017.

Results and concluding remarks

For the Portuguese part of Minho and Lima river basins, the prolonged drought indicator showed that the more severe drought episode, in intensity and duration, occurred between 2004/2005 – 2005/2006 in both river basins.

In the Spanish part of the two basins there were two large periods of prolonged drought that took place in 2004/2005 – 2005/2006 and 2011/2012. In the Minho river basin, the two episodes had similar intensity and duration. In the Lima river basin, the 2004/2005 – 2005/2006 was the longest episode, however the 2011/2012 was the episode with greater intensity.

A comparison between Portuguese and Spanish parts of the river basins was made regarding the evolution of the drought indicators. In the Minho river basin case, the indicators considered for Spain for the referred comparison corresponded to Low Minho Spanish territorial unit.

Through the comparison between the two Portuguese and Spanish river basins parts it can be concluded that:

- in general, despite different intensities and durations, there is a certain agreement between the periods of prolonged drought in the Spanish part and in the Portuguese part of both basins between 1980/1981 and 2016/2017;
- the prolonged drought episodes were more frequent in the Spanish parts than in the Portuguese parts, but both international basins were affected by the major drought events, namely those occurred in 2004/2005 – 2005/2006, 2011/2012 and 2016/2017. In this last event, the duration and intensity of the drought event were similar in both parts of Minho and Lima river basins.

Regarding the scarcity indicators, the corresponding evaluation for the Portuguese part of the Minho and Lima river basins is currently being carried out, and is planned to be concluded by spring 2019.

Acknowledgments: RISC_ML (Reference: 0034_RISC_ML_6_E), project co-financed by the European Regional Development Fund (ERDF) through the Interreg V-A Spain-Portugal (POCTEP) 2014-2020 program.

References

CHMS (2017) Plan Especial de Actuación en Situacones de Eventual Sequía de la Parte Española de la Demarcación Hidrográfica del Miño-Sil. https://www.chminosil.es/es/chms/planificacionhidrologica/nuevo-plan-especial-de-sequia/consulta-publica-plan-especial-de-sequia

Maia R, Serrano S (2017) Drought Planning and Management in the Iberian Peninsula. In: Wilhite D, Pulwarty R, Drought and Water Crises: Integrating Science, Management, and Policy, 1st ed, Taylor & Francis Group, pp 481-505.

RISC_ML. (2018) Prevención de Riesgos de Inundaciones y Sequías en la Cuenca Internacional del Miño-Limia. http://risc-ml.eu

11th World Congress on Water Resources and Environment (EWRA 2019)
"Managing Water Resources for a Sustainable Future", 25-29 June 2019, Madrid, Spain

Flood inundation studies to protect the national highways

S. Mohan, S. Akash*
Environmental and Water Resources Engineering/department of Civil Engineering, Indian Institute of Technology Madras, Chennai, India
** e-mail: akashsinha08@hotmail.com*

Introduction

Rapid urbanization has a direct impact on land use/cover change which results in low infiltration and consequently high runoff during a flood event. Recently, the city of Chennai in 2015 has witnessed a severe flood in 2015. And its impact was magnified due to irregular urbanization and poor maintenance of drainage system. Based on local observation, the flood water in the region near Thiruvottyuir- Ponneri – Panchetti Road (TPP road) of Chennai city, between Vichur road and Kosasthalaiyar river, remained stagnate for about 2 months after the flood event. Several factors are to be blamed, namely, the sequence of the flood event, huge flow coming to the area from Kosasthaliyar river, high urbanization, blockage of storm-drainage passage and poor condition of culverts. All these factors summed up and had created the problem. As most of the road drainage and urban drainage projects are designed for a return period of 5 to 10 years or 25 to 50 years, there is no fault on the design aspect. The city of Chennai and its suburb - recorded multiple torrential rainfall events during November-December 2015 that caused inundation of the coastal districts of Chennai, Kancheepuram, and Tiruvallur. It is estimated that about 90% of mean annual rainfall of Chennai, occurred in just 20 days. Some reports claim that the 2015 extreme rainfall event in Chennai was found to be rare with a return period close to 100 years. This flood has two peaks, one on 16th Nov of 369 mm and the other on 2nd of Dec, 2015 of 291 mm.

Materials and methods

As a part of preliminary studies, sub-catchment map of the flooded region is made using Digital Elevation Map (DEM), SRTM data of resolution 90 m. The entire region is delineated into sub catchment using ArcGIS 10.3.1.

The runoff generated from the storm is first estimated using empirical formula (Dicken's formula; Ryve's formula and Inglis formula) and then using synthetic unit hydrograph method, based on the "Guidelines for the design of small bridges and culvert", IRC- SP13, "Manual of Estimation of Design Flood, (CWC 2001)" and "Report of "Lower Eastern coast 4(b), (CWC 1987)".

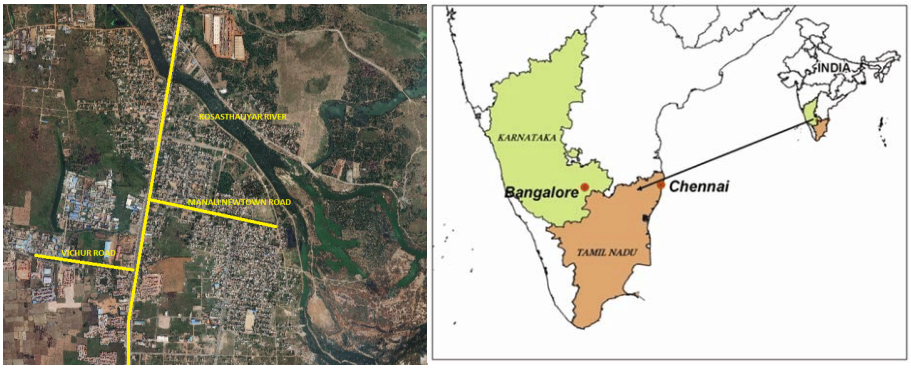

Figure 1. Study Area near Kosasthalyiar River in Chennai

These methods are based on the studies done earlier which do not consider the recent effect of urbanization in the runoff. Moreover, these methods do not consider antecedent moisture condition (AMC) also. As the area has witnessed sequences of the flood in a matter of 20 days, the infiltration capacity of the region will keep on decreasing. Due to which the runoff generation will increase for later events.

SCS-CN (Soil Conservation Service – Curve Number) method was applied for the present study to estimate the amount of runoff generated in the nearby area. This method adopted based on the work of Ahmad et al., (2015) where precipitation (P) and potential maximum retention (S). The final equation for runoff calculation is given by:

$$Q = (P-Ia)^2/(P-Ia+S) \quad (1)$$

For Indian condition Ia = 0.3S. The only parameter needed is the curve number which can be obtained directly from SCS developed by USDA Natural Resource Conservation Service or can be computed for areas having composite geology. Area-weighted composite curve number for various conditions of land use and hydrologic soil conditions are computed as follows:

$$CN_{eq}=(\sum CN_i \times A_i)/A \quad (2)$$

where A_i represent areas of a polygon having curve number values CN_i and A is the total area. Based on CN for AMC II, CN for AMC I and III was estimated. The land use and land cover of the study area estimated from ArcGIS 10.3.1. It shows that more than 75% of the area is either residential or block, leaving only 25% for major infiltration. Based on land use and land cover, Equivalent curve number is estimated for each sun catchment for different AMC condition.

Results and concluding remarks

The Upper Sub-catchment includes all the runoff generation area west of TPP road. This entire runoff is supposed to be drained through the two culverts at Chainage of 7/705 of TPP road which is further diverted through a canal running parallel to the TPP road to the nearest stream. The canal current capacity is taken from the TPP report. As per the report, presently there is two culvert at a Chainage of 7/705 of size 3.8 × 1.8 m. The canal is having a normal discharge capacity of 0.16 m^3/sec/m. Hence, the total water that the culvert can discharge through two culverts is 28356.48 cubic meter in a day.

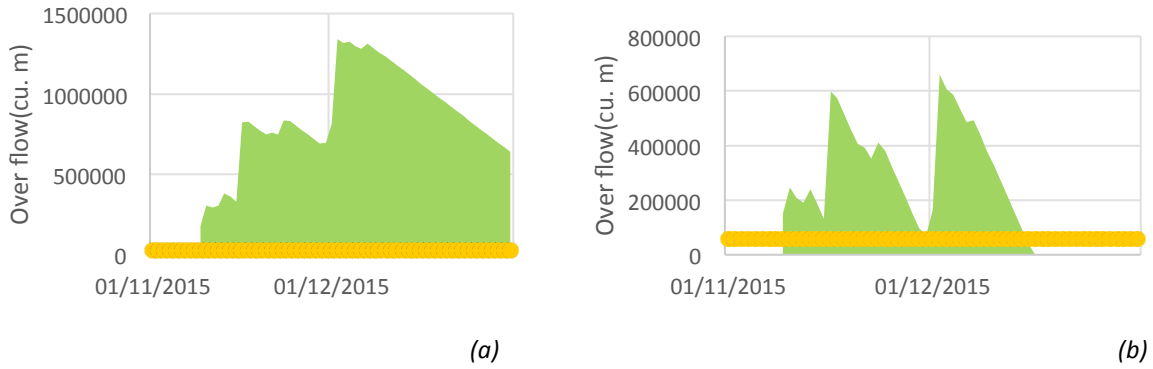

Figure 2. Scenario analysis based on current design and proposed design on TPP road

The above analysis is made on the assumption that the culvert is working at its full capacity. It is evident from Figure 2(a) that even if the culvert operates at its capacity, the flood water will remain stagnant until the end of December. It is proposed to construct one more culverts of the same dimension as of current one. The proposed structure will add to discharge capacity of 0.75 m^3/sec. The results show (Figure 2(b)) that the flood water will get drained out of the system by 15th of December.

Acknowledgments: The author(s) appreciate the technical support received from Tamil Nadu Road Development Company Ltd. (TNRDCL).

References

Ahmad I, Verma V, Verma M (2015) Application of Curve Number Method for Estimation of Runoff Potential in GIS Environment. 2nd International Conference on Geological and Civil Engineering, pp 16–20. https://doi.org/10.7763/IPCBEE

CWC (1987) East Coast subzone 4(a), (b) & (c)

CWC (2001) Manual on Estimation of Design Flood.

11th World Congress on Water Resources and Environment (EWRA 2019)
"Managing Water Resources for a Sustainable Future", 25-29 June 2019, Madrid, Spain

A methodology for the assessment of hydrological risk of river levee overtopping at ungauged sites

M. Isola[1,2*], E. Caporali[1], L. Garrote[2], L. Mediero[2]
[1] Department of Civil and Environmental Engineering, University of Florence, Firenze, Italy
[2] Department of Civil Engineering: Hydraulics and Energetics, Universidad Politécnica de Madrid, Madrid, Spain
* e-mail: matteo.isola@unifi.it

Introduction

Overtopping has been identified as the main cause of failure for a river levee (Vorogushyn et al. 2010). It typically occurs when the river discharge exceeds the design value of the levee during a flood event or, broadly, if either the river water level exceeds the levee crest or the flow overtops a weak levee segment. Risk assessment of levee overtopping is necessary for assessing levee stability and flood risk management planning.

The complexity of routing processes in some hydraulic structures, such as river levees and dams, requires the representation of the full flood hydrograph. Consequently, a multivariate analysis on flood variables is useful for their design. Besides, regional analyses improve at-site quantile estimates obtained at gauged sites, especially when short flow series exist, and provide estimates at ungauged sites where flow records are unavailable.

The main goal of this research is to develop a methodology that combines a multivariate analysis of flood variables with a regional flood frequency analysis, in order to assess the overtopping hydrological risk at both ungauged and gauged sites. The results showed that the multivariate distribution of the hydrological flood variables can be obtained when the aim is to assess the levee failure level for a given return period.

Materials and methods

The bivariate flood frequency distributions at the sites considered in the study were obtained through a copula approach, following the regional multivariate methodology proposed by Requena et al. (2016). The fitted copulas were used to generate a large set of synthetic peak-volume flood pairs. Synthetic hydrographs were generated following the methodology of Isola et al. (2018), to ascribe a given shape to each synthetic peak-volume pair. The set of synthetic hydrographs was routed through the river reach, identifying the hydrographs that exceed the overtopping threshold condition (Damme et al. 2016), expressed in terms of overtopping flood volume and duration. A curve in the bivariate peak-volume space was obtained from all hydrographs that strictly satisfy the threshold condition. Such curve represents a failure threshold, called critical overtopping flood hydrograph (COFH) (Isola et al. 2018).

Moreover, the copula model allows us to estimate the return periods (e.g. Kendall return period), which give the probability of exceedance of a given flood hydrograph in a river without considering the overtopping levee failure. Specifically, the purpose of this methodology is to combine the relationship among the return level of river levee failure and the multivariate return period of the hydrological variables in order to improve the risk estimation for river levee against overtopping. Ombrone Pistoiese River located in Poggio Caiano municipality (Tuscany, Italy).

Results and concluding remarks

The proposed procedure is useful for practitioners to estimate quantiles and select design hydrological events by using a multivariate regional frequency analysis of flood hydrological variables, in order to assess the overtopping risk for a river levee.

Quantile curves can be obtained at an ungauged target site located in a given homogenous region through the discharge and volume data collected at a set of nearby gauged sites, supplying an estimate at a

location where no flood data exist. Furthermore, a large set of synthetic flood hydrographs needed for extending short series of observations can be obtained via the regional approach. It can be useful in performing levee design or hydrological safety analyses based on the routed return period approach. Hence, in this research the multivariate regional approach is used for estimating the confidence interval of the probability of overtopping levee failure.

The proposed approach can be useful in levee design, as it improves estimations provided by the flood event-based return periods, taking into account the levee characteristics that influence on the risk of overtopping. In addition, this study could be replicated in terms of flood damage risks. Therefore, the proposed methodology can procure useful information to estimate the Design Flood Hydrograph.

Acknowledgments: We would like to acknowledge the Hydrological Service of Tuscany Region for providing the data.

References

Damme MV, Ponsioen L, Herrero M, Peeters P (2016) Comparing overflow and wave-overtopping induced breach initiation mechanisms in an embankment breach experiment. FLOODrisk 2016 - 3rd European Conference on Flood Risk Management, Vol. 03004, Lione, 422 1–9

Isola M, Caporali E, Garrote L (2018) Hydrological risk analysis for the characterization of overtopping for a river levee. 5th IAHR EUROPE CONGRESS ''New challenges in hydraulic research and engineering'', June 12-14, 2018, Trento

Requena AI, Chebana F, Mediero L (2016) A complete procedure for multivariate index-flood model application. Journal of Hydrology 535:559–580. doi: 10.1016/j.jhydrol.2016.02.004

Vorogushyn S, Merz B, Lindenschmidt KE, Apel H (2010) A new methodology for 514 flood hazard assessment considering dike breaches. Water Resources Research 46(8):1–17

11th World Congress on Water Resources and Environment (EWRA 2019)
"Managing Water Resources for a Sustainable Future", 25-29 June 2019, Madrid, Spain

Fuzzy Linear Regression for assessment of drought effects on groundwater level in a coastal unconfined aquifer

Ch. Papadopoulos*, M. Spiliotis, I. Gkiougkis, F. Pliakas, B. Papadopoulos
Department of Civil Engineering/School of Engineering, Democritus University of Thrace, Xanthi, Greece;
** e-mail: cpapadp@civil.duth.gr*

Introduction

Drought is a natural phenomenon characterised by a significant decrease of water availability during a significant period of time and over a large area (Nalbantis and Tsakiris 2009). Drought is in fact, a relative, rather than absolute, condition. It occurs either in areas with significant rainfall, or in areas with low rainfall and virtually under all climatic regimes (Spiliotis et al. 2016). Since the evaluation of effects of hydrological drought on aquifer systems is a complicated issue, it is of particular importance to assess the response of groundwater level to precipitation shortages in order to better understanding the phenomenon. This can be carried out using simulation models, however, they are data demanding methods. Investigation of drought impacts on groundwater dynamics can be also approached by statistical manner. Yan et al. (2018) applied a multiple linear regression model for predicting groundwater levels in an unconfined aquifer.

Fuzzy logic is a relatively recent mathematical approach that can incorporate the uncertainty resulting from the modelling of water bodies. In this work, a fuzzy multiple linear regression model (FMLR) is applied in a coastal unconfined aquifer in order to produce a fuzzy relation between the depth of water table (*D*) and precipitation (*P*), potential evapotranspiration (*EP*) and the mean streamflow (*Q*) of Nestos River, North Greece. In order to assess the applicability of the fuzzy model, two measures of suitability are used. Fuzzy linear regression instead of crisp linear regression is preferred for two reasons: first of all, due to the fact that there is not enough data, and secondly due to the complexity of the groundwater processes. In general, the fuzzy regression model produced a fuzzy band which contains all the observed data. In the case of crisp data, the fuzziness arises from the use of the fuzzy coefficients, which are selected to be symmetric triangular fuzzy numbers.

Materials and methods

The Tanaka model (1987) is considered with the use of symmetric triangular fuzzy numbers (Figure 1a) as coefficients*:*

$$\tilde{D}_j = \tilde{A}_0 + \tilde{A}_1 P_j + \tilde{A}_2 EP_j + \tilde{A}_3 Q_j \quad j = 1,2,\ldots,\mathrm{m} \tag{1}$$

According to the Tanaka (1987) method, the total spread of the fuzzy output, *J* is minimized

$$J = \min\left\{ mc_0 + \sum_{j=1}^{m} \left(c_P \left| P_j \right| + c_{Ep} \left| EP_j \right| + c_Q \left| Q_j \right| \right) \right\} \tag{2}$$

under the inclusion constraints, that is, the requirement that all the data must be included within the produced fuzzy band, which is generated from the optimization problem. The decision variables of the equivalent optimization problem are the centres (*r)* and the widths (*c*) of the fuzzy coefficients.

In order to check the applicability of the model the total spread of the fuzzy output, *J* (Papadopoulos and Sirpi 1999) is examined. In addition, the Theil's Inequality Coefficient U with respect to the central values of the fuzzy regression (where $\mu = 1$), is also examined:

$$U = \sqrt{\frac{1}{m}\sum_{j=1}^{m}\left(D_{r,j} - D_j\right)^2} \Bigg/ \left(\sqrt{\frac{1}{m}\sum_{j=1}^{m}\left(D_{r,j}\right)^2} + \sqrt{\frac{1}{m}\sum_{j=1}^{m}\left(D_j\right)^2} \right) \ (\mathrm{j} = 1,2,\ldots,m) \tag{3}$$

where $D_{r,j}$ is the produced central value of the depth of groundwater and D_j is the observed value regarding

the j[th] observation. The closer *U* is to zero, the more predictive the model is (Yorucu 2003).

Results and concluding remarks

The proposed methodology was applied to a coastal unconfined aquifer in the eastern part of the Nestos River Delta, Prefecture of Xanthi, Greece. The depths of water table in four wells were used as dependent variable D_j while measurements were taken every three months during 10/2006 - 09/2008 (Gkiougkis 2018).

The results show that *P* and *Q* affect in a negative way on *D* (Figure 1b and Table 1), while *EP* is positively related to *D*. The uncertainties also are negligible regarding the coefficient of the rainfall influence. It is obvious, that small values of *J* indicate high predictability behaviour for the generated fuzzy band. In contrast, when the total fuzziness is high (the number of data is common for all cases), then the values of the Theil index values increase (as in the case of the first two wells in Table 1).

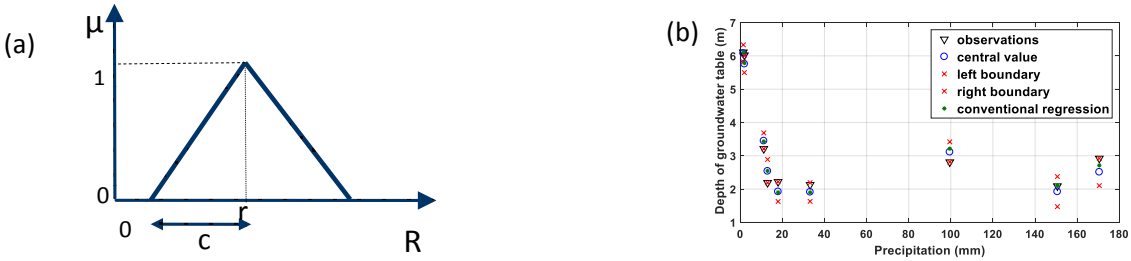

Figure 1. Representation of the fuzzy solution: (a) fuzzy symmetrical triangular number, (b) Projection of the generated fuzzy and conventional multiple regressions in the case of the "194 well".

Table 1. Results of the fuzzy regression regarding the examined wells.

Wells	**Fuzzy coefficients of**								**J**	U
	Constant term		**P**		**EP**		**(mean) Q**			
	r_0 (centre)	c_0 (width)	r_1 (centre)	c_1 (width)	r_2 (centre)	c_2 (width)	r_3 (centre)	c_3 (width)	**Total fuzziness**	Theil's measure
177	0.7371	0.4752	-0.0048	0	0.0456	0.0101	-0.0281	0	10.29	0.12
185	1.0877	0.6665	-0.0019	0	0.0390	0.0091	-0.0481	0	11.38	0.13
190	0.9507	0.5188	-0.0030	0	0.0403	0.0027	-0.0500	0	6.30	0.08
194	2.2853	0.1977	-0.0011	0	0.0260	0	-0.0442	0.0075	2.85	0.04

Acknowledgments: «This research is co-financed by Greece and the European Union (European Social Fund - ESF) through the Operational Programme «Human Resources Development, Education and Lifelong Learning» in the context of the project "Strengthening Human Resources Research Potential via Doctorate Research" (MIS-5000432), implemented by the State Scholarships Foundation (IKY)».

References

Gkiougkis I (2018) Seawater intrusion assessment in coastal aquifers in a deltaic environment: the case of Nestos River Delta. (Doctoral thesis). Department of Civil Engineering, Democritus University of Thrace, Xanthi

Nalbantis I, Tsakiris G (2009) Assessment of Hydrological Drought Revisited. Water Resources Management 23(5):881-897. https://doi.org/10.1007/s11269-008-9305-1

Papadopoulos B, Sirpi M (1999) Similarities in fuzzy regression models. Journal of Optimization Theory and Applications 102(2):373–383. https://doi.org/10.1023/A:1021784524897

Spiliotis M, Mediero L, Garrote L (2016) Optimization of Hedging Rules for Reservoir Operation During Droughts Based on Particle Swarm Optimization. Water Resources Management 30(15):5759-5778. https:/doi.org/10.1007/s11269-016-1285-y

Tanaka H (1987) Fuzzy data analysis by possibilistic linear models. Fuzzy Sets and Systems 24(3):363–375. https://doi.org/10.1016/0165-0114(87)90033-9

Yan S, Yu S, Wu Y, Pan D, Dong J (2018) Understanding groundwater table using a statistical model. Water Science and Engineering 11(1):1-7. https://doi.org/10.1016/i.wse.2018.03.003

Yorucu V (2003) The Analysis of Forecasting Performance by Using Time Series Data for Two Mediterranean Islands. Review of Social, Economic and Business Studies 2:175-196. http://www.researchgate.net/publication/255584205

11th World Congress on Water Resources and Environment (EWRA 2019)
"Managing Water Resources for a Sustainable Future", 25-29 June 2019, Madrid, Spain

Assessment of the realisations of EURO-CORDEX projections in the simulation of rainfall regimes in Spain.

C. Garijo*, L. Mediero
Department of Civil Engineering: Hydraulics, Energy and Environment, ETSI de Caminos, Canales y Puertos, Universidad Politécnica de Madrid, Madrid, Spain.
** e-mail: c.garijo@upm.es*

Introduction

Climate model projections are usually utilised to assess how the climate will change or develop in the future. Climate models are simplified representations of the Earth's climate system, that allow us to know the possible evolution of climate in the future (Garijo and Mediero 2018). Climate models are forced with the expected evolution of a set of variables, such as greenhouse gas emissions, to assess how climate change will affect climatic variables, such as precipitation. Global Climate Models (GCM) usually have a gross spatial resolution. Thus, regionalization methods are used to obtain results at a higher spatial resolution. In Spain, there are two main data sources of climate change projections under the Fifth Assessment Report (AR5) of the IPCC: AEMET ('Agencia Estatal de Meteorología', in Spanish) and CORDEX. AEMET generated climatic projections in a set of existing rain-gauging stations throughout Spain by statistical regionalisation. The CORDEX project offers several realisations of Regional Climate Models (RCM), producing climatic data over a mesh focused on a given area of the planet. For example, EURO-CORDEX focuses on Europe (Jacob et al. 2014).

Despite several studies were carried out in recent years assessing how climate models simulate the current climate (Frei et al. 2003; Jacob et al. 2007; Mascaro et al. 2018), few studies were focused on Spain. A comparison between AEMET projections and observations at rain-gauging stations was conducted by Garijo et al. (2018), finding that such projections characterise better the mean climate behaviour than the extremes. However, no studies examine how EURO-CORDEX model simulations fit observed data over the Iberian Peninsula, and, therefore, how proper simulations of EURO-CORDEX climate models are for consequent studies. In this manuscript, EURO-CORDEX projections are investigated, to assess how precipitation simulated by climate models fit the actual behaviour of observed precipitation time series. Such assessment is based on a set of statistics that represent the spatial and temporal distribution of rainfall.

Materials and methods

The Spanish part of the Iberian Peninsula and the Balearic Islands, in southern Europe, are considered as the area of study. Regarding climate change projections, the data used in the study were supplied by the CORDEX project, specifically by its European domain (EURO-CORDEX). Daily rainfall time series were obtained from one of the data-nodes of the project. EURO-CORDEX supplies outputs of the RCMs by cells with a spatial resolution of 0.11°. A total of 12 models were selected, with a varying control period either 1951-2005 or 1971-2005, depending on the model. In addition, observed data were supplied by AEMET, consisting in daily precipitation time series collected in a network of 1742 rain gauging stations over the study area. The Portuguese part of the Iberian Peninsula was not considered due to the lack of available information.

The first step in a study about climate change, or where climate change data is used, should be to assess how good the data used are. In this study, this step is conducted through the comparison between observed and simulated data, for daily rainfall time series. To compare simulated rainfall series supplied by climate models with observations, a set of statistics are used. Not only average behaviour of rainfall is assessed, but also extreme precipitation, as well as seasonal behaviour are analysed, both for average and maximum precipitation. Finally, additional statistics, such as days without precipitation are also included in

the study. The set of selected statistics were calculated for all the cells for each of the 12 climate models, as well as for the 1742 stations for observed rainfall. As climate models have different control periods, statistics of the observed series were computed twice, according to the period used by the climate model to be compared.

After all statistics were obtained, relative differences or errors were computed, in order to conduct a comparison among different errors. Thus, for each model, the error was estimated comparing the statistic obtained from the observed precipitation time series at a given station with the statistic obtained in the nearest cell in the mesh of EURO-CORDEX. Therefore, for each model, 1742 values are obtained for each statistic. After that, in each gauging site, the average error and the coefficient of variation of all errors (CVe) throughout all climate models were calculated. Not only the general behaviour can be assessed, but also the extent of the errors. For example, if the average error at one station is 0 but the CVe is high, the models do not fit well to that statistic individually, as different errors are compensated each other.

Results and concluding remarks

The comparison between climate model simulations and observations in the control period was conducted in the Spanish Iberian Peninsula and the Balearic Islands, due to the lack of information in the Portuguese Iberian Peninsula. Conclusions that arise from such comparison indicate that climate models of EURO-CORDEX reproduce better the maximum rainfall magnitudes than the average characteristics of rainfall. However, EURO-CORDEX projections worsen their characterization of the most extreme events, as errors in the coefficient of skewness of annual maximum series are higher, indicating a worse characterization of the right tail of the distributions. However, it is important to shed some light on the variability among models, not only on average values among climate models. Though a general pattern can be extracted, the variability is high enough that final conclusions should be given with caution.

Regarding statistics that test rainfall intensity magnitudes, models do not simulate accurately the most intense precipitations. In addition, climate model cannot characterise separate storms bursts due to a common bias called drizzle.

Comparing this study to previous works, such as Garijo et al. (2018) some differing results were found. While regarding maximum rainfalls, EURO-CORDEX climate models show a better behaviour, AEMET regionalizations show a better fit to the observed rainfall series in terms of average rainfall. Thus, depending on the type of study to be carried out in Spain, it would be better to use either one climate projection source or the other. Furthermore, results of this study show that EURO-CORDEX models have some biases that are needed to correct before using them. However, the errors found are not as higher as expected, especially at its spatial resolution. Therefore, EURO-CORDEX models are a suitable tool to assess climate change studies.

Acknowledgments: The authors acknowledge funding from the project CGL2014-52570-R 'Impact of climate change on the bivariate flood frequency curve' of the Spanish Ministry of Economy and Competitiveness. The authors also thank the Spanish Centre of Hydrographic Studies of CEDEX, the Agencia Estatal de Meteorología (AEMET) and last but not least EURO-CORDEX project for providing climate data, respectively, used in this paper.

References

Frei C, Christensen JH, Déqué M et al. (2003) Daily precipitation statistics in regional climate models: Evaluation and intercomparison for the European Alps. J Geophys Res 108:4124. http://doi.org/10.1029/2002JD002287

Garijo C, Mediero L, Garrote L (2018) Usefulness of AEMET generated climate projections for climate change impact studies on floods at national-scale (Spain). Ingeniería del agua 22(3):153-166

Garijo C, Mediero L, (2018) Influence of climate change on flood magnitude and seasonality in the Arga River catchment in Spain. Acta Geophysica 66. http://doi.org/10.1007/s11600-018-0143-0.

Jacob D, Bärring L, Christensen OB et al. (2007) An inter-comparison of regional climate models for Europe: model performance in present-day climate. Clim Change 81:31–52. http://doi.org/10.1007/s10584-006-9213-4

Jacob D, Petersen J, Eggert B et al. (2014) EURO-CORDEX: new high-resolution climate change projections for European impact research. Reg Environ Chang 14:563–578. http://doi.org/10.1007/s10113-013-0499-2

Mascaro G, Viola F, Deidda R (2018) Evaluation of precipitation from EURO-CORDEX regional climate simulations in a small-scale Mediterranean site. J Geophys Res Atmos 123:1604–1625. http://doi.org/10.1002/2017JD02746

11th World Congress on Water Resources and Environment (EWRA 2019)
"Managing Water Resources for a Sustainable Future", 25-29 June 2019, Madrid, Spain

Projecting meteorological drought by SPI in Gediz basin, Turkey, under RCP8.5 scenario

U. Kirdemir[1*], U. Okkan[2]
[1] Civil Engineering Department, Dokuz Eylul University, Izmir, Turkey
[2] Civil Engineering Department, Balikesir University, Balikesir, Turkey
* e-mail: umut.kirdemir@gmail.com

Introduction

In recent years, climate change has become the major reason of many problems such as water scarcity, agricultural infertility, severe flood, drought events and etc. Among these, water scarcity and drought are highly interrelated such that every type of drought occurs by the reason of reduction of water existing in the earth. That is, when the precipitation falls under the normal level, which differs from region to region, then the drought event is experienced at that time. Increasing surface temperature due to climate change caused the surface water to be evaporated more than before and irregular precipitation regimes were experienced as well. It makes possible to experience instant severe droughts and upon considering the detrimental effects of severe droughts, it is important to take measure in order to manage the water resources in any possible drought hazard. In this respect, there are several studies in which estimations are made about the drought occurrence foreseen in the future time period. For instance, Park et al. (2015) carried out a drought projection study using Effective Drought Index in Korea region by the end of the twenty first century under Representative Concentration Pathway 8.5 (RPC8.5) scenario. Li et al. (2008) tried to estimate drought characteristics by the year 2100 over Amazon region by utilizing Standardized Precipitation Index. By the reason that drought characteristics show an unstable pattern all around the world and in Turkey as well, in the study, it was aimed to make climate projections in order to estimate possible future drought events for the period 2015-2050 for a basin of Turkey. The possible effects of climate change was investigated in Gediz Basin which is located in Turkey under RCP8.5 scenario of IPCC. A statistical downscaling strategy was applied in order to project future precipitation between 2015-2050 and frequencies of meteorological drought events were estimated by Standardized Precipitation Index for varying time periods. The details about study region, methodology and results are given in sections given below.

Materials and methods

Gediz Basin is located in Aegean Region of Turkey where typical Mediterranean climate characteristics prevails. The drainage area of the basin is 17125 km^2 and agricultural sector is the major user of the surface water in the basin. The mean annual temperature is 15°C and the total areal precipitation over the basin is in the order of 550 mm. 39 meteorological stations observing precipitation in the basin for the period between 1980-2005 were utilized. ERA-Interim reanalysis dataset for selection of precipitation predictor of the basin and twelve general circulation models (GCMs) for climate projections were used. Twelve atmospheric variables at different atmospheric levels (200 hPa, 500 hPa, 850 hPa) were utilized in both reanalysis dataset and GCMs in order to evaluate the precipitation of the related region. The GCM data capturing the pessimistic representative concentration pathway (RCP) scenario were used for future projections such that the related scenario was referred to as RCP8.5 scenario hereinafter. The detailed information about meteorological stations, ERA-Interim variables and GCMs can be accessed from Okkan and Kirdemir (2018). Statistical downscaling methods were employed in order to downscale the coarse-resolution GCM data into finer scale. Artificial neural networks (ANN) and least square support vector machines (LSSVM) methods were employed such that the selected predictor variable *prate* by all possible regressions method was the input of the related methods. Due to the fact that the GCMs have inherent bias, it was not adequate only to downscale the GCMs. Hence a bias correction procedure namely quantile

mapping method (QM) was employed. Thus, physically and statistically plausible precipitation projections were derived. Moreover, utilization of individual GCMs results in uncertainty in model selection, hence, Bayesian Model Averaging method was implemented in order to obtain combination of twelve GCMs. Probabilistic weights of each GCM were obtained for wet and dry periods, separately.

Standardized Precipitation Index is a drought digitization method taking into account only precipitation data of the related region. The drought indices are calculated by means of the distributional pattern of the observed precipitation (requires at least 20 and 30-year observations) and the standardized z values fitting to standard normal distribution correspond to a drought classification. The drought analysis can be carried out for different time intervals such as 1-month (SPI-1), 3-month (SPI-3), 6-month (SPI-6), 9-month (SPI-9), 12-month (SPI-12) or 24-month (SPI-24) periods. Subsequent to the precipitation projections were derived under RCP8.5 scenario, the above-mentioned Standardized Precipitation Index (SPI) was utilized for 3, 6 and 12-month time intervals so that it was possible to estimate the drought frequency/duration/intensity between 2015-2050 periods by predicted precipitation time series.

Results and concluding remarks

In the study, ANN and LSSVM methods were employed separately and their results were evaluated by means of several statistical performance criteria. According to the results, the models showed adequate performances in simulating precipitation patterns of the each meteorological station. However, the best model results were utilized for each meteorological stations and the bias correction procedure was applied for the related time series. Subsequent to the QM and BMA implementations, the ultimate projections were obtained for the time period 2015-2050. When compared to the historical time period 1980-2005, it was foreseen decrease of 17% in precipitation in the related future time period. Upon evaluating the past precipitation records of Gediz Basin, it was seen that the basin experienced the normal conditions by 34%, 28% and 23% of the historical time period for SPI-3, SPI-6 and SPI-12 respectively. The 50%, 54% and 46% of the time period was experienced in near normal or dry conditions (drought index is lower than 0) and wet conditions occurred in approximately 18%, %17 and 31% of the related time period for SPI-3, SPI-6 and SPI-12 respectively. However, when the projected time series were evaluated under distribution pattern of historical precipitation, it was seen that the frequency of near normal and dry drought events increased for SPI-3, SPI-6 and SPI-12 such that it corresponded to the 65%, 64% and %67 of the future time period under RCP8.5 scenario respectively. The frequency of the normal conditions were foreseen to decrease by half and insignificant part of the future period was foreseen to experience wet conditions with the frequency of about 5% for all time intervals. In addition to SPI analysis, the authors consider for the further researches the use of drought indices such as Reconnaissance Drought Index (Tsakiris and Vangelis 2005) or Standardized Precipitation Evapotranspiration Index (Vicente-Serrano et al. 2010) in order to take into consideration water losses from the earth surface.

Acknowledgments: The research leading to this study is funded by the Scientific and Technological Research Council of Turkey (TUBITAK) under Grant No. 114Y716

References

Li W, Fu R, Juárez RIN, Fernandes K (2008) Observed change of the standardized precipitation index, its potential cause and implications to future climate change in the Amazon region. Philos Trans R Soc B Biol Sci 363:1767–1772

Okkan U, Kirdemir U (2018) Investigation of the Behavior of an Agricultural-Operated Dam Reservoir Under RCP Scenarios of AR5-IPCC. Water Resour Management 32(8):2847–2866. doi: 10.1007/s11269-018-1962-0

Park CK, Byun HR, Deo R, Lee BR (2015) Drought prediction till 2100 under RCP 8.5 climate change scenarios for Korea. J Hydrol 526:221–230. doi: 10.1016/j.jhydrol.2014.10.043

Tsakiris G, Vangelis H (2005) Establishing a drought index incorporating evapotranspiration. Eur Water 9/10:3–11

Vicente-Serrano SM, Beguería S, López-Moreno JI (2010) A multiscalar drought index sensitive to global warming: The standardized precipitation evapotranspiration index. J Clim 23:1696–1718

11th World Congress on Water Resources and Environment (EWRA 2019)
"Managing Water Resources for a Sustainable Future", 25-29 June 2019, Madrid, Spain

Climatic and anthropogenic factors affecting river discharge in Piranhas-Açu basin in Brazilian Semiarid: Trend test and change-point analysis

L. Falcao[1*], T. M.C. Studart[1,2], M.M. Portela[2]
[1] Hydraulic and Environmental Engineering Department (DEHA), Federal University of Ceará, Fortaleza, Brazil
[2] Civil Engineering Research and Innovation for Sustainability (CERIS), Instituto Superior Tecnico (IST), University of Lisbon (UL), Portugal
* e-mail: lucasfalcaomuniz@gmail.com

Introduction

The Piranhas-Açu River Basin is located in the Brazilian semiarid and has an area of 43,681.50 km^2, partially inserted in the states of Paraíba (60%) and Rio Grande do Norte (40%). It presents low rainfall (below 900 mm), with high temporal variability (with recurrent and sometimes multiannual droughts), high evaporation (above 2,000 mm), an unfavorable hydrogeological context, and intermittent rivers. The water security for the basin's population (around 1.4 million inhabitants) and the economic activities during periods of water scarcity are heavily dependent on the existent infrastructures.

In water resources planning studies, the primary step is to assess the water availability, based on the existent hydrological time series. In Piranhas-Açu Basin these studies always used the data from two river gauges stations - São Fernando (code 37570000) and Jardim de Piranhas (code 37470000) - which together control an area of 31,310 km² (about 70% of the area of the Piranhas-Açu Basin).

The hydrological time series at those stations are supposed to meet a set of ideal conditions, such as being consistent and trend-free (Adeloye and Montaseri 2002). Consistency implies that all the collected data belong to the same statistical population; trend-free means that there is no significant correlation between the observations and time. However, even a mere visual analysis of the annual discharge series at these two river gauges stations shows a similar anomalous behavior in the early 1980s, with notorious decrease of the river discharges after that period. Given the importance of the discharge series when addressing the present and the future water availability in the basin, this study intends to investigate the causes of such decrease – if natural, anthropogenic or both. For this purpose, trend analysis and change point detection were applied to some of the hydrometeorological series in São Fernando Basin.

Materials and methods

São Fernando gauge station is located in Seridó River and has a drainage area of 9,700 km² (98.9% of Seridó River basin area) (Figure 1). The station has daily discharges records from Jan/1963 to Dec/2014.

To analyze the rainfall regime, 77 rain gauges were considered. The data was provided by the Brazilian meteorological entities. The Thiessen Polygon method was used to calculate the weighted rainfall.

The Hargreaves Method was applied to compute the monthly evapotranspiration. The records of humidity and temperature were obtained from the historical daily database for Cruzeta Climatological Station from the National Institute of Meteorology – INMET (Figure 1). Silveira et al. (2011) showed that Hargreaves and Penman-Monteith methods present similar results for the Brazilian semiarid.

For filling the missing values of the rainfall series, the method based in linear correlation, was applied. For each monthly gap in a given rain gauge, the method identifies the candidate rain gauges that can be used for filling it. These gauges are next ranked according to the correlation coefficient between paired series for that particular month at the rain gauge with the gap and at the candidate rain gauges. The one with higher correlation coefficient is used to fill the gap based on a linear regression model. After filling the missing values, the 40 rain gauges schematically located in Figure 1, with complete series from 1963 to 2014 (52 years) were used in the rainfall analysis. The few temperature and humidity gaps at Cruzeta Climatological Station were filled with the respective monthly means.

To characterize the trends, two statistical tests were applied to the weighted monthly rainfall in São Fernando Basin: The Mann-Kendall and Sen' Slope tests. Mann-Kendall is a nonparametric test, highly

recommended for the analysis of hydro-meteorological time series (Wang 2011). The significance level adopted was of 5%. The Sen Slope is a classical statistical test that provides estimates of the trends.

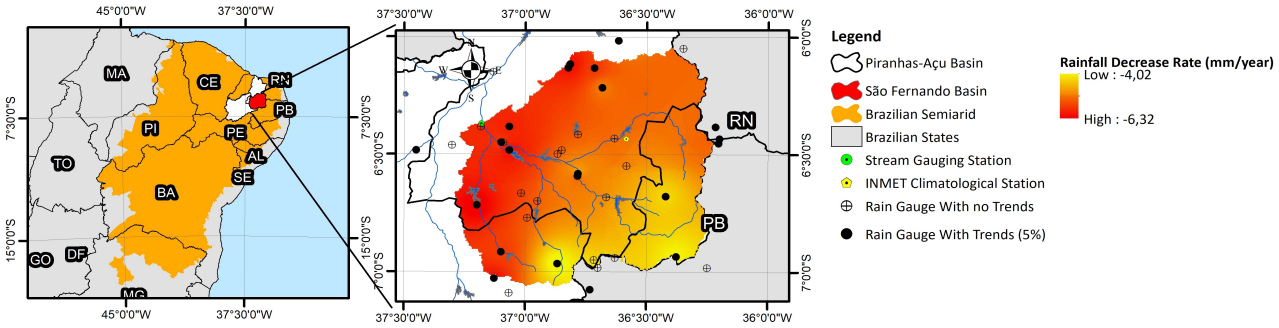

Figure 1. São Fernando Basin in Piranhas-Açu Basin. Location of the stations studied and map of the rainfall trends.

The change point methodology used derives the asymptotic distribution of the likelihood ratio test statistic for the most significant change in the mean (Villarini et al. 2009).

Results and concluding remarks

Figure 2 presents the annual time series of discharge and weighted rainfall in São Fernando Basin from Jan/1963 to Dec/2014. It shows that both time series have a similar pattern until early 1980. After this period, the river discharges exhibit a pronounced decrease, which is not perceived in rainfall.

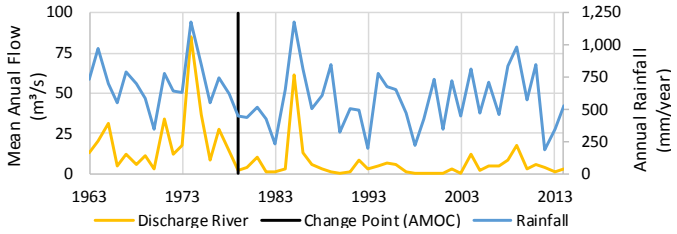

Figure 2. Annual series in São Fernando Basin from January 1963 to December 2014.

The rainfall demonstrates a significant decrease in most rain gauges (21 gauges). The rate of decrease of the annual rainfall varies from 4.0 to 6.3 mm/year, in the rain gauges, and is of about 3.98 mm/year, in terms of weighted value. The spatial variation of the rainfall trends are shown in Figure 1.

The temperature rise in some periods of the year, with an increase in its annual value of 0.019 °C/year. Except for January and February, the humidity exhibits a downward trend with a rate of 0.124%/year, and the potential evapotranspiration an increase of 4.27 mm/year.

As a result of change point analysis applied to the river discharges, the year of 1979 was highlighted (see Figure 2). After that year, the mean annual discharge was only 5.81 m³/s, i.e., 70% of the average in the initial period. The mean annual values of the different hydrological variables before and after that year were also compared. The decrease rate in rainfall and humidity, combined with the increase rate in potential evapotranspiration and temperature appear not be enough to explain the decrease of 70% in the mean annual discharge after 1979, clearly indicating that the abrupt decrease in discharges are not only due to natural conditions, but also, and even mainly, to anthropic actions. Accordingly, the complete series at São Fernando station should not be used in future studies about water resources, as it was always done.

References

Adeloye AJ, Montaseri M (2002) Preliminary streamflow data analyses prior to water resources planning study. Hydrologic Science. Journal 47(5):679–691

Silveira CS, Souza JL, Farias JV, Araújo BAM, Studart TMC (2011) Análise espacial da evapotranspiração no estado do Ceará: análise comparativa entre métodos. XIX Simpósio Brasileiro de Recursos Hídricos. Associação Brasileira dos Recursos Hídricos, ABRH, Maceió, AL, Brasil.

Wang W, Peng S, Yang T, Shao Q, Xu J, Xing W (2011) Spatial and Temporal Characteristics of Reference Evapotranspiration Trends in the Haihe River Basin, China. Journal of Hydrological Engineering 10:239-252

Villarini G, Serinaldi F, Smith JA, Krajewski WF (2009) On the stationarity of annual flood peaks in the continental United States during the 20th century. Water Resources Research 45:W08417

11th World Congress on Water Resources and Environment (EWRA 2019)
"Managing Water Resources for a Sustainable Future", 25-29 June 2019, Madrid, Spain

Comparative study on the estimation of flood peaks based on the peaks-over-threshold method and annual maximum method

G. Onuşluel Gül, A. Gül*
Department of Civil Engineering, Dokuz Eylül University, İzmir, Turkey
** e-mail: ali.gul@deu.edu.tr*

Introduction

Flood frequency estimates are needed in design of hydraulic structures and other engineering solutions such as flood protection systems, culverts and bridges. Annual Maximum (AM) series, which are the maximum rates of flood flow observed within a year period, are greatly considered in estimating flood quantities. Another arrangement of data used for similar purposes is the peaks-over-threshold (POT) series, also referred to as partial duration series by some researchers.

The study by Langbein (1949), which can be considered as the leading research on the subject, presented results of flood recurrence intervals computed through both annual maxima and partial duration series. Davison and Smith (1990) stated that this approach has many advantages when POT flood data is basically used. The Flood Estimation Handbook (Robson and Reed 1999) states that the main advantage of the POT use over the AM series associates with the case of relatively short data series. Bezak et al. (2014) compared POT and AM series in Slovenia and they concluded that the POT method gave better results than AM although POT approach was little more complex.

In this study, flood frequency analysis was performed by using peak values above the threshold for a streamflow station identified in the Seyhan Basin, where the incidence of floods and the risk of flooding are both found to be remarkably high. The threshold value was determined by employing four different approaches. Generalized Pareto (GP) distribution as the frequently used model in partial continuity series has been tested for compliance with the observed values in the analysis time span. After checking the suitability of the model, the confidence intervals of the parameters were established and 2, 5, 10, 25, 50 and 100-year flood peaks and corresponding confidence intervals were determined. In the last step, confidence intervals of parameters and quantiles were additionally computed to allow comparative assessments between the POT and AM uses through the estimated flood peaks.

Materials and methods

The station 1801-Göksu Himmetli selected for the study on the Seyhan River is one of the oldest stations in the basin with solid historical data availability. The data-available period of 1935-2004 was entirely used in the study. While the drainage area of the basin is 20731 km², the station located at 665m elevation a.s.l. has a drainage area of 2596.8 km^2.

Ribatet (2006) has developed a program that runs in statistical calculation environment (R) in order to carry out statistical analysis of POT series. The POT package here includes the determination of threshold value, calculation of distribution parameters, testing of model fit and determination of confidence intervals of parameters and quantile estimations. The step of determining the threshold value is critical to the results of the analysis. Choosing a very high threshold value causes an increase in variance due to a decrease in bias but a small number of values above the threshold value, while selecting a very low threshold value causes the number of observed floods to increase in numbers and decreases the variance as increasing the bias included. The optimum value of the threshold is determined by four different methods: threshold choice plot, mean residual life plot, L-moments plot and dispersion index graph. In the study, the parameters of GP distribution were calculated in three different ways, namely the Maximum Likelihood Estimation (MLE), Probability Weighted Moments (PWM) and Moments (MOM) methods from nine different methods in POT package. In order to check the fitted model, probability/probability plot, quantile/quantile plot, density plot and return level plot are used in the package.

Results and concluding remarks

In hydrologic assessments, the use of AM series may lead to some loss of information due to taking count of the largest considered maximum in a year when disregarding the second or third maxima. While POT use may help overcome this problem, problem solving task becomes more complicated, requiring prior attention on the analyses to be conducted, when the POT series are employed in hydrologic studies instead of the AM data. On the other hand, the stochastic dependence within the POT data would be considerable, for example, especially based on the fact that the original time series can be autocorrelated themselves.

Based on the comparative use of flood data in both format, arranged as peak discharges over an analyzed threshold which were isolated from daily series against the annual maximum discharges corresponding to each individual year, it was determined in the presented study that the threshold value for POT could be taken as 76 m^3/s by trying different values through the four methods for assigning the threshold. According to the MLE method, the scale and shape parameters were determined as 51.07 and 0.102, respectively. In the next step, the fitted model was checked (Figure 1) and the associated confidence limits of parameters and quantiles were computed. As a result of the flood frequency analysis using the AM values, Gumbel distribution was determined as the most suitable distribution. The results of the flood frequency analysis performed separately by using the AM values and POT were compared and it was found that the flood peaks computed by the POT method corresponding to the different recurrence intervals were 20% less in average than the values computed by using AM series.

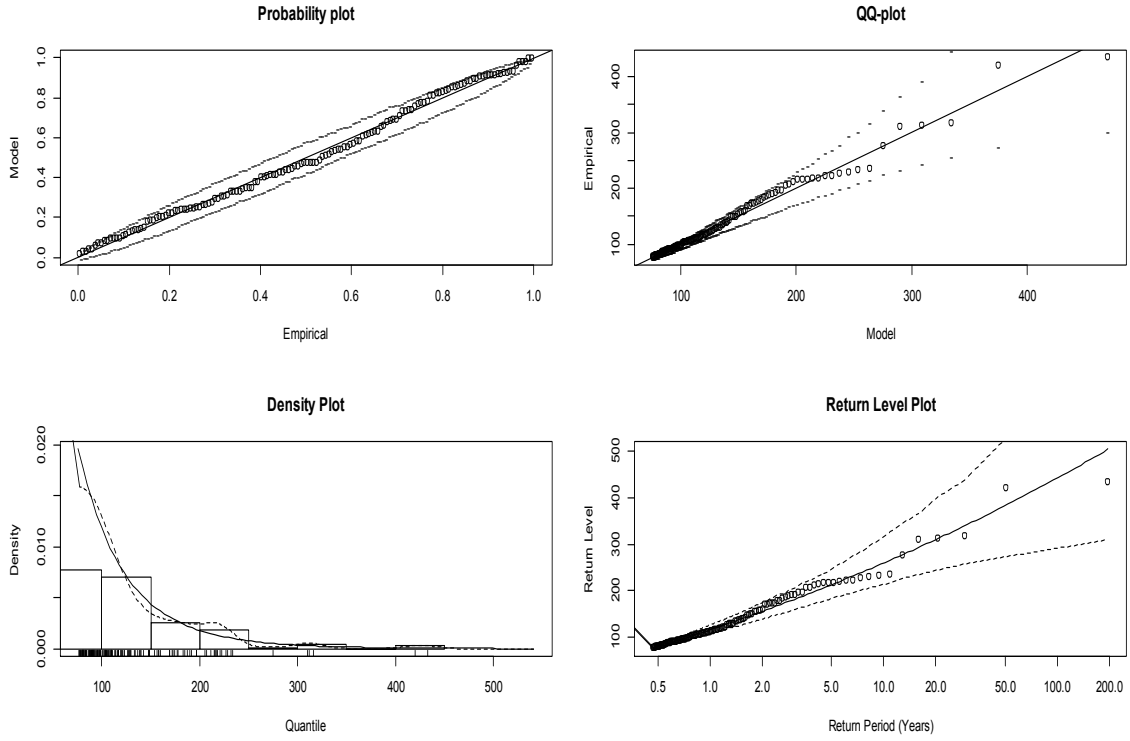

Figure 1. Testing of goodness of the model.

References

Bezak N, Brilly M, Šraj M (2014) Comparison between the peaks-over-threshold method and the annual maximum method for flood frequency analysis. Hydrological Sciences Journal 59(5):959-977

Davison AC, Smith RL (1990) Models for exceedances over high threshold s. J.Royal Statist. Soc. B. 52(3):393-442

Langbein, WB (1949) Annual floods and the partial-duration flood series. Transactions, American Geophysical Union 30(6):879–881

Ribatet M (2011) A User's Guide to the POT Package (Version 1.4)

Robson AJ, Reed DW (1999) Statistical procedures for flood frequency estimation. Volume 3 of the Flood Estimation Handbook. Wallingford: Centre for Ecology & Hydrology

Tavares LV, Da Silva JE (1983) Partial duration series method revisited. Journal of Hydrology 64 (1–4):1–14

11th World Congress on Water Resources and Environment (EWRA 2019)
"Managing Water Resources for a Sustainable Future", 25-29 June 2019, Madrid, Spain

Regional frequency analysis of droughts in Küçük Menderes Basin

G. Onuşluel Gül*, A. Kuzucu, A. Gül
Department of Civil Engineering, Dokuz Eylul University, İzmir, Turkey
** e-mail: gulay.onusluel@deu.edu.tr*

Introduction

Drought is a natural disaster that is defined as the period of time that falls below the average precipitation. Food and Agriculture Organization (FAO) (2017) indicated that agriculture in Turkey is the most vulnerable sector to drought and Aegean is one of the regions that are predicted to suffer most from more frequent and intense droughts in the future. In efforts for obtaining the frequencies of drought events, it can be more accurate to analyze all data samples collectively rather than using a single sample. The relationship between physical and statistical assessments of the regions and their estimated frequency distributions are expressed through regional frequency analysis. Vicente-Serrano et. al. (2004) investigated droughts temporally and spatially and used regional frequency distributions based on L-moments using the Standardized Precipitation Index (SPI). Santos et al. (2011) used annual maximum and partial duration series and calculated the return periods of droughts. Nunez et al. (2011) created maps of spatial distribution using L-coefficient of variation (L-CV) and L-skewness.

In the presented study, the regional frequency analysis of droughts based on L-moments for the period of 1972-2016 in Küçük Menderes Basin was implemented based on annual drought severities obtained from the 6 month-SPI values. None of the 11 meteorological stations in the basin was discordant and the region was determined as homogeneous. The goodness-of-fit tests resulted that the Generalized Pareto (GP) distribution was the best fit distribution. Finally, the quantile estimates and growth curve were obtained by using the GP distribution.

Materials and methods

Küçük Menderes Basin with a drainage area of about 3225 km² is located in the Aegean Region located in the West of Turkey. In the river basin, the climate is dominated by the Mediterranean climate that associates with hot and dry summers and mild winters with substantial precipitation. The basin has great significance in terms of agriculture and 42% of the basin is cultivated (Onuşluel Gül et al. 2017).

In the presented study, annual drought severities were determined for 11 meteorological stations using 6 month-SPI values for the period of 1972-2016 in Küçük Menderes Basin, considering the threshold value for SPI as "0" (considering SPI<0). The regional frequency analysis based on L-moments was applied in four steps proposed by Hosking and Wallis (1997): (1) screening of the data, (2) identification of homogeneous regions, (3) choice of a frequency distribution and (4) estimation of the frequency distribution. The discordancy measure (D_i) which provides an initial screening of the data considers three L-moment ratios (L-CV, L-skewness and L-kurtosis). Acceptance of a homogenous region is tested by using the heterogeneity measure which compares the between-site variations in sample L-moments for the group of sites with what would be expected for a homogeneous region. Hosking and Wallis (1997) recommended that the region is accepted as homogeneous in case of $H_1 < 2$, possibly heterogeneous in case of $2 < H1 < 3$ and as heterogeneous in case of $H_1 > 3$. The goodness-of-fit statistic (Z^{DIST}), which indicates how well the theoretical L-kurtosis of the fitted distribution matches the regional average L-kurtosis of the observed data (Santos et al. 2011), is computed for the homogeneous region for the distributions, separately, Generalized Logistic, Generalized Extreme-Value (GEV), Lognormal, Pearson Type III, and Generalized Pareto. If $|Z^{DIST}|$ is less than 1.64, the distribution is acceptable. The quantiles of the regional frequency distribution are calculated using the regional L-moment algorithm. Error bounds for the estimated regional growth curves are obtained by simulation.

Results and concluding remarks

A drought risk assessment for Küçük Menderes basin was performed based on the regional frequency analysis of the annual severity series obtained by using the 6-month SPI series. L-moment ratios were calculated using annual drought severities for each site and given by Table 1. Considering 11 sites as a single region, the discordancy statistics (D_i) were calculated and compared with the critical value of D_i for each site, and none of the sites was accepted as discordant. Since the value of H_1 (computed as -1.36) is less than 2, the region was accepted as homogeneous.

Table 1. L-moment ratios and D_i values

Site Name	N (year)	Mean	L-CV	L-skewness	L-kurtosis	t_5	D_i
Manisa	42	4.675	0.488	0.345	0.221	0.063	0.840
İzmir	43	4.420	0.530	0.363	0.170	0.102	0.320
Çeşme	44	4.383	0.568	0.413	0.229	0.151	2.610
Kuşadası	43	4.555	0.478	0.267	0.149	0.119	1.050
Aydın	41	4.651	0.492	0.319	0.148	0.090	0.080
Salihli	44	4.658	0.519	0.305	0.048	-0.033	1.950
Seferihisar	44	4.108	0.510	0.388	0.160	0.017	1.740
Ödemiş	42	4.464	0.517	0.333	0.123	0.045	0.260
Sultanhisar	44	4.262	0.479	0.267	0.126	0.104	0.780
Selçuk	44	4.264	0.464	0.298	0.190	0.146	0.950
Nazilli	44	4.365	0.497	0.344	0.151	0.088	0.400

Both Generalized Pareto and Pearson Type III distributions were found to be acceptable for the regional frequency distribution, since the absolute values of Z^{DIST} (0.33 and 0.37, respectively) were less than 1.64. In the study, Generalized Pareto was selected as the regional frequency distribution. The quantiles and growth curve were obtained based on this distribution. The study allowed determining the frequency of the most significant droughts in the basin.

References

Food and Agriculture Organization of the United Nations (FAO) (2017) Drought characteristics and management in Central Asia and Turkey. Water for Food Daugherty Global Institute University of Nebraska.

Hosking JRM, Wallis JR (1997) Regional Frequency Analysis. Cambridge University Press, New York

Núñez JH, Verbist K, Wallis JR, Schaefer MG, Morales L and Cornelis WM (2011) Regional frequency analysis for mapping drought events in north-central Chile. Journal of Hydrology 405:352-366

Santos JF, Portela MM and Pulido-Calvo I (2011) Regional Frequency Analysis of Droughts in Portugal. Water Resources Management 25:3537–3558

Onuşluel Gül G, Gül A, Kuzucu A (2017) Analysis of Drought in Küçük Menderes River Basin Using SPI and SPEI Drought Indices. STAHY Workshop

Vicente-Serrano SM, González-Hidalgo JC, Luis M, Raventós J (2004) Drought patterns in the Mediterranean area: the Valencia region (eastern Spain). Climate Research 26:5–15

11th World Congress on Water Resources and Environment (EWRA 2019)
"Managing Water Resources for a Sustainable Future", 25-29 June 2019, Madrid, Spain

Estimation of local drought frequency in a small dam using the daily evapotranspiration rate and precipitation

M. Mathlouthi[1*], F. Lebdi[2]
[1] Research Laboratory in Sciences and Technology of Water in National Agronomic Institute of Tunisia, 43 Avenue Charles Nicolle, 1082 Tunis, Tunisia
[2] National Agronomic Institute of Tunisia (INAT), 43 avenue Charles Nicolle, 1082 Tunis, University of Carthage, Tunisia
* e-mail: Majid_Mathlouthi@yahoo.fr

Introduction

Dry spell can be defined as a sequence of dry days including days with less than a rainfall threshold value. A practical procedure to analyze rainfall event time series under semi-arid climatic conditions is the event-based concept. This design of analysis is favoured over continuous type data generation method. It is to simulate wet and dry spells separately by fitting their durations to an appropriate probability distribution such as the negative binominal or geometric distribution (Semenov et al. 1998; Mathlouthi and Lebdi 2008), or empirical distribution (Rajagopalan and Lall 1999). The characteristics of multi-day wet and dry spells is often important for investigating likely scenarios for agricultural water requirements, reservoir operation, for analyses of antecedent moisture conditions (Mathlouthi and Lebdi 2008), and a watershed runoff generation. In virtue, this paper is focused on the modelling of rainfall occurrences under climate Mediterranean by wet-dry spell approach for operation dam with basis different from that of observations carried out with regular time's intervals. The event-based concept allow the synthetic rainfall data generation. This used, for example, for reservoir simulation studies, the estimation of irrigation water demand and the study of the effects of a climatologically change. This paper concentrates solely on the characterization of the events of the dry spell in a Dam North of Tunisia.

Materials and methods

The data used in this analysis are the daily precipitation records at Ghezala dam located in Northern Tunisia. The rainy season starting at September and lasting until the beginning of May. The mean of annual rainfall is 680 mm. Except in occasional wet years; most precipitation is confined to the winter months in this basin. The dry season lasts from May to August. Daily values of precipitation are quite variable.

A rainfall *event* is an uninterrupted sequence of wets periods. The definition of event is associated with a rainfall threshold value which defines *wet*. As this limit 3.6 mm d^{-1} has been selected. This amount of water corresponds to the expected daily evapotranspiration rate, marking the lowest physical limit for considering rainfall that may produce utilizable surface water resources. In this approach, the process of rainfall occurrences is specified by the probability laws of the length of the wet periods (storm duration), and the length of the dry periods (time between storms or inter-event time). The rainfall event *m* in a given rainy season *n* will be characterized by its duration $D_{n,m}$, the temporal position within the rainy season, the dry event or inter-event time $Z_{n,m}$ and by the cumulative rainfall amounts of $H_{n,m}$ of $D_{n,m}$, rainy days in mm:

$$H_{n,m} = \sum_{i=1}^{Dn,m} h_i \quad (1)$$

where h_i is positive and represent the daily precipitation totals in mm. Note that for at least one h_i >3.6 mm.

Results and concluding remarks

Approximately 33% of the events last at most one day. The persistence of uninterrupted sequences of rainy days sometimes lasting nearly two weeks (the maximum observed duration is 13 days). However, the

frequency of such long-duration events decreases rapidly with increasing duration. An arithmetic mean of 2.79 days and a standard deviation of 1.87 were obtained. The geometric pdf appears most adequate for the fitting.

The regression analysis display that the dry event can be assumed to be independent from the rainfall event and the rainfall depth per event. Thus the distribution of the dry event (interevent time), which can only assume integer values, follows an unconditional probability distribution function. The negative binomial pdf has been found as best fitted to describe the distribution of the dry event. Tithe shortest interruption (one day) is the most frequent one. Almost a fifth of the observed dry events are only one day long. Dry periods up to 30 or even more days may be recorded (a 56 days maximum is recorded). The arithmetic mean and the standard deviation for the dry event are respectively 7.3 days and 7.9; for the longest dry event there are 30.2 days and 3.6.

The time series of the beginning of the first rainfall event in the year was analysed. The best fitting of this random variable is a law of the leaks (Fig. 1). It was concluded that on average the first rainfall event occurs in the mid-September whereas the probability of surpassing this value is 0.52 for a biennial return period. In the extreme case, the hydrological year starts about the first decade of October.

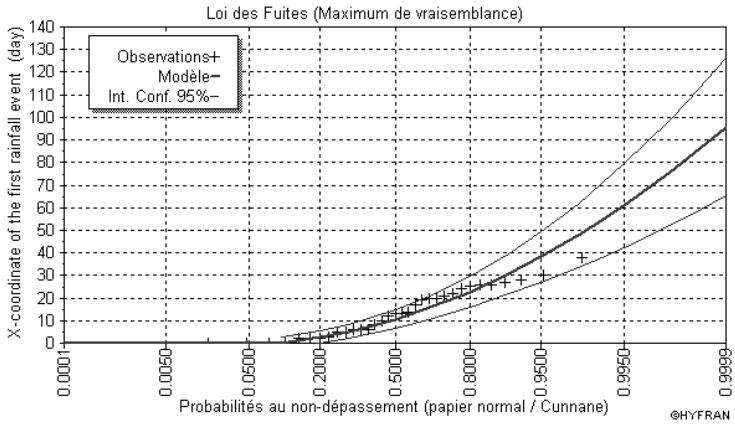

Figure 1. Fitting leaks law for the chronological position of the first rainfall event in rainy season

The case study confirms the concept of the independence of rainfall and dry event duration. The dry spell phenomenon in this region seems to be particularly well described by fitting a pdf to the length of the interevent time. The negative binomial pdf provides an excellent fit for the prolonged dry periods between subsequent rainfall events. Conceptually, in a true Poisson process, the time “without event” should follow the exponential pdf or, in a discrete case, the geometric pdf (Fogel and Duckstein 1982). It is relevant to note that this “flaw” could be eliminated by defining the interevent time as the dry event. Consequently, the present role of the interevent time would be taken over by the rainfall events duration. The theoretical requirements of the fitted geometric pdf are satisfied.

Event-based analysis has been used to generate synthetic rainfall event time series. By coupling this with a rainfall-runoff model, one obtains synthetic streamflow series to be used for reservoir simulation studies and design flood estimations. As another application, the study of the effects of a climatologically change.

References

Fogel MM, Duckstein L (1982) Stochastic precipitation modelling for evaluating non-point source pollution in statistical analysis of rainfall and runoff. In: Proceedings of the International Symposium on Rainfall-Runoff Modelling, 1981, Statistical Analysis of rainfall and runoff, Water Resources Publications. Littleton, Colo., USA, pp 119-136

Mathlouthi M, Lebdi F (2008) Event in the case of a single reservoir: the Ghèzala dam in Northern Tunisia. Stochastic Environ. Res. and Risk Assessment 22:513–528

Rajagopalan B, Lall U (1999) A k-nearest-neighbor simulator for daily precipitation and other weather variables. Water Resour. Res. 35:3089-3101

Semenov MA, Brooks RJ, Barrow EM, Richardson CW (1998) Comparison of WGEN and LARS-WG stochastic weather generators for diverse climates. Clim. Res. 10:95-107

11th World Congress on Water Resources and Environment (EWRA 2019)
"Managing Water Resources for a Sustainable Future", 25-29 June 2019, Madrid, Spain

Considering the use of crop evapotranspiration (ET_c) in Reconnaissance Drought Index (RDI)

D. Tigkas*, H. Vangelis, G. Tsakiris
Centre for the Assessment of Natural Hazards and Proactive Planning & Laboratory of Reclamation Works and Water Resources Management, School of Rural and Surveying Engineering, National Technical University of Athens, Greece
** e-mail: ditigas@mail.ntua.gr*

Introduction

Agricultural or vegetation-agricultural drought is a term used for describing the effects of drought on agriculture and plant development. Various drought indices have been developed over the years for assessing drought characteristics, while many of them are suitable for agricultural drought characterisation (Sivakumar et al. 2011). A key parameter used in agricultural drought indices is soil moisture, however many indices based on meteorological data have been also proved efficient for identifying agricultural drought conditions. The Reconnaissance Drought Index (RDI; Tsakiris et al. 2007) is one of the widely used meteorological drought indices, employed satisfactorily in agricultural drought studies, while a modified version of the index (Effective RDI - eRDI) has recently been developed (Tigkas et al. 2017). The structure of RDI is similar to the well-known Standardised Precipitation Index (SPI); however, RDI takes also into account the evapotranspiration, apart from precipitation, forming a more robust conceptual base in representing the water balance of the system under study.

The formulation of RDI, as a meteorological drought index, is originally based on the concept of reference evapotranspiration, which provides a general measure of the evaporative atmospheric demand, based on the climatic conditions. However, in agricultural drought studies focusing on specific crops, it would be more accurate to employ crop evapotranspiration instead, which takes into account crop characteristics. In this paper, the use of crop evapotranspiration in RDI calculation in such cases is discussed, while the significance of this amendment is assessed.

Material and methods

RDI has three forms, providing different information and insights regarding drought and climatic conditions of the region under study. The initial form (α_k) is expressed as the ratio of precipitation to reference evapotranspiration, accumulated for a period of k months. Based on the timeseries (N years) of α_k, a normalised series (RDI_n) may be derived (second form), expressed as the ratio of the α_k to the arithmetic mean ($\overline{\alpha_k}$) for N years, minus 1. The third form of the index (standardised RDI; RDI_{st}) is calculated through a standardisation procedure of α_k values, producing a normally distributed timeseries with a mean of zero and standard deviation of unity.

Allen et al. (1998) addressed several shortcomings of previous evapotranspiration definitions and approaches, defining precisely the properties of the reference surface and the conditions for calculating reference evapotranspiration (or reference crop evapotranspiration), using the revised FAO Penman-Monteith (FAO P-M) method. According to Vangelis et al. (2013), FAO P-M can be ideally employed for RDI calculation; however, temperature based methods, such as Hargreaves or FAO P-M using only temperature data, can be also applied, without significant effects on RDI_{st} results.

The FAO P-M method, apart from calculating evapotranspiration from the reference surface, can be used for the direct calculation of any crop evapotranspiration (ET_c), as the surface and aerodynamic resistances (included in FAO P-M equation) are crop specific. The evapotranspiration rates of the various crops are related to the evapotranspiration rate from the reference surface using crop coefficients (K_c). ET_c is calculated by multiplying ET_o by the K_c of the crop under study.

The use of evapotranspiration in RDI intends to represent the potential (maximum) evaporative demand, therefore ET_c should be considered under standard conditions, i.e. without limitations on crop

development under the given climatic conditions, related to water availability, crop density, soil conditions and plant pressures by diseases, weeds or insects. In addition, considering ET_c under standard conditions has the advantage of allowing the transferability of K_c values derived by previous studies to different locations (Pereira et al. 2015).

Results and concluding remarks

There are two main approaches for calculating ET_c, either by using single or double crop coefficient. Here, the single K_c approach is employed, combining in one coefficient the difference in evapotranspiration between the cropped and reference surface, since it is sufficient for the purpose of the study without introducing further computational complexity. The values of K_c can be represented by curves, which are typically divided in four segments corresponding to the initial ($K_{c\text{-}ini}$), development ($K_{c\text{-}dev}$), mid-season ($K_{c\text{-}mid}$) and late-season ($K_{c\text{-}end}$) crop growing stages.

The RDI was calculated using ET_o and ET_c for four indicative crops (winter wheat, tomato, olive and cotton) under Mediterranean conditions, in three regions of Greece (Crete, Thessaly and Thrace), using meteorological data for a timeseries of 45 years. The average annual precipitation for each region is 484, 418 and 542 mm, while the average annual reference evapotranspiration is 1024, 1263 and 1083 mm, respectively. The reference periods for RDI calculation correspond to the typical growing season of each crop, while the respective crop coefficients are based on the values presented by Allen et al. (1998). The calculation of RDI performed using Drought Indices Calculator (DrinC) software (Tigkas et al. 2015).

As expected, the RDI series based on ET_o and ET_c, respectively, have very high correlation ($r > 0.99$) for each crop and region. However, their variation level between specific values is different, depending on the form of RDI, as well as the region and crop under study. More specifically, the Root Mean Square Error (RMSE) for tomato (growing season Apr. – Aug.) and cotton (growing season May – Oct.) is relatively low, up to 0.007 and 0.015, respectively, for all regions and RDI forms. Though, for olives (growing season during the entire year) RMSE reaches 0.315 (Thessaly) to 0.470 (Thrace) for α_k form, while for RDI_n and RDI_{st} remains low (up to 0.013). For winter wheat (growing season Nov. – Jun.), RMSE values for α_k is between 0.201 (Thessaly) and 0.336 (Thrace), while for RDI_n is between 0.011 to 0.015 and for RDI_{st} is higher, from 0.039 to 0.047.

Based on the results, it is deduced that the use of either ET_o or ET_c in RDI calculation may not have significant effect on its outcomes for specific crops, a fact that is related to their growing season, as well as the climatic conditions of the study area. However, the differences in calculation outcomes may be significant in other cases, with greater variations expected for α_k form of RDI, while RDI_n and RDI_{st} may present lower, though not always insignificant variations. Further research considering other crops and regions with different climatic conditions may provide further insights on the matter.

References

Allen RG, Pereira LS, Raes D, Smith M (1998) Crop evapotranspiration - Guidelines for computing crop water requirements. FAO Irrigation and Drainage paper 56. FAO, Rome

Pereira LS, Allen RG, Smith M, Raes D (2015) Crop evapotranspiration estimation with FAO56: Past and future. Agricultural Water Management 147: 4-20. http://doi.org/10.1016/j.agwat.2014.07.031

Sivakumar M, Stone R, Sentelhas PC, Svoboda M, Omondi P, Sarkar J, Wardlow B (2011) Agricultural Drought Indices: Summary and Recommendations. In: Sivakumar et al. (eds) Agricultural Drought indices proceedings of an expert meeting. 2 - 4 June 2010, Murcia, Spain. World Meteorological Organization, Geneva, Switzerland, pp 172-197

Tigkas D, Vangelis H, Tsakiris G (2015) DrinC: a software for drought analysis based on drought indices. Earth Science Informatics 8(3): 697-709. http://doi.org/10.1007/s12145-014-0178-y

Tigkas D, Vangelis H, Tsakiris G (2017) An Enhanced Effective Reconnaissance Drought Index for the Characterisation of Agricultural Drought. Environmental Processes 4(suppl 1): 137-148. http://doi.org/10.1007/s40710-017-0219-x

Tsakiris G, Pangalou D, Vangelis H (2007) Regional drought assessment based on the Reconnaissance Drought Index (RDI). Water Resources Management 21(5): 821-833. http://doi.org/10.1007/s11269-006-9105-4

Vangelis H, Tigkas D, Tsakiris G (2013) The effect of PET method on Reconnaissance Drought Index (RDI) calculation. Journal of Arid Environments 88: 130-140. http://doi.org/10.1016/j.jaridenv.2012.07.020

11th World Congress on Water Resources and Environment (EWRA 2019)
"Managing Water Resources for a Sustainable Future", 25-29 June 2019, Madrid, Spain

Drought occurrence probabilities based on copulas

J. Pontes Filho[1*], T.M.C. Studart[1,2], M.M. Portela[2], F.A. Souza Filho[1]
[1] Hydraulic and Environmental Engineering Department (DEHA), Federal University of Ceará, Fortaleza, Brazil
[2] Civil Engineering Research and Innovation for Sustainability (CERIS), Instituto Superior Tecnico (IST), University of Lisbon (UL), Portugal
* e-mail: dehon@alu.ufc.br

Introduction

The Standardized Precipitation Index (SPI) is a helpful index for meteorological drought characterization, however, it is not suitable for drought warning. Aiming at exploring its forecasting capabilities, the concept of precipitation threshold for drought recognition developed by Portela et al. (2014) can be used. In each rain gage, if the cumulative precipitation in a given time-span falls below the precipitation threshold for that time-span, a drought with a severity (from moderate to extreme), defined in accordance with the threshold, will occur. For a rain gage, a time period and a drought severity, the precipitation thresholds are obtained based on the precipitation series for that time period by inverting the SPI calculation, which means that they simply give the SPI value back to the precipitation field.

Portugal presents the largest concentration of rainfall from October to March; therefore, it was considered that it was relevant to obtain the probability of drought occurrence starting in October (beginning of the hydrological year) and adopting two reference dates - March (end of rainy season) and September (end of the hydrological year) - corresponding to SPI time scales 6 and 12.

In mathematical terms, the definition of drought, in this study is: if N is the number of months of the time span to which the precipitation threshold P_t refers (defined in accordance with the time scales of the SPI6 and SPI12), n is the initial months of that time-span ($1 \leq n \leq N-1$) and P_n the cumulative precipitation in those n-months, then a drought will occur by the end of the N-month period if the precipitation in the remaining (N-n) months $P_{(N-n)}$ is not enough to meet the threshold:

$$Pn+P(N-n) \leq Pt \quad (1)$$

Consider, for example, that at the end of December (n=3) of a given year, the probability of an occurrence of a drought in a moderate severity (MD) from October to March (N=6) is required. Given the observed cumulative precipitation from October to December (P_n with n=3), the question is: *what is the probability that the cumulative precipitation from January to March (still unknown), added to cumulative precipitation from October to December, being below the drought threshold (P_t), for that severity*?

$$P(P_n+P_{(N-n)} \leq P_t \mid P_n) \quad (2)$$

It is a problem of conditional probability that aims at assigning a probability to the rainfall (and, accordingly, to the drought) in a given period provided that the precipitation in the beginning of that period is already known. This work presents the application of copulas to solve such problem.

Materials and methods

Santa Marta da Montanha (SMM) rainfall gauge, in the north of mainland Portugal, was selected for the present study. The monthly records from 1913 to 2018 were obtained via a public Portuguese databasis (*Sistema Nacional de Informação de recursos Hídricos, SNIRH)*.

To analyze the drought occurrences, the SPI time spans considered were 6 and 12 months. The thresholds for the drought intensities were those proposed by Agnew (2000).

The programming language R was used to calculate copulas, which are capable to model dependency structure of marginal distributions in a flexible way. In order to select an appropriate copula, the Akaike information criterion (AIC) were used.

According to Nelsen (2006), if $F_{1,2,\ldots,n}(x_1,x_2,\ldots,x_n)$ is a multivariate function with n random variables correlated (X_1, X_2, ..., X_n) with respective marginal distributions $F_1(x_1)$, $F_2(x_2)$, ..., $F_n(x_n)$, then,

$$H(x_1, x_2, ..., x_n) = C[F_1(x_1), F_2(x_2), ..., F_n(x_n)] = C(u_1, ..., u_n) \quad (3)$$

where, $F_k(x_k) = u_k$ for k = 1, ..., n, with $u_k \sim u(0,1)$ and $C(u_1, ..., u_n)$ being the copula function. Given a bivariate copula C (u_1, u_2), a bivariate cumulative distribution function - CDF $H(x_1, x_2)$ and marginal CDFs $F_1(x_1)$ and $F_2(x_2)$ with $H(x_1,x_2) = C(F_1(x_1), F_2(x_2))$, then the conditional probability is given by,

$$P(X1 < x1|X2 = x2) = \frac{P(X<x,Y=y)}{P(Y=y)} = \frac{\partial}{\partial u2} C(F1(x1), F2(x2)) \quad (4)$$

Results and concluding remarks

The knowledge of the probability of drought occurrence is extremely relevant to forecast drought events and mitigate their impacts. Using copulas, the conditional probability of an occurrence of a drought of a given severity can be continuously reevaluated at the end of each month, serving as a monitoring tool. Table 1 presents the conditional probability of moderate drought (MD), severe drought (SD) and extreme drought (ED) occurrence in SMM adopting the hydrological year 2017/2018 for purposes of demonstration. Using the inverse CDF, the thresholds from Oct-Mar (SPI6) and Oct-Sep (SPI12) were determined. The monthly precipitation on the hydrological year 2017-2018 and the monthly average precipitation are also show.

Table 1. Conditional probability of MD, SD and ED occurrence in hydrological year 2017/2018 in SMM.

		Oct	Nov	Dec	Jan	Feb	Mar	Apr	May	Jun	Jul	Aug	Sep
Monthly rainfall (mm)	recorded	43.1	40.4	173.0	109.0	58.6	273.5	166.8	79.4	91.2	22.5	2.5	1.1
	average	133.3	160.9	190.1	197.5	135.2	161.7	126.0	115.5	54.8	22.9	22.9	61.2
Accumulated rainfall (mm)		43.1	83.5	256.5	365.5	424.1	697.6	864.4	943.8	1035.0	1057.5	1060.0	1061.1
Threshold (mm)	Moderate						791.0						1238.4
	Severe						628.1						1027.9
	Extreme						509.7						865.2
		Drought occurrence probability											
Moderate	Oct - Mar	0.35	0.56	0.63	0.69	0.98	Drought						
	Oct - Sep	0.36	0.57	0.63	0.67	0.87	0.70	0.81	0.90	0.75	0.75	0.86	Drought
Severe	Oct - Mar	0.25	0.43	0.29	0.30	0.66	No Drought						
	Oct - Sep	0.25	0.35	0.29	0.26	0.54	0.14	0.14	0.08	0.02	0.02	0.06	No Drought
Extreme	Oct - Mar	0.17	0.28	0.09	0.09	0.17	No Drought						
	Oct - Sep	0.16	0.20	0.09	0.05	0.18	0.01	0.01	0.00	0.00	0.00	0.00	No Drought

The results of Figure 1 show the applicability of copulas for monitoring and detection of drought events. It showed a good performance in following the tendency of a *MD* event in 2017/2018 hydrological year, with the probability of occurrence of a MD in March ranging from 63% (on Dec/2017) to 98% (on Feb/2018); a moderate drought was consolidated in SMM on March. The method also had a good performance on forecasting a MD event on the end of the hydrological year (Sep/2018).

Figure 1 also shows that the conditional probability of occurrence of a *SD* between Oct/2017 and Mar/2018 given the cumulative precipitation occurred from Oct/2017 to Feb/2018, was 66%; however, the *SD* did not consolidate. It can be seen, nevertheless, that the threshold for this type of drought is 628.1 mm and the cumulative precipitation from Oct/2017 to Feb/2018 was 424.1 mm. An anomalous precipitation (273.5mm) occurred on Mar/2018 (the average monthly precipitation on March is 161.7 mm) and the cumulative precipitation in that period became 69.5 mm above the threshold necessary to classify this event as *SD*.

It can be observed that copula presented a good performance in detecting a MDs, however it was not capable to distinguish the severity of the event, once SD and ED are very sensitive to an individual precipitation value in the month of analysis. Rainfall thresholds for these classes are lower and can be easily exceeded by few millimeters of precipitation.

As was demonstrated in this study, copulas provide a promising method for characterizing the complicated dependence structure on cumulative precipitation and can be a powerful tool for imminent drought occurrence recognition.

References

Agnew CT (2000) Using the SPI to identify drought. Drought Network News 12(1):6–12

Nelsen RB (2006) An Introduction to Copulas. 2ª ed. [s.l.] Springer.

Portela MM, Santos JF, Matos JP, Silva AT (2014) Application of the standardized precipitation index, SPI, to the establishment of precipitation thresholds for drought recognition. International Journal of Environmental Engineering and Natural Resources, IJEENR 1(1):19-35

11th World Congress on Water Resources and Environment (EWRA 2019)
"Managing Water Resources for a Sustainable Future", 25-29 June 2019, Madrid, Spain

How many storms are needed to estimate the maximum annual flood? A continuous, fully-distributed, physically-based model approach

I. Gabriel-Martin*, A. Sordo-Ward, D. Santillán, L. Garrote
Departamento de Ingeniería Civil: Hidráulica, Energía y Medio Ambiente, Universidad Politécnica de Madrid, Spain
** e-mail: i.gabriel@upm.es*

Introduction

In order to estimate extreme flood hydrographs accurately by stochastic approaches, it is necessary to carry on hydrologic simulations of thousands of years. By using continuous fully distributed simulation models we are able to derive flood frequency distributions from the continuous hourly streamflow obtained at any desired point in the drainage network of the basin. This approach has the advantage of estimating the variables for the entire period of simulation. However, continuous models tend to be more complex than event-based models, with computational efforts that could be very intensive, even by using high performance computing and parallelization processes. Event-based simulations require much shorter simulation times. Among other disadvantages, the maximum annual rainfall does not necessarily have to produce the maximum annual flood. Furthermore, different properties of storm events could affect in the derivation of flood frequency curves: rainfall temporal distribution, event duration, maximum intensity, total storm depth, etc. Therefore, the estimation of high return period flood frequency curves by using event-based models is a challenge.

This paper focuses on addressing this challenge by analysing the results obtained by coupling a continuous stochastic weather generator with a continuous distributed physically-based hydrological model. The objective is to propose a criterion for the selection of the minimum number of storm events per year to guarantee a correct derivation of the flood frequency curve for high return periods, according to its maximum annual peak-flow, maximum annual volume, and the bivariate analysis of both variables. The outcomes of this research would be useful for event-based model applications.

Materials and methods

We applied the methodology to Peacheater Creek, a 64 km^2 watershed located in Oklahoma, USA. First, a set of 5,000 years of hourly weather was generated using AWE-GEN (Fatichi et al. 2011). AWE-GEN is a statistical hourly model capable to reproduce statistical properties of several weather variables including precipitation, cloud cover, shortwave incoming radiation, air temperature, vapour pressure, wind speed and atmospheric pressure. We calibrated AWE-GEN by using a set of 20 years of observed hourly weather data in Westville, a weather station located within the basin.

Afterwards, we used the 5,000 year weather time series to force the hydrological model tRIBS, which has been previously calibrated for the case study basin (Ivanov et al. 2004). tRIBS is a continuous physics-based, distributed-parameter hydrological model that includes parameterizations of rainfall interception, evapotranspiration, infiltration with continuous soil moisture accounting, lateral moisture transfers in the unsaturated and saturated zones and kinematic-wave runoff routing. By using the model with a spin-up period of ten years, we obtained a set of 5,000 years of continuous flow at the basin outlet, which we used to derive the peak-flow and volume flood frequency curves.

Simultaneously, we separated the independent storm events from the set of 5,000 years of hourly rainfall by applying the exponential method (Restrepo-Posada and Eagleson 1982). Afterwards, the obtained storm events were catalogued and ranked within the year of occurrence following three main criteria: total rainfall depth, maximum intensity, and storm duration. The biggest rainfall event of each year was identified as rank one, the second one as rank two, and so on.

Finally, for each criterion, we identified the rank of the storm event that generated the maximum peak-flow and maximum flood volume of each year within the 5,000-year time-series. Following a similar

approach to Sordo-Ward et al. (2016), we analysed the relationship between the storm rank and the maximum annual flood, in terms of peak-flow and volume of flood events.

Results and concluding remarks

By applying the methodology to the Peacheater Creek basin, we analysed the influence of the number of storms considered each year on the estimation of the flood frequency curve (Figure 1). Specifically:

- The criterion of ranking by total rainfall depth is strongly correlated with the maximum annual flood peak-flow and volume. Selecting the three largest storms each year results into a probability of achieving the maximum annual peak-flow of 86% (Figure 1a), whereas the maximum annual volume is reached with a probability of 93% (Figure 1b). If the five largest total depth storms per year are selected, this probability increases to 95% (Figure 1a) and 99% (Figure1b) respectively.
- The flood frequency curve for high return periods (100 ≤ return period ≤ 500 years) can be derived with more than 90% of accuracy by considering the largest total depth storm per year, for the maximum annual peak-flow (Figure 1c), maximum annual volume (Figure 1d) and, simultaneously, maximum annual peak-flow and volume (Figure 1e).
- If the three largest storms each year are selected, the probability of achieving simultaneously a hydrograph with the maximum annual peak flow and the maximum annual volume for a return period higher than ten years is over 90% (Figure 1e), being the return period calculated from the maximum annual peak flows series.
- Coupling a continuous weather simulator with a continuous hydrological model permits to account for the variability of initial soil moisture states.

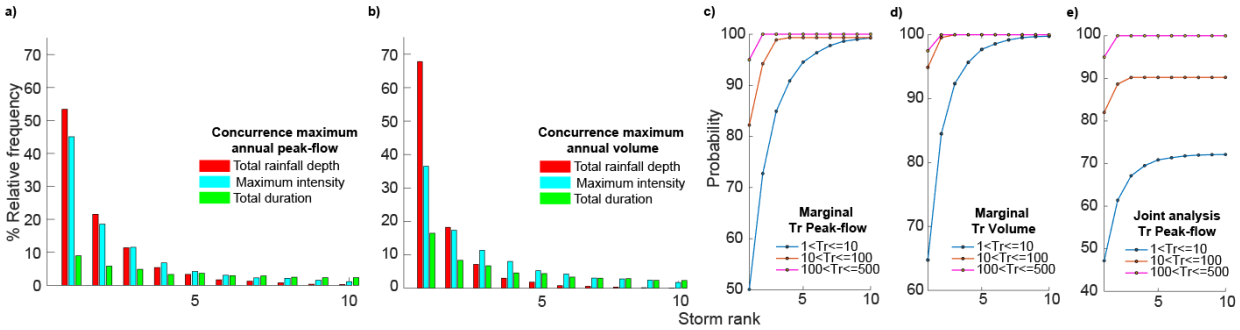

Figure 1. Relative frequency in which a storm of a specific rank generates the annual maximum peak-flow (a) or volume (b) depending on the criteria selected. For the total rainfall depth criteria, probability that a storm of a specific order or lower concurs with the maximum peak flow of a year (c), maximum volume of a year (d), and simultaneously, with the event of maximum annual peak-flow and volume (e, classified by the return period (Tr) of peak-flow)

Acknowledgements: The authors acknowledge the computer resources and technical assistance provided by the Centro de Supercomputación y Visualización de Madrid (CeSViMa) and the funds from Universidad Politécnica de Madrid in the framework of "Programa propio: Ayudas para contratos predoctorales para la realización del doctorado en sus escuelas, facultad, centro e institutos de I+D+i", "Programa propio: ayudas a proyectos de I+D de investigadores posdoctorales" and "Consejo Social: XVI Convocatoria de ayudas del consejo social para el fomento de la formación y la internacionalización de doctorandos".

References

Fatichi S, Ivanov VY, Caporali E (2011) Simulation of Future Climate Scenarios with a Weather Generator. Advances in Water Resources 34(4):448-467. http://doi.org/10.1016/j.advwatres.2010.12.013

Ivanov VY, Vivoni ER, Bras R, Entekhabi D (2004) Catchment Hydrologic Response with a Fully Distributed Triangulated Irregular Network Model. Water Resources Research 40(11):1-23. http://doi.org/10.1029/2004WR003218

Restrepo-Posada P, Eagleson P (1982) Identification of independent storms. Journal of Hydrology 55(1-4):303-319. http://doi.org/10.1016/0022-1694(82)90136-6

Sordo-Ward A, Bianucci P, Garrote L, Granados A (2016) The Influence of the Annual Number of Storms on the Derivation of the Flood Frequency Curve through Event-Based Simulation. Water 8(8):1-19. http://doi.org/10.3390/w8080335

11th World Congress on Water Resources and Environment (EWRA 2019)
"Managing Water Resources for a Sustainable Future", 25-29 June 2019, Madrid, Spain

Assessment of extreme hydrological phenomena in the eastern Slovakia

M. Zelenakova[1*], T. Solakova[1], M. M. Portela[2], Z. Vranayová[3], P.Purcz[4], D. Simonová[5]
[1] Department of Environmental Engineering, Technical University of Kosice, Kosice, Slovakia
[2] Department of Civil Engineering, Technical University of Lisbon, Lisbon, Portugal
[3] Department of Applied Mathematic, Technical University of Kosice, Kosice, Slovakia
[4] Department of Architectural Engineering, Technical University of Kosice, Kosice, Slovakia
[5] Slovak Hydrometeorological Institute, Kosice, Slovakia
* e-mail: martina.zelenakova@tuke.sk

Introduction

Observations since 1950 and the 21st century climatic projections provide evidence that drought is a recurring climatic feature in several parts of Europe, particularly in the Mediterranean (Hoerling et al. 2012), but also in Western, Southeast and Central Europe (Mishra and Singh 2010). More frequent droughts occur in Scandinavia (Hisdal et al. 2006), in Eastern Europe (Spinoni 2015) and Russia (Parry et al. 2012). Trends over the past 60 years have shown increasing, longer and more intense drought in these regions, while a negative trend has been seen in north-eastern Europe. In a changing climate, it is likely that this trend will be strengthened in the 21st century and will affect a wide range of socio-economic sectors.

Frequency risk analysis is conducted to determine the likelihood of its occurrence and to evaluate its potential negative impacts on fauna and flora, human society, the national economy, and to identify its characteristics (Mishra and Singh 2010). Various methods have been designed to identify, characterize and monitor the drought phenomenon, but among the most widely used we include drought indices, which are a special combination of indicators including meteorological, hydrological and other data. Depending on the type of drought, the most appropriate index is chosen (Tsakiris et al. 2007). The index value is the only number that plays a significant role in assessing the risk of drought and classifies its severity usually into 5 degrees: 1) slight drought, 2) mild drought, 3) severe drought, 4) extreme drought, 5) exceptional drought (Mishra and Singh 2010). This classification is essential for proper planning and management of control measures to mitigate the impacts of drought. Comprehensive lists of drought indices are listed and delineated in the following articles: Heim (2002) and Mishra and Singh (2010).

Materials and methods

Modarres (2007) introduced Standardized Streamflow Index (SSI). In this method, daily or monthly streamflow data can be applied and normalization is used associated with Standardized Precipitation Index (SPI) as same as Standardized Drought Index (SDI) calculation. SSI can be calculated for both observed and forecasted data and it can give a perspective for drought and wet periods. SSI is a probability-based index and this makes SSI sensitive to the aspects and assumptions that regulate probabilistic hydrology. The range of SSI values along with their classifications was stated by Nalbantis and Tsakiris (2009).

The calculation for different time scales allows the application of SPI and SSI in several spheres of water management or agriculture. Shorter time scales (1 - 3 months) well interpret changes in soil moisture and river flow. They are, for example, suitable for assessing the impact of drought on agricultural yields. Moderate time scales (6-12 months) reflect changes in water accumulation in water reservoirs and long-time scales reflect changes in groundwater reserves (Vicente-Serrano et al. 2010).

For the presented research – for the calculation of the SSI (Standardized Streamflow Index), the Slovak Hydrometeorological Institute provided daily flows for 7 river stations – Bardejov, Červený Kláštor, Humenné, Ižkovce, Medzev, Svidník, Ždiar for the period 1972-2014. Evaluated river stations have unchanged hydrological flow regime by human activity (construction of water structures, excessive water consumption and others).

Results and concluding remarks

The occurrence and identification of the basic parameters of short-term hydrologic drought was calculated using SSI-1 and SSI-3 from 1 to 3-month mean flow values collected over a 43-year time period. The greatest record of events of short-term hydrological events was in the decade 1982-1991, with long-term hydrological drought with an intensity less than -1 occurring 21 times in the decade: 1982-1991 and decade 1992-2001. The total dry period for river stations ranges from 64 to 89 months and the number of droughts ranges from 21 to 51. The longest drought from the evaluated stations was recorded at the Svidník and Medzev station. The severity of droughts ranges from -101.17 to -128.8, the maximum severity of hydrological drought is in Svidník and the minimum in Ižkovce. Average return time of drought is from 9.14 months to 14.4 months, short-term hydrological drought can be expected in Humenné every 9 months and in Medzev approximately every 14.5 months. The maximum duration of hydrological drought was in 1986 in Ždiar and lasted 7 months and in Humenné in 1983 with a 10-month duration. The results also show that the occurrence of the short-term deficit of the flows is mainly in summer and autumn months.

The long-term occurrence of mild hydrologic drought was identified by a 12-month and 24-month SSI. The total period of long-term hydrological drought for river stations ranges from 70 to 94 months, and the number of droughts ranges from 8 to 22. It is also important to note that the number of events for the SSI-24 is decreasing. In the water stations: Červený Kláštor, Humenné, Svidník and Ždiar, the longest drought from the evaluated stations was recorded. The severity of the droughts ranges from -108.6 to -136.6, the maximum severity of hydrological drought is in Bardejov and Ždiar and the minimum in Humenné. Average drought recovery time ranges from 23.6 months to 60 months, long-term hydrological drought can be expected in Červený Kláštor about every 2 years and Medzev approaching every 5 years. The maximum duration of hydrological drought was 2002 in Medzev and lasted 25 months and in Červený Kláštor in 1983 with a 37-month duration. The highest average intensity is recorded in Medzev. It also follows from the results that the occurrence of long-term flow deficit is mainly in summer and winter months.

Determining the vulnerability of the site to hydrological drought is an important basis for the proper management of water resources at the time of this phenomenon, as well as the elimination of its impacts on fauna and flora as well as by human action through effective measures. The planning and anticipation of adverse impacts of drought events in the river basin depends mainly on information on its magnitude, severity and duration. This information can be obtained through drought monitoring, which is usually done using drought indices, which provide quantitative information on drought characteristics.

Acknowledgments: This work has been supported by projects SRDA SK-PT-18-0008, SKHU/1601/4.1/187 and SEGA 1/0217/19.

References

Heim R (2002) A Review of Twentieth-Century Drought Indices Used in the United States. American Meteorological Society 1146-1165

Hisdal H, Roald LA, Beldring S, Demuth S, Gustard A, Planos E, Seatena F, Servat E (2006) Past and future changes in flood and drought in the Nordic countries. IAHS Publication 308

Hoerling M, Eischeid J, Perlwitz J, Quan X, Zhang T, Pegion P (2012) On the increased frequency of Mediterranean drought. Journal of Climate 25(6):2146-2161

Mishra K, Singh P (2010) A review of drought concepts. Journal of Hydrology 391(1):202-216

Modarres R (2007) Streamflow drought time series forecasting. Stochastic Environmental Research and Risk Assessment 21:223–233

Nalbantis I, Tsakiris G (2009) Assessment of hydrological drought revisited. Water Resour. Manage. 23:881—897

Parry S, Hannaford J, Lloyd-Hughes B, Prudhomme C (2012) Multi-year droughts in Europe: analysis of development and causes. Hydrology Research 43(5):689-706

Spinoni J, Naumann G, Vogt J, Barbosa P (2015) The biggest drought events in Europe from 1950 to 2012. Journal of Hydrology: Regional Studies 3:509-524

Tsakiris G, Loukas A, Pangalou D, Vangelis H, Tigkas D, Rossi G, Cancelliere A (2007) Drought characterization. In: Iglesias A, Moneo M, López-Francos A (eds.) Drought management guidelines technical annex. Zaragoza: CIHEAM/EC MEDA Water, 85-102

Vicente-Serrano SM, López-Moreno JI, Beguería S, Lorenzo-Lacruz J, Azorin-Molina C, Morán-Tejeda E (2012) Accurate Computation of a Streamflow Drought Index. Journal of Hydrologic Engineering 17(2):229-358

11th World Congress on Water Resources and Environment (EWRA 2019)
"Managing Water Resources for a Sustainable Future", 25-29 June 2019, Madrid, Spain

A proposed framework for flood risk assessment in cultural heritage sites upon specific ultra-detailed stage-damage functions

J. Garrote[1*], A. Díez-Herrero[2], C. Escudero[3], I. García[3]
[1] Department of Geodynamics, Stratigraphy and Paleontology, Complutense University of Madrid, Spain
[2] Geological Hazards Division, Geological Survey of Spain (IGME), Madrid, Spain
[3] Risk and Emergencies Management in Cultural Heritage, Castilla & Leon Regional Goverment, Valladolid, Spain
* e-mail: juliog@ucm.es

Introduction

River floods are possibly the natural phenomenon that has the greatest impact on the actual deterioration of cultural heritage. That is why the study of flood risk becomes essential in any attempt to manage cultural heritage (archaeological sites, historic buildings, art-works, etc.). In this context, this paper proposes a methodological framework for flood risk analysis in cultural heritage locations (BICs) in central Spain. The analysis is implemented in two phases: a first phase of estimating the level of qualitative risk at a regional scale; and a second phase of calculating the damages on patrimonial assets in a quantitative way, at a local scale. The first phase is based on a flood risk matrix for patrimonial assets, fed by spatial information from a GIS. The developed risk matrix outweighs previous proposals of this type (Ortiz et al. 2016; Arrighi et al. 2018), making it more versatile and useful.

For the second phase of analysis, several BICs (of different typology) with high susceptibility to flooding have been selected, for which ultra-detailed magnitude-damage functions have been developed. These functions have to adjust to the unique characteristics of the assets they represent, although they may be similar to functions developed for other types of buildings (i.e. Pistrika et al. 2014; Blanco-Vogt and Schanze 2014; Godfrey et al. 2015), and also present unique characteristics. Finally, the proposed methodological framework allows us to quantify the damages (tangible, both direct and indirect) associated with each scenario (return periods) considered, which cover ordinary and extraordinary events.

Materials and methods

Flood Risk – Cultural Heritage Matrix development: The development of a risk matrix for heritage buildings is an analytical methodology that has been used previously in the last decade (Ortiz et al. 2016; Arrighi et al. 2018). However, the complexity of the matrix developed in this work significantly exceeds that of previous matrices and it is based on 7 variables (three linked to the hazard factor and four linked to the vulnerability factor), from which six levels of potential risk are defined (qualitatively). The process of estimating the level of risk can be considered as an iterative process dependent on the T-year return period flood (Figure 1), and the spatial relationship between BICs and flood prone areas.

Development of ultra-detailed Stage-Damage Functions: For the development of magnitude-damage functions, the city of Zamora has been taken as a study area, and a detailed catalogue of cultural heritage was prepared. Economic losses have been considered both in the continent (buildings) and in the content (movable heritage, such as sculptural, pictorial or documentary assets). These patrimonial assets have been classified into different categories (Figure 2), depending mainly on the type of material used for their construction; considering their vulnerability and the effective potential damage depending on water depth, flow velocity and the time of permanence of the flood (flash floods vs. deluge floods).

Results and concluding remarks

A total of 11 BICs are affected by the 500-year return period flood, including the old town of Zamora, 8 churches, 1 convent and 1 museum. The numerical and cartographic results of this work are influenced by many of the limitations already pointed out by Pistrika et al. (2014) with respect to the deficiency in the quality of the information available regarding flood damage to buildings. This limits the quality of the

results obtained and increases their associated uncertainties.

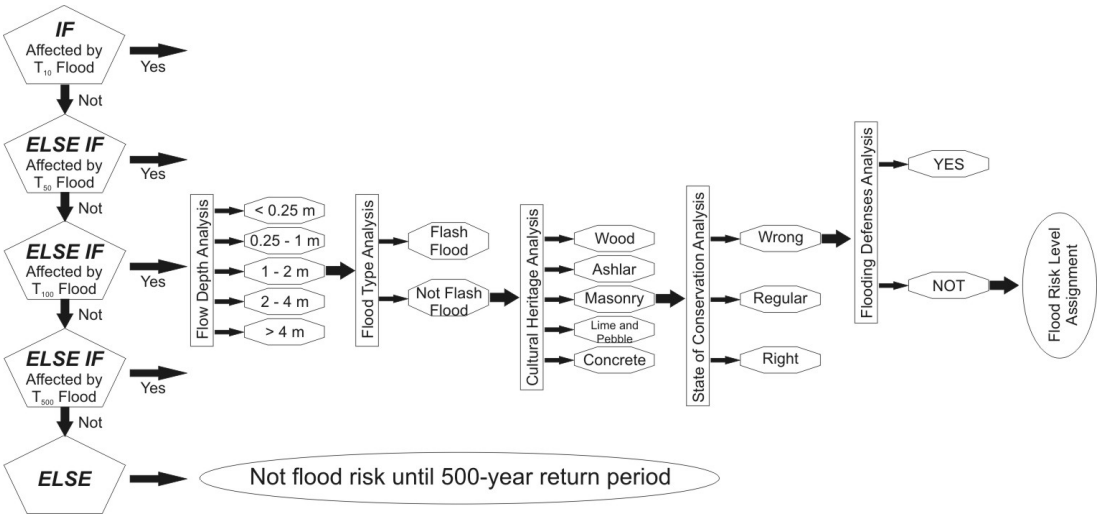

Figure 1. Flow chart for Flood Risk assessment in Cultural Heritage.

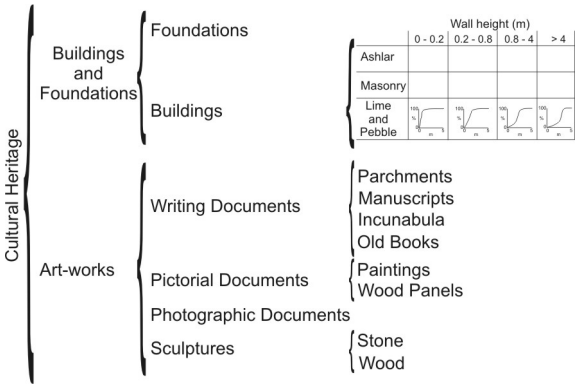

Figure 2. Diagram of the Cultural Heritage typologies.

In addition, in the case of sculptural and pictorial assets, evaluation of their exposure to floods is complicated (due to the possibility of being moved to safe areas). Despite these circumstances, the development of specific magnitude-damage functions for each heritage element has proved essential for a correct estimation of flood risk in cultural heritage, and as an aid to preventive conservation and rescue in emergencies.

Acknowledgments: This study was supported by the project DRAINAGE, CGL2017-83546-C3-R (MCIU/AEI/FEDER, UE).

References

Arrighi C, Brugioni M, Castelli F, Franceschini S, Mazzanti B (2018) Flood risk assessment in art cities: the exemplary case of Florence (Italy). Journal of Flood Risk Management 11: S616–S631. http://dx.doi.org/10.1111/jfr3.12226

Blanco-Vogt A, Schanze J (2014) Assessment of the physical flood susceptibility of buildings on a large scale – conceptual and methodological frameworks. Natural Hazards and Earth System Sciences 14(8):2105-2117. http://dx.doi.org/10.5194/nhess-14-2105-2014

Godfrey A, Ciurean RL, van Westen CJ, Kingma NC, Glade T (2015) Assessing vulnerability of buildings to hydro-meteorological hazards using an expert based approach – An application in Nehoiu Valley, Romania. International Journal of Disaster Risk Reduction 13:229–241. http://dx.doi.org/10.1016/j.ijdrr.2015.06.001

Ortiz R, Ortiz P, Martín JM, Vázquez MA (2016) A new approach to the assessment of flooding and dampness hazards in cultural heritage, applied to the historic centre of Seville (Spain). Science of the Total Environment 551–552:546–555. http://dx.doi.org/10.1016/j.scitotenv.2016.01.207

Pistrika A, Tsakiris G, Nalbantis I (2014) Flood Depth-Damage Functions for Built Environment. Environmental Processes 1(4):553–572. http://dx.doi.org/10.1007/s40710-014-0038-2

11th World Congress on Water Resources and Environment (EWRA 2019)
"Managing Water Resources for a Sustainable Future", 25-29 June 2019, Madrid, Spain

SOON: The Station Observation Outlier fiNder

S. Dal Gesso[1*], E. Arnone[1], M. Venturini[1], M. Cucchi[1], M. Petitta[1,2,3]
[1] Amigo s.r.l., Rome, Italy
[2] ENEA, SSPT-MET-CLIM, Rome, Italy
[3] EURAC, Institute for Applied Remote Sensing, Bolzano, Italy
* e-mail: sara.dalgesso@amigoclimate.com

Introduction

In the climate change era, it is fundamental to monitor the availability of water resources. One of the possible causes for a change in the water availability is related to variations in the meteorological conditions. To track this change, ground-based observations are one of the commonly used measurements (e.g. Klein Tank and Können 2003). However, these datasets might include both extreme but realistic values and erroneous information. A necessary but not trivial preliminary process for exploiting the observations is to filter the former while retailing the latter (e.g. Jiménez 2010).

The Station Observation Outlier fiNder (SOON) is a highly innovative algorithm, that identifies errors in large dataflows. SOON can be used on historical datasets as well as in real-time dataflows. A first prototype has been tested on 8 years (2007-2014) of hourly data recorded by about 10000 stations around Europe, which includes 7 meteorological variables: temperature, dewpoint temperature, pressure, precipitation, wind speed, wind gusts, and cloudiness. The dataset belongs to the Ubimet archive and has been provided within the EDI incubator programme.

Materials and methods

The idea behind SOON is that data flows can be simultaneously screened from different perspectives. This approach maximizes the exploitation of the available information. At the same time, the process becomes resilient to the absence of information. More practically, SOON detects the errors through machine learning (ML) by checking the internal consistency of the dataflow from a temporal, spatial and parametric perspective. To implement the ML modelling, the dataset is split into the training and the test dataset, corresponding to the periods 2007-2013 and 2014, respectively.

SOON is constituted by three modules:

1. *Data Pre-processing:* preparation of dataset for the ML modelling, i.e. (i) filtering of unphysical measurements based on realistic ranges; (ii) assigning to each station the corresponding pre-defined cluster, calculated through a K-means technique with K=20 (MacQueen 1967) on the basis of the geographic location, elevation, and monthly values of average temperature and cumulated precipitation; (iii) calculating the standardized variables based on the average and standard deviation computed over the training set.
2. *ML modelling:* application of Random Forest (RF; Breiman 2000) regressor to predict hourly values at each station. Three types of RF models are built to leverage the three information domains, i.e. time, space and parameter consistency. Models are built cluster by cluster and differs mainly in the inputs. The time consistency is evaluated on the basis of the last 24 hours of observations, the space consistency through the measurements of the five nearest neighbor stations, and the parametric consistency based on the values of previously identified correlated variables.
3. *Errors Detection:* error identification on the basis of a *score.* For each information domain, the score is computed as the difference between the prediction and the observation divided by three times the root mean squared error (RMSE) calculated over the training set. The final score is the weighted average of the three previously defined scores. Finally, values overcoming 1 are detected as errors. The weights are estimated by exploring a synthetic dataset, which includes artificial random errors. More specifically, the weight is defined as the product of Area Under Curve (AUC) of the Receiver Operating Characteristic (ROC) curve and the sensitivity at the threshold, i.e. 1.

Results and concluding remarks

SOON identifies as errors between 0.5 and 1% of the data of 2014. An example timeseries is displayed in Figure 1. The variation of temperature (T) observed at one station over 2014 is depicted as a grey line. The data that are identified as outliers by the initial filtering of the pre-processing module, and by the temporal, spatial and parametric components are highlighted with different colors. Finally, the observations that are classified as errors through the final score are shown as red circles. It is noticeable that the most evident errors are identified correctly. It is also worth stressing that not all the observations that are classified as outliers by one of the ML components present a final score that is beyond the threshold. In this sense, SOON reduces the effects of likely limitations in the reliability of the ML modelling components, and of using possible erroneous values as inputs of the RF regressors. In other cases, the classification of the different ML components are not all available. In this respect, SOON maximizes the available information, and enables the error identification even in fragmented datasets.

As a future development, SOON will be further extended by including a module that distinguishes between errors and extreme but realistic observations. To this end, the extreme value theory will be employed. With this final module, SOON will become a unique trans-sectoral tool for identifying errors in any type of instrumental network, including weather stations and smart water sensors.

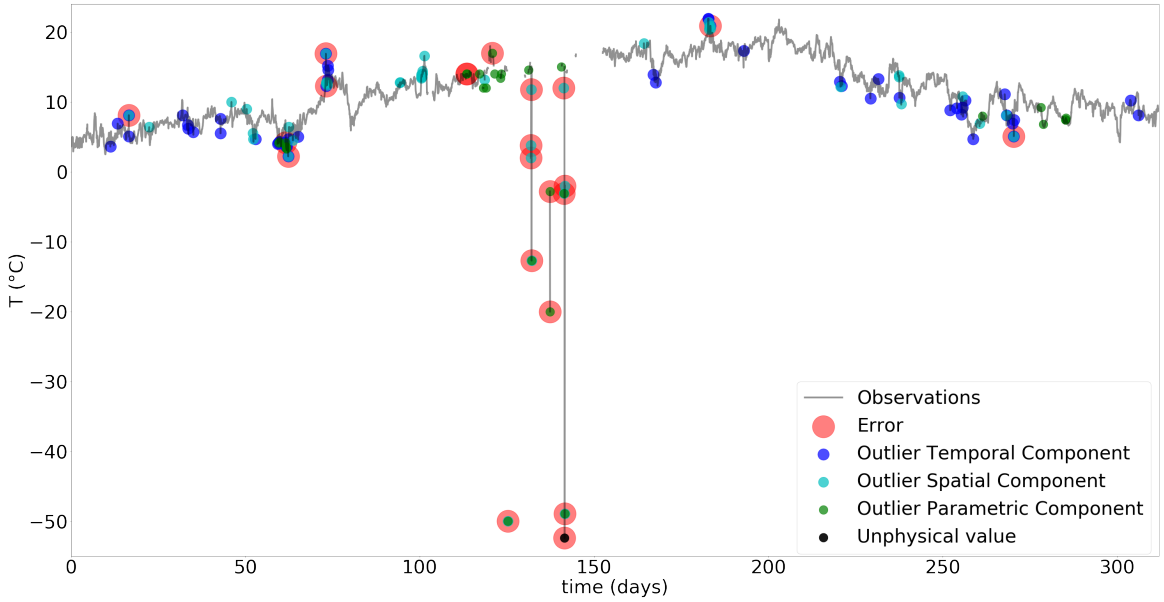

Figure 1. Example timeseries of Temperature for one station. The red dots indicate the errors identified by SOON.

References

Klein Tank AM, Können GP (2003) Trends in Indices of Daily Temperature and Precipitation Extremes in Europe, 1946–99. Journal of Climate 16:3665–3680. https://doi.org/10.1175/1520-0442(2003)016<3665:TIIODT>2.0.CO;2

Jiménez PA, González-Rouco JF, Navarro J, Montávez JP, García-Bustamante E (2010) Quality Assurance of Surface Wind Observations from Automated Weather Stations. Journal of Atmospheric and Oceanic Technology 27:1101–1122. https://doi.org/10.1175/2010JTECHA1404.1

MacQueen JB (1967) Some Methods for classification and Analysis of Multivariate Observations. Proceedings of the Fifth Berkeley Symposium on Mathematical Statistics and Probability, Volume 1: Statistics, 281-297, University of California Press, Berkeley, Calif., 1967. https://projecteuclid.org/euclid.bsmsp/1200512992

Breiman L (2000) Some infinity theory for predictor ensembles. Technical Report 579, Statistics Dept. UCB

11th World Congress on Water Resources and Environment (EWRA 2019)
"Managing Water Resources for a Sustainable Future", 25-29 June 2019, Madrid, Spain

A joint remote-sensing based index for drought identification and characterization in the Caribbean Islands

B. Monteleone[1*], B. Bonaccorso[2], M. Martina[1]
[1] Scuola Universitaria Superiore IUSS Pavia, Pavia, Italy
[2] Department of Engineering, Università di Messina, Messina, Italy
* e-mail: beatrice.monteleone@iusspavia.it

Introduction

Drought is a natural hazard originating from a lack of precipitation. Its impacts are delayed, non-structural and spread over large areas (Wilhite 2000). Drought characterization, through the determination of onset, offset, severity, intensity and duration, is crucial to manage and reduce the risk related to this extreme event. More than 100 indices have been proposed to monitor drought, each one with its aim and specificity. A single drought monitoring variable is insufficient to effectively determine drought features. Severity and intensity should be monitored at frequent time-steps. In addition, drought monitoring can be a hard task in countries with sparse gauges and few meteorological stations on the ground.

The present study proposes a new index, SP&VH, developed by combining two of the most common variables used in drought monitoring: the Standardized Precipitation Index (SPI; Mckee et al. 1993) and the Vegetation Health Index (VHI; Kogan 1990), derived from satellite-based data. The new index shows some interesting features: it is remote-sensing based, weekly updated and it can be computed over the entire globe at a proper spatial resolution. The index has been validated against text-based information retrieved for a specific case study (Haiti).

Materials and methods

Haiti was chosen as case study, since the country was affected by intense droughts that caused huge loss of crops and deeply affected the population. Events were identified starting from text-based information and are reported in Table 1.

Table 1. Drought events in Haiti. Information retrieved from governmental reports, NGOs, newspapers and other.

Year	Department	Affected people	% population
1981	South, Grand Anse, West	103000	2
1982-1983	South, South East, North West, North East	333000	5.75
1984-1985	North West	13500	2
1986	All island		
1990-1992	All island	1000000	14
1997	North West, North, North East	50000	0.64
2000	All island		
2003	North West	35000	0.41
End 2009	North West		
2011-2012	North, North West, North East, Artibonite, Centre		
2013	All island	>143000	1.5
2014-2017	All island	3600000	33

SPI was computed at weekly time-steps based on precipitation retrieved from the CHIRP dataset (Funk et al. 2015). CHIRP has global coverage, daily temporal resolution and 0.05° spatial resolution. Its records started in 1981. VHI was retrieved from the NOAA STAR (NOAA 2011). The dataset has global coverage, weekly temporal resolution and 4 km spatial resolution.

SPI was selected, as recommended by the WMO, to identify drought periods. VHI can be seen as a measure of drought impacts on the ground, since it accounts for vegetation stress and includes the effects

of temperature, being a combination of the Vegetation Condition Index and the Temperature Condition Index.

Both indices have normal distribution, therefore it is fair to combine them by using a bivariate normal distribution function, which is then standardized through a normal quantile transformation, following an approach used for instance to develop the Joint Drought Index (Kao & Govindaraju 2010) or the Multivariate Standardized Drought Index (Hao and AghaKouchak 2013). SP&VH model was validated by plotting joint probability values against the empirical copula values.

Drought events identified with SP&VH were compared against reported events.

The Receiver Operating Characteristic (ROC) curve, as described by Hanley and McNeil (1982) was employed to test the index.

Results and concluding remarks

SPI3 was chosen due to its stronger correlation with VHI with respect to other aggregation timescales. The new index performed slightly better than SPI and VHI considered alone (**Error! Reference source not found.**); hit rates and false alarm rates, computed for the period 1981-2018 starting from the confusion matrix, were respectively 0,82 and 0,26 for SP&VH, 0,72 and 0,34 for SPI3 and 0,79 and 0,31 for VHI. SP&VH helped in reducing the number of false alarms and increasing the number of events that were correctly classified (drought and non-drought periods).

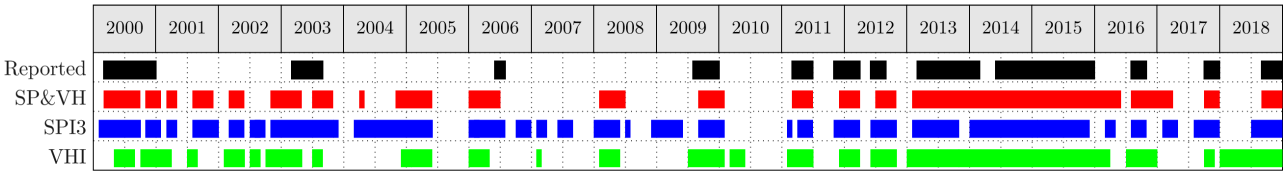

Figure 1. Comparison between performances of SP&VH, SPI3 and VHI with respect to reported events.

The new index, given its ability in the identification of start and end date of a drought event, can provide useful information to decision-makers when establishing drought management policies.

References

Funk C, Peterson P, Landsfeld M, Pedreros D, Verdin J, Shukla S et al. (2015) The climate hazards infrared precipitation with stations - A new environmental record for monitoring extremes. Scientific Data 2:1–21. https://doi.org/10.1038/sdata.2015.66

Hanley AJ, McNeil B (1982) The meaning and use of the Area under a Receiver Operating Characteristics (ROC) Curve. Radiology 143:29–36. https://doi.org/10.2196/jmir.9160

Hao Z, AghaKouchak A (2013) Multivariate Standardized Drought Index: A parametric multi-index model. Advances in Water Resources 57:12–18. https://doi.org/10.1016/j.advwatres.2013.03.009

Kao S, Govindaraju RS (2010) A copula-based joint deficit index for droughts. Journal of Hydrology 380(1–2):121–134. https://doi.org/10.1016/j.jhydrol.2009.10.029

Kogan FN (1990) Remote sensing of weather impacts on vegetation in non-homogeneous areas. International Journal of Remote Sensing 11(8):1405–1419

McKee TB, Doesken NJ, Kleist J (1993) The relationship of drought frequency and duration to time scales. AMS 8th Conference on Applied Climatology 179–184

NOAA (2011) STAR—Global Vegetation Health Products. National Oceanic and Atmospheric Administration (NOAA). https://www.star.nesdis.noaa.gov/smcd/emb/vci/VH/vh_ftp.php

Wilhite DA (2000) Drought as a natural hazard: Concepts and definitions. Drought: A Global Assessment, pp 3–18

11th World Congress on Water Resources and Environment (EWRA 2019)
"Managing Water Resources for a Sustainable Future", 25-29 June 2019, Madrid, Spain

The relationship between precipitation depth and weather circulation patterns over Sicily

G. Cipolla[1*], A. Francipane[1], S. Blenkinsop[2], H.J. Fowler[2], L.V. Noto[1]
[1] *Department of Engeneering, University of Palermo, Palermo, Italy*
[2] *School of Civil Engineering and Geosciences, Newcastle University, Newcastle upon Tyne, UK*
** e-mail: giuseppe.cipolla04@unipa.it*

Introduction

Some weather circulation patterns (WPs) derived by the UK Met Office and defining a certain type of atmospheric circulation over Europe have been recently used to analyse the relationship of the regional UK precipitation and drought with respect to the atmospheric circulation over Europe (Richardson et al. 2018).

In this study, we attempt to find out one or more relationships between precipitation depth and weather patterns over a non UK-centred domain, such as Sicily (Italy), which is characterized by a totally different climate as compared to the climate of UK. Since the island has been affected by many floods in the last years, occurred as a consequence of extreme rainfall events, it would be very important to understand if there exist some European WPs that are responsible for causing extreme rainfall events in the island. This aspect could be very helpful in reducing the flood risk, since it would make possible to prevent extreme rainfall events, almost likely leading to floods, by simply preventing the atmospheric circulation with a meteorological model.

Materials and methods

In order to achieve the aims of this study, two different databases have been here used. The first one is a database of rainfall annual maxima (AMAX) at the durations of 1, 3, 6, 12, and 24 hours and has been provided by the *Osservatorio delle Acque - Regione Siciliana*. In order to ensure a reasonable statistical analysis at the gauge level, all of the gauges with less than ten years of data have been discarded from the original database. The resulting dataset is made of 280 raingauge stations (spread over the entire island) with recorded data that range between 1930 and 2016. The second database is made of the occurred WPs over Europe, at the daily scale, between 1850 and 2016. The possible WPs in the database are eights and are designed to be used at the monthly and seasonal timescales (Neal et al. 2016). Among the eight WPs, the WP1 and WP2 present the highest frequency of occurrence with positive mean sea level pressure (MSLP) anomalies in the northern part of Europe and negative MSLP anomalies in the south of Europe, where Sicily is located, and negative MSLP anomalies to the north of Europe and positive MSLP anomalies to the southern part of the continent, respectively.

Starting from the two databases above described, some statistical analyses have been carried out to search possible relationships between the annual maxima for fixed durations and the weather circulation patterns for Sicily. The methodology of this study is perfectly suitable with the INTENSE project (Blenkinsop et al. 2018).

Results and concluding remarks

In an attempt to link together the two databases, the AMAX from all the gauges, for each of the available five durations, have been firstly associated to one of the eight WPs, on the base of the day of occurrence of the AMAX and of the WP. Furthermore, the same procedure has been applied to a sample of those values of AMAX higher than a R-Med value (i.e., the AMAX that has a probability of not being exceeded equal to 50%). These analyses highlighted the noticeable contribution of WP1 to the occurrence of all the pooled AMAX at all durations (Figure 1a) and to the occurrence of those values greater than R-Med threshold value. Moreover, the AMAX values recorded under WP2 increase their frequency of occurrence as the duration increases.

In order to investigate the seasonality of the AMAX, the original database has been split into two datasets and each event of these has been linked to a WP. In particular, the first dataset includes the AMAX occurred from May to October (broadly the convective rainfall season in Sicily), while the second one contains the events occurred from November to April. The two datasets have been named *summer half year* and *winter half year* (Pińskwar et al. 2018), respectively. The results showed that most of the AMAX values occurring during the *summer half year* are characterized by the shortest durations (i.e., 1 and 3 hours) and happen mainly under WP1, while in the *winter half year* the biggest part of AMAX with long duration (i.e., 12 and 24 hours) occurring under WP1 and WP2 (and also other WPs) have almost the same frequencies of occurrence (Figure 1b).

Finally, in order to take into account also the frequency of each WP occurrence, the conditional probability of all the pooled AMAX given the frequency of occurrence of all WPs, has been calculated using the Bayes' theorem. The application of the Bayes' theorem showed that the AMAX for all the durations are mostly caused by the occurrence of WP1, with an almost constant frequency value for all the durations (similar to what happens in Figure 1a).

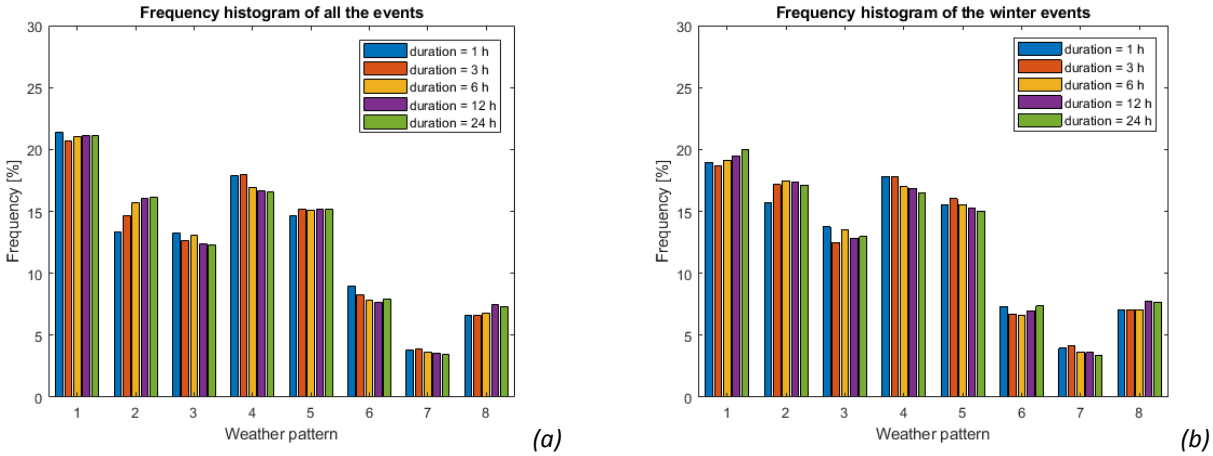

Figure 2. (a) Weather type frequency histogram for AMAX at all durations. (b) Frequency histograms for all the annual maxima in winter half year (NDJFMA)

In conclusion, the first results of such an analysis seem to stress the importance of some WPs, as compared to other ones, in forecasting the occurrence of the AMAX in some regions of Europe affected by the flood risk. In this way, this connection could be very useful to have some useful information concerning the occurrence of a flood by simply looking at the current and forecasted atmospheric circulation pattern.

References

Neal R, Fereday D, Crocker R, Comer RE (2016) A flexible approach to defining weather patterns and their application in weather forecasting over Europe. Meteorological Applications 23:389-400. doi: 10.1002/met.1563

Richardson D, Fowler HJ, Kilsby CG, Neal R (2018) A new precipitation and drought climatology based on weather patterns. International Journal of Climatology 38:630-648. doi: 10.1002/joc.5199

Blenkinsop S, Fowler HJ, Barbero R, Chan SC (2018) The INTENSE project: using observations and models to understand the past, present and future of sub-daily rainfall extremes. Advances in Science and Research 15:117-126. https://doi.org/10.5194/asr-15-117-2018

Pińskwar I, Choryński A, Graczyk D, Kundzewicz ZW (2018) Observed changes in extreme precipitation in Poland: 1991–2015 versus 1961–1990. Theoretical and Applied Climatology 135:773-787. https://doi.org/10.1007/s00704-018-2372-1

11th World Congress on Water Resources and Environment (EWRA 2019)
"Managing Water Resources for a Sustainable Future", 25-29 June 2019, Madrid, Spain

Variance of pipe flow-series as surrogate reliability measures in design of water distribution networks

S. Rathi*, R. Gupta
Department of civil Engineering,Visvesvaraya National Institte of Technology, Nagpur, India
** e-mail: shwetanabira12345@rediffmail.com*

Introduction

Water distribution systems (WDSs) are designed to provide consumers adequate quantity of water with sufficient pressure and of acceptable quality at all the times under a range of operating conditions. How best a network satisfies to achieve this objective is termed as its reliability. Reliability is classified into different types as described in previous studies such as mechanical reliability, hydraulic reliability and water quality reliability. Hydraulic reliability refers to network tolerance for demand changes. Mechanical reliability refers to how well WDS can perform under abnormal situations such as pipe bursts and pump failure conditions. Water quality reliability measures refer to quality of water delivered to consumers under any mechanical or hydraulic uncertainty over time. Reliability based design of water distribution network is an active area of research and is a challenging task as it requires complex sampling and iteration procedures. Focussing on this aspect, recently various reliability surrogate measures are introduced by different researchers for hydraulic reliability and mechanical reliability of WDS. These surrogate measures mainly aims at simplifying the reliability considerations in design. The improvement in surrogate measures shows improvement in performance of network under failure and uncertain conditions.

In previous studies different reliability surrogate measures are proposed such as Entropy reliability indicator (ERI), Resilience index (RI), Network resilience index (NRI), Modified resilience index (MRI), Mixed reliability surrogate measures, Surplus power factor, Hydraulic reliability and pipe failure tolerance, Available power index (API) and Diameter sensitive flow entropy etc suggested to simplify reliability-based design process. These reliability surrogate measures are mainly classified into two main categories such as power based indices and Entropy based method. Recently many researchers have compared different reliability surrogate measures to identify the most reliable ones. The improved values of these surrogate measures during design are observed to improve the ability of network to sustain failure. Most of the surrogate reliability indicators are based on logical metrics and they have been shown to improve network reliability when applied to assist in network design. However, each indicator may have its own disadvantage (Atikson et al. 2014, Tanyimboh et al. 2016, Liu et al. 2017). The usefulness of surrogate reliability measures have been typically justified by their application against some bench-mark problems. The effect of failure of any pipe on the network will be least, if all pipes have same hydraulic capacities. However, achieving same hydraulic capacities is not possible during design, and it is observed that uniformity in pipe capacities at junction nodes results in higher reliability. Several researchers suggested uniformity in diameter of different pipes at the node or in the loop to improve the reliability of the network. Martinez (2007) suggested calculating pipe flows by minimizing the variance of pipe flows in series in their reliability-based minimum cost formulation. Thus, reliability is indirectly considered through minimizing the variance of pipe flow series. In order to simplify the flow allocation process, Martinez (2007) proposed an analytical method to obtain pipe flows that provided a minimum variance of flow series. Rathi et al. (2018) illustrated that there are an infinite set of possible flow distributions for any looped network that will satisfy the node flow continuity equations and hence there are an infinite set of possible variances. Among all flow distributions, three flow distributions are selected so as to satisfy mass balance at each node and found that the condition used in analytical method is not sufficient. Rathi et al. (2019) suggested a new optimization formulation based on Genetic Algorithm (GA) which directly relates variance of pipe-flow series with network reliability. GA is used for fixing the flow distribution in network without any prior knowledge of flow direction in the network. After fixing the flow distribution using GA, a Linear

programming (LP) is used to design a network and reliability is measured in terms of demand satisfaction ratio (DSR). A level-one redundant system is designed for Water Main System of Washington D.C. and observed that less costly design solutions is found for achieving the same level of reliability as compared to all other previous applications. Therefore, herein the main objective of the study is to compare a design based on newly proposed reliability surrogate measure variance of pipe flow series with design based on other surrogate reliability measures. It has the advantages of being easy to calculate for existing system and easy to incorporate into cost optimisation design procedures. This study further describes the use and merits of variance of pipe flow series as a surrogate measure of reliability.

Materials and methods

Variance defined as average of square of deviation from mean in a series is obtained by considering the magnitude of pipe flows in a series. Equation (1) shows new modified formulation for minimisation of variance of pipe-flow series subjected to the condition shown by equation (2). In our previous study it is observed that minimization of variance brings more uniformity in pipe flows and capacity of network is affected least when a pipe is failed and isolated for repairs.

Problem of minimizing the variance of pipe flow series is defined as:

$$Min\ V_Q = \frac{1}{N}\left(\sum_{x=1}^{N}\left(|Q_x| - \overline{Q_x}\right)^2\right) \tag{1}$$

subjected to: $\sum_{\substack{x\ connected \\ at\ node\ j}} Q_x - q_j = 0$, for all j = 1, . . ., J (2)

$$\overline{Q_x} = \frac{1}{N}\sum_{1}^{N}|Q_x| \tag{3}$$

In this study, a comparisons of design based on minimization of variance are made with designs based on other surrogate reliability measures on a sample network.

Results and concluding remarks

Rathi et al. (2019) suggested a new GA based approach for minimizing the variance of pipe flow series is observed more efficient for the design of level-one redundant system of Water Main of Washington D.C. and provided least costly design solutions as compared to others. Herein a study is carried out to compare the design based on minimization of variance of other surrogate reliability measures on a sample problem and it is observed that a variance of pipe flow series can be considered as a new reliability surrogate measures under mechanical reliability and hoped to consider as good reliability surrogate measures under hydraulic reliability.

References

Atikson et al. (2014) Reliability indicators for water distribution system design: Comparison. Journal of Water Resources Planning and Management 142(2):160-168. https://doi.org/10.1061/(ASCE)WR.1943-5452.0000304

Liu H, Savic DA, Kapelan Z, Creaco E, Yuan Y (2017) Reliability Surrogate Measures for Water Distribution System Design: Comparative Analysis. Journal of Water Resources planning and Management, 143(2):04016072. https://doi.org/10.1061/(ASCE)WR.1943-5452.0000728

Martínez J (2007) Quantifying the economy of water supply looped networks. Journal of Hydraulic Engineering, 133(1):88-97. doi: 10.1061/(ASCE)0733-9429(2007),133:1(88)

Rathi et al. (2018) Directional Dependency of Minimum Variance of Flow Series in Looped Water Distribution Networks. Vol 1, 2018 WDSA / CCWI Joint Conference

Rathi et al. (2019) Minimizing the Variance of Flow Series using Genetic Algorithm for Reliability-based design of Looped Water Distribution Networks. Engineering Optimization, doi: 10.1080/0305215X.2019.1598984

Tanyimboh et al. (2016) Comparison of surrogate measures for the reliability and redundancy of water distribution systems. Water Resources Management 30:3535-3552. doi: 10.1007/s11269-016-1369-8

11th World Congress on Water Resources and Environment (EWRA 2019)
"Managing Water Resources for a Sustainable Future", 25-29 June 2019, Madrid, Spain

Assessing operational reservoir rules for evaluating flood risk scenarios using a Monte Carlo bivariate framework: A case study in Sicily

A. Candela[1], G.T. Aronica[2*]
[1] Dipartimento di Ingegneria, Università di Palermo, Palermo, Italy
[2] Dipartimento di Ingegneria, Università di Messina, Messina, Italy
* e-mail: garonica@unime.it

Introduction

Dams have a positive role within the water management strategies providing drinking water, hydroelectric power, flood control, recreation and many other benefits to people or local economies. However, dams can pose significant risks to people living downstream should they fail. Due to increased development, consequences of dam reservoir incorrect operational management have become much higher in the last decades. Risk assessments also should consider all artificial structures holding water (i.e. dams and reservoirs) which represent potential sources of flooding in the case of possible failure of the structure and during operational flood control.

In Italy, national laws and various technical guidelines have highlighted the need to set up specific operational reservoir management rules for managing flooding risk downstream dam reservoirs.

Also, scientific literature emphasize the importance of specific operational rules for flooding safety downstream to dam reservoirs with a specific focus on probability of occurrence of routed flood hydrograph (Hardesty et al. 2018).

The return period should be defined in terms of occurrence of dam overtopping or downstream damages, instead of in terms of natural probability of occurrence of flood, to take into account the influence of reservoir and dam characteristics on the flood hydrograph routing process (Mediero et al. 2010). Standard hydrological approaches for solving the above problems are usually based on well-established univariate frequency analysis methods and the iso-frequency hypothesis. Hence, the risk related to a specific event can be over- or underestimated if only the return period of either the peak or volume is analysed. These negative aspects can be overcome by using bivariate flood frequency analysis for the reliable evaluation of the entire flood hydrograph associated with a specific return period (Bocchiola and Rosso 2014; Klein et al. 2010, Requena et al. 2013; Candela et al. 2014).

Further, adopting Monte Carlo simulation method the storm temporal distribution, spatial distribution, duration, and depth can be simulated numerically to overcome the mathematical complexity in the derivation of the design flood hydrograph (Aronica and Candela 2007).

Materials and methods

In this section, the proposed procedure is described in detail. First, the methodology to calculate flood hydrographs is reported, then the flood risk evaluation through (HEC-RAS) hydraulic simulations to estimate the inundation risk at the infrastructure location under different operation strategies of an upstream reservoir. The entire procedure can be summarised as follows: (1) derivation of single synthetic rainfall events starting from Monte Carlo generation of rainfall by using a bivariate copulas analysis; (2) synthetic bivariate inflow hydrographs calculation by using a conceptual fully distributed model starting from synthetic hyetographs, (3) flood hydrograph routing through the reservoir taking in account the initial level (as empirical distribution of initial water storage levels recorded in several years); (4) flood risk mapping and evaluation through 2D hydraulic simulation. The procedure was applied to the case study of the Castello reservoir, located in the southwestern part of Sicily (Italy). It dams the river Magazzolo with a drainage area of 81 km^2, forming an artificial lake with a reservoir volume of 26 Mm^3 (Figure 1).

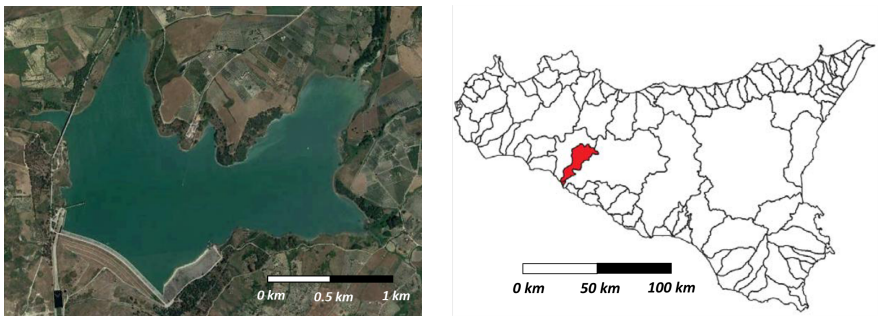

Figure 1. Castello dam and Magazzolo catchment

Results and concluding remarks

Following the above outlined procedure, stochastic inflow bivariate hydrographs has been generated using the methodology outlined. The inflow hydrographs routed through the reservoir allowed to obtain the outflow hydrographs from the spillway (peak flows, volumes and total duration) for different initial conditions in terms of water storage (Figure 2). Finally, outflow hydrographs for different reservoir conditions have been used for deriving flood hazard and risk maps downstream. Results demonstrate the framework's potential and the effects of different water management scenarios on the flood risk of the downstream infrastructure.

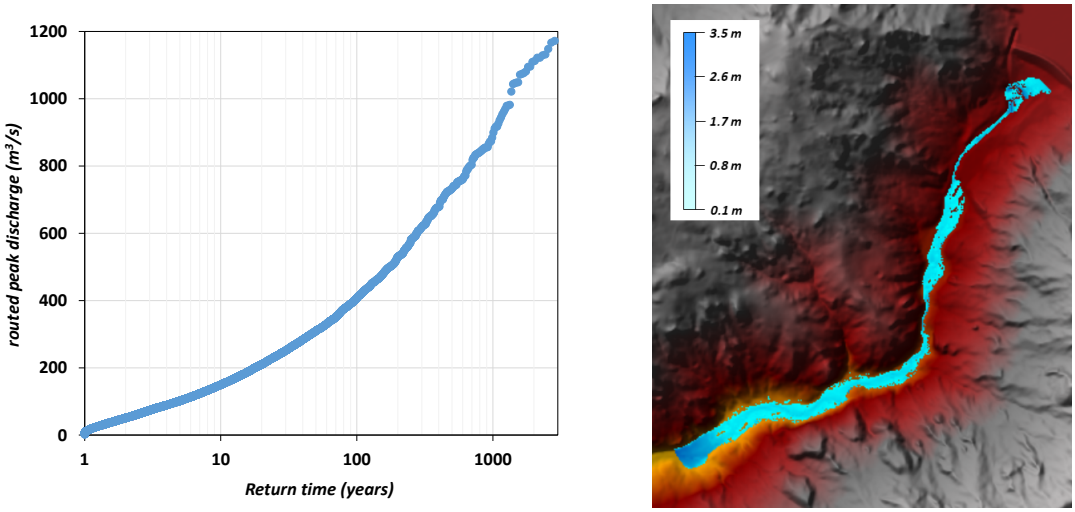

Figure 2. Routed flood discharge frequency (left). Flood hazard map for given reservoir condition (right)

References

Aronica GT, Candela A (2007) Derivation of flood frequency curves in poorly gauged catchments using a simple stochastic hydrological rainfall-runoff model. Journal of Hydrology 347(1-2):132-142

Bocchiola D, Rosso R (2014) Safety of Italian dams in the face of flood hazard. Advanced Water Resources 71:23–31

Candela A, Brigandì G, Aronica GT (2014) Estimation of synthetic flood design hydrographs using a distributed rainfall–runoff model coupled with a copula-based single storm rainfall generator. Natural Hazards Earth System Science 14:1819–1833

Klein B, Pahlow M, Hundecha Y, Schumann A (2010) Probability analysis of hydrological loads for the design of flood control systems using copulas. Journal of Hydrological Engineering ASCE 15:360–369

Mediero L, Jimenez-Alvarez A, Garrote L (2010) Design flood hydrographs from the relationship between flood peak and volume. Hydrological Earth System Science 14:2495–2505

Requena AI, Mediero L, Garrote L (2013) A bivariate return period based on copulas for hydrologic dam design: accounting for reservoir routing in risk estimation. Hydrological Earth System Science 17:3023–3038

Sage H, Xinyi S, Efthymios N, Emmanouil A (2018) A Numerical Framework for Evaluating Flood Inundation Hazard under Different Dam Operation Scenarios - A Case Study in Naugatuck River. Water 10:1798. doi: 10.3390/w10121798

11th World Congress on Water Resources and Environment (EWRA 2019)
"Managing Water Resources for a Sustainable Future", 25-29 June 2019, Madrid, Spain

Approaching drought through human perception based on the sense of sound

I. Tsevreni[1], M. Tsevreni[2], N. Proutsos[3], D. Tigkas[4*]
[1] Department of Early Childhood Education, University of Thessaly, Volos, Greece
[2] Department of Political Science and Public Administration, National and Kapodistrian University of Athens, Greece
[3] Institute of Mediterranean Forest Ecosystems, Helenic Agricultural Organization "DEMETER", Athens, Greece
[4] Lab. of Reclamation Works and Water Resources Management, National Technical University of Athens, Greece
* e-mail: ditigas@mail.ntua.gr

Introduction

Drought is a natural hazard with severe effects in many parts of the globe. A distinctive difference between drought and other natural hazards is the fact that it cannot be directly conceptualised by human senses, in contrast to other hazards, such as floods, tsunamis, forest fires, etc., which can be perceived through vision or hearing. In this paper, an approach of drought both with static and dynamic terms is attempted, inspired by the concept of "hyperobject", in which the association of human beings to certain environmental manifestations is seen as a phenomenological relation between humans and objects (Morton 2013). By reminding the necessity of the philosophical basis of the natural sciences, and also trying to reduce the gap between natural sciences and humanities, a dialectic relation between "system and lifeworld" can be introduced (Habermas 1987), as a means of interrelating statistical and content analysis, modelling and hermeneutics, static and dynamic approaches.

Drought events are typically assessed through statistical analyses of certain parameters and indices, related to climatic drivers of the phenomenon or environmental factors that represent its effects (Tigkas et al. 2019). An alternative way of approaching the condition and 'health' of ecosystems can be achieved using and evaluating the sense of sound. To this end, the potential and the benefits of approaching drought and its impacts using soundscape analysis is considered and discussed.

Materials and methods

Natural sounds or their absence serve as an excellent 'universal' variable, indicating the condition of an ecosystem and reflecting the dynamic of human-nature relationship. The exploration of the soundscape of an ecosystem through ecoacoustics can help to comprehend its ecological significance or the threats it confronts. In the framework of acoustic ecology, a soundscape is the sonic environment (Scafer 1994), while, according to soundscape ecology, it represents the biological, geophysical and anthropogenic sounds that are produced by a landscape, reflecting significant ecosystem processes and human activities (Pijanowski et al. 2011). Recent advances in data analysis and technological improvements in sound-related hardware and software have significantly broadened the applications in which ecoacoustics can be used.

Although ecoacoustics deal with several aspects of ecosystems, there are only few studies associated with climatic issues, which are mainly focusing on climate change effects (e.g. Krause and Farina 2016; Llusia et al. 2013). There are various drought impacts that can be identified in an ecosystem, such as streamflow reduction, flora and fauna stress, etc. The categorisation of the sounds depending on their source may provide the means for isolating and measuring variations and specific attributes that can be used for identifying the level of drought impacts. Three main sound categories can be distinguished: biophony (sounds produced by living organisms), geophony (sounds produced by the geophysical environment) and anthropophony (sounds produced by human activities) (Krause and Farina 2016). Identifying variations in specific categories can be used to assess the magnitude of drought episodes. For instance, geophonies produced by the sound of a river may indicate the level of drought effects on streamflow; specific variations on biophonies may be associated with stress levels of various species, etc.

Several tools of ecoacoustics can be used for analysing audio waveforms and provide means for further

statistical processing for identifying drought effects on an ecosystem. For example, the Acoustic Complexity Index (ACI) is an algorithm created to produce a direct quantification of the complex biotic songs by computing the variability of the intensities registered in audio-recordings, despite the presence of constant human-generated-noise (Pieretti et al. 2011). It is noted that, similarly to a typical drought analysis, a sufficient timeseries of data must be available, to identify the variation patterns in specific ecosystems.

Results and concluding remarks

The use of ecoacoustics in approaching drought is illustrated through an indicative example, based on data of a study by Krause and Farina (2016) and a comparison with typical drought analysis tools. More specifically, Krause and Farina (2016) analysed time series (2002 – 2015) of recordings from Sugarloaf Ridge State Park, located between the Sonoma and Napa valleys, California, USA, using ecoacoustic methods to survey the impacts of climate change on biodiversity. Through their analysis, the ACI of geophonies and biophonies at the study area were produced. The above study was selected due to the fact that it is based on a consistent series of recordings, using a calibrated protocol, in the same location and season of the year (mid-April), for a sufficient number of years. Additionally, the geophonies are principally constructed from the sound of a stream.

The above ACI outcomes are now compared with standard drought analysis tools, to examine whether they correspond to specific drought episodes. For this purpose, the drought conditions for each year (mid-April) are considered, based on US Drought Monitor (NDMC et al. 2018) and the values of the Standardised Precipitation Evapotranspiration Index (SPEI) from the SPEI global database (Begueria and Vicente-Serrano 2017). It is noted that SPEI calculation is based on FAO Penman-Monteith method.

The results show that ACI for both geophonies and biophonies are generally in line with drought conditions according to US Drought Monitor, with very low ACI values corresponding to the multi-year drought period 2013-2015. However, there is also a low ACI value for the year 2011, during which there were normal conditions. Regarding SPEI and ACI relationship, ACI values have better correlation with short reference periods (3 to 6-month) of SPEI. Indicatively, Pearson correlation value for SPEI-4 and ACI-geophonies is 0.47, while for SPEI-4 and ACI-biophonies is 0.34. The above indicate that the variations in geophonies and biophonies can be associated with drought episodes, while the timescales that seems to represent more accurately the magnitude of the effects coincides, approximately, to the first months of the hydrological year.

The above approach indicates the potential of ecoacoustics to be used for identifying drought impacts in an ecosystem. It appears that there is a dynamic basis for using the sense of sound to monitor and evaluate drought. This could be a starting point for further research on reconsidering and redefining drought, taking into account ontological and phenomenological dimensions.

References

Begueria S, Vicente-Serrano SM (2017) SPEIbase v.2.5 [Dataset]. http://dx.doi.org/10.20350/digitalCSIC/8508

Habermas J (1987) Lifeworld and System: A critique of functionalist reason. The theory of communicative action, vol. 2, Beacon Press, Boston

Krause B, Farina A (2016) Using ecoacoustic methods to survey the impacts of climate change on biodiversity. Biological Conservation 195:245–254. http://doi.org/10.1016/j.biocon.2016.01.013

Llusia D, Marquez R, Beltran JF, Benitez M, Do Amara J (2013) Calling behaviour under climatic change: geographical and seasonal variation of calling temperaturesin ectotherms. Global Change Biology 19(9):2655-2674

Morton T (2013) Hyperobjects: Philosophy and ecology after the end of the world. The University of Minnesota Press, Minneapolis, MN, USA

National Drought Mitigation Center (NDMC), US Department of Agriculture (USDA), National Oceanic and Atmospheric Association (NOAA) (2018) United States Drought Monitor. https://droughtmonitor.unl.edu

Pieretti N, Farina A, Morri D (2011) A new methodology to infer the singing activity of an avian community: The Acoustic Complexity Index (ACI). Ecological Indicators 11(3):868-873

Pijanowski BC, Villanueva-Rivera LJ, Dumyahn SL, Farina A, Krause B, Napoletano BM, Gage SH, Pieretti N (2011). Soundscape ecology: the science of sound in the landscape. BioScience 61(3):203–216

Scafer, R. M. (1994) Soundscape: Our Sonic Environment and the Tuning of the World. Destiny Books, Rochester, VT

Tigkas D, Vangelis H, Tsakiris G (2019) Drought characterisation based on an agriculture-oriented standardised precipitation index. Theoretical and Applied Climatology 135(3-4):1435-1447. http://doi.org/10.1007/s00704-018-2451-3

11th World Congress on Water Resources and Environment (EWRA 2019)
"Managing Water Resources for a Sustainable Future", 25-29 June 2019, Madrid, Spain

A regional depth-duration-frequency formulation for sub-hourly extreme rainfall estimates in Sicily under scale invariance

B. Bonaccorso*, G. Bringandì, G.T. Aronica
Department of Engineering, University of Messina, Messina, Italy
** e-mail: bbonaccorso@unime.it*

Introduction

Depth (or intensity)-duration-frequency (DDF or IDF) curves are commonly applied in hydrology to derive storms of fixed duration and return period for hydraulic infrastructures design and risk assessment. Usually, annual maxima rainfall (AMR) data from 1 to 24-hour duration are used to develop IDF curves. However, design of urban drainage systems or flood risk assessment in small mountain catchments often requires knowledge of very short-duration rainfall events (less than 1 hour), whose data are usually unavailable or too scarce for estimating reliable DDF curves (Nguyen et al. 1998; Aronica and Freni 2005; Borga et al. 2005). Regularities in the temporal pattern exhibited by storm records, known as scaling properties (Gupta and Waymire 1990; Koutsoyiannis and Foufoula-Georgiu 1993; Willems 2000), could help in characterizing extreme storms at partially gauged sites better than the application of traditional statistical techniques (Burlando and Rosso 1990).

In this work, a scaling approach for estimating the distribution of sub-hourly extreme rainfalls is presented with the aim of taking advantage both from high resolution rain gauges with short functioning period and from low resolution rain gauges with longer data samples. First, simple scaling versus multiple scaling assumption is verified for AMR data from 10 minute to 24 hour duration recorded by the gauge network of the Regional Agrometeorological Service of Sicily Region. Then, regional DDF curves under a scale-invariant framework are developed to estimate T-year sub-hourly extreme rainfalls at sites where only rainfall data for longer durations (≥ 1 hour) are available. Finally, validation of sub-hourly estimates with respect to historical observations shows the validity of the proposed approach for practical purposes, which provides reliable results through a parsimonious analytical formulation of DDF curves.

Materials and methods

Two rain gauge networks are used, producing respectively hourly and 10 min records. The hourly rainfall data are manually read from recorder charts of the rain gauges operated by the Water Observatory of Sicily Region (WOS), during the period 1928–2015. The 10 min dataset is provided by an automatic rain gauge network operated by the Sicilian Agrometeorological Service (SIAS), with records covering at most the 2002–2018 period. Starting from this dataset, we create new datasets at 10, 20, 30, 40, 50, 60, 180, 360, 720 and 1440 min durations respectively, by first aggregating over moving windows of corresponding width, and then by extracting AMR series at each duration and station. To ensure the accuracy in estimating extreme rainfall statistics, only rain gauges with record lengths longer than 15 years are chosen.

A GEV simple scaling model is assumed to develop the DDF scaling formulas. Under this assumption, the location, scale and shape parameters of AMR series of the GEV distribution for two different time scales d and $D_0=\lambda \cdot d$ are related as follows:

$$\mu_d = \mu_{D_0} \cdot \left(\frac{d}{D_0}\right)^k \quad \sigma_d = \sigma_{D_0} \cdot \left(\frac{d}{D_0}\right)^k \quad \text{and} \quad \xi_d = \xi_{D_0} \tag{1}$$

Therefore, the T-year GEV quantile of annual maxima rainfall of duration d, is given by:

$$h(d,T) = \left(\frac{d}{D_0}\right)^k \cdot \left\{\mu_{D_0} - \frac{\sigma_{D_0}}{\xi_{D_0}} \cdot \left[1 - \left(-\ln\left(1-\frac{1}{T}\right)\right)^{-\xi_{D_0}}\right]\right\} \tag{2}$$

In the present study, a reference duration D_0 equal to 1 hour is considered. The location, scale and

shape parameters at D_0 in Eq. (2) can be estimated from the 1-hour AMR series at WOS stations, while the scaling exponent *k* is transferred from SIAS stations to WOS stations by spatial interpolation.

Results and concluding remarks

Following Yu et al. (2004), the Probability Weighted Moments (PWMs) method is used to test the assumption of simple scale versus multiple scale invariance. This analysis reveals that the simple scaling regime holds from 20 to 60 minutes for 66 sub-hourly stations out of 69. For each sub-hourly station, the scaling exponent is computed as the mean of the slope values of linear regression relationships between the log-transformed values of PWMs and rainfall durations for various orders of PWMs. These values are, then, spatially interpolated by the Inverse Distance Weighted method (see Fig. 1, left hand side), so that *k* values can be assessed also for ungauged or partially gauged sites.

Hence, the regional GEV simple scaling model is tested on 20 long AMR series at hourly WOS stations for which 30 min records are also available. As an example, the matching between 30 min regional scaling quantiles and sample quantiles obtained for Acireale station, whose *k* estimate is equal to 0.49, is examined in Fig. 1 (right hand side). According to the Q-Q plots derived for all the considered sub-hourly stations, the suitability of the model to the samples may be outlined.

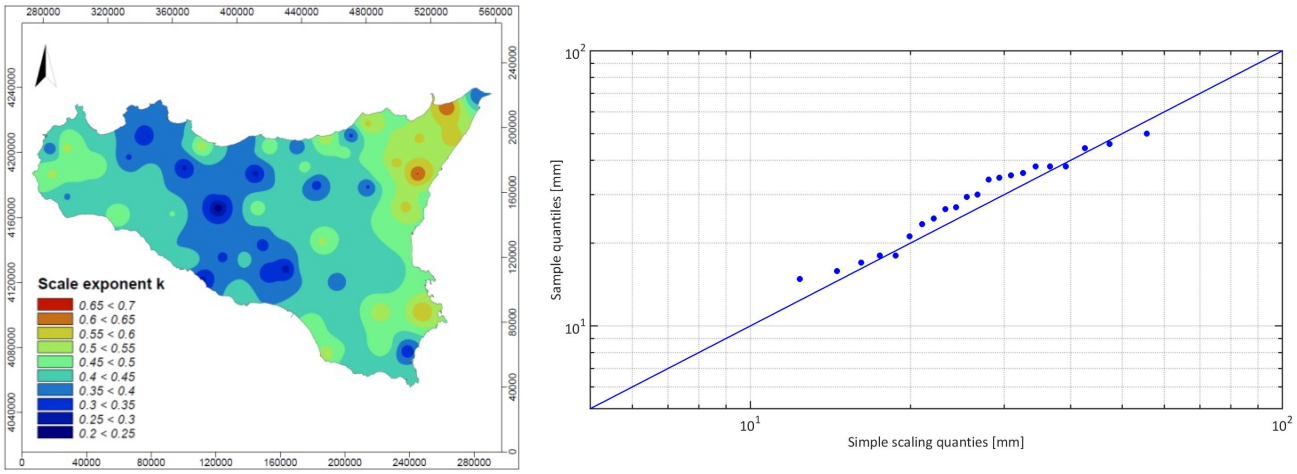

Figure 1. Spatial variation of k (on the left). Q-Q plot of 30-min AMR quantiles at Acireale station (on the right).

Derived results indicate that the proposed scaling approach could provide reliable sub-hourly AMR estimates in ungauged sites. Further research is underway to establish relationships between K values and geographical information.

References

Aronica GT, Freni G (2005) Estimation of sub-hourly DDF curves using scaling properties of hourly and sub-hourly data at partially gauged site. Atmospheric Research 77(1–4 SPEC. ISS.):114–123

Borga M, Vezzani C, Dall Fontana G (2005) Regional rainfall depth-duration-frequency equations for an alpine region. Natural Hazards 36(1–2):221–235

Burlando P, Rosso R (1996) Scaling and multiscaling models of depth–duration–frequency curves for storm precipitation. J. Hydrol. 187:45–64

Gupta VK, Waymire EC (1990) Multiscaling properties of spatial rainfall and river flow distributions. J. Geophys. Res.: Atmos. 95(D3):1999–2009

Koutsoyiannis D, Foufoula-Georgiu E (1993) A scaling model of storm hyetograph. Water Resour. Res. 29(7):2345–2361

Nguyen VTV, Nguyen TD, Wang H (1998) Regional estimation of short duration rainfall extremes. Water Science and Technology 37(11):15–19

Willems P (2000) Compound intensity/duration/frequency relationships of extreme precipitation for two seasons and two storm types. J. Hydrol. 233(1–4):189–205

Yu PS, Yang TC, Lina CS (2004) Regional rainfall intensity formulas based on scaling property of rainfall. J. Hydrol. 295 (1–4):108–123

11th World Congress on Water Resources and Environment (EWRA 2019)
"Managing Water Resources for a Sustainable Future", 25-29 June 2019, Madrid, Spain

Effect of shape parameters on earthen embankment failure due to overtopping

R.M. Kansoh[1*], M. Elkholy[2], G. Abo-Zaid[1]
[1] Irrigation Engineering and Hydraulics Department, Alexandria University, Alexandria, Egypt
[2] Civil and Environmental Engineering Department, Beirut Arab University, Tripoli, Lebanon
* e-mail: rkansoh@yahoo.com

Introduction

Selection of the appropriate mixtures of earthen embankments plays an important role in reducing the chances of failure of such crucial structures by overtopping, internal erosion or seepage, etc. In this study, the failure of compacted homogeneous non-cohesive earthen embankment due to overtopping has been experimentally investigated. Evolution of the breach shape is tracked using a sliding rod technique method together with an image processing technique utilizing a high-definition camera. Time of failure of the embankments is evaluated for different downstream slopes, crest width and embankment heights.

Lots of works have been done on modelling the shape of earthen embankments of non-cohesive sediments during the erosion process like the ones by: Singh and Scrlats (1988), where they developed simple analytical models for dam breach erosion; Visser (1998) identified three stages of erosion for earthen embankment of non-cohesive soil and developed a mathematical model; Coleman et al. (2002) experimentally studied breaching due to overtopping using different sizes of soil; Zhu et al. (2006) observed that erosion occurs first at locations close to the toe of the embankment; Schmocker and Hager (2010) studied overtopping through dikes of uniform non-cohesive sediment. They found that side wall has small effect on dikes with width of 0.1m and this effect disappeared for width of 0.2 m; Pickert et al. (2011) calculated a number of laboratory experiments to study failure mechanism of the breach process of homogenous non-cohesive embankment due to overtopping using different types of soil; Zhu et al. (2011) investigated physicals models and studied head cut erosion during embankment breach and studied the characteristics of embankment dam breach; Tabrizi et al. (2015) investigated embankment failure on a homogenous, non-cohesive and non-compacted soil; they used a sliding-rod technique to measure breach evolution shape, outflow and the water surface and Tabrizi et al. (2017) investigated the effect of soil compaction energy using different compaction levels on embankment breach process due to overtopping.

The objective of this paper is to investigate the effects of the downstream slope, crest width and embankment height on embankment breach process due to overtopping.

Materials and methods

Experimental measurements of the profile of an earthen embankment due to overtopping are done in the Hydraulic Laboratory of Alexandria University. A trapezoidal embankment of uniformly distributed sediment is constructed in a flume in different layers; each is 0.1 m thick and is compacted with a standard proctor test, a pilot channel is cut through the embankment crest to allow water to pass over to initiate the overtopping process. The tests started by pumping water into the flume until the required height, for each experiment. Five different mixtures are tested, one for pure sand (S), second for pure gravel (G1 and G2) and others for sand-gravel mixtures (SG1, SG2 and SG3). Two high-definition cameras are used, one on the side of the flume to record the erosion process for the different studied cases and the other on the downstream end to track the water level above the rectangular weir at the end of the flume to later estimate the discharge and aid in the hydrograph analysis.

Results and concluding remarks

The results show that the downstream slopes have a major effect in changing the failure modes of the embankment. Figure 1 shows the shape of the embankment as function of time, where X* and Z* are the

normalized horizontal and vertical distances, respectively. For small downstream slope of 5:1 (H:V), and 10:1, the erosion of the downstream slope takes place along a pivot point located above the bed of the embankment where the base length of the embankment increases by time. However, for higher values, the pivot point is located on the base of the embankment and the base length of the embankment decreases by time till it reaches equilibrium.

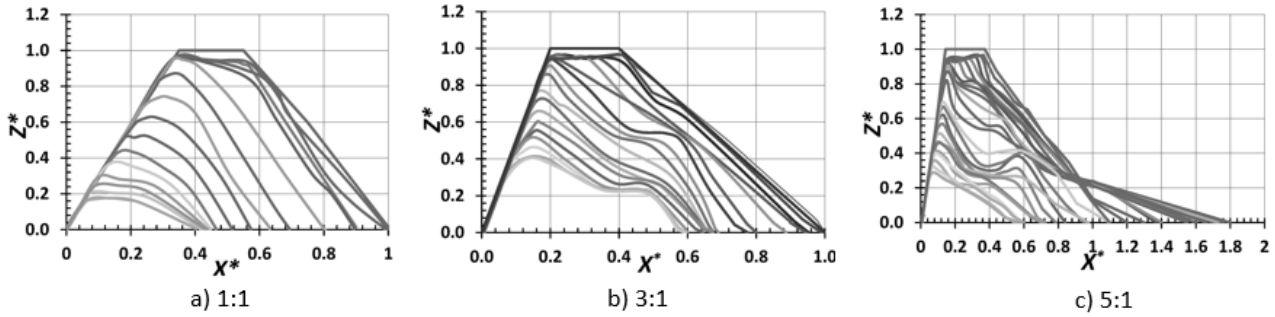

Figure 1. Effect of changing the downstream slope on erosion process.

Also, it is found that using mixtures of gravel/sand materials affect the time of failure. Increasing the percentage of sand to gravel from 0.5 to 2% causes an exponential increase of the time of failure by 63%. The 3D breach shape and the parameters noted in the experiments are shown and illustrated in details.

References

Coleman SE, Andrews DP, Webby MG (2002) Overtopping breaching of noncohesive homogeneous embankments. Journal of Hydraulic Engineering 128(9):829-838

Pickert G, Weitbrecht V, Bieberstein A (2011) Breaching of overtopped river embankments controlled by apparent cohesion. Journal of Hydraulic Research 49(2):143-156.

Schmocker L, Hager WH (2010) Overtopping and breaching of dikes—breach profile and breach flow. In: Proceedings of the International Conference on Fluvial Hydraulics - Riverflow 2010, pp. 515-522

Singh VP, Scarlatos PD (1988) Analysis of gradual earth-dam failure. Journal of Hydraulic Engineering 114(1):21-42

Tabrizi AA, Elalfy E, Elkholy M, Chaudhry MH, Imran J (2017) Effects of compaction on embankment breach due to overtopping. Journal of Hydraulic Research 55(2):236-247

Tabrizi AA, Elalfy E, LaRocque LA, Chaudhry MH, Imran J (2015) Experimental modeling of levee failure process due to overtopping. In: Annual Meeting of the Association of State Dam Safety Officials (ASDSO), September 2015, New Orleans, LA, USA

Visser PJ (1998) Breach growth in sand-dikes. Delf University of Technology

Zhu Y, Visser PJ, Vrijling JK (2006) Laboratory observations of embankment breaching. Proceedings of the 7th International Conference on HydroScience and Engineering, September 10-13, 2006, Philadelphia, USA

Zhu Y, Visser PJ, Vrijling JK, Wang G (2011) Experimental investigation on breaching of embankments. Science China Technological Sciences 54(1):148-155

11th World Congress on Water Resources and Environment (EWRA 2019)
"Managing Water Resources for a Sustainable Future", 25-29 June 2019, Madrid, Spain

Self-financing the purchase of water for environmental purposes through a public water bank

C. Gutiérrez-Martín*, J.A. Gómez-Limón, N. Montilla-López
WEARE Research Group, Department of Agricultural Economics, Universidad de Córdoba, Córdoba, Spain
** e-mail: carlos.gutierrez@uco.es*

Introduction

In closed basins, where it is not possible to further increase water supply, the environment is often negatively affected by an excessive extraction of water, which jeopardizes the maintenance of the associated ecosystems. This problem is especially acute during drought periods. Given this situation, there are different ways to recover water for the environment instead of consumptive uses (Crase et al. 2012), including market instruments for the acquisition of water rights through buy-backs (e.g. Wheeler et al. 2013) or allocation trading (Hanak and Stryjewski 2012) from the agricultural sector. These economic instruments are implemented and managed by water banks, institutions usually of public nature which centralizes all market operations, both purchases and sales.

Although market instruments are more cost-effective than investments in infrastructure when recovering water for environmental purposes (Wheeler and Cheesman 2013), public budget constraints are a major obstacle to the establishment of water banks for environmental purposes (Burke et al. 2004). To overcome this problem, the innovative solution provided by this work is to develop a water bank with the twofold objective of reallocating water within the agricultural sector and recovering a share of the purchased water for the environment during drought periods (allocation trade), without any public spending on environmental purchases (i.e., self-financing the purchase of water for environment).

Materials and methods

The starting point for our proposal is a water bank for the reallocation of water within the agricultural sector. Figure 1a explains a situation in which the water bank, acting as a monopoly, buy temporal water rights (allocations) from willing sellers to subsequently reallocate them at the same price to willing buyers. The objective of this water bank would be to maximize the water use efficiency that, following economic theory, is reached in the equilibrium point where supply and demand curves intersect so that quantities (Q_p and Q_{sa}) and prices (P_p and P_s) are equal both for purchases and sales. Acting in this way, the performance of this water bank is the same than a competitive spot water market.

The efficiency generated by the water bank purchases is calculated through the *producer surplus* (S_p), measuring the profit beyond the marginal value of water that a water user obtains when he or she sells his/her water allocation to the bank instead of using it (if water is sold at a price P_p as shown in Figure 1a, then S_p is equivalent to the $P_pAP_p{}^0$ area). On the other hand, the efficiency generated by the water bank sales is calculated through the *consumer surplus* (S_{sa}), accounting for the surplus that water users gain when they purchase the water from the bank at a price lower than their marginal value of water (if water is bought at a price P_s, then S_{sa} can be measured as the $P_{sa}{}^0BP_s$ area).

Starting from this point, the public water agency may use the monopoly power of the water bank to create a gap (Q_{se}) between Q_p and Q_{sa} which will be recovered for the environment as shown in Figure 1b. However, similar to consumer surplus for purchases by productive users (S_{sa}), there is another kind of consumer surplus for the resources recovered for environmental uses (*environmental surplus*, S_e), which can only be assessed if the social demand for environmental water is taken into account. This surplus can be measured as the extra benefit that society gains when environmental water is obtained from the water bank at a cost below its marginal social value (V), which is determined by society's demand curve for environmental water $Q_{se}(V)$. For the shake of simplicity, the environmental demand is supposed linear, intersecting the ordinate axis at V^0 and the abscissa representing the gap between stream flows in a

situation of water scarcity and the average stream flows. Introducing society's demand curve for environmental water into the analysis, this demand must be added to the productive water demand to give an aggregate demand $Q_s(P_s)$ for productive and environmental water at any price P_s (equal to the marginal value of water for the environment, V).

To recover water for environmental purposes, compared with the situation described in Figure 1a, a lower quantity of water Q_p is purchased at a lower price (P_p), and later only a share of this volume bought (Q_{sa}) is sold back to irrigators at a higher price P_s, while another share (Q_{se}) is recovered for the environment. The gap between quantities and prices in the water purchase and sale makes possible that the expenditure in the purchase of water equals the revenue from sales, reaching a financial balance that avoid the use of any additional public funding.

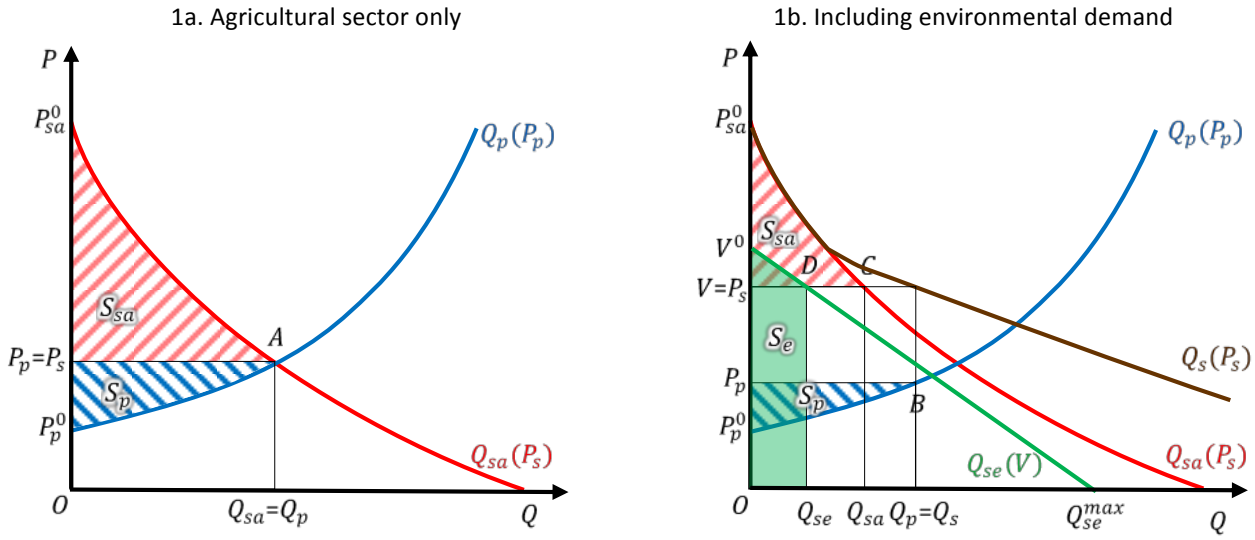

Figure 1. Equilibria reached by the water bank maximizing total efficiency.

Results and concluding remarks

We can conclude that the proposed self-financed water bank with the twofold objective of reallocating water between farmers and recovering water for environmental purposes can be considered an interesting policy option from an efficiency point of view. It is remarkable that, for high social values of environmental water (where the maximum environmental value lies somewhere above the competitive market equilibrium price), the proposed water bank outperforms a water bank that only reallocates water within the agricultural sector, since the gains in environmental surplus (S_e) are higher than the losses in purchase and sale surpluses (S_p and S_{sa}). Finally, it should be noted that this design of water bank can be easily modelled using mathematical programming to evaluate the ex-ante performance in a case study knowing the shape of the supply and demand curves.

References

Burke SM, Adams RM, Wallender WW (2004) Water banks and environmental water demands: Case of the Klamath project. Water Resources Research 40(9):W09S02. http://doi.org/10.1029/2003WR002832

Crase L, O'Keefe S, Kinoshita Y (2012). Enhancing agrienvironmental outcomes: Market-based approaches to water in Australia's Murray-Darling Basin. Water Resources Research 48(9):W09536. http://doi.org/10.1029/2012WR012140

Hanak E, Stryjewski E (2012) California's water market, by the numbers: Update 2012. Public Policy Institute of California, San Francisco, USA

Wheeler SA, Cheesman J (2013) Key findings from a survey of sellers to the restoring the balance programme. Economic Papers 32(3):340-352. http://doi.org/10.1111/1759-3441.12038

Wheeler SA, Garrick D, Loch A, Bjornlund H (2013) Evaluating water market products to acquire water for the environment in Australia. Land Use Policy 30(1):427-436. http://doi.org/10.1016/j.landusepol.2012.04.004

11th World Congress on Water Resources and Environment (EWRA 2019)
"Managing Water Resources for a Sustainable Future", 25-29 June 2019, Madrid, Spain

Effects of the 2016-2018 drought on Pequenos Libombos reservoir (Maputo, Mozambique): A comparative analysis

M. Bermúdez[1,2*], M. Álvarez[1], J. Puertas[1], E. Peña[1*], R.J. Araneda[1]
[1] Water and Environmental Engineering Group (GEAMA), Universidade da Coruña, A Coruña 15071, Spain
[2] Environmental Fluid Dynamics Group, Andalusian Institute for Earth System Research, University of Granada, Spain
* e-mail: mbermudez@udc.es

Introduction

Droughts are amongst the most destructive natural hazards and occur throughout the world. Mozambique, a country within Southern Africa region, is one of the poorest countries and is classified as a Least Developed Country (LDC) with the tenth-lowest Human Development Index (HDI) in the world. At the same time, Mozambique is highly exposed to drought conditions, specially its south and central provinces. During the period 1970-2017, Mozambique experienced roughly 12 droughts that killed more than 100000 people, affected more than 20 million and caused economic damage by 50000 10^3 USD (EM-DAT 2018). As a consequence, the socio-economics impacts of droughts on the population and infrastructure are compounded by the widespread deep poverty and lack of resilience.

In this study we analysed the last drought event experienced in the region (years 2016-2018), and compared it with other relevant past drought events. We then evaluated its impact on Pequenos Libombos (PL) reservoir storage. The PL reservoir, located on the Umbeluzi River, has a total capacity of 392 million m^3, and is the main source of urban water supply (~ 80 %) to Maputo city and the villages of Matola and Boane. The ultimate objective of this study is to investigate the possibility of implementing a Drought Early Warning System (DEWS) for monitoring and management PL reservoir, and to facilitate the implementation of effective emergency response programmes to reduce the impact of drought (WMO 2014).

Materials and methods

In order to characterize drought, we used the Standardised Precipitation Index (SPI), as recommended by the World Meteorological Organization (WMO 2012). Precipitation data were obtained from the gridded monthly observed dataset CRU TS 4.01 at 0.5° horizontal resolution (Harris et al. 2014). This dataset does not include at present years 2017 and 2018, which were taken from the GPCC monitoring analysis (Schneider et al. 2015). Based on this data, we computed the SPI at 11 times scales (between 3 and 36 months). A comparative analysis of the 2016-2018 drought was conducted in relation to the most severe drought events that occurred in the last 30 years. The relation between drought events and El Niño Southern Oscillation (ENSO) was also analysed.

PL monthly reservoir storage data for the period 1990-2018 were provided by the Water Resources Department of the Southern Regional Water Management Administration (ARA-Sul) of Mozambique. These monthly storages were standardized (SS) by subtracting the mean long-term storage and dividing by the long term standard deviation, in order to allow direct comparison with SPI values. The SPI series for different time scales and the SS series were compared over period 1990-2018 by means of Pearson correlation coefficient (R).

Results and concluding remarks

The results showed that the SPI was able to identify the main drought events that affected the PL reservoir basin during the last 30 years, according to the historical drought records reflected in the international disaster database EM-DAT. An acceptable relationship at 28-month time scale between SPI and the SS was found (R ~ 0.6).

Since 2015, southern Mozambique has experienced the strongest El Niño phenomenon in its history with peak anomalies of 2.8 (very strong category). The drought characteristics (DC) of the 2016-2018 event

show a mean severity of -1.1 and maximum intensity of -1.73 (severe drought category) with a 30-month duration. As a consequence, the SS of PL reservoir reached its historical minimum. With only 19 % of its storage capacity, severe water supply restrictions were imposed during 2017 and 2018 in the metropolitan area of Greater Maputo and the region´s main irrigation systems.

In the comparative analysis with other historical drought events, special attention is given to the drought episode occurred in 1997 year. The DC of this event indicate that it was even more severe than the 2016-2018 drought, with a mean severity of -1.3, a maximum intensity of -1.98 and a 51 month-duration. This drought also developed during the warm phase of ENSO, El Niño 1998, which was classified as strong, although slightly weaker than El Niño 2016. Notably, the SS was comparatively less affected than by the 2016-2018 drought, reaching -0.89 (11/1992), which represents 53% of the storage capacity of PL reservoir.

A time lag of 10 months was found between El Niño peaks and the maximum intensity of drought events, based on 28-month SPI. The drought events identified by SPI in this study coincide with de warm phase of ENSO, and a strong relationship between the ENSO and drought in the PL reservoir exists, at least in relation to the analysed events.

The different effects of drought on the reservoir across events can be related, among others, to the management and operation of the PL reservoir, as well as the remarkable population growth experienced by the Greater Maputo during the last 30 years. At present, regardless of drought conditions, the PL reservoir is insufficient to meet the needs of water supply and the water authorities of Mozambique are searching for new alternatives. Meanwhile, this study opens the possibility of implementing a DEWS that facilitates the operational management of the PL reservoir, and can contribute to the development of preparedness plans and emergency response programmes to increase the coping capability and reduce the impact of drought in the province of Maputo. The severe drought of 2016-2018 has resulted in an increase of responsibilities for women and an exacerbation of their vulnerabilities (CARE 2016). The adoption of the proposed measures can have a beneficial impact on civil society, especially on women and girls, who represent more than 83% of the Mozambican population.

Acknowledgments: The authors would like to acknowledge the Spanish Regional Government of Galicia (Galician Cooperation Agency and Augas de Galicia foreign action office) for funding the project COOPERACION GALEGA PR815A-2017-5. The authors would also like to thank the assistance provided by the technical staff of Water Resources Department of Southern Regional Water Management Administration (ARA-Sul). María Bermúdez gratefully acknowledges funding from the European Union's Horizon 2020 research and innovation programme under the Marie Skłodowska-Curie grant agreement Nº 754446 and UGR Research and Knowledge Transfer Found – Athenea3i.

References

CARE (2016) Hope dries up? Women and Girls coping with Drought and Climate Change in Mozambique results in an increase of responsibilities for women. Maputo, Mozambique: CARE International in Mozambique. Retrieved from http://careclimatechange.org/wp-content/uploads/2016/11/El_Nino_Mozambique_Report_final

EM-DAT (2018) The Emergency Events Database - Université catholique de Louvain (UCL) - CRED - www.emdat.be, Brussels, Belgium

Harris I, Jones P D, Osborn T J, Lister D H (2014) Updated high-resolution grids of monthly climatic observations—the CRU TS3.10 dataset. International Journal of Climatology 34:623–42

Schneider U, Becker A, Finger P, Meyer-Christoffer A, Ziese M (2015) GPCC Monitoring Product: Near Real-Time Monthly Land-Surface Precipitation from Rain-Gauges based on SYNOP and CLIMAT data. https://doi.org/10.5676/DWD_GPCC/MP_M_V5_100

WMO (2012) Standardized Precipitation Index User Guide. WMO-No.1090, Geneva

WMO (2014) National Drought management Policy Guidelines: A Template for Action. Integrated Drought Management Programme (IDMP) Tools and Guidelines Series 1. WMO, Geneva, Switzerland and GWP, Stockholm, Sweden

Scenario analysis for energy optimization of pumping plants in complex water supply systems

J. Napolitano*, G.M. Sechi
Department of Civil and Environmental Engineering and Architecture, University of Cagliari, Cagliari, Italy
** e-mail: jacopo.napolitano@unica.it*

Introduction

The management of complex water supply systems needs a close attention to economic aspects concerning high costs related to energetic management (Pasha and Lansey 2014). Specifically, the optimization of water pumping plants activation schedules is an important issue, especially managing strategic and costly water transfers under drought risk (Asefa et al. 2014; Matheus and Tullos 2016). In such management context and under uncertainty conditions, it is crucial to assure simultaneously energy savings and water shortage risk alleviating measures. The model formulation needs to highlight these requirements duality: to guarantee an adequate water demands fulfilment respecting an energy saving policy.

The obtained results should allow the water system's Authority to get a robust decision policy, defining optimal rules and, specifically, the definition of optimal activation triggers for water pumping stations.

Materials and methods

This problem modelling approach has been developed using a two stages scenario analysis (Pallottino et al. 2004) with a cost-risk balancing approach (Gaivoronski et al. 2012; Napolitano et al. 2016), achieving simultaneously an energetic and operative costs minimization and assuring an adequate water demand level fulfilment for users. The water supply system has been schematized through a single-period flow network graph (basic graph) (Diestel 2005) and by its replicates obtaining the multi-period graph (Pallottino et al. 2004).

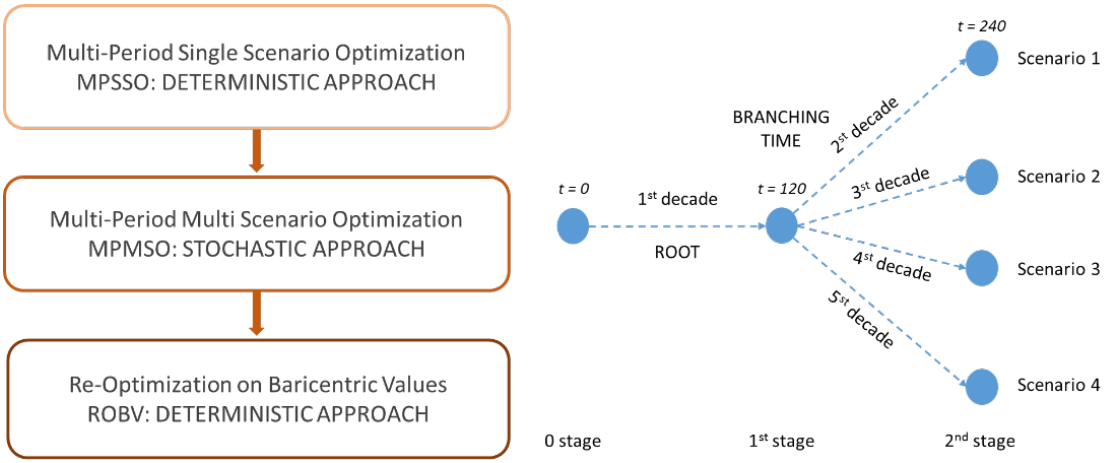

Figure 1. Main modelling steps and scenario tree aggregation

The optimization procedure (summarized in the flowchart shown in Figure 1) aims to identify the pump activation thresholds, mainly using reservoirs' storage volumes as trigger values in the pumps-activation decision. For each pump station, two seasons' activation thresholds should be identified, in order to define a barycentric seasonal value. These trigger values refer specifically to the dry (in Mediterranean countries months from April to September) and the wet (months from October to March) hydrological semester.

The scenario optimization model has been implemented using the software GAMS (2008) interfaced with CPLEX solvers specifically designed for modelling mixed integer optimization problems.

Results and concluding remarks

An application of the proposed optimization approach has been tested considering the draft of a real supply system located in a drought-prone area in South-Sardinia (Italy).

By applying the scenario-optimization process, a robust decision strategy for seasonal trigger values of pumps activation was retrieved. Reference scenarios were settled considering the regional hydrological database (RAS 2006) modified in order to take into account climatological trends in last decades and water resource reductions. As drafted in Figure 1, the database has been organized considering 4 hydrological scenarios of different criticism, where each one has been of 20 years, 240 monthly periods with the branching time located at the 120^{th} period.

The scenario-optimization methodology confirmed its potentiality when applied to the real-case. It allowed identifying two seasonal optimal activation thresholds for each pumping plant located in the water system. Moreover, the cost-risk balancing approach minimized the O&M costs and contextually restricted risks and conflicts between users in shortage conditions.

Costs and penalties have been evaluated in a simulation phase through an economic post-processor taking into account water shortages penalties and pumping costs. Deficit occurrences could remain into "planned shortages", which the user is asked to accept under drought conditions or into "unplanned shortages", which could occur in very critical scenarios, due to severe and not expected lack of resource.

In order to build a model more adherent to the reality, the effectiveness of the obtained results has been tested interacting with the regional water system's Authority by comparison with the occurred management behaviour.

References

Asefa T, Clayton J, Adam A, Anderson D (2014) Performance evaluation of a water resources system under varying climatic conditions: reliability, resilience, vulnerability, and beyond. Journal of Hydrology 508:53-65. https://doi.org/10.1016/j.jhydrol.2013.10.043

Diestel R (2005) Graph Theory. Springer-Verlag, New York

Gaivoronski AA, Sechi GM., Zuddas P (2012) Balancing cos-risk in management optimization of water resource systems under uncertainty. Physics and Chemistry of the Earth 42-44:98-107. https://doi.org/10.1016/j.pce.2011.05.015

GAMS (2008) A user's guide. GAMS Development Corporation, Washington DC, USA

Mateus MC, Tullos D (2016) Reliability, sensitivity, and vulnerability of reservoir operations under climate change. Journal of Water Resources and Planning Management 143:257-265. 10.1061/(ASCE)WR.1943-5452.0000742

Napolitano J, Sechi GM, Zuddas P (2016) Scenario optimization of pumping schedules in a complex water supply system considering a cost-risk balancing approach. Water Resource Management 30:5231-5246. https://doi.org /10.1007/s11269-016-1482-8

Pasha MFK, Lansey K (2014) Strategies to develop warm solutions for real-time pump scheduling for water distribution systems. Water Resource Management 28(12):3975-3987. https://doi.org/10.1007/s11269-014-0721-0

RAS (2006) Piano stralcio di bacino regionale per l'utilizzo delle risorse idriche. Regione Autonoma della Sardegna, Italy

11th World Congress on Water Resources and Environment (EWRA 2019)
"Managing Water Resources for a Sustainable Future", 25-29 June 2019, Madrid, Spain

Importance of updating hydrologic frequency analysis in countries with short hydrometric records: Case study, Oman

A.M. Al Qurashi
Oman Society of Engineers
** e-mail: aisha10q@hotmail.com*

Introduction

The Sultanate of Oman has a distinctly arid climate. Average annual rainfall ranges from 50 mm to 350 mm with less than 100 mm nationwide and with high temporal and spatial variability. Other typical arid zone characteristics include flash flooding, the absence of base flow, sparsity of plant cover and high transmission, evaporation and evapotranspiration losses. There is no wet or dry season, except in the southern Dhofar Governorate near the city of Salalah, where the khareef monsoon brings a very localised 3-month wet period from June to August.

The Sultanate is experiencing rapid development and needs to improve floodplain planning and management. Reliable rainfall and flood frequency data are required for risk analysis for new development. Several, standard approaches to hydrological frequency analysis were found to be inapplicable in this arid region due to short record periods and some special hydrological characteristics (Al-Qurashi et al. 1997). The paper shows the necessity of updating frequency analysis in arid areas, describes the experience in Oman, and discusses the difficulties encountered.

Materials and methods

Three standard methods and variations of them were tested to analyse flood data for selected stations. The first involved peak-over-threshold (POT), or partial series data, with log return period plotting using the same number of events as years of data (Al-Qurashi et al. 1997).

The second approach utilized annual series data with log-Pearson III, where the third utilized annual series data with Gumbel method. It was found that the large number of zero or near zero events, particularly in the annual series, had to be discarded from best line-fitting.

One of the objectives of the exercise was to attempt to assess regional flood characteristics throughout Oman, making a standardised approach desirable. It was found that best line-fitting from the 50% point upwards was generally appropriate (Pilgrim 1987). In the case of the POT analysis, straight line fitting was shown to be generally more suitable and avoided too much emphasis on individual highest events which curve-fitting would introduce.

It was noted that, the station-year approach is useful where, as for Oman, the data period is very short. However, in Oman, occasional heavy storms tend to be widespread events covering most of the north or south of the country. Hence, it is not reasonable to assume that flood and storm events are independent events at each hydrometric station, and this largely precludes use of the station-year approach.

The POT method was also used for rainfall frequency analysis but in this case, all points (not just above the 50% rank, as in flood peak analysis) were used in best line-fitting. It was noticed that using the same method for Dhofar resulted in poor line-fitting. As Dhofar coast is subjected to occasion cyclones, it might be advisable to separate the different storm types, so that very mixed statistical populations can be avoided.

Results and concluding remarks

Flood and rainfall characteristics of Oman vary from north to south and from the cyclone-affected coast line to the interior, requiring differing analytical treatment.

Records show that prior to 2007, the greatest storm and flood known to affect Muscat occurred in June 1890 nearly 130 years ago. It was a full-blown cyclone which dumped 286 mm on Muscat. More recently

Cyclone Gonu (June 2007) produced a 1-day rainfall of over 700 mm in Wadi Dayqah and about 1,033 mm in 34 hours at Jabal Asfar. Until recently the highest 1-day recorded rainfall in Dhofar Governorate was 333 mm, but in May 2018 Cyclone Mukunu produced 1-day rainfall 663 mm and about 864 mm in 72 hours at Shibob Rainfall Station.

Table 1 illustrates the effect of updating rainfall and flood frequency analyses and highlights the implications for selection of design storms for hydraulic analysis and flood risk assessments, using different period of records.

Table 1. Flood peak frequency for Wadi Miglas (Muscat Governorate) for different period of records

Station	Wadi	Station ID	Period of Record	Area km²	Mean (MAF) m^3/s	Flood Peak Frequencies - m^3/s Return Period - yrs 5	10	20	50	100	200
Quriyat	Miglas	FA877343AD	79-06	554	112	281	463	644	884	1065	1247
			79-07*		240	523	1136	1750	2561	3174	3788
			79-2010**		287	591	1297	2004	2938	3645	4352
			79-2010***		113	254	430	605	837	1012	1188

Note :

*Including Gonu

**: Including Gonu and Phet

***: Excluding Gonu and Phet

The results show that flood peak frequencies for different record periods are very sensitive to updated analysis. Flood peak frequencies values of the 5-year return period increased from 281 to 591 m^3/s by including both Gonu and Phet events and from 1,065 to 3,645 m^3/s for the 100-year. These frequencies decrease for both return periods if both the Gonu and Phet events are excluded, which shows how important it is to also include severe events when updating frequency analyses.

In areas with short record periods, it is important to update frequency analyses periodically to check that 100-year or 200-year predicted floods are within the realms of reality and also recognize the potential impact of major events.

For arid regions, where most of the time it is dry, long record periods are required to establish flood and storm characteristics. A few occasional severe storm events or unusual droughts can dominate short period data and lead to potentially misleading projections. (Al-Qurashi et al. 1997). In areas with short record periods, regular updating of hydrologic frequency analyses provides a rational check on rainfall and flood frequency projections.

References

Al Qurashi AM, Kaul F, Calma T (1997) Constraints in traditional hydrological frequency analysis methods when applied to Oman. Third Gulf Water Conference, Muscat, Sultanate of Oman

Al-Qurashi AM (2013) Achieving Sustainable Water Resources Management in the Sultanate of Oman. Oman Power and Water Summit, Muscat, Oman

Pilgrim DH (1987) Australian rainfall and runoff: a guide to flood estimation. The Institution of Engineers, Australia

11th World Congress on Water Resources and Environment (EWRA 2019)
"Managing Water Resources for a Sustainable Future", 25-29 June 2019, Madrid, Spain

A robust method to update local IDF curves and flood maps using global climate model output and weather typing based statistical downscaling

M. Bermúdez[1,2], L. Cea[2*], E. Van Uytven[3], P. Willems[3], J. Puertas[2]
[1] *Environmental Fluid Dynamics Group, Andalusian Institute for Earth System Research, University of Granada, Spain*
[2] *Environmental and Water Engineering Group, Universidade da Coruña, Spain*
[3] *Department of Civil Engineering – Hydraulics Section, KU Leuven, Belgium*
** e-mail: mariabermudez@ugr.es*

Introduction

Global warming is changing the magnitude and frequency of extreme precipitation events. This requires updating local rainfall intensity-duration-frequency (IDF) curves and flood hazard maps according to the projected changes. This is however far from straightforward, given our limited ability to model the effects of climate change on the temporal and spatial variability of rainfall at small scales.

In this study we develop a robust method to update local IDF relations for sub-daily rainfall extremes using Global Climate Model (GCM) data. A weather typing statistical downscaling method is applied to climate projections, and IDF curves for the future climate are determined. A hydrological-hydraulic modelling chain is then used to quantify the changes on flood risk maps induced by the IDF changes.

Materials and methods

The proposed methodology was applied to estimate the impact of future climate change on precipitation extremes and flood risk in the coastal town of Betanzos, located in a 437 km^2 basin in the NW of Spain. A 10-minute resolution basin-averaged rainfall series covering the period 2001-2017 was computed using measured data from a pool of 11 stations. The Lamb circulation type (LCT) classification of Trigo and DaCamara (2000) was used to characterize the daily large-scale atmospheric circulation. Daily mean sea level pressure (SLP) to calculate historical LCTs frequency was extracted from the ERA Interim dataset (period 1979-2015). High precipitation events were extracted from the historical time series, and the number of events associated to each LCT was evaluated.

A set of 97 GCM runs was used in this study to assess future LCTs' occurrence (period 2071-2100), and a weather type statistical downscaling method was applied to obtain time series of precipitation for future scenarios. WTs and temperature were used as large-scale predictors, while the local-scale predictant was the daily precipitation accumulation. Analog days were identified in the historical data to form the downscaled precipitation dataset.

The Gumbel extreme value distribution was used to evaluate the IDF curves from the precipitation data. For this purpose, the rainfall series were divided into segments according to the WTs, such that each subseries contained the rainfall events associated to a particular WT only. In this way, IDF relations were developed for each WT separately and then composed into a single IDF curve. This was done for the historical precipitation data and for the future precipitation series obtained from each of the 97 GCMs considered in this study.

From the future IDFs, the 50-year synthetic design storm was built using the Alternating Block Method. A calibrated HEC-HMS hydrological model of the basin was used to compute the 50-year flood hydrograph, which was then introduced in the 2D hydrodynamic model Iber (Bladé et al. 2014) to evaluate inundation hazard maps in the urban area of Betanzos.

Results and concluding remarks

The analysis of extreme events and LCT frequencies showed that the majority of intense precipitation events occur in winter and autumn, associated with weather types cyclonic (C), west (W) and southwest (SW). The analysis of future LCTs shows a large spread in the frequency change estimates. The median

predictions show a decrease in the C types throughout the year, and a slight increase of SW and W types in winter. For most of the seasons and LCTs, changes are stronger for higher Representative Concentration Pathways (RCP) scenarios.

The downscaled rainfall projections show a wide spread among GCMs, which consequently results in large uncertainty in IDF relationships. The median IDF curves for future period, calculated from all the downscaled GCMs, show an increase in rainfall intensity for all rainfall durations (Figure 1). This results in increased flood hazard in the urban area compared with current estimates for the same return period.

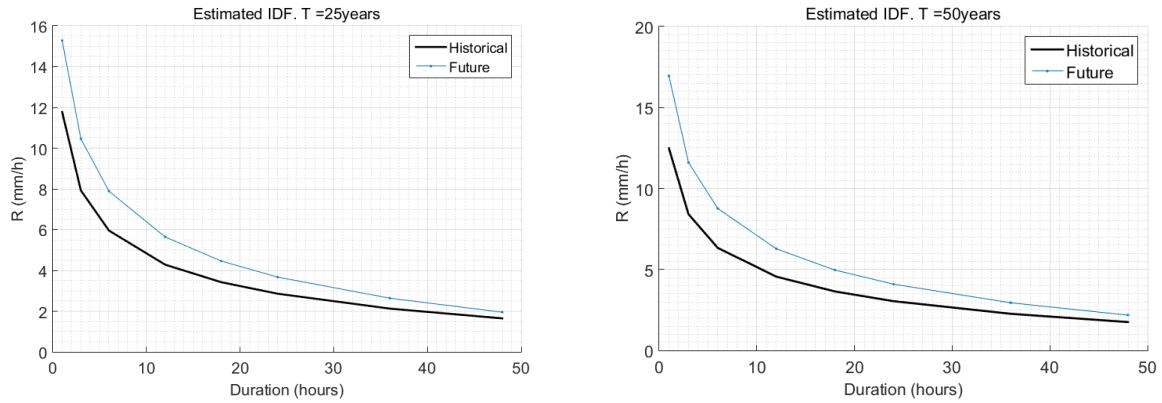

Figure 1. Historical and projected median IDF curves showing 25-year (left) and 50-year (right) recurrence interval precipitation intensities.

The results show that existing IDF standards need to be updated to reflect potential changes in future extreme rainfall intensities. Although the results presented use the best available information concerning future climate change, huge uncertainties remain. Therefore, besides updating IDF relations, engineering design guidelines that incorporate climate change need to ensure flexibility to adjust to future conditions and adaptability to unexpected change.

Acknowledgments: M. Bermúdez gratefully acknowledges funding from the European Union's Horizon 2020 research and innovation programme under the Marie Skłodowska-Curie grant agreement Nº 754446 and UGR Research and Knowledge Transfer Found – Athenea3i. E. Van Uytven is financially supported by a PhD fellowship of the Research Foundation -Flanders. We thank ECMWF project for making their data available.

References

Trigo RM, DaCamara CC (2000) Circulation weather types and their influence on the precipitation regime in Portugal. International Journal of Climatology 20(13):1559-1581

Bladé E, Cea L, Corestein G, Escolano E, Puertas J, Vázquez-Cendón ME, Dolz J, Coll A (2014) Iber: herramienta de simulación numérica del flujo en ríos. Revista Internacional de Métodos Numéricos para Cálculo y Diseño en Ingeniería 30(1):1-10

11th World Congress on Water Resources and Environment (EWRA 2019)
"Managing Water Resources for a Sustainable Future", 25-29 June 2019, Madrid, Spain

Rain gauge network extension using a simulated annealing heuristic: main challenges in calibration of algorithm parameters

A. Chebbi[1,3], M.C. Cunha[2*], Z. Bargaoui[3]
[1] Higher Institute of Applied Sciences and Technology of Sousse, University of Sousse, Taffala City (Ibn Khaldoun), 4003 Sousse, Tunisia
[2] INESC Coimbra, Department of Civil Engineering, University of Coimbra, Coimbra, Portugal
[3] National School of Engineering of Tunis, Laboratory of Modelling in Hydrology and Environment, Tunis, Tunisia
* e-mail: mccunha@dec.uc.pt

Introduction

Rain gauge networks help to quantify the spatial distribution of rainfall intensity and estimate rainfall statistics, which can then be used to design hydraulic structures and manage water and environmental resources. In this paper, a simulated annealing (SA) algorithm is analysed to optimise the augmentation of a rain gauge network. Simulated annealing is a stochastic global optimization technique based on some internal parameters. It is worth noting that the effectiveness of solutions based on SA mainly depends on how carefully one determines these control parameters. This fact has been emphasized since early works on the application of SA to the management of environmental systems (Cunha 1999, Nunes et al. 2004 and Chebbi et al. 2017). The contribution of this paper is to set out a methodology to calibrate internal (control) parameters of the SA algorithm in the specific context of a rain gauge augmentation and considering observed short duration (1 h) maximum rainfall intensity fields. Thus, the main contribution of this work is a tuning of SA control parameters to improve the speed of solution convergence without compromising accuracy.

Materials and methods

Rainfall networks are actually part of flood and environmental warning systems and flood forecasting systems. The network density (number of observation sites per km²) and configuration (geographical location of the observation sites) are key factors that impact on areal rainfall estimation accuracy. We first define a general purpose underlying the network extension project (see a literature review on this subject in Chebbi et al. 2011). This objective is to improve the accuracy of estimating the areal distribution of maximum 1h- rainfall intensity observed during the event. In fact, one hour intensity is a suitable duration for discharge prediction in moderate size catchments. Two well documented rainy events were considered to derive the rainfall spatial variability features. Kriging tools are used for spatial interpolation (Chebbi et al. 2013). The semi-variogram is adopted to reflect the spatial variability of the maximum 1h-intensity field which is considered as a regionalized variable Z. We also assume that Z is a stationary random function with known mean m and variance σ^2. The semi-variogram is defined as one half of the variance between two locations separated by h, where h is the inter-distance vector and x is the location vector. The experimental semi-variogram is computed from data pairs of observations measured at each station over the course of the event for specific distance lags and directions. Here we consider a global variogram, taking all directions together. The sample variogram is then fitted to a variogram model. Ordinary Kriging (OK) is selected to interpolate rainfall intensity in non-sampled locations x_i. The computation points are the nodes of a squared grid covering the study domain. The optimization problem is the minimizing of the objective function (OF) defined here as the average kriging variance of error over grid nodes σ_i^2.

$$OF = \sum_{i=1}^{n} \sigma_i^2 \Big/ n \tag{1}$$

where n is the number of grid nodes.

Simulated annealing was introduced by Kirkpatrick et al. (1983) as an algorithm for solving well known combinatorial optimization problems. There are recent review articles that provide a good overview of the theoretical development of simulated annealing and its application in various hydrological and hydraulic systems problems (e.g., Zeferino et al. 2009 and Vieira and Cunha 2017). Many efforts have been dedicated to get the most optimal SA parameters for these optimization problems. In this work, we propose a new approach for tuning the control parameters of the simulated annealing algorithm used to search for the optimal location of new rain gauges. In fact, this paper examines both effects of the number of new locations and the variogram model on the SA internal parameters**.** Four SA control parameters are investigated (elasticity of acceptance *EA* which is linked to initial temperature, cooling rate factor α, minimum chain length n_1 and limit percentage of accepted moves P_{lim}). Four criteria are adopted to calibrate these parameters using various replicates of Monte Carlo runs: the percentage of solution acceptance, the decrease in the value of objective function at optimum, the number of iterations and the number of optimal solutions.

Results and concluding remarks

A sensitivity analysis of the optimal SA tuning parameters to the variogram structure of the rainfall field and to the number of new locations to be selected has been undertaken. We used factorial experiments to compute the effect of a given SA parameter on the percentage of solution acceptance and the number of iterations to obtain the optimal objective function (standing for computation time) as well as the decrease in the value of objective function at optimum (standing for solution quality). The important differences in their spherical variogram models (60 km range for the first versus 160 km range for the second as well as 21 $(mm/h)^2$ sill for the first versus 1000 $(mm/h)^2$ for the second) give more relevance to the conclusions of the study. The impacts of the network size and variogram structure on SA parameter tuning were considered separately. The results underline the fact that SA parameters do vary with respect to the spatial variability of the rainfall pattern, and, to lesser degree, in relation to the number of decision variables. The cooling rate α = 0.9 is found the best The values of elasticity of acceptance (*EA*) can be set to 0.9 in case of large augmentation in network size whatever the variability; 0.95 in case of small augmentation and small spatial variability, and 0.99 in case of small augmentation size and high spatial variability. The minimum chain length was found to be n_1=5 in case of high variability and large augmentation and n_1=10 in the other cases. The limit of accepted moves P_{lim} was P_{lim}=5% for high variability and large augmentation and P_{lim}=1% in the other cases. Although a large collection of ranges and sills has been covered by the two case studies, the selection of other hypothetical variogram features should be undertaken in future research.

References

Chebbi A, Bargaoui ZK, Cunha MC (2011) Optimal extension of rain gauge monitoring network for rainfall intensity and erosivity index interpolation. Journal of Hydrologic Engineering 16(8):665–676. https://doi.org/10.1061/(ASCE)HE.1943-5584.0000353

Chebbi A, Bargaoui ZK, Cunha, M C (2013) Development of a method of robust rain gauge network optimization based on intensity-duration-frequency results. Hydrology and Earth Systems Sciences 17:4259–4268. https://doi.org/10.5194/hess-17-4259-2013

Chebbi A, Bargaoui ZK, Abid N, Cunha MC (2017) Optimization of a hydrometric network extension using specific flow, kriging and simulated annealing. Journal of Hydrology 555:971-982. https://doi.org/10.1016/j.jhydrol.2017.10.076

Cunha MC (1999) On solving aquifer management problems with simulated annealing algorithms. Water Resources Management 13(3):153-169. https://link.springer.com/article/10.1023%2FA%3A1008149626428

Kirkpatrick S, Gelatt, CD, Vecchi MP (1983) Optimization by Simulated Annealing. Science 220(4598):671680. DOI: 10.1126/science.220.4598.671

Nunes LM, Cunha MC, Ribeiro L (2004) Groundwater monitoring networks optimization with redundancy reduction. Journal of Water Resources Planning and Management, ASCE130 (1):33-43. http://dx.doi.org/10.1061/(ASCE)0733-9496(2004)130:1(33)

Zeferino J, Antunes A, Cunha MC (2009) An efficient simulated annealing algorithm for regional wastewater systems planning. Computer-Aided Civil and Infrastructure Engineering 24(5):359–370. https://doi.org/10.1111/j.1467-8667.2009.00594.x

Vieira J, Cunha MC (2017) Nested Optimization Approach for the Capacity Expansion of Multiquality Water Supply Systems under Uncertainty. Water Resources Management 31(4):1381-1395. https://doi.org/10.1007/s11269-017-1584-y

11th World Congress on Water Resources and Environment (EWRA 2019)
"Managing Water Resources for a Sustainable Future", 25-29 June 2019, Madrid, Spain

Effects of non-uniform flow in the mixing layer in compound channels

J. Fernandes
Hydraulics and Environmental Department, National Laboratory for Civil Engineering, Lisbon, Portugal
e-mail: jnfernandes@lnec.pt

Introduction

The alluvial valleys of rivers usually have a compound channel cross section during flood events. This configuration leads to much more complex flow mechanisms when compared to a single channel flow namely with the existence of a mixing layer and large-scale coherent structures in the interface between the main channel and the floodplain (*i.e*. subsections). Uniform flow in compound channels has been extensively studied (e.g. Shiono and Knight 1991). Due to the non-prismatic nature of rivers, non-uniform flow is the most common situation such as converging or diverging floodplains or meandering channels. Non-uniform flows can also be observed in prismatic geometries with unbalanced inflow conditions.

This last configuration is studied in the present paper. The influence of the non-uniformity of the flow in a straight compound channel is carefully analysed in an experimental study carried out for different relative depths and subsection discharges. For each flow case, the longitudinal profile of water depth and the longitudinal development of the flow mechanisms (e.g. shear layer, turbulence intensities) are characterized.

Materials and methods

The experiments took place in a compound open-channel flume located at the National Laboratory for Civil Engineering (LNEC). The schematic view and the flow conditions are shown in Figure 1.

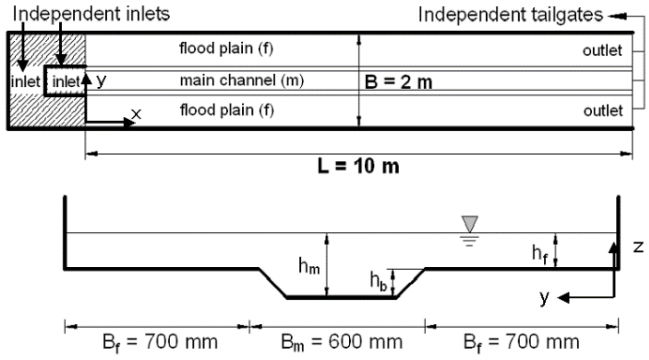

Flow case reference	h_r (-)	$\left(Q_{fp} - Q_{fp}^{unif}\right)/Q_{fp}^{unif}$ (%)	Q_{mc} (l.s^{-1})	Q_{fp} (l.s^{-1})	Q (l.s^{-1})
hr020s–19		–19%	44.3	9.1	
hr020s*		0	42.2	11.2	
hr020s+19	0.2	19%	40.1	13.3	53.4
hr020s+38		38%	37.9	15.5	
hr020s+53		53%	36.3	17.1	
hr030s–19		–19%	59.2	21.4	
hr030s*		0	54.2	26.4	
hr030s+19	0.3	19%	49.2	31.4	80.6
hr030s+38		38%	44.2	36.4	
hr030s+53		53%	40.2	40.4	

Figure 1. Top view and cross section of the compound channel and flow condictions.

The flume is 10 m long, 2 m wide, and is made of polished concrete with a bottom slope of 1.1 mm/m. The symmetric cross section is composed of two floodplains and one trapezoidal main channel with a bank slope of 45° and with a height, h_b, of 100 mm (further details are available in Fernandes et al. 2014).

Firstly, distribution of the subsection discharge for uniform flow was calibrated. As independent inlets for each subsection were used, non-uniform flow conditions were achieved by changing the uniform flow upstream discharge distribution between the main channel and the floodplains and keeping constant the total flow discharge. The downstream boundary condition, *i.e*., the position of the tailgates for each relative depth was established for uniform flow. Considering that Q_{fp}^{unif} is the floodplain discharge for a uniform flow, each non-uniform flow is identified by the percentage of variation in the floodplain discharge in the upstream cross section compared to uniform flow conditions, $\left(Q_{fp} - Q_{fp}^{unif}\right)/Q_{fp}^{unif}$ (at the upstream section).

Three flow cases with overfeeding of the floodplain were studied, +19%, +38%, and +53%, leading to a mass transfer from the floodplains towards the main channel. The underfeeding of the floodplains (–19%) results in a mass transfer in the opposite direction. These four non-uniform conditions were analysed for relative depths (ratio between floodplain and main channel flow depths) 0.2 and 0.3. The velocity

measurements were made with a Vectrino ADV and the measuring cross sections are located at x = 1.1, 3.0, 5.0 and 7.5 m.

Results and concluding remarks

For a given relative depth and cross section, the floodplain flow depth increases from non-uniform –19% to +53%. Considering the symmetric flows (relatively to uniform flow conditions) +19% and –19%, the water surface profile for non-uniform flow –19% is further from equilibrium all along the flume for both relative depths. This result indicates an asymmetry in the exchange of mass and/or momentum between the subsections, depending on the direction of these exchanges.

Figure 2 presents the depth-averaged lateral distribution of the velocity and Reynolds shear stress.

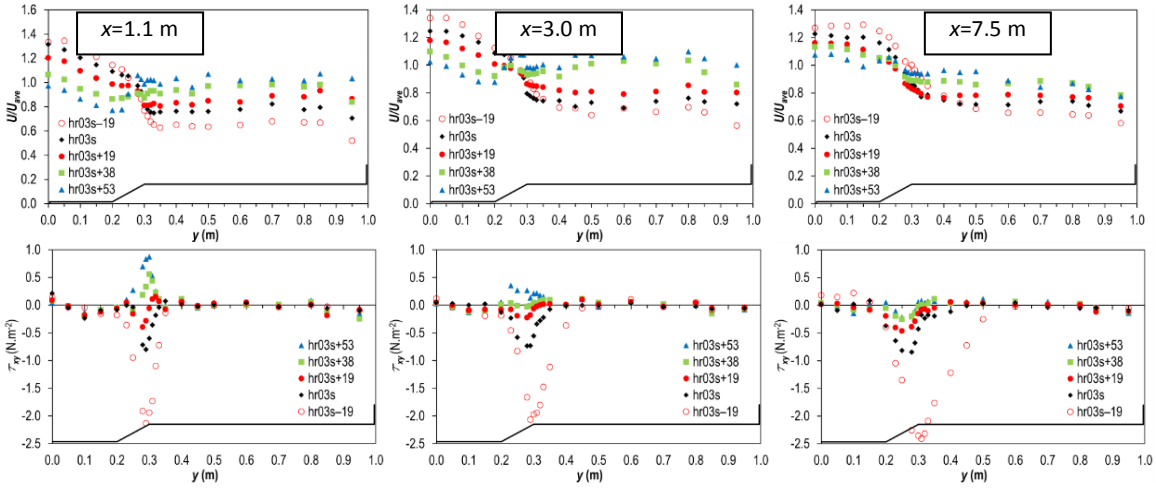

Figure 2. Sectional distribution of depth-averaged streamwise velocity and Reynolds shear stress (x=1.1 m; 3.0 m, 7.5 m for h_r = 0.3).

The two flow cases +38% and +53% differ from the other non-uniform flows, since the flow is supercritical in the floodplain in the most upstream measuring cross section, with a ratio $U_{fp}/U_{mc} > 1$. The other non-uniform flows with an excess in floodplain flow present a large plateau of U across the floodplain. Within the shear layer in the main channel, the lateral gradients $\partial U/\partial y$ decrease as the overfeeding of the floodplain grows. The deficit in floodplain flow leads to a lateral spread of the mixing layer.

For uniform flow the shear layer does not change significantly throughout the longitudinal direction. For flow case hr03s+53, positive lateral shear stress is a consequence of an untypical velocity distribution in a compound channel, where flow is faster in the floodplain. In the longitudinal direction the depth-averaged lateral shear stress increases and becomes closer to uniform flow. The shear layer turbulence is highly altered by the lateral mass exchange. The high shear region is both laterally and vertically stretched by the transverse flow. As the lateral mass exchange increases, the magnitude of lateral shear stress peak decreases.

With a lateral mass exchange coming from the main channel (non-uniform +19%), the high shear region is slightly shifted in the direction of the floodplain, when comparing compared to uniform flow and non-uniform flow –19%. Between the two relative depths, the trend observed with uniform flows is kept. For a given non-uniform flow, lower relative depths results in higher shear.

Acknowledgments: The author acknowledges the support to Grant SFRH/BPD/114768/2016 and Project MixFluv – Mixing Layers in fluvial systems (PTDC/ECI-EGC/31771/2017) by FEDER and Science and Technology Foundation.

References

Fernandes JN, Leal J, Cardoso AH (2014) Improvement of the Lateral Distribution Method based on the mixing layer theory. Advances in Water Resources 69:159–167

Shiono K, Knight DW (1991) Turbulent open channel flows with variable depth across the channel. Journal of Fluid Mechanics 222:617–646

11th World Congress on Water Resources and Environment (EWRA 2019)
"Managing Water Resources for a Sustainable Future", 25-29 June 2019, Madrid, Spain

Employing innovative technologies and procedures are critical in meeting growing water demands in the arid regions of the world

R.A. Sahi
Consultancy services, STTS Limited, Toronto, Canada
e-mail: riazasahi@gmail.com

Introduction

It is now recognized that water is an intricate part of nature and that for developed and developing countries it is more than just a resource. This is especially true for countries with arid landscapes. In the Middle East, particularly Saudi Arabia, the key environmental challenge is short water supply, because natural recharge of an aquifer can be almost negligible due to rain scarcity (Sahi 1997). As a result, one option is to increase desalinated water production, which is enormously expensive and causes massive environmental pollution. The other option is to transfer water in between aquifers, which is also not an easy solution due to difficult terrains and limited potential of other aquifers. Thus, the salient goal of groundwater resource management has long been improvement of the resource through the use of innovative well development technologies and procedures (Sahi 2018).

There is extensive and theoretically diverse management and exploration literature concerning groundwater resources, but it is inconclusive on the role of newly developed innovative technologies and well development procedures in managing groundwater resources and achieving sustainability. Indeed, this vast body of literature focuses more on resource selection and water consumption rather than on improving the resource itself.

Materials and methods

In this research, new innovative well completion technologies and well development procedures have been devised, which improve the resource's efficiency more than 32% using the existing pumping equipment and without involving any additional cost. Moreover, the life of the resource is extended by over 20%. These are essential steps towards sustainable development. Furthermore, these procedures use a mixed scientific approach that will open up new frontiers for resolving groundwater management and sustainability issues through efficiency improvement (Sahi 2018).

Results and concluding remarks

Innovative well completion technologies and development procedures will play a dynamic role in the groundwater exploration and development field in the future, specifically as part of sound water policy. This will be particularly significant in the Middle East, where aquifers are very deep and are continuously being depleted with little sign of replenishment. These procedures are highly technical and need the necessary expertise, without which the full benefits will not be achieved. Therefore, unless new technologies and procedures are applied to develop future groundwater resources, it will be always difficult to compute the full potential of any new resource effectively. It will assist the managers in achieving higher production with extended resource life to meet ever-growing demand for water and achieving viable sustainability goals in the arid regions of the world (Sahi 2018).

Table 1. Productivity improvement results

Ref Wells	Specific Capacity with Standard Procedures	Specific Capacity with Innovative Procedures	Percentage Increase in Specific Capacity
MD-1	14.61 GPM/ft	19.8 GPM/ft	35.5
MD-2	14.8 GPM/ft	19.9 GPM/ft	34.45
MD-3	13.5 GPM/ft	18.2 GPM/ft	34.81

Table 2. Cementing bond log improvement results

Ref Wells	Previous Bonding Strength	New Bonding Strength	Percentage Increase
MD-1	61.1	82.3	21.2
MD-2	62.4	82.8	20.4
MD-3	60.3	82.9	22.6

References

Sahi RA (1997) Water Resource Development. In: Water Technology Conference, March 24, Doha, Qatar

Sahi RA (2018) How water security and sustainability challenges are emerging in Pakistan. In: International Conference on Water Security, March 22, Toronto, Canada

11th World Congress on Water Resources and Environment (EWRA 2019)
"Managing Water Resources for a Sustainable Future", 25-29 June 2019, Madrid, Spain

Uncertainty quantification in a dam break flood study due to breach parameters

V. Bellos[1*], V. Tsakiris[2], G. Kopsiaftis[1], G. Tsakiris[1]
[1] School of Rural and Surveying Engineering, National Technical University of Athens, Athens, Greece
[2] SEEMAN Environmental PC, Athens, Greece
* e-mail: vmpellos@mail.ntua.gr

Introduction

The dam break study of this communication uses two interrelated sub-models: a) the dam breach sub-model and b) the hydrodynamic routing sub-model. The first sub-model generates the flood hydrograph from the dam which is derived for a specific set of the parameters describing the breach process. This is also the input for the hydrodynamic model, with which simulates the flood wave propagation in the computational domain. Due to complexity, dam breach parameters are characterised by significant uncertainties, which are propagated to the output of the dam-breach sub-model and the consequent hydrodynamic model. Therefore, it is not safe to derive a unique solution for the flood hydrograph, without taking into account the uncertainty of the simulated results. In this study, a forward uncertainty analysis is implemented in order to quantify and propagate uncertainty introduced by the dam breach parameters, in a real-world case study.

Materials and methods

The case-study of our analysis refers to a dam under study in Crete, Greece (Papadiana dam, located in Tavronitis river), at the west part of the island. The spillway stage is at +326.0 m, whereas the bottom of the dam at +237.0 m. The type of the dam is Roller-Compacted Concrete (RCC). Although RCC dam is a hybrid case between earthfill and concrete dam, the static behaviour and therefore the failure mechanism, resembles more to gravity dam.

The linkage of the two sub-models is obtained in the framework of the HEC-RAS software. For the dam-breach sub-model, seven parameters, describing the process of the breach (geometry of the breach and required time for the completion of the breach), are specified. The final form of the breach is assumed to have a trapezoidal shape. The downstream boundary conditions generating the flood hydrograph due to the failure, have the form of the weir equation $Q=CLH^{3/2}$, where C is the discharge coefficient, L is the spillway length and H is the hydraulic head above the breach. For the hydrodynamic sub-model, one-dimensional (1D) approach is adopted.

The seven parameters which are included in our analysis are: a) the final width of the breach at the bottom of the breach W; b) the final elevation of the bottom of the breach E; c) the left side slope of the breach L; d) the right side slope of the breach R; e) the breach weir coefficient C, f) the required time for the completion of the breach t; g) the water stage in the reservoir when failure starts S.

Results and concluding remarks

For the uncertainty analysis, the Monte Carlo method is used in which 10000 random combinations of the seven parameters are generated, covering the parametric space using the Latin Hypercube Sampling technique. The intervals of the parameters are the following: W[100,200] m, E[251,270] m, L[0,2], R[0,2], C[1.2-1.6] $m^{1/2}/s$, t[0.2-0.5] h, S[300-326] m. In Figure 1, the uncertainty band of the derived flood hydrograph in the dam location after the failure and the distribution of the flood peaks are shown. The distribution fitted to the data is the normal distribution with mean μ=30679.7 m^3/s and standard deviation σ=3845.2 m^3/s.

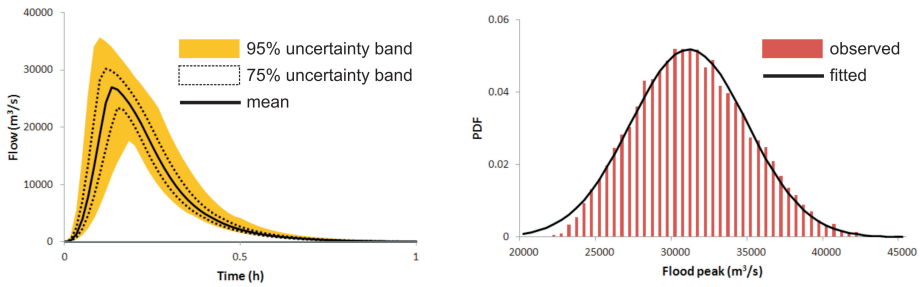

Figure 1. Uncertainty band for several confidence intervals (left) and the pdf of the flood peaks (right)

In the second phase the propagation of this uncertainty through the 1D hydrodynamic sub-model is investigated. For this purpose, the Weibull distribution is fitted to the flood peaks and the maximum simulated water stages in four control points at the river. Figure 2 depicts the comparison of the probability distribution function between observed and fitted data, at these four control points. In order to check the evolution of uncertainty through the flood wave propagation, the ratio *s*/*m* is calculated for each point of the route to the sea. Table 1 summarises the values for defining the metric *s*/*m*. The parameters *k* and *λ* are the parameters of Weibull distribution. The *m* and *s* are functions of *k* and *λ*.

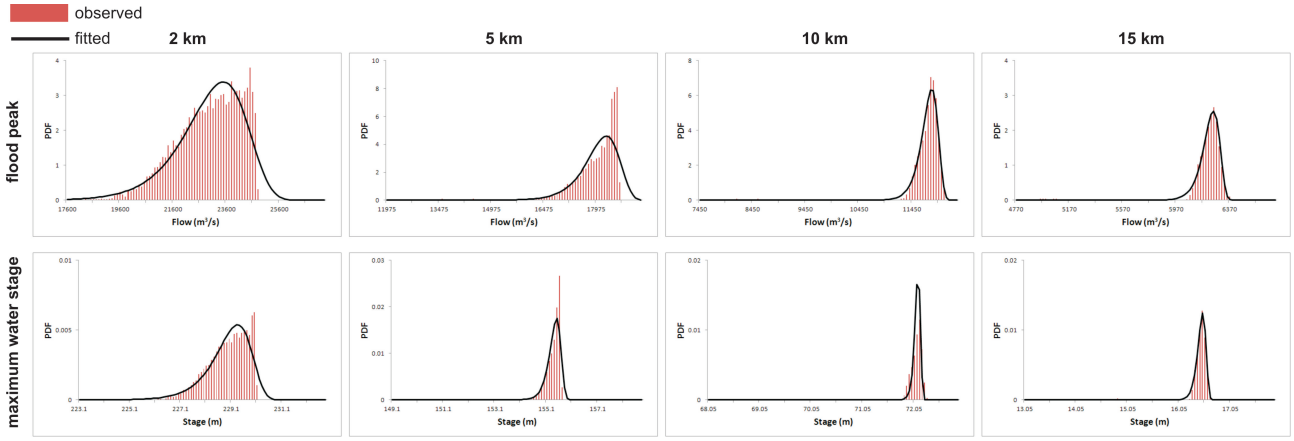

Figure 2. Comparison of pdfs of observed and fitted flood peaks and maximum water stages in four control points

Table 1. Calculation of the ratio s/m for the four control points

Control point	*k*	*λ*	*m*	*s*	*s*/*m*	*k*	*λ*	*m*	*s*	*s*/*m*
	flood peak					*maximum water stage*				
2 km	21.6	23474.0	22895.0	1315.7	**0.057**	336.2	229.3	228.9	0.9	**0.0038**
5 km	40.6	18233.1	17984.3	559.0	**0.031**	749.8	155.4	155.3	0.3	**0.0017**
10 km	82.3	11801.3	11720.2	181.0	**0.015**	1500.0	72.1	72.1	0.1	**0.0009**
15 km	108.9	6237.2	6204.7	72.6	**0.012**	228.2	16.5	16.4	0.1	**0.0056**

It is concluded that dam breach parameters are sources of significant uncertainties regarding the characteristics of the flood created. However, according to the ratio *s*/*m*, it seems that during the propagation of the flood wave through the hydrodynamic model, uncertainty decreases. The latter is probably due to the mechanism of diffusion (Tscheikner-Gratl et al. 2019) which occurs during the propagation of the flood wave. It is also concluded that water stage results are less uncertain than the corresponding of flood peak results, since momentum equation is non-linear whereas continuity equation is linear. The increase of uncertainty in the last control point for water stage is probably due to the influence of the downstream boundary condition.

References

Tscheikner-Gratl F, Bellos V, Schellart A et al. (2019) Recent insights on uncertainties present in integrated catchment water quality modelling. Water Research 150(1):368-379

11th World Congress on Water Resources and Environment (EWRA 2019)
"Managing Water Resources for a Sustainable Future", 25-29 June 2019, Madrid, Spain

Method for water sustainability assessment of multipurpose reservoirs: A case study

A.B.S. Estácio*, V.C. Porto
Hydraulic and Environmental Engineering Department, Federal University of Ceará, Fortaleza, Brazil
** e-mail: alysonbrayner@gmail.com*

Introduction

Besides the increase of water demand, Climate Change intensifies the emergence of studies on Water Security. Bigas (2013), based on UNESCO's definition (UNESCO-IHP 2012), synthetized Water Security as the capacity of a population to safeguard sustainable access to adequate quantities of acceptable quality water for sustaining livelihoods, human well-being, and socio-economic development, for ensuring protection against waterborne pollution and water-related disasters, and for preserving ecosystems in a climate of peace and political stability. The great number of aspects related with this definition points to the complexity of modeling Water Security assessment. Focusing in reservoirs management, Ribeiro and Pizo (2011) related Water Sustainability to the maintenance of a balance between water supply and demand, in a way that the water body exploitation is smaller than its regeneration. Although someone can claim a strictly quantitative interpretation of water management in this statement, it can be strongly useful to Water Sustainability assessment in dry regions, where the low availability of water volumes is the most limiting aspect.

Considering the increasing demand for modeling Water Security, the aim of this study is to propose a method for Water Sustainability assessment in a multipurpose reservoir. As case study the method proposed is applied to Araras reservoir in the northeast of Brazil, a dry region with historic water supply issues.

Materials and methods

Simulation of reservoir operation is used to quantify the water risk associated to Araras exploitation and to assess its sustainability. Using the reconstructed inflow series from 1920 to 2012, besides the evaporation rates and the reservoir topography, it is possible to reproduce the water balance over time and observe the system's response depending on the operation rates adopted.

Two indexes are used to quantify the water risk (or the water sustainability) of the system: the reliability (R) and the permanence below a certain storage level X ($P_{<X}$). The reliability is defined by Hashimoto, Stedinger and Loucks (1997) as the ratio between the number of events with satisfactory value and the total number of events in the simulated time. Here a satisfactory value is considered when the storage level allows the outflow predefined by the operation. The permanence $P_{<X}$, in turn, is defined as the percentage of the total time simulated in which the reservoir has a storage below a certain level X, where X is a percentage of total volume.

The method proposed considers a main purpose for the reservoir, that should be more strictly assured, and secondary purposes, that should also be observed. The method is basically composed by two steps:

- Verification of sustainability for the main purpose.
- Assessment of other uses supply by safeguard operation optimization.

In the first step, the simulation considers as outflow the expected demand (q) for the main purpose. Then, according to reliability and permanence (below 10% of the total volume) values, the system is classified as: multipurpose, allowing only the main purpose or improper. In this case study the criteria for this classification is presented in Table 1.

If in the second step the reservoir is classified as multipurpose the simulations are launched considering a safeguard level (n). Bellow n the reservoir operates with outflow q, otherwise a higher outflow q_{sup} is allowed. Using a Nelder-Mead algorithm, a value to n is reached to maximize q_{sup} respecting the constraints

$P_{<10\%} \leq 10$ %, $R_q \geq 98$ % and $R_{qSUP} \geq 90$ %, where $P_{<10\%}$ is the permanence below 10 % of the total volume, R_q is the reliability of q and R_{qSUP} is the reliability of q_{sup}.

Table 1. Verification of sustainability for the main purpose - criteria

Classification	Conditions		
Multipurpose	$R \geq 98$ %	and	$P_{<10\%} \leq 10\%$
Only the main purpose	$90\ \% \leq R < 98$ %	and	$P_{<10\%} \leq 10\%$
Improper	$R < 90$ %	or	$P_{<10\%} > 10\%$

Results and concluding remarks

The simulation of the reservoir operation considering an outflow equivalent to the urban demand q = 0.3 m^3/s (main purpose of Araras) results in the storage series represented in Figure 1.

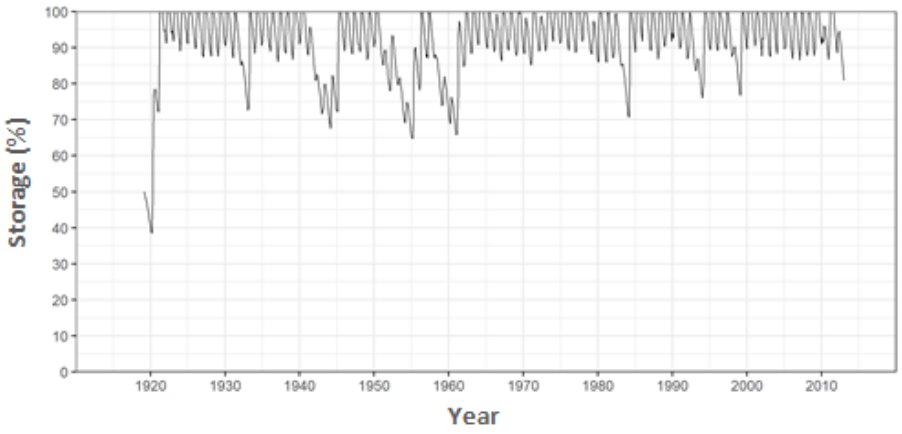

Figure 1. Storage series of Araras with outflow equivalent to the urban demand.

Figure 1 shows that if the climatic conditions of the past were repeated, Araras would be able to assure the urban demand. Since this demand was assured in all simulated time with no storage lower than 10%, Araras is classified as a multipurpose reservoir.

Maximizing the outflow, it's possible to assure q_{sup}= 10.0 m^3/s, with a safeguard level n = 10% and assured $P_{<10\%}$ = 10 %, R_{qSUP} = 90 % and R_q = 100 % of simulated time.

This method appears to be efficient in estimate water supply, allowing the water resources manager to insert his perception of the tolerable risk. Combining this method with an evaluation of climatic and demand scenarios is a potential tool for water resources management.

Acknowledgments: This study was financed in part by Coordenação de Aperfeiçoamento de Pessoal de Nível Superior – Brazil (CAPES) and Conselho Nacional de Desenvolvimento Científico e Tecnológico - Brazil (CNPq).

References

Bigas H (2013) Water Security and the Global Water Agenda: a UN-Water Analytical Brief. United Nations University - Institute for Water, Environment and Health, Hamilton

Hashimoto T, Stedinger JR, Loucks DP (1982) Reliability, resiliency, and vulnerability criteria for water resource system performance evaluation. Water Resources Research 18(1):14-20. https://doi.org/10.1029/WR018i001p00014

Ribeiro CR, Pizzo H S (2011) Avaliação da Sustentabilidade Hídrica de Juiz de Fora/MG. Mercator - Revista de Geografia da UFC 21(10):171-188. http:// doi.org/10.4215/RM2011.1021.0012

UNESCO-IHP (2012) Strategic Plan of the Eighth Phase of IHP (IHP-VIII, 2014-2021). Paris

II. Water Quality and Water Treatment

11th World Congress on Water Resources and Environment (EWRA 2019)
"Managing Water Resources for a Sustainable Future", 25-29 June 2019, Madrid, Spain

Selection of variables to be sampled in water quality monitoring networks

F. Barbaros[1*], N. B. Harmancioglu[2]
[1] Civil Engineering Department, Dokuz Eylul University, Izmir, Turkey
[2] EA-TEK, International R&D, Engineering, Software and Consultancy Company, DEU Technopark, Izmir, Turkey
* e-mail: filiz.barbaros@deu.edu.tr

Introduction

The selection of water quality variables to be sampled is a highly complicated issue with significant cost implications since there are several variables to choose from. Essentially, there are five significant issues that need to be stressed regarding variables to be monitored: (a) variable selection should be based on objectives of monitoring; that is, the type and nature of information required for water quality assessment must be identified first; (b) the selection of variables should be realized by a systematic approach as a monitoring network itself is a family of systematically operated monitoring stations; (c) variable to be monitored, i.e., constituents and pollutants, should be selected so as to identify the biochemical composition of the aquatic ecosystem (constituents), including those that characterize the natural driving forces and the anthropogenic impact (pollutants) representing the modifying forces; (d) a number of investigations has to be carried out before making the selection among a large number of variables (e.g. water quality criteria, pollution inventories and impacts, water use, etc.); (e) economics of monitoring play a significant role in selection of variables to be sampled.

Practically, there are no standard methods that may be used in either the selection of variables or the assessment of an already selected list of variables monitored. To this end, the current paper proposes an approach that may facilitate the selection or assessment procedure. The study presents the above methodology in-depth and demonstrates it on the case of a monitoring network in Gediz basin of Turkey.

Materials and methods

The proposed approach is based on a study by Chapman (1992), where three groups of variables are considered:

a) base variables to be monitored at every station (requires basin-scale analysis);
b) variables that need to be monitored with respect to water use (requires site-specific analysis);
c) variables that need to be monitored with respect to impact assessment (again requires site-specific analysis).

The second and third groups are further divided into industrial and non-industrial water-use and impact assessment variables. Harmancioglu et al. (1999) and SUMER (2003) have further developed this approach to define:

a) variables that need to be sampled at every station in a basin-wide network;
b) variables that need to be sampled specifically at each station.

This methodology considers basin characteristics and local features at each station to determine the variables to be monitored. Next, all variables are ordered with respect to their significance. Finally, the list is screened once more by regression to reduce the number of variables if strong correlations exist among them. Other considerations such as the cost of sampling, temporal variability of the variable considered, and easiness of sampling, are also used in this reduction process.

Results and concluding remarks

Base variables reflect the quality of the natural or unpolluted streams or river reaches and are determined at basin scale. They depend on the local geological, biological and climatological characteristics of a basin, which dominate ion balances, mineral quality and biological nature of the aquatic environment.

A list of base variables observed in every monitoring station in the Gediz basin is given in Table 1. The number of asterisks shown next to each variable indicates the significance of that variable in defining the background water quality, i.e., variables with three asterisks are the most important and those with one asterisk have the least significance for the monitoring programme.

Table 1. Base variables.

Variables	Significance	Variables	Significance
General		**Organic Matter**	
Temperature	***	Total organic carbon	**
Color	**	COD	**
Suspended solids	***	BOD	***
Turbidity/transparency	*	**Ions**	
Conductivity	**	Sodium	*
pH	***	Potassium	*
Dissolved oxygen	***	Calcium	*
Chlorophyll a	*	Magnesium	**
Nutrients		Chloride	**
Ammonia	*	Sulphate	*
Nitrate/nitrite	**		
Phosphorus/phosphate	**		

The next step of the analysis is site-specific and is carried out separately for each monitoring station, considering relevant water use oriented and impact oriented variables that are descriptive of the site represented by that station. Finally, the list of base variables is merged with site-specific variables to obtain a final ordered list for the particular station as in Table 2.

Table 2. Ordered list of base and specific variables for Station 006 (Menemen Bridge) in the Gediz River basin.

Variables to be sampled	Significance	Variables to be sampled	Significance
pH	***	Phosphorus/phosphate	**
Dissolved oxygen	***	Total organic carbon	**
Temperature	***	COD	**
BOD	***	Turbidity/transparency	*
Suspended solids	***	Chlorophyll a	*
Color	**	Ammonia	*
Magnesium	**	Sodium	*
Chloride	**	Potassium	*
Conductivity	**	Calcium	*
Nitrate/nitrite	**	Sulphate	*

For further reduction in the variables to be sampled, regression and principal component analyses are also applied, and the results confirm that the above methodology provides a logical approach to selection of monitoring variables. This selection is significant with respect to assessment of water quality in the area and the costs that accrue from monitoring.

References

Chapman D (1992) Water Quality Assessments. Published on behalf of UNESCO, WMO and UNEP, Chapman & Hall, London, 648 p

Harmancioglu NB, Fistikoglu O, Ozkul SD, Singh VP, Alpaslan N (1999) Water Quality Monitoring Network Design. Kluwer Academic Publishers, Water Science and Technology Library, Volume 33, 290 p

SUMER (2003) Assessing the Performance of DSI's (State Hydraulic Works of Turkey) Water Quality Monitoring Networks – II, Research Project granted by TUBITAK (The Scientific and Technical Research Council of Turkey) and realized jointly by DSI and DEU, Project Code: TUBITAK YDABAG-100Y102, 2001-2003

11th World Congress on Water Resources and Environment (EWRA 2019)
"Managing Water Resources for a Sustainable Future", 25-29 June 2019, Madrid, Spain

Diapir as the main point of salty pollution in Kakan subwatershed, Central Zagros Mountains, IRAN

M. Farzin
Department of Natural Resources, Yasouj University, Yasouj, Iran
e-mail: m.farzin@yu.ac.ir

Introduction

In arid and semi-arid areas, salinization and saline-surface crusts are the main sources of pollution of water and soil (Goldstein et al. 2017; Goudie 2013). Diapir (Salt Dome) can be considered as the source of water and soil salinization. In Iranian rivers, one of the most important reasons of decreasing the water quality is the existence of single, separate and sometimes continuous diapirs along the rivers. Even small diapir can has a great influence on the destruction of water and soil resources. In southern Iran, there are several rivers that quality of its water has been decreased because of passing besides the diapirs (e.g. Mond, Kol and Dalaki Rivers) (Zarei et al. 2014a). This research studied the destructive effects of a small and important diapir on water and soil in the Kakan sub watershed, Central Zagros Mountains, Iran.

Materials and methods

The study region is located on High Zagros Mountains, in northeast of Yasouj city (Kakan), Iran. In general, the climate of the region is cold. Kakan is considered to be Zagros snowfalls; there are a high discharge in wet seasons there. There are several brine springs from a diapir (salt dome) in the slopes of the middle part of the watershed that its water directly enter the main stream (Figure 1).

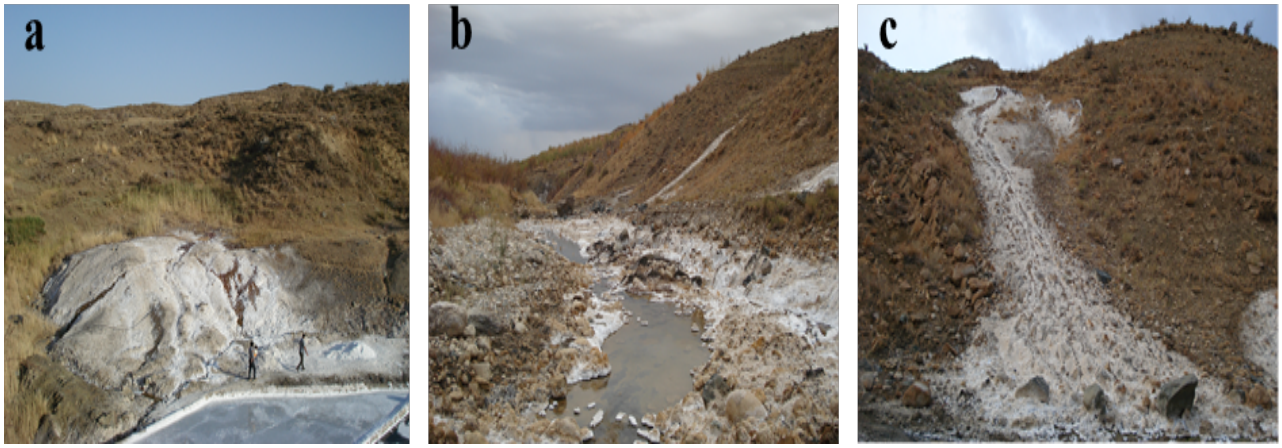

Figure 1. (a) Saline spring, (b) Saline stream, (c) Diapirism.

In order to determine the quality of river water and to investigate the changes on water chemical properties with effect of diapir in the watershed, water sampling was carried out from the upstream to the downstream of the river (to outlet of the watershed). Furthermore, in order to study soil chemical properties of different geological units and also affected soils by saline irrigation in the study area, soil sampling was carried out at a depth of 20 cm on several points on middle of the each geological unit.

Results and concluding remarks

Water samples were divided into two groups, before and after the diapir (Table 1). The results show that the levels of Ec, Cl and Ca^{2+} + Mg^{2+} variables in the samples after the diapir are relatively higher than before that. This situation can be attributed to the entrance of saline water into the river, entrance of the salts accumulated around the main stream, and low water velocity in the river.

Ec values measured in irrigated soil samples are very high compared to other samples. According to the soil samples properties, it can be concluded that the salinity of the saline river is completely influenced by the diapirism phenomenon which has shown itself as brine springs.

Table 1. Average water properties along the stream.

	EC (mmho/cm)	HCO_3^- (mEq)	$Ca^{2+} + Mg^{2+}$ (mEq)	SO_4^- (mEq)	Cl^- (mEq)
Before diapir	400	4.13	6.8	46.6	4
After diapir	55000	4	23.7	29.5	1193

Table 2. Average soil chemical properties.

	EC (mmho/cm)	HCO_3^- (mEq)	$Ca^{2+} + Mg^{2+}$ (mEq)	SO_4^- (mEq)	Cl^- (mEq)
Non irrigated soils	268	2.14	3.2	65.5	0.77
Irrigated soils (agriculture)	3200	2.6	4	60.8	9.15

In many cases, diapirs are the point sources of the water pollution which are considered as the most important contaminant factor (e.g. Zarei et al. 2014b; Kloppmann et al. 2001). The diapir in the study area that is located in margin of the river, serves salinity factor for the salinization of water and soil on its own. Although the activity of a diapir depends on the concentration and sedimentation of salt by the tectonic factors inside the dome and the viscosity of the salt (Zurab and Koyi 2008), the diapir of the studied area can be more destructive depending on the weather conditions (droughts); therefore it can cause severe degradation to the region. By water salinization of the river, soil of the agricultural lands on downstream is affected by irrigation that reduces soil fertility and yield. The analysis of water and soil properties shows that the effect of diapir on the soil and water resources is completely negative. In the studied sub watershed, anyway, the diapir is a destructive factor.

References

Goldstein HL, Breit GN, Reynolds RL (2017) Controls on the chemical composition of saline surface crusts and emitted dust from a wet playa in the Mojave Desert (USA). Journal of Arid Environment 140:50-66. https://doi.org/10.1016/j.jaridenv. 2017.01.010

Goudie AS (2013) The Human Impact on the Natural Environment: Past, Present, and Future. John Wiley & Sons, the Atrium, UK

Kloppmann W, Ne´grel PH, Casanova J, Klinge H, Schelkes K, Guerrot C (2001) Halite dissolution derived brines in the vicinity of a Permian salt dome (N German Basin), Evidence from boron, strontium, oxygen, and hydrogen isotopes. Geochim Cosmochim Acta 65(22): 4087–4101. https://doi.org/10.1016/S0016-7037(01)00640-8

Zarei M, Sedehi F, Raeisi E (2014a) Hydrogeochemical characterization of major factors affecting the quality of groundwater in southern Iran, Janah Plain. Chemie der Erde 74(4):671-680. https://doi.org/10.1016 /j.chemer.2014.03.005

Zarei M, Raeisi E, Merkel BJ, Kummer N-A (2014b) Identifying sources of salinization using hydrochemical and isotopic techniques, Konarsiah, Iran. Environmental Earth Sciences 70(2):587-604. https://doi.org/10.1007/s12665-012-2143-8

Zurab C, Koyi H (2008) The control of salt supply on entrainment of an anhydrite layer within a salt diapir. Journal of structural Geology 30:1192-1200. https://doi.org/10.1016/j.jsg.2008.06.004

11th World Congress on Water Resources and Environment (EWRA 2019)
"Managing Water Resources for a Sustainable Future", 25-29 June 2019, Madrid, Spain

Comparative assessment of phytoplankton diversity and water quality of two different lagoons in Istanbul (Turkey)

N. Yilmaz[1*], C.H. Yardimci[1], M. Elhag[2]
[1] Department of Freshwater Resources and Management, Istanbul University Faculty of Aquatic Sciences, Istanbul, 34134, Turkey
[2] Department of Hydrology and Water Resources Management, Faculty of Meteorology, Environment & Arid Land Agriculture, King Abdulaziz University Jeddah, 21589, Kingdom of Saudi Arabia
* e-mail: nyilmaz@istanbul.edu.tr

Introduction

Lagoon systems are considered as one of the special aquatic ecosystems because they are hosting a diversity of species. They form an important habitat for freshwater and marine life forms. Additionally, lagoons are significant areas for all aquatic organisms and shelter areas for birds (Yilmaz 2015; Yilmaz et al. 2018).

The aim of the study is to compare the water pollution status of Kamil Abduş (Tuzla Lake) and Kucukcekmece lagoons according to phytoplankton diversity, water quality parameters and nutrient concentrations. Both lagoons are located in Istanbul and connected to Marmara Sea. Due to physical, chemical and biological changes, the two coastal lagoons are negatively affected, and the emerging changes can be used as indicators of water pollution.

Materials and methods

Samples were collected from February 2016 to January 2017 from Kamil Abduş Lagoon and from May 2008 to August 2008 from Kucukcekmece Lagoon in monthly periods using Nansen bottles. Selected sampling stations at Kamil Abduş Lagoon were located near Tuzla Shipyard and greenhouses, and also the connecting channel to Marmara Sea. Sampling sites at Kucukcekmece Lagoon were situated along the channel surrounding the lake and at Marmara Sea.

The samples were fixed with Lugol's iodine for phytoplankton identification. Phytoplankton species were counted with an inverted microscope according to Lund et al. (1958). The taxonomic identification of phytoplankton species was done according to several comprehensive reviews. All the recorded species were checked in AlgaeBase site (Guiry and Guiry 2018). Salinity, electrical conductivity and pH were measured with a WTW Multi 340i/set in the field. Nitrite (NO_2), nitrate (NO_3) and orthophosphate (PO_4) concentrations in the water were analyzed at the laboratory according to standard methods (Greenberg 1984). Chlorophyll- *a* concentrations were estimated according to Parsons and Strickland (1963).

Results and concluding remarks

A total of 32 taxa were recorded in Kamil Abduş Lagoon and 28 taxa were identified in Kucukcekmece Lagoon. In both lagoons, it was determined that the Bacillariophyta division was the richest group in terms of species diversity. The following species were recorded in both lagoons: *Aulocoseira italica* (Ehr.) Simonsen, *Cocconeis placentula* Ehr., *Cyclotella atomus* Hust., *Cymbella affinis* Kütz., *Ulnaria acus* (Kutz.) M.Aboal, *Ulnaria ulna* (Nitzsch) P.Compere of Bacillariophyta; *Monoraphidium falcatus (*Corda) Ralfs and *Scenedesmus* sp. of Chlorophyta; *Merismopedia glauca* (Ehr.) Naeg., *Microcystis aeruginosa* (Kütz.) Kütz and *Oscillatoria tenuis* C.Agarth Gomont of Cyanobacteria; *Euglena gracilis* G. A. Klebs and *Trachelomonas hispida* (Perty) F. Stein of Euglenozoa; *Peridinium bipes* F.Stein and *Prorocentrum micans* Ehr. of Miozoa.

Measured chlorophyll-*a* concentrations varied between 0.46 and 349.20 µg/L in Kamil Abduş Lagoon and 4.45 to 40.36 µg/L in Kucukcekmece Lagoon. In conclusion, based on measured nutrients and chlorophyll-*a* concentrations, and recorded eutrophic phytoplankton species, Kamil Abduş Lagoon was found near eutrophic state. According to high chlorophyll-*a* concentrations and recorded pollution

indicator phytoplankton species Kucukcekmece Lagoon was found in the eutrophic state (Yilmaz 2015; Yilmaz et al. 2018).

Table 1. Measured maximum and minimum physicochemical parameters and chlorophyll-a concentrations in the two lagoons.

	KUCUKCEKMECE LAGOON	KAMIL ABDUS LAGOON
pH	6.27- 8.31	7.29 - 9.22
Salinity (‰)	11.8 – 24.9	4.20 - 25.40
Conductivity (mS/cm)	19.7 – 39.2	7.74 - 58.40
Chlorophyll- *a* (µg/L)	4.45- 40.36	0.46 - 349.20
NO_2 (µg/L)	0.27 -5.63	0.1 - 2431
NO_3 (µg/L)	1.109 – 15.034	0.7 - 2480
PO_4 (µg/L)	0.061 – 0.083	31 - 3087

Acknowledgments: This work was supported by Scientific Research Project Coordination Unit of Istanbul University. Project number: BEK-2017-25150.

References

Greenberg A (1985) Standard Methods for the Examination of Water and Wastewater. 16th ed., American Public Health Association, Washington, DC, USA

Guiry MD, Guiry, GM (2017) AlgaeBase. World-Wide Electronic Publication, National University of Ireland, Galway. 2017. Available online: http://www.algaebase.org

Lund JWG, Kipling C, Le Cren ED (1958) The inverted microscope method of estimating algal numbers and the statistical basis of estimations by counting. Hydrobiologia 11:143–170

Parsons TR, Strickland JDH (1963) Discussion of spectrophotometric determination of marine plant pigments, with revised equations for ascertaining chlorophylls and carotenoids. J. Marine Res. 21:155–163

Water Pollution Control Regulations (Su Kirliliği ve Kontrol Yönetmeliği) (2004) Official Journal of the Publication: Ankara, Turkey (in Turkish)

Yilmaz N (2015) Diversity of phytoplankton in Kucukcekmece Lagoon channel, Turkey. Maejo Int. J. Sci. Technol. 9(01), 32-42. doi: 10.14456/mijst.2015.4

Yilmaz N, Yardimci CH, Elhag M, Dumitrache CA (2018) Phytoplankton Composition and Water Quality of Kamil Abduş Lagoon (Tuzla Lake), Istanbul-Turkey. Water 10:603. doi: 10.3390/w10050603

11th World Congress on Water Resources and Environment (EWRA 2019)
"Managing Water Resources for a Sustainable Future", 25-29 June 2019, Madrid, Spain

Investigation of diapirism effect on Mond River, Bushehr - Iran, using remote sensing

M. Farzin[1*], S. Menbari[2]
[1] Department of Natural Resources, Yasouj University, Yasouj, Iran
[2] Yazd University, Iran
* e-mail: m.farzin@yu.ac.ir

Introduction

One-third of Earth and two-thirds of Iran located in arid and semiarid conditions which plays an important role in evolution of desertification. Salinization of soil and water resources widely occurs in arid and semiarid areas (Goldstein et al. 2017; Goudie 2013). One of the main natural causes of desertification is outcrop of salt dome which directly and indirectly has role in desertification (Dehghani 2002). The salt domes can imbrue Surface and underground water resources in various ways in which this pollution is in large quantity (Bostani 2006). Study water quality in upstream and downstream of the salt domes, shows that crossing water through various lands causes physical and chemical changes on water. Spreading of evaporation and salt formations, vaporization due to the weather heat and extension of the salt domes in many parts of Iran, especially in Zagros folded, are important causes in salinization of water resources in Iran (Zarei et al. 2014). One of the aspects of land performance loss (desertification) in Bushehr can be considered as salinity increase in Mond River and subsequently reduces in the biological potential of soil and vegetation. The study of circumstance of Jashak Salt Dome role in reducing the quality of karstic water, destruction of basic resources and intensifying of desertification is necessary.

Materials and methods

In this study, River variation is determined using data achieving from five sampling stations and investigating water quality factors. Then the most affecting area of salt dome on water quality degradation is studied. Five chemical parameters of water quality including pH, SALT percent, TDS, CL and EC of samples on 5 stations are analysed. Also, for detecting the effect of Salt Domes, the ASTER sensor data in the visible area, near infrared, middle infrared and the algorithm of Principal Component Analysis (PCA) and three indexes used. In the selection of satellite image, we aimed to select the hottest month of a year to have the maximum evaporation from soil surface and regions around rivers; because of the over-accumulation of salts on the soil surface leads to observe this region more clearly in satellite images. For this purpose, first, the corrections were done. Then, the PCA technique was used to compress data and improve the visual quality of images. Therefore, the best principle component with the maximum information was extracted. Salinity indices include normalized difference salinity index (NDSI), salinity index (SI), and relative saline condition index (RSCI]. The aim of presenting the three indices was to maximize the difference between the spectral reflections of effective regions and their backgrounds in order to have a high-quality image.

Results and concluding remarks

Analysing the quality parameters in 5 sampling stations shows the serious effect of salt dome on crossing river. For instance on sloping surface the outgoing water from Jashak salt dome are penetrating in ground surface and causes water and soil salinization. Also Climatic factors such as water and wind cause high erosion in dome and has affected the downstream area of study. Amount of electrical conductivity and salinity in studied seasons before and after of the dome show a lot of changes. Thus, in Bordekhoon reaches 47,700 micromho per cm. Concentration of dissolved salts in river mirage for cause erosion capability less salt dome about is half of the coastal section of the river. The soils, which are affected by salt dome show high reflections in satellite image due to the presence of salt on the soil surface, as a result, can be recognized easily. The indices can reduce unwanted effects and increase the information relevant to

regions affected by a salt dome. In evaluating the remote sensing data of principal component analysis (PCA), the sixth component showed better variations to determine the salt dome affected regions. Besides, the results of using salinity indices indicated (SI Index) better compatibility with areas affected by salt domes. The result shows that quality changes due to presence of Jashak salt dome significantly effects on salinization of adjacent plains of Mond River and consequently desertification of area is increased dramatically.

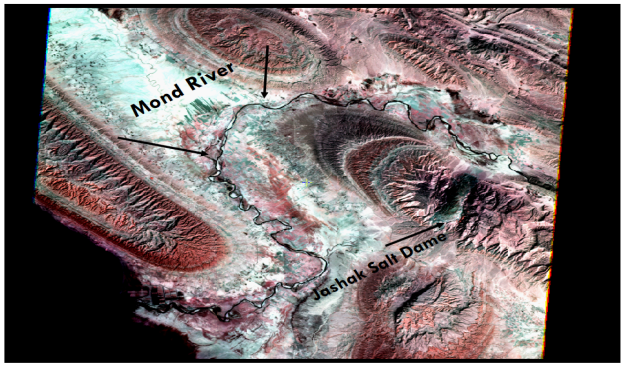

Figure 1. Sattelite image of salt dome and Mond river in Bushehr

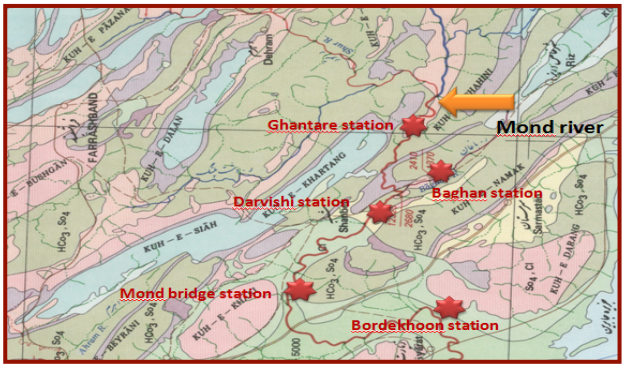

Figure 2. Location of five stations on Mond River

Figure 3. pc6 for Aster image

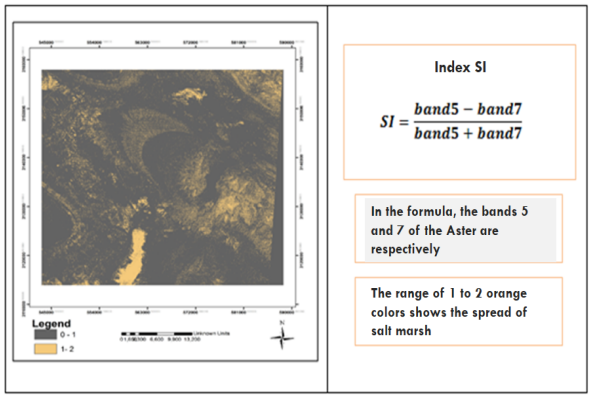

Figure 4. SI index

References

Boustany S, Kompani Z, Noshadi M (2006) Effect of salt domes on the water resources in the gulf region Dahrom. Forests and Rangeland Journal 78: 84-93. In Persian

Dehghan AH (2002) The geological phenomenon of the desertification. Forests and Pasture Quarterly 70:93-95 (in Persian)

Goldstein HL, Breit GN, Reynolds RL (2017) Controls on the chemical composition of saline surface crusts and emitted dust from a wet playa in the Mojave Desert (USA). Journal of Arid Environment 140: 50-66. https://doi.org/10.1016/j.jaridenv. 2017.01.010

Goudie, A.S (2013) The Human Impact on the Natural Environment: Past, Present, and Future. John Wiley & Sons, the Atrium, UK.

Zarei M, Sedehi F, Raeisi E (2014) Hydrogeochemical characterization of major factors affecting the quality of groundwater in southern Iran, Janah Plain. Chemie der Erde 74(4): 671-680. https://doi.org/10.1016 /j.chemer.2014.03.005

11th World Congress on Water Resources and Environment (EWRA 2019)
"Managing Water Resources for a Sustainable Future", 25-29 June 2019, Madrid, Spain

A sustainable technique of Pd-doping on TiO_2 using plant-based electron donor analytes for photocatalytic wastewater treatment

V. Rao Chelli[1], Y. Mundhada[2], A.K. Golder[2*]
[1] RTG-Refining R&D, Reliance Industries Limited, Jamnagar, Gujarat, India
[2] Department of Chemical Engineering, Indian Institute of Technology Guwahati, Assam-781039, India
* e-mail: animes@iitg.ac.in

Introduction

Titania (TiO_2) is considered to be one of the most versatile semiconductor photocatalysts and its typical applications include sterilization, removal of odour, detoxification of hazardous chemicals and water purification. The primary limitation of TiO_2 is that the photocatalytic activity is confined within UV light with a band gap of 3.2 eV. For pure TiO_2, the free electron (e^-) and hole (h^+) pair generated can recombine at a faster rate (~20 ns) resulting in a lower quantum yield (Rao and Golder 2016). Whereas, metal-doped semiconductors such Pd-doped TiO_2 exhibit a high Schottky barrier, and it acts as e^- traps at a metal /semiconductor interface assisting the separation of e^-/h^+ pair. In general, the techniques of Pd-doping on TiO_2 involve energy-intensive processes like physical vapour deposition, chemical reduction, photo-deposition, etc.

Herein, we make use of plant-based electron-donor compounds for Pd-doping on TiO_2 for the harvesting of visible for the photocatalytic wastewater treatment. Leaves of *Oxalis Corniculata*, a local creeping woodsorrel are a rich source of ascorbic acid, flavonoids, glycosides, tannins, etc. These analytes were extracted in aqueous media and applied for Pd-doping on TiO_2 at room temperature and pressure. The physiochemical attributes of this functional catalyst were determined and tested for the decomposition of phenol by illuminating diffused visible light.

Materials and methods

Oxalis Corniculata plant grows naturally at the premises of Indian Institute of Technology Guwahati. The clean leaves were crushed and mixed (1:10 w/v) with deionized water under continuous stirring, and heated at <90°C for 10 min. This extract was clarified by the membrane filtration (2 µm).

On the other side, an amount of 2 g TiO_2 (P25-TiO_2: surface area 66.5 m^2/g and pore diameter 17.7 nm) was mixed with $PdCl_2$ (Pd(II): 0.25-2% w/w) by sonication (15 min) followed by magnetic stirring (45 min) at 320 rpm. TiO_2/Pd(II) residue was centrifuged, washed (ethanol/water) and vacuum-dried, and it was then introduced into the clarified extract (20 mL) for the direct Pd-doping on TiO_2 with a reaction time of 24 h at room temperature and pressure. The doped catalyst (symbolized as TiO_2/Pd) was centrifuged (4500 rpm), washed (ethanol/water) and dried for detail characterizations and photocatalytic applications. The true Pd-loading was determined by measuring the residual Pd(II) concentrations in solutions.

In the catalytic activity test, an amount of 0.1 g/L TiO_2/Pd was used for phenol (20 mg/L) decomposition in a simple batch photo-reactor made of borosilicate glass (100 mL) at 25 ± 2°C using a 100 W light source (λ_{mean}=525 nm) up to a reaction time of 120 min. The concentration of phenol was recorded spectrophotometrically during the reaction (Solid-Spec 3700/3700DUV, Japan).

Results and concluding remarks

The spectral response of both pure TiO_2 and TiO_2/Pd was recorded at the very beginning, and it was found that the absorption edge of TiO_2 in the visible wavelength was gradually shifted to a higher absorbance of 0.5 at 450 nm with a true Pd-loading of 1.33% (TiO_2/Pd-1.33) from its absorbance of zero for TiO_2. However, a higher dopant concentration (>1.82% w/w) caused a reduction in the optical absorption in the visible range. The band gap energy was calculated from the indirect transition model and it was found that the band gap was decreased to 2.3 eV for TiO_2/Pd-1.33 from 3.0 eV for TiO_2/extract-control (Rao and

Golder 2016). It implies that the proposed technique enabled TiO_2/Pd-1.33 for the photocatalytic activity within the visible light spectrum. TiO_2/extract-control showed a minor band gap reduction in comparison to pure TiO_2 due to the adsorption of pigmenting agents present in the extract which was also confirmed by the thermogravimetric analysis of doped catalysts.

The X-ray diffraction analysis was used to acquire the information on the incorporation of Pd into the lattice structure of TiO_2. From the broadening of the diffraction pattern of the peak (101) at 2θ = 25.2°, the crystallite size was determined using Scherer's equation, and there was a slight increase in the crystallite size with Pd-doping (30.35 nm for TiO_2/Pd-1.33 from 22.97 nm for TiO_2) with a marginal decrease in the surface area (by 15%). We found a partial phase transformation from anatase to rutile (79.8 to 72.1%) due to Pd-doping on TiO_2. It corroborates the enlargement in the interplanar d-spacing from 0.3514 to 0.354 nm (maximum) with TiO_2/Pd-1.33 as Pd ions substituted Ti from the TiO_2 lattice structure and formed Ti–O–Pd bonds (Behnajady and Eskandarloo 2013). Further, the lattice strains were calculated from the Williamson-Hall's equation ($\beta\cos\theta = \frac{k\lambda}{L} + 4\varepsilon\sin\theta$) (Chelli et al. 2018).

The symbols in this equation signify as, *β*=full width at half maximum, ε= lattice strain, *k*= shape factor, *L*= crystallite size, and λ= wavelength of Kα(Cu) radiation. The value of ε was determined from the slope of the best fit line, and it reduced to 0.0374 for TiO_2/Pd-1.33 from 0.0386 for TiO_2 (Figure 1a).

The photocatalytic activity of these functional catalysts is shown in Figure 1b. There was only 8% phenol removal for TiO_2 which was mostly resulted from its adsorption. Phenol decomposition efficiency was found to be directly related to the decrease in the band gap up to the dopant concentration of 1.33% (w/w), and the highest phenol decomposition of 85% was achieved with TiO_2/Pd-1.33 (Figure 1b). A higher Pd-loading (>1.82% w/w) slowed down the rate of phenol decomposition due to a higher band gap.

The quantum yield (QY) was determined from the number of phenol molecules decomposed per incident photon. The highest % QY was found to be 32.3% in 120 min of reaction time using TiO_2/Pd-1.33 and, it was only 3.04% with TiO_2.

Therefore, it can be concluded that plant-based electron analytes present in *Oxalis Corniculata* leaves are effective for the incorporation of Pd into the lattice structure of TiO_2 (i.e. doping) with a reduced band gap of 2.3 eV and a high QY of 32.3% with clear superiority over many earlier studies.

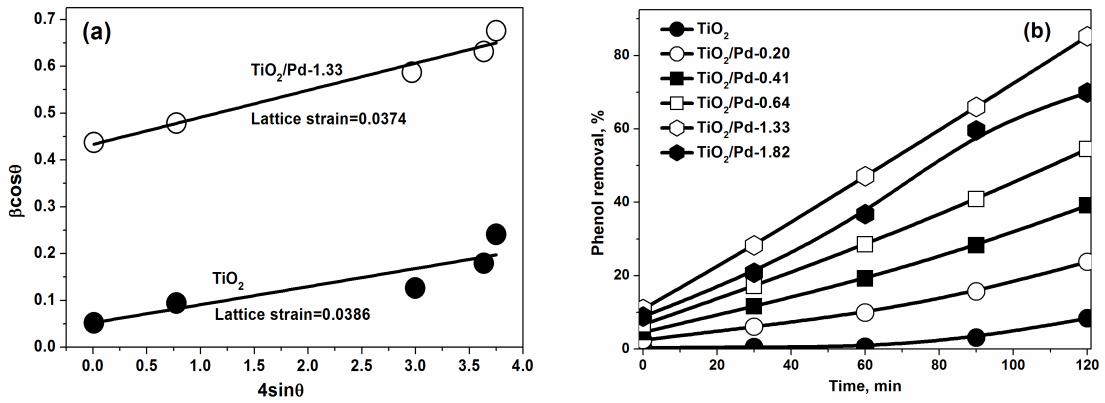

Figure 1. (a) Variation of βcosϑ with 4sinϑ (Williamson-Hall plots) and (b) Phenol decomposition kinetics with different TiO_2/Pd catalysts.

References

Behnajady MA, Eskandarloo H (2013) Silver and copper co-impregnated onto TiO_2-P25 nanoparticles and its photocatalytic activity. Chem. Eng. J. 228:1207–1213

Borodziński A, Bond GC (2008) Selective hydrogenation of ethyne in ethene rich streams on palladium catalysts. Part 2: steady-state kinetics and effects of palladium particle size, carbon monoxide, and promoters. Catal. Rev. Sci. Eng. 50:379–469

Chelli VR, Chakraborty S, Golder AK (2018) Ag-doping on TiO_2 using plant-based glycosidic compounds for high photonic efficiency degradative oxidation under visible light. J. Mol. Liq. 271:380–388

Rao CV, Golder AK (2016) Development of a bio-mediated technique of silver-doping on titania. Colloids Surfaces A Physicochem. Eng. Asp. 506: 557–565

11th World Congress on Water Resources and Environment (EWRA 2019)
"Managing Water Resources for a Sustainable Future", 25-29 June 2019, Madrid, Spain

Initiating efficient Sb(V) removal for drinking water by a mechanism of reduction/adsorption sequence

T. Asimakidou[1], G. Vourlias[1], K. Kalaitzidou[2], M. Mitrakas[2], K. Simeonidis[2*]
[1] Department of Physics, Aristotle University of Thessaloniki, Thessaloniki, Greece
[2] Department of Chemical Engineering, Aristotle University of Thessaloniki, Thessaloniki, Greece
* e-mail: ksime@physics.auth.gr

Introduction

The aqueous soluble forms of antimony are considered as emerging water pollutants regulated by strict legislation especially referring to their long-term exposure through drinking water consumption (Simeonidis et al. 2018; Martinez-Boubeta and Simeonidis 2019). In spite of the low number of incidents with high antimony concentrations in groundwater, the low regulation limit of 5 μg/L signifies its high toxicity and the global raised concern by authorities (European Union Council 1998). Similarly to arsenic, antimony species are met in the oxidation states +3 and +5 with Sb(V) being the dominant form in well-oxygenated resources. Unfortunately, the sorption behaviour of Sb(V) on typical inorganic adsorbents is much different than corresponding arsenic ones, following their larger dimensions and the octahedral geometry of the oxy-ionic form $Sb(OH)_6^-$ in natural water. As a consequence, efforts to develop an antimony-specified adsorbent result in practically zero efficiencies especially when referring to drinking water concentrations and the case of Sb(V) (Simeonidis et al. 2017). On the other hand, adsorption of Sb(III) is much more favourable on typical metal hydroxide adsorbents.

In an attempt to overcome the difficulties related to the efficient capture of Sb(V), this work introduces an alternative approach based on the intermediate reduction to the Sb(III) followed by its non-reversible adsorption on typical iron oxy-hydroxides (Figure 1). To this direction, an iron oxy-hydroxide (FeOOH) optimized for high Sb(III) uptake was combined either with iron oxide (Fe_3O_4) or tin oxy-hydroxide ($Sn_6O_4(OH)_4$) nanoparticles that serve as a reducing agents and a carrier of the FeOOH. The synergy of the two phases in the nanocomposite enables a much better performance for Sb(V) removal in compliance with the drinking water regulations and the requirements for long-term chemical stability and low-cost preparation.

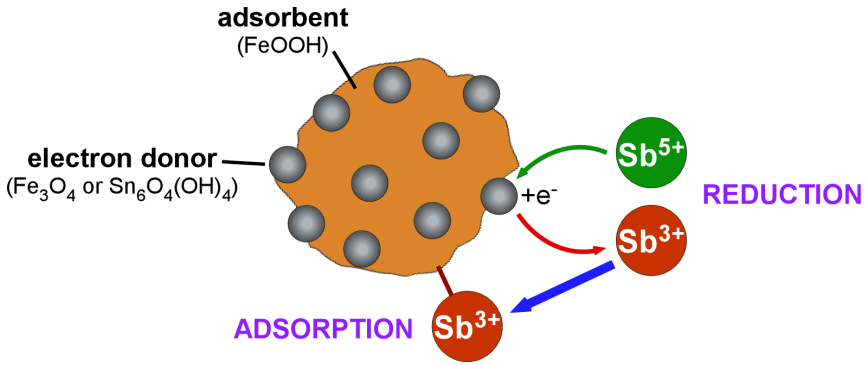

Figure 1. Mechanism of Sb(V) uptake on the developed nanocomposites.

Materials and methods

The studied Fe_3O_4/FeOOH and $Sn_6O_4(OH)_4$/FeOOH nanocomposites were synthesized in a two-stage continuous flow reactor by the sequential precipitation of iron and/or tin salts under different acidity and oxidative conditions. In the first tank, the iron oxy-hydroxide was prepared by the precipitation of $FeSO_4$ at a pH value of 6 and a redox of 300 mV controlled by the addition of NaOH and H_2O_2 solutions, respectively. Then, the product was introduced in the second reactor where the formation of Fe_3O_4 or $Sn_6O_4(OH)_4$

nanoparticles take place. For each case, the precipitation of $FeSO_4$ and $Fe_2(SO_4)_3$ at alkaline conditions or the precipitation of $SnCl_2$ at acidic conditions was applied. The final product was collected from the outflow of the second reactor and was washed with distilled water, centrifuged and dried at room temperature. To modify the percentage of electron donor phase the quantities of reagents in the second stage were varied proportionally.

The structural characterization of the adsorbents was performed by powder X-ray diffractometry (XRD) assisted by thermogravimetric measurements (TG-DTA) while scanning electron microscopy (SEM) was used to identify the morphology. As an indicator of the reducing potential of the nanocomposite, the percentage of Fe^{2+} or Sn^{2+} was determined by $KMnO_4$ titration. The efficiency of developed nanocomposites as Sb(V) adsorbents was evaluated by adsorption experiments carried at pH 7 and residual concentrations in the range 0-700 μg/L using a natural-like water prepared according to the National Sanitation Foundation (NSF) standard. The capacity corresponding to a residual concentration equal to the maximum contaminant level 5 μg/L (Q_5-index) was used as an evaluation criterion between samples. X-ray photoelectron spectroscopy (XPS) was applied to identify the antimony speciation in the surface of the adsorbent obtained after the removal process in Sb(V)-spiked solution.

Results and concluding remarks

The reducing potential of the nanocomposites increases almost proportionally to the percentage of Fe_3O_4 and $Sn_6O_4(OH)_4$. Titration measurements indicate that Fe^{2+} and Sn^{2+} represent a significant part in the total mass of Fe_3O_4 and $Sn_6O_4(OH)_4$ approaching 20 and 85 %wt., respectively. The ability of such phases to operate as electron donors enables the reduction of Sb(V) to Sb(III) oxy-ions which are then captured by the iron oxy-hydroxide that shows higher affinity to antimonite species. It is important to note that the efficiency of these adsorbents is extended to the low residual concentrations range including the drinking water regulation limit for antimony. Suggestively, the uptake capacity of the Fe_3O_4/FeOOH (50 %wt.) corresponding to a Sb(V) residual concentration of 5 μg/L is found to be 0.4 mg/g However, further increase in the Fe_3O_4 content does not improve efficiency. The magnetic response of Fe_3O_4 is another important advantage of this system related to the possibility for alternative application schemes in water treatment based on magnetic separation.

Optimum composition in the $Sn_6O_4(OH)_4$/FeOOH nanocomposite is observed at much lower tin oxy-hydroxides percentages <30 % wt. This is attributed to the combination of higher reducing potential but much lower affinity of $Sn_6O_4(OH)_4$ to the secondary formed Sb(III) species. XPS studies verify the occurring of the assumed “reduction-adsorption” mechanism introduced by the studied nanocomposites. In particular, the majority of adsorbed antimony is found in the trivalent state and mostly located in the neighborhood of Fe^{3+} ions indicating their attachment to the FeOOH surface. Such preliminary results set the application of reducing-FeOOH nanocomposites among the first adsorption processes with practical interest in Sb(V) removal.

Acknowledgments: This scientific work was implemented within the frame of the action “Supporting Postdoctoral Researchers” of the Operational Program “Development of Human Resources, Education and Lifelong Learning 2014-2020” of IKY State Scholarships Foundation and is co-financed by the European Social Fund and the Greek State.

References

European Union Council (1998) Council Directive 98/83/EC of 3 November 1998 on the quality of water intended for human consumption. Official Journal of the European Community L330:0032-0054

Martinez-Boubeta C, Simeonidis K (2019) Magnetic nanoparticles for water purification. In: Thomas S et al. Nanoscale materials in water purification. Elsevier, Amsterdam, Netherlands, pp 521-552

Simeonidis K, Papadopoulou V, Tresintsi S, Kokkinos E, Katsoyiannis IA, Zouboulis AI, Mitrakas M (2017) Efficiency of iron-based oxy-hydroxides in removing antimony from groundwater to levels below the drinking water regulation limits. Sustainability 9:218. http://doi.org/10.3390/su9020238

Simeonidis K, Martinez-Boubeta C, Zamora-Perez P, Rivera-Gil P, Kaprara E, Kokkinos E, Mitrakas M (2018) Nanoparticles for heavy metal removal from drinking water. In: Dasgupta N et al. Environmental nanotechnology, Volume 1. Springer International Publishing, Cham, Switzerland, pp 75-124

11th World Congress on Water Resources and Environment (EWRA 2019)
"Managing Water Resources for a Sustainable Future", 25-29 June 2019, Madrid, Spain

Assessment of heavy metals pollution in groundwater of Ardabil aquifer, Iran

M. Rahimi, V. Rezaverdinejad*
Department of Water Engineering, Urmia University, Urmia, Iran
** e-mail: v.verdinejad@gmail.com*

Introduction

Any changes in quality and quantity of water resources can lead to environmental problems (Nosrati and Eeckhaut 2012; Agca et al. 2014). Increase in pollutants production, including heavy metals is one of the increasingly serious problems (Kheir et al. 2010). Heavy metals are a part of metals and metalloids that even at small concentrations are toxic and hazardous, thus they are at first rank of pollutants and in recent years they have attracted a lot of attention as environmental pollutants effecting human health and living organisms (Merzaee et al. 2015). Although, metals such as Cu, Mn, and Zn are necessary for the activity of some enzymes in the human body, at concentrations above the permissible limit may cause physiological disorders. Cd, Cr, and Pb are toxic for human even at low concentrations (Alam et al. 2012). Currently, heavy metals are the most important environmental pollutants in Iran, and due to agricultural and industrial activities, their concentrations in groundwater of Iran are increasing. Ardabil province is one of the industrial centers of Iran and it is also an important agricultural area. For this reason, in recent years, groundwater in this region has been in danger of pollution as a result of industry and use of chemical fertilizers. The aim of this study was to analyze the state of pollution from heavy metals. For this purpose, by using GIS software, the concentration of heavy metals in the study area was zoned and the quality situation of water for drinking consumption was evaluated according to standards of the World Health Organization (WHO), the Environmental Protection Agency of the United States of America (EPA), and the Institute of Standards and Industrial Research of Iran (ISIRI). Then, the sources of these pollutants were determined.

Materials and methods

The study area is Ardabil aquifer which is located in Ardabil province. Ardabil province with an area about 17953 km^2 is located in north western Iran. This province is located between 37.45^o to 39.42^o north latitudes and 48.55^o to 47.30^o east longitudes. The studied aquifer region includes Ardabil and Namin cities that have an area about 1153 km^2. Ardabil province is one of the industrial centers of Iran because of having facilities such as industrial parks and access to markets in neighbouring countries. Additionally, due to suitable climate and soil fertility, this province is considered a centre of agriculture of Iran, where the use of chemical fertilizers in agricultural fields is impacting groundwater quality. In most of the rivers in the study area, maximum flows occur in April and minimum flows in October. Groundwater of Ardabil is in unconfined and semi-confined aquifer. In recent years, groundwater pollution of the study area has significantly increased. In the present study, the pollution of Ardabil aquifer groundwater was investigated in terms of heavy metals.

For monitoring heavy metals pollution, 76 wells were considered in the study area and sampling and testing were conducted twice a year, during dry and wet seasons of 2012. The dry season sampling was conducted in October 2012, when the level of groundwater was minimum. The wet sampling was conducted in April 2012 under maximum groundwater level conditions. From the 76 existing wells, 32 were drinking wells and 44 were agricultural wells. The following elements were measured: Hg, Cd, Cr, Cu, Fe, Mn, Ni, Pb, Zn, As, and Sb. The heavy metals were measured according to standards methods and using atomic absorption.

Results and concluding remarks

Statistics of maximum, minimum, standard deviation (SD) and mean concentration of each heavy metal in groundwater of the study area are presented in Table 1.

Table 1. Statistics of heavy metal concentrations (mg/L) in Ardabil aquifer (n=76)

Parameter	Dry season				Wet season				Permissible limit		
	Minimum	Maximum	Mean	SD	Minimum	Maximum	Mean	SD	EPA	WHO	ISIRI
Hg	0.000	0.312	0.038	0.064	0.000	0.116	0.026	0.029	0.002	0.006	0.006
Cd	0.000	1.559	0.025	0.198	0.000	0.750	0.013	0.088	0.005	0.003	0.003
Cr	0.000	1.280	0.075	0.174	0.000	0.167	0.041	0.054	0.100	0.050	0.050
Cu	0.000	3.890	0.388	0.702	0.000	1.140	0.253	0.244	1.300	2.000	2.000
Fe	0.064	28.552	2.365	4.708	0.156	18.190	3.527	3.305	0.300	0.300	0.300
Ni	0.000	1.559	0.104	0.210	0.000	0.284	0.047	0.065	0.100	0.070	0.070
Mn	0.000	20.143	0.655	2.559	0.000	2.357	0.641	0.471	0.050	0.400	0.400
As	0.000	1.559	0.048	0.198	0.000	0.942	0.042	0.112	0.010	0.010	0.010
Zn	0.205	15.520	2.102	3.642	0.000	6.270	0.281	0.742	5.000	15.000	15.000
Pb	0.000	0.088	0.007	0.016	0.000	1.381	0.059	0.202	0.015	0.010	0.010
Sb	0.000	0.332	0.040	0.067	0.000	0.332	0.025	0.047	0.006	0.020	0.020
Se	0.000	0.157	0.034	0.038	0.000	0.141	0.024	0.029	0.050	0.040	0.010

The increase in production of pollutants such as heavy metals is one of the increasingly serious problems in the society. Heavy metal pollution is dangerous not only for physical and chemical properties of soil, but also for human health through entering the food change and groundwater. The results of the research showed that the concentrations of Cd, Cu, and Zn in this area are below the permissible limits, but other elements (Hg, Fe, Ni, Mn, As, Cr, Pb, Sb, Se) in most parts of the aquifer have concentrations above the permissible limit. The concentrations of Cd, Pb, Cr, Fe, Hg, As, Mn, Ni, Se, Sb in wet season are respectively: 6.57, 21.33, 22.6, 97.3, 66.67, 61.33, 62.67, 26.67, 21.33, 37.33 percentages and above the permissible limit. Also, in dry season these values are respectively: 1.31, 22.58, 27.4, 97.3, 45, 40.32, 89.33, 40.32, 38.7 and 50 percentages and above the permissible limit. The reasons for having high values of heavy metals are: using various chemical fertilizers in agriculture and their leaching in soil profile and entering into groundwater, sewage from industrial parks and using sinkholes instead of purification and sewage disposal. The zoning maps of heavy metals showed most of the regions have pollution above the permissible limit. Consuming polluted water with heavy metals may lead to serious human health problems and can cause different intoxications and cancers. Therefore, it is recommended to stop using the wells for drinking, or remove heavy metals by using modern methods such as nano-filtration, ultra-nano-filtration, reverse osmosis, etc. Also, it is recommended to develop permanent monitoring network for investigating groundwater quality of the region.

References

Ağca N, Karanlık S, Ödemiş B (2014) Assessment of ammonium, nitrate, phosphate, and heavy metal pollution in groundwater from Amik Plain, southern Turkey. Environmental Monitoring Assessment 186(9):5921–5934. doi: 10.1007/s10661-014-3829-z

Alam M, Rais S, Aslam M (2012) Hydrochemical investigation and quality assessment of groundwater in rural areas of Delhi, India. Environmental Earth Science 66:97–110

EPA U (2002) Edition of the drinking water standards and health advisories. US 417 Environmental Protection Agency Washington eDC DC

ISIRI (2009) Chemical specifications of drinking water. No. 1053, 5th ed., Institute of Standards and Industrial Research of Iran, Tehran (in Persian)

Kheir RB, Greve MH, Abdallah C, Dalgaard T (2010) Spatial soil zinc content distribution from terrain parameters: A GIS-based decision-tree model in Lebanon. Environmental Pollution 158(2):520-528

Nosrati K, Eeckhaut MVD (2012) Assessment of groundwater quality using multivariate statistical techniques in Hashtgerd Plain, Iran. Environmental Earth Science 65:331–344

WHO (2011) Guidelines for drinking-water quality. 4th ed, World Health Organization, Geneva, Switzerland

11th World Congress on Water Resources and Environment (EWRA 2019)
"Managing Water Resources for a Sustainable Future", 25-29 June 2019, Madrid, Spain

Performance evaluation of Forward Osmosis - Reverse Osmosis hybrid system for treatment of produced water from oil production fields

N. Balouti[1], S.M. Abedan Dehkordi[2*]
[1] Department of Petroleum Engineering, Amirkabir University of Technology, Tehran, Iran
[2] Department of Chemical Engineering, Amirkabir University of Technology, Tehran, Iran
* e-mail: smehdi_abedan@aut.ac.ir

Introduction

As the population is rapidly growing, developing low-energy water treatment techniques for unconventional sources is crucial to sustain water and energy resources and meet increasing water demand. Although most of the installed water treatment plant are currently using RO techniques to produce clean water, reverse osmosis still remains an energy-intensive process (Munirasu et al. 2016). Furthermore, membrane fouling decreases RO performance by posing periodic plant downtime and increases maintenance cost due to use of cleaning chemicals (Chekli et al. 2016). Hence, novel low-cost treatment technologies that could surmount these issues will play a significant role in sustaining the water and energy sources.

Recently, forward osmosis is gaining interest as a novel low-cost water treatment technology due to their significantly lower fouling potential and energy consumption compared to the conventional pressure-driven membranes. However, one of the major obstacles that barricades the common industrial use of FO process is the extraction of clean water from the diluted draw solution (Kim et al. 2018), which a hybrid system coupling RO to the FO membrane could predictably overcome.

This study investigated the optimizing of the FO-RO hybrid process performances in treatment of produced water (PW) from oil production fields.

Materials and methods

Feed solution (FS) was obtained from various petroleum production wells in Abteymour oil field, Iran. Seawater obtained locally from Persian Gulf, was used as the draw solution (DS).

Flat-sheet asymmetric FO membrane made of cellulose triacetate (CTA) with a thickness of 50 µm from Hydration Technology Innovations Company (HTI) were employed. Active layer facing feed solution (ALFS) was applied on the membrane in order to avoid the aggravated fouling in the support layer due to pore-clogging (Motsa et al. 2014). Purchased membranes were cut to fit the set-up scale with active membrane area of 50 cm^2 and stored in DI water for 24 hours prior to use in each experiment.

Lab-scale cross-flow FO and RO systems were used, as described elsewhere (Kim et al. 2015). After the initial flux was stabilized, changes in mass was recorded over time by a computer and a digital mass scale (A&D, Australia) to measure the water flux of permeate.

Results and concluding remarks

The Performance of the FO-RO hybrid system for treatment of produced water is investigated by evaluating the effects of three different operating factors (osmotic pressure driven force, produced water pH and flow rate) on the total water flux.

Osmotic pressure driven force is known to strongly affect the water flux in the FO process. Produced water with different TDS was used to investigate the role of osmotic pressure on the water and solute transport across the membrane. As the difference between the TDS of FS and DS was increased, a higher flux was resulted, where for PW with TDS of 9500, 13100 and 18000, the obtained flux was 11, 8.5 and 4.8, respectively.

The results also showed that the water flux obtained at lower pH (pH = 4.4) was highest while at pH 6.5 the lowest flux was obtained. This indicates that although the pH of the produced water does not directly

affect the water flux, the influence of pH on the membrane fouling potential indirectly alters the permeate flux, which is in good agreement with previous studies (Yung et al. 2014). The produced water at lower pH contains more amount of organic compounds with higher molecular weight compared to other pH conditions. In fact, in experiments with higher pH of produced water as feed solution, pore blockage caused by smaller size foulant penetrating through the membrane pores significantly decreased the water flux and thus the system performance.

Three different cross-flow rates (200, 500 and 800 mL/min) were employed in this study to investigate the influence of flow rate on the overall water flux. The result indicates that the flux increases when a higher cross-flow velocity is applied in FO process. At the lowest velocity, the minimum flux was obtained due to the acceleration of fouling cake layer formation which increases the concentration polarization on the feed side facing of membrane active layer. Subsequently, higher water flux is obtained while FO system is operated under higher cross-flow rate which further supports the statement related to procrastination of foulant cake layer formation in higher PW velocity.

Acknowledgments: The authors acknowledge Mehrtash Sepahan Co. for the financial supports and providing facilities for conducting this study.

References

Chekli L, Phuntsho S, Kim JE (2016) A comprehensive review of hybrid forward osmosis systems: Performance, applications and future prospects. Journal of Membrane Science 497:430-449. https://doi.org/10.1016 /j.memsci.2015.09.041

Kim DI, Kim J, Kyong Shon H (2015) Pressure retarded osmosis (PRO) for integrating seawater desalination and wastewater reclamation: Energy consumption and fouling. Journal of Membrane Science 483:34-41. https://doi.org/10.1016/j.memsci.2015.02.025

Kim JE, Phuntsho S, Chekli L (2018) Environmental and economic assessment of hybrid FO-RO/NF system with selected inorganic draw solutes for the treatment of mine impaired water. Desalination 429:96-104. https://doi.org/ 10.1016/j.desal.2017.12.016

Motsa M, Mamba B, D'Haese A (2014) Organic fouling in forward osmosis membranes: The role of feed solution chemistry and membrane structural properties. Journal of Membrane Science 460:99-109. https://doi.org/10.1016/j.memsci.2014.02.035

Munirasa S, Abu Haija M, Banat F (2016) Use of membrane technology for oil field and refinery produced water treatment - A review. Journal of Process Safety and Environmental Protection 100:183-202. http://doi.org/ 10.1016/j.psep.2016.01.010

Yun T, Kim YJ, Lee S, Hong S, Kim, GI (2014) Flux behaviour and membrane fouling in pressure-assisted forward osmosis. Desalination and Water Treatment 52(4-6):564-569. https://doi.org/10.1080 /19443994.2013.827322

11th World Congress on Water Resources and Environment (EWRA 2019)
"Managing Water Resources for a Sustainable Future", 25-29 June 2019, Madrid, Spain

Optimum allocation of the pollutant load distributions based on a linked simulation-optimization approach

M.T. Ayvaz[1*], D. Sadak[1], A. Elci[2], M. Dilaver[3], S. Ayaz[3]
[1] Department of Civil Engineering, Pamukkale University, Denizli, Turkey
[2] Department of Environmental Engineering, Dokuz Eylül University, Izmir, Turkey
[3] Environment and Cleaner Production Institute, TUBITAK Marmara Research Center, Kocaeli, Turkey
* e-mail: tayvaz@pau.edu.tr

Introduction

Allocation of the pollutant load distributions among different sources in a watershed is an important problem in environmental management studies. According to the European Union Water Framework Directive (2000/60/EC) (WFD), the concentration of conventional, priority and specific pollutants should be lower than the mandated Environmental Quality Standards (EQS) to protect the aquatic environment and human health. In order to maintain these EQS values throughout the entire surface water system, pollutant loads are allocated to different pollution point sources usually applying a trial-and-error approach. Although this kind of an allocation approach can be easily implemented to the pollution sources in upstream locations, it may be difficult to do so for downstream locations since the flowing water is already polluted downstream while all EQS values are satisfied upstream. Therefore, it is required to apply a systematic solution approach for allocating the pollutant loads among different source locations based on the given EQS values.

The main objective of this study is to propose a linked simulation-optimization approach for allocating the pollutant loads among different source locations on a river basin. In the proposed approach, the pollutant concentration distribution of the river system is simulated using the AQUATOX water quality model (Park et al. 2008) based on the hypothetical but realistic values for hydraulic parameters and point source loadings. Since this AQUATOX-based simulation model cannot be integrated into the optimization model in its present form, model outputs are obtained by using a concentration-response matrix (CRM) (Su et al. 2019) instead of forward running the AQUATOX model. The developed CRM is then integrated into an optimization model where a heuristic differential evolution (DE) optimization method (Storn and Price 1997) is used. The performance of the proposed linked simulation-optimization approach is evaluated for different pollutant load scenarios and the identified results are interpreted in detail.

Materials and methods

This study is a part of a research project entitled "Identification of Receiving Water Body Based Discharge Limits Kucuk Menderes River Basin (Turkey) Case Study" which is supported by the Scientific and Technological Research Council of Turkey (TUBITAK). In the context of this project, water quality samples will be collected from different monitoring points every 2 months for one year and analyzed for different parameters suggested by WFD. After obtaining these parameter distributions, an AQUATOX-based water quality model will be set up by calibrating the model parameters based on the collected data. It should be noted that site and laboratory studies of the project are in their initial phase and development of the AQUATOX-based water quality simulation model for the entire river basin is underway. Thus, in this study, the model is set up on a sub-watershed of the Kucuk Menderes river basin by considering hypothetical but realistic hydraulic parameters and point source loadings. After completing all site and laboratory studies, the model will be replaced with the calibrated one based on the collected and analyzed data.

The AQUATOX model in the proposed approach will be used to determine pollutant concentration responses of pollutant loads from 4 point sources (two industrial sites, one domestic wastewater treatment plant, and one tributary) at the monitoring locations. Since the optimization process requires repetitive computations to generate load distributions, the AQUATOX model must be executed automatically for each

optimization cycle. Although this kind of integration appears to be sensible, integration of the AQUATOX to an optimization model is not possible in the present form. Therefore, a CRM is formed by calculating the concentration responses of the river system for the unit pollutant load values from the source locations. Note that the formed CRM is used to calculate the 5-day carbonaceous biological oxygen demand ($CBOD_5$) as the pollutant concentration for any given monitoring location. The formed CRM is then integrated into a DE-based optimization model. DE is a powerful heuristic optimization method and can solve various engineering optimization problems without requiring any derivative information and specialized initial solution. The objective of DE in the proposed approach is to determine the pollutant loads of the 4 source locations by minimizing the error between the simulated and EQS concentrations for the $CBOD_5$ parameter at the monitoring sites. This optimization procedure requires satisfying some constraints which are considered by means of the penalty function approach.

Results and concluding remarks

The conceptual model of the proposed approach is shown in Figure 1. As can be seen, observed $CBOD_5$ concentrations at monitoring points 3 and 4 are greater than the associated EQS value. According to WFD, $CBOD_5$ concentrations should be below the EQS value for all surface water bodies in the river basin. This goal is achieved by means of the proposed simulation-optimization approach by allocating pollutant loads among 4 source locations based on their load assignment weights. The performance of the proposed approach is then evaluated by considering different load assignment weights. The identified results indicate that the proposed approach can successively allocate the pollutant loads among source locations by maintaining the maximum $CBOD_5$ concentrations below EQS limit values for the entire surface water system being studied.

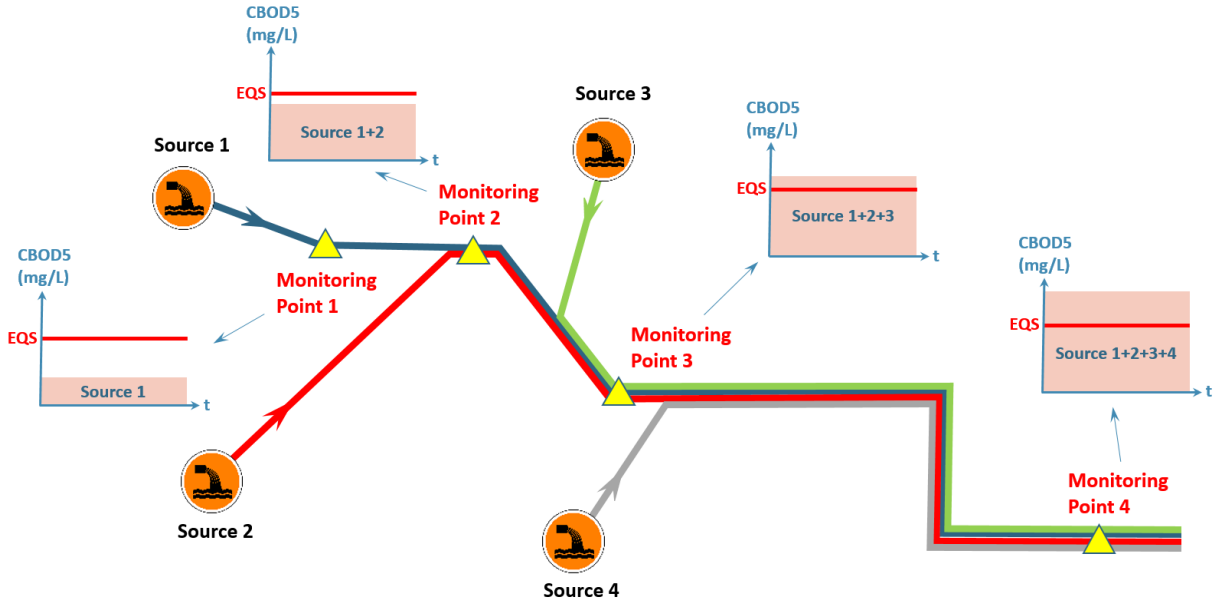

Figure 1. A conceptual model of the proposed simulation-optimization approach

Acknowledgments: This study is funded by The Scientific and Technological Research Council of Turkey (TUBITAK) under Project Number 116Y413/116Y414/116Y415.

References

Park RA, Clough JS, Wellman MC (2008) AQUATOX: Modeling environmental fate and ecological effects in aquatic ecosystems. Ecological Modelling 213:1–15

Su Y, Li K, Liang S, Lu S, Wang Y, Dai A, Li Y, Ding D, Wang X (2019) Improved simulation–optimization approach for identifying critical and developable pollution source regions and critical migration processes for pollutant load allocation. Science of the Total Environment 646:1336–1348

Storn R, Price K (1997) Differential Evolution – A Simple and Efficient Heuristic for global Optimization over Continuous Spaces. Journal of Global Optimization 11:341-359

11th World Congress on Water Resources and Environment (EWRA 2019)
"Managing Water Resources for a Sustainable Future", 25-29 June 2019, Madrid, Spain

Determination of rate of pollution decay coefficient in Talar river, Iran

R. Sadeghi-Talarposhti, K. Ebrahimi*, A.H. Hourfar, S.H. Hoseini-Ghafari
Department of Irrigation & Reclamation Eng, University of Tehran, Karaj, Iran
** e-mail: EbrahimiK@ut.ac.ir*

Introduction

Determining the accurate rate of pollution decay coefficient is an important issue in water quality management due to its effects on oxygen consumption in rivers. The main purpose of this paper is to determine the decay rate coefficient (Kc) of Talar River, Iran, by means of field experiments and to specialize empirical equations in spring and summer. Former studies on this topic have been published by Yeli Zink et al. (2016) for simulation of parameters in three stations including COD, NH_4-N and TP and hydraulic characteristics by QUAL2K model; the results of two methods to obtain the decay rate coefficient have been compared. Later, Feria Diaz et al. (2017) estimated the decay rate coefficient and the re-aeration coefficient of Sinu River in northwestern Colombia. The main parameters included BOD, DO, temperature and hydraulic characteristics; the values of Kc are between 0.1 and 0.37 according to Streeter and Phelps equation.

Recently, Abdollahi et al. (2018) evaluated the best equations of the re-aeration rate coefficient, among 29 most used equations based on the dissolved oxygen modelling for Karoon River, Iran, at different seasons (2010-2011). Using Qual2Kw5.1 software, the relevant modelled re-aeration rate coefficients for each season were equal to 0.62, 0.23, 0.33 and 1.59 (d^{-1}), respectively. Moghimi-Nezad et al. (2018) studied the seasonal variation of self-purification capacity of Karoon River, Iran. Results indicated that the decrease of nitrate in January and February and the decrease of BOD for all months except October up to 30% had the most positive effects on river water quality. The 30% decrease of wastewater flow rate containing pathogens had the most positive effects on the river water quality.

Materials and methods

In this study Kc was estimated for spring and summer by means of field experiments and new reformed coefficient of empirical equation for Talar River, Iran, was achieved. Talar River is sited in 52'31" E and 35'45" N branching from Alborz Mountains discharging to Caspian Sea with average annual flow rate of approximately 9.2 m^3/s.

Experimental data were collected and recorded in May and August 2018, at 5 stations located along the river at an interval of 1000 m. The main parameters included BOD, DO, EC, pH, Nitrate, Phosphate and temperature.

Results and concluding remarks

The measured parameters of five stations are shown as a sample in Table 1 for the spring. Considering the results of experiments, Kc was determined by Streeter and Phelps analytic model in reverse method. Coefficients of empirical equations resulted for Talar River, Iran, by employing calculated Kc values and intended parameters in empirical equations. The following Eqs. (1) and (2) resulted for Ka and Kc:

$$Ka = 1.490\ Kc\ (L'/D') + 0.937\ (\Delta D/\Delta T.D') + 1.16 \quad (1)$$

$$Kc = 0.2899\ (H)^{-1.764} \quad H<0.75 \quad (2)$$

where Ka and Kc are the re-aeration and decay rate coefficients (d^{-1}), respectively; L' and D' correspond to the average of the last carbonaceous BOD and the average of the oxygen deficit between two adjacent stations (mg/L); ΔD is the change in the dissolved oxygen between the adjacent stations (mg/L); ΔT is the average time used by the mass of water to pass through the adjacent stations (day); and H refers to the depth of water in the river (m).

Table 1. Value of measured quality parameters for five stations of Talar River, spring 2018.

Parameter	**Station 1**	**Station 2**	**Station 3**	**Station 4**	**Station 5**
DO (mg/L)	6.5	7.1	7.59	7.95	8.21
BOD_5 (mg/L)	6.3	5.1	3.9	3.4	3.0
EC (µS/cm)	1018	1012	1009	999	988
pH	7.01	7.30	7.21	7.20	7.17
Nitrate (mg/L)	0.606	0.881	0.983	0.751	0.606
Phosphate (mg/L)	0.119	0.113	0.146	0.181	0.363

In Figure 1, changes of oxygen deficit (DO) is illustrated for four ranges between the above mentioned five stations, where Kc_1, Kc_2, Kc_3, and Kc_4 corresponds to ranges between station 1 to 2, 2 to 3, 3 to 4 and 4 to 5, respectively and km 0 belongs to station 1. Results show that the values of DO along the river are at critical conditions. Kc curves are increasing along the river for all four ranges along the river. Moreover, no decrease along the river could be seen; so there will not be any considerable problem in this season due to the values of BODs.

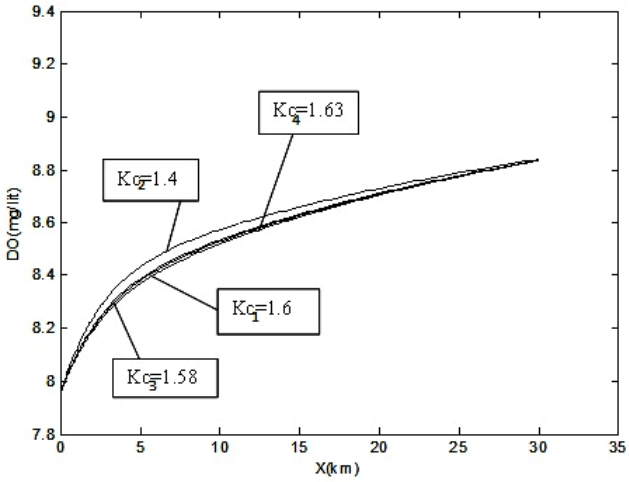

Figure 1. Changes in DO, Talar River, Spring 2018.

Acknowledgments: The authors are grateful to University of Tehran for providing facilities for conducting the present research.

References

Feria-Diaz JJ, Nader-Salgado D, Meza-Perez SJ (2017) Rates of deoxygenation and reaeration for the Sinú River. Ingeniería y Desarrollo 35(1):1-17. doi: 10.14482/inde.35.1.8940

Zhang Y, Yang H, Wang Z (2016) Simulating Water Quality of Wei River with QUAL2K Model, a Case Study of Hai River Basin in China. The 3rd International Conference on Industrial Engineering and Applications, vol 68. https://doi.org/10.1051/matecconf/20166814005

Streeter HW, Phelps EB (1958) A Study of the Pollution and Natural Purification of the Ohio River. U.S. Publ. Health Service Bull., 1925, 146:1–75

Abdollahi B, Ebrahimi K, Araghi-Nejhadz Sh, Liaghat AM (2018) Annual Investigation of the Karoon River Re-aeration Rate Coefficient. Iranian J. Soil and Water Research 49(4):925-943. doi: 10.22059/ijswr.2018245357.667789

Moghimi-Nezad S, Ebrahimi K, Karachian R (2018) Investigation of Seasonal Self-purification Variations of Karoon River, Iran. Amirkabir J. Civil Eng. 49(4):193-196. doi: 10.22060/ceej.2016

11th World Congress on Water Resources and Environment (EWRA 2019)
"Managing Water Resources for a Sustainable Future", 25-29 June 2019, Madrid, Spain

ENFOCAR: An approach to evaluate chemical mixtures formed during water disinfection

C. Aznar-Luque, E. Pérez-Albadalejo, C. Porte, C. Postigo*
Water and Soil Quality Research Group, Department of Environmental Chemistry, Institute of Environmental Assessment and Water Research (IDAEA-CSIC), Barcelona, Spain
** e-mail: cprqam@cid.csic.es*

Introduction

Disinfection of water is one of the major triumphs in public health of the 19th century because it contributed to reducing the number of deaths due to waterborne diseases. Since its discovery, this practice has been commonly used to ensure the safety of drinking and reclaimed water. However, during the reaction of chemical disinfectants (such as chlorine) with pathogenic organisms and any organic and inorganic matter present in water, a large suite of disinfection byproducts (DBPs) is formed.

The main concerns regarding the presence of DBPs in disinfected water are related to their potential toxicity. Many of these compounds (most of them halogenated) were found to be highly genotoxic and cytotoxic to Chinese hamster ovary (CHO) mammalian cells in *vitro* assays (Richardson et al. 2007). Moreover, they have been associated with the appearance of negative effects at reproductive and developmental level, and even with a high incidence of bladder cancer in several epidemiological studies (Nieuwenhuijsen et al. 2009).

However, the DBP mixture formed during disinfection processes has not been completely characterized and the toxic effects of the mixture are also largely unknown. Thus, preventive measures call for minimizing of toxic DBPs in disinfected waters to protect public and environmental health. For this, analytical approaches that allow identifying the most toxic DBPs in disinfected water so that they can be minimized have to be developed.

ENFOCAR, a project funded by the second edition of the ComFuturo Programme (a compromise between public and private entities to foster science and future), was designed to attain this challenge. This work presents the results obtained in the first stage of the project.

Materials and methods

The approach selected to identify the most relevant compounds in the DBP mixture is based on an "effect-directed analysis" (EDA) (Burgess et al. 2013). This approach allows simplifying the mixture in different fractions. The toxicity of each fraction needs to be evaluated with an in vitro bioassay so that chemical characterization efforts can be focused in toxic fractions.

First, a representative DBP mixture extract has to be obtained from water by using a generic extraction protocol. For this, the recoveries of organic chemicals (>80) belonging to different chemical classes (i.e., pharmaceuticals, plasticizers, oestrogens, pesticides, haloacetic acids, haloacetamides and haloacetonitriles) were evaluated after extracting fortified waters containing these compounds with different SPE generic-purpose sorbents (i.e., extraction mixture of DAX8 over XAD2 resins, ENV+, Oasis HLB, TELOS ENV; TELOS PSDV, ENVI-carb, DPA-6S) and using liquid-liquid extraction (LLE) with MTBE. Analyte recovery was evaluated by means of liquid chromatography and gas chromatography coupled to mass spectrometry.

The compatibility of the best generic extraction protocol selected with the in vitro assay was also evaluated. The in vitro assay selected was a human placental cell line (JEG-3) (Pérez-Albadalejo et al. 2017), based on previous reports regarding the potential reprotoxicity of these compounds. Since the toxicity of DBPs to this cellular model was not investigated before, the cytotoxic and oxidative stress (ROS) response of the model to various haloacetic acids was also evaluated.

The best extraction protocol was preliminary applied to the extraction of a real sample of chlorinated

reclaimed water. Characterization of DBP mixtures was done by means of LC and GC coupled to high resolution mass spectrometry.

Results and concluding remarks

The best extraction performance was observed for the Telos ENV sorbent. However, due to the different selectivity of extraction of the SPE approach as compared to the LLE approach, both approaches were used to extract the sample of reclaimed water. Extracts obtained were analysed by means of LC and GC coupled to high resolution mass spectrometry and features obtained are currently being evaluated.

Next steps will be focused on the toxicological characterization of these extracts and the fractionation of the extract by means of HPLC in order to identify the toxicity drivers. Furthermore, the toxicological response of the DBP mixture and its fractions will be compared to that obtained for the haloacetic acids tested.

Acknowledgments: C. Postigo acknowledges the financial support by Fundación General CSIC (Spanish ComFuturo Programme). This work was supported by the Government of Catalonia (Consolidated Research Groups 2017 SGR 01404- Water and Soil Quality Unit).

References

Burgess RM, Ho KT, Brack W, Lamoree M (2013) Effects-directed analysis (EDA) and toxicity identification evaluation (TIE): Complementary but different approaches for diagnosing causes of environmental toxicity. Environmental Toxicology and Chemistry 32:1935-1945

Nieuwenhuijsen MJ, Grellier J, Smith R, Iszatt N, Bennett J, Best N, Toledano M (2009) The epidemiology and possible mechanisms of disinfection by-products in drinking water. Philosophical Transactions of the Royal Society A 367:4043-4076

Pérez-Albadalejo E, Fernandes D, Lacorte S, Porte C (2017) Comparative toxicity, oxidative stress and endocrine disruption potential of plasticizers in JEG-3 human placental cells. Toxicology in vitro 38:41-48

Richardson SD, Plewa MJ, Wagner ED, Schoeny R, Demarini DM (2007) Occurrence, genotoxicity, and carcinogenicity of regulated and emerging disinfection by-products in drinking water: a review and roadmap for research. Mutation Research 636:178-242

11th World Congress on Water Resources and Environment (EWRA 2019)
"Managing Water Resources for a Sustainable Future", 25-29 June 2019, Madrid, Spain

Microalgae-bioremediation of water containing pesticides: The experience of the BECAS project

E. López-García[1], M.V. Barbieri[1], C. Postigo[1], R. Ávila[2], P. Blánquez[2], M. Rambla-Alegre[3], V. Sola[4], T. Vicent[2], M. López de Alda[1*]

[1] *Water and Soil Quality Research Group, Department of Environmental Chemistry, Institute of Environmental Assessment and Water Research (IDAEA-CSIC), Barcelona, Spain*

[2] *Departament d'Enginyeria Quimica, Biologica i Ambiental, Universitat Autonoma de Barcelona (UAB), Cerdanyola del Valles, Spain*

[3] *IRTA, Ctra Poble Nou, km 5.5, 43540, Sant Carles de la Ràpita, Spain*

[4] *Comunitat d'Usuaris d'Aigües de la Vall Baixa i del Delta del Llobregat (CUADLL), El Prat de Llobregat, Spain*

** e-mail: mlaqam@cid.csic.es*

Introduction

Large volumes of pesticides are produced and used for different purposes worldwide, being the most relevant one the control of agricultural pests. Agriculture has been appointed as the main anthropogenic activity that negatively affects the quality of environmental waters. Due to their chemical diversity, pesticides, once in the environment, may cause very different acute and chronic damages in aquatic organisms, including endocrine disruptive effects, and effects at reproductive and developmental level (FAO 1997). To reduce their presence in the environment, and thus, their potential impacts, there is a need for developing novel technologies capable of removing them at their source. Non-biological processes based on adsorption on granular activated carbon (García Portillo et al. 2014) or advanced oxidation processes (Carar et al. 2004) have been proposed for this purpose. However, these technologies are expensive and their efficiency is usually matrix-dependant. Based on this, the BECAS project, funded by the Spanish State Research Agency (AEI) and the European Regional Development Fund (ERDF), aims at developing bioremediation systems to biodegrade hardly naturally-biodegradable pesticides commonly found in water bodies. Thus, the present work aims at presenting the objectives and progress of the BECAS project in this regard, with special emphasis on the experiments conducted to investigate the capability of microalgae to treat pesticide-containing waters.

Materials and methods

During the first stage of the project, analytical tools based on mass spectrometry detection were developed for the multi-residue analysis of pesticides in waters. These methodologies were applied to characterize the pesticides present in waters and sediments of three agricultural areas of Catalonia (NE Spain) with different crops and irrigation techniques: Lower Llobregat River basin, Ebro River Delta and Mas Badia.

Environmental risk of pesticides detected in these areas was evaluated using toxic units and risk indexes, using toxicity data reported in peer-reviewed literature. Structure-activity relationship models were used to estimate toxicity of pesticides for which literature data were not available.

Microalgae-based biodegradation experiments were conducted with three pesticides (acetamiprid, propanil and bentazone) that were selected upon their occurrence on the areas monitored. For this, 250 mL Erlenmeyer flasks containing 100 mL of microalgae biomass from a pilot-plant tubular photobioreactor Hom-Diaz et al. 2017) (2.1 ± 0.4 g dry weight/L) and the pesticide (1 mg/L) were used. Flasks were continuously exposed to light and orbital shaken at 25ºC. For each pesticide, four different cultures, in triplicate were done, so that, adsorption, photodegradation, and microalgae degradation could be differentiated.

Pesticide degradation and formation of transformation byproducts in the different cultures at time zero, 2 days and 7 days of the experiment was investigated by means liquid chromatography coupled to high-

resolution mass spectrometry, using a hybrid quadrupole-Orbitrap (Q-Exactive).

Results and concluding remarks

According to the monitoring studies carried out, pesticide presence was more relevant in the Ebro River Delta than in the Lower Llobregat River basin, both in water and sediments. The occurrence of pesticides in Mas Badia area is currently under study. The environmental risk assessment will show the relevance of the type and abundance of pesticides found in these areas.

The results obtained in degradation experiments showed that microalgae were only capable of degrading propanil and acetamiprid but not bentazone. While propanil was fully degraded after 2 days of treatment, 50% of acetamiprid still remained in solution after that time. On the contrary, bentazone concentration did not change after 7 days of treatment. Control cultures indicated that pesticides were not adsorbed on the biomass.

Mass spectrometry data suggest the formation of TPs during the degradation processes of propanil and acetamiprid. Identification of these TPs is ongoing.

Acknowledgments: This work has received funding from the Government of Catalonia (2017 SGR 01404 and 2017 SGR 00014), the Spanish State Research Agency (AEI) and the European Regional Development Fund (ERDF) through the project BECAS (grant number CTM2016-75587-C2-2-R), and the European Union's Horizon 2020 Research and Innovation Programme under grant agreement No. 727450. This presentation only reflects the authors' views and the Commission is not responsible for any use that may be made of the information it contains.

References

FAO (1997) Lucha contra la contaminación agrícola de los recursos hídricos. Capítulo 4 – Los plaguicidas, en cuanto contaminantes del agua; E.D. Ongley, FAO, Burlington, pp 59-76. http://www.fao.org/docrep/W2598S/w2598s00.htm

García Portillo M, Avino ES, Vicente JO, De Andres RL, Jimenez MAS, Blanco JPL (2004) Purification system for wastewater coming from fruit and vegetable processing plants and phytosanitary treatment in the field. United States Patent US6709585B1

Carra I, Sánchez Pérez JS, Malato S, Autin O, Jefferson B, Jarvis P (2014) Performance of different advanced oxidation processes for tertiary wastewater treatment to remove the pesticide acetamiprid. Journal of Chemical Technology and Biotechnology 91: 72-81

Hom-Diaz A, Jaén-Gil A, Bello-Laserna I, Rodríguez-Mozaz S, Vicent T, Barceló D, Blánquez P (2017) Performance of a microalgal photobioreactor treating toilet wastewater: Pharmaceutically active compound removal and biomass harvesting. Science of the Total Environment 592:1–11

11th World Congress on Water Resources and Environment (EWRA 2019)
"Managing Water Resources for a Sustainable Future", 25-29 June 2019, Madrid, Spain

Study of scale formed by southern Algeria groundwater on irrigation PVC pipe by degassing CO_2 water

R. Ketrane
LECVE «Laboratoire Electrochimie Corrosion Valorisation Energétique», Département de Génie des Procédés-Université de Béjaia, Route de Targa Ouzemmour, Béjaia (06000), Algeria
e-mail: rachid.ketrane@gmail.com

Introduction

In Algeria desert, groundwater recovered from two water aquifers (Complex Terminal and Continental Intercalary) is the main source of drinking water and of irrigation for agricultural development (Larbes 2003). The temperature of the groundwater pumped from large depths varies from 25 to 73 °C. This groundwater, which has a strong mineralization, leads to a very strong hardness. The high temperature and the strong mineralization promote formation of scale deposits on drain water pipes and cooling towers (Larbes 2003; Bouchkima 2003). This phenomenon has serious technical and economic consequences. Very little works are devoted to southern Algeria groundwater (Ketrane et al. 2010).

Scale deposition kinetics is generally long under natural conditions. Therefore, different techniques have been proposed to accelerate the phenomenon in the laboratory. In this study, the $CaCO_3$ precipitation is provoked by degassing dissolved CO_2 in a cylindrical cell made of polyvinyl chloride (PVC), a material that is widely used in irrigation pipes in Algeria.

The aim of this work is to artificially reconstitute at laboratory level the precipitation conditions of scale formed from geothermal waters in a very short period while taking into account the main parameters (hardness and temperature of the water).

Materials and methods

In this study, $CaCO_3$ precipitation is provoked by degassing water dissolved CO_2 in a cylindrical cell. The experiments are conducted in set up designed in our laboratory (Figure 1).

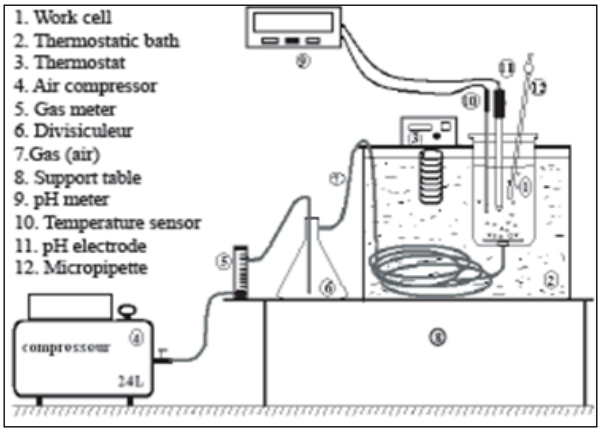

Figure 1. Device of the experimental controlled degassing CO_2 technique

To initiate the precipitation of $CaCO_3$, the calcocarbonic equilibrium ($CaCO_3$-CO_2-H_20) is displaced by outgassing the dissolved CO_2 by bubbling with a continuous flow of gas poor in CO_2 (8 L/min) according to:

$$Ca^{2+} + 2HCO_3^- \rightleftharpoons CaCO_3 + CO_2 + H_2O$$

The $CaCO_3$ precipitation is studied on plastic material substrate made of polyvinyl chloride (PVC) which is a material widely used in irrigation pipes. The experimental solution used is calcocarbonically pure water (CCP water) of hardness at 30, 50 and 70 °f (1 °f = 10 mg/L of dissolved $CaCO_3$) at 30 °C. The kinetic study

consisted in following over time the solution pH as well as the concentration of free Ca^{2+} ions in the water.

Results and concluding remarks

The kinetic study on the PVC substrate has shown that germination time decreases with the water hardness (30, 50 and 70 °f) at 30 °C. Moreover, the precipitation rate increases with the water hardness. As expected, increased hardness of water accelerates the scale precipitation.

The maximum pH values are inversely proportional to the hardness. In fact, maximum pH values reached for 70, 50, 30 °f are 8.04, 8.18 and 8.46, respectively. In addition, maximum pH value is reached more quickly when the water is hard. This means that the supersaturation is reached more quickly for waters that have a higher hardness.

The $CaCO_3$ amounts determined by measuring free ion calcium and by filtration of the solution at the end of the experiments (2 hours) shows that the heterogeneous precipitation (on the wall of the substrate) of $CaCO_3$ is more important (94% of total mass of the scale) than the homogeneous precipitation in solution (6% of total mass of the scale).

Finally, SEM observations showed that formed calcium carbonate precipitated mainly in the form of calcite, a crystallographic form that is the most thermodynamically stable and the most adherent to the walls.

References

Bouchkima B (2003) L'eau de la nappe albienne du sud algérien. Journées Techniques et Scientifiques sur la Qualité des Eaux du Sud, El-Oued Algeria. Vol. III, pp 39–51

Ketrane R, Leleyter L, Baraud F, Jeannin M, Otavio Gil O, Saidani B (2010) Characterization of natural scale deposits formed in southern Algeria groundwater. Effect of its major ions on calcium carbonate precipitation. Desalination 262:21–30

Larbes A (2003) Le système aquifère du Sahara septentrional. Journées Techniques et Scientifiques sur la Qualité des Eaux du Sud, El-Oued Algeria. Vol. I, pp. 25–34

11th World Congress on Water Resources and Environment (EWRA 2019)
"Managing Water Resources for a Sustainable Future", 25-29 June 2019, Madrid, Spain

Water quality assessment using a modified water quality index: A case study of El Abid River, Morocco

I. Karaoui*, A. Arioua, M. Hssaisoune
Sultan Moulay Slimane University, Béni Mellal, Morocco
** e-mail: I.karaoui@usms.ma*

Introduction

The anthropogenic activities, has an impact on the river quality in the global scale, in many cases that still had to be fully quantified (Meybeck 2005). Whilst, our ability to understand the size of anthropogenic damages are reduced by the limit availability of long term water quality data-sets, and the lack of methods which allows the better understanding of the quality parameters, later on fail to have the best knowledge of the river global quality (Burt et al. 2014).

The question that is repeated all the time is How to compare the quality of different water sources, which cannot be done easily by comparing the list of constituents in each sample. The traditional approaches are based on a comparison of experimentally values obtained in laboratory with existing local standards and giving the same coefficient or importance to all the parameters used for this determination. In many cases, this methodology allows identifying of contamination sources and may be essential for verifying legal compliance. However, it does not give an exact view on the overall water quality while we are comparing samples (Abbasi and Abbasi 2012).

To answer to this complicated question, some researchers have made strides towards employing applied mathematical computational indices (defined as WQI), which seek to address this vexing problem and to communicate information on water quality trends in a single number (like a grade; Pesce and Wunderlin 2000).

Despite the overabundance of WQI indices which have been used and developed, it is not possible to say which index is the best or even a list of ten best indices. In general, physicochemical variables are considered in a similar way, only the statistical integrations of parameters among this method are in different ratios. For example, 20 parameters were involved in NSF-WQI to assess water quality in the Suquı'ıa River (Pesce and Wunderlin 2000) while in Bagmati River only 18 (Kannel et al. 2007). Indeed, a modification into NSF-WQI is necessary to reduce the redundant variables that are much correlated.

Materials and Methods

In order to evaluate El Abid River water quality, a one year physicochemical and pollution parameters measurements have been used to check the seasonal surface quality variation and develop a new index that aims to better describe the global quality estimation in the study area. The El Abid River watershed is located in the central part of Morocco, in a distance of 60 km South of Béni Mellal city.

Based on analytic results, an NSF-WQI index was calculated for the most contrasting periods, dry season and wet season. The NSF-WQI is an arithmetic weighted index that classifies the water quality according to a scale of 0-100 with the interval 100-80% are considered as '' very bad quality", while 0-20% as "Excellent quality" (Sapkal and Valunjkar 2013).

The NSF-WQI index results are subjected to a Principal Component Analysis (PCA) to determine the correlated parameters that have the same effect on NSF-WQI index variation. Those parameters are tested to check their impact on NSF-WQI results while we eliminate them.

Results and concluding remarks

Based on Pearson's law (n) correlation results (Table 1), the electrical conductivity (EC) has a high correlation with chloride (Cl^-) (R^2=0.728), while organic matter (OM) and biological oxygen demand (BOD) are almost correlated (R^2=0.980). The total hardness (TH) has a correlation of R^2= 0.628 and R^2=0.687

consecutively with sulphate (SO_4^{2-}) and total alkalinity (TA).

Table 1. Pearson (n) correlation matrix for parameters used in NSF-WQI index

Variables	pH	EC	BOD	OM	DO	Cl^-	NO_3^-	SO_4^{2-}	PO_4^{3-}	TH	TA
pH	**1**	-0,156	-0,217	-0,217	-0,057	0,072	0,280	-0,252	-0,073	-0,392	-0,369
EC		**1**	0,349	0,349	-0,171	0,729	0,248	0,351	-0,023	0,517	0,257
BOD			**1**	0,980	-0,035	0,220	-0,265	0,392	0,379	0,131	-0,136
OM				**1**	-0,035	0,220	-0,265	0,392	0,379	0,131	-0,136
DO					**1**	-0,111	-0,059	-0,039	0,037	-0,068	0,013
Cl^-						**1**	0,181	-0,040	0,068	0,010	-0,071
NO_3^-							**1**	0,036	-0,191	0,372	0,284
SO_4^{2-}								**1**	0,050	0,628	0,278
PO_4^{3-}									**1**	-0,126	-0,185
TH										**1**	0,688
TA											**1**

Based on the PCA results, a first WQI_{min} can be made based on the SO_4^{2-} and TH elimination, due to their high correlation with TA. The BOD use instead of OM, and the EC employment rather than Cl^-. The relative weights of the eliminated parameters are added into the weight factor of the correspondence correlated parameter.

The comparison between WQI_{min} and NSF-WQI results (Figure 1) shows that both indices are not graphically much different. Statistically their correlation has an R^2 = 0.89; S.D. = 4.67; RMSE= 2.96), the only variation is seen in some data set from summer season and Oum Er-Rbia River (P12-13).

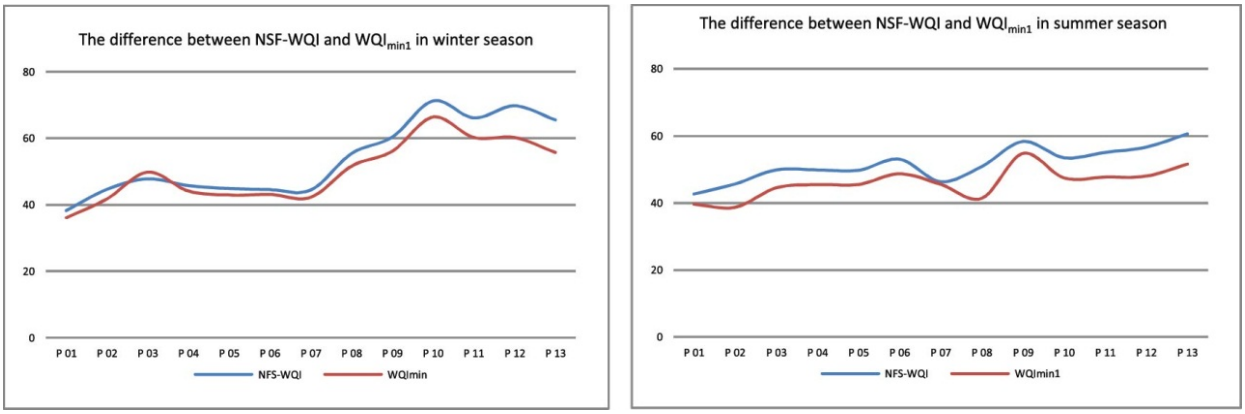

Figure 1. Difference between winter and summer in the proposed index (WQImin1) and NSF-WQI

The NSF-WQI and proposed index WQI_{min} use were verified according to Moroccan standards as a useful tool for assessing and classify spatial and temporal changes in water quality. This new proposed index WQI_{min} is seeking to minimize as much as possible the cost of the chemicals products used in standard NSF-WQI index, and to give a precise surface water evaluation.

References

Abbasi T, Abbasi SA (2012) Why Water-Quality Indices. In: Water Quality Indices, Elsevier, pp 3–7. Retrieved from http://linkinghub.elsevier.com/retrieve/pii/B9780444543042000014

Burt TP, Howden NJK, Worrall F (2014) On the importance of very long-term water quality records. Wiley Interdisciplinary Reviews: Water 1(1):41–48

Kannel PR, Lee S, Lee Y-S, Kanel SR, Khan SP (2007) Application of water quality indices and dissolved oxygen as indicators for river water classification and urban impact assessment. Environmental Monitoring and Assessment 132(1):93–110

Meybeck M (2005) Looking for water quality. Hydrological Processes 19(1):331–338

Pesce SF, Wunderlin DA (2000) Use of water quality indices to verify the impact of Córdoba City (Argentina) on Suquía River. Water Research 34(11):2915–2926

Sapkal RS, Valunjkar SS (2013) Development and sensitivity analysis of water quality index for evaluation of surface water for drinking purpose. International Journal of Civil Engineering and Technology 4(4):119-134

11th World Congress on Water Resources and Environment (EWRA 2019)
"Managing Water Resources for a Sustainable Future", 25-29 June 2019, Madrid, Spain

Selenium removal from water by adsorption onto FeOOH

K. Kalaitzidou[1], K. Simeonidis[2], M. Mitrakas[1*]
[1] Department of Chemical Engineering, Aristotle University of Thessaloniki, 54124, Thessaloniki, Greece
[2] Department of Physics, Aristotle University of Thessaloniki, 54124, Thessaloniki, Greece
* e-mail: manasis@eng.auth.gr

Introduction

Selenium is released in the environment by natural sources and anthropogenic activities that include the use of a wide variety of selenium based materials and runoff drainage (Ma et al. 2018). Regarding selenium in surface and groundwater selenite [SeO_3^{2-}], and the more soluble selenate [SeO_4^{2-}] are the most commonly encountered species (Hayashi et al. 2009). Excessive selenium consumption results to neurological and dermatological effects attributed to its toxicity when accumulated (Barron et al. 2009).

Many technologies have been studied on selenium removal, while adsorption is considered a very competitive method due to efficient removal and low cost. In the present study adsorbents commercially available GFH and Bayoxide as well as laboratory synthesized FeOOHs were evaluated through batch experiments with the same initial concentration (100 μg/L Se(IV) or Se(VI)). Experiments showed near zero Se(VI) uptake for all the adsorbents studied. Iron oxy-hydroxides (FeOOHs) were evaluated by adsorption isotherms and achieved optimal results on Se(IV) adsorption. The experimental data were better fitted to Freundlich adsorption model and the maximum adsorption capacity of 3.1 μg Se(IV)/mg adsorbent was achieved by the FeOOH synthesized at pH 2.5, which mainly consisted of schwertmannite (oxy-hydroxy-sulfate ($Fe_{16}O_{16}(OH)_{10}(SO_4)_3 10H_2O$). It is noticeable that adsorption of Se(IV) was mainly related with surface charge density and affected by the presence of sulfates and specific surface area.

Materials and methods

The examined FeOOHs were synthesized according the procedure which is described in detail in Tresintsi et al. (2012), by oxidation-hydrolysis of $FeSO_4 \cdot H_2O$ under high redox potential and pH values in the range of 2.5-8. Batch adsorption experiments were carried out in order to record the respective isotherms for the evaluation of adsorbents' efficiency. An amount of 10-60 mg of fine powdered samples was dispersed in 200 mL of phosphate solutions at pH 7 in 300 mL conical flasks. The flasks were placed in an orbital shaker and stirred for 24 h at 20°C. After 24 h contact time filtration at 0.45 μm follows and residual concentration of selenium is determined. The adsorbents were evaluated through their adsorption capacity at the equilibrium concentration of 10 μg Se/L, which is abbreviated as Q_{10}, henceforth (European Union 1998). Initial and residual concentrations were determined by Graphite Furnace Atomic Absorption Spectrophotometry, by a Perkin-Elmer AAnalyst 800 instrument. Stock solutions of Se(IV) and Se(VI) were prepared from analytical reagent grade Na_2SeO_3 and $NaSeO_4$, respectively, dissolved in distilled water. Working standards were freshly prepared by proper dissolution of stock the solutions in NSF water (prepared by dissolving 252 mg $NaHCO_3$, 12.14 mg $NaNO_3$, 0.178 mg $NaH_2PO_4 \cdot H_2O$, 2.21 mg NaF, 70.6 mg $NaSiO_3 \cdot 5H_2O$, 147 mg $CaCl_2 \cdot 2H_2O$ and 128.3 mg $MgSO_4 \cdot 7H_2O$ in 1 L of distilled water) containing the interfering ions commonly encounter in natural waters.

Results and concluding remarks

Adsorption isotherms reflect the equilibrium between the concentrations of selenium in the solution and onto the surface of the adsorbent at a given temperature. The results were better fitted to Freundlich model. As already mentioned experiments showed near zero Se(VI) uptake for all the adsorbents studied, which spotlights the weakness of adsorption process to meet drinking water regulation limit of 10 μg/L for Se(VI) removal. Figure 1 shows that the experimental results for adsorption capacities for Se(IV) removal of the batch experiments for the studied FeOOHs at pH 7. The respective Q_{10} adsorption capacities are shown

in Table 1 alongside with the main characteristics of the examined FeOOHs.

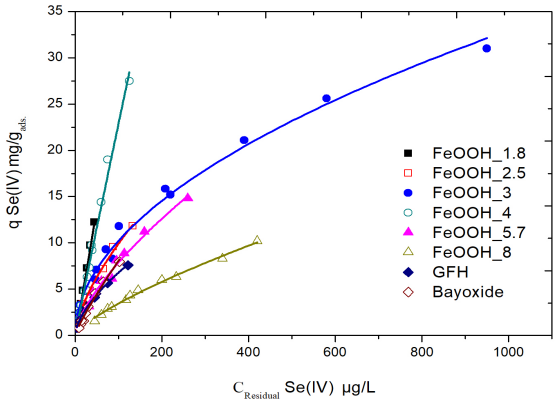

Figure 1. Adsorption isotherms for Se(IV) uptake onto FeOOHs.

Table 1. Adsorbents characteristics and adsorption capacities.

Adsorbent	q_{10} mgSe(IV)/gFeOOH	%Fe	BET m^2/g	C_{tot} mmol/g	IEP	pH_{PZC}	Bulk density
GFH	1.6	54.2	237	1.0	7.1	5.2	1.28
Bayoxide	1.0	52	135	0.8	7.4	7.8	0.41
FeOOH-2	2.7	38.6	100	2.8	5.7	2.6	0.46
FeOOH-2,5	3.1	44.8	48	3.25	6.9	2.7	0.54
FeOOH-3	2.7	44.9	53	2.45	7.2	2.9	0.54
FeOOH-4	2.4	50.4	120	2.23	7.1	2.9	0.49
FeOOH-5,7	1.7	50.1	168	1.42	7.3	4.2	0.49
FeOOH-8	1.4	50.2	226	1.04	6.6	7.9	0.48

The most important remark of this study is that there is a strong correlation between total surface charge of OH^- group and adsorption capacity. Figure 2 shows this correlation.

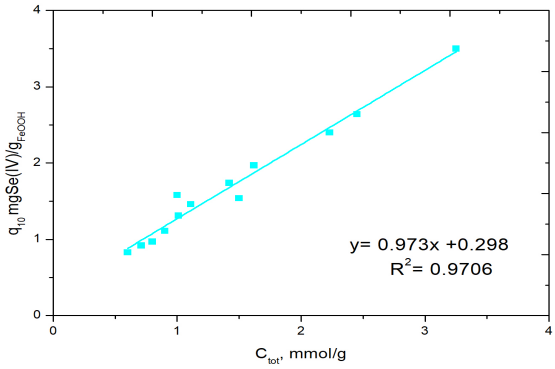

Figure 2. Adsorption capacity Q_{10} of FeOOHs versus C_{total}.

References

Barron E, Migeot V, Rabouan S, Potin-Gautier M, Seby F, Hartemann P, Levi Y, Legube B (2009) The case for re-evaluating the upper limit value for selenium in drinking water in Europe. Journal of Water and Health, 07(4):630-642. https://doi:10.2166/wh.2009.097

Hahashi H, Kanie K, Shinoda K, Muramatsu A, Suzuki S, Sasaki H (2009) pH-dependence of selenate removal from liquid phase by reductive Fe(II)–Fe(III) hydroxysulfate compound, green rust. Chemosphere 76:638-643. https://doi:10.1016/j.chemosphere.2009.04.037

Ma Z, Shan C, Liang J, Tong M (2018) Efficient adsorption of Selenium(IV) from water by hematite modified magnetic nanoparticles. Chemosphere 193:134-141. https://doi.org/10.1016/j.chemosphere.2017.11.005

Tresintsi S, Simeonidis K, Vourlias G, Stavropoulos G, Mitrakas M (2012) Kilogram-scale synthesis of iron oxy-hydroxides with improved arsenic removal capacity: Study of Fe(II) oxidation-precipitation parameters. Water Research 46(16):5255-5267. http://dx.doi.org/10.1016/j.watres.2012.06.049

The Council of the European Union (1998) Council Directive 98/93/EC of November 1998 on the equality of water intended for human consumption. Off. J. Eur. Communities 330:32–54

11th World Congress on Water Resources and Environment (EWRA 2019)
"Managing Water Resources for a Sustainable Future", 25-29 June 2019, Madrid, Spain

On the use of DPSIR model for defining the water quality determinants of groundwater abstraction in coastal aquifer

S. Hani[1*], S. Lallahem[2], A. Hani[1], L. Djabri[1], H. Chaffai[1], N. Bougherira[1]
[1] Department of Geology, Badji Mokhtar Annaba University / Water resource and sustainable development Labory, Annaba, Algeria
[2] IXSANE, 11 B Avenue de l'Harmonie, HUB Innovation La Haute Borne, 59493 Villeneuve d'Ascq, France
* e-mail: hani.samir@outlook.fr

Introduction

Water resources management in semi-arid Mediterranean countries with scarce water resources is a complex challenge (Sharma 1998, Jones et al. 2010). It requires new concepts and techniques if management should be based on sound scientific findings in order to optimize and conserve the precious water resources (Rajurkar et al. 2004).

In regards to integrated water resources management (IWRM), no systematic comprehensive multidisciplinary works have been developed so far and even they seem to have shortcomings. Therefore, many scholars explicitly have called for additional work to substantiate this aspect.

In this research, a relation between groundwater abstraction and socioeconomic variables in the Annaba coastal aquifer has been developed based on a cause–effect relationship tackling the life cycle of water resources management. The driver-pressure-state-impact-response (DPSIR), EEA, was selected as a well-established framework to develop the possible socio-economic variables (Lallahem and Hani 2016).

Materials and methods

Annaba region, in Algeria, is currently facing an acute shortage of freshwater supply and water is seen as one of the most critically stressed resources. The regional aquifer system is limited in the west by the Edough metamorphic complex, in the south by Fetzara Lake and the eastern extension of the Cheffia Numidian mountains, in the north by the Mediterranean Sea, and finally in the east by the Bouteldja Numidian massifs.

The total area of the Annaba region is 760 km^2. The study area is divided into 21 main sectors. The population of Annaba is expected to double by 2020 to reach 2 millions. This will worsen the already precarious situation. However, the current withdrawals are very far from meeting demand in terms of quantity and quality: domestic water supply is only 100 liters per capita per day (L c^{-1} d^{-1}), com-pared with 150 L c^{-1} d^{-1} recommended by the World Health Organization (WHO) standards. Over-exploitation of the aquifer has led to falling groundwater levels and deteriorating water quality due to seawater intrusion. Furthermore, groundwater quality is made worse through the infiltration of sewage, polluted surface water, solid waste leachates, and agricultural chemicals. Chloride and nitrate contents of the water are very high, at many locations exceeding maximum levels established by the WHO for drinking water. During recent years, water resource shortages and water pollution have severely hindered the socio-economic development in many parts of Annaba. Considering the potential doubling of population by year 2020, water demand will increase to reach 300 hm^3 $year^{-1}$ by that time. This projected value will definitely exceed the sustainable capacity of the aquifer.

The tools chosen for this research were ANN, expert opinion and judgment, health risk assessment, basic statistics, and multivariate techniques. The software selected were the STATISTICA package version 6.0, STATISTICA Neural Networks (SNN) Release 4.0 E and RISC WorkBench. There are five steps in the proposed methodology for developing a conceptual integrated water model:

- Step 1: This first step expresses the creation of the ANN model, the characterization and prioritization of the effective variables, and the establishment of the modeling prediction relationships.

- Step 2: This indicates the analysis of the questionnaire undertaken to explore the expert opinion and judgment of various stakeholders using descriptive statistics. The results of Step (2) were compared with the results of the ANN in Step (1) to examine the understanding and knowledge of the local experts about the actual baseline conditions of water sector.
- Step 3: Transformation of data variables that were not normally distributed, and calculation of the correlation matrix, were carried out in Step (3) for the variables selected from Step (1).
- Step 4: Three techniques of multivariate analysis were undertaken in Step (4) for the selected variables, to classify them with the relevant municipalities.
- Step 5*:* This final step explains the health risk assessment of the Annaba Wastewater Treatment Plant as a contaminated hotspot. It assessed the health risks associated with the current disposal of wastewater on the sea shore close to the bathing areas. The chemicals identified as carcinogenic risks were fed back into the CWIMSAM model.

Results and concluding remarks

In this research, a new conceptual water integrated model has been developed based on cause–effect relationships. The new model depicts the most important elements and science related to water, and indicates that water resource development and management must be within the ecological sustaining limits of the available natural water resources. The new conceptual water integrated model was applied to the life cycle of water resources management in the Annaba region.

The effective variables have been characterized and prioritized using multi-criteria analysis with ANN, risk assessment techniques, and expert opinion and judgment. The selected variables have been classified and organized using the multivariate techniques of cluster analysis, principal component and classification analysis, and factor analysis.

The conclusions of data analysis using the techniques of ANN, basic statistics, multivariate, health risk assessment, and expert opinion and judgment can be summarized as follows:

- All water policy and management responses are significant. Sustainable coastal aquifer management must take into consideration technical engineering as well as managerial interventions such that top priority should be given to the reuse of treated wastewater in agriculture followed by desalination of water.
- Cadmium is the only chemical that has carcinogenic risk for both adults and children and its concentration has to be reduced by 20%. The total carcinogenic risk of cadmium for both adults and children is close to two cases per million. Cadmium has the highest total hazard.
- Index, followed by Chromium VI, whilst copper has the lowest for both adults and children. The total hazard index resulting from all chemicals in the two exposure routes is higher in the case of adults than for children. The dermal contact exposure route has a higher total hazard index compared with the ingestion exposure route.
- Coastal municipalities as well as municipalities located close to the northern border of Annaba region are characterized with high Cl concentration. This is due to seawater intrusion in coastal municipalities.

References

Jones N, Evangelinos K, Gaganis P, Polyzou E (2010) Citizens'perceptions on water conservation policies and the role of social capital, Water Resour. Manage. 25:509–522

Lallahem S, Hani A (2016) Artificial neural networks for defining the water quality determinants of groundwater abstraction in coastal aquifer. The International Conference on Technologies and Materials for Renewable Energy, Environment and Sustainability

Rajurkar MP, Kothyari UC, Chaude UC (2004) Modeling of the daily rainfall runoff relationship with artificial neural network. J. Hydrol. 285:96-113

Sharma KD (1998) The hydrological indicators of desertification. Arid Environ. 39:121–132

11th World Congress on Water Resources and Environment (EWRA 2019)
"Managing Water Resources for a Sustainable Future", 25-29 June 2019, Madrid, Spain

Fig leaves (*Ficus carica*) as adsorbents for removal of 4-bromoaniline (4BA) from aqueous solutions: Modelling and optimization

H. Tizi*, T. Berrama, Z. Bendjama
Laboratory of Industrials Processes Engineering Science, Mechanical Engineering and Processes Engineering Faculty, University of Sciences and Technology Houari Boumediène, PO Box 32, El-Alia, 16111, Bab-Ezzouar, Algiers, Algeria
** e-mail: thayet2@yahoo.fr*

Introduction

Aniline and its derivatives are organic intermediaries which are considered as potential pollutants. Their presence in water at very low concentrations is harmful to aquatic life (Han et al. 2006). Adsorption is one of the purification and separation techniques used in this area. Algeria produces annually 56910 tones of fig; therefore, a large amount of fig leaves is generated, and the conversion of this waste into adsorbent allows the valorization of agricultural residue.

The main purpose of the present work is to describe an application of statistical method for modelling and optimization of the conditions of the 4-bromoaniline (4BA) adsorption by an agricultural by-product, locally available (fig leaves), treated by sodium hypochlorite (NaOCl).

Materials and methods

All adsorption tests were carried out in batch mode according to the same experimental protocol. The aliquots were withdrawn at regular times and were subjected to vigorous centrifugation (Nahita-Centrifuge model 2698). The residual 4BA concentration was analyzed by a double-beam spectrophotometer (UV–Visible, SAFAS, EASYPEC II 320 D) at 240 nm.

Results and concluding remarks

The operational parameters of 4BA adsorption on the treated fig leaves were put in equation of first degree by using the method of the experimental design. In this method, each parameter takes two values coded higher level (+1) and low level (-1). Five parameters were be reviewed and their maximum and minimum values are grouped in Table 1.

Table 1. Range values of parameters

Parameter	Designation	Nivel (-1)	Nivel (+1)
Speed agitation (rpm)	X_1	300	350
Adsorbent concentration ($g.L^{-1}$)	X_2	0.5	1
Initial concentration of 4-BA ($mg.L^{-1}$)	X_3	50	100
Initial pH of the solution	X_4	6.8	7.2
Temperature (°C)	X_5	28	30

We carried out a complete factorial of 2^5 following the experimental matrix. The answers (Y) represent the yields of 4BA elimination on the prepared adsorbent. The results were treated by Yates method (Atikler et all. 2006; Cannillos et al. 2006; El Hannafi et al. 2008; Goupy and Creighton 2006; Gülşah and Laçin 2006; Jincai and Lua 2006; Sílvia and Rui 2008). The general model was simplified; indeed the calculation of the standard deviations showed that certain coefficients of the general model are influencing whereas others are not. The model obtained can be written as:

$$Y = 44.04+9.18X_2-6.20X_3-2.29X_4-2.34X_5-1.31X_1X_2-2.31X_2X_3-1.62X_2X_4-1.75X_1X_3X_4-2.47X_2X_3X_4+0.94X_2X_3X_5 \quad (1)$$

In order to determine the best conditions for fixing 4BA, we chose the temperature and the speed agitation as key parameters. These parameters will not change significantly the response value. The speed agitation (ω) can be selected chosen between 300 and 350 rpm, without changing significantly value yield.

Working at moderate speeds avoids the formation of vortex; then the experimental field can be represented by three parameters instead of five. The experimental range can be represented by a geometrical form (cube) (Figure 1); each vertex represents an average yield.

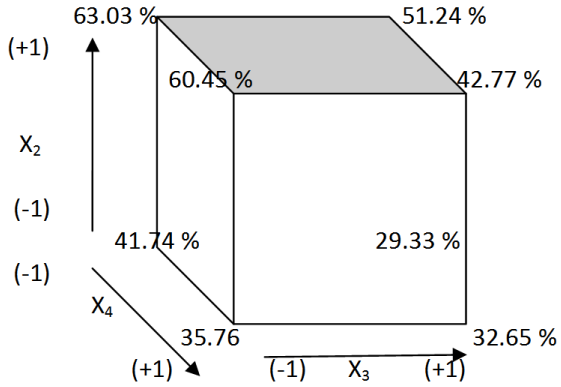

Figure 1. Variation yield average in different conditions

The best average yields of 4BA elimination on the adsorbent are obtained on two faces of the cube corresponding to: (X_2 = +1, X_3 = -1 to + 1, X_4 = -1 to + 1) and (X_3 = -1, X_2 = -1 to + 1, X_4 = -1 to + 1).

The results indicate that the adsorbent concentration (X_2) and the initial concentration (X_3) are the most influential parameters with probability of the order of 10^{-8} and 10^{-6} respectively.

The best experimental performance of 4BA elimination on the adsorbent was obtained with: Adsorbent concentration (X_2) = 1g L^{-1}; Initial concentration (X_3) = 50 mg L^{-1}; Initial pH (X_4) = 6.8; Temperature (X_5) = 28°C; Speed agitation (X_1) = 300 rpm.

In conclusion, the principal objective of this study was the development of a new adsorbent of vegetable origin starting from an agricultural waste. The operational parameters of the 4BA adsorption have been studied by using the method of the experimental design; a first degree model has been established. Statistical design of experiments for the 4BA adsorption was an efficient technique to quantify the effect of variable parameters.

The kinetic study showed that the equilibrium time varies between 40 and 45 min. Sorption kinetic data revealed that 4BA adsorption followed the pseudo second order equation (R^2 = 0.997). The value of k_2 was found to be 0.004 g $mg^{-1}min^{-1}$. The experimental results obtained with the fig leaves are in concord with the Freundlich model. The best experimental performance of 4BA elimination on the fig leaves was obtained with: Adsorbent concentration (X_2) = 1g L^{-1}; Initial concentration (X_3) = 50 mg L^{-1}; pH (X_4) = 6.8; Temperature (X_5) = 28 °C; Speed agitation (X_1) = 300 rpm.

References

Atikler U, Demir H, Tokali F, Tihminliog LF, Boalko Se D, Ulku S (2006) Optimisation of the effect of colemanite as a new synergetic agent in an intumescent system, Polym. Degrad. Stabil. 91:1563–1570

Cannillos V, Carlierb E, Manfredinia T, Montorsia M, Siligardia C (2006) Design and optimisation of glass-celsian composites. Compos. Part A 37:23-30

El Hannafi N, Boumakhla MA, Berrama T, Bendjama Z (2008) Elimination of phenol by adsorption on activated carbon prepared from the peach cores: modelling and optimisation. Desalina. 223:264–268

Goupy J, Creighton L (2006) Introduction aux plans d'expériences, DUNOD, Paris, pp 67–92

Gülşah KE, Laçin O (2006) Statistical modelling of acid activation on cotton oil bleaching by Turkish bentonite. J. Food Engine. 75:137–141

Han Y, Quan X, Chen S, Zhao H, Crui C, Zhao Y (2006) Electrochemically enhanced adsorption of aniline on activated carbon fibre. Separ. Purific. Techno. 50(3):365-372

Jincai S, Lua AC (2006) Influence of carbonisation parameters on the transport properties of carbon membranes by statistical analysis.J. Membr. Sci. 278:335-343

Sílvia CRS, Rui ARB (2008) Adsorption modelling of textile dyes by sepiolite. Applied Clay Sci. 42:137–145

11th World Congress on Water Resources and Environment (EWRA 2019)
"Managing Water Resources for a Sustainable Future", 25-29 June 2019, Madrid, Spain

Study on the optimization of the PV performance of SolWat: A hybrid technology for simultaneous clean water and electricity production

N. Pichel[1,2*], M. Vivar[3], M. Fuentes[3]
[1] *Nanotechnology and Integrated BioEngineering Centre, Ulster University, Northern Ireland B37 0QB, United Kingdom*
[2] *IMDEA Water Institute, Alcalá de Henares 28805, Spain*
[3] *Grupo IDEA, EPS Linares, Universidad de Jaén, Linares 23700, Spain*
** e-mail: nataliapichelccamb@gmail.com*

Introduction

SolWat is a new hybrid photochemical and photovoltaic (PV) technology for simultaneous solar water disinfection (SODIS) and electricity production (Vivar at al. 2010). It was developed based exclusively on using solar energy for two final applications: (1) visible and near-infrared light to generate renewable electricity; (2) far-infrared and UV (UVA-UVB) light for bacteria inactivation. SolWat comprises a PV module and a water disinfection reactor that is fully integrated into a single unit. The PV module acts as the base of the water disinfection reactor with a water layer on top that is transparent to visible and near-infrared light. Water disinfection occurs between the water disinfection reactor´s glass cover and the PV module.

The feasibility of this concept has been demonstrated in previous works (Pichel et al. 2016, 2017), which show that the hybrid system (PV + SODIS) achieves the same electrical and disinfection results as two independent systems (PV module and a disinfection reactor separately) during 6 h of experimentation. Pichel et al. (2018) have also demonstrated that under strong climate conditions, *E. coli*, total coliforms, *Enterococcus spp.* and *Clostridium perfringens* were completed inactivated after 3 hours of solar treatment, reducing the treatment time recommended for conventional SODIS reactors (6 h) by half. The cited works show that the PV module integrated into SolWat does not lead to major losses caused by the reduced solar irradiation received (lower current, I) as such losses are compensated by the cooling effect of the water layer being purified on top of the module (higher voltage, V). Accordingly, the refrigerated effect of water being purified on the PV module at the start of the treatment process is maximum. Thus the SolWat energy output could benefit from lower temperatures in short treatment times if properly optimised in combination with a smart water disinfection process strategy on top. This work aims to study the effect of the water disinfection reactor on the electrical performance of the photovoltaic module integrated into the SolWat system on different hydraulic retention times (HRT).

Materials and methods

The experiment was conducted in the rooftop facilities of IMDEA Water (Alcalá de Henares, Spain) in September 2018. Three hybrid SolWat systems, plus a single PV module acting as reference, were placed on a fixed solar structure, and were tilted 40° (the latitude of Alcalá de Henares is 40° N) and N-S oriented. A pyranometer was also located on the same structure. The hybrid systems were filled with Milli-Q water (initially at room temperature, 25°C) and exposed to natural sunlight for 6 h. However, each SolWat system was subjected to different hydraulic retention times: (1) SolWat A, HRT of 6 h, the system was filled once at the beginning of the experiment and emptied at the end; (2) SolWat B, HRT of 3 h, the system was filled and after 3 h emptied, to be refilled with new Milli-Q water; (3) SolWat C, HRT of 2 h, the system was filled and emptied 3 times during the 6-hour experimentation period.

Si-a thin film PV modules (Xunzel, Spain) of 7 W were selected to conduct the study. Four solar panels with the same characteristics were acquired, of which three were selected to manufacture the SolWat systems, with one per HRT (6, 3 and 2 h), plus one module acting as the control. Having initially degraded (60 kW h/m^2) and electrically characterised the PV modules, the manufacturing process of the water disinfection reactors started. Firstly, an aluminium frame was built and fixed to the frame of the solar panels to create the space for the water disinfection treatment. The aluminium frame included the water

temperature sensors and connectors to provide the system with water inputs and outputs. A water layer of 18 mm high was established for all the systems, which gave a final reactor capacity of 1.8 litres. Secondly, borosilicate glass (2 mm thick) with high transmittance for UVA-UVB, visible and infrared spectrum (Pichel et al. 2017) was used to cover the water disinfection reactors. Finally, they were filled by a pump that propelled water through a network of pipes.

The electrical performance of the three PV modules integrated into the SolWat systems and the single PV module were evaluated simultaneously by a PV-KLA 4.4 I-V Curve Analyser. The monitored parameters included global irradiance (Kipp & Zonen CMP 21 pyranometer: 280-3000 nm), ambient temperature (PT100 sensor with a shield protector), water temperature (NTC immersion sensors 10K) and back modules´ temperature (PT100 sensors). Data were recorded every 60 s by an Agilent 34972 datalogger.

Results and concluding remarks

Photovoltaic performance was assessed at average global irradiance levels of 898 W/m^2 (maximum of 1,041 W/m^2) and at an average ambient temperature of 30.4°C (maximum of 32.7°C). After 6 h of sun exposure, the generated energy output of the reference PV module was 31.2 Wh, SolWat A 27.4 Wh, SolWat B 27.6 Wh and SolWat C 29.6 Wh. The final power output of the reference PV module was higher than the hybrid systems, regardless of HRT. However, these differences can also be attributed to the different efficiencies of the four panels under STC (standard test conditions), without the water disinfection reactor on top, which they were also different, being slightly higher for the reference panel: 5.6%, 4.7%, 4.6% and 4.8%, respectively. Relative measurements would need to be use instead of absolute measurements to evaluate the effect of the different HRT. In fact, if each module´s electrical losses were compared to its electrical output under STC, the real effect would be seen. In this case, electrical losses were minimum for the system with the shorter HRT (19.7%), followed by the system with a 3-hour HRT (22.1%) and a 6-hour HRT (24.6%), and were maximum for the single PV module acting as the reference (28.9%). This means that the PV module actually benefits from the cooling effect of water on its front surface.

This is better understood by observing the average working temperature of all four modules: while the temperature for the reference PV module was of 57.9°C, the PV modules integrated into the SolWat systems worked at lower temperatures, which were lower when HRT was shorter: 53.2°C SolWat A, 51.6°C SolWat B and 49.2°C SolWat C. The module temperature is, along with the received irradiance, the major cause of losses in PV modules, resulting in a decreased power output when the module temperature increases. When the hybrid systems were completely filled with new Milli-Q water (initially at 25°C), the modules´ temperatures dramatically dropped by about 20°C.

To conclude, this work demonstrated that a PV module integrated into a SolWat system would be able to produce even more energy than a single PV module working at short HRTs, due to the cooling effect of water being purified on top.

Acknowledgments: M. Vivar acknowledges funding from the Spanish Ministry of Economy and Competitiveness, Grant number RYC-2015-17306.

References

Vivar M, Skryabin I, Everett V, Blakers A (2010) A concept for a hybrid solar water purification and photovoltaic system. Solar Energy Materials and Solar Cells 94(10):1772-1782. doi: 10.1016/j.solmat.2010.05.045

Pichel N, Vivar M, Fuentes M (2016) Performance analysis of a solar photovoltaic hybrid system for electricity generation and simultaneous water disinfection of wild bacteria strains. Applied Energy 171:103-112. doi: 10.1016/j.apenergy.2016.03.050

Pichel N, Vivar M, Fuentes M (2017) Performance study of a hybrid photovoltaic and solar water disinfection system considering climatic variations over a year. Energy Conversion and Management 144:312-321. doi: 10.1016/j.enconman.2017.04.080

Pichel N, Vivar M, Fuentes M (2018) Results from a first optimization study of a photovoltaic and solar disinfection system (SOLWAT) for simultaneous energy generation and water purification. Energy Conversion and Management 176:30-38. doi: 10.1016/j.enconman.2018.09.017

11th World Congress on Water Resources and Environment (EWRA 2019)
"Managing Water Resources for a Sustainable Future", 25-29 June 2019, Madrid, Spain

Assessing two step cascade technology for removing carbon and nitrogen from domestic wastewater

E. Nabil[1], M. Roushdi[1*], F. Ghobrial[2]
[1] Environment and Climate changes Research Institute, National Water Research Center, Egypt
[2] Faculty of Engineering, Ain Shams University, Egypt
* e-mail: mahmoudroushdi@yahoo.com

Introduction

The Domestic Wastewater treatment plants in Egypt are mainly depended upon the activated sludge process for the biological treatment. The capacity of these plants in Egypt is approaching 10 million m^3/day, where most of these plants (75%) is using the activated sludge process while the remaining 25% is conducted through trickling filters and oxidation ponds (Abdel-Shafy and Mansour 2013). However, these treatment systems have the ability only to remove some of the pollutants, especially carbon, while other pollutants such as Nitrogen and Phosphorus could not be removed. Nutrients are causing significant impacts since they are responsible for stimulate the growth of algae in water.

Thus, it was necessary to remove nutrients in effective and economic way. Cascade technology with step feeding (anoxic-oxic) is one of biological nitrogen removal technologies, which characterized by: high chemical oxygen demand and nitrogen removal (Nabil et al. 2017). The present study aims at improving both carbon and nitrogen removal efficiency in municipal wastewater treatment plants using cascade technology. Accordingly, a laboratory experimental scale model consists of two steps cascade with step feeding pilot plant, each step consist of anoxic and oxic zone, has been implemented and tested to assess the impact of influent flow rate distribution between the two anoxic zones on the system performance and to identify the optimum design criteria.

Materials and methods

A pilot plant was designed, constructed and operated following Metcalf and Eddy (2003). Synthetic wastewater with specific properties similar to municipal wastewater was used. The experiment took place at the National Water Research Center compound at Delta Barrage, Egypt.

Each stage consists of anoxic and aerobic zone. The volumes of anoxic and aerobic compartments ratio (V_{anoxic}/V_{oxic}) was put at fixed ratio of 35%. Air compressor was used for supplying air to the aerobic compartments. The wastewater was continuously fed to the reactor and the flow rates were controlled through adjustable dosing pumps. Another dosing pump was used for pumping the return sludge to the reactor, pilot plant components and flow chart of the system are shown in Figure 1.

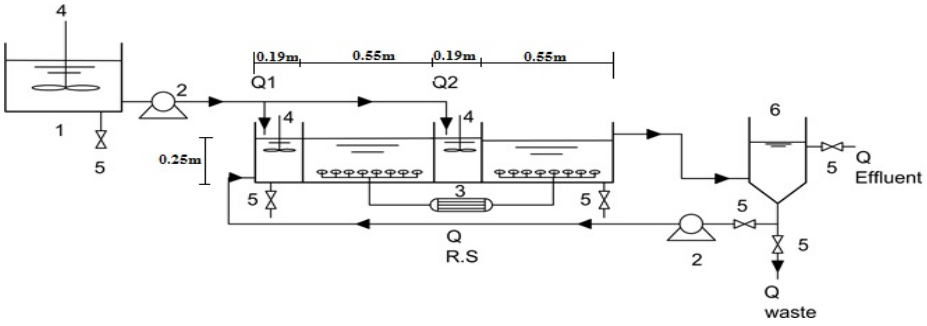

Figure 1. Schematic diagram of the step feed biological nitrogen removal process (1- Feeding tank; 2- Dosing pumps; 3- Air pump; 4- Stirrer; 5- Sluice value; 6- Feeding tank)

The operation conditions of the system were: dissolved oxygen at denitrification and nitrification zones were not less than 0.5 mg/l and 2.5 mg/l respectively, pH varied from 7 to 8.5, the volume of Anoxic to the

volume of Oxic zone ratio (V_{Anox} /V_{Oxic}) was 35 %, the flow distribution ratios were as shown in Table 1.

Table 1. Flow conditions of experimental work (Q1: Discharge in first step, Q2: Discharge in second step)

Stages	Stage 1	Stage 2	Stage 3
Flow conditions	Q1: Q2= 62.5:32.5 %	Q1: Q2= 75:25 %	Q1: Q2= 87.5:12.5 %

Results and concluding remarks

The steady state of the system achieved at mixed liquor suspended solids (MLSS) more than 4000 mg/l, as the pilot plant was designed. During the operation stages, average MLSS was 4025 mg/l, 4065 mg/l and 4093 mg/l, respectively. These values mean that the system was operated in stable state. To make activation to the system, some of sludge was returned to the first point in the first nitrification zone, the average MLSS in the returned sludge were 11700 mg/l, 11840 mg/l and 11910 mg/l, respectively.

The maximum COD removal reached to a maximum value of 96% with an average value of 90% to the increase in temperature, which it reached to 37 ^{o}C. The optimum consumption of carbon within the denitrification zones was achieved in stage 2. A decline in removal from 96 % to 73 % occurred in stage 3 at the same temperature (37 ^{o}C) due to the different flow distribution, which led to decrease in the required carbon available for the second denitrification zone. In addition, the maximum BOD removal reached to a maximum value of 97% with an average removal of 92% in stage 2 at the same temperature (37 ^{o}C). Thus, stage 2 with the flow distribution ratio of (75:25 %) achieved the highest removal efficiency.

TKN removals at different temperatures are shown in Figure 2-a. The autotrophic nitrifiers growth rate is typically increasing at 25-35 °C. Accordingly, the denitrification rate is increasing with temperature increasing until reaching up to 40 °C (Zhu et al. 2007).

It was concluded that, the best removal efficiencies of pollutants were at the second stage (Q1: Q2= 75:25 %) with removal efficiencies of 96%, 97%, and 93% for COD, BOD and TKN, respectively. Results of other flow distribution ratios indicate that increasing the volume of carbon source which contained in the influent wastewater discharged into the first denitrification zone, increases the TKN removal within a certain range. Beyond this range, the TKN removal gradually decreases due to decrease of carbon discharged to the second step which would be needed for the second step denitrification. Figure 6b shows the maximum removals of COD, BOD and TKN, at different flow distribution ratios.

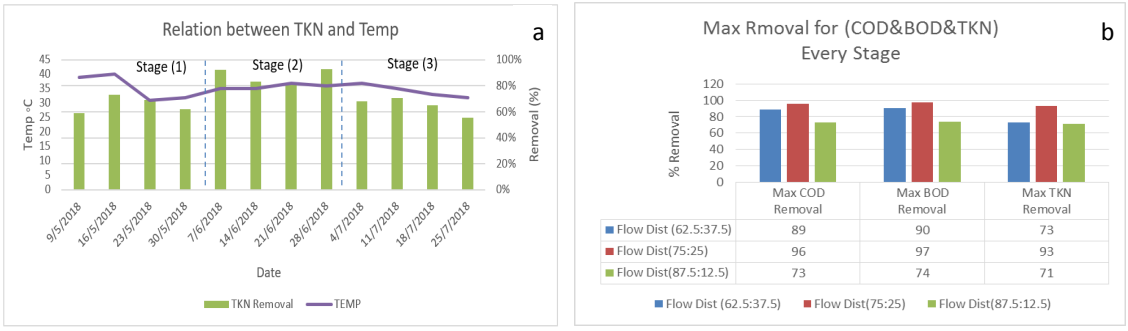

Figure 2. Removal efficiencies of COD, BOD and TKN: (a) Removal efficiencies of TKN (b) Maximum removal efficiencies of COD, BOD and TKN

References

Abdel-Shafy H, Mansour M (2013) Overview on water reuse in Egypt: Present and Future. Sustainable Sanitation Practice 14(1):17-25

Metcalf and Eddy (2003) Wastewater Engineering: Treatment and Reuse. 4th ed., McGraw Hill, New York, USA

Nabil E, Roushdi M, Ghobrial F (2017) Enhancing Nitrogen Removal from Wastewater Using Two Step Cascade. International Conference of Water Resources and Climate Change: Anthropogenic and Climate Impact on Variability of Water Resources, 2-4 October 2017, Hammamet, Tunisia

Zhu Y, Peng S, Wang S, Mam B (2007) Effect of influent flow rate distribution on the performance of step-feed biological nitrogen removal process. Chem. Eng. J. 131:319-328

11th World Congress on Water Resources and Environment (EWRA 2019)
"Managing Water Resources for a Sustainable Future", 25-29 June 2019, Madrid, Spain

Assessment of groundwater safety around contaminated water storage sites

I. Radelyuk[1,2*], K. Tussupova[1,3], K. Zhapargazinova[2]
[1] Department of Water Resources Engineering, Lund University, Lund, Sweden
[2] Department of Chemistry and Chemical Technology, Pavlodar State University, Pavlodar, Kazakhstan
[3] Department of Public Health, Karaganda State Medical University, Karaganda, Kazakhstan
[*] e-mail: ivan.radelyuk@tvrl.lth.se

Introduction

Safe drinking water is one of the sustainable development goals for humanity. Previous work (Tussupova et al. 2016) shows that more than 50% of people in rural Kazakhstan use groundwater for domestic purposes.

Wastewater from oil refineries in Kazakhstan contains high concentrations of harmful substances. Current methods of wastewater treatment as well as condition of treatment units at oil refineries (which were built during soviet area) in Kazakhstan do not let reach the safe concentrations of contaminants for ecological systems. Moreover, existing conditions of recipients of their discharge lead to infiltration of pollutants through the soil to groundwater, which creates potential threats to public health. This study investigates the presence of different chemicals in the observed wells around recipients and assesses them from a point of view of national and international water quality guidelines.

Materials and methods

The study area is located in north-east Kazakhstan. Groundwater from nine observed wells were sampled and analysed between 2014 and 2018 twice a year, during the rainy and dry seasons. Nineteen parameters, including pH, total petroleum hydrocarbons (TPH), total dissolved solids (TDS), chlorides (Cl^-), sulfates (SO_4^{2-}), ammonia (NH_4^+), total hardness (TH) and sodium (Na^+) were evaluated. Concentrations of substances were compared with Kazakhstani (KZ) standards for drinking water and those of the World Health Organisation (WHO) to evaluate the suitability of groundwater quality for drinking and domestic purposes.

Results and concluding remarks

High concentrations of TPH were identified in all wells. The concentrations exceed KZ and WHO recommended limit for TPH equal 0.1 mg/L (Table 1). Measured TDS values varied from 643 to 36392 mg/L with an average 5499 mg/L, thereby exceeding, in most cases, the KZ and WHO maximum permissible levels of 1000 mg/L. The TH in the groundwater samples varied between 2.0 and 377.5 mmol/L. Based on the Todd classification, all groundwater samples could be classified as very hard water. The Cl^- concentrations was between 15.0 and 24757 mg/L, with the majority of groundwater samples exceeding WHO permissible limit of 350 mg/L. SO_4^{2-} concentrations exceeded the normal by 18 times. There is a possible health-related concerns regarding K^+ and Na^+ content in groundwater because concentrations in wells was exceeding permissible WHO and KZ limits. Finally, individual exceedance of surfactants, NO_2^-, NO_3^-, NH_4^+ were identified. According to WHO (2017), for such 8 substances water would normally be rejected by consumers.

The higher concentrations of some parameters, such as TPH, Na^+, Cl^-, SO_4^{2-}, TDS and TH and their potential effects on human health, indicate that additional research should be carried out to investigate the groundwater flow and evaluate potential relationships between a public health in the region and the quality of consumed water. Moreover, additional measurements are needed to evaluate presence and concentrations of toxic hydrocarbons in groundwater.

Table 1. Concentrations of different chemicals in the groundwater around the recipient pond.

	Unit	Range	Mean	SD	Median	Limits*
pH	Standard	6.87-9.14	8.6	0.3	8.6	6-9
TPH	mg/L	0.11-0.89	0.41	0.18	0.39	0.1
TDS	mg/L	643-36392	5499	700	1629	1000
Cl^-	mg/L	15-24757	2305.9	739.6	253.4	350
SO_4^{2-}	mg/L	89-9400	1183	304	325	350
NH_4^+	mg/L	0.0-10.9	1.2	1.8	0.5	0.2
TH	mmol/L	2.0-377.5	40.2	9.0	6.8	7.0
Na^+	mg/L	66-9200	1193.8	291.2	435.0	200.0

* WHO recommendations and Kazakhstani requirements for drinking water

References

Tussupova K, Hjorth P, Berndtsson R (2016) Access to Drinking Water and Sanitation in Rural Kazakhstan. International Journal of Environmental Research and Public Health 13(11):1115. https://doi.org/10.3390/ijerph13111115

WHO (2017) Guidelines for drinking-water quality. WHO Press, Geneva

11th World Congress on Water Resources and Environment (EWRA 2019)
"Managing Water Resources for a Sustainable Future", 25-29 June 2019, Madrid, Spain

Investigating the need for inclusion of water quality objectives in water distribution network design optimisation models

M.S. Nyirenda[1,2], T.T. Tanyimboh[1*]
[1] School of Civil and Environmental Engineering, University of the Witwatersrand, Johannesburg, South Africa
[2] GIBB (PTY) Ltd, Woodmead North Office Park, 54 Maxwell Drive, Woodmead, South Africa
* e-mail: tiku.tanyimboh@wits.ac.za

Introduction

The design of water distribution networks (WDNs) is a complex problem that has been the focus of computational optimisation research over many decades. The works of Savic and Walters (1997), Walski (1987), Siew and Tanyimboh (2011) (among others) have all contributed to creating a robust body of knowledge on systems and optimisation procedures to achieve the best hydraulic and cost-efficient design of a WDN which includes the design of service reservoirs. However, these and other optimisation procedures have not incorporated water quality objectives in the design optimisation of WDNs. This is thought to result in potentially negative effects such as long residence times, low chlorine residual as well as the production of harmful disinfection by-products (Clark and Haught 2005). Disinfection by-products are formed when a disinfectant reacts with naturally occurring inorganic and organic substances. Research (Ghebremichael et al. 2008) has also indicated that long residence times are a major contributing factor in the formation of disinfection by-products. Low chlorine residuals can lead to bacterial regrowth and ultimately waterborne diseases (Clark and Haught 2005), while disinfection by-products are reportedly carcinogenic and thought to cause reproductive and developmental problems (Nieuwenhuijsen 2005; Richardson et al. 2002). This research aims to investigate the deleterious effects of service reservoirs on water quality and the benefits of water quality-based criteria in the WDN design optimisation models, with the ultimate aim of informing decision-making and designs of service reservoirs in the future.

Materials and methods

This paper looks at two optimisation procedures: "Penalty-Free Multi-objective Evolutionary Algorithm" (PF-MOEA) and "Fuzzy Multi-objective Optimisation" (FMO) presented by Siew et al. (2016) and Vamvakeridou-Lyroudia et al. (2005) respectively applied to a benchmark water distribution network. These methods are both multi-objective which allows the user to optimise a WDN for multiple criteria like overall hydraulic performance and overall cost which was used in both cases. However, one of the solutions suggested by the PF-MOEA (Solution 2) utilised an additional tank depletion criterion which selects a tank size that will empty and re-fill every 24 hours. This is thought to decrease water age in the system and aid proper mixing of the water in the tanks. The Anytown Network (Walski 1987) is a benchmark water distribution network design, rehabilitation and upgrading problem which was considered for the purposes of the post-optimisation water quality investigations. The final design solutions to the Anytown Network for each procedure was analysed for water quality in EPANET 2. Water age, chlorine residual and tri-halomethanes concentrations were utilised as the water quality indicators during the water quality analyses. A first order kinetics model was used with bulk and wall reaction rate constants assumed to be 0.5/day and 0.1 m/day, respectively (Seyoum and Tanyimboh 2014). Hydraulic and water quality time steps of 1 minute were used in an extended period simulation of 3 days of operation. Comparisons between the results produced by each optimisation procedure were carried out. The results are only presented for the last 24 hours here, allowing the simulations to stabilise.

Results and concluding remarks

The water quality analyses performed on the FMO and PF-MOEA optimisation solutions of the Anytown network yielded the results in Table 1. The table presents a summary of the minimum and maximum values

of the water quality parameters as produced by each optimisation model. The optimisation approach with better water quality results will present lower water ages, lower concentrations of tri-halomethanes (THMs) and higher concentrations of chlorine. A recommended minimum chlorine concentration of 0.2 mg/l (WHO 2017) should also be observed. From the table it is seen that PF-MOEA consistently performs better with lower water ages and lower concentrations of THMs. FMO on the other hand presents worse results of water ages than those of PF-MOEA. One of the reservoirs in the FMO solution has a chlorine concentration of 0 mg/l over 47 hours in the 72 hour simulation period. This is consistent with the original literature for the procedure (Vamvakeridou-Lyroudia et al. 2005) which states that the reservoir does not fully utilise its operational volume over the simulation period. By contrast, in the PF-MOEA solution, the minimum chlorine concentration of 0 mg/l observed in one of the reservoirs occurs over approximately 1 hour and 18 minutes within the 72-hour simulation. It is interesting to note that, with respect to water quality, even though PF-MOEA encourages tank depletion only, all of the water quality parameters are better than FMO which does not include any water quality related objectives.

Table 1. Summary of water quality results

		Maximum water age (hrs)	Minimum chlorine concentration (mg/l)	Maximum THM concentration (µg/l)
PF-MOEA	Service Reservoirs	38.8	0.00	53.1
	Demand nodes	19.5	0.39	28.4
FMO	Service Reservoirs	43.3	0.00	67.6
	Demand nodes	23.3	0.14	37.6

The results point to the need of including water quality in design and optimisation procedures. This seems to result in better designs which can decrease negative effects such as longer residence times and lower chlorine concentrations. These initial results will have to be confirmed by analysing more networks and other enhanced design procedures and by including more effective measures of the results.

References

Clark R, Haught R (2005) Characterizing pipe wall demand: implications for water quality modelling. Journal of Water Resources Planning and Management 31(3):208-217

Ghebremichael K, Gebremeskel A, Trifunovic N et al. (2008) Modelling disinfection by-products: coupling hydraulic and chemical models. Water Science and Technology. Water Supply 8(3):289–295

Nieuwenhuijsen M (2005) Adverse reproductive health effects of exposure to chlorination disinfection by-products. Global NEST Journal 7(1):128-144

Richardson S, Simmons J, Rice G (2002) Disinfection by-products: the next generation. Environmental Science and Technology 36(9):198A - 205A

Savic DA, Walters G (1997) Genetic algorithms for least-cost design of water distribution networks. Journal of Water Resources Planning and Management 123(2):67-77

Seyoum AG, Tanyimboh TT (2014) Pressure dependent network water quality modelling. J. Water Management 167(6):342-355. doi: 10.1680/wama.12.00118

Siew C, Tanyimboh TT (2011) Design of the "Anytown" network using the penalty-free multi-objective evolutionary optimisation approach. Proceedings of the 13th Annual Water Distribution Systems Analysis Conference, Palm Springs, California, pp 190-198

Siew C, Tanyimboh TT, Alemtsehay SG (2016) Penalty-free multi-objective evolutionary approach to optimization of Anytown water distribution network. Water Resources Management 30(11):3671-3688

Vamvakeridou-Lyroudia LC, Walters GA, Savic DA (2005) Fuzzy multi-objective optimization of water distribution networks. Journal of Water Resources Planning and Management 131(6):467-476

Walski TM (1987) Discussion of multi-objective optimization of water distribution networks. Civil Engineering Systems 4(1):215-217

World Health Organization (2017) Guidelines for Drinking-water Quality: Fourth edition incorporating the first addendum. World Health Organization, Geneva

11th World Congress on Water Resources and Environment (EWRA 2019)
"Managing Water Resources for a Sustainable Future", 25-29 June 2019, Madrid, Spain

Fate of fluoroquinolone-resistant *Salmonella* in full-scale wastewater treatment plant and effect of chlorine disinfection

P. Kumalo, O. O. Awolusi*, S. Kumari, F. Bux
Institute for Water and Wastewater Technology, Durban University of Technology, South Africa
** e-mail: oluyemia@dut.ac.za*

Introduction

Antibiotics have revolutionised medicine and several deaths have been prevented. However, the modern medicine is currently facing a major problem due to increasing development of resistance to commonly used antibiotics, and alarming spread of antibiotic resistant bacteria and genes (Bouki et al. 2013). Significant concentrations of antibiotic resistant bacteria (ARB) and antibiotic resistant genes (ARG) have been reported in wastewater. Among these, antibiotic resistant *Salmonella* has been reported in the treated wastewater effluent (Goldstein et al. 2012). Duffy et al. (2012) linked *Salmonella* antibiotic resistance with an increasing infection rate which may lead to high levels of hospitalization, prolong illness, and presents higher risk of invasive diseases with treatment difficulties.

Chlorination is one of the widely used disinfection processes in wastewater treatment plants (WWTP) due to its simple application and cost effectiveness. This may be effective in decreasing ARB, however, the fate of ARG during chlorination in full-scale WWTP is still unclear. In 2017, WHO listed fluoroquinolone-resistant *Salmonella* (FRS) among high priority pathogens for further surveillance and research, both among humans and in the receiving aquatic environment. This study, therefore, investigated the fate of FRS in full-scale WWTP and the effect of chlorination inactivation on their antibiotic-resistant genes.

Materials and methods

Samples from wasted sludge, influent and effluent wastewater were taken from a full-scale WWTP (Durban, South Africa) treating domestic and hospital effluents. The sampling was done over a period of six months. The modified standard National Committee for Clinical Laboratory Standards (NCCLS) agar dilution method was used for isolating fluoroquinolone-resistant *Salmonella* spp. (FRS) in the samples, as described by Iyigundogdu et al. (2017). The identity of the isolates was further confirmed based on PCR and sanger sequencing. The concentrations of FRS at different treatment stages of the WWTP were investigated with the aim of evaluating the potential role of the WWTP in FRS discharge into the environment.

Lab-scale reactors were also used to evaluate the chlorination disinfection on the kanamycin and ciprofloxacin resistant *Salmonella* spp. in phosphate-buffered saline (PBS) and pre-chlorinated wastewater effluent from the WWTP. Initial chlorine concentrations of 0.0, 0.1, 0.3, 0.5, 1.0 and 3.0 mg Cl_2/L were used in the PBS set-up whilst 0.0, 0.5, 3.0, 5.0 and 10.0 mg Cl_2/L were used in the secondary wastewater experiment at 3, 5, 10, 20, 40 and 60 min.

After inactivation experiments, the isolates were recovered using membrane filtration and cultured using standard pour plate method. DNA was also extracted from chlorinated samples (PBS and pre-chlorinated secondary effluent), then PCR was used to confirm the presence of kanamycin resistant and ciprofloxacin-resistant genes. DNA was extracted using the Powersoil extraction kit (Qiagen, USA) as per the manufacturer's manual. The PCR were performed in a total reaction volume of 25 µL as described by Huddleston et al. (2006) using primer sets *ame aph*, Fluoroquinolone *gyrA* and *parC* (Sekyere and Amoako 2017).

Results and concluding remarks

There was a significant reduction in the antibiotic resistance bacterial population in the treated effluent being discharged from the WWTP, however, it was a different scenario for the wasted sludge. It was noted that both Kanamycin- and Ciprofloxacin-resistant *Salmonella* spp. have been reduced in the treated

wastewater to 13% and 12%, respectively. However, Kanamycin-resistant *Salmonella* spp. was about 56% in the wasted sludge whilst Ciprofloxacin-resistant *Salmonella spp*. was about 106%. This could be an indication of accumulation in the wasted sludge.

In some of the isolates, genes conferring the resistance to the antibiotic could not be detected, even though the isolates showed resistance to the antibiotics phenotypically. This may be due to resistance to antibiotic being conferred by more than one type of genes. Chlorination was more effective in PBS compared to secondary wastewater as revealed in this experiment. About 100% log reduction was achieved at >1 mg OCl^-/L and >40 min in PBS, and >5 mg OCl^-/L for >40 minutes in secondary effluent. The *ame aph (3')-III* and *gyrA* genes were detected in chlorinated suspensions of kanamycin and ciprofloxacin-resistant *Salmonella* spp., even non-viable samples. Chlorine disinfection could not effectively destroy ARGs despite inactivation of the ARB. However, ARGs could not be detected at high chlorine concentration and long contact times >3 mg OCl^-/L at >40 minutes in PBS and >5 mg OCl^-/L at 60 min in secondary effluent. This result suggests that ARB and ARGs may persist after chlorine inactivation in WWTPs and may be discharged into the receiving aquatic environment. Therefore, it is essential to introduce new disinfection technologies that can remove ARB together with ARGs in wastewater treatment facilities.

Acknowledgments: The authors will like to acknowledge Durban University of Technology and NRF-South African Research Chairs Initiative (SARChI).

References

Iyigundogdu ZU, Demir O, Asutay AB, Sahin F (2017) Developing novel antimicrobial and antiviral textile products. Applied Biochemistry and Biotechnology 181(3):1155-1166. https://doi.org/10.1007/s12010-016-2275-5

Goldstein RER, Micallef SA, Gibbs SG, Davis JA, He X, George A, Kleinfelter LM, Schreiber NA, Mukherjee S, Sapkota A (2012) Methicillin-resistant Staphylococcus aureus (MRSA) detected at four US wastewater treatment plants. Environmental Health Perspectives 120(3):1551. https://doi.org/10.1289/ehp.1205436

Duffy LL, Dykes GA, Fegan N (2012) A review of the ecology, colonization and genetic characterization of Salmonella enterica serovar Sofia, a prolific but avirulent poultry serovar in Australia. Food Research International 45(2):770-779. https://doi.org/10.1016/j.foodres.2011.04.024Get

Bouki C, Venieri D, Diamadopoulos E (2013) Detection and fate of antibiotic resistant bacteria in wastewater treatment plants: a review. Ecotoxicology and Environmental Safety 91:1-9. https://doi.org/10.1016/j.ecoenv.2013.01.016

Huddleston JR, Zak JC, Jeter RM (2006) Antimicrobial susceptibilities of Aeromonas spp. isolated from environmental sources. Applied and Environmental Microbiology 72(11):7036-7042. https://doi.org/10.1128/AEM.00774-06

Sekyere JO, Amoako DG (2017) Genomic and phenotypic characterisation of fluoroquinolone resistance mechanisms in Enterobacteriaceae in Durban, South Africa. PloS one 12(6):e0178888. https://doi.org/10.1371/journal.pone.0178888

11th World Congress on Water Resources and Environment (EWRA 2019)
"Managing Water Resources for a Sustainable Future", 25-29 June 2019, Madrid, Spain

Simulation model of wastewater treatment plant with automatic control

J. Caravaca-Vilchez[1], J. Murillo[1*], A. Navas-Montilla[1], S. Lopez Barcos[2], M.J. Tárrega Martí[2]
[1] Fluid Mechanics, University of Zaragoza, Zaragoza, Spain
[2] Departamento Aguas Residuales, Global Omnium
* e-mail: Javier.Murillo@unizar.es

Introduction

The activated sludge process is widely used in wastewater treatment plants to reduce pollutant levels in contaminated wastewaters, which mainly come from industrial and municipal sector (Nelson et al. 2009). In the activated sludge process, there is a large variety of microorganisms capable of degrading organic matter, reducing nutrient content and transforming toxic components into harmless products. In recent decades, many authors have attempted to develop biological models to increase our understanding of the influence of process modifications on treatment process efficiency (Petersen et al. 2002). The Activated Sludge Model No. 1 (ASM1) presented by the IAWQ (International Association on Water Quality) is generally accepted as the state-of-the-art. The ASM1 describes the oxygen and nitrogen demand in microbial growth processes, including nitrification, denitrification and removal of organic matter mechanisms (Henze et al. 1987).

The main objective of this study is to understand the secondary treatment of wastewater plants and its equipment operation by focusing on the biological relationships between species and the hydrodynamics that governs them, especially in transient cases. In this study, a coupled hydrodynamic and biological model that includes an automatic regulation faithful to reality has been designed, unlike common commercial models where the regulation is not included.

Materials and methods

The main equipment which are used in the secondary treatment of wastewater plants are bioreactors, secondary clarifiers, a recirculation line, a purge discharge, sludge thickeners and dehydrators. In this study, the sludge thickeners and dehydrators are not considered because their contribution is negligible in terms of effluent concentrations. The plant layout is depicted in Figure 1.

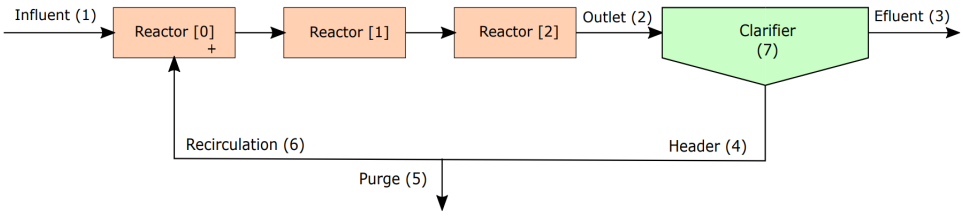

Figure 1. Plant layout

The secondary treatment of wastewater plant presents three bioreactors where the ASM1 processes are mainly carried out. In this study, bioreactors are represented by a 0D model, which implies the concentrations are the same in its entire volume. The first of them operates under anoxic conditions and presents a submersible mixer, which is responsible for ensuring the homogenisation of the mixture. The other reactors operate under aerobic conditions due to the presence of an Orbal system, which is responsible for providing the oxygen needed to prevent the decrease of autotrophic and heterotrophic bacteria. The Orbal system operation is regulated by an on/off control, which regulates the oxygen concentration considering ammonium-ammonia concentration in the third reactor.

Concerning the secondary clarifiers, the ASM1 processes are also carried out within them. The clarifier volume is considered constant because the volume variations of the clarifier are negligible as compared

with the total volume. In the clarifier, the particulate components are partially deposited by sedimentation, which means most solids come back to the first reactor through the recirculation line, including both autotrophic and heterotrophic bacteria. However, a small fraction of these solids come out of the plant through the effluent. In the first case, the concentration of the particulate components in the effluent are calculated using a clarifier yield. In the second case, the clarifier performance considering the sedimentation velocity of the sludge is simulated using a model based on the solids-flux theory. The flux theory represents the mass balance model in the clarifier (Gavrila et al. 2007) as follows

$$\frac{\partial(C)}{\partial t} = -u\frac{\partial(C)}{\partial z} + \frac{\partial(vC)}{\partial z} + D_a\frac{\partial^2(C)}{\partial z^2}, \quad (1)$$

where z is the height coordinate, C represents the suspended solids concentration, v is the zone-settling velocity of the activated sludge calculated using Vesilind model, u represents the total velocity in the clarifier and D_a is the pseudo-diffusivity coefficient (2.15 m²/h).

The advective part of Eq. (1) is solved using Godunov's scheme, which is an explicit method based on the use of Riemann solvers. On the other hand, the diffusion term is integrated implicitly using Thomas' algorithm. This prevents the reduction of the time step for time integration.

Note that the purge flow is regulated by a pump which is controlled by an on/off system. This pump regulates the purge flow considering the biological sludge production, which is estimated through the ratio between the generated suspended solids in the reactor and the DBO eliminated every 3 days.

Results and concluding remarks

The results of the model described in the previous section have been compared to real information measured in a wastewater treatment plant with an Orbal system. The real DBO, DQO and total nitrogen concentration in the effluent (blue line) and the simulation results using the clarifier yield (green line) and the solid flux theory (red line) are depicted in Figure 2.

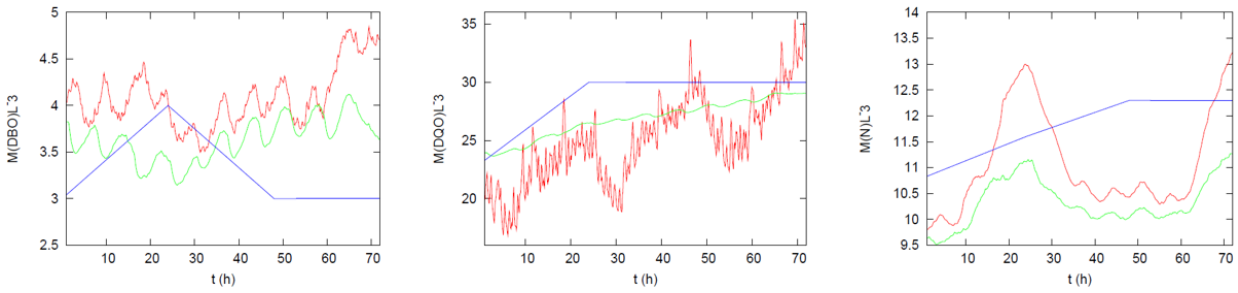

Figure 2. DBO, DQO and total nitrogen concentrations

As can be observed, reasonable results are obtained using both methods to simulate the clarifier performance. DBO and DQO concentration in the effluent are closer to reality using the clarifier yield than using the model based on the solids-flux theory. Nevertheless, total nitrogen concentration in the effluent is closer to reality using the model based on the solids-flux theory than using the clarifier yield.

On one hand, the oxygen regulation and the recirculation line are indispensable to ensure ammonia-ammonium and organic matter elimination through nitrification and denitrification process and organic matter oxidation. On the other hand, a purge regulation is needed in order to avoid an accumulation of inert particulate products.

References

Gavrila B, Gruia I (2007) Simulated suspended solids concentrations of secondary clarifiers in the activated sludge process using Comsol Multiphysics Program. European COMSOL Conference 2007, Grenoble

Henze M, Gujer W, Mino T, van Loosdrecht M (2000) Activated sludge models ASM1, ASM2, ASM2d and ASM3. IWA Publishing, London

Nelson MI, Sidhu HS (2009) Analysis of the activated sludge model (number 1). Applied Mathematics Letters 22(5):629-635

Petersen B, Gernaey K, Henze Mogens, Vanrolleghem PA (2002) Evaluation of an ASM1 model calibration procedure on a municipal-industrial wastewater treatment plant. Journal of Hydroinformatics 4(1):15-38

11th World Congress on Water Resources and Environment (EWRA 2019)
"Managing Water Resources for a Sustainable Future", 25-29 June 2019, Madrid, Spain

Feasibility study for power and water cogeneration plant in south coast of Iran

A. Poursarvandi[1*], R.H. Khoshkho[1,2]
[1] R&D Office, Monenco Iran Consulting Engineers, Tehran, Iran
[2] Faculty of Mechanical and Energy Engineering, Shahid Beheshti University, Tehran, Iran
* e-mail: poursarvandi.ali@monencogroup.com

Introduction

On the basis of the International Water Management Institute (IWMI), countries are divided into two water scarcity categories: physically water scarce and economically water scarce. Iran is approaching physical water scarcity based (Nepomilueva 2014). There are generally two ways to manage water crisis: supply side solutions (desalination, wastewater reuse, infrastructure upgrade) and demand side solutions (tariffs management, agricultural use management) (CEBC 2017). Among these ways, desalination is the most used solution in Persian Gulf region and is techno-economically analysed in this paper.

Seddigh et al. (2014) analysed nine different desalination scenarios in terms of energy consumption including MED, MSF, SWRO, MED+SWRO hybrid (3 scenarios), MSF+SWRO hybrid (3 scenarios). Results show that the SWRO scenario has the least energy consumption and energy consumption for hybrid scenarios are almost same (Seddigh et al. 2014). Kotagama et al. (2016) made a comparison between desalination process and wastewater treatment process in terms of unit water production cost. Techno-economic analysis was done for both scenarios. The cost of produced water is 1.2 USD/m^3 for desalination and 0.29 USD/m^3 for wastewater treatment considering site condition (Kotagama et al. 2016). Hosseinpour (2016) compared three different water and power cogeneration scenarios using DEEP and DE-TOP softwares. Levelized cost was calculated for unit production of water and unit production of electricity (Hosseinpour 2016). Osman (2016) conducted a comprehensive thermo-economic study based on the exergy accounting method to evaluate the performance of a combined gas/steam power generation system integrated with a hybrid MSF/SWRO desalination plants. The total power generated is 2,645.5 MW and total water production is 1,000,000 m^3/d. Results shows that water production cost varying from \$0.8258/m^3 to \$2.259/m^3 and the per unit electricity generation cost varying from \$0.02266/kWh to \$0.0966/kWh, as the oil price is increased from \$6/bbl to \$72/bbl, respectively (Osman 2016). Golkar et al. (2017) studied two main scenarios for power and water cogeneration. First scenario includes two 170 MW GT + one 160 MW ST + 143,000 m^3/day MED and second scenarios includes one 170 MW GT + one 95 MW ST + 143,000 m^3/day SWRO. Technical and economical modeling of each scenario was done and levelized water costs were calculated. Results show that levelized water cost in SWRO plant is lower than MED plant. For Persian Gulf FOB gas price, MED water cost is 1.16 \$/m3 and SWRO water cost is 0.99 \$/m3 (Golkar et al. 2017). Power and water cogeneration plant is studied in this paper. Power block consist of 25 MW GT and water block consist of MED/SWRO.

Materials and methods

Previous studies on water demand and determining desalination plants specification showed that it is better to build distributed desalination with small and medium capacity. So medium range gas turbine (25 MW) could be a suitable choice for power block of cogeneration plants in south of Iran (NWW 2015). Gas turbine exhaust could be used to produce steam and there are two major options for using produced steam in desalination process. First option is using gas produced steam in thermal desalination plant such as MED and the second option is using produced steam in a steam turbine for electricity generation and using SWRO technology in water block. So the first scenario is 25 MW GT + HRSG + 9,000 m^3/day MED and second scenario is 25 MW gas turbine+ HRSG + ST + 9,000 m^3/day SWRO desalination.

The technical specification for main equipment of each scenario has been determined. Gas turbine

model is TUGA MGT30 with 25 MW nominal power output and 36% efficiency at ISO condition. Each MED unit capacity is 4500 m^3/day and GOR of 8.56. Steam turbine nominal capacity is 10 MW and SWRO recovery ratio is 35%. Two scenarios has been technically modelled using thermoflow software and their performance parameters have been computed.

Direct and indirect capital cost and also running cost including fixed operation cost and variable operation cost (electricity, chemical, etc.) has been estimated for each scenario. A financial model has been developed and cost of produced water has been calculated assuming IRR of 12%.

Results and concluding remarks

Below table shows technical and financial result of study. As can be seen produced water cost using MED unit is less than SWRO unit. However further calculation show that the cost of produced water using SWRO decrease by increasing water production capacity. The cost is almost equal to MED scenario for 18,000 m^3/day SWRO capacity and it will be 1.06 for 27,000 m^3/day SWRO capacity. In conclusion, the desalination technology depends on the water production capacity. MED units is better for small capacity, MED and SWRO have almost same water production cost for medium capacity and SWRO units is better for large capacity.

Table 1. Technical and financial result of study

	MGT30+MED	MGT30+ST+SWRO
Nominal installed capacity (MW)	25	35
Net power output (MW)	19.17	28.22
Auxiliary power consumption (MW)	2.24	3.14
Electrical efficiency (%)	29.6	43.67
Produced water cost (USD/m3)	1.13	1.60

Acknowledgments: We acknowledge the MAPNA group - Investment Project Division for financial and technical support.

References

Clean Energy Business Council (2014) Water and energy in MENA; challenges, opportunities and potential

Golkar B, Khoshkho R, Poursarvandi A (2017) Techno-economical Comparison of MED and RO Seawater Desalination in a Large Power and Water Cogeneration Plant in Iran. Water Resources in Arid Areas: The Way Forward. Springer

Hosseinpour M (2016) Economic analysis of water and power cogeneration plant using DEEP and DE-TOP softwares. National conference on power engineering and nuclear power plants, Tehran

Kotagama H, Ahmed M, Al-Haddabi M (2016) Cost evaluation of desalination and sewage treatment based on plants operated in Oman and use of software models. Desalination and Water Treatment 57(19):8649-8656. 10.1080/19443994.2015.1027274.

National Water & Wastewater Engineering Company (2015) Comprehensive study for determining desalination plant specification in south of Iran, Tehran

Nepomilueva D (2017) Water scarcity indexes; Water availability to satisfy human needs. Helsinki Metropolia University of Applied Sciences

Osman H (2016) Thermoeconomic analysis of combined power cycle integrated with MSF/SWRO desalination plant, Desalination and Water Treatment 57(55):26552-26561

Seddigh H, Golkar B, Poursarvandi A (2014) Technical Study of Thermal-Membrane Hybrid Desalination Configurations. 2nd International training workshop and conference on desalination, Tehran

11th World Congress on Water Resources and Environment (EWRA 2019)
"Managing Water Resources for a Sustainable Future", 25-29 June 2019, Madrid, Spain

Technical and financial assessment of water supply for a petrochemical company: A case study

A. Fouladitajar*, M.R. Pourghasem, M. Danaye Manavi
Power Generation Deputy, Monenco Iran Consulting Engineers Company, Tehran, Iran
** e-mail: fouladi.amir@monencogroup.com*

Introduction

Iran, being a country in the arid and semi-arid region of the world with increasing population, temporal and spatial disparity of precipitation, growing water consumption and development of industries, faces different challenges of water supply. Therefore, providing water is one of the most important concerns of Iran's today society, and treatment of unconventional water and its use in the industry is of great importance. Considering the urgent and growing need of industries for water, including the petrochemical industry, and the lack of local water resources, different scenarios are needed to ensure providing process water. In this paper, two scenarios for water supply in Kazeroun Petrochemical Company (KPC) were studied: 1) advanced treatment of treated municipal wastewater effluent of Kazeroun city; 2) Nargesi dam water.

In recent years, there has been a considerable growth in application of membrane technology in effective treatment of different kinds of wastewaters. There are several conventional methods such as gravity settling (Beydoun et al. 1998), dissolved and induced air flotation (Al-Shamrani et al. 2002), coagulation and flocculation (Bensadok et al. 2007), coalescence and centrifugation which have been used to treat contaminated water. In most cases, these methods are not efficient enough to meet the standard requirements of water used in petrochemical complexes. To meet the standards, hybrid combinations of the aforementioned methods with advance membrane technologies have shown promising results (Valizadeh et al. 2015). The main objective of this study was to technically and financially investigate which scenario can be the best option for water supply in KPC.

Materials and methods

In order to supply 5 million m^3 per year from two different sources, the following activities were done:

Section I - Water transmission from two scenarios (Nargesi Dam/Wastewater Treatment Facility of Kazeroun City) to the plant was technically and economically studied and activities including mapping and designing the route, conceptual design of the pumping stations and pipelines, land exploitation, and estimation of the cost of main transmission equipment were done. After the conceptual design of transmission line, its cost was evaluated and the best option was selected.

Section II – The conceptual design of pretreatment and advanced treatment systems were carried out for both water resources (scenarios). Technical and economic studies for both scenarios were examined and finally the preferred option was selected.

Section III – In this section, water market studies, contractual provisions for both scenarios, and providing financial model were done. With regard to the preliminary contracts with two water suppliers, the water price was evaluated using a financial model (calculating important parameters like Fixed and O&M costs, cash flow, internal rate of return (IRR), Net present value (NPV), etc.) and the cost of treated water per cubic meter (including water price, transmission, and treatment) was calculated in both scenarios. Finally, a financial model was provided to select the best option.

Results and concluding remarks

After mapping and designing the possible transmission routes, the capital cost of the transmission line and pump station(s) were estimated. Then, the treatment systems were designed. Based on the water analysis from two sources, different treatment units were designed. In the case of wastewater treatment

plant, equalization pond, clarifier, neutralization pit, self-cleaning filter, ultrafiltration (UF), cartridge filter, RO system, and electro-deionization (EDI) were used. Since almost 90% of the treated water is used in cooling towers, the effluent of the clarifier were sent directly to cooling tower, and the rest, was sent to the advanced treatment system (UF+RO). This resulted in a reasonable cost which is illustrated in Table 1.

Table 1. Cost of water treatment for the first scenario (wastewater treatment plant)

#	Description	Cost (USD)	Product flow rate	Unit	Final Cost ($/m^3)	Contribution (%)
1	Total Fixed Cost	4,912,850	150	MMm^3 (for 30 years)	0.03	3.8
1-1	Transmission Fixed Cost	4,745,230	150	MMm^3 (for 30 years)	0.03	3.6
1-2	Treatment Fixed Cost	168,300	150	MMm^3 (for 30 years)	0.00	0.2
2	Total O&M Cost	263,300	5	MMm^3/yr	0.06	6.5
2-1	Transmission O&M Cost	238,100	5	MMm^3/yr	0.05	5.4
2-2	Treatment O&M Cost	25,230	5	MMm^3/yr	0.01	1.0
Total Cost of Transmission and Treatment					0.09	10.3
3	Cost of Wastewater				0.79	89.7
Total Cost of treated water (US $/m^3)					0.88	100.0

In the case of dam water, the Total Suspended Solids (TSS) concentration was pretty low (TSS= 0.31 mg/L); therefore, there were no need to use any kinds of clarifier. On the contrary, the salinity of water was quite high (TDS=2560 mg/L) which needed a double pass RO system to meet the standards of EDI system entrance, to produce boiler feed. In addition, a single pass RO system was designed for treat the water for cooling towers.

The fixed cost and O&M cost of both transmission line and treatment system (for the first scenario: advanced treatment of municipal wastewater treatment effluent of Kazeroun city) is given in Table 1, and the final cost of treated water per cubic meter has been calculated. The same was done for the second scenario, but the results are not presented in detail. The final total cost of treated water per cubic meter for the case of Dam Water was calculated to be 0.42 US$/m^3, showed to be the preferred option.

Nowadays, continuous improvement strategies for increasing the quality of treated wastewater effluent are applied to meet the required standards; therefore, use of a new and more efficient approach is imperative. It was technically shown that the treatment of waters from non-conventional sources is challenging but possible, which usually requires advanced technology and high cost.

References

Beydoun D, Guang D, Chhabra P, and Raper, A (1998) Particle settling in oil-in-water emulsions. Powder Technology 97(1):72–76. https://doi.org/10.1016/S0032-5910(97)03404-9

Al-Shamrani A, James A, Xiao H, (2002) Separation of oil from water by dissolved air flotation. Colloids and Surfaces A: Physicochemical and Engineering Aspects 209(1):15–26. https://doi.org/10.1016/S0927-7757(02)00208-X

Bensadok K, Belkacem M, Nezzal G (2007) Treatment of cutting oil/water emulsion by coupling coagulation and dissolved air flotation. Desalination 206 (1-3):440–448. https://doi.org/10.1016/j.desal.2006.02.070

Valizadeh B, Zokaee Ashtiani F, Fouladitajar A, Dabir B, Baraghani S, Armand S B, Salari B, Kouchakiniya N (2015) Scale-up economic assessment and experimental analysis of MF–RO integrated membrane systems in oily wastewater treatment plants for reuse application. Desalination 374:31-37. https://doi.org/10.1016/j.desal.2015.07.017

11th World Congress on Water Resources and Environment (EWRA 2019)
"Managing Water Resources for a Sustainable Future", 25-29 June 2019, Madrid, Spain

Ecological status of Greek lakes based on different biological quality elements – criticism on the one out - all out approach

C. Ntislidou[1*], D. Latinopoulos[2], O. Petriki[3], V. Tsiaoussi[4], I. Kagalou[2], M. Lazaridou[1], D.C. Bobori[1]
[1] School of Biology, Aristotle University of Thessaloniki, Thessaloniki, Greece
[2] School of Civil Engineering, Democritus University of Thrace, Xanthi, Greece
[3] Institute of Marine Biological Resources and Inland Waters, Hellenic Centre for Marine Research, Anavissos, Greece
[4] Greek Biotope Wetland Centre (EKBY), The Goulandris Natural History Museum, Thermi, Greece
* e-mail: ntislidou@bio.auth.gr

Introduction

Since 2000, the Water Framework Directive (EC 2000) has brought a new era to the management of aquatic ecosystems in Europe. Besides aiming at achieving good ecological status for surface water bodies, it focuses, using a holistic way to the assessment of ecological quality, to their protection and the mitigation of their degradation. The initial milestone of this achievement by 2015 was very ambitious, thus an extension was necessary to reach it by the end of the second (2015-21) or/and the third (2021-27) management cycles. The WFD demands the ecological status to be assessed using different biological quality elements (BQEs: phytoplankton, aquatic flora, fish and benthic macroinvertebrates) and to be expressed in a five quality scale corresponding to an ecological quality ratio (EQR). It further suggests for this assessment all BQEs to be incorporated using the one out-all out (OAOA) approach (CIS 2003).

In Greece, until recently, there were gaps in the assessment of the ecological quality of lakes with WFD-compatible indices. Four new national indices, applicable in the broader Mediterranean area, were developed reflecting the local peculiarities. The aims of the present study are: a) to juxtapose the ecological quality of the Greek lakes assessed by the Greek Lake Benthic invertebrate Index (GLBiI, Ntislidou et al. 2018) with the assessments from indices based on other BQEs and, b) to test and criticize the strictness of the OAOA approach in ecological status assessments.

Materials and methods

The GLBiI is based on benthic macroinvertebrates and is composed by three metrics; the number of taxa and the Simpson's diversity index in the profundal and sublittoral lake zones, and the relative contribution of Chironomidae (%) of the profundal zone. This index was used to estimate the ecological quality of 17 Greek lakes, where 2 of them are very shallow (mean depth <3 m), 8 are shallow (mean depth: 3-9 m) and 7 deep (mean depth > 9 m). Human activities degrade the studied lakes, with fishery and irrigation being dominant. The EQR results for these lakes are presented along with the rest of the available formal national assessment indices: i) GLFI (Greek Lake Fish Index; Petriki et al. 2017) is based on the relative numerical abundance of introduced fish species and the relative biomass of omnivorous ones, ii) HeLM index (Hellenic Lake Macrophytes; Zervas et al. 2018) is composed by a modified trophic index and maximum colonization depth and iii) HeLPhy index (Hellenic Phytoplankton; Tsiaoussi et al. 2017) which combines 4 metrics: total phytoplankton biovolume, cyanobacterial biovolume, a modified Nygaard index and Chlorophyll α concentration.

Results and concluding remarks

The use of multiple BQEs for ecological quality assessments, according to the WFD, is an asset for the outcomes' credibility, since each BQE assesses different lake areas (Lyche-Solheim et al. 2013). In our testing, the ecological quality was identical in 23.5% (4 lakes) of the lakes examined. It should be noted that in several cases, there were no available results (Table 1). Comparing GLBiI and GLFI, 4 deviations out of 11 lakes were found. The most important divergence was observed in the case of Lake Chimaditis. When GLBiI was compared to HeLM index, a mismatch of 57% (8 out of 14 lakes in common) was recorded attributed

perhaps to HELM's response to eutrophication of the littoral zone (Zervas et al. 2018). Similar outcomes were noticed from the comparison with HeLPhy (60%, Table 1).

Table 1. Ecological quality of 17 Greek lakes, based on multimetric indices (GLBil, GLFI, HeLM and HeLPhy). Classification results are presented according to WFD quality colour scale and EQR values are mentioned in the cells.

Lake	GLBil	GLFI	HeLM	HeLPhy	OAOA	Median	Average
Volvi	0.41	0.58	0.70	0.45	0.41	0.52	0.54
Doirani	0.69		0.77	0.56	0.56	0.69	0.67
Vegoritis	0.54	0.60	0.75	0.66	0.54	0.63	0.64
Petron	0.54	0.53			0.53	0.54	0.54
Zazari	0.26	0.30	0.32	0.24	0.24	0.28	0.28
Chimaditis	0.14	0.61			0.14	0.38	0.38
Kastoria	0.45	0.38	0.68	0.47	0.38	0.46	0.50
Megali Prespa	0.65		0.76	0.69	0.65	0.69	0.70
Mikri Prespa	0.43	0.57	0.71	0.76	0.43	0.64	0.62
Pamvotis	0.59	0.27	0.20	0.41	0.20	0.34	0.37
Amvrakia	0.61	0.80	0.76	0.89	0.61	0.78	0.77
Ozeros	0.53	0.42	0.45	0.71	0.42	0.49	0.53
Lysimachia	0.39	0.47	0.59	0.56	0.39	0.52	0.50
Trichonis	0.68		0.76	0.73	0.68	0.73	0.72
Yliki	0.34			0.77	0.34	0.56	0.56
Paralimni	0.51		1.00	0.89	0.51	0.89	0.80
Kourna	0.67		1.00	0.90	0.67	0.90	0.86

The OAOA approach, selecting the "worst case", showed the poorest ecological quality status, whereas the median indices' EQRs were better in total. The OAOA is in cases avoided, since it may downgrade the ecological status of a water body due to its strictness (Caroni et al. 2013) and over-estimate the precautionary principle. The approach for status classification should be reconsidered in the future. Nonetheless, the recorded differences are crucial for lake management, since each index comprises unique information that every BQE adds (Kelly et al. 2016), and is associated with the sampling methods, the weights given, the habitats addressed and the BQEs' response time.

References

Caroni R, van de Bund W, Clarke RT, Johnson RK (2013) Combination of multiple biological quality elements into waterbody assessment of surface waters. Hydrobiologia 704(1):437-451. https://doi.org/10.1007/s10750-012-1274-y

CIS (2003) Overall approach to the classification of ecological status and ecological potential. Guidance document n 13

EC (2000) Directive 2000/60/EC of the European Parliament and of the Council of 23 October 2000 establishing a framework for Community action in the field of water policy

Kelly MG, Birk S, Willby NJ et al. (2016) Redundancy in the ecological assessment of lakes: Are phytoplankton, macrophytes and phytobenthos all necessary? Science of the Total Environment 568:594-602. https://doi.org/10.1016/j.scitotenv.2016.02.024

Lyche-Solheim A, Feld CK, Birk S et al. (2013) Ecological status assessment of European lakes: a comparison of metrics for phytoplankton, macrophytes, benthic invertebrates and fish. Hydrobiologia 704(1):57-74. https://doi.org/10.1007/s10750-012-1436-y

Ntislidou C, Lazaridou M, Tsiaoussi V, Bobori DC (2018) A new multimetric macroinvertebrate index for the ecological assessment of Mediterranean lakes. Ecological Indicators 93:1020-1033. https://doi.org/10.1016/j.ecolind.2018.05.071

Petriki O, Lazaridou M, Bobori DC (2017) A fish-based index for the assessment of the ecological quality of temperate lakes. Ecological Indicators 78:556-565. https://doi.org/10.1016/j.ecolind.2017.03.029

Tsiaoussi V, Mavromati E, Kemitzoglou D (2017) Report on the development of the national method for the assessment of the ecological status of natural lakes in Greece, using the biological quality element "phytoplankton". 1st revision. Greek Biotope / Wetland Centre and Special Secretariat for Waters, Ministry of Environment, Thermi, Greece

Zervas D, Tsiaoussi V, Tsiripidis I (2018) HeLM: a macrophyte-based method for monitoring and assessment of Greek lakes. Environmental Monitoring and Assessment 190(6):326. https://doi.org/10.1007/s10661-018-6708-1

11th World Congress on Water Resources and Environment (EWRA 2019)
"Managing Water Resources for a Sustainable Future", 25-29 June 2019, Madrid, Spain

Biodegradation potential of bacteria capable of growing in an imazalil-rich wastewater

I. Alexandropoulou[1], Z. Mavriou[1], P. Melidis[1], D.G. Karpouzas[2], S. Ntougias[1*]
[1] Laboratory of Wastewater Management and Treatment Technologies, Department of Environmental Engineering, Democritus University of Thrace, Vas. Sofias 12, 67132 Xanthi, Greece
[2] Laboratory of Plant and Environmental Biotechnology, Department of Biochemistry and Biotechnology, University of Thessaly, Biopolis, 41500 Larissa, Greece
* e-mail: sntougia@env.duth.gr

Introduction

Imazalil is a systemic imidazole fungicide, with a half-life in soil of four to five months (USEPA 2002). Although it is stable for at least 8 weeks in neutral to acidic aqueous solutions, it decays when it is exposed to high temperature and light.

Imazalil is applied to suppress a range of fungi affecting fruits, vegetables and ornamentals. Moreover, imazalil is widely used as postharvest fungicide for the protection of fruits like citrus and bananas in order to prevent storage decay (Sepulveda et al. 2015). Several technologies, like dipping, spraying, waterfalling or candle mixing (Erasmus et al. 2011; Pérez et al. 2011; Altieri et al. 2013), are employed for imazalil application in fruits and vegetables. Imazalil mode of action includes the inhibition of ergosterol biosynthesis in certain fungi, like *Penicillium* spp. On the other hand, imazalil exhibits toxicity against various aquatic organisms, like zebrafish (Jin et al. 2016).

Moreover, the wide use of imazalil as post-harvest fungicide in fruit processing industry has resulted in the production of high-strength imazalil-containing wastewaters. However, the recalcitrant nature of such effluents resists biodegradation in the conventional activated sludge systems (Santiago et al. 2018). A range of chemical methods have been recently applied at laboratory scale to treat these recalcitrant effluents, like Fenton and advanced oxidation processes (Santiago et al. 2018). However, such approaches have not been adopted for full-scale applications since the cost of chemicals minimize their applicability.

On the other hand, microorganisms that are specialized in the degradation of imazalil are limited, a fact that restricts the adoption of biological methods to face the treatment of imazalil-rich effluents generated by the fruit processing agro-industry. Thus, the scope of this work was to isolate and molecularly identify novel microbiota capable of growing in synthetic wastewater containing high concentration of imazalil in order to serve as starter culture in biological systems treating such fungicide-rich effluents.

Materials and methods

To obtain effective imazalil-degrading microbiota, the residue of a storage tank receiving imazalil-rich effluent was served as the inoculum. To isolate potential imazalil-degrading microbiota, ten-fold dilution plating was performed in defined medium consisting of commercially available imazalil formulation. In particular, the dilution series were performed in a solution consisting of the appropriate nitrogenous inorganic compounds, phosphate salts and trace elements (in the absence of any carbonaceous compound). The aforementioned solution was also used for the preparation of solid media, where 1.7 w/v bacteriological agar served as the solidifying agent. After sterilization and prior agar solidification, 250 mg/L imazalil was added to serve as the carbon source.

To phylogenetically characterize the isolated microorganisms, DNA was extracted by using the Macherey-Nagel "NucleoSpin Tissue" kit. The genomic DNA obtained from the microbial isolates was amplified by using universal primers for the 16S rRNA gene, as previously described (Remmas et al. 2018). In brief, a thermocycling protocol consisting of a primary denaturation step of 2 min at 94°C, followed by 35 cycles of 30 sec denaturation at 94°C, 30 sec primer annealing at 52°C and 90 sec DNA extension at 72°C, was implemented. A final DNA elongation step at 72°C for 10 min was carried out to accomplish the PCR

reaction. All sequencing reactions were performed at Eurofins Genomics (Germany) by using universal 16S rRNA gene primers.

Results and concluding remarks

In total, 20 bacterial strains capable of growing in imazalil-containing medium were isolated. Performance of phylogenetic analysis showed that they were representatives of the order *Rhizobiales* (class *Alphaproteobacteria*) and the family *Pseudomonadaceae* (class *Gammaproteobacteria*), which both include various effective degraders. Therefore, it is concluded that the selection pressure applied during storage of imazalil-rich fruit processing waste resulted in the proliferation of a well-adapted bacterial community capable of coping with the severe conditions established by the accumulation of post-harvest fungicides.

Acknowledgements: This research (carried out within the frame of the research project entitled "Development and implementation of novel biobased methods for the treatment of pesticide-contaminated wastewaters from agro-industries, MIS 5030360") has been co-financed by the European Union and Greek national funds through the Operational Program Competitiveness, Entrepreneurship and Innovation, under the call RESEARCH – CREATE – INNOVATE (project code: T1EDK-02566).

References

Altieri G, Di Renzo GC, Genovese F, Calandra M, Strano MC (2013) A new method for the postharvest application of imazalil fungicide to citrus fruit. Biosystems Engineering 115(4):434-443. https://doi.org/10.1016/j.biosystemseng.2013.04.008

Erasmus A, Lennox CL, Jordaan H, Smilanick JL, Lesar K, Fourie PH (2011) Imazalil residue loading and green mould control in citrus packhouses. Postharvest Biology and Technology 62(2):193-203. https://doi.org/10.1016/j.postharvbio.2011.05.006

Jin Y, Zhu Z, Wang Y, Yang E, Feng X, Fu Z (2016) The fungicide imazalil induces developmental abnormalities and alters locomotor activity during early developmental stages in zebrafish. Chemosphere 153:455-461. https://doi.org/10.1016/j.chemosphere.2016.03.085

Pérez E, Blanco O, Berreta C, Dol I, Lado J (2011) Imazalil concentration for in vitro monitoring of imazalil resistant isolates of Penicillium digitatum in citrus packinghouses. Postharvest Biology and Technology 60(3):258-262. https://doi.org/10.1016/j.postharvbio.2011.01.002

Remmas N, Melidis P, Voltsi C, Athanasiou D, Ntougias S (2017) Novel hydrolytic extremely halotolerant alkaliphiles from mature landfill leachate with key involvement in maturation process. Journal of Environmental Science and Health 52(1):64-73. https://doi.org/10.1080/10934529.2016.1229931

Santiago DE, González-Díaz O, Araña J, Pulido Melián E, Pérez-Peña J, Doña-Rodríguez JM (2018) Factorial experimental design of imazalil-containing wastewater to be treated by Fenton-based processes. Journal of Photochemistry and Photobiology A: Chemistry 353:240-250. https://doi.org/10.1016/j.jphotochem.2017.11.038

Sepulveda M, Cuevas II, Smilanick JL, Cerioni L, Rapisarda VA, Ramallo J (2015) Improvement in imazalil treatments in commercial packinglines to control green mold on lemon fruit. Scientia Horticulturae 192:387-390. https://doi.org/10.1016/j.scienta.2015.06.021

U.S. Environmental Protection Agency (2002) Imazalil: the Revised HED Toxicology Chapter for the Reregistration Eligibility Decision Document (RED)(2002)PC Code 111901, Case 816389. HED Document No. 0050434. U.S. EPA, Office of Pesticide Programs, Washington DC

11th World Congress on Water Resources and Environment (EWRA 2019)
"Managing Water Resources for a Sustainable Future", 25-29 June 2019, Madrid, Spain

Exploring the spatiotemporal water quality variations and their influencing factors in a large floodplain lake (Poyang Lake) in China

B. Li*, G. Yang
Key Laboratory of Watershed Geographic Sciences, Nanjing Institute of Geography and Limnology, Chinese Academy of Sciences, Nanjing, China
** e-mail: bli@niglas.ac.cn*

Introduction

Floodplain lakes are natural fragmented systems with periodic hydrological connections and are constantly suffered from pollution and eutrophication. Evaluating water quality variations in the floodplain in space and under different hydrological conditions and exploring their driving forces are vital to establish possible management actions that can intervene in the recovery and preservation of floodplain ecosystems. Many scholars have used multivariate statistical approaches, fuzzy theory, WQI indices to identify underlying patterns in water quality alterations (Wold et al. 1987; Yidana et al. 2008; Sener et al. 2017). Nevertheless, complexity and uncertainty problems exist during evaluation (Wong and Hu 2014). Fuzzy matter–element method (FME) can efficiently solve these problems by combining fuzzy boundaries and matter–element theory.

Poyang Lake is the largest freshwater lake in China and is a typical floodplain lake characterized by dramatic water level fluctuations. Water quality parameters in this kind of system are highly dynamic and different from those in other lentic lakes due to large seasonal variations in surface area and water level (Sokly et al. 2018). It is essential to reveal the spatiotemporal patterns of water quality and their influencing factors to inform guidelines for water management in large floodplain lakes.

Materials and methods

Poyang Lake receives water from precipitation and the inflow of five main tributaries and water of the lake drains into the downstream Yangtze River through a narrow channel. The prevailing climate is subtropical monsoon, causing a substantial water level fluctuation between 8 m and over 20 m from dry to wet season. The data used in the present study contains monthly water quality data in 18 sampling sites from the lake body and its inflow rivers from 2010 to 2015. Cluster analysis was initially used to identify the clusters with high external and internal heterogeneity. FME model was then used to evaluate the water quality status of the lake.

The FME model based on classical and extension mathematics is commonly used to solve uncertain and contradictory problems. According to FME theory, a compound fuzzy matter-element can be generated by m water quality evaluation objects (water samples), n feature vectors C_n (indices), the corresponding fuzzy value u_{ij} and k water quality classifications G_j (see detail in Li et al. 2017). A rank feature value was finally obtained to represent the water quality status, with high value denoting bad water quality and vice versa.

Results and concluding remarks

No statistically remarkable differences were found between the water quality of the lake and inflow rivers, whereas the water quality of the eastern part of the lake showed significant difference with other sampling sites, which may be a result of receiving discharge from the relatively polluted upstream Lean River. The pollution hotspot region in the eastern part of the Poyang Lake was also reported by Li using a two-dimensional water quality model (Li et al. 2018). In addition, despite poor water quality in cluster II, water quality of sampling sites in the cluster I showed relatively desirable water quality, denoting the high transportation and degradation capability of the floodplain lake.

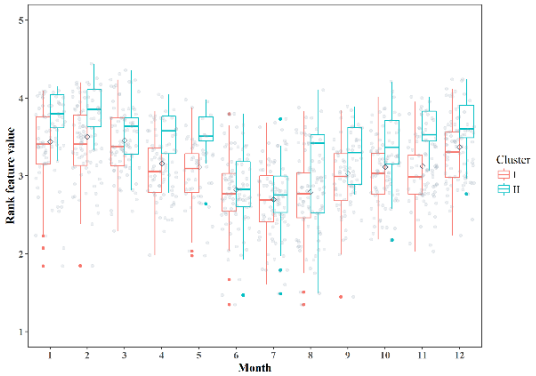

Figure 1. Seasonal boxplots of water quality rank feature values between clusters I and II (east part of the lake)

Figure 2 shows the spatial variations of FME values in 18 sampling sites during different seasons. Similarly, Poyang Lake exhibited the most desirable water quality during summer whereas poorest water quality during winter. A total of 38.8%, 16.7%, and 11.1% of the sampling sites during winter, spring, and autumn were classified as "poor" status in Poyang Lake, respectively. The relatively desirable water quality of Poyang Lake during wet season was mainly attributed to high dilution and biological degradation processes. Notably, Water level variation exhibited significant negative correlation with FME rank feature values, which indicated that water quality was more likely to be desirable in high water level periods.

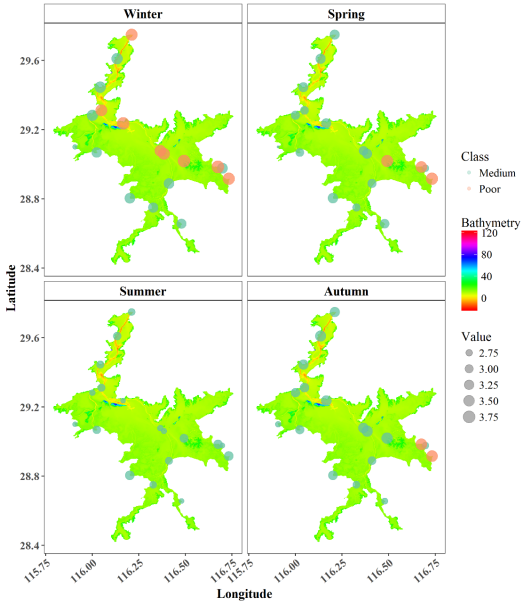

Figure 2. Spatial variations in FME values during different seasons in Poyang Lake

Acknowledgments: This work was financially supported by the Key Research Program of the Chinese Academy of Sciences (KFZD-SW-318) and the National Scientific Foundation of China (41801092).

References

Li B, Yang G, Wan R et al. (2017) Dynamic water quality evaluation based on fuzzy matter–element model and functional data analysis, a case study in Poyang Lake. Environ Science and Pollution Research 24(23):19138-19148

Sener S, Sener E, Davraz A (2017) Evaluation of water quality using water quality index (WQI) method and GIS in Aksu River (SW-Turkey). Science of the Total Environment 584:131-144

Sokly S, Heejun Y, Ty S et al. (2018) Sediment dynamics in a large shallow lake characterized by seasonal flood pulse in Southeast Asia. Science of the Total Environment 631:597-607

Wold S, Esbensen K, Geladi P (1987) Principal component analysis. Chemometrics and Intelligent Laboratory 2:37-52

Yidana SM, Ophori D, Banoeng-Yakubo B (2008) A multivariate statistical analysis of surface water chemistry data - The Ankobra Basin, Ghana. Journal of Environment Management 86(1):80-87

Wong H, Hu BQ (2014) Application of improved extension evaluation method to water quality evaluation. Journal of Hydrology 509:539-548

11th World Congress on Water Resources and Environment (EWRA 2019)
"Managing Water Resources for a Sustainable Future", 25-29 June 2019, Madrid, Spain

Polypropylene based nanocomposite membrane with a novel self-assembled coating for seawater treatment via membrane distillation

R. Kumar*, M. Ahmed, G. Bhadrachari, J. Thomas
Water Research Center, Kuwait Institute for Scientific Research, P.O. Box, 24885, 13109 Safat, Kuwait
** e-mail: rajeshakumar15@yahoo.com*

Introduction

MD is an emerging technology which is competing with other desalination technologies, where there is an urgent need to bring down the energy consumptions during the desalination process. Recently, a lot of interest in commercialization efforts for MD has been realized. As an example, Aquaver Company recently commissioned the world's first seawater MD-based desalination plant in Maldives. The plant uses waste grade heat available from a local power plant and has a capacity of 10,000 L/day. For Kuwait, seawater desalination is the only source of pure water for potable and domestic use. The development of low-cost desalination technology such as MD has a direct positive impact on the country's economy. However, the membrane fouling is a particular concern due to necessity of hydrophobic membrane for MD process. The concept of a mixed-matrix membrane, where a small filler material is dispersed throughout a larger polymeric matrix, has improved mechanical, chemical, and thermal stability, as well as enhanced separation (Behera et al. 2007; Rittigstein et al. 2007).

In this current study a novel approach of self-assembly techniques has been used for the coating of superhydrophobic layer over the microporous polypropylene (PP) support for seawater treatment application. The hydrophobic fluorinated silica nanoparticles were synthesized and isolated by reacting tetraethyl orthosilicate (TEOS) with excess heptadeca- fluoro-1,1,2,2-tetrahydrodecyl) triethoxysilane.

Materials and methods

PVDF Kynar® HSV 900 was procured from Arkema Inc., Heptadeca- fluoro-1,1,2,2-tetrahydrodecyl) triethoxy silane was purchased from ABCR GMBH, Germany, Tetraethyl orthosilicate and polyethylene glycol (Mw= 600 Da) were procured from Sigma Aldrich Co., ethanol, sodium chloride and 25% solution of aqueous ammonia were purchased from Merck Co.

The synthesis of hydrophobic silica nanoparticles (HSN) includes a reported protocol in the literature with modifications in the stoichiometric ratio of the reactants (Hongxia et al. 2008). In a typical procedure, tetraethyl orthosilicate (20 mL), with Heptadeca- fluoro-1,1,2,2-tetrahydrodecyl) triethoxysilane (10 mL) was dissolved in 100 mL of ethanol at 25-26 °C. Then the reaction mixture was charged with a solution of ammonium hydroxide/ethanol solution (25 ml 28% $NH_3 \cdot H_2O$ in 75 mL ethanol) at 25-26 °C. The turbid solution could stir at 25-26 °C for 12 h to ensure complete fluoro coating of the Silica nanoparticles. The stirring was stopped to settle down the precipitated HSN particles, the supernatant was separated by decanting, the precipitates were washed with ethanol (2x100 mL) followed by washing with deionized water (1x100 mL) and dried at 80 °C for 5 h.

The HSP were dispersed in the coating solution consisted of trimesoyl chloride, trimethylamine and hexane compositions. The coating layer thickness was limited to 100-150 µm by selecting the proper compositions of the TEA and TMC. The coating layer with HSP was effectively formed over the PP support via self-assembly of the hydrolyzed TMC molecules as trimesic acid molecules stabilized by intermolecular hydrogen bonding. The membranes were characterized using porometer, liquid entry pressure, atomic force microscope from Nanosurf France, scanning electron microscope from Zeiss, and contact angle measurements.

Results and concluding remarks

SEM and AFM analysis: The SEM analysis as presented in Figure 1 revealed that the coating of HSN particle layer over the surface of PP membrane resulted in a drop in the pore size of the membrane surface.

The coated particles were highly hydrophobic in nature and contact angle study confirmed that the increase in contact angle value was from 80° to 155° leading to a superhydrophobic surface. Also, it is notable that the self-assembled TMC layer has aided the HSN molecules to attach firmly on the membrane surface. The AFM images revealed a slight increase in the surface roughness value for the coated membrane from 110 nm to 130 nm (Figure 2), however the increased roughness was less severe compared to the loading composition of the HSN particles. The nascent PP membranes showed a liquid entry pressure (LEP) value of 110 kPa, while for the coated membrane its value was increased to 160 kPa. The increase in LEP enhanced the seawater desalination performance of the coated membrane by offering less wetting to the membrane surface.

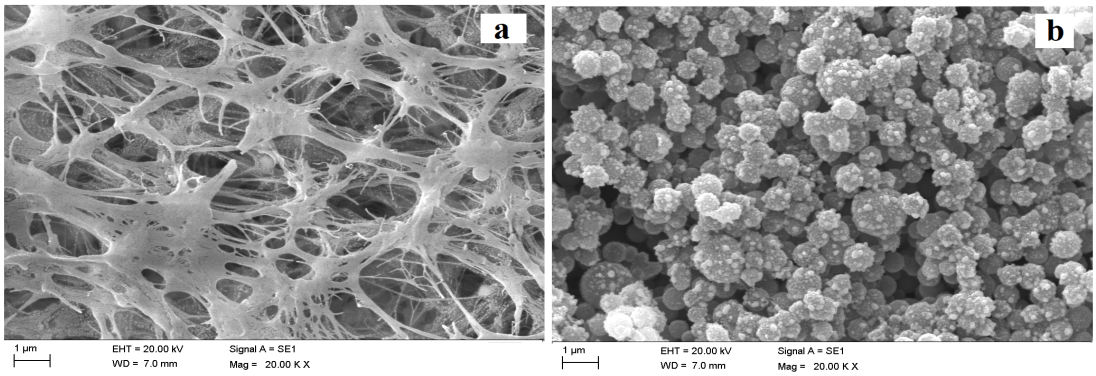

Figure 1. a) Surface image of PP membrane, b) surface image of coated PP membrane with HSN particles.

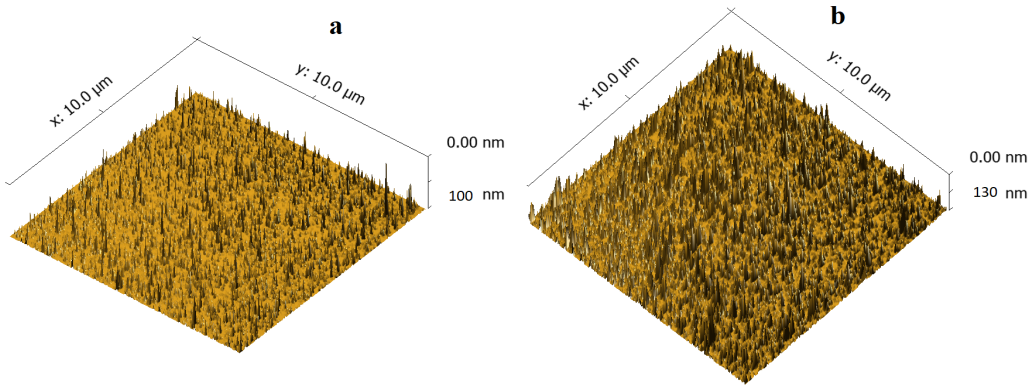

Figure 2. AFM images of a) PP membrane, b) coated PP membrane with HSN particles.

The application of membranes was tested for membrane distillation application in direct contact membrane distillation (DCMD) configuration using hot feed of 35 g/L aqueous sodium chloride solution, and cold deionized water as permeate. The maximum transmembrane permeate flux of 46.7 kg/m^{2}h with >99% salt rejection was obtained at 80°C demonstrating the future potential application towards seawater desalination.

Acknowledgements: Authors are thankful to the Kuwait Foundation for Advancement of Sciences and Kuwait Institute for Scientific Research (KISR) for financially supporting this research activity.

References

Behera D, Banthia AK (2007) BisGMA/TiO2 organic-inorganic hybrid nanocomposite. Polymer-plastics Technology and Engineering 26(1):10-12. doi: 10.1080/03602550701575821

Rittigstein P, Priestley RD, Broadbelt LJ, Torkelson JM (2007) Model polymer nanocomposites with known interlayer spacing provide understanding of confinement effects in real nanocomposites. Nature Materials 6(1):278-282. doi: 10.1038/nmat1870

Hongxia W, Jian F, Tong C, Jie D, Liangti Q, Liming D, Xungai W, Tong L (2008) One-step coating of fluoro-containing silica nanoparticles for universal generation of surface superhydrophobicity. Chemical Communications 7:877–879. doi: 10.1039/B714352D

11th World Congress on Water Resources and Environment (EWRA 2019)
"Managing Water Resources for a Sustainable Future", 25-29 June 2019, Madrid, Spain

WaterSpy: Utilizing photonics technology for drinking water quality analysis

G. Kopsiaftis[1*], A. Doulamis[1], N. Doulamis[1], A. Voulodimos[2], M. Bimpas[1], A. Angeli[1], N. Bakalos[1], A. Giusti[2], P. Philimis[2], P. Demosthenous[2]
[1] Department of Rural and Surveying Engineering, National Technical University of Athens, Greece
[2] Cyprus Research and Innovation Center Ltd (CyRIC), Cyprus
* e-mail: gkopsiaf@central.ntua.gr

Introduction

Drinking water microbiology has for more than 100 years been dominated by a conservative approach caused by a limited understanding of the indigenous bacterial flora. This was mainly due to the lack of sensitive, fast and realistic methods to detect and quantify both the indigenous microbial cells and the presence of relevant pathogens. For the past time, routine monitoring and hygiene assessment focused on the detection of (1) cultivable heterotrophic microbes as a measure of the general microbiological quality of water, and (2) the detection of indicators for faecal pollution using plating methods. However, the microbial cells in drinking water are significantly higher, compared to those that can be cultured on synthetic growth media. Some 90–99%, or even more, of the bacterial cells detected in aqueous and terrestrial environments cannot be cultivated in the laboratory with the methods presently used, which creates a huge discrepancy between cultivable and total cell counts, commonly referred to as "the great plate count anomaly".

This paper presents the basic principles and the preliminary results of a research project (WaterSpy) which aims at addressing some of the aforementioned limitations through the development of a novel, compact, cost-effective photonic device, operating in the spectral range of 6-10 μm and suitable for pervasive water quality sensing. In particular, the aim of this research is to develop a device that will require less than a few hours for a full water sample analysis of 100 mL, in search for three heterotrophic bacterial cells (E. coli, Salmonella and P. aerruginosa).

Materials and methods

The research work is established on the following basic pillars: 1) the *Fourier-transform infrared spectroscopy (FT-IR)* technique, 2) the *Quantum cascade lasers (QCLs)* technology, 3) the *Molecular Recognition Elements (MREs)* and 4) the *Ultrasound* techniques.

The FT-IR method is used to obtain an infrared spectrum of absorption of the three examined bacteria (Schäwe 2011). The differences in the spectra for these bacteria is determined through Attenuated Total Reflection (ATR) experiments. It should be noted that there has been a growing interest in expanding spectroscopic methods beyond 2 μm range of infrared (IR) spectrum and up to the 12 μm wavelength. This specific region of IR spectrum is home to many vibrational and rotational absorptions of compounds and molecules related to water quality and contaminants. Unfortunately, water itself is a very strong absorber of infrared light. Thus, since available infrared light sources provide only insufficient power, the proposed method is restricted to strongly confined laboratory settings. In particular, in order to address this challenge, photonics technology was utilized to develop a device able to operate in the mid-infrared (6-10 μm).

The proposed solution has the following main features: 1) the development of advanced QCL sources coupled with innovative, fibre-coupled, fast and sensitive, High-Operating-Temperature (HOT) photodetectors, in order to detect the fingerprint regions of selected analytes of high priority in freshwater 2) the development of an antibody-based mechanism (smart surface) to capture the bacteria on the microfluidic channel's surface, in order to further increase detection accuracy and specificity 3) the use of Attenuated Total Reflection (ATR) techniques, to maximize the Signal-to-noise ratio (SNR), without the

need for any further sample preparation procedure, 4) the use of molecular recognition elements (MREs) of high specificity for binding on the surface the target bacteria, in order to maximize the SNR and bind even the single bacteria of the targeted strains and 5) the use of a novel sample pre-concentration technique, based on ultrasounds (Freitag 2018).

Results and concluding remarks

All individual components of the device have been developed and tested (e.g. Freitag 2018). The preliminary results were promising. However, it was found that infrared spectroscopy by itself would not be sufficient to meet the requirements of measuring 1 bacterium in 100 mL of water. Therefore, it was concluded that, besides sample pre-concentration, an additional amplification step of the target bacteria should be performed, such as incubation. After the preliminary sample pre-concentration, the sample will be passed into a heated syringe-based incubator. In this module, the bacteria will be combined with a broth to enable their growth. After 6h of incubation (time interval to be optimised), the sample will be handed over to the acoustofluidic cell for the final analysis. The first version of this incubation module has already been developed and the first cultivation experiments will be performed in the near future. Moreover, an ultrasound enhanced assay is deployed, which increases the detection capabilities. In this assay, a multibounce ATR element is used, while UV-VIS spectroscopy is used to provide an assessment of the number of bacteria in the used samples. Initial results (without incubation) are presented in Figure 1.

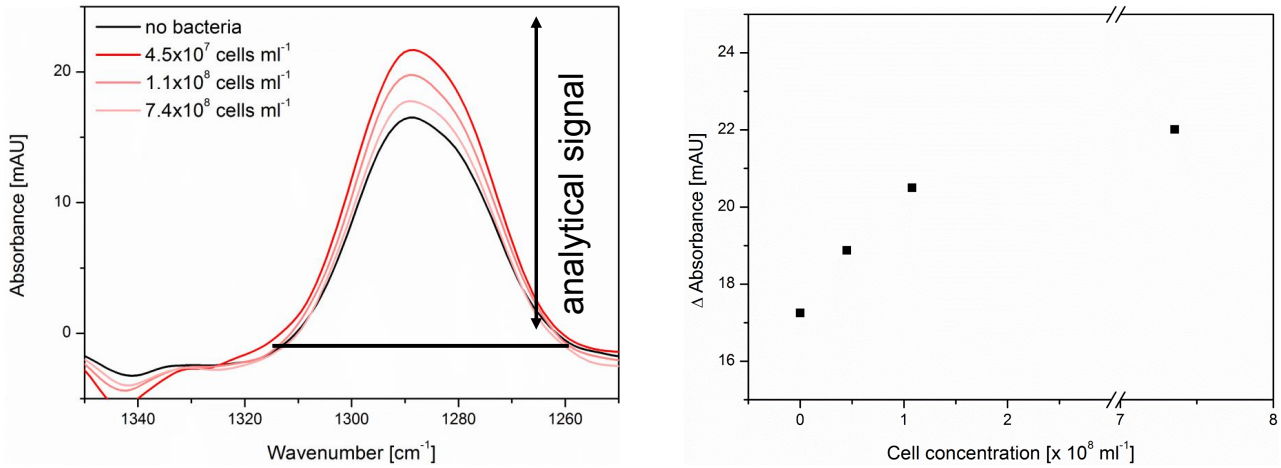

Figure 1. Initial Results

Apart from the innovation of the device and the related technological achievements, the proposed method is expected to have a significant impact in public health, since it will ensure the safety of citizens through the reduction of vulnerabilities and consequences of attacks. Furthermore, the fast and effective detection of pollutants will help saving large amounts of water by preventing pollutants' propagation.

Acknowledgments: The research leading to these results has received funding from the European Union's Horizon 2020 Research and Innovation Programme under grant agreement no. 731778 (WaterSpy project).

References

Brandstetter M, Genner A, Anic K, Lendl B (2010) Tunable external cavity quantum cascade laser for the simultaneous determination of glucose and lactate in aqueous phase. Analyst 135(12):3260-3265

Freitag S, Schwaighofer A, Radel S, Lendl B (2018) Towards ultrasound enhanced mid-IR spectroscopy for sensing bacteria in aqueous solutions. In: Microfluidics, BioMEMS, and Medical Microsystems XVI (Vol. 10491, p. 104910M). International Society for Optics and Photonics

Schäwe R, Fetzer I, Tönniges A, Härtig C, Geyer W, Harms H, Chatzinotas A (2011) Evaluation of FT-IR spectroscopy as a tool to quantify bacteria in binary mixed cultures. Journal of Microbiological Methods 86(2):182-187

11th World Congress on Water Resources and Environment (EWRA 2019)
"Managing Water Resources for a Sustainable Future", 25-29 June 2019, Madrid, Spain

Design of experiment for chromium (VI) removal with PVC / Aliquat 336 polymeric inclusion membrane in MF-FSMC module

S. Bey[1*], H. Semghouni[1], A. Criscuoli[2], A. Figoli[2], F. Russo[2], M. Benamor[1], E. Drioli[2]
[1] Laboratoire des Procédés Membranaires et des Techniques de Séparation et de Récupération (LPMTSR), Faculté de Technologie, Université de Bejaia,06000, Algerie
[2] Institue on Membrane Technology (ITM-CNR), University of Calabria, 87030 Rende (CS) Italy
* e-mail: saidbey06@yahoo.com

Introduction

In the two recent decades, membrane contactors have attracted attention in the separation of metal ions from aqueous solutions. These systems, and in particular liquid membranes, can offer an alernative in many fields according to their higher performance compared to other systems. Polymer inclusion membranes (PIMs) are a type of liquid membranes (Lopez et al. 2010; Kaya et al. 2016) composed of a liquid phase and a base polymer. They are considered to be an atractive green alternative for solvent extraction (Ines et al. 2017). PIMs have been in use for long time and their development is constantly increasing (Kebiche et al. 2010; Anane et al.2015). PIMs allow extraction and backextraction to occur simultaneously in one step using simple systems.

In this work, we explore for the first time the use of polymeric inclusion membrane base on PVC/Aliquat-336 into multiframe flat sheet membrane contactor (MF-FSMC). The investigation focuses on the transport of Cr(VI) and the design of experiment (DOE) for the feed and receiving phase, which was used to optimize the extraction parameters.

Material and methods

Membrane preparation: Polymeric inclusion membranes were prepared by dissolving a certain quantity of polyvinyle chloride (PVC) in tetra hydrofurane (THF) (Fontás et al. 2005). After that, Aiquat-336, quaternary ammonium extractant, was added and agitated vigorously to obtain a homogeneous polymeric solution. The content of Aliquat-336 in the membrane was varied at the ratio PVC/Aliquat-336 of: 1/0.5, 1/1 and 1/1.5. The mixed polymeric solutions were poured in a petri dish and the solvent was allowed to evaporate slowly at room temperature.

Extraction experiment: Chromium (VI) transport was carried out in a multiframe flat sheet membrane contactor (MF-FSMC) moule, recently designed. Concentrations of 10, 30 and 50 ppm were used in the feed solution and sodium chloride at 1 M in sodium hydroxide at 0.1 M was used as receiving phase. All the experiments were carried out at a fixed flux rate of 0.3 mL/s.

Results and discussion

PIMs based on PVC and trioctyl methyl ammonium (Aliquat336) were prepared by varying the ratio PVC/Aliquat-336. The investigated ratio PVC/Aliquat-336 were 1/0.5, 1/0.75 and 1/1. The produced membranes were characterized and successfully applied for chromium (VI) extraction from aqueous solution using a novel multiframe flat sheet membrane contactor module consisting on ten parallel chambers alternating source and receiving phases. Several techniques were used to characterize the produced membranes, such as SEM, ATG and FTIR. SEM pictures show a homogeneous dense structure and two step degradation in ATG thermograms confirming the incorporation of Aliquat336 into the membrane matrix. In this configuration, high chromium recovery factors were obtained with initial concentrations of 10 ppm and 1 M of NaCl at 20°C.

To determine the interaction between different parameters, a full factorial design of experiment was used for the feed and stripping solutions. The study focuses on the evaluation of the effect of temperature (T), Aliquat336 and Cr (VI) concentration in the feed phase on the efficiency of the system. The results show

that the interaction between Aliquat336 and temperature was the most important parameter. Moreover, the analysis of the variance shows an insignificant effect of [Aliquat336], T and interactions T*[Cr(VI)], [Cr(VI)]*[Aliquat336] on the extraction efficiency of Cr(VI) in the source phase. However, a significant effect was observed for [Cr(VI)] and interactions [Aliquat336]*T, [Cr(VI)]*[Aliquat336]*T. In the case of receiving phase, an insignificant effect was observed for [Aliquat336] and interactions [Aliquat336]*T and [NaCl]*[Aliquat336]*T. However, a significant effect is considered for [NaCl], T and the two interactions T*[NaCl] and [NaCl]*[Aliquat336]. Mathematical models established seem to represent correctly the experiments, correlating well predictions and experimental data, represented by the following equations:

Feed phase:

$$S = 87.033 + 2.645\,[Cr] + 0.129\,[Aliq] - 0.967\,T + 0.077\,[Cr]*[Aliq] + 0.530\,[Cr]*T + 3.667\,[Aliq]*T - 3.530\,[Cr]*[Aliq]*T \quad (1)$$

Receiving phase:

$$R = 43.872 + 7.945\,[NaCl] + 1.717\,[Aliq] + 5.329\,T + 3.397\,[NaCl]*[Aliq] - 2.674\,[NaCl]*T - 0.921\,[Aliq]*T + 0.676\,[NaCl]*[Aliq]*T \quad (2)$$

where S =represents the source phase and R = represents the receiving phase.

As a result, the optimal values of different parameters are [Cr(VI]=10 ppm, PVC/Aliquat336 = 1/0.5 and T=20°C for the feed phase and the extraction efficiency is greater than 93%. For the receiving phase, the optimal values of the different parameters are: [NaCl]=2 M, PVC/Aliquat336 = 1/1 and T=50°C for re-extraction efficiency of 59%.

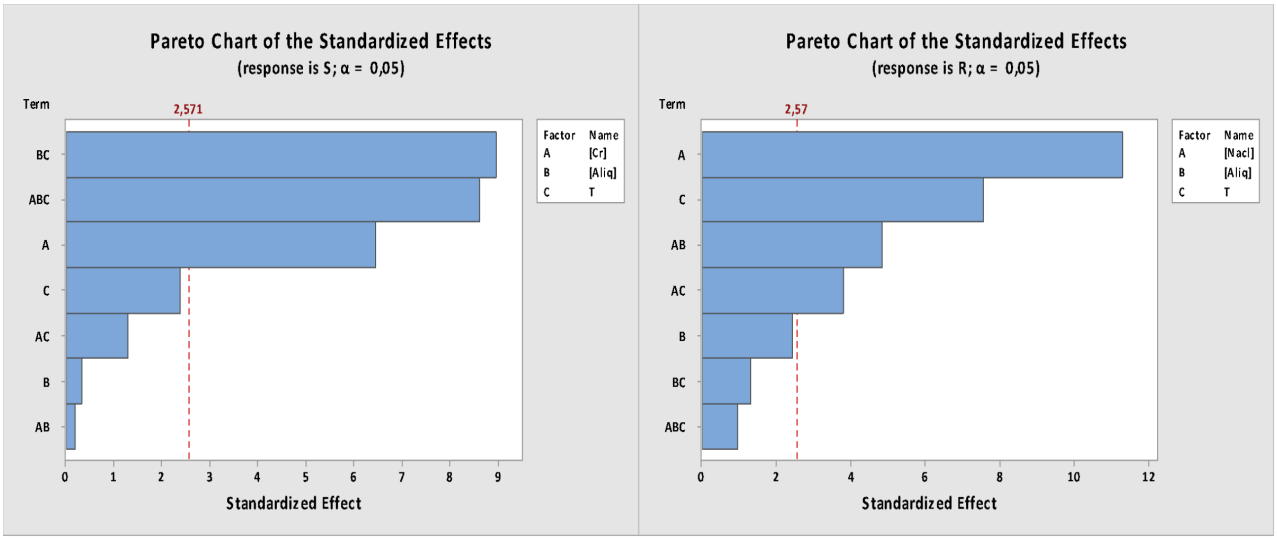

Figure 1. Pareto chart of the effects for extraction efficiency of Cr(VI) as response to the feed (left) and receiving phases (right).

References

Annane K, Sahmoune A, Montels P, Tingry S (2015) Polymer inclusion membrane extraction of cadmium(II) with Aliquat 336 in micro-channel cell. Chemical Engineering Research and Design 9(4):605–610

Fontás C, Tayeb R, Tingry S, Hidalgo M, Seta P (2005) Transport of platinum(IV) through supported liquid membrane (SLM) and polymeric plasticized membrane (PPM). Journal of membrane science. 263:96–102

Ines M, Almeida GS, Cattrall Robert W, Kolev Spas D (2017) Polymer inclusion membranes (PIMs) in chemical analysis - A review. Analytica Chimica Acta 987:1-14

Kaya A, Onac C, Korkmaz AH, Yilmaz A, Atar N (2016) Removal of Cr(VI) through calixarene based polymer inclusion membrane from chrome plating bath water. Chemical Engineering Journal 283:141–149

Kebiche-Senhadji O, Tingry S, Seta P, Benamor M (2010) Selective extraction of Cr(VI) over metallic species by polymer inclusion membrane (PIM) using anion(Aliquat 336) as carrier. Desalination 258:59–65

Lopez-Lopez JA, Mendiguchía C, Pinto JJ, Moreno C (2010) Liquid membranes for quantification and speciation of trace metals in natural waters. Trac-Trends Anal. Chem. 29:645-653

11th World Congress on Water Resources and Environment (EWRA 2019)
"Managing Water Resources for a Sustainable Future", 25-29 June 2019, Madrid, Spain

Utilization of water hyacinths for the extraction of heavy metals from contaminated water - organic acid assisted phytoremediation

R. Sallah-Ud-Din*, R. Saeed, M. Farid
Department of Environmental Sciences, University of Gujrat, Gujrat, Pakistan
** e-mail: raishamsalahuddin@hotmail.com*

Introduction

Concentrated urbanization and the demand for better to best products to enhance quality of life is boosting the intense industrialization, which is ultimately posing burden on nature's resources (Rizwan et al. 2017). Open discharges of industrial effluent enriched with inorganic toxicants are merging into rivers and streams, reaching to agricultural land; its utilization for crop cultivation is now common and preferable practice by the farmers in Pakistan (Ali et al. 2015). According to Mohiuddin et al. (2010) and Adress et al. (2015), fertile lands are getting polluted with heavy metals (HMs) concentrations transported within unprocessed industrial effluent. This contamination is threatening by inclusion into the entire food web and causing damage among biota. Among HMs, several are prominently fond in industrial wastewater, i.e., chromium (Cr), cadmium (Cd), lead (Pb), zinc (Zn), silver (Ag), and copper (Cu).

Phytoremediation is green, solar driven and efficient technique which can be further modified with acid amendments that act as chelating agent in HM removal and in supporting plant function (Farid et al. 2018). This study was designed to evaluate the potential of water hyacinths (*Echhornia crassipes*) being hyperaccumulator on the extraction of Cr (stable) and Cd (mobile) from water. These two metals are collectively discharged from metal plating industry. Application of citric acid (CA), an organic acid, was the modification of this technique to get better outcomes in terms of water treatment. Effects of Cr, Cd and CA on physiology of water hyacinths were also estimated.

Materials and methods

Fresh water hyacinths of equal size were collected from marsh water and were kept floating in glass containers (10 per glass containers) containing 25 L of water and provided with 8 treatments (three replicates) of Cr, Cd and CA individually and in combined application including control. The experiment ran for 30 days at 25°C with continuous aeration and sufficient sunlight.

After 30 days, plants were cut and separated into three organs, i.e., roots, stems and leaves, for the determination of:

- Agronomic traits
- Growth parameter
- Chlorophyll and carotene contents
- Physico-chemical characteristics
- Anti-oxidant enzymes analysis
- Heavy metals concentrations
- Accumulation
- Bio-concentration factor
- Translocation factor
- Remaining metal in water according to protocols followed by Sallah-Ud-Din et al. (2017).

Results and concluding remarks

This investigation suggested water hyacinth as significant hyperaccumulator for both metals, Cd followed by Cr. It is also understood that Cd exerted more toxic effect on plant's morphological, biochemical and physiological characteristics as compared to the Cr but this toxicity got magnified with the combined application of both metals (Figure 1). The magnified toxic effect on Cd application is in line with the previous findings by Kumar et al. (2017), that the mobility of Cd makes it more bioavailable to the roots

of plants ultimately more removable from water compared to Cr. Meanwhile, CA proved to be a good amendment in alleviating metal caused toxic effects exerted by Cr, Cd or Cr+Cd. Significant was the effect of CA in making metal bioavailable to plants in the case of Cr and more in the case of Cd. Citric acid ultimately enhanced accumulation of HMs in all organs of plants, ensuring efficiency in terms of phytoextraction from the contaminated water and proving their potential hyperaccumulator capacity to treat wastewater.

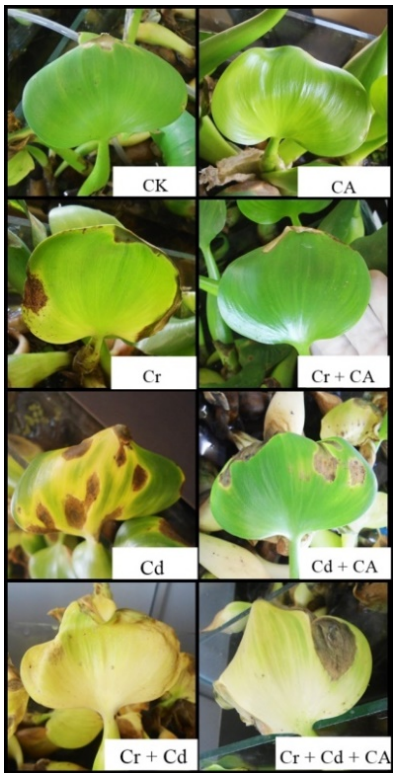

Figure 1. Effects of different treatments on water hyacinth leaf greenery / Chlorophyll contents.

References

Adrees M, Ali S, Rizwan M, Ibrahim M, Abbas F, Farid M, Zia-ur-Rehman M, Irshad MK, Bharwana SA (2015) The effect of excess copper on growth and physiology of important food crops: a review. Environmental Science and Pollution Research 22(11):8148-8162. doi: 10.1007/ s11356-015-4496-5

Ali S, Chaudhary A, Rizwan M, Anwar HT, Adrees M, Farid M, Irshad MK, Hayat T, Anjum SA (2015) Alleviation of chromium toxicity by glycinebetaine is related to elevated antioxidant enzymes and suppressed chromium uptake and oxidative stress in wheat (Triticum aestivum L.). Environmental Science and Pollution Research 22(14):10669-10678

Farid M, Ali S, Zubair M, Saeed R, Rizwan M, Sallah-Ud-Din R, Azam A, Ashraf R, Ashraf W (2018) Glutamic acid assisted phyto-management of silver-contaminated soils through sunflower; physiological and biochemical response. Environmental Science and Pollution Research 25(25):25390-25400

Kumar SS, Kadier A, Malyan SK, Ahmad A, Bishnoi NR (2017) Phytoremediation and rhizoremediation: uptake, mobilization and sequestration of heavy metals by plants. In: Plant-Microbe Interactions in Agro-Ecological Perspectives, Springer, Singapore, pp 367-394

Mohiuddin KM, Zakir HM, Otomo K, Sharmin S, Shikazono N (2010) Geochemical distribution of trace metal pollutants in water and sediments of downstream of an urban river. International Journal of Environmental Science & Technology 7(1):17-28

Rizwan M, Ali S, Abbas F, Adrees M, Zia-ur-Rehman M, Farid M, Gill RA, Ali B (2017) Role of organic and inorganic amendments in alleviating heavy metal stress in oil seed crops. Oil Seed Crops: Yield and Adaptations under Environmental Stress 12:224-235

Sallah-Ud-Din R, Farid M, Saeed R, Ali S, Rizwan M, Tauqeer HM, Bukhari SAH (2017) Citric acid enhanced the antioxidant defense system and chromium uptake by Lemna minor L. grown in hydroponics under Cr stress. Environmental Science and Pollution Research 24(21):17669-17678

11th World Congress on Water Resources and Environment (EWRA 2019)
"Managing Water Resources for a Sustainable Future", 25-29 June 2019, Madrid, Spain

Modeling surface water quality with limited data: A calibration approach applied to the Middle Tagus Basin (Spain)

A. Bolinches[1,2*], L. De Stefano[1,2], J. Paredes-Arquiola[3]
[1] Universidad Complutense de Madrid, Facultad de Ciencias Geológicas, Ciudad Universitaria, Madrid, Spain
[2] Water Observatory, Botín Foundation
[3] Research Institute of Water and Environmental Engineering, Universitat Politècnica de València, València, Spain
* e-mail: abolinch@ucm.es

Introduction

The ecological and chemical status of a river results from the combination the quality of its waters and the magnitude of the flow that circulates in its riverbed. In densely populated regions or in areas with intensive agriculture the understanding of the origin and behaviour of pollutants reaching the river is particularly important in order to improve the ecological status of surface water bodies. This requires the development of water quality models that reproduce the response of the river to different pressures starting from measurements of Waste Water Treatment Plant (WWTP) effluents and estimation of diffuse pollution from agricultural sources, and from observations of flow and concentration of pollutants in the receiving waters. Typically, observations on a regular basis (daily, weekly) of quantity and quality of pressures and receiving waters have been used to callibrate the model coefficients. However, very often the available observations are too sparse to allow such an approach. There is still limited research investigating how to calibrate the models when the available data is not dense enough to confront pressures and observations on similar dates and locations. Thus, this study aims to define how to calibrate the coefficients describing the evolution of the model with sparse observational data. This will be achieved through the exploitation of the statistical properties of the available data. A specific goal function is developed to maximize model performance.

The model is applied to Middle Tagus Basin (central Spain), which is an interesting case study for several reasons. Firstly, several surface water bodies in the area have nitrogenous and phophorous concentrations that exceed the limits set according to the European Water Framework Directive (WFD). Secondly, this area receives a large volumen of waste water from the densely polulated metropolitan area of Madrid. Thirdly, urban point pressure is combined with the diffuse pollution from agriculture, without a clear understanding of the relative contribution of each pressure on the final concentrations in the river. Last but not least, the basin is subject to a water transfer (Tagus-Segura water transfer) that detracts an average of 350 hm^3/year from the Tagus headwaters to transfer to the Mediterranean coast, further limiting the Tagus' capacity to dilute the pollution originating in the Madrid region.

Materials and methods

The study considers the main urban rivers of Madrid Region (Jarama, Henares and Manzanares) from their headwaters in the Guadarrama mountains to their outlet in Tagus and the Tagus river from its junction with the Jarama to the city of Toledo (map in Figure 1). These bodies of water support the pressure of more than 5.1 million people through the effluents of WWTPs, and the diffuse pollution of more than 250,000 ha of agricultural land. Available data includes:

- Water flow historical record (ROEA network) from the Spanish Ministry of Environment
- Physico-chemical pollutants concentration historical record (CEMAS network) and WWTP effluents quantity and quality provided by Tagus River Basin Authority
- Nitrogen surplus from agriculture as reported by Spain to the European Commission in accordance with directive 91/676/EEC requirements.

The period from 2009 to 2015 is chosen since it is the closest to the current infrastructure setup with highest density of observations. Only steady state is taken into account, and due to the low density of

observations of water quality in the river (a measurement every three months) only summer months with lower flow variability can be characterized. These months correspond to the lowest precipitations and highest agriculture detractions therefore for a near to constant pressure they represent the most critical pollution load case.

The concentration of physico-chemical pollutants (dissolved oxygen, biological oxygen demand, ammonium, nitrates and phosphates) in the surface water bodies of the area of study is simulated with a steady-state model. Simulated pollutant concentrations are allowed to evolve in the water stream following first order reactions: degradation of BOD5 and nitrification of ammonium with dissolved oxygen consumption, phosphate sedimentation, and reaeration.

Results and concluding remarks

Reaction coefficients and diffuse pollution load were calibrated with the observations of pollutant concentration in the rivers. Since there is not enough data to calculate a factor (Nash-Sutcliffe, R2 coefficient of determination) comparing observed and simulated data at equal time lapses (Santhi et al. 2001, Moriasi et al. 2007), a calibration goal function (1) was developed to compare the average values taking into account the variability of the observed data. Pollution load factors for nitrates and phosphates were calibrated using a similar approach as the quantity of diffuse pollution coming from agricultural sources is unknown.

$$\min_k \frac{[mean(obs)-sim]^2}{stdev(obs)} \quad (1)$$

Percentage Bias factor was used to measure the model performance, giving a good fit for nutrients according literuture standard values. The diagram in figure 1 shows the evolution of the ammonium along the Jarama and Tagus rivers. It can be observed that the water transfer implies an increase of an average of 50% in the concentration of ammonium in this section of the Tagus river.

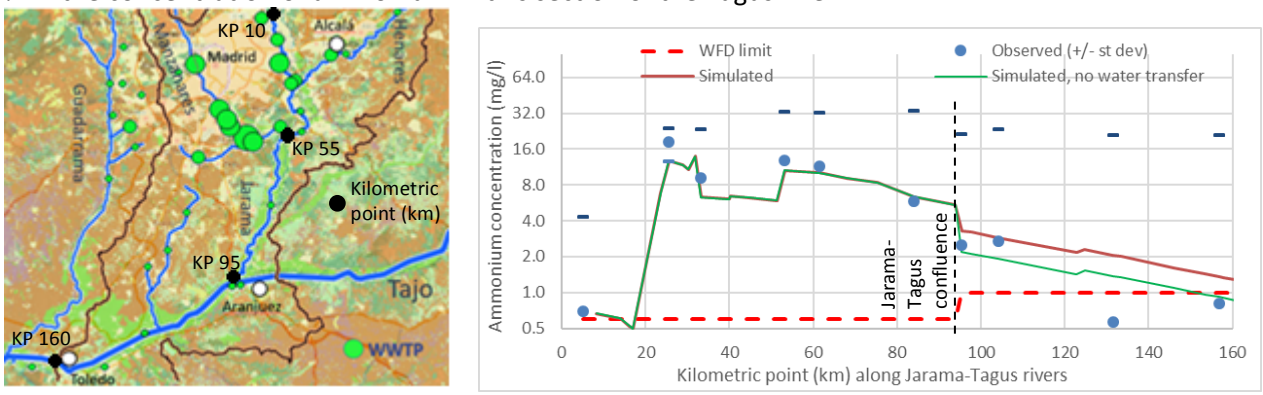

Figure 1. Area of study and evolution of ammonium.

Preliminary results show that a reduction of the water volumes transferred from the Tagus headwaters to the Mediterranean coast would have a positive impact on the river water quality – due to increased dilution capacity - but would not alone solve the existing water quality problems. High ammonium, nitrate and phosphate concentrations in the Jarama river upstream of its junction with the Tagus should be addressed to achieve the good status of the surface water bodies. The model shows that the pollution from urban WWTP (as opposed to the pollution from agricultural sources) accounts for more than 80% of the concentration observed in the river. Current research is focusing on how and how much anthropic pressures on the studied water bodies should decrease in order achieve the water quality standards required by the Water Framework Directive.

References

Moriasi DN, Arnold JG, Van Liew MW, et al. (2007) Model evaluation guidelines for systematic quantification of accuracy in watershed simulations. Trans ASABE 50:885–900. doi: 10.13031/2013.23153

Santhi C, Arnold JG, Williams JR, et al. (2001) Validation of the swat model on a large river basin with point and nonpoint sources. J Am Water Resour Assoc 37:1169–1188 https://doi.org/10.1111/j.1752-1688.2001.tb03630.x

11th World Congress on Water Resources and Environment (EWRA 2019)
"Managing Water Resources for a Sustainable Future", 25-29 June 2019, Madrid, Spain

ENFOCAR: An approach to evaluate chemical mixtures formed during water disinfection

C. Aznar-Luque, E. Pérez-Albadalejo, C. Porte, C. Postigo*
Water and Soil Quality Research Group, Department of Environmental Chemistry, Institute of Environmental Assessment and Water Research (IDAEA-CSIC), Barcelona, Spain
** e-mail: cprqam@cid.csic.es*

Introduction

Disinfection of water is one of the major triumphs in public health of the 19th century because it contributed to reducing the number of deaths due to waterborne diseases. Since its discovery, this practice has been commonly used to ensure the safety of drinking and reclaimed water. However, during the reaction of chemical disinfectants (such as chlorine) with pathogenic organisms and any organic and inorganic matter present in water, a large suite of disinfection byproducts (DBPs) is formed.

The main concerns regarding the presence of DBPs in disinfected water are related to their potential toxicity. Many of these compounds (most of them halogenated) were found to be highly genotoxic and cytotoxic to Chinese hamster ovary (CHO) mammalian cells in *vitro* assays (Richardson et al. 2007). Moreover, they have been associated with the appearance of negative effects at reproductive and developmental level, and even with a high incidence of bladder cancer in several epidemiological studies (Nieuwenhuijsen et al. 2009).

However, the DBP mixture formed during disinfection processes has not been completely characterized and the toxic effects of the mixture are also largely unknown. Thus, preventive measures call for minimizing of toxic DBPs in disinfected waters to protect public and environmental health. For this, analytical approaches that allow identifying the most toxic DBPs in disinfected water so that they can be minimized have to be developed.

ENFOCAR, a project funded by the second edition of the ComFuturo Programme (a compromise between public and private entities to foster science and future), was designed to attain this challenge. This work presents the results obtained in the first stage of the project.

Materials and methods

The approach selected to identify the most relevant compounds in the DBP mixture is based on an "effect-directed analysis" (EDA) (Burgess et al. 2013). This approach allows simplifying the mixture in different fractions. The toxicity of each fraction needs to be evaluated with an in vitro bioassay so that chemical characterization efforts can be focused in toxic fractions.

First, a representative DBP mixture extract has to be obtained from water by using a generic extraction protocol. For this, the recoveries of organic chemicals (>80) belonging to different chemical classes (i.e., pharmaceuticals, plasticizers, oestrogens, pesticides, haloacetic acids, haloacetamides, and haloacetonitriles) were evaluated after extracting fortified waters containing these compounds with different SPE generic-purpose sorbents (i.e., extraction mixture of DAX8 over XAD2 resins, ENV+, Oasis HLB, TELOS ENV; TELOS PSDV, ENVI-carb, DPA-6S) and using liquid-liquid extraction (LLE) with MTBE. Analyte recovery was evaluated by means of liquid chromatography and gas chromatography coupled to mass spectrometry.

The compatibility of the best generic extraction protocol selected with the in vitro assay was also evaluated. The in vitro assay selected was a human placental cell line (JEG-3) (Pérez-Albadalejo et al. 2017), based on previous reports regarding the potential reprotoxicity of these compounds. Since the toxicity of DBPs to this cellular model was not investigated before, the cytotoxic and oxidative stress (ROS) response of the model to various haloacetic acids was also evaluated.

The best extraction protocol was preliminary applied to the extraction of a real sample of chlorinated

reclaimed water. Characterization of DBP mixtures was done by means of LC and GC coupled to high resolution mass spectrometry.

Results and concluding remarks

The best extraction performance was observed for the Telos ENV sorbent. However, due to the different selectivity of extraction of the SPE approach as compared to the LLE approach, both approaches were used to extract the sample of reclaimed water. Extracts obtained were analysed by means of LC and GC coupled to high resolution mass spectrometry and features obtained are currently being evaluated.

Next steps will be focused on the toxicological characterization of these extracts and the fractionation of the extract by means of HPLC in order to identify the toxicity drivers. Furthermore, the toxicological response of the DBP mixture and its fractions will be compared to that obtained for the haloacetic acids tested.

Acknowledgments: C. Postigo acknowledges the financial support by Fundación General CSIC (Spanish ComFuturo Programme). This work was supported by the Government of Catalonia (Consolidated Research Groups 2017 SGR 01404- Water and Soil Quality Unit).

References

Richardson SD, Plewa MJ, Wagner ED, Schoeny R, Demarini DM (2007) Occurrence, genotoxicity, and carcinogenicity of regulated and emerging disinfection by-products in drinking water: a review and roadmap for research. Mutation Research 636:178-242

Nieuwenhuijsen MJ, Grellier J, Smith R, Iszatt N, Bennett J, Best N, Toledano M (2009) The epidemiology and possible mechanisms of disinfection by-products in drinking water. Philosophical Transactions of the Royal Society A 367:4043-4076

Burgess RM, Ho KT, Brack W, Lamoree M (2013) Effects-directed analysis (EDA) and toxicity identification evaluation (TIE): Complementary but different approaches for diagnosing causes of environmental toxicity. Environmental Toxicology and Chemistry 32:1935-1945

Pérez-Albadalejo E, Fernandes D, Lacorte S, Porte C (2017) Comparative toxicity, oxidative stress and endocrine disruption potential of plasticizers in JEG-3 human placental cells. Toxicology in vitro 38:41-48

11th World Congress on Water Resources and Environment (EWRA 2019)
"Managing Water Resources for a Sustainable Future", 25-29 June 2019, Madrid, Spain

Metal pollution in Blyde and Steelpoort rivers of the Olifants River System, South Africa

A. Addo-Bediako*, M.R. Mohosana
Department of Biodiversity, University of Limpopo, Sovenga, 0727, South Africa
** email: abe.addo-bediako@ul.ac.za*

Introduction

The Olifants River System is one of the most polluted river systems in South Africa. It has been systemically impaired following an increase in economic development and urbanisation over the years and is contaminated with metals, chemicals and organic pollutants (Addo-Bediako et al. 2014).

The Blyde and Steelpoort rivers are important tributaries of the Olifants River. The human activities in the catchments have resulted in release of pollutants into the rivers, including heavy metals. There is, therefore, increasing concern regarding the long-term impact of pollution on the rivers and the health of rural communities in the catchments, especially those still reliant on untreated water for drinking or other aquatic resources from the rivers (Oberholster et al. 2010). The study assessed heavy metal pollution in water and sediments of the two rivers, using pollution indices such as enrichment factor (EF) and geo-accumulation index (*I*geo), and to identify pollution sites. The comparative study of these two rivers is important to prioritise pollutants and sources of pollutants entering the Olifants River from their catchments, which is essential to design proper management programmes.

Materials and methods

The physico-chemical constituents of water, such as temperature, pH, dissolved oxygen, total dissolved solids (TDS), electrical conductivity and salinity were measured in the field by using a YSI equipment (Model 554 Datalogger with a 4 m multiprobe). Water and sediment samples were collected at seven sites in the Blyde River (S1, S2, S3, S4, S5, S6 and S7), and four sites in Steelpoort River (S1, S2, S3 and S4). The sample sites were selected to cover the different land use (agricultural, mining, industrial etc.) in the catchments. Water samples were collected in 100 mL acid pre-treated polyethylene bottles and stored at 4^{o}C prior to analysis. Surface sediment samples were collected at a depth of 0-10 cm using a hand trowel. The samples were placed in plastic bags and transported to the laboratory and remained frozen prior to analysis. Heavy and trace metals, metalloids were analysed at an accredited (ISO 17025) chemical laboratory (WaterLab) in Pretoria, using inductively coupled plasma-emission spectrometry (ICP-OES) for the following metals, As, Cr, Fe, Mn, Ni, Pb and Zn.

Statistical analysis was carried out using Statistica (Version 10) with a level of statistical significance set at $p < 0.05$. Analysis of variance (ANOVA) was used to investigate differences of mean pollutant concentrations among the two rivers.

Results and concluding remarks

Results of the analyses indicated differences in physicochemical variables among the different land-use categories. The pristine sites of both rivers exhibited significantly higher levels of dissolved oxygen, but lower TDS, conductivity and turbidity, as compared to the agricultural, mining and industrial sites (ANOVA: $p<0.05$). Thus, the pristine sites had relatively good water quality and impacted sites had poor water quality.

The concentrations of all the metals (Cr, Fe, Mn, Ni, Pb and Zn) were higher at Steelpoort River than Blyde River, except of As. The mean concentrations of the metals except Ni exceeded the surface water standard in both rivers. All the metals were available at high concentrations in the sediments, suggesting that sediments serve as reservoirs of metals in rivers. The metals showed significant variation between rivers ($p<0.05$), with higher values at Steelpoort River than Blyde River. There were also significant

variations among the sites, with higher values at highly polluted midstream (near mining and industries) of the Steelpoort River, while at the Blyde River, higher values were at sites close to agricultural activities.

According to the EF classifications, most of the metals showed deficiency to minimal enrichment in both rivers. However, Cr showed a moderate (>2) to a significantly high (>-5) enrichment at midstream (S3) and downstream (S4) of the Steelpoort River, while Mn shows a moderate (>2) enrichment at BS3 and BS6 of the Blyde River. These high values are strongly linked to the human activities near the sites.

The *Igeo* value of heavy metals showed that sediments have background concentration for all the metals at most of the sites in the Blyde River, while in the Steelpoort River, the metals in the sediments with the exception of As and Pb exceeded the background concentrations for most of the sites. The heavy metals in the Blyde River sediments are classified mainly as unpolluted (class = 1), considering the calculated *Igeo* values. However, sediments of the Steelpoort River are contaminated with Cr, Fe, Mn, Ni and Zn and fall in class 1 to class 4, indicating moderately polluted to heavily polluted sediments for these metals (Table 1).

The results show that the Steelpoort River is enriched with heavy metals and may serve as a source of metal pollution of the Olifants River, while the Blyde River continues to provide water of good quality to the Olifants River. We conclude that the high concentrations of certain metals in the Steelpoort River may pose health risk to the rural communities which rely on the river for drinking water and food (e.g., fish). There is, therefore, a need to implement proper management strategies to reduce pollution in Steelpoort River.

Table 1. Geo–accumulation index for heavy metal in sediments of Blyde and Steelpoort rivers

Igeo	As	Cr	Fe	Mn	Ni	Pb	Zn
BS1	-2.80	-0.88	-1.10	-1.10	-1,41	-2.90	-1.60
BS2	-3.51	-1.42	-1.31	-1.43	-2.10	-2.14	-2.10
BS3	-3.23	-2.61	-2.87	-1.60	-3.33	-2.23	-2.52
BS4	-2.69	-1.13	-0.48	-0.32	-0.96	-2.50	-1.13
BS5	-3.48	-2.23	-2.71	-2.20	-3.22	-2.67	-2.58
BS6	-2.49	-1.90	-2.52	-0.89	-2.40	-2.41	-3.20
BS7	-2.40	**0.68**	-0.15	-0.91	-0.90	-2.40	-1.10
SS1	-3.12	-1.21	**1.70**	**0.85**	-1.62	-3.23	-2.31
SS2	-0.50	**2.21**	**1.82**	**0.85**	**0.50**	-0.15	-0.20
SS3	-4.10	**3.41**	**0.96**	**0.40**	**0.26**	-3.10	**0.61**
SS4	-4.32	**1.82**	**0.55**	**0.43**	**0.85**	-3.20	**0.10**

References

Addo-Bediako A, Marr S, Jooste A, Luus-Powell WJ (2014) Are metals in the muscle tissue of Mozambique tilapia a threat to human health? A case study of two impoundments in the Olifants River, Limpopo, South Africa. Annales de Limnologie – International Journal of Limnology 50:201-210. https://doi.org/10.1051/limn/2014091

Oberholster PJ, Botha A, Chamier J, De Klerk AR (2013) Longitudinal trends in water chemistry and phytoplankton assemblage downstream of the Riverview WWTP in the upper Olifants River. Ecohydrology and Hydrobiology 13:41-51. https://doi.org/10.1016/j.ecohyd.2013.03.001

11th World Congress on Water Resources and Environment (EWRA 2019)
"Managing Water Resources for a Sustainable Future", 25-29 June 2019, Madrid, Spain

Catalytic ozonation of 4-chlorobenzoic acid and benzotriazole under a continuous flow system

G. Metaxakis[1], E. Kaprara[1*], S. Psaltou[2], A. Zouboulis[2], M. Mitrakas[1]
[1] Department of Chemical Engineering, School of Engineering, Aristotle University of Thessaloniki, Thessaloniki, Greece
[2] Department of Chemistry, School of Sciences, Aristotle University of Thessaloniki, Thessaloniki, Greece
* e-mail: kaprara@auth.gr

Introduction

The increasing worldwide consumption of chemical products has led to an increasing chemical pollution of surface and ground waters (Margot et al. 2015). Municipal wastewaters are contaminated by a wide range of chemicals, including pharmaceuticals, personal care products, steroid hormones and plasticizers, usually termed as micropollutants, due to their low concentrations (pg/L to ng/L) in aquatic ecosystems (Psaltou et al. 2018). These compounds are poorly removed by conventional treatment processes and they tend to concentrate in environmental matrices having serious effects on human health and aquatic life. Catalytic ozonation is considered to be one of the advanced oxidation processes (AOPs) commonly applied for degradation of micropollutants, that has advantages over simple ozonation as it eliminates its side effects and improves its oxidation efficiency (Psaltou et al. 2018).

In this study heterogeneous catalytic ozonation is tested in a continuous flow system for the removal of two characteristic micropollutants, 4-chlorobenzoic acid (p-CBA) and benzotriazole (BTA).

Materials and methods

Experiments of catalytic ozonation were performed in a continuous flow pilot unit (Figure 1) comprised of two columns in row, one filled with hydrophobic polyethylene terephthalate (PET) pellets, which served the dilution of ozone to water by offering adequate contact surface, and a column filled with granules of a hydrophilic Mn-feroxyhyte synthesised according to Tresintsi et al. (2014). Prior to experiments, the unit's functional variables were tested in order to optimise its operation. The initial concentrations of micro-pollutants ranged from 2 to 3 μM, pH value from 6 to 7, while at optimum conditions, the pilot unit provided a capacity of 2 mg O_3/L.

Batch mode experiments were also performed in order to quantify PET and Mn-feroxyhyte adsorption capacity for micropollutants. The initial concentration of micropollutants in these experiments was 4 μM.

Figure 1. Catalytic ozonation continuous flow pilot unit

Results and concluding remarks

Batch adsorption experiments determined an adsorption capacity of Mn-feroxyhyte around 5.5% and 7.5% for p-CBA and 2.4% and 9.8% for BTA, at pH values 6 and 7, respectively, while PET's adsorption capacity did not exceed 2%, suggesting that adsorption had an insignificant contribution in micropollutant removal.

During catalytic ozonation experiments for p-CBA removal in the continuous flow system, a contact time of 1.7, 3.85 and 7.7 minutes was achieved at water flows of 0.45, 0.20 and 0.10 L/min, respectively, in the PET column, and 2.4, 5.45 and 11 minutes, respectively, in the Mn-feroxyhyte column. Similarly, contact times for BTA removal were 3.85 and 7.7 minutes in PET column and 5.45 and 11 minutes in Mn-feroxyhyte column for water flows of 0.20 and 0.10 L/min, respectively.

Regarding the removal capacity of continuous flow system for micropollutants, experiments with p-CBA revealed a degradation rate of 71% at the PET column, while the additional treatment in the Mn-feroxyhyte column resulted in an aggregate rate of 85%. In the case of BTA, the degradation rate in continuous flow experiments reached 78% in the PET column and 90% at the completion of treatment in the Mn-feroxyhyte column.

Acknowledgments: This research has been co-financed by the European Union and Greek national funds through the Operational Program Competitiveness, Entrepreneurship and Innovation, under the call RESEARCH – CREATE – INNOVATE (project code: T1EDK-02397).

References

Margot J, Rossi L, Barry DA, Holliger C (2015) A review of the fate of micropollutants in wastewater treatment plants. WIREs Water 2:457–487

Psaltou S, Stylianou S, Mitrakas M, Zouboulis A (2018) Heterogeneous catalytic ozonation of p-chlorobenzoic acid in aqueous solution by FeMnOOH and PET. Separations 5(3):42-53

Tresintsi S, Simeonidis K, Mitrakas M (2014) Mn-feroxyhyte: The role of synthesis conditions on As(III) and As(V) removal capacity. Chemical Engineering Journal 251:192-198

11th World Congress on Water Resources and Environment (EWRA 2019)
"Managing Water Resources for a Sustainable Future", 25-29 June 2019, Madrid, Spain

Performance of different types of vegetation in wetland systems for wastewater treatment: Life-size test in La Almunia de Doña Godina

O. Ruiz*, A. Acero, B. Russo, M. Lapuente, A. Jimenez
Grupo de Ingeniería Hidráulica y Ambiental (GIHA), Escuela Politécnica de La Almunia (EUPLA), Universidad de Zaragoza, Spain
** e-mail: oruiz@unizar.es*

Introduction

In 2018, the wastewater treated in Aragón was around 89%, and the other 11% included a great part of the Aragon' villages. Almost 1,400 villages out of a total of 1,505 villages in Aragon have less than 1,000 inhabitants representing only 14% of the population. The construction of a conventional treatment system is economically unfeasible for them and they have to look for a better solution. Our project arises in this framework, a life-size test to help the regional wastewater authorities in the selection of the best solution for small villages for a low-cost treatment plant based on wetlands.

To carry out this project, a wetland pilot treatment plant has been built, in real scale, in the WWTP of La Almunia de Doña Godina (Zaragoza) for 50 inhabitants. The test treatment plant is designed for the minimal maintenance and management necessities and with a minimal investment in infrastructure. The operation of the pilot plant shows the relationships of the pollutants for an effective treatment, the bulrush optimal answer in the first line of the ponds and the minimum infrastructure requirements for a good performance.

Materials and methods

Two wetlands have been built in the available space in the WWTP of La Almunia; one was a horizontal subsurface flow wetland and the other a free-surface flow wetland. La Almunia is a village in the Jalón river basin in the province of Zaragoza (Spain). From the climate point of view, the area is characterized by a continental Mediterranean climate, with scarce rainfall occurring in spring and autumn.

The WWTP of La Almunia consists of primary treatment, for removal of coarse objects, grit and fats, active sludge biological treatment and two secondary clarifiers. The wetlands gather the raw water after the grit removal in order to avoid creating another point of waste generation. The water is pumped to a pit divider where the two treatment lines begin. In the divider pit, a weir guaranties that the same flow feeds each line.

The two lines are divided into three independent ponds in series, one following the other, where the water arrives consecutively. A set of chambers and pipes allows the order in which the water enters the lines to be varied, allowing pond 1 to be the first, second or third in the order in which the water is treated, so that the performance of the plant in each situation can be tested.

The configuration of the line 1 is: Treatment by floating macrophytes; Plants: Cattail, Reed, Bur reed (Ty*pha Latifolia, Phragmites, Sparganium*); Flotation system: Burlap mantle, Burlap sacks, Polystyrene (various types). The configuration of the line 2 is: Treatment by horizontal subsurface flow constructed wetlands; Plants: Cattail, Reed, Rush (*Typha Latifolia, Phragmites, Scirpus Lacustre*)

Both lines have three ponds of trapezoidal section of 10.50 m long, 2.30 m wide and 0.60 m deep with 0.20 m of freeboard. After the ponds, the treated water comes back to the main treatment plant avoiding insufficiently treated water discharges. The water quality in the inlet and the outlet is analysed every day for BOD_5, SS, N and P, and the condition of the plants and the pumping pit is also checked.

The floating macrophyte uses solar energy through the photosynthesis of macrophyte plants. These plants are naturally floating and form a carpet of roots and rhizomes that occupy the volume of the canal, forcing the water to circulate through the roots. These roots contain microorganisms that degrade organic matter and eliminate phosphorus and nitrogen (de Miguel Beascoechea et al. 2000). The subsurface flow wetlands include a gravel bed that supports the root structure of the emergent vegetation. The flow

crosses the gravel bed (Ministerio de Medio Ambiente y Medio Rural y Marino 2010).

The system built for this study of the different types of wetlands allows us to analyse with a real flow and a real pollutant load, the following aspects:

- Comparision between floating macrophytes and horizontal subsurface flow constructed wetlands
- Performance of diverse types of macrophytes
- Performance of the vegetation with different amount of pollutant loads
- Performance of the vegetation with different support systems
- Study of flotation elements
- Minimum infrastructure requirements

Results and concluding remarks

During these first months of research we have been able to reach some initial findings about the operation of the unconventional treatment systems used in this project:

- The grid removal is not enough as primary treatment before de ponds, the sludge received created problems in the first pond of the lines. A simple primary clarifier was designed and installed before the divider pit solving the sludge problems that required the emptying and cleaning of two ponds.
- Regarding the vegetation, the cattail (*Typha Latifolia*) has offered very good results in both systems. The reed (*Phragmites*) has turned out to be more sensitive to low temperatures, but with the elevated temperatures it began to grow and already covers a floating wetland. The rush (*Scirpus Lacustre*), after a replanting in summer, have not been the appropriate plant and have been replaced by cattail. Bur reed (*Sparganium*) has a satisfactory performance in flotation although the possibility of changing its flotation system to one with larger holes that improve its growth is being studied.
- About the performance of the vegetation respect the polluting load, the cattail is the plant that better supports the incoming of high loads in the wetland.
- The flotation elements designed for wetland 2 had sunk. We replaced them by polystyrene plates but less dense than the installed in wetland 3. The new type of plates has more holes and larger ones, in them, and the vegetation has grown better. Therefore, it is studied to implement this system also for the bur reed in wetland 3. In addition, low density polystyrene presses the plant less.
- As for the optimal flotation system for each vegetation, the reed and bur reed grow well in the polystyrene plates, but this system does not work with the cattail. The cattail supported by polystyrene plates would end up overturning. These overturns are minimized in the 15 cm thick low-density polystyrene.

Acknowledgments: This project is carried out because of the interest in the use of soft and sustainable treatment techniques of the Instituto Aragonés del Agua (Aragonese Water Institute). The IAA finances the project, operation and maintenance for two years, renewable.

References

Aina M, Kpondjo N, Adounkpe J, Chougourou D, Mpudachirou M (2012) Study of the Purification Efficiencies of three Floating Macrophytes in Wastewater Treatment. International Research Journal of Environment Sciences 1(3):37-43

Brix H (1994) The Role of Wetlands for the Control of Pollution in Rural Areas. Design and Use of Constructed Wetlands. Curso CI HEAM-IAWQ. Zaragoza

Crites R, Middlebrooks E, Reed S (2006) Natural Wastewater Treatment Systems. CRC Press, Taylor & Francis Group

de Miguel Beascoechea E, de Miguel Muñoz J, Curt Fernández de la Mora MD (2000) Manual de fitodepuración. Filtros de macrofitas en flotación. J. Fernández Gonzalez (ed.), Madrid

Ministerio de Medio Ambiente y Medio Rural y Marino (2010) Manual para la implantación de sistemas de depuración en pequeñas poblaciones. Ministerio de Medio Ambiente y Medio Rural y Marino

Sipaúba-Tavares,LH, de Souza Braga FM (2008) Constructed wetland in wastewater treatment. Universidad Estadual de Maringá

Soler C, Crespi R, Soler E, Pugliese M (2018) Evaluación de humedales artificiales de flujo libre superficial con macrófitas acuáticas flotantes. Ingeniería del Agua

III. Hydrological Processes

11th World Congress on Water Resources and Environment (EWRA 2019)
"Managing Water Resources for a Sustainable Future", 25-29 June 2019, Madrid, Spain

Hydraulic conductivity spatiotemporal variability in watersheds

K.X. Soulis*, P. Londra, G. Metaxas, G. Kargas
Department of Natural Resources Manag. and Agricultural Eng., Agricultural University of Athens, Greece
** e-mail: soco@aua.gr*

Introduction

Saturated hydraulic conductivity (*Ks*) is a key parameter in hydrology, though its variability in space and time is far from being completely understood up to now (Rienzner and Gandolfi 2014). *Ks* varies extensively across spatial and temporal scales due to heterogeneities in soil, vegetation, and cover characteristics. The spatial variability of *Ks* is a function of both the method and the scale of measurement (Kargas et al. 2017). Accordingly, field estimated values of *Ks* are fully representative only of the point and the time at which the measurement is taken (Rienzner and Gandolfi 2014). Furthermore, relationships between *Ks* and other soil characteristics are not strong enough to provide sufficiently accurate predictions of its value (Chirico et al. 2007). The fact that soil properties vary on a scale of a few meters, complicates hydrological processes modeling in larger areas such as watersheds (Dingman 2002). Thus, the small-scale values that it is possible to measure and the effective values required in models are actually different quantities (Beven 2012).

Apart of the heterogeneities related to soil and cover properties, disturbances such as wildfires, floods etc. that are also part of natural ecosystems dynamics may influence *Ks* spatial and temporal variability (Zimmermann and Elsenbeer 2008; Kargas et al. 2016; Soulis 2018). Human induced changes may play a significant role in altering hydrologic response in natural watersheds as well (Soulis et al. 2015). Forest fires cause widespread and abrupt changes that may have a marked effect on hydrological response. The impacts of forest fires on the hydrological cycle can be direct, due to the destruction of the vegetation cover, as well as indirect by altering the hydraulic properties of the soil (Soulis et al. 2012; Zhou et al. 2015).

In order to investigate the spatial and temporal variability of *Ks* at multiple scales in natural watersheds, six measurement campaigns covering a 14 years period were performed in a small-scale experimental watershed in Greece. The watershed was also affected by a major forest fire that provided the additional opportunity to investigate as well the effect of major disturbances in spatial and temporal variability of *Ks*.

Materials and methods

The study was performed in the Lykorrema stream small scale experimental watershed (7.84km^2), which is located in the east side of Penteli Mountain, Attica, Greece. The experimental watershed is characterized by sharp relief and its climate is Mediterranean semi-arid with precipitations mostly occurring in the autumn–spring period. The average annual precipitation for the study period (2005-2018) was 670 mm and the average annual temperature 16.3 ^{o}C. Geologically, the watershed is dominated by schists and a small part is covered by marbles. As regards to soils, it is mainly covered by coarse soils (Sandy Loam and Sandy Clay Loam). The land cover consists of a mixed vegetation cover, including young pine trees, bushes, pasture, and a few scattered tufts of old trees. A more detailed description is provided by Soulis (2018). During the last 40 years, the study area has experienced three major fires in 1982, 1995, and 2009.

Spatiotemporal variability of *Ks* was investigated at multiple scales based on six measurement campaigns covering a 14 years period (2005-2018). The first campaign was carried out at the summer of 2005, 10 years after the last major forest fire event. In this campaign both undisturbed and disturbed samples from the surface soil layer were collected in 24 positions (three samples for each position) in the watershed, while field infiltration measurements with a double ring infiltrometer were also made in three positions. The coordinates of each sampling position were registered with a GPS. For each sample, *Ks* was measured with a constant-head permeameter and saturation water content, bulk density, and soil texture were also determined. The second campaign was carried out soon before the forest fire of August 2009 at two characteristic positions, while the third and the fourth campaigns were carried out at the same two

positions soon after the forest fire (just after the fire, and after the first autumn rainfalls). The last two campaigns were carried out at the end of summer 2017 and at the end of the winter 2018, at three characteristic locations (two positions were the same for all the campaigns). At the last two campaigns sampling was made at three spatial scales (three samples in a 1 m^2 small plot, three small plots in a 250 m^2 large plot, and three large plots in the entire watershed).

The obtained results were statistically analysed in various ways in order to identify the spatial and temporal variability of *Ks* and its relation with soil texture and other parameters.

Results and concluding remarks

According to the results of the 1st campaign, *Ks* in the watershed ranged between 254 cm/h and 5 cm/h (most values were between 11 and 40 cm/h). The average value was 33 cm/h, the median 25 cm/h, and the standard deviation (STD) 47 cm/h. The above results highlight the huge spatial variability of *Ks* in such a small watershed. It is also interesting that the variation of *Ks* does not seem to be correlated with soil texture and stoniness, which were more uniform (e.g. STD for sand percentage was only 5.3%). This is in agreement with Chirico et al. (2007).

Interestingly the *Ks* values measured just after the forest fire (3rd campaign) were close to the *Ks* values measured soon before the fire (2rd campaign) and within the range of *Ks* values of the 1st campaign (the *Ks* values at the two sampling sites were 9 cm/h and 15 cm/h, while STD is 4 cm/h and 9 cm/h respectively). In contrast, the *Ks* values measured after the first autumn rainfalls (4rd campaign) were significantly lower (*Ks* ≈ 3.5 cm/h and 2.5 cm/h; STD ≈ 3.7 cm/h and 0.7 cm/h, respectively). This observation is in accordance with the rainfall-runoff data recorded before and after the fire (Soulis et al. 2012; Soulis 2008).

The results of the 5th and 6th campaigns indicated that there aren't any obvious differences between summer and winter and that 8 years after the fire *Ks* values were more similar to the 1st campaign. Furthermore, it is interesting that the STD values obtained for the three examined scales were similar, indicating a similar spatial variability across scales. Specifically, in the 5th campaign *Ks* ranged between 288 cm/h and 5 cm/h, the average value was 69 cm/h, the median 29 cm/h, and the STD 85 cm/h. The corresponding values for the 6th campaign were 236, 5, 54, 28, 63 cm/h. The STD values obtained for the three scales were 53, 59, and 75 cm/h for the small plot, the large plot, and the watershed scales.

References

Beven K (2012) Rainfall-Runoff Modelling: The Primer, Second Edition. John Wiley & Sons Ltd, doi: 10.1002/9781119951001

Chirico GB, Medina H, Romano N (2007) Uncertainty in predicting soil hydraulicproperties at the hillslope scale with indirect methods. Journal of Hydrology 334:405-422

Dingman SL (2002) Physical Hydrology Second Edition, Prentice-Hall Inc., p 409

Kargas G, Kerkides P, Sotirakoglou K, Poulovassilis A (2016) Temporal variability ofsurface soil hydraulic properties under various tillage systems. Soil and Tillage Research 158:22-31

Kargas G, Londra P, Agapitou E, Sotirakoglou K (2017) Spatial and temporal variability of saturated hydraulic conductivity of upper soil layer. 10th Congress of the Hellenic Society of Agricultural Engineers, Athens

Rienzner M, Gandolfi C (2014). Investigation of spatial and temporal variability of saturated soil hydraulic conductivity at the field-scale. Soil and Tillage Research 135:28-40. doi:10.1016/j.still.2013.08.012

Soulis KX Valiantzas JD (2012) SCS-CN parameter determination using rainfall-runoff data in heterogeneous watersheds-the two-CN system approach. Hydrology and Earth System Sciences 16:1001-1015. doi:10.5194/hess-16-1001-2012

Soulis KX (2018) Estimation of SCS Curve Number variation following forest fires. Hydrological Sciences Journal 63(9): 1332-1346. doi: 10.1080/02626667.2018.1501482.

Soulis KX, Dercas N, Papadaki CH (2015) Effects of forest roads on the hydrological response of a small-scale mountain watershed in Greece. Hydrological Processes, doi: 10.1002/hyp.10301

Soulis KX, Dercas N, Valiantzas JD (2012) Wildfires impact on hydrological response – the case of Lykorrema experimental watershed. Global NEST Journal 14(3):303-310

Zhou Y, Zhang Y, Vaze J, Lane P, Xu S (2015) Impact of bushfire and climate variability on streamflow from forested catchments in southeast Australia. Hydrological Sciences Journal 60(7–8):1340–1360. doi: 10.1080/ 02626667.2014.961923

Zimmermann B, Elsenbeer H (2008) Spatial and temporal variability of soil saturated hydraulic conductivity in gradients of disturbance. Journal of Hydrology 361(1-2):78-95. doi:10.1016/j.jhydrol.2008.07.027

11th World Congress on Water Resources and Environment (EWRA 2019)
"Managing Water Resources for a Sustainable Future", 25-29 June 2019, Madrid, Spain

Rainfall-runoff modelling with application of wavelet neural networks in arid and semi-arid regions. Case study: GharehAghaj basin, Southern Iran

Z. Zarezadeh, M. Rahnemaei*
Department of Water Resources Engineering, Islamic Azad University, Shiraz, Iran
** e-mail: mehrdad_rah@yahoo.com*

Introduction

Iran, with an annual average of 220 mm/year of precipitation, is among the world's driest countries. Rainfall-runoff modelling plays an important role in water resource management. The Wavelet Analysis (WA) will have shown their reliability in various water-related studies, especially for modelling. Important studies in this field have been presented by Maheswaran and Khosa (2012), Wang and Ding (2003), Kuo et al. (2007) and Jamali A (2016). The goal is to establish a correlation between the rainfall-runoff time series with development of WNN.

Materials and methods

It is assumed that the watershed area, like a black box, transforms rainfall into runoff. On two selected hydrometric stations in Fars Province, Iran (Aliabad-e-Khafr and Kavar-Band-Bahman, with 32 years recorded rainfall and runoff) data, statistical evaluation and control were performed (normality, homogeneity and randomness tests) by SPSS software. All data were converted into intervals 1 and 0. The rainfall signal is presented with a mother wavelet so in WNN decompositions of "HAR" and "SYM 3" were performed with degradation rates of 1 and 2. Three layers of the neurons were selected (two hidden layers and one output layer). After modelling, the root mean square errors (RMSE) were calculated. Also, the linear correlation coefficient of the computational vs. observational data (R^2) was tested. Calibration and verification operations were followed. All calculations were performed using the Neural Network-code and coding toolkit in the 2016 MATLAB software. 25% and 75% of the data were used for training (calibration) and verification, respectively. Figure 1 shows the calibration graphs.

Results and concluding remarks

For rainfall-runoff modeling at the Aliabad-e- Khafr , the $RMSE_v$ and $RMSE_c$ (v for verification and c for calibration) in wavelet Neural Network methods are given in Table 1. The highest R^2 and lowest RMSE shows the least error. The same modeling was also performed for the data of the Band-e-Bahman-e-Kavar. Again, R^2 and RMSE (Table 2) show the optimal performance of the WNN. Due to the errors in the modeling of the computational and observational data were well adapted. Totally, the model performed satisfactorily in this dry region as with an area in the north of the Fars Province with a 3 fold depth of annual precipitation. Because of the laws in the way of writing, we have to choose the best simulation results using wavelet got 4 modes and side tables, chart, we have the best mode to suit the lowest $RMSE_V$.

Table 1. Results of rainfall-runoff modelling using wave guide-neural network at Ali abad-e-khafr station

Wavelet function	Degree of decomposition	ANN structure	First layer hidden layer transfer function	Second layer hidden layer transfer function	R^2_c	$RMSE_c$	R^2_v	$RMSE_v$
SYM3	2	20-17	Logarithmic	Tangent	0.8436	0.0536	0.7949	0.0400

Table 2. Results of rainfall-runoff modeling using waveguide-neural network at Kavar-Band-Bahman Station

Wavelet function	Degree of decomposition	ANN structure	First layer hidden layer transfer function	Second layer hidden layer transfer function	R^2_c	$RMSE_c$	R^2_v	$RMSE_v$
Haar	2	17-20	Logarithmic	Tangent	0.7341	0.0701	0.6987	0.0298

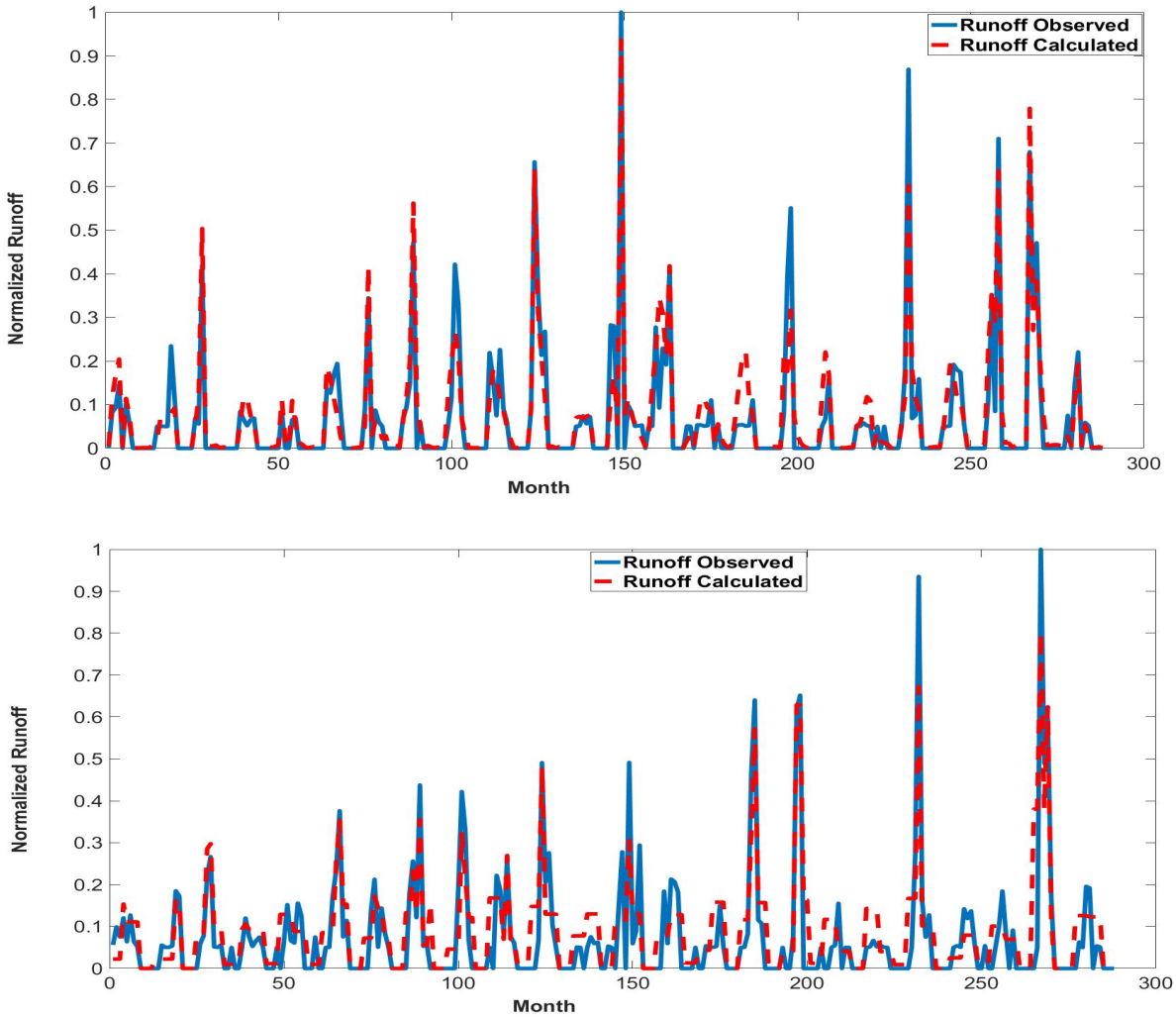

Figure 1.The observed vs. estimated runoff by calibration using the wavelet-neural network (the Haar wavelet) with the degree of decomposition 2 (above: Kavar-Band-Bahman station, below: Aliabad Khafr station)

References

Jamali A (2016) Rainfall-Runoff Modeling with Neural Network-Wavelet combined Model in Droudzan Basin .Islamic Azad University. Water Resources Dept.

Kuo J-T, Hsieh M-H, Lung W-S, She N (2007) Using artificial neural network for reservoir eutrophication prediction Ecological Modelling 200(1):171-177

Maheswaran R, Khosa R (2012) Comparative study of different wavelets for hydrologic forecasting. Computers and Geosciences 46:284-295. https://doi.org/10.1016/j.cageo.2011.12.015

Wang W, Ding S (2003) Wavelet network model and its application to the prediction of hydrology. Nature and Science 1:67-71. doi: 10.1139/S03-071

11th World Congress on Water Resources and Environment (EWRA 2019)
"Managing Water Resources for a Sustainable Future", 25-29 June 2019, Madrid, Spain

Prediction of suspended sediment yield in the Saf Saf catchment, northeast of Algeria

K. Khanchoul*, Z.A. Boukhrissa
Department of Geology, Soils and Sustainable Development Laboratory, Badji Mokhtar University-Annaba, Algeria
** e-mail: kamel.khanchoul@univ-annaba.dz*

Introduction

The scarcity or discontinuity on sediment transport measurements reduces knowledge about soil loss and its impact on human life. In some cases, such in the northeast of Algeria, several researchers have found difficulties to apply the most suitable methods to estimate sediment yield (Achite and Ouillon 2016; Khanchoul and Jansson 2008; Megnounif et al. 2013). Evaluating sediment yield in Algeria is often difficult due to the inexistent or low accuracy of suspended sediment concentrations.

The present work represents an assessment of suspended sediment yield in the Saf Saf catchment over 39 years (from 1976 to 2014). Long-term annual suspended sediment loads are estimated using non-linear power model, developed on mean discharge class technique as sediment rating curves.

Materials and methods

The Saf Saf catchment is located on the ridge of the Tell mountains and has an area of 322 km^2 at the gauging station of Khemakhem. The Saf Saf catchment has 63% of its area covered by weathered or un-consolidated geologic formations that generate very erodible soils viz. marly limestone of Senonian, gypseous-sandy clay and clayey conglomerate of continental Miocene age and the lower Numidian clay. The basin has 66% of its area cultivated with wheat and barley. Forest and shrubs cover 30% of the Saf Saf catchment. Based on recorded daily rainfall of the 39-year period, the study catchment can be characterized by irregular annual precipitation, with a mean annual rainfall of 617 mm and a mean annual temperature of 22°C.

Hydrological data have been monitored routinely for years by the National Agency of Hydraulic Resources. The Khemakhem hydrometric dataset includes records of daily water discharge (Q) and suspended sediment concentration (C). Suspended sediment concentration samples were transported in one-litre plastic bottles for laboratory analysis. The sediment concentration of each sample was calculated by filtration method, evaporating the sample, and then weighing the remaining sediment. On the other hand, water samples were taken for measurement of suspended sediment concentration several times a year, which make more than 3000 hourly data sets in 39-year period (1976-2014).

In the absence of sufficient suspended sediment concentration (SSC) measurements, Sediment rating curves method has been used to predict suspended sediment concentrations for subsequent flux calculations, and determining long-term suspended sediment loads (Khanchoul et al. 2012). The most commonly used sediment rating curve was a power function as:

$$C = aQb \quad (1)$$

where *a* and *b* are regression coefficients.

The used regression analysis has provided a fairly low coefficient of correlation (r = 0.50). The developed regression on all separate measurements have strongly underestimated the true sediment load. Due to this underestimation of sediment load, a further interesting prediction about the suspended sediment transport could be extracted from the water discharge class method. Optimization of rating curve method was validated by comparing the predicted against observed values on scatter plots. We might use a non parametric correction for the transformation bias. To test the validation of the sediment rating curve technique, an error of estimation of observed and predicted values was computed for different predictions on validation datasets.

Results and concluded remarks

The use of the discharge class method to develop sediment rating curves has provided good results, as the sum of the daily suspended sediment discharges with measured concentration values were close to the sum of those calculated with concentrations predicted with sediment rating curve technique. The best-fit power function line through the data has given a high coefficient of correlation (r = 0.93) and the suspended sediment estimates at the high water discharges were accurately represented because the vast majority of the sediment was transported during these very high discharge events.

The error in the sum of loads by using the relationship between daily suspended sediment concentration and water discharge compared with the sum of loads from 850 datasets with measurements, has demonstrated that sediment loads calculated by using a single rating curve have underestimated the load by only 10.71% after correction for bias.

Based on the sediment rating curve, the calculated mean annual specific suspended sediment yield in the Saf Saf basin during the period 1976-2014 was equal to 477 T km^{-2} $year^{-1}$, which corresponds to an annual sediment load of $6x10^6$ tonnes. Suspended sediment loads for the period prior to 1998 has given a mean annual sediment yield of 826 T km^{-2} $year^{-1}$, indicating that sediment production and transport were considerably higher and which was generated from more surface runoff (Q > 6 m^3/s) and intensive soil erosion. The four years 1984, 1985, 1993 and 1995, with the highest annual loads in Saf Saf River, yielded 66% of the total suspended sediment load of the 39 year period.

In spite of the fairly low runoff compared to other basins of the northeastern part, the annual average suspended sediment concentrations of flood events are consistently high in the study basin. In fact, other physical conditions than runoff might play a major role in such a high erosion. One cause certainly was the greater general steepness of the topography. Another reason for the high erosion in the basin was the high percentage of cultivated land. Moreover, the cultivated land in the Saf Saf basin was to a great extent found on slopes >23%, with clayey loamy regosols, which were easily eroded. Landslides, bank and gully erosion were frequent. The monthly suspended sediment load values during the study period were higher in the winter season, with a contribution of 78%.

As a conclusion, pasture and open shrubland in the Saf Saf catchment are still suffering from overgrazing. The steep slopes in the basin and the high drainage density mean were the reasons for a high delivery of the eroded material to the streams, and the high gradient of the stream channels means a high delivery of the sediment within the drainage net down to the measuring station.

This work has helped to highlight the contribution of the geomorphic conditions to explain the erosion in the catchment by building a regression model offered by some suspended sediment-water discharge measurements. Nevertheless, more sediment samplings must be conducted in the future to provide better sediment load predictions.

References

Achite M, Ouillon S (2016) Recent changes in climate, hydrology and sediment load in the Wadi Abd, Algeria (1970–2010). Hydrology and Earth System Sciences 20(4):1355-1372. https://doi.org/10.5194/hess-20-1355-2016

Khanchoul K, Jansson MB (2008) Sediment rating curves developed on stage and seasonal means in discharge classes for the Mellah wadi, Algeria. Geografiska Annaler: Series A, Physical Geography 90(3):227-236. https://doi.org/10.1111/j.1468-0459.2008.341.x

Khanchoul K, Boukhrissa ZA, Acidi A, Altschul R (2012) Estimation of suspended sediment transport in the Kebir drainage basin, Algeria. Quaternary International 262:25-31. https://doi.org/10.1016/j.quaint.2010.08.016

Megnounif A, Terfous A, Ouillon S (2013) A graphical method to study suspended sediment dynamics during flood events in the Wadi Sebdou, NW Algeria (1973–2004). Journal of Hydrology 497:24-36. https://doi:10.1016/j.jhydrol.2013.05.029

11th World Congress on Water Resources and Environment (EWRA 2019)
"Managing Water Resources for a Sustainable Future", 25-29 June 2019, Madrid, Spain

Physics based distributed integrated hydrological model for Yerli sub-catchment, Maharashtra, India

V.D. Loliyana[1*], P.L. Patel[2]
[1] Department of Civil and Construction Engineering, Rustomjee Academy for Global Careers, Partner University - University of Wolverhampton (UK), Dahanu, Maharashtra, India
[2] Department of Civil Engineering, SVNIT Surat, Gujarat, India
* e-mail: viraj.nishi@gmail.com

Introduction

In India, irrigation accounts for nearly 80% of water demand followed by the demands from drinking, industry, and energy sectors. The depleting water resources, under changing climatic conditions and increasing population across the globe, is a major challenge for meeting the demands of domestic, agricultural and industrial sectors. Prediction of water availability in space and time is prerequisite for irrigation planning, rain water harvesting and conservation measures, particularly in arid and semi-arid regions. The Yerli sub-catchment (area of 15881 km^2) of Purna river catchment in upper Tapi river basin, Maharashtra, India has been selected as study region for present research investigation. The average annual rainfall and potential evapotranspiration (PET) of Purna river catchment are 785 mm and 1715 mm respectively. Thus, climate in the catchment is classified as 'Semi-arid' region as its aridity index (ratio of average annual rainfall to PET) is ≈ 0.46. The requirement of an extensive physics-based distributed hydrological model is essentially needed for prediction of stream flows, groundwater levels and water balance in the catchment for better management of water resources. While going through literature, it is revealed that integrated physics based distributed hydrological model were applied in the past only for experimental or smaller catchments area (<5000 km^2), without considering the fully distributed hydrological parameters or multiple geological layers. Further, the research studies reported, so far, are in scarce which could consider the calibration of distributed MIKE SHE model under multi-objective framework, comprehensive validation of model using observed stream flows, groundwater levels and water balance for relatively larger catchments with distributed Manning's roughness coefficient for overland flow. The investigation presented here has been planned to showcase the development of a fully distributed physics based model for a water scarce region while simulating stream flows, groundwater levels and water balance in the catchment.

Materials and methods

The MIKE SHE/MIKE 11 (DHI 2017), a distributed physics based coupled integrated hydrological model (grid size 500 m × 500 m) has been calibrated using continuous stream flow of eight years (1991-1998) and by incorporating distributed vegetation, soil and geologic parameters within the study region. The remaining six years (1999-2004) data has been used for validation of the calibrated model. The calibrated and validated model for Yerli catchment is further used for assessing the performance of model in prediction of stream flows at Gopalkheda and Lakhpuri stream gauging stations within the catchment. The simulated groundwater well heads are also compared with observed heads at different locations (hilly as well as plain areas) in the catchment. Lastly, total water balance of the catchment is estimated for period of 1991-2004 (Loliyana 2018). Table 1 depicts the nature of data used for present investigation.

Results and concluding remarks

The simulated runoff and groundwater levels have been found to highly sensitive with respect to saturated hydraulic conductivity of unsaturated zone, horizontal and vertical hydraulic conductivity of saturated porous media. The simulated groundwater well levels from the distributed model are also compared with observed water levels at different locations (hilly, transition and plain areas) within the

catchment. At the end, total water balance of the sub-catchment is estimated for period 1991-2004 from simulated hydrological parameters using aforesaid fully distributed hydrological model. The performance of calibrated model has been found satisfactorily in prediction of stream flows at catchment outlet (RMSE = 100.98 m^3/s, r = 0.81, NSE = 0.68 and EI = 0.99) and groundwater levels (RMSE = 8.97 m to 9.08 m) within the catchment. The analyses of water balance revealed that fully distributed coupled MIKE SHE/MIKE 11 model could simulate better dynamics of water balance components (water balance errors 0.86% and 1.09% for 1991-1998 and 1999-2008 periods) during calibration and validation periods. The application of MIKE SHE in carrying out detailed hydrological water balance study, plays an important role in evaluating the irrigation demands, and deciding the magnitude of water that can be stored for irrigation/ domestic/ industrial uses in sub-sequent dry season. This would consequently facilitate the irrigation management and encourage the farmers to adopt suitable cropping pattern within the agriculture fields.

Table 1. Required data, its source and data type for modelling

Input Data	Data Source	Data Type For Modelling
Topography	SRTM DEM 30 m data	Distributed map
Precipitation	IMD station data	Semi Distributed map (Station Based)
Potential ET	IMD station data	Time series (Station Based)
Vegetation	Derived from land use classification	Distributed map
Leaf Area Index (LAI)	From literature	Constant
Root Depth (RD)	From literature	Constant
River Network	SoI Toposheets	Digitized GIS shape files
Cross section	CWC gauging cross-section data	Chainage – Elevation series
Soil Types	NBSSLUP, Nagpur	Distributed map
Geology Map	GSI, Nagpur	Distributed map
Discharge and water level	CWC gauging stations	Time series
Exploratory and observation wells	CGWB, Nagpur	Distributed map Time series

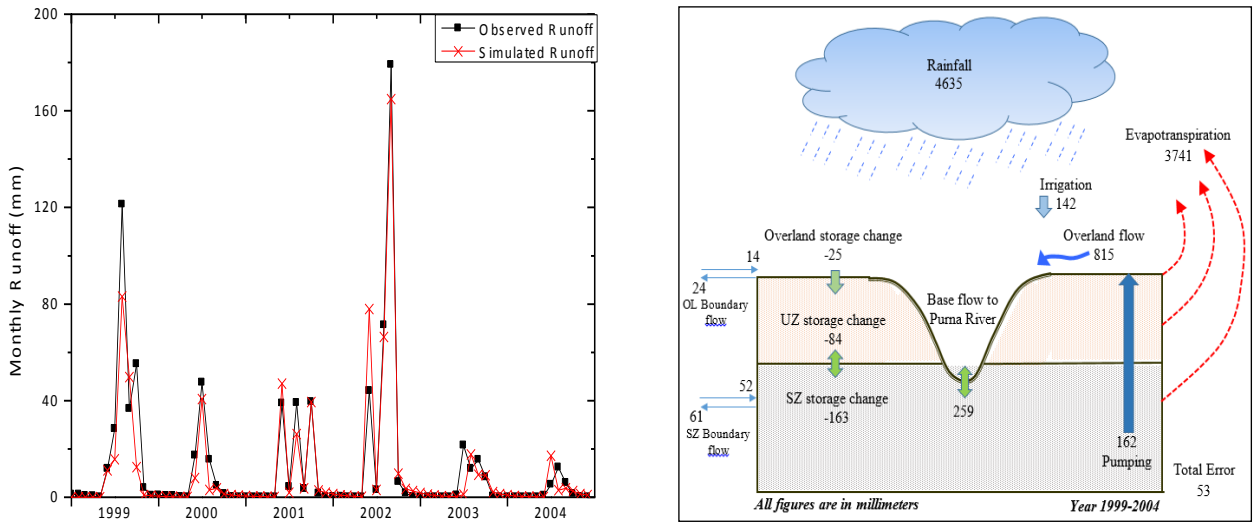

Figure 1. Comparison of observed and simulated monthly runoff and simulated total water balance within the study area for validation period 1999-2004

Acknowledgments: Authors are thankful to World Bank assisted CoE, TEQIP-II, MHRD-India for providing the funding to this research. Also, special thanks to IMD, CWC, CGWB, SOI, GSI and NBSSLUP for providing data for present investigation.

References

DHI (Danish Hydraulic Institute) (2017) MIKE-SHE User (Volume-I) and Reference Manual (Volume-II)

Loliyana VD (2018) Development of a physics based distributed integrated hydrological model for prediction of water availability in a semi-arid region in India. PhD Thesis, SVNIT Surat, Gujarat, India

11th World Congress on Water Resources and Environment (EWRA 2019)
"Managing Water Resources for a Sustainable Future", 25-29 June 2019, Madrid, Spain

Pan evaporation modelling in Central India using soft computing techniques

H. Sanikhani[1*], R. Mirabbasi[2], O. Kisi[3]
[1] Department of Water Engineering, Faculty of Agriculture, University of Kurdistan, Sanandaj, Iran
[2] Department of Water Engineering, Faculty of Agriculture, Shahrekord University, Shahrekord, Iran
[3] Faculty of Natural Sciences and Engineering, Ilia State University, Tbilisi, Georgia
* e-mail: h.sanikhani@uok.ac.ir

Introduction

Pan evaporation (Epan) is an important parameter in water budget estimations and in modeling crop water response in different weather conditions. It has been widely used as an index of evapotranspiration, lake and reservoir evaporation, potential or reference crop evapotranspiration and irrigation scheduling. Because evaporation is a nonlinear, stochastic and complex process, it is difficult to derive an accurate formula to represent all the physical processes involved (Moghadamnia et al. 2009). In recent years, application of artificial intelligence (AI) techniques, such as multivariate adaptive regression splines (MARS), least square support vector regression (LSSVR) and M5 tree model in estimation of hydrological parameters have been widely considered by the most of researchers.

The main objective of the present study is to evaluate the performance of M5 tree, LSSVR and MARS methods in estimating long-term monthly Epan in central India (i.e. Madhya Pradesh state).

Materials and methods

Study area: The study area is Madhya Pradesh (MP) state located in central India between latitude 21.2° - 26.87°N and longitude 74.03° - 82.816° E and covers a total area of 308,252 km^2. In this study, the long-term monthly mean Epan data and their geographic characteristics for a total of 45 stations distributed uniformly across the study area in MP state for a period of 110-year (1901- 2010) were applied to develop and evaluate the data-intelligent models. Epan values were calculated by taking the average of 110 years data. Each station has 12 Epan values corresponding to 12 months.

Multivariate Adaptive Regression Splines (MARS): Multivariate adaptive regression splines (MARS) was introduced by Friedman (1991) as a new method for nonlinear regression modeling of high dimensional data. So, diverse issues and information can be dealt with MARS. Piecewise basis functions are used to define relationships between predictors and a response variable.

Least Square Support Vector Regression (LSSVR): Vapnik (1995) introduced the support vector regression (SVR) based on the statistical learning theory that follow minimization of structural risk. Then, Suykens et al. (2002) proposed the LSSVR. The LSSVR unlike SVRs uses linear equations instead of quadratic equations and therefore has higher computational accuracy compared to classic SVR.

For a given dataset including $\{x_i, y_i\}_{i=1}^{N}$ where $x_{i\in R^p}$ as input vectors and $y_i \in R$ as output vector, the nonlinear regression function can be written as follow for solving the problems:

$$y(x) = w^T.\varphi(x) + b \quad (1)$$

where *w* and *b* denote the values of weights and bias of regression function, respectively. *φ(x)* is the nonlinear mapping of inputs in feature space with high dimension.

M5 Tree Model: This model is based on tree classification for creating the relationship between dependent and independent variables. This model proposed by Quinlan (1992) is a combination of linear regression and regression tree and can be applied for quantitative and qualitative datasets. For M5 tree model, the data domain is divided to subspace (so called leaf) and used numerical label for each leaf and can be applied for estimation of continues numerical variables. Each regression tree includes root, branches, nodes and leaves, similar to a tree.

Results and concluding remarks

The ability of five different soft computing methods, M5 tree, MARS and LSSVR, was compared in estimating long-term monthly Epan. The inputs of the considered models are the month number of the year and the geographical data (longitude, latitude, altitude). The results were evaluated according to the commonly used statistics; determination coefficient (R^2), mean absolute errors (MAE) and root mean square errors (RMSE).

Table 1 reports the summary of test process of M5 tree, MARS and LSSVR models in estimating long-term Epan. In the applications, the M5 tree, MARS and LSSVR models were employed using the MATLAB toolboxes M5PrimeLab (Jekabsons 2016a), ARESLab (Jekabsons 2016b) and LS-SVMlab (Pelckmans et al. 2002), respectively. For the M5 tree, MARS and LSSVR models, the RMSE ranges are 0.05-0.24, 0.08-0.40 and 0.06-0.24 mm and the MAE ranges are 0.05-0.18, 0.07-0.36 and 0.05-0.23 mm, respectively. The LSSVR (RMSE=0.116 mm, MAE=0.095 mm, R^2=0.996) performs superior to the other methods in the testing phase. The LSSVR model shows the lowest RMSE (0.06 mm) and MAE (0.05 mm) for the Seoni Station and Sidhi Station has the worst accuracy (RMSE=0.26 mm and MAE=0.23 mm) for this method. The LSSVR model has the highest accuracy in 7 stations out of 11, while the both M5 tree and MARS models give the highest accuracy in only 2 stations.

Table 1. Summary of the testing process of M5 tree, MARS and LSSVR models

Station	M5 tree			MARS			LSSVR		
	RMSE (mm)	MAE (mm)	R^2	RMSE (mm)	MAE (mm)	R^2	RMSE (mm)	MAE (mm)	R^2
SEHORE	0.10	0.09	0.993	0.08	0.07	0.996	0.10	0.08	0.995
SEONI	0.07	0.06	0.999	0.10	0.08	0.994	0.06	0.05	0.997
SHAHDOL	0.10	0.08	0.998	0.10	0.08	0.994	0.16	0.13	0.995
SHAJAPUR	0.14	0.13	0.996	0.15	0.13	0.997	0.09	0.07	0.996
SHEOPUR	0.21	0.18	0.980	0.40	0.36	0.906	0.16	0.12	0.993
SHIVPURI	0.16	0.12	0.986	0.34	0.29	0.933	0.09	0.07	0.996
SIDHI	0.24	0.17	0.972	0.17	0.15	0.984	0.26	0.23	0.995
TIKAMG.	0.12	0.08	0.991	0.27	0.23	0.956	0.09	0.07	0.996
UJJAIN	0.11	0.10	0.997	0.14	0.12	0.996	0.11	0.09	0.996
UMARIA	0.05	0.05	0.998	0.10	0.08	0.996	0.06	0.05	0.998
VIDISHA	0.18	0.14	0.979	0.15	0.13	0.992	0.10	0.08	0.994
Mean	0.135	0.109	0.990	0.182	0.156	0.977	0.116	0.095	0.996

The results indicated that the LSSVR outperforms the other considered models with respect to R^2, MAE and RMSE in modeling long-term Epan. The ranks of the considered models in estimating long-term Epan with respect to accuracy are: LSSVR, M5 tree and MARS.

References

Friedman JH (1991) Multivariate adaptive regression splines (with discussion). The Annals of Statistics 19(1): 79-141.

Jekabsons G (2016a) M5PrimeLab: M5' Regression Tree and Model Tree ensemble toolbox for Matlab/Octave ver. 1.7.0. Institute of Applied Computer Systems Riga Technical University, Latvia. Available: http://www.cs.rtu.lv/jekabsons/Files/M5PrimeLab.pdf

Jekabsons G (2016b) ARESLab Adaptive Regression Splines toolbox for Matlab/Octave ver. 1.13.0. Institute of Applied Computer Systems Riga Technical University, Latvia. Available: http://www.cs.rtu.lv/jekabsons/Files/ARESLab.pdf

Moghadamnia A, Gousheh MG, Piri J, Amin S, Han D (2009) Evaporation estimation using artificial neural networks and adaptive neuro-fuzzy inference system techniques. Advances in Water Resources 32:88-97

Pelckmans K, Suykens JAK, Van Gestel T, De Brabanter J, Lukas L, Hamers B, De Moor B, Vandewalle J (2002) LS-SVMLab: a Matlab/C toolbox for Least Squares Support Vector Machines. Available: www.esat.kuleuven.be/sista/lssvmlab/

Quinlan JR (1992) Learning with continuous classes. Proceedings of the Fifth Australian Joint Conference on Artificial Intelligence, Hobart, Australia, 16-18 November, World Scientific, Singapore, pp 343–348

Suykens J, De Brabanter J, De Moor B, Vandewalle JAK, Van Gestel T (2002) Least squares support vector machines. Vol 4, World Scientific, Singapore

Vapnik V (1995) The Nature of Statistical Learning Theory. Springer, New York

11th World Congress on Water Resources and Environment (EWRA 2019)
"Managing Water Resources for a Sustainable Future", 25-29 June 2019, Madrid, Spain

Characterization of meteorological drought at various time scales in the Lobo watershed, Côte d'Ivoire

B. Koffi[1*], K.L. Kouassi[1], M.S. Angulo[2], Z.A. Kouadio[1]
[1] Jean Lorougnon Guédé University, BP 150 Daloa, Côte d'Ivoire
[2] Laboratory of Planetology and Geodynamics, University of Nantes, Faculty of Science and Technology
* e.mail: koffiberen@gmail.com

Introduction

Drought and desertification phenomena that affected many African countries south of the Sahara have not spared Côte d'Ivoire, especially since the 1970s (Goula et al. 2006). These phenomena have resulted in major climatic disruptions, including a significant decrease in rainfall in various regions of the country and particularly in the Lobo catchment area, which is an area with high agricultural activity (Yao 2015). Like other regions of the country, it is experiencing climatic disturbances caused by the deterioration of climatic parameters, including precipitation and temperature. For example, monitoring meteorological drought using the Standardized Precipitation Index (SPI) at various time scales is a vital and important element in assessing drought risk (Gumus and Algin 2017; Oloruntade et al. 2017). As some global change scenarios indicate that the occurrence and impact of droughts are likely to increase in the coming years (IPCC 2013), it is essential to be able to analyse drought weather sequences in order to propose mitigation or adaptation measures to populations if necessary.

Materials and methods

An analysis of the monthly rainfall data was done using the DrinC software, which is a program developed by Tigkas et al. (2015). The method used is the calculation of SPI at different time scales: short (1 month), medium (6 months) and long term (12 months). The Gamma probability distribution has been used for precipitation.

$$SPI = \frac{P_i - P_m}{\sigma} \quad (1)$$

where P_i: rain of the year i; P_m: average rainfall of the series on the time scale considered; σ: standard deviation of the series on the time scale considered.

The drought event occurs when SPI is continuously negative and reaches an intensity of -1.00 or less; the event ends when SPI becomes positive; the positive sum of SPI for all months during a dry event is equal to the magnitude (amplitude) of the drought.

The cumulative drought frequency (F) was obtained by dividing the cumulative dry sequence population by the total rainfall year population. The magnitude and severity determined the intensity of the meteorological drought. The extreme value of the SPI was considered as a reference value for drought intensity.

Results and concluding remarks

The analysis of meteorological drought index values for different time scales using SPI at the Vavoua, Daloa and Zuenoula stations revealed that the Lobo catchment area experienced a significant rainfall deficit after 1970, with peaks in March 1991, December 2003 and August 1984 in the short term; in the medium term peaks were observed in March 1993, December 2003 and November 2003 and in the long term drought peaks were observed in March 1984, September 2003 and August 1973. These peaks were characterized by extremely severe types of droughts. These results confirm the research carried out by Mahé et al. (2001) in West Africa. In Côte d'Ivoire, the work of Meledje et al. (2015) and Soro et al. (2014) showed that the decades 1970-1979, 1980-1989 and 1990-1999 were dry periods. This rainfall decrease

intensified during the 1980s and 1990s, before increasing slightly in the 2000s.

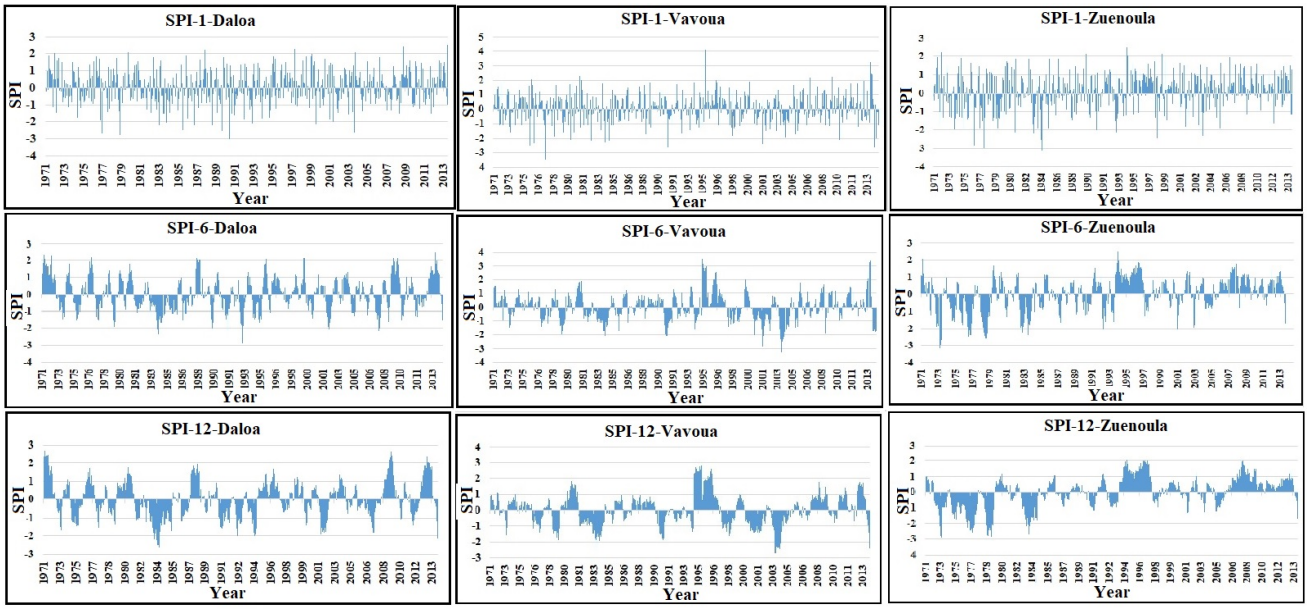

Figure 1. Evolution of meteorological drought in the short, medium and long term using the standardized precipitation index at Daloa, Vavoua and Zuenoula stations.

In terms of intensity and frequency of drought sequences, the results obtained are different in the short, medium and long term, whatever the time scale. These analyses show the effects of the study time scale on the characterization of dry sequence parameters. The longer the time chosen, the more historical data, the more little the statistical index varies and makes it possible to define dry episodes with greater precision. Hence the need to use long-term time scales to better characterize drought sequences.

Acknowledgments: We would like to thank the IRD for allowing us to carry out this study thanks to a scholarship.

References

Goula BTA, Savané I, Brou K, Vamoryba F, Gnamien B (2006) Impact de la variabilité climatique sur les ressources hydriques des bassins de N'Zo et N'Zi en Côte d'Ivoire (Afrique tropicale humide). Vertigo 7(1) :1‑12

Gumus V, Algin HM (2017) Meteorological and hydrological drought analysis of the Seyhan–Ceyhan River Basins, Turkey: Drought analysis of the Seyhan–Ceyhan River Basins, Turkey. Meteorological Applications 24(1):62‑73. https://doi.org/10.1002/met.1605

IPCC (2013) Climate Change 2013: The Physical Science Basis. In Contribution of Working Group I to the Fifth Assessment Report of the Intergovernmental Panel on Climate Change.

Mahé G, L'hote J, Olivry C, Wotling W (2001) Trends and discontinuities in regional rainfall of West and Central Africa. Hydrological Sciences Journal 42(1):211‑226

McKee TB, Doesken NJ, Kleist J (1993) The relationship of drought frequency and duration to time scales.

Meledje NH, Kouassi KL, N'Go YA, Savane I (2015) Characterization of dry period in the transfrontier Bia watershed in Côte d'Ivoire and Ghana: contribution of Markov chains. Cahiers Agricultures 3:186-197. https://doi.org/10.1684/agr.2015.0755

Oloruntade AJ, Mohammad TA, Ghazali AH, Wayayok A (2017) Analysis of meteorological and hydrological droughts in the Niger-South Basin, Nigeria. Global and Planetary Change 155:225‑233. https://doi.org/10.1016/j.gloplacha.2017.05.002

Soro GE, Anouma DGL, Goula BTA, Srohorou B, Savane I (2014) Caracterisation des sequences de secheresse météorologique a diverses echelles de temps en climat de type soudanais : cas de l'extreme Nord-Ouest de la Côte d'Ivoire. Larhyss Journal 18:107‑124

Tigkas D, Vangelis H, Tsakiris G (2015) DrinC: a software for drought analysis based on drought indices. Earth Science Informatics 8(3):697‑709. https://doi.org/10.1007/s12145-014-0178-y

Yao AB (2015) Evaluation des potentialités en eau du bassin versant de la Lobo en vue d'une gestion rationnelle (Centre-Ouest de la Côte d'Ivoire). Université Nanguy Abrogoua, 225 p

11th World Congress on Water Resources and Environment (EWRA 2019)
"Managing Water Resources for a Sustainable Future", 25-29 June 2019, Madrid, Spain

Analysis of the variation of the hydrological response of Luján river sub-basin, Albuera stream, in the province of Buenos Aires

T. Bran, P. Palmeyro, I. Arzuaga, M. Torrero, S. Viñes*
School of Engineering and Agricultural Sciences, Catholic University of Argentina, Buenos Aires, Argentina
** e-mail: susanavines@yahoo.com.ar*

Introduction

The Albuera creek basin, a tributary of the Lujan River, is located in the Malvinas Argentinas district, in Buenos Aires province. This area has experienced an important industrial and population growth in the last decades, mainly due to its proximity to Buenos Aires city. Given the huge importance of the basin, not only as a hydric resource but also as a broader socioenvironmental factor, this paper will focus on analyzing the ombrothermic diagrams, water balances, and the correlation between precipitation and runoff, in order to determine variations in the water flow response with time due to the effect of global warming and the reduction of the drainage surface caused by the urbanization of the area. Since the creek has no gouging measurements, the precipitation data obtained from the Don Torcuato Aero and San Miguel stations are used to analyze whether there is a hydrologic excess in the basin and its magnitude. Thus, the elaboration and analysis of the water balances allow us to evaluate if the hydrologic system of the Albuera basin has excess and what incidence it has on flow variations.

Materials and methods

The climatological data of the stations of San Miguel (Lat. -34° 33'0'', Long. -58° 44'0'', height 26 masl) for the period 1933-2017, and of Don Torcuato Aero (Lat. -34° 29'0'', Long. -58° 37'0'', height 4 masl) for the period 1963-2006, corresponding to the statistics provided by the National Meteorological Service, was employed at an initial phase to calculate the water balances. Gaussen's ombrothermic diagrams were made and analyzed to determine the existence and duration of dry periods, following the guidelines presented by Castillo and Castellví Sentis (2001).

Given that it is a watercourse which does not have gaps, the information provided by the water balance will allow to establish the existence or not of water excesses and depending on them, in the case that effectively there is, it will allow quantifying the flow rate precipitation. In a river basin, the flow of a river, defined as the volume of surface runoff per unit of time (Bruniard 1992; Monsalve Sáenz 1999) depends on factors such as climate, vegetation, and the soil-substrate complex. That is, processes such as precipitation, evaporation, interception, transpiration, infiltration, and storage directly affect the flow. Likewise, factors of human nature, such as those related to anthropogenic intervention, influence surface runoff. Therefore, it is essential to assess the river's response to these factors (Heras 1972; Pedraza 1996; Monsalve Sáenz 1999). Therefore, the elaboration of the water balances allows to evaluate if the water system of the Albuera stream presents excesses and its incidence in the variability of the flow.

The water balances are made and analyzed using the method of Thornthwaite and Mather (1957) for the localities of San Miguel (periods 1933-2017) and Don Torcuato (periods 1963-2005). The analysis of the water balance of the San Miguel station for the period 1981-1990 showed a greater wet period. The water balance for this case shows us that the use is of 39.82 mm (Fig. 1). The excess period (215.71 mm) occurs in the months of July to November and in December and January, rainfall begins to fall and potential evapotranspiration gradually increases, using water stored in the soil, compensate for the need for water. Without exhausting reserves, it is replenished in the months of February to March and enters a new period of excess (165.20 mm), which runs from April to June (Fig. 1).

The above-described analysis was complemented with a numerical hydrological simulation of the sub-basin employing the public domain software HEC-HMS developed by the U.S. Army Corps of Engineers. Through this numerical model, the different zones of the sub-basin were represented and the peak

discharge flow at the end of the sub-basin for different average recurrence intervals (2, 10, 50, 100 years) was obtained. A sensibility analysis is included in order to observe how this peak discharge flow varies with curve number values for different soil types. In the same line, numerical modeling of the sub-basin is performed employing the software HEC-RAS, also developed by the U.S. Army Corps of Engineers, to study the evolution of flood surface and contour with increasing average recurrence intervals. Maps showing the flood surface in each case and the current urban area potentially vulnerable to this situation are included.

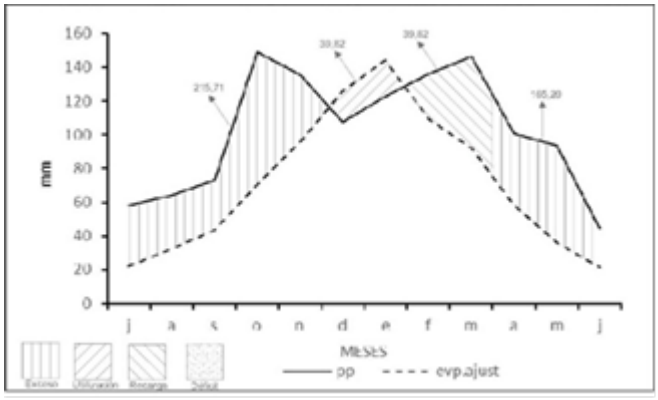

Figure 1. Water balance for the San Miguel station period 1981-1990.

Results and concluding remarks

From the water balances elaborated and analyzed regarding the basin of the Albuera stream, for the period 1933-2012, we can observe the predominance of humid periods that include from autumn to spring inclusive, and short dry periods during the summer. Although rainfall falls during this period and evapotranspiration increases, there is no water deficit, so the deficit is zero in the basin studied.

The decrease in the time of concentration of water by the progressive urbanization of the area, as a result of paving, urbanization, etc., added to the great excesses that occur in this basin, lead to conclude that water balances constitute a tool of great importance in the decision-making process and in the water management of the basin.

Finally, the comparison between the behaviour of the sub-basin for different average recurrence intervals and the change in the use of the soil within the sub-basin, including the important growth in the urbanization of the area surrounding the stream, allow us to conclude that the vulnerable population to floods in the zone has worryingly increased in the last decades and that actions from different level governments and social actors involved are highly required to prevent this vulnerability, especially regarding the invest in hydraulically infrastructure.

References

Bruniard E (1992) Hidrografía, Procesos y tipos de escurrimiento superficial. Ceyne, Buenos Aires

Campo de Ferreras AM, Capelli de Steffens AM, Díez PG (2004) El clima del Suroeste Bonaerense. Universidad Nacional del Sur, Bahía Blanca

Castillo FE, Castellví Sentis F (2001) Agrometeorología. Mundi Prensa, España. 520 pp

Gaussen H (1954) Théories et classifications des climats et microclimats. VIII Congrés Int. Bot. Act. 7 et 3. CNRS. 125-130

Gaussen H (1955) Expresión des milieux par des formules écologiques. Colloque Inter. CNRS. 257-269

Heras R (1972) Manual de hidrología, principios básicos en hidrología. Dirección General de Obras Hidráulicas, Centro de Estudios Hidrográficos, Madrid

Monsalve Sáenz G (1999) Hidrología en la Ingeniería. Alfaomega, Colombia

Pedraza Gilsanz J de (1996) Geomorfología, principios, métodos y aplicaciones. Ed. Rueda, Madrid

Remenieras G (1974) Tratado de Hidrología Aplicada. ETA, Barcelona

Servicio Meteorológico Nacional (1986) Estadísticas Meteorológicas 1981-1990, Nº 36. S.M.N., Buenos Aires

11th World Congress on Water Resources and Environment (EWRA 2019)
"Managing Water Resources for a Sustainable Future", 25-29 June 2019, Madrid, Spain

Entropy based regional precipitation prediction in case of Gediz basin

Ö. Bozoğlu, F. Barbaros*, T. Baran
Civil Engineering Department, Faculty of Engineering, Dokuz Eylul University, Izmir, Turkey
** e-mail: filiz.barbaros@deu.edu.tr*

Introduction

The Shannon's entropy concept defined to measure the information content of hydrological processes in hydrology and water resources, is used as an objective criterion in planning of water resources systems.

The purpose of the presented study is to determine the expected value of long-term annual total precipitation by using entropy theory. The frequency analysis of the observed long-term total monthly precipitation is carried out for these purposes and entropy values are determined by the histogram of frequency which are called "Intensity Entropy - IE".

In the case study of Gediz Basin, 44 precipitation stations with long-term data are evaluated for determining the IE values. The results show that the annual total precipitation values have strong statistical relations between the IE values (r = 0.99) on the Gediz catchment basis. Consequently, IE values can be used to define regional information for the expected value of annual total precipitation, which have the same meaning of potential water resources availability of the Gediz basin.

Materials and methods

According to the information entropy theory defined by Shannon (1948), the negative expected value of the logarithm of the probability density function of the variable is the uncertainty or disorder of the variable or its probability distribution. When considering the intensity (or quantity) of monthly precipitation as a random variable and taking p_i as its probability of occurrence in a series of precipitation, the IE can be estimated using Eq. 1.

$$H = \sum_{i=1}^{k} p_i \log p_i \quad (1)$$

The probabilities for a particular precipitation are expressed in a discrete form by taking into account all available monthly precipitation values and their probability of occurrence. IE is assessed in the following steps: *(a)* The monthly precipitation data in the m-year sets are listed together under one data set without any sequence attribute; *(b)* The entire range of monthly precipitation are divided into n classes at the same class interval, *(c)* The frequency fi for each class i is counted then to make a frequency distribution tablefifi, *(d)* The relative frequency (fi/N)fi/N for each class i is calculated in a discrete form for the entire range of monthly precipitation with a probability density function and *(e)* Based on these relative frequencies, IE values are calculated using the following equation ; where n is the number of classes, and f_i is the frequency for class i. Here, the unit of IE is "napier" with the logarithmic base of e and given as in Eq. 2.

$$IE = \sum_{i=1}^{k} \frac{f_i}{N} ln \frac{f_i}{N} \quad (2)$$

Expected rainfall values increases in the form given in Figure 1 with increasing IE results. This suggests that IE have positive correlation with the expected precipitation and can therefore be an alternative to the prediction of total amount precipitation (Maruyama et al. 2005). IE can be used to define the regional information even if stations have different observation periods. Another advantage of the method is that there is no need to complete the missing observation years, to define elevation – precipitation relations and orographic maps. It is considered that observations are random and so there is no autocorrelation between them (Temiz and Baran 2012).

On the other hand, it is known that the selection of Δx is a crucial problem, such that each specified class interval size gives a different reference level of zero uncertainty with respect to which the computed entropies. While researchers approximate the discrete probabilities p_i by using $f(x)\Delta x$, where $f(x)$ is the relative

class frequency and Δx, the size of class intervals for continious varibles, various entropy measures become relative to the discretizing interval Δx and change in value as Δx changes (Baran et al. 2017). Hence, to define the regional information same class intervals are used for all frequency analyses.

Results and concluding remarks

The presented study is carried out with the available precipitation data in Gediz basin, which is located in the western part of Turkey within the borders of the Aegean region. The average annual precipitation in Gediz Basin is approximately 635 mm. In Turkey's 26 major river basins, the Gediz basin is the 20th with a drainage area of 17,500 km^2 and the 21st with an annual surface water potential of 1.95 billion m^3. These values are 2.2 % of the country's surface area and 1.7 % of the country's water potential (SHW 2005). Evaluated precipitation data of 44 precipitation observation stations are the stations of State of Meteorological Works (DMI) and State Water Works (DSI) for Gediz River Basin. IE values are calculated in the explained steps as previously and the annual total precipitation values versus IE values relationship (r = 0.99) are obtained as:

$$P = 52{,}58.\, e^{1{,}12IE} \tag{3}$$

The regional IE distribution of Gediz basin, which was achieved through basin-wide interpolation of the IE values by the Spline algorithm, are presented in Figure 2. By using Fig. 2 and Eq. 3, researchers can estimate total annual precipitation, which also means gross water potential in long-term period.

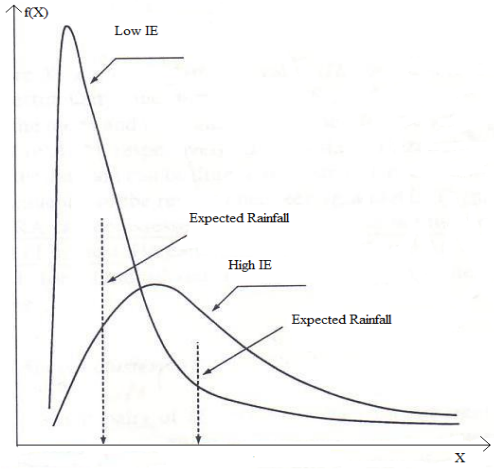

Figure 1. Expected precipitation with IE.

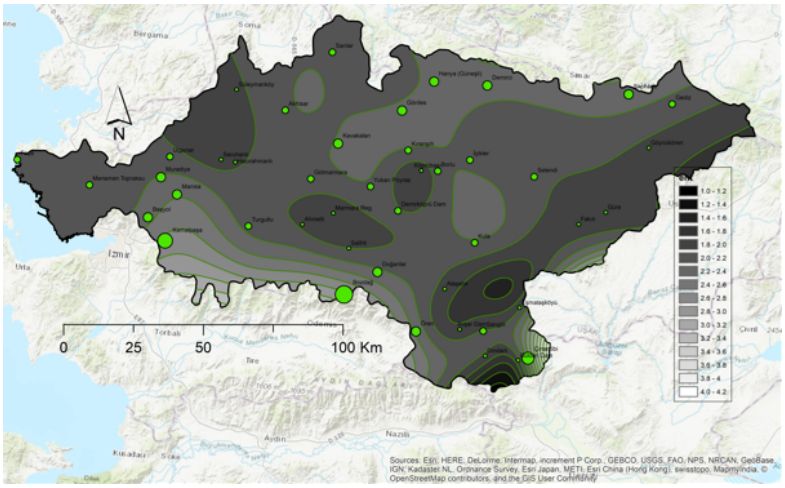

Figure 2. Intensity Entropy (IE) distribution in Gediz Basin.

Acknowledgement: Authors would like to acknowledge to Assoc. Prof. Dr. Ali GÜL for his great contribution to the mapping process of the manuscript.

References

Baran T, Harmancıoğlu N, Çetinkaya CP, Barbaros F (2017) An Extension to the Revised Approach in the Assessment of Informational Entropy. Entropy 19(634). doi: 10.3390/e19120634.

Maruyama T, Kawachi T, Singh VP (2005) Entropy-based Assessment and Clustering of Potential Water Resources Availability. Journal of Hydrology 309:104-113

Shannon, C.E. (1948) Mathematical Theory of Information. In The Mathematical Theory of Information, the University of Illinois Press: Urbana, IL, USA, 27:170-180

SHW (2005) Environmental Master Plan of Gediz Basin. II. Directorate of State Hydraulic Works, İzmir

Temiz Ö, Baran T (2012) Determination of Expected Value for Monthly Total Precipitation by Entropy Based Method Case Study: Gediz Basin. 10th International Congress on Advances in Civil Engineering, Paper no: 769, 10 p

11th World Congress on Water Resources and Environment (EWRA 2019)
"Managing Water Resources for a Sustainable Future", 25-29 June 2019, Madrid, Spain

Development of a distributed hydrological software application employing novel velocity-based techniques

K. Risva*, D. Nikolopoulos, A. Efstratiadis
Department of Water Resources and Environmental Engineering / School of Civil Engineering, National Tecnhical Univerisity of Athens, Athens, Greece
** e-mail: conrisva@gmail.com*

Introduction

The aim of this study is the development of an event-based distributed hydrological model, incorporating novel methodologies for estimating the effective rainfall and flow routing across the terrain and the hydrographic network (Risva 2018). We present two modelling configurations of the model, one for extracting the flood hydrograph (separating interflow) and one for the full hydrograph, at the basin outlet.

Materials and methods

First, we distinguish between the effective from the gross rainfall, at a cell basis, thus extracting the spatial distribution of surface runoff during the simulation period. The underlying model is based on an improved NRCS-CN scheme, which uses a spatially distributed reference CN value for the cells, and two lumped (i.e. common for the entire basin) dimensionless parameters, one for representing the antecedent soil moisture conditions (AMC) of the basin at the beginning of the storm event, and one for estimating the initial rainfall abstraction (Savvidou et al. 2018). The proposed scheme contains several novelties, regarding the estimation of the reference CN value (i.e. the value that refers to average soil moisture conditions and initial rainfall abstraction as 20% of maximum potential retention) from spatial data, estimation of the infiltration losses (Efstratiadis et al. 2014) and the event's CN adjustment at a cell basis against the two model parameters.

For the propagation of runoff to the basin outlet, two surface flow types are considered: an overland flow across the catchment's terrain, and a channel flow along the river network. These two types are synthesized by employing a velocity-based approach, to form the flood hydrograph (Grimaldi et al. 2012). This approach implements an original methodology for assigning realistic velocity values along the river network, also accounting for the novel concept of the varying (i.e. dependent on runoff intensity) time of concentration (Antoniadi 2016; Michailidi et al. 2018) for different rainfall events.

The proposed approach takes advantage of regional relationships and literature values for assigning appropriate values to all model attributes, except for the two lumped parameters of the rainfall-runoff transformation, which are either manually assigned or inferred through calibration, provided that observed flow data are available. In the last case, it is essential to extract the sub-surface flow component (interflow) from the total hydrograph, which may be done through several approaches of varying complexity. Here we propose an empirical method, requiring the fitting of a lumped hydrological model the observed hydrograph, which explicitly accounts for the contribution of interflow to total runoff.

An alternative, more integrated approach, aims at enhancing the distributed model with additional functionalities, in order to obtain the full hydrograph at the basin outlet. In this context, we have also developed a more generic version of the modelling framework, in which the NRCS-CN procedure is combined with a continuous soil moisture accounting scheme, thus generating both the surface (overland) runoff as well as the interflow through the unsaturated zone. Apparently, the augmented version of the model requires more parameters, since more processes are accounted for within the simulation procedure.

For the schematization of the model domain, the user needs to formulate two spatial layers, a grid-based partition of the basin to equally-dimensioned square cells, and a graph-based configuration of the hydrographic network, comprising of junctions and interconnected river segments. Both layers can be easily extracted on the basis of a digital elevation model (DEM) of the basin, using typical tools that are

available in any GIS environment.

In order to develop our models we use the high - level interpreted programming language Python, is used, along with many GIS and computational packages. In addition to coding the two versions of the hydrological model, a GUI interface (Figure 1) is co-developed so as to make a user – friendly software, allowing the user to enter all the necessary inputs, visualize them, select the surface or the augmented model, perform simulation and optimization procedures and assess the simulated hydrographs.

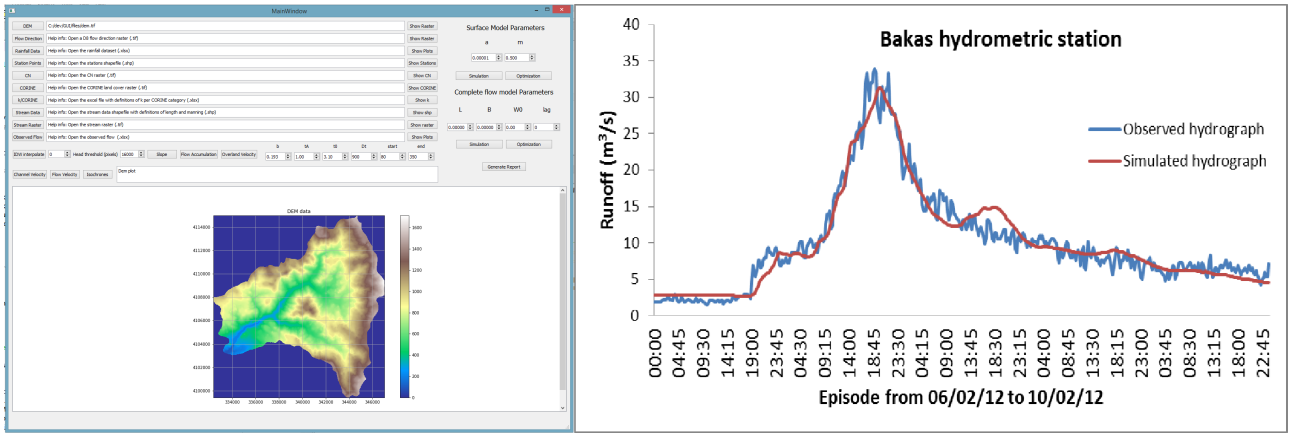

Figure 1. Left: The GUI of the hydrological software, showing the import of the basin's DEM model. Right: Simulated hydrograph from the 06/02/12 rainfall event with NSE of 0.95.

Results and concluding remarks

The software is used to simulate two rainfall events in the Nedontas river basin, in Greece (Table 1 and Figure 1). The results seen on indicate that the output hydrograph of both models simulates with good efficiency the observed one in the selected events. Two distributed models were developed, characterized by very good performance in their application in the given study area. The innovations that contribute to the methodology developed include the incorporation of a modern GIS method to assess the CN index by geospatial information, usage of an empirical adjustment of CN to any humidity conditions before the rainfall event and temporally varying channel flow velocities. In conclusion, it is a sophisticated and parsimonious approach, as opposed to many other distributed models that require a variety of parameters for their operation.

Table 1. Results at Nedontas river Basin for two rainfall events.

	Event 06/02/2012	Event 16/01/2013
NSE (surface model)	0.90	0.70
NSE (augmented model)	0.95	0.87

References

Antoniadi S (2016) Investigation of the time - response variability of river basins. National Technical University of Athens

Efstratiadis A, Koukouvinos A et al. (2014) Description of regional approaches for the estimation of characteristic hydrological quantities, DEUCALION-Assessment of flood flows in Greece under conditions of hydroclimatic variability: Development of physically-established conceptual-probabilistic. Athens

Grimaldi S, Petroseli A, Tauro F, Porfiri M (2012) Time of concentration: A paradox in modern hydrology. Hydrol. Sci. J., 57(2):217–228. https://doi.org/10.1080/02626667.2011.644244

Michailidi E (2018) Flood risk assessment in gauged and ungauged basins in a multidimensional context. Universita Degli Studi di Brescia

Risva K (2018) Development of a distributed hydrological software application employing novel velocity-based techniques. MSc thesis, Department of Water Resources & Environmental Engineering – National Technical University of Athens, 166 p

Savvidou E et al. (2018) The Curve Number Concept as a Driver for Delineating Hydrological Response Units. Water 10(2):194. https://doi.org/10.3390/w10020194

11th World Congress on Water Resources and Environment (EWRA 2019)
"Managing Water Resources for a Sustainable Future", 25-29 June 2019, Madrid, Spain

Field and laboratory toolbox for unsaturated zone hydrological studies

E. Zavridou, K. Marakantonis, A. Kallioras*
Dept. of Mining and Metallurgical Engineering, National Technical University of Athens, Athens, Greece
** e-mail: kallioras@metal.ntua.gr*

Introduction

Different methods are applied to extract water from soil such as azeotropic distillation (Allison and Hughes 1983; Revesz and Woods 1990; Thorburn et al. 1993), cryogenic microdistillation (Dawson and Ehleringer 1993), vacuum distillation (Fontes et al. 1986), centrifugation (Edmunds and Bath 1976), mechanical squeezing (White et al. 1985) and equilibration (Scrimgeour 1995). Recent work of Orlowski et al. (2016) has pointed out the differences between these soil water extraction techniques. In this study, field and lab technologies were developed and tested for investigating the hydrological process within the unsaturated zone. A multi-level undisturbed soil sampling, using a portable direct push vibro coring technology, along with azeotropic distillation, were used to determine soil water isotopic concentration. The sampling sites were located in Marathon plain, in the NE part of Attica peninsula, Greece, where the mean annual rainfall is 500 mm. The investigated area consists of upper unconsolidated sedimentary deposits among other aquifer formations.

Materials and methods

Undisturbed materials from the unsaturated zone were collected using a portable direct push vibro-coring set from the surface to various depths up to 1000 mm at 50 different locations. Sampling was carried out in June 2018 from unconsolidated soils. Each soil core weighed approximately 500 g, and was sealed and placed in polyethylene bags, off one part was used for grain-size analysis while the other for pore water extraction with azeotropic distillation process.

Grain size analysis is a crucial tool for describing unconsolidated materials and sediments. Sediments with a grain size larger than 75 μm were separated by sieving analysis while sediments smaller than 75 μm were determined by a sedimentation process using a hydrometer (ASTM Standard D422-3, C136 – 06). Gravimetric water content was determined by oven drying at 105 ^{o}C for 24 h.

The soil water was extracted from each sample by azeotropic distillation with an immiscible organic solvent such as toluene. Azeotrope is a solution of at least two different liquids at a boiling point specific for that component. The toluene and water present a boiling point of 110.6 ^{o}C and 100 ^{o}C respectively and form a toluene water azeotropic mixture at 84.1 ^{o}C. The removal of water was done using a distillation apparatus which consists of a heating mantle, a flask, a condenser and a specially designed receiving funnel. The toluene, with a smaller density than that of water (0.865 g/mL and 0.998 g/mL respectively), was condensed in the condenser and was returned back into the boiling flask, while the water was collected at the base of a distilling receiver and was removed through a stopcock from the bottom. The entire distillation process, which should be carried out in a fume hood, takes between 40 – 50 min per sample and the total amount of the soil water is between 15-30 mL. The extracted water was collected and stored in tightly sealed bottles to prevent evaporation. The water extracted from the undisturbed soil samples was used for the determination of chloride concentration and of different isotopic signals such as ^{18}O and ^{2}H which have been used to determine the origin and the age of porewaters. The chloride concentration of the extract was measured by a simple titration in accordance with titrate $AgNO_3$ 2.256N of HACH. The chloride concentration of extracted water was expressed as meq/L.

Results and concluding remarks

According to USDA soil texture classification system, the soil samples in the upper 1 m in the area of Marathon presented the following texture: 40% of the samples were silty loam, 30% were sandy loam, 28%

characterized as loamy, while loamy fine sandy soils constituted the 2% of the samples. The biggest amount of gravimetric water content was observed, as expected, in smaller grain size soils. The determination of chloride concentration via azeotropic distillation has shown high chloride concentration values. These results indicate low recharge rates through the unsaturated zone because chloride accumulates in the subsurface as a result of evapotranspiration and the existence of human practices such as application of fertilizer and irrigation. The ^{18}O and ^{2}H values of extracted porewater indicate the contribution of soil water from sandy and silt loam soils. This research is part of a methodological framework that is under formation in order to develop a technically sound toolbox for unsaturated zone measurements.

References

Allison GB, Hughes MW (1983) The use of natural tracers as indicators of soil-water movement in a semi-arid region. Journal of Hydrology 60(1-4):157-173. doi: 10.1016/0022-1694(83)90019-7

ASTM Standard C136 - 06. Standard Test Method for Sieve Analysis of Fine and Coarse Aggregates, ASTM International, West Conshohocken, PA, doi: 10.1520 /C0136-06

ASTM Standard D422 - 63e1. Standard Test Method for Particle-Size Analysis of Soils, ASTM International, West Conshohocken, PA, doi: 10.1520/D0422.

Dawson TE, Ehleringer JR (1993) Isotopic enrichment of water in the woody tissues of plants: Implications for plant water source, water uptake, and other studies which use the stable isotopic composition of cellulose. Geochimica et Cosmochimica Acta 57(14):3487-3492. doi: 10.1016/0016-7037(93)90554-A

Fontes JC, Yousfi M, Allison GB (1986) Estimation of long-term diffuse groundwater discharge in the Northenr Sahara using stable isotope profiles in soil water. Journal of Hydrology 86:315-327. doi: 10.1016/0022-1694(86)90170-8

Orlowski N, Pratt D, McDonnell J (2016) Intercomparison of soil pore water extraction methods for stable isotope analysis. Hydrol. Process. 30:3434-3449. doi: 10.1002/hyp.10870

Revesz K, Woods PH (1990) A method to extract soil water for stable isotope analysis. Journal of Hydrology 115(1-4):397-406. doi: 10.1016/0022-1694(90)90217-L

Scrimgeour CM (1995) Measurement of plant and soil water isotope composition by direct equilibration methods. Journal of Hydrology 172:261-274. doi: 10.1016/0022-1694(95)02716-3

Thorburn PJ, Walker GR, Brunel J-P (1993) Extraction of water from Eucalyptus trees for analysis of deuterium and oxygen–18: laboratory and field techniques. Plant, Cell and Environment 16(3):269-277. doi: 10.1111/j.1365-3040.1993. tb 00869.x

White JWC, Cook ER, Lawrence JR, Wallace SB (1985) The D/H ratios of sap in trees: implications for water sources and tree ring D/H ratios. Geochimica et Cosmochimica Acta 49(1):237-246. doi: 10.1016/0016-7037(85)90207-8

11th World Congress on Water Resources and Environment (EWRA 2019)
"Managing Water Resources for a Sustainable Future", 25-29 June 2019, Madrid, Spain

Post-2010 forest fire hydrological changes in the Upper Nahal Oren basin, Mt. Carmel Israel: A comparison to pre-fire rates

N. Greenbaum*, L. Wittenberg, D. Malkinson, M. Inbar
Department of Geography and Environmental Studies, University of Haifa, Haifa, Israel
** e-mail: noamgr@geo.haifa.ac.il*

Introduction

Wildfires, in general, increase overland flow (Shakesby 2011). At the catchment scale, the affected overland flow parameters are: (a) higher total runoff, (b) higher runoff coefficient, and (c) shorter lag time to runoff generation and to peakflows. These hydrological impacts of wildfire gradually decrease with time depending on rehabilitation of the vegetation, litter and soil (Shakesby 2011; Shakesby and Doerr 2006). Pre-fire conditions are commonly not monitored and the relatively short (2-3 years) post-fire studies usually terminates before the full recovery of the area is exceeded (Shakesby 2011).

Lavabre et al. (1993), in a 85%-burnt catchment of 1.46 km^2 in southeastern France, estimated a 30% increase in annual runoff and an increase in the frequency of the larger flows during the first year after the fire.

Candela et al. (2005) reported higher rainfall-runoff ratio, more rapid flows and shorter lag time between rainfall and flood peak.

Ferreira et al. (2005), in a 1.1 km^2 burnt catchment in central Portugal, reported on runoff coefficients of up to 48.5% explained by rapid transmission of throughflow and baseflow water bypassing the more water-repellent areas into the channel.

Mayor et al. (2007), in a 2.1 ha burnt catchment in eastern Spain, documented a three-order magnitude increase of total runoff in a 7-year, post-fire study. Annual runoff coefficients were 2.3-2.8%, whereas event runoff coefficients were up to 10.3%. Maximum peakflows, were documented during the second and third years after the fire, decreasing only at the fourth year and reaching very low values during the sixth and seventh years.

Material and methods

The Upper Nahal Oren catchment −18 km^2 is a typical mountainous, ephemeral stream system of Mt. Carmel draining its western flanks into the Mediterranean Sea with a general channel gradient of 3%. The carbonate rocks exposed in the basin and the resulting karstic nature of catchment cause low drainage density of 3.2 km/ km^2 and existence of groundwater aquifer. The landuse at the basin includes: natural and planted forests composed of oaks and pines - 61%; agriculture - 17%, and 22% - urban area of the village of Isfiya located at the eastern water divide of the catchment.

The Mediterranean type climate at Mt. Carmel characterized by dry and hot summers and rainy winters (695 mm/yr at the Bet Oren gaging station).

Floods in Nahal Oren generate after a cumulative rainfall of 120-150 mm (Wittenberg et al. 2007). Large floods result from rainstorms of >100 mm. The flows in the ephemeral channel of Nahal Oren, are commonly characterized by rapid rise in water level, a peak discharge within a few tens of minutes, and a swift recession followed by a relatively long "tail". Runoff volumes are typically tens to a few hundred thousand m^3. The typical lag time is generally a few hours, depending on the antecedent soil moisture and rainstorm characteristics. Flow event duration ranges between several hours to several days, thereafter the channel returns to its previous dry condition. The duration and recession of the floods is relatively long due to the drainage of the relatively large water storage of the basin and the increased discharge of two springs during winter, which feed a temporal base flow lasting up to 2-3 weeks after large floods. Annual rainfall-runoff ratio is 3-4% (Wittenberg et al. 2007).

Rainfall and flows in the Mediterranean, ephemeral, mountainous stream of Upper Nahal Oren basin (18 km^2) are monitored using 4 rain-gauges and a hydrometric station at the outlet, since 2001. The 2010 fire burnt 2500 hectares, – about 35% of the basin area, all of which are forested or open areas. This configuration enables a comparison between the hydrological characteristics of the basin pre- and post-fire, as well as to follow the resilience of the basin and returning to the natural rates due to the rehabilitation of the vegetation cover.

Results and concluding remarks

The results indicate that: (a) The first floods during the 3 years after the fire (2010-2013) generated after rainfall amounts of 52-65 mm and after 23-55 mm (39 mm in average), for the following winter floods in comparison to 120-150 mm and 50-60 mm, respectively, prior to the fire. Since 2014, these values increased again to >100 mm for the first flood and to 40-62 mm for the following floods. (b) The number of flow events >0.2 $m^3 s^{-1}$ increased from 2-6 flows per year (3.8 flows/yr in average) pre-fire (2001-2010) to 5.7 flows/yr post-fire (2011-2013) right after the fire (an increase of about 50%). During the years -2014-2016, the average number of flows returned to 3.7 flows/yr. (c) Post-flood base flows shortened from an average of 7.2 days pre-fire to about 2.7 days post-fire. The flows during 2010-12 had no base-flows at all.

These results show that the Upper Nahal Oren Basin became more responsive to rainfall after the fire i.e., generates runoff after smaller rainfall amounts for the first seasonal flood as well as for the following winter floods. These are explained by the absence of the vegetation cover, the disturbance/disappearance of the organic A horizon of the soil, the exposure of the finer B or C horizons and the soil water repellency/hydrophobicity development of layer (Doerr et al. 2000; Tessler et al. 2012), all of which result in decrease of infiltration. These contribute to shortening of the lag time between rainfall and flows and an increase in rainfall/runoff ratio. The decrease in post-flood base-flow duration is explained by the decrease in deep infiltration into the shallow and alluvial aquifers, which in turn, result in decrease in discharge of the springs and seepages along the channel.

The resilience of the various hydrological characteristics of the basin after the fire took 3-5 years until they returned to the natural, pre-fire values along with the recovery of the vegetation cover.

References

Candela A, Aronica G, Santoro M (2005) Effects of forest fires on flood frequency curves in a Mediterranean catchment. Hydrological Science Journal 50:193-206

Doerr SH, Shakesby RA, Walsh RPD (2000) Soil hydrophobicity: its causes, characteristics and hydro-geomorphological significance. Earth Science Reviews 51:33-65

Ferreira AJD, Coelho COA, Boulet AK, Leighton-Boyce G, Keizer JJ, Ritsema CJ (2005) Influence of burning intensity on water repellency and hydrological processes at forest and shrub sites in Portugal. Australian Journal of Soil Research 43:327-336

Lavabre J, Torres DS, Cernesson F (1993) Changes in the hydrological response of a small Mediterranean basin a year after a wildfire. Journal of Hydrology 142:273-299

Mayor AG, Bautista S, Llovet J, Bellot J (2007) Post-fire hydrological and erosional responses of a Mediterranean landscape: seven years of catchment-scale dynamics. Catena 71:68-75

Shakesby RA (2011) Post-wildfire soil erosion in the Mediterranean: Review and future research directions. Earth Science Reviews 105:71-100

Shakesby RA, Doerr SH (2006) Wildfire as a hydrological and geomorphological agent. Earth Science Reviews 74:269-307

Tessler N, Wittenberg L, Greenbaum N (2012) Soil water repellency persistence after recurrent forest fires on Mount Carmel, Israel. International Journal of Wildland Fires, http://doi.org/10/1071/WF12063

Wittenberg L, Kutiel H, Greenbaum N, Inbar M (2007) Short-term changes in the magnitude, frequency and temporal distribution of floods in the Eastern Mediterranean region during the last 45 years — Nahal Oren, Mt. Carmel, Israel. Geomorphology 84:181-191

11th World Congress on Water Resources and Environment (EWRA 2019)
"Managing Water Resources for a Sustainable Future", 25-29 June 2019, Madrid, Spain

Towards reducing model error in flow predictions in ungauged basins via a Bayesian approach

C. Prieto[1,2,3*], N. Le Vine[2,4], D. Kavetski[5], E. García[1], C. Álvarez[1], R. Medina[1]
[1] Environmental Hydraulics Institute "IHCantabria", Universidad de Cantabria, Santander, Spain
[2] Department of Civil and Environmental Engineering, Imperial College London, UK
[3] Department of Civil Engineering, Bristol University, UK
[4] Swiss Re, Armonk, NY, USA
[5] School of Civil, Environmental and Mining Engineering, University of Adelaide, SA, Australia
* e-mail: prietoc@unican.es

Introduction

Flow predictions in ungauged basins (PUBs) remain an elusive challenge in hydrological sciences and engineering, even with the advances achieved during the "PUB decade" (Hrachowitz et al. 2013). Meeting this challenge is made difficult by the uncertainty in the "regionalization" model used to transpose hydrological data from gauged to ungauged basins (e.g. Wagener and Wheater 2006), and by the uncertainty in the hydrological model used to predict streamflow in the ungauged basin (Clark et al. 2011). Traditionally, regionalization proceeded by transferring the parameters of a hydrological model from gauged basins to the ungauged basin. A more recent approach to regionalization is to extrapolate the hydrological characteristics (flow indices) of a catchment rather than its fitted hydrological model parameters (see Wagener and Montanari 2011). Many advances have been made in the last decade in flow indices selection (e.g. using principal components analysis; Olden and Poff 2003) and regionalization (e.g. regression via Random Forest instead of linear regression; Snelder et al. 2009). Once regionalized flow indices are available, conditioning the hydrological model parameters on regionalized flow indices via a Bayesian approach has proven to be advantageous to quantify and reduce the uncertainty in the hydrological model streamflow predictions (e.g. Bulygina et al. 2009; Blöschl et al. 2013). The approach rests on the assumptions that both regionalization model and hydrological model are adequate for a selected ungauged catchment; and hence requires devising tests to evaluate the assumptions (Wagener and Montanary 2011).

Our study has the following objectives:

1. Incorporate new developments in flow indices selection and regionalization into a Bayesian framework to condition hydrological model parameters and flow predictions in ungauged catchments; and
2. Develop two statistical tests (DistanceTest and InfoTest) to evaluate a priori (i.e. prior to any conditioning of hydrological model parameters) the adequacy of hydrological and/or regionalization models for a catchment. The methodological developments are shown for catchments in Northern Spain.

Materials and methods

First, 103 flow indices available in gauged catchments are reduced to the most significant Principal Components (PCs) via the broken stick method (Jackson 1993). Second, a probabilistic regionalization model relating catchment descriptors to catchment flow PCs is developed using Random Forests augmented with a residual error model. Third, the derived regionalization model is applied to ungauged basins to predict the corresponding flow PCs using available catchment descriptors. Fourth, a selected hydrological model, PDM (Moore 2007), is applied to estimate flow PCs (with uncertainty) for the ungauged catchments, when model parameters are sampled from an a priori parameter ranges. Fifth, the adequacy of the regionalization, the hydrological model, and their combination are evaluated via two proposed statistical tests - DistanceTest and InfoTest. DistanceTest quantifies whether a model (regionalization,

hydrological, or their combination) is likely to reproduce catchment flow index PCs, and InfoTest evaluates how much information is added by a model over a prior knowledge about catchment flow index PCs. A model is defined as adequate if it passes both tests. Sixth, provided the adequacy tests are passed for both regionalization and hydrological models in a selected ungauged catchment, the hydrological model parameters are conditioned on the regionalized flow index PCs to predict the time series of flows in the ungauged catchment.

Results and concluding remarks

Application of the techniques in Norther Spain yielded the following findings:

1. 103 flow indices can be reduced to 4 PCs to explain 87% of flow index variance;
2. The regionalization error is 12-16% of the observed flow PCs;
3. The regionalization model is adequate in 75% of the catchments, while the hydrological model is inadequate in most of the catchments;
4. Improving regionalization model when hydrological model passes the adequacy tests leads to an improvement in flow prediction;
5. However, improving regionalization model when hydrological model is *not* adequate does not result in better predictions.

Therefore, the model adequacy tests may be considered as a prerequisite to attain meaningful and high quality flow predictions in ungauged catchments. Finally, the adequacy tests allow identifying the major source of predictive error - hydrological model, regionalization model, or both. In the case study presented here, the hydrological model is identified as a dominant source of error, and hence priority should be given to hydrological model improvements before adjusting the regionalization model.

References

Blöschl G, Sivapalan M (1995) Scale issues in hydrological modelling - a review. Hydrological Processes 9(3-4):251–290. doi: 10.1002/hyp.3360090305

Bulygina N, McIntyre N, Wheater H (2009) Conditioning rainfall-runoff model parameters for ungauged catchments and land management impacts analysis. Hydrology and Earth System Sciences 13(6):893-904. doi: 10.5194/hess-13-893- 1182 2009

Clark MP, Kavetski D, Fenicia F (2011) Pursuing the method of multiple working hypotheses for hydrological modeling, Water Resour. Res. 47:W09301, 1205. doi: 10.1029/2010WR009827

Hrachowitz M, Savenije HHG, Blöschl G et al. (2013) A decade of Predictions in Ungauged Basins (PUB) – a review. Hydrological Sciences Journal 58(6):1198-1255. doi: 10.1080/02626667.2013.803183

Jackson DA (1993) Stopping Rules in Principal Components Analysis: A Comparison of Heuristical and Statistical Approaches. Ecology 74:2204-2214. 1251 doi: 10.2307/1939574

Moore RJ (2007) The PDM rainfall-runoff model. Hydrology and Earth System Sciences 11(1):483-499. doi: 10.5194/hess-11-483-2007

Olden JD, Poff NL (2003), Redundancy and the choice of hydrologic indices for characterizing streamflow regimes. River Res. Applic. 19:101–121. doi: 10.1002/rra.700

Snelder TH, Lamouroux N, Leathwick JR, Pella H, Sauquet E, Shankar U (2009) Predictive mapping of the natural flow regimes of France. Journal of Hydrology 373(1):57-67

Wagener T, Wheater HS (2006) Parameter estimation and regionalization for continuous rainfall-runoff models including uncertainty. Journal of Hydrology 320:132–154

Wagener T, Montanari A (2011) Convergence of approaches toward reducing uncertainty in predictions in ungauged basins, Water Resour. Res. 47:W06301. doi:10.1029/2010WR009469

11th World Congress on Water Resources and Environment (EWRA 2019)
"Managing Water Resources for a Sustainable Future", 25-29 June 2019, Madrid, Spain

Application of an analytical model framework to obtain summer streamflow distribution in Swiss catchments

A.C. Santos[1,2], M.M. Portela[2*], A. Rinaldo[3], B. Schaefli[4]
[1] *Ecole Polytechnique Fédérale de Lausanne (EPFL), Lausanne, Switzerland*
[2] *Civil Engineering Research and Innovation for Sustainability (CERIS), Instituto Superior Tecnico (IST), University of Lisbon (UL), Portugal*
[3] *Dipartimento di Ingegneria Civile Edile e Ambientale, Universit a degli studi di Padova, Padova*
[4] *Faculty of Geosciences and Environment, University of Lausanne, Lausanne, Switzerland*
** e-mail: maria.manuela.portela@tecnico.ulisboa.pt*

Introduction

In hydrology, the probability distribution of daily streamflow is usually represented as flow duration curves (FDCs) instead of a probability density functions (pdfs). FDCs assign an exceedance probability to each discharge value, which corresponds to the complement of the cumulative distribution function (cdf).

Daily FDCs can be obtained in different manners, the most straightforward method being the assignment of empirical probabilities to observed ranked streamflow data (yielding empirical FDCs). Alternatively, they can be obtained from hydrological models that are useful in cases of lack of data, or to understand the processes that drive streamflow production and to predict the effects of changes in those conditions. Among the existing methods, there is the analytical model framework proposed by Botter et al. (2007) that is simple, relatively easy to compute and requires few data but is still physically based.

Materials and methods

The model framework was applied to obtain FDCs for the summer streamflows (from June 1st to August 31st) in the 25 Swiss catchments schematically represented in Figure 1. The catchments are under natural conditions and present a wide range of hydrological regimes (Santos et al. 2018). The application of the model requires daily discharge and precipitation data, as well as land use data to calculate the precipitation losses.

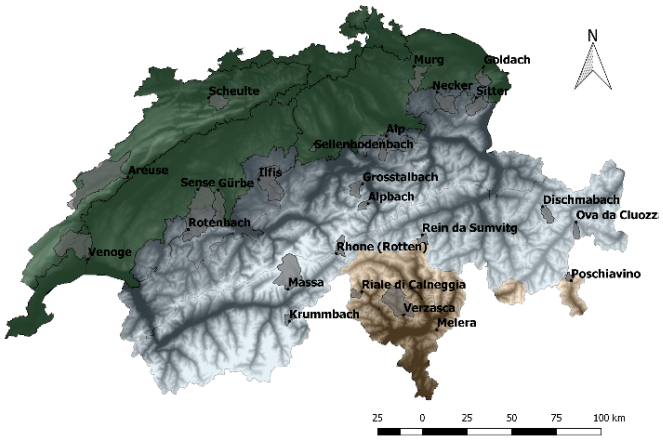

Figure 1. Schematic location of the 25 Swiss case studies.

The analytical model framework for probabilistic characterization of rainfall-drive daily discharges developed by Botter et al. (2007) is based on a previous model proposed by Rodriguez-Iturbe et al. (1999) that represents the dynamics of soil moisture at a point as a result of a deterministic state-dependent loss function, combined with stochastic increments triggered by rainfall events.

Assuming a linear recession model, the FDCs follow a gamma distribution characterized by few parameters: the mean depth of daily precipitation, the frequency of precipitation events that produce

discharge, the area and the mean residence time (the inverse of the recession coefficient) of the catchment. Later this framework extended to nonlinear recession models (Botter et al. 2009).

The parameters of the model related to precipitation (i.e., the frequency and the average depth of the discharge-producing rainfall events) were estimated directly from the observed data whereas the recession parameters were estimated using a traditional recession analysis method (RAM) and by maximum likelihood estimation (MLE) for both the linear and the nonlinear recession models.

The performance of the model framework was assessed by the maximum difference between the values of the empirical and of the modeled cumulative distributions (i.e. Kolmogorov-Smirnov distance).

Results and concluding remarks

Figure 2 exemplifies the results achieved based on three case studies with different hydrological regimes for linear and nonlinear models with recession parameters estimated by RAM or MLE.

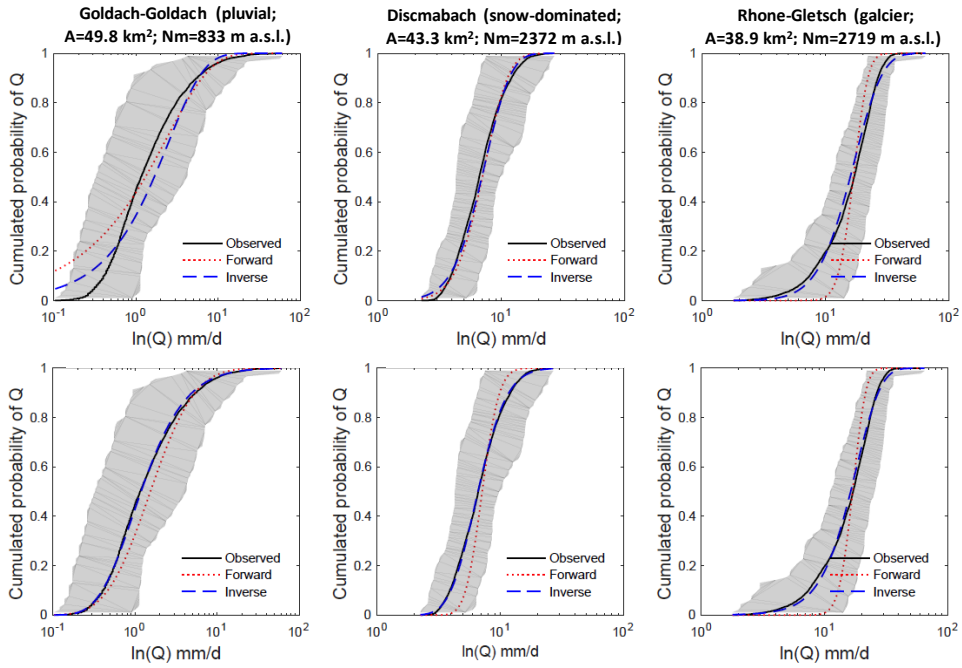

Figure 2. Results from the linear (top) and the nonlinear (bottom) models for the summer discharges in three catchments. The shaded area between the cdf envelopes represents the natural variability of the discharges (for each catchment between brackets: hydrological regime, area and mean elevation).

The results achieved show that the analytical model framework applied to estimate summer streamflow probability distributions in several Swiss case studies performs well across a wide range of discharge regimes. Given that the original framework was developed by Botter et al. (2007) for purely rainfall-driven regimes, the new contribute to expand its applicability to mountainous regions increases its interest. The detailed comparison between the performance of the linear and the nonlinear model formulation shows that the description of Swiss summer flows strongly benefits from using a nonlinear storage-discharge relationship, in particular for catchments with summer low flow.

References

Botter G, Porporato A, Rodriguez-Iturbe I, Rinaldo A (2007) Basin-scale soil moisture dynamics and the probabilistic characterization of carrier hydrologic flows: Slow, leaching-prone components of the hydrologic response. Water Resources Research 43:w02417. doi: 10.1029/2006WR005043

Botter G, Porporato A, Rodriguez-Iturbe I, Rinaldo A (2009) Nonlinear storage discharge relations and catchment streamflow regimes. Water Resources Research 45(10). doi: 10.1029/2008wr007658

Rodriguez-Iturbe I, Porporato A, Ridol_L, Isham V, Cox DR (1999) Probabilistic modelling of water balance at a point: the role of climate, soil and vegetation. Proceedings of the Royal Society A: Mathematical, Physical and Engineering Sciences, 455(1990):3789-3805. doi: 10.1098/rspa.1999.0477

Santos AC, Portela MM, Rinaldo A, Schaefli B (2018) Analytical flow duration curves for summer streamflow in Switzerland. Hydrology and Earth System Sciences 22(1):2377-2389. https://doi.org/10.5194/hess-22-2377-2018

11th World Congress on Water Resources and Environment (EWRA 2019)
"Managing Water Resources for a Sustainable Future", 25-29 June 2019, Madrid, Spain

Slackwater sediment in a gully network records the increase in maximum probable precipitation due to climate change (Jaén, Spain)

J.D. del Moral-Erencia, P.J. Jiménez-Ruíz, F.J. Pérez-Latorre, P. Bohorquez*
Departamento de Ingeniería Mecánica y Minera, Universidad de Jaén, 23001 Jaén, Spain
** e-mail: patricio.bohorquez@ujaen.es*

Introduction

The number and magnitude of flash floods in southern regions of Spain affected by the Mediterranean climate have increased, becoming a problem of great social interest due to the damages and derived economic losses (European Environment Agency 2017). Critical elements at risk may include water channel, sewerage, levee and transport infrastructure that affect the normal functioning of society. The probable maximum precipitation (*PMP*) is a key input parameter regarding the civil engineering calculations of such systems which involve the modelling of the rainfall-runoff process, flow routing and generation of flooding maps (Sánchez and Lastra 2011). The observed increase in *PMP* also implies a higher probable maximum flood (*PMF*), flow velocity and stage, which rise the erosive potential of the flow and sediment transport. Here, we propose a simple method to calculate the *PMF* and *PMP* associated to extreme hydrological events using remotely sensed slackwater sediments as key input data (Bohorquez 2016).

Materials and methods

We consider two kinds of hydrological problems: Direct and Inverse problems. On the one hand, the input hydrological data of the *direct problem* is the known discharge or precipitation, which requires the availability of streamflow records or rain gauge data, respectively. The main output data of the computational model is the inundated area by the flood. On the other hand, in the *inverse problem* we know the flooded area from satellite imagery but the water discharge and precipitation are unknowns (ungauged basin).

The most relevant study case is the inverse problem that we solve in the following steps:

- First, we propose a novel way to determine the observed inundation area, A_{obs}, through slackwater deposits detected in high-resolution satellite imagery (pixel size < 1 m). Hence, the flooded area can be delimited post-event by using available remote sensed flood evidence.
- Second, by applying standard methods of paleohydrology, we then infer the peak water discharge required to inundate the observed area, *Q*, as an output (Bohorquez 2016). To this end, we run the numerical simulation by prescribing the value of *Q*, which yield a modelled inundation area A_{mod} as a function of *Q*. The numerical simulation of flooding areas is done with a two-dimensional, unsteady, shallow-water model implemented in IberPlus (García-Feal et al. 2018).
- Third, we search the optimal value of *Q*, denoted by *PMF*, that maximises the critical success index. *CSI* measures the quality of the simulated inundation area (Bohorquez and del Moral-Erencia 2017):

$$CSI = (A_{obs} \cap A_{mod}) / (A_{obs} \cup A_{mod}) \quad (1)$$

  Note that *CSI* determines the overlap between the observed and simulated flooded areas, varying in the 0-1 range. A value close to 0 indicates that no correlation exists between simulation and reality, while 1 implies a perfect agreement. In this work, we achieved values as high as *CSI*=0.9.
- Subsequently, the spatial-averaged *PMP* is obtained from the drainage area of the upstream basin, A_{drain}, and the inferred *PMF* under the condition of water repellency of surface soils:

$$PMP = PMF/A_{drain} \quad (2)$$

- Finally, the minimum accumulated precipitation is $TPMP = T \times PMP$, where the time of concentration *T* is estimated from the kinematic wave (or rational) method by Morgali and Linsley (1965). Note that a longer duration of the real rainfall event with intensity *PMP* yields the same *PMF*.

Results and concluding remarks

We analysed three sub-basins of the Guadalquivir River (southern Spain) dedicated to agricultural lands which have experienced an increase of runoff and streamflow in the last decades. In the margins of the gully floodplains, fine sediments have deposited through time, allowing us to quantify the most extreme hydrological event based on a complete set of orthophotos since 1946 following a methodology analogous to our urban area studies (Bohorquez 2016; Bohorquez and del Moral-Erencia 2017). Sediment deposits resulted from recent flash floods in December 2009 and May 2011, but their fast temporal scale and high variability in space impede the measurement of relevant hydrological variables.

The application of the inverse method provides *PMF* and *PMP* at multiple spatial scales, as summarised in Table 1. The size of the drainage areas (0.4-555 km^2) and *PMF* (1.5-533 m^3/s) varies in three orders of magnitude, showing the general capability of our formulation. The precipitation intensity exhibits a strong dependence on the location of the study site, even for the same hydrological event. In December 2009, the lowest value arose in Porcuna (2.9 mm/h) while a higher intensity of 10.6 mm/h was inferred in the neighbour sub-basin of Arjona. Surprisingly, in the upper reach of Ibros basin, the strength of the precipitation in May 2011 reached the maximum of 37.4 mm/h. Such a hydrological event caused significant damages.

Table 1. Estimated values of water discharge and precipitation at the Salado de Porcuna, Salado de Arjona and Ibros Basins in Southern Spain. In Arjona and Ibros we solved the inverse problem sequentially and analysed multiple sub-basins with different sizes (denoted from I to IV).

	A_{drain} (km^2)	PMF (m^3/s)	PMP (mm/h)	T (h)	TPMP (mm)	GTPMP (mm)
Porcuna	670	533	2.9	7.1	20.2	36.3
Arjona	307	460	5.4	5.6	30.2	38.3
I	87.2	195	8.1	5.6	45.1	38.2
II	191	180	3.4	5.6	19.0	37.5
III	15.3	45	10.6	5.6	59.3	42.4
IV	13.7	40	10.5	5.6	58.9	40.5
Ibros	23.3	170	26.3	1.9	49.1	61.1
I	0.41	1.5	13.0	1.9	24.3	31.4
II	0.66	4.5	24.6	1.9	46.0	80.6
III	1.54	4.1	9.6	1.9	17.9	33.7
IV	0.26	2.7	37.4	1.9	71.0	98.5

Overall, the values inferred with the indirect approaches are similar to those measured with rain gauges by the regional Government of Andalusia, see the modelled (TPMP) and recorded accumulated precipitation (GTPMP) in Table 1. TPMP is lower than GTPMP because the time of concentration *T* given by the rational method is a lower bound of the event duration. Also, we compared with the Spain05 database that provides the precipitation in a daily format for the period 1971-2011 with a resolution of 0.11 degree, but the spatial resolution of Spain05 is too coarse to capture the extreme hydrological events studied in the current work.

Acknowledgements: This work was supported by the Spanish Ministry of Science, Innovation and Universities (MICINN/FEDER, UE) under Grant SEDRETO CGL2015-70736-R. J.D.d.M.E. was supported by the PhD scholarship BES-2016-079117 (MINECO/FSE, UE) from the Spanish National Programme for the Promotion of Talent and its Employability (call 2016).

References

European Environment Agency (2017) Climate change, impacts and vulnerability in Europe 2016: An indicator-based report. Publications Office of the European Union, Luxembourg

Sánchez FJ, Lastra J (2011) Guía metodológica para el desarrollo del Sistema Nacional de Cartografía de Zonas Inundables. Ministerio de Medio Ambiente, Medio Rural y Marino

Bohorquez P (2016) Paleohydraulic reconstruction of modern large floods at subcritical speed in a confined valley: proof of concept. Water 8 (12):567. doi:10.3390/w8120567

Bohorquez P, Del Moral-Erencia JD (2017) 100 years of competition between reduction in channel capacity and streamflow during floods in the Guadalquivir River (Southern Spain). Remote Sensing 9(7):727. doi:10.3390/rs9070727

García-Feal O, González-Cao J, Gómez-Gesteira M, Cea L, Domínguez MJ, Formella A (2018) An accelerated tool for flood modelling based on Iber. Water 10(10):1459. doi:10.3390/w10101459

11th World Congress on Water Resources and Environment (EWRA 2019)
"Managing Water Resources for a Sustainable Future", 25-29 June 2019, Madrid, Spain

Mapping risk of gully erosion in Mediterranean olive groves affected by climate change (Jaén, Spain)

P.J. Jimenez-Ruiz, P. Bohorquez*, J.D. del Moral-Erencia, F.J. Perez-Latorre
Departamento de Ingeniería Mecánica y Minera, Universidad de Jaén, 23001 Jaén, Spain
** e-mail: patricio.bohorquez@ujaen.es*

Introduction

Runoff intensity and gully dimension have achieved undesirable levels in southern olive crops of Spain as a consequence of the increase in the magnitude of extreme hydrological events by climate change (European Environment Agency 2017), agriculture use and soil management in the crops (Burguet et al. 2016). Both factors together with the water repellence of surface soils have induced a transport capacity of surface water higher than the catchment sediment budget, and this deficit has provoked non-sustainable soil erosion rates. The precise quantification of the extent and volume of the gully drainage network exhibits several technical difficulties that can now be overcome using the approach developed in the current work.

Using as input parameter the probable maximum precipitation (PMP), which can be derived with the paleohydrological methods proposed in our companion talk and previous works (Bohorquez and del Moral-Erencia 2017), a high-resolution DEM (Digital Elevation Model) based on LiDAR (Light Detection and Ranging) elevations, and a physically-based distributed hydrological model (García-Feal et al. 2018), we are able to locate the drainage gully network and measure its surface area and the local gully depth with unprecedented accuracy. Also, we can identify the critical areas at high-risk of erosion as well as the transport capacity of fine sediments due to soil erosion. The current methods are not limited to a particular study site and, hence, could be applied in many Mediterranean olive groves with similar soil degradation by erosion.

Materials and methods

To apply the proposed procedure, we may distinguish two types of sites:

- Gauged basin with known maps of probable maximum precipitation. Such a map is a key input data to the distributed hydrological model that solves for the local values of the flow depth and velocity vector in each cell of the computational mesh, as explained below.
- Ungauged basin with unknown precipitation or subject to a sudden, extreme hydrological event as flash floods. By applying standard methods of paleohydrology, we have shown in a companion work how to infer the spatial-averaged PMP in the basin or, more accurately, the map of PMP based on the recursive analysis of the multiple sub-basins.

The next step consists of running a two-dimensional, unsteady, rainfall-runoff, shallow-water model implemented in the free software IberPlus (García-Feal et al. 2018). In the pilot basin of Ibros (Jaén, Southern Spain), that covers a 12x4 km^2 drainage area, we worked with a 2 m spatial resolution (10 M cells). We created a 2 m DEM from a LiDAR point cloud with the spatial resolution lower than 1.4 m and root-mean-square (maximum) error of 0.2 m (0.4 m). Also, we conducted a sensitivity analysis using a 5 m coarser mesh. To speed up the numerical simulation, we simulated in a Tesla K40 GPU (Graphics Processing Unit).

Subsequently, we post-processed the hydraulic data. On the one hand, the map of bank-full flow depth serves to characterise the gully dimensions that were sculpted by surface waters during past, extreme hydrological events. On the other hand, contour maps of the dimensional shear stress (or Shields parameter) determine the location of the areas at high risk of erosion of sand-mud cohesive mixture (or non-cohesive sediments). Finally, the evaluation of the soil erosion rate in the basin is undertaken through Walder's (2015) dimensionless erosion laws which may account for possible uncertainties of the critical shear stress for the inception of erosion.

Results and concluding remarks

On May 2011, the Ibros basin experienced the most severe flash flood ever documented due to a brief (< 3 h) and intense rainfall (mean $\mathrm{PMP} = 26.2$ mm·h^{-1}) produced by reduced area storms. Steep slopes along the streams (3.5%) and across the basin (17.6%) induced high-speed flows ($1.4 < v < 3.8$ m·s^{-1}). The hydrological variables of such flash flood had to be reconstructed using paleohydrology because the short duration, the non-uniform distribution of the precipitation ($10 < \mathrm{PMP} < 37$ mm·h^{-1}) and the small area (25.6 km^2) impeded in-situ measurements. Also, conventional tillage of the olive groves over 94.6% of the drainage area favoured sediment entrainment, leading to suspended load in the main torrents.

Flood maps of local flow depth allowed the automatic detection of the gully bankfull depth for the inferred PMP (see Figure 1a). Gullies occupy 17.9% of the drainage area and a volume of 0.47 M m^3 (1.26 Mt of sediment). Furthermore, the map of the shear stress yields a potential area of sand erosion of 22.3% for sands and 23.7% for cohesive sediments. The 7% of the areas at risk of erosion lie outside of the existing gullies. The sensitive analysis regarding the spatial resolution of the computational grid shows a slight underestimation of the actual gully area (13.7% vs 17.9%) and erosion risk areas (16.2% vs 22.3%). Also, we quantified the effects of an increase in rainfall to the maximum value 37 mm·h^{-1} reconstructed in the upper basin for the May 2011 episode and found out at risk about 27.3-28% of the basin. Extreme rainfalls may lead to an unprecedented increase in gullies shortly.

Lastly, we used Walder's (2015) equation to evaluate the soil erosion rate, which yields the mean value E=0.117 mm/h in overland flows (> 5 cm deep). As we are able to quantify the local values of E, one can thus establish a proper criterion to detect the most dangerous area at high risk of erosion, as shown in Figure 1b.

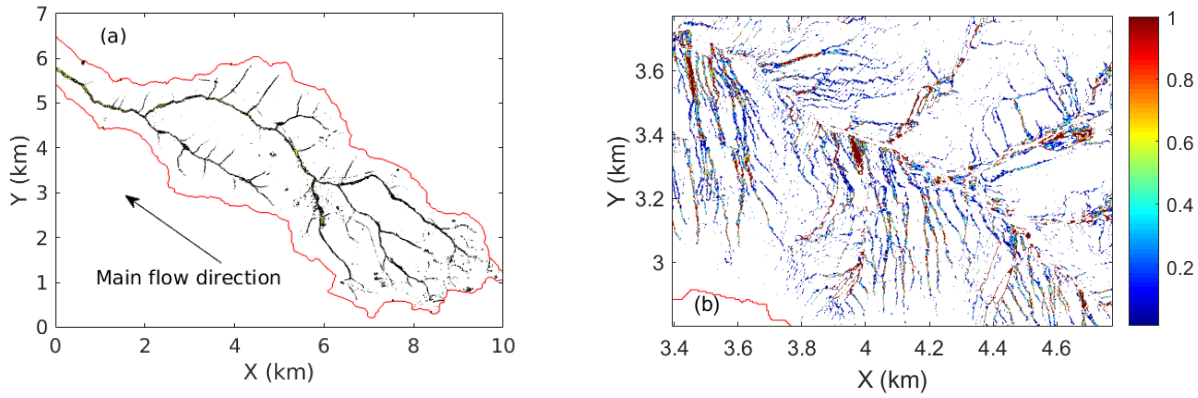

Figure 1. (a) Visualization of the main torrents and gullies deeper than 0.2 m in black. (b) Zoom of the soil erosion rate E (mm/h) in overland flows shallower than 5 cm. Areas at high risk of erosion are coloured in red.

Acknowledgements: This work was supported by the Spanish Ministry of Science, Innovation and Universities (MICINN/FEDER, UE) under Grant SEDRETO CGL2015-70736-R. P.R.J. was supported by the European Social Fund and the University of Jaén. J.D.d.M.E. was supported by the PhD scholarship BES-2016-079117 (MICINN /FSE, UE) from the Spanish National Programme for the Promotion of Talent and its Employability.

References

European Environment Agency (2017) Climate change, impacts and vulnerability in Europe 2016: An indicator-based report. Publications Office of the European Union, Luxembourg

Burguet M, Taguas EV, Cerdà A, Gómez JA (2016) Soil water repellency assessment in olive groves in Southern and Eastern Spain. Catena 147:187-195. doi:10.1016/j.catena.2016.07.005

Bohorquez P, Del Moral-Erencia JD (2017) 100 years of competition between reduction in channel capacity and streamflow during floods in the Guadalquivir River (Southern Spain). Remote Sensing 9(7):727. doi:10.3390/rs9070727

García-Feal O, González-Cao J, Gómez-Gesteira M, Cea L, Domínguez MJ, Formella A (2018) An accelerated tool for flood modelling based on Iber. Water 10(10):1459. doi:10.3390/w10101459

Walder JS (2015) Dimensionless erosion laws for cohesive sediment. Journal of Hydraulic Engineering 142(2):04015047. doi:10.1061/(ASCE)HY.1943-7900.0001068

11th World Congress on Water Resources and Environment (EWRA 2019)
"Managing Water Resources for a Sustainable Future", 25-29 June 2019, Madrid, Spain

Determination of reservoir inflows from river basin using Soil and Water Assessment Tool (SWAT) and SWAT-CUP: A case study

C. Praveen Kumar[1], V.D. Regulwar[1,2], S.N. Londhe[2], V. Jothiprakash[1*]
[1] Department of Civil Engineering, Indian Institute of Technology (IIT) Bombay, Mumbai, 400076, India
[2] Department of Civil Engineering, Vishwakarma Institute of Information Technology, Pune, 411048, India
* e-mail: vprakash@iitb.ac.in

Introduction

In this study, Soil and Water Assessment Tool (SWAT), a widely used semi distributed model (Arnold et al. 1998; Srinivasan et al. 2010; Saraf and Regulwar 2018) is adopted for estimating streamflow in Upper Godavari (UG) basin, a sub basin of Godavari river, India. The UG basin receives less rainfall compared to other sub basins of Godavari catchment, which is a major source of water for agricultural dominant land within the basin. Availability of large storage capacity in small groups of reservoirs in the catchment, improper measurements of runoff, gaps in runoff observations gives additional challenges to model the river system. Therefore, there is a strong need to determine exact potential of the watershed up to Jayakwadi dam located at the outlet of the UG basin. Secondly, streamflow estimations in large river catchments is becoming a serious issue in recent decades due to the obstruction of natural river flow by large storage structures constructed across the rivers. Improper estimation can lead to the false results which can further take hydrologic modellers near to the non-realistic results leading to failure of water resources management (Ikhar et al. 2018). Hence, the main objective of the present study is to estimate the streamflow in UG basin using SWAT model by considering several large reservoirs located within the catchment. Further, quantification of parameter uncertainty in hydrological modeling is necessary to obtain its sensitivity information. SWAT requires a large number of input parameters, which complicates model parameterization and calibration. SWAT-CUP provides a decision-making framework that incorporates a semi-automated approach (SUFI2, ParaSol) using both manual and automated calibration and incorporating sensitivity and uncertainty analysis especially with reservoir details.

Materials and method

The Godavari River originates in the Western Ghats of central India near Nashik in Maharashtra State. The Longitude and Latitude of Upper Godavari (UG) ranges from 73° 24' to 83° 4' E and 16° 19' to 22° 34' N respectively. It flows for 1,465 km, first eastwards across the Deccan Plateau then turns southeast, to flow into the Bay of Bengal. The Godavari River from start to Jayakwadi dam named as UG basin is studied. There are around six large reservoirs in the upstream of Jayakwadi dam and their presence are considered in SWAT model. The hydrologic cycle of the SWAT model is based on the water balance equation:

$$SW_t = SW_o + \sum_{i=1}^{t} (R_{day} - Q_{surf} - E_a - w_{seep} - Q_{gw}) \quad (1)$$

where SW_t is the final soil water content, SW_o is the initial soil water content, *t* is the time (days), R_{day} is the amount of precipitation on day *i*, Q_{surf} is the amount of surface runoff on day *i*, E_a is the amount of evapotranspiration on day *i*,. The water balance equation for reservoirs impoundments shown in Equation 2:

$$V = V_{stored} + V_{flow\ in} - V_{flow\ out} + V_{pcp} - V_{evap} - V_{seep} \quad (2)$$

where V is the water storage in the reservoir at the end of each day; V_{stored} is the water stored volume in the reservoir at the beginning of a day; $V_{flow\ in}$ and $V_{flow\ out}$ is the volume of water entering and flowing out of the reservoir during a day, respectively; and V_{pcp}, V_{evap}, and V_{seep} is the precipitation, evaporation and

seepage, respectively. In SWAT, with the help of delineated watershed, the LULC, SOIL and SLOPE map is generated to create HRUs. After feeding the weather data into SWAT, model parameters were optimised by studying its sensitivity analysis and model is run to get the simulated streamflow. SUFI2, an uncertainty algorithm of SWAT-CUP has been adopted to study parameter sensitivity analysis. The model performance has been analysed using the statistics of NSE and R^2 during the calibration and validation process.

Results and concluding remarks

In this study, the UG basin considered as the study area. The SWAT model can be used without considering reservoirs or including reservoirs located in the basin into model simulations. For realistic estimation of runoff at the outlet of the Jayakwadi dam, six major dams namely Gangapur, Mukane, Mula, Bhandardara, Darana and Pachagoan which holds the significant quantity of water within the basin has been considered while carrying SWAT modeling. The salient features, inflow and outflow of the major dams, the rainfall and temperature data is used to estimate streamflow using SWAT model up to Jayakwadi Dam. The six most sensitive parameters were identified by studying parameter sensitivity analysis using sequential uncertainty fitting algorithm (SUFI-2). The proposed evaluation criteria for uncertainty analysis in this study includes *R*-factor, *P*-factor, computation efficiency, and performance of best estimates. The SWAT model has been calibrated during 1961 to 2009 and validated with the observed data during 2010 to 2013. The time series and scatter plot between observed and SWAT simulated streamflow showed in Figure 1. The performance of model is evaluated using the statistics of R^2 and *NSE*, it is observed to be 0.52 and 0.52 during calibration and 0.65 and 0.64 during validation, respectively (Table 1).

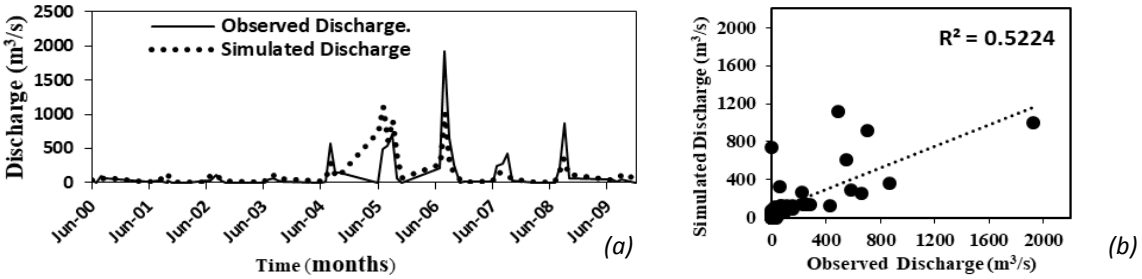

Figure 1. (a) Time series and (b) Scatter plot of observed and SWAT simulated runoff during calibration period.

Table 1. Performance measures of SWAT model.

Performance measures	Calibration	Validation
R^2	0.52	0.65
NSE	0.52	0.64

Acknowledgments: Authors greatly acknowledge the support of Command Area Development Authority (CADA), Aurangabad, Maharashtra, India for providing reservoirs data. The authors also extend their thanks to India Meteorological Department (IMD), Pune for providing weather data in Upper Godavari basin.

References

Arnold JG, Shriniwasan R, Muttiah RS, Williams JR (1998) Large Area Hydrologic Modelling Assessment Part 1: Model Development. Am. Water. Resour. Assoc. 34(1):73-89

Abbaspour KC, J Yang, I Maximov, R Siber, K Bogner, J Mieleitner (2007) Modelling hydrology and water quality in the pre-alpine/alpine Thur watershed using SWAT. J. Hydrol. 333(2–4):413–430. https://doi.org/10.1016/j.jhydrol.2006.09.014

Ikhar PR, Regulwar DG, Kamodkar RU (2018) Optimal reservoir operation using soil and water assessment tool and genetic algorithm. ISH Journal of Hydraulic Engineering 24(2):249-257. doi: 10.1080/09715010.2017.1417754

Narsimlu B, AK Gosain, BR Chahar (2013) Assessment of future climate change impacts on water resources of Upper Sind River Basin, India using SWAT model. Water Resour. Manage. 27:3647–3662. https://doi.org/10.1007/s11269-013-0371-7

Saraf VR, Regulwar DG (2018) Impact of Climate Change on Runoff Generation in the Upper Godavari River Basin, India. doi: 10.1061/ (ASCE) HZ.2153-5515.0000416

Srinivasan R, X Zhang, J Arnold (2010) Swat ungauged: Hydrological budget and crop yield predictions in the upper Mississippi river basin. Am. Soc. Agric. Biol. Eng. 53(5):1533-1546

11th World Congress on Water Resources and Environment (EWRA 2019)
"Managing Water Resources for a Sustainable Future", 25-29 June 2019, Madrid, Spain

Soil water content measurements with Time Domain Reflectometry (TDR)

A. Papadopoulos*, P. Kofakis, A. Kallioras
School of Mining & Metallurgical Engineering, National Technical University of Athens, Athens, Greece
** e-mail: papadopoulosa@metal.ntua.gr*

Introduction

Time Domain Reflectometry (TDR) constitutes an integrated and well-known technique for soil water content measurements. The main feature of the method is its ability to properly measure the bulk dielectric constant of the soil from the initially measured propagation velocity of a high frequency electromagnetic pulse travelled along the waveguides embedded in that soil (Todoroff et al. 2001). The dielectric constant is typically related to the volumetric water content through an empirical calibration equation (Topp et al. 1980).

The main objective of this study is to expand the manufacturing process of TDR waveguides, to test different constructing materials of the probes and improve the installation techniques of the sensors both in laboratory and field studies. A supplementary goal of the research team is to investigate and monitor the hydrological processes taking place along the height of the vadose zone, through the extracted TDR measurements (Kallioras et al. 2016) An integrated experiment consisting of a cylindrical column and various TDR configurations is established in the premises of Athens Water Supply and Sewerage Company (EYDAP S.A.), as well as in two field agricultural locations in the suburbs of Athens.

Materials and methods

The whole experiment in EYDAP S.A. is integrated within a plexiglass cylindrical column of known dimensions. The column is filled with homogeneous and fine grained quartz sand and is installed on a heavy metallic platform. Both commercial, for point soil moisture measurements, and custom-made TDR sensors are installed against the walls and in the middle of the column respectively. Several infiltration experiments have been made with wetting of the column from above using a sprinkler configuration, while a number of studies have been conducted with wetting of the sand from a hole at the bottom of the column and an upward water front. During the infiltrations, successive measurements of soil moisture profiles within critical saturation conditions and along the length of the column have been recorded. The main characteristic of the resulted TDR waveforms is that the projected travel time of each waveform increases as the dielectric permittivity of the soil increases, due to the higher water content.

The characteristic curve of the quartz sand used in this experiment, which was created originally by the researchers of this study, in conjunction with the results from the TDR measurements, contributed greatly to the delineation of the hydrological processes inside the column during the infiltration and wetting experiments.

A great deal of thought has been invested in improving the manufacturing process and selecting the appropriate constructing materials to developing custom-made TDR waveguides, in terms of qualitative measured results, financial viability and labor. The results so far, have pointed an inclination to high density polyethylene (HDPE) materials for probe construction and flat enameled copper wires for serving as waveguides, while the whole construction process lasts no more than a few hours and can be made by any number of people, as it is relatively simple and requires no physical strength.

A number of experiments has been conducted in the field to test the custom-made probes under real soil conditions and improve the installation technique of the probes underground. TDR is a rather sensitive geophysical method and requires immediate contact between the waveguides and the surrounding soil to provide appropriate results. Undisturbed soil is another factor needs to be taken into consideration, as measurements in a highly disturbed soil will provide results that do not correspond well to the real

conditions of the ground. The installation made in one of our sites using a large and heavy borehole machinery disturbed the surrounding soil around the borehole and several preferential flow paths were created. As a result, the corresponding TDR measurements were highly affected and nearly unusable. On the other hand, when a small hand-operated auger was employed the corresponding results were decent and usable.

Results and concluding remarks

TDR is an appropriate stand-alone or complementary method for qualitative soil water content measurements. It relies on impedance changes and can accurately provide dielectric constant measurements. Its main advantage is its ability to provide real time and continuous measurements of soil water contents, while its most important drawback is that it is highly affected by saline and clay soils and requires an immediate and undisturbed contact between the waveguides and the surrounding material under examination. Several custom-made TDR probes have been constructed and many laboratory and field experiments have been conducted to test the viability of those probes and compare them with commercial ones, as well as to delineate the hydrological processes inside the column and the field vadose zone. The outcome is quite encouraging as the water content is nicely recorded and presented and the results are close to those of the commercial probes and in fact, because the custom ones are tailor-made, can be used in a wider range of applications.

References

Kallioras A, A Khan, M Piepenbrink, H Pfletschinger, F Koniger, P Dietrich, C Schuth (2016) Time-domain reflectometry probing systems for the monitoring of hydrological processes in the unsaturated zone. Hydrogeol J. 24:1297-1309

Todoroff P, Lan Sun Luk J-D (2001) Calculation of in situ soil water content profiles from TDR signal traces. Meas. Sci. Technol. 12:27-36

Topp GC, JL Davis, Annan AP (1980) Electromagnetic determination of soil water content: Measurements in coaxial transmission lines. Water Resourc. Res. 16:574-582

IV. Urban Water Management

11th World Congress on Water Resources and Environment (EWRA 2019)
"Managing Water Resources for a Sustainable Future", 25-29 June 2019, Madrid, Spain

Testing the existence of an Environmental Kuznets Curve for urban water use at river basin scale

A. Expósito[1*], M.P. Pablo-Romero[1,2], A. Sánchez-Braza[1]
[1] Department of Economic Analysis, Universidad de Sevilla, Sevilla, Spain
[2] Universidad Autónoma de Chile, Santiago de Chile, Chile
* e-mail: aexposito@us.es

Introduction

Existing literature has usually highlighted the existence of an inverted U-shaped Environmental Kuznets Curve (EKC) to describe the relationship between economic development and water use levels. EKC shows that water use increases in a first stage of economic development, and decreases after achieving a certain threshold level of income (or development) (Zhao 2017). The study of this relationship offers relevant information for water resources management and planning, especially in those locations where water scarcity and competition for limited water resources constitute serious challenges (e.g., in closed river basins, such as our case study). Despite the study by Katz (2015), which analyses EKC existence individually for agricultural, industrial and domestic sectors, to the best of our knowledge, there has been no systematic study at a river basin scale. In our analysis, urban water includes those water withdrawals for residential (or domestic) and service (public and private) uses, though it might also include water use from small industries, depending on the specific municipality. Using data from a wide sample of municipalities of the Guadalquivir basin (southern Spain), this study aims to carry out a systematic analysis of the relationship between urban water use and indicators of economic development (i.e., income and employment) at river basin scale. The analysis includes other determinants that might also have an impact on urban water use, such as electricity consumption, population density, age and educational level. Thus, this study goes beyond the simple testing for the existence of an EKC for urban water use.

Materials and methods

This study uses data of 336 Andalusia municipalities of the Guadalquivir river basin, including big cities such as Seville, Cordoba and Granada, but also small towns. Data refer to the period 2005 to 2014. Two economic development indicators have been used to analyze their impact on urban water use: income level of the population and total employment. Other variables have been also considered. Data have been collected from the Guadalquivir basin authority and SIMA database (2018).

The water use function to be analyzed in this study may be expressed as follows:

$$W_{it} = A_{it} + \beta_1 Y_{it} + \beta_2 Y_{it}^2 + \beta_3 Y_{it}^3 + \beta_4 EMP_{it} + \beta_5 E_{it} + \beta_6 AG_{it} + \beta_7 EA_i + \beta_8 D_{it} + \beta_9 UR_i + u_{it} \quad (1)$$

where W refers to the urban water use in per capita terms in logs, Y refers to the income per capita in logs, EMP refers to the employment in the municipality related to total population in percentage values, E refers to the electricity consumption per capita in logs, AG refers to the average age in logs, EA to the educational attainment in percentage values, D refers to the density in logs, UR to the percentage urban surface, A represents the sum of the time effect and individual effect, and i and t denote Guadalquivir municipalities and years, respectively. Finally, u is a random error term.

For the study of the stochastic nature of the variables, the Pesaran CD (Pesaran 2004) test was used to test the existence of cross-sectional dependence among the variables. As the results show that this dependence exits, a second generation panel unit root test was used to determinate the order of integration of the time series variables. The CIPS test (Pesaran 2007) shows that variables may be considered stationary in all trends, when considering specification with trends. Therefore, it is adequate to estimate the model in levels for the transformed variables. According to the autocorrelation and homoscedasticity tests performed, the feasible generalized least squares model (FGLS) and the generalized

method of moments (GMM) have been used for estimation.

Results and concluding remarks

Results show that income is a main driver and has a positive effect on urban water use (Table 1). Nevertheless, results do not support the existence of an urban water EKC, or an N-shaped path between the considered variables. Instead, a growing water elasticity with respect to income is observed. Since competition among alternative uses is expected to increase, these results have significant policy implications for the management of the river basin. Measures oriented to reinforce policy measures designed to control demand, along with investments in reducing water conveyance losses would be desirable. With respect to other considered determinants of urban water use, employment rate and energy consumption show non-significant parameters in the estimates. Regarding urbanization and population density, the estimated coefficients show significant positive and negative values, respectively. This shows that effective cross-compliance measures between land and water policy are required, since changes in land uses do impact on the sustainability of urban water use patterns. Regarding population characteristics, population age has positive impacts on the urban water use. On the contrary, higher educational levels tend to reduce the water use, as the educational level is usually related to environmental concerns and attitudes.

Table 1. Results of estimates

	FGLS		GMM	
	Squared	**Cubic**	**Squared**	**Cubic**
Y	0.088*** (0.021)	0.084*** (0.022)	0.151** (0.067)	0.150** (0 .065)
Y^2	0.048*** (0.015)	0.048*** (0.015)	0.054 (0.185)	0.067* (0.039)
Y^3	-	0.010 (0.012)	-	0.178 (0.194)
EMP	0.025 (0.058)	0.024 (0.058)	-0.245 (0.372)	-0.256 (0.372)
E	-0.003 (0.010)	-0.003 (0.010)	0.064 (0.070)	0.064 (0.070)
AG	0.287** (0.127)	0.295** (0.127)	1.810*** (0.640)	1.895*** (0.666)
EA	-5.221*** (0.689)	-5.23*** (0.688)	-6.888*** (1.042)	-7.131*** (1.020)
D	-0.803*** (0.036)	0.802*** (0.036)	-0.614*** (0.166)	-.0579*** (0.161)
UR	0.365*** (0.015)	0.365*** (0.015)	0.329*** (0.057)	0.320*** (0.055)
Kleibergen-Paap rk Underidentification test	-	-	19.904***	19.901***
Kleibergen-Paap rk Weak teidentification test	-	-	29.778***	29.771***
Hansen Overidentification test	-	-	1.934	1.905

Note: All estimates include time dummies. Standard errors are shown in parenthesis, *** denotes significant level at 1%, ** for 5% and * for 10%. Source: Own elaboration.

References

Katz D (2015) Water use and economic growth: Reconsidering the environmental Kuznets curve relationship. J Clean Prod 88:205–213. http://doi.org/10.1016/j.jclepro.2014.08.017

Pesaran MH (2004) General diagnostic tests for cross section dependence in panels. Cambridge Working Papers WP0435. Faculty of Economics, University of Cambridge, Cambridge, UK

Pesaran MH (2007) A simple panel unit root test in the presence of cross section dependence. J Appl Economet, 22(2):265–312

SIMA (2018) Multiterritorial Information System of Andalusia. Junta de Andalucía, Sevilla, Spain

Zhao J (2017) The cubic water Kuznets curve: patterns of urban water consumption and water policy effects. Water Policy 19(1):28–45. http://doi.org/10.2166/wp.2016.146

11th World Congress on Water Resources and Environment (EWRA 2019)
"Managing Water Resources for a Sustainable Future", 25-29 June 2019, Madrid, Spain

Quantifying the impact on stormwater management of an innovative ceramic permeable pavement solution in Benicàssim (Spain)

J.T. Castillo-Rodríguez[1*], I. Andrés-Doménech[1], M. Martín[1], I. Escuder-Bueno[1], S. Perales-Momparler[2]
[1] Research Institute of Water and Environmental Engineering, Universitat Politècnica de València, Spain
[2] Green Blue Management, Valencia, Spain
* e-mail: jecasrod@upv.es

Introduction

This contribution briefly describes the first results obtained from an innovative ceramic permeable pavement developed as part of the LIFE CERSUDS project in the city of Benicàssim (Spain).

This pavement, composed by modules built from ceramic tiles in stock, allows water infiltration, runoff treatment and water reuse as part of a Sustainable Urban Drainage System (SUDS) built in 2018.

A monitoring programme from September 2018 until July 2019 is currently ongoing. Outcomes from data gathering for the first three months have shown positive results regarding the impact of the system on improving stormwater management in the study area, reducing peak runoff rates and the volume of water which is conducted to the existing drainage system downstream the demonstrator.

Materials and methods

The LIFE CERSUDS (Ceramic Sustainable Urban Drainage System) project is a European project executed in the 2016-2019 period and co-funded by the European Commission, which proposes an innovative permeable ceramic pavement, based on findings of a previous research project (IMDIC 2010).

One of the results from this previous project was a permeable urban pavement based on the use of low commercial value ceramic pieces in stock. These pieces are cut in strips, thus turning ceramic material into an opportunity for providing a permeable material for paving actions.

The ceramic permeable modules have been tested and manufactured within the LIFE CERSUDS project to provide an innovative solution for permeable pavements, installed in a street of the city of Benicàssim in Castellón, Spain (Figure 1).

The demonstrator, executed between February and June 2018, is 200 m long and has a variable width ranging from 10 to 27 m and a 1.5% descending longitudinal slope. The complete intervention area is 3200 m^2. The demonstration site is located in a low-density residential area, characterized by several municipal sport facilities which make the street not only a frequent connection point between the beach and the city center, but also an area linked to strategic public facilities.

The case study has included the implementation of a sustainable drainage system along the street which allows water infiltration and collection, following international references for SUDS design (e.g. Woods-Ballard et al. 2015). The ceramic permeable pavement, in combination with drainage cells and geotextiles, provides runoff treatment and reduction of water flows to the existing drainage network (Figure 1). In addition, the system includes a rainwater harvesting tank, with a volume of approximately 10 m^3, aiming at reusing water for irrigation at the demonstration site.

The demonstrator monitoring will be carried out from September 2018 to July 2019, for analysing its performance in terms of runoff quantity and quality management. The first results were gathered from September to November 2018.

Results and concluding remarks

Based on previous experiences (e.g. Andrés-Doménech et al. 2018), a monitoring period of 9 months have been set for analysing system performance in terms of runoff quantity and quality.

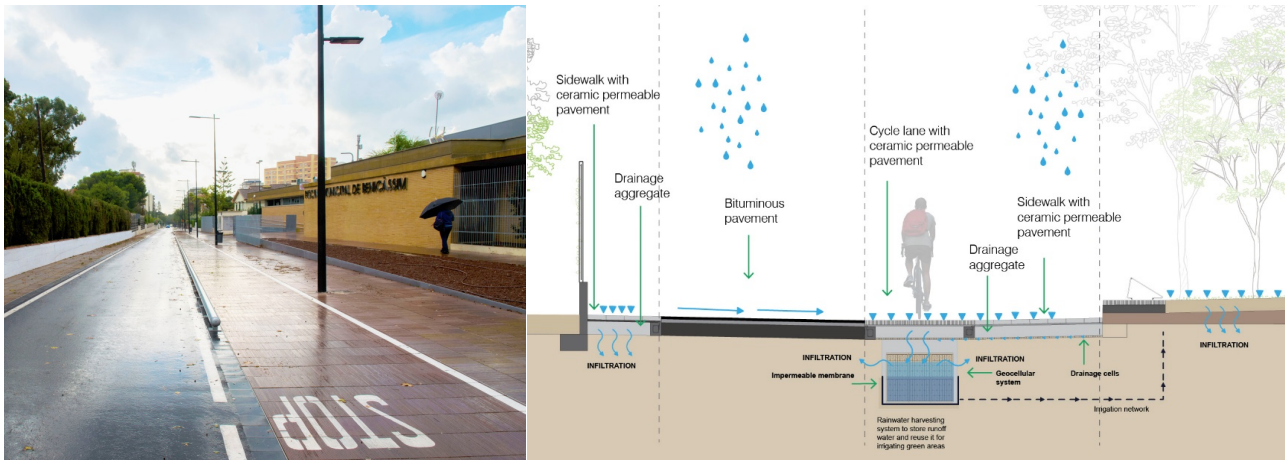

Figure 1. View and cross section of the sustainable drainage system performed in Benicàssim (Spain).

A total of 15 rainfall events have been registered during the first three months of monitoring. Only in 5 of the 15 registered events, exceeding runoff water reached the downstream drainage network. Outcomes from data analysis for these five events are summarized in Table 1.

Table 1. Results of the first monitoring period at the demonstrator in Benicàssim (Spain)

Event	Rainfall (mm)	Rainfall volume at demo site (l)	Runoff volume to DS network (l)	Reduction of runoff volume to DS network (%)	Maximum adjusted flow rate* (mm/h) A	Maximum rainfall intensity (mm/h) B	Relation A/B (%)
18/Sep/2018	22.2	73260	16415	*78%*	4.59	36	*13%*
18/Oct/2018	48.8	161040	119359	*26%*	46.90	144	*33%*
19/Oct/2018	38.4	126720	8580	*93%*	1.86	48	*4%*
18/Nov/2018	22.2	73260	3889	*95%*	3.77	48	*8%*
19/Nov/2018	14.8	48840	982	*98%*	1.05	12	*9%*

** Registered flow rate in the downstream (DS) point of the demonstrator, divided by the area managed by the SUDS.*

It can be concluded from these preliminary results that the system performs as expected, allowing water infiltration and reducing the amount of runoff water that finally reaches the downstream drainage network. Further information will be gathered in the upcoming months to better characterize system performance in terms of stormwater management.

This new permeable pavement system will help to boost a more sustainable urban development, combining sustainable stormwater management, and reuse of materials and runoff water for irrigation. This demonstration case study represents a reference example of urban retrofitting actions which integrate social, economic and environmental aspects.

Acknowledgments: The LIFE CERSUDS project is financed by the LIFE Programme 2014-2020 of the European Union for the Environment and Climate Action under the project number LIFE15 CCA/ES/000091.

References

Andrés-Doménech I, Hernández-Crespo C, Martín-Monerris M, Andrés-Valeri VC (2018) Characterization of wash-off from urban impervious surfaces and SuDS design criteria for source control under semi-arid conditions. The Science of the Total Environment 612:1320-1328. doi: 10.1016/j.scitotenv.2017.09.011.

IMIDIC (2010) Reutilización y reciclado de productos obsoletos o deshechos de fabricación para la generación de nuevos productos. Project financed by the Valencian government in 2010. Ref. IMIDIC/2010/73

Woods-Ballard B, Wilson S, Udale-Clarke H, Illman S, Scott T, Ashley R, Kellagher R (2015) The SUDS Manual (C753). London, UK

11th World Congress on Water Resources and Environment (EWRA 2019)
"Managing Water Resources for a Sustainable Future", 25-29 June 2019, Madrid, Spain

A comparison of sediment incipient motion and incipient deposition in open channels

M.J.S. Safari[1*], H. Aksoy[2]
[1] Department of Civil Engineering, Yaşar University, Izmir, Turkey
[2] Department of Civil Engineering, Istanbul Technical University, Istanbul, Turkey
* e-mail: jafar.safari@yasar.edu.tr

Introduction

Sediment threshold and two relevant concepts; incipient deposition and incipient motion are important in the sediment transport technology. There are inherent difficulties and inconsistencies in the definition of sediment threshold. The issue can be linked to the fact that entrainment of sediment particles is a random process depending on the fluctuating flow field as well as the size and relative positioning of sediment particles on the bed. Sediment incipient deposition and incipient motion are considered as self-cleansing design criteria for drainage systems design, which are quite important in urban hydrology and urban water management practice (Safari et al. 2018).

Studies on incipient deposition are rare in the literature (Loveless 1992; Aksoy et al. 2017) in comparison with incipient motion studies. It is a concept closely-related to the incipient motion (ASCE 1966; Loveless 1992) but not exactly the same (Safari et al. 2018). In order to demonstrate the difference between the incipient motion and incipient deposition, two basic approaches, velocity and shear stress, are available. Based on the importance and needs highlighted above, this study experimentally investigates sediment motion in a trapezoidal rigid boundary channel to determine velocity and shear stress required for the incipient motion and incipient deposition. The difference between the two concepts is expected to be better explained in this study for a clear definition of sediment threshold. It is also expected to contribute in the hydraulic design of urban drainage systems as a practical concern.

Materials and methods

The experimental apparatus was composed of a support structure, channel, a tank to prevent fluctuations, sediment feeder, tailgate and sand trap at the downstream section of the channel (Safari 2016). Channel was mounted on the support structure having 12 m-long with trapezoidal cross-section and 30 cm-bottom width and 60 degree-outer angle for the side walls. Uniform flow was established in the channel by adjusting the tailgate at the channel downstream outlet. Experiments were conducted according to the sediment motion cycle composed of decreasing velocity and increasing velocity half cycles as shown in Figure 1. In the experiments, the channel bed slope was adjusted for different nine cases to change from 0.00147 to 0.01106. As sediment, four sizes of uniform sediment with median diameter of 0.15 mm, 0.58 mm, 1.08 mm and 1.52 mm were used.

With this experimental procedure, four sediment transport modes were evaluated namely: non-deposition, incipient deposition, deposition and incipient motion. In the non-deposition mode of sediment transport, sediment particles move in the flow either as suspended load or bed load. Oppositely, sediment particles are all at rest at the non-motion mode. Flow conditions in which sediment particles begin to deposit or to move were also determined in the experiments. The former is related to incipient deposition while the latter is about incipient motion. An absolute separation of sediment motion modes from each other is impossible even with very high precision-measurement instrumentation. It is particularly worth mentioning that an important difficulty arises due to various definitions of the incipient motion in the literature. Due to this fact, it is essential to predefine each sediment motion mode for the consistency of experimental results. In this study, the fourth definition of Kramer (1935) on incipient motion, that is "general transport", was considered.

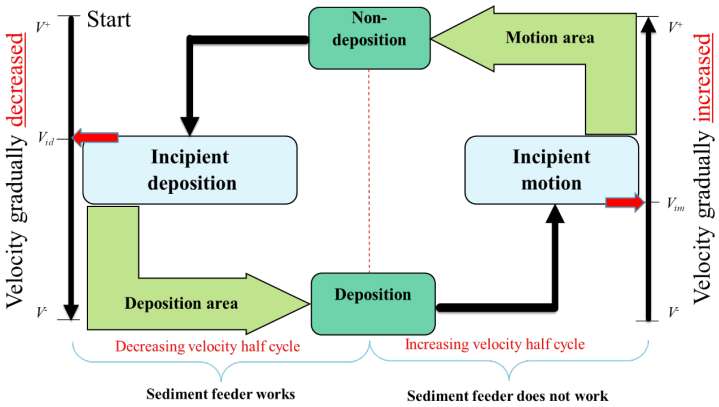

Figure 1. Sediment motion cycle.

Results and concluding remarks

Experimental data collected for incipient motion and incipient deposition in the flow within the trapezoidal cross-section channel were analysed based on the shear stress and velocity approaches. The Shields (1936) and Yalin (1972) criteria are used for the shear stress approach; the Yang (1973), and Novak-Nalluri (1984) methods for the velocity approach. Incipient motion and incipient deposition data demonstrate that flow characteristics such as velocity, dimensionless shear stress and particle Froude number are higher in incipient deposition than incipient motion. Comparison of experimental data with Shields, Yalin and Yang curves shows that higher hydrodynamic forces are required for the incipient motion of sediment particles in loose boundary channels than rigid boundaries. Velocity approach-based incipient motion and incipient deposition models developed in this study as well as their corresponding models available in the literature behave differently due to the fact that each model is proposed for a specific channel cross-section. It may therefore be concluded that channel cross-section is an essential factor in determining the threshold condition of sediment motion and deposition in rigid boundary channels. This is an issue to be studied with utilizing different cross-sections in the experiments. Most importantly, this study can be considered as a step to remove inconsistencies on the definition of sediment threshold. Based on the observations and results of this study, sediment threshold is considered a critical range between the upper boundary-incipient deposition and lower boundary-incipient motion in which sediment particles in motion tend to deposit and stationary particles tend to move.

Acknowledgments: This study was supported by the Scientific and Technological Research Council of Turkey (TUBITAK) under the project 114M283.

References

Aksoy H, Safari MJS, Unal NE, Mohammadi M (2017) Velocity-based analysis of sediment incipient deposition in rigid boundary open channels. Water Science and Technology 76(9):2535–2543

ASCE Task Force on Sediment Transportation Mechanics (1966) Incipient of motion. Journal of the Hydraulics Division, ASCE 92(HY2):291-314

Kramer H (1935) Sand mixtures and sand movement in fluvial levels. Trans ASCE, 100:798-838

Loveless JH (1992) Sediment transport in rigid boundary channels with particular reference to the condition of incipient deposition. PhD Thesis, University of London, UK

Novak P, Nalluri C (1984) Incipient motion of sediment particles over fixed beds. Journal of Hydraulic Research 22(3):181-197

Safari MJS (2016) Self-cleansing drainage system design by incipient motion and incipient deposition-based models. PhD Thesis, Istanbul Technical University, Turkey

Safari MJS, Mohammadi M, Ab Ghani A (2018) Experimental studies of self-cleansing drainage system design: a review. Journal of Pipeline Systems Engineering and Practice ASCE 9(4):04018017

Shields A (1936) Application of similarity principles and turbulence research to bed-load movement. Soil Conservation Service

Yalin MS (1972) Mechanics of sediment transport. Pergamon Press, New York

Yang CT (1973) Incipient motion and sediment transport. Journal of the Hydraulics Division ASCE 99(10):1679-1704

11th World Congress on Water Resources and Environment (EWRA 2019)
"Managing Water Resources for a Sustainable Future", 25-29 June 2019, Madrid, Spain

Modelling the effects of intermittent water supply on quality deterioration in terms of disinfection by-products formation

S. Mohan, G.R. Abhijith*
Environmental and Water Resources Engineering, Department of Civil Engineering, Indian Institute of Technology Madras, Chennai – 600 036, India
** e-mail: gnrabhijith@gmail.com*

Introduction

Nearly one billion of the world population is depending on the intermittent water supply (IWS) systems for meeting their water demands. In contrast to Continuous water supply (CWS) systems, the quality deterioration problem is more serious in IWS systems. Low water velocities, low pressures and water stagnation associated with intermittent operation increases the chances of recontamination during the non-supply periods (Kumpel and Nelson 2014). Maintaining high levels of chlorine is the most common strategy adopted to remediate the recontamination and regrowth problems, especially in developing countries. However, chlorination possesses the dilemma of risk trade-off because of the increased public attention attained recently by the Disinfection By-Products (DBPs), especially trihalomethanes (THMs), due to its bioaccumulation characteristics and increased carcinogenic risk. The Eulerian and Lagrangian based modelling techniques, with the assistance of computer packages such as EPANET 2.0 and its multi-species extension, EPANET-MSX, are extensively adopted to optimize the chlorination processes (Seyoum and Tanyimboh 2017). But the conventional models consider the distribution pipelines as fully pressurized and do not significantly detail the chlorine decay and THMs formation during the emptying phases commonly associated with IWS systems. To model the effects of alternating schedules of supply and non-supply on the temporal and spatial distributions of chlorine and THMs in distribution pipelines, more improved modelling techniques have to be developed. In the present work, a conceptually improved hydraulic simulation model, incorporating partial flow regimes, and a multi-species reactive-transport model, based on a novel Cellular Automata (CA) approach considering both advection and dispersion mechanisms, are integrated. The integrated model is applied to a benchmark problem to demonstrate the effects of the intermittent operation on chlorine decay and THM formation in WS systems.

Materials and methods

The benchmark single sourced WS system proposed by Bhave and Gupta (2006) was used to demonstrate the application of the integrated model. The only source node with elevation 90 m is a fill and draw type overhead reservoir with base diameter 5 m and maximum water level 10 m. For simulating continuous operation, the pressure-dependent analysis approach by Abdy Sayyed et al. (2015) was used by approximating a static HGL of 100 m at the source node. While for intermittent operation, the pumping duration was selected as 8 hours (from 6 am to 2 pm) and the pumping rate was fixed at 500.4 m^3/h. The outflows were modelled as uncontrolled orifice-based demands. The desirable pressure head at the four nodes was taken as 7 m. The concentrations of chlorine and THM in the pumped water was considered as 1.0 mg/L and 25 µg/L, respectively. At every demand node, the water outlet point was approximated to be situated at the middle of the incoming pipe. The empirical model developed originally by Sohn et al. (2004) for THM formation and recently used by Seyoum and Tanyimboh (2017) was selected to model the formation of THMs in the distribution pipelines.

The overall methodology framework adopted is given in Figure 1. The simulations were run by keeping the time step as 10 s for 120 hours until steady-state chlorine and THM concentrations were attained at all the demand nodes. The clock time 6 am was taken as the start time of simulation.

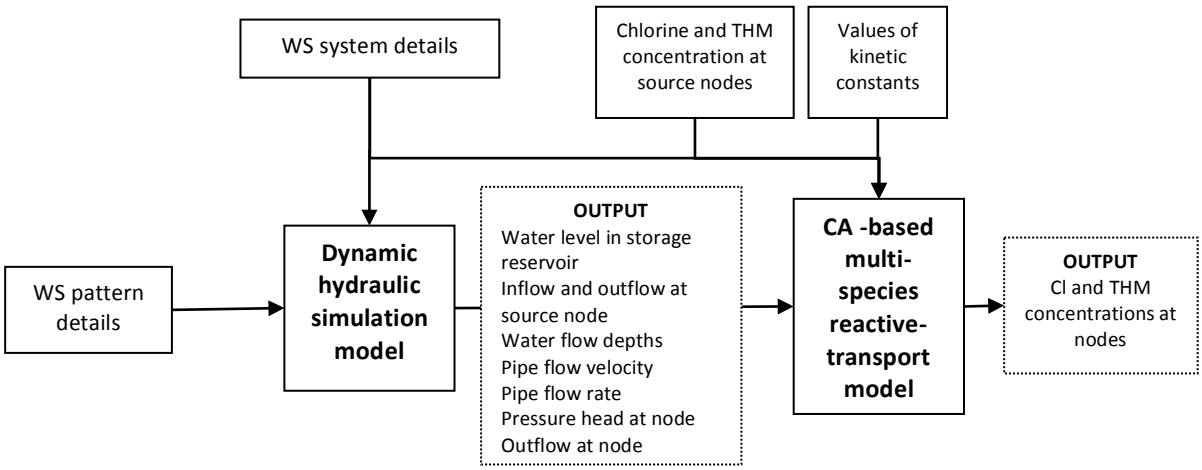

Figure 1. Overall methodology framework

Results and concluding remarks

The temporal variations of chlorine and THM concentrations for the last 24 hours of simulation, corresponding to the intermittent operation, are shown in Figure 2.

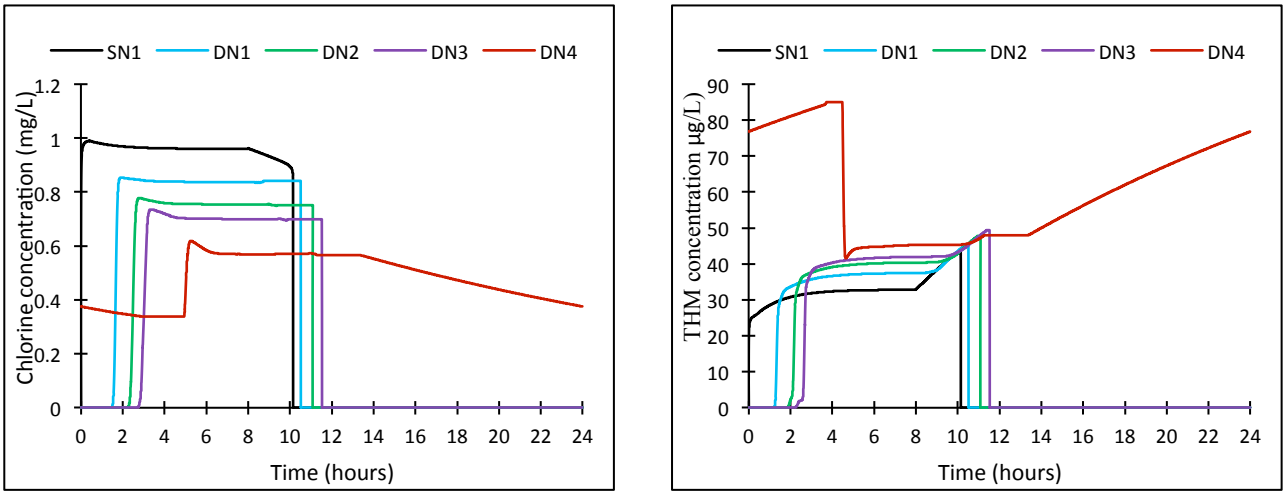

(a) *(b)*

Figure 2. Temporal variations of (a) chlorine and (b) THM at the source and demand nodes

The chlorine and THM profiles for DN4 were observed to be different from the other four nodes. This is attributed to the presence of stagnant water in node DN4. Due to stagnation, the chlorine decay and THM formation continued after the supply periods. Subsequently, THM concentration as high as 84 µg/L was observed before the start of the flushing phase at node DN4. For the other three demand nodes, higher chlorine and lower THM concentrations were found during intermittent operation compared to continuous operation. This may be attributed to higher flow velocities contributed by uncontrolled consumption.

References

Abdy Sayyed MAH, Gupta R, Tanyimboh TT (2015) Noniterative application of EPANET for pressure dependent modelling of water distribution systems. Water Resour Manag 29:3227–3242. doi: 10.1007/s11269-015-0992-0

Bhave PR, Gupta R (2006) Analysis of Water Distribution Networks, 3rd ed. Narosa Publishing House Pvt. Ltd.

Kumpel E, Nelson KL (2014) Mechanisms affecting water quality in an intermittent piped water supply. Environ Sci Technol 48:2766–2775. doi: 10.1021/es405054u

Seyoum AG, Tanyimboh TT (2017) Integration of hydraulic and water quality modelling in distribution networks: EPANET-PMX. Water Resour Manag 31:4485–4503. doi: 10.1007/s11269-017-1760-0

Sohn J, Amy G, Cho J, et al. (2004) Disinfectant decay and disinfection by-products formation model development: chlorination and ozonation by-products. Water Res 38:2461–2478. doi: 10.1016/j.watres.2004.03.009

11th World Congress on Water Resources and Environment (EWRA 2019)
"Managing Water Resources for a Sustainable Future", 25-29 June 2019, Madrid, Spain

Multi-criteria decision support framework for water sensitive stormwater management in an urban residential complex

R.N. Nyawo[1,2], T.T. Tanyimboh[1*]
[1] *School of Civil and Environmental Engineering, University of the Witwatersrand, Johannesburg, South Africa*
[2] *KTN Consulting Engineers and Project Managers, Johannesburg, South Africa*
** e-mail: tiku.tanyimboh@wits.ac.za*

Introduction

The stormwater from urban catchments is often managed as a potential flood hazard and is disposed of as rapidly as possible; in so doing quantity is managed whilst quality is ignored (Fisher-Jeffes and Armitage 2012). This is the widely used stormwater management approach in South Africa, which is based on the conventional drainage system. There is, however, a growing movement to treat stormwater as a renewable resource as opposed to a nuisance; the aim is to reduce the impacts of pluvial events in urban catchments and create areas that mimic "pre-development" dynamics, encourage ecosystem development and restore water quality (McGrane 2015; Parker et al. 2009).

This study, ultimately, seeks to develop a practical and robust decision support framework for the sustainable management of stormwater in an urban residential complex. The multi-criteria analysis approach under development is based on four main criteria with ten sub-criteria comprising a mixture of qualitative and quantitative indicators.

Sustainable drainage systems (SuDS) are not widely used in South Africa; however most stormwater management by-laws recommend the use of SuDS. The study, therefore, further seeks ultimately to establish the implementation constraints of SuDS in South Africa with particular reference to the City of Johannesburg (CoJ), as a secondary aim. A conventional drainage system has been designed to represent the prevailing practice. The ultimate goal is to compare the conventional system to alternatives such as sustainable and hybrid systems.

Materials and methods

A 7.15 ha greenfield site, subdivided into stands 1 (4.5 ha) and 2 (2.65 ha), in the City of Johannesburg's largest township (Soweto), which is earmarked for government-subsidized residential housing (comprising three storey units) in 2019, was adopted for this study. Existing information for the site such as GIS data, topographical survey, geotechnical report, existing services and layout plan for future development was collected and analysed. Analysis of the existing data is followed by the development of three stormwater management alternatives namely: Conventional, Sustainable (SuDS) and Hybrid Drainage Systems.

The final stage of the study entails the development of sub-criteria for each design alternative and comparing the results using the Analytical Hierarchy Process (AHP). The Analytical Hierarchy Process (AHP) is one method of Multi-Criteria Decision Making and is one of the most inclusive approaches. This method formulates the problem as a hierarchical system and seamlessly combines a mixture of quantitative and qualitative criteria (Taherdoost 2017). AHP has proved a theoretically sound, extensively tested and accepted methodology (Bhushan and Rai 2004; Tanyimboh and Kalungi 2008, 2009).

Results and concluding remarks

The peak flows are calculated using the Rational Method as prescribed in the South African National Roads Agency Drainage Manual (SANRAL 2013). The results for the Conventional Drainage System for both stands are shown in Table 1. The peak flows for different return periods increase after development due to a reduction in infiltration rates by an increase in impermeable surfaces i.e. roofs, driveways, parking, etc.

Table 1. Pre- and post-development peak flows for stands 1 and 2.

		Peak flows for various return periods					
	Return Periods (Years)	2	5	10	25	50	100
Stand 1	Pre-development flows (m^3/s)	0.124	0.171	0.241	0.354	0.618	0.882
	Post-development flows (m^3/s)	0.481	0.709	0.977	1.203	1.593	1.951
	Percentage increases (%)	288	315	305	240	158	121
Stand 2	Pre-development flow (m^3/s)	0.076	0.123	0.185	0.255	0.418	0.616
	Post-development flow (m^3/s)	0.300	0.441	0.608	0.749	0.992	1.215
	Percentage increases (%)	295	259	229	194	137	97

The proposed system is sized to accommodate runoff based on a return period of five years. The stormwater pipes collect runoff from the buildings and parking areas and convey this flow plus the overland flow from the upstream area to the existing stormwater system downstream. The system comprises 1.4 km of concrete pipes ranging from 300 mm to 600 mm in diameter, 17 grid inlets, six kerb inlets and 23 manholes. The total post-development peak stormwater discharge rate of 1.15 m^3/s for both stands, for a 5-year recurrence interval design storm event, exceeds the pre-development peak stormwater discharge rate of 0.294 m^3/s from the site for the same design storm event. Self-evidently, the conventional drainage system does not reduce the post-development peak flow to pre-development conditions as specified in the CoJ Stormwater Management By-laws (CoJ 2010). The multi-criteria decision support framework for stormwater management under development considers three different design alternatives based on the conventional, SuDS and hybrid systems and applies the AHP to determine the best option.

SuDS are not widely used in South Africa although CoJ stormwater management by-laws recommend their use. The achievement of adequate water management necessitates an integrated, trans-disciplinary and multi-stakeholder approach. Although the scope of this study is limited to the Civil Engineering Sector (Stormwater Drainage), it further seeks to establish the implementation constrains of SuDS.

References

Bhushan N, Rai K (2004) Strategic decision making: applying the analytic hierarchy process. CREAX Information Technologies Pty Ltd, Bangalore

City of Johannesburg Metropolitan Municipality (CoJ) (2010) Local Government: Municipal Systems Act, 2000 (Act No. 32 of 2000). Stormwater Management By-laws. http://openbylaws.org.za/

Fisher-Jeffes L, Armitage NP (2012) Charging for stormwater in South Africa. Water Institute of Southern Africa (WISA) 39(3):429-436. http://dx.doi.org/10.4314/wsa.v39i3.13

McGrane JM (2015) Impacts of urbanisation on hydrological and water quality dynamics, and urban water management: a review. Hydrological Sciences Journal 61(13):2296-2311. https://doi.org/10.1080 /02626667.2015.1128084

Parker N, Gardner T, Goonetilleke A, Egodawatta P, Prasanna K, Giglio D (2009) Effectiveness of WSUD in the 'real world'. In Proceedings of The 6th International Water Sensitive Urban Design Conference and the 3rd Hydropolis: Towards Water Sensitive Cities and Citizens, 5-8 May 2009, Perth, Western Australia

South African National Roads Agency Limited (SANRAL) (2013) Drainage Manual, 6th ed. p 3-1 – 3-60. SANRAL, Pretoria

Taherdoost H (2017) Decision making using the analytic hierarchy process (AHP): a step by step approach. International Journal of Economics and Managements Systems 2:244-246

Tanyimboh T, Kalungi P (2008) Holistic planning methodology for long-term design and capacity expansion of water networks. Water Science and Technology – Water Supply 8(4):481-488. https://doi.org/10.2166/ws.2008.105

Tanyimboh T, Kalungi P (2009) Multi-criteria assessment of optimal design, rehabilitation and upgrading schemes for water distribution networks. Civil Engineering and Environmental Systems 26(2):117-140. https://doi.org/10.1080/10286600701838626

11th World Congress on Water Resources and Environment (EWRA 2019)
"Managing Water Resources for a Sustainable Future", 25-29 June 2019, Madrid, Spain

Effects of spatial correlation of demands on the cost and resilience of water distribution networks: A new design optimization approach

T.T. Tanyimboh[1,3*], S. Saleh[2,3]
[1] School of Civil and Environmental Engineering, University of the Witwatersrand, Johannesburg, South Africa
[2] Department of Civil Engineering, University of Tripoli, Libya
[3] Department of Civil and Environmental Engineering, University of Strathclyde, Glasgow, UK
* e-mail: tiku.tanyimboh@wits.ac.za

Introduction

Design optimization procedures for water distribution systems generally assume that the nodal demands follow the same diurnal pattern, which implies that the demands are fully synchronised and perfectly correlated. However, it is well known that in practice the spatial correlation of the demands is not perfect; i.e. the cross-correlation is less than unity. This study investigates the effects of the widespread assumption that demands are perfectly correlated on the overall performance and capital cost of water distribution systems. A new optimal design approach that considers the cross-correlation of the nodal demands was developed herein. Essentially, the novelty of the research is that the optimization procedure incorporates the spatial properties of the demands in terms of the cross-correlation while preserving the diurnal demand patterns. Thus, in addition to the cross-correlation effects, the nodal demand patterns are assumed to be independent and unique and are addressed explicitly using extended period simulation.

Materials and methods

The method developed is demonstrated on the benchmark network in Figure 1. All pipes are 1000 m long with a Hazen-Williams coefficient of 130. The minimum residual pressure required at the demand nodes is 30 m. There are 14 discrete pipe diameter options (Alperovits and Shamir 1977). For perfect cross-correlation, the diurnal patterns of the nodal demands are perfectly synchronized as illustrated in Figure 2 with a time lag between the respective nodal peaks of zero. For a given maximum time lag between the nodes, the time lag was divided by $N - 1$; N = number of demand nodes. For large networks the demand nodes may be grouped if necessary. For a time lag of 15 minutes, for example, there are five periods of 3 minutes each. The diurnal patterns of the demand nodes were assumed to start at different times, i.e. 0, 3, 6, 9, 12 and 15 minutes. For example, the demand pattern of node 1 may start at 00:00 a.m.; node 2 at 00:03 a.m.; node 3 at 00:06 a.m. etc. Any suitable mapping scheme or approach (e.g. historical, socio-economic, random, etc.) may be used. To evaluate the overall correlation for each time lag, the correlation coefficients of all the pairs of nodes were averaged. The (averages of the) correlation coefficients for the time lags considered are shown in Table 1. For each time lag, the initial capital cost of the network was minimized. Strictly, the time lag herein refers to the maximum time lag between any two nodes.

The Non-dominated Sorting Genetic Algorithm II (Deb et al. 2002) was used with two objectives. The initial capital cost was minimized. The pressure deficit at the critical node (i.e. the node with the largest deficit) was minimized by being reduced to zero to yield feasible solutions. The decision variables were the pipe diameters. The constraints were the conservation of mass and energy and minimum node pressure equations. The constitutive equations were satisfied by simulation in EPANET 2 (US EPA). Five independent optimization runs were executed for each time lag using random initial populations of size 100 and 5,000 generations. The crossover and mutation probabilities were 1.0 and 0.03125, respectively.

Results and concluding remarks

The results achieved are summarised in Table 1. The hydraulic capacity reliability and failure tolerance (FT) were calculated using the methodology developed by Tanyimboh and Templeman (1998, 2000). The Cullinane *et al.* (1992) pipe failure model was used. Head-driven simulation with PRAAWDS (Tanyimboh and

Templeman 2010) was used to simulate the pipe failure effects on the network's hydraulic performance.

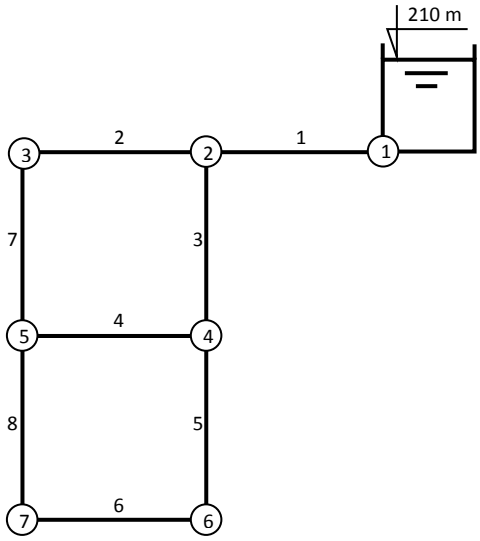

Figure 1. Layout of the network

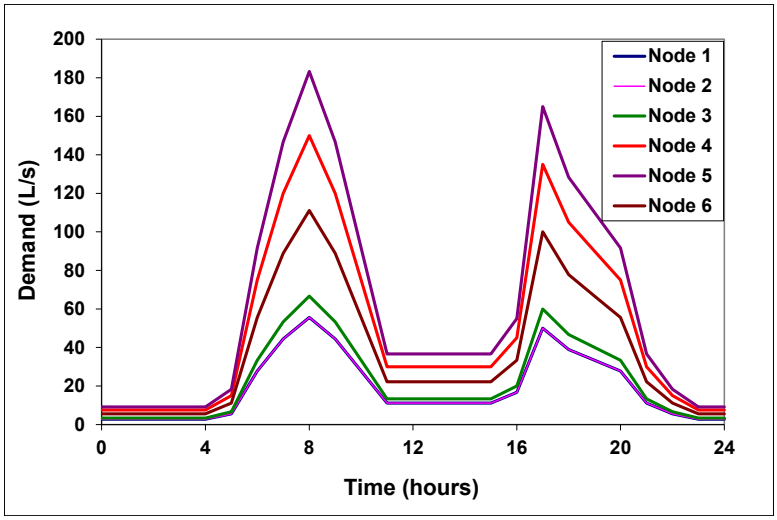

Figure 2. Daily demand variations with zero time lag

The results show that the cost increases with the cross-correlation, and thus incorporating the spatial properties of the demands with reference to cross-correlation is a pre-requisite to the development of economical designs. Similarly, the performance in terms of hydraulic reliability and failure tolerance improves as the cross-correlation increases. Conversely, when the cross-correlation is less than unity, the individual demand patterns are not fully synchronized and so the peak of the total demand decreases; this results in designs with reduced flow-carrying and re-routing capacities. It can be seen also that, generally, the mean diameter increases as the cross-correlation increases. Thus, the optimal design of water distribution systems should consider the relevant trade-offs based on the degree of cross-correlation.

Table 1. Properties of the optimal designs achieved for the cross-correlation levels considered

Time lag (mins.)	Correlation coefficient	Cost (10^3)	Surplus head (m)	Reliability	FT	Diameters of the pipes indicated (mm)								
						1	2	3	4	5	6	7	8	Mean
0	1.000	985	0.002	0.99971	0.935	558.8	457.2	508.0	25.4	508.0	203.2	457.2	355.6	384
15	0.996	868	0.004	0.99970	0.841	558.8	406.4	508.0	304.8	457.2	76.2	355.6	355.6	378
30	0.983	858	0.002	0.99968	0.932	558.8	406.4	508.0	25.4	508.0	304.8	355.6	152.4	352
45	0.964	822	0.003	0.99965	0.926	558.8	304.8	508.0	152.4	508.0	304.8	254.0	25.4	327
60	0.939	814	0.002	0.99967	0.958	558.8	355.6	508.0	25.4	508.0	355.6	304.8	25.4	330
120	0.797	630	0.001	0.99946	0.885	508.0	457.2	457.2	25.4	406.4	152.4	355.6	254.0	327
180	0.622	616	0.001	0.99894	0.768	508.0	254.0	508.0	355.6	406.4	25.4	254.0	355.6	333
240	0.444	597	0.001	0.99783	0.532	508.0	406.4	457.2	25.4	406.4	203.2	355.6	254.0	327

Besides feasibility, the surplus head at the critical node is a measure of the optimality of the solutions. FT denotes failure tolerance.

Acknowledgments: This research was funded by the UK EPSRC (Grant Number EP/G055564/1).

References

Alperovits E, Shamir U (1977) Design of optimal water distribution systems. Water Resources Research 13(6):885-900

Cullinane MJ, Lansey KE, Mays LW (1992) Optimization-availability-based design of water distribution networks. J. Hydraulic Engineering 118:420-441

Deb K, Pratap A, Agarwal S, Meyarivan T (2002) A fast and elitist multiobjective genetic algorithm: NSGAII. Transactions on Evolutionary Computations 6(2):182-197

Tanyimboh TT, Templeman AB (2000) A quantified assessment of the relationship between the reliability and entropy of water distribution systems. Engineering Optimization 33(2):179-199

Tanyimboh TT, Templeman AB (1998) Calculating the reliability of single-source networks by the source head method. Advances in Engineering Software 29(7-9):499-505. doi: 10.1016/S0965-9978(98)00016-7

Tanyimboh TT, Templeman AB (2010) Seamless pressure-deficient water distribution system model. J. Water Management 163(8):389-396. doi: 10.1680/wama.900013

11th World Congress on Water Resources and Environment (EWRA 2019)
"Managing Water Resources for a Sustainable Future", 25-29 June 2019, Madrid, Spain

Evaluation of water losses in drinking water distribution networks in Turkey

C. Coskun Dilcan[1], G. Capar[1*], A. Korkmaz[2], Ö. İritas[2], Y. Karaarslan[2], B. Selek[3]
[1] Water Management Institute, Ankara University, Ankara, Turkey
[2] General Directorate of Water Management, Republic of Turkey Ministry of Agriculture and Forestry, Ankara, Turkey
[3] Republic of Turkey Ministry of Agriculture and Forestry, Ankara, Turkey
* e-mail: gcapar@ankara.edu.tr

Introduction

Water resources are under pressure due to many factors such as increasing demand in developing and rapidly growing economies, climate change, population increase and human activities. According to the 4th World Water Development Report; 1.8 billion people would suffer from water scarcity and two-thirds of the world's population would experience water stress in 2025 (United Nations 2012). Hence, access to clean and safe water becomes much more important in terms of sustainable urban water management. Turkey is not a water-rich country and climate change is expected to impact the water resources adversely. It is of crucial importance to improve water efficiency in all sectors, including household services.

Losses in the drinking water distribution systems, i.e., non-revenue water, is defined as the difference between the amount of water supplied to the drinking water line and the amount of water consumed by the users (World Bank 1996). Water losses in water supply and distribution systems are divided into two groups as physical and apparent/commercial losses (WHO and UNICEF 2000). According to the World Bank, approximately 45 billion m^3 of water per day is lost in drinking water networks which can meet the water need of approximately 200 million people (Kingdom et al. 2006). In spite of increasing demand for water, its loss in distribution networks results in water inefficiency as well as significant economic losses. These facts lead to the conclusion that losses in water distribution networks must be thoroughly monitored and precautions must be taken for improving urban water management in the world and Turkey.

Materials and methods

The information and sources used as scientific material are based on legal regulations of Turkey and the literature review on the topic. In this study, the water leakages and losses in water distribution networks in the world and Turkey has been compared. In this context, Turkey's responses towards the issue and the studies carried out on legal regulations were investigated and the findings were reported in Results section.

Results and concluding remarks

The development level of countries is a determinant factor among the reasons why the physical and administrative water losses vary widely from country to country. In developed countries, water losses in drinking water networks vary between 10-20%, while these rates are observed to be much higher in developing countries (Kingdom et al. 2006). The non-revenue water values recorded in 2010 are less than 10% for some countries like Germany, the Netherlands and Australia and higher than 60% in countries such as Bosnia and Herzegovina, Albania and Armenia. This ratio is approximately 45% in Turkey while about 25% is seen in Russia and China (Muhammetoglu and Muhammetoglu 2017). Table 1 provides a comparison of non-revenue water levels of some cities from Turkey and other countries. The cities in Turkey were classified as large or small with respect to their population, i.e., 750.000 capita. It is clear that a solid conclusion cannot be drawn from the data, as some large cities have low level of non-revenue water whereas some small cities have high losses. The main reason of the leakage problem is the ageing of water distribution networks. Although the problematic parts of worn networks are renewed, problems arise again after a while. In some cities of Colombia, Mexico and Philippines, microbiological impurities were detected

in addition to the leakages. It is obvious that deteriorated pipelines are an important problem and threat in terms of pathogen attack in drinking water systems.

Table 1. Non-revenue water percentages from some cities in Turkey and around the world

Population*	Cities from Turkey	Non-revenue water (%)	Cities from World	Non-revenue water (%)
>750.000	Istanbul (World Bank 2016)	24	Mexico City, Mexico (Lee and Schwab 2005)	37
	Ankara (World Bank 2016)	42	Calcutta, India (Lee and Schwab 2005)	25
	Antalya (World Bank 2016)	33	Manila, Philippines (Lee and Schwab 2005)	58
	Tekirdag (World Bank 2016)	17	Abidjan, Coˆ te d'Ivoire (World Bank 1996)	17
	Eskisehir (World Bank 2016)	35	Damascus, Syria (World Bank 2003)	64
	Ordu (World Bank 2016)	69	Dubai, UAE (World Bank 2003)	15
	Sanlıurfa (World Bank 2016)	57	Makkah, Saudi Arabia (Lee and Schwab 2005)	56
<750.000	Bolu, (Ozturk et al. 2007)	75		
	Isparta (Ozturk et al. 2007)	55		
	Igdır (Ozturk et al. 2007)	35		

*Population values belong to the year of reference work

In Turkey, a new regulation named "Control of Water Losses from Drinking Water Supply and Distribution Systems" (Official Gazette 2014) and a technical procedure was issued by the Turkish Ministry of Agriculture and Forestry in 2014-2015 to establish some policies. This regulation forces the metropolitan and provincial municipalities to reduce water losses down to 30% within 5 years starting from 2014, and to 25% within the following 4 years. According to the annual water loss reports of metropolitan and provincial municipalities, average water loss rate was 36%. In Turkey, there are 25 municipalities with a significant decrease in water loss rates by years and 20 municipalities with a water loss rate below 30%. In light of this information, it may be concluded that a decrease in water loss rate from 36% to 25% in a city with a population of 1 million would save about 8 million m^3 water, which equals to the annual water requirement of a small city with a population of 110,000 capita.

It is clear that we need to focus on infrastructure investments as well as control and monitoring systems in order to decrease the water loss rates. The main precautions to reduce water losses are monitoring, control and measurement of the network continuously, technical personnel training in international norms, prevention of informal water use and renewal of equipment and network. Efficiency improvements, such as the reduction of non-revenue water losses in drinking water supply are crucial for integrated urban water management. While leakages in distribution network are more common in developing countries, this situation is an obstacle for the protection of financial investments and the government budget. On the other hand, it has vital importance for the sustainable supply of drinking water, protection of human health and ensuring water security.

References

Lee EJ, Schwab KJ (2005) Deficiencies in drinking water distribution systems in developing countries. Journal of Water and Health 3(2):109-127

Muhammetoglu H, Muhammetoglu A (2017) Handbook on the Control of Water Losses in Drinking Water Supply and Distribution Networks (in Turkish), Republic of Turkey Ministry of Forest and Water Affairs, General Directorate of Water Management

Official Gazette (2014) http://www.resmigazete.gov.tr/eskiler/2014/05/20140508-1.htm (accessed in February 2019)

Ozturk I, Uyak V, Cakmakci M, Akca L (2007) Dimensions of Water Loss Through Distribution System and Reduction Methods in Turkey. International Congress On River Basin Management, pp 245-255

United Nations (2012) Managing Water under Uncertainty and Risk. World Water Development Report 4 Volume 1. Retrieved from http://www.unwater.org/publications/managing-water-uncertainty-risk/

WHO & UNICEF (2000) Joint Monitoring Programme Global Water Supply and Sanitation Assessment 2000 Report. Iseman Creative, Washington, DC

World Bank (1996) Indicators: Water and Wastewater Utilities. 2nd ed. World Bank, Washington, DC

World Bank (2003) Unaccounted for Water. http://web.worldbank.org/WBSITE/EXTERNAL/COUNTRIES/MENAEXT/EXTMNAREGTOPWATRES/0,,contentMDK:22356658~pagePK:34004173~piPK:34003707~theSitePK:497164,00.html

World Bank (2016) Turkey Sustainable Urban Water Supply and Sanitation. Report No. 110547-TR. Retrieved from http://www.worldbank.org/en/country/turkey/publication/turkey-sustainable-urban-water-supply-and-sanitation-report

11th World Congress on Water Resources and Environment (EWRA 2019)
"Managing Water Resources for a Sustainable Future", 25-29 June 2019, Madrid, Spain

How to account for uncertainty in optimization of urban systems

O. Marquez-Calvo[1], D.P. Solomatine[1,2*]
[1] *Hydroinformatics Chair, IHE Delft Institute for Water Education, Delft, Netherlands*
[2] *Water Resources section, Delft University of Technology, Delft, Netherlands*
** e-mail: d.solomatine@un-ihe.org*

Introduction

Water sector started to use mathematical optimization algorithms in the 1960s (see, e.g. Maier et al. 2014). However, in typical settings, the issue of uncertainty was not considered, and only relatively recently one can find studies with the explicit consideration of uncertainty in multi-objective optimization of water systems. This type of optimization is often (albeit not always) referred to as robust optimization. Notion of robustness is treated in different studies in various ways and is determined by the particular needs of a case study or the authors' preferences.

Multi-Objective Optimization (MOO) of urban systems is a mature technology. In MOO, when the objective function is not known analytically, the most popular approach is using randomized search, and the most widely used group of methods is evolutionary optimization.

Some of the published literature on MOO techniques which take uncertainty into account (e.g. Kapelan et al. 2005), however, in our opinion (Marquez-Calvo and Solomatine 2019) the problem formulations used do indeed take uncertainty into account, but it can be seen that uncertainty is in a way 'hidden' and cannot be directly estimated. The problem of robustness is not formulated explicitly and varies in different case studies; besides, the process of probabilistic uncertainty propagation to the final solutions is typically not explicit either. This prompted the development of a new algorithm for robust optimization.

Materials and methods

We define Robust optimization in multiple objectives as an optimization method modified in such a way that it generates a solution or a set of solutions that have minimum (or limited) variability of the objective functions when some elements or parameters of the modelled real system vary due to their uncertainty.

The main idea of the proposed method entitles Robust Optimization and Probabilistic Analysis of Robustness (ROPAR) in the following (Marquez-Calvo and Solomatine 2019):

- the uncertainties is assumed probabilistic with the known distribution (pdf) (in urban flood context this is e.g. rainfall intensities and duration);
- various realisations of uncertainty (rainfall events) are sampled; for each of the realisations the multi-objective optimization problem is solved and a Pareto set of optimal solutions generated;
- resulting uncertainty (pdfs) is analysed for various levels of objective functions, as presented on Figure 1.

Additionally, we have developed several ways of identifying the robust solution but optimizing the objective function describing the robustness, e.g. understood in "average risk" or minimax risk" sense.

Results and concluding remarks

ROPAR approach was tested on a number of cases, from benchmarks used in MOO studies, to urban drainage systems and water distribution networks. We used NSGAII and AMGA algorithms as the main (deterministic) optimization engines. In contrast to the known methods, ROPAR allows for explicit handling of uncertainty and showing how uncertainty is propagated to a set of Pareto optimal solutions. It allows for determining the bounds on the values of objective functions and decision variables corresponding to different levels of robustness.

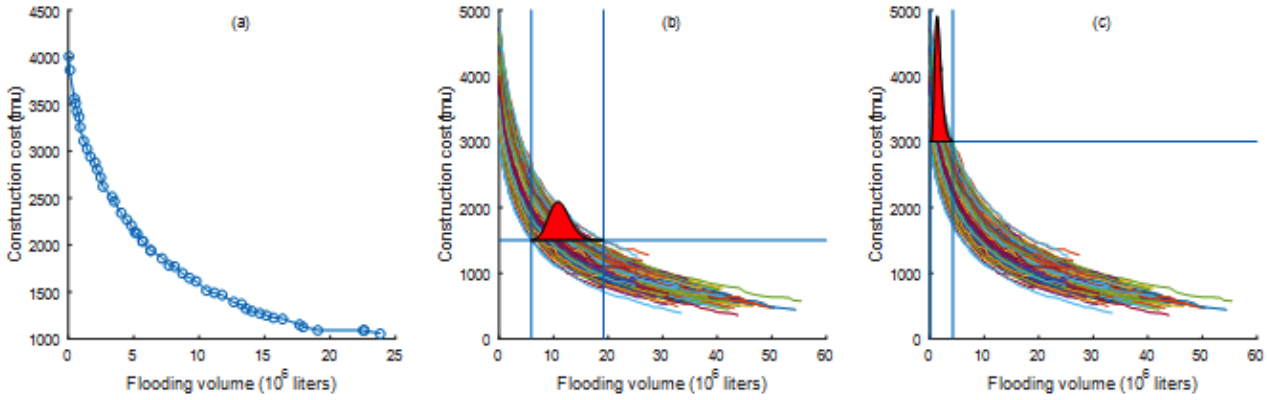

Figure 1. The main idea of probabilistic analysis in ROPAR, on an example of a drainage network optimization. (a) example of solving MOO problem assuming no uncertainty; (b, c) N realisations of an uncertain variable (e.g. rainfall) are sampled and MOO problem is solved N times, resulting in N Pareto optimal sets. For the two assumed value of construction costs allow for building two empirical distributions of the corresponding urban flood volume (Marquez-Calvo and Solomatine 2019)

Acknowledgments: The first author thanks the Mexican government for its support for funding his PhD programme through CONACYT programme at IHE Delft.

References

Kapelan ZS, Savic DA, Walters GA (2005) Multiobjective design of water distribution systems under uncertainty. Water Resources Research 41:1-15

Maier HR, Kapelan Z, Kasprzyk J, Kollat J, Matott LS, Cunha MC, Dandy GC, Gibbs MS, Keedwell E, Marchi A, Ostfeld A, Savic D, Solomatine DP, Vrugt JA, Zecchin AC, Minsker BS, Barbour EJ, Kuczera G, Pasha F, Castelletti A, Giuliani M, Reed PM (2014) Evolutionary algorithms and other metaheuristics in water resources: Current status, research challenges and future directions. Environmental Modelling & Software 62:271-299

Marquez-Calvo O, Solomatine DP (2019) Approach to robust multi-objective optimization and probabilistic analysis: the ROPAR algorithm. J. Hydroinformatics 21(3):427-440

11th World Congress on Water Resources and Environment (EWRA 2019)
"Managing Water Resources for a Sustainable Future", 25-29 June 2019, Madrid, Spain

Development of a hybrid biofilter for stormwater treatment and for the remediation of nitrate-contaminated groundwater

A. Brenner[1,2*], A. Aloni[1], H. Cohen[1], O. Gradus[1], A. Mor[1], O. Koren[1], S. Shandalov[1], Y. Zinger[2]
[1] *Unit of Environmental Engineering, Faculty of Engineering Sciences, Ben-Gurion University of the Negev, Beer-Sheva 8410501, Israel*
[2] *The Center for Water Sensitive Cities in Israel, KKL Eshtaol 9977500, Israel*
** e-mail: brenner@bgu.ac.il*

Introduction

The application of biofiltration systems for stormwater harvesting is a common practice for areas with rainfall distribution over the entire year, as applied successfully In Australia (Wong 2006; Zinger et al. 2013). However, a modified application is required in semi-arid countries such as Israel, which suffers a prolonged dry period (with no drop of rain) during 7-8 months of the year. This requires to use a hybrid system for both stormwater harvesting during winter, and for groundwater remediation (reduction of high nitrate levels) during summer. A representative illustration of this concept is shown in Figure 1.

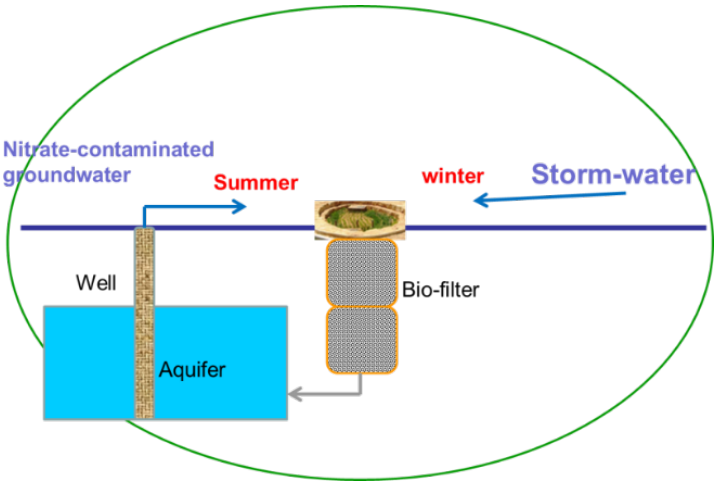

Figure 1. The concept of a hybrid biofilter application in Israel.

Materials and methods

For the examination of groundwater remediation two columns were operated. Each column was built of PVC and had height of 120 cm, and diameter of 23.5 cm. The columns were filled with quartz sand in three layers: bottom 2.5-3.5 mm (7 cm height), middle 0.8-1.5 mm (8 cm height), and a top layer of 0.4-0.6 mm (45 cm height). The top 30 cm of the smallest sand layer was mixed with two types of solid carbon sources: one column with cotton (Aloni and Brenner 2017), and the other with *Eucalyptus* wood-chips (Australian practice). A nitrate solution (KNO_3) forming concentration of 100 mg/L in tap water, served as the feed solution which was pumped continuously to the top of the columns. The hydraulic load applied was 36 mm/h (38 L/d per column).

For the study of stormwater treatment, seven similar columns were constructed and operated. The experiments were done using a synthetic mixture for the simulation of a typical Israeli stormwater, containing organic matter (TOC 5 mg/L), Ammonia (5 mgN/L), phosphate (2 mgP/L), sodium (20 mg/L), chloride (20 mg/L), and alkalinity (30 mg/l as CaCO3). Three types of plants were used on top of four columns: *Agapanthus, Tolbaghia, and Vetiver*.

Results and concluding remarks

Results are presented herein for the two modes of operation, namely, remediation of nitrate-contaminated water by biological denitrification in one stage, and treatment of simulated stormwater in a second stage. In the first stage, two columns were operated continuously several months and demonstrated efficient nitrate removal (as shown in Fig. 2), and low accumulation of nitrite and TOC (not shown).

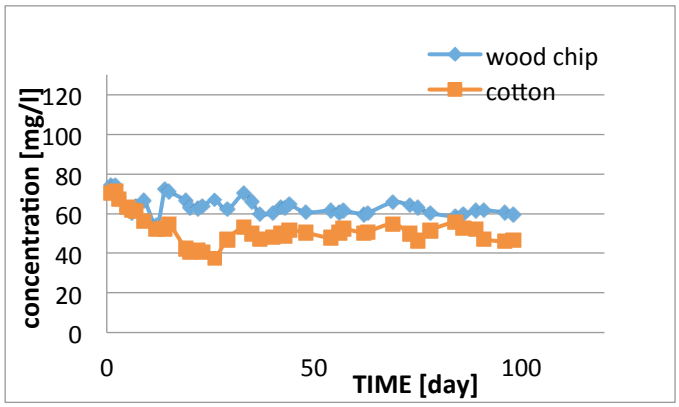

Figure 2. Nitrate outlet concentrations for the cotton and wood-chips columns.

For the second stage, the overall results demonstrated complete nitrification in all columns, complete removal of phosphate in low hydraulic loads, and partial removal of nitrate and organic matter. The results for total N removal are shown in Fig. 3 and demonstrate the combined effect of the vegetation.

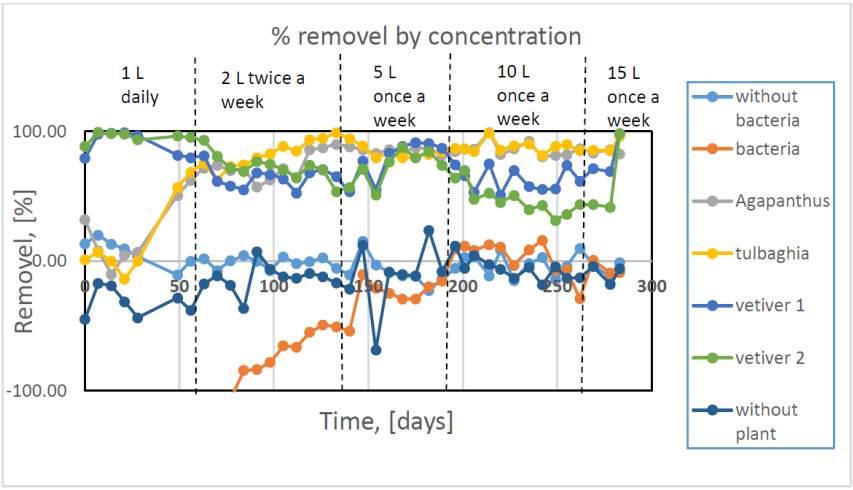

Figure 3. Total N removal percent based on concentration change in the tested columns.

In summary, operation of biofilters during a long period to simulate treatment of stormwater and bioremediation of nitrate-contaminated groundwater, proved the feasibility of the concept offered.

Acknowledgments: The authors wish to express their thanks to Keren Kayemet Leisrael (JNF) for funding this research study.

References

Aloni A, Brenner A (2017) Use of cotton as a carbon source for denitrification in biofilters for groundwater remediation. Water 9:714-725

Wong TH (2006) An Overview of Water Sensitive Urban Design Practices in Australia. Wat. Pract. Tech. 1:1–8

Zinger Y, Blecken GT, Fletcher TD, Viklander M, Deletic A (2013) Optimising nitrogen removal in existing stormwater biofilters: Benefits and tradeoffs of a retrofitted saturated zone. Ecol. Eng. 51:75–82

11th World Congress on Water Resources and Environment (EWRA 2019)
"Managing Water Resources for a Sustainable Future", 25-29 June 2019, Madrid, Spain

Monte-Carlo simulations for capacity planning and reservoir management for urban water supply systems

S. Burak[1*], A.H. Bilge[2], F. Samanlioglu[2]
[1] Marine Environment Department Institute of Marine Sciences and Management, Istanbul University, Istanbul, Turkey
[2] Department of Industrial Engineering, Kadir Has University, Istanbul, Turkey
* e-mail: sburak@istanbul.edu.tr

Introduction

Appropriate and efficient management of urban water infrastructure is the key issue for the sustainability of water services. Demographic pressure on the one hand, climatic disturbances on the other, necessitate dynamic adaptation tools in order to comply with hydro-climatic variabilities and resulting uncertainties. Dam reservoirs are the most important elements of the water infrastructure system to be managed rationally, especially in cases of inter-basin water transfer. Water management systems based on historical hydrological data overlook expected future changes in the climatic systems, hence these can no longer be the only source of information to plan for variabilities and extremes (Ludwig et al. 2014). Therefore, pro-active and flexible measures which take into account changing conditions, deserve an in-depth assessment.

In a previous work, we studied future performance of the water supply system in Istanbul, Turkey, that consists of dam reservoirs and water transfer systems. Based on the demographic growth model that we have used, we have seen that the system would fail in the steady state, that is estimated to be reached over a 100-year horizon. In the present work, we study steady state capacity planning and operational performance of an urban water supply system consisting of dam reservoirs and water transfer systems, under stochastic natural inflow, taking into account variabilities in its statistical properties.

Simulations on an annual basis are used to determine capacity planning, basically for water transfer infrastructure. Then, simulations for the operational principles of the water transfer are used to determine a trade-off between the necessity of water shortage and excessive discharge. The management of the dam reservoir system is interpreted as an inventory management problem and system performance is described within this framework.

Materials and methods

A discrete model for reservoir management is proposed as follows. Let W_n be the amount of water present in the reservoir at the beginning of the period n. The amount at the next period is defined as

$$W_{n+1}=W_n+A_n+(Y_n^{(1)}+Y_n^{(2)}+Y_n^{(3)}) - (H_n^{(1)}+H_n^{(2)}+H_n^{(3)}) - D_n, \quad (1)$$

where, A_n denotes the natural inflow; the $Y_n^{(i)}$'s denote external inputs such as water transfer and/or non-conventional water, (e.g. treated effluent, desalinated water); the $H_n^{(i)}$'s denote the amount of water delivered for specific usages, such as urban use, irrigation or hydro-power generation and D_n denotes the amount of discharged water, including spared amount for environmental flow. The restrictions on these parameters are as follows.

- The storage capacity is bounded by W_M that depends on the total inflow to the catchment basin. Storage capacity at a specific period is denoted $W_{max,n} < W_M$. Any inflow exceeding $W_{max,n}$ should be discharged. On annual operational scheme, $W_{min,n}<W_n<W_{max,n}$, where $W_{min,n}$ is the dead storage capacity. Our monthly operational scheme is characterized by a critical storage level $W_{c,n}$, $W_{min,n}<W_{c,n}<W_n$ that corresponds to the amount of storage that will ensure successful operation of the system.
- The inflow during the period n, denoted by A_n, is a random variable, obeying Gamma and Gaussian distributions for monthly and annual precipitations, respectively. The statistical parameters are

computed using 105 years of data recorded at Kandilli Observatory, Istanbul, Turkey (BOUN-KOERI 2017). Inflows are computed using runoff coefficients and climate scenarios are implemented by adjusting the parameters of these random variables.

- External inputs $Y_n^{(i)}$, are limited by the design parameters, as $Y_n^{(i)} < Y_{max,n}^{(i)}$, denoting operational or structural constraints.
- The water quantity supplied for specific purposes $H_n^{(i)}$, are bounded by the demand $S_n^{(i)}$, i.e, $H_n^{(i)} < S_n^{(i)}$. Ideally, one should have $H_n^{(i)} = S_n^{(i)}$, but this may not be possible due to water scarcity.
- The amount of water that has to be discharged D_n, has to meet the environmental flow demand, i.e, $D_n > D_{e,n}$.

Simulation on annual basis: In the steady state, the water demand S_{max} is assumed to be constant, the reservoir capacity W_{max} is fixed and water transfer can be used to supplement the inflow with $Y_{max}=k(S_{max}-m(A))$, where k is a constant and m(A) is the expected value of the inflow. We apply the algorithm presented in (Burak et al. 2017) to the situation described above and run Monte Carlo simulations to determine the parameter k, for realizations keeping water rationing at an acceptable level.

Simulation on monthly basis: In monthly operational framework, we start with a fixed system capacity, optimized as above, and use the algorithm presented in (Burak et al. 2018), to determine the critical reservoir level, $W_{c,n}$, again with the purpose to minimize discharge, water transfer and water rationing.

Results and concluding remarks

Prerequisite for customer satisfaction is uninterrupted water supply, even under deficient hydrological conditions. In such cases, water transfer is used to compensate for the deficient water quantity which corresponds to the gap between demand and expected inflow to the storage system. Bearing in mind that, beyond its economic burden, water transfer touches delicate environmental issues, therefore, it has to be operated at minimal levels. Our simulations show that, due to irregularities in the inflow, higher quantities of water transfer would be necessary in order to operate the system without any interruption in the water supply. On the other hand, much lower real and environmental costs would occur if reasonable amounts of water shortages are tolerated.

In order to quantify these situations, we run Monte-Carlo simulations with effectively 10^7 replications, for water transfer capacities corresponding to the parameter values k=0.95, 1.00 and 1.05 respectively. The simulations are repeated for ratios of standard deviation over the mean of the inflow ranging from 20% to 50% to take into account climatic variability.

Table 1. Percentage of water rationing as a function of water transfer capacity and of the parameter $\eta=std(A_n)/m(A_n)$.

Water Transfer Capacity	**k=0.95**	**k=1**	**k=1.05**
η=0.20	2.8764	0.3359	0.0013
η=0.30	3.0574	0.7963	0.0782
η=0.40	3.4429	1.3853	0.3825
η=0.50	4.0131	2.0794	0.9717

Simulations on monthly bases are used to determine optimal critical storage level Wc,n by combining Monte Carlo simulations with inventory management techniques (Petersson et al. 2007).

Acknowledgments: This work is partially supported by the Istanbul University and Kadir Has University.

References

BOUN-KOERI (2017) Monthly precipitation in Istanbul. Bogaziçi University Kandilli Observatory and Earthquake Research Instutute, Istanbul

Burak S, Bilge A, Dernek D (2017) A network model simulation proposal for river basin management plans (RBMPs) in Turkey. Paper presented at the 10th World Congress of EWRA, 5-9 July 2017, Athens

Burak S, Bilge A, Dernek D (2018) Assessment and simulation of water transfer for Greater Istanbul using a network model. Water Resources Management (submitted)

Ludwig F, van Slobbe E, Cofino W (2014) Climate change adaptation and integrated water resource management in the water sector. Journal of Hydrology 518:235-242. http://dx.doi.org/10.1016/jhydrol.2013.08.010

Petersson E, Giupponi C, Feas J (2007) Decision support for strategic water management: Mdss in the large dam context. International Water Resources Association 32(2):265-279

11th World Congress on Water Resources and Environment (EWRA 2019)
"Managing Water Resources for a Sustainable Future", 25-29 June 2019, Madrid, Spain

Water quality vulnerability assessment and determination of critical control points in drinking water supply systems

S. Tsitsifli[1*], V. Kanakoudis[1*], D. Tsoukalas[2]
[1] Department of Civil Engineering, University of Thessaly, Volos, Greece
[2] School of Science and Technology, Hellenic Open University, Patras, Greece
* e-mail: tsitsifli@uth.gr

Introduction

Water supply systems are extremely vulnerable to risks caused unintendedly or being intended by human activities. Unintended risks exist due to operational conditions (such as disinfection by-products), extreme weather phenomena (e.g. floods) or other disasters (e.g. earthquakes) and aging of the water supply system. As water supply systems include kilometres of pipes and numerous pumps, valves, tanks and other important equipment, their complexity makes them extremely vulnerable to physical, chemical, biological and cyber threats. The threats' nature varies greatly depending on the geographic location, the population and the accessibility of the infrastructure.

The paper focuses on the vulnerability assessment and is connected to normal operating conditions. It is important to determine the critical control - vulnerable points in a water supply system and connect these points to physical, chemical and/or biological hazards.

Materials and methods

Vulnerability assessment of a water supply system takes into consideration the whole supply system (surface or groundwater intake), transmission, treatment and distribution system, up to the customer's tap. Risk determination in water supply systems is performed using HACCP and water safety plans methodologies, which are risk assessment tools used in many water utilities around the world (Damikouka et al. 2007; Havellar 1994; Khaniki et al. 2009; Martel et al. 2006; Nadebaum et al. 2004; Tavasolifar et al. 2012).

A typical flow diagram of the water supply system includes the following stages: (a) water intake (from surface water or groundwater sources); (b) transmission of water to the treatment plant; (c) water pre-treatment and treatment phases including coagulation, flocculation, sedimentation, filtration, ozonation etc. (in case of surface water) or treatment of groundwater when needed; (d) disinfection; (e) storage; (f) distribution network; and (g) customers' taps. The exact flow diagram of the water supply system depends on the water treatment needed based on water quality parameters.

The determination of hazards in the water supply system is very important. Surface water and groundwater can carry or be contaminated with pathogenic micro-organisms and chemical residues due to the existence of waste sources near the groundwater aquifers or surface water abstraction sources, such as solid waste, fertilizers used in agricultural activities etc. During the drinking water transfer from the pumping systems to the untreated water storage tank, the water can be contaminated with pathogenic micro-organisms, chemical residues and impurities (Martel et al. 2006; Nadebaum et al. 2004; National Water Quality Management Strategy 2004). In all pipeline systems the formation of biofilm, corrosion, possible leakages, etc. can adversely affect the physico-chemical and microbiological safety of water. Chemical and biological risks exist in the whole treatment process of drinking water. Disinfection is used to eliminate any possible biological threat. However, disinfection can be responsible for the formation of by-products, being responsible for severe impacts in human health. The selection of disinfection method, the determination of disinfection dose and the existence of disinfectant residual are critical factors in disinfection process. Finally, a variety of physical, chemical and microbiological hazards could occur in the drinking water distribution network up to the final consumption points (Martel et al. 2006). These hazards are due to corrosion, leakages and pipes' materials. There is still the possibility of existence of impurities

within the pipes due to leakage.

Results and concluding remarks

The analysis above is helpful for the determination of the critical control points in a water supply network. Every stage of the water supply system is examined taking into consideration the probability of occurrence of the risk as well as its severity. The water intake source is considered as a critical control point for biological (CCP1B-surface water & CCP2B-groundwater) and chemical hazards (CCP1C-surface water & CCP2C-groundwater). Pre-treatment stage is a critical control point for chemical hazards, while the treatment stage is responsible for the possible occurrence of biological (CCP3B) and chemical hazards (CCP4C). Also, final disinfection is defined as a critical control point for both biological (CCP4B) and chemical (CCP5C) hazards. Drinking water storage is likely to contaminate and develop biological hazards (CCP5B) while drinking water distribution up to the final consumption points can be defined as a critical control point for all types of hazards (CCP6B, CCP6C and CCP1F). The critical control points determination is a hard task and it depends on each water supply system characteristics. At this study the authors are trying to provide general guidelines.

At this paper the vulnerable - critical control points of a water distribution network are identified using the HACCP methodology. An effective vulnerability assessment can serve as a guide to the water utility by providing a prioritized plan for security upgrades, modifications of operational procedures, and/or policy changes to mitigate the risks and vulnerabilities to the utility's critical assets.

Acknowledgments: The research is elaborated within the framework of the invitation "Granting of scholarship for Post-Doctoral Research" of the University of Thessaly, which is being implemented by the University of Thessaly and was funded by the Stavros Niarchos Foundation.

References

Damikouka I, Katsiri A, Tzia C (2007) Application of HACCP principles in drinking water treatment. Desalination 210(1-3):138-145. https://doi.org/10.1016/j.desal.2006.05.039

Havellar HA (1994) Application of HACCP to drinking water supply. Food Control 5(3):145-152. https://doi.org/10.1016/0956-7135(94)90074-4

Khaniki GRJ, Mahdavi M, Mohebbi MR (2009) HACCP application for treatment of drinking water for Germi in Iran. Journal of Food, Agriculture & Environment 7(2):709-712

Martel K, Kirmeyer G, Hanson A, Stevens M, Mullenger J (2006) Application of HACCP for Distribution System Protection. American Water Works Association, USA

Nadebaum P, Chapman M, Morden R, Rizak S (2004) A Guide to Hazard Identification & Risk Assessment for Drinking Water Supplies. Research report II. CRC for Water Quality and Treatment, Australia

National Water Quality Management Strategy 2004 Australian Drinking Water Guideline 6. National Health and Medical Research Council, Australian Government

Tavasolifar A, Amin MM, Ebrahimi A, Jalali M (2012) Implementation of hazard analysis and critical control points in the drinking water supply system. International Journal of Environmental Health Engineering 1(3):1-7

11th World Congress on Water Resources and Environment (EWRA 2019)
"Managing Water Resources for a Sustainable Future", 25-29 June 2019, Madrid, Spain

Water losses management in the urban network of Algiers

K. Sebbagh*, A. Safri, Z. Moula
Environmental, Geotechnical and Hydraulic Laboratory (LEG-HYD), University of Science and Technology Houari Boumediene—(USTHB), Algiers, Algeria
** e-mail: karima.sebbagh@gmail.com*

Introduction

The Sustainable management of water distribution networks is a crucial challenge facing water utilities around the world. The World Bank study estimated that more than 32 billion cubic meters of treated water are lost each year to fleeing urban water supply systems through the world (Kingdom et al. 2006), Regarding the Algiers network, the Algerian Water and Sanitation Company (SEAAL) estimated in 2017 that the percentage of overall loss was 44%.

The work carried out in this document boils down to proposing a methodology that aims at pre-locating and detecting leaks in a drinking water supply system using a model calibrated and built using the GIS to optimize the use of resources and improve constancy of supply. The application of the FAVAD concept and the Genetics Algorithms (GA) are appropriate solutions for this kind of resolution. In order to test and validate the proposed approach, many pilots were tested in Algiers, where the total pipe length vary between 12 and 87 km, the results of these optimization were quite satisfactory (Sebbagh et al. 2018).

Materials and methods

Leaks in water systems generally appear due to the aging of the infrastructure, generated or amplified by corrosion, or to mechanical constraints which are particularly exposed by the increase in operating pressure. Many experimental researches have reported that the reduction of the pressure, induces the reduction of the leaks (Babel et al. 2009).

In this context we used the features of the Epanet hydraulic model using additional demand in the consumption node to simulate water leaks in a drinking water distribution system. this method is the best solution for the representation of leaks according to (Al-Ghamdi 2011; Cobacho et al. 2014).

When simulating a leak in EPANET, the parameter that represents the coefficient of flow rate through a valve is the emitter. This emitter represents a valve open to the atmosphere, it is a simple element of the node. The Equation (1) that represents the methodology mentioned above is the FAVAD concept:

$$Q(t)\text{total} = \sum [(Q_{DBi} * Cc\ (t)) + (Ci * Pi\text{^}N1)] \quad (1)$$

where $[Q_{DBi} * Cc\ (t)]$ is the hourly consumption demand and (Ci*Pi^N1)] is the leakage rate at node i, Ci is the discharge (emitter) coefficient, Pi is the simulated pressure at node i and N1 is the exponent emitter representative of entire network in EPANET.

The use of the equation above makes it possible to correctly represent the behavior of the leaks in a hydraulic model. The goal research is therefore the determination of the parameters Ci of each node of the hydraulic model and N1 representative of the whole network in order to be able to determine a leak rate specific to each node over a time t and to be able to pre-locate and detect the leaks on a distribution network.

A decision support tool has been developed for pre-locating leaks in Matlab in interface with EPANET and using the EPANET Toolkit's dynamic link library (DLL).

The input data for the tool for the calibration of the model are:

- A file (.inp) named from the hydraulic model concerned.
- Specification of the time that corresponds to the Minimum Night Flow (MNF), in order to calculate the quantities of leaks on each node at this time.
- Definition of GA parameters as population size, generation number, number of elites, crossing rate, etc., according to the user's choice (Sivanandam and Deepa 2018).

The output data are:

- A distribution of the emitter coefficients in each node of the network and the allocation of a single exponent of the emitter for the whole network, following the definition of the fitness function and the respect of the constraints of the GA.

Results and concluding remarks

The calibration of the model (flow and pressure) was successfully carried out using the programming tool. It was tested and validated by minimizing the fitness function, comparing the pressure and flow rate values measured with the results of the simulation.

During the calibration process, the coefficients Ci and the emitter exponent N1 were adjusted as calibration parameters of the flow rate and of pressure measurements.

The programming tool simulates and distributes leakage coefficients (Ci) on each network node and simulation of the emitter exponent N1 by optimizing the Genetic Algorithms. The calculation of the magnitude of the leaks at the time corresponding to the (MNF) on each node of the network is done through the use of the Equation (1). It is proposed to target critical points of leakage, thus contributing to help utilities in their efforts to reduce physical losses. The identification does not always necessarily tip accurately on the location of the leak, but it significantly reduces the uncertainty and thus allows leak detection teams in the field to obtain better detection rates more quickly in areas where leaks have been pre-located.

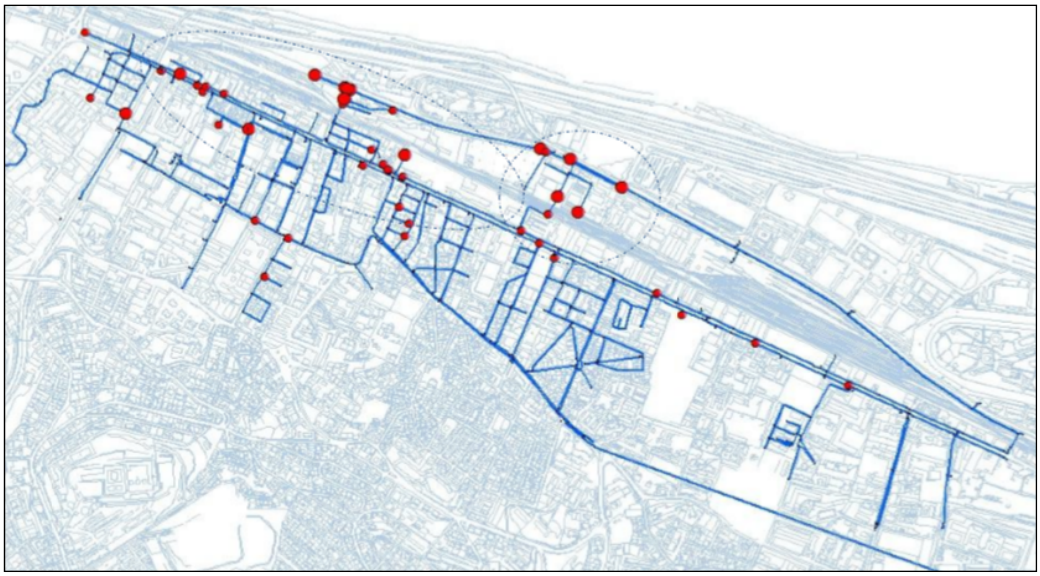

Figure 1. leaks pre-located and detected on a network of 30 km in Algiers.

References

Al-Ghamdi AS (2011) Leakage–pressure Relationship and leakage detection in intermittent water distribution systems. J. Water Supply Res. Technol. Aqua 60:178–183. http://doi:10.2166/aqua.2011.003

Babel MS, Islam MS, Gupta AD (2009) Leakage Management in a low-pressure water distribution network of Bangkok. Water Sci. Technol. Water Supply 9:141–147. doi:10.2166/ws.2009.088. 4

Cobacho R, Arregui F, Soriano J, Cabrera E Jr (2014) Including leakage in network models: An application to calibrate leak valves in EPANET. J. Water Supply Res. Technol. Aqua 64:30. doi:10.2166/aqua.2014.197

Kingdom B, Liemberger R, Marin P (2006) The challenge of reducing Non-Revenue Water (NRW) in developing countries. In The World Bank, Water Supply and Sanitation Sector Board Discussion Washington, Paper NO (08); World Bank Group, Washington, DC, USA

Sebbagh K, Safri A, Zabot M (2018) Pre-Localization approach of leaks on a water distribution network by optimization of the hydraulic model using an evolutionary algorithm. Proceedings 2:588; doi:10.3390/proceedings2110588

Sivanandam SN, Deepa SN (2018) Introduction to Genetic Algorithms. Springer, Berlin Heidelberg New York

11th World Congress on Water Resources and Environment (EWRA 2019)
"Managing Water Resources for a Sustainable Future", 25-29 June 2019, Madrid, Spain

Regional rainfall design parameters of Sustainable Urban Drainage Systems based on a stochastic approach. Case study: United States of America

A. Fanti[1*], Á. Sordo-Ward[2], R. Jodrá-López[2], L. Garrote[2], E. Caporali[1]
[1] Department of Civil and Environmental Engineering, University of Florence, Florence, Italy
[2] Department of Civil Engineering: Water, Energy and Environment, Universidad Politécnica de Madrid, Madrid, Spain
*e-mail: andrea.fanti1@stud.unifi.it

Introduction

Nature Based Solutions are becoming increasingly established as a solution for Flood Risk Management. Guidelines (e.g. WWF 2017; Woods Ballard et al. 2016) were developed in order to spread commonly adopted practices, including design methods for these facilities. Some solutions are designed to reduce storm runoff in urban environments. In these cases, standard design criteria specify that infiltration should be equal to or greater than 80% of rainfall volume.

This study is focused on the regional definition of hydrologic design of parameters for Sustainable Urban Drainage Systems (hereinafter cited as SuDS) in order to improve rainwater management. Design parameters are derived from local rainfall regime. Rainfall series are characterized by their main attributes, such as magnitude, intensity (mean/max.), duration, time between events, among others. The goal is to obtain a satisfactory performance of the facility under design conditions, specified in terms of relevant variables associated to different return periods. The objective of this study is to estimate the rainfall parameters for the design of SuDS at a regional scale and based on a stochastic approach.

Materials and methods

The methodology proposed in this work is based on a continuous rainfall record 20 years or longer at high time resolution (10 or 15 minutes). A Minimum Time between Storms (hereinafter cited as MTS), is defined first, used to single out individual events in the analysis period. The main variables characterizing each event are derived from the rainfall record, including rainfall depth, maximum rainfall intensity and duration. Hydrological parameters for SuDS design are derived from the observed probability distributions of these main variables. The design goal is usually to be able to process a certain fraction of the events or a certain fraction of total rainfall volume. For instance, the criterion set by normatives and guidelines (Woods Ballard et al. 2016) consist to treat at least the 80% of the storms (N80) or the 80% of total rainfall (V80) at the specified location. Hydrologic design consists on identifying the values of critical variables that satisfy this condition.

The analysis is carried out on data from the United States gauge station network. A set of 138 stations from contiguous states was chosen with a semi-random criterion. The first group was chosen from the list of most populated cities according to censuses. These are mostly clustered in the East and Southern coast. In order to obtain uniform coverage of the contiguous US, another group was randomly chosen from the cities with longer length of available record. The final group was composed of 138 stations. For each station, Mean Annual Rainfall (that is the average annual value of total precipitation, hereinafter cited as MAR), position, elevation, among others, were compiled. Koppen-Geiger climatological classifications (Kottek et al. 2006) was used to divide the group of stations in homogeneous subgroups. High-resolution rainfall data from these stations was processed to derive the probability distributions of main variables to produce a database of hydrological SuDS parameter values, including rainfall depth for V80 and N80 design criteria. The spatial distribution of the resulting hydrologic design criteria was analysed, using several geographical covariates to test alternative predictive schemes.

Results and concluding remarks

There is an evidence of correlation between hydrological parameters for SuDS design and other hydrological and climatological parameters (elevation, mean annual rainfall, climatological classification, etc.). Figure 1 shows the scatter plot of V80 rainfall depth versus Mean Annual Rainfall, showing evidence for a linear relationship, although highly spreaded. Climate zones (shown with different colours) also play a role.

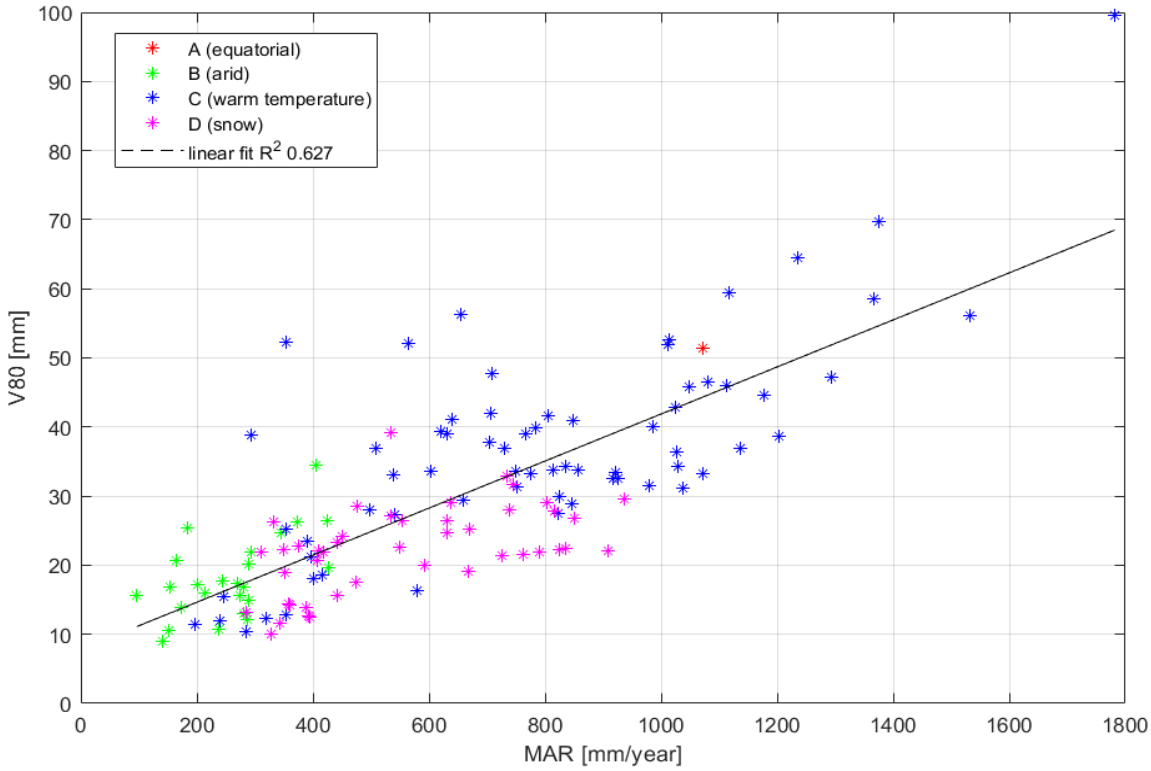

Figure 1. The 80% of total cumulated precipitation of total events in analysis period (V80) calculated with Accumulated Precipitation Criteria versus the Mean Annual Rainfall (MAR). Stations are here divided according Köppen-Geiger climatological division map (Kottek et al. 2006).

Analogous correlations were obtained for other percentages of minimum infiltration, for both approach criteria (N80, V80 and higher percentages). There is evidence of other non-linear correlations between such design variables with elevation. Again, climate zones play a role in these relations. These correlations encourage further analyses to test the existence of other possible multi-variates correlations in order to develop hydrological design parameters on a regional scale.

Acknowledgments: Funding from the ERASMUS+ Program is acknowledged allowing the first author to work on this research within his traineeship with the Research Group on Hydroinformatics and Water Management of the Universidad Politécnica de Madrid.

References

Woods Ballard B, Wilson S, Udale-Clark H, Illman S, Scott T, Ashley R, Kellagher R, Secondsurname B (2016) The SuDS Manual. CIRIA, Griffin Court, 15 Long Lane, London

Kottek M, Grieser J, Beck C, Rudolf B, Rubel F (2006) World Map of the Köppen-Geiger climate classification updated. Meteorol. Z. 15:259-263. doi: 10.1127/0941-2948/2006/0130.

WWF (World Wide Fund for Nature) (2017) Natural and Nature-Based Flood Management: A Green Guide (Flood Green Guide). https://www.worldwildlife.org/publications/natural-and-nature-based-flood-management-a-green-guide

11th World Congress on Water Resources and Environment (EWRA 2019)
"Managing Water Resources for a Sustainable Future", 25-29 June 2019, Madrid, Spain

RISKNOUGHT: A cyber-physical stress-testing platform for water distribution networks

D. Nikolopoulos[1*], G. Moraitis[1], D. Bouziotas[2], A. Lykou[1], G. Karavokiros[1], C. Makropoulos[1,2]
[1] Department of Water Resources and Environmental Engineering, School of Civil Engineering, National Technical University of Athens, Iroon Politechniou 5, 157 80 Zografou, Athens, Greece
[2] KWR, Water Cycle Research Institute, Groningenhaven 7, 3433 PE Nieuwegein, the Netherlands
* e-mail: nikolopoulos.dio@gmail.com

Introduction

Cyber-Physical systems (CPS) consist of two layers, one comprised of the physical processes, and one computational and networking layer (Lee 2008). Modern water systems (distribution network, treatment plants, etc.) are CPS, as the physical system is supervised and operated by sensors and actuators through SCADA (Supervisory Control And Data Acquisition) in real-time. Advantages of CPS are automation, increased reliability and efficiency. However, a major disadvantage of the networking, communication and remote control of CPS is the susceptibility to cyber and physical attacks (or combinations) (Rasekh et al. 2016). Indeed, various incidents of cyber-physical attacks have threatened real-world water CPS, making them among the most targeted critical infrastructure (ICS-CERT 2016), e.g. like the 2000 Maroochy Water Services incident.

As water CPS are critical for human society, life and health, there is an immediate need of developing robust tools able to assess performance under cyber-physical threat scenarios. Influential work in this new field is implemented by Taormina et al. (2017), with the characterization of cyber-physical attacks in water distribution systems and the development of an EPANET-based modelling environment of such attacks.

In this work, we present the development of a stress-testing modelling platform for Cyber-Physical water distribution systems, able to simulate both the cyber layer information flow and the physical processes.

Materials and methods

Our modelling platform called RISKNOUGHT (risk + nought, to risk nothing) is EPANET-based as it is a proven tool for water distribution network simulations. We use the WNTR toolbox (Klise et al. 2017) which provides the functionality of simulating and analysing systems and model input/output. WNTR has a built-in hydraulic simulation engine using the same equations as EPANET and is also able to use EPANET's engine. The advantage of WNTR simulation engine is the ability to perform Pressure Driven Analysis, which is essential for simulating the inability of meeting demands due to disrupted system operation under a cyber-physical attack. Hence, we use WNTR's simulation engine as the basis of the physical layer of the system.

On top of the physical layer we develop the cyber infrastructure objects: sensors, actuators, Programmable Logic Controllers (PLC), central SCADA and Historian (the database of the SCADA) and their respective connections (wireless, optical fiber etc.). These objects form the control logic of the network by interacting with each other. The control logic explicitly and directly controls the state of the physical layer in each simulation time step. For example: A sensor in a tank senses its level (the actual tank head of the hydraulic simulation in this particular time-step) transmits this information to a PLC, which accordingly to its specified set of instructions sends a signal to an actuator to turn a pump off (setting the pump to off in the hydraulic network). The actuator transmits an ACK ("acknowledged") signal back to the PLC and the PLC reports all inputs and actions to the supervisory SCADA, which stores data in the Historian.

We have developed methods of various interactions between both layers that can simulate a comprehensive list of cyber-physical threat scenarios on a wide range of attack vectors throughout the CPS. This includes:

- Attacks that target sensors, like manipulating readings, making them appear offline or physically

destroy them etc.

- Attacks that target actuators, like intercepting signal from PLCs and sending fake ACK messages, making them offline, performing Denial Of Service attacks, alter behaviour etc.
- Attacks on PLCs, like altering/deleting the instruction sets, making them offline etc.
- Attacks on master SCADA and Historian units, like disrupting communications with the slave PLCs, making the whole cyber system offline, altering database values etc.
- Physical attacks on the hydraulic system, like destroying pumps, valves, pipes etc.

More than one attacks are possible to affect multiple components of the system, and start times and duration of the events can be described, using a novel scenario planner tool that sets the environment for the cyber-physical simulation. By using the scenario planner we can conduct a thorough stress-testing of the system with a multitude of different attack combinations and system states in order to identify vulnerabilities and assess performance.

Consequences of the cyber-physical attacks, including cascading effects on the physical layer, can be quantified through the use of selected Key Performance Indicators, in multiple dimensions (e.g. demand coverage, recovery time, Customer Minutes lost), depicting the criticality of the CPS service failure.

Results and concluding remarks

We present a cyber-physical stress-testing platform able to simulate both the cyber and physical layers of a water distribution network and assess performance versus a wide range of cyber-physical attacks. The use of the platform is presented by utilizing the C-Town water distribution system, which is based on a real-world medium-sized network (Ostfeld et al. 2012), already used as benchmark for similar purposes. It is suggested that such tools are crucial for preparing water utilities to shield their systems from potential threats of the evolving digital landscape.

Acknowledgments: STOP-IT has received funding from the European Union's Horizon 2020 research and innovation programme under grant agreement No 740610. The publication reflects only the authors' views and the European Union is not liable for any use that may be made of the information contained therein.

References

ICS-CERT (Industrial Control Systems-Cyber Emergency Response Team) (2016) NCCIC/ICS-CERT year in review: FY 2015. Rep. No. 15-50569. DC: ICS-CERT, Washington

Klise KA., Hart DB, Moriarty D, Bynum M, Murray R, Burkhardt J, Haxton T (2017) A software framework for assessing the resilience of drinking water systems to disasters with an example earthquake case study. Environmental Modelling and Software 95(1):420-431. http://doi.org/10.1016/j.envsoft.2017.06.022

Lee EA (2008) Cyber physical systems: Design challenges. 11th IEEE Int. Symp. on Object Oriented Real-Time Distributed Computing (ISORC), IEEE, New York, 363. http://doi.org/10.1109/ISORC.2008.25.

Ostfeld A, Salomons E, Ormsbee L, Uber JG (2012) Battle of the water calibration networks. Journal of Water Resources Planning and Management 138(5):523-532. https://doi.org/10.1061/(ASCE)WR.1943-5452.0000191

Rasekh A, Hassanzadeh A, Mulchandani S, Modi S, Banks MK (2016) Smart water networks and cyber security. Journal of Water Resources Planning and Management 142(7):01816004. http://doi.org/10.1061/(ASCE)WR.1943-5452.0000646

Taormina R, Galelli S, Tippenhauer NO, Salomons E, Ostfeld A (2017) Characterizing cyber-physical attacks on water distribution systems. Journal of Water Resources Planning and Management 143(5):04017009. https://doi.org/10.1061/(ASCE)WR.1943-5452.0000749

11th World Congress on Water Resources and Environment (EWRA 2019)
"Managing Water Resources for a Sustainable Future", 25-29 June 2019, Madrid, Spain

Modelling water quantity in low impact development solution for stormwater management in residential area: A case study

D.J. Carvalho[1*], M.E.L. Costa[1], C.S. Conserva[2], L.M.S. Andrade[2], S. Koide[1]
[1] Civil and Environmental Engineering Department, Faculty of Technology, University of Brasília, Brasília, Brazil
[2] Faculty of Architecture and Urbanism, University of Brasília, Brasília, Brazil
* e-mail: d.junqueirac@gmail.com

Introduction

Conventional solutions for stormwater management have been causing a series of problems to the environment and the urban population. These solutions include designing drainage systems with large conduits that aim to rapidly convey the water downstream. However, due to the large volume of runoff generated by the surface impermeabilization and the presence of pollutants, problems such as flooding and diffuse pollution of the receiving water bodies often occur. In Brazil, despite the studies that show that this type of solution is outdated and that there are technologies that can be applied to minimize the impacts, the traditional approach is still used in the design of new stormwater systems (Souza et al. 2012).

Low impact development (LID) solutions are sustainable alternatives to stormwater management that have various benefits, including the reduction of runoff volume, the increase of infiltration and possibly the enhancement of the water quality. Solutions like this have been showing positive results in a number of applications around the world (WWAP 2018). There are different types of LID practices, for example, rain gardens and infiltration swales, but all of them require proper planning and integration with the urban design. In the study of the application of LID solutions, modelling has been shown to be a useful tool, being performed to quantify the practice's benefits (Shamsi 2010; Méndez 2018). Thus, this study aimed to compare the performance of a traditional and a low impact development solution in terms of water quantity by hydraulic and hydrological modelling applied to a new development area to be constructed.

Materials and methods

The studied area corresponds to a residential region in the Federal District, Brazil, that has not been implemented yet due to concerns about the impact on the lake that is immediately downstream. Important information about the future infrastructure were available, as the drainage system project and the urban design.

The area will accommodate 1,415 land parcels with total area of 223.5 hectares. The designed drainage network uses a traditional solution, composed by 525 conduits with diameters varying from 0.6 to 3 meters, integrated with two detention ponds near the outfall of the watershed. The slope ranges mostly between 3 and 8% and the soils can be classified as SCS hydrological soil group A, with good infiltration capacity.

Since the development has yet not been implemented, modifications in the project can be considered. Therefore, in addition to the existing proposal for the drainage system an alternative project that added LID solutions to the stormwater management was adapted over the original development proposal and studied. The LID practices adopted were the vegetative swales, that were distributed along the contour lines in the area. Side slope of 1:3 proportion (vertical / horizontal) and 1-meter depth swales were adopted. Surface slope paths within the swale were assumed to be small considering that the projected swales followed the topography.

The Storm Water Management Model (SWMM) was used by means of the PCSWMM software to model the solutions. The SCS method was chosen to quantify the runoff and infiltration and the Curve Number coefficient was estimated to each subcatchment using weighted average based on the projected land use. Dynamic wave was adopted for flow routing and a design storm with a 10-year return period and 24-hour duration was used for the simulations as suggested by the local Authority for drainage networks design.

Results and concluding remarks

The simulation with the design storm event allowed to evaluate the tendencies of the hydrological processes in the study area for a precipitation of high return period, besides the performance of the detention ponds and the reduction of peak flow provided by them. The total precipitation depth generated in the 24 hours of the event was 97.6 mm. From this depth, less than 42% of the water infiltrated in the scenario with the proposed project and the other part became surface runoff or was stored along the area. With the LID solution scenario, the infiltration amounted 78% of the precipitation depth, which represents a significant improvement and indicates a reduction of the generated runoff and increase in groundwater recharge, very important to this site. Table 1 shows the results found for the simulated scenarios.

Table 1. Modelling results for each scenario and comparison between the LID and the Proposed Project.

	Proposed Project	LID solution	LID x Proposed Project
Peak flow	6.5 m^3/s	0.53 m^3/s	- 92%
Runoff volume	93.5 x 10^3 m^3	18.1 x 10^3 m^3	- 81%
Infiltration volume	87.7 x 10^3 m^3	164.8 x 10^3 m^3	+ 88%

The peak flow presented for the Proposed Project scenario is the value obtained for sum of the detention ponds outflows. The detention ponds reduced the peak flow value from 45 m^3/s at the inlet to 6.5 m^3/s at the outlet, showing great efficiency. However, less than half of the total storage volume available was used in both of them and this simulation indicates that they are oversized. In the LID scenario the detention ponds were not necessary because the peak flow was already reduced to an acceptable value.

About the drainage system, it was verified that in the Proposed Project scenario some of the conduits were undersized, causing surcharging and even flooding in certain points of the system. For the LID solution scenario, only small conduits were necessary to collect the outflow from the vegetative swales. The LID devices functioned as expected, but regarding the total swale depth available, less than 50% of it was occupied, reaching the maximum of 0.34 meters of depth in one swale.

Modelling results showed that the conventional solution leads to substantial impacts on the hydrological cycle in the area, which can be mitigated by the application of LID solution. The detention ponds can reduce peak values, however, it did not help the reestablishment of the natural processes within the area, as did the vegetative swales. Both the conventional drainage network project and the LID addition project need alterations and the use of the SWMM model was a useful tool to study these stormwater management scenarios.

It is important to point out that the LID solution proposed still has grounds for improvement. Some important steps of the modelling process such as calibration were not performed in this study since there was no data for this. In addition, continuous simulation is required to evaluate the performance of the proposed LID more accurately. Therefore, it is important to proceed with investigation with the LID solutions including the acquisition of field data and the simulation with long time series of local precipitation.

Acknowledgments: FAPDF, CAPES and FINEP for the support and Chi Water for the PCSWMM license.

References

Méndez DFP (2018) Hydraulic Analysis of Urban Drainage Systems with Conventional Solutions and Sustainable Technologies: Case Study in Quito, Ecuador. Journal of Water Management Modeling 26:C440. https://doi.org/10.14796/JWMM.C440

Shamsi UM (2010) Low Impact Development for Stormwater Quantity and Quality. Journal of Water Management Modeling R236-13:199-209. https://doi.org/10.14796/JWMM.R236-13

Souza CF, Cruz MAS, Tucci CEM (2012) Desenvolvimento Urbano de Baixo Impacto: Planejamento e Tecnologias Verdes para a Sustentabilidade das Águas Urbanas. Revista Brasileira de Recursos Hídricos 17(2):9-18. https://doi.org/10.21168/rbrh.v17n2.p9-18

WWAP (United Nations World Water Assessment Programme)/UN-Water (2018) The United Nations World Water Development Report 2018: Nature-Based Solutions for Water. UNESCO, Paris

11th World Congress on Water Resources and Environment (EWRA 2019)
"Managing Water Resources for a Sustainable Future", 25-29 June 2019, Madrid, Spain

Water supply network rehabilitation: A case study

G. Viccione
Department of Civil Engineering, University of Salerno, Fisciano, Italy
e-mail: gviccion@unisa.it

Introduction

Serino, Southern Italy, known by the locals as "il paese dell'acqua" which translated reads as "the town of waters", suffers recurrent water shortages due to the obsolescence of the local water supply network. Such a circumstance sets up a paradox since the "Serino aqueduct" alone supplies Naples, the capital of Campania Region and its neighbourhood, with a discharge of approximately 1–3.5 m^3/s (Fiorillo et al. 2007). Belonging to the well known Terminio karst aquifer, moderately conditioned by groundwater abstraction (Pagnozzi et al. 2017), Serino springs have being exploited since long time. Consider that the Serino aqueduct, also known as Aqua Augusta, was built during the Augustus period, almost certainly at the end of the 1st century B.C., when Marco Agrippa was the curator aquarum of the Roman Empire (De Feo and Napoli 2007). Karst aquifers represent a fundamental resource as they supply drinkable water to about a quarter of the world's population including European cities such as London, Paris, Rome and Vienna (Ford and Williams 2007).

The rehabilitation of water supply networks is a crucial aspect of sustainable urban development in a scenario where strategies for limiting the effects of climate change have to be taken into account to preserve water quality. Unfortunately, most water utilities do not developed a long-term decision making approach to prevent the aging of pipes and degradation of hydraulic manufacts. It is common to take decisions on a year-to-year base which elements of the water supply system should be rehabilitated or, even worse, on impeding emergency calls. Numerous rehabilitation strategies have been presented in the literature, e.g. Engelhardt et al. (2000), Scholten et al. (2014), Shin et al. (2016), as well as related applications (Aşchilean and Giurca 2018; Viccione et al. 2018).

The purpose of the paper is to discuss the rehabilitation of a water supply network with reference to a case study.

Materials and methods

The water distribution network (WDN) of Serino, made up of four independent networks as depicted in Figure 1.a, is supplied by three springs and two wells, (conceptual scheme in Figure 1.b), serving a population of about 7000 (Table 1) with a total demand for water of 57 l/s whereas the available actual flow rate is only 35-40 l/s during the drought season. It was built between the fifties and sixties with the "Mezzogiorno Development Fund" which provided incentives for infrastructures in Southern Italy. The continuous maintenance interventions led to the displacement of pipes and artworks of different materials: cast iron, steel and more recently HDPE. The water balance shows water leakages reaching peaks of 60% due to the age of the system and fragmented repairs. In addition, there are - however few - main pipelines working as distributing and conveying water at the same time. Some feeding tanks are going through a poor state of maintenance while others have not enough volume capacities to adequately serve the network with recurrent service interruptions.

Table 1. Main features of sub-water networks.

Feeding Tank	San Gaetano	Subravai	Guanni	Canale
Serving population [ab.]	4125	1392	892	522
Total length of pipes [km]	27	11	5	5
Covered Area [km^2]	4.96	1.56	0.58	0.86
Density [ab./km^2]	752	1112	1578	891
Elevation range [m a.s.l.]	367-502	410-586	407-472	401-553

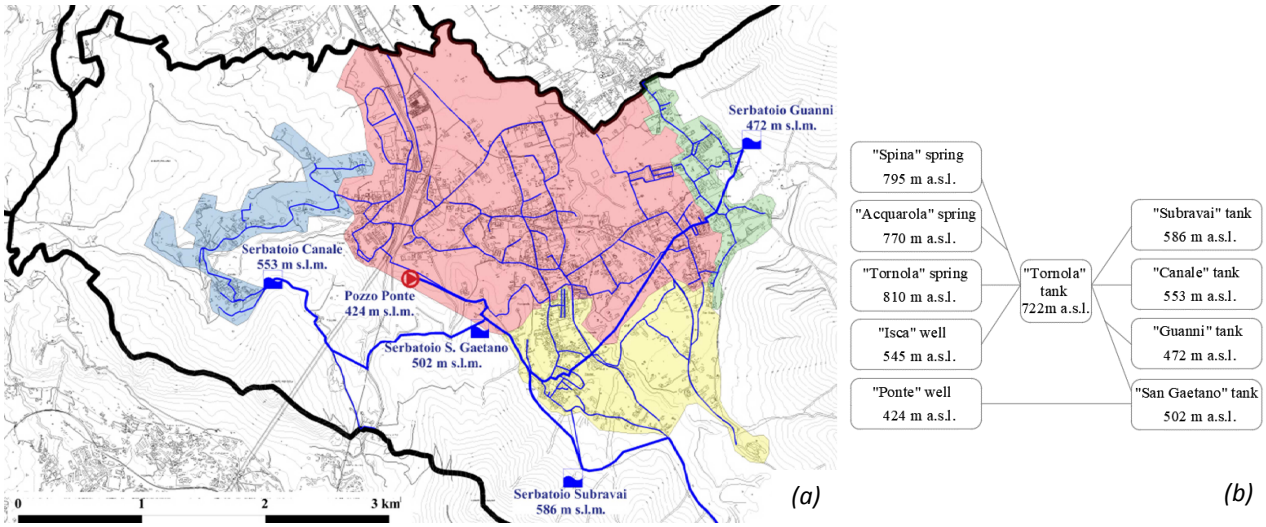

Figure 1. (a) Layout of the water supply network of Serino, Italy; (b) Conceptual scheme

Results and concluding remarks

As the local water distribution networks should have an acceptable level of reliability the following actions was considered:

- The "Isca" water lifting pump system can reach a higher water flow rate peak of 42 l/s (up to 50% more), as shown by a recent geological investigation of the aquifer. The new pump station of 190 kW, implying an energy consumption increase of 72% and an initial investment of 55000 Eur, will replace the actual pump, being operational since the nineties and not to be energy efficient.
- The WDN of Serino was automatically implemented (Viccione 2010) and executed in EpaNet solver, showing areas at higher altitude with piezometric heads lower than 10 m and areas at lower altitudes with piezometric heads exceeding 80 m. The level of service was then restored by identifying District metered areas (DMAs), using Pressure Reducing Valves (PRV) taking into account the hydraulic and network topology constraints (availability of water resource, streets, tanks) while minimizing the total cost, made of capital investment, maintenance and rehabilitation costs.

References

Aşchilean I, Giurca I (2018) Choosing a water distribution pipe rehabilitation solution using the analytical network process method. Water (Switzerland) 10(4):484. http://doi.org/10.3390/w10040484

De Feo G, Napoli RMA (2007) Historical development of the Augustan Aqueduct in Southern Italy: Twenty centuries of works from Serino to Naples. Water Science & Technology Water Supply 7(1):131-138. http://doi.org/10.2166/ws.2007.015

Engelhardt MO, Skipworth PJ, Savic DA, Saul AJ, Walters GA (2000) Rehabilitation strategies for water distribution networks: a literature review with a UK perspective. Urban Water 2:153-170. http://doi.org/10.1016/S1462-0758(00)00053-4

Fiorillo F, Esposito L, Guadagno FM (2007) Analyses and forecast of water resources in an ultra-centenarian spring discharge series from Serino (Southern Italy). Journal of Hydrology 336:125-138. http://doi.org/10.1016/j.jhydrol.2006.12.016

Ford D, Williams P (2007) Karst hydrogeology and geomorphology. Wiley J. & Sons Ltd

Pagnozzi M, Esposito L, Fiorillo F, Ventafridda G. (2017) Analysis of recharge processes in some karst systems, Southern Italy. Rendiconti Online Societa Geologica Italiana 43:23-27

Scholten L, Scheidegger A, Reichert P, Mauer M, Lienert J (2014) Strategic rehabilitation planning of piped water networks using multi-criteria decision analysis. Water Research 49:124-143

Shin H, Joo C, Koo J (2016). Optimal Rehabilitation Model for Water Pipeline Systems with Genetic Algorithm. Procedia Engineering 154:384-390. http://doi.org/10.1016/j.proeng.2016.07.497

Viccione G, Amato R, Martucciello M (2018) Hydropower Potential from the AUSINO Drinking Water System. Proceedings 2:688. http://doi.org/10.3390/proceedings2110688

Viccione G (2010) Una procedura per la generazione da CAD dei file di input per Epanet. L'Acqua 2:185-188

11th World Congress on Water Resources and Environment (EWRA 2019)
"Managing Water Resources for a Sustainable Future", 25-29 June 2019, Madrid, Spain

On the potential of the first flush concept for sizing criteria of stormwater control practices

S. Todeschini*, S. Manenti
Department of Civil Engineering and Architecture, University of Pavia, Pavia, Italy
** e-mail: sara.todeschini@unipv.it*

Introduction

The behaviour of pollutant load in wet-weather runoff has been widely investigated in the last decades. These studies demonstrated that the early runoff in a storm event is often more contaminated than the subsequent part of the hydrograph, a phenomenon known as first flush. Unfortunately, the notion of first flush has been adopted with reference to a plurality of detection methodologies (Bertrand-Krajewski et al. 1998; Ma et al. 2002), most of them hardly usable for the design and sizing stormwater quality control measures.

This paper studies in deep the first flush concept with the aim of exploiting the potential of this phenomenon for an effective and economical implementation of stormwater quality control practices. In this analysis the first flush notion is associated to a first flush volume and related pollutant loads instead of proportions, as these quantities are actually needed for the definition of sizing criteria and for a critical evaluation of the rules imposed by regulations. Different pollutants are tested since an effective improvement of current stormwater practices requires the knowledge and the peculiarity of the dynamics of various pollutant types. This is an important insight of the adopted procedure since traditional approaches have often shown problems in the first flush assessments on different pollutants (McCarthy 2009).

Materials and methods

A newly developed sound quantitative methodology (Bach et al. 2010) is applied for the assessment of the first flush on discrete water quality data of different pollutant types (i.e., total suspended solids TSS, chemical oxygen demand COD, total phosphorus TP, total nitrogen TN, Pb and Zn) collected during a long lasting monitoring campaign in an urban catchment of Pavia, Italy (Papiri et al. 2008).

The assessment method start by finding the average catchment pollutant concentrations for a given increment of runoff volume using a number of event pollutographs. The non-parametric Wilcoxon Rank Sum Test (Gibbons and Chakraborti 2011) is then used to establish a catchment's characteristic pollutograph, identifying: i) the initial and background pollutant concentrations; ii) the first flush strength, assessed by the probability value from the Wilcoxon Rank Sum Test applied to the population of the initial and last group; iii) the corresponding first flush volume, which is defined as the required runoff volume to reduce a catchment's stormwater pollutant concentrations to background levels.

A sensitivity analysis is carried out both on the slice size and the level of statistical significance for the Wilcoxon Rank Sum Test; a common sense solution is then proposed in order to overcome some ambiguities that can arise from the analysis.

The robustness and the advantages of the adopted procedure are also tested by comparing the results obtained from the adopted procedure to the results from a previous study quantifying the magnitude of the first flush in the examined catchment by means of the Mass First Flush Ratio method (Barco et al. 2008).

Results and concluding remarks

The adopted procedure allows identifying the first flush phenomenon for all the examined pollution parameters with a 5% significance level, while some pollutant does not meet the test requirements at 1% significance level. Pollutants exhibit different number of slice groups and, therefore, different first flush

volume, confirming the peculiarities of the dynamics of each pollution parameter in wet-weather runoff. Some tendency is observed between the strength and the volume of the first flush.

All pollutants exhibit a strong reduction in concentration compared to the initial value after 3 mm runoff, but the achievement of background levels for all parameters requires the transit of 6 mm runoff (as shown for TSS in Figure 1). These values do not differ much from usual Italian design criteria for wet-weather detention tanks arising from regional regulations (e.g., for Lombardia Region: Regional Law 12 December 2003, N.26 and Regional Regulations 24 March 2006, N. 3 and 4), which impose storage capacities ranging from 25 to 50 m^3 per contributive impervious hectare.

The sensitivity analysis shows the crucial role of the monitoring protocol and event selection criteria for enhancing the robustness of the methodology. The strength and the advantages of the adopted procedure are also highlighted by comparison with the widely used Mass First Flush Ratio method. The adopted approach proves therefore fruitful to guide decisions and sizing criteria for stormwater quality control measures.

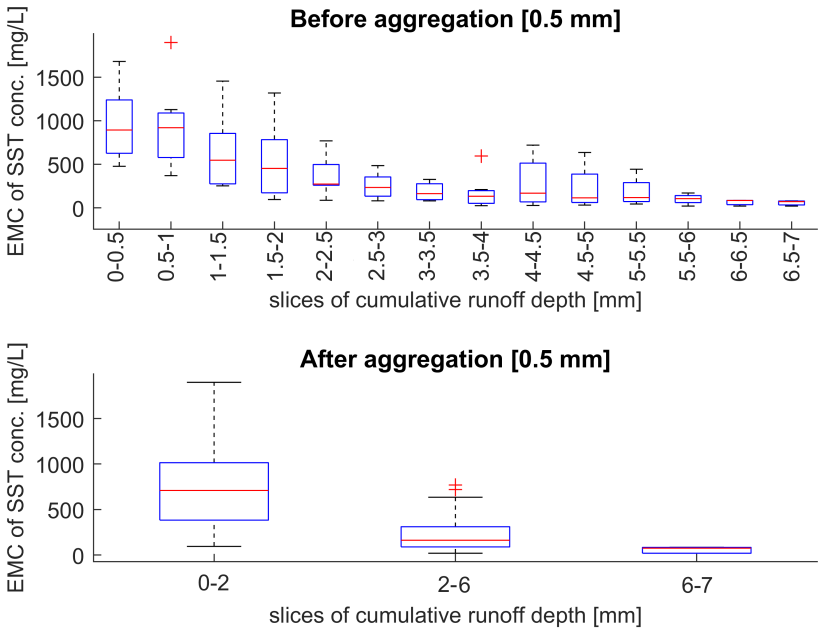

Figure 1. Ungrouped (slice size 0.5 mm) and grouped (5% significance level) box and whisker plots for TSS concentration data.

References

Bach PM, McCarthy DT, Deletic A (2010) Redefining the stormwater first flush phenomenon. Water Research 44:2487-2498

Barco J, Papiri S, Stenstrom MK (2008) First flush in a combined sewer system. Chemosphere 71:827–833

Bertrand-Krajewski JL, Chebbo G, Saget A (1998) Distribution of pollutant mass vs volume in stormwater discharges and the first flush phenomenon. Water Research 32:2341–2356

Gibbons JD, Chakraborti S (2011) Nonparametric Statistical Inference, 5th ed., Chapman & Hall/CRC Press, Taylor & Francis Group, Boca Raton, FL

Ma JS, Khan S, Li YX, Kim LH, Ha S, Lau S-L, Kayhanian M, Stenstrom MK (2002) First flush phenomena for highways: how it can be meaningfully defined. In: Proceedings of the 9th International Conference on Urban Drainage (ICUD), Portland, Oregon

McCarthy DT (2009) The first flush of E. coli in urban stormwater runoff. Water Science and Technology 60(11):2749–2757

Papiri S, Ciaponi C, Todeschini S (2008) The experimental urban catchment of Cascina Scala (Pavia): rainfall, runoff and quality of sewer discharges from 1987 to 2006. Aracne, Rome, Italy (in Italian)

11th World Congress on Water Resources and Environment (EWRA 2019)
"Managing Water Resources for a Sustainable Future", 25-29 June 2019, Madrid, Spain

Urban water supply management in critical conditions using fuzzy PROMETHEE V technique

M. Ghandi, A. Roozbahani*
Department of Irrigation and Drainage Engineering, Aburaihan Campus, University of Tehran, Tehran, Iran
** e-mail: roozbahany@ut.ac.ir*

Introduction

Drinking water supply management in pre-crisis conditions is crucial topic. Many different natural and unnatural disasters, including earthquakes, droughts, floods, terrorist attacks and water pollution, cause the great damages to the urban water supply networks. Prioritizing the effective strategies by expert decision-makers before any of such events can greatly mitigate their consequences. It is also essential to minimize the strategy-related costs as urban crisis management organizations have limited budgets. PROMETHEE V is a widely-applied category of MCDM which uses net flow calculations to optimize the selection of the best subset of measures facing limitations such as maximum budget available to the government, human resources and etc. For example, Morais and De Alemeida (2007) proposed a leakage management strategy in water distribution networks, using the PROMETHEE V. Fontana and Morais (2013) used the PROMOTHEE V to select water leakage reduction scenarios considering system constraints, such as water loss and budget limitation.

The current research introduced Fuzzy PROMRTHEE V technique for the first time to select the most applicable drinking water supply risk management alternatives in critical conditions for Tehran city, capital of Iran with considering the budget limitations, diversity of expert opinions and criteria such as Water supply reliability, Implementation cost, Implementation simplicity, social satisfaction and water quality.

Materials and methods

The general structure of the proposed model is presented in Figure 1.

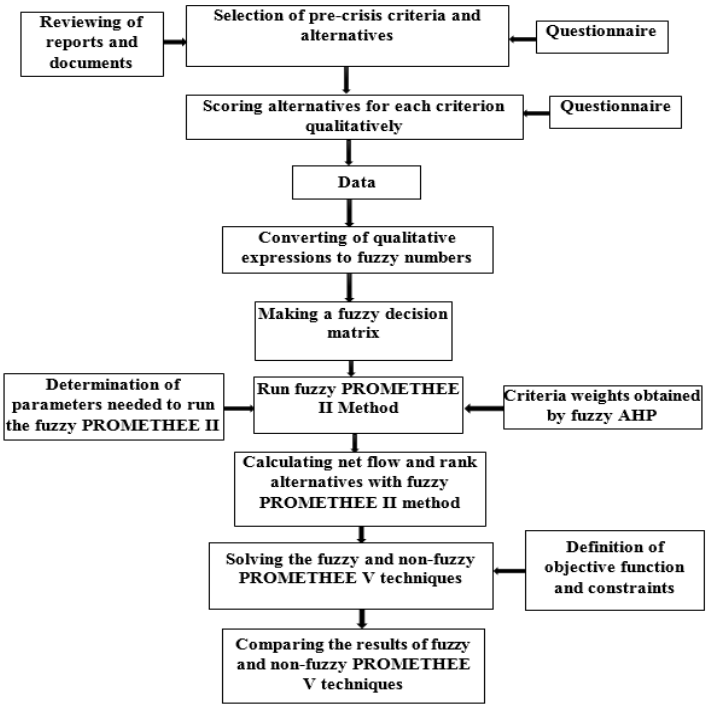

Figure 1. Flowchart of Fuzzy PROMETHEE V method

Results and concluding remarks

In this study, 5 criteria and 10 alternatives for water supply management in pre-crisis conditions were determined for Tehran city in Iran with population of 11,050,000 people by preparing the questionnaires. As mentioned before, the first step is to consider the problem without any limitation and to solve and rank alternatives using PROMETHEE II. After investigating the budget limitations for alternatives, coefficients of the objective function and fuzzy net flow were calculated using the PROMETHEE II and the budget limitation as the problem's constraint was defined, resulting in the formation of a fuzzy optimization problem, which was solved using fuzzy method and one non-fuzzy method (Table 1).

Table 1. The results of fuzzy and non-fuzzy PROMETHEE V

Method	Feasible alternatives	Not feasible alternatives	Z
Fuzzy PROMETHEE V	A2,A3,A5,A6,A7,A9	A1,A4,A8,A10	Z= 11.97
Non-fuzzy PROMETHEE V	A2,A3,A4,A5,A6,A7,A9	A1,A8,A10	Z= 8.39

Results from solving the model with fuzzy and non-fuzzy methods showed that the Z value of the objective function in the non-fuzzy PROMETHEE V was 8.39; whereas, this value increased to 11.97 using the fuzzy PROMETHEE V technique. These results showed that the fuzzy PROMETHEE V is more practical to control emergency conditions and enables decision makers to adopt applied alternatives more carefully. The final selected alternatives are: Enhancing the safety of chlorine capsules and changing the water chlorination system (A2), Strengthening passive defence in supply, transportation and distribution systems (A3), Planning to use popular forces and holding maneuvers (A5), Preparing portable water treatment systems (A6), Equipping water supply systems with emergency power (A7), Management of consumption, promoting the water-saving culture and encouraging people to store emergency water (A9). The proposed model can be also used to plan scenarios during and after the crisis in vulnerable cities.

References

Fontana ME, Morais DC (2013) Using Promethee V to select alternatives so as to rehabilitate water supply network with detected leaks. Water resources management 27(11):4021-4037. https://doi.org/10.1007/s11269-013-0393-1

Kumar A, Kaur J, Singh P (2011) A new method for solving fully fuzzy linear programming problems. Applied Mathematical Modelling 35(2):817-823. https://doi.org/10.1016/j.apm.2010.07.037

Morais DC, de Almeida AT (2007) Group decision-making for leakage management strategy of water network. Resources, Conservation and Recycling 52(2):441-459. https://doi.org/10.1016/j.resconrec.2007.06.008

11th World Congress on Water Resources and Environment (EWRA 2019)
"Managing Water Resources for a Sustainable Future", 25-29 June 2019, Madrid, Spain

Developing quantitative metrics to manage water resources for a sustainable future

H. Tavakol-Davani[1*], T.J. Sun[1], S.J. Burian[2]
[1] *Department of Civil & Environmental Engineering, San Diego State University, San Diego, CA, USA*
[2] *Department of Civil & Environmental Engineering, University of Utah, Salt Lake City, UT, USA*
** e-mail: htavakol@sdsu.edu*

Introduction

Sustainable water resources management has received attention from researchers with different backgrounds, including water resources engineers and sustainability experts, recently. On one hand, water resources engineers have been identifying ways to achieve hydrologic goals through implementation of recent environmentally-friendly approaches, e.g. Green Infrastructure – without quantifying the life cycle environmental impacts of the infrastructure. On the other hand, sustainability experts have been applying the ISO Life Cycle Assessment (LCA) to quantify the life cycle environmental impacts of water infrastructure in implementation, operation and maintenance phases – without considering the important water resources engineering aspects through hydrologic and hydraulic (H&H) analysis. In fact, defining proper system elements and boundaries for watershed-scale sustainability studies requires both H&H and LCA specialties, which reveals the necessity of performing an integrated, interdisciplinary study presented in this paper.

Materials and methods

Application of Green Infrastructure is trending in water resources management (Tavakol-Davani et al. 2018; U.S. EPA 2014), although a quantitative method for evaluating sustainability benefits of water infrastructure is missing. This paper presents a watershed-scale study using the standard LCA method (ISO 14044 2006) informed by a hydrologic and hydraulic (H&H) analysis system. The proposed system – called uWISE (urban Water Infrastructure Sustainability Evaluation) – is able to quantify the sustainability benefits of the water infrastructure for the planning horizon. The uWISE framework uses an H&H model to simulate the system and a LCA model to translate the quantity and consumed energy into life cycle impacts (Figure 1).

For the present paper, the U.S. EPA SWMM 5.1 was used as the H&H model for the application of the uWISE, and Rainwater harvesting (RWH) was considered as the water infrastructure of interest. Hourly continuous precipitation data was used for this application. For the LCA portion, the functional unit (FU) was defined as 1 m^3 reduction of Combined Sewer Overflow (CSO) over the life cycle of facilities. The system boundary consists of the operational phases of the WTP and WWTP. TRACI (the Tool for the Reduction and Assessment of Chemical and other environmental Impact) assessment method was used in this study to represent environmental impacts per material and energy consumptions. Among the TRACI impact categories, Global Warming Potential (GWP) and Eco-toxicity Water (ETW) were selected. The uWISE framework was applied to study the City of Toledo's stormwater drainage system in the State of Ohio. Toledo's collection system serves approximately 310 km^2. The proposed RWH system was considered to supply toilet flushing demands in buildings.

Results and concluding remarks

According to the uWISE results in Figure 2.a, supplying toilet flushing demand by RWH may add a GWP burden caused by the additional combined sewage treatment volume (18.9 million kg CO_2e) – now captured instead of being discharged to water bodies as a CSO. Further analyses confirmed that the high energy consumption for treating combined sewage is the main cause of this observation.

For the uWISE results in terms of ETW (Figure 2.b), the reduced CSO volume provided by RWH could avoid a significant environmental impact (727 million CTU eco), while the added burden of combined

sewage treatment and avoided burden of potable water treatment were in equilibrium (≈200 million CTU eco).

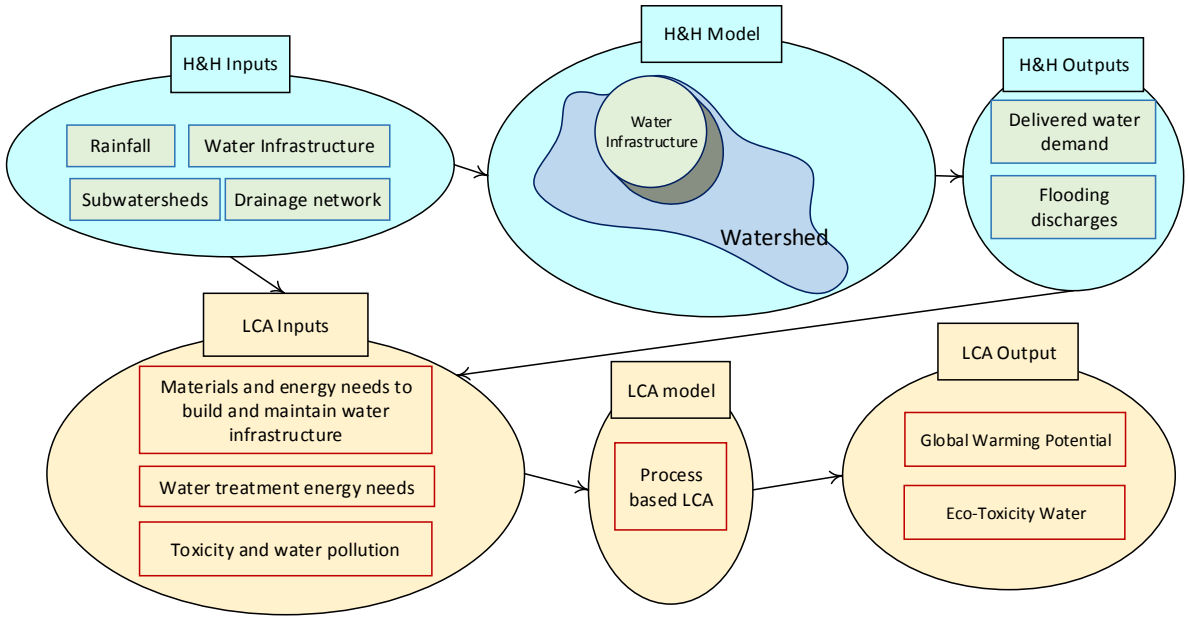

Figure 1. The uWISE framework for sustainability evaluation of water infrastructure.

These results show only a couple of examples of how to bring the water resources engineering and sustainability expertise together. With this integration, uWISE is able to contribute moving the current vague definition of sustainable water resources management towards onto a globally standard concept, since it is established based on an ISO standard for sustainability evaluation. In the illustrated example, the uWISE framework provided broader information on the RWH strategies, and indicated the potential positive and negative sustainability impacts.

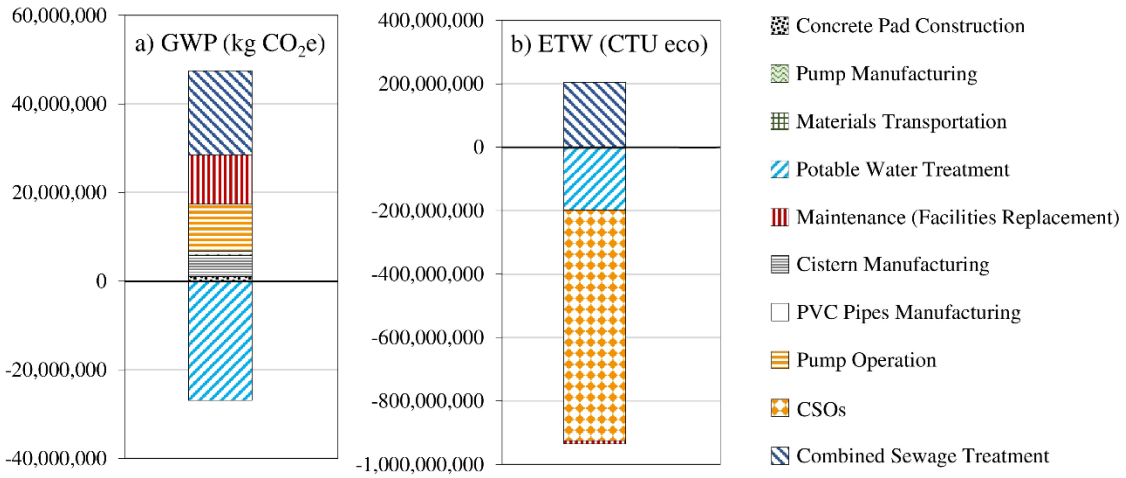

Figure 2. uWISE results over the entire 75 years life cycle of facilities (changes from the existing conditions).

Acknowledgments: This paper presents a part of a research project funded by the U.S. National Science Foundation (NSF) through grants CBET-1235855 and 1236660.

References

Tavakol-Davani H, Burian SJ, Butler D, Sample D, Devkota J, Apul D (2018) Combining Hydrologic Analysis and Life Cycle Assessment Approaches to Evaluate Sustainability of Water Infrastructure. Journal of Irrigation and Drainage Engineering 144(11):05018006. doi: 10.1061/(ASCE)IR.1943-4774.0001340

U.S. EPA (2014) Greening CSO plans: Planning and modeling green infrastructure for combined sewer overflow (CSO) control. EPA-832-R-14-001, Washington, DC

11th World Congress on Water Resources and Environment (EWRA 2019)
"Managing Water Resources for a Sustainable Future", 25-29 June 2019, Madrid, Spain

A flexible approach for the design of water distribution systems using Multi-Criteria Decision Analysis

M.C. Cunha[1*], J.Marques[1], D. Savić[2]
[1] INESC Coimbra, Department of Civil Engineering, University of Coimbra, Coimbra, Portugal
[2] University of Exeter, Exeter, UK
* e-mail: mccunha@dec.uc.pt

Introduction

Many water utilities have been facing growing challenges such as lack of networks hydraulic capacity due to urban population growth and the ageing of infrastructure due to low investment in network upgrading. This gives rise to decreasing pressure, widening the gap between demand requirements and water delivered, and thus reinforcement processes are needed. All these challenges arise at a time of mounting preoccupations with climate variability and high consumer expectations of water services. The rehabilitation and reinforcement of existing water distribution networks (WDNs) are generally costly interventions and the high reliability and safety requirements of these infrastructures means that a thorough study must be undertaken to support decision making. The state of the art in this field shows that there is no literature on the analysis of alternative designs for the reinforcement of existing networks, considering phased interventions during the planning horizon and thus providing flexible networks able to adapt to new information. Therefore, this work proposes a multi-criteria decision analysis (MCDA) as a useful tool for supporting the definition of the best ranked flexible reinforcement solutions for WDNs, using a phased design scheme and multiple plausible future demand scenarios (Maier et al. 2016), and considering different criteria to cover all the issues at stake (investments, environmental and hydraulic performance through a vulnerability index). Most of the literature on using MCDA in the rehabilitation of water supply systems area is concerned with the prioritization of individual pipes or network areas that are proposed for rehabilitation, rather than with defining design interventions, such as new parallel pipe installations of a specific size that needs to be implemented.

The novel methodology proposed is implemented through a comprehensive structure comprising three main steps. The first step establishes the alternatives, criteria and weights. In the second step, the criteria are evaluated on the basis of a set of demand increase generated scenarios. Finally, in the third step, the alternatives are ranked by the PROMETHEE method (Mareschal 2013), a sensitivity analysis is conducted on the results and a supplementary analysis is performed using the SAW method (Banihabib et al. 2017). The traditional formulations that only consider a single phase fixed plan are here replaced by a flexible design approach able to deal with uncertainty related to future demand changes.

Materials and methods

The methodology proposed in this study, intending to define flexible solutions for the reinforcement of WDNs capable of accommodating new information emerging during the planning horizon, is divided into 3 steps. It has been developed so that the reinforced network implemented in the first phase can be revaluated in the subsequent phases if new information becomes available. Therefore, from the outset the infrastructure is designed to include unknown future circumstances as time unfolds. For this purpose, a phased planning horizon scheme (see Marques et al. (2018) for the concept of phased design) is proposed considering a set of possible future demand that the network might have to cope with, during its lifespan.

In the first step, the main components required to perform the MCDA are established. An optimization model is shaped to help to construct each alternative considering a cost minimization for a phased reinforcement of the WDN taking a set of predefined future demand increase scenarios into account. Criteria are established for expressing intervention purposes of decision makers (investments, environmental and hydraulic performance through a vulnerability index). The weight sets embodying the

relative importance that can be given to criteria by the decision makers are also defined in this first step. For each criterion a weighting factor is defined, expressed as a value from 0 to 1 where 0 represents the least important and 1 the most important criterion to be fulfilled.

In the second step, the criteria are used to evaluate how each alternative reinforcement design, already defined, works under a set of multiple plausible future demand increase scenarios. This assessment is an input for performing the MCDA.

Finally, the third step comprises ranking the alternatives according to the weight sets, using the outranking method PROMETHEE. A sensitivity analysis on the weight values is performed and a compensatory method SAW is also implemented to analyse possible ranking differences.

The phased design provides solutions for short time intervals (compared with the full planning horizon) and this enables the network configuration to be adapted if conditions turn out to be different from those predicted. With this approach we will be guided towards a robust solution. This means that after the application of the MCDA method we will be informed of the alternatives that perform best for different scenarios simultaneously. Water utilities are very concerned to provide consumers with the best services by keeping the infrastructure in a state such that it can perform well under different future conditions.

The procedure can be repeated up to the last phase. This means that the infrastructure is prepared from the outset for the introduction of unknown circumstances as time unfolds.

Results and concluding remarks

The application of the methodology is illustrated by a case study based on the work of Schaake and Lai (1969) and consists of reinforcing the New York tunnel water system. The network uses large pipe diameters and the reinforcement consists of increasing the capacity by constructing pipelines parallel to the existing ones to enable the network to meet the water demand growth with enough pressure. To get a picture of how an alternative design is sensitive to the weights given to criteria, the concept of stability intervals for the weights is used. There is less sensitivity to changes in the weights relative to hydraulic performance. Decision makers should be informed about the influence that changing weights has on the final results. The supplementary analysis carried out with the SAW method made it possible to compare the ranking of those solutions and the PROMETHEE solution rankings, thus giving decision makers new insights into the selection of alternatives, through methods using different views. The results of the case study show that complete outranking of the PROMETHEE method tends to cancel out the high strengths of solutions with very good values for criteria, with the high weaknesses being related to the very poor values for others, even for different combinations of weight sets attributed to criteria.

The phased intervention scheme proposed in this work makes it possible to review the process and adapt the projected designs as new information becomes available during the planning horizon. The results for the specific case study show the value of MCDA in that it provides decision makers with insightful information.

Acknowledgments: The authors thank also the Portuguese public agency Fundação para a Ciência e a Tecnologia through the strategic project UID/Multi/00308/2019 granted to INESCC.

References

Banihabib ME, Hashemi-Madani F-S, Forghani A (2017) Comparison of Compensatory and non-Compensatory Multi Criteria Decision Making Models in Water Resources Strategic Management. Water Resources Management 31(12):3745–3759. https://doi.org/10.1007/s11269-017-1702-x

Maier HR, Guillaume JHA, van Delden H, Riddell GA, Haasnoot M, Kwakkel JH (2016) An uncertain future, deep uncertainty, scenarios, robustness and adaptation: How do they fit together? Environmental Modelling and Software 81:154–164. https://doi.org/10.1016/j.envsoft.2016.03.014

Mareschal B (2013) Visual PROMETHEE manual. VPSolutions, 192 p. https://doi.org/10.13140/RG.2.1.4004.3042

Marques J, Cunha M, Savić D (2018) Many-objective optimization model for the flexible design of water distribution networks. Journal of Environmental Management 226:308–319. https://doi.org/10.1016/j.jenvman.2018.08.054

Schaake JC, Lai D (1969) Linear programming and dynamic applications to water distribution network design. MIT, 222 p

11th World Congress on Water Resources and Environment (EWRA 2019)
"Managing Water Resources for a Sustainable Future", 25-29 June 2019, Madrid, Spain

Best Management Practices (BMP) as an alternative for flood and urban storm water: The study case of a watershed in the city of Rome (Italy)

F. Recanatesi[1*], C. Giuliani[2], M. Piccinno[2], B. Cucca[1], M. N. Ripa[1]
[1] Department of Agricultural and Forestry Sciences (DAFNE), Tuscia University, Viterbo, Italy
[2] Sapienza University, Rome, Italy
* e-mail: fabio.rec@unitus.it

Introduction

In the present paper, the positive impact of introducing Best Management Practices (BMPs) at urban scale is assessed, with particular regard to the decreasing of flood prone areas. A suburban watershed of the metropolitan area of Rome has been selected for a study case, as its soil sealing rate can be considered paradigmatic at this scale. Starting from the analysis of rainfall events occurring between 2008 and 2011 which caused millions of euros worth of damage, and using a high resolution data set in GIS environment, two scenarios, with and without BMP introduction, are evaluated applying a rainfall-runoff model and a bidimensional hydraulic model. From a comparison of the flood maps with and without the introduction of BMPs, it was determined that in 90% of the circumstances the employment of the BMPs would completely remove the hydraulic risk, while in the remaining 10% the BMP would at least reduce the areas subjected to flooding.

Materials and methods

An urban watershed (centroid coordinates 41°43'58"N; 12°22'23" E) in the Metropolitan Area of Rome (Italy) was selected to demonstrate how to apply urban BMPs in stormwater management, figure 1. The study area extends over approximately 2.744 ha and consists of contiguous and discontinuous urban fabric (51.2%), industrial or commercial units (6.4%), green or bare soil in urban areas (2.2%), road and public car parking (10.1%) and a protected area (the Castelporziano Nature Reserve) (30.1%) (Recanatesi et al. 2013, 2015). As in other similar peri-urban areas, the development of urban infrastructures has increased its environmental vulnerability to urban stormwater runoff. Indeed, from 2008 to 2011 five storm events occurred in the study area, causing considerable damage, whose average cost was more than 15 million €.

To address the need to find measures which could prevent the repetition of similar damage by reducing runoff volume at the outlet of the study area, we combined a high resolution data set with the development of a hydrological/hydraulic model. In particular we have provided: (i) a digital elevation model (DEM) with 1 m resolution was then realized interpolating over 15,000 Lidar points; (ii) the Corine Land Cover map was updated to classify different rate of soil sealing; (iii) in order to understand the behaviour of runoff and to detect the areas vulnerable to hydraulic risk, we photo-interpreted the whole road network assigning an elevation value to each stretch of road; (iv) Five critical rainfall events, occurred between 2008 and 2011, were selected based on floods occurring in the study area; (v) The hydrologic modelling was performed applying the EBA4SUB (Event Based Approach for Small and Ungauged Basins) software (Petroselli et al. 2015); (vi) The flood routing was developed employing the bi-dimensional hydraulic model FLO-2D (http://www.flo-2d.com/).

Results and concluding remarks

The present paper analyzes at watershed scale how the BMPs can help in reducing the territory hydraulic risk for a peri-urban environment characterized by high rates of sealed soil. In the study area eight watersheds characterized by the possibility of designing an urban BMP for stormwater management in proximity of each outlet were selected, and five observed rainfall events were modelled for each watershed employing a hydrological model and a bi-dimensional hydraulic model. In doing so, a flood map was delineated, in terms of extension, flow depths and volumes. The hypothesized design of the watershed

BMP would allow a part of the design hydrograph to be stored and later released in safety, so that flooding would have a lower impact on the territory, hence reducing the hydraulic risk of the study area. From a comparison of the flood maps with and without the employment of the proposed BMPs, it can be seen that in 90% of the circumstances the employment of the BMPs would completely remove the hydraulic risk, while in the remaining 10% the BMP would at least reduce the areas subjected to flooding.

The results contribute to a clearer understanding as to why and how these green infrastructures should be taken into serious consideration by planners and by environmental policy makers with view to mitigating the effects of soil sealing, which is one of the most limiting factors to a correct urban development. Indeed, in urban and peri-urban contexts, high soil sealing rates lead to an increment of flood prone areas, due to an uncontrolled urbanization and territory impermeabilization. The employment of the BMPs can definitely help in reducing such hydraulic risk.

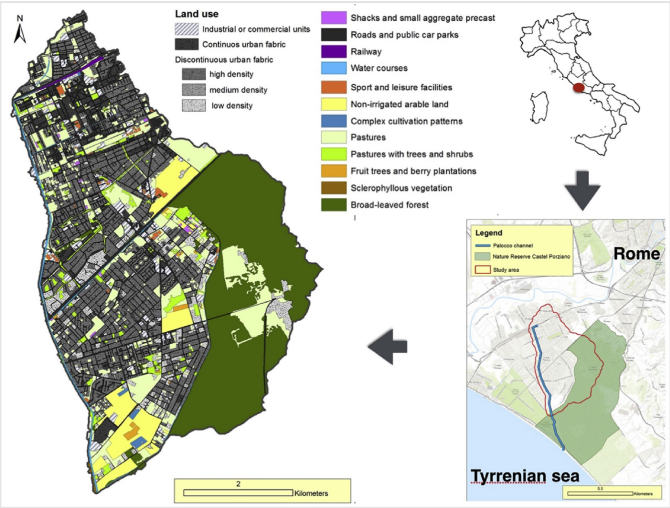

Figure 1. Land use and location of the study area.

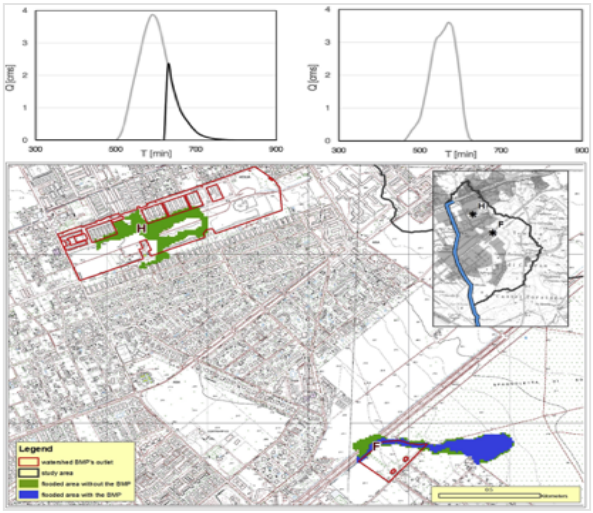

Figure 2. Case studies F (left) and H (right). BMP: hatched area. Flooded area with the BMP: green area. Flooded area without the BMP: blue area.

Acknowledgments: This research performed thanks to the environmental monitoring program for the "Presidential Estate of Castelporziano" promoted out by the National Academy of Sciences - (Rome) and coordinate by the Scientific Committee of Castelporziano.

References

Petroselli A, Grimaldi S (2015) Design hydrograph estimation in small and fully ungauged basin: a preliminary assessment of EBA4SUB framework. J. Flood Risk Manag. http://dx.doi.org/10.1111/jfr3.12193

Recanatesi F, Tolli M, Ripa MN, Pelorosso R, Gobattoni F, Leone A (2013) Detection of landscape patterns in airborne LIDAR data in the nature reserve of Castelporziano (Rome). J. Agric. Eng. 44:472-477

Recanatesi F (2015) Variations in land-use/land-cover changes (LULCCs) in a peri-urban Mediterranean nature reserve: the estate of Castelporziano (Central Italy). Rend. Fis. Acc. Lincei 26(S3):517-526

11th World Congress on Water Resources and Environment (EWRA 2019)
"Managing Water Resources for a Sustainable Future", 25-29 June 2019, Madrid, Spain

Development of new and seamless surrogate measure of hydraulic reliability of water distribution systems

S.H.A. Saleh[1*], T.T. Tanyimboh[2]
[1] Civil Engineering Department/Faculty of Engineering, University of Tripoli, Tripoli, Libya
[2] School of Civil and Environmental Engineering, University of the Witwatersrand, Johannesburg, South Africa
* e-mail: ssaleh1974@yahoo.com

Introduction

Water distribution systems represent an essential infrastructure component that is subject to operational failures, upgrading and rehabilitation processes during operation period. The traditional approach to achieving optimal designs of a water distribution system considers minimizing the construction cost that satisfies the pressure requirements within the system. The resulting designs are characterized with small pipe sizes that have little or no spare capacity to compensate for the effects of component failures or water demand increase. The hydraulic reliability and failure tolerance are considered measures of robustness that evaluate the ability of the system to meet water demands under both normal and failure operating conditions. However, these reliability measures are difficult to evaluate (Wagner et al. 1988) and accordingly their inclusion in optimization processes becomes computationally impractical. As a result, a number of surrogate measures that aim to substantially reduce the computational effort at the cost of accuracy have been suggested. These, for example, include flow entropy, resilience index and surplus power factor.

The flow entropy, when increased, has revealed to: produce designs with improvements in the hydraulic reliability; make use of the arrangements of flow paths in layout optimization; Saleh and Tanyimboh 2014); produce high uniformity of pipe diameters in line with increase in the reliability; provide strong positive correlation with hydraulic reliability and failure tolerance (Tanyimboh and Templeman 2000); and result in an increase in the overall capacity of the system. However, the fact that flow entropy is highly dependent on pipe flow directions gives rise to some computational issues associated with maximizing entropy of water distribution designs. These particularly include: the huge search space of maximum entropy designs; solving a system of non-linear equations for multiple source systems; the confinement of the huge solution space into a narrow domain makes very different designs have marginally or very similar flow entropy value. In this paper, a new surrogate measure that addresses the aforementioned issues is proposed. The new measure uses total flow paths throughout the system as a measure of hydraulic reliability of water distribution systems. The incorporation of the proposed measure into an optimization approach of a benchmark network has shown encouraging results. These findings can be summarized as: the elimination of solving any type of equations in evaluating surrogate hydraulic reliability and thus the optimization process are more efficient; the strong correlation between flow entropy and total flow paths; the similar values of total flow paths for similar maximum flow entropy designs; the very different values of total flow paths for marginally different maximum entropy designs which in turn facilitate recognizing marginally different designs during search process.

Materials and methods

The performance and efficiency of the proposed measure of hydraulic reliability is tested by developing two optimization models. The first model uses maximum flow entropy (MFE) as the driving objective towards maximizing hydraulic reliability in the optimization process, while the second model uses total flow paths (TFP) as the driving objective in the optimization process. Besides the aforementioned objectives, the objectives of minimizing both cost and hydraulic infeasibility are incorporated in both models to ensure achieving cost effective and hydraulically feasible designs respectively. A multi-objective penalty-free approach was developed to simultaneously optimize all of the objectives. The non-dominated sorting

genetic algorithm NSGA-II is used as the optimization tool in the optimization process. The decision variables are the pipe diameters to be selected from the domain of the available discrete pipe sizes. The hydraulic simulator EPANET 2 is used to analyze each generated design for pipe flow rates and directions.

The maximum flow entropy model uses pipe flow rates in calculating maximum flow entropy, while using pipe flow directions in calculating maximum entropy of pipe flows. The calculation of maximum flow entropy in multiple source networks, which is mostly the case in real systems, requires solving non-linear equation(s). The Alpha-method (Yassin-Kassab et al. 1999) that reduces to the solution of a single non-linear equation in two-source networks is used in calculating maximum flow entropy. The bisection method is used to numerically solve the non-linear equation. In contrast, the total flow paths model uses only pipe flow directions and therefore does not require solving any type of equations in evaluating hydraulic reliability. In other words, only a sorting and counting algorithm of total flow paths is required.

Results and concluding remarks

To assess the performance of the proposed measure, the two models are tested on an actual real world system from literature in the city of Ferrara-I (Creaco et al. 2010, 2012) and compared for the aspects of efficiency and performance. The efficiency of each model is evaluated in terms of the computational time consumed and number of generated designs to reach stable convergence. The performance is measured by comparing the resulting designs considering all of the objectives incorporated in the optimization process. The results showed that the model of total flow paths outperformed the maximum flow entropy model in that it achieved a best design in terms of maximum flow entropy value and better optimal front (Figure 1). The main findings include the strong correlation between TFP and MFE (Figure 2), better visualization of MFE designs when expressed in terms of TFP, similarity of TFP values for similar MFE designs, and obvious difference between TFP and MFE values for marginally different MFE designs. The main conclusion of this study is that total flow paths could replace maximum flow entropy as a measure of hydraulic reliability of water distribution systems.

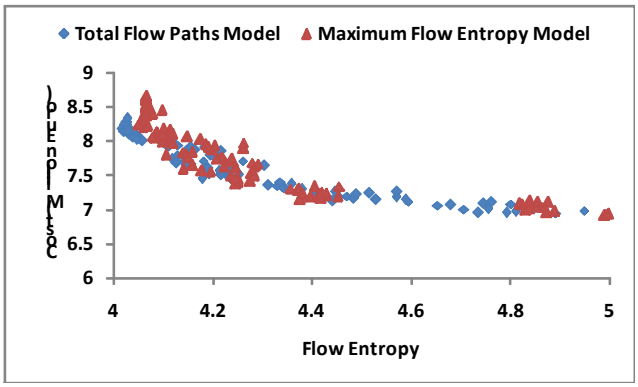

Figure 1. Optimal fronts of the two models

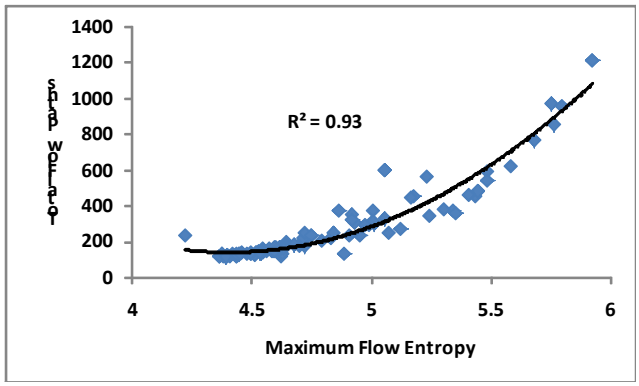

Figure 2. Correlation between TFP and MFE

References

Saleh SHA, Tanyimboh TT (2014) Optimal design of water distribution systems based on entropy and topology. Journal of Water Resources Management 28(11):3555–3575

Tanyimboh T, Templeman A (2000) A quantified assessment of the relationship between the reliability and entropy of water distribution systems. Journal of Engineering Optimization 33(2):179–199

Creaco E, Franchini M, Alvisi S (2010) Optimal placement of isolation valves in water distribution systems based on valve cost and weighted average demand shortfall. Journal of Water Resources Management 24(15):4317–4338

Yassin-Kassab A, Templeman AB, Tanyimboh TT (1999) Calculating maximum entropy flows in multi-source, multi-demand networks. Journal of Engineering Optimization 31(6):695–729

11th World Congress on Water Resources and Environment (EWRA 2019)
"Managing Water Resources for a Sustainable Future", 25-29 June 2019, Madrid, Spain

Preliminary estimation of spatial and temporal synchronization of water demands in the capital city of Libya

S.H.A. Saleh*, M. Alsharif, A.A. Elkebir, E. Wheida
Civil Engineering Department/Faculty of Engineering, University of Tripoli, Tripoli, Libya
** e-mail: ssaleh1974@yahoo.com*

Introduction

Water supply systems represent an essential component of the infrastructure in urban populations worldwide. Water distribution systems are designed by sizing system components so that they meet current and future demands to be provided at minimum required levels of water pressure and quality. The cost of establishing newly-designed water supply systems is largely dedicated to the supply and placement of pipelines. The sizing of pipelines is highly dependent on the amount of water demands allocated to distribution nodes of the system under consideration. The current demand allocation practices normally imply that there is perfect spatial synchronization among the aggregated demands, which is not essentially the case in practice. This assumption indicates that most users follow a single diurnal pattern, which means that such users react simultaneously and in exactly the same way during normal and peak demand conditions. However, the way users react in real-world systems highly depends on many factors that differ from one user to another such as social habits and financial constraints. Recent studies anticipated that low levels of spatial demand synchronization can result in significant savings of the capital cost of water supply systems. In this paper, an investigation on the actual demand spatial synchronization is carried out using field measurements of diurnal demand patterns for different users in a residential area located in the city of Tripoli. Results showed that users react independently and the correlation is far away from the perfect case.

The impacts of the spatial synchronization of water demands on the hydraulic performance and cost of water distribution networks have been studied by a number of researchers. A chance-constrained optimization model applied to a simple network (Tolson et al. 2004) showed that, for a fixed level of hydraulic reliability, network cost increases with the level of spatial synchronization between demands. Additionally, the study pointed out that a higher level of cross correlation between network demands has the effect of producing larger fluctuations in nodal pressure accompanied with more frequent low-pressure failures. A multi-objective evaluation models were tested on the New York tunnels problem under synchronized demands confirming that network cost increases with level of demand synchronization when fixing level of hydraulic reliability (Kapelan et al. 2005; Babayan et al. 2005). A systematic synchronization analysis was conducted to gain a better understanding of the relationship between synchronized demands, network cost, and hydraulic performance (Filion et al. 2006). The results of these studies showed that, in systems without tank storage, the level of synchronization between nodal demands is proportional to variability of nodal pressures. The aim of this paper is to investigate the level of spatial synchronization of water demands in a real system, namely in the capital city of Libya. The results of the study pointed out that the level of synchronization is not strong and a demand analysis should be carried out to accurately model network for better hydraulic performance and to achieve more cost-effective designs.

Materials and methods

The method of study was first started by instantaneously collecting data of residential water demands in a residential area at the East part of the city of Tripoli, Libya. Twenty single-family houses were randomly selected and numbered from 1 to 20. The reason for selecting this area was that the houses equipped with metering devices, which are not the case in different areas of the city. For the purpose of collecting continuous data with high-resolution of time intervals, recording cameras were installed on the service line for each house within the month of October 2017. Then, these indoor residential demand data was

converted into single rectangular pulses with one hour time interval each by aggregating the water demand consumed within this selected interval. The water demands are averaged and demand multipliers were calculated with respect to the average demand. A diurnal demand pattern that relates the demand multiplier to the corresponding time interval was determined for each house. To visually investigate the level of synchronization among all sets of residential houses, all demand patterns were plotted together. The synchronization level was quantified by calculating the correlation coefficients for recognized minimum, maximum, and average time shifts of peak multipliers. This is to demonstrate how strongly water demands are spatially correlated. Finally, all demands were aggregated to explore whether such demands could be represented by a single pattern or not.

Results and concluding remarks

The results have obviously showed that the level of synchronization in all cases is far from the perfect case (level of synchronization is far away from the correlation coefficient of +/-1.0) among all of the demand patterns. Moreover, some correlation coefficients have negative values suggesting that there is no synchronization at all between these water users. The findings can be summarized in that the assumption that synchronization between network demands exists need to be reconsidered in network modelling. This means that applying a single peaking factor to all network demands in extended period simulation need to be re-evaluated. Further analysis is highly required to confirm such a conclusion. Second, should this is the case in real systems that demands are not strongly synchronized, it may be necessary for water utilities to conduct an analysis on the level of spatial synchronization of water demands. This is to better increase the accuracy of network modelling for design and rehabilitation work. From economical viewpoint, increasing the accuracy between demands estimated in design stage and those observed in the real system could help utilities save design costs by building smaller pipe sizes and other network components. Additionally, establishing accurate demand patterns could help reduce the implications of underestimated design in avoiding low pressure zones.

References

Babayan AV, Savic DA, Walters GA (2005) Multiobjective Optimization for the Least-Cost Design of Water Distribution System Under Correlated Uncertain Parameters. EWRI 2005: Impacts of Global Climate Change, EWRI, May 15-19, 2005, Anchorage, Alaska

Filion YR, Adams BJ, Karney BW (2006) Cross Correlation of Demands in Water Distribution Network Design. Journal of Water Resources Planning and Management 133(2):137-144

Tolson BA, Maier HR, Simpson AR, Lence BJ (2004) Genetic Algorithms for Reliability-Based Optimization of Water Distribution Systems. Journal of Water Resources Planning and Management 130(1):63-72

Kapelan Z, Savic DA, Walters GA (2005) An Efficient Sampling-Based Approach for the Robust Rehabilitation of Water Distribution Systems Under Correlated Nodal Demands. EWRI 2005: Impacts of Global Climate Change, EWRI, May 15-19, 2005, Anchorage, Alaska

11th World Congress on Water Resources and Environment (EWRA 2019)
"Managing Water Resources for a Sustainable Future", 25-29 June 2019, Madrid, Spain

Evaluating the investment needs for water and sanitation assets renewal: The case of the Spanish urban water cycle

P. Gracia-de-Rentería[1*], F. Ezbakhe[2], A. Guerra[3], A. Pérez Zabaleta[1], A. Pérez Foguet[2], M. Ballesteros[1]

[1] *Aquae Chair in Water Economics, Spanish National Distance Education University (UNED), Madrid, Spain*
[2] *Research Group on Engineering Sciences and Global Development (EScGD), Department of Civil and Environmental Engineering, Universitat Politècnica de Catalunya (UPC), Barcelona, Spain*
[3] *Spanish Water Association of Water Supply and Sanitation (AEAS), Madrid, Spain*
** e-mail: catedraeconomiadelagua@cee.uned.es*

Introduction

There is a consensus on the growing needs for water infrastructure investment aimed at covering current services and future challenges. Many water supply and sanitation assets are deteriorated and close to the end of their life cycle, which reduces efficiency and increases not only financial costs, but also environmental and social costs. In this context, it is essential to analyse the investment needs for renewing these assets in an appropriate manner, and compare it with the current investment levels.

The importance of adequate water supply and sanitation asset management has led some international and national organizations to undertake this type of analysis (see, for example, OECD 2006; Bluefield Research 2016). However, most European countries (including Spain) have not carried out this type of evaluation. Therefore, the objective of this study is to analyse, for the first time in the case of Spain, the investment needs for water and sanitation assets renewal in the urban water cycle. Additionally, this study proposes a novel methodological framework that could be applied to other countries and case studies.

Materials and methods

For estimating the investment needs in Spain's urban water cycle, two types of assets are distinguished: (i) networks (adduction, water distribution and sewerage) and (ii) singular infrastructures (drinking-water pumping stations, drinking-water treatment plants, water tanks, wastewater pumping stations, stormwater tanks, and wastewater treatment plants). The methodological framework of this study encompasses main 3 steps (as seen in Figure 1).

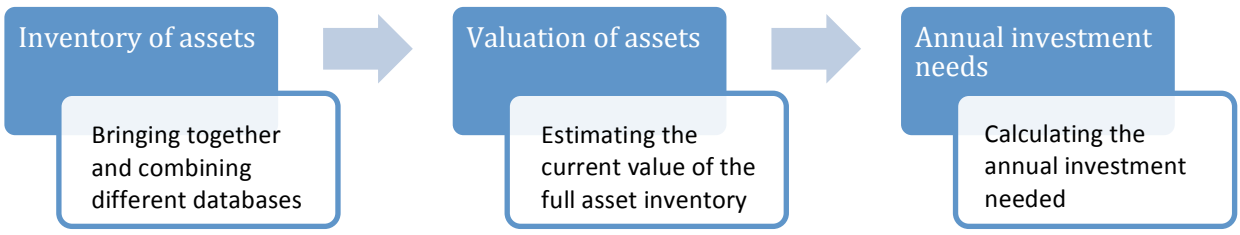

Figure 1. Summary of the methodological framework for estimating the investment needs.

The first step consists in completing an inventory of the different assets included in the urban water cycle, by combining information from different official databases (Ministerio de Política Territorial y Función Pública 2017; AEAS 2018; EEA 2018; Ministerio de Sanidad, Consumo y Bienestar Social 2018).

The second step aims at estimating the current value of the full asset inventory. The aim is to define the total costs of construction and installation. For the network assets, Spanish municipalities were first clustered according to their characteristics. Then a total of 100 technical and tender projects were analysed to determine the cost of pipelines per linear meter in each cluster. Finally, the total value of the networks was calculated based on the composition and the price of the pipelines in each cluster. For the singular infrastructures, 166 different technical projects were analysed to define the econometric relationship between the cost of each infrastructure and its main characteristic (that is, the water flow for drinking-

water treatment plants, the electric power of pumps for pumping stations, and the capacity for the rest of the infrastructures). The total value was obtained from the results of the linear regression for each infrastructure to the inventory.

The last step involves obtaining the annual investment needed to renew and rehabilitate the full inventory in a sustainable way. It is obtained by dividing the value of the different assets between their renewal periods. For network assets, we considered the value and the renewal period for different pipeline materials (fibre cement, concrete, PVC, amongst others). For singular infrastructures, we considered the value and the renewal period of the different components (urbanisation, civil work, electromechanical equipment, and instrumentation and equipment).

Results and concluding remarks

Table 1 summarizes the main results. The adduction, water distribution and sewerage networks have a length of 23,789km, 248,245 km, and 189,203 km, respectively. Moreover, Spain has 1,640 drinking-water treatment plants, 29,305 water tanks, 456 stormwater tanks and 2,184 wastewater treatment plants.

Table 1. Inventory, value, annual investment needs and comparison with the current investment level (in € million).

	Inventory	Value	Annual investment needs	Current investment level
Adduction network	23,789 km.	5,138	n.a.	n.a.
Water Distribution network	248,245 km.	33,606	503	140
Sewerage network	189,203 km.	120,774	2,078	106
Drinking water pumping stations	n.a.	686	15	9
Drinking water treatment plants	1,640 units	7,454	176	85
Water tanks	29,305 units	12,188	202	33
Wastewater pumping stations	n.a.	1,170	45	34
Stormwater tanks	456 units	1,413	23	4
Wastewater treatment plants	2,184 units	14,466	524	41
TOTAL OF THE INVENTORY		**196,895**	**3,566**	**452**

The value of the full asset inventory amounts to € 196,895 million, where more than 61% corresponds to the sewerage network. Indeed, 81% of the value of the inventory corresponds to the networks, whereas only 19% corresponds to singular infrastructures. Furthermore, 70% of the value of the inventory relates to the sanitation phase, while only 30% is located in the water supply phase.

In order to renew the entire inventory in a sustainable way, local entities, which are responsible of providing these services, should invest a total of € 3,566 million per year. However, the current investment barely reaches 12% of it. This is especially worrisome in the case of the sewerage networks since, although they are most valued assets, only 5% of what would be necessary is being invested in their renewal. Similarly, the current investment in wastewater treatment plants represents 8% of the necessary investment. On the contrary, the investment that is being made in drinking water treatment plants, drinking-water pumping stations, and wastewater pumping stations represents 48%, 60% and 75% of the required investment levels, respectively.

These results highlight the need to substantially increase the investments in water and sanitation assets in Spain, in order to sustain them and achieve a suitable degree of efficiency in the urban water cycle.

References

AEAS (2018) XV Estudio Nacional de Suministro de Agua Potable y Saneamiento en España. Asociación Española de Abastecimiento y Saneamiento y Asociación de Gestoras de Agua, Madrid

Bluefield research (2016) Europe municipal water infrastructures: Utility strategies and CAPEX forecast, 2016-2025. Bluefield Research, Barcelona

EEA (2018) Waterbase - UWWTD: Urban Waste Water Treatment Directive – reported data. European Environment Agency, Copenhagen

Ministerio de Política Territorial y Función Pública (2017) Encuesta de Infraestructura y Equipamientos Locales. Ministerio de Política Territorial y Función Pública, Madrid

Ministerio de Sanidad, Consumo y Bienestar Social (2018) Calidad de agua de consumo humano en España, 2016. Ministerio de Sanidad, Consumo y Bienestar Social, Madrid

OECD (2006) Infrastructure for 2030. Telecom, land transport, water and electricity. OECD Publishing, Paris

11th World Congress on Water Resources and Environment (EWRA 2019)
"Managing Water Resources for a Sustainable Future", 25-29 June 2019, Madrid, Spain

Multi-criteria assessment of flood hazard in urban drainage systems

I.M. Kourtis[1*], C.-A. Papadopoulou[2], H. Vangelis[1], V.A. Tsihrintzis[1]
[1] Lab. of Reclamation Works and Water Resources Management, National Technical University of Athens, Greece
[2] Lab. of Natural Geography and Environmental Impact, National Technical University of Athens, Greece
* e-mail: gkourtis@mail.ntua.gr

Introduction

The aim of the present work is to provide a simplified but reliable methodology for the estimation of urban flood hazard, based on a hydrologic-hydraulic model and by utilizing Multi-Criteria Decision Analysis (MCDA). A number of manholes are ranked as to their vulnerability to flood on the basis of two different MCDA methods and the relative results are compared. The methodology proposed herein is demonstrated in a part of a subcatchment of a combined drainage network, in Athens, Greece, but it is easy to be implemented in other, both rural and urban, basins.

The nodes of the drainage system that are most vulnerable to flood are determined based on eight indices: (i) conveyance (calculated using Manning equation for conduits) (m^3/s); (ii) subcatchment area (m^2); (iii) subcatchment width (m); (iv) subcatchment average slope (%); (v) Manning coefficient of the impervious part of the subcatchment ($s/m^{1/3}$); (vi) Manning coefficient of the pervious part of the subcatchment ($s/m^{1/3}$); (vii) impervious area of the subcatchment (%); and (viii) SCS runoff Curve Number.

Four manholes (alternatives) are evaluated with respect to the aforementioned indices (evaluation criteria) as to their vulnerability to flood. The manholes are ranked from the most "risky" to the less "risky". To this end, two different MCDA methods are applied, the Weighted Summation method and the Electre II method, while criteria weights are estimated by using the Analytic Hierarchy Process (AHP) and the respective Saaty scale (Saaty 1977). Both Weighted Summation and Electre II are discrete quantitative methods dealing with quantitative data on the basis of alternative consequences and priorities (weights) assigned to the evaluation criteria (Janssen 1992).

Materials and methods

The methodology proposed herein constitutes a simplification of the original model developed by Bellos et al. (2017). The model was developed using Storm Water Management Model (SWMM) (Tsihrintzis and Hamid 1998; Kourtis et al. 2017; 2018). Prior to applying the proposed methodology, the model was automatically calibrated using measured rainfall and flow in one sewer of the combined drainage network (Kourtis et al. 2017). Then, the methodology was applied using five synthetic design storms derived using the IDF curve of Eq. (1) (Mimikou et al. 2000), with return periods of T = 2, 5, 10, 25 and 50 years, which were developed using the Alternating Block Method for t = 2 hours of storm duration:

$$I = 15.39\, T^{0.276}\, t^{-0.725} \quad (1)$$

where I is the rainfall intensity (mm/h), T is the return period (years), and t is the rainfall duration (h).
The rainfall depths that resulted from Eq. (1) were 22.55, 29.04, 35.16, 45.27 and 54.82 mm for the respective return periods.

After defining the values of the relative indices, a MCDA followed in order for the nodes to be classified according to their vulnerability to flood. The indices represented the evaluation criteria while the nodes represented the alternatives. First of all, criteria weights were defined through pair wise comparisons (AHP method – Expert Choice software). Second, the Weighted Summation method was applied (DEFINITE software) and resulted in a first rank of the nodes for all return periods. For each alternative, a total score was estimated by multiplying its scores by the respective criterion weight. The sum of the weighted scores for all criteria is the result of the Weighted Summation method for each alternative (A_i).

$$A_{i\,WSM} = \sum_{j=1}^{N} a_{ij} w_j \quad (2)$$

where: a_{ij} the consequence of the alternative i in terms of criterion j and w_j the weight of criterion j.

The Electre II method was also applied. Electre is an outranking method based on pair wise comparisons

of alternatives per criterion and the construction of dominance relations (Roy 1991). Dominance relations are defined using concordance and discordance indices (Janssen 1992).

Results and concluding remarks

According to the results derived from AHP, the most important criterion (index) is that of impervious area of the subcatchment (0.248) while the less important criterion is Manning coefficient of the pervious part of the subcatchment (0.012) (Total sum of weights = 1). Regarding the ranking of the nodes, indicative results from the application of Weighted Summation and Electre II methods for T = 10 years are presented in Figure 1 and Table 1.

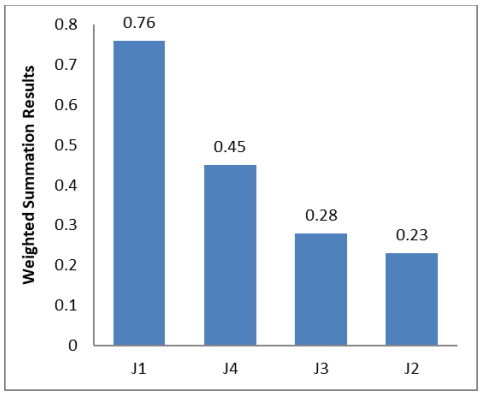

Figure 1. Weighted Summation (indicative results).

Table 1. Electre II – concordance matrix.

	J1	**J2**	**J3**	**J4**
J1		0.91	0.72	0.68
J2	0.09		0.81	0.28
J3	0.28	1.00		0.28
J4	0.40	0.72	0.72	
Ranking	J1 > J4 > J3 >J2			

The results of the two methods resemble as they both classify the manhole J1 as the most "risky" followed by manhole J4. The respective classification of the manholes, for all return periods, regarding their probability to flood is: J1 > J4 > J3 > J2. Such kind of classification can support a safer design of the urban drainage systems.

Acknowledgments: This research is co-financed by Greece and the European Union (European Social Fund-ESF) through the Operational Programme «Human Resources Development, Education and Lifelong Learning» in the context of the project "Strengthening Human Resources Research Potential via Doctorate Research" (MIS-5000432), implemented by the State Scholarships Foundation (IKY).

References

Bellos V, Kourtis IM, Moreno-Rodenas A, Tsihrintzis VA (2017) Quantifying roughness coefficient uncertainty in urban flooding simulations through a simplified methodology. Water 9(12):944

Janssen R (1992) Multiobjective decision support for environmental management. Springer, Netherlands

Kourtis IM, Kopsiaftis G, Bellos V, Tsihrintzis VA (2017) Calibration and validation of SWMM model in two urban catchments in Athens, Greece. In International Conference on Environmental Science and Technology, 31 August to 2 September, Rhodes Island (CEST2017_00709): 1-6

Kourtis IM, Tsihrintzis V.A. Baltas E. (2018) Simulation of low impact development (LID) practices and comparison with conventional drainage solutions. Proceedings 2(11):640. doi: 10.3390/proceedings2110640.

Mimikou M, Baltas E, Varanou E (2000) A study of extreme storm events in Athens greater area. Proceedings of a Symposium, The extreme of extremes, Extraordinary Floods 2000, IAHS Publ. No. 271, Reykjavik, Iceland

Roy B (1991) The outranking approach and the foundations of the ELECTRE methods. Theory and Decisions 31(1):49-73

Saaty TL (1977) A scaling method for priorities in hierarchical structures. Journal of Mathematical Psychology 15(3):234-281

Tsihrintzis VA, Hamid R (1998) Runoff quality prediction from small urban catchments using SWMM. Hydrological Processes 12(2):311-29

V. Agricultural Water Management

11th World Congress on Water Resources and Environment (EWRA 2019)
"Managing Water Resources for a Sustainable Future", 25-29 June 2019, Madrid, Spain

Utilization of tea factory solid wastes towards polyphenols extraction

S. Saha, C. Das*
Department of Chemical Engineering, Indian Institute of Technology Guwahati, Assam, PIN 781039, India
** e-mail: cdas@iitg.ac.in*

Introduction

Tea industry generates a huge amount of solid waste during various tea-processing units which needs proper treatment. Phenolic compounds represent the most plentiful constituents in tea leaves as well as tea processing solid wastes as it has antioxidant activities (Todisco et al. 2002). The particular use of tea factory solid waste for the extraction of total polyphenols towards solid waste management is a novel and innovative approach. With the view to minimize the solvent cost of processing, health hazards and adverse environmental effects, the blending of eco-compatible techniques with non-toxic and reusable solvents, like de-ionized water, is receiving utmost importance during extraction of polyphenols from various solid waste materials. Ethanol, methanol, acetone, ethyl acetate and de-ionized water, were used and compared during extraction of polyphenols from tea factory solid waste. The influence of temperature (30-70°C) on recovery of total polyphenols using de-ionized water was also explored. The effects of different solid waste content in water (0.5 to 2.5 g) at a various contact times of 10 to 90 min on the extraction of polyphenols from tea factory solid waste were verified. Response surface methodology (RSM) was used to achieve the optimum extraction of total polyphenols.

Materials and methods

Extraction methodology to recover polyphenols using different solvents: The tea factory solid waste was obtained from M/s. Sindhu Tea Private Limited, Golaghat Assam, India. Different organic solvents to water ratio (1:4, 2:3, 3:2, 4:1 and 5:0) such as, methanol, ethanol, acetone and ethyl acetate on the extraction of total polyphenols were prepared during solid-liquid extraction. The de-ionized (DI) water was chosen for the extraction of total polyphenols as DI water has significant effect on removing hydrolysable coloured components from the tea factory solid waste materials (Cay et al. 2004). To identify the effects of solid waste content in the different solvents, a series of dried solid waste was fixed, like 0.5 to 2.5 g in 50 mL, according to the different parametric conditions. Extraction time was maintained from 10 to 90 min in all the cases. The stirring speed was fixed at 52.36 rad s^{-1}. The extraction temperature was studied by varying the temperature from 30 to 70°C, whereas, for the different organic solvents extraction, the temperature was maintained at 28±2°C. The total polyphenols (mg L^{-1} GAE) were determined by spectrophotometer (Make: HITACHI High-Tech Science Corporation, Tokyo, Japan; Model: U-5100 UV/VIS) using gallic acid as standard (absorbance at 765 nm), according to the Folin-Ciocalteu method (R^2=0.987) (Das et al. 2017).

Response surface methodology to optimize the process parameters: To optimize the extraction parameters, response surface methodology was applied. Three process parameters, i.e., the solid content (g), temperature (°C) and extraction time (min) have been considered as input variables. The total polyphenols has been chosen as output response. Design expert software 7.0.1 was used to analyse the results. The maximum and minimum range of three inputs viz., the solid content, temperature and extraction time were 1 and 3 g, 30 and 90°C, 10 and 90 min, respectively.

Results and concluding remarks

The effects of five different solvents and solvent-water mixture, namely, methanol, ethanol, acetone, ethyl acetate, and DI water on the extraction of polyphenols are shown in Figure 1. It is clearly observed from Figure 1a that extraction of polyphenols increases with solvent concentration up to solvent to water ratio of 4:1 (vol: vol). The solvent-water mixture intensifies the extraction efficiency by increasing the total components. Upon further increase in solvent concentration for the ethanol and acetone from 3:2 to 4:1,

the extraction of total polyphenols was almost constant, whereas, it is also shown in Figure 1a, that ethanol gives the maximum extraction of total polyphenols among the five solvents. During the extraction of secondary plant compounds namely, phenolic substances, ethanol and water mixture presents significant extraction efficiency due to the high solubility of phenolic compounds in the ethanol-water liquid phase. The extraction efficiency of pure water with various temperatures is shown in Figure 1b. It is noticed that with increasing extraction temperature from 30 to 70° C, the extraction of total polyphenols increases for all the solid contents.

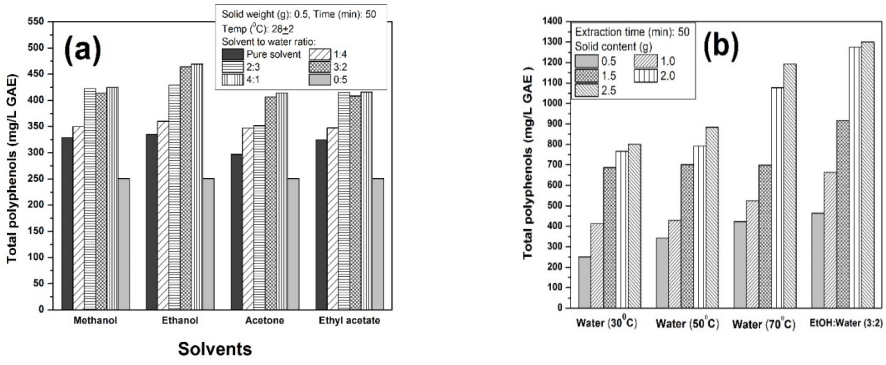

Figure 1. (a) The effect of various solvents on the extraction of total polyphenols from tea factory solid waste at extraction time (50 min), temperature (28±2°C) and solid weight (0.5 g) (b) The comparative study between the ethanol-water mixture (28±2°C) and the de-ionized water (30-70°C) on the total polyphenols extraction.

Figure 2 represents the three-dimensional response surface analysed diagram of the effects of the extraction time and the solid waste content on recovery of total polyphenols. The extracted amount rises with increasing extraction time at constant solid waste content. The analysed optimum parametric conditions using response surface methodology are as follows: solid content (g): 2.45 g; extraction time (min): 68.06 min; extraction temperature: 67.33°C. According to the design expert software, the predicted value of total polyphenols is 1270.34 mg L^{-1} GAE.

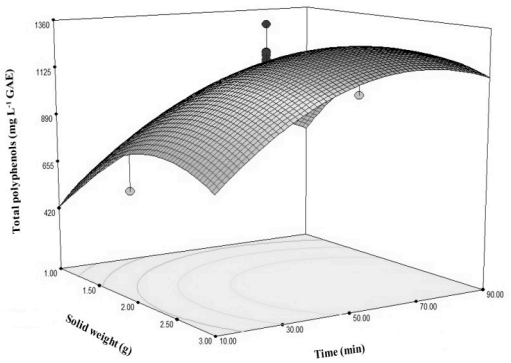

Figure 2. The combined effect of extraction time (min) and solid weight content (g) at a constant temperature of 60°C on the extraction of total polyphenols.

References

Cay S, Uyanik A, Ozasik A (2004) Single and binary component adsorption of copper (II) and cadmium (II) from aqueous solutions using tea-industry waste. Separation Purification Technology 38:273-280

Das AB, Goud VV, Das C (2017) Extraction of phenolic compounds and anthocyanin from black and purple rice bran (Oryza sativa L.) using ultrasound: A comparative analysis and phytochemical profiling. Industrial Crops and Products 95:332-341

Todisco S, Tallarico P, Gupta BB (2002) Mass transfer and polyphenols retention in the clarification of black tea with ceramic membranes. Innovative Food Science and Emerging Technologies 3:255-262

11th World Congress on Water Resources and Environment (EWRA 2019)
"Managing Water Resources for a Sustainable Future", 25-29 June 2019, Madrid, Spain

Evaluation of the Square Root Time model in estimating the evaporation from a bare loam soil

G. Kargas, P. Londra*, E. Karistinou, D. Katsipis, K. Soulis
Department of Natural Resources Management and Agricultural Engineering, School of Agricultural Production, Infrastructure and Environment, Agricultural University of Athens, Athens, Greece
** e-mail: v.londra@aua.gr*

Introduction

Evaporation is an important component parameter of the hydrological balance, especially in dry and semi-dry areas. The phenomenon of soil water evaporation, when there is no high underground water level, occurs in three distinct stages (Philip 1957; Ritchie 1972). Several mathematical models have been proposed to assess evaporation from a bare soil. Black et al. (1969), applying a simplified version of the equation of one-dimensional unsaturated water flow on homogeneous soil under isothermal conditions, showed that the evaporation rate of soil water from a bare soil, E, is inversely proportional to the square root of time, t, (Eq. 1) and the cumulative evaporation, E_c, is proportional to the square root of time, t (Eq. 2):

$$E = \alpha t^{-0.5} \quad (1)$$

$$E_c = \alpha t^{0.5} \quad (2)$$

$$\alpha = 2\left(\theta_i - \theta_o\right)\left(\frac{D}{\pi}\right)^{0.5} \quad (3)$$

where θ_i is the initial soil moisture content, assumed constant for t=0 and x>0 (two days after rainfall event), θ_o is the moisture content at soil surface (x=0), assumed constant for t>0, and D is the soil water diffusivity. This approach as described by equations (1) and (2) is referred to as the Square Root Time (SRT) model (Torres and Calera 2010). The parameter α can be deduced from the experimental data using the slope of the line provided by the cumulative evaporation and the square root of time. Although this model has the advantage of simplicity, it has the disadvantage that the evaporation rate is never zero.

In the present study, the application of the SRT model is examined in a bare (absence of natural vegetation) loam soil after three intense rainfall events during the dry period over the years 2015, 2016 and 2018 in Athens - Greece.

Materials and methods

Experiments were conducted on a loam soil in the experimental field of the Agricultural University of Athens (Athens, Greece). Soil moisture profile was determined by the dielectric profile probe PR2 (Delta –T Device Ltd 2008) at the depths 10, 20, 30, 40, 60 and 100 cm. The profile probe is inserted into the access tube which has been permanently installed into the center of experimental plot.
The soil moisture θ was determined using the equation:

$$\theta = \frac{\sqrt{\varepsilon} - b_o}{b_1} \quad (4)$$

where ε is the soil dielectric constant, and the parameters b_0 and b_1 have the values 1.6 and 8.4, respectively, by the manufacturers.

For the calculation of the water depth (mm) stored in the soil profile, a numerical integration was performed (Kargas et al. 2012):

$$\int_{a}^{b}\theta dz=\frac{b-a}{2v}\left[\theta(a)+2\theta(n_1)+2\theta(n_2)+....+2\theta(n_{n-1})+\theta(b)\right] \quad (5)$$

where v is the number of the space steps (finite differences) the whole soil depth is divided, a is zero denoting the soil surface and b is 100 cm, n_1, n_2… n_{n-1} are soil depths. In our calculations Δz=5 cm (Kargas et al. 2012). Also, a rain gauge was placed in the same experimental field for recording the height and intensity of rainfall.

Measurements of soil moisture profiles were obtained after each intense rainfall event during the period between early spring and early autumn at the years, 2015, 2016 and 2018. Three events of heavy rainfall with water heights of 44.2, 22.8 and 25.4 mm, respectively, were selected. These events were happened at the dates 27/03/2015, 15/03/2016 and 8/7/2018. Measurements of soil moisture profiles were recorded initially on a daily basis and then at more sparse time intervals.

Results and concluding remarks

The water stored in the soil profile up to a depth of 30 cm two days after each rainfall event was 60.42, 38.5 and 38.3 mm in years 2015, 2016 and 2018, respectively. The soil moisture contents (θ_i) were 0.19 m^3m^{-3} (2015), 0.112 m^3m^{-3} (2016) and 0.154 (2018). As an example, it can be mentioned that recording of soil moisture profiles revealed that the phenomenon of evaporation is observed up to a depth of approximately 20 cm for the period from 10/7/2018 to 27/7/2018, i.e. 17 days.

From the experimental results it was shown that the relationship between cumulative evaporation and square root of time, $E_c(t^{0.5})$, is strongly linear with high values of the coefficient of determination R^2 (0.985, 0.945 and 0.870 in years 2015, 2016 and 2018, respectively). The slope values, α, of the linear relationship $E_c(t^{0.5})$ were 3.34, 1.5 and 2.7 $mmd^{-0.5}$ for the years 2015, 2016 and 2018, respectively. From these results the dependence of the slope value α on the soil moisture content θ_i is shown in the following linear relationship

$$\alpha=23.4\theta_i\text{-}1.05 \quad (6)$$

Torres and Calera (2010) applied the SRT model using experimental data of a loam soil and estimated a slope value α=5.41 $mmd^{0.5}$ for θ_i=0.28 m^3m^{-3}. Using Eq. (6) obtained by our experimental data on a loam soil and applying θ_i=0.28 m^3m^{-3}, a value of α=5.5 $mmd^{0.5}$ was calculated, which is almost the same to the experimental one. Also, from Eq. (6), the value of θ_i in which the slope α is zero (in other words the evaporation practically stops) can be calculated. Based on the few relevant experimental data, this θ_i value is 0.045 m^3m^{-3}. This value may vary depending on the soil type and climate.

The results showed the dependence of the cumulative evaporation from the initial soil moisture content. The greater the initial soil moisture content, the greater the cumulative evaporation at the end of the experiment is.

References

Black TA, Gardner WR, Thurtelly GW (1969) The prediction of evaporation, drainage and soil water storage for a bare soil. Soil Science Society of America Journal 33:655-660. doi: 10.2136/sssaj1969.03615995003300050013x

Delta Device Ltd (2008) User Manual for the Profile Probe. Delta Device Ltd, Cambridge, UK

Kargas G, Kerkides P, Sotirakoglou K, Poulovassilis A (2016) Temporal variability of surface soil hydraulic properties under various tillage systems. Soil and Tillage Research 158:22-31. http://dx.doi.org/10.1016/j.still.2015.11.011

Philip JR (1957) Evaporation and moisture and heat fields in the soil. Journal of the Atmospheric Sciences 14:354-366. DOI: 10.1175/1520-0469(1957)014<0354:EAMAHF>2.0.CO;2

Ritchie JT (1972) Model for predicting evaporation from a row crop with incomplete cover. Water Resources Research 8(5):1204-1213. https://doi.org/10.1029/WR008i005p01204

Torres EA, Calera A (2010) Bare soil evaporation under high evaporation demand: a proposed modification to the FAO-56 model. Hydrological Sciences Journal 55(3):303-315. https://doi.org/10.1080/02626661003683249

11th World Congress on Water Resources and Environment (EWRA 2019)
"Managing Water Resources for a Sustainable Future", 25-29 June 2019, Madrid, Spain

Optimization of pumps working as turbines under economic criteria in water irrigation networks to improve sustainability: Case study

M. Pérez-Sánchez[1], H. Montero[1], F.J. Sánchez-Romero[2], P.A. López-Jiménez[1*]
[1] Hydraulic and Environmental Engineering Department, Universitat Politècnica de València, 46022 Valencia, Spain
[2] Rural and Agrifood Engineering Department, Universitat Politècnica de València, 46022 Valencia, Spain
* e-mail: palopez@upv.es

Introduction

Hydraulic is a renewable source of energy with a promising future. Its growth is expected in the next years, in which a considerable part of this energy can be obtained due to the energetic recovery in pressure water systems for irrigation or potable water distribution (Emec et al. 2015). Contrary to hydraulic power stations, the main goal of these systems is not energy generation (which means that they are multipurpose systems) but energy recovery, allowing to reduce operating costs or even to obtain benefits from the energy sale.

It is necessary to adjust the pressure in irrigation or potable water distribution systems for consumption. For this purpose pressure reducing valves are often used. If these valves are replaced with pumps working as turbines (PATs) not only pressure regulation can be achieved, but also a recovery of energy can be obtained, that otherwise would not be exploited.

In this research, an existent energy recovery optimization methodology based on the installation of PATs is applied to an irrigation network located in a town in Valencia local region. Through this methodology, it is possible to find out the installed power and recovered energy in this particular irrigation network according to the number of PATs to be installed. With this information, a viability analysis is performed in order to select the best combination. Then, the methodology searches in a PATs catalogue the machines that optimize the energetic recovery. Finally, the profitability of the real case is evaluated and it is decided to install two groups of PATs, which allow a total energy recovery near 40 MWh/year.

This energy can be even increased when variable conditions are considered for the management of the installed machines, under economic criteria for optimization. To do so, simulated annealing is introduced in order to select the final machines performance. Flow, head and power will be known for the selected PATs, even when variable speed of the machines is considered.

Materials and methods

In this research, an existent methodology based on optimizing the management of irrigation water networks is used (Pérez-Sánchez et al. 2018). Nevertheless, a novelty is introduced in this particular case: the consideration of variable velocities in the machines in order to determine the more interesting PAT to install, considering not the total performance of the system, but the total recovered power in the different functioning conditions. The proposed methodology is based on the next steps: (i) Determination of consumption patterns to know flows over time, using the methodology proposed by Pérez-Sánchez et al. (2016); (ii) Calibration strategy for defining flows and pressure consumption in the network model for all the pipes and lines; (iii) Energy balances along the network; (iv) Definition of the maximum power lines for machine selection, using experimental curves to define the flow-head and efficiency curves, considering the empiric method proposed by Pérez-Sánchez et al. (2018) and using real curves of manufacturer; (v) Definition of PATs location in the network by means of simulated annealing analysis along the network; (vi) Simulation of network performance in different conditions using EPANET; (vii) Final selection of machines: location an performance under variable conditions seeking the maximum obtained power.

Results and concluding remarks

The previously presented methodology has been used in the irrigation network located in a township located in the province of Valencia (Spain), particularly in the 'Canyoles water system' (Figure 1a). The pressurized network supplies 383 ha where the main crop is citrus and the water is stocked up in a reservoir. The total length of the used pipes is 44 km where the diameters are between 32 and 500 mm with different materials. Finally, the network has 404 irrigations points, supplying the different crops.

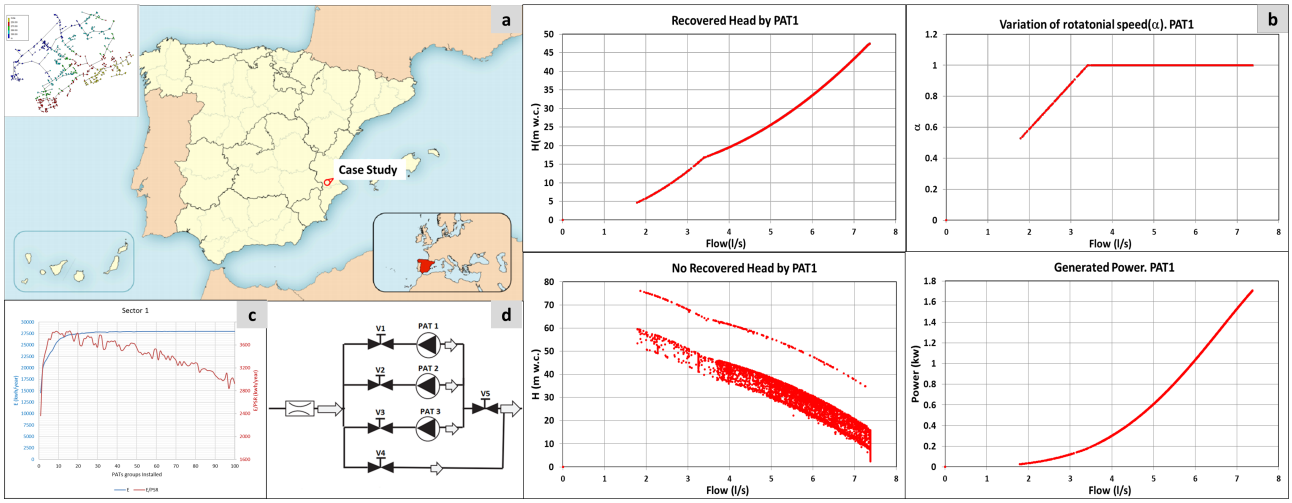

Figure 1. (a) Canyoles Network (b) Example of recovered head, power and rotational speed as a function of flow for PAT1 (c) Comparison between objective functions as a function of number of installed PAT groups (d) Scheme of PAT installation in paralell.

The system was optimized considering objective function of energy and economic criteria. The optimization considered the theoretical possible energy to recover, number of turbine groups in parallel (Figure 1d), the real curves of PATs as well as the real cost to develop the civil investment (Figure 1c). The installation of two groups of turbines (in lines 2004 and 2070) was the best solution among all possible positions. The best solutions were chosen developing a particular feasibility analysis. This analysis considered the financial indicators (NPV, IRR and payback period), calculated for difference hypothesis (sold price and different r). This analysis showed the best solution in sector two, establishing the minimum sold price in 0.06€/kwh and the payback period was 19. For these values, the Net Present Value (NPV) was 16445€ and Internal Rate Return (IRR) 4.33%. The flow variability forced to consider the use of parallel group of turbines since the flow oscillate between 0 and 160 l/s. The energy analysis showed the theoretical recovered energy were 108.4 MWh/year when the consumed flow was 1.18 Hm^3 (0.092 kwh/m^3). Considering real machines, when the real curves of PATs, the variation of rotational speed and the recovery strategy was defined (Figure 1b), the total recovered energy was 41.7 MWh/year (38.8% of the theoretical energy) and the turbine volume was 83.3%. The present manuscript show the novelty of considering a real study of the investment needs, real curves and calibrated flow in the lines as well as the feasibility of these recovery systems to improve the sustainability of the water systems. This action could be carried out by the water managers inside of their daily management of the resource, with surely very promising recovery energy ratios

References

Emec S, Bilge P, Seliger G (2015) Design of production systems with hybrid energy and water generation for sustainable value creation. Clean Technol. Environ. Policy 17:1807–1829. doi: 10.1007/s10098-015-0947-4

Pérez-Sánchez M, Sánchez-Romero FJ, López Jiménez PA, Ramos HM (2016) Modeling Irrigation Networks for the Quantification of Potential Energy Recovering: A Case Study. Water 6(8):1-26. doi: 10.3390/w8060234

Pérez-Sánchez M, Sánchez-Romero FJ, López Jiménez PA, Ramos HM (2018) PATs selection towards sustainability in irrigation networks: Simulated annealing as a water management tool. Renewable Energy 116(234). doi: 249. 10.1016/j.renene.2017.09.060

Pérez-Sánchez M, López Jiménez PA, Ramos HM (2018) Modified Affinity Laws in Hydraulic Machines towards the Best Efficiency Line. Water Resources Management 3(32):829-844. doi: 10.1007/s11269-017-1841-0

11th World Congress on Water Resources and Environment (EWRA 2019)
"Managing Water Resources for a Sustainable Future", 25-29 June 2019, Madrid, Spain

Comparison of reference evapotranspiration estimations: Simplified Penman's formulae versus reduced FAO Penman-Monteith

J.D. Valiantzas
Department of Natural Resources Management & Agricultural Engineering, Agricultural University of Athens, Geece
e-mail: ival@aua.gr

Introduction

Reference evapotranspiration, ET_0 (mm/d), is a major component of the hydrologic cycle and its estimate is widely used in hydrological and irrigation engineering applications. The FAO-56 Penman-Monteith equation suggested by Allen et al. (1998) (hereinafter referred to as FAO56-PM) is a model for estimating reference evapotranspiration proved well for various locations and climatic conditions. The FAO56-PM requires numerous reliable weather measurements of wind speed, u (m/s); solar radiation, R_S (MJ/m^2/d); relative humidity *RH (%)*; and air temperature T (^{o}C). Frequently measured wind data are lacking or are of low or questionable quality (Allen 1996) and there is no method to predict wind speed with total confidence. Valiantzas (2006, 2013) developed algebraic formulas simplifying Penman's equation that compute ET_0 without requiring u data

This study focuses on a new version of simplified ET_0 formula suggested by Valiantzas (2018) that does not require wind data. Comparisons were conducted using daily weather data obtained from 21 stations with the objective to assess the effects on the performance of the new ET_0 formula (and the other two formulas) versus the reduced set FAO Penman Monteith procedure (hereinafter referred to as reduced-PM) not requiring wind data also. Comparisons were also conducted when local long-term average wind speed value, $U_{av}\,(\mathrm{m/s})$, is incorporated as an additional input.

Materials and methods

Databases: The daily data-set used for comparisons was extracted from 21 weather stations in California, Florida, Arizona and Greece. Some stations are characterized by an arid, semiarid climate and other by a humid climate and cover a wide range of the long term average wind ranged from 1.0 to 4.0 m/s.

ET_0 methods: (a) The first simplified Penman's ET0 formula, the Eq. 1 bellow, was derived by Valiantzas (2006); (b) Later Valiantzas (2013) suggested the Eq. 2 bellow not requiring Ra; (c) Valiantzas (2018) based on further simplification of the Penman's radiation term suggested a new formula for estimating ET0 from T and RH data alone. Then the new version formula, the Eq. 3 bellow, is obtained:

$$ET_0 = 0.0393R_S(T+9,5)^{0.5}-2.4(R_S/R_a)^2+(T+20)(1-RH/100)(0.066\,U_{av}^{0.6}-0.23) \quad (1)$$

$$ET_0 = 0.0393R_S(T+9,5)^{0.5}-0.19\,R_S^{0.6}f^{0.15}+0.48(T+20)(1-RH/100)U_{av}^{0.7} \quad (2)$$

$$ET_0 = 0.0347R_S((T+10)^{0.5}-40/R_a)+0.066(T+20)(1-RH/100)U_{av}^{0.6} \quad (3)$$

where f (rad) is the latitude of the station; (d) Finally the reduced form of the FAO56-PM procedure suggested by Allen et al. (1998) (hereinafter referred to as reduced-PM) when wind data are missing is included in comparisons.

Note that for places where an estimation of U_{av} is not available the 4 methods are applied using the default value of U_{av} = 2 m/s.

Results and concluding remarks

The four methods were compared with the "reference" FAO56-PM. The statistical results of the comparisons the long term average ratio, rt, the traditional coefficient of determination, R^2, and the root square mean error RMSE are evaluated for the 21 stations, using both estimations of u= 2m/s and u= U_{av}. A

summary of these results is presented in Table 1. Table 1 show that the new Eq. 3 produced more accurate ET_0 estimations than the other 3 methods when u= 2m/s. The Eq. 3 produced lower scatter in the regression fit than the other three methods for almost all the21 stations, with average for all the stations of R^2 = 0.921, a lower average RMSE and lower bias (rt). Eq. (3) yields an average RMSE that is about 15% lower than average RMSE of reduced-PM. When the 4 methods were applied with u= U_{av} then Eqs. 1 and 3 have almost the same performance whereas the reduced-PM yielded the poorest results (Table 1). The bias of all methods is significantly reduced when U_{av} is additionally considered. A thorough examination indicates that Eq. (3) performed significantly better than reduced-PM in most stations. In 5 stations with humid climate the reduced-PM performed better. However, these 5 stations are characterized by an excessively low impact of wind on ET_0 calculation. Under these conditions the FAO-56 PM and the reduced-PM practically degenerate to the same equation. Hargreaves and Allen (2003) reported that the comparison of the reduced-PM with the FAO56 –PM method is conditioned because both the approximate and the reference methods have the same mathematical form. This is more clearly shown in Fig. 1a concerning the station of Davis/CA with strong impact of wind, where Eq.3 (RMSE=0.54 mm/d) is significantly more accurate than reduced-PM (RMSE=0.68 mm/d). On the contrary in De Laveaga/CA with low impact of wind, Fig 1b, the reduced-PM performed better than Eq. 3. To avoid this situation, the CIMIS-Penman scheme estimating hourly ET_0 (considered as the standard method for estimating ET_0 in California) is used as the "reference" method. Comparisons indicated that the reduced –PM produced the lowest accuracy results for all stations (Table 1).

Table 1. Average for all the stations RMSE (mm/d) values of the four approximate methods.

	Eq.1	Eq. 2	Eq. 3	reduced-PM
Methods with u= 2m/s vs FAO56-PM	0.586	0.601	0.547	0.646
Methods with u= U_{av} vs FAO56-PM	0.486	0.537	0.491	0.526
Methods with u= U_{av} vs Penman CIMIS	0.565	0.549	0.562	0.746

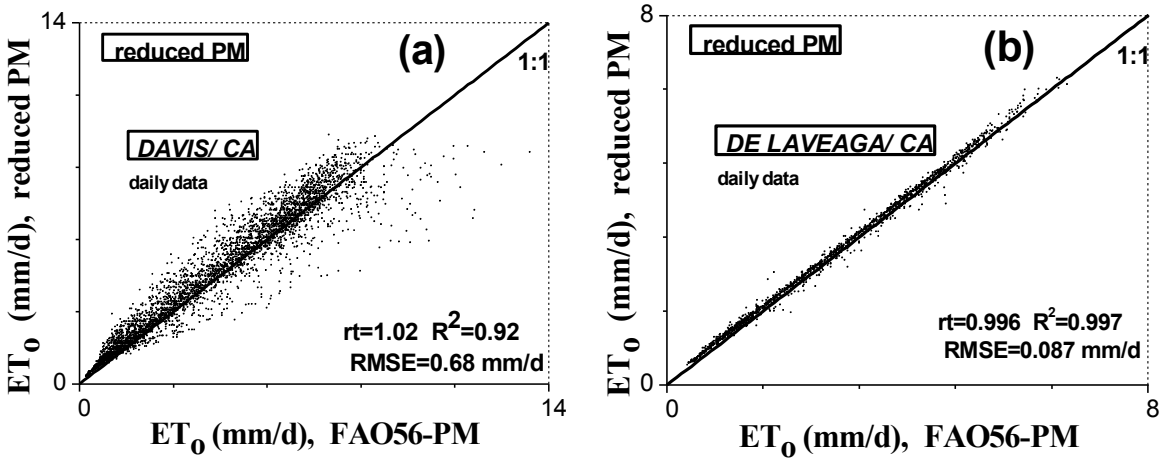

Figure 1. Daily values of reference evapotranspiration estimated by reduced-PM for (a) Davis (b) De Laveaga

References

Allen RG, Pereira LS, Raes D, Smith M (1998) Crop evapotranspiration-Guidelines for computing crop water requirements-FAO Irrigation and Drainage Paper 56. FAO, Rome

Hargreaves GH, Allen RG (2003) History and evaluation of Hargreaves evapotranspiration equation. Journal of Irrigation and Drainage Engineering 129(1):53-63

Valiantzas JD (2006) Simplified versions for the Penman evaporation equation using routine weather data. Journal of Hydrology 331(3-4):690-702. https://doi.org/10.1016/j.jhydrol.2006.06.012

Valiantzas JD (2013) Simple ET0 forms of Penman's equation without wind and/or humidity data. I: theoretical development. Journal of Irrigation and Drainage Engineering 139(1):1-8 https://doi.org/10.1061/(ASCE)IR.1943-4774.0000520

Valiantzas JD (2018) Temperature-and humidity-based simplified Penman's ET0 formulae. Comparisons with temperature-based Hargreaves-Samani and other methodologies. Agricultural Water Management 208:326-334. https://doi.org/10.1016/j.agwat.2018.06.028

11th World Congress on Water Resources and Environment (EWRA 2019)
"Managing Water Resources for a Sustainable Future", 25-29 June 2019, Madrid, Spain

Hydro-economic modelling approaches for agricultural water resources management in a Greek watershed

A. Alamanos[1*], N. Mylopoulos[1], A. Loukas[1,2], D.Latinopoulos[3], S. Xenarios[4]
[1] Department of Civil Engineering, University of Thessaly, Laboratory of Hydrology and Aquatic Systems Analysis, Volos, Greece
[2] Department of Rural and Surveying Engineering/Aristotle University of Thessaloniki, Thessaloniki, Greece
[3] Faculty of Engineering, School of Spatial Planning and Development, Aristotle University of Thessaloniki, Thessaloniki, Greece
[4] Graduate School of Public Policy, Nazarbayev University, Astana, Republic of Kazakhstan
* e-mail: alamanos@civ.uth.gr

Introduction

The combination of economic insights with hydrology and engineering processes offers a more realistic and coherent framework for integrated water resources management (Medellín-Azuara et al. 2009). So far, Hydro-Economic Models (HEMs) have been used mainly for agricultural concerns and water allocation policies (Blanco-Gutiérrez et al. 2013). Comparative studies of HEMs have been carried out using efficiency criteria (Krause et al. 2005). Cornelissen et al. (2013) assessed the suitability of different model types for simulating scenarios of future discharge behaviour in the context of climate and land use change, and Bekchanov et al. (2015) provided a review of HEMs features and applications. But to our knowledge no study has compared the performance of the same model under different conditions, yet. This study presents two different approaches of setting a HEM in Lake Karla watershed, a rural area in Central Greece. The two ways concern different situations of: data availability (a limited-data and a complete-data version), scopes (a preliminary and a complete version) and different desirable results, while their common outputs are compared. The novelties of this study are: the attempt to show how flexible should be the settings of a model (depending on the needs of the desired results and the data availability), and the attempt to provide the optimum approach, in order to express simpler engineering and economic terms to achieve a better local management.

Materials and methods

The first HEM version provides the water balance, the irrigation water cost, the farmers' utility, the irrigation water value using the "Net Income Change" method, and other economic indices (Alamanos et al. 2016, 2017). The second version provides the water balance, the net profits from the agricultural activity (utility), and the full cost of water, according to the Water Framework Directive (WFD) 2000/60/EC. Table 1 shows their main features.

Table 1. Comparing the characteristics of the two HEM's versions.

Version 1	Version 2
Incomplete data and recordings (hydrological and economic). Thus, the scope was a preliminary understanding of the system.	Complete and reliable official data per farm. The aim was to prepare the ground for the implementation of the economic objectives of the WFD.
4 main crops were used, because of limited data.	11 crops, as they were classified from official data.
Tools: GIS, CROPWAT, WEAP (weap21.org), economic model.	Tools: GIS, CROPWAT, WEAP (weap21.org), economic model.
The watershed is divided into 10-19 irrigation zones. This division offered higher precision, spatial integration of the results and "covered" the weakness of the limited data that were used for the analysis.	The watershed is divided into 3 zones depending on the supply source (water bodies), as it is convenient and useful to evaluate the full cost of water regarding the quantitative and qualitative degradation of each water body of the watershed.

Results and concluding remarks

Both versions were examined under demand management scenarios. Some basic outputs of the two versions are shown in Table 2, indicatively.

Table 2. Comparing some of the results of the two HEM's versions.

Management Scenarios	Annual water demand (hm^3) Version 1/ Version 2	Annual unmet demand (hm^3) Version 1/ Version 2	Farmers' Utility (v1)/Net Profits(v2) (mil. €)
1 (baseline scenario – BAU)	343.9 / 374.1	131.9 / 160.4	44.745 / 47.313
1a (reducing losses on Scen.1)	248.7 / 284.9	94.5 / 71.2	44.745 / 47.313
1b (drip irrigation on Scen.1)	311.7 / 356.2	111.4 / 142.5	44.745 / 47.313
2 (operation of a new reservoir)	322.0 / 373.2	109.3 / 99.5	44.143 / 49.395
2a (crop replacement on Scen.2)	309.8 / 351.8	97.1 / 78.2	41.143 / 47.328
2b (crop replacement on Scen.2)	308.8 / 363.9	97.8 / 90.3	41.962 / 48.681
2c (reducing losses on Scen.2)	247.2 / 284.2	55.1 / 10.5	44.143 / 49.395
2d (drip irrigation on Scen.2)	303.6 / 355.3	97.5 / 81.7	44.143 / 49.395

It should be noted that the first version does not "cancel" the second or vice versa. Furthermore, the second version cannot be considered as an updated version, but just as another way to illustrate better outputs such as full cost of water, compared to the irrigation cost and water value of the first version. The paper sets the bases for the evaluation of hydro-economic factors and their connection with the net profit of the stakeholders, something that still is not concerned by the local authorities. Considering more parameters that combine environmental and economic objectives, it is easier to provide guidelines for an efficient and flexible management, where water and economy will operate supplementary and not competitively.

Acknowledgments: The preparation of the article has been co-financed -via a programme of State Scholarships Foundation (IKY) - by the European Union (European Social Fund - ESF) and Greek national funds through the action entitled "Scholarships programme for postgraduates studies -2nd Study Cycle" in the framework of the Operational Programme" Human Resources Development Program, Education and Lifelong Learning" of the National Strategic Reference Framework (NSRF) 2014 – 2020.

References

Alamanos A, Fafoutis C, Papaioannou G, Mylopoulos N (2017) Extension of an integrated hydroeconomic model of Lake Karla basin, under management, climate and pricing scenario analysis. Proceedings of the Sixth International Conference on Environmental Management, Engineering, Planning & Economics, June 25-30, 2017, Thessaloniki, Greece, pp 368-357

Alamanos A, Xenarios S, Mylopoulos N, Stålnacke P (2016) Hydro-economic modeling and management with limited data: the case of Lake Karla Watershed, Greece. European Water 54:3-18

Bekchanov M, Sood A, Jeuland M (2015) Review of hydro-economic models to address river basin management problems: structure, applications and research gaps. Colombo, Sri Lanka: International Water Management Institute. 60 p (IWMI Working Paper 167). doi: 10.5337/2015.218

Blanco-Gutiérrez I, Varela-Ortega C, Purkey DR (2013) Integrated assessment of policy interventions for promoting sustainable irrigation in semi-arid environments: A hydro-economic modelling approach. J Environ Manage (128):144–160. doi: 10.1016/j.jenvman.2013.04.037

Cornelissen T, Diekkrüger B, Giertz S (2013) A comparison of hydrological models for assessing the impact of land use and climate change on discharge in a tropical catchment. Journal of Hydrology 498:221–236. doi:10.1016/ j.jhydrol.2013.06.016

Krause P, Boyle DP, Base F (2005) Comparison of different efficiency criteria for hydrological model assessment. Adv. Geosci. 5:89-97. doi.10.5194/adgeo-5-89-2005

Medellín-Azuara J, Mendoza-Espinosa LG, Lund JR, Harou JJ, Howitt RE (2009) Virtues of simple hydro-economic optimization: Baja California, Mexico. Journal of Environmental Management 90(11):3470-3478. doi: 10.1016 /j.jenvman.2009.05.032

Water Evaluation And Planning System, Stockholm Environment Institute (SEI) - weap21.org

11th World Congress on Water Resources and Environment (EWRA 2019)
"Managing Water Resources for a Sustainable Future", 25-29 June 2019, Madrid, Spain

Biogas production from domestic waste and wastewater using bacterial species isolated from animal husbandry

P. Shrivastava[1], R. Shrivastava[1], A. Vishwanath[1], P. Bhakre[1], K. Samal[1,2], S.R. Geed[1], K. Mohanty[2], C. Das[2*]

[1] Department of Chemical Engineering, Madhav Institute of Technology & Science, Gwalior,M.P.- 474005 India
[2] Department of Chemical Engineering, Indian Institute of Technology Guwahati, Assam - 781039 India
* e-mail: cdas@iitg.ac.in

Introduction

The biogas is one of the potential alternative energy sources. Biogas consists majorly of methane gas (55-75%) and carbon dioxide gas (45-25%), depending on the nature of feed used (Sreekrishnan et al. 2004; Weiland 2010; Zhang et al. 2014). Anaerobic conditions are required for the sustenance of microbes, which feed the organic waste to produce biogas. The anaerobic process takes place through pathways such as hydrolysis, acidogenesis, acetogenesis and methanogenesis. Previous studies have shown that a buffer system created by ammonia and volatile fatty acids leads to higher methane generation. It is also seen that thermophilic bacteria favours more methane generation as compared to mesophilic bacteria (Jingura and Matengaifa 2009; Banks et al. 2011).

This work demonstrates the isolation of bacterial species and their application in biogas production. The feed slurry was made of domestic waste and wastewater. For the production of biogas, a bioreactor was designed and fabricated considering anaerobic conditions. The experiments were performed to produce methane rich biogas with various co-substrates and pretreated feed. Pretreatment of food waste along with cattle manure, wastewater, sludge or green waste helped in high yields of methane.

Materials and methods

The microbial consortia were isolated from animal husbandry waste by serial dilution, which was further purified using nutrient agar plating. Biochemical and molecular characterization of isolated species were done. The most efficient microbes were used for biogas production. Experiments were performed to optimize the process parameters, such as pH, temperature and kitchen waste content as feed. The bio-reactor was fabricated as shown in Figure 1. The slurry of domestic waste used as feed and the degradation experiment were performed for 25 days. The biogas and leachate were analysed by GC and GC-MS, respectively.

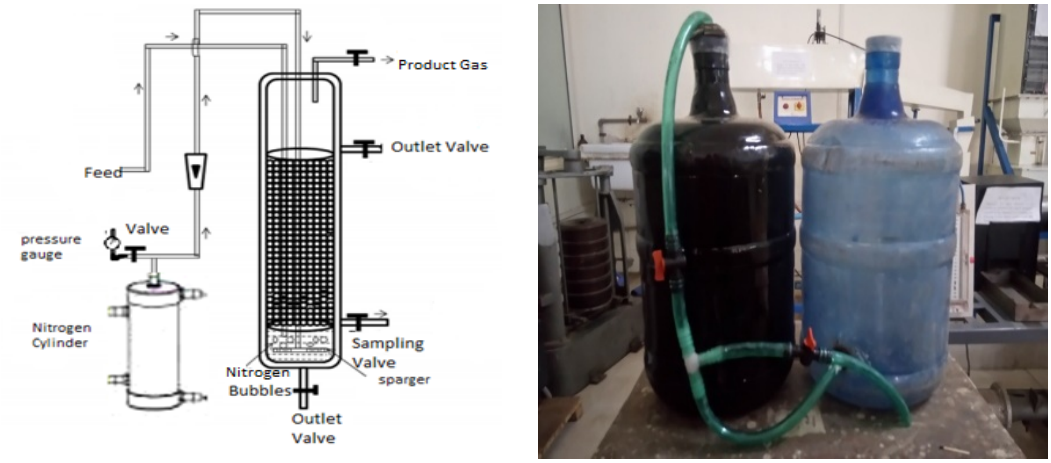

Figure 1. Schematic of the bio-reactor set-up for biogas production.

Results and concluding remarks

The bacterial isolates were motile and rod-shaped in nature. The isolated microbes exhibited positive results for gram staining and motility. The sequences of isolated bacterial nucleotides were outsourced by Tri Scientific Hyderabad India. The obtained nucleotide sequences were deposited in NCBI GenBank database under the accession number MH180813 Sp 1, MH180814 Sp 2, MH180815 Sp 3. Phylogenetic investigation of obtained nucleotide sequences were performed using MEGA-6 software and identified as *Tepidimicrobium* CHEM 1, *Defluviitoga* CHEM 2, and *Tepidanaerobacter* CHEM 3.

The gas produced in the batch experiments was analyzed using GC (M/s. Thermo-Fisher, 7610, USA) as shown in Figure 2. The chromatograph confirmed presence of methane, hydrogen, oxygen, nitrogen and carbon dioxide in the produced biogas. The residual degraded food substrate (extracted in organic solvent) was analyzed using GC-MS (Shimadzu, QP2010 Ultra, Japan) to distinguish metabolites and confirmation of biodegradation of feed. Figure 3 shows the GC-MS analysis results of the 21st day biodegraded sample. The peaks of bis(trimethylsiloxy)-butane, 1,1,4-dibromotetradecane, Oxalic acid, 3,5difluorophenyl nonyl-ester, 4 bromophenyl- undecyl-ester, 2,5-bis-(1-1 dimethylethyl-phenol) and m-hydroxy-ethyl ester were found at residence times of 24.91, 19.23, 24.66, 25.85, 14.51 and 14.717 min, respectively. The corresponding percentage areas under the peak curves in the obtained chromatograph were 0.15, 0.12, 0.18, 0.66, 1.88 and 0.15.

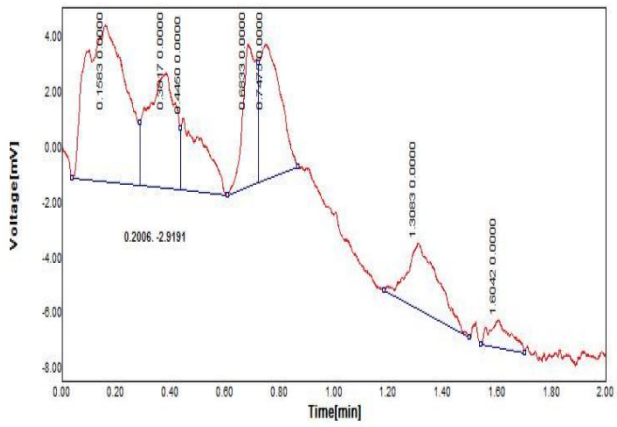

Figure 2. GC analysis of produces biogas.

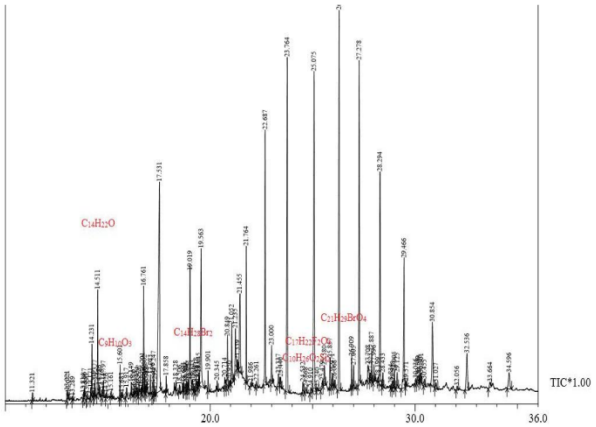

Figure 3. GC-MS analysis of leachate sample

Cow dung was most efficient bacterial source for decomposition of domestic waste for the production of biogas. The initial biogas generation was observed after 8 days start-up of experiments. The process parameters were optimized as pH 7.0±1, food waste contents 50% and temperature 30±2^{o}C. The results of GC-MS confirmed the presence of metabolites that indicates the biodegradation of waste food substrate. The isolated microbes have exhibited the higher potential for promoting the production of methane gas which further enriches the calorific value of the biogas.

References

Banks CJ, Chesshire M, Heaven S, Arnold R (2011) Anaerobic digestion of source-segregated domestic food waste: performance assessment by mass and energy balance. Bioresource Technology 102(2):612-620

Jingura RM, Matengaifa R (2009) Optimization of biogas production by anaerobic digestion for sustainable energy development in Zimbabwe. Renewable and Sustainable Energy Reviews 13(5):1116-1120

Sreekrishnan TR, Kohli S, Rana V (2004) Enhancement of biogas production from solid substrates using different techniques-a review. Bioresource Technology 95(1):1-10

Weiland P (2010) Biogas production: current state and perspectives. Applied Microbiology and Biotechnology 85(4):849-860

Zhang C, Su H, Baeyens J, Tan T (2014) Reviewing the anaerobic digestion of food waste for biogas production. Renewable and Sustainable Energy Reviews 38:383-392

11th World Congress on Water Resources and Environment (EWRA 2019)
"Managing Water Resources for a Sustainable Future", 25-29 June 2019, Madrid, Spain

Combined use of river basin network model and analytic hierarchy process in assessing sustainability of water allocation scenarios

B. Srdjevic[1*], Z. Srdjevic[1], B. Blagojevic[1], R. Bajcetic[2]
[1] Faculty of Agriculture, Department of Water Management, University of Novi Sad, Novi Sad, Serbia
[2] Public Water Management Company Vode Vojvodine, Novi Sad, Serbia
* e-mail: bojans@polj.uns.ac.rs

Introduction

In recent years two projects has been completed in Vojvodina Province (Republic of Serbia), aimed to explore long-term strategies for managing water resources in regional hydrosystems Krivaja and Nadela. Systems are simulated over multiyear periods with river basin network model ACQUANET (Brasilian version of MODSIM) (LaLaina 2015; Labadie 1995). The model creates capacitated artificial network for given systems and optimally balance water distribution accross the network in a single month. End-of-month status is conveyed to the beginning of the next month and optimal balancing of water distribution is performed again. This way, model performs a multi-year simulation of system performance with imbedded monthly optimizationsis. In each month distribution strategy is defined by water demands and their priorities including physical and operational constraints imposed over the system. One run of the model corresponds to single scenario of water allocation. Model output offers rich information about system performance in many aspects. Of special interest is how much water is distributed to the users, e.g. did defficits occurred and how big they are. The other, not less impoortant, is information to what extent defined targets at reservoirs (e.g. operating rule curves) are met. Concerning only these two issues is sufficient to validate defined strategy for operating the system on long term basis, that is to assess system performance and effects of simulated water allocation scenario.

If appropriate 'coupling module' is developed and programmed, output of the network model can be used for additional computations and analyses of system's performance indicators such as reliability, resilience, vulnerability, firm yield, dispersions of simulated reservoirs' levels from rule curves, etc. (Srdjevic and Srdjevic 2017; Sandoval-Solis et al. 2011). Once such analyses are completed, each scenario can be considered as an alternative operational strategy for the system. By alocating weights to performance indicators, a decision matrix can be created for standard multi-criteria assessment of scenarios, their thorough validation and the final ranking.

Materials and methods

Two network models are created for hydrosystems Krivaja and Nadela (Figure 1). The Krivaja system has four surface reservoirs, while the other one (Nadela) does not have reservoirs. In both systems there are small and medium sized irrigation systems, needs for industrial supply, collecting facilities of used (partially purifed) waters, draining systems from agricučltural land etc. Systems are operated separately by regional water management companies, authorised by the global public water management company 'Vode Vojvodine'. Worth to mention is that Krivaja and Nadela are important parts of a global state-owned Danube-Tisza-Danube hydrosystem with more than 20.000 km long network of open firt, second and third order canals and subsurface pipelines.

Network models for two systems are applied for many operational scanarios to explore capabilities of the systems in meeting multi-years demands of different priorities, mostly conflicting. Coupling module followed multiple simulation runs to calculate performance indicators for two systems under different scenarios odf operation, i.e. with different demands, rule curves at reservoirs, dufferent priority schemes etc.

For comparing quality of scenarios with respect to calculated performance indicators, simple additive and product weighting multicriteria methods are initially used, followed by more sophisticated methods

TOPSIS (Technique for Order of Preference by Similarity to Ideal Solution) and CP (Compromise Programming). At a later stage, evaluation of scenarios is continued with the Analytic hierarchy process (AHP) (Saaty 1980) as an appropriate method for either individual or group decision making. This method is selected because it is easier to familiarize decision maker(s) with its logic and way of structuring the problem hierarchy consisting of: (1) goal (at the top) - to rank the scenarios; (2) performace indicators as criteria set (intermediate level); and (3) scenarios as alternatives (the bottom level).

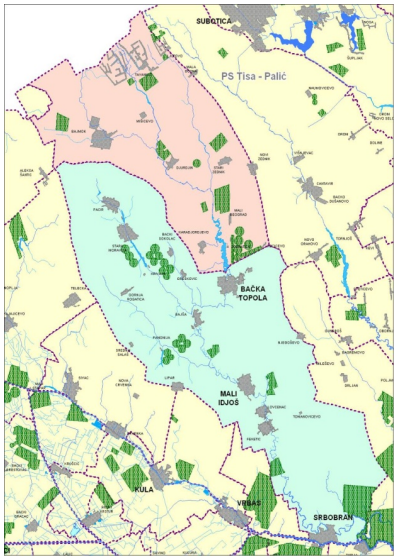

Figure 1a. Regional hydrosistem Krivaja

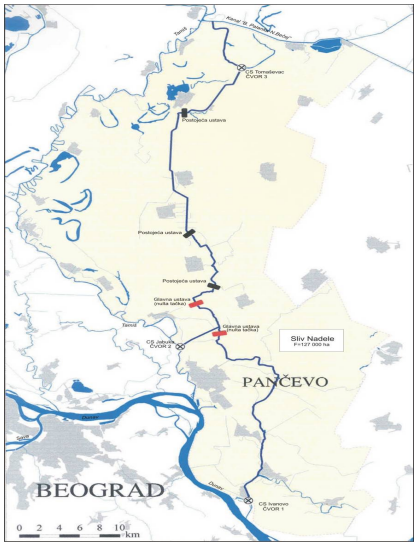

Figure 1b. Regional hydrosistem Nadela

Results and concluding remarks

Combining network model ACQUANET (to simulate water allocation), coupling module (to calculate indicators of system performance) and analytic hierarchy process (to evaluate quality of scenarios) ensured consistent methodological approach to identification of best (most desirable) water allocation strategy for each of two regional hydrosystems. Repeated application of ACQUANET model for two systems and their best scenarios, optimal in multi-criteria sense, finally indicated possibilities for minor changes in operational strategies. These fine-tunning changes enabled additional systems' capabilities to met specified long term targets in water allocation to the users with different demands regarding quantities of needed water and a ways of its use (consumptive and non-consumptive), spatial and temporal distribution of demands, priorities of users, and other visible and non-visibe impacts (e.g. political influence). We believe that the methodology is applicable elsewhere, especially in environments where asessment of water management scenarios may help to identify desired and sustainable long term-solutions.

Acknowledgments: The work is supported in part by the Ministry of Education, Science and Technological Development of Serbia, Grant #174003: Theory and application of Analytic hierarchy process in multi-criteria decision making under conditions of risk and uncertainty (individual and group context).

References

Labadie JW (1995) MODSIM–River basin network model for water rights planning, Documentation and User Manual, Colorado State University, Fort Collins, USA

LaLaina RP (2015) AcquaNet – Modelo integrado para análise de sistemas complexos em recursos hídricos. Universidade de Sao Paulo, Brasil

Saaty TL (1980). The analytical hierarchy process, McGraw Hill, New York

Sandoval-Solis S, McKinney DC, Loucks DP (2011) Sustainability index for water resources planning and management. Water Resources Planning and Management 2011:381–390

Srdjevic Z, Srdjevic B. (2017) An extension of the sustainability index definition in water resources planning and management. Journal Water Resources Management 31:1695–1712. http://doi.org/DOI 10.1007/s11269-017-1

11th World Congress on Water Resources and Environment (EWRA 2019)
"Managing Water Resources for a Sustainable Future", 25-29 June 2019, Madrid, Spain

Searching for the most accurate method for riverine nutrient load estimation as a function of monitoring frequency

D. Park[1*], M. Markus[2], M.-J. Um[3], K. Jung[1]
[1] Department of Civil and Environmental Engineering, Konkuk University, Seoul, Republic of Korea
[2] Illinois State Water Survey, Prairie Research Institute, University of Illinois, Champaign, IL, USA
[3] Department of Civil Engineering, Kyonggi University, Suwon, Republic of Korea
* e-mail: drpark@konkuk.ac.kr

Introduction

Accurate calculations of seasonal, annual, and long-term nutrient loads passing a given monitoring station are critical in designing appropriate remediation management strategies. Determining nutrient loads typically combines frequently (daily) monitored discharge data and relatively less frequently (monthly or quarterly) monitored nutrient concentration data. As a result, the determination of nutrient loads is an estimation problem subjected to many potential sources of uncertainty, including data and modeling errors. A wide variety of load estimation modeling approaches have been developed and used to estimate loads of various water quality constituents. These different approaches generally could be divided into averaging, ratio, and regression estimators. The residual adjustment techniques such as the composite method have been introduced to utilize the autocorrelation in concentration residuals. Similar to the composite method, Verma et al. (2012) proposed triangular and rectangular shape functions to account for residuals in the vicinity of observed concentrations, using proportional and residual adjustment methods. To remove the effects of random variations of streamflow on estimated concentrations and flux, Hirsch et al. (2010) suggested a new approach, weighted regression on time, discharge, and season (WRTDS), now called as Exploration and Graphics for RivEr Trends (EGRET).

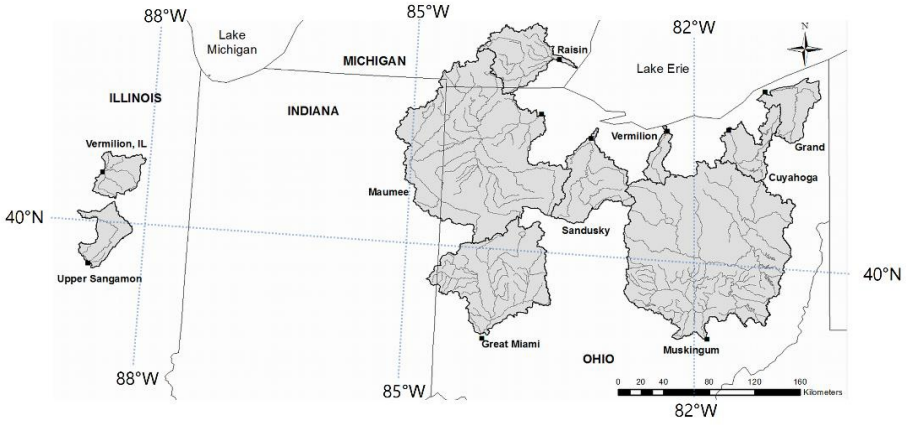

Figure 1. Location of applied watersheds and corresponding monitoring stations

Materials and methods

Data were available for the eight watersheds in the Lake Erie and Ohio River basins (Ohio watersheds), for monitoring periods ranging from 8 to 32 years. Data preprocessing was conducted to eliminate water years with considerable missing concentration and flow data. The study analyzed two pollutants: nitrate plus nitrite nitrogen (NO3-N + NO2-N), and total phosphorus as P (TP). Six watersheds, namely Cuyahoga, Grand, Maumee, Raisin, Sandusky, and Vermilion, drain into Lake Erie. Two watersheds, Great Miami and Muskingum, drain southwards into the Ohio River basin as we can see from Figure 1. The seven-parameter log linear model relies on the correlation between discharge and load, and requires the estimation of the following parameters: a constant, a quadratic fit to the logarithm of discharge, a quadratic fit to time, and a

sinusoidal function to remove the effects of annual seasonality (Cohn et al. 1992). Two general approaches were compared in this study to examine trends in annual nitrate loads and concentrations. The first approach includes the rating curve estimator (Cohn 1995), coupled with several residual adjustment techniques (Verma et al. 2012). The second approach was based on the WRTDS (EGRET) (Hirsch et al. 2010). In the subsequent sections, these approaches are described in more detail.

Results and concluding remarks

RMSE values were computed for the 5-parameter, 6-parameter and 7-parameter regressions along with the different error correction techniques applied to them for low, medium and high frequency sampling for the Maumee River watershed. Each RMSE value was calculated by averaging results from 100 iterations (each iteration had random samples as model inputs). Figure 2 shows RMSE results for nitrate concentration estimations from various method and sampling scenarios. The color of the boxes corresponds to the magnitude of the RMSE with the values increasing from green to yellow. Overall, the 5-parameter regression incorporating triangular residual correction method shows the most accurate results in the Maumee river watershed.

		Station	Maumee				
		Nutrient	NO23	**concentration**			
		# of Sampling	6 per year	264.000			
RMSE		# of Iteration	100	no 5weeks consideration			
Maumee Station	Regression	Composite_residual	Composite_proportional	Triangular_residual	Triangular_proportional	Rectangular_residual	Rectangular_proportional
5 params	3.23	2.58	5.21	2.47	3.37	2.82	5.99
6 params	3.23	2.60	5.32	2.51	3.46	2.84	6.12
7 params	3.21	2.59	5.18	2.50	3.39	2.84	5.95
		Station	Maumee				
		Nutrient	NO23	**Daily Load**			
NO23		# of Sampling	6 per year				
RMSE		# of Iteration	100.000	no 5weeks consideration			
Maumee Station	Regression	Composite_residual	Composite_proportional	Triangular_residual	Triangular_proportional	Rectangular_residual	Rectangular_proportional
5 params	39,435	31,467	59,604	29,966	36,792	33,688	65,348
6 params	40,200	31,949	60,891	31,116	38,094	34,136	66,809
7 params	39,770	31,729	59,911	30,657	37,453	33,922	65,793
		Station	Maumee				
		Nutrient	NO23	**Annual Load**			
NO23		# of Sampling	6 per year				
RMSE		# of Iteration	100.000	no 5weeks consideration			
Maumee Station	Regression	Composite_residual	Composite_proportional	Triangular_residual	Triangular_proportional	Rectangular_residual	Rectangular_proportional
5 params	3,729,805	3,631,920	13,363,988	2,704,427	5,758,767	3,789,419	13,791,220
6 params	3,736,354	3,611,628	13,402,496	2,747,409	5,748,417	3,775,387	13,834,046
7 params	3,641,796	3,615,894	13,311,204	2,722,053	5,690,207	3,774,251	13,749,333

Figure 2. RMSEs in estimating nitrate concentrations using the 5-parameter, 6-parameter and 7-parameter regression equations along with various correction techniques applied to them. Evaluation was performed for low, medium and high frequency sampling using data from the Maumee River watershed.

Acknowledgments: This research was supported by Basic Science Research Program through the National Research Foundation of Korea (NRF) funded by the Ministry of Science, ICT & Future Planning (No.2019R1A2C1007447), and by the Korea Environmental Industry & Technology Institute (KEITI) grant funded by the Ministry of Environment (No.RE201901080).

References

Hirsch RM, Moyer DL, Archfield SA (2010) Weighted regressions on time, discharge, and season (WRTDS), with an application to Chesapeake Bay river inputs. J. Am. Water Resour. Assoc. 46:857–880

Cohn TA (1995) Recent advances in statistical methods for the estimation of sediment and nutrient transport in rivers. Review of Geophysics 33(S2):1117–1123

Cohn TA, Caulder DL, Gilroy EJ, Zynjuk LD, Summers RM (1992) The validity of a simple statistical model for estimating fluvial constituent loads: An empirical study involving nutrient loads entering Chesapeake Bay. Water Resour. Res. 28(9):2353–2363

Verma S, Markus M, Cooke RA (2012) Development of error correction techniques for nitrate-N load estimation. J. Hydrol. 432:12–25

11th World Congress on Water Resources and Environment (EWRA 2019)
"Managing Water Resources for a Sustainable Future", 25-29 June 2019, Madrid, Spain

Irrigation scheduling of cool and warm season turfgrass irrigated with sprinkler irrigation method

S. Bezirgan*, A. Halim Orta
Department of Biosystem Engineering, Faculty of Agriculture, Namık Kemal University, 59030 Tekirdağ, Turkey
** e-mail: suleymanbezirgan@gmail.com*

Introduction

The natural areas per capita are decreasing, especially in the cities because of the increase in the world population. Human beings are looking for ways to create more and more quality green areas, in order to meet this need with the intense stress of city life. The most important role of keeping the green landscape is only possible with irrigation. The recreation areas that could be created with high investment costs are likely to be of targeted quality, however, if irrigation is done with proper technique and effective maintenance, sustainability can be achieved. The most common plant used in recreation areas, the turfgrass has over 1200 species and varieties. Each type of grass has its own characteristics and these characteristics play an active role in the applied area (Orta 2017).

Due to the population growth of the cities in Thrace region, the amount of recreation areas needed is increasing every year. However, in almost all green areas, cool climate lawns are being used and because of high water requirements, it is causing a negative pressure on water resources. In this study, irrigation scheduling has carried out of cool and warm season turfgrasses under the sprinkler irrigation method and thus, the plant water consumption was determined and compared. In addition, by taking local conditions into consideration, the most suitable estimation method of reference evapotranspiration for cool and warm season turfgrasses was determined.

Materials and methods

This study had taken place in the trial fields of Agricultural Production and Research Center (TURAM) of Silivri Municipality, that lies upon Tekirdağ-İstanbul provincial border (41°03′N; 28°00′E; 46 m a.s.l.). The field experiment was carried out during the summer period of 2017. The soil of the area was classified as C2S1 according to US Salinity Laboratory (US Salinity Laboratory Staff 1954). The slope varies between 2-7% from East to West. Meteorological parameters were measured by the automated meteorological station located just near the experimental field and there was a manual pluviometry in the field to ensure the station in terms of precipitation.

The experiment was designed in Split-Plots (SP) in a Randomized Complete Block Design (RCBD) with three replications. Main treatments were two different species; C_1: Cool-Season turfgrass (10% Poa pratensis, 25% Festuca rubra var. rubra, 30% Lolium perenne, 35% Festuca arundinacea) and C_2: Warm-Season (*Cynodon dactylon L. Pers.*) turfgrasses. Sub-treatments are three different irrigation strategies as a threshold ($S_{0\text{-}30}$:30%, $S_{0\text{-}50}$:50%, and $S_{0\text{-}70}$:70%). These thresholds corresponded, respectively, to 30%, 50% and 70% of total available soil moisture depletion at 0-30 cm of the effective root zone and returning soil moisture back to field capacity (Figure 1).

Irrigation amounts are adjusted, based on the observations of soil moisture, due to usage of %30, %50 and %70 of water capacity at effective root depth. The amount of soil water in the 0.30 m top layer was used to initiate irrigation. The plots were irrigated at nearly 10-15cm depth by pop-up spray type sprinklers with flow rates of 87.25 litres per 90° angle per hour at an operating pressure of 2,1 bar were used and the lateral spacing were determined by head to head spacing with nozzles of 2,5 m irrigation radius.

The soil water level was monitored daily by using a soil moisture profile probe (PR2/6, Delta company, UK) with a soil moisture meter (HH2, Delta company, UK) for 0.10, 0.20, 0.30, 0.40, and 0.60 m depths during the whole growing season (May-September). Soil moisture meter with PR2/6 profile probe is calibrated by using the gravimetric method as described by Blake (1965). Evapotranspiration for 10-days

period was calculated based on the results of only the PR2/6 by applying the water balance method to the upper 0.60 m soil layer (Heerman 1985).

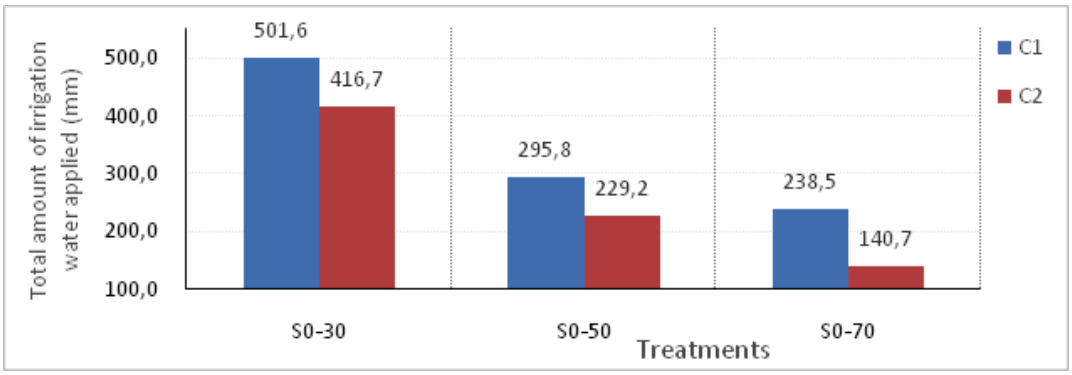

Figure 1. Total amount of irrigation water for all treatments during the measurement period.

Results and concluding remarks

As a result, irrigation interval for cool climate grass mixtures was determined as 2 days and for warm climate grass as 12 days. Crop evapotranspiration values of cool climate grass mixtures were measured as 610,45 mm, 384,89 mm and 317,81 mm. Crop evapotranspiration for warm climate grass is 488,78 mm, 324,36 mm and 211,00 mm. Generally, for both types of grass, different irrigation amounts affected the yield significantly (Figure 2).

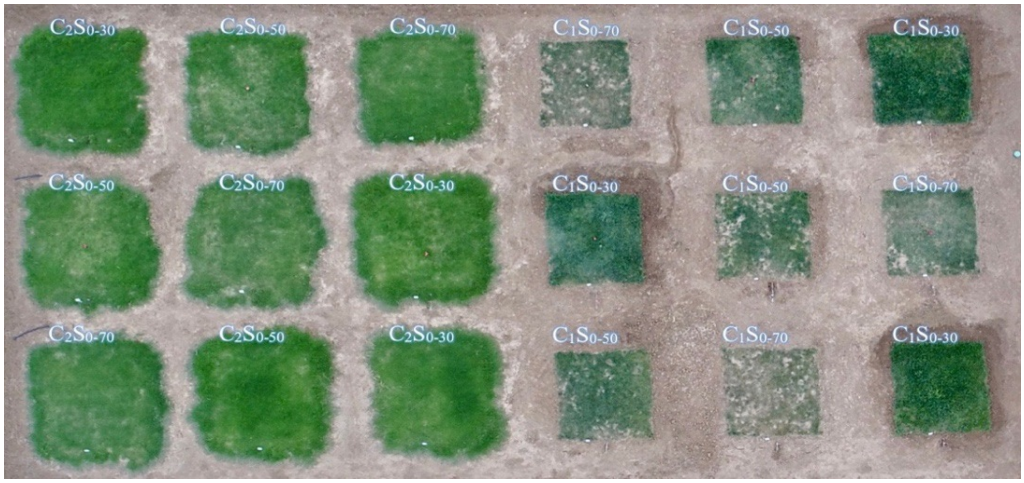

Figure 2. View of study area.

The most suitable estimation method for warm season turfgrass evapotranspiration was FAO modifications of A class evaporation pan, for cool season turfgrass evapotranspiration was Blaney-Criddle method.

References

Akpınar A, Cankurt M (2015) Assessing the Association between the Amount of Green Space Per Capita and Mortality in Turkey. Journal of Adnan Menderes University Agricultural Faculty 12(2):101-107

Avcıoğlu R (1997). Grass Technique - Cultivation, Planting and Maintenance of Green Areas. Ege University, İzmir

Blake GR (1965) Bulk Density Methods of Soil Analysis. Part I. Am. Soc. Agron. 9:374-390

Heerman DF (1985) ET in irrigation management. In: Proceedings of the National Conference on Advances in Evapotranspiration, ASAE Publication, pp 323–334

Orta AH (2017) Irrigation in the Recreation Areas. Nobel Akademik Yayıncılık. Tekirdağ

US Salinity Laboratory Staff (1954) Diagnosis and Improvement of Saline and Alkali Soils. Soil Science Society of America Journal, Washington

11th World Congress on Water Resources and Environment (EWRA 2019)
"Managing Water Resources for a Sustainable Future", 25-29 June 2019, Madrid, Spain

Participatory water governance to protect drinking water resources in an agricultural peri-urban area

M.V. Barbieri[1], C. Postigo[1], R. Roda[2], E. Isla[2], G. Frances[2], A. Casanovas[2], E. Queralt[3], V. Sola[3], J. Martín-Alonso[4], A. De la Cal[4], M.R. Boleda[4], E. López-García[1], A. Ginebreda[1], D. Barceló[1], M. López de Alda[1*]

[1] *Water and Soil Quality Research Group, Department of Environmental Chemistry, Institute of Environmental Assessment and Water Research (IDAEA-CSIC), Barcelona, Spain*
[2] *Parc Agrari del Baix Llobregat, Barcelona, Spain*
[3] *Comunitat d'Usuaris d'Aigües de la Vall Baixa i del Delta del Llobregat (CUADLL), El Prat de Llobregat, Spain*
[4] *Aigües de Barcelona, Empresa Metropolitana de gestió del Cicle Integral de l'Aigua, S.A. (ABEMGCIA), Barcelona, Spain*
** e-mail: mlaqam@cid.csic.es*

Introduction

The European Horizon 2020 project WaterProtect aims at developing new solutions and tools to adopt the correct management practices and mitigation measures to protect drinking water resources from agriculture and other human activities (Belsman et al. 2018). Experiences from seven different areas of study (action labs) in Europe will be used to achieve this goal. One of these action labs is the lower basin of the Llobregat River (NE Spain).

The Spanish action lab is located in the metropolitan area of the city of Barcelona. This is a densely populated area, and consequently with a high drinking water demand. Aquifers in the area and the Llobregat River are the water resources available to produce drinking water. Moreover, both groundwater and surface water are highly exploited to sustain other water demands in the area such as agriculture, and different industrial activities. The quality of these water resources is also threatened by urban and industrial activities (4 wastewater treatment plants) and to a less extent by agriculture (Marcé et al. 2012).

Based on a multi-actor participatory approach, different actions have been conducted in the Spanish action lab to get the different water actors involved and evaluate the current water governance framework, with the aim of proposing and implementing a new model of water governance that contributes to a better water management in the area and protect drinking water resources.

Materials and methods

Water governance and best management practices currently in place in the Lower Llobregat River basin were analyzed using through individual surveys and discussion groups in which all relevant water actors in the area participated (water producers, water users, farmers, water administrators, researchers, etc).

Water governance aspects that were analyzed included:

- Territorial characteristics and water resources of the area
- Activities that may impact the quality of water resources
- Water actors, their roles, and their perception of water quality and things that should be improved
- Governmental organization
- Relationships among different actors
- Actor arrangements
- Water policy and related legislation, informal rule and voluntary agreements
- Economic and social incentives to protect water quality
- Best management practices currently in place
- Projects and activities done in the past to improve water quality

A participatory monitoring approach was used to assess the information on water quality currently available and to identify knowledge gaps regarding the occurrence of pesticides and nitrates in the area.

For this, historical data were evaluated as well as the monitoring plans of the different water actors.

A practical collaborative open access tool that integrates and geo-references water quality information in the area has been also designed to increase the trust level among users.

Results and concluding remarks

The analysis of the governance system currently in place in the Spanish action lab allowed identifying aspects that could contribute to improving water management in the area. Many of them involve the construction of new infrastructure (irrigation channels, infiltration ponds). However, some of them could be adopted without additional economic investment.

Five agricultural best management practices (BMPs) were selected to reduce the impact of agriculture on water quality. All of them aim at reducing pesticide and nitrate contamination of drinking water resources. These BMPs are being promoted among farmers through various training and information workshops.

Two techniques for bioremediation of water polluted with pesticides are also being tested. One of them consists of constructed channels that contain fungi for in-situ bioremediation of irrigation drainage waters. The other one is algae ponds that treat pesticide-containing waters.

Finally, meeting the drinking water demand of this area in the future requires increasing the use of reclaimed water. Safety of this practice for public health can be achieved through Sanitation Safety Planning, a step-by-step risk-based approach endorsed by the World Health Organization to assist in the implementation of the 2006 WHO Guidelines for Safe Use of Wastewater, Excreta, and Greywater in Agriculture and Aquaculture (WHO 2006). Wastewater has been used to some extent in the Lower Llobregat River basin for crop irrigation. However, the creation of a working group to design the Sanitation Safety Plan is relevant to increase the volume of reclaimed water used in the future, the social acceptance of this practice, and the trust of farmers on this water resource. It is important to highlight, that this is the first time ever that Sanitation Safety Planning is applied in a real system, at least, in a real system where the volume of wastewater reused is relevant (about 6 Hm3 per year). The adoption of Sanitation Safety Planning within the water governance system of the Lower Llobregat River basin will contribute to protecting public health and also the environment in this area, as reclaimed water produced can be also used for aquifer recharge and sustain delta lagoons. Moreover, it will give an opportunity for new generations to become farmers and extend agricultural activity in the municipalities involved, because the current situation does not allow obtaining market competitive products.

Acknowledgments: This work has received funding from the EU's Horizon 2020 Research and innovation Programme through the WaterProtect project (grant agreement No. 727450).

References

Belmans E, Campling P, Dupon E, Joris I, Kersealers E, Lammens S, Messely L, Pauwelyn E, Seuntjens P, Wauters E (2018) The multiactor approach enabling engagement of actors in sustainable use of chemicals in agriculture. In: Capri E, Alix A (editors), Sustainable Use of Chemicals in Agriculture. Advances in chemical Pollution, Environmental Management and Protection, vol 2, pp 23-62

World Health Organization (2006) Guidelines for the safe use of wastewater, excreta and greywater. Available at. https://goo.gl/f3T4j9

Marcé R, Honey-Rosés J, Manzano A, Moragas L, Catllar B, Sabater S (2012) The Llobregat River basin: a paradigm of impaired rivers under climate change threats. In Sabater S, Ginebreda A and Barceló D (editors) The Llobregat: the story of a polluted Mediterranean River. The Handbook of Environmental Chemistry 21, Springer, Berlin, Heidelberg, pp 1-26

11th World Congress on Water Resources and Environment (EWRA 2019)
"Managing Water Resources for a Sustainable Future", 25-29 June 2019, Madrid, Spain

Modified budget of net anthropogenic nitrogen inputs to large watersheds: application in Lower Mondego (Portugal)

J. Vieira[1*], M.C. Cunha[1], R. Luís[2]
[1] INESC Coimbra, Department of Civil Engineering, University of Coimbra, Coimbra, Portugal
[2] University of Coimbra, Coimbra, Portugal
* e-mail: jvieira@dec.uc.pt

Introduction

Nitrogen budgets have been developed in the last two decades to estimate net nutrient contribution to watersheds accounting for all inputs (e.g., fertilizer use, biological fixation, livestock and human consumption, and atmospheric deposition) and outputs (e.g, incorporation in crops and animals, and atmospheric releases). The nitrogen budget (NANI - Net Anthropogenic Nitrogen Input) was first introduced by Howarth et al. (1996). A positive NANI represents that nutrient inputs to the watersheds are greater than nutrient outputs. A positive budget means nitrogen that can accumulate in the landscape and contribute to surface or groundwater contamination, to leaching, and erosion. Hong et al. (2012, 2017) detailed that NANI accounting has been shown good relationship with nutrient export in streamflow on large scale, multi-year average.

In this paper, the authors present an adaptation to the NANI budget described in Hong et al. (2012, 2017) with an application to a watershed (Lower Mondego – Portugal) with relevant agricultural activity. In the remainder of this paper, the authors present the nitrogen budget as defined in Hong et al. (2012, 2017), the adaptation proposed and the results from the application of the modified nutrient budget to the case study area.

Materials and methods

Hong et al. (2012, 2017) defined NANI by the sum of four major components, all in the same units:

$$NANI = FERT_N + BNF_N + DEP_N + NFFI_N \quad (1)$$

where $FERT_N$ (e.g., kg-N/ha/year) is the fertilizer nitrogen (N) application, BNF_N (kg-N/ha/year) is the biological fixation of atmospheric N by microorganisms which enjoy a symbiotic relationship with leguminous plants, DEP_N (kg-N/ha/year) is the atmospheric N deposition, and $NFFI_N$ (kg-N/ha/year) is N contained in net food and feed imports. While $FERT_N$, BNF_N and DEP_N are defined usually by simple expressions (e.g., $FERT_N$ is determined usually from statistics of commercial fertilizers and N content), the $NFFI_N$ is defined in Hong et al. (2012, 2017) as a budget it self:

$$NFFI_N = C_{a,N} - P_{a,N} + C_{h,N} - P_{c,N} \quad (2)$$

where $C_{a,N}$ and $C_{h,N}$ are the animal and human N consumption (or demand), respectively, and $P_{a,N}$ and $P_{c,N}$ are the animal and crops N production (or incorporation), respectively (all in kg-N/ha/year). In Eqs. (1) and (2), $FERT_N$, BNF_N, DEP_N, $C_{a,N}$ and $C_{h,N}$ are positive fluxes adding N to the watersheds, while $P_{a,N}$ and $P_{c,N}$ are negative fluxes removing N from the watersheds.

The first modification to the N budget described in Hong et al. (2012, 2017) is based on the hypothesis that the nitrogen in excess that can accumulate in the landscape related to the agricultural activities is approximated as follows:

$$EXCESS_{c,N} = FERT_N - P_{c,N} \quad (3)$$

From Eq. (3), one can say that the nitrogen in excess related with the agricultural activities corresponds to the nitrogen from fertilizers not uptaken by crops. As an alternative and expedite approach, the authors propose here to estimate $EXCESS_{c,N}$ (kg-N/ha/year) by theoretical nitrogen needs of each crop to be

supplied from fertilizers use and an efficiency on fertilizer uptake by crops as follows:

$$EXCESS_{c,N} = \sum_{crop} TH\_NEEDS_{crop,N} \times \frac{1 - EF_{crop,N}}{EF_{crop,N}} \quad (4)$$

where $TH\_NEEDS_{crop,N}$ (kg-N/ha/year) are theoretical N needs of each crop for a given yield and $EF_{crop,N}$ (dimensionless) is the efficiency on N fertilizer uptake by crops. Theoretical N needs are available in the literature, and the approach given by Eq. (4) can be useful when statistics about fertilizer sales are not available.

Additionally, by representing the nitrogen excreted by animals in one single term, $E_{a,N}$ (kg-N/ha/year):

$$E_{a,N} = C_{a,N} - P_{a,N} \quad (5)$$

the modified NANI (NANI*, also in kg-N/ha/year) proposed by the authors can be written as follows:

$$NANI^* = \sum_{crop} TH\_NEEDS_{crop,N} \times \frac{1 - EF_{crop,N}}{EF_{crop,N}} + BNF_N + DEP_N + C_{h,N} + E_{a,N} \quad (6)$$

Results and concluding remarks

The modified nitrogen budget (NANI*) was applied in Lower Mondego basin (1740 km^2) for the periods 1986-1989, 1990-1999, 2000-2009 and 2010-2016 (average pressures considered in each period) at the sub-basin scale (the sub-basins were defined by the watersheds of the main tributaries of Mondego river in the case study area).

In general, the higher values of NANI* (>80 kg N/ha/year) were found in sub-basins with significant agriculture and livestosck with greater contribution from components $EXCESS_{c,N}$ and $E_{a,N}$.

The mean values of NANI* (50-80 kg N/ha/year) were observed in more urbanized sub-basins, also with an important contribution of component $C_{h,N}$.

The lower values of NANI* (<50 kg N/ha/year) were found in sub-basins in which the land use is mainly forest land. In these sub-basins, the greater contribution in percentage to the value of NANI* is from components $EXCESS_{c,N}$ and $E_{a,N}$ but the absolute values are significantly lower than in the sub-basins with significant agriculture and livestock.

In a multi-period analysis, NANI* showed a trend of increase in most sub-basins from period 1986-1989 to period 1990-1999. Then, the value of NANI* decreased successively in all sub-basins in the two remaining periods (2000-2009 and 2010-2016). From the source data used to the application of NANI*, this behaviour can be explained by the decrease of agriculture (reduction of crop areas) and livestock (reduction of the number of animals grown in the case study area).

The nutrient balance presented in work allowed a first characterization of the anthropogenic pressures that interact with the nitrogen cycle on Lower Mondego basin. Subsequent studies will be pursued to investigate the relationship between spatial and temporal trends of NANI* and riverine nitrogen fluxes in the watershed.

Acknowledgments: This research was supported by LEAP (LEgacies of Agricultural Pollutants) project (WaterJPI/005/2015). The authors thank also the Portuguese public agency Fundação para a Ciência e a Tecnologia through the strategic project UID/Multi/00308/2019 granted to INESCC.

References

Hong B, Swaney DP, Morth C, Smedberg E, Hagg HE, Humborg C, Howarth RW, Bouraoui F (2012) Evaluating regional variation of net anthropogenic nitrogen and phosphorus inputs (NANI/NAPI), major drivers, nutrient retention pattern and management implications in the multinational areas of Baltic Sea basin. Ecological Modelling 227:117-135. https://doi.org/10.1016/j.ecolmodel.2011.12.002

Hong B, Swaney DP, McCrackin M, Svanbach A, Humborg C, Gustafsson B, Yershova A, Pakhomau A (2017) Advances in NANI and NAPI accounting for the Baltic drainage basin: spatial and temporal trends and relationships to watershed TN and TP fluxes. Biogeochemistry 133(4):245-261. https://doi.org/10.1007/s10533-017-0330-0

Howarth RW, Billen G, Swaney D, Townsend A, Jaworski N, Lajtha K, Downing JA, Elmgren R, Caraco N, Jordan T, Berendse F, Freney J, Kudeyarov V, Murdoch P, Zhao-Liang Z (1996) Regional nitrogen budgets and riverine N & P fluxes for the drainages to the North Atlantic Ocean: Natural and human influences. Biogeochemistry 35(1):75-139. https://doi.org/10.1007/BF02179825

11th World Congress on Water Resources and Environment (EWRA 2019)
"Managing Water Resources for a Sustainable Future", 25-29 June 2019, Madrid, Spain

Water management in Turkey: The effects of climate change on agriculture and the economy

C. Sánchez Cerdà[1,2], T. Pilevneli[2], G. Capar[2*]
[1] Department of Biology, Healthcare and the Environment Barcelona University Barcelona Spain
[2] Ankara University Water Management Institute Ankara Turkey
* e-mail: gcapar@ankara.edu.tr

Introduction

In Turkey, like other Mediterranean countries, the effects of climate change threaten the country's water resources, causing the agricultural and economic sector to be at a critical point in its prosperity. In Turkey, agriculture is an important sector in the economy, as it represents 27% of the total labour force and in certain rural areas it represents almost 100% of it (Cakmak et al. 2008). Moreover, it plays an important role in exports and is essential to supply the 80 million Turkey inhabitants.

The aim of this work is to assess how climate change would affect water availability in Turkey and investigate its consequences on the country's agricultural and economic sector.

Materials and methods

For this study, the existing information and projections of climate change in Turkey were analysed. First, the current situation of water resources in Turkey and the availability of these in future were assessed by studying the projections of the climate change in the country. A downscaling of the RCP scenario 4.5 and RCP 8.5 were made by the Ministry of Agriculture and Forestry (former Ministry of Forestry and Water Affairs) for their "Climate Hydro. Climate Changes Impact on Water Resources Project" (Ministry of Agriculture and Forestry 2014). The projection period covers the years between 2015-2100 and the reference period is 1961-2000. With this project it is possible to know how temperature, rainfall and water availability will vary in each river basin for the projected periods and scenarios.

Second, it was studied how the variation on water resources will affect the water availability for agriculture. To carry out this study eight main crops were chosen and their water footprints were assessed. The selected crops were wheat, cotton, olives, hazelnuts, grapes, tobacco, oranges and lemons. Data on their production and harvest by region were obtained from the Turkish Statistics Institute (Turkstat 2018). Their water footprints were studied considering the green, blue and grey water footprint, where the data was obtained from Twente Water Centre (Mekonnen et al. 2011).

Thirdly, an economic evaluation was carried out. To do so, the prices for tone of each crop were obtained (Turkstat 2018) and an estimation of the income for the harvest of each crop by region was obtained. Then it was discussed how this income will be affected if there is a change in the harvest of the selected crops.

Results and concluding remarks

To estimate the variation of water resources in Turkey due to climate change effects, it is necessary to integrate the variables of precipitation and temperature for each projected period studied. It was observed that the regions in the north of the country that would have an increase in their water resources will increase, while in the south there will be a decrease (Table 1).

The agricultural study (Sánchez Cerdà 2018) enabled to see how the regions that are most likely to be affected by climate change due to the increase in temperatures and the decrease in precipitation are also the ones that produce most of the crops and therefore where there is more water consumption (Aegean region, Mediterranean region Central Anatolia region and Southeast Anatolia region) (Table 2). In this way, and in response to the decrease in water resources that is projected with climate change, it is necessary to rethink the country's agricultural system, promoting rainfed agriculture in regions where water resources

are most committed and increase or initiate the growth of crops that require more irrigation in areas that will see their water resources increased with climate change.

Table 1. Water resources for each region of Turkey for the projected periods (elaborated with data from the Ministry of Agriculture and Forestry 2014).

	2015-2040 Km^3/year	2041-2070 Km^3/year	2071-2100 Km^3/year
Marmara Region	14.05	14.05	14.05
Aegean Region	14.19	14.19	14.19
Mediterranean Region	38.53	38.53	38.53
Southeast Anatolia Region	27.21	26.21	25.21
Central Anatolia Region	8.15	8.15	8.15
East Anatolia Region	40.68	39.68	38.68
Black Sea Region	48.98	48.98	48.98
Whole Turkey	191.79	189.79	187.79

Table 2. Water consumption of the selected crops for each region (km^3) (elaborated with data from Mekonnen et al. 2011 and Turkstat 2018)

	Wheat	Cotton	Olives	Hazelnuts	Grapes	Tobacco	Lemons	Oranges	Total
Marmara Region	7.662	0.001	0.952	0.952	0.140	0.089	000001	0.00011	9.00
Aegean Region	3.705	1.027	2.280	0.400	1.318	2.263	0.016	0.092	11.10
Mediterranean Region	4.099	0.428	1.163	0.243	0.347	0.059	0.240	0.47	7.05
Southeast Anatolia Region	8.810	2.848	0.106	0.419	0.441	0.409	---	---	13.03
Central Anatolia Region	17.557	---	0.009	0.155	0.238	0.112	---	---	18.07
East Anatolia Region	2.785	0.001	---	0.072	0.070	0.096	---	---	3.02
Black Sea Region	3.967	---	0.001	0.005	0.017	0.257	0.0001	0.00054	4.25
Whole Turkey	48.58	4.31	4.51	1.45	2.57	3.29	0.26	0.56	

Although more exhaustive economic cost-benefit studies are needed, the data obtained from the economic evaluation show that the regions that will be "favoured" by climate change due to an increase in their water resources are also the ones that will be most economically "benefited", as they will have the possibility to: 1) harvest large areas, and 2) harvest crops that consume a lot of water but have a high economic value. On the other hand, the regions that will see their water resources diminished will also see their income reduced, because 1) they will need to reduce the harvested areas, and 2) they will have to change the crops for others that consume less water but have a lower economic value.

References

Cakmak EH et al. (2008) Macro-Micro feedback links of irrigation water management in Turkey. The World Bank Development Research Group Sustainable Rural and Urban Development Team. Policy Research Working Paper 4781. http://documents.worldbank.org/curated/en/698961468108847250/pdf/WPS4781.pdf

Mekonnen M et al. (2011) The green, blue and grey water footprint of crops and derived crop products. Hydrology and Earth System Sciences 15:1577–1600. http://waterfootprint.org/media/downloads/Mekonnen-Hoekstra-2011-WaterFootprintCrops.pdf

Ministry of Agriculture and Forestry (2014) Clima Hydro. Climate Changes Impact on Water Resources Project. http://iklim.ormansu.gov.tr/Eng/

Sánchez Cerdà C (2018) Water management in Turkey: the effects of climate change on agriculture and the economy. Master's Degree Thesis in Science and Integrated Water Management, University of Barcelona

Turkish Statistical Institute (Turkstat) (2018) Available at: http://www.turkstat.gov.tr/UstMenu.do?metod=temelist

11th World Congress on Water Resources and Environment (EWRA 2019)
"Managing Water Resources for a Sustainable Future", 25-29 June 2019, Madrid, Spain

On farm water-use efficiency investments: Perennials and climate change

D. Adamson*, A. Loch
Centre for Global Food & Resources, Faculty of Professions, University of Adelaide, Australia
** e-mail: david.adamson@adelaide.edu.au*

Introduction

Water-use efficiency (WUE) has been embraced by policy makers as it allows producers to generate the same level of a desired output with less inputs (i.e. water) by substituting in other non-binding factors of production (land, labour, capital) (Arrow et al. 1961). However, WUE can ties existing technology into long term investments that can take time to pay off, exposing capital to the vagaries of risk and uncertainty.

The world's supply of water is finite and uncertain. Historic misallocation of finite water resources has created insecurity, inequality, and negative externalities. The combination of increased water demand and uncertain supply can amplify private capital investment risk exposure that, when scaled, can result in larger irreversible capital losses. We can represent water supply uncertainty as the adoption of alternative management responses when droughts and/or floods occur (Adamson et al. 2017). In this case the response to a realised supply of water can create non-convex management solutions to protect capital investments (Baumol and Bradford 1972). However, our understanding of adaption to climate change is incomplete and the risk to long term investments is likely to increase.

The purpose of this paper is to explore a possible strategy to mitigate capital risk exposure at multiple scales by combining the state contingent analysis (SCA) (Chambers and Quiggin 2000) with cost-benefit analysis (CBA). The strategy enables an alternative representation of uncertainty, coupled with an improved understanding of how private investors adapt to realised water supply, to enhance our appreciation of why water-use efficiency investments may fail. This new approach is tested against four investment choices in improving WUE on farm. The paper assumes that the farmer only invests in options that improve WUE once water has reached the farm gate.

Materials and methods

We propose that the combination of SCA within a modified CBA framework provides an effective approach to understand the risk and uncertainty of upgrading irrigation infrastructure. The benefit of the SCA approach is that it separates uncertainty (Ω) into a set of mutually exclusive and real states of nature ($S \in \Omega$). In this case water supply is the uncertainty signal, and the states of nature (s) are normal, drought and wet. For each s a set of management options are defined that include a s specific bundle of inputs that produces a s described output. Thus, when a s is revealed, ambiguity is removed as now the decision maker has complete awareness of how to respond. While the decision maker has a preconceived belief about the frequency of each s occurring, the decision maker cannot influence which s occurs.

This paper extends the work by Adamson et al. (2017) by modifying the traditional Just-Pope stochastic production functions into a SCA representations. The major advance in this new representation provides far greater clarity of how water inputs protect capital investments in each state of nature, in Equation1. Now output (z) by state of nature (s) is a combination of additive risk from natural soil fertility (ζ) and two multiplicative risk signals for water inputs (x): that is, those inputs required to keep the production system alive (g) in all s, and water inputs required to generate outputs (h). Note, g=0 for all annual crops.

$$z_s \leq \zeta_s + g(x)_{s,\varepsilon} + h(x)_{s,\varepsilon}. \quad (1)$$

Consequently, if $g(x)$ units of water are not provided irreversible losses of capital directly invested in that production system (e.g. rootstock, trellising, and some irrigation equipment) is lost. This new equation is then tested against the irrigator's choice of investing in alternative technologies to improve WUE efficiency.

The paper explores how investments strategies alter in response to WUSE subsidies and how the return

on those investments alter in response to climate change. Based from lessons learnt by Adamson et al. (2009), climate change is represented by changing the frequency of states of nature occurring. The case study is based on investing in an almonds crop in California, USA.

Results and concluding remarks

The results illustrate that subsidies are already required to improve the adoption of WUE technology. Technology that reduces $g(x)_s$ provides growers with some space for dealing with droughts. However, climate change is expected to make all future returns on investments negative. Consequently, current and future long-term investments in perennial crops are likely to face irreversible losses. Therefore, policies that incentives the adoption of WUE, and perennials may create irreversible capital outcomes. Policy makers then need a greater awareness of the minimum amount of water required to keep a connected system function to preserve economics, social and natural capital.

Acknowledgments: Funding provided (DE160100213) "Optimising the National Benefits from Restoring Environmental Flows" & DE150100328 “Minimising transaction costs in the Murray-Darling Basin”

References

Adamson D, Loch A, Schwabe K (2017) Adaptation responses to increasing drought frequency. Australian Journal of Agricultural and Resource Economics 61:385-403

Adamson D, Mallawaarachchi T, Quiggin J (2009) Declining inflows and more frequent droughts in the Murray–Darling Basin: climate change, impacts and adaptation. Australian Journal of Agricultural and Resource Economics 53:345-366

Baumol WJ, Bradford DF (1972) Detrimental Externalities and Non-Convexity of the Production Set. Economica 39:160-176

Chambers RG, Quiggin J (2000) Uncertainty, production, choice, and agency: The state-contingent approach. Cambridge University Press, New York

11th World Congress on Water Resources and Environment (EWRA 2019)
"Managing Water Resources for a Sustainable Future", 25-29 June 2019, Madrid, Spain

Italian approach to quantify water for irrigation

R. Zucaro, M. Ferrigno*, V. Manganiello
Council for Agricultural Research and Economics, Research Centre for Agricultural Policies and Bioeconomy (CREA-PB), Rome, Italy
** e-mail: marianna.ferrigno@crea.gov.it*

Introduction

According to Water Framework Directive 2000/60/CE (WFD) and the user-pay principle, water pricing policies should be implemented which encourage the efficient use of resources, even at fixed rates depending on the volumes actually used. The Italian context is characterized by a great variability both in the characteristics of the territory and in irrigation systems (Zucaro 2014) and, as a consequence of this variability, the quantification of irrigation volumes, and the relevant regulatory provisions already in place at regional level, lacks in uniformity (INEA 2001).

The challenge was to define a suitable approach to apply the Union legislation and, at the same time, sufficiently flexible and simple to be effectively applied in any national contexts. The purpose of this work is to describe the scientific approach for drafting the Italian national Guidelines for the quantification of irrigation volumes by Regions, and subsequent technical document, and the strategy adopted to allow the full application of Guidelines at local levels.

Materials and methods

The purpose of Italian national Guidelines for the quantification of irrigation volumes by Regions (MiPAAFT 2015) was to identify homogeneous criteria by which the Italian Regions regulate how to quantify water volumes used by end-users for irrigation purposes in order to promote the quantification through the use of water meters and the application of water prices based on the volumes actually used. The technical support to draft the guideline has been provided by a working group. It has been established at the Ministry of Agriculture (MiPAAFT), supported by CREA Research Centre for Agricultural Policies and Bioeconomy and also participated by the Ministry of the Environment, Regions and Autonomous Provinces (APs), River Basin Districts Authorities, Agricultural Associations, ISTAT (National Institute of Statistics), ANBI (Association for Land Reclamation and Irrigation). Experts from research institutions endured the scientific debate inside the group. The drafting of Guidelines also responded to the need of a unique database for collecting and processing information on irrigation.

In the drafting of Guidelines was also decided to guarantee a strong link with River Basin District planning, which constitute (according to the WFD) the geographic reference unit for water management and protection, in order to optimize the management of water resources and crisis situations.

With the approval of Guidelines, the drafting working group was confirmed and transformed into a Permanent Table, coordinated by MiPAAFT with the technical support of CREA Research Centre for Agricultural Policies and Bioeconomy, whose purpose was to keep coordination between all stakeholders involved in the drafting of Guidelines, also in their subsequent transposition by the Regions and APs (provided as ex-ante conditionality in Rural Development Plans at regional level), to monitor the implementation of the Guidelines also with reference to the collection and management of data on irrigation volumes and to draft documents designed to standardize estimation methods where the Guidelines provide for its use.

Drafting of Guidelines has numerous innovative aspects; both the approach (adaptation of regional dispositions to the peculiar territorial needs) and the content (coordinating guideline provisions with the River Basin District planning) represent a novelty.

Results and concluding remarks

Taking into account the highlighted differences and peculiarities of the irrigation systems in Italy,

Guidelines provide common indications for the quantification of irrigation volumes, through measurement or estimation, defining the minimum cases in which the Regions and Autonomous Provinces (APs) establish the obligation to measure withdrawals, uses and return flows, for both collective irrigation and self-supply (Figure 1). Guidelines are integrated by a technical document (MiPAAFT 2016) drawn up within the Permanent Table and concerning common estimation methodologies for withdrawals and uses by collective irrigation, withdrawals and uses by self-supply, return flows and releases, to be used in alternative to the direct measurements, where required or permitted. Their use is now consolidated over time, but Guidelines address their application in a uniform and coordinated manner on the national territory and providing adequate technical support for the subjects concerned to the quantification of irrigation volumes.

Furthermore, Guidelines identify SIGRIAN - National Information System for Water Management in Agriculture (http://sigrian.entecra.it/sigrianmap/sigria/SigriaStart.php) as the Italian national reference database for the collection and share of data resulting from the monitoring of water volumes for irrigation, in order to make them available to Administrations and other Bodies responsible for water management.

For its elements of generality and flexibility of application, it is believed that the approach used for the drafting of national Guidelines and the subsequent regional transposition can be applied in other contexts equally characterized by great variability of irrigation systems, also different from the Italian ones.

Table 1 summarize the indications of the Guidelines and of the mentioned technical document, for collective irrigation and self-supply.

Table 1. Common indications for collective irrigation and self supply

<table>
<tr><th colspan="2" rowspan="2">GUIDELINES INDICATIONS</th><th colspan="3">ELEMENT TO BE MONITORED - COLLECTIVE IRRIGATION</th><th colspan="3">ELEMENT TO BE MONITORED - SELF-SUPPLY</th></tr>
<tr><th>Withdrawals</th><th>Uses</th><th>Return flows</th><th>Withdrawals</th><th>Uses</th><th>Return flows</th></tr>
<tr><td rowspan="2">WHAT</td><td>Obligation to meter</td><td>>100 l/s (threshold) (Regions may define a different threshold)</td><td>Head of irrigation district</td><td>>100 l/s (where relevant)</td><td rowspan="2">As by regional regulation</td><td>At users level, as by regional regulation</td><td>As defined by Regions, if relevant</td></tr>
<tr><td>Cases of exclusion</td><td>No one above threshold</td><td>As defined by Regions (advisory services, unfeasibility, etc.)</td><td>Where not relevant</td><td>by Region (where not possible or not relevant)</td><td>As defined by Regions, if relevant</td></tr>
<tr><td rowspan="2">HOW</td><td>Measurement (different types of meters)</td><td>I-II level (even in real time if necessary)</td><td>IV level</td><td>As and if required</td><td>At users level</td><td>At users level</td><td>As defined by regions, if relevant</td></tr>
<tr><td>Estimation</td><td>under threshold and over 50 l/s</td><td>where metering is not, or not yet, possible (if quantification is necessary)</td><td>under threshold or when metering is not, or not yet, possible (where relevant)</td><td colspan="2">When metering is not, or not yet, possible or not relevant (if quantification is necessary) Aggregated data for municipalities and water bodies (*)</td><td>As defined by Regions, if relevant</td></tr>
<tr><td rowspan="3">WHO</td><td>Collection</td><td colspan="3">Irrigation agencies</td><td colspan="3">Regions (according to regional data base, existing or to be implemented)</td></tr>
<tr><td>Validation</td><td colspan="3">Regions (after transmission to SIGRIAN)</td><td colspan="3">Regions</td></tr>
<tr><td>Transmission to SIGRIAN</td><td colspan="3">Irrigation agencies</td><td colspan="3">Regions (after validation)</td></tr>
<tr><td rowspan="2">WHEN</td><td>Collection</td><td>Monthly volume (during irrigation season)</td><td>Total volume (during irrigation season)</td><td>Total volume (during irrigation season)</td><td>Total volume (during irrigation season)</td><td>Total volume (during irrigation season)</td><td>Total volume (during irrigation season)</td></tr>
<tr><td>Transmission to SIGRIAN</td><td>LW(*) Once per month during irrigation period SW(*) Twice, during irrigation season Once per year for other uses</td><td>Once at the end of irrigation season</td><td>Once at the end of irrigation season</td><td>Once per year</td><td>Once at the end of irrigation season</td><td>Once at the end of irrigation season</td></tr>
<tr><td colspan="2">NOTES</td><td colspan="3">(*) LW - Large withdrawals (≥1000 l/s according to national law, Royal Decree 1775/33) SW - small withdrawals (< 1000 l/s according to national law, Royal Decree 1775/33)</td><td colspan="3">(*) For the purpose of estimation, it was considered for self-supply: i) uses= withdrawals; ii) return flows not relevant.</td></tr>
</table>

References

Zucaro R (2014) Atlas of Italian Irrigation systems. INEA, Rome

Istituto Nazionale di Economia Agraria (2001) Quadro normativo in materia di acque ad uso irriguo. INEA, Rome

MiPAAFT (2015) Italian national Guidelines for the quantification of irrigation volumes by Regions

MiPAAFT (2016) Estimation methodology of irrigation volumes withdrawals, uses and return flows.

11th World Congress on Water Resources and Environment (EWRA 2019)
"Managing Water Resources for a Sustainable Future", 25-29 June 2019, Madrid, Spain

Smart on-farm irrigation of Chia-Nan irrigation association of Taiwan

F.N.-F. Chou[1*], H.-C. Lee[1], S.-J. Luo[2], C.-W. Wu[1]
[1] Department of Hrdraulic and Ocean Engineering, National Cheng Kung University, Tainan, Taiwan
[2] Management Section, Southern Water Resources Office, Water Resources Agency, Kaohsiung, Taiwan
* e-mail: hyd4691@mail.ncku.edu.tw

Introduction

The Chia-Nan Irrigation Association adopts a precision rotation irrigation system and accompanied with enhanced irrigation management to improve irrigation efficiency. The current irrigation system of the Irrigation Association has been in existence and operated for a long time. There is a certain degree of rapport with the peasants. However, there still are difficulties that the current system often encounters in practice are:

- Some farmers do not plant crops according to farming pattern.
- Even if crops such as rice are grown according to the pattern, however, it was not planted at the time set by the irrigation system.
- Part-time farmers do not cooperate with precision rotation irrigation plans to draw water,
- The government fully subsidies the water fee which led some upstream farmers to divert water as much as possible and result uneven water allocation.
- Equipment such as division box may be easily adjusted by farmers. It results in water allocation errors.

Climate change exacerbates the extreme events of hydrological trends. Demands of domestic and public water supply continue to grow. The current and future water situations of southern Taiwan are in a high-risk state of imbalance between supply and demand. The Chia-Nan Irrigation Association has strengthened irrigation management to save water under ordinary conditions. When a severe drought occurs, the water situation is even worse. Some paddy fields irrigation must be ceased for transferring water to support the stabilization of water supplies for other purposes. The competent authority promotes the smart irrigation system in response to this challenge. It is expected to improve the efficiency of water allocation and assist local ditch managers to save effort and time by refining the on-farm irrigation practice of the Irrigation Association.

Materials and methods

The general configuration of the smart on-farm irrigation system includes:

- Set up the water level-flow sensing device at the end of each adjacent water supply ditch in the irrigation area.
- Real-time onsite hydrologic and climate data can be transferred to the cloud database instantaneously by technology of Internet of Things (IOT) and transmission equipment.
- A central smart management platform (SMP) is developed to evaluate whether water allocated is appropriate based on real-time sensing data. It may recommend corresponded water volume adjustment strategy.
- The SMP returns the recommended strategy of water adjustment to the local operator by also using the IOT technology and transmission equipment. In addition, control system such as division box can be remotely controlled by the SMP directly to adjust the amount of water distribution in a rotation area,
- If there is a surplus of water under the proper allocation in a rotation area, SMP may adjust a series of gates of the upstream channels to save surplus water in different upstream storage facilities.

Results and concluding remarks

This smart irrigation system with technology such as the IOT can provide assistance to implement what is not easy to be carried out of the current system. SMP recommends water allocation strategy based on local real-time sensing data. This strategy may be modified with reference to the feedback from the Irrigation Association personnel, ditch manager and farmers. The experience and knowledge of local ditch managers can be incorporated into the system with the SMP. The functions of the built-in smart irrigation system include:

- On-farm water supply and ditch flow monitoring equipment

Irrigation system is equipped with water measuring facilities at every entrance gate of a rotation area to ensure that the required amount of water is supplied according to the irrigation plan. However, the amount of water drained out from the rotation area has not been observed before. The inflow and outflow of each small water supply ditch of unit zones of paddy field of a rotation area has also not been measured.

The smart irrigation system adds water level monitoring equipment to the existing water gates, at the end of each small water supply ditch and at the outlet of drainage system of the rotation area. The measuring equipment monitors the amount of water flowing out from each single unit zone to improve the accuracy of water supply to the rotation area and water distribution between single unit zones. The SMP will issue instant alerts based on detected abnormal water flow out from a single unit zone to improve management efficiency of ditch manager.

- Control equipment used to check or divert water in the water supply ditch

Precision rotation operation includes supplying water to the small ditch of a single unit zone and the rotation of the blocks in the single unit zone alternatively. To facilitate the rotation irrigation of single unit zones, division boxes with checks are installed in every small and medium water supply ditch to allow the ditch manager distributing water. There is also a check slot and board prepared at about 40 meters in distance in a small water supply ditch to raise the water level for diverting water into each block. It helps to carry out rotation irrigation of all blocks in a single unit zone.

This study also cooperates with research and developing water division and control equipment, labor-saving and lockable gate mechanical control equipment for ditches while promoting smart irrigation. All developed equipment has the function of automatic operation or remote control such that the ditch manager can save time and effort in distributing water.

- Automatic control equipment of inlet water gates of a rotation area

The inlet gates of small and medium water supply ditches in a rotation area are mechanical water gates before. It is manually and laboriously operated by personnel of the workstation of Irrigation Association. The ditch flow is adjusted once every ten days in general. However, in conjunction with strengthening irrigation management operations, the operating frequency is significantly increased in recent years.

The smart irrigation system improves water gate to be motorized and combined with functions such as manual operation, automatic adjustment and remote control. The rebuilt electricized water gate saves time in operation compared to the original mechanical water gate. However, it still maintains manual operation option to allow the unit to operate without power. Automatic adjustment or remote control can save the travel time of workstation personnel if it is further equipped with monitoring equipment.

The smart irrigation system can help the workstation of Irrigation Association to instantly grasp the distribution of water in the field. It can effectively improve the efficiency of on-farm irrigation through maneuver adjustment.

To properly allocate the amount of on-farm water, division boxes and gate opening can be adjusted more accurately according to the sensing data of water level and discharge at the end outlet of each irrigation ditch of the rotation area. Secondly, remote control automation equipment saves time and effort of workstation personnel and ditch manager to perform water allocation operations. In the long run, workstation personnel or ditch manager can take advantage of this smart irrigation system to use less effort but improve the effectiveness of on-farm water allocation operation.

References

Chou F, Lee H (2018) Strategies of water intake of paddy block and gate regulation of irrigation ditches of the experimental paddy field. In: Improving irrigation water saving management technique: a case study in Chia-Nan irrigation area (Phase II). Southern Water Resources Office, Water Resources Agency, Taiwan, pp 133-170

VI. Water-Energy-Food Nexus

11th World Congress on Water Resources and Environment (EWRA 2019)
"Managing Water Resources for a Sustainable Future", 25-29 June 2019, Madrid, Spain

Evolution of water use, consumption and energy in the Spanish irrigated sector

J. Espinosa-Tasón, C. Gutiérrez-Martín, J. Berbel*
Department Agricultural Economics, WEARE Group, Universidad de Córdoba, Spain
** e-mail: berbel@uco.es*

Introduction

This study describes the evolution of the main variables for Spanish irrigated sector: water use, consumption, and energy use at national level, considering that most of the basins have reached closure (Molle et al. 2010). The response to the context of growing water demand with limited supply has been the modernization of irrigated areas with the transformation of furrow irrigated areas to drip and sprinkler and a resulting increase of irrigation efficiency (IE). The change of irrigation system is linked to increase in energy use. This trajectory has been explained at river basin level (Berbel et al. 2013) and the effects of modernization at national level by Berbel et al. (2019). The study is conducted at national level for the period 1950-2017 with a detailed analysis of the evolution of irrigation efficiency and energy consumption.

Materials and methods

Different sources have been used either for the observed original data or the estimation of non-observed variables when necessary.

Observed variables have been gathered mainly from Statistical National Institute (water abstraction volume), Ministry of Agriculture (irrigated area by system) and Ministry of environment (groundwater piezometric level) for the period 1950-2017. Basic statistical techniques (minimum squares or time series) have been used to estimate missing data.

1) Observed variables
   a) Total irrigated area (ha) from 1950 and irrigated area by system (furrow, sprinkler, drip) (1988-2017).
   b) Total irrigation water abstraction (m^3) by irrigation system (1999-2017).
   c) Pumping lift (m) data were derived from a sample of water table depth from the Ministry of Environment Database.
2) Parameters required for the model are based on frequent values found in literature.
   a) Irrigation efficiency by system, we use average typical values of: furrow, 60%; sprinkler, 80% and drip, 90%.
3) The remaining key variables are estimated based upon technical parameters and the original data.
   a) Water consumption as the product of water use (m^3) by irrigation system efficiency.
   b) Return flows as the difference between water use and water consumption.
   c) Energy consumption based on the equation [1] (Daccache et al. 2014)

$$Energy\ (kWh) = \frac{Volume\ (m^3) \cdot TH\ (m)}{367 \cdot \mu_{pump} \cdot \mu_{motor}} \quad (1)$$

Equation (1) estimates energy use as a function of water abstracted (m^3) and total elevation TH (m). Pump efficiency of μ_{pump}=0.8 and motor efficiency μ_{motor} of 0.4 for fuel powered and 0.9 for electric motors was defined. Total height is the sum of system pressure where typical operating pressures for drip (1 bar) and a sprinkler (3 bar) were assumed plus 20% of distribution losses and finally a pumping lift was assumed for groundwater (weighted average defined in 1.b above) and surface water (5m).

Results and concluding remarks

Figure 1 illustrates the trajectory towards basin closure and the key variables are summarized in Table 1.

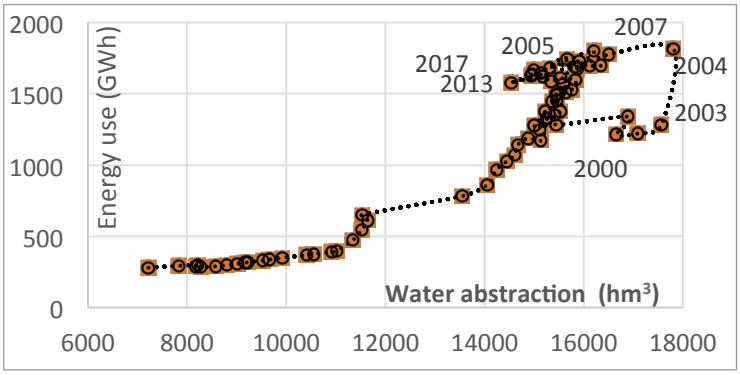

Figure 1. Water abstraction and energy consumption by the irrigation in Spain 1950-2017. (Note: desalinization and reclaimed water supply not included)

Table 1. Estimated water withdrawal, water consumption, irrigated area and energy consumption in Spain. (Note: desalinization and reclaimed water supply not included)

	Year				Annual growth		
	1950	**1980**	**2004**	**2017**	***1950-1980***	***1980-2004***	***2004-2017***
Irrigated area (ha)	1 179	2 656	3 264	3 734	*2.7%*	*0.9%*	*1.0%*
Water abstraction (hm^3)	7 221	15 220	17 808	14 998	*2.5%*	*0.7%*	*-1.3%*
Water consumption (hm^3)	4 332	9 624	12 936	11 460	*2.7%*	*1.2%*	*-0.9%*
Energy consumption (GWh)	279	1.376	1.815	1.667	*5.3%*	*1.2%*	*-0.7%*
Irrigation efficiency	0.60	0.63	0.73	0.76	*0.2%*	*0.6%*	*0.4%*
Energy use kWh/m^3	0.04	0.09	0.10	0.11	*2.8%*	*0.5%*	*0.7%*
per area water use (m^3/ha)	6 125	5 731	5 456	4 017	*-0.2%*	*-0.2%*	*-2.4%*

Observation of Spanish irrigation main variables shows three phases of water economy: *Expansion* (1950-1980), all variables growth at high rates; *Closure* (1980-2004), water withdrawal reaches maximum; *Modernization* (2004-2017), effects of water conservation are visible as water withdrawal is reduced 16% vs 2004, although energy consumption and irrigated area keep growing and water consumption is reduced only 11% vs 2004. Recently, in the period 2015-2017 although water abstraction remained stable, water consumption and energy use grow 1% and 2% respectively in the last period.

The analysis of main variables does not confirm any rebound effect at national level as some authors have argued (Berbel and Mateos 2014). Data shows a strong water energy nexus, when pressurized systems are adopted as a response to water scarcity. Although water withdrawal has been reduced, impact in water consumption has been smaller and the irrigated area keeps growing so that long term sustainability of the system is not guaranteed.

Acknowledgments: The authors have received financial support from MINECO-Grant: AGL-2014-53417-R.

References

Berbel J, Expósito A, Gutiérrez-Martín C, Mateos L (2019) Effects of the irrigation modernization in Spain 2002-2015. Water Resources Management 33(5):1835–1849

Berbel J, Mateos L (2014) Does investment in irrigation technology necessarily generate rebound effects? A simulation analysis based on an agro-economic model. Agricultural Systems 128:25-34

Berbel J, Pedraza V, Giannoccaro G (2013) The trajectory towards basin closure of a European river: Guadalquivir. International Journal of River Basin Management 11(1):111-119

Daccache A, Ciurana JS, Rodriguez Diaz JA, Knox JW (2014) Water and energy footprint of irrigated agriculture in the Mediterranean region. Environmental Research Letters 9(12):120414

Molle F, Wester P, Hirsch P (2010) River basin closure: Processes, implications and responses. Agricultural Water Management 97(4):569-577

11th World Congress on Water Resources and Environment (EWRA 2019)
"Managing Water Resources for a Sustainable Future", 25-29 June 2019, Madrid, Spain

Water-Energy-Food nexus framework for quantifying the embedded water and energy in food production: A case study of Lebanon

A. Karnib*, H. Haidar
Lebanese University, Hadath Campus, Baabda, Lebanon
** e-mail: karnib.ali@gmail.com*

Introduction

Over 70% of global water withdrawals are used for agricultural sector (WWAP 2017). Studies of water and energy resources embedded in irrigated crops (water and energy footprints) are under critical discussion regarding the difficulty of linking the estimated footprints to: i) the different useable water resources (surface water, groundwater, desalination water and/or recycled water); ii) the irrigation technologies used in producing the crops (surface irrigation, sprinkler irrigation, micro irrigation); iii) the technologies used in energy use and production (fossil fuels, biofuels, electricity and renewable energy). To respond to these crucial gaps, the quantification of the embedded water and energy in agriculture and food production necessitates a water-energy-food (WEF) nexus framework where the used resources, production technologies and the complex series of direct and indirect interlinkages between WEF systems may be evaluated (Karnib 2018, 2017a, b; Hoff 2011). Karnib (2018) describes the practical and theoretical notions of the direct and indirect effects of the WEF nexus approach.

The present study provides a preliminary quantification of useable water (UW; useable water is related to exploitable surface water, groundwater, desalination water and/or recycled water sources) and useable energy (UE; useable energy is related to fossil fuels, biofuels and electricity energy sources expressed as secondary energy) embedded in Lebanon's agriculture production. The study evaluates, within a water-energy-food nexus framework, the entire series of direct and indirect UW and UE embedded in irrigated crops production. The quantitative evaluation of UW and UE embedded in food production are advantageous policy parameters for informing water and food security management; in fact, they are useful for analysing the trade-off between food production and water and energy savings through food trade.

Materials and methods

The technology-oriented feature of the Q-Nexus Model is used to develop the water, energy and food nexus case study of Lebanon (Karnib 2018, 2017a, b). In this model, the water, energy and food sectors are categorized by a set of production technologies. The model allows to recognize the direct and indirect interconnections that exist between WEF sectors and to track and evaluate the embedded water and energy by source of resources and technology used for crops production. The following set of WEF production technologies are considered in this study:

i) water sector production technologies (MCM/year): surface water extraction, groundwater extraction grouped into different depth levels, desalination and reuse of treated wastewater;
ii) energy sector production technologies (GWh/year): diesel oil and electricity (imports, steam turbine once through using seawater, gas turbine, hydro, solar photovoltaic, wind);
iii) food sector production technologies (kt/year): the selected irrigated crops presented in Table 1 using surface, sprinkler and micro irrigation systems.

The following information are collected or estimated to build the nexus system based on the Q-Nexus Model requirements: i) the end use demand of the different WEF production technologies mentioned above (households, rest of the economy, losses and exports); ii) the intersectoral WEF allocation and production intensities.

Results and concluding remarks

Table 1 presents the selected irrigated crops quantities produced for the year 2014 in Lebanon, these values are estimated by the author based on data available at FAO AQUASTAT and FAOSTAT (FAO 2018a,b). The Q-Nexus Model (WEF nexus tool) is used to evaluate the direct and indirect UW and UE embedded in the irrigated crops mentioned above, the results are presented in Table 1.

Table 1. Irrigated crops quantities and the embedded direct and indirect UW and UE for the year 2014

	Produced quantities (kt) (Irrigated)	Embedded UW (MCM)			Embedded UE (GWh)		
		Direct	Indirect	Total	Direct	Indirect	Total
Wheat	55.82	42.538	0.024	42.562	5.815	77.419	83.234
Barley	12.12	9.232	0.005	9.237	1.136	16.802	17.938
Maize	10.47	7.978	0.004	7.982	1.036	14.520	15.556
Other cereals	101.25	77.153	0.043	77.196	10.020	140.419	150.439
Vegetables	151.8	57.835	0.032	57.867	8.697	105.259	113.956
Potatoes	483.65	73.708	0.059	73.767	75.577	134.151	209.728
Other roots and tubers	104.77	15.967	0.013	15.980	16.372	29.061	45.433
Leguminous crops	54.36	103.556	0.056	103.612	7.928	188.473	196.401
Bananas	84.54	21.473	0.006	21.479	4.403	16.736	21.139
Citrus	394.12	100.106	0.028	100.134	20.529	78.020	98.549
Other fruits	732.02	185.933	0.052	185.985	38.129	144.912	183.041
Olives	18.75	7.144	0.004	7.148	0.781	13.002	13.783
Total	-	702.623	0.326	702.949	190.423	958.774	1149.197

As shown in Table 1, the total embedded UW and UE (direct and indirect) are 702.949 MCM and 1149.197 GWh respectively. The simulation shows that the direct quantities of the embedded UW and UE are 702.623 MCM and 190.423 GWh respectively; but these direct water and energy quantities required additional indirect quantities. The indirect water quantity accounts for 0.326 MCM while the indirect energy quantity accounts for 958.774 GWh. The high indirect energy quantities are resulted from the energy used for groundwater abstraction.

The use of the WEF Q-Nexus Model allows to evaluate the direct and indirect embedded UW and UE quantities in food production, in addition, it permits to disaggregate the embedded water and energy quantities according to the water and energy sources and production technologies. The evaluated embedded UW and UE can be used for supporting policy making and informing about the trade-off between water, energy and food security and food trade.

References

FAO (2018a) Aquastat Database. Food and Agriculture Organization of the United Nations (FAO). http://www.fao.org/nr/water/aquastat/main/index.stm

FAO (2018b) FAOSTAT Database. Food and Agriculture Organization of the United Nations (FAO). http://www.fao.org/faostat/en/#data

Hoff H (2011) Understanding the Nexus. Background Paper for the Bonn 2011 Conference: The Water, Energy and Food Security Nexus, Stockholm Environment Institute (SEI), Stockholm

Karnib A (2017a) Quantitative Assessment Framework for Water, Energy and Food Nexus. Computational Water, Energy, and Environmental Engineering Journal 6:11-23

Karnib A (2017b) Evaluation of Technology Change Effects on Quantitative Assessment of Water, Energy and Food Nexus. Journal of Geoscience and Environment Protection 5:1-13

Karnib A (2018) Bridging Science and Policy in Water-Energy-Food Nexus: Using the Q-Nexus Model for Informing Policy Making. Water Resources Management 32(15):4895-4909

WWAP (United Nations World Water Assessment Programme) (2017) The United Nations World Water Development Report 2017, Wastewater: The Untapped Resource. UNESCO, Paris

11th World Congress on Water Resources and Environment (EWRA 2019)
"Managing Water Resources for a Sustainable Future", 25-29 June 2019, Madrid, Spain

Impact of e-flow methods on energy production of a run-of-river hydropower plant and fish habitat

A. Kuriqi[1*], A. Sordo-Ward[2], A.N. Pinheiro[1], L. Garrote[2]
[1] CERIS, Instituto Superior Técnico, Universidade de Lisboa, Lisbon, Portugal
[2] Department of Civil Engineering: Hydraulics, Energy and Environment, Technical University of Madrid, Madrid, Spain
* e-mail: alban.kuriqi@tecnico.ulisboa.pt

Introduction

Several studies reported that run-of-river (RoR) hydropower plants cause considerable alteration of natural flow regime in the diverted river reach, which may result in degradation of the habitat condition (Anderson et al. 2015). Usually, the environmental flow methods (EFMs) applied for environmental flow releases (e-flow) in case of RoR hydropower plants are arbitrarily defined and not consistently applied (Anderson et al. 2015). The most widely applied methods are so-called static approaches, e.g., %MAF, NNQ, Q_{75} and so on (Tharme 2003). So far, dynamic approaches, e.g., %Q-Daily (%Q-D) or a combination of the %Q-D with static approaches are rarely applied. Razurel et al. (2016) applied %Q-D in several RoR hydropower plants located in Alpine rivers, and they concluded that dynamic approaches increase energy production while still preserving essential parameters of the natural flow regime. The main objective of this study is to assess the impact of several EFMs on energy production, e-flow releases and finally the implication on the fish habitat. Also, to show the potential of the dynamic approaches EFMs application in case of Mediterranean rivers.

Materials and methods

The study site area is located in the Ocreza river, Tagus basin, East Portugal (39°44' 07.05''N, 7°44' 16.51''W). The analysis conducted in this study is based on a hypothetical RoR hydropower plant. Computation of energy production and flow alteration was based on 30 years of mean daily flow data. The indicators of hydrological alteration (*IHA*) approach proposed by Richter et al. (1996) was used to characterise the flow alteration.

The biological information about the fish species, river bathymetry, physical and hydraulic information was collected through extensive field works (Rivaes et al. 2017). Iberian barbel (*Luciobarbus bocagei*) was selected as target fish species to assess the impact on the fish habitat. Flow-habitat relationship was evaluated based on the Instream Flow Incremental Methodology (Tharme 2003). For this purpose, River-2D model was used to conduct the hydrodynamic and habitat modelling.

The fish habitat suitability expressed as Weighted Usable Area (WUA) was analysed considering two life stages (i.e., juvenile and adults) regarding natural flow regime (NFR) and for each e-flow release, scenario obtained by applying the eight hydrological based EFMs. Daily timeseries of WUA for both, natural and altered flow regime were generated considering 30 years of mean daily flow data. Also, the energy production from each e-flow scenario was analysed. Finally, a sensitivity analysis was performed to compare the impact of the different e-flows methods on energy production, flow alteration and fish habitat.

Results and concluding remarks

Results show that energy production, e-flow releases, and WUA varied significantly among the EFMs. As expected, the summer period (i.e., July, August, September) was the most critical period regarding the e-flow releases and water allocation for energy production (Figure 1). Among the EFMs, 5% and 25%MAF restrict the energy production significantly (Figure 1a), but allow for the highest e-flow releases (Figure 1b) by resulting in near-natural habitat condition for both life stages of the target fish (Figure 1c, d). NNQ provides the highest energy production but allows less e-flow releases, which resulted in a significant

reduction of the WUA for both life stages of the fish. The other methods allow quite similar energy production with slight differences between them and as a result very similar e-flow release. Concerning the available habitat, Q_{84} causes the highest reduction of the WUA, while Q_{75}, 1/3ASF, 10%Q-D+NNQ and 20%Q-D cause quite a similar reduction of the WUA among them.

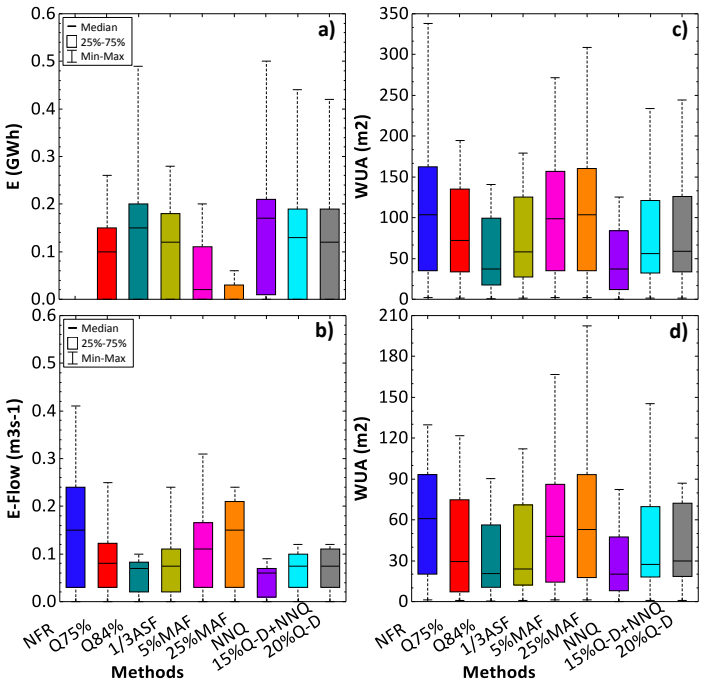

Figure 1. Energy production, e-flow release and WUA during the summer season regarding the eight EFMs: a) boxplots of inter-annual energy production b) boxplots of inter-annual e-flow compared to the NFR, c) boxplots of WUA-adults and d) boxplots of WUA-juvenile related to the NFR and altered flow regime.

However, it is worth to mention that 10%Q-D+NNQ and 20%Q-D are the only EFMs that provide relatively high energy production compared to the other EFMs applied in this study and a minimum threshold of the e-flow releases similar to the natural flow regime. Also, these two methods preserve essential flow parameters (i.e., the rate of change, frequency, timing and duration) which has a crucial role in several hydromorphological processes that form adequate habitat condition for fish and other biotas as well (Richter et al. 1996). Summarising, our results demonstrate that dynamic approaches; 10%Q-D+NNQ and 20%Q-D are very promising methods to define such e-flow releases to support the sustainable development of the renewable energy sector in case of the RoR hydropower plant.

Acknowledgements: A. Kuriqi was supported by a PhD scholarship granted by Fundação para a Ciência e a Tecnologia, I.P. (FCT), Portugal, under the PhD Programme FLUVIO–River Restoration and Management, grant number: PD/BD/114558/2016

References

Anderson D, Moggridge H, Warren P, Shucksmith J (2015) The impacts of 'run-of-river' hydropower on the physical and ecological condition of rivers. Water Environ. J. 29(2):268-276. https://doi.org/10.1111/wej.12101

Razurel P, Gorla L, Crouzy B, Perona P (2016) Non-proportional repartition rules optimise environmental flows and energy production. Water Resour. Manag. 30(1):207-223. https://doi.org/10.1007/s11269-015-1156-y

Richter BD, Baumgartner JV, Powell J, Braun DP (1996) A method for assessing hydrologic alteration within ecosystems. Conserv. Biol. 10(4):1163-1174. https://doi.org/10.1046/j.1523-1739.1996.10041163.x

Rivaes R, Boavida I, Santos JM, Pinheiro AN, Ferreira MT (2017) Importance of considering riparian vegetation requirements for the long-term efficiency of environmental flows in aquatic microhabitats. Hydrology and Earth System Sciences 21(11):5763-5780. https://doi.org/10.5194/hess-21-5763-2017

Tharme RE (2003) A global perspective on environmental flow assessment: emerging trends in the development and application of environmental flow methodologies for rivers. River Res. Appl. 19(5-6):397-441. https://doi.org/10.1002/rra.736

11th World Congress on Water Resources and Environment (EWRA 2019)
"Managing Water Resources for a Sustainable Future", 25-29 June 2019, Madrid, Spain

Integrated nexus model for sustainable urban sanitation system

T. Zinati Shoa*, M. Barjenbruch, A. Wriege-Bechtold
Department of Urban Water Management, Technical University of Berlin, Gustav-Meyer Allee 25, 13355 Berlin
** e-mail: t.zinati@campus.tu-berlin.de*

Introduction

Within the framework of sustainable development, it is important to find ways of reducing natural resource consumption and to change towards closed-loop management of nutrient, energy and water resources (Meinzinger 2010). The municipal wastewater sector in urban water management consume high amount of energy to remove nutrient and pollutant and release the treated water to nature. Even though conventional wastewater treatment resolves hygiene and aquatic environment related problems, it does not have control on generated wastewater at the source and does not consider resource recycling (Otterpohl 2002). As alternative to conventional wastewater, many approaches based on source separated sanitation system have been introduced (Larsen et al. 2009; Otterpohl et al. 2002; Zeeman et al. 2008). Although the technical feasibility of source separated sanitation systems in different pilot projects (Larsen and Lienert 2007; Peter-Fröhlich et al. 2007) have been successfully proved, nevertheless there is still lack of knowledge to more resource-oriented sanitation system alternative. This study aims to develop an integrated nutrient-energy flow analysis model to compare different developments of source separation systems that could be sustainably more feasible than conventional treatment of wastewater. It focuses on innovative systems and leading-edge technologies that are commercially available and have the potential to improve sustainability criteria in the short or mid-term.

Materials and methods

Conventional and source separated urban sanitation systems are compared in terms of their resource recovery potential including nutrient, energy and water demand in a settlement with 50,000 inhabitants in Germany. The evaluation has been done with sustainability indicators for resource demand and emission to air, water and soil.

A range of required wastewater treatment processes (emphasizing on processes, which lead to nutrient/energy production) is defined. The required parameter is set for each flow (including greywater, blackwater and urine) and corresponding processes.

The material flow model is set up using SIMBA# software and SAmpSONS Simulator tool (Schütze et al. 2018) a preliminary version for visualisation of material flow of new sanitation system. The model is developed by transferring corresponding processes into mathematical equations. The model equations not only integrate mass and nutrients flow but also the sustainability indicator of various systems. The validation and calibration have been completed.

In order to comparatively assess these systems, four different concepts have been set up including conventional system, concept 1 with nutrient recovery from urine storage, concept 2 nutrient recovery from precipitation of separated urine, concept 3 separation of greywater and energy production from undiluted wastewater.

The simulated concepts involve the processing of different wastewater fraction, transport, and energy supply. The resulting substance flow model is evaluated with a set of indicators including nutrient recovery, effluent quality, and energy and water balance in investigated sanitation concepts.

Results and concluding remarks

Figure 1 presents the energy demand equivalent and CO_2 equivalent emission in different urban sanitation concepts. The conventional system does not provide any potential of nutrient recovery, while the concept 2 with precipitation process from urine show the highest amount of possibility of nutrient

recovery for the replacement of mineral fertilizer.

Although source separation concepts are showing high potential for resource recovery and reduction of CO_2 emission, these concepts are still immature and risky in term of application in urban areas. Therefore, the developed model in this study offers the identification of such opportunities and by simulating a more realistic picture of the impact of this improvement before a decision is made.

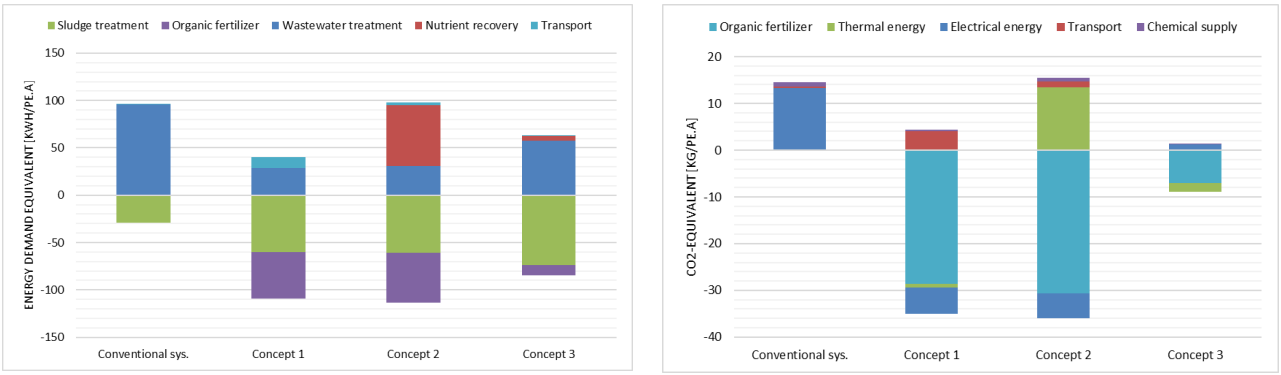

Figure 1. Energy demand and CO_2 equivalent of different concepts

Using the results of this study, the urban planner and the decision maker will be better prepared to implement successful strategies to increase efficiency of sanitation system. A general assessment of source separated sanitation system is not possible only based on process engineering technology. Although other aspects connected to source separation system may be more difficult to solve. However, it is important to evaluate carefully the new approaches in terms of their sustainability, including environmental, economic and social impacts. Source separating technologies are still considered immature and risky by most wastewater professionals.

Acknowledgments: Erasmus Mundus Lot 3 and UWI (Urban Water Interface) research training group at the technical university of Berlin are acknowledged for the financial support of this project.

References

Meinzinger F (2010) Resources efficiency of urban sanitation systems: a comparative assessment using material and energy flow analysis. Ph.D. thesis, Hamburg University of Technology, Institute of Wastewater Management and Water Protection, Hamburg, Germany

Otterpohl R (2002) Options for alternative types of sewerage and treatment systems directed to improvement of the overall performance. Water Sci Technol 45(3):149–158

Peter-Fröhlich A, Pawlowski L, Bonhomme A, Oldenburg M (2007) EU demonstration project for separate discharge and treatment of urine, faeces and greywater—part I: results. Water Sci Technol 56(5):239–249

Peter-Fröhlich A, Bohomme A, Oldenburg M, Gnirss R, Lesjean B (2007) Sanitation concepts for separate treatment of urine, feces, and greywater (SCST)-results, Kompetenzzentrum Wasser Berlin gGmbH, Berlin, Germany

Schütze M, Wriege-Bechtold A, Zinati Shoa T, Söbke H, Wißmann I, Schulz M, Veser S, Londong J, Barjenbruch M, Alex J (2018) Simulation and Visualization of Material Flows in Sanitation Systems for Streamlined Sustainability Assessment. Journal Water Science & Technology (submitted)

Zinati Shoa T, Barjenbruch M, Wriege-Bechtold A (2017) Source separation technologies, opportunities for sustainable wastewater management. European Water 58:111-117

11th World Congress on Water Resources and Environment (EWRA 2019)
"Managing Water Resources for a Sustainable Future", 25-29 June 2019, Madrid, Spain

Investigating the behaviour of water shortage indices for performance evaluation of a water resources system

F.N.-F. Chou[1], N.T.T. Linh[1,2*]
[1] Department of Hydraulic and Ocean Engineering, National Cheng Kung University, Tainan, Taiwan
[2] Thuy Loi University, 175 Tay Son, Dong Da, Hanoi, Vietnam
* e-mail: linhntt@tlu.edu.vn

Introduction

Population growth and socioeconomic development over the past several decades are imposing intense global pressures on finite water resources. Besides, the climate change becomes more especially important concern for water resources planning and management. Therefore, comprehensive water policies are essential for adapting to the increasing demand and water resources planning and management has become especially important in recent years.

The major purpose of the present study is using composite water shortage indices for assessing modified management policy of hydropower generation; and exploring various scenarios of water supply conditions. The water resource performance is evaluated using the water shortage characteristics, such as duration, magnitude, and frequency. Based on the water shortage characteristics of reservoir yield description, the water supply reservoir performance for various optimization operation policies can be easily compared.

Materials and methods

In general, system analysis models can be classified as simulation models, optimization models and combination of simulation were obtained to solve the optimize reservoir problem. This simulation–optimization approach is adopted here for optimal generated hours. A simulation model GWASIM model, which is based on Network Flow Programming, is employed to simulate the system performance base on the current condition of the hydrology, reservoir and water demand. The GWASIM which referencing MODSIM of Colorado State University is simulation model was developed based on Network Flow Programming was applied to expose the characteristic of the case study. In this study the BOBYQA algorithm of Powell (2009) is applied to find out and solve the above problems using the trust region method that forms quadratic models by interpolation. This model is expected in solving large scale problem with derivative–free algorithm.

Suppose the object studied is mainly on hydropower generation potential which is manifested by hydropower hour generation. Maximizing hydropower generation with satisfying water supply is objective of this study according to historical inflows of the reservoir.

Results and concluding remarks

The proposed approach was applied to Be river cascade reservoirs system. The study consisted of 3 hydro plants in among of 4 reservoirs. The study case has resulted in a relaxed problem with 36 continuous variables and over 64,000 constraints. Reliability of the existing system was presented by from various scenarios for different reliability of domestic and industrial water supply conditions. The optimal operating policy obtained from the simulation-optimization model is compared with the actual reservoir operation in the last decade, i.e., from water years 1978– 2010 The actual annual energy was compared to the optimized scenario with DPD constraint is 1000, 1500, 2520, 3618, and it is found that the optimized policies are superior in a way improving annual energy and lighting water shortage for the dry periods.

Table 1. Annual hydropower production from various scenarios for different DPD conditions

Simulation result			Optimized result			
Hour demand	**Energy**	**DPD**	**Scenarios**	**Energy**	**DPD**	**Difference energy**
Hour demand	12.23	3873	Scenario 1	12.91	1000	5.60%
			Scenario 2	12.93	1500	5.72%
			Scenario 3	12.85	2520	5.11%
			Scenario 4	12.72	3618	4.04%

Thus, the optimal operation policy obtained from simulation-optimization model offers advantage over the existing operation condition of the same system.

References

Arunkumar R, Jothiprakash V (2012) Optimal reservoir operation for hydropower generation using non-linear programming model. Journal of the Institution of Engineers (India): Series A 93(2):111-120

Bonner V (1989) HEC-5: Simulation of flood control and conservation systems (for microcomputers). Model-Simulation: Hydrologic Engineering Center, Davis, CA USA

Cheng C.-T, Wang W-C, Xu D-M, Chau K (2008) Optimizing hydropower reservoir operation using hybrid genetic algorithm and chaos. Water Resources Management 22(7):895-909

Chou FN-F, Wu C-W (2007) A network flow model for evaluating water supply strategies in Taiwan. In: Proceedings of the International Conference on Water Resources Management, IASTED, Honolulu, Hawaii

Draper AJ, Munévar A, Arora SK, Reyes E, Parker NL, Chung FI et al. (2004) CalSim: Generalized model for reservoir system analysis. Journal of Water Resources Planning and Management 130(6):480-489

Fu X, Li A, Wang L, Ji C (2011) Short-term scheduling of cascade reservoirs using an immune algorithm-based particle swarm optimization. Computers & Mathematics with Applications 62(6):2463-2471

Hydraulics D (1991) RIBASIM River basin simulation. Project completion report to Water Resources Commission, Taipei, Taiwan

Iwan K, Legowo S (2013) Determination of the Cascade Reservoir Operation for Optimal Firm-Energy Using Genetic Algorithms. Aceh International Journal of Science and Technology 2(2)

Kadowaki M, Ohishi T, Martins LS, Soares S (2009) Short-term hydropower scheduling via an optimization-simulation decomposition approach. Paper presented at the PowerTech, 2009 IEEE Bucharest

Labadie J (1995) MODSIM: River basin network flow model for conjunctive stream-aquifer management. Program User Manual and Documentation, Colorado State University

VII. Ecosystems and Environmental Processes

11th World Congress on Water Resources and Environment (EWRA 2019)
"Managing Water Resources for a Sustainable Future", 25-29 June 2019, Madrid, Spain

Fine sediment budget modelling during storm based events in the Rivers Bandon and Owenabue, Ireland

J.T. Garcia[1*], J.R. Harrington[2], J. Park[3]
[1] Technical University of Cartagena, R&D Group HIDR@M, Spain
[2] School of Building & Civil Engineering, Cork Institute of Technology, Ireland
[3] K-water Institute, Korea Water Resources Corporation (K-water), P.O. Box 34350, 200 Sintanjin-Ro, Daedeok-Gu, Daejeon, Republic of Korea
* e-mail: juan.gbermejo@upct.es

Introduction

Fine sediments transported in rivers during storm based events can represent an important part of the total transported fine sediments by a river during the year (Harrington and Harrington 2012a). Fine sediments are recognized as a vector for the transfer of nutrients and contaminants through river systems (Harrington and Harrington 2012b, 2014). The monitoring and modelling of the fine sediment concentration in riverine systems is of much importance to understand dynamics of suspended sediments flux and to evaluate the compliance with the European Union Water Framework Directive, the Freshwater Fish directive and the Habitats Directive. The Rivers Bandon and Owenabue located in County Cork (Ireland) are time-continuous monitored by turbidity probes. Automatic and manual suspended sediment sampling are also taken. Besides, suspended sediment rating curves have previously been studied (Harrington and Harrington 2013). The current work evaluates several models to estimate the fine sediment budget during storm based events in the Rivers Bandon and Owenabue over a period of a year using the formulation proposed by Park and Hunt (2018) as a framework, that serves for the integration of other formulations such as presented by Vansickle and Beschta (1983) and Garcia et al. (2017). A simplified application of the Krone (1962) and Partheniades (1962) models for erosion and deposition of cohesive soils is also proposed for the River Bandon. First results show good agreement between modelled and observed data as first steps to calibrate a model that will allow simulation of different scenarios with application to Irish rivers.

Materials and methods

From the data of flowrate and turbidity at 15-minutes intervals in the periods 10/02/2010 to 09/02/2011 in case of the Bandon and from 15/09/2009 to 15/09/2010 for the Owenabue the formulation proposed by Park and Hunt (2018) was applied. This is an empirical formulation that was previously evaluated for several study cases including the Rivers Bandon and Owenabue. During storm events, this is also coupled to a formulation proposed by VanSinckle and Beschta (1983), based on an exponential function for sediment output from the bed, that needs a sediment rating curve in the form of a power function according to Harrington and Harrington (2013), $SSC = aQ^b$, where constants *a* and *b* represent the linear regression of the logarithmic transformation. The formulation presented by Garcia et al. (2017) was also evaluated. This was developed originally for urban runoff during combined sewer overflows and uses statistical indeces based on linear regressions traced between suspended sediment curves and hydrograph characteristics. The Krone (1962) and Partheniades (1962) formulations are also evaluated. These are based on the shear stress on the bottom of the stream bed. Shear stress was obtained from a calibrated hydraulic model of the River Bandon (Gamble and Harrington 2016).

Results and concluding remarks

The formulations were evaluated at 15-minutes time intervals along the simulation period and results of budget of sediment supply associated to storm events are presented in Figures 1 and 2. Suspended sediment associated with dry periods was subtracted according to the Park and Hunt (2018) proposal. The formulations were adjusted to the measured data according to the empirical and statistical variables of

each formulation and in case of Krone-Partheniades a shear stress according to the hydraulic model was selected. Values modelled are in accordance with observed, as a promising first attempt to validate a model that in the future will allow characterisation for different rainfall scenarios.

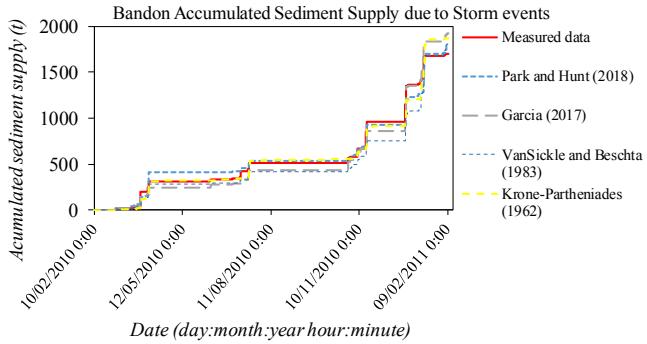

Figure 1. Accumulated sediment supply in tonnes during storm events in the river Bandon.

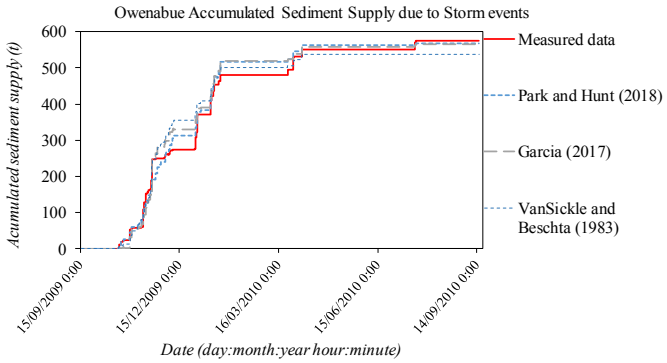

Figure 2. Accumulated sediment supply in tonnes during storm events in the river Owenabue.

Acknowledgments: The authors acknowledge the funding received through the Visiting Researchers Programme from Technical University of Cartagena UPCT, Spain in the period August to December 2018.

References

Harrington ST, Harrington JR (2012a) The influence of storm based events on the suspended sediment flux in a small scale river catchment in Ireland. Monitoring, Simulation, Prevention and Remediation of Dense and Debris Flows IV, 4, 173

Harrington JR, Harrington ST (2012b) Sediment and nutrient behaviour on the River Bandon, Ireland. River Basin Management 7:215-226

Harrington ST, Harrington JR (2014) Dissolved and particulate nutrient transport dynamics of a small Irish catchment: the River Owenabue. Hydrology and Earth System Sciences 18(6):2191-2200

Harrington ST, Harrington JR (2013) An assessment of the suspended sediment rating curve approach for load estimation on the Rivers Bandon and Owenabue, Ireland. Geomorphology 185:27-38

Park J, Hunt JR (2018) Modeling fine particle dynamics in gravel-bedded streams: storage and re-suspension of fine particles. Science of the Total Environment 634:1042-1053

Vansickle J, Beschta RL (1983) Supply-based models of suspended sediment transport in streams, Water Resour. Res. 19(3):768-778

García JT, Espín-Leal P, Vigueras-Rodriguez A, Castillo LG, Carrillo JM, Martínez-Solano PD, Nevado-Santos S (2017) Urban Runoff Characteristics in Combined Sewer Overflows (CSOs): Analysis of Storm Events in Southeastern Spain. Water 9(5):303

Krone RB (1962) Flume studies of the transport of sediment in estuarial shoaling processes, final report, Hydraul. Eng. Lab. and Sanit. Eng. Res. Lab., Univ. of Calif., Berkeley

Partheniades E (1962) A study of erosion and deposition of cohesive soils in salt water. University of California, Berkeley

Gamble J, Harrington JR (2016) Sediment Transport Modelling on the River Bandon. Civil Engineering Research Association of Ireland conference, CERI, NUI Galway, pp 631-636

11th World Congress on Water Resources and Environment (EWRA 2019)
"Managing Water Resources for a Sustainable Future", 25-29 June 2019, Madrid, Spain

Evaluation of management strategies under the WFD: Application of fuzzy ELECTRE method

L. Panagiotou, M. Spiliotis*, I. Kagalou
Department of Civil Engineering, Democritus University of Thrace, Kimmeria Campus, 67100 Xanthi, Greece
** e-mail: mspiliot@civil.duth.gr*

Introduction

It has been recognized that the continued deterioration of freshwater is not sustainable and also it has been realized that less modified freshwater ecosystems provide significant economic and social benefits to society. The largest water-related policy that exists at this moment in Europe is the Water Framework Directive 2000/60/EC (WFD, EC 2000) introducing a framework for a ''catchment - basin approach'' concerning integrated water management at a European level. WDF calls for at least Good Ecological Status (GES) in all surface waters by 2015 or, at the least, by 2027. If the ecological status is less than good, stakeholders have to apply Programme of Measures (PoMs) to manage anthropogenic pressures in order to improve ecosystem health until good status is achieved. Regarding the Greece, Kanakoudis et al. (2015) highlighted serious weak issues regarding the qualitative assessment of the RBMPs which affects the prioritization of PoMs. Furthermore, since the uncertainty in water management is clearly illustrated in the WFD (Refsgard et al. 2007) the incorporation of uncertainty methods in the planning process is considered as very important (Gottardo et al. 2011). In the context of several PoMs (alternatives) prioritization, as a part of the planning process required for the implementation of WFD is dealt in this work. Hence, a fuzzified version of the ELECTRE multicriteria method has been applied in a Mediterranean lake (Lake Pamvotis-Greece) taking into account the need of a simultaneous evaluation of heterogeneous information (biological, physico-chemical, social and economic), the need for commensurate solutions and furthermore, in order to incorporate the inherent uncertainty which appears in this kind of problems.

Materials and methods

Lake Pamvotis (NW Greece) is a shallow Mediterranean lake receiving water from karst springs, streams, and urban runoff. Substantial water quality deterioration was described during the last decades (Kagalou et al. 2003) while it's classified as "bad ecological status" in terms of WFD (Special Secretariat for Water, Hellenic Ministry of Environment and Energy 2017).

The most important pressures in the study area come from agriculture and livestock farming, housing and tourism, and hydromorphology alterations across the littoral zone. Taking into account the requirement for 'good ecological status', the current eutrophication status of the lake and the suggested PoMs included in the River Basin Management Plan (RBMP) for the entire Water District following six alternatives are modulated: *Alt.1)* Reduction of livestock waste by treatment, *Alt.2)* improvement of the inflow's water quality applying Natural Based Solution, *Alt.3)* Restoration hydraulic balance among the near by springs and the lake, *Alt.4)* Reduction of water abstractions, *Alt.5)* Improve ecosystem services, *Alt.6)* Restriction of hydromorphological alterations.

In order to describe the multi-aspects of the examined water systems, six criteria are adopted: *Cr.1)* Reach the WFD for good status, *Cr.2)* P(phosphorous)- reduction, *Cr.3)* Increase of water quality, *Cr.4)* Increase of renewal time, *Cr.5)* Economic Impact, *Cr.6*) Social Impact (the weights are equal to *0.25, 0.15, 0.15, 0.15, 0.15, 0.15* respectively). The pay-off matrix of the proposed alternatives with respect to the selected criteria is shown in Table (1). Qualitative judgments are selected to describe the scores of the criteria (negative, mild negative, average, mild satisfactory, satisfactory) which are finally evaluated as fuzzy numbers in the scale between one and five. The use of qualitative criteria and consequently, the quantification of them by using fuzzy numbers is obvious due to the complexity of the environmental problems. By supposing equal support sets and symmetrical trapezoidal numbers, the spreads themselves

easily modulate the preference thresholds of the Fuzzy ELECTRE method (e.g. Tsakiris and Spiliotis 2011).

The fuzzy ELECTRE multicriteria method is based on the binary comparison over all criteria. The main principle of the method is the concordance and non-discordance principle (Perny and Roy 1992). The fuzzy approach enables us to express the grey region of the monocriterion comparison between the alternatives and furthermore, to achieve a suitable aggregation of the monocriterion scores (Spiliotis et al. 2015). The monocriterion comparison is based on the soft preference relation as it was founded by Perny and Roy (1992). Indeed, it is obvious, that since a fuzzy evaluation of the multicriteria exists, then the multicriteria approach must incorporate the aforementioned grey region of the binary comparison. In addition, the use of the non-discordance principle leads to commensurate solutions. To simplify the decision, the scoring function is used (Tsakiris and Spiliotis 2011) in order to exploit the binary comparisons. Eventually, the scoring function takes into account all the binary comparison concluding to a score for each alternative.

Table 1. A calibration relationship between alternatives and criteria by use of fuzzy numbers

Alternatives	Cr.1	Cr.2	Cr.3	Cr.4	Cr.5	Cr.6	Scoring function
Alt.1	$\tilde{4}$	$\tilde{3}$	$\tilde{3}$	$\tilde{1}$	$\tilde{2}$	$\tilde{3}$	- 0.5833
Alt.2	$\tilde{4}$	$\tilde{5}$	$\tilde{4}$	$\tilde{3}$	$\tilde{3}$	$\tilde{4}$	+ 0.4167
Alt.3	$\tilde{4}$	$\tilde{3}$	$\tilde{3}$	$\tilde{3}$	$\tilde{2}$	$\tilde{3}$	- 0.2500
Alt.4	$\tilde{4}$	$\tilde{1}$	$\tilde{1}$	$\tilde{2}$	$\tilde{4}$	$\tilde{1}$	- 0.1667
Alt.5	$\tilde{3}$	$\tilde{3}$	$\tilde{3}$	$\tilde{5}$	$\tilde{4}$	$\tilde{5}$	+ 0.3333
Alt.6	$\tilde{4}$	$\tilde{3}$	$\tilde{3}$	$\tilde{5}$	$\tilde{2}$	$\tilde{4}$	+ 0.2500

Results and concluding remarks

Based on the scoring function, the *Alt.2* is promised and secondly the *Alt. 5.* The results seem reasonable since the second alternative has a high score regarding the first primary criterion and secondly it is characterized from a balanced evaluation of the other criteria. Indeed, the “improvement of the inflow's water quality applying Natural Based Solution” has mild impacts to the economy and the society whist it has positive impacts to the other criteria (Table 1). The *Alt.5* has also a very balanced evaluation among the criteria.

Based on the previous, it can be concluded that the developed Fuzzy ELECTRE method is suitable for environmental problems, since it incorporates the inherent uncertainty of the environmental problems, and moreover, the non-discordance principle can lead to commensurate and more environmentally, economically and societal sustainable decisions.

References

Kagalou I, Papastergiadou E, Tsimarakis G, Petridis D (2003) Evaluation of the trophic state of Lake Pamvotis Greece, a shallow urban lake. Hydrobiologia 506(1-3):745–752. https://doi.org/10.1023/B:HYDR.0000008603.69847.9e

Kanakoudis V, Tsitsifli S, Azariadi T (2015) Overview of the River Basin Management Plans developed in Greece under the context of the Water Framework Directive 2000/60/EC focusing at the economic analysis. Water Resour. Manag. 29(9):3149-3174. https://doi.org/10.1007/s11269-015-0988-9

Gottardo S, Semenzin E, Giove S, Zabeo A, Critto A, de Zwart D, Ginebreda A, von der Ohe PC, Marcomini A (2011) Integrated risk assessment for WFD ecological status classification applied to Llobregat river basin (Spain). Part I—Fuzzy approach to aggregate biological indicators. Science of the Total Environment 409:4701–4712. https://doi.org/10.1016/j.scitotenv.2011.07.052

Perny P, Roy B (1992) The use of fuzzy outranking relations in preference modeling. Fuzzy Sets and Systems 49:33- 53. https://doi.org/10.1016/0165-0114(92)90108-G

Refsgaard JC, van der Sluijs JP, Hojberg AL, Vanrolleghem A (2007) Uncertainty in the environmental modelling process-a framework and guidance. Environ Modell Soft 22:1543–1556. doi: 10.1016/j.envost.2007.02.004

Special Secretariat for Water, Hellenic Ministry of Environment and Energy (2017) http://wfdver.ypeka.gr/en/management-plan

Spiliotis M, Martín-Carrasco F, Garrote L (2015) A fuzzy multicriteria categorization of water scarcity in complex water resources systems. Water Resour Manag 29(2):521–539. https://doi.org/10.1007/s11269-014-0792-y

Tsakiris G, Spiliotis M (2011) Planning Against Long Term Water Scarcity: A Fuzzy Multicriteria Approach. Water Resour. Manag. 25:1103–1129. http://doi 10.1007/s11269-010-9692-y

11th World Congress on Water Resources and Environment (EWRA 2019)
"Managing Water Resources for a Sustainable Future", 25-29 June 2019, Madrid, Spain

The environmental impacts of flow regulation in Spain

S. García de Jalón[1*], M. González del Tánago[2], D. García de Jalón[2]
[1] Basque Centre for Climate Change – BC3. Building 1, 1st floor, Scientific Campus of the University of the Basque Country. Barrio Sarriena, s/n, 48940 Leioa, Spain
[2] Department of Natural Resources and Systems, Universidad Politécnica de Madrid, E.T.S.I. Montes, Forestal y del Medio Natural, 28040, Madrid, Spain
* e-mail: silvestre.garciadejalon@bc3research.org

Introduction

Water available for irrigation, hydroelectric production and urban or industrial supplies frequently requires flow regulation by dams and reservoirs which alters natural patterns of flow regimes and severely affects river ecosystems. At present, more than two thirds of river discharge that flows across the world is obstructed by more than 40,000 large dams. Vörösmarty et al. (2003) estimated that more than 50% of the sediment flow produced in watersheds is trapped in artificial reservoirs. Nilsson et al. (2005) found that the flow of water from reservoirs and reservoirs was one of the most frequent sources of environmental impacts in rivers (Poff et al. 2007).

This study presents an approach to assess the environmental impact of flow regulation based on the intensity of the hydrological alteration of the natural flow regime. We propose a dynamic approach that is determined by the hydrologic alteration that the river suffers at every time instant (changes in river flow due to flow regulation) in the Spanish rivers.

Materials and methods

This study uses daily flow data from river gauging stations in Spain. The requirements for selecting the river gauging stations were that there had to be continuous daily flow data available for more than 10 years before the construction of the dam and for the considered post-dam operation period. Monitoring stations that met these requirements within the Spanish basins were selected (http://ceh-flumen64.cedex.es/anuarioaforos). The method developed for the assessment of flow regulation impact caused by large reservoirs follows three main steps:

The first step was to define the admissible range of flow variability under natural flow regimes. This range was calculated by using data from the non-regulated period (pre-dam) for each river.

The second step measured the environmental impact of flow regulation according to the inferred hydrological alteration (changes in magnitude, timing and duration of flows). This was calculated by quantifying differences between current circulating flows and their admissible range of variability (see García de Jalón et al. 2017a for further information). The environmental impact was calculated for each day during the evaluated post-impact period as the divergence between the current circulating flows and the reference admissible flow variability. Thereby the estimated environmental impact could be due to either discharges higher than the upper limit of the admissible area (high-flow impact) or discharges lower than the lower limit (low-flow impact). In the assessment, not only changes in the magnitude and timing of flows but also flow duration are considered. Both calculations, the admissible range of flow variability based on pre-dam data and the environmental impact of flow regulation based on post-dam data, were calculated using the R package 'FlowRegEnvCost' (García de Jalón et al. 2017b).

The third step classified the river reaches into groups, or 'clusters', that were internally homogeneous (i.e., the environmental impacts in each cluster were 'closely related'). The estimated admissible range of flows in natural regimes (pre-dam period) and flow impacts during the post-dam period were separately classified using a hierarchical cluster analysis technique (MacQueen 1967; Anderberg 1973). The identified groups of patterns of flow variability and flow regulation impacts were compared and characterized according to differences in hydrologic regime (i.e., magnitude, duration and seasonality of the impact) and main water use. Several statistical tests (MANOVA, ANOVA and Tukey's HSD tests) were used to test

whether admissible ranges of flow variability and low-flow and high-flow impacts differed among the river basins and among the identified clusters.

Results and concluding remarks

This study shows that the estimated admissible range of flow variability under natural flow regimes considerably varies among regulated rivers in Spain. However, in most rivers the admissible range is generally broad from late October to early June and very narrow from July to September. This pattern is characteristic of Mediterranean basins, where precipitation can be highly variable between late autumn and late spring and is very low during summer (de Luis et al. 2010; Deitch et al. 2017).

From the hierarchal cluster analysis, the calculated dendrograms and scree plots illustrate that three main clusters or rivers can be identified in relation to the estimated daily flow regulation impacts in the post-dam period. The first identified cluster was named 'constant low-intensity' and includes rivers in which both low-flow and high-flow impacts are typically not very large in magnitude, or if they are large, then the duration and the frequency of the impact is relatively short. Although they can be produced at any time of the year, high-flow impacts are often produced from July to early September, and low-flow impacts occur during the rest of the year. The second cluster was named 'seasonal'. In those rivers, there is a clear difference between the months with high-flow impacts and the months with low-flow impacts. During the summer months, high-flow impacts are rather strong, and low-flow impacts are produced very rarely. The period of high-flow impacts is notably longer in rivers with 'constant low-intensity' impacts and usually lasts from late June to late October. The last cluster was named 'constant high-intensity'. This cluster is a combination of 'constant low-intensity' and 'seasonal' rivers. Low-flow impacts can be produced at any time of the year; nevertheless, they are typically generated between late September and June. High-flow and low-flow impacts are relatively strong from November to April and from July to August, respectively.

Overall the study demonstrates that the proposed approach can be useful for regionalizing natural flow regimes of different river types as a first step to guide environmental flow standards. The approach also allows the identification of differences in the magnitude of hydrological impacts, which can be translated to environmental costs in monetary terms. The methodology offers a new spare-parameter approach of assessing hydrological impacts of flow regulation that better responds to the requirements of the Water Framework Directive and should be tested in other regions.

References

Anderberg MR (1973) Cluster Analysis for Applications. Probability and Mathematical Statistics. Academic Press, Inc.

de Luis M, Brunetti M, Gonzalez-Hidalgo JC, Longares, LA, Martin-Vide J (2010) Changes in seasonal precipitation in the Iberian Peninsula during 1946–2005. Global Planet. Change 74(1):27-33

Deitch, MJ, Sapundjieff MJ, Feirer ST (2017) Characterizing precipitation variability and trends in the world's Mediterranean-Climate areas. Water 9(4):259

García de Jalón S, González del Tánago M, Alonso C, García de Jalón D (2017a) The environmental costs of water flow regulation: an innovative approach based on the 'polluter pays' principle. Water Resources Management 31(9):2809–2822

García de Jalón S, Martínez-López J, González del Tánago M, Alonso C, García de Jalón D (2017b) FlowRegEnvCost: The Environmental Costs of Flow Regulation. R package version 0.1.1. Available at: https://cran.r-project.org/web/packages/FlowRegEnvCost/index.html, and https://github.com/garciadejalon/FlowRegEnvCost

MacQueen JB (1967) Some Methods for classification and Analysis of Multivariate Observations. Proceedings of 5th Berkeley Symposium on Mathematical Statistics and Probability. 1. University of California Press, pp 281–297

Nilsson C, Reidy CA, Dynesius M, Revenga C (2005) Fragmentation and flow regulation of the world's large river systems. Science 308(5720):405-408

Poff NL, Olden JD, Merrit DM, Pepin DM (2007) Homogenization of regional river dynamics by dams and global biodiversity implications. PNAS 104(14):5732-5737

Vörösmarty CJ, Meybeck M, Fekete B, Sharma K, Green P, Syvitski JP (2003) Anthropogenic sediment retention: major global impact from registered river impoundments. Global and Planetary Change 39:169–190

11th World Congress on Water Resources and Environment (EWRA 2019)
"Managing Water Resources for a Sustainable Future", 25-29 June 2019, Madrid, Spain

Assessment of bedload transport in sand-gravel bed rivers by using nonlinear fuzzy regression

M. Saridakis, M. Spiliotis, V. Hrissanthou*
Department of Civil Engineering, Democritus University of Thrace, Kimmeria Campus, 67100 Xanthi, Greece
** e-mail: vhrissan@civil.duth.gr*

Introduction

When a channel's sediment transport capacity exceeds the rate of sediment supply from upstream, the channel starts to degrade. Because of the nonuniformity of the bed material size, finer materials will be transported at a faster rate than the coarser materials, and the remaining bed material will become coarser. This coarsening process will stop once a layer of coarse material completely covers the streambed and protects the finer materials beneath it from being transported. After this process is completed, the streambed is armored and the coarser layer is called the armor layer (Yang 1996). Three phases, regarding the stability of the armor layer, can be distinguished: During phase 1, bed load composed of fine sediments supplied from upstream passes over the immobile armor layer. Phase 2 designates the breakup of the armor layer; during this phase, coarse grains can participate in transport and the availability of fine sediments from the subsurface is increased. During phase 3, all grain sizes are in motion (Recking 2010). All three phases depend on the value of the stream discharge. Because of the nonlinearity of the dependence of the sediment transport rate on the stream discharge, as well as because of the inherent uncertainties in the sediment transport phenomenon generally, an attempt is made in this study to approach the above three phases of the armor layer evolution by means of the nonlinear fuzzy regression.

Materials and methods

The uncertainties in sediment transport prediction arise from the role of turbulence in sediment entrainment (Spiliotis and Hrissanthou 2018), the inadequate data, the difficulties during the sediment transport measurements and the complexity of the phenomenon itself. In addition, in sand-gravel bed rivers, the breakup of the bed armor layer complicates the prediction and moreover leads to a significant nonlinear behaviour (Spiliotis et al. 2017). For these reasons, a nonlinear fuzzy regression is implemented to achieve a fuzzy relation between the sediment transport rate and stream discharge.

First of all, in case of polynomial form, a fuzzy linear regression formulation can be obtained by substituting some nonlinear terms with auxiliary variables. This approach holds only in case that the independent variables are crisp numbers. Therefore, the nonlinear fuzzy regression can conclude to a fuzzy linear regression problem with many variables.

Next, the fuzzy linear regression of Tanaka (1987) is used. In general, the fuzzy regression analysis gives a fuzzy functional relationship between the dependent and independent variables (Papadopoulos and Sirpi 1999; Tsakiris et al. 2006). In contrast to the statistical regression, the fuzzy regression model of Tanaka (1987) has no error term, while the uncertainty is incorporated in the model with the use of fuzzy numbers (Spiliotis and Hrissanthou 2018). The data of the fuzzy regression can be either fuzzy or crisp. Usually, the data are rather crisp numbers (observed data), and thus, the uncertainty arises from the used fuzzy model, that is, the fuzzy coefficients.

The inclusion property of the produced fuzzy band, that is, the requirement that all the data must be included within the produced fuzzy band creates the constraints. Additional constraints can be added, for instance, in order to avoid negative values, which, in our case, have no physical meaning.

Results and concluding remarks

Two cases will be presented in this work. The first one is the Blackmare Creek, located in the State of Idaho, USA. The second case is the Little Buckhorn Creek, which also is located in the State of Idaho, USA.

The results are shown in Figure 1. As it can be seen from Figure 1, all the data are included within the produced fuzzy band. For illustrative purposes, the fuzzy relation regarding the bed load transport rate in Little Buckhorn Creek is listed:

$$\tilde{m}_{G,j} = -0.5679 \cdot Q_j^4 + (0.7039, 0.0245) \cdot Q_j^3 - 0.2027 \cdot Q_j^2 + 0.0222 \cdot Q_j + (-0.0003, 0.0004) \quad (1)$$

where m_G [kg/(s·m)] is the bed load transport rate and Q (m^3/s) represents the stream discharge. The brackets in Equation (1) represent fuzzy symmetrical triangular numbers. The first term in the brackets symbolizes the central value and the second term the semi-spread. An interesting perspective is that, as it can be seen from Equation (1), some coefficients appear without uncertainty.

In a similar manner with the crisp polynomial regression, we should avoid either the overtraining (by considering a high polynomial order) or the undertraining (by considering a low polynomial order). In both cases, the linear model is unsuitable. For instance, in the second case, it is concluded that, even if the addition of a polynomial term reduces the uncertainty, incompatible results with the physical process are produced (overtraining).

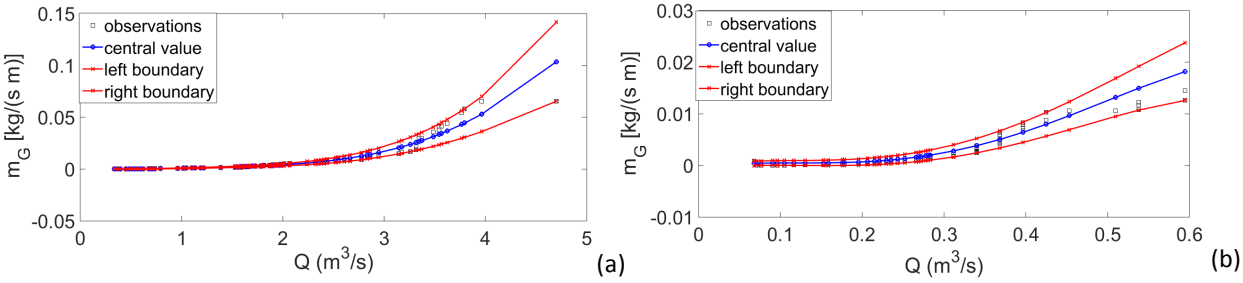

Figure 1. Graphical representation of the fuzzy polynomial regression for the bed load transport rate m_G [kg/(s m)] with respect to the stream discharge Q (m^3/s), for (a) Blackmare Creek, (b) Buckhorn Creek.

An interesting point of view is that, as it seems from Figure 1, three regions can be distinguished. The first and the third regions have an absolutely different behaviour. In the first region, the uncertainties are not significant, whilst the bed load transport rate is rather constant and not important. In the third region, the uncertainty is significant, whilst the bed load transport rate increases rapidly since all grain sizes are in motion. Between the two regions, the region 2 with mild uncertainty corresponds to the breakup of the armor layer.

References

Kitsikoudis V, Spiliotis M, Hrissanthou V (2016) Fuzzy regression analysis for sediment incipient motion under turbulent flow conditions. Environmental Processes 3(3):663–679. https://doi.org/10.1007/s40710-016-0154-2

Papadopoulos B, Sirpi M (2004) Similarities and distances in fuzzy regression modeling. Soft Computing 8(8):556–561. https://doi.org/10.1007/s00500-003-0314-y

Recking A (2010) A comparison between flume and field bed load transport data and consequences for surface-based bed load transport prediction. Water Resources Research 46:W03518. doi: 10.1029/2009WR008007

Spiliotis M, Hrissanthou V (2018) Fuzzy and crisp regression analysis between sediment transport rates and stream discharge in the case of two basins in northeastern Greece. In: Hrissanthou V and Spiliotis M (eds), Conventional and Fuzzy Regression: Theory and Engineering Applications; Nova Science Publishers: New York, USA, pp 2-49

Spiliotis M, Kitsikoudis V, Hrissanthou V (2017) Assessment of bedload transport in gravel-bed rivers with a new fuzzy adaptive regression. European Water 57:237–244

Tanaka H (1987) Fuzzy data analysis by possibilistic linear models. Fuzzy Sets and Systems 24:363-375. https://doi.org/10.1016/0377-2217(89)90431-1

Tsakiris G, Tigkas D, Spiliotis M (2006) Assessment of interconnection between two adjacent watersheds using deterministic and fuzzy approaches. European Water 15/16:15-22

Yang CT (1996) Sediment Transport: Theory and Practice. McGraw-Hill

11th World Congress on Water Resources and Environment (EWRA 2019)
"Managing Water Resources for a Sustainable Future", 25-29 June 2019, Madrid, Spain

Understanding the behaviour of sandbars of River Brahmaputra and its utilization

G. Talukdar*, A. Kumar Sarma
Civil Engineering Department, Indian Institute of Technology Guwahati, Guwahati, India
** e-mail: gauravtalukdar01@gmail.com*

Introduction

The Brahmaputra River, originating from the Mansarovar Lake in the northern Himalayas is governed by its high discharge, catastrophic flooding and dynamic nature flowing through China, India and Bangladesh. The river is braided with varying morphology and has meandering course in the plains with frequent formation of sandbars. The dwellers residing in the floodplains rely on the normal flood which brings fresh sediments to the floodplains favouring agriculture and farming. The river has been widening and changing its cross section with slow migration with time (Gilfellon et al. 2003). The morphodynamic behaviour of rivers in terms of planform and land use change is crucial and land use changes affects various processes like the ecological activities, sedimentation and erosion processes.

River sandbars are an important habitat for various species of birds, fishes and reptiles. The sandbars of Brahmaputra River have been utilized for various human activities like farming, cropping, pottery making, mask making etc. for their livelihood. These are some of the prime sources of income for the people residing near the river. Hence, optimally utilizing the ecosystem is of great importance, so that the river is not exploited causing adverse effects in the near future and achieve maximum benefit from it. In Large Rivers like Brahmaputra, the water level rises and drops depending upon the weather and climatic conditions throughout the whole season. During June-September, the river experiences severe flooding while during the months of January-May, the water level recedes exposing the vast areas of sandbars. Henceforth, to optimally utilize these sandbars, a study of the entire reach is necessary, so as to also understand the changes this gigantic river exhibits. Thus, a hydrodynamic model study is required to simulate different flows during different time period all through the year. The use of 1D and 2D models was intensified and broadened in the 1970s and later. MIKE 21C model was developed for simulating the 2D flows and morphological changes in rivers (Morianou et al. 2016). Geoinformatics study will be helpful in understanding the changing course of the river. Combining the knowledge derived from both studies, the objective is to optimally utilize the Riverine ecosystem in such a way that it benefits the dwellers who depend on it, as well as the socioeconomic development of the society.

Materials and method

The bed forms of the river Brahmaputra keeps on changing and to study these spatiotemporal changes as well as prior to the application of the model, an understanding about the bed forms, deposition and movement is necessary. Hence, for the study, Landsat MSS and TM, Google imagery and LISS IV imageries (2018) have been used. From the imagery (Figure 1), it can be seen that there is formation of a sandbar which is unutilized and barren, and through proper study and field surveys, it can be utilized for various beneficiary activities favouring upliftment of the poor.

In view of the model development, the bathymetry of the river is essential and hence a field survey within a certain river reach of 11 km is carried out. The hydrodynamic model, MIKE 21C (DHI M 2011) was applied and simulated for the conditions representing different seasons. The computational grid is extended over the entire reach and the boundary conditions are specified at the upstream and downstream portion.

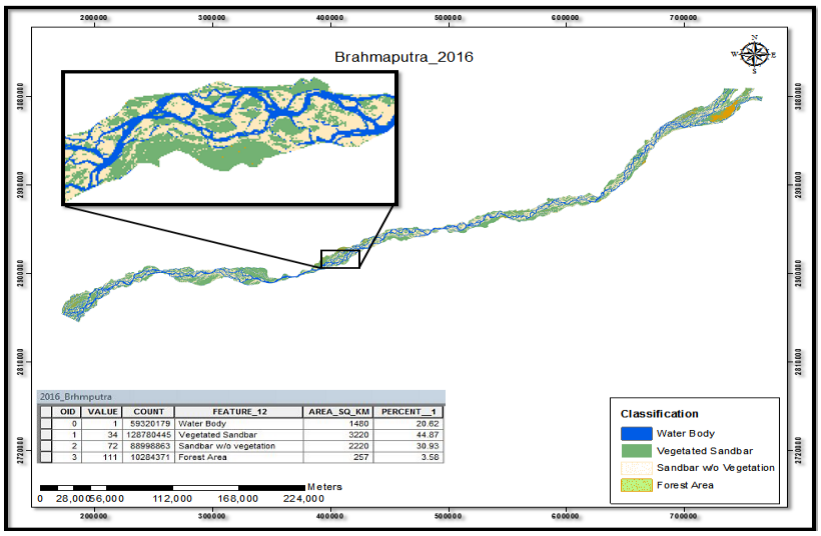

Figure 1. Classification depicting vegetated and non-vegetated sandbars

Results and concluding remarks

Three different scenarios were taken into account over the surveyed reach of the Brahmaputra River to understand the flow variations for the entire season, i.e., low, medium and high flow in the months of February, May and July, respectively.

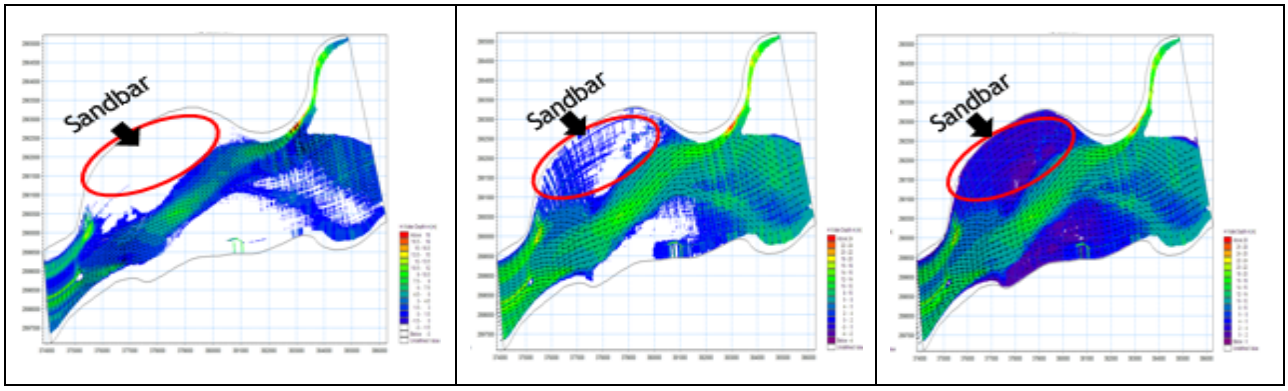

Figure 2. Simulated water depth for low, medium and high flow using MIKE 21C

Observations from the model study (Figure 2) shows that the area of sandbar is completely submerged during the high flow period (July) and exposed during the low flow period (February). Hence, a notable observation from the study is that after the flood recedes during the month of October, there is a time span of around 7 months until the next flood. Thus, the exposed sandbars of the entire River can be utilized in an optimal way within this time. Interestingly, classifications done along with the geoinformatics study has proved that there has been traces of activities carried out in the sandbars of River Brahmaputra. While observing the sandbar utilization from 1976 – 2016, it has been found that the vegetated sandbar has an increasing trend comparative to sandbar without vegetation. However, whether these actvities are optimally carried out or what other actvities are favourable under those conditions, are of interest and needs to be studied.

References

DHI M (2011) A Modelling System for Rivers and Channels. Reference Manual. DHI Water & Environment, Denmark

Gilfellon GB, Sarma JN, Gohain K (2003) Channel and bed morphology of a part of the Brahmaputra River in Assam. Journal-Geological Society of India 62(2):227-236

Morianou GG, Kourgialas NN, Karatzas GP, Nikolaidis NP (2016) Hydraulic and sediment transport simulation of Koiliaris River using the MIKE 21C model. Proceedia Engineering 162:463-470

11th World Congress on Water Resources and Environment (EWRA 2019)
"Managing Water Resources for a Sustainable Future", 25-29 June 2019, Madrid, Spain

The role of soil moisture and vegetation cover on biomass growth in water-limited environments

J. Lozano-Parra[1*], S. Schnabel[2], M. Pulido[2], Á. Gómez-Gutiérrez[2], J.F. Lavado-Contador[2]
[1] Instituto de Geografía, Pontificia Universidad Católica de Chile, Santiago, Chile
[2] Research Institute for Sustainable Land Development, University of Extremadura, Cáceres, Spain
* e-mail: jlozano@outlook.es

Introduction

Soil water directly affects biomass production and food security, particularly in ecosystems conditioned by water availability. Nevertheless, close to half of the global surface is composed of arid, semiarid, and dry subhumid lands. Improved knowledge of feedbacks between ecohydrological processes, such as those occurred between soil moisture and spatiotemporal variations of biomass growth, would enable better decisions-making and contribute to the sustainability of these ecosystems.

The development of herbaceous plants depends on the balance of positive and negative effects of limiting factors, such as water, light, temperature, nutrients, and space (Callaway 2007). Nevertheless, because of the characteristics of the Mediterranean climate and the configuration of the landscape, such factors present a high variability that influences the phenology and productivity of natural grasses. Despite this, the use of large-scale soil water measurements and its relationships with climate, vegetation and biomass production under natural conditions is still infrequent. Furthermore, soil moisture measurements have been largely neglected to carry out drought monitoring and its use is scarce. The objective of this study was to define the response and sensitivity of annual pastures to soil water availability under the influence of two vegetation covers and during two contrasting growing seasons, wet and dry. The study was conducted in 3 privately owned farms located in Spain. They were selected because are representative of savanna-like rangeland with a Mediterranean climate, consisting of grasslands with scattered tree cover that result from tree clearing and livestock grazing.

Materials and methods

Soil water content was monitored by means of capacitance sensors which continuously registered with a temporal resolution of 30 minutes during two complete hydrological years (from 2010 to 2012). They were installed at 5, 10 and 15 cm, and the fourth sensor was installed 5 cm above the bedrock depending on soil thickness. The sensors were gathered in Soil Moisture Stations (SMS) in two main contrasting situations: open spaces (Grassland) and below tree canopies (Tree). A total of 12 SMS were installed and distributed between the 3 study areas representative of savanna-like rangeland with a Mediterranean climate. Pasture production and growth were recorded by biomass cuts and by manual measurements of its height, respectively. Soil hydrological properties were determined by the porous medium method and the pressure membrane. An agricultural drought index was calculated in order to determine the soil water deficit index (SWDI) of each SMS as described by Lozano-Parra et al. (2018). Climate variables were continuously measured with a 5 min resolution by meteorological instruments installed in the three study areas. They were used to calculate the reference evapotranspiration (ETo) at daily scale for each site. The data mining technique Multivariate Adaptive Regression Spline was used to modelling the growing of pastures and to identify and rank the factors influencing in its growth.

Results and concluding remarks

This study highlights the importance of the near-surface soil layer (i.e. the one located in the upper 15 cm of the soil profile) for ecohydrological processes and as the main zone for water supply to annual pastures. This layer was more decisive than deeper ones as a water resource for pastures, since was able to satisfy the water demand during the growing season. Soil water deficits were longer and more intense

beneath the tree canopies than in grasslands, and this situation was more pronounced during drier environmental conditions. Severe or extreme soil water deficits in the upper soil layer during the growing season may suppose a yield decrease >40% compared to years when water is not a limiting factor (Figure 1), being this decrease greater beneath the tree canopies (>50%) than in grasslands. Statistical analysis proved that factors affecting plant growth were different between dry and wet growing seasons. Under drier conditions, the influence of the water balance at short-term on pasture growth was more noticeable than under wet conditions. Precipitation inputs played a key role because relative losses of soil moisture due to evapotranspiration were greater than in wet situations. The influence of vegetation covers on pasture growth was more prominent during dry stages, presumably because rainfall interception by trees is greater during dry periods.

Savanna-like rangelands usually present a canopy cover between 21-40% and occupy important extensions (about 3 million ha in Spain and Portugal, 4 million ha in California and significant extensions in other areas, such as South Africa, Australia or Chile). If dry episodes become more frequent in the present century due to climate change, important surface, especially under trees, could become drier, less productive, and therefore more prone to land degradation.

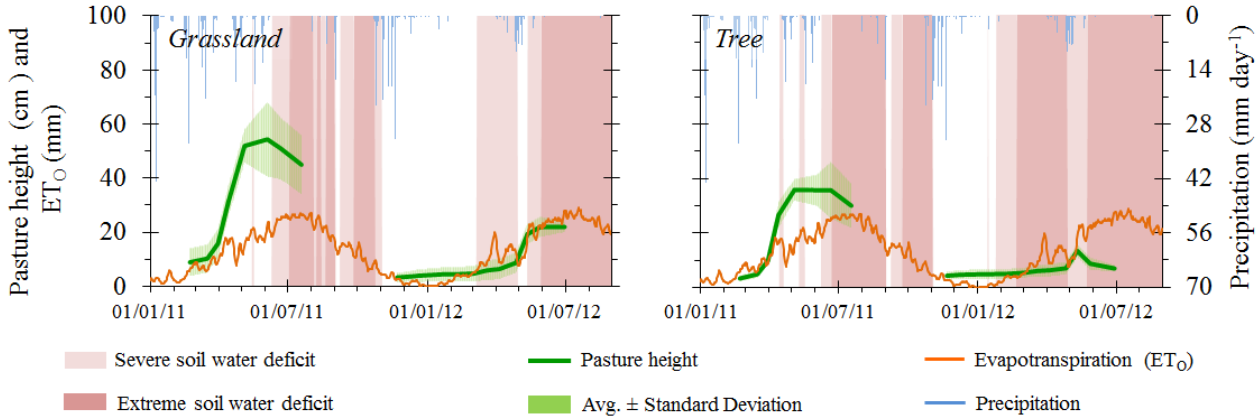

Figure 1. Aboveground pasture growth (cm) under the influence of two vegetation covers, tree and grassland, during two contrasting hydrological years (2010-11 and 2011-12). Shades represent different values for soil water deficit index (SWDI) in surface (first 15 cm). The clearest depicts severe agricultural drought and the darkest depicts extreme agricultural drought. Orange line depicts the reference evapotranspiration (mm) calculated as a 5 days sum.

Acknowledgments: This research was funded by the Fondo Nacional de Desarrollo Científico y Tecnológico [CONICYT/FONDECYT 11161097] and by the Programa de Cooperación Internacional para la Formación de Redes Internacionales de Investigación [REDI170640], both granted by the Government of Chile.

References

Callaway RM (2007) Positive interactions and interdependence in plant communities. Springer, The Netherlands

Lozano-Parra J, Schnabel S, Pulido M, Gómez-Gutiérrez Á, Lavado-Contador JF (2018) Effects of soil moisture and vegetation cover on biomass growth in water-limited environments. Land Degradation and Development 29(12):4405-4414. https://doi.org/10.1002/ldr.3193

11th World Congress on Water Resources and Environment (EWRA 2019)
"Managing Water Resources for a Sustainable Future", 25-29 June 2019, Madrid, Spain

The river continuum theory in the high-mountain tropical Andes

J.J. Vélez[1*], L.A. Galindo-Leva[2], A. Londoño[3], B. Guzman[2], M.F. Ocampo[3], E. Jiménez[2]
[1] Civil Engineering Department, Universidad Nacional de Colombia Sede Manizales, Manizales, Colombia
[2] Engineering and Architecture Faculty, Universidad Nacional de Colombia Sede Manizales, Manizales, Colombia
[3] Chemical Engineering Department, Universidad Nacional de Colombia Sede Manizales, Manizales, Colombia
* e-mail: jjvelezu@unal.edu.co

Introduction

The river continuum theory is based on the concept of dynamic equilibrium, in which stream forms are balanced between physical parameters, width, depth, velocity, physical-chemical parameters, sediment transport, and biological factors. The characterization of the case study at Rioclaro River is intended to determine the dynamics of hydrobiological continuity throughout the three main zones of the river, the upper, middle and lower zones, before it discharges into the Chinchiná River. Each zone has variant characteristics but is embraced within the same river system. Different factors must be studied in each zone, such as climate, geology, topography, vegetation, channel physiognomy, natural and anthropic disturbance types and intensities, and the quantity and quality of its water. The intention of this investigation is to determine the dynamics of hydrobiological continuity along the Rioclaro River, a high-mountain river located in the Colombian Andes. The Rioclaro River has rarely been anthropically examined, and has neither been characterized within regional Chinchiná River studies, nor the investigations carried out by environmental authorities for basin planning and management (POMCA of the Chinchiná River). It is concluded that continuum river theory has been proven in high-mountain tropical Andes Rivers.

Materials and methods

The Rioclaro river basin has an area of 244.58 km², and is located on the western slopes of Nevado Santa Isabel. It forms part of those areas under the paramo and Los Nevados National Park jurisdiction. The water resource contributes approximately 48% of its average flow, at the mouth, to the Chinchiná River, which is directly related to extraordinary wetland richness, and corresponds to 60% of wetland extension in the entirety of the Chinchiná River Basin.

The proposed methodology is carried out in accordance with the previously established objectives:

- A database with secondary information will be obtained as a baseline for current characteristics, so as to compare them with other currents.
- Monitoring campaigns will be performed, in order to obtain sediment and biota and physical-chemical river characteristics in four locations along the river: two in the upper, one in the middle, and one in the lower zone.
- In order to establish the continuum river concept in these three zones (high, medium, and low), secondary information and collected data will be employed, which observe the relationship between biota and abiotic variables, such as climate.

Results and concluding remarks

Discharge was between 0.039 m³/s and 4.2 m³/s, with good solid transport along the channel. Water temperature was between 7 °C and 23 °C, had sufficient oxygenation, between 5.5 and 8 mg O_2/l., a good distribution of macronutrients, as well as metal contributions, both in sediments and water, which reflects the impact of volcanic fluids.

Two integrated samplings were taken at four sites in the basin, so as to simultaneously assess physical variables (topography, channel morphology, discharge, sediment load) and physical-chemical conditions, such as dissolved oxygen, turbidity, pH, and conductivity, among other characteristics, including certain metals and biotic aspects, such as trophic functional groups, abundance, and richness, and aspects of

tolerance of contamination of aquatic macroinvertebrate communities.

The characterization of the Rioclaro River shows a longitudinal succession of functional macroinvertebrates groups, in the three main zones of the Rioclaro River, the upper zone or headland, middle, and the low zone, which is concordant with the continuum river concept (Vannote et al. 1980).

According to the results found for Rioclaro, the most significant biotic variable correlations were presented, with respect to flow, as expected. Brooks et al. (2005) argues that flow is correlated with many river physical-chemical characteristics, including water temperature, channel geomorphology, and habitat diversity, and therefore, is considered a key variable that limits the distribution and abundance of the aquatic biome, and regulates the ecological integrity of lotic systems. Flow results are based on the fact that small-scale differences in hydraulic conditions, created by combinations of water velocity, depth, and substrate roughness, determine habitat heterogeneity, and as such, play an important role in the spatial distribution of macroinvertebrate assemblages.

Data have been reported regarding the shortage or absence of shredders in the tropical zones of Neotropical systems. Similarly, there is information available which details microbial activity in leaf processing in Malaysian rivers, due to the near absence of these invertebrates (Wantzen and Wagner 2006). However, in a recent study of Colombia (Quindío), Chara-Serna et al. (2011) identified that the community of aquatic insects in streams of the La Vieja River Basin is composed mainly of collectors and crushers. These are the groups with the largest number of individuals, and which account for 86% of the population, which coincides with the results obtained for Rioclaro. This result confirms the importance of leaf litter, or coarse particulate organic matter, as a food resource for the insect community studied, and therefore, as a source of energy in these aquatic environments.

Perhaps the most relevant conclusion of the present investigation is the importance of having a baseline for the implementation of future climate change studies. This allows for the proposal of adequate adaptation strategies for high-mountain tropical rivers. Further, Rioclaro River shows a longitudinal succession of functional groups, which is concordant with the concept of the river as a continuum. The ecological continuity found in Rioclaro demonstrates a low level of alteration, which reflects a healthy river. Additionally, integrated sampling made it possible to characterize the river, as demonstrated by the excellent indicators of quantity, quality, sediments, and biota that were collected during the monitoring campaigns. It is important to highlight that minimal anthropic intervention was achieved for this high-mountain Andean River.

Acknowledgments: We would like to especially thank the Universidad Nacional de Colombia Sede Manizales (UNAL) research office (DIMA) for supporting this study, throughout the project entitled “Caracterización hidrológica de un río de montaña andino poco intervenido para Línea Base en el marco del Cambio Climático”. Additionally, we recognize IDEA UNAL for having supplied data.

References

Brooks JR, HR Barnard, R Coulombe, JJ McDonnell (2010) Ecohydrologic separation of water between trees and streams in a Mediterranean climate, Nat. Geosci. 3(2):100–104. doi: 10.1038/ngeo722

Chará-Serna, AC Encalada, JN Davies, S Lamothe, A Cornejo, AOY Li, LM Buria, VD Villanueva, M.C Zúñiga, CM Pringle (2011) Global Distribution of a Key Trophic Guild Contrasts with Common Latitudinal Diversity Patterns. Ecology 92(9):1839-1848

Vannote RL Minshal GW, Cummins KW, Sedell KR, Cushing CE. (1980) The River Continuum Concept. Can. J. Fish. Aquat. Sci. 37:130-137. https://doi.org/10.1139/f80-017

Wantzen KM, R Wagner (2006) Detritus Processing by Invertebrate Shredders: a Neotropical–Temperate Comparison. Journal of the North American Benthological Society 25(1):216-232

11th World Congress on Water Resources and Environment (EWRA 2019)
"Managing Water Resources for a Sustainable Future", 25-29 June 2019, Madrid, Spain

Bilbao city ICMLive flood early-warning and monitoring system

P. Batanero[1*], E. Martinez[1], I. Martinez[2]
[1] Innovyze, Madrid, Spain
[2] INECO, Madrid, Spain
* e-mail: paloma.batanero@gmail.com

Introduction

The city of Bilbao is located in a high-risk flooding area, at the end of a very fast and steep catchment (Nervión-Ibaizábal River), under the direct influence of the Cantabrian Sea tidal levels.

Over the last 50 years there have been several flood events, the most serious occurred in 1983, which resulted in great economic and personal losses for the city. Since then, Bilbao has been searching for an effective tool to prevent and be aware in advance of this kind of incidents.

In recent years, technology has reached a development point where it is possible to effectively monitor and simulate the hydraulic condition of Bilbao. This paper presents the new Flood Early-Warning and Monitoring System that has been developed under the lead of Bilbao City Council. It will serve as a powerful Decision Support System and enable a better flood risk management for the City Crisis Committee. This project has been a 3-year process which involved many parties within public and private sectors, being a great example of mutual collaboration and team.

Materials and methods

Figure 1 shows an aerial view of Bilbao urban area, where the Nervión-Ibaizábal channel is indicated on its way, which crosses the whole city: from Southeast to Northwest, towards its coastal outlet.

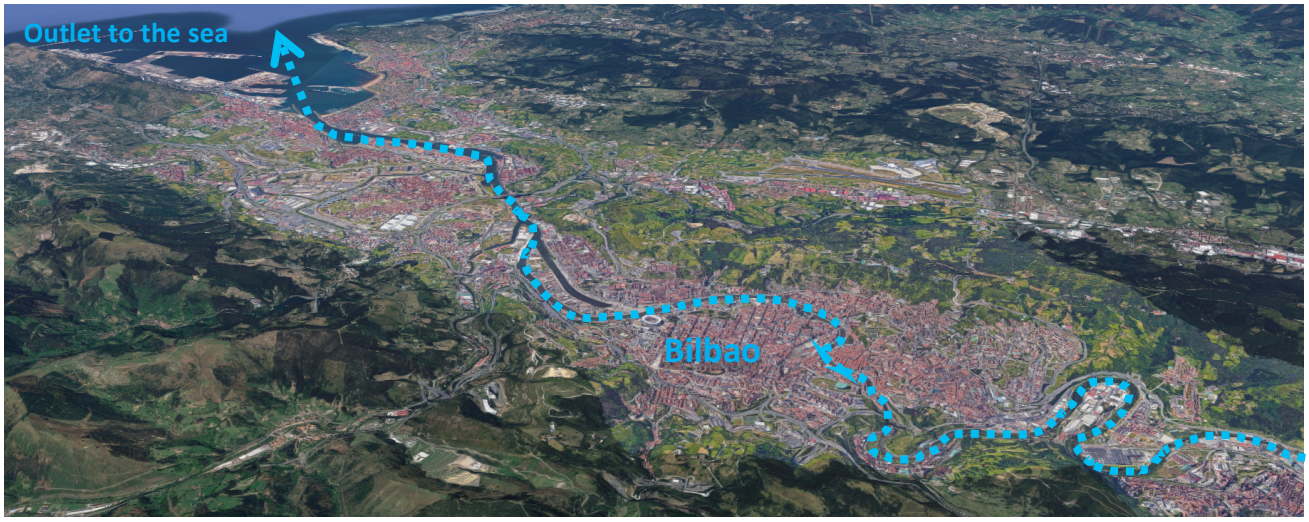

Figure 1. Aerial view of the urban area: Nervión-Ibaizábal path along the city towards the Cantabrian Sea.

Since the great flood of August 1983, Bilbao has felt exposed to the harshness of extreme rainfall and tide. This date marked a before and after in the hydrological and hydraulic management of the city, whose final step is the implementation of a flood early warning and monitoring system, which is described in this paper. The phases of this project have been:

- Delimitation of the contributing areas to be included in the system.
- Construction of the mathematical model within ICMLive.
- Optimisation process of the model: 2D mesh correction, removal of smaller pipes, simplification of ungauged basins.

- Connection to an automatic SCADA database of registered and forecast values.
- Definition of alerts to be monitored.
- Start-up and deployment of the system.

Aimed to become a digital twin of the hydrological and hydraulic processes of the city, will be able to: provide assessment on flood impacts, help on the design of corrective elements, on the elaboration of action protocols and improve communication and coordination between City administrations. In Figure 2 there is a summary of the actions that this system is able to do.

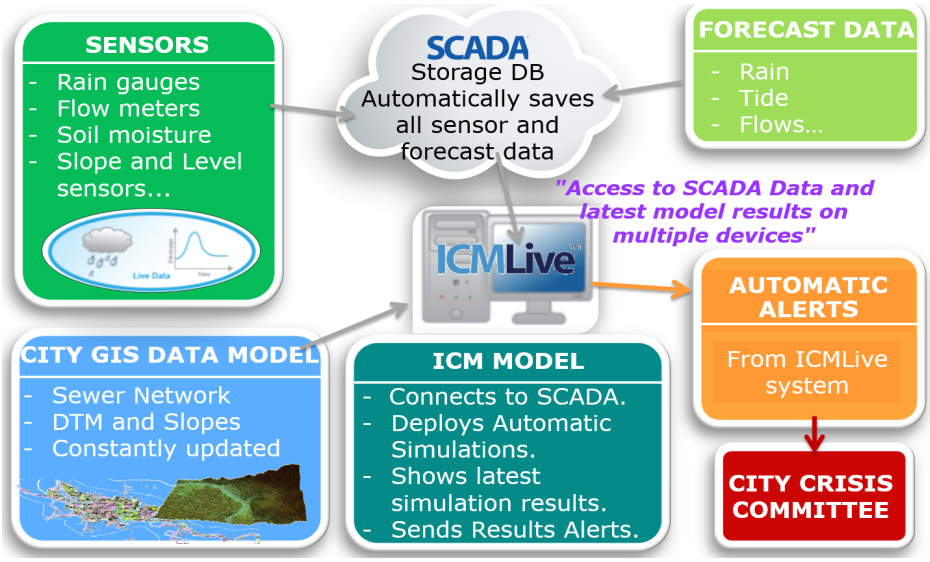

Figure 2. Bilbao city ICMLive flood early-warning and monitoring system summary.

Concluding remarks

Bilbao City Early Warning and Flood Decision Support System will provide clear benefits to municipality management:

- Maintained over time, it supplies a great tool to better understand the hydraulic behaviour of a system as complex as the city of Bilbao.
- It Improves the visualization and understanding of what is about to happen in the city.
- It helps to interpret the risk that the city will have to face in the coming hours.
- It changes the way to manage urban risk: from sheer interpretation of meteorological and tidal warnings, to simulate, in a calibrated mathematical environment (ICMLive), a future scenario based on the current (registered) status of the city and the next hours forecasts, obtaining a final status within a sufficient timeframe to react and reduce the damage.
- Automatic exports of alert lists, graphics and flood plants prevent serious events from being unnoticed and, therefore, human failure.
- Finally, it limits individual responsibility, allowing the management to be carried out by a team that does not know all the behaviour history of the hydraulic system of the city.

Acknowledgments: Noelia Izquierdo and Pedro Izaga from Bilbao City Council. Also Raul Requena from Bilbao IT city services (Cimubisa), José Antonio Aranda & Pedro Anitua from Emergencies and Meteorology of the Basque Government, José María Sanz De Galdeano, Christian Stocker & Rubén Santos from the Basque Water Agency, Juan Manzano Cano, from the Spanish Meteorological Agency and Xabier Aguirre & Iñaki Gonzalez, from the Bilbao-Bizkaia Water Consortium.

References

Alcrudo F, Mulet J (2005) Urban inundation models based on the ShallowWater equations. Numerical and practical issues. In: F. Benkhaldoun, D. Ouazar & S. Raghay (eds), Hermes Science

Batanero P, Martinez E (2017) Early-Warning and Monitoring Real-Time Systems in Rural and Urban Catchments. 1st HydroSenSoft Congress, Madrid, Spain

11th World Congress on Water Resources and Environment (EWRA 2019)
"Managing Water Resources for a Sustainable Future", 25-29 June 2019, Madrid, Spain

Water quality of Greek reservoirs: The impact of land cover and water resources management on phytoplankton

V. Navrozidou*, A. Apostolakis, S. Katsavouni, E. Mavromati, V. Tsiaoussi
The Goulandris Natural History Museum, Greek Biotope Wetland Centre (EKBY), 14th km Thessaloniki - Mihaniona, 57001 Thermi, Greece
** e-mail: vnavrozidou@ekby.gr*

Introduction

Natural and artificial lakes (reservoirs) are ecosystems of major importance; however, environmental pressures such as eutrophication, global warming and overexploitation of water resources put a pressure on them (Gaglio et al. 2017). Phytoplankton is an important element of aquatic ecosystems and a significant indicator of water quality as it responds directly to eutrophication pressure (Hajnal and Padisák 2008). The objectives of this study are: i) to present recent data on phytoplankton communities of Greek reservoirs; and ii) to investigate their correlation with land cover of river basin and water resources management.

Materials and methods

Sampling campaigns were carried out during the warm season of years 2013-2016 at 25 reservoirs in Greece. Phytoplankton samples were collected from the euphotic zone and were preserved with lugol's solution. Quantitative analysis was performed using the Utermöhl method (Utermöhl 1958). The 2012 Corine Land Cover spatial datasets were downloaded from the Copernicus Land Monitoring Service. For a subset of 23 reservoirs, data for residence time were collected (EYDAP S.A., PPC S.A., etc.). Statistical analyses were performed with R (R Core team 2014).

Results and concluding remarks

Biovolume values of Greek reservoirs ranged from 0.02 mm^3/L to 35.25 mm^3/L; 64% of these values where <1 mm^3/L and 22.5% ranged between 1.00 and 3.13 mm^3/L. Three reservoirs (Adriani, Karla and Kerkini) displayed both high biovolume values and high variations between the years (6.40 - 35.25 mm^3/L). Phytoplankton was mostly formed by cyanobacteria in these three reservoirs; Cylindrospermospis raciborskii, Aphanizomenon spp. and Anabaena spp. were the most dominant.

Low values of total phytoplankton and cyanobacteria biovolume were observed in reservoirs located in river basins with a high cover of natural and semi-natural areas (Figure 1). This is expected as most reservoirs are located on mountainous and semi-mountainous areas, where forest and forested areas prevail and human settlements are scarce (Mavromati et al. 2018). On the contrary, high phytoplankton values appeared in river basins with a relatively large cover of intensive agriculture (>30%) (Figure 1).

Values of residence time varied considerably throughout the investigation period, ranging from 0.004 to 4.42 years, according to water resources management decisions. Although phytoplankton biovolume is thought to be related to residence time, in this dataset, this relationship was neither significant nor strong (R^2=0.015, p>0.05).

Land cover of river basins has considerable impact on the physicochemical features of natural and artificial lakes in Greece (Mavromati et al. 2018). Surface inflows transfer nutrients from agriculture and other uses, enhancing eutrophication in aquatic ecosystems (Toporowska et al. 2018). This is also indicated by the phytoplankton results of Greek reservoirs in the present study. We recommend to focus management actions at river basin scale. An enlarged dataset from the continuation of monitoring may be required to better understand the link between phytoplankton and residence time in Greek reservoirs.

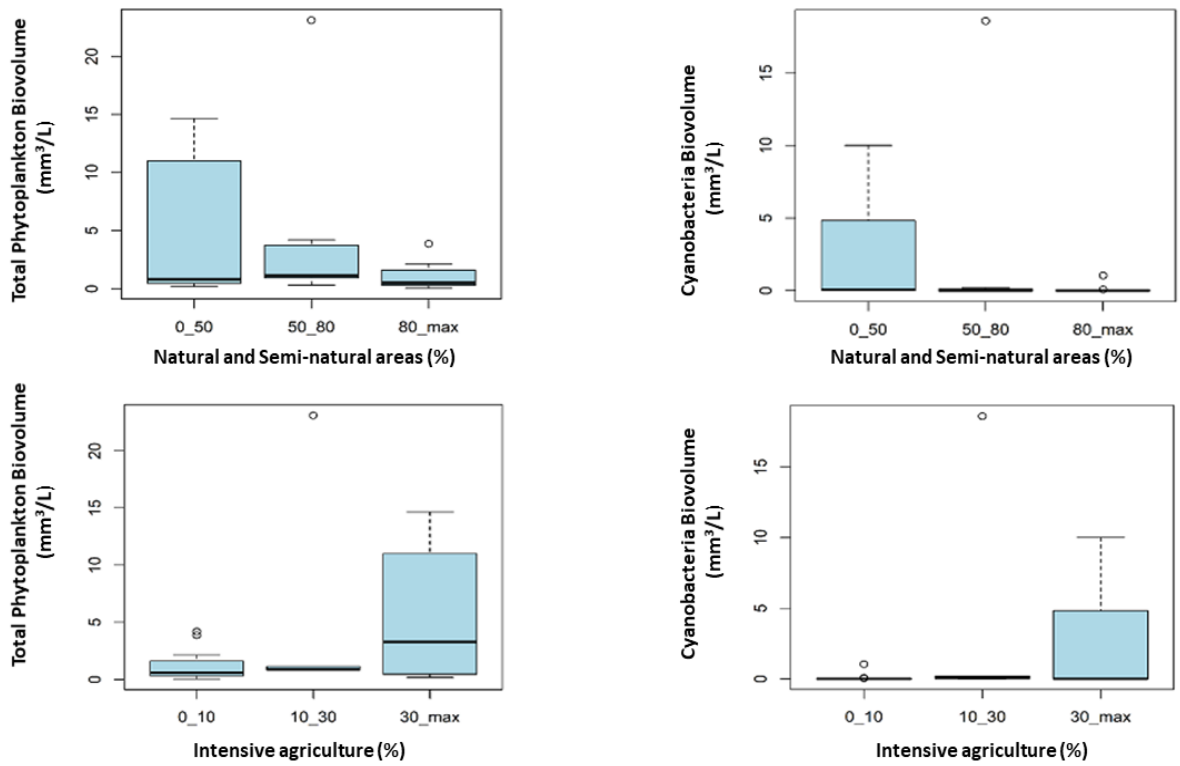

Figure 1. Box and Whisker Plots of natural semi-natural areas and intensive agriculture in relation to total phytoplankton biovolume and cyanobacteria biovolume.

Acknowledgments: This study was co-financed by the European Union Cohesion Fund (Partnership Agreement 2014-2020, MIS 5001204). Monitoring was implemented by The Goulandris Natural History Museum, Greek Biotope/Wetland Centre (EKBY), in the context of the National Water Monitoring Network for Greek lakes (JMD 140384/2011). Data used in this report come also from Acts MIS 371010, 371138, 371140, 371144, 371145 financed by the European Regional Development Fund. Part of the phytoplankton analysis was conducted by E. Chalalambous. Part of the phytoplankton analysis was commissioned by EKBY to the Aristotle University of Thessaloniki (conducted by M. Moustaka and M. Katsiapi).

References

Gaglio M, Aschonitis VG, Gissi E, Castaldelli G, Fano EA (2017) Land use change effects on ecosystem services of river deltas and coastal wetlands: case study in Volano–Mesola–Goro in Po river delta (Italy). Wetlands Ecology and Management 25(1):67-86. https://doi.org/10.1007/s11273-016-9503-1

Hajnal E, Padisák J (2008) Analysis of long-term ecological status of Lake Balaton based on the ALMOBAL phytoplankton database. Hydrobiologia 599:259-276. https://doi.org/10.1007/s10750-007-9207-x

Mavromati E, Kagalou I, Kemitzoglou D, Apostolakis A, Seferlis M, Tsiaoussi V (2018) Relationships among land use patterns, hydromorphological features and physicochemical parameters of surface waters: WFD Lake Monitoring in Greece. Environ. Process. 5(Suppl 1):139–151. https://doi.org/10.1007/s40710-018-0315-6

Toporowska M, Ferencz B, Dawidek J (2018) Impact of lake-catchment processes on phytoplankton community structure in temperate shallow lakes. Ecohydrology 11:e2017. https://doi.org/10.1002/eco.2017

Utermöhl H (1958) Zur Vervollkommn ung der quantitativen Phytoplankton. Methodik. Mit. Int. Verein. Theor. Angew. Limnology 9:1-38. https://doi.org/10.1080/05384680.1958.11904091

11th World Congress on Water Resources and Environment (EWRA 2019)
"Managing Water Resources for a Sustainable Future", 25-29 June 2019, Madrid, Spain

Measuring changes in water level fluctuations and the associated effect on the distribution of wetland vegetation in Poyang Lake, China

R. Wan[1*], G. Yang[1,2], X. Dai[1]
[1] Nanjing Institute of Geography and Limnology, Chinese Academy of Sciences, Nanjing, China
[2] Nanjing Branch of Chinese Academy of Sciences, Nanjing, China
* e-mail: rrwan@126.com

Introduction

The effect of water-level fluctuations (WLF) on vegetation distribution and the makeup of wetland environments is of growing interest as hydrological regimes become even more profoundly modified by human actions and climate change(Coops et al. 2003; Leira and Cantonati 2008). It is necessary to develop a scientifically defensible and empirically testable relationship between changes in WLF and the corresponding ecological responses on a regional scale.

Poyang Lake wetland is a hypertrophic Ramsar wetland that experiences dramatic seasonal WLF (The Ramsar Convention 2017). In recent years, scholars have observed extreme shifts in the seasonal WLF of the lake and clear degradation of the vegetation (Dai et al. 2015; Wan et al. 2018). Hence, it is critical to identify key seasonal WLF and determine their relationships with various types of vegetation. Two urgent questions are addressed in this study: (1) At what time scale does WLF alteration have the most significant linear continuum impact on the distribution of wetland vegetation? (2) What possible critical thresholds of WLF indicators could lead to shift changes in the wetland ecosystem?

Materials and methods

The dynamic monitoring of the distribution of sedge belts from 1993 to 2010 in the Poyang Lake wetland was carried out through analysis of the vegetation maps (unpublished data), which were interpreted from the Landsat TM images by the Nanjing Institute of Geography and Limnology, Chinese Academy of Sciences. Diurnal water level observations of Poyang Lake from 1993 to 2010 were obtained from the Hydrological Bureau of Jiangxi Province.

In order to analyze the possible alteration of various WLF patterns, 38 ecologically meaningful hydrological parameters were selected. They were used in the Classification and Regression Tree (CART) model to determine the vulnerability and the brief life-spans of sedge belts in the Poyang Lake wetland exposed to the stress of water-level fluctuations.

The rationale of the CART model is to separate the data into two subsets so that the records within each subset are more homogeneous than in the previous subset. It is a recursive process—each of the two subsets is then split again, and the process will repeat until a homogeneity criterion is reached (Qian 2011). The least-squared deviation (LSD) method was used to measure the impurity of various subsets. The Minimal Cost Complexity Pruning (MCCP) method (Knoll et al. 1994) was used in this study to measure and reduce both the complexity and the misclassification risk of using the tree.

Results and concluding remarks

The results show that there were two final water level fluctuation patterns that were entered into the CART model: the 20-day WLF and those of the last retreating season (Figure 1). The 20-day WLF were found to have the greatest impact on variation in the spring sedge belts in this area. When the AWI at day 20 was higher than 10.64 m, the area of spring sedge belts would experience an obvious increase of approximately 423.4 km^2. However, when the level was lower than 10.64 m, the changes in the distribution of spring sedge belts was mainly dependent on the WLF of the last retreating season, i.e. the second most important water level fluctuation pattern. When the water level amplitude of the last retreating season was higher than 5.22 m, the area of spring sedge belts experienced a dramatic decline of approximately 201.5 km^2.

When the water level amplitude of the last retreating season was lower than 5.22 m, the area of spring sedge belts remained in an intermediate state within the optimum range, in which the average value was approximately 267.7 km^2. Consequently, the previous 20-day WLF and those of the last retreating season significantly impact the most important eco-hydrological processes in Poyang Lake wetland. More specially, the 10.64 m of antecedent water-level index (AWI) at day 20 and 5.22 m of the water level amplitude during the last retreating season may be the thresholds beyond which catastrophic changes could be triggered.

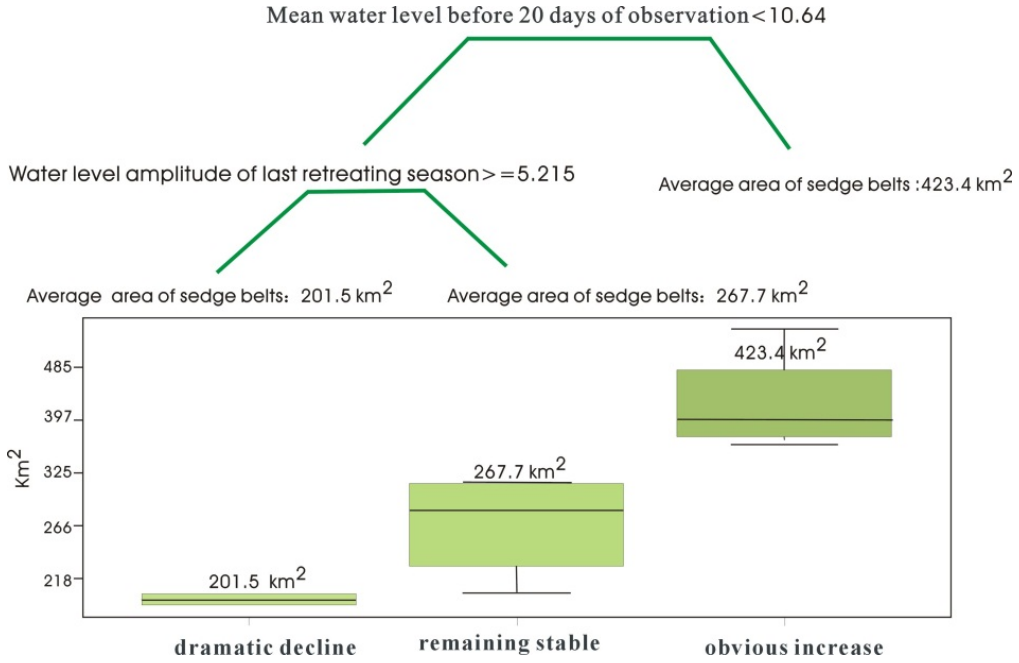

Figure 1. The probable critical water level fluctuation thresholds which could trigger dramatic change in area spring sedge belts in Poyang Lake wetland from 1993 to 2010.

Overall, sedge belts exposed to rapid water level changes could adjust their distribution after nearly 30 days in response to their new environment. Continuous exposure to high water levels lasting up to 20 days and falling to extremely low levels during the retreating season could trigger catastrophic changes in the distribution of spring sedge belts. To a certain extent, because the WLF of Poyang Lake may be significantly altered in the near future, the surrounding wetland communities may become even more vulnerable. Therefore, it would be wise to include studies of hydro-pattern restoration of the Poyang Lake wetland in future management planning.

Acknowledgments: This research received financial support from the National Basic Research Program of China (‘‘973’’Program, 2012CB417006) and the National Science Foundation of China (Grant No.41571107).

References

Coops H, Beklioglu M, Crisman TL (2003) The role of water-level fluctuations in shallow lake ecosystems - workshop conclusions. Hydrobiologia 506(1-3):23-27. doi: 10.1023/B:Hydr.0000008595.14393.77.

Knoll U, Nakhaeizadeh G, Tausend B (1994) Cost-sensitive pruning of decision trees. In: Machine Learning: ECML-94. Springer, pp 383-386

Leira M, Cantonati M (2008) Effects of water-level fluctuations on lakes: an annotated bibliography. Hydrobiologia 613:171-184. doi: 10.1007/s10750-008-9465-2.

Qian SS (2011) Environmental and ecological statistics with R. CRC Press

The Ramsar Convention (2017) The List of Wetlands of International Importance. http://www.ramsar.org/sites/default/files/documents/library/sitelist.pdf

Wan R, Dai X, Shankman D (2018) Vegetation response to hydrologic changes in Poyang Lake, China. Wetlands. https://doi.org/10.1007/s13157-018-1046-1

11th World Congress on Water Resources and Environment (EWRA 2019)
"Managing Water Resources for a Sustainable Future", 25-29 June 2019, Madrid, Spain

A thorough investigation of energy recovery from tannery effluent in the context of circular economy

E. Kokkinos*, V. Proskynitopoulou, E.N. Peleka, A. Zouboulis
Department of Chemistry, Aristotle University of Thessaloniki, Greece
** e-mail: kokkinosevgenios@yahoo.gr*

Introduction

The tanning wastewater effluent raises environmental concerns since it consists a complex mixture of organic and inorganic pollutants. Physicochemical and biological methods are applied to treat such a wastewater, so solids and potentially hazardous substances to be isolated. The produced sludge from the previous treatment is rich in organic matter and Cr(III), a metal which is primarily used in tanning process. Certain alternatives have been proposed, tested and implemented for the exploitation and/or safe disposal of tannery sludge on a pilot and industrial scale. Land application after stabilization, composting, anaerobic digestion, combustion for energy recovery, pyrolysis, chromium recovery and employment in ceramics are some of the proposed methods. The main treatment process of sludge is dehydration, in order to reduce its volume and achieve the appropriate moisture content required for landfill disposal. However, there is no universal solution for the reuse/management of sludge, while legislation and practices vary from country to country (UNIDO 2011). A proper tannery sludge management is crucial for the sustainable operation of a relevant plant and according to European Union guidelines, energy recovery from tannery sludge are recommended, fulfilling the principles of circular economy (EU 2013). Therefore, aim of this study is to explore the possibility of energy recovery through tannery sludge combustion and to define the optimum conditions in order to fully exploit its potential.

Materials and methods

Air dried sludge was obtained from the main tannery wastewater treatment plant located in the industrial area of Thessaloniki in Northern Greece. The sludge was homogenized by grounding and sieving the initial weakly adhered particles at a diameter size below 0.5 mm. Combustion test was performed in a Differential Thermogravimetric Analyser (TG-DTA), with which weight loss and heat flow recorded as a function of temperature (range 50-850 ^{o}C, air flow 20 mL/min and heating rate 20 ^{o}C/min). Additionally, a portion of the sludge was incinerated in an electric furnace under the optimum combustion conditions (namely 400 ^{o}C for 1 h under air), as revealed by the TG-DTA diagram. The resulting tannery sludge ash was considered as the second sample and it aimed to simulate the corresponding ash after combustion for energy recovery. Also, the higher heating value at constant volume (HHV) was determined using adiabatic oxygen bomb calorimeter, via the equivalent method ASTM D 4809. Approximately 1 g of tannery sludge was pelletized in a hand press and placed into the instrument.

Chemical characterization conducted by acid digestion, where 0.5 g samples' fine powder placed in a 100 mL PTFE beaker with 20 mL of concentrated HNO_3 and refluxed on a heated source at 95 ^{o}C for 24 h. Afterwards, 10 mL of 1N HCl were added and heated for 2 h without cover, until no brownish fume was obtained. Metals (Cr_{total}, Ca, Mg, etc.) concentration was determined by Flame Atomic Absorption Spectrophotometry. Cr(VI) concentration was determined by the standard 1,5-diphenylcarbazide method and quantified using a UV spectrophotometer at 540 nm. Organic matter was measured by a TOC analyzer, while samples' pH and electrical conductivity were determined by extracting with deionized water in a suspension ratio liquid to solid equal to 50. Humidity defined by the weight loss of the samples at 120 ^{o}C for 24h and the corresponding loss due to combustion of the sludge was determined by weaving before and after the process.

Results and concluding remarks

Figure 1 presents the mass loss as a function of temperature (TG-black). Initially, water was removed from sludge up to 250 °C, both naturally adsorbed (50-150 °C) and crystalline (150-250 °C), which requires higher energy. The process is endothermic and the corresponding peak is shown in the heat flow diagram (DTA-red). In the range 250-550 °C, two exothermic peaks appeared due to the combustion of organic matter. The double peak was attributed to the complexity of its composition, resulting multiple stages in the process (Li et al. 2015). In the same range part of the mass loss attributed to $CaCO_3$ decomposition.

The experimental determination of tannery sludge's potential for combustion revealed a HHV at 2 MJ/Kg. An overall low value comparing with sludge from other sources (e.g. typical sewage sludge lays in the range 16-21 MJ/Kg), but high enough for energy recovery using the appropriate incinerator (Saxena and Jotshi 1996). The difference is attributed to the proportionally lower organic carbon. Furthermore, as shows Fig. 1, the ignition temperature for tannery sludge was at 250 °C and the first stage of organic matter combustion begun. But in order to fully exploit the produced exothermic energy, the combustion should be carried out at 400 °C, in which temperature the second stage of the process was maximized. The acceptance of this temperature as the optimum for tannery sludge combustion was also determine the thermal conditions of the second's sample treatment, the corresponding ash.

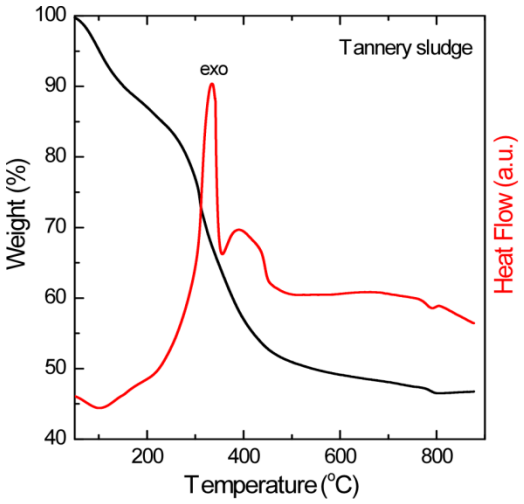

Figure 1. TG-DTA diagram of tannery sludge.

The combustion of tannery sludge was responsible for an overall 50% weight decrease, mainly attributed to moisture and organic matter loss. Their content was diminished in the ash and on the other hand metals' content doubled since no affect by the specific temperature level occurred (Table 1). Moreover, both samples proved to be strongly alkaline materials but the amount of leachable ions after combustion were extremely higher than before, according to electrical conductivity measurements. Another interesting fact was that tannery sludge contains only Cr(III) while the corresponding ash a mixture of Cr(III) and Cr(VI) in ratio 1:1. This feature could be used as an advantage in order to recover chromium from the ash due to high Cr(VI) solubility, in the frame of its sustainable management.

Table 1. Physicochemical characteristics of tannery sludge and corresponding ash.

	Moister	Organic matter	Cr(III)	Cr(VI)	Ca	Mg	pH	Conductivity (mS/cm)
			%					
Tannery sludge	11	22	14.4	-	14.8	2.4	9.1	0.96
Corr. Ash	2.4	1.3	14.3	14.6	29.7	4.9	9.2	7.35

Acknowledgments: We acknowledge support of this work by the project "INVALOR: Research Infrastructure for Waste Valorization and Sustainable Management" (MIS 5002495) which is implemented under the Action "Reinforcement of the Research and Innovation Infrastructure", funded by the Operational Programme "Competitiveness, Entrepreneurship and Innovation" (NSRF 2014-2020) and co-financed by Greece and the European Union (European Regional Development Fund).

References

UNIDO (2011) Introduction to treatment of tannery effluents. What every tanner should know about effluent treatment. UNIDO, Vienna

EC (2013) Best available techniques (BAT) reference document (BREF) on Tanning of Hides and Skins. European Commission, Seville

Li Z, Du Y, Chen Z, Sun D, Zhu C (2015) Synthesis and characterization of cobalt doped green ceramic pigment from tannery sludge. Ceramics International 41:12693-12699. https://doi.org/10.1016/j.ceramint.2015.06.101

Saxena SC, Jotshi CK (1996) Management and combustion of hazardous wastes. Progress in Energy and Combustion Science 22:401-425. https://doi.org/10.1016/S0360-1285(96)00007-X

11th World Congress on Water Resources and Environment (EWRA 2019)
"Managing Water Resources for a Sustainable Future", 25-29 June 2019, Madrid, Spain

Promoting urban integration through green infrastructure incorporation to improve climate governance in cities

N. Proutsos[1*], C. Tsagari[1], G. Karetsos[1], A. Solomou[1], E. Korakaki[1], E. Avramidou[1], N. Gounaris[2], K. Kontos[2], C. Georgiadis[2], A.B. Kontogianni[2], D. Vlachaki[2]
[1] Institute of Mediterranean Forest Ecosystems, Hellenic Agricultural Organization DEMETER, Athens, Greece
[2] Homeotech Co, Thessaloniki, Greece
* e-mail: np@fria.gr

Introduction

Urban green and blue spaces are recognized as driving factors for mitigation and adaptation of climate change impacts in cities, generating environmental, economic and social benefits, supporting biodiversity conservation, reducing the effects of heat waves and other extreme events (flooding, drought, etc.). The optimal placement and selection of green infrastructure can decrease the negative effects of land use and climate changes on hydrology and water quality and thus improve the well-being of citizens (Liu et al. 2016). Important, also, is the impact of increasing temperature and decreasing precipitation trends on human health (Patz et al. 2005). In this frame, mitigation and adaptation to climate change, actions on a regional level are necessary and local governors have established a great number of groups and networks in order to achieve the goals of reducing carbon emissions and increase awareness resilience and sustainability (Castan Broto 2017): e.g. ICLEI-Local Governments for Sustainability and Energy Cities in 1990, R20 Regions of Climate Action and NRG4SD-Global Network of Regional Governments for Sustainable Development in 2002, UCLG-United Cities and Local Governments in 2004, C40 Cities-Climate Leadership, the World Mayors Council and the Covenant of Mayors in 2005 etc. From the same perspective, the European Union has already taken initiatives to face climate change and established a number of financing tools in order to support projects for climate change mitigation and adaptation such as the "Climate Change Action" with main priorities focused on reducing greenhouse gas emissions, increasing resilience to climate change, communication, cooperation and dissemination on climate change mitigation. One of the recent projects co-funded by the EU is LIFE17 GIC/GR/000029 GrIn: "Promoting urban integration of GReen INfrastructure to improve climate governance in cities".

Materials and methods

Urban open spaces should be considered as vital elements of the urban landscape/ecosystem with specific environmental functions and contribution to climate change mitigation and adaptation and not as isolated units. The LIFE GrIn project aims to incorporate the climate change adaptation and mitigation perspectives and green infrastructure management and conservation with local governance in cities, through the establishment of an integrated policy framework focusing on Urban Green Areas (UGAs) and promoting urban integration. The main objectives of the project are to:

- establish an integrated policy framework for the management, monitoring and evaluation of UGAs based on cooperative planning and best practices in urban forestry, satisfying public values and promoting urban adaptation to climate change
- integrate and promote European policies in relation to climate change adaptation and mitigation, as well as sustainable urban planning and design
- quantify and multiply the impact of UGAs on climate-related problems in cities (heat waves, heat island effect, increased runoff during heavy precipitation etc)
- promote the incorporation of sustainable urban forest management for climate change adaptation and mitigation in the Covenant of Mayors and other EU policies
- improve citizens' quality of life through the mitigation of the effects of climate change and the multifunctional planning of UGAs and conserve nature and biodiversity in cities

- raise public and decision-makers awareness regarding the necessity and benefits of taking action on climate change adaptation/mitigation at municipal level and promote active participation

The objectives of the project will be realised through the development of a sustainable urban forest management framework with participatory planning that combines public perception and values of UGAs with management practices addressing climate change. Supportive and well-tailored governance that covers horizontal and vertical engagement and broad stakeholder participation is a basic condition for all steps of the adaptation planning, implementation and monitoring process as is awareness and tailored knowledge creation (EEA 2016).

The LIFE GrIn partnership includes: the Hellenic Agricultural Organization DEMETER-Institute of Mediterranean Forest Ecosystems, the Homeotech Co, the Central Union of Hellenic Municipalities, the Greek Municipalities of Amarousion and Heraklion and the Hellenic Ministry of Environment and Energy.

Results and concluding remarks

The expected results from the implementation of the project (years 2017 to 2021) are the following:

- Assessment of the current climate related risks and threats in two Greek municipalities and evaluation of the existing Green Infrastructure in relation to its contribution to climate change mitigation and adaptation, as well as its ecological quality and other functions
- Capacity-building at municipal level for the creation, management and monitoring of integrated networks of green infrastructure, especially UGAs
- Current CO_2 sequestration by UGAs and its increase in the two cities by the end of the project
- Reduction of greenhouse gas emissions through better planning that reduces maintenance needs
- Establishment of guidelines and indicators to incorporate climate into the management of UGAs
- Implementation of climate inclusive management framework for the establishment of new or reformation of existing UGAs i.e. structure improvement or formation of green networks in the cities
- Committing 10 Municipalities to elaborate and apply integrated management plans following the strategic planning principles produced by the project, in order to affect more than 1 million citizens
- UGAs quality improvement through better tree health, species composition and green coverage
- Establishment of a cooperation platform that will incorporate quantified data on green infrastructure and its contribution to climate change adaptation and mitigation and also best practices and guidelines to support replication
- Regulatory act to incorporate climate change into the management framework of UGAs in Greece
- Extension of the commitment of one additional Municipality (Heraklion) to the New Covenant of Mayors to reduce CO_2 emissions by at least 40% by 2030 and to adopt an integrated approach to tackle mitigation and adaptation to climate change (Mayors Adapt)
- Incorporation of green infrastructure data for the two participating Greek cities in the European Environment Agency platform - Interactive map based on Green Infrastructure indicators.

Acknowledgments: The GrIn project “Promoting urban Integration of GReen INfrastructure to improve climate governance in cities” LIFE17 GIC/GR/000029, is co-funded by the European Commission under the Climate Change Action-Climate Change Governance and Information component of the LIFE Programme.

References

Castan Broto V (2017) Urban Governance and the Politics of Climate change. World Development 93:1-15. http://dx.doi.org/10.1016/j.worlddev.2016.12.031

EEA (2016) Urban adaptation to climate change in Europe 2016-Transforming cities in a changing climate. EEA Report No 12. European Environment Agency, Copenhagen. doi: 10.2800/021466

Liu Y, Theller LO, Pijanowski BC, Engel BA (2016) Optimal selection and placement of green infrastructure to reduce impacts of land use change and climate change on hydrology and water quality: An application to the Trail Creek Watershed, Indiana. Science of the Total Environment 553:149-163. http://dx.doi.org/10.1016/j.scitotenv.2016.02.116

Patz JA, Campbell-Lendrum D, Holloway T, Foley JA (2005) Impact of regional climate change on human health. Nature 438:310–317. doi:10.1038/nature04188

11th World Congress on Water Resources and Environment (EWRA 2019)
"Managing Water Resources for a Sustainable Future", 25-29 June 2019, Madrid, Spain

Incorporating biological components to analyse the hydrological variability for ecological flow recommendations

C. Papadaki[1], V. Bellos[2], K. Soulis[3], E. Dimitriou[1*]
[1] Hellenic Centre for Marine Research, Institute of Marine Biological Resources and Inland Waters, Greece
[2] Laboratory of Reclamation Works and Water Resources Management, School of Rural and Surveying Engineering, National Technical University of Athens, Greece
[3] Department of Natural Resources Management and Agricultural Engineering, Division of Water Resources Management, Agricultural University of Athens, Greece
* e-mail: elias@hcmr.gr

Introduction

For a proper water management policy, hydrological variability is one of the main issues that should be taken into account (Cartwright et al. 2017). Living organisms depend on the variability of the flow regime, a fact that has well been established by several researchers worldwide (Acreman 2016; Poff et al. 2006; Naiman et al. 2008). Nevertheless, the human intervention to natural streamflow regime is rising without, most of the time, incorporating sufficient biological information. In several cases, overly simplistic "rules of thumb", such as minimum flow standards, have been adopted for defining allowable degrees of hydrologic modification, based on the legislative framework of each country. Although these methods provide general guidelines to the policy makers, they still do not provide a sufficient framework, which can ensure the biological integrity. To overcame this limitation, statistical analysis of hydrological data series (usually more than 10 years), derived either by gauging stations or by hydrological models, coupled with habitat suitability models (Papadaki et al. 2017), is proposed, for representing environmental water requirements in a more adequate way, regardless of policy restrictions.

In this study a combination of the aforementioned approaches was made for estimating a Suitable Range of Discharges (SRD), using the West Balkan trout (*Salmo farioides*, Karaman 1938) (hereafter W. B. trout) as biological component. Moreover, the number of days per month the SRD occurred was estimated, based on daily hydrological simulated data series from a previous study (Papadaki et al. 2016) for summer conditions (June to October). Finally, a comparison of the SRD against the current Greek legislation framework of ecological flows was made.

Materials and methods

To select a representative river reach, habitat mapping procedures (Dolloff et al. 1993) during low flow conditions (i.e. summer 2016) was performed for a 1.5 km section of Acheloos river, located in the upper part of the river at central western mountainous region of Greece. For estimating the Weighted Usable Area (WUA0.5), which is an ecological index of habitat suitability, the well-known hydraulic model HEC-RAS coupled with habitat suitability criteria for two W. B. trout sizes (small sized 5-15 cm Total Length (TL), large sized >15 cm TL), for thirteen discharge scenarios, ranging from 0.5 to 18 m^3/s was used. WUA0.5 is a threshold index which takes into account only the suitable conditions for the target species (Papadaki et al. 2016). A selection among the aforementioned discharge scenarios was made for estimating the SRD (and not just a minimum flow threshold), which is both compatible with the Greek legislation regarding ecological flow rules and the fulfillment of the specific species habitat requirements, based on the normalization of the WUA0.5 index. Greek legislation establishes a minimum flow as a percentage of the natural flow regime, according to the highest value of the following rules: a) 30% of the mean monthly flows of June, July and August, b) 50% of the mean monthly flow of September. To identify the SRD, a script written in Fortran language was developed. SRD was estimated taking into account only the discharge scenarios under which the normalized WUA0.5 index was higher than 60% for both sizes of the W.B. trout (table 1). Finally, based on daily discharge simulations from a previous study (Papadaki et al. 2017) the

monthly median discharges (m^3/s) and monthly 25% and 75% interquartile ranges of discharges (m^3/s) for the months (June to October) were estimated.

Results and concluding remarks

SRD ranged from 2.5 m^3/s to 9 m^3/s under which the habitat requirements of the W.B. trout can remain in good conditions, based on WUA0.5 index. It is noted that SRD is compatible with the current Greek legislative framework.

Table 1. Number of days SRD occurred, together with monthly median discharge (med in m^3/sec) and interquartile ranges (25% and 75% in m^3/s), (-): zero number of days.

Month	June				July				August				September				October		
Year	No Days	Med	25 %	75 %	No Days	Med	25 %	75 %	No Days	Med	25 %	75 %	No Days	Med	25 %	75 %	No Days	Med	25 %	75 %
1986	–	20.6	15.2	35.3	7	10.9	9.0	12.8	28	5.0	4.0	6.9	27	3.0	3.0	4.0	24	3.0	2.0	3.4
1987	10	9.6	8.0	12.3	25	5.0	4.0	6.8	30	3.0	2.0	3.0	13	2.3	2.0	4.0	18	7.5	5.0	14.0
1988	29	4.0	3.0	5.0	23	2.0	2.0	2.6	5	1.8	1.0	2.0	6	1.0	1.0	2.0	7	1.0	1.0	2.0
1989	24	5.0	4.0	7.0	25	3.0	2.0	6.5	12	2.0	1.0	2.3	2	1.0	0.9	1.0	11	2.5	1.4	6.0
1990	30	4.0	3.0	5.0	7	2.0	1.0	2.0	3	1.0	1.0	1.5	2	1.0	0.8	1.0	7	0.9	0.6	7.5
1991	6	11.8	9.0	13.7	20	9.0	8.0	11.7	23	5.0	4.0	6.0	26	3.0	3.0	4.0	16	4.4	2.0	8.3
1992	37	7.0	5.3	8.0	13	5.0	4.0	6.0	21	3.0	2.0	4.0	5	1.0	1.0	2.0	10	3.0	1.0	11.3
1993	4	12.6	9.3	15.1	31	5.3	5.0	6.8	30	3.0	3.0	3.3	10	2.0	1.0	2.0	6	1.3	1.0	2.1
1994	22	7.0	6.0	8.8	27	4.0	3.6	5.0	24	2.6	2.0	3.1	5	2.0	1.0	2.0	7	2.0	1.0	4.7
1995	23	7.0	6.0	8.0	30	4.0	4.0	5.0	17	7.0	3.3	13.0	19	7.5	5.3	10.6	31	3.5	3.0	4.9
1996	7	11.7	9.1	16.7	29	5.1	5.0	6.0	30	3.0	3.0	3.7	18	6.0	3.0	14.3	4	14.7	12.2	22.2
1997	28	5.0	4.0	6.1	31	3.0	3.0	3.0	14	2.0	2.0	3.0	1	1.0	1.0	1.0	6	7.5	1.3	36.0
1998	–	14.6	12.0	20.8	29	6.0	5.0	7.5	30	4.0	3.0	4.0	19	4.0	2.2	14.8	19	7.5	5.5	13.5
1999	25	6.0	5.1	8.0	30	4.0	3.0	4.6	14	2.0	2.0	2.0	7	2.0	1.0	2.0	8	2.2	1.0	10.6
2000	29	5.0	3.7	5.0	23	2.0	2.0	3.0	3	1.0	1.0	2.0	10	1.2	1.0	3.0	15	4.0	2.0	8.0
2001	29	5.0	4.5	6.4	30	3.0	2.0	3.8	9	2.0	2.0	3.0	5	1.0	1.0	2.0	1	1.0	0.9	1.0
2002	21	7.0	6.0	9.0	27	4.0	3.0	5.0	18	6.0	4.0	16.5	–	45.4	31.6	109.2	–	34.2	30.1	41.1
2003	26	5.5	5.0	7.0	29	3.0	3.0	3.8	16	2.0	2.0	3.0	16	4.0	3.0	6.8	11	23.7	5.8	40.2
2004	–	15.6	12.6	20.9	22	8.0	6.9	9.0	31	4.0	3.0	5.0	22	3.1	3.0	9.5	12	10.9	4.3	20.6

SRD adequately describe the flow requirements of the specific fish species. This type of approach may be a supportive tool for environmental flow assessments in the context of the WFD 2000/60/EC. More research should be conducted for understanding the mechanisms associated with the biological responses of all ecosystem components to the hydrological variability. This preliminary application highlights the need for further science-based eco-hydrologic approaches, taking into account both the local biodiversity and EU water management policies.

References

Acreman M (2016) Environmental flows—basics for novices. Wiley Interdisciplinary Reviews: Water 3(5):622-628. https://doi.org/10.1002/wat2.1160

Cartwright J, Caldwell C, Nebiker S, Knight R (2017) Putting flow-ecology relationships into practice: A decision-support system to assess fish community response to water-management scenarios. Water 9(3):13–16. http://doi.org/10.3390/w9030196

Dolloff CA, Hankin DG, Reeves GH (1993) Basin wide Estimation of Habitat and Fish Populations in Streams. USFS Southeastern Forest Experiment Station, Asheville. https://doi.org/10.2737/SE-GTR 83

Naiman RJ, Latterell JJ, Pettit NE, Olden JD (2008) Flow variability and the biophysical vitality of river systems. Comptes Rendus Geoscience 340(9-10):629-643. https://doi.org/10.1016/j.crte.2008.01.002

Papadaki C, Soulis K, Muñoz-Mas R, Ntoanidis L, Zogaris S, Dercas N, Dimitriou E (2016) Potential impacts of climate change on flow regime and fish habitat in montane rivers of the southwestern Balkans. Science of the Total Environment 540:418-428. https://doi.org/10.1016/j.scitotenv.2015.06.134

Papadaki C, Soulis K, Ntoanidis L, Zogaris S, Dercas N, Dimitriou E (2017) Comparative Assessment of Environmental Flow Estimation Methods in a Mediterranean Mountain River. Environmental Management 60(2):280-292. https://doi.org/10.1007/s0026

Poff NLR, Olden JD, Pepin DM, Bledsoe BP (2006) Placing global stream flow variability in geographic and geomorphic contexts. River Research and Applications 22:149–166. https://doi.org/10.1002/rra.902

VIII. Groundwater Hydrology, Contamination and Management

11th World Congress on Water Resources and Environment (EWRA 2019)
"Managing Water Resources for a Sustainable Future", 25-29 June 2019, Madrid, Spain

An ensemble modelling approach for groundwater salinity prediction

A. Lal*, B. Datta
Department of Civil Engineering, College of Science & Engineering, James Cook University, Townsville, Australia
** e-mail: alvin.lal@my.jcu.edu.au*

Introduction

In recent years, the use of prediction models in hydrology has increased considerably. In the context of saltwater intrusion modelling studies, prediction models are largely used as approximate simulators in coupled simulation-optimization approach to develop computationally feasible optimal aquifer management strategies. A number of prediction models such as artificial neural network (Bhattacharjya et al. 2007), genetic programming (Sreekanth and Datta 2011a) and support vector machine regressions (Lal and Datta 2018) have been used to approximate saltwater intrusion processes in a coastal aquifer system. Performance of a prediction model can be improved using ensemble models instead of the standalone prediction model (Petrakova et al. 2015). Recently, Sreekanth and Datta (2011b) and Roy and Datta (2017) have utilized ensemble genetic programming and multivariate adaptive regression spline, respectively to develop prediction models capable of approximating saltwater intrusion numerical models.

In this study, a relatively new technique, support vector machine regression (SVMR) based data-driven models are used to predict salinity concentration at selected monitoring wells in a coastal aquifer. The main aim is to demonstrate the accuracy of ensemble SVMR models when compared to the standalone SVMR models. The outcome from this study would enable researchers and water resources engineers choose the best possible tool (either ensemble or standalone SVMR model) for reliable prediction of groundwater salinity levels in coastal aquifers.

Materials and methods

An illustrative coastal aquifer was modelled using FEMWATER computer package. The aquifer was about 2.5 km^2 and comprised of 8 freshwater wells (FWs) and 3 barrier wells (BWs). The FWs were used for fresh groundwater extraction and the BWs (installed near the shoreline) were used to hydraulically control saltwater intrusion. Salinity concentration in the aquifer was monitored at 3 different monitoring wells (MWs). The 3D view of the study area is presented in Figure 1. The 60 m aquifer was divided equally into 3 layers. The coastal side boundary of the aquifer was treated as a constant head (0 m at both ends) and constant concentration (35 kg/m^3) boundary. The remaining two sides of the aquifer were assigned as no flow boundaries. Hydraulic conductivity of the aquifer was considered homogenous (15 m/d) but anisotropic in the x, y and z directions. A constant groundwater recharge rate (0.00054 m/d) was specified to the entire model domain.

A set of 700 input and output patterns were used to construct and evaluate the performances of the standalone and ensemble SVMR models. Out of the 700 datasets, 500 were used to construct (400 to train and 100 for testing) the models. The additional 200 datasets (referred to as independent sets) were used to evaluate the prediction capabilities of the constructed models. A random set of input transient pumping patterns from all operating wells in the aquifer were obtained using Latin Hypercube sampling methodology. These input pumping patterns were implemented into the numerical simulation model to obtain the corresponding concentration datasets at the MWs. The accumulated input-output datasets from a particular monitoring well is utilized to train and test a SVMR model capable of predicting salinity concentrations for that particular monitoring well. Hence, for each monitoring well in the aquifer, a separate SVMR model was developed. For ensembles, each ensemble SVMR model consisted of 10 standalone SVMR models. These standalone SVMR models were developed using different realizations of the input-output datasets obtained through random sampling without replacement. The standalone models were combined into ensembles using the simple average ensemble methodology. The prediction

performances of the developed ensemble SVMR models are compared with the best performing model in the ensemble (BPM_En) and assessed using various mathematical indices such as root mean square error (*RMSE*), coefficient of correlation (*R*) and Nash-Sutcliffe coefficient (*NSE*).

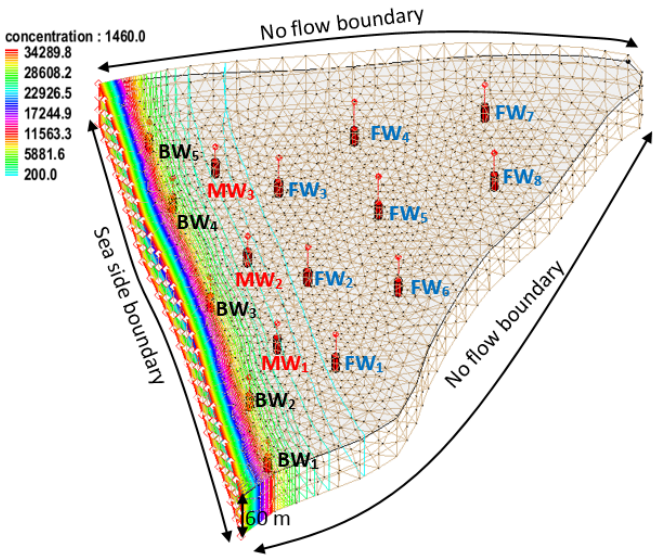

Figure 1. Illustrative coastal aquifer numerical simulation model.

Results and concluding remarks

The ensemble SVMR models are compared in terms of various mathematical error indices against the BPM_En. The results are presented in Table 1.

Table 1. Performance evaluation results using the independent datasets.

	Models	MW_1	MW_2	MW_3
RMSE	BPM_En	0.39	0.28	0.51
	Ensemble	0.30	0.23	0.46
R (%)	BPM_En	98	96	98
	Ensemble	99	99	99
NSE	BPM_En	0.99	0.99	0.99
	Ensemble	0.99	1	1

These results establish that the ensemble SVMR models had better prediction capabilities than the BPM_En. Hence, instead of the standalone models, the ensemble SVMR models can be used as a reliable (more accurate) approximate simulator of the saltwater intrusion processes.

References

Bhattacharjya RK, Datta B, Satish MG (2007) Artificial neural networks approximation of density dependent saltwater intrusion process in coastal aquifers. Journal of Hydrologic Engineering 12:273-282

Lal A, Datta B (2018) Development and Implementation of Support Vector Machine Regression Surrogate Models for Predicting Groundwater Pumping-Induced Saltwater Intrusion into Coastal Aquifers. Water Resources Management 32(7):2405–2419

Petrakova A, Affenzeller M, Merkurjeva G (2015) Heterogeneous versus homogeneous machine learning ensembles. Information Technology and Management Science 18:135-140

Roy DK, Datta B (2017) Multivariate Adaptive Regression Spline Ensembles for Management of Multilayered Coastal Aquifers. Journal of Hydrologic Engineering 22:04017031

Sreekanth J, Datta B (2011a) Comparative evaluation of genetic programming and neural network as potential surrogate models for coastal aquifer management. Water Resources Management 25:3201-3218

Sreekanth J, Datta B (2011b) Coupled simulation-optimization model for coastal aquifer management using genetic programming-based ensemble surrogate models and multiple-realization optimization. Water Resources Research 47:W04516

11th World Congress on Water Resources and Environment (EWRA 2019)
"Managing Water Resources for a Sustainable Future", 25-29 June 2019, Madrid, Spain

The arsenic and uranium ratios in sediment and groundwater samples as an indicator for contaminated areas from different sources

J. Wurl[1*], L. Mendez-Rodriguez[2], M. Schneider[3], L. Thomas[3]
[1] Universidad Autonoma de Baja California Sur, Km 5.5 Carretera al Sur, Departamento Academico de Ciencias de la Tierra, La Paz, Baja California Sur. C.P. 23080, Mexico
[2] Centro de Investigaciones Biológicas del Noroeste S. C., Km. 1 Carretera a San Juan de La Costa "EL COMITAN" La Paz, Baja California Sur. C.P. 23205, Mexico
[3] Institut fuer Geologische Wissenschaften, Malteserstraße 74-100, Freie Universitaet Berlin, 12249 Berlin, Germany
* e-mail: jwurl@uabcs.mx

Introduction

The contamination of sediments and groundwater from the remains of historic gold mining has been widely documented for San Antonio - El Triunfo mining district in Mexico, where main health problems result from elevated As concentrations. Based on a spatial analysis of groundwater and surface water anomalies, in combination with the temporal observation of the concentrations in runoff water, Wurl et al. (2018) recognized different zones in the southern part of the mining district zones where impact from natural geogenic anomalies and contamination due to historic mining activity can be distinguished. Former studies show that high concentrations in As, Pb, Hg, and Cd can also be observed at locations at greater distances from the SA–ET district (Marmolejo-Rodríguez et al. 2011), and may not be explained as resulting from hydrological drainage from the SA–ET (Gutiérrez-Caminero et al. 2015). Gutiérrez-Caminero et al. (2015) used lead isotope ratios to obtain the isotopic fingerprint for the San Antonio-El Triunfo mining district, which allowed recognizing an additional source of toxic elements related to fault-bounded hydrothermal activities. The purpose of this study was to distinguish between different sources of potentially toxic elements in a wider zone around the Antonio - El Triunfo mining district, using arsenic and uranium ratios obtained from source rock, sediment and groundwater analyses.

Materials and methods

The content of total and dissolved metals, including arsenic and uranium, was analyzed in 10 surface water and 30 groundwater samples, taken in the southern part of the San Antonio - El Triunfo mining district using Inductively Coupled Plasma Mass Spectrometry (ICP-MS according to EPA 6020-A-2007). In the field, water temperature, specific conductance, redox potential, pH and dissolved oxygen were measured. Analysis from another 38 wells located in the Los Planes basin (CNA 2003) were included in the interpretation, in order to define the influential radius of the mining-related contamination. A geochemical database of relevant volcanic and metamorphic rocks, which are present within the study area (Schaaf et al. 2000; Perez-Vendzor 2013) was interpreted in order to recognize the sources of different element anomalies. Another 133 sediment samples, reported by SGM (2017), which had been collected from the main creeks of the study area and analyzed by inductively coupled plasma atomic emission spectroscopy, allowed recognizing the distribution path via sediment transport.

Results and concluding remarks

Surface- and groundwater: More than 90 percent of the total uranium is dissolved. In the eight surface water samples from the San Antonio - El Triunfo mining district, an average concentration of 0.0052 mg/L dissolved uranium was obtained; no sample reached the safety limit of 0.009 mg/L proposed by UNSCEAR (2000) (minimum 0.0034 mg/L, maximum 0.0075 mg/L). In the 30 groundwater analyses, a higher average value of 0.0109 mg/L (minimum <0.0002 mg/L, maximum 0.120 mg/L) was observed; the highest uranium values correspond to fracture zones in Diorite and Granodiorite. The concentrations of uranium in the groundwater were in 30% of the cases higher than the safety limit recommended by UNSCEAR and in 7% of

cases higher than the safety limit of 0.030 mg/L, as recommended by US-EPA (2011). The total uranium concentration, analyzed in 38 wells from the Los Planes basin (CNA 2003), were lower, with an average of 0.0059 mg/L (minimum 0.0008 mg/L, maximum 0.0259 mg/L. In 13% of the groundwater samples from the Los Planes basin the uranium concentration was above the safety limit recommended by UNSCEAR and in all cases, less than the safety limit, recommended by US-EPA 2011.

Sediments and rock samples: In sediment samples from the Los Planes watershed, uranium concentration varies between 1.43- 7.35 ppm; the zone with elevated uranium concentrations coincides with the location of wells with elevated total uranium concentration. These elevated uranium levels can be traced back to an anomaly in Diorites of the eastern mountain range "Sierra la Gata".

Seven sediment samples with the highest arsenic concentrations (50.5 ppm to a maximum of 685 ppm) are related to the remains of historic gold mining and show relatively low uranium concentrations (1.86 – 2.27 ppm U, but there is a significant correlation coefficient of 0.73 ($p<0.05$ one-tailed).

Based on the groundwater flow lines, the area influenced by arsenic contamination, a zone, influenced by thermal water, a coastal zone with sea water infiltration and the area with elevated uranium concentrations were distinguished and the corresponding As – U ratios calculated. This allowed estimating the influences of each in the mixing zone in between these well-defined areas. The arsenic - uranium ratios can give important information on sources and mixtures in groundwater. Therefore it is advisable to include uranium in water analysis of wells in granitic and metamorphic rocks.

Acknowledgments: The article was elaborated, based on analyses documented in the report Wurl et al. (2011), contracted by the Concordia Project Mining Company and SEMARNAT-CONACyT 249423.

References

Gutiérrez-Caminero L, Weber B, Wurl J, Carrera-Muñoz M (2015) Tracing toxic elements sources using lead isotopes: An example from the San Antonio–El Triunfo mining district, Baja California Sur, México. Applied Geochemistry 59:23-32

Marmolejo-Rodríguez AJ, Sánchez-Martínez MA, Romero-Guadarrama JA, Sánchez-González A, Magallanes-Ordóñez VR (2011) Migration of As, Hg, Pb, and Zn in arroyo sediments from a semiarid coastal system influenced by the abandoned gold mining district at El Triunfo, Baja California Sur, Mexico. Journal of Environmental Monitoring 13(8):2182-2189

Pérez-Venzor JA (2013) Geological-geochemical study of the eastern edge of the Los Cabos Block, Baja California Sur, México. Dissertation. UNAM México (in Spanish)

Schaaf P, Böhnel H, Pérez-Venzor JA (2000) Pre-Miocene palaeogeography of the Los Cabos Block, Baja California Sur: geochronological and palaeomagnetic constraints. Tectonophysics 318:53-69

SGM (Servicio Geologico Mexicano) (2017) GeoInfoMex, El Banco de Datos del SGM. http://mapasims.sgm.gob.mx

UNSCEAR (Comité Científico de Naciones Unidas sobre los Efectos de la Radiación Atómica) (2000) Sources and effects of ionizing radiation: report to the General Assembly, with scientific annexes. United Nations, New York. http://www.unscear.org/docs/reports/annexd.pdf

US-EPA (La Agencia de Protección Ambiental de EE.UU.) (2007) Method 6020A. Inductively Coupled Plasma-Mass Spectrometry. Washington, DC

US-EPA (La Agencia de Protección Ambiental de EE.UU.) (2011) Expert Elicitation Task Force: White Paper. Science and Technology Policy Council, Washington DC, p 141

WHO (2005) Uranium in Drinking Water. Background Document for development of WHO guidelines for Drinking Water Quality. WHO/SDE/03.04/118

Wurl J, Imaz Lamadrid M, Mendez-Rodriguez L, Acosta Vargas B (2018) Arsenic concentration in the surface water of a former mining area: The La Junta Creek, Baja California Sur, Mexico. International Journal of Environmental Research and Public Health 15(3):437

11th World Congress on Water Resources and Environment (EWRA 2019)
"Managing Water Resources for a Sustainable Future", 25-29 June 2019, Madrid, Spain

Modeling discontinuous aquifers using modified response matrix approach

S. Mohan, K. Neenu*
Environmental and Water Resources Engineering, Department of Civil Engineering, Indian Institute of Technology Madras, Chennai – 600 036, India
** e-mail: kneenu@gmail.com*

Introduction

The water resource management models that combine simulation and optimisation modules are based on the algorithms of embedded approach or response matrix approach (Psilovikos 2006). In the embedded approach the governing equation of groundwater flow is treated as the constraint (Aguado and Remson 1974), whereas in response matrix approach, the response of the system for unit stress at pre-defined locations are found out by multiple runs of the simulation model and the developed influence coefficient matrix is incorporated into the constraint set of the optimisation model (Gorelick 1983) Response matrix is based on the principle of superposition, so this method works well in linear systems. The embedded models contain all the values of the output from the simulation model along the entire domain in space and time, thus many decision variables and constraints will be unnecessarily used in the management model (Peralta and Azarmnia 1991). The initial computational effort for the response matrix is high, but once the matrix is developed, the computational efforts can be drastically reduced in the later stages of modeling (Seo et al. 2018).

Response matrix is widely used for simulating confined aquifers due to its linear relationship between pumping and drawdown. The confining units may have some discontinuities, due to which the linear relationship may not hold valid. In such cases, the standard response matrix may not be giving accurate results. To account for the nonlinear behaviour of the aquifer due to the discontinuous formation, this study aims at modifying the existing response matrix by incorporating the second order term of Taylor series expansion using Newmark Beta method.

Materials and methods

Response matrix uses the first term of Taylor series expansion to express the relation between drawdown and pumping, as given in Eq. (1). In the Modified Response Matrix, the second order term is also considered, which is expanded using the Newmark β Method (Eq. 2). The value of β ranges from 0 to 0.5. The second order term is considered as the difference of response matrices for a selected pumping rate and a weighted matrix for an equivalent pumping. If the system were completely linear, then this difference would be zero. Thus, the component of non-linearity is incorporated by this term.

$$\Delta h = \frac{\partial h}{\partial Q}.Q + \frac{1}{2!}.\frac{\partial^2 h}{\partial Q^2}.Q^2 + \frac{1}{3!}.\frac{\partial^3 h}{\partial Q^3}.Q^3 + ... \quad (1)$$

$$\Delta h = (\frac{\partial h}{\partial Q})_Q.Q + \{(\frac{1}{2} - \beta)(\frac{\partial^2 h}{\partial Q^2})_Q + \beta(\frac{\partial^2 h}{\partial Q^2})_{Q+\Delta Q}\}.Q^2 \quad (2)$$

$$\frac{\partial^2 h}{\partial Q^2} = \frac{[RM]_{nQ} - n[RM]_Q}{\Delta Q} \quad (3)$$

where Δh is the Drawdown, Q is the Pumping Rate, $[RM]_{nQ}$ is Response Matrix for pumping at n times the unit rate and $[RM]_Q$ is Response Matrix for unit pumping rate.

To check the applicability of this method a hypothetical case was chosen from the literature (Thangarajan and Singh 2016) consisting of an unconfined aquifer of 6000 m x 12000 m with a thickness of

35 m. Nine well locations, as specified in the model, was used for generating the response matrix and modified response matrix. Visual MODFLOW was used as a tool to generate the matrix by multiple simulation runs. Once the two matrices were generated, Pumping rates were assigned at all the nine locations and the drawdown obtained through Response matrix, modified response matrix and MODFLOW are compared in Figure 1.

Results and concluding remarks

From Figure 1, it can be observed that the Modified Response Matrix gives drawdown values close to that obtained from the simulation model MODFLOW. The deviations in the drawdown values obtained from the response matrix and modified response matrix from MODFLOW are listed in Table 1.

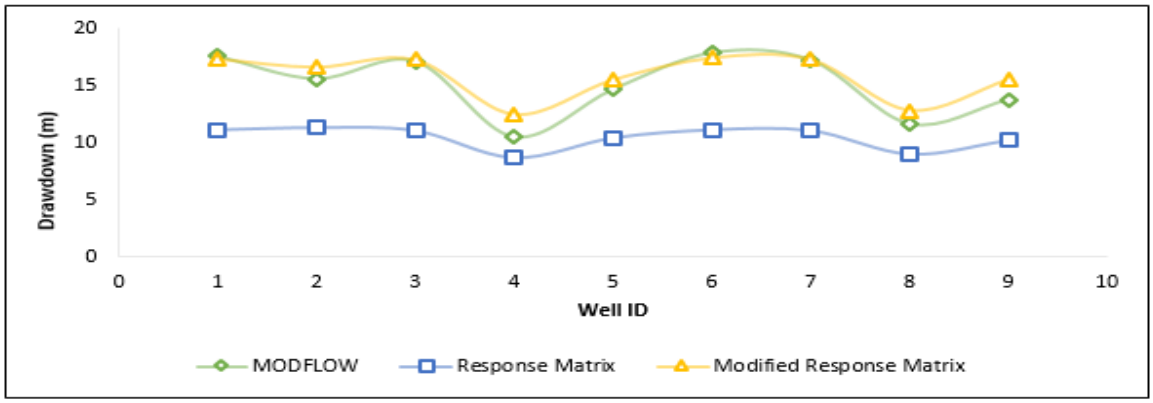

Figure 1. Comparison of Response Matrix and Modified Response Matrix

Table 1. Comparison of the performance of Response Matrix and Modified Response Matrix

Error Index	Response Matrix	Modified Response Matrix
RMSE	4.96	1.07
R^2	0.89	0.96
NSE	-2.86	0.819

It was observed that the RMSE got reduced from 4.96 to 1.07 by using Modified Response Matrix. NSE for modified response matrix was 0.819, which indicates good fit. Thus, it can be concluded that the Modified Response Matrix can be used for replacing the simulation model from the simulation-optimization framework, thereby reducing the computational cost.

References

Aguado E, Remson I (1974) Groundwater Hydraulics in Aquifer Management. Journal of the Hydraulics Division 100:103-118

Gorelick SM (1983) A Review of Distributed Parameter Groundwater Management Modeling Methods. Water Resour Res 19:305–319

Psilovikos A (2006) Response matrix minimization used in groundwater management with mathematical programming: A case study in a transboundary aquifer in Northern Greece. Water Resour Manag 20:277–290. doi: 10.1007/s11269-006-0324-5

Peralta RC, Hossein Azarmnia ST (1991) Embedding and Response Matrix Techniques for Maximizing Steady-state Groundwater Extraction, Computational Comparison. 357–364

Seo SB, Mahinthakumar G, Sankarasubramanian A, Kumar M (2018) Conjunctive Management of Surface Water and Groundwater Resources under Drought Conditions Using a Fully Coupled Hydrological Model. 144:1–11. doi: 10.1061/(ASCE)WR.1943-5452.0000978

Thangarajan M, Singh VP (2016) Groundwater Assessment, Management and Modeling, Taylor & Francis Group, London, New York

11th World Congress on Water Resources and Environment (EWRA 2019)
"Managing Water Resources for a Sustainable Future", 25-29 June 2019, Madrid, Spain

Nitrate concentration and transport simulation of a rural basin aquifer under the strict compliance to the E.U. Nitrates Directive (91/676/EEC)

P. Sidiropoulos[1*], N. Mylopoulos[1], L. Vasiliades[1], A. Loukas[2]
[1] Department of Civil Engineering, University of Thessaly, Volos, Greece
[2] School of Rural and Surveying Engineering, Aristotle University of Thessaloniki, Thessaloniki, Greece
* e-mail: psidirop@civ.uth.gr

Introduction

One of the major global threats of groundwater resources of rural basins is the nitrate contamination from the excessive use of nitrogenous fertilizers at cultivated areas (Almasri and Kaluarachchi 2007). This phenomenon has been created by the consecutive need of agricultural product maximization due to population growth (Rutting et al. 2018). Problems regarding the safeguarding public health are raised when nitrate contaminated groundwater is used for potable needs. For this reason, the World Health Organization recommended a health-based guideline value for nitrate of 50 mg/L for drinking-water. European Union, through the Nitrates Directive (91/676/EEC), set "threshold" values on nitrate fertilization of crops (kg/ha) to prevent nitrate contamination of groundwater. Furthermore, a stricter "threshold" value has been set for continuous existence of nitrate concentration in groundwater, that of 25 mg/L by Nitrates Directive.

The study estimates the spatially distributed nitrate concentrations of Lake Karla aquifer of Eastern Thessaly with the use of simulation models through two scenarios regarding nitrate fertilization of crops: i) the current status; and ii) the strict compliance with the Nitrates Directive. For that reason, a modelling system has been applied, which has been proposed by Sidiropoulos et al. (2018). The study highlights the importance of the full compliance with Nitrates Directive requirements by the farmers of rural basins, where the groundwater resources are used for potable needs; otherwise the public health is threatened.

Materials and methods

Lake Karla watershed is a rural basin located at the southern eastern part of the most cultivated region of Greece, Thessaly. The aquifer covers an area of 500 km^2 and it is entirely located in Eastern Thessaly plain, where water demanding crops prevail. The long-term intense agricultural activities, the lack of any surface water body and of an organized irrigation network have led to aquifer's quantitative and qualitative degradation. Almost more than 80% of the total groundwater consumption is used to agriculture (Mylopoulos and Sidiropoulos 2016). Thessaly region is one of the seven vulnerable zones, with respect to nitrogen pollution from agricultural run-offs, which have been identified in Greece, according to the requirements of the Directive 91/676/EEC (transposed into national legislation with Joint Ministerial Decision 161890/1335/1997). Nevertheless, farmers to succeed crop product maximization do not follow the requirements of the E.U. Nitrates Directive regarding nitrate fertilization.

The methodology starts with the classification of crop types at the study area of aquifer with the use of a Geographical Information System (GIS). The nitrate loading for each type of crop has been estimated: i) for the current status scenario as Wichmann (1992) proposed; and ii) for the second scenario, according to the E.U. Nitrates Directive guideline. Table 1 presents the nitrate loading of prevailed crop types for each scenario. Nitrate leaching to aquifer is achieved through water infiltration from surface to subsurface system and has been estimated as proposed by Shamrukh et al. (2001).

The modelling system applied, consists of a monthly semi-distributed hydrological model (UTHBAL) for the assessment of groundwater recharge, a groundwater simulation model (Modflow) and a groundwater transport and a dispersion simulation model (MT3DMS). The modelling system has been calibrated and successfully implemented at Lake Karla watershed by Sidiropoulos et al. (2018). The simulation has been conducted for a thirteen year period from 1995 to 2007.

Table 1. Nitrate loadings per crop for the two scenarios.

	Nitrate loading (kg/ha) - Scenario 1	Nitrate loading (kg/ha) - Scenario 2
Cotton	160	70
Wheat	160	40
Vegetables	60	40
Trees of almonds, walnuts, peanuts, etc.	200	120
Alfalfa	30	30
Maize	250	150
Sugar beet	180	120
Other trees	150	70

Results and concluding remarks

Two cross sections (West-East, North-South) of the study area have been chosen for the presentation of the results. These sections cross the most nitrate polluted area of the aquifer and the area where the wells for the supply of drinking water to the nearby city of Volos are located and operate over the last 20 years. The results indicate that the values of nitrate concentration exceed the limit of 25 mg/L, at many parts of the study area, for the first scenario. It is crucial to mention that this limit is exceeded at the supply wells area. On the contrary, the values of nitrate concentration are lower than the limit for the entire study area for the second scenario (Figure 1).

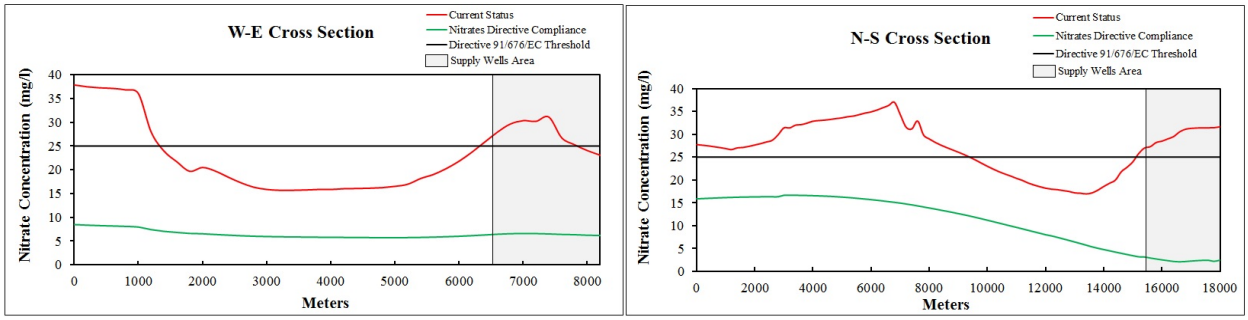

Figure 1. W-E and N-S cross sections presented the values of nitrate concentration for the two scenarios.

The study proves that the E.U. Nitrates Directive requirements are not taken into consideration and this fact has led to the violation of the limit of 25 mg/L threatening public health. To reverse this phenomenon, drastic measures must be taken by the water resources management authorities. Also, the nitrate vulnerable zones of the aquifer must be identified and delineated.

Acknowledgments: The scientific publication was held within the framework of the invitation "Granting of scholarship for Post-Doctoral Research" of the University of Thessaly, which is being implemented by the University of Thessaly and was funded by the Stavros Niarchos Foundation.

References

Almasri MN, Kaluarachchi JJ (2007) Modeling nitrate contamination of groundwater in agricultural watersheds. Journal of Hydrology 343(3-4):211-229. http://doi.org/10.1016/j.jhydrol.2007.06.016

Mylopoulos N, Sidiropoulos P (2016) A stochastic optimization framework for the restoration of an over-exploited aquifer. Hydrological Sciences Journal 61(9):1691-1706. http://doi.org/10.1080/02626667.2014.993646

Rütting T, Aronsson H, Delin S (2018) Efficient use of nitrogen in agriculture. Nutrient Cycling in Agroecosystems 110(1):1-5. http://doi.org/10.1007%2Fs10705-017-9900-8

Shamrukh M, Corapcioglu MY, Hassona FAA (2001) Modeling the effect of chemical fertilizers on groundwater quality in the Nile Valley aquifer. Groundwater 39(1):59-67. https://doi.org/10.1111/j.1745-6584.2001.tb00351.x

Sidiropoulos P, Tziatzios G, Vasiliades L, Papaioannou G, Mylopoulos N, Loukas A (2018) Modeling flow and nitrate transport in an over-exploited aquifer of rural basin Using an integrated system: the case of Lake Karla Watershed. Proceedings of 3rd EWaS International Conference on “Insights on the Water-Energy-Food Nexus”, Lefkada Island, Greece, 27–30 June 2018, 2, 667. http://doi.org/10.3390/proceedings2110667

Wichmann W (1992) IFA World Fertilizer Use Manual. International Fertilizer Association, Paris

11th World Congress on Water Resources and Environment (EWRA 2019)
"Managing Water Resources for a Sustainable Future", 25-29 June 2019, Madrid, Spain

Geostatistical interpolation as a prior model improves accuracy: A comparative synthetic study

L. Sarada*, B.V.N.P. Kambhammettu
Department of Civil Engineering, Indian Institute of Technology Hyderabad (IITH), India
** e-mail: ce14resch11002@iith.ac.in*

Introduction

The determination of storage and conductivity properties of aquifers is important in the context of groundwater conservation. This problem is highly undetermined and hence difficult.

Hydraulic Tomography (HT) combined with pilot point inversion seems to be a promising technique to determine the hydraulic conductivity and specific storage of spatially heterogeneous aquifers (Butler et al. 1999; Illman et al. 2007, 2008; Berg and Illman 2015). In Pilot point inversion, a relatively small number of pilot points are placed at suitably chosen sites in the aquifer. The hydraulic parameters are then calculated at the pilot points. A geostatistical algorithm like ordinary Kriging is then used to reconstruct the true picture of the hydraulic parameters. The position of pilot points is crucial. Using a prior model to choose pilot points appears to improve accuracy (Brauchler et al. 2003, 2011; Hu et al. 2011; Jimenez et al. 2013). In this study the permeability values at the observation sites are used to estimate the hydraulic conductivity at these points. Ordinary Kriging is then used to interpolate the conductivity to the rest of the aquifer. This procedure produces an approximate picture of the zones of the aquifer which is then used to place the pilot points judiciously. The inversion results are compared with a uniform distribution of pilot points (without a prior model). The comparison is made rigorous through cross-validation (done in two ways).

Materials and methods

This work involves a synthetic study of a weathered granitic aquifer. These kinds of aquifers are typically found in the Deccan Plateau region of India. The aquifer considered is two-dimensional with dimensions 25m x 10m. Dirichlet boundary conditions of constant heads are imposed on the vertical boundaries and a no-flow condition on the horizontal boundaries. The hydraulic parameters are chosen uniformly at random from typical known values. In order to perform HT, crosshole pumping tests are conducted in 3 wells with 4 isolated zones each. Four crosshole pumping tests are performed and the inversion is done simultaneously. The "observed" drawdown responses are simulated using the software HydroGeoSphere (HGS). The model-independent inversion tool Parameter Estimation (PEST) is used in conjunction with HGS to solve the inversion problem of determining the hydraulic parameters of the aquifer. The simulation is done in the transient mode. The statistics of the "true" Hydraulic conductivity are summarized in Table 1.

Table 1. Statistics of the synthetic Hydraulic Conductivity (metres/second)

Statistic	Value
Minimum	7.45E-7
Maximum	5.62E-4
Mean	6.04E-5
Standard Deviation	1.19E-4

In the aforementioned synthetic model, the values of hydraulic conductivity at the observation locations are assumed to be known (in the field they are typically estimated by performing permeability tests). These values are then statistically interpolated using ordinary Kriging. Pilot points are chosen to be located around but not exactly on the observation/pumping sites. In addition, pilot points are also placed somewhat near the boundaries to capture the effects of the boundary conditions. The prior model obtained by interpolation of known values in the wells is used to choose pilot points liberally in the interiors of hydraulic conductivity zones. Cross-validation is performed in two ways – by running the forward model

for more time and calculating the total Root Mean Square (RMS) validation errors at all pilot points, and by collecting data at two validation wells and measuring the RMS error at these wells. This inversion scheme is then compared with a direct inversion through PEST by placing pilot points uniformly without a prior model. The performance of the inversion schemes is judged by taking both validation methods into account.

Results and concluding remarks

The inversion depending on a Kriging based prior model appears to do vastly better than the control, i.e., a uniform selection without a prior (Table 2). However, there is one puzzling feature of the data. The spatial (well-based) validation error of the uniform selection scheme appears to be a little lower than that of the Kriging based scheme whereas the temporal validation error is very high for the uniform selection scheme. Indeed, well validation is strongly dependent on the position of the wells (which coincidentally happen to be placed in just the right locations where the control scheme performs well). The temporal validation errors take into account the entire aquifer and therefore provide a better perspective.

Table 2. RMS Validation errors of Drawdowns (metres)

Inversion Scheme	Well validation error	Temporal validation error
Kriging based prior	5.65	0.17
Uniform selection	3.99	14.72

Acknowledgments: The authors thank the President and CEO of Aquanty, Dr. Steven Berg for technical support and guidance in using the software HydroGeoSphere (HGS).

References

Berg SJ, Illman WA (2015) Comparison of hydraulic tomography with traditional methods at a highly heterogeneous site. Groundwater 53(1):71-89. https://doi.org/10.1111/gwat.12159

Brauchler R, Liedl R, Dietrich P (2003) A travel time based hydraulic tomographic approach. Water Resources Research 39(12):1370. https://doi.org/10.1029/2003WR002262

Brauchler R, Hu R, Dietrich P, Sauter M (2011) A field assessment of high-resolution aquifer characterization based on hydraulic travel time and hydraulic attenuation tomography. Water Resources Research 47(3):W03503. https://doi.org/10.1029/2010WR009635

Butler JJ, McElwee CD, Bohling GC (1999) Pumping tests in networks of multilevel sampling wells: Motivation and methodology. Water Resources Research 35(11):3553-3560. https://doi.org/10.1029/1999WR900231

Hu R, Brauchler R, Herold M, Bayer P (2011) Hydraulic tomography analog outcrop study: Combining travel time and steady shape inversion. Journal of Hydrology 409(1-2):350-362. https://doi.org/10.1016/j.jhydrol.2011.08.031

Illman WA, Liu X, Craig A (2007) Steady-state hydraulic tomography in a laboratory aquifer with deterministic heterogeneity: Multi-method and multiscale validation of hydraulic conductivity tomograms. Journal of Hydrology 341(3-4):222-234. https://doi.org/10.1016/j.jhydrol.2007.05.011

Illman WA, Craig AJ, Liu X (2008) Practical issues in imaging hydraulic conductivity through hydraulic tomography. Groundwater 46(1):120-132. https://doi.org/10.1111/j.1745-6584.2007.00374.x

Jiménez S, Brauchler R, Bayer P (2013) A new sequential procedure for hydraulic tomographic inversion. Advances in Water Resources 62:59-70. https://doi.org/10.1016/j.advwatres.2013.10.002

11th World Congress on Water Resources and Environment (EWRA 2019)
"Managing Water Resources for a Sustainable Future", 25-29 June 2019, Madrid, Spain

Analyzing the groundwater age and flow fractions in subsurface hydrologic systems

N. Ayinippully Nalarajan[1*], S. Kumar Govindarajan[2], I.M. Nambi[1]
[1] Environmental and Water Resources Engineering, Department of Civil Engineering, Indian Institute of Technology Madras, Chennai – 600 036, India
[2] Department of Ocean Engineering, Indian Institute of Technology Madras, Chennai – 600 036, India
* e-mail: leadmethru@gmail.com

Introduction

The calculation of groundwater ages has been an essential step in groundwater management as a tool to evaluate different aspects of the protection and sustainability of water supply wells. Groundwater age data provides information about the recharge ages of the aquifer and hence its susceptibility to contamination and the estimates of renewable groundwater resources (Kazemi et al. 2006). Groundwater age simulations have been discussed by, among others, Varni and Carrera (1998), Castro and Goblet (2005), Cornaton and Perrochet (2006) and Molson and Frind (2012).

Groundwater age modeling thus helps to gain insight into solutions of problems concerned with both quantity as well as the quality of groundwater reserves. The concept of capture fraction (CF), introduced by Potter et al. (2008), indicate the certainty or strength of capture of flow by a pumping well. The present study couples the knowledge from the groundwater age model and capture fraction to understand the variation of ages with the strength of capture, by the pumping well, within its capture zone. This idea can, in turn, help easily outline impressions of the transient effects on the groundwater ages.

Materials and methods

The present work computes capture fraction (Potter et al. 2008) to obtain the well capture zone and solves the groundwater age model sequentially for the analyses. Figure 1 encapsulates the methodology adopted.

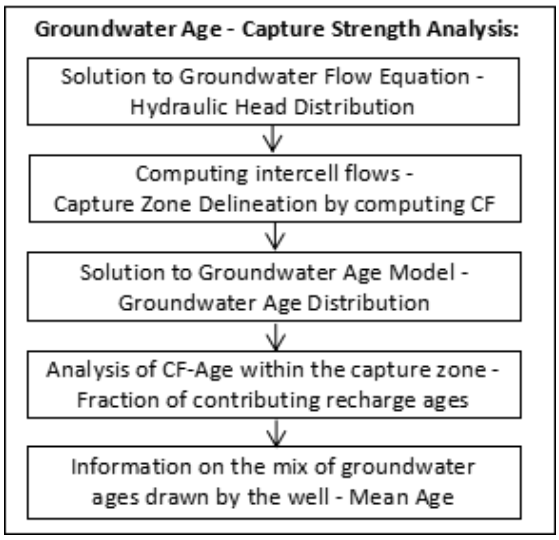

Figure 1. Flowchart of the adopted methodology

The method was coded in Python and applied to a simple hydrogeology setup, representing a homogeneous confined aquifer, with a pumping well at the center of the domain. The pumping rates were varied to simulate a transient sink in the system. The following equations have been used for groundwater flow and age transport modeling (Anderson et al. 2015; Goode 1996):

$$\frac{\partial}{\partial x}\left(T_x \frac{\partial h}{\partial x}\right)+\frac{\partial}{\partial y}\left(T_y \frac{\partial h}{\partial y}\right)=S\frac{\partial h}{\partial t}-R \quad (1)$$

$$\frac{\partial}{\partial x_i}\left(D_{ij} \frac{\partial A}{\partial x_j}\right)-v_i \frac{\partial A}{\partial x_i}+1=0 \quad (2)$$

where h is the hydraulic head in meter, T is the transmissivity in square meter per day, S is the storativity of the aquifer, R is the volumetric flux in cubic meter per day per unit volume representing sources and/or sinks of water, D_{ij} is the macrodispersion tensor, v_i is the velocity vector, and +1 is the source term expressing the growth of the age mass at the rate of 1 day/day.

Results and concluding remarks

Figure 2 shows the well capture zone, along with the cell CF, and the groundwater ages obtained from the model.

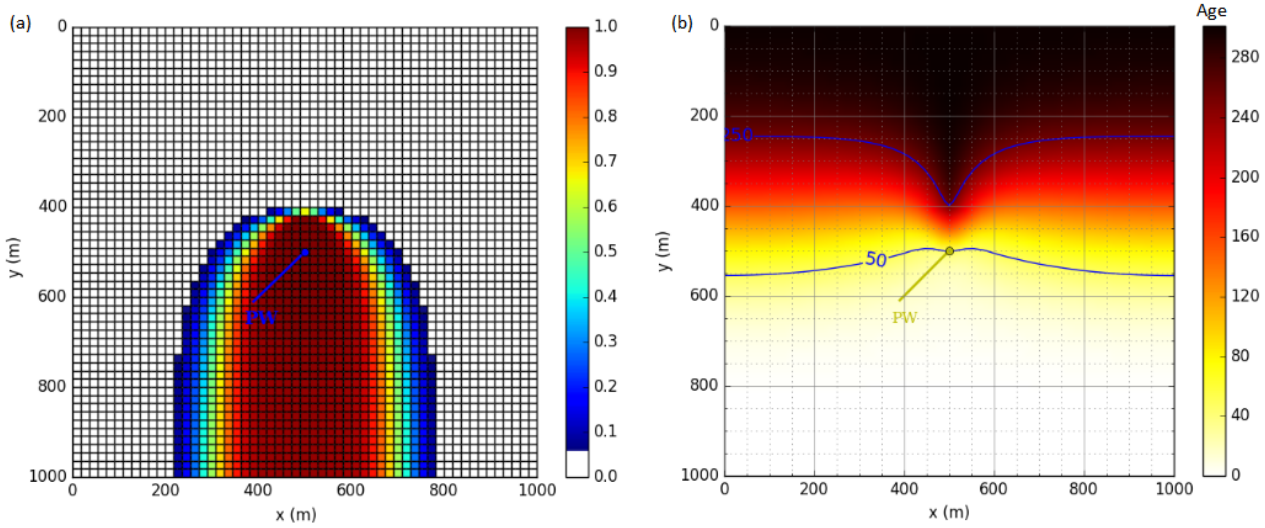

Figure 2. (a) Isopleths of capture fraction - well capture zone, (b) Groundwater age distribution

The examination of CFs with the groundwater ages, within the capture zone, will yield the mean age resulting from the mixing of the incoming recharge and the existing flows to the well. This union of information can, successively, help infer the effect of transients during the simulation period.

References

Anderson MP, Woessner WW, Hunt RJ (2015) Applied Groundwater Modeling: Simulation of Flow and Advective Transport. Academic Press

Castro MC, Goblet P (2005) Calculation of ground water ages-A comparative analysis. Ground Water 43(3):368–380. doi: 10.1111/j.1745-6584.2005.0046.x

Cornaton F, Perrochet P (2006) Groundwater age, life expectancy and transit time distributions in advective–dispersive systems; 2. Reservoir theory for sub-drainage basins. Advances in Water Resources 29:1292–1305. doi: 10.1016/j.advwatres.2005.10.010

Goode D (1996) Direct simulation of groundwater age. Water Resources Research 32(2):289–296. doi: 10.1029/98wr02536

Kazemi GA, Lehr JH, Perrochet P (2006) Groundwater Age. John Wiley & Sons, New Jersey

Molson JW, Frind EO (2012) On the use of mean groundwater age, life expectancy and capture probability for defining aquifer vulnerability and time-of-travel zones for source water protection. Journal of Contaminant Hydrology 127(1-4):76–87. doi: 10.1016/j.jconhyd.2011.06.001

Potter ST, Moreno-Barbero E, Divine CE (2008) MODALL: A Practical Tool for Designing and Optimizing Capture Systems. Ground Water 46(2):335–340. doi:10.1111/j.1745-6584.2007.00410.x

Varni M, Carrera J (1998) Simulation of groundwater age distributions. Water Resources Research 34(12):3271–3282. doi: 10.1029/98wr02536

11th World Congress on Water Resources and Environment (EWRA 2019)
"Managing Water Resources for a Sustainable Future", 25-29 June 2019, Madrid, Spain

Estimation of the flow parameters in unsaturated zone using shuffled frog leaping algorithm

M. Das*, B.G. Rajeev Gandhi, R. Kumar Bhattacharjya
Civil Engineering Department, Indian Institute of Technology Guwahati, Guwahati, India
** e-mail: mamtadas4@gmail.com*

Introduction

A major portion of the precipitation which falls onto the earth's surface eventually enters into the ground by the process of infiltration. This infiltrated water flows through the unsaturated zone and finally reaches the groundwater table. As a result, there is a change in soil moisture content within this zone. Due to the nonlinear behaviour of the process, the modelling of water flows through the unsaturated zone is highly complex and time-consuming. In order to develop an accurate simulation model in field scale along with the natural boundary condition, it is necessary to incorporate the soil and hydraulic parameters of the medium. But there are some parameters which are difficult to measure at the desired scale. Thus inverse optimization based parameter estimation techniques can be useful for developing the flow model in the unsaturated zone. In this technique, the numerical flow model for the unsaturated zone is coupled with the optimization model for finding the soil and hydraulic parameters. The optimization model can be solved using an optimization algorithm. However, due to the non-linear nature of the response function, the gradient based classical optimization algorithms are sometime not capable of finding the global optimal solution of the problem. On the other hand, the meta-heuristic optimization algorithms are proven to be effective algorithms in solving the inverse optimization model. One of such efficient meta-heuristic algorithm is Shuffled Frog Leaping Algorithm. In this study, a simulation-optimization based parameter estimation procedure is developed using Shuffled Frog Leaping Algorithm.

Materials and methods

A one-dimensional unsaturated flow model is developed under transient state condition. The model numerically simulates the mixed form of the Richards equation by finite-difference approximations using MATLAB. Since the equation is highly nonlinear and makes the computation more complex, a modified Picard iterative method is used to overcome the nonlinearity.

Governing Equation: Mixed form of the Richards equation for transient state condition (Tim and Mostaghimi 1991):

$$\frac{\partial\theta(h)}{\partial t}=\frac{\partial}{\partial z}\left[K(h)\left(\frac{\partial h}{\partial z}+1\right)\right] \tag{1}$$

h is the pressure head [L], θ is the volumetric water content [L^3L^{-3}], t is time [T], z is the spatial coordinate [L] and K is the unsaturated hydraulic conductivity function [LT^{-1}]. For the parameterization, the constitutive relations of $\theta(h)$ and $K(h)$ as given by van Genuchten (1980) is considered to develop the model.

$$\theta(h)=\theta_r+\frac{\theta_s-\theta_r}{\left(1+|\alpha h|^n\right)^m} \tag{2}$$

$$K(h)=K_s\frac{1-|\alpha h|^{n-2}\left[1+\left(|\alpha h|^n\right)\right]^{-m}}{\left[1+|\alpha h|^n\right]^{2m}} \tag{3}$$

where, m, n and α are unsaturated soil parameters. After the development of the simulation model in the unsaturated zone it is coupled with an optimization algorithm to estimate the flow parameters. The optimization algorithm solves the absolute error between the observed and the simulated heads. The

decision variables are the parameters that are to be estimated (5 parameters in this case). The objective function is defined as follows.

$$f = \sum_{n=1\ to\ Z}^{t=1\ to\ T} \left| OH_n^t - SH_n^t \right| \tag{4}$$

Shuffled Frog Leaping Algorithm is used as the optimization algorithm for estimating the parameters. This algorithm is based on the food search by an army of frogs in the swamp. They search for food by leaping onto the nearest possible rock and also communicating with the rest of the frogs for betterment. Thus, they develop a strategy where each individual leaps in their best possible way to get the maximum food with less time. The algorithm developed replicating this process is called the Shuffled Frog Leaping Algorithm (SFLA). The principle and philosophy of this algorithm is a combination of Shuffled Complex Evolution (SCE) and Particle Swarm Optimization (PSO). It is a population-based metaheuristic algorithm and a memetic algorithm. Fig. 1 shows the flowchart of the Shuffled frog leaping algorithm.

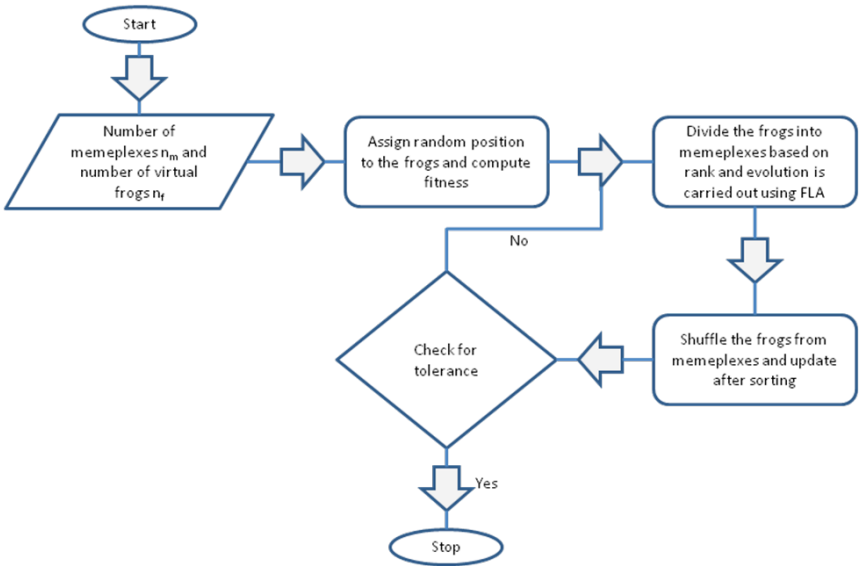

Figure 1. Shuffled frog leaping algorithm flowchart

Results and concluding remarks

The code developed for simulating the flow process in the unsaturated zone is validated using the finite-element 1D model HYDRUS 1D (Šimunek et al. 2012). The model predictions are in excellent agreement with the reported predictions. The parameter estimation algorithm developed is used to estimate the parameters, *i.e.* saturated moisture content (θ_s), residual moisture content (θ_r), saturated hydraulic conductivity (K_s), α and n are unsaturated soil parameters. The result obtained from the simulation-optimization model is given in the Table 1. From the obtained results it is clear that the predicted value of the parameter match reasonably well with the actual flow parameters.

Table 1. Estimation of the flow parameters

Parameters	θ_s	θ_r	**α**	**n**	**K_s**
Actual	0.3680	0.1020	0.0335	2.0000	0.00922
Predicted	0.3664	0.1052	0.0330	2.0038	0.00912

References

Eusuff M, Lansey M, Pasha F (2006) Shuffled frog-leaping algorithm: a memetic meta-heuristic for discrete optimization. Engineering Optimization 38(2):129-154. doi: 10.1080/03052150500384759

Šimunek J, Sejna M, Saito H, Sakai M, van Genuchten MT (2012) The HYDRUS-1D software package for simulating the one-dimensional movement of water, heat, and multiple solutes in variably-saturated media, Version 4.15, Riverside, California

Tim SU, Mostaghimi S (1991) Model for predicting virus movement through soils. Ground Water 29(2):251–259

Van Genuchten MT (1980) A closed-form equation for predicting the hydraulic conductivity of unsaturated soils. Soil Science society of America Journal 44(5):892-898

11th World Congress on Water Resources and Environment (EWRA 2019)
"Managing Water Resources for a Sustainable Future", 25-29 June 2019, Madrid, Spain

Study of water infiltration in soil by Richards equations in 3D: Summary and methodology validation

A. del Vigo[1*], S. Zubelzu[2], L. Juana[2]
[1] Universidad Politécnica de Madrid, E.T.S.I. de Agrónomos, Ciudad Universitaria s/n (28040) Madrid, Spain
[2] Dpto. Ingeniería Hidráulica. E.T.S.I. de Agrónomos, Ciudad Universitaria s/n (28040) Madrid, Spain
* e-mail: avigo@nebrija.es

Introduction

Study of water infiltration and its applications has been a notorious importance research field in the last two centuries. Resolution of Richard's equation has provided analytical (Philip 1969; Warrick 1974) and numerical models (Sayah et al. 2016) on one-, two-, or three dimensions that have described this phenomenon with reasonable accuracy in homogeneity ideal conditions. Even, there exist commercial software available (Šimůnek et al. 1998) that predict quite satisfactory water infiltration flow under ideal conditions. However, there still exist many situations that demand to develop new programs that let us reach even more accuracy to understand this phenomenon.

A scheme based on finite differences was developed in order to study 3-D water soil infiltration for axisymmetric conditions, via Richard's equation. The routine was validated throughout several paths: analytical solutions, numerical models and experiments that are summarized here. Preliminary results are also presented.

Materials and methods

Approximation via explicit finite differences scheme was been developed to solve axisymmetric Richards equation. A code based on matrix computations of the variables is presented here (Inf_3d). This scheme, is based on van Genuchten-Mualem characterization soils (Mualem 1976; Van-Genuchten 1980) that relates the hydraulic conductivity with water content.

A first validation with commercial software HYDRUS is presented (Figure 1); a second a validation with analytical results is given as well (Figure 2).

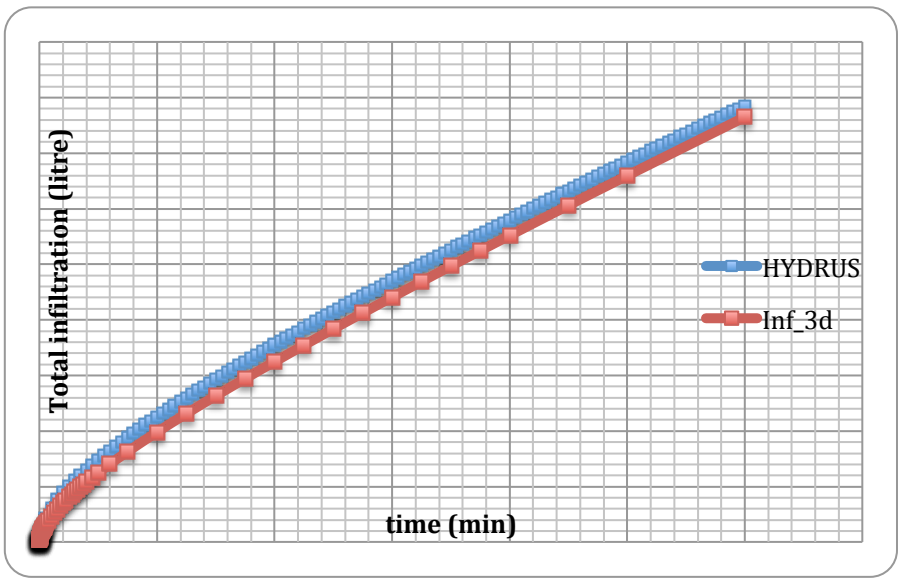

Figure 1. Infiltration comparison with time between commercial software Hydrus, and our simulations for a 6 cm radius saturated puddle in surface.

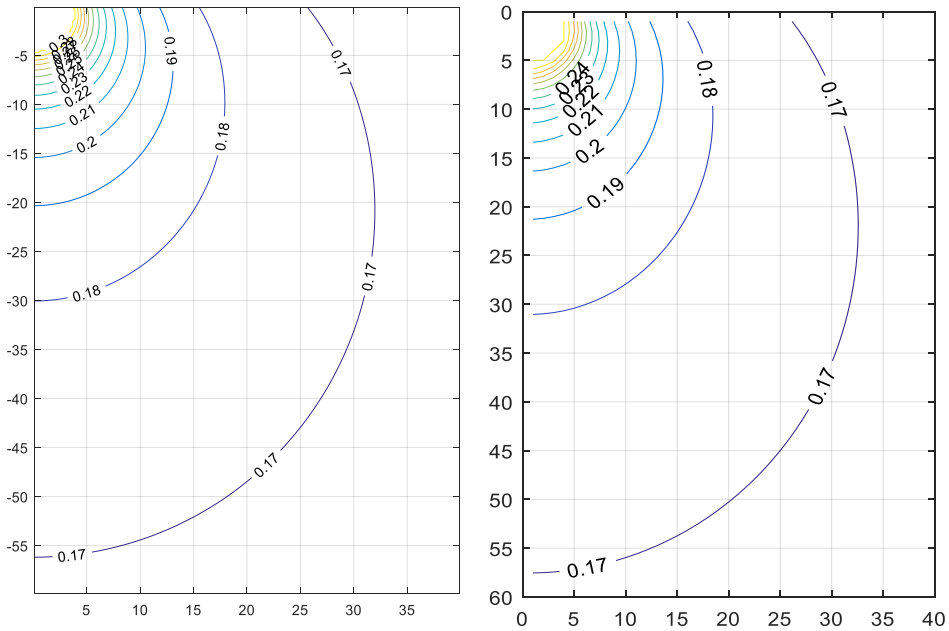

Figure 2. Water content comparison after 60 minutes of irrigate. (a) Analytical solution, (b) Inf_3d.

Results and concluding remarks

A summary of validation parameters are given in Table 1. Loam soil was used for validation with Hydrus; the rest of floor features may be found in the bibliography (Van Genuchten 1980; Warrick 1974).

Table 1. Summary of validation. Parameters used in the simulations.

	θ_0	θs	dr	dz	dt_{min}	Z_{max}	R_{max}
HYDRUS	0.2	0.43	1 cm	1 cm	0.000166 min	50 cm	50 cm
Analytical sol.	0.1653	0.3	1 cm	1 cm	0.000166 min	50 cm	50 cm

A satisfactory agreement is found in these and other performed tests, what confirms that our routine may be considered as an appropriate tool, to get new results in the theory of water infiltration.

References

Lomen DO, Warrick AW (1974) Time-dependent linearized infiltration: II. Line source. Soil Sci. Soc. Amer. Proc. 38:568

Mualem Y (1976) A new model for predicting the hydraulic conductivity of unsaturated porous media. Water Resource Journal 12:513

Philip JR (1969) Theory of Infiltration. Advances in hydro-science. Academic Press, New York

Sayah B et al. (2016) Development of one-dimensional solutions for water infiltration. Analysis and parameters estimation. Journal of Hydrology 535:226-234

Šimůnek J el al. (1998) The HYDRUS code for simulating the one-dimensional movement of water, heat, and multiple solutes in variably-saturated media. Research Report No. 144, U.S. Salinity Laboratory, USDA-ARS, Riverside, California

Van Genuchten MT (1980) A closed-form equation for predicting the hydraulic conductivity of unsaturated soils. Soil Science Society of America Journal (44):892

Warrick AW (1974) Time-dependent linearized infiltration: I. Point source. Soil Sci. Soc. Amer. Proc. (34):383

11th World Congress on Water Resources and Environment (EWRA 2019)
"Managing Water Resources for a Sustainable Future", 25-29 June 2019, Madrid, Spain

Agronomic and groundwater nitrate contamination modelling in rural basin, central Greece

P. Sidiropoulos[1*], G. Tziatzios[1], L. Vasiliades[1], N. Mylopoulos[1], A. Loukas[2]
[1] Department of Civil Engineering, University of Thessaly, Volos, Greece
[2] School of Rural and Surveying Engineering, Aristotle University of Thessaloniki, Thessaloniki, Greece
* e-mail: psidirop@civ.uth.gr

Introduction

Nowadays, numerical simulation tools are applied widely in the hydrogeology field with the purpose of describing and investigating the groundwater flow, the ground water budget, as well as the fate and transport of contaminants in subsurface environment (Karatzas 2017). In addition to this, there is plenty of literature dealing with the interaction of surface water and groundwater. On the other hand, a knowledge gap exists on the interaction among surface water, unsaturated zone and finally groundwater. As a result, the exploitation of agronomic simulation tools is utilized in order to add the necessary knowledge among the interaction of surface water - soil - groundwater system (Peña-Haro et al. 2009).

Lake Karla watershed is selected as field of study. The plain of Lake Karla is situated at the southern eastern part of eastern hydrogeological basin of Thessaly. It constitutes the main agricultural region of the Greek territory, and therefore, it is intensively cultivated, irrigated and fertilized using nitrogenous substances (Sidiropoulos et al. 2018). There is lack of relative bibliography about the interaction of agronomic simulation, surface and groundwater hydrology in Greece compared with Europe. In this paper, agronomic simulation is examined for two cultivated periods, 2009 and 2015.

Materials and methods

The proposed modelling approach is illustrated in Figure 1. It is developed based on physical processes, which take place in surface – soil – ground water system and are in close interaction to each other. Each of these processes is simulated using 6 different numerical simulation models.

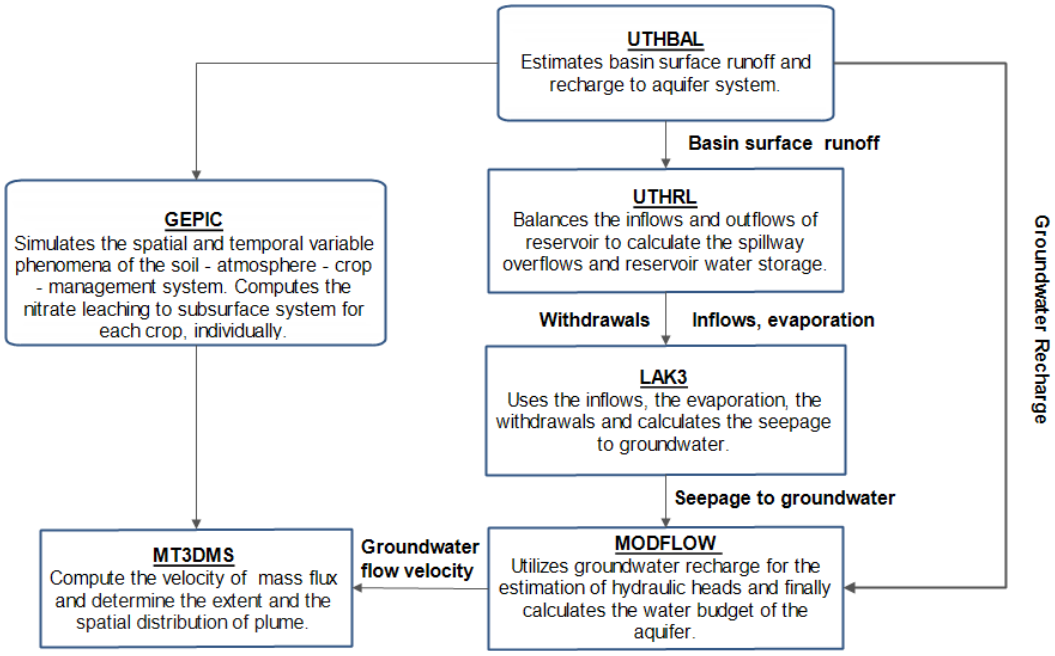

Figure 1. The methodological approach of the modelling system.

Results and concluding remarks

Agronomic simulation consists a noticeable tool for the study of groundwater quality in agricultural regions. Percent nitrate leaching results, field by field, for the two periods are presented in Figure 2. The nitrate loss rate ranges from 0 to 44 %. Differences are very small in the area of cultivated land in the two periods. On the contrary, there is a different crop type strategy in 2015, which have led to the decrease of nitrate loss to the subsurface. The crops that prevailed in the area in 2009 were crops with high nitrogen requirements such as cotton, wheat and maize. Therefore, in addition to policies of good agricultural practice which should be applied, in order to reduce nitrate leaching to the subsurface, it is important to also change the current crop pattern and turn to cultivations which do not require high rate of nitrogen fertilizing such as almond trees, walnut trees, pistachios etc.

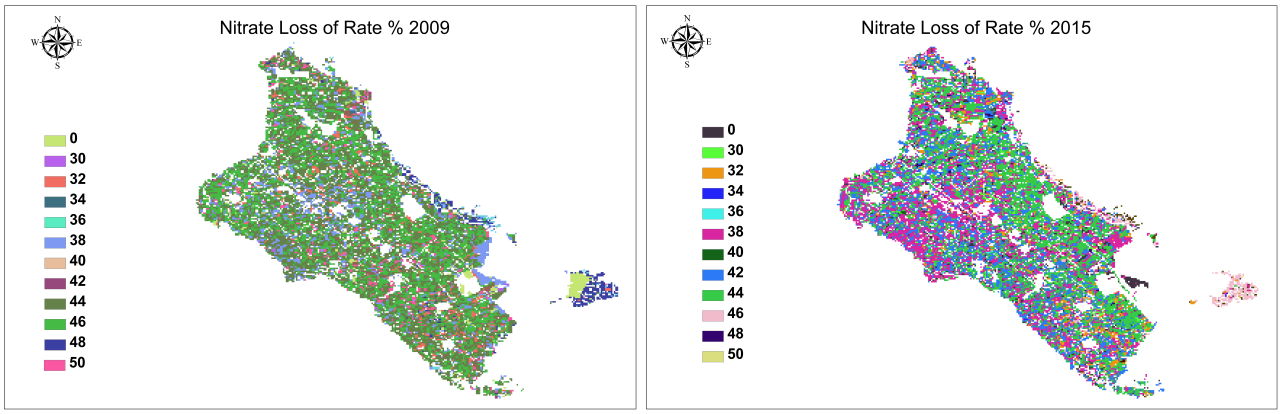

(a) *(b)*

Figure 2. Nitrate loss of rate (%) a) portrays the nitrate loss of rate for 2009 cultivated period and b) illustrates the nitrate loss of rate for 2015 cultivated period

Acknowledgments: Dr. Pantelis Sidiropoulos is a post-doctoral scholar of Stavros Niarchos Foundation and the University of Thessaly. Part of the scientific publication was held within the framework of the invitation "Granting of scholarship for Post-Doctoral Research" of the University of Thessaly, which is being implemented by the University of Thessaly and was funded by the Stavros Niarchos Foundation. Georgios Tziatzios has been co-financed - via a programme of State Scholarships Foundation (IKY) - by the European Union (European Social Fund - ESF) and Greek national funds through the action entitled “Scholarships programme for postgraduates studies -2nd Study Cycle” in the framework of the Operational Programme “Human Resources Development Program, Education and Lifelong Learning” of the National Strategic Reference Framework (NSRF) 2014 – 2020. We are immensely grateful to Mrs Konstantina Konovesi and Mr. Konstantinos Lois from OPEKEPE as well as to Georgia Pappa and Ioannis Chrysiados from the Ministry of Agricultural Development and Food, for the cultivation and land use data series.

References

Karatzas GP (2017) Developments on Modeling of Groundwater Flow and Contaminant Transport. Water Resources Management 31:3235-3244. https://doi.org/10.1007/s11269-017-1729-z

Peña-Haro S, Velazquez PM, Sahuquillo A (2009) A hydro-economic modelling framework for optimal management of groundwater nitrate pollution from agriculture. Journal of Hydrology 373:193-203. doi: 10.1016/ j.jhydrol.2009.04.024

Sidiropoulos P, Tziatzios G, Vasiliades L, Papaioannou G, Mylopoulos N, Loukas A (2018) Modeling Flow and Nitrate Transport in an Over-Exploited Aquifer of Rural Basin Using an Integrated System: The Case of Lake Karla Watershed. Proceedings of 3rd EWaS International Conference on “Insights on the Water-Energy-Food Nexus”, Lefkada Island, Greece, 27–30 June 2018, 2, 667. http://doi.org/10.3390/proceedings2110667

Hellenic Ministry of Rural Development and Food (2015) Greek Payment Authority of Common Agricultural Policy (C.A.P.) Aid Schemes (OPEKEPE). Integrated Cultivation Management System for 2006-2015

11th World Congress on Water Resources and Environment (EWRA 2019)
"Managing Water Resources for a Sustainable Future", 25-29 June 2019, Madrid, Spain

Coastal aquifer characteristics determination based on in-situ observations: River Neretva Valley aquifer

I. Lovrinovic[1], V. Srzic[1*], M. Vranjes[1], M. Dzaja[2]
[1] Department of Water Resources, Faculty od Civil engineering, Architecture and Geodesy, University of Split, Split, Croatia
[2] HIGRA, HIdrological observations, Split, Croatia
* e-mail: veljko.srzic@gradst.hr

Introduction

Saltwater intrusion in coastal aquifers has been widely investigated in last few decades primarily due to the negative effects to the agricultural yield in coastal areas. To mitigate salt-water intrusion, traditional surveys like geo-electric and/or seismic reflection/refraction are often used with a goal to identify necessary aquifer characteristics. Compared to abovementioned techniques, which can be financially high demanding, tidal methods are shown to be successful and effective for determination of coastal aquifer parameters in many coastal areas around the world (Zhou et al. 2006; Xia et al. 2007; Zhou 2008).

Although the hydrogeological site characterization procedure of river Neretva valley started in 1960s, no completely clear picture has been conducted up to date. To handle the problem of the saltwater intrusion and piezometric state dynamics, a monitoring system has been established during last 10 years within the area. In this paper we take into consideration: i) available "soft" aquifer data: borehole information and slug test results, and ii) observed data of long-term sea level oscillations and piezometric head observed in a borehole positioned 85 m away from the coastline towards inland, to determine river Neretva Valley aquifer parameters, respectively: hydraulic diffusivity, storativity and transmissivity. To our best knowledge, this is the first paper dealing with determination of Neretva aquifer parameters determination although the area is of great agricultural importance.

Materials and methods

Findings rely on continuous observations of long-term sea level oscillations and piezometric head oscillations within the borehole located inside the area of interest. We start our analysis with inspection of the features of the observed time series in frequency domain. The analyses demonstrate significant correlation of the long-term sea level oscillations and piezometric head oscillations thus emphasizing sea level as a main driving force for the groundwater oscillations.

To determine aquifer parameters, we use analytical tidal method approaches (Jiao and Tang 1999; Dong et al. 2012) relying on previously known solutions of groundwater head oscillation under different conditions to capture for observed piezometric head features within the aquifer (Figure 1). Hereby, sea level is used in two different ways depending on the applied tidal method capability: i) observed sea level signal and ii) approximation of the observed sea level signal with appropriate number of frequency components whose parameters are determined via Monte Carlo approach.

Tidal efficiency and time lag values have been determined directly from observed time series, while slug test and borehole geological information are used to verify appropriate geological setup which has been investigated within the conducted laboratory experiment.

Finally, tidal methods are applied with incorporated soft aquifer data to define river Neretva Valley aquifer parameters. The proposed methodology couples in-situ observations, analytical and experimental approach.

Results and concluding remarks

Main results arose from the conducted analyses can be summarised as follows: i) river Neretva Valley aquifer is shown to be under significant influence of sea level oscillations; ii) the analysis has been done for

the dry hydrological period thus neglecting external influence (e.g. rainfall, irrigation system, etc.), iii) results demonstrate qualitatively good approximation of results obtained under laboratory conditions to mimic nature of tidal propagation through aquifer thus enabling determination of aquifer characteristics when coupled by proper analytical approach, iv) determined Tidal efficiency equals to 0.3, while Time lag corresponds to 2.50 hours, v) obtained aquifer parameters correspond to values typically found within dominantly gravely to gravely-sand aquifers.

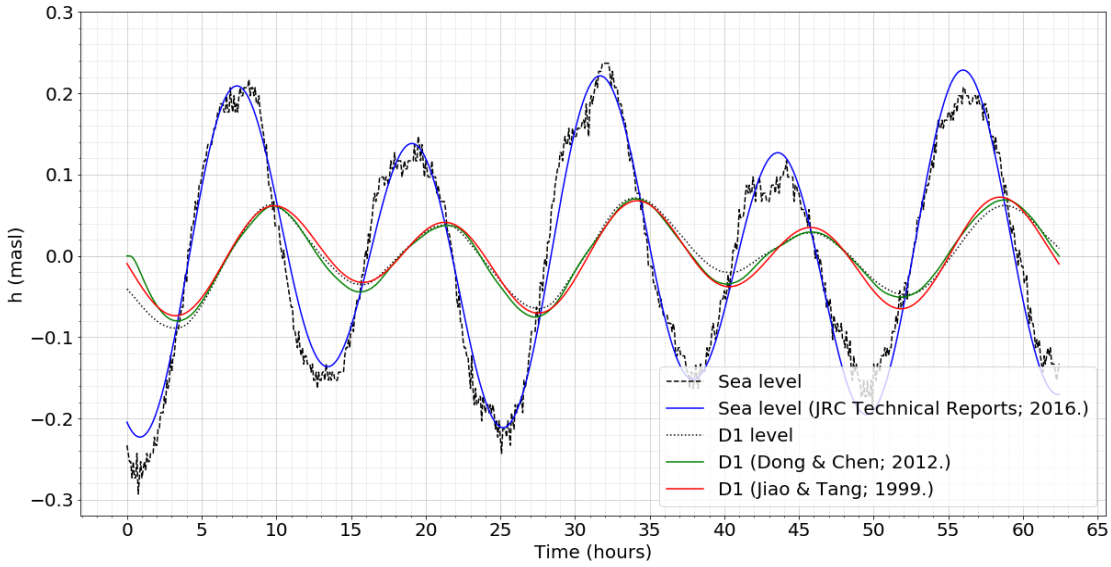

Figure 1. Observed and modelled sea level and borehole piezometric head oscillations

References

Jiao JJ, Tang Z (1999) An analytical solution of groundwater response to tidal fluctuation in a leaky confined aquifer. Water Resources Research 35(3):747-751

Zhou X, Chuanxia R, Yanyan Y, Bin F, Yecheng O (2006) Tidal effects of groundwater levels in the coastal aquifers near Beihai, China. Environmental Geology 51:517-525. doi: 10.1007/s00254-006-0348-4

Xia Y, Li H, Boufadel MC, Guo Q, Li G (2007) Tidal wave propagation in a coastal aquifer: Effects of leakages through its submarine outlet-capping and offshore roof. Journal of Hydrology 337:249-257. doi:10.1016?j.jhydrol.2007.01.036

Zhou X (2008) Determination of aquifer parameters based on measurements of tidal effects on a coastal aquifer near Beihai, China. Hydrological Processes 22:3176-3180. doi: 10.1002/hyp.6906

Dong L, Chen J, Fu C, Jiamg H (2012) Analysis of groundwater-level fluctuation ina acoastal confined aquifer induced by sea-level variation. Hydrogeology Journal 20:719-726. doi: 10-1007/s10040-012-0838-2

Annunziato A, Probst P (2016) Continuous harmonics analysis of sea level measurements: Description of a new method to determine sea level measurement tidal components. JRC Technical Reports, EUR 28308 EN. doi: 10.2788/4295

11th World Congress on Water Resources and Environment (EWRA 2019)
"Managing Water Resources for a Sustainable Future", 25-29 June 2019, Madrid, Spain

Origin of an industrial pollution in Berrahal aquifer system, Algeria

A. Hani*, H. Khelfaoui, H. Chaffai, S. Hani, N. Bougherira, L. Djabri
Department of Geology, Badji Mokhtar Annaba University / Water resource and sustainable development Laboratory, Annaba, Algeria
** e-mail: haniazzedine@hotmail.com*

Introduction

Industrial effluents mixed with water are one of the independent sources of the environment's toxicity. They do not only affect water quality, but they also have a negative impact on the microflora of the ground and the watery ecosystem (Arminder et al. 2010). In addition to the concentration of metals in subterranean water influenced by anthropic activities such as mining and metal extraction (Coynel et al. 2007), the contamination of subterranean water by heavy metals was the subject of several scientific works because of their low biodeterioration and their toxic effects.

Currently, industrial effluents in the area of Berrahal contain important quantities of organic and inorganic chemicals and other polluting substances (Khelfaoui et al. 2013). The majority of the companies are not connected to any network of cleansing, and even if such thing exists, this does not function in a suitable way. Consequently, these liquid industrial effluents, which are strongly colored and toxic, run out with free air and join at Lake Fetzara, so they contribute later to the contamination of surface and subterranean waters. Around the industrial park of Berrahal, the degree of contamination was very intense in certain sectors. Formerly, the area had an agricultural function, and none of the production facilities made a provision to reduce industrial effluents. The soil was regarded as a medium ready to absorb all kinds of products (heavy metals, waste) without having to deteriorate its normal function. Agricultural production decreased considerably, and aquatic life in Lake Fetzara became strongly polluted and eventually disappeared. In this study, we come to clear up the impact of these industrial activities on the area as well as identify the potential points responsible for the deterioration of water quality through the use of statistical methods based on principal component analysis (PCA) and discriminant factorial analysis (DFA).

Materials and methods

The town of Berrahal is located 30 km west of the city center of Annaba in the extreme northeast of Algeria. The industrial park of Berrahal is located at the southwest of Berrahal at a distance of approximately 2 km; it has an area of 1.21 km^2, is surrounded by some secondary agglomerations (Guiche and Tacha), and currently comprises 82 plots and 28 active companies.

As a whole, the low hills of the area of Berrahal form the southern repercussion of Edough, giving rise to the small solid mass of Berrahal which is the continuity of the solid mass of Edough; it is spread out in slopes with a north–south orientation. The process of individualization of this small solid mass and its installation in the regional context is due to the violent folding that has affected the area.

Edough is almost made up of rocks that underwent a degree of variable metamorphism, justified by the order of appearance indicating metamorphic minerals such as chlorite, andalusite, kyanite, sillimanite, and garnets. To identify and locate the aquiferous systems, one will have to use the stratigraphic columns of three drillings established in this area and will have to define the relations between various water tables which are presented as follows:

- The unconfined aquifer consists of fine sand and gravel. It has a thickness that does not exceed 10 m in the east part of Berrahal, whereas it reaches 20 m in the western part.
- The semi-confined aquifer made up of cipolin is located on the level of fissured metamorphic limestone and is separated from the unconfined aquifer by a thin layer of gravelly clay (3 m) which constitutes the roof in the eastern part of the studied zone. The formation of gneiss and mica schists constitutes the substratum of this aquifer, which has a thickness of about 2 m.

Results and concluding remarks

PCA thus reveals three types of water quality in the area of Berrahal: the first one has natural chemical composition, the second has high mineralization, and the third is polluted by organic substances marked by BOD_5 and NO_2. According to the first classification of DFA, it is clearly visible that G2 (which represents the points beside the industrial park) and G3 (which carries all of the industrial wastes) are the groups where high mineralization and bad quality in organic matters of water in the area of Berrahal originated, whereas G1 has kept its quality quite distinctly from its neighbouring sources of pollution. The additional samples are generally affected and appear the same as with the samples of their assigned groups. For the misclassified samples, only point 1P17, which is reallocated from G2 to G1, is perfectly strict since it is on a high piezometric level on the watershed, which maintains to be relatively far from pollution.

For DFA of the second and third classifications, all indicators of pollution and bad water quality that are organic or mineral appear at groups Gr1 and Gr3 (agroalimentary and soap factory and hydrocarbons), and that shows the effect of the two types of activity on the underground water quality of Berrahal. The samples of G2 (metals) that intercalate within the three other groups are in a state of transition, which seems to eventually deteriorate the natural water quality of G1 if a rapid intervention for the treatment of industrial wastewaters of companies and the establishment of a suitable network of cleansing is done. The spatial distribution of samples of the first experiment on the piezometric map of the area as well as the reassignment of the misclassified samples show that samples of natural water (G1), which are relatively far from the industrial park (in the south), are vulnerable to pollution coming from wastewater of industrial activities, whereas those at the centre of the area are at a great risk to be polluted (Figure 1).

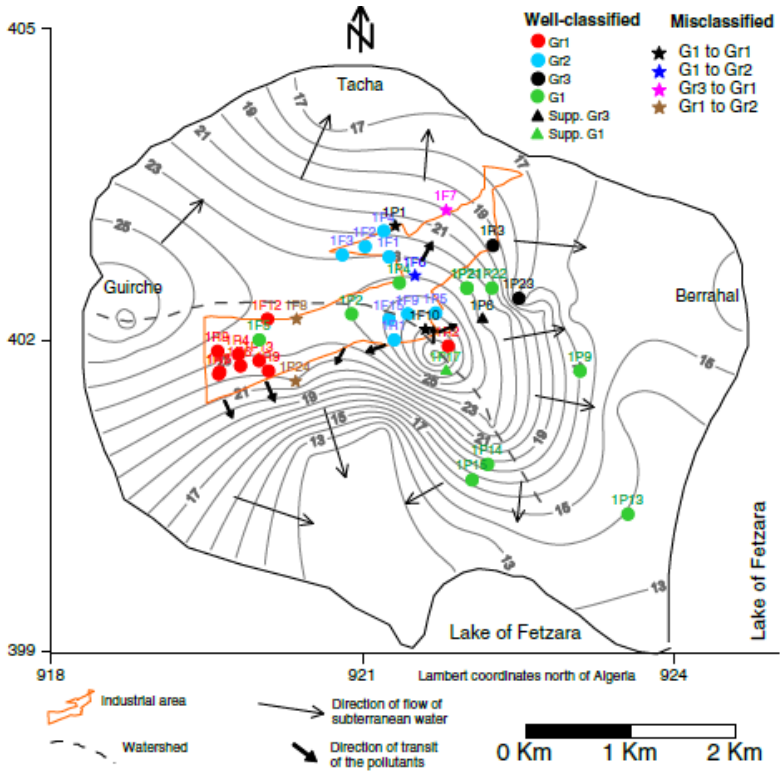

Figure 1. Distribution of well-classified and misclassified samples on the piezometric bottom of the area. Classification by industrial activity type according to the chemical composition of natural water

References

Arminder K, Siddharth V, Sumit R, Ankit B, Jharna G, Ranjeet ST, Komal KG (2010) Physicochemical analysis of the industrial effluent and to their impact on the soil microflora. Procedia Environ Sci 2:595–599

Coynel A, Schafer J, Dabrin A, Rirardot NR, White G (2007) Groundwater contributions to metal transport in small river affected by mining and smelting waste. Water Res 41:3420–3428. doi:10.1016/ j.watres.2007.04.019

Khelfaoui H, Chaffai H, Mudry J, Hani A (2013) Use of discriminant statistical analysis to determine the origin of an industrial pollution type in the aquiferous system of the area of Berrahal, Algeria. Arab J Geosci 6:4517–4527

11th World Congress on Water Resources and Environment (EWRA 2019)
"Managing Water Resources for a Sustainable Future", 25-29 June 2019, Madrid, Spain

Upward transport of trichloroethylene vapour in a soil column

C.-S. Fen*, C. Tsoa, P. Yen
Department of Environmental Engineering and Science, Feng Chia University, Taichung, Taiwan, ROC
** e-mail: csfen@fcu.edu.tw*

Introduction

Vapour phase migration of volatile organic compounds (VOCs) from contaminated groundwater or soil into overlying buildings, termed as vapour intrusion (VI), has received increased attention in many countries during the last two decades, because long-term indoor exposure even at relatively low vapour concentrations may cause human health problems. In particular, VI of Trichloroethylene (TCE) may also pose acute health risk to persons residing or working in the buildings (Hosangadi et al. 2017). Many mathematical models have been developed and used as a tool in conjunction with field investigation data, as part of a multiple-lines-of-evidence approach for evaluating VI pathways. However, these models so far lack validation (Yao et al. 2013), which limits the confidence of these models in prediction.

For vapour phase migration originating from liquid, sorbed or dissolved VOCs in subsurface under natural conditions, gas diffusion and advection both can be important. Particularly, dense vapours or light hazardous gases mixed in the air may substantially alter the density of gas mixtures in the subsurface and induce density-driven transport. Vapour phase diffusion is usually described by Fick's law which has been adopted in most of the gas phase transport models. The dusty gas model (DGM) equations, however, are more complete and rigorous for multicomponent gas diffusion in porous systems.

The purpose of this study is to investigate flux mechanisms controlling upward transport of a dense vapour in soils and to assess the predictability of gas phase transport models on this scenario. We conducted experiments to investigate vertically upward transport of TCE vapour in a soil column. Pressure difference between the column ends and TCE vapour concentration at the column ends were measured. Two gas phase transport models, Michigan Soil Vapour Extraction Remediation (MISER; Abriola et al. 1997) and DGM-based Gas Phase Transport (DGPT; Fen 2014), were applied to simulate the transport scenario of the experiment. MISER and DGPT are based on Fick's law and the DGM equations, respectively, for gas phase diffusion.

Materials and methods

The whole set of the transport experiment consists of a glass column packed with quartz sand, a pressure differential to record gas pressure differences between the column ends and two glass cells at each end of the column. Each of the glass cells was sealed with the column end by the use of bolt clips and grease. The soil column is 11 cm in length and was placed vertically. The transport experiment was started with injecting a volume amount of TCE liquid (96% pure) into the cell at the bottom of the column. Gas samples were then taken periodically from both ends of the soil column and from the cell at the top of the column for measuring TCE concentration.

We simulated vertically upward migration of TCE vapour through the soil column as a one-dimensional closed system: a closed top (the downstream end) and a constant TCE vapour concentration assigned at the bottom of the column (the upstream end).

Results and concluding remarks

The transport experiment was conducted several times. We found that gas mixture in the cell where TCE liquid retained at the bottom of the column did not attain a saturated TCE vapour concentration (around 0.5 g/L) for each experiment lasting over 8 hours. TCE concentration measured at the bottom of the column was 0.031 g/L when the connected cell is 5 cm in height and 0.08 g/L when the cell is 2.5 cm in height. Even the upstream vapour concentration was measured as low as 0.031 g/L, the downstream TCE concentration

hardly approached this level. The result of gas pressure measurement showed that gas pressure at the upstream end of the column is more than that at the downstream one for only 0.2~0.7 Pa.

TCE vapour migration upwardly in the column was simulated with MISER and DGPT by assigning the upstream end of the column at a constant TCE vapour concentration of 0.031 (or 0.08 g/L) and a closed top boundary. Temporal evolution of the TCE vapour concentration at the downstream end predicted by MISER was somewhat lagged behind the one predicted by DGPT. However, for an opened column system, Fen et al. (2018) showed that the downstream evolution profile predicted by MISER was ahead of the DGPT result. These predicted profiles gradually reached the concentration level as the upstream one for 8-hour transport simulations. It was shown that, as the upstream concentration was greater, the deviation between the model predicted downstream profile and the measured one was more substantial. We suspected that leaking occurred from the sampling septum located on the cell at the downstream end of the column during the transport experiment. Thus, the upward transport of the TCE vapour was under a semi-opened condition in our experiment. In addition, the gravitational force needs to be considered to predict vapour phase transport. Without considering the gravitational force, we may over-predict vapour phase transport of dense vapour migrating upwardly in an opened system and may under-predict it in a closed system.

Acknowledgments: Financial support for this study was provided by the Ministry of Science and Technology in Taiwan (contract no. 106-2221-E-035-008-MY3).

References

Hosangadi V, Shaver B, Hartman B, Pound M, Kram M, Frescura C (2017) High-frequency continuous monitoring to track vapor intrusion resulting from naturally occurring pressure dynamics. Remediation 27:9-25. doi: 10.1002/rem.21505

Yao Y, Shen R, Pennell KG, Suuberg EM (2013) A review of vapor intrusion models. Environmental Science Technology 47:2457-2470

Abriola LM, Lang J, Rathfelder K (1997) Michigan soil vapor extraction remediation (MISER) model: a computer program to model soil vapor extraction and bioventing of organic chemicals in unsaturated geological material, U.S. Environmental Protection Agency, Office of Research and Development, National Risk Management Research Laboratory, Cincinnati, OH

Fen CS (2014) Assessing vadose zone biodegradation by a multicomponent gas transport model. Vadose Zone Journal 13(1). doi: 10.2136/vzj2012.0179

Fen CS, Sun Y, Cheng Y, Chen Y, Yang W, Pan C (2018) Density-driven transport of gas phase chemicals in unsaturated soils. Journal of Contaminant Hydrology 208:46-60

11th World Congress on Water Resources and Environment (EWRA 2019)
"Managing Water Resources for a Sustainable Future", 25-29 June 2019, Madrid, Spain

Numerical model of groundwater flow using MODFLOW: Application to western Bursa, Turkey

S. Korkmaz[1*], M.Z. Keskin[2]
[1] Department of Civil Engineering, Uludağ University, Bursa, Turkey
[2] Orhangazi Municipality, Directorate of Reconstruction and Urbanization, Bursa, Turkey
* e-mail: skorkmaz06@gmail.com

Introduction

Several pieces of software are available in the field of groundwater modeling. Among them are: MODFLOW (McDonald and Harbaugh 1988), MIKE-SHE (Refsgaard and Storm 1995) and MODHMS (Panday and Huyakorn 2004). MODFLOW is the most widely used model. For example, Gaur et al. (2011) used Geographic Information Systems (GIS) for watershed management and MODFLOW for groundwater modeling in the study of the Banganga River basin. Wang et al. (2015) modeled the effect of precipitation density on groundwater levels with MODFLOW. Korkmaz et al. (2016) modeled the underground and surface water flow of Eskişehir basin with MODFLOW for transient conditions. Nkhonjera et al. (2017) investigated the importance of direct and indirect effects of climate change on groundwater of the Olifants River basin by basin modeling. Boughariou et al. (2018) modeled the aquifer behavior in the Sfax region of Tunisia by using GIS and MODFLOW 2000 under climate change and high consumption conditions. Liu et al. (2018) conducted basin modeling with MODLFOW in order to investigate the effects of intensive agricultural activities on the groundwater dynamics in the oasis regions of the arid inland river basins in northwestern China.

The aim of this study is to develop a numerical model of groundwater distribution in the part of Susurluk Basin located within the boundaries of Karacabey and Mustafakemalpaşa districts of Bursa, Turkey. Within this scope, daily water levels of 5 observation wells between years 2013 and 2015 were acquired. Daily precipitation and evapotranspiration values of the stations in the region were obtained from the General Directorate of Meteorology. In GIS environment, the wells were marked as points and boundaries of the basin were determined using a topographic map and Digital Elevation Model. Maps of aquifer boundaries and well locations were transferred to MODFLOW and a grid with a resolution of 150 m x 150 m was generated. By entering precipitation and evapotranspiration values of the years 2013-2015, the groundwater level distribution of the basin was computed. Hydrologic parameters were estimated.

Materials and methods

Initially, the data of 5 observation wells were acquired from State Hydraulic Works. Three of these wells are located in Karacabey and two in Mustafakemalpaşa districts in Bursa. The data includes hourly water and barometric pressures recorded between 2013 and 2015. The external parameters that affect the groundwater level of the basin are precipitation and evapotranspiration. Daily precipitation and evapotranspiration values measured between 2013 and 2015 at observation stations in Karacabey and Mustafakemalpaşa were obtained from the General Directorate of Meteorology.

Basin delineation was done in GIS environment. Aster GDEM raster files with a resolution of 30 m x 30 m were used to determine the basin area. The raster file was converted to point heights for use in MODFLOW. Hydrological analysis of the basin was performed using the ArcHydro toolbar. Shape files were created and the wells, rivers, lakes and meteorological stations in the basin are plotted on the map.

Numerical modeling was done in GMS program. GMS is a program that provides graphical interface for MODFLOW. GMS generates and records input data for and visualizes the output from MODFLOW. Files transferred from the GIS environment to the GMS appear as shape files. These files were transferred to the newly created conceptual model in order to transfer the spatial data to MODFLOW grid. The grid cell size was 150 m in x-direction, 150 m in y-direction, and cell number 1 in z-direction.

MODFLOW 2005 was used for modeling and model type was selected as transient state. LPF (Layer Property Flow) was selected as the flow package and PCGN was selected as the solver. Point elevations were used as surface elevations in MODFLOW. The rivers in the basin were modeled with the RIV1 package. In order to use the RIV1 package, the conductivity value (C, m^2/day) must be entered. In addition, water surface elevation and river bottom elevation should be entered for the river. The water surface elevation of the lake in the northeast of basin was entered as specified head using the CHD1 package. DRN1 package was used to model the drains in the basin. In DRN1 package, the conductivity value (C) of the channel and the bottom elevation of the drain must be specified. RCH1 package was used for precipitation in the basin and EVT1 package was used for evapotranspiration (ET). EVT1 package requires the maximum ET rate and the extinction depth to which the evapotranspiration will be applied.

The constant head boundary condition was used for rivers along the eastern, northern, and southeastern boundaries of the basin. Other boundaries were specified as impermeable boundaries. Hydraulic conductivity was determined by calibration using the PEST (Parameter Estimation) model within the range of 5 to 500 m/day. In PEST simulations, the observed groundwater levels were compared with the values calculated by MODFLOW. After the calibration was completed, the groundwater distribution of the basin was determined for all years.

Results and concluding remarks

In this study, a numerical model of groundwater distribution in the Susurluk basin within the boundaries of Karacabey and Mustafakemalpaşa districts of Bursa province was developed. In GIS environment, the basin hydrological features were drawn as shape files in GIS environment and then transferred to the MODFLOW interface, namely, GMS. The necessary data was mapped to MODFLOW grid. Modeling of the basin was made in transient state. Hydraulic conductivity values were determined using the PEST model. Generally, an agreeable fit was observed between simulated and observed hydraulic heads. In days of excessive precipitation and low evaporation groundwater levels increased. An important part of the basin is composed of alluvial lands, and hence, the high hydraulic conductivity caused the water to spread more easily in the aquifer creating a fluctuation within a tight range.

References

Boughariou E, Allouche N, Jmal I, Mokadem N, Ayed B, Hajji S, Khanfir H, Bouri S (2018) Modeling aquifer behaviour under climate change and high consumption: Case study of the Sfax region, southeast Tunisia. Journal of African Earth Sciences 141:118-129

Gaur S, Chahar BR, Graillot D (2011) Combined use of groundwater modeling and potential zone analysis for management of groundwater. International Journal of Applied Earth Observation and Geoinformation 13(1):127-139

Korkmaz S, Pekkan E, Güney Y (2016) Transient analysis with MODFLOW for developing water-diversion function. Journal of Hydrologic Engineering 21(6):1-11

Liu M, Jiang,Y, Xu X, Huang Q, Huo Z, Huang G (2018) Long-term groundwater dynamics affected by intense agricultural activities in oasis areas of arid inland river basins, Northwest China. Agricultural Water Management 203(30):37-52

McDonald MG, Harbaugh AW (1988) A modular three-dimensional finite-difference ground-water flow model. Techniques of Water-Resources Investigations, U.S. Geological Survey, Denver, 586

Nkhonjera GK, Dinka MO (2017) Significance of direct and indirect impacts of climate change on groundwater resources in the Olifants River basin: A review. Global and Planetary Change 158:72-82

Panday S, Huyakorn PS (2004) A fully coupled physically-based spatially-distributed model for evaluating surface/subsurface flow. Advences in Water Resources 27:361-382

Refsgaard JC, Storm BJ (1995) MIKE SHE. In: Computer Models of Watershed Hydrology, Singh VP (ed), Water Resources Publications, Littleton, Colorado, USA, pp 809-846

Wang H, Gao JE, Zhang M, Li X, Zhang S, Jia L (2015) Effects of precipitation intensity on groundwater recharge based on simulated precipitation experiments and a groundwater flow model. CATENA 127:80-91

11th World Congress on Water Resources and Environment (EWRA 2019)
"Managing Water Resources for a Sustainable Future", 25-29 June 2019, Madrid, Spain

A hybrid GIS-Shannon Entropy framework for artificial recharge in arid regions plain

S.A. Sajadi[1*], S. Shojaie[2], M. Kholghi[1]
[1] Department of Irrigation & Reclamation Engineering, University of Tehran, Karaj, Tehran, Iran
[2] Department of Geology, College of basic science, Islamic Azad University of Zahedan, Zahedan, Iran
* e-mail: s_ahmadsajadi@ut.ac.ir

Introduction

Nowadays, due to the rapid expansion in agriculture and industrial practices, and a downward trend in precipitation in arid and semi-arid regions of the world, including but not limited to Iran, aquifers, and groundwater resources have been harmed immensely. Accordingly, the aforementioned factors have caused a significant drop in aquifers' water tables and degraded the quality of these natural resources. Using stormwater run-offs as a source to artificially recharge aquifers can be seen as an approach to sustain groundwater resources. However, given the expensive nature of artificial recharge projects, it is crucial to opt for a suitable charging place (Kalantari et al. 2010). Most practiced frameworks for locating these charging places are challenging and time-consuming, which causes making errors along the way inevitable. Utilizing geographic information system (GIS) and multi-attribute decision-making methods proved to be a practical and efficient approach for these site selection process (e.g., Senanayake et al. 2016; Selvarani et al. 2017).

Artificial recharge of aquifers can be seen as a sustainable remedy to cope with the looming water crisis in Iran (Madani 2014). Gezir plain, located in southern part of Iran, for instance, is one of these cases where the deterioration of the aquifer's water quality and dramatic drop of its water-table have forced the local authorities to ban extracting water from this aquifer even for drinking and sanitation purposes. In this study, however, a combination of geographic information system (GIS) and Shannon's Entropy were utilized to select the most suitable location for artificial recharge wells in Gezir plain.

Materials and methods

Considering the case studies' geographic characteristics, socio-economic conditions, environmental concerns, and based on the advice of experts, the following criteria were used as evaluation factors: Hydraulic conductivity, type of alluvial deposits, the depth of the water table, land use, topography, type of soil, and the chemical component of the water (i.e., EC of the water). Using GIS, these criteria were combined. But one must first attempt to quantify the importance of each evaluation factor (i.e., assign the proper weight) in the site selection process.

Since the introduction of the Entropy concept (Shannon 1948), it was employed as an effective instrument to cope with uncertainty and instability (Pourghasemi et al. 2012). In essence, this multi-attribute decision-making method tend to assign the highest weight (e.g., associated with the most critical criterion) to an evaluation criterion with the highest dispersity in its values. For further information on this method and its mathematical instruction, the readers can refer to Pourghasemi et al. (2012).

Results and concluding remarks

The first step is to incorporate the experts' assessment into the weights assigned to each evaluation criteria using the concept of Shannon's Entropy. Table 1 summarized the assigned weights. And using these weights the artificial recharge zones of the region was delineated (Figure 1). The green areas illustrate the areas that are considered *excellent* for artificial recharge sites.

Table 1. The weight of evaluation criteria computed using the Shannon Entropy method.

Evaluation Criterion	Information Entropy	Assigned Weight
Topography	0.921	0.161
Depth of the Water Table	0.928	0.147
Alluvial Deposits Type	0.926	0.151
Soil Type	0.921	0.161
Hydraulic Conductivity	0.895	0.231
Land Use	0.926	0.151
EC	0.992	0.017

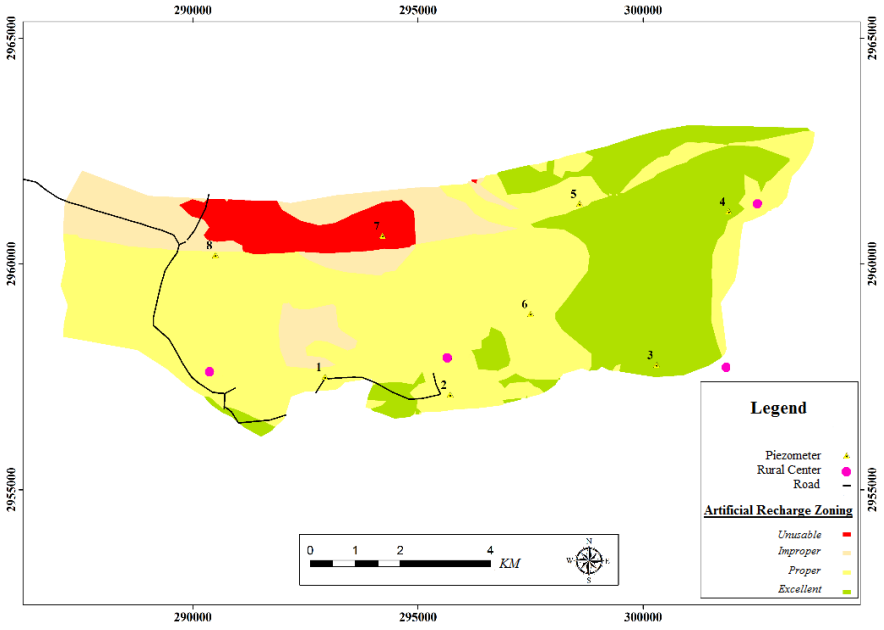

Figure 1. Prioritizing and zoning the artificial recharge sites.

The results indicate that, approximately, 25% of the region can be considered *excellent* for artificial recharge sites. Given the unprecedented water-related challenges in the area, this could be interpreted as an opportunity for the regions' water resources. These sites would the most suitable locations to harness the stormwater run-offs to artificially recharge the excused aquifers of the region. These recharge sites could, potentially, have a positive impact on the water quality of groundwater systems as well. This study, thus, demonstrated the capability of the hybrid approach (i.e., employing GIS and multi-attribute decision-making methods such as Shannon's Entropy) in coping with the uncertainty and complexity of decision-making in the challenging field of groundwater planning and management.

References

Kalantari N, Rangzan K, Thigale SS, Rahimi MH (2010) Site selection and cost-benefit analysis for artificial recharge in the Baghmalek plain, Khuzestan Province, southwest Iran. Hydrogeology journal 18(3):761-773. https://doi.org/10.1007/s10040-009-0552-x

Madani K (2014) Water management in Iran: what is causing the looming crisis? Journal of environmental studies and sciences 4(4):315-328. https://doi.org/10.1007/s13412-014-0182-z

Pourghasemi HR, Pradhan B, Gokceoglu C (2012) Remote sensing data derived parameters and its use in landslide susceptibility assessment using Shannon's entropy and GIS. Applied Mechanics and Materials 225:486-491. https://doi.org/10.4028/www.scientific.net/AMM.225.486

Selvarani AG, Maheswaran G, Elangovan K (2017) Identification of artificial recharge sites for Noyyal river basin using GIS and Remote Sensing. Journal of the Indian Society of Remote Sensing 45(1):67-77. https://doi.org/10.1007/s12524-015-0542-5

Senanayake IP, Dissanayake D, Mayadunna BB, Weerasekera WL (2016) An approach to delineate groundwater recharge potential sites in Ambalantota, Sri Lanka using GIS techniques. Geoscience Frontiers 7(1):115-124. https://doi.org/10.1016/j.gsf.2015.03.002

Shannon CE (1948) A mathematical theory of communication. Bell system technical journal, 27(3):379-423. https://doi.org/10.1002/j.1538-7305.1948.tb01338.x

11th World Congress on Water Resources and Environment (EWRA 2019)
"Managing Water Resources for a Sustainable Future", 25-29 June 2019, Madrid, Spain

Investigation of sharp-interface modifications, as surrogates of the variable density models

G. Kopsiaftis[1*], V. Christelis[2], A. Werner[3], A. Mantoglou[1]
[1] Lab. of Reclamation Works and Water Resources Management, National Technical University of Athens, Greece
[2] British Geological Survey, Environmental Science Centre, Keyworth, Nottingham, UK
[3] Flinders University, Adelaide, Australia
* e-mail: gkopsiaf@survey.ntua.gr

Introduction

Seawater intrusion (SWI) in coastal aquifers is a physical phenomenon which consists of several processes. SWI models usually consider only some of them, depending on the accuracy required for each application or the available computational resources. Two modelling approaches are considered here: 1) the variable density (VD) model, which assumes a dispersion zone between saltwater and freshwater and 2) the sharp-interface (SI) model, which assumes an abrupt interface that separates saltwater from freshwater.

The VD model is a more accurate representation of SWI but it is based on the numerical solution of a coupled differential equation system that significantly increases the computational burden (Werner 2017). On the other hand, the simplified SI model, considered in this study, is based on the Ghyben-Herzberg approximation and the single-potential formulation of Strack (1976). Several papers discuss the accuracy of these two models in simulating SWI (Pool and Carrera 2011; Llopis-Albert and Pulido-Velazquez 2014; Lu and Werner 2013; Koussis et al. 2015), or their performance in pumping optimization of coastal aquifers (Christelis and Mantoglou 2016; Kopsiaftis et al. 2019).

The present study investigates the prediction skills of the SI model based on recent proposed modifications of the density ratio, to account for the solute transport mechanisms' effect on the SWI extent. In past studies, a single density modification was adopted for the entire aquifer simulation domain. Here, a multiple modification approach is developed, where an individual density ratio is identified for each one of the pumping wells in the aquifer. First, a calibration process is employed which aims to minimize the discrepancies between the SI toe and the 0.5 kg/m^3 iso-chlore line from the VD simulation, by finding an optimal density ratio. Then, a regression model is built to apply a local correction on the SI model and test its performance against SWI predictions from the VD model.

Materials and methods

A steady-state SI model is employed in the current paper, which is based on the solution of the following differential equation

$$\frac{\partial}{\partial x}\left(K\frac{\partial \phi}{\partial x}\right)+\frac{\partial}{\partial y}\left(K\frac{\partial \phi}{\partial y}\right)+N-Q(x,y)=0 \tag{1}$$

where ϕ is the flow potential and K is the aquifer's hydraulic conductivity and $Q(x,y)$ is the total pumping rate.

The potential at the toe location could be estimated by the following equation:

$$\phi_\tau = \left[\frac{\varepsilon(\varepsilon+1)}{2}\right]d^2 \tag{2}$$

where ε is the density difference ratio defined as follows:

$$\varepsilon=\frac{\rho_s-\rho_o}{\rho_o} \tag{3}$$

where ρ_s and ρ_o stand for the maximum seawater density and freshwater density, respectively. It should be noted that the most usual value for ε is 0.025 (Strack 1976).

In the current paper the value of ε is modified, based on an optimization framework, in order to minimize the distance between the SI toe and the 0.5 kg/m^3 iso-chlore line. The position of the critical iso-chlore is calculated using a variable density model. The estimation of the optimal ε value is performed not for the entire aquifer, but only for the position of each well separately, in order to reduce the computational cost.

The procedure described above is applied on a hypothetical unconfined aquifer of rectangular shape with size 7 km x 3 km x 25 m. The aquifer is pumped by 10 wells, scattered along the entire aquifer. A data set consisting of 4,000 variable density simulations was created, using the SEAWAT numerical code. The position of the critical iso-chlore line is calculated from the concentration results. The 4,000 pumping rate sets are created using the Latin Hypercube Sampling (LHS) statistical method. Then, the Strack flow potential is calculated for the same pumping rate sets.

References

Christelis V, Mantoglou A (2016) Coastal Aquifer Management Based on the Joint use of Density-Dependent and Sharp Interface Models. Water Resour Manage 30:861–876. doi: 10.1007/s11269-015-1195-4

Kopsiaftis G, Christelis V, Mantoglou A (2019) Comparison of Sharp Interface to Variable Density Models in Pumping Optimisation of Coastal Aquifers. Water Resources Management. doi: 10.1007/s11269-019-2194-7

Lu C, Werner AD (2013) Timescales of seawater intrusion and retreat. Advances in Water Resources 59:39–51. doi: 10.1016/j.advwatres.2013.05.005

Pool M, Carrera J (2011) A correction factor to account for mixing in Ghyben-Herzberg and critical pumping rate approximations of seawater intrusion in coastal aquifers. Water Resources Research 47:W05506. doi: 10.1029/2010WR010256

Strack ODL (1976) A single-potential solution for regional interface problems in coastal aquifers. Water Resources Research 12:1165–1174. doi: 10.1029/WR012i006p01165

Werner AD (2017) Correction factor to account for dispersion in sharp-interface models of terrestrial freshwater lenses and active seawater intrusion. Advances in Water Resources 102:45–52. doi: 10.1016/j.advwatres.2017.02.001

Llopis-Albert C, Pulido-Velazquez D (2014) Discussion about the validity of sharp-interface models to deal with seawater intrusion in coastal aquifers. Hydrological Processes 28(10):3642-3654

Koussis AD, Mazi K, Riou F, Destouni G (2015) A correction for Dupuit–Forchheimer interface flow models of seawater intrusion in unconfined coastal aquifers. Journal of Hydrology 525:277-285

11th World Congress on Water Resources and Environment (EWRA 2019)
"Managing Water Resources for a Sustainable Future", 25-29 June 2019, Madrid, Spain

A lagging-theory model for slug test in a confined aquifer with sensitivity analysis

C.-S. Huang[1], Y.-C. Lin[2], C.-P. Li[2], H.-D. Yeh[2*], M.-H. Chuang[3]
[1] State Key Laboratory of Hydrology-Water Resources and Hydraulic Engineering, Center for Global Change and Water Cycle, Hohai University, Nanjing 210098, China
[2] Institute of Environmental Engineering, National Chiao Tung University, 1001 University Road, Hsinchu, Taiwan
[3] Department of Urban Planning and Disaster Management, Ming Chuan University, Taoyuan, Taiwan
* e-mail: hdyeh@mail.nctu.edu.tw

Introduction

Slug test is a commonly used aquifer test for determining aquifer hydraulic parameters. The parameters can be estimated by applying a suitable mathematical model coupled with an optimization method. Several scholars have developed analytical models describing the flow for slug tests in confined aquifers (e.g., Cooper et al. 1967; Bredehoeft and Papadopulos 1980; Butler and Zhan 2004). Lin and Yeh (2017) introduced two lag times to reflect the effects of inertial and non-interconnected pores on confined flow for a constant-rate pumping test. This study proposes a new analytical model considering the lag times for the slug test to demonstrate the relative importance of the aquifer parameters and estimate them from a field test data.

Materials and methods

The dimensionless parameters are defined as $s_D = s/s_0$, $s_{wD} = s_w/s_0$, $r_D = r/r_w$, $t_D = c_t t$, $\tau_{sD} = c_t \tau_s$, $\tau_{qD} = c_t \tau_q$, $c_t = T/(Sr_w^2)$ where subscript *D* represents a dimensionless symbol, s is the aquifer drawdown, s_0 is the initial drawdown in the test well, s_w is the drawdown in the well, T and S are respectively the aquifer transmissivity and storativity, r is the radial distance from the center of the well, r_w is the radius of the well, t is time since the test beginning, τ_q and τ_s are the lag times of the water flow and the hydraulic gradient, respectively. The dimensionless flow equation with two lag times can be expressed as:

$$\mathrm{T}\left(1+\tau_{\mathrm{s}}\frac{\partial}{\partial \mathrm{t}}\right)\left(\frac{\partial^2 \mathrm{s}}{\partial \mathrm{r}^2}+\frac{1}{\mathrm{r}}\frac{\partial \mathrm{s}}{\partial \mathrm{r}}\right)=\mathrm{S}\left(1+\tau_{\mathrm{q}}\frac{\partial}{\partial \mathrm{t}}\right)\frac{\partial \mathrm{s}}{\partial \mathrm{t}}\left(1+\tau_{sD}\frac{\partial}{\partial t_D}\right)\left(\frac{\partial^2 s_D}{\partial r_D^2}+\frac{1}{r_D}\frac{\partial s_D}{\partial r_D}\right)=\left(1+\tau_{qD}\frac{\partial}{\partial t_D}\right)\frac{\partial s_D}{\partial t_D} \quad (1)$$

The initial conditions of the dimensionless drawdown and water flow before the test are:

$$\mathrm{s}(\mathrm{r},\mathrm{t}=0)=\frac{\partial \mathrm{s}(\mathrm{r},\mathrm{t}=0)}{\partial \mathrm{t}}=0 s_D=0 \text{ and } \frac{\partial s_D}{\partial t_D}=0 \text{ at } t_D=0 \quad (2)$$

The initial water level in the test well is:

$$s_{wD}=1 \text{ at } t_D=0 \quad (3)$$

The inner boundary condition with wellbore storage effect is written as:

$$\frac{\partial s_D}{\partial r_D}=c_w\frac{\partial S_{wD}}{\partial t_D} \text{ at } r_D=1 \quad (4)$$

where c_w = 0.5/S. The remote boundary condition is:

$$lim_{r_D\to\infty}\, s_D=0 \quad (5)$$

Applying the Laplace transform to Eqs. (1) – (5) yields the Laplace-domain solution of the dimensionless drawdown expressed as:

$$\bar{s}_D(r_D,p)=\frac{c_w K_0(r\lambda)}{c_w p K_0(\lambda)+\lambda K_1(\lambda)} \quad (6)$$

$$\lambda=\sqrt{p(1+p\tau_{qD})/(1+p\tau_{sD})} \quad (7)$$

where the overbar represents the Laplace domain and p is the Laplace parameter.

Results and concluding remarks

The measured drawdown data from the slug tests for wells LA-87B conducted by Greene et al. (1999) in the Minnelusa aquifer are analysed by the present, Cooper et al. (1967) and Su et al. (2015) solutions. Each of these three solutions is coupled with the Levenberg-Marquardt algorithm to analyse the measured drawdown for estimating the aquifer properties. Before the parameter estimation, the local sensitivity analysis (Kabala 2001) is used to assess the sensitivity of the drawdown to the variation in each of aquifer parameters in the present model. Figure 1a shows T is the most sensitive parameter followed by S, τ_s, and τ_q, indicating T is the key factor in the present model. Figure 1b displays the curves predicted by the present solution with T = 4.96×10^{-6} m^2/min, S = 0.82, τ_q = 234.51 min, and τ_s = 13.53 min, the Su et al. (2015) solution with T = 7.93×10^{-6} m^2/min, S = 0.78, β_1 = 0.72, β_2 = 0.92, b_2 = 1.84, and the Cooper et al. (1967) solution with T = 9.34×10^{-6} m^2/min, S = 0.01. Note that β_1 and β_2 in Su et al. model denote the order of fractional derivatives for immobile and mobile zones, respectively; b_2 is the ratio of the mobile zone to the total porosity. The estimated results indicate Cooper et al. (1967) solution cannot agree to the measured drawdown. The present solution gives smaller standard error of estimate (SEE = 6.09×10^{-3} m) and mean error (ME = 1.09×10^{-4} m) than those of Su et al. solution (SEE = 1.07×10^{-2} m, ME = 4.40×10^{-4}), indicating our model with the lag times leads to better-predicted curves. As concluded, the present solution with the lagging theory has demonstrated its applicability to the analyses of field slug test data.

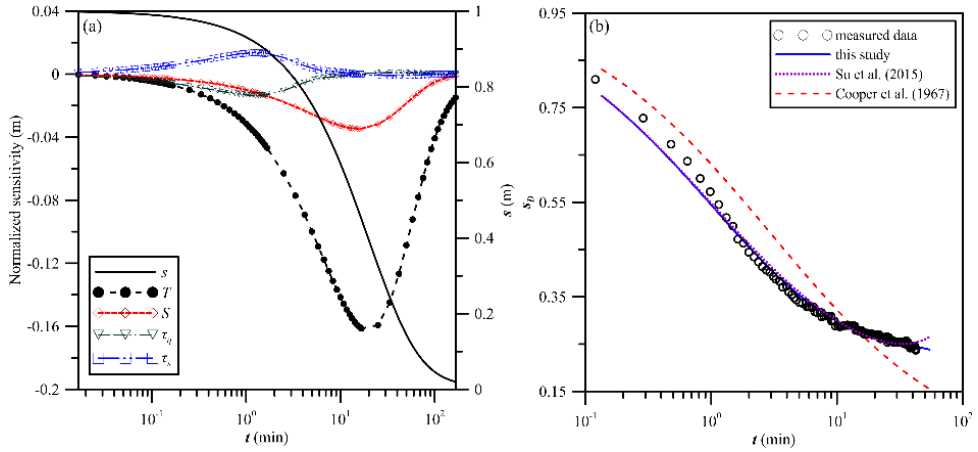

Figure 1. The curves of (a) the temporal distributions of the normalized sensitivity and (b) the drawdown predicted by three analytical solutions and the measured drawdown from the test wells LA-87B in the Minnelusa aquifer.

Acknowledgments: Research leading to this extended abstract has been partially supported by the grants from the Fundamental Research Funds for the Central Universities (2018B00114), the National Natural Science Foundation of China (51809080) and the Taiwan Ministry of Science and Technology under the contract numbers MOST 107-2221-E-009-019-MY3.

References

Bredehoeft JD, Papadopulos IS (1980) A method for determining the hydraulic properties of tight formations. Water Resources Research 16(1):233-238

Butler Jr JJ, Zhan X (2004) Hydraulic tests in highly permeable aquifers. Water Resources Research 20:W12402

Cooper HH, Bredehoeft JD, Papadopulos IS (1967) Response of a finite-diameter well to an instantaneous charge of water. Water Resources Research 3(1):263-269

Greene EA, Shapiro AM, Carter JM (1999) Hydrogeologic characterization of the Minnelusa and Madison aquifers near Spearfish, South Dakota Rep. US Dept. of the Interior, US Geological Survey, Branch of Information Services

Kabala ZJ (2001) Sensitivity analysis of a pumping test on a well with wellbore storage and skin. Advances in Water Resources 24(5):483-504

Lin YC, Yeh HD (2017) A Lagging Model for Describing Drawdown Induced by a Constant-Rate Pumping in a Leaky Confined Aquifer. Water Resources Research 53(10):8500-8511

Su N, Nelson PN, Connor S (2015) The distributed-order fractional diffusion-wave equation of groundwater flow: Theory and application to pumping and slug tests. Journal of Hydrology 529:1262-1273

11th World Congress on Water Resources and Environment (EWRA 2019)
"Managing Water Resources for a Sustainable Future", 25-29 June 2019, Madrid, Spain

Numerical groundwater flow model of Jordan

M. Dahabiyeh[1], M. Gropius[2*]
[1] Ministry of Water and Irrigation (MWI), Amman, Jordan
[2] Federal Institute for Geosciences and Natural Resources (BGR)
* e-mail: mark.gropius@bgr.de

Introduction

Jordan is considered one of the most water scarce countries in the world. Groundwater is the most important source of the Jordanian water supply. Population growth, rising use of water for irrigation purposes and illegal abstractions have increased the stress on existing groundwater resources.

In the framework of the technical cooperation project "Groundwater Resources Management of Jordan", the Federal Institute for Geosciences and Natural Resources (BGR) and the Jordanian Ministry of Water and Irrigation (MWI) have developed a numerical groundwater flow model of Jordan in order to assess and to quantify all relevant groundwater resources of Jordan. The aim of the model is to provide a comprehensive understanding of all groundwater resources and will be used as a tool to predict future developments of the groundwater resources and to investigate water management options.

Materials and methods

The conceptual model comprises the geologic rock units from Ram to Basalt and Alluvium with aquifers and aquitards hydraulically distinguished. The groundwater flow regime for lower sandstone aquifers is understood to be driven by an inflow to the Ram Aquifer from Saudi Arabia and Iraq and a discharge to the Dead Sea. The upper limestone and basaltic aquifers are naturally recharged by precipitation and discharged at wadis and springs (Margane et al. 2002). Both aquifer systems reveal significantly different flow directions and groundwater heads.

The numerical groundwater flow model has been built using MODFLOW-NWT code (Harbaugh 2005; Niswonger et al. 2010) and comprises nine layers representing the relevant hydrogeological units identified in the conceptual model (Figure 2). Due to the regional scale of the model domain, a regular grid with a uniform cell size of 2000 m times 2000 m has been established. Boundary conditions include the groundwater inflow at the model boundary and the outflow at wadis, springs, the Dead Sea and about 5000 official pumping wells.

Only few observed groundwater level data were available for times prior to an extensive development of groundwater exploitation. Therefore, groundwater level data from available monitoring wells were averaged from 1960 to 1990. The long-term averages were used for the steady state calibration. Groundwater levels, flow directions and water balance at steady state are in good accordance to observed values and findings of previous investigations and studies performed on a regional scale.

The parameter settings and resulting hydraulic heads of the steady state calibration reflect the pre-development conditions and were used as initial conditions for the transient modelling.

Results and concluding remarks

The transient groundwater model simulates the 1960 - 2017 period. The results reproduce observed hydraulic processes like the reversed flow directions in Azraq area, the drying out of Azraq springs and the decline of baseflow discharging at Zarqa river. The transient groundwater model results reflect the observed decline of groundwater levels as well as the vast heterogeneity of its temporal development throughout Jordan and the different aquifers. Looking at individual monitoring wells, calculated drawdown and temporal trends are often in good accordance with the observed data at early simulation times. However, calculated heads do not reproduce the exacerbated decline observed later. This indicates that groundwater abstractions applied in the groundwater model according to the known licensed abstraction

rates are inferior to the ones taking place actually. The groundwater model outlines those areas, where officially unknown abstractions have to be taken into consideration. The use of landuse data and estimated crop demand to define groundwater abstraction rates instead of applying the licensed abstraction rates leads to calculated groundwater heads that are consistent with the observed groundwater levels.

Considering the scale of the model domain and the limitations due to the applied generalizations, the groundwater flow model is assumed suitable to investigate long-term variations for future groundwater resources planning.

The groundwater flow model has been applied to predict long-term groundwater development in Jordan showing a further decline of groundwater levels and revealing areas with reduced groundwater availability in future. Especially areas in the North of Jordan are affected by a significant groundwater level decrease but also major groundwater abstraction sites in the South of Jordan are subject to a significant drop of groundwater levels of more than 2 m drawdown per year. These model-based predictions shall be included to the strategic groundwater resources management and shall support the planning of measures to mitigate adverse developments.

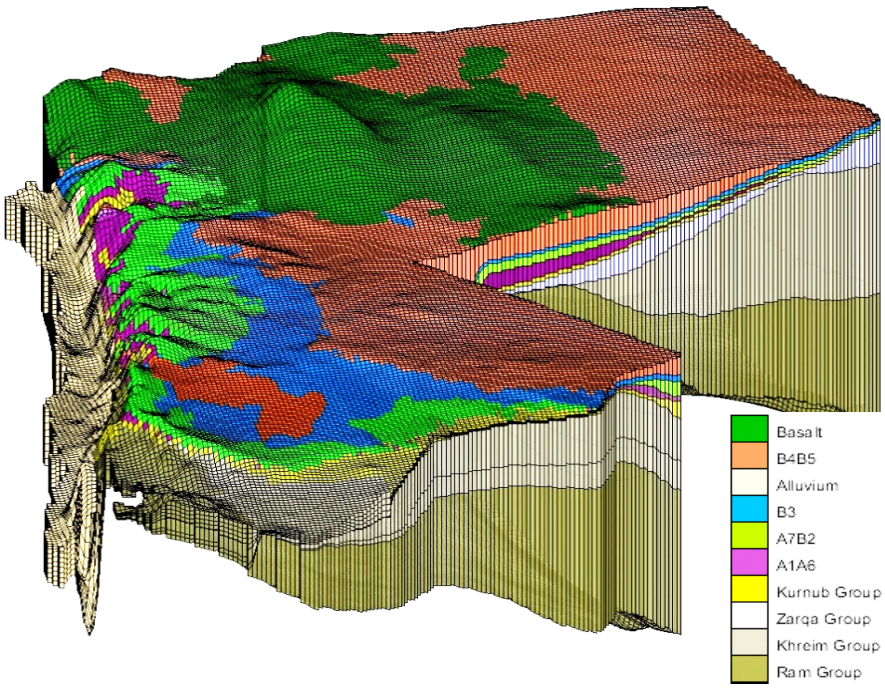

Figure 2. 3D view of the groundwater flow model (model cells color coded according to hydrogeological units).

Acknowledgments: The project "Groundwater Resources Management, Jordan" is part of the German-Jordanian technical cooperation financed by the Federal Ministry for Economic Cooperation and Development.

References

Harbaugh AW (2005) MODFLOW-2005, the U.S. Geological Survey modular ground-water model -- the Ground-Water Flow Process. U.S. Geological Survey Techniques and Methods 6-A16

Margane A, Hobler M, Almomani M, Subah A (2002) Contributions to the hydrogeology of Northern and Central Jordan. Bundesanstalt fuer Geowissenschaften und Rohstoffe und den Staatlichen Geologischen Diensten in der Bundesrepublik Deutschland (ed), Geologisches Jahrbuch. Reihe C (Hydrogeologie, Ingenieurgeologie). Stuttgart Schweizerbart

Niswonger RG, Panday S, Ibaraki M (2011) MODFLOW-NWT, A Newton formulation for MODFLOW-2005. U.S. Geological Survey Techniques and Methods 6-A37, 44 p

11th World Congress on Water Resources and Environment (EWRA 2019)
"Managing Water Resources for a Sustainable Future", 25-29 June 2019, Madrid, Spain

Detecting seawater intrusion using 3D electrical resistivity imaging technique in Dibdibba aquifer at Basrah Governorate south of Iraq

F.H. AL-Menshed
Geophysics Division, General Commission for Ground Water, Baghdad, Iraq
e-mail: ffffhkh@yahoo.com

Introduction

The area where the field work was conducted lies to the east of Safwan and to the north of Um Qasir towns, along the west bank of khor Al-Zubair, at the southwest of Basrah Governorate, south of Iraq.

Khwedim et al. (2017) indicated that seawater intrusion may have occurred in the coastal zone of the research area because of the high concentrations of arsenic, selenium, SO_4^{-2} and Cl^{-1} in well water samples near the shore line of Khor Al-Zubair.

Abdulameer et al. (2018) detected (in general) sea water intrusion in the studied area by using 2D electrical resistivity imaging survey but they did not present quantitative information about the exact position and the distance of this intrusion expansion inland. So, as a main objective, this study will be a step forward of the previous studies in the area by focusing on getting quantitative information about the exact position of the sea water intrusion and detecting its expansion distance inland. Accordingly, this study is essential for sustainable management of coastal groundwater system in the research area.

Materials and methods

Three-dimensional (3D) electrical resistivity imaging survey was conducted to determine the location and depth of salt water intrusion. This is the first time in Iraq a 3D imaging survey used for delineating sea water intrusion.

Five large two-dimensional (2D) electrical resistivity profiles oriented from southwest to northeast direction, perpendicular to The Khor Al-Zubair shore line and covering an area of about 48 km^2 were made. Each profile was 2400 m long with 10 m electrodes spacing. The distance between the profiles was approximately 5000 m.

Wenner-Schlumberger electrode array was used for data acquisition because it can show higher and more uniform model sensitivities for mapping 3D features and it is recommended for a higher resolution when transferred from 2D profiles. The 2D electrical surveys were performed using an IRIS SYSCAL Pro Switch 120 electrodes resistivity-meter. Measured 2D datasets were collated into one 3D data file using the software package Prosys II V.03.02.02 (www.iris-instruments.com). The 3D forward and inverse modelling was done using the RES3DINVx32 Ver. 2.23.24 (www.Geotomo software.com).

Results and concluding remarks

The main objective of this study which was to delineate the sea water intrusion was completely achieved by resistivity imaging method supported by hydrogeological, hydrochemical and lithological information. The intrusion appeared as a very low resistivity zone starting from the location of Khor Al-Zubair at the northeasterly direction of the studied area and extended inland along a distance reaching about 2.5km intruding the semi-confined part of the Dibdibba aquifer as in Figure (1). Also, the 3D inversion and modeling have allowed obtaining a good delineation of the main water bearing bed in the study area. The results showed the existence of three major zones. The upper zone represented the uppermost aquifer system which appears as a relatively high resistivity zone (more than 75 Ωm) with thickness reaching about 25 m. This zone is considered to be the upper unconfined part of Dibdibba aquifer saturated with relatively slightly brackish water TDS <10000 mg/L. The second zone had a resistivity ranging between (75 Ωm – 9 Ωm) and thickness reaching about 60 m. It is considered to be the semi-confined part of Dibdibba aquifer saturated with undesired saline groundwater (TDS >10000 mg/L). The third zone has a lowest resistivity

(less than 9 Ωm). It may represent very saline water leaking up from the underlined beds of Fatha formation. The Jojab clay separating bed between the two parts of Dibdibba aquifer is also distinguished at a depth reaching about 25 m.

Results and conclusions of this study may be extrapolated to the same cases in arid and semi-arid coastal aquifers where groundwater resources are vital to the population.

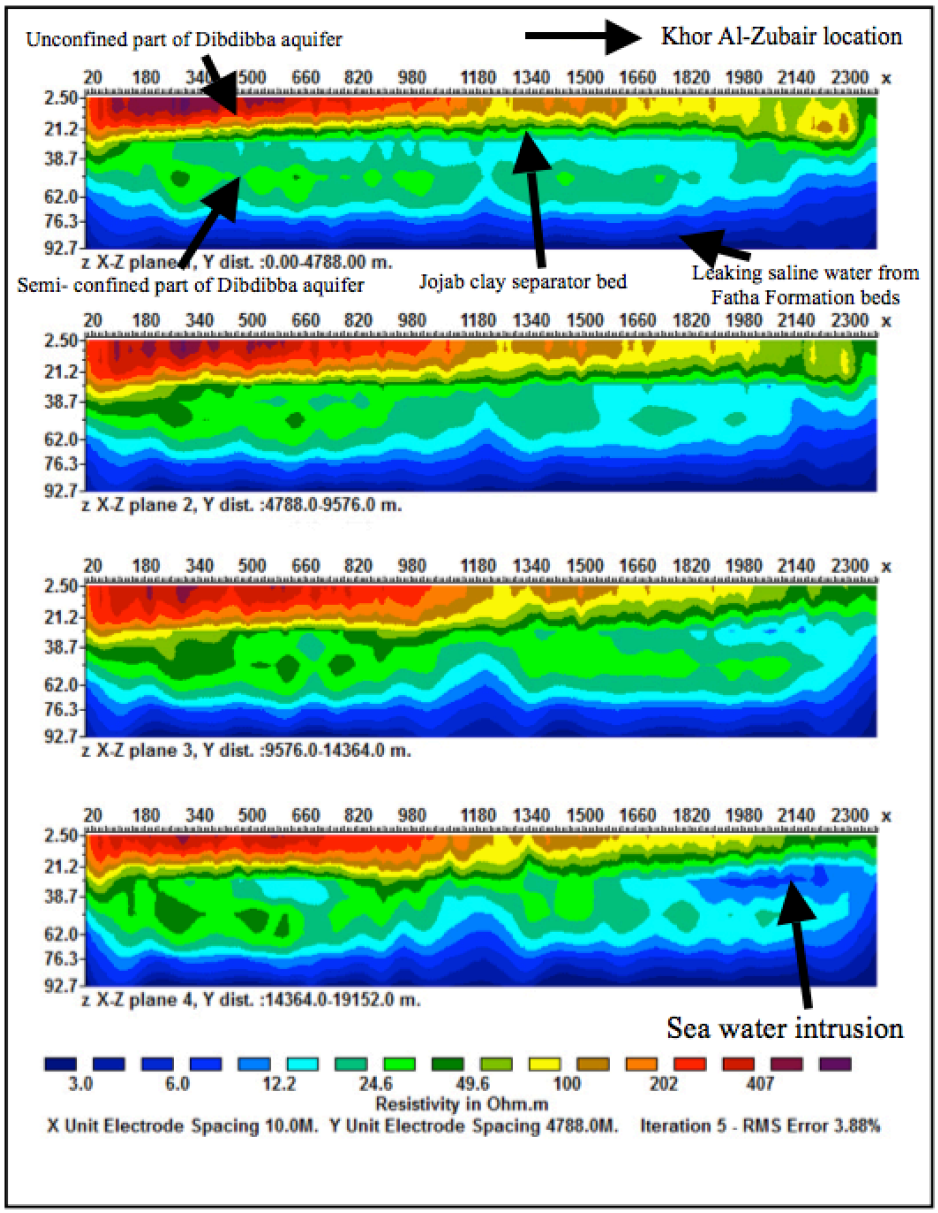

Figure 1. High resolution X-Z plain 3D resistivity models show the investigated water bearing bed in the studied area and the location of sea water intrusion.

References

Abdulameer A, Thabit JM, AL-Menshed FH, Merkel B (2018) Investigation of seawater intrusion in the Dibdibba Aquifer using 2D resistivity imaging in the area between Al-Zubair and Umm Qasr, southern Iraq. Environ Earth Sci 77:619. doi: 10.1007/s12665-018-7798-3

Khwedim K, Schneider M, Ameen N, Abdulameer A, Winkler A (2017) The Dibdibba aquifer system at Safwan–Zubair area, southern Iraq, hydrogeology and environmental situation. Environ Earth Sci 76:155

11th World Congress on Water Resources and Environment (EWRA 2019)
"Managing Water Resources for a Sustainable Future", 25-29 June 2019, Madrid, Spain

Optimal location of subsurface dams in arid regions using geographic information system and analytic hierarchy process

S.S. Mehdizadeh*, M. Ghoroqi, A. Naqizadeh
Department of Civil Engineering, Central Tehran Branch, Islamic Azad University, Tehran, Iran
** e-mail: Saj.Mehdizadeh@iauctb.ac.ir*

Introduction

Subsurface dams store water underground by means of an obstacle inserting on the way of groundwater flow. The main advantages of retaining groundwater by subsurface dams are the low amount of evaporation, minimum environmental problems and low construction cost. In recent years, researches have investigated about the proper location of subsurface dams (e.g. Telmer and Best 2004; Forzieri et al. 2008; Ishida et al. 2008; Ouerdachi et al. 2012 and Cantalice et al. 2016). The results of these studies suggest that access road to dam location, quality and quantity of rainfall, bedrock depth, soil permeability and chemical quality of water play significant role in finding optimal location of subsurface dams. However, limited field-scale studies have been introduced considering all effective factors for subsurface dam best location. Weighting and priority of related parameters also need more investigations. In this study, all indexes that influence on subsurface dam location are first determined. Afterward, a real plain in arid areas of Iran is selected and the spatial priority of each index is defined by the geographic information system (GIS). Each element is then compared to each other two using analytic hierarchy process (AHP) based on completed questionnaires by experts and ultimately the best location of the subsurface dam is derived.

Material and methods

The arid Ardakan plain is located in Yazd province at center of Iran. The area of the plain is 8050 km^2. The lowest point of the basin has 970 m elevation from sea level and the average elevation is obtained as 1565 m. Relevant indexes are determined as follows:

Porosity: High effective porosity leads to high-retained volume of groundwater behind dam axis due to an increase in the void of soils that should be saturated after dam construction.

The permeability of bedrock: Low permeable bedrock should be chosen for dam position in order to reduce leakage amount.

Shallow sub-surface flows in the bed of waterway: The existence of shallow sub-surface flows is necessary for dam reservoir. If the aquifer is located in depth, it is difficult, costly and needs technical equipment to recognize the hydrogeological features of soil strata.

Fault: Construction of subsurface dam beneath riverbed with active fault should be avoided. Faults are appropriate path to drain groundwater and direct it to out of reach regions.

Wells and qanats: None of wells or qanats should be demolished or be exposed to severe decline of water. Hence, regions where there are wells or qanats are improper places for subsurface dam construction.

Riverbed slope: Areas with steep riverbed are not usually a suitable place to construct subsurface dams. Large reservoir volume is not formed in these areas. Moreover, the magnitude of groundwater velocity is usually high in these areas that leads to surpassing erosion to sedimentation. It is considered as another negative aspect of a steep slope.

Groundwater: Groundwater volume is the main criteria in optimal site selection of subsurface dams that is accompanied by the chemical quality of subsurface flow.

Axis length: It is desired to have a reservoir with maximum capacity but with the least possible dam length.

Social and economic factor: This includes the amount of required water in term of drinking, agricultural or industrial demand. The distance of dam location to roads and villages should also be considered in this

factor.

The determined indexes are then normalized in the AHP decision tree with digits ranges from zero to one. By this method, suitable pixels on each map (separately for each index) have a numeric value close to one and the improper zones have a numeric value close to zero. Weighting and determination of each indexes priority are then carried out by means of comparison between each pair of indexes.

Results and concluding remarks

The final map of optimal subsurface dam location has been categorized into a permanently not suitable, currently not suitable, marginally suitable, moderately suitable region, and highly suitable regions according to the Figure 1. Improper zones are mostly located in areas that wells or qanats outnumbered. The proper regions are close to zones with the most water demand. The permeability and length of dam axis are also minimum in these regions. Southern areas with slope lower than 6% are also considered as potentially suitable regions. The proposed areas are sufficiently far from saline soils to extract high quality water after dam construction. In term of population congestion, residential southern region have rather priority to other zones where the required water demand of indigenous is appreciably supplied.

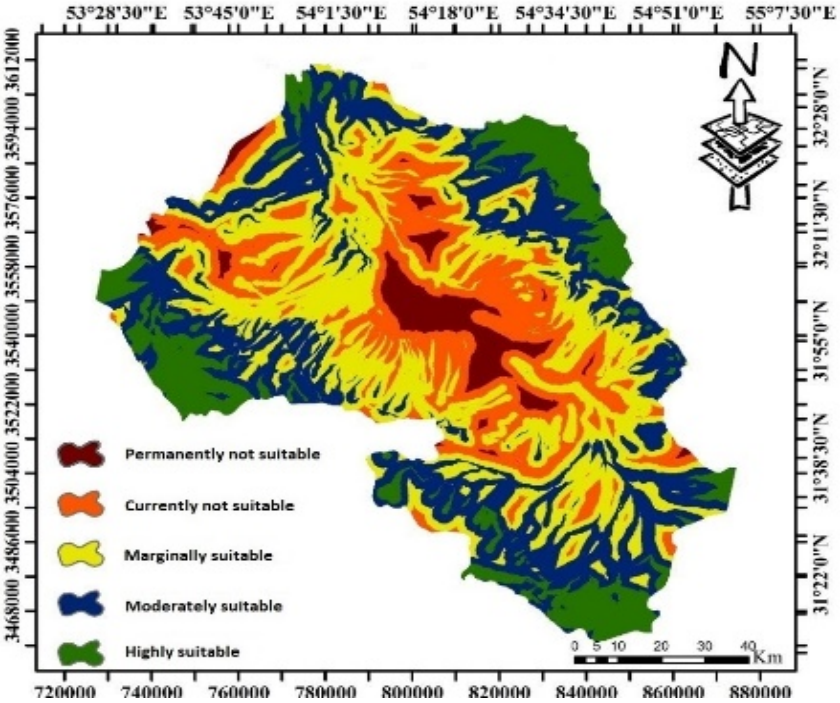

Figure 1. Map of optimal site selection for subsurface dam in the studied area

References

Cantalice JER, Piscoya VC, Singh VP, Da Silva YJ, De FC Barros M, Guerra SM, Moacyr Filho C (2016) Hydrology and water quality of an underground dam in a semiarid watershed. African Journal of Agricultural Research 11(28):2508-2518. https://doi.org/10.5897/AJAR2016.11163

Forzieri G, Gardenti M, Caparrini F, Castelli F (2008) A methodology for the pre-selection of suitable sites for surface and underground small dams in arid areas: A case study in the region of Kidal, Mali. Physics and Chemistry of the Earth, Parts A/B/C 33(1-2):74-85. https://doi.org/10.1016/j.pce.2007.04.014

Ishida S, Tsuchihara T, Yoshimoto S, Imaizumi M (2011) Sustainable use of groundwater with underground dams. Japan Agricultural Research Quarterly JARQ 45(1):51-61. https://doi.org/10.6090/jarq.45.51

Ouerdachi L, Boutaghane H, Hafsi R, Tayeb TB, Bouzahar F (2012) Modeling of underground dams Application to planning in the semi arid areas (Biskra, Algeria). Energy Procedia 18:426-437. https://doi.org/10.1016/j.egypro.2012.05.054

Telmer K, Best M (2004) Underground dams: a practical solution for the water needs of small communities in semi-arid regions. TERRA 1(1):63-65

11th World Congress on Water Resources and Environment (EWRA 2019)
"Managing Water Resources for a Sustainable Future", 25-29 June 2019, Madrid, Spain

Identifying the sources of reactive contaminants in groundwater aquifers using simulation-optimization approach

A. Anshuman*, T.I. Eldho
Department of Civil Engineering, IIT Bombay,Mumbai,India
** e-mail: aatishanshuman@gmail.com*

Introduction

Groundwater aquifers are being polluted by a number of sources. Most of the times, the sources of pollution are unknown. Identification of these sources is essential for the remediation process to be carried out optimally (Guneshwor et al. 2018). Source identification problem is considered ill-posed as the transport process of the contaminant through the aquifer is irreversible. Different strategies such as concentration response matrix (Guneshwor et al. 2018), surrogate model (Zhao et al. 2016) and linked simulation-optimization model (Singh and Datta 2006) are reported in previous studies to deal with the problem. In these studies, the type of contaminant considered is conservative. However, in field conditions the contaminant released may be reactive i.e. it may change its form through its transport process under the influence of hydraulic head. In this study, a coupled flow and transport model based on the meshfree radial point collocation method (RPCM) is used to simulate reactive transport. The model is more computationally efficient compared to traditional mesh/grid based methods such as the finite element method (FEM), finite difference method (FDM) etc. Further, the model is linked with particle swarm optimization (PSO) model through a concentration-response matrix (CRM) to identify the pollution sources. The main objectives of the work are to determine the location of sources and solute fluxes injected into the aquifer from the sources.

Materials and methods

The transport in groundwater is governed by advection-dispersion-reaction equation. The transport process depends on the velocity field which is obtained by the flow model by solving the governing equation for flow in confined/unconfined aquifers. Flow and transport models are constructed based on RPCM in which the problem domain is represented using a group of scattered nodes. The RPCM flow model is used to obtain steady state heads which are further used to estimate nodal velocities and dispersion coefficients using the local support domain. The RPCM reactive transport model is then used to compute the responses at the observation wells which are arranged in the form of CRM. The detailed description of the construction of CRM is explained in Gorelick et al. (1983). In the source identification problem, the possible sources of pollution are identified and the fluxes released from the sources are computed. Hence the sources corresponding to zero release flux are not actual sources. The PSO optimization model is coupled with the CRM to obtain the unknown fluxes from the sources. The model is applied to a hypothetical problem (Figure 1a) which is modified from a scenario presented in Singh and Dutta (2006). Instead of a conservative contaminant, Tritium is considered which is radioactive with a half-life of approximately 12 years. Here a steady state analysis is presented where only the location and solute flux injected are considered as unknown. The aquifer is assumed to be polluted through possible sources (S1 and S2). Three cases are solved which are given by 1) S1 releases unknown flux and S2 is not the source, 2) S2 releases unknown flux and S1 is not the source, and 3) both S1 and S2 are sources and release unknown fluxes. The methodology employed for all three cases is presented in Figure 1b. The objective function for the optimization model is given by Equation 1.

$$\text{Minimize } \sum_{i=1}^{n} (C_i^{obs} - C_i^{pred})^2 \quad (1)$$

where C^{obs} is the observed concentration which is obtained at observation wells by running forward simulation in RPCM reactive transport model and C^{pred} is the SO model predicted concentration at the

observation wells. The SO model is run repeatedly until the convergence criteria i.e. tolerance value of the objective function or, the maximum number of iterations is met.

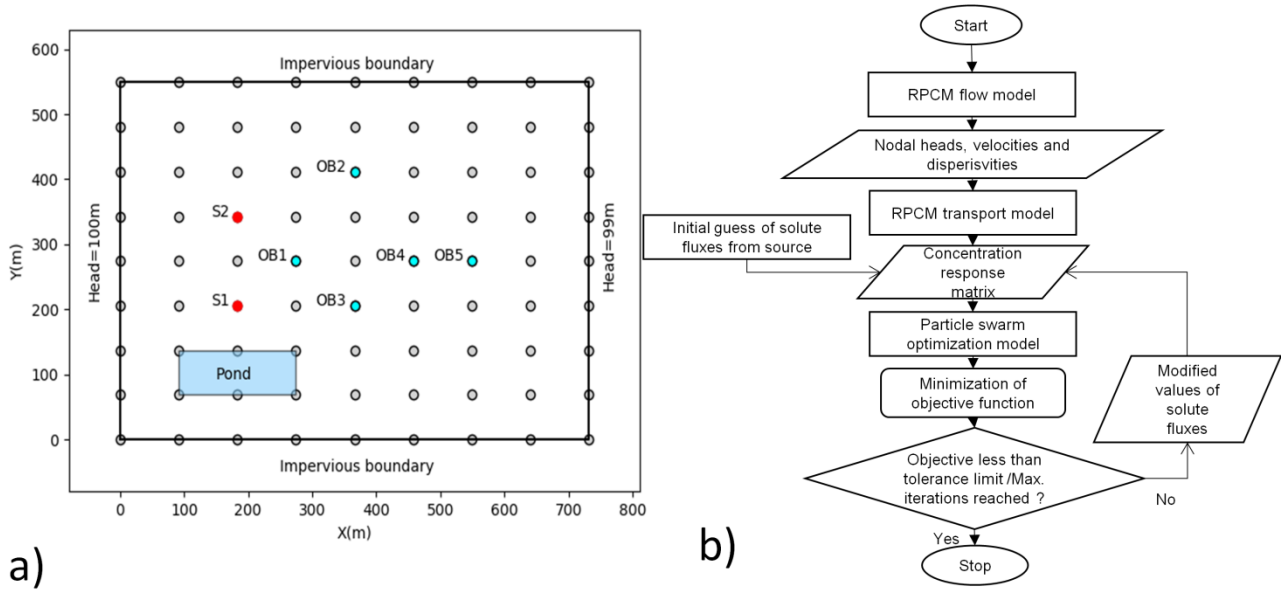

Figure 1. a) Study area for the problem; b) Flowchart of simulation-optimization model.

Results and concluding remarks

The estimated fluxes at S1 and S2 are presented in Table 1. As it is observed, the simulation-optimization model predicts the fluxes very accurately. The use of CRM increases reduces the computational effort to a great extent.

Table 1. Comparison of observed and predicted fluxes for all three cases.

Source location	Case 1		Case 2		Case 3	
	Actual flux(mg/l)	Predicted flux(mg/l)	Actual flux(mg/l)	Predicted flux(mg/l)	Actual flux(mg/l)	Predicted flux(mg/l)
S1	500	499.99	0	0	500	500.0
S2	0	0	1000	999.99	1000	999.999

In this study simulation-optimization approach using CRM has been successfully applied for the identification of the sources of a reactive contaminant. The similar approach may be used for steady state problems involving real aquifers.

Acknowledgments: This study is supported by Board of Research in Nuclear Sciences (BRNS) under project code 16BRNS002. Authors are thankful to BRNS for the support.

References

Gorelick SM, Evans B, Remson I (1983) Identifying sources of groundwater pollution: An optimization approach. Water Resources Research 19(3):779-790

Guneshwor L, Eldho TI, Kumar AV (2018) Identification of Groundwater Contamination Sources Using Meshfree RPCM Simulation and Particle Swarm Optimization. Water Resources Management 32(4):1517-1538

Singh RM, Datta B (2006) Identification of groundwater pollution sources using GA-based linked simulation optimization model. Journal of hydrologic engineering 11(2):101-109

Zhao Y, Lu W, Xiao C (2016) A Kriging surrogate model coupled in simulation–optimization approach for identifying release history of groundwater sources. Journal of contaminant hydrology 185:51-60

11th World Congress on Water Resources and Environment (EWRA 2019)
"Managing Water Resources for a Sustainable Future", 25-29 June 2019, Madrid, Spain

Optimal use of groundwater for irrigation purposes in Al-Salhubia area, Al-Muthana Governorate, south Iraq

A.A. Obeed Al-Azawi[1*], A.M. Al-Shamma'a[2]
[1] General Commission for Groundwater, Ministry of Water Resources, Iraq
[2] University of Baghdad, College of Science, Dept. of Earth Science, Iraq
* e-mail: ali.obeed67@gmail.com

Introduction

In this paper, the emphasis was on the investment of groundwater in crop irrigation. Generally, the growth of human populations and the increasing demand for water often corresponds to different purposes with the change in land use. The study area considered a desert area, which lack surface water; therefore, much of the southern desert of Iraq depends in large part on groundwater as a main source of water for their water supply system. A 2002 Investigation dealt with optimum management model of ground water resources in Safuan-Zubair area, and the Karbala desert area south of Iraq (AL-Abadi 2002; Al-Mussawy 2013). An optimization model for a multi-year planning horizon is formulated, developed, applied, and interpreted for developing available groundwater resources in Al-Salhubia area of the southern of Iraq, by using the Optimization GAMS model, which will be used for the prediction of groundwater in the area by using the different scenarios within the next ten-years through joining between groundwater and agriculture. Three scenarios were developed, in which pumping patterns are optimized over a 10-year time horizon. For the first scenario the model is run with an upper bound allowed to increase in land area by 20% over current observed cultivation levels. For the second scenario the model is run with an upper bound on total annual pumping allowed to increase by 10% from current levels. For the third scenario the model is run with maximum total pumping allowed to increase by 20% from current levels. Results show that total water pumped for all scenarios are less than the total recharge of the study area, indicating that pumping appears to be up-scalable for future development.

An important gap remain in the search for optimal groundwater and use patterns in our study of southwestern Iraq in the search for policy interventions to promote more optimal water use patterns. The aim of the present study is to fill some of the gaps not previously examined by the previous studies. Bearing that in mind, our objectives are to; the first aim is to determine the amount of groundwater utilization in crop irrigation and compare it with the amount of groundwater storage, and the second aim is discussed the problems concerning aquifer sustained recharge and assesses the type of groundwater system management for long-term utilization. Optimally, sustainable management strategies may be developed by decision makers to utilize groundwater resources.

Materials and methods

Study area: The study area is located in the stable zone of Iraq in southwestern Al-Samawa. The Basin has a land area of just over 3,000 square kilometers (80 km in length and 37.5 km in width). It is located about 70 km southwest Al-Samawa City and southwest of the Euphrates River (Figure 1). The main aquifer in Al-Salhubia basin is located within the Dammam Formation is exposed in most of the study area and it is one of the most important aquifers in southwestern Iraq (Figure 2). It is composed of variable carbonate rocks mainly limestone, dolomitic limestone and dolomite, with marl and evaporates. It is characterized by the presence of cavities and karstified canals in addition to fractures, fissures and joints that caused the formation to have high transmissivity and permeability in most areas.

Optimization model for irrigation application: The optimization model used in this study was built for modeling and solving optimization mathematical problems, where, this model can treat many objectives in the same time (i.e. given of multi-objective function)(Rashid 2014). Therefore, the studied area has been divided into one irrigation cell according to the discharge of the wells. The optimization procedure for the

study area has three goals, first, to maximize pumping rate with minimize of drawdown, second, to maximize perennial yield (safe yield) with maximize pumping rate, and with minimize of drawdown, and third to maximize net benefit with minimize of costs.

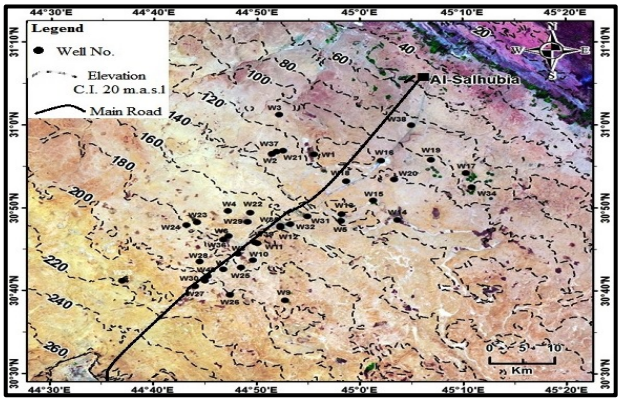

Figure 1. Location map of the studied area

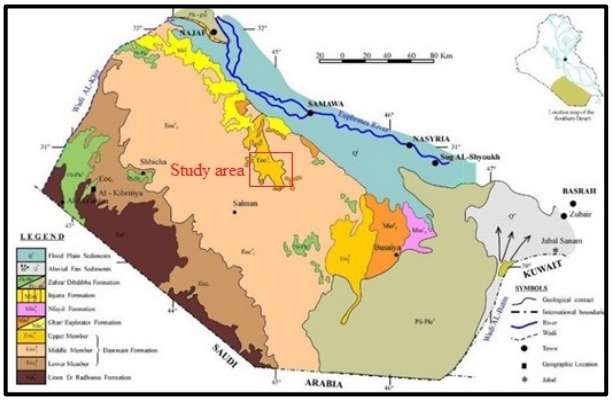

Figure 2. Geological map of the studied area.

Table 1. Optimum model Scenarios for three parameters for ten years period (2016-2025).

Year	Optimization model Scenarios								
	Water pumped ($M m^3$)			Perennial (safe)Yield ($M m^3$)			Drawdown (m)		
	First	Second	Third	First	Second	Third	First	Second	Third
2016	9.81	10.55	10.55	33.60	37.70	37.70	0.73	0.82	0.82
2017	5.94	10.34	12.66	12.15	36.53	49.40	0.26	0.80	1.1
2018	3.75	6.86	9.81	0.00	17.27	33.62	0.00	0.40	0.74
2019	3.75	3.75	6.73	0.00	0.00	16.53	0.00	0.00	0.36
2020	3.75	3.75	3.75	0.00	0.00	0.00	0.00	0.00	0.00
2021	3.75	3.75	3.75	0.00	0.00	0.00	0.00	0.00	0.00
2022	3.75	3.75	3.75	0.00	0.00	0.00	0.00	0.00	0.00
2023	3.75	3.75	3.75	0.00	0.00	0.00	0.00	0.00	0.00
2024	3.75	3.75	3.75	0.00	0.00	0.00	0.00	0.00	0.00
2025	3.75	3.75	3.75	0.00	0.00	0.00	0.00	0.00	0.00

Results and concluding remarks

The results show that the optimal pumping rate for all scenarios are less than the total recharge, and the maximum water extractions are a little than the perennial yield of the aquifer for all scenarios (Table 1). Therefore, the maximum water extraction does not exceed perennial yield for the study area, a conservation of groundwater storativity will exist and it will encourage the future utilization of groundwater in the study area.

References

AL-Abadi AA (2002) Optimum management model of ground water resources in Safwan – Zubair area South of Iraq. In: Sience college, 110, University of Basra, Iraq

Al-Mussawy WH (2013) Optimum management modules of groundwater use in Karbala Desert Area, Iraq. In: College of Engineering 210, University of Al-Mustansiriyah, Baghdad, Iraq

Rashid H, Al-Shukri H, Mahdi H (2014) Optimal management of groundwater pumping of cache critical groundwater area, Arkansas. Applied Water Science 5(3):209–219

11th World Congress on Water Resources and Environment (EWRA 2019)
"Managing Water Resources for a Sustainable Future", 25-29 June 2019, Madrid, Spain

Identification of groundwater zones and subsurface lithology in Saint Martin's Island using vertical electrical sounding

M.M. Uddin*, I.M. Shofiqul, M. Minhazur Rahman, M. Tahmidur Rahman
Department of Civil and Environmental Engineering, Shahjalal University of Science and Technology, Bangladesh
** e-mail: mun_cee@yahoo.co.uk*

Introduction

Schlumberger electrode array of vertical electrical sounding (VES) survey has been used in the study to delineate the thickness of the shallow aquifer and its possible interaction with the sea water in Saint Martin's Island in Bangladesh. The present study area has an increasing demand for additional and sustainable water resources due to the daily need of water for economic development and demographic growth. Groundwater exploration and management is an important issue in the study area for its sustainable development. In this study, VES surveys were carried out using surface Schlumberger electrode array to provide accurate interpretation of the possible interaction between coastal shallow aquifer and seawater. The difference in resistivity is associated with the variations in lithology, groundwater saturation, and salinity. The greater the distance between the current electrodes, the dipper the investigation (Roy and Apparao 1971). The interpretation of VES curves reveals low resistivity zones characterizing the study area. These zones reflect saline water intrusion in the island.

The main objectives of the study were to identify the subsurface lithology, to identify the productive zone, i.e., to determine the existence of a potable aquifer and to create a subsurface map based on VES.

Materials and methods

Vertical Electrical Soundings were carried out at several stations. The method had been based on the estimation of the electrical conductivity or resistivity of the medium. The estimation was performed based on the measurement of voltage of electrical field induced by the distant grounded current electrodes. This was subsequently done on all the point data obtained for each VES station to give the set of apparent resistivity value supplied for computer program for the geoelectrical parameters. Schlumberger configuration using Microprocessor based signal stacking digital resistivity meter of IGIS, Hyderabad (Model SSR -MP1) was used to deploy. The apparent resistivity for this configuration was computed with the following formula:

$$\rho a = \pi \nabla \mathrm{V}/\mathrm{I} * [\{(AB/2)\text{^}2 - (MN/2)\text{^}2\}/MN] \quad (1)$$

where, AB=Spacing of current electrode, MN= Spacing of potential electrode, ΔV= Potential difference

Both survey procedures, i.e., resistivity profiling and resistivity sounding have been carried out. The detailed geological, geomorphological and hydrogeological properties were analyzed by interpretation and analysis of VES data by quantitative methods using IPI2 WIN (Bobachev 2002) and Surfer 9.0 software. Quantitative interpretation of geoelectrical sounding curves is complicated due to the well-known principle (Van Overmeeren 1989) of equivalence. A maximum electrode spacing AB/2 of 120 m was employed to delineate the subsurface lithology and groundwater potentials.

Results and concluding remarks

Based on interpreting curve, a lithological model, 3D subsurface view of water zone and water table contour map are proposed for St. Martin's Island. The subsurface undulation is remarkable by these illustrations. Moreover, tube well data are compared to the modeling result. In the lithology section, it is seen that the water table at location 2 are between 4.52-12.6 m from the surface (Table 1). The water table at location 3 is between 1.18-8.04 m from the surface and a fresh-water bearing sand zone is situated between 8.04-8.71 m from the surface. At location 4, the water table is between 1.5-21.6m from the

surface. The water table at location 8 and location 9 is between 2.09-17.3 m and 1.14-2.93 m, respectively.

Table 1. Summary of VES data interpretations with positions.

VES No.	Curve Type	Layer No.	Resistivity	Thickness	Depth	Lithology	Location
1	H	1	3.76	0.659	0.659	Sandy Soil	Northeast
		2	0.869	6.18	6.84	Clay	
		3	2296			Hard bed rock	
2	K	1	1.81	4.52	4.52	Clay	West side of
		2	66.2	8.06	12.6	Fresh water sand	Restaurant
		3	0.0378			Clay	Belavhumi
3	AK	1	0.38	1.18	1.18	Clay	South side of
		2	1.71	6.86	8.04	Silty sand	Restaurant
		3	15251	.0673	8.71	Sand with fresh water	Belavhumi
		4	2.76			Clay/Sand with saline water	
4	A	1	1.16	1.5	1.5	Clay	Bangla Boss Rd
		2	103	20.1	21.6	Silty sand	1st
		3	207			Hard bed rock	
5	A	1	1057	1.13	1.13	Clay	Bangla Boss Rd
		2	1.9×10^5	2.38	3.51	Silty sand	2nd
		3	3.5×10^6			Hard bed rock	
6	A	1	808	1.65	1.65	Clay	Bangla Boss Rd
		2	85431	1.86	3.51	Silty sand	3rd
		3	2.3×10^6			Hard bed rock	
7	A	1	2519	1.08	1.08	Clay	Bangla Boss Rd
		2	6.9×10^6	20.3	21.4	Silty sand	4th
		3	9.6×10^6			Hard bed rock	
8	K	1	1.4	2.09	2.09	Clay	East side of
		2	49.6	15.2	17.3	Fresh water sand	Bangla Boss Rd
		3	1.5			Clay	5th
9	K	1	9.62	1.14	1.14	Clay	Between Neel
		2	1.1×10^5	1.79	2.93	Fresh water sand	Digante Resort and
		3	503			Clay	SomudroBilash

Vertical Electrical Sounding proved to be important tools for mapping the freshwater-saltwater interface and for studying conductive bodies and subsurface geological structures. A total of nine VES have been conducted and cross-sections have been generated by IPI 2 WIN yielding four major lithological zones identified in Saint Martin's Island. According to the nature of electrical field curves, qualitative interpretation (1D) was applied and four types were classified, which are H, K, A, and AK. It is revealed that 88.89% of the total soundings are interpreted by 3-layer modes, while the other 11.11% by 4 layer model. Both A and K curve type have about 77.78% of the total soundings, while H type occupied by 11.11% and AK type occupied by 11.11% of the total soundings. Most of the saline water formation is in the north side of the island. The fresh-water zone which lies at the eastern part of the study area, where the aquifer thickness is about 1.18 m, has increased to about 8.04 m.

References

Bobachev CJMSU (2002) IPI2Win: A windows software for an automatic interpretation of resistivity sounding data.

Reena G, Murugan M (2017) Geophysical Investigation from Thiruporur to Mahaballipuram Using Resistivity Method. International Journal of Engineering and Techniques 3(5):36-54

Roy A, Apparao A (1971) The two-electrode system of resistivity prospecting. In: Symposium on 'Exploration techniques for metalliferous deposits', Khetri, Rajasthan, India

Van Overmeeren RJG (1989) Aquifer boundaries explored by geoelectrical measurements in the coastal plain of Yemen: A case of equivalence. Geophysics 54(1):38-48

11th World Congress on Water Resources and Environment (EWRA 2019)
"Managing Water Resources for a Sustainable Future", 25-29 June 2019, Madrid, Spain

Conceptualization and simulation of an integrated pump & treat and Aquifer Storage and Recovery (ASR) pilot scheme in a saline aquifer

M. Perdikaki[1*], A. Kallioras[1], C. Makropoulos[2], K. Dimitriadis[3]
[1] School of Mining and Metallurgical Engineering, National Technical University of Athens, Athens, Greece
[2] School of Civil Engineering, National Technical University of Athens, Athens, Greece
[3] Geoservice LTD, Athens, 11147, Greece
* e-mail: mperdikaki@metal.ntua.gr

Introduction

Managed Aquifer Recharge (MAR) is an increasingly used technique for water storage, for the improvement of groundwater quality and/or the reduction of seawater intrusion in an aquifer (Bouwer 2002). In many European countries and the circum-Mediterranean, a number of MAR plants, of several scales, have been developed in order to enhance reuse and storage of the existing freshwater resources (Sprenger et al. 2017; García-Menéndez et al. 2018).

A pilot-scale Aquifer Storage and Recovery (ASR) unit was constructed in the alluvial saline aquifer of Marathon plain (at the NE coast of Attica, Greece), in order to detect the rehabilitation ability of the aquifer in terms of seawater intrusion and freshwater storage. The MAR scheme was developed in accordance with innovative and practical concepts, called Subsurface Water Solutions or Technologies (SWS or SWT) that were generated especially for coastal areas suffering from seawater intrusion and freshwater resources deficiency (subsol.org; Zuurbier et al. 2017). After the unit was constructed, different experiments were conducted to explore any improvements in the salinity and the piezometry of the groundwater. The simulation of the experimental unit, using MODFLOW-2005 USGS code is presented along with several scenarios that were produced, in ModelMuse 3.10 platform, in order to determine the best water injection-abstraction scheme.

Materials and methods

The aim of the Marathon SWS approach, was the utilization of deep groundwater resources of better quality from the karstic aquifer, in order to recharge the upper saline unconsolidated formation. The karstic water is injected into the alluvial formation through a Horizontal Directional Drilling Well (HDDW), at the same time groundwater is abstracted simultaneously from a lower level of the alluvial aquifer through a vertical well. The main goal of the pilot scheme is the formulation of a seawater intrusion barrier along the coast. More details of the experimental scheme can be found in Perdikaki et al. (2018).

The conceptualization of the experiment includes:

- Two confined layers of different hydraulic conductivity (k): Layer 1: 3 m ($k = 7.13\ E^{-7}$ m/s), Layer 2: 20 m ($k = 3.1E^{-6}$ m/s)
- Grid: 2 by 2 m
- Domain: 280x400 m^2 (the surrounding area of the experiment)
- Boundary Conditions:
  - Time-Variant Specified-Head Package (CHD): coast
  - General-Head Boundary Package (GHB): Northern boundary
  - Well Package (WEL): horizontal well (injection), vertical well (pumping)

Results and concluding remarks

The results of the simulation showed an acceptable coincidence with the experimental observations. After the simulation, different ASR scenarios were developed (Table 1), in accordance with the pilot scheme special features. The simulation process and results for each scenario are presented in Table 1.

Table 1. Model scenarios and results.

Scenarios	Simulation process	Simulation results
Scenario A	▪ Injection: 2.5 m^3/h in the HDDW ▪ Pump: No pump ▪ Simulation period:40 days ▪ EC 3400μS/cm ▪ Starting Head: 0.8 m	▪ Overflow:14 days ▪ Hydraulic Head at day 14: 3m ▪ Min EC At day 14: 2569 μS/cm ▪ Hydraulic Head at day 40: 0.8 m ▪ Min EC at day 40: 2850 μS/cm
Scenario B	▪ Injection: 2.5 m^3/h in the HDDW ▪ Pump: 1 m^3/h from the vertical well ▪ Simulation period:70 days ▪ EC: 3400μS/cm ▪ Starting Head: 0.8 m	▪ Overflow:34 days ▪ Hydraulic Head at day 34: 3m ▪ Min EC at day 34: 1737 μS/cm ▪ Hydraulic Head at day 70: 0.8 m ▪ Min EC at day 70: 2213 μS/cm
Scenario C	▪ Injection: 2.5 m^3/h in the HDDW ▪ Pumping 1 $m^3$from different depths of the vertical well ▪ Simulation period:70 days ▪ EC: 3400μS/cm ▪ Starting Head: 0.8 m	▪ Same results as scenario B
Scenario D	▪ Injection: 2.5 m^3/h in the vertical well ▪ Pumping:2.5 m^3/hfrom the HDDW	▪ Well overflow from the first day

Considering the above results, the best ASR scheme for the rehabilitation of the system is Scenario B, as more freshwater is injected in the aquifer and the electrical conductivity can be held in a lower level for longer periods.

Acknowledgements: This research is a part of SUBSOL-bringing coastal SUBsurface water SOLutions to the market Project. SUBSOL has received funding from the European Union's Horizon 2020 research and innovation programme under grant agreement No 642228.

References

Bouwer H (2002) Artificial recharge of groundwater: hydrogeology and engineering. Hydrogeology Journal 10(1):121-142

García-Menéndez O, Ballesteros BJ, Renau-Pruñonosa A, Morell I, Mochales T, Ibarra PI, Rubio FM (2018) Using electrical resistivity tomography to assess the effectiveness of managed aquifer recharge in a salinized coastal aquifer. Environmental Monitoring and Assessment 190(2):100

Perdikaki M, Kallioras A, Monokrousou K, Christoforidis C, Iossifidis D, Bizani E, Zafeiropoulos A, Dimitriadis K, Raat K, van den Berg G, Makropoulos C (2018) Integrated subsurface water solutions for coastal wetland restoration through integrated pump & treat and aquifer storage and recovery (ASR). In: Multidisciplinary Digital Publishing Institute Proceedings 2(11):665

Sprenger C, Hartog N, Hernández M, Vilanova E, Grützmacher G, Scheibler F, Hannappel S (2017) Inventory of managed aquifer recharge sites in Europe: historical development, current situation and perspectives. Hydrogeology Journal 25(6):1909-1922

SUBSOL Subsurface Water Solutions. http://www.subsol.org/ (accessed on 20/02/2019)

Zuurbier KG, Raat KJ, Paalman M, Oosterhof AT, Stuyfzand PJ (2017) How subsurface water technologies (SWT) can provide robust, effective, and cost-efficient solutions for freshwater management in coastal zones. Water Resources Management 31(2):671-687

IX. Geoinformatics, Remote Sensing and Water Resources

11th World Congress on Water Resources and Environment (EWRA 2019)
"Managing Water Resources for a Sustainable Future", 25-29 June 2019, Madrid, Spain

Detection of vegetation water requirement of a Mediterranean wetland by satellite imagery

M.C. Gunacti*, C.P. Cetinkaya
Department of Civil Engineering, Dokuz Eylul University, Izmir, Turkey
** e-mail: mert.gunacti@deu.edu.tr*

Introduction

Wetlands are hotspots in the catchments due to their contribution to biodiversity and their various ecological benefits. However, they are sensitive to hydro-meteorological and man-made conditions in the catchments. Especially, coastal delta wetlands are affected directly by upstream anthropogenic activities such irrigation, wastewater disposal, etc. Monitoring (Ozesmi and Bauer 2002; DeVries et al. 2017; Kaplan and Avdan 2017; Nhamo et al. 2017) and assessing the water requirements of the wetlands (Peyman and Massoud 2006; Dabrowska-Zielinska et al. 2010) is a key issue to maintain the ecological equilibrium of these sites. The presented study investigates the vegetation water requirement of a RAMSAR site called "Bird Paradise" situated in Gediz River Delta on Aegean coast of Turkey. "Bird Paradise" is a diverse wetland with different land covers such salt and inland marshes, phrygana, permanent crops, salines and lagoons; therefore, it inhabits a large variety of species in flora and fauna (Yilmaz and Erdem 2011). Furthermore, it is on the outlet of the Gediz River Basin where the agricultural activities are intense and the major water consumer is irrigation. Irrigational water demand is therefore the main competitor for the vegetation water requirement of the site, which has substantial importance for the ecology of "Bird Paradise". Gediz riverbed was changed at the beginning of the 20th century so no natural freshwater is available to feed marshes and lagoons; however, governmental authorities allocated freshwater through irrigation channel of Menemen Left Bank Irrigation Association in order to meet water requirement of the wetland vegetation. During dry seasons irrigation schedule is tight and generally wetland does not receive enough water.

The study aims to determine near-real time vegetation water requirements of the RAMSAR site in order to assist water allocation and distribution challenges encountered. Study examines the irrigational season, which is between May-September for Gediz River Basin, since irrigation competes with water supply of the wetland. The vegetation water need is determined by GIS tools and meteorological data available.

Materials and methods

In the study, satellite images of the RAMSAR site has been processed to acquire crop coefficient (K_c) maps of the area. Since the site is on Mediterranean region, the empirical equations developed by Cuesta et al. (2004) whose study has also been on same climate, has been utilized on the conversion of Normalized Difference Vegetation Index (NDVI) to K_c.

$$K_c = 1.15NDVI+0.17 \quad (1)$$

After the reference evapotranspiration (ET_0) has been calculated by the meteorological data according to FAO-56 Penman-Monteith equation (Allen et al. 1998), vegetation water requirements of the site throughout the irrigation season has been estimated by the equation developed by Moran et al. (1997).

Results and concluding remarks

Vegetation water requirements of Bird Paradise has been calculated for the irrigation season of 2016 and 2017 (Table 1). Results show that, water requirement of Bird Paradise can be determined by satellite imagery, furthermore a 5-10 day prediction can be applied. This asset can help Menemen Left Bank Irrigation Association managers to schedule irrigation practices and allocate enough water to the wetland.

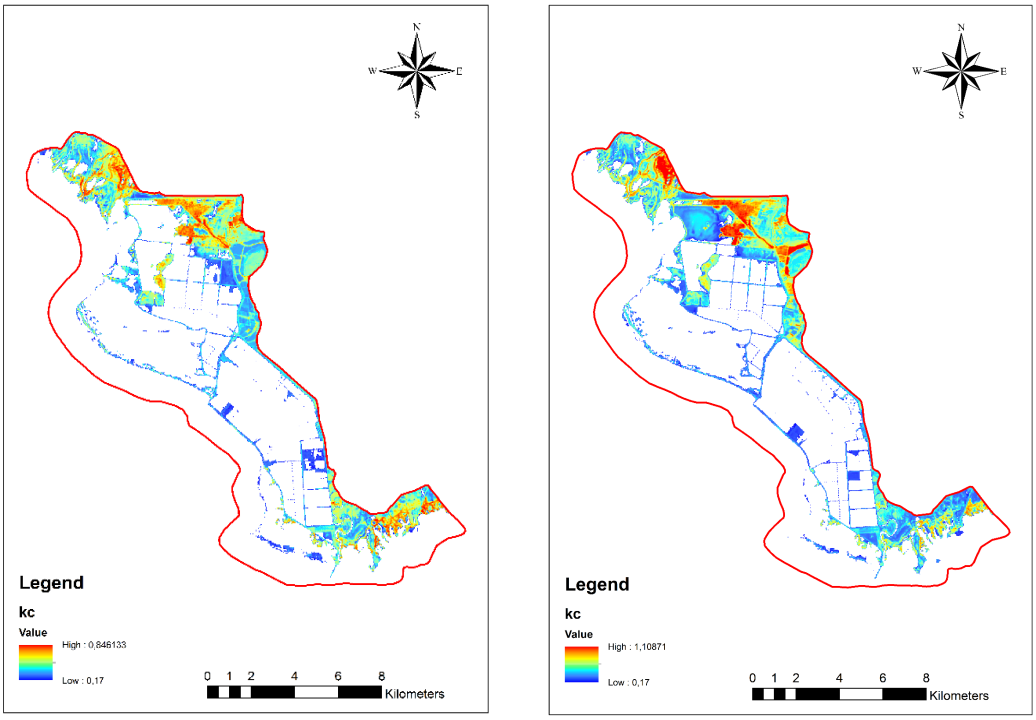

Figure 1. Produced Kc maps of Izmir Bİrd Paradise of 2016 and 2017, respectively.

Table 1. Monthly vegetation water requirement of Izmir Bird Paradise (m^3/month).

	2016	2017
May	2393987	1898316
June	4153946	4525225
July	4870890	6044422
August	4388217	6388510
September	3192496	4291397

References

Allen RG, Pereira LS, Raes D, Smith M (1998) Crop evapotranspiration – guidelines for computing crop water requirements. FAO Irrigation and Drainage paper 56, FAO, Rome

Cuesta A, Montoro A, Jochum AM, López P, Calera A (2005) Metodología operativa para la obtención del coeficiente de cultivo desde imágenes de satélite. ITEA, 101

Dabrowska-Zielinska K, Budzynska M, Kowalik W, Turlej K (2010) Soil moisture and evapotranspiration of wetlands vegetation habitats retrieved from satellite images. Hydrol. Earth Syst. Sci. Discuss. 7:5929-5955

DeVries B, Huang C, Lang MW, Jones JW, Huang W, Creed IF, Carroll ML (2017) Automated Quantification of Surface Water Inundation in Wetlands Using Optical Satellite Imagery. Remote Sens. 9(807):1-22. doi: 10.3390/rs9080807

Kaplan GJ, Avdan U (2017) Mapping and monitoring wetlands using sentinel-2 satellite imagery. ISPRS Annals of Photogrammetry, Remote Sensing and Spatial Information Sciences 4:271-277

Moran MS, Inoue Y, Barnes EM (1997) Opportunities and limitations for image-based remote sensing in precision crop management. Remote Sens. Environ. 61:319-346

Nhamo L, Magidi J, Dickens C (2017) Determining wetland spatial extent and seasonal variations of the inundated area using multispectral remote sensing. Water SA 43(4):543-552. http://dx.doi.org/10.4314/wsa.v43i4.02

Ozesmi SL, Bauer ME (2002) Satellite remote sensing of wetlands. Wetlands Ecology and Management 10:381-402

Peyman DA, Massoud T (2006) Estimation of Free Water Evaporation from Hamun Wetlands Using Satellite Imagery. Int. J 10(10):1-5

Yilmaz O, Erdem U (2011) Gediz Deltası'nin Uzaktan Algilama Teknikleri Uygulanarak Alan Kullanim Kararlari Uzerine Arastirmalar. Journal of Tekirdag Agricultural Faculty 8(1):53-63

11th World Congress on Water Resources and Environment (EWRA 2019)
"Managing Water Resources for a Sustainable Future", 25-29 June 2019, Madrid, Spain

Assessment of reservoir sedimentation using LANDSAT imagery and HEC-HMS model in Kodar reservoir watershed of Chhattisgarh State, India

C.L. Dewangan, I. Ahmad*
Dept. of Civil Engineering, National Institute of Technology Raipur, G.E. Road, Raipur, Chhattisgarh - 492010, India
** e-mail: iahmad.ce@nitrr.ac.in*

Introduction

Scientific planning for soil conservation requires knowledge of the relations between those factors that cause loss of soil and those that help to reduce such losses (Wischmeier and Smith 1978). With the change in precipitation pattern especially in terms of intensity over a short span of time, observed in past decade, results in soil erosion and ultimately causing sediment deposition in the reservoirs. Chhattisgarh state of India is having number of irrigation project for storing water in the form of reservoirs constructed before 1980's. With the development of State, percentage of forest land decreases and agricultural land area is increased. Due to this development, runoff is carrying more sediment in the reservoirs causing decrease in the designed storage. For better understanding of soil erosion causing reservoir sedimentation, remote sensing and GIS technique along with established model can be used to estimate the sediment load can be successfully applied for proper management of watershed prone to soil erosion causing decrease in reservoir capacity. A number of studies have been reported for reservoir sedimentation assessment using remote sensing and GIS technique (Ahmad and Verma 2013; Gibson et al. 2010; Jain et al. 2002).

In the present study, Kodar reservoir project, situated in Mahasamund district of Chhattisgarh State, is assessed for sediment deposition and its causes. The reservoir is reported 30% deficit to actual irrigation in the last five years. Agriculture is the dominant land use in the watershed and consists of sandy, sandy loam and silty loam type of soil which is more prone to soil erosion due to intense rainfall. A number of parametric models have been developed to forecast soil erosion at drainage basins, yet Universal Soil Loss Equation, popularly known as USLE model is most widely used empirical formula for estimating annual soil loss from agricultural basins (Ahmad and Verma 2013). Across the country, there is no provision of sediment load observation in the small streams and watershed area. Same situation is prevailing in Chhattisgarh state also. The study demonstrates the combined approach of Remote Sensing imagery and HEC-HMS model for assessing the Kodar reservoir sedimentation.

Materials and methods

For assessing the reservoir sedimentation HEC-HMS model is used, it is physically based empirical model intended to simulate the precipitation runoff, water quality, soil erosion and sediment transport forms in an extensive variety of geographic areas (Chu and Steinman 2009; Scharffenberg and Fleming 2010). Modified Universal Soil Loss Equation (Subramanya 2013) model is included in the model to calculate the soil erosion in the sub basin of the watershed. Figure 1 represents the methodological flowchart of HEC-HMS model.

Following data were utilized for reservoir sedimentation assessment procured from various sources: rainfall, temperature, designed area-elevaion-capapcity table, inflow, release, geometry of river and its tributaries, roughness coefficient, width and depth of silt deposition, soil type, imagery, DEM, topographic sheets, land use, etc.

The evaluation of revised capacity and conveyance of sedimentation in the reservoir are vital perspectives for proper reservoir operation. Landsat 8OLI and Landsat 7ETM imageries of different dates covering the entire range of live storage in Kodar reservoir have been utilized as a part of the study. For estimation of revised capacity at various levels of Kodar reservoir, NDWI strategies for image classification has been utilized to separate the water pixels from other land utilization. The revised capacities between the levels and cumulative revised capacities at various levels have been processed and compared with

designed capacities to assess the loss in storage due to sedimentation.

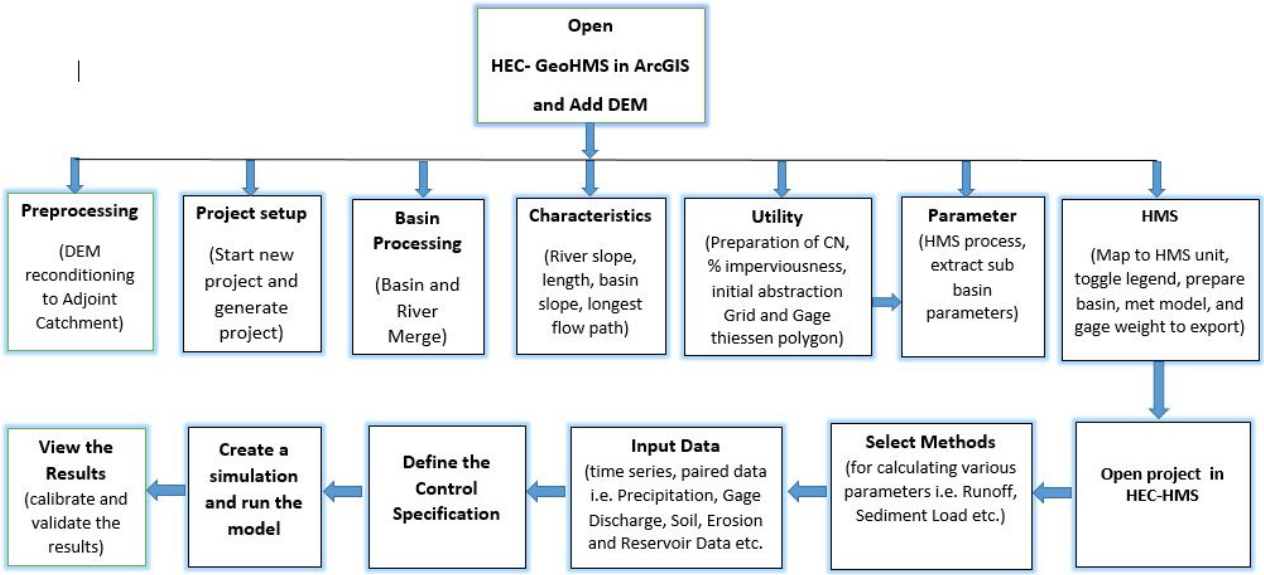

Figure 1. HEC-HMS Model

Results and concluding remarks

The sedimentation study of Kodar reservoir demonstrated that 21.44 MCM of live storage has been lost in 36 years (1981-2016). Considering the uniform loss in the storage, it can be recognized that 0.60 MCM of live storages are lost every year. HEC-HMS model simulated 1.11 million tons of average sediment load deposited during year 2012-2014 and is validated with the total sediment deposited using from remote sensing imagery and annual rainfall. The average annual soil loss from the Kodar reservoir watershed is 5.50 t/ha/year. Looking in to the future water requirement of the state, the existing reservoir should have sufficient capacity to fulfil the requirement of domestic, agricultural and industrial need. The study can be applied to the other reservoirs so that proper watershed treatment plan can be established before the alarming situation.

Acknowledgments: The authors acknowledge the support provided by State Data Centre, Water Resources Department Chhattisgarh Raipur, India, for providing necessary data and support to complete this work.

References

Ahmad I, Verma MK (2013) Application of USLE model & GIS in estimation of soil erosion for Tandula reservoir. International Journal of Emerging Technology and Advanced Engineering 3(4):570-576

Chu X, Steinman A (2009) Event and continuous hydrologic odeling with HEC-HMS. Journal of Irrigation and Drainage Engineering 135(1):119-124

Gibson SA, Pak JH, Fleming MJ (2010) Modeling watershed and riverine sediment processes with HEC-HMS and HEC-RAS. In: Watershed management conference 2010. ASCE Madison, Wisconsin, pp 1340–1349

Jain SK, Singh P, Seth SM (2002) Assessment of sedimentation in Bhakra reservoir in the Western Himalayan region using remotely sensed data. Hydrological Sciences Journal 47(2):203–212

Scharffenberg WA, Fleming MJ (2010) Hydrologic Modeling System HEC-HMS: user's manual version 3.5. US Army Corps of Engineers, Institute for Water Resources, Hydrologic Engineering Centre, Davis, CA

Subramanya K (2013) Engineering hydrology. McGraw-Hill, Delhi, India

Wischmeier WH, Smith DD (1978) Predicting Rainfall Erosion Losses. Agricultural Handbook No. 537. USDA-Science and Education Administration. Washington DC

11th World Congress on Water Resources and Environment (EWRA 2019)
"Managing Water Resources for a Sustainable Future", 25-29 June 2019, Madrid, Spain

Tropical Rainfall Measuring Mission performance in the measurement of precipitation for the Muriaé sub-basin

R.L. Frota*, F.A. Souza Filho, L.Z.R. Rolim, G.A. Reis, V.C. Porto
Department of Hydraulic and Environmental Engineering, Federal University of Ceará, Brazil
** e-mail: renata.locarno@hotmail.com*

Introduction

Remote sensing by satellites applied to Water Resources has gained visibility. A popular example of this application is the use of the satellite TRMM - Tropical Rainfall Measuring Mission that studies clouds, rainfall, heat flow, lightning and other aspects of the water cycle contributing to climate research in various locations around the world. The TRMM provides images in almost real time: they change every three hours and its resolution is 25 km. Thus, this work aims to analyze the performance of the data obtained by the TRMM through comparison between them and the average precipitation obtained through the Thissen method, using data from the National Agency of Water (ANA). The study area is the basin bounded by the fluvial station Itaperuna (58940000) belonging to the Muriaé River, Paraíba do Sul Basin, in southeast Brazil.

Materials and methods

Within this area we have six pluviometric stations. The historical series of precipitation obtained from the pluviometric stations were used for the period from 2000 to 2016. The average monthly precipitation in the basin was determined by the Thissen method. After obtaining the average monthly precipitation, it was possible to calculate the annual cumulative precipitation. This data is to be used in the comparison. Scripts developed on the software R were used to decode TRMM information. Within the sub-basin area, sixteen points were observed in a 4x4 mesh, where each was considered a pluviometer. Thus, an arithmetic mean was obtained to acquire the average daily precipitation. Consequently the monthly average and the annual accumulation were also obtained.

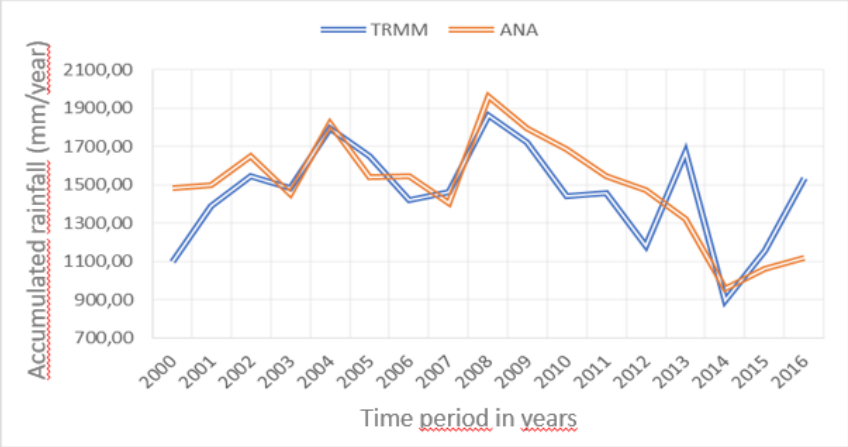

Figure 1. Comparative graph of cumulative precipitation.

Results and concluding remarks

From the data manipulation of the rainfall stations (ANA) and TRMM it was possible to observe, according to Figure 1, that the values are close. However, in five years (2000, 2010, 2012, 2013 and 2016), there was a significant disparity, reaching a 37% percentage difference in the year 2016. The correlation between the values is equal to 0.70 which means a good similarity between the two curves.

These differences may be due to systematic errors which are susceptible to the pluviometers. We can

consider data losses due to equipment wetting, evaporation and aerodynamic effects. In addition, the measurement is executed manually which makes it susceptible to human failure. Another problem is the scarcity and reliability of the data, being some or even several days without measurement. The spatial distribution of pluviometers is also a significant factor. Additionally, it must be considered that the satellite can present errors due to the overlap of clouds because it considers the cloud's reflectance and this fact can result in some imprecision.

After the study it is possible to verify that Tropical Rainfall Measuring Mission data are satisfactory when used in the Paraíba do Sul basin.

Acknowledgments: The authors thank National Council for the Improvement of Higher Education (CAPES), National Council for Scientific and Technological Development (CNPq) and Cearense Foundation for Scientific and Technological Development Support (FUNCAP) for the financial support.

References

Blacutt lA, Herdies dL, de Gonçalvez LGG, Vila DA, Andrade M (2015) Precipitation comparison for the CFSR, MERRA, TRMM3B42 and combined scheme datasets in Bolivia. Atmos. Res., 163:117-131

Clarke RT, Buarque DC, de Paiva RCD, Collischonn W (2011) Issues of spatial correlation arising from the use of TRMM rainfall estimates in the Brazilian Amazon. Water Resour. Res. 47:W05539

Collischon B, Collischon W, Tucci C (2006) Analysis of the precipitation field generated by the TRMM satellite on São Francisco Basin until Três Marias. I Simpósio de Recursos Hídricos do Sul-Sudeste, 27-29 de Agosto, Curitiba, PR.

De Gonçalves LGG, Shuttleworth WJ, Nijssen B, Burke EJ, Marengo JA, Chou SC, Houser PR, Toll DL (2006) Evaluation of Model-Derived and Remotely Sensed Precipitation Products for Continental South America. J. Geophys. Res. 111:D16113

Magionni V, Meyers PC, Robinson MD (2016) A review of merged high-resolution satellite Precipitation product accuracy during the Tropical Rainfall Measuring Mission (TRMM). Era, J. Hydrometeorol. 17:1101-1117

11th World Congress on Water Resources and Environment (EWRA 2019)
"Managing Water Resources for a Sustainable Future", 25-29 June 2019, Madrid, Spain

Crop water requirement prediction and observation of potential productivity on the scope of a Mediterranean agricultural plot

M.C. Gunacti[1*], A. Gul[1], C.P. Cetinkaya[1], D. Kahraman[2], F. Kıdoğlu[2], S. Ozcelik[2]
[1] Department of Civil Engineering, Dokuz Eylul University, Izmir, Turkey
[2] UTAEM, Ministry of Agriculture and Forestry, Izmir, Turkey
* e-mail: mert.gunacti@deu.edu.tr

Introduction

Over the past century there has been a dramatic increase in water scarcity and drought in arid and semi-arid territories even in the Northern Hemisphere, that nowadays have become a topic of increasing research attention also in European Union. Despite Europe's being considered as having adequate water resources, water scarcities and droughts become an increasingly frequent and widespread phenomenon in the scale of the European Union. The imbalance caused by water demand much over the available water resources is a major drawback. In addition, consequences of climate change are expected to produce more negative impacts on water availability, adding pressures to the most stressed EU regions including the Mediterranean. During recent years, Earth Observation (E.O.) from space has become the most important source of data for monitoring much of the land surface-atmosphere processes and in particular the hydrology of agricultural and forestry areas. Nowadays, E.O. data are implemented in operative applications for the management of land and water resources (D'Urso et al. 2015). Implementations such as land and water resources monitoring (Behera et al. 2018; Jódar et al. 2017), water quality monitoring (Imen et al. 2018) have been possible in a more efficient manner with thanks to remote sensing.

Individually, FATIMA (FArming Tools for external nutrient Inputs and water MAnagement) is one of the joint research efforts which used the E.O. data in order to monitor and manage the agricultural resources in a more effective and efficient way. The project was funded by the European Commission under the Horizon 2020 programme of research and innovation. It is a multi-national project with 9 active participating countries. In the project, satellite data from Landsat-8 and Sentinel-2 sources were used to monitor pilot plots where various crops have been traditionally cultivated. In the process of 3 years in the project, each harvest provided new outputs about forecasting crop water requirements (CWR) and each plot's yielded variability. Crop monitoring and CWR services have been available since 2015 on the internet platform so-called spiderWEBgis which has been developed by Universidad de Castilla-La Mancha (UCLM) and data sourced by each pilot area. This paper presents the methodological framework of potential productivity map and accuracy of the CWR prediction throughout the irrigation season of the Turkish pilot area considered in the FATIMA project.

Materials and methods

In the study, satellite images of the pilot area have been processed to acquire crop coefficient (K_c) distribution maps. The empirical equations developed by Cuesta et al. (2004), where Mediterranean climate was also targeted, has been utilized in converting Normalized Difference Vegetation Index (NDVI) to K_c as follows:

$$K_c = 1.15NDVI+0.17 \quad (1)$$

After the reference evapotranspiration (ET_0) has been calculated by the meteorological data according to FAO-56 Penman-Monteith equation (Allen et al. 1998), daily transpirations of the pilot has been estimated by the equation developed by Moran et al. (1997). Accumulated daily transpirations from crop emergence until maturity were interpreted as proxy to the potential productivity map, which can later be transferred to biomass through multiplication by water productivity.

Results and concluding remarks

The study results indicate that there has been a total difference of approximately 250 mm between the physically-applied and methodologically-predicted irrigations in the season for the plot 1WU1. Differences were observed to increase in early and later stages of the crops phenology (Figure 1). Potential productivity map, which was produced from the accumulation of the transpirations throughout the season, indicates relatively more productive areas in the plot in red and less productive areas in green (Figure 2).

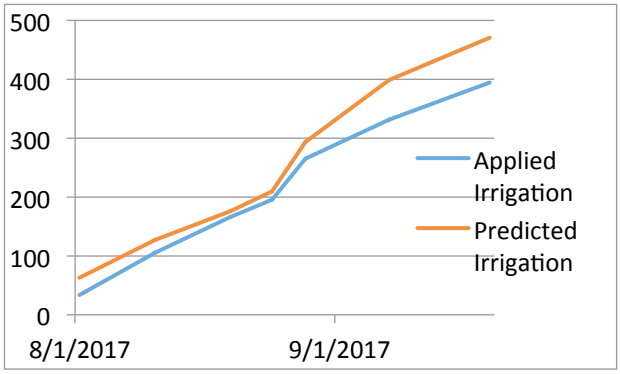

Figure 1. Applied and predicted irrigations of plot 1WU1 of season 2016

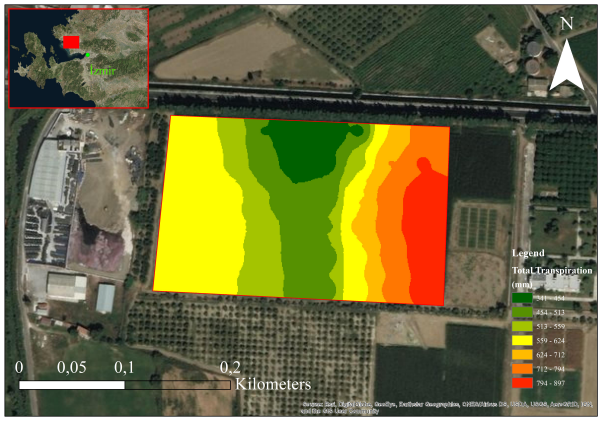

Figure 2. Potential productivity map of pilot plot 1WU1 for season 2016

Acknowledgments: This study has been formed by the findings of the Turkish Pilot of Project "FATIMA" of Horizon 2020 Programme of Research and Innovation of European Commission with collaboration of Turkish partner UTEAM (International Agricultural Research and Training Center of Ministry of Agriculture and Forestry of Turkey).

References

Allen RG, Pereira LS, Raes D, Smith M (1998) Crop evapotranspiration – guidelines for computing crop water requirements. FAO Irrigation and Drainage paper 56. FAO, Rome.

Behera MD, Gupta AK, Barik SK, Das P, Panda RM (2018) Use of Satellite remote sensing as a monitoring tool for land and water resources development activities in an Indian tropical site. Environ Monit Assess 190(401):1-21

Cuesta A, Montoro A, Jochum AM, López P, Calera A (2005) Metodología operativa para la obtención del coeficiente de cultivo desde imágenes de satélite. ITEA, 101

D'Urso G, Vuolo F, Chirico GB, De Michelle C (2015) Earth Observation for Monitoring Irrigation Demand. Agrociencia Uruguay 19(3):76

Jodar J, Carpintero E, Martos-Rosillo S, Ruiz-Constan A et al. (2018) Combination of lumped hydrological and remote-sensing models to evaluate water resources in a semi-arid high altitude ungauged watershed of Sierra Nevada (Southern Spain). Science of the Total Environment 625:285-300

Moran MS, Inoue Y, Barnes EM (1997) Opportunities and limitations for image-based remote sensing in precision crop management. Remote Sens. Environ. 61:319-346

Imen S, Chang N, Yang YJ, Golchubian A (2018) Developing a Model-Based Drinking Water Decision Support System Featuring Remote Sensing and Fast Learning Techniques 12(2):1358-1368

11th World Congress on Water Resources and Environment (EWRA 2019)
"Managing Water Resources for a Sustainable Future", 25-29 June 2019, Madrid, Spain

Sugarcane yield prediction at farm scale using remote sensing and artificial neural network

M. Rahimi Jamnani[1*], A. Liaghat[1], N. Sadeghi Loyeh[2]
[1] Department of Irrigation and Reclamation, University of Tehran, Karaj, Iran
[2] Department of Irrigation and Drainage, University of Tehran, Tehran, Iran
* e-mail: mostafarahimi@ut.ac.ir

Introduction

Accurate predictions of regional yield for sugarcane agro-industries are of vital importance for formulating harvesting, milling and forward selling decisions, while at a block scale they provide growers with an understanding of both in-crop variability and total production (Robson et al. 2016). Lack of a reliable model and inadequate image processing equipment analysers lead the sugarcane agro-industries toward yield prediction through manual sampling (destructive), which is not only associated with sampling problems but also requires spending money and labour. Moreover, vegetation models require agronomic and meteorological data, which are not easily available due to their wide spatial distribution. Many plant indices based on canopy spectral reflectance have shown the ability to estimate crop physiological properties accurately; including plant, biomass and crop yield (Tucker et al. 1979; Zhao et al. 2003). Current rates of sugar production in Iran could not meet the demands, so that the unsatisfied demand shall be supplied by imports (ISFS 2017). By increasing the farm yield and achieving higher sugar purity, one can attenuate the need for imports.

Numerous studies have been performed on finding relationships between remotely sensed vegetation indices and yield across sugarcane farms, most of which have been performed on regional scale. Bégué et al. (2010) used SPOT4 and SPOT5 images and assumed an exponential relationship between maximum NDVI and sugar yield, ending up with a R^2 value of 0.78. Lofton et al. 2012 Predicted sugarcane yield based on NDVI and stipulated that the best time for estimating sugarcane yield is the interval between 601 and 750 Growing Degree-Days. Fernandes et al. (2017) used NDVI time series of MODIS images. The result showed that R^2 was 0.63 for the Stacking method, anticipating the crop forecast by three months before the harvest.

The present research is aimed at identifying the appropriate date for acquiring best satellite images to achieve maximum correlation between vegetation indices and end of season yield at farm scale. The research further looks for the optimal model and the best vegetation index for predicting irrigated sugarcane yield.

Materials and methods

Imam Khomeini Sugarcane Agro-Industry is developed in Khuzestan Province, Iran and including 530 farms with a total area of 15,800 hectares. The average annual precipitation of 237 mm and average altitude is 30 meters based on MSL. In this area, different cultivars of sugarcane are irrigated with furrow irrigation system. In general, local soil is heavy and dominantly composed of silty clay loam and silty clay. The most important challenges affecting sugarcane growth in study area are soil salinity and water scarcity.

For the purpose of this research, two scene of LANDSAT8 were used and investigations were performed during four crop season from 2013 to 2017.

Three indices were used to estimate sugarcane yield, namely Normalized Difference Vegetation Index (NDVI), Green Vegetation Index (GVI), and Green Normalized Difference Vegetation Index (GNDVI). NDVI is an index to measure health and greenness of plant. GVI refers to green vegetation index, which minimizes the effects of background soil and emphasizing green vegetation. GDNVI is mostly similar to NDVI, except that here we measure green spectrum rather than red. In each farm, Average values of vegetation indices were measured using 25 Landsat images in development growth stage for four seasons. After calculating

vegetation indices for each farm (Average pixel values), multivariate linear regression (MLR) and Artificial Neural Network (ANN) models were examined to estimate sugarcane farm yields. Furthermore, two methods were used to find the optimal model: (a) modelling based on acquiring a single image during plant development stage and calculating vegetation indices for each farm, and (b) modelling based on acquiring multiple images during plant development stage and calculating vegetation indices for each date and use in models.

Results and concluding remarks

The results show that maximum values of the vegetation indices have occurred from 235 to 260 days after last harvest (late August to mid-September) which marks the end of the vegetation growth stage. Irrigation is cut off at the end of the vegetation growth stage in order to increase sugar content and make vegetation indices decrease after their peak. Farm data including Harvesting year, ratoon age, variety, soil type and average vegetation index used as input for both MLR and ANN model then various scenarios were tested to achieve the best model. Compared to the MLR model, ANN model exhibited better performance. Differences in growth stage among sugarcane farms at each image results in reduced linear correlation between vegetation indices and farm yield. Based on results, using multi images during a season was found to impose no significant effect on the value of the coefficient of correlation, while decreasing the value of RMSE. GVI provided better predictability compared to GNDVI and NDVI in all scenarios. Using June, July and August images together make best results (coefficient of correlation: R = 0.897; root mean square error RMSE = 6.1 ton/ha; normalized root mean square error: NRMSE = 0.053).

The prediction of sugarcane yield with before August images increases the risk of poor water distribution or other stress after august, therefore, vegetation indices have a lower correlation with yield. In contrast, prediction of sugarcane yields with images acquired after August also showed lower correlation with vegetation indices, due to the plant stress caused by stopping irrigation from mid-September. Therefore, it can be generally concluded that, the vegetation indices show maximum correlation with plant yield when it reaches its maximum value which is about three month before harvest. As the date of acquired images gets farther from the harvesting date, the risk of various stresses such as water scarcity increases and reducing the correlation between vegetation indices and farm yield.

References

Bégué A, Lebourgeois V, Bappel E, Todoroff P, Pellegrino A, Baillarin F, Siegmund B (2010) Spatio-temporal variability of sugarcane fields and recommendations for yield forecast using NDVI. International Journal Remote Sensing 31:5391–5407. http://doi.org/10.1080/01431160903349057

Fernandes JL, Ebecken NF, Esquerdo JD (2017) Sugarcane yield prediction in Brazil using NDVI time series and neural networks ensemble. International Journal of Remote Sensing 38(16):4631-4644. http://doi.org/10.1080/01431161.2017.1325531

Iranian Sugar Factories Syndicate, Available online: http://www.isfs.ir/

Lofton J, Tubana SB, Kanke Y, Teboh J, Viator H, Dalen M (2012) Estimating Sugarcane Yield Potential Using an In-Season Determination of Normalized Difference Vegetative Index. Sensors 12(6):7529-7547. http://doi.org/10.3390/s120607529

Robson A, Abbott C, Lamb D, Bramley R (2012) Developing sugar cane yield prediction algorithms from satellite imagery. In: 34th Annual Conference Australian Society of Sugar Cane Technologists, Cairns

Tucker CJ (1979) Red and photographic infrared linear combinations for monitoring vegetation. Remote Sens. Environ 8(2):127–150. http://doi.org/10.1016/0034-4257(79)90013-0

Zhao D, Reddy KR, Kakani KG, Read J, Carter GA (2003) Corn growth, leaf pigment concentration, photosynthesis, and leaf hyper-spectral reflectance properties as affected by nitrogen supply. Plant and Soil 257:205–217

11th World Congress on Water Resources and Environment (EWRA 2019)
"Managing Water Resources for a Sustainable Future", 25-29 June 2019, Madrid, Spain

Automatic generation of a TIN discrete model for rainfall-runoff transformation and hydraulic propagation based on DEM data

M. Sinagra[1*], C. Nasello[1], T. Tucciarelli[1], T. Moramarco[2]
[1] Department of Engineering, University of Palermo, Palermo, Italy
[2] Research Institute for Hydro-geological Protection, National Research Council, Perugia, Italy
* e-mail: marco.sinagra@unipa.it

Introduction

Rainfall-runoff transformation inside a catchment basin can be split in the hydrological formation of net rain and in the propagation of the same rain over the basin. Propagation is strongly affected by the catchment topography and this information is usually found in the Digital Elevation Model (DEM) of a rectangular area including the area of the catchment basin. Unfortunately, small errors in the ground level measurements can lead to large errors in the hydrograph estimation, mainly due to the formation of several artificial minima where large volumes of water remain stored during the rain. To avoid this inconvenient, it is possible to modify the DEM in order to guarantee a minimum negative slope in at least one of the eight directions connecting each cell with the neighbour ones, in spite of a small deviation from the measured data.

Call $\mathbf{S}_i$ the set of cells in the upstream tree of cell *i*. Call $\mathbf{S}_{imin}$ the set of cells inside the contour of the catchment basin. The drainage area D_i of cell *i* is given by the sum of the areas of the cells of set $\mathbf{S}_i$. A hydrologic network with a density smaller than the maximum one can be easily obtained from the set $\mathbf{S}_{imin}$ by removing all the cells of the set $\mathbf{S}_i$ corresponding to a drainage area D_i smaller than a fixed minimum value. A practical way to fix this minimum area is to fix a minimum percentage *r* of the total catchment area, called threshold ratio. Call $\mathbf{S}^r_{imin}$ the resulting set of cells. We get an hydrologic network with a density associated to the fixed ratio *r* by connecting the centre of each cell *m* with *iout*(*m*), where *iout*(*m*) is the neighbour cell along the most negative descending direction.

A numerical SW model using all the DEM cells as computational cells would be quite demanding from a computational point of view. In the following, a Triangular Irregular Network (TIN) which satisfies the extended Delaunay property (Aricò et al. 2011) is created on the basis of the proposed hydrologic network. In the proposed TIN all the edges of the network are either sides of triangles, or are split in smaller edges aligned in the same direction, in order to save the Delaunay property of the mesh. The mesh will have the maximum density close to the hydrologic network, but the triangular shape of the elements allows a strong reduction of the mesh density in areas with higher slope. The ground elevation of the nodes is given by a bilinear or piece-wise linear interpolation of the DEM corrected elevations at the centre of the cells. This correction is further improved to avoid the creation of artificial minima due to the existence of triangle sides linking nodes located far from each other.

Materials and methods

We compute the sub-optimal solution of our problem as combination of two intermediate solutions, named "upper" and lower" solutions. The upper solution *zu* is a feasible solution of the original problem, where at least one direction with a minimum slope does exist for each cell, except for the lowest one, and all the corrected elevations are higher than or equal to the measured ones. This type of solution has already been proposed by many authors, like Zhu et al. (2013). In the following, a very simple and fast iterative formula is proposed for its computation.

The "upper" solution is often a good sub-optimal solution of our problem, but it always overestimates the optimal one, with an artificially flat area covering each artificial minimum. If a positive error is given in the elevation datum of a cell *i* inside a riverbed, all the upstream part of the riverbed will be artificially raised, up to the elevation of cell *i*. To avoid this inconvenient, many authors like Martz et al. (1999) or

Grimaldi et al. (2007), try to "breach" the artificial dam created by the positive errors or to simulate the natural erosion process for the removal of the artificial deposit.

To improve the sub-optimal solution, we search instead a "lower" solution with corrected elevations *zl* always smaller than the measured ones. In the search of the lower solution we maintain negative (i.e. descending) the sign of the slope in the direction from cell *i* to the cell *iout(i),* previously computed in the search of the "upper" solution, for all the cells *i* of the catchment basin.

The final solution is found for each cell *i* of the basin through a linear combination of the lower and the upper solution, such that:

$$z_i = \alpha(C_i) zl_i + (1-\alpha(C_i)) zu_i \text{ if } i \in \mathbf{A} \quad (1)$$

$$z_i = z_i^* \text{ if } i \notin \mathbf{A} \quad (2)$$

where $\alpha(C_i)$ is a suitable coefficient depending on the location of cell *i*, $\mathbf{A}$ is the set of cells where the upper solution is strictly higher than the lower solution and z_i^* is the measured elevation. Observe that each value of α, for $0 \le \alpha \le 1$, provides a feasible solution of the original minimization, because both upper and lower solutions are feasible, as well as any linear combination of them.

The corrected elevation $\mathbf{z}$ is the basis for the computation of the hydrologic network. This network can be thought as the ensemble of the segments connecting the centres of cells *i*, *iout*(*i*). These segments will have only four possible directions: the x direction, the y direction and the two diagonal directions. The final hydrologic network is the network resulting from the segments connecting all the cells with a drainage area greater than the minimum value corresponding to the fixed threshold ratio.

The strong advantage of this network is that it is an optimal basis for the generation of a TIN to be used as spatial discretization in a shallow water hydraulic model. In the sought after TIN all the edges of the hydrologic network are set as internal boundaries and overlap triangular edges. Because all the edges have a descending slope, this implies that artificial obstructions, like artificial topographic minima or river "cutting edges" will not be met by the simulated channel flow. Because the length of the edges is very small, it is important to use a TIN with heterogeneous mesh density, decreasing along with the distance from the segments of the hydrologic network.

Results and concluding remarks

The proposed algorithm is applied to a small gauged basin of the Tiber river, where both discharges and rain depths in a selected number of locations are available for several events. The DEM data are automatically managed to get both the hydrologic network and the computational mesh, used as input by the MAST-2D model along with the net rain measured in three different events. Computed flooded areas are compared with photos made immediately after those events, with a good match between observed and computed data.

References

Aricò C, Sinagra M, Begnudelli, L, Tucciarelli T (2011) MAST-2D diffusive model for flood prediction on domains with triangular Delaunay unstructured meshes. Advances in Water Resources 34 (11):1427-1449

Zhu D, Ren Q, Xuan Y, Chen Y, Cluckie I (2013) An effective depression filling algorithm for DEM-based 2-D surface flow modelling, Hydrol. Earth Syst. Sci. 17:495–505

Martz L, Garbrecht J (1999) An outlet breaching algorithm for the treatment of closed depressions in a raster DEM, Comput. Geosci 5:835-844

Grimaldi S, Nardi F, Di Benedetto F, Instanbulluoglu E, Bras R (2007) A physically based method for removing pits in digital elevation models. Adv. Water Resour. 30:2115-2158

11th World Congress on Water Resources and Environment (EWRA 2019)
"Managing Water Resources for a Sustainable Future", 25-29 June 2019, Madrid, Spain

Contribution of remote sensing for the estimation of the sedimentation of the Beni Haroun reservoir (W. Mila, Algeria)

F.Z. Tebbi*, H. Dridi, M. Kalla, H. Baazi
Natural Hazards and Territory Planning Laboratory LRNAT, Earth Sciences and Universe Institute, Geography and Territory Planning Department Mostefa Benboulaid Batna 2 University, Fesdis, Batna, Algeria
** e-mail: f.tebbi@univ-batna2.dz*

Introduction

Sedimentation reduces reservoir storage and the benefits derived therefrom (Annandale et al. 2016). Once a reservoir is in operation, sediment accumulation is measured by performing repeated hydrographic surveys. However, these measurements are very costly and time consuming. In the last few years, it becomes very easier to quantify sedimentation in a reservoir using Remote Sensing (Donchyts et al. 2017; Foteh et al. 2018). Temporal changes in water spread area are analyzed to assess sediment deposition in reservoirs requiring less time. In present study, sedimentation of Beni Haroun Reservoir is carried out using Remote Sensing approach using Google Earth Engine (GEE) cloud computing platform.

Materials and methods

Beni Haroun Dam is located in the confluence of Rhumel Wadi at East and Enndja Wadi at West in Mila town, some 70 km West of Constantine Town, is a rectilinear Rolled Compactec Gravity dam of 118 m high. It is a great strategic hydraulic complex, with a capacity of 960 million cubic meters. It supplies drinking water to several districts in the including Jijel, Constantine, Oum el Bouaghi, Batna and Khenchela. It also provides a significant amount of irrigation water for a few hundred hectares.

Google Earth Engine offers the opportunity to perform global-scale geospatial analysis at no cost. The most convenient way to use GEE is through its web-based code editor for interactive algorithm development based on Earth Engine JavaScript API. Recently available Sentinel-2 Multi Spectral Instrument (MSI) imagery were used to estimate the water spread area of the reservoir at different reservoir levels and several dates. Original Reservoir Area-capacity curve and different water level changes were obtained from the Algerian Agency of Dams and Transfers of Beni Haroun reservoir (ANBT) (2015-2018). Satellite data (Oct. 2015 to 4 July 2018) were used to assess temporal and spatial patterns of the water spread area of the reservoir. Available Satellite images of 2017 year and correspondent water levels at Beni Haroun reservoir used to assess its sedimentation. Water level has been recorded between 197.13 m and 200.29 m. The Normalized Difference Water Index (NDWI) was first suggested by McFeeters (1996) to detect surface waters in wetland environments and measure surface water dimensions. NDWI method used in this paper uses the green and NIR bands.

$$NDWI = \frac{Green - NIR}{Green + NIR} \quad (1)$$

As a result, water features have positive values and are enhanced. Vegetation and soil features usually have zero or negative values and are suppressed.

Results and concluding remarks

Normalized Difference Water Index time series from 2015 to 2018 are obtained from a written script GEE. Then, time series chart of correspondent water spread areas can be produced (Figure 1).

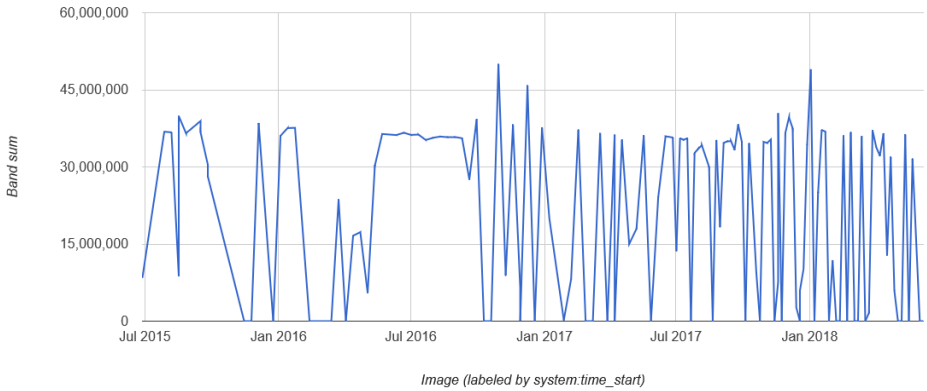

Figure 1. Water spread areas time series (04/2015 to 06/2018) Sentinel 2.

New reservoir capacity between two successive reduced levels and water levels is calculated using trapezoidal formula as:

$$V = \frac{h}{3}\left(A_1 + A_2 + \sqrt{A_1 A_2}\right) \quad (2)$$

Progressive volumes were computed and compared with the design volumes for the same levels. The reduction in volume was attributed to the estimation of present storage capacity and capacity loss due to sedimentation (Foteh et al. 2018). Using the Prismoidal formula, the revised capacity between the maximum (200.29 m) and minimum (197.13 m) observed levels is obtained jointly with Elevation-Area-Capacity curve (Figure 2.). The loss in live storage capacity since base period (2007) to the year 2017 based on Remote Sensing is about 0.5 hm^3/year.

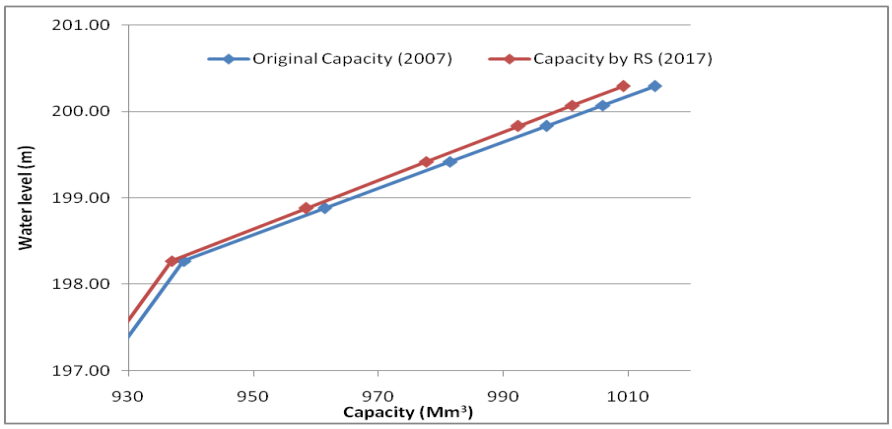

Figure 2. Original (hydrographic) and revised (remote sensing) elevation-capacity curves

Thus, original live storage capacity of Beni Haroun Reservoir 997.900 hm^3 is reduced to 992.800 hm^3. Benefits of utilizing GEE for implementation Remote Sensing gives information of the capacities only in the water level fluctuation zone, which generally lies in the live zone of the reservoir. On the basis of analysis of Remote Sensing, sedimentation at Beni Haroun Reservoir seems to be more important on the side of Endja River.

References

Annandale GW, Morris GL et al. (2016) Extending the Life of Reservoirs: Sustainable Sediment Management for Dams and Run-of-River Hydropower, World Bank Publications.

Donchyts G, Giesen NVD et al. (2017) Reconstruction of reservoir and lake surface area dynamics from optical and SAR satellite imagery. International Workshop on the Analysis of Multitemporal Remote Sensing Images (MultiTemp). Brugge, Belgium.

Foteh R, Garg V et al. (2018) Reservoir Sedimentation Assessment through Remote Sensing and Hydrological Modelling. Journal of the Indian Society of Remote Sensing 46(11):1893–1905

McFeeters SK (1996) The use of the Normalized Difference Water Index (NDWI) in the delineation of open water features. International Journal of Remote Sensing 17(7):1425-1432

11th World Congress on Water Resources and Environment (EWRA 2019)
"Managing Water Resources for a Sustainable Future", 25-29 June 2019, Madrid, Spain

Groundwater over-abstraction in Jordan: Impact and outlook

R. Bahls[1*], A. Subah[2], K. Holzner[1], R. Al-Roud[2], M. Alhyari[3]
[1] Federal Institute for Geosciences and Natural Resources, Hanover, Germany
[2] Ministry of Water and Irrigation, Amman, Jordan
[3] Federal Institute for Geosciences and Natural Resources, GWRM-Project, Amman, Jordan
* e-mail: rebecca.bahls@bgr.de

Introduction

Groundwater is the most important component of the Jordanian water supply, but falling groundwater levels in monitoring wells as well as drying out of production wells and springs are indicators of an extremely critical situation for the resource. It is quite challenging to take the step from single point observations to a regional quantification of resources due to low observations densities and complex geology. Planning without reliable data is less effective. Therefore, it is very important to regularly assess and analyze the groundwater situation in the country.

One of the most used aquifers countrywide, and thus at risk, is the A7/B2. Population growth, increased use of water for irrigation and illegal extraction has aggravated the situation: the continuous decline of groundwater levels leads to a further extension of potentially unsaturated areas.

In a joint cooperation project between the Ministry of Water and Irrigation (MWI) and the Federal Institute for Geosciences and Natural Resources (BGR), a nationwide groundwater inventory, the second after 1995, has been conducted to collect the latest available data. A first product out of this exercise is the groundwater contour map for the A7/B2 aquifer, which is the base for thematic maps presenting the depth to water level, drawdown since 1995, and saturated thickness. All results are used by decision makers trying to assure a continuous water supply in Jordan.

Materials and methods

Current groundwater level measurements in 42 observation points have been taken and analyzed. Additionally, 99 measurements from turned off pumping wells and 119 extrapolated historical data sets were used as supporting points to draw the contour lines. The data distribution shows that there is a huge gap of observation points in the eastern part of the country. To be able to produce adequate maps, an area of data certainty was defined based on the most eastern monitoring points available. Based on the ANUDEM 5.3 program developed by Michael Hutchinson (1988, 1989, 1996, 2000 and 2011), the groundwater contour lines were rasterized, using ArcGIS.

The different thematic maps were produced based on the combination of the groundwater contour map and the structural map (Brückner 2018).

Results and concluding remarks

Natural groundwater flow conditions within the A7/B2 aquifer are affected by high abstraction rates, especially in the northern part of Jordan, where a regional groundwater drawdown cone seems to have developed. Between Mafraq and Azraq the groundwater flow direction has been inverted. Instead of flowing towards the Azraq oasis (1995), now it flows towards the regional depression cone caused by the abstraction wells around Mafraq.

Unsaturated areas west of Mafraq had already been mapped before 1995 (Margane 1995, 2002). However, these areas have significantly expanded towards the west since then. Large zones along the outcrop areas have become potentially unsaturated. Furthermore, the declining groundwater levels result in the deterioration of the groundwater quality.

The map of groundwater level difference between 1995 and 2017 shows that almost the whole country is affected by a continuous drawdown. In critical areas (along the eastern side of the highlands and north of Amman), the drawdown is more than 100 meters. The actual annual groundwater production is the main

reason for a strong drawdown in certain areas. Furthermore, in areas with a very high drawdown and a small number of legal wells, the possibility of a high density of illegal wells needs to be taken in consideration. This is especially the case North and West of Irbid, where private wells are scarce but drawdown is high. The analysis of satellite images show a wide area used for agriculture.

Because the A7/B2 aquifer is partly unsaturated, wells have to be deepened into underlying aquifers, e.g. A4 or A1/A2. Considering the available information and assuming that the abstraction rate will stay at the same level, the drawdown will continue and the extension of unsaturated areas will consequently increase. That would result in a significant increase of spending for water production through deeper wells and electricity costs due to pump rise of more than 300 m out of the subsurface. Following the development of the last years, it is more likely that the abstraction rate will increase, which would accelerate the extension of unsaturated areas.

Acknowledgments: The project "Groundwater Resources Management, Jordan" is part of the German-Jordanian technical cooperation financed by the Federal Ministry for Economic Cooperation and Development.

References

Brückner F (2018) Update of Structure Contour Maps of Ajloun and Belqa Groups which is part of the BGR project "Improved Groundwater Resources Management in Response to the Syrian Refugee Crisis", Hanover, Germany

Hutchinson M (1988) Calculation of hydrologically sound digital elevation models. In: 3rd International Symposium on Spatial Data Handling, Sydney, Australia

Hutchinson M (1989) A new procedure for gridding elevation and stream line data with automatic removal of spurious pits. Journal of Hydrology 106:211–232

Hutchinson M (1996) A locally adaptive approach to the interpolation of digital elevation models. In: Proceedings of 3rd International Conference/Workshop on Integrating GIS and Environmental Modeling, National Center for Geographic Information and Analysis, Santa Barbara

Hutchinson M (2000) Optimising the degree of data smoothing for locally adaptive finite element bivariate smoothing splines. ANZIAM Journal 42(E):C774–C796

Hutchinson M, Xu T, Stein J (2011) Recent Progress in the ANUDEM Elevation Gridding Procedure. In: Geomorphometry 2011, T. Hengel et al. (eds), Redlands, California, USA, pp 19–22

Margane A (2002) Contributions to the hydrogeology of northern and central Jordan. Geologisches Jahrbuch C 68:3-51

Margane A, Almomani M, Hobler M (1995) Groundwater Resources of Northern Jordan. Vol.2: Groundwater Abstraction Groundwater Monitoring, Part 1: Groundwater Abstraction in Northern Jordan, BGR, Amman

11th World Congress on Water Resources and Environment (EWRA 2019)
"Managing Water Resources for a Sustainable Future", 25-29 June 2019, Madrid, Spain

Evaluating the performance of a hydrodynamic model using SAR images

A. Gkouma, I. Zotou*, V. Bellos, V. Karathanassi, V.A. Tsihrintzis
School of Rural and Surveying Engineering, National Technical University of Athens, 9 Iroon Polytechniou St., Zografou, 15780 Athens, Greece
** e-mail: iwannazwtou@central.ntua.gr*

Introduction

The evaluation of the performance of flood models is a difficult task, mainly due to the lack of in-situ data. In this context, the contribution of Remote Sensing is crucial. Flood simulation, incorporating Remote Sensing techniques, constitutes a subject which has been widely discussed (e.g., Yan et al. 2013; Patro et al. 2009; Di Baldassarre et al. 2011) demonstrating the high potential of using satellite data to evaluate the flood model results. Specifically, the ability of microwave irradiation to penetrate cloud cover, and thus, effectively detect floods has rendered the use of radar imagery decisive in flood mapping (Horritt 2000).

The present study employs satellite Synthetic Aperture Radar (SAR) images to test the performance of a hydrodynamic model. The methodology was applied in a real-world case study, namely a 25-km reach of Pineios River, Thessaly, Greece. Two Sentinel-1 SAR images depicting the area of interest before and at the last day of a specific precipitation event were selected. After appropriate processing of the SAR images, the extent of the flooded area was extracted. The flood extent was also determined by simulating the flood flow on a selected reach of the main river, using the well-known HEC-RAS software. Inundation extents as derived from both processes were compared based on an index indicating the measure of fit between the results predicted by the model and the satellite data (Horritt 2000).

Materials and methods

The individual stages of the whole process applied in this study are briefly described below:

Satellite data processing: At this stage, two Sentinel-1 images of pixel spacing equal to 10 meters covering the study area were acquired via ESA's Open Access Hub. S1 SAR products were Ground Range Detected (GRD), Interferometric Wide (IW) images, both having a VV polarization. Two satellite C-band SAR scenes were acquired on the 22nd of February 2018, and on the 28th of February 2018, the last day of a 6-day precipitation event, respectively. The exact time of the second scene was at 04:40 a.m. Satellite images were processed using SNAP software. The main processing techniques were applied on both images in the following order: (a) multi-looking processing, radiometric and geometric correction; (b) single image filtering (Lee filter was applied only on the second image); (c) conversion of the images into decibel (DB) images; (d) delineation of training polygons and extraction of their statistics; (e) determination of a threshold value for a 95% confidence level; (f) image classification for determining water surfaces. The flooded areas were extracted by the subtraction of the classified images.

Hydrologic-hydrodynamic simulation: The same result was attempted to be reproduced through hydrodynamic simulation of the flow using the 1D unsteady routine of HEC-RAS. The software requires as input a flow hydrograph for the storm event at the upper boundary of the reach, which was generated through the hydrologic simulation of the upstream drainage area using the HEC-HMS software. For the rainfall-runoff sub-model, the SCS Unit Hydrograph method was used, whereas for the routing sub-model, the Muskingum method was selected. The flow hydrograph derived from the above process was applied as an upstream boundary condition, in order to perform the unsteady flow simulation using HEC-RAS. The output of the model consists of the flood extent in a specific time moment, which is identical with the satellite image acquisition, namely 04:40 a.m. EET.

Quantification of model performance: At this stage, model-predicted inundation extent was tested against that extracted from the satellite image. For this purpose, both images were first converted to binary form (flooded or not flooded). The surface area of intersection and union between the shoreline predicted by the model (S_{mod}) and that observed from the satellite image (S_{obs}) were calculated, and then, the

following index was applied to quantify model performance:

$$F = \frac{(S_{mod} \cap S_{obs})}{(S_{mod} \cup S_{obs})} \times 100 \mathrm{F} = \frac{(\mathrm{S_{mod}} \cap \mathrm{S_{obs}})}{(\mathrm{S_{mod}} \cup \mathrm{S_{obs}})} \times 100 \quad (1)$$

Results and concluding remarks

The comparison between model prediction and extracted flood areas from SAR images are illustrated in Figure 1.

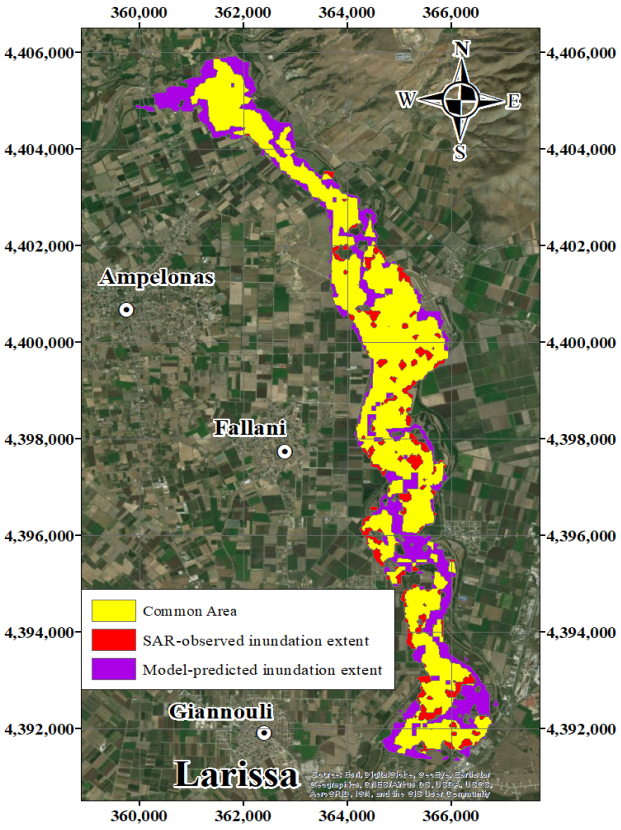

Figure 1. Model-predicted and SAR-derived inundation extent

According to the area-based measure of fit, it was found that model prediction coincides by 62.2 % with the extent extracted from the SAR image, indicating a relative overestimation of the flooded area by the model. Nevertheless, it can be seen that the model represents sufficiently the main features of the observed inundation area. Discrepancies appearing between the two flooded areas are mostly due to the uncertainty in input data (inflow from HEC-HMS software and topography) and the input parameters of HEC-RAS.

For future research, an extensive uncertainty analysis needs to be implemented, in order to investigate the influence of each uncertainty component to the final results. Besides, apart from the "modelling errors", errors arise from the SAR processing ("observation errors") as well. This is an additional factor which needs to be further examined and taken into account in model results evaluation.

References

Di Baldassarre G, Schumann G, Brandimarte L, Bates P (2011) Timely low resolution SAR imagery to support floodplain modeling: a case study review. Surveys in Geophysics 32(3):255–269

Horritt MS (2000) Calibration of a two-dimensional finite element flood flow model using satellite radar imagery. Water Resources Research 36(11):3279–3291

Patro S, Chatterjee C, Singh R, Raghuwanshi N (2009) Hydrodynamic modeling of a large flood-prone river system in India with limited data. Hydrological Processes 23(19):2774–2791

Yan K, Di Baldassarre G, Solomatine D (2013) Exploring the potential of SRTM topographic data for flood inundation modelling under uncertainty. Journal of Hydroinformatics 15(3):849-861

X. Global Change and Water Resources

11th World Congress on Water Resources and Environment (EWRA 2019)
"Managing Water Resources for a Sustainable Future", 25-29 June 2019, Madrid, Spain

Analysis of the characteristics of dry and wet spells in a Mediterranean region

T. Caloiero[1*], R. Coscarelli[2]
[1] CNR-ISAFOM, Rende (CS), Italy
[2] CNR-IRPI, Rende (CS), Italy
* e-mail: tommaso.caloiero@isafom.cnr.it

Introduction

Climate change could increase the risk of future hydrological extremes over large regional areas and trigger further pressure on water resource availability. In particular, the variability of daily precipitation, characterized by dry and wet spells, is a useful indicator in the representation of weather pattern. In fact, if a dry/wet spell brings too insufficient /much amount of precipitation, an extreme drought/flood event could happen (Li et al. 2017). In this century, numerous analyses related to dry/wet spells have been performed in countries such as in China (She et al. 2012), Switzerland (Schmidli and Frei 2005), Greece (Nastos and Zerefos 2009), India (Singh and Ranade 2010), Croatia (Cindrić et al. 2010), Italy (Caloiero et al. 2016, 2018) Iberian Peninsula (Lana et al. 2008) and Iran (Sarhadi and Heydarizadeh 2014). The majority of these studies is related to the spatial distribution and temporal trend in the dry/wet spells and mainly evidence an increase in the mean and largest dry periods (Caloiero et al. 2015).

In this study, the overall characteristics of dry/wet spells during 1951–2006 were analysed, considering both yearly and seasonal scale.

Materials and methods

A dry or wet spell is defined as the number of consecutive days with a daily precipitation amount below or above a certain threshold which should be first determined. Two types of thresholds are used in recent studies, i.e. a constant value (usually 0.1, 1, 5, 10 mm) or spatially varying values based on percentiles or daily mean rainfall (Li et al. 2017). In the present study, a day with precipitation amount greater than the threshold of 0.1 mm is defined as a wet day, otherwise it is defined as a dry day. With the dry/wet spells defined, some relevant indices were used to analyse the dry/wet spells with different lengths, and the precipitation amount from different wet spells. These indices are: (i) the mean and maximum lengths of dry/wet spells; (ii) the number of dry/wet spells with different lengths over the whole study period of 1951–2006 and (iii) the contributions of dry/wet spell with different lengths to the total number of dry/wet days.

The area under investigation is the Calabria region (southern Italy), which covers an area of about 15,000 km^2 (Figure 1). The study area is located within the Mediterranean basin and is characterized by particular climatic conditions. The Mediterranean climate characterizes this area; the winter season is a rather mild and rainy period, whereas the summer season is very hot and dry. The database used in this study was the one presented in Brunetti et al. (2012) in which available precipitation time series have been tested for time series homogeneity and missing data have been filled. The database consists of 129 daily precipitation series, in the period 1951–2006, with an average density of 1 station per 138 km^2 (Figure 1).

Results and concluding remarks

Considering the spatial distribution of the mean dry spell lengths, the study area can be divided in two parts: the western side of the region with mean values ranging between six and eight days, and the eastern side with the highest mean values (between eight and ten days). Similar results between the two sides of the region have been obtained for the maximum dry spell length. In particular, the longest dry spells (more than 200 days) have been identified in the most economically important agricultural areas of the region, in which long dry periods can be quite harmful to crops because of water or moisture shortage. As regards the

wet spell, opposite results have been obtained with respect to the dry spell, with the highest mean and maximum values identified in the western side of the region. Generally, the mean and maximum lengths of dry and wet spells have similar spatial patterns as those of annual mean precipitation, thus suggesting that the lengths of dry and wet spells are related to local climate.

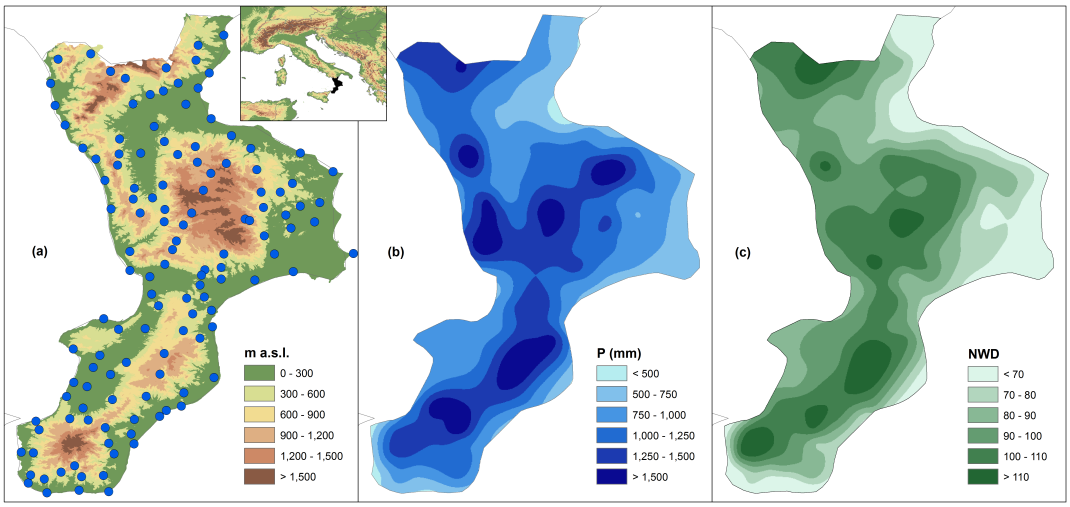

Figure 1. Location of the selected 129 rain gauge on a DEM (a) and spatial patterns of the mean annual rainfall (b) and mean annual number of wet days (c) during the period 1951–2006 over Calabria.

The analysis of the number of dry and wet spells for each length allowed to evaluate the decaying rates decrease. Finally, the contributions of each dry/wet spell with specific length to the total number of dry/wet days were further quantified through dividing the product of the number of certain spell and its spell length by the total number of dry/wet days. As a results, the greatest contributions to the total number of dry days have been obtained for the 2-day spell while the 7-day spell is the mainly contributor to the total number of wet days. These results are linked to the humid characteristics of the Calabria region. In fact, overall, the drier the climate, the shorter wet spells contribute more to the total number of wet days, and the longer dry spells contribute more to the total number of dry days (Li et al. 2017). In summary, the characteristics of dry/wet spells are closely related to local climatology.

References

Brunetti M, Caloiero T, Coscarelli R, Gullà G, Nanni T, Simolo C (2012) Precipitation variability and change in the Calabria region (Italy) from a high resolution daily dataset. Int J Clim 32:57–73

Caloiero T, Coscarelli R, Ferrari E, Sirangelo B (2015) Analysis of dry spells in southern Italy (Calabria). Water 7:3009

Caloiero T, Coscarelli R, Ferrari E, Sirangelo B (2016) An Analysis of the Occurrence Probabilities of Wet and Dry Periods through a Stochastic Monthly Rainfall Model. Water 8:39

Caloiero T, Coscarelli R, Ferrari E, Sirangelo B (2018) Occurrence Probabilities of Wet and Dry Periods in Southern Italy through the SPI Evaluated on Synthetic Monthly Precipitation Series. Water 10:336

Cindrić K, Pasarić Z, Gajić-Čapka M (2010) Spatial and temporal analysis of dry spells in Croatia. Theor Appl Climatol 102:171–184

Lana X, Martínez MD, Burgueño A, Serra C, Martín-Vide J, Gomez L (2008) Spatial and temporal patterns of dry spell lengths in the Iberian Peninsula for the second half of the twentieth century. Theor Appl Climatol 91:99–116

Li Z, Li Y, Shi X, Li J (2017) The characteristics of wet and dry spells for the diverse climate in China. Global Planet Change 149: 14–19

Nastos PT, Zerefos CS (2009) Spatial and temporal variability of consecutive dry and wet days in Greece. Atmos Res 94:616–628

Sarhadi A, Heydarizadeh M (2014) Regional frequency analysis and spatial pattern characterization of dry spells in Iran. Int J Climatol 34:835–848

Schmidli J, Frei C (2005) Trends of heavy precipitation and wet and dry spells in Switzerland during the 20th century. Int J Climatol 25:753–771

She D, Xia J, Song J, Du H, Chen J, Wan L (2012) Spatio-temporal variation and statistical characteristic of extreme dry spell in Yellow River Basin, China. Theor Appl Climatol 112:201–213

Singh N, Ranade A (2010) The wet and dry spells across India during 1951–2007. J Hydrometeorol 11:26–45

11th World Congress on Water Resources and Environment (EWRA 2019)
"Managing Water Resources for a Sustainable Future", 25-29 June 2019, Madrid, Spain

System dynamics for integrated management of the Jucar River Basin

A. Rubio-Martín*, H. Macian-Sorribes, M. Pulido-Velazquez, A. Garcia-Prats
Research Institute of Water and Environmental Engineering (IIAMA), Universitat Politècnica de València, Valencia, Spain
** e-mail: adrumar@upv.es*

Introduction

System dynamics (SD) is a theory of system structure and a set of tools for representing complex systems and analyzing their dynamic behaviour (Forrester 1961). In SD, the relation between structure and behaviour of the system is more a consequence of the relation between variables, time delays, amplifications and structural relationships between elements than of the individual components themselves (Simonovic 2001). SD facilitates holistic understanding of water resource systems as it allows to see how the different elements of the system actually relate to one another and permits experiments with changing relations within the system when different decisions are included (Mirchi et al. 2012). The typical purpose of a SD model is to realize how and why the dynamics of concern are generated and to look for managerial policies that can improve the situation (Saysel et al. 2002).

Over the past 50 years, SD tools have been applied to fields as diverse as economics, ecology, politics, sociology and resource management. Its application to the field of water resources has grown significantly over the last two decades, facilitating the enhancement of models by adding social, economic and ecological components. However, its application to the operation of complex multireservoir systems has been very limited so far.

Climate services use data and models to support climate informed decision making. Climate service development requires the involvement of users to create a product that responds to their specific needs. SD models provide a platform where different users and realities can be represented, allowing the users to interact and experiment with their inputs. User-tailored climate services often derive from these management models incorporating climate data as well as other socio-economic variables of interest for the user.

Materials and methods

In this contribution, we have developed a SD model for the Jucar River Basin, one of the most vulnerable basins in the western Mediterranean region with regard to droughts. The software Vensim Pro has been used for the creation of the model. The system has three main reservoirs, which allows for a multiannual management of the storage that compensates the highly variable streamflow from upstream. The model developed consists of five interlinked subsystems:

- Topology of the system network, including the 3 main reservoirs, water seepage and evaporation, inflows and catchments.
- Monthly operating rules of each reservoir. The rules were derived from the expert knowledge eluded from the operators of the reservoirs.
- Monthly urban, agricultural and environmental water demands.
- State index of the system and drought mitigation measures triggered depending on the state index.
- Mancha Oriental aquifer and stream-aquifer interaction with the Jucar River.

The SD model of the Jucar River Basin is able to capture the complexity of the water resource system as it combines physical, social and political (managerial) features.

Results and concluding remarks

The comparison between observed and simulated series showed that the model provides a good representation of the observed reservoir operation and total deficits (Figure 1). Results for the model are

also similar to the ones obtained by previous water resource models developed with commonly used tools like Aquatool.

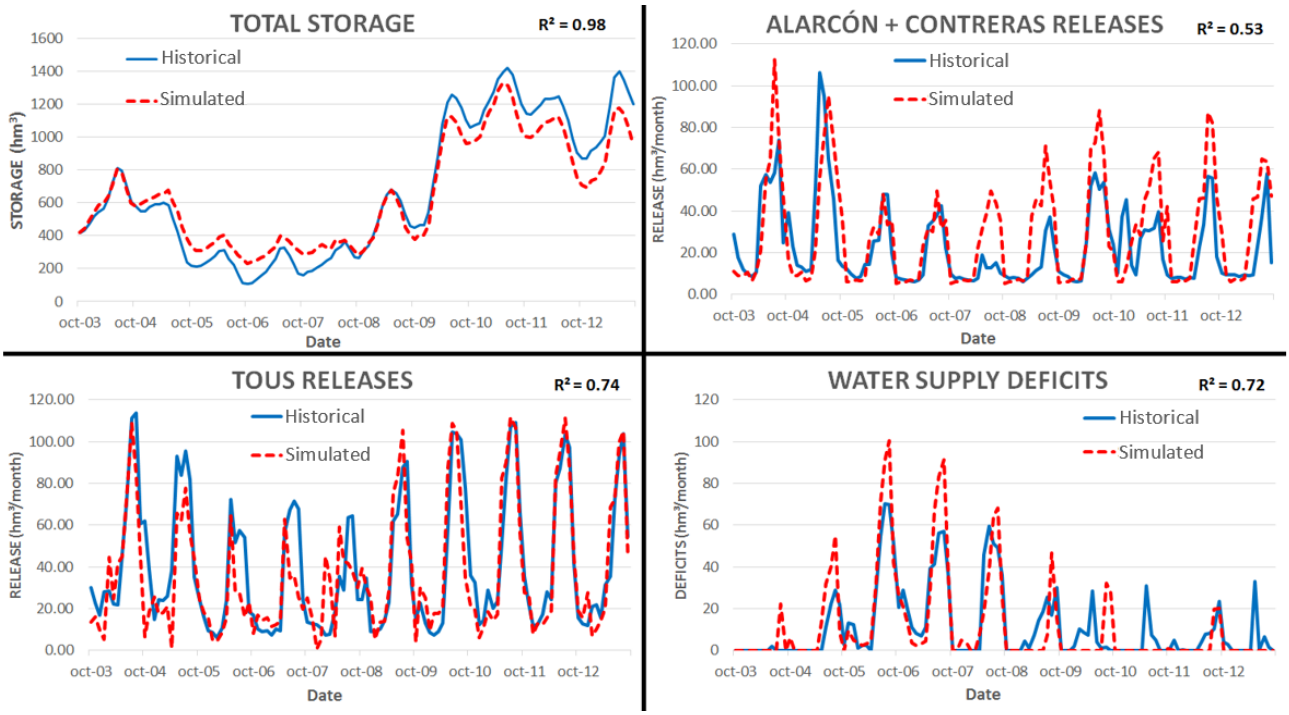

Figure 1. Comparison of results between simulated and observed values.

The interdisciplinary and open nature of the methodology allows to add new variables and dynamics to the model that are rooted on non-physical system components, including management (operating rules), political (drought mitigation measures), and social (population and demand growths) aspects. The structure-behaviour link of SD models allows analysis of how changes in one part of the system might affect the behaviour of the system as a whole. This allows testing how the system will respond under varying sets of conditions, including climate change scenarios. Different climate services for water management and climate change adaptation can be developed using as a template this SD model.

Acknowledgments: The European Research Area for Climate Services programme (ER4CS) supports this study under the INNOVA project (grant agreement: 690462).

References

Ahmad S, Simonovic SP (2001) Modeling dynamic processes in space and time: a spatial system dynamics approach. In: Phelps D, Sehlke G (eds) World water congress 2001 bridging the gap: meeting the world's water and environmental resources challenges, May 2001, Orlando. doi: 10.1061/40569(2001)88

Mirchi A, Madani , Watkins Jr D, Ahmad S (2012) Synthesis of System Dynamics Tools for Holistic Conceptualization of Water Resources Problems. Water Resour Manage 26:2421–2442. doi: 10.1007/s11269-012-0024-2

Saysel A, Barlas Y, Yenigün O (2002) Long-term sustainability in an agricultural development project: a system dynamics approach. doi: 10.1004/jema.2002.0585

11th World Congress on Water Resources and Environment (EWRA 2019)
"Managing Water Resources for a Sustainable Future", 25-29 June 2019, Madrid, Spain

Robust climate change adaptation strategies for the largest irrigated system in the European Union

D. Haro*, L. Palazón, S. Beguería
Estación Experimental de Aula Dei, Consejo Superior de Investigaciones Científicas, Zaragoza, Spain
** e-mail: dharo@eead.csic.es*

Introduction

With a total irrigated area of 127,210 ha divided in 58 irrigators associations, the Riegos del Alto Aragón (RAA) irrigation district is currently the largest irrigated area in Spain and in the European Union. It is by far the largest water user within the Gallego-Cinca system in the Ebro River, which also supplies water to 588 livestock operations, 10 industrial polygons, and 110 populated areas. Although there are plans to increase the irrigated area another additional 47,000 ha, the system is already close to its average resource limit and some supply restrictions took place in the last years. Additionally, the effects of climate change on future water resources produced in the Pyrenees (the major source of water for irrigation in the system), as well as market prices, national and international trade and agricultural policies, among other variables, are surrounded by a high level of uncertainty that difficult investment decision-making.

This communication presents the advances on implementing a multi-model multi scenario methodology to assess different climate change adaptation strategies in the RAA irrigation district. This methodology is the first step in the implementation of a robust decision making framework for adaptation in a water resources system with important agricultural actors.

Materials and methods

In situations of 'deep' or 'severe' uncertainty, current research argues that robustness should be preferred over optimality (McPhail et al. 2018). A 'robust' system performs satisfactorily, or satisfices selected performance criteria, over a wide range of uncertain futures rather than performing optimally over the historical period or a few scenarios (Lempert et al. 2006).

In the case of RAA, a number of portfolios of adaptation strategies, or measures, were assessed against a large number of regional climate datasets by combining a hydrologic and a water allocation model. The Soil and Water Assessment Tool (SWAT; Arnold et al. 2012) was used to build and calibrate a rainfall-runoff model of the Gallego-Cinca headwaters, where most of the system's resources are generated and the major regulation infrastructures are located. The outputs from the SWAT model are afterwards inputs to a water allocation model built with AQUATOOL (Andreu et al. 1996) that will simulate the management of the system's reservoirs and the distribution of water to the different demands. Each portfolio is a combination of various measures oriented to enhance adaptation to climate change of the system (e.g. additional storage, irrigation modernisation, or crops adaptation), that can take different intensities that will be reflected in different aspects of the two models used in the simulation process.

The composition of portfolios was achieved through stakeholder participation. Through a series of group dynamics, different adaptation alternatives were identified, ranked and validated. These were later translated into model additions and modifications for their evaluation.

Results and concluding remarks

Robustness metrics were calculated for each portfolio under each climate scenario. These will allow comparing the performance of the different portfolios as well as the trade-offs between different alternatives and provide guidance to decision makers about which adaptation options are more robust under a highly uncertain future.

Evaluating the performance of adaptation strategies under a large number of scenarios allows incorporating the inherent uncertainty of climate change into the decision making process. This makes

possible to find alternatives that perform satisfactorily over a larger number of situations instead of optimally within a single or a few scenarios. Additionally, this process has the potential to provide stakeholders with a better understanding of the system's dynamics as well as on the point of view of the problems of other competing water users.

Acknowledgments: The authors acknowledge EU Interreg-POCTEFA programme (EFA201/16/PIRAGUA) and EU ERA-NET WaterWorks 2015 (INNOMED) for providing funding for this research.

References

Andreu J, Capilla J, Sanchís E (1996) AQUATOOL, a generalized decision-support system for water-resources planning and operational management. Journal of Hydrology 177(3-4):269-291. https://doi.org/10.1016/0022-1694(95)02963-X

Arnold JG, Moriasi DN, Gassman PW, Abbaspour KC, White MJ, Srinivasan R, Santhi C, Harmel RD, van Griensven A, van Liew MW, Kannan N, Jha MK (2012) SWAT: Model Use, Calibration, and Validation. Transactions of the ASABE 55(4):1491-1508

Herman JD, Reed PM, Zeff HB, Characklis GW (2015) How Should Robustness Be Defined for Water Systems Planning under Change? Journal of Water Resources Planning and Management 141(10):04015012. https://doi.org/10.1061/(asce)wr.1943-5452.0000509

Lempert RJ (2003) Shaping the next one hundred years: new methods for quantitative, long-term policy analysis. Rand Corporation

McPhail C, Maier HR, Kwakkel JH, Giuliani M, Castelletti A, Westra S (2018) Robustness Metrics: How Are They Calculated, When Should They Be Used and Why Do They Give Different Results? Earth's Future 6(2):169-191. https://doi.org/10.1002/2017EF000649

11th World Congress on Water Resources and Environment (EWRA 2019)
"Managing Water Resources for a Sustainable Future", 25-29 June 2019, Madrid, Spain

Climate change effects for severe rainfall events in Madrid region

A. Lastra de la Rubia*, M. Ortega Castro, J. Botello Herranz
Canal de Isabel II, Madrid, Spain
** e-mail: alastra@canaldeisabelsegunda.es*

Introduction

The adequate management of water resources involves, amongst others, the anticipation of future changes in the climate in order to develop plans that minimise disruptions and build systems that withstand those uncertain events. Changes in rainfall events affect particularly urban drainage networks in that their sizing and behaviours depends specially on temporal and spatial distribution of those events.

The aim of the present abstract is to describe the results obtained from the study *Climate Change scenarios for severe rainfall events in Madrid Region* (Lastra et al. 2017) carried out by Canal de Isabel II, in which regional climate change factors affecting future rainfalls have been obtained. This work is one of the first examples at the international level of application in the field of urban drainage of the new RCP scenarios proposed in the abovementioned report.

Materials and methods

For several years now, the scientific community have been raising concerns about the Climate Change, its implications for the human activity and the need to anticipate its evolution in order to adapt the available resources to new scenarios. In this sense, the last report of the Intergovernmental Panel on Climate Change (IPCC 2014), provided a series of future scenarios of climate change under which global simulations of different climate models have been generated. These simulations, of a global nature, must undergo a process of "regionalisation" for their results to be used on a local scale.

The Advanced Rainfall Study of Extreme Precipitation Estimation in Madrid Region, which has provided the basis for this document, has been grounded on different General Circulation Models (CGM), a specific "regionalisation" technique (Spatial Downscaling) called FICLIMA (Ribalaygua et al. 2013), elaborated and validated in Spain by the Foundation for Climate Research (FIC), and four radiative forcing scenarios (Representative Concentration Pathways or RCP). As a result, future scenarios of climate change on precipitation in Madrid region have been generated. The combination of the models used and the scenarios available for each of them have provided a range of thirty-one possible future climate evolutions that extend to 2100.

Since the RCP must cover the entire existing range and also provide interim information, a set of four RCP were chosen that included both the extreme values and two intermediate values, separated enough from each other, so that the results obtained from them also yielded different results. The new scenarios are RCP 2.6, RCP 4.5, RCP 6.0 and RCP 8.5 (numbers referring to radiative forcing reached in 2100) (Meinshausen et al. 2011).

The potential effects of climate change in Madrid region have been quantified through the calculation of climate change coefficients that express the quotient between rainfall intensity for a given return period and a certain duration (Willems et al. 2011), corresponding to a future climate scenario, and the equivalent rainfall intensity in the present climate for the same return period and the same duration.

In order to obtain coefficients of climate change for intensities with shorter than daily durations, a careful selection of meteorological observatories for the region of Madrid has been carried out to be able to guarantee the obtaining of the local future climate scenarios, in the best way possible in each point, analysing the available data, validating the FICLIMA methodology and the climate models.

Results and concluding remarks

Duration, intensity and frequency of rainfall events affect significantly the behaviour of drainage

networks. Since the sizing of the infrastructure is done considering short return periods (in Madrid typically 10 years), future changes in the occurrence and characteristics of these events should be considered.

The variations between the design conditions and the changing reality influenced by the climate change represent current and future challenges for water service providers. Those variations should be forecasted as precise as possible so that floods and discharges to the natural environment can be minimised and managed correctly.

Climate change coefficients have been obtained for each time horizon and each RCP scenario, for daily and hourly rainfall. In general, there is an increase in extreme rainfall events as opposed to a decrease in average annual precipitation, which indicates a substantial reduction in the occurrence of weak and moderate rain and an increase in rainfall episodes of heavy rain. Results are summarised in Figure 1. Climate change coefficients are greater than one in all studied scenarios and horizons, so it is expected that hyetograph peaks are greater for the future rainfall events.

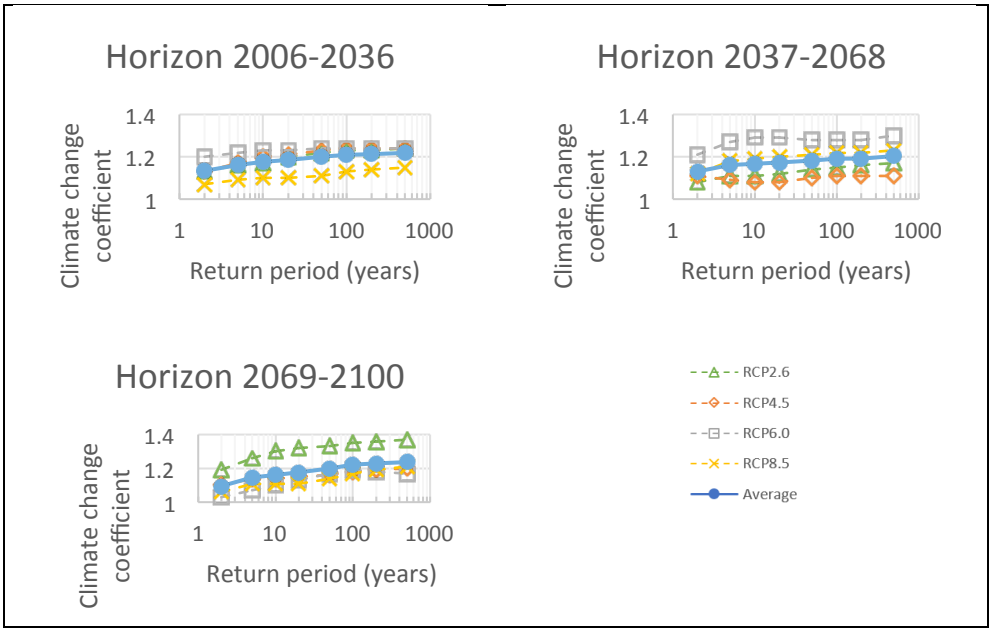

Figure 1. Climate change coefficient for maximum annual precipitation of one-hour duration, for each of the three climate horizons. Median value of the data for each climate model and observatory.

Acknowledgments: This work was carried out in collaboration with Paula González Laynez, Beniamino Russo, Raúl Rodríguez-Solá, Jaime Ribalaygua, Aqualogy's Urban Drainage Office, the Department of Astronomy and Meteorology of the Universitat de Barcelona, the Department of Physics and Nuclear Engineering of the Universitat Politècnica de Catalunya and the Foundation for Climate Research.

References

IPCC (2014) Climate Change 2014: Synthesis Report. Contribution of Working Groups I, II and III to the Fifth Assessment Report of the Intergovernmental Panel on Climate Change [Core Writing Team, R.K. Pachauri and L.A. Meyer (eds.)]. IPCC, Geneva, Switzerland, 151 p

Lastra de la Rubia A, González Laynez P, Russo B, Rodríguez-Solá R, Ribalaygua J (2018) Climate Change Scenarios for severe rainfall events in Madrid Region, Booklet 27. Madrid, Madrid, Spain: Research & Development & Innovation. Canal de Isabel II

Meinshausen M, Smith SJ, Calvin K, Daniel JS et al. (2011) The RCP greenhouse gas concentrations and their extensions from 1765 to 2300. Climatic Change 109(1-2):213-241. doi: 10.1007/s10584-011-0156-z

Ribalaygua J, Torres L, Pórtoles J, Monjo R, Gaitán E, Pino MR (2013) Description and validation of a two-step analog/regression downscaling method. Theoretical and Applied Climatology 114(1-2):253-269. doi: 10.1007/s00704-013-0836-x

Willems P, Vrac M (2011) Statistical precipitation downscaling for small-scale hydrological impact investigations of climate change. Journal of Hydrology 402(3-4):193-205. doi: 10.1016/j.jhydrol.2011.02.030

11th World Congress on Water Resources and Environment (EWRA 2019)
"Managing Water Resources for a Sustainable Future", 25-29 June 2019, Madrid, Spain

Integrating top-down and bottom-up approaches for climate change adaptation in the Jucar river basin (Spain)

P. Marcos-Garcia*, M. Pulido-Velazquez
Research Institute of Water and Environmental Engineering (IIAMA), Universitat Politècnica de València, Spain
** e-mail: patmarg5@upv.es*

Introduction

In the Mediterranean region, drought events are relatively frequent due to the irregular hydrology of the area, water scarcity issues and aquifer overuse. In this context, climate change could exarcebate the current situation, decreasing the water resources (Marcos-Garcia and Pulido-Velazquez 2017) and increasing the magnitude, frequency and intensity of the droughts (Marcos-Garcia et al. 2017), due to the combined effects of precipitation reduction and potential evapotranspiration increase. In order to confront the climate change impacts in water resources systems, three possible strategies are possible (Gleick 2011): the "wait and see" approach, which is the less expensive one in the short term but could involve the highest risks in the mid and long terms; the assessment of "no regret" adaptation options under a wide variety of future climate conditions and; the design and building of new infrastructure to tackle the rising uncertainty due to climate change, which could be costly and potentially unsuitable. However, although the assessment of cost-efficient adaptation programs could be regarded as the most desirable strategy, its practical implementation is far from being an easy task.

In broad terms, there are two main ways of designing adaptation programs at the basin scale: the "top-down" and the "bottom-up" approaches. The traditional top-down approach involves a chain of models, starting by Global Climate Models (GCM), which are downscaled for a particular region through Regional Climate Models (RCM). Wilby and Dessai (2010) defined this process as a "cascade of uncertainty", because uncertainty is propagated and enlarged from one step to the following one. On the contrary, the bottom-up approach is primarily focused on the local stakeholders' responses to face up the global change challenges. Here, we propose a methodology to mix up both approaches, in order to select a cost-effective program of adaptation measures for the Jucar river basin, a complex water resources system located in Eastern Spain.

Materials and methods

The case study is the Jucar River Basin, a Mediterranean basin of 22,261 km in Eastern Spain. The system is highly regulated through 3 main reservoirs: Alarcon and Contreras, in parallel in the upper basin and Tous, downstream. Agriculture is the most prominent water user in the basin (with a share of about 80% of the total demand), and its principal withdrawals (UDAs) are located in the lower part basin (except for groundwater irrigation in Mancha Oriental). Water availability has historically been a main issue in the basin, where a frail equilibrium between resources and demands already exists.

Figure 1 shows the general framework applied to the case study. Regarding the top-down approach (left), we used several combinations of GCMs and RCMs and two climate change scenarios: the RCP 4.5 and 8.5 in the short term (2011/40) and in the midterm (2041/70). The climate output (precipitation and temperature at the monthly scale) from these models was bias-corrected using a quantile-mapping technique. The next step was to calibrate and validate a conceptual, lumped hydrological model and simulate the future inflows using the previously corrected climate variables as inputs. In relation to the bottom-up approach (right), the global socioeconomic scenarios (Shared Socioeconomic Pathways, SSPs) were first adapted at the regional level through several semi-structured interviews conducted with local experts. The next step was to develop the main elements of these scenarios into plausible narratives that could be used in the workshops. Concretely, two workshops were celebrated with local farmers from the main agricultural areas (La Ribera del Júcar and La Mancha Oriental), and a third one with the main stakeholders at the basin scale. In the farmers' workshops, the participants were asked to discuss the

narratives to make it plausible at the local scale, to foresee the evolution of the agricultural sector in those contexts and to propose potential adaptation measures. In the third workshop, the stakeholders assessed both quantitatively and qualitatively the measures proposed by the farmers regarding its suitability to be implemented at the basin scale. Finally, the future inflows obtained from the top-down approach and the adaptation measures selected in the bottom-up approach were integrated in a decision support system (DSS). The DSS consisted in a hydroeconomic model of the basin which, through an optimization algorithm, is able to select the combination of adaption measures more cost-efficient under the future scenarios.

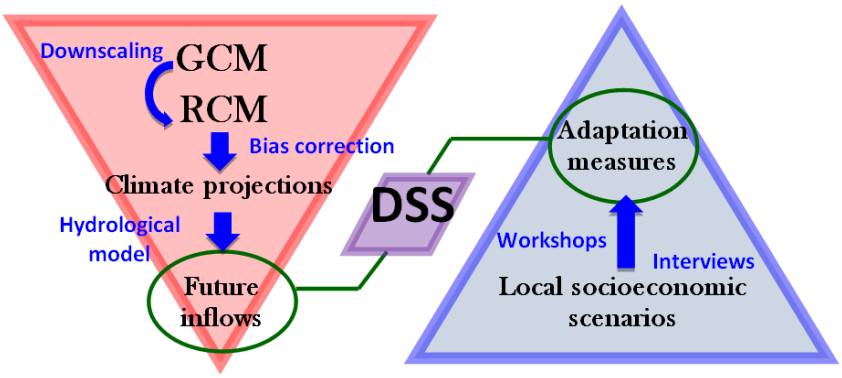

Figure 1. Mixed top-down and bottom-up approach. General framework.

Results and concluding remarks

From the top-down approach, we found that there is a high uncertainty regarding the decrease of the system inflows in the future, which arises mainly from the climate models but also from the selected hydrological model. Moreover, climate change seems to pose higher impacts in the headwaters than in the coastal area. Regarding the bottom-up approach, we found that the most appealing adaptation measures for the stakeholders are the improvement of water governance (regulation and control of water rights), improvement of the irrigation efficiency and the use of non-conventional resources (water reuse and desalinated water). Nevertheless, economic instruments and potentially conflictive measures (such as water transfers) were considered the less attractive measures. The combination of the two approaches has provided valuable insights on the strengths and weaknesses of the system to confront climate change challenges, and the use of a hydroeconomic model has allowed to include the economic dimension of water management, as demanded by the Water Framework Directive.

Acknowledgments: This study has been supported by the IMPADAPT project (CGL2013-48424-C2-1-R) with Spanish MINECO (Ministerio de Economía y Competitividad) and European FEDER funds. Patricia Marcos-Garcia is also supported by a FPI grant from the PhD Training Program (BES-2014-070490) of the former MINECO.

References

Gleick PH (2011) Water planning and management under climate change. J. Contemp. Water Res. Educ. 112:1–5

Marcos-Garcia P, Pulido-Velazquez M (2017) Cambio climático y planificación hidrológica: ¿es adecuado asumir un porcentaje único de reducción de aportaciones para toda la demarcación? Ingeniería del Agua 21(1):35-52 (in Spanish with English summary)

Marcos-Garcia P, Lopez-Nicolas A, Pulido-Velazquez M (2017) Combined use of relative drought indices to analyze climate change impact on meteorological and hydrological droughts in a Mediterranean basin. Journal of Hydrology 554:292-305

Wilby RL, Dessai S (2010) Robust adaptation to climate change. Weather 65:180–185

11th World Congress on Water Resources and Environment (EWRA 2019)
"Managing Water Resources for a Sustainable Future", 25-29 June 2019, Madrid, Spain

Reservoir performance under climate change: validating the storage-yield-reliability approach

A. Granados*, A. Sordo, I. Gabriel-Martin, L. Garrote
Department of Civil Engineering: Hydraulics, Energy and Environment, Universidad Politécnica de Madrid, Spain
** e-mail: a.granados@upm.es*

Introduction

Reservoir storage has been the predominant strategy to address hydrologic variability in water scarce regions. The reliability of water supply can be significantly enhanced if enough water is stored in reservoirs to overcome supply deficit during low flow periods. Many reservoir sizing techniques have been developed to define the minimum reservoir capacity required to supply a given demand at a certain location with enough reliability (Vogel 1987; Vogel et al. 2007). These techniques usually normalize reservoir storage and yield dividing by mean annual flow to account for local conditions. For a given required reliability, the relationship between storage and yield depends on hydrologic variability, which is usually accounted through the coefficient of variation of annual flows. The resulting relations are usually known as Storage-Yield-Reliability (S-Y-R) curves.

Anticipated changes in the mean and coefficient of variation of annual flows due to climate change will affect reservoir performance. The impacts may be estimated through the analysis of S-Y-R relations. In this work we analyse the observed and projected performance of storage reservoirs in Europe. The objective is to explore the validity of the S-Y-R approach to predict climate change impacts on regulated water supply systems.

Material and methods

We defined S-Y-R relations for a single reservoir with a simple model that simulates reservoir operation. For each reservoir configuration, the model was forced with an ensemble of synthetic hydrologic inputs with increasing variability. The inputs were generated from streamflow series of different hydrologic regimes. The series were perturbed to change their mean and variability while keeping the same temporal sequence, following the algorithm presented by (Chavez et al. 2013). All series were perturbed to have a common mean of 1000 hm^3/yr. Variability was described through the coefficient of variation of annual flows and seasonal range, defined as the ratio between the minimum and maximum seasonal averages. We explored a range of coefficient of variation between 0.15 and 1.10 and a range of seasonal range between 0.2 and 0.7. The simulations provided the maximum constant demand that can be supplied with a given reliability for a range of reservoir capacities between 0 and 3.5 times the mean annual flow. The sensitivity analysis was designed to determine the influence of reservoir capacity, coefficient of variation and seasonal range on reservoir performance. The results were synthesized in average curves, describing the yield associated to the reservoir as a function of the coefficient of variation of flows. These curves were compared with simple analytical approaches, like the Gould-Dincer method (McMahon 2007).

We compared the results obtained for a single reservoir with empirical water availability estimates for the river network of Europe. We used the WAAPA model to simulate the operation of the system of reservoirs located upstream of every node in the river network. The system was operated to maximize water availability. Model topology for WAAPA was taken from the GTOPO HYDRO1K dataset, accessible in USGS Earth Explorer (https://earthexplorer.usgs.gov/). Reservoir data were obtained from the ICOLD World Register of Dams. The model includes 2301 dams with storage larger than 5 hm^3. Hydrologic forcing was derived from the results of the PCRGLOB-WB model runs of the ISIMIP project, which were downloaded from the PIK node of the Earth System Grid Federation (ESGF) (https://esg.pik-potsdam.de/search/isimip-ft/). We selected the run forced with GFDL-ESM2NM climatic model and the time slice from 1960 to 1999 to characterize current conditions.

Results and discussion

Results are summarized in Figure 1. The figure shows the relation between yield and coefficient of variation for varying reservoir storage volumes. Yield and storage volumes are normalized by mean annual flows. The plot on the left of Figure 1 shows data derived from two different sources. The lines represent the result of applying the analytical Gould-Dincer method for uncorrelated normally distributed inflows. The solid circles present the result of the sensitivity experiments performed with the single reservoir model and perturbed streamflow series. In both cases, each range of reservoir storage volumes is represented by a different colour code. The plot on the right shows the results of the water availability model for Europe. It also represents normalized yield in each location as a function of coefficient of variation, but the storage volume corresponds to the total reservoir capacity upstream of that location.

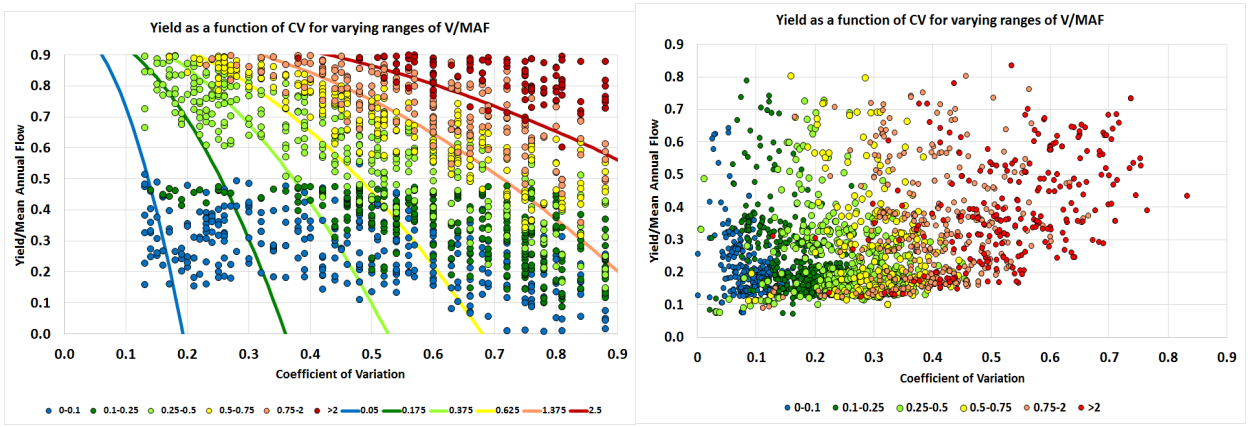

Figure 1. Normalized yield versus coefficient of variation for different values of normalized storage. Left: data from single-reservoir simulations (solid circles) and analytical results from Gould-Dincer method (lines). Right: data from systems of reservoirs derived from the European water availability model.

The differences between the two sets of data are apparent. In the case of single reservoirs, the results obtained in the sensitivity experiments differ significantly from the results of the analytical model, except in the case of large storage volumes. This is due to the fact that the Gould-Dincer model works only with annual flows and is only intended for very large reservoirs where carryover storage is significant. If the reservoir volume is small compared to mean annual flow, the reservoir performs within-the-year regulation and the yield may be much larger than predicted by the analytical expression. The plot on the right is showing the actual distribution of reservoir storage over Europe. Colour codes are segregated mostly by coefficient of variation and they show a different tendency from what is predicted by theory. The reason for this is that storage requirements are determined by streamflow variability. Small reservoir volumes are usually enough if the coefficient of variation is small, but larger variability in the flow requires larger reservoir volumes. The analysis of the S-Y-R relations can also provide the basis for the prediction of impacts on reservoir performance due to changes in mean or variability due to climate change.

Acknowledgments: We acknowledge support from Universidad Politécnica de Madrid through ADAPTA project and his program for young researchers.

References

Chavez-Jimenez A, Lama B, Garrote L, Martin-Carrasco F, Sordo-Ward A, Mediero L (2013) Characterisation of the Sensitivity of Water Resources Systems to Climate Change, Water Resources Management 27:4237-4258

McMahon TA, Pegram GGS, Vogel RM et al. (2007) Review of Gould–Dincer reservoir storage–yield–reliability estimates. Advances in Water Resources 30:1873-1882

Vogel, RM (1987) Storage-Reliability-Resilience-Yield Relations for Over-Year Water-Supply Systems Water Resources Research 31(3):645-654

Vogel, RM, Sieber J, Archfield SA et al. (2007) Relations among storage, yield, and instream flow. Water Resources Research 43(5):W05403

11th World Congress on Water Resources and Environment (EWRA 2019)
"Managing Water Resources for a Sustainable Future", 25-29 June 2019, Madrid, Spain

Assessment of GCM and scenario uncertainty to project streamflow under climate change

Das Subhadarsini, N.V. Umamahesh*
National Institute of Technology, Warangal, Telangana, India
** e-mail: uvnanduri@gmail.com*

Introduction

The ongoing processes of global heating and climate change controlled by different driving forces such as greenhouse gases, aerosol, and others are highly uncertain on regional and local spatial scales. In India, the climate projections indicate that the increase in temperature (precipitation) is by 3 ^{o}C (10% - 20 %) over central India by the end of this century. Therefore, it is vital to assess the importance of climate change on a river basin. In order to measure potential changes at local level, the reduction scale of GCM (Global Climate Model) outputs are necessary. But, the different estimated outputs from the downscaled GCM data contain different heights of uncertainties.

Mujumdar and Ghosh (2008) modelled GCM and scenario uncertainty by calculating the possibilistic mean of the CDFs (Cumulative Distribution Function) for 3 standard time slots 2020s, 2050s and 2080s and their results indicated that the probability of incidence of extremely high flow events was likely to decrease in the future. Ghosh and Mujumdar (2009) used ensemble averaging with the assignment of weights to GCMs based on model evaluation to address uncertainty of GCM. They modelled the uncertainty with imprecise probability. The derived imprecise CDFs of monsoon rainfall for three 30-year time slices i.e. 2020s, 2050s and 2080s, with A1B, A2 and B1 scenarios were used for the prediction of monsoon rainfall, showing a possible decreasing trend in the future in Orissa. Das and Umamahesh (2015) estimated the forth-coming scenario of monsoon precipitation on different IMD grid points using the statistical downscaling of the monthly precipitation of simulations with the RCP (Representative Concentration Pathways) 4.5 scenario of (NorESM1-M) and (CanESM2) of fifth phase of Coupled Model Inter-comparison Project (CMIP5) over Godavari River Basin, India. Kim and Noh (2016) used a rainfall-runoff model and RCP climate change scenarios data to generate future climate scenarios and daily runoff for the Geum River consisting of three weirs along the main stream. Finally, analyses of changes in runoff by the indicators of the hydrologic alteration (IHA) program showed that climate change is likely to lead to an increase of the future runoff ratio and that weirs contributed to an increase in the minimum discharge and a decrease in the maximum discharge. Hengade and Ghosh (2018) also evaluated the likely effects on the hydrology condition by the predicted daily precipitation for future years (2011-2099) for a large river basin, Godavari River Basin, India under scenarios, i.e. RCP4.5 and RCP8.5. Here, a statistical scaling model which was based on the non-parametric kernel regression was used to produce future daily precipitation and the Variable Infiltration Capacity (VIC) macro-scale hydrological model was taken for hydrological simulations.

A single trajectory derived from a single GCM with single climate change scenario cannot represent a future hydrologic scenario. In the present study, the objective is to project the impact of climate change on the flows in Godavari river basin. Arc SWAT (Soil & Water Assessment Tool) is used for hydrologic modelling of the basin. The possibility theory is used to get the weighted average of the future projections of meteorological data obtained from six high resolution GCMs under two different scenarios. The projected meteorological data is required for projecting the flows in the river basin for assessing the impact of climate change.

Materials and methods

The Arc SWAT 2012 version is used for simulations of streamflow over Indravati Sub-basin, Godavari Basin, India. Weather data with a resolution of ($0.5^{o}\times0.5^{o}$) are collected from all GCM (ACCESS, CCSM4, CNRM, GFDL, MPI, NORESM) with scenarios RCP 4.5 and RCP 8.5 for both historical (1970-2005) and future

(2006 - 2099) from Indian Institute of Tropical Meteorology (IITM), Pune. The observed stream flow data of Indravati sub-basin at Pathegudam outlet point is collected from Water Resource Information System (WRIS). Observed temperature and precipitation data with resolution of ($0.5^{o}\times0.5^{o}$) from 1960-2013 are collected from IMD(India Meteorological Department) .

The steps illustrating the complete details of the methodology are as follows:

Step-1: Set up SWAT model by using prepared temperature and precipitation data and GIS data [DEM (Digital Elevation Model), LULC (Land Use Land Cover) map and Soil map].

Step-2: Set up calibrated model after calibration and validation of the model by using SWAT-CUP [SWAT-Calibration and Uncertainty Program (SUFI2 Algorithm-Sequential Uncertainties Fitting Version-2)].

Step-3: Bias-correct (by using quantile Mapping) all the GCM Model and its scenario (RCP4.5 and RCP8.5) data.

Step-4: By taking bias-corrected data into SWAT with calibrated model parameters, runoff is predicted for recent past years (2006-2013) when there are indications of climate forcing. Possibilities as a weightage factor (i.e. performance measure (C)), which is similar to Nash–Sutcliff Efficiency (NSE) are computed for each GCM and its scenarios.

Step- 5: Due to the property of possibility distribution i.e. there should be at least one scenario simulated by any of the GCMs with a possibility value 1, the results which are derived from the equation of 'C' for all the six GCMs with associated scenarios are normalized first.

Step-6: Considering the possibilities for all GCMs and its scenarios, future (2020-2040, 2041-2070, 2071-2099) streamflows are predicted.

Results and concluding remarks

The model is setup with best fitted values of the sensitive parameters after many iterations of calibration and validation. The values of P-factor and r-factor which has been used to evaluate the strength of calibration (validation) are 0.44 (0.26) and 0.21 (0.21), respectively, and the values of coefficient of correlation (R^2) and Nash–Sutcliff Efficiency (NSE) which measures uncertainty for calibration (validation) are 0.65 (0.58) and 0.64 (0.57) respectively which confirm a approximately good performance of the model.

After calculating the performance measure C for all 6 GCMs with RCP4.5 and RCP8.5 based on their prediction of streamflow in the recent period, it indicates that CCSM4 (RCP4.5 and RCP 8.5) with –ve C value fails to predict whereas MPI 4.5 and NORESM4.5 GCMs with small C value predict very poor results. So, by ignoring these above GCMs, possibilities are assigned to other models after normalization.

Then the possibilistic mean CDF (Fpm) is computed by using the possibility values and the CDFs of streamflow obtained for each GCM with scenario for the time slices 2020-2040, 2041-2070, 2071-2099. The possibilistic mean CDFs for years 2020-2040, 2041-2070, 2071-2099 comparing with the CDF of observed stream flow of 2006-2013 indicate that the value of streamflow at which the possibilistic mean CDF reaches the value of 1 for years (2020-2040), (2041-2070), (2071-2099) are lower than that of baseline period 2006-2013. The streamflow reduces for time slices (2020-2040) and (2041-2070) and then increases to some extent for (2071-2099). The study indicates that the stream flows in Indravati sub-basin are likely to decrease in future.

References

Das J, Umamahesh NV (2015) Multisite Downscaling of Monsoon Precipitation over the Godavari River Basin under the RCP 4.5 Scenario. World Environmental and Water Resources Congress 2015, doi:10.1061/9780784479162.105

Ghosh S, Mujumdar PP (2009) Climate change impact assessment: Uncertainty modeling with imprecise probability. Journal of Geophysical Research 114:D18113. https://doi.org/10.1029/2008JD011648

Hengade N, Eldho TI, Ghosh S (2018) Climate change impact assessment of a river basin using CMIP5 climate models and the VIC hydrological model. Hydrological Sciences Journal 63:596-614. doi: 10.1080/02626667.2018.1441531

Kim S, Noh H, Jung J, Jun H, Kim HS (2016) Assessment of the Impacts of Global Climate Change and Regional Water Projects on Streamflow Characteristics in the Geum River Basin in Korea. Water 8:91. doi: 10.3390/w8030091

Mujumdar PP, Ghosh S (2008) Modeling GCM and scenario uncertainty using a possibilistic approach: Application to the Mahanadi River, India, Water Resources Research 44:W06407. doi: 10.1029/2007WR006137

11th World Congress on Water Resources and Environment (EWRA 2019)
"Managing Water Resources for a Sustainable Future", 25-29 June 2019, Madrid, Spain

Prediction of future water resources sustainability of the Yellow River under climate change

H. Cui*, X. Wang
Key Laboratory of Land Surface Pattern and Simulation, Institute of Geographic Sciences and Natural Resources Research, Chinese Academy of Sciences, Beijing 100101, China
** e-mail: cuihj@igsnrr.ac.cn*

Introduction

As a typical drought-prone region, the Yellow River basin (YRB) has long been over exploited with highly concentrated population and farmland, but with very limited resources. The water resources is one of the key constraints of the sustainable development of this region. However, unfortunately, due to both human activities and climate change, the precipitation of this basin has been found continuously decreased during last several decades, while the streamflow showed a significant decreasing trend as well. As a result, the lack of the availability of the water resources in the YRB is increasingly severe. It is of importance to predict the future water resources sustainability under climate change.

According to the US EPA (2007) classification, the flow condition can be categorized using the flow duration curve, which is plotted a gauging station representing streamflow values from high to low against the percentage of time these values are either equalled or exceeded, where 60% to 90% means dry conditions, and 90% to 100% for low flows. The flow duration curve (FDC) is always computed empirically, and Singh et al. (2014a, b) first introduced the entropy theory to estimate the FDC, where they defined the entropy parameter for each station, so that the FDC for different recurrence intervals can be easily predicted. The main advantages of the use of the entropy theory for computing the FDC are: (1) the parameters are based on observations and no fitting is needed; (2) the theory permits a probabilistic characterization of the flow duration curve.

To that end, the entropy-based FDC curve will be applied to estimate the flow condition of the Yellow River basin and to predict the future condition based on the entropy parameter under climate change scenarios.

Materials and methods

Six streamflow stations (Table 1) are selected from the YRB for predicting the FDC and analysing the future availability of water resources. Among these stations the Tangnaihai station is located at the source of the Yellow River and least affected by human activities, and the human impacts are negligible.

Table 1. Streamflow stations used in this study

No.	Gauge/sub-region	Latitude (°N)	Longitude (°E)	Drainage area (104 km^2)
1	Tangnaihai	35.50	100.15	12.21
2	Wubu	37.45	110.72	6.56
3	Hejin	35.57	110.80	3.87
4	Huaxian	34.58	109.77	5.97
5	Sanmenxia	34.82	111.37	4.75
6	Huayuankou	34.92	113.65	4.18

Considering the temporally averaged discharge Q at one station as a random variable, the procedure for deriving flow duration curves based on the entropy theory, comprises (1) definition of the Shannon entropy, (2) specification of constraints, (3) maximization of entropy (4) derivation of the probability distribution of discharge, (5) determination of Lagrange multipliers, and (6) derivation of the flow duration curve. The procedures for computing entropy-based FDC are identical to the study by Singh et al. (2014a),

while the future FDC are predicted with different climate change scenarios. To that end, the simulated future runoff from the DBH model projected by GCM models under RCP scenarios are used for generating the future FDC, with which the water resources sustainability is discussed.

Results and concluding remarks

The FDC of the YRB is estimated and predicted using the entropy theory from observed data for the past and simulated land-surface model, respectively. From the FDC computed from the six stations, the average return period of the low flow condition is around 30 months, which is less than three year, while it will be shorten to 20-25 months under different RCP scenarios. Besides, the water resources sustainability is under more threats for the downstream than for the upstream stations.

Acknowledgments: This study is funded by National Natural Science Foundation of China (41877454).

References

Singh VP, Byrd A, Cui H (2014a) Flow Duration Curve Using Entropy Theory, J Hydrol Eng 19:1340-1348

Singh VP, Cui H, Byrd AR (2014b) TSALLIS entropy-based flow duration curve, Transactions of the ASABE 57(3):837-849

US Environmental Protection Agency (US EPA) (2007) An approach for using load duration curves in the development of TMDL. EPA-841-B-07-006, Watershed Branch, Office of Wetlands, Oceans and Watersheds, USEPA, Washington DC

11th World Congress on Water Resources and Environment (EWRA 2019)
"Managing Water Resources for a Sustainable Future", 25-29 June 2019, Madrid, Spain

Simulating maximum temperature for future time series on lower Godavari basin, Maharashtra State, India by using SDSM

Y.J. Barokar[1*], V.R. Saraf[2], D.G. Regulwar[1]
[1] Department of Civil Engineering, Government College of Engineering, Aurangabad, Maharashtra State, India
[2] Government College of Engineering, Jalgaon, Maharashtra State, India
* e-mail: yogeshbarokar@gmail.com

Introduction

Global warming is causing changing pattern of temperature. Study of changing temperature pattern for future period can be helpful in the mitigation of changing cropping pattern. SDSM is a freely available tool which helps to downscale climate variables such as temperature and precipitation for future series. Statistical relationship between predictors and predictands is used by SDSM for downscaling climate variables.

Downscaling can be carried out dynamically or statistically but statistical downscaling is preferable than dynamic downscaling (Wilby et al. 2001). In downscaling half of the work has been done for comparing different types of downscaling techniques and remaining has been done for other sectors (Wilby and Dowson 2013). Downscaling is helpful in other sectors such as downscaled precipitation can be useful for calculation of discharge values using SWAT model for future time period (Saraf and Regulwar 2018) also downscaling by SDSM helps to study extreme temperature events (Mahmood and Babel 2014). In this study area selected for downscaling maximum temperature is Lower Godavari Basin, Maharashtra State, India (Latitude: 19°11', Longitude: 76°33'). Downscaling of maximum temperature has been done by using SDSM and GCMs selected for study are HaCM3 and CanESM2 (CMIP5). Downscaling has been done under A2a and B2a scenarios of HadCM3 and under RCP 2.6, RCP 4.5 and RCP 8.5 of CanESM2. Statistiacal results for Calibration and validation period have been tabulated. Results under all scenarios of both GCMs have been plotted for three future series as 2020s (2011-2040), 2050s (2041-2070) and 2080s (2071-2099) for comparison. Both models show increasing trend of maximum temperature over selected area for all three future series.

Materials and methods

Observed data of maximum precipitation obtained from Indian Meteorological Department (IMD), Pune. This data is available at high spatial resolution 0.50° × 0.50° (Latitude × Longitude) for the period 1961-2013. Predictor data of GCMs were extracted from the website http://www.cics.uvic.ca/scenarios given by Canadian Institute for Climate Studies (CICS).

The methodology of the study is divided into seven steps:

1. *Quality Control*: Which helps to identify missing values,
2. *Screen Variables*: Specific set of predictors can be selected form this step,
3. *Calibrate Model*: This step makes statistical relation between predictor and predictand,
4. *Weather Generator*: In this step we can verify our calibrated model,
5. *Summary Statistics*: It gives statistics file for selected data set,
6. *Scenario Generator*: It generates climatic variable values for future series. Basic equation used in this step to downscale the maximum temperature is as given below:

$$U\mathrm{i} = \Upsilon_0 + \sum_{j=1}^{n}(\Upsilon\mathrm{j} + \mathrm{Xij} + €\mathrm{i}) \quad (1)$$

where Ui is the temperature, Xij indicates predictors, € is the model error, i corresponds to day and Υ is regression coefficients,

7. *Compare Results*: In this step we can compare results and plot them in graphical format.

Results and concluding remarks

Statistical results of downscaling under all scenarios are given in Tables 1 and 2.

Table 1. Statistical comparison of observed and downscaled mean monthly Tmax under base line period

Model	R^2
HadCM3_A2a (Under base line period 1961-2000)	0.97
HadCM3_B2a (Under base line period 1961-2000)	0.96
CanESM2_Historical (Under base line period 1961-2005)	0.90

Table 2. Future change in mean annual Tmax (with respect to base line period)

Model	Scenario	Future	Tmax (^{o}C)
HadCM3	A2a	2020s	0.92
		2050s	1.92
		2080s	3.17
	B2a	2020s	0.97
		2050s	1.60
		2080s	2.39
CanESM2	RCP 2.6	2020s	1.05
		2050s	1.44
		2080s	1.36
	RCP 4.5	2020s	1.21
		2050s	1.64
		2080s	1.85
	RCP 8.5	2020s	1.19
		2050s	2.07
		2080s	3.05

From the above results we can say, HadCM3_A2a and HadCM3_B2a gives slightly higher coefficient of determination than CanESM2_Historical. Result for future series shows that all the scenarios of both GCMs gives increasing trend of Tmax with respect to the base line period. RCP 2.6, RCP 4.5 and RCP 8.5 give higher increase in Tmax than that of A2a and B2a.

References

Wilby RL, Dawson CW, Barrow EM (2001) SDSM-a decision support tool for the assessment of regional climate change impacts. Environmental Modelling and Software 17:147-159

Wilby RL, Dawson CW (2013) The Statistical Downscaling Model: Insights from one decade of application, International Journal of Climatology 33:1707-1719. doi: 10.1002/joc.3544.

Saraf VR, Regulwar DG (2018) Impact of Climate Change on Runoff Generation in the Upper Godavari River Basin, India. Journal of Hazardous, Toxic and Radioactive Waste, ASCE, ISSN 2153-5493 doi: 10.1061/(ASCE)HZ.2153-515.0000416.

Mahmood R, Babel MS (2014) Future changes in extreme temperature events using the statistical downscaling model (SDSM) in the trans-boundary region of the Jhelum river basin. Journal of Weather and Climate Extremes, http://dx.doi.org/10.1016/j.wace.2014.09.001

11th World Congress on Water Resources and Environment (EWRA 2019)
"Managing Water Resources for a Sustainable Future", 25-29 June 2019, Madrid, Spain

Assessing lake vulnerability to climate change using the coupled MIKE SHE/MIKE 11 model: Case study of Lake Zazari in Greece

D. Papadimos[1], K. Demertzi[1*], D. Papamichail[2]
[1] *Goulandris Natural History Museum, Greek Biotope/Wetland Centre, Thermi, Thessaloniki, Greece*
[2] *Department of Hydraulics, Soil Science and Agricultural Engineering, Aristotle University of Thessaloniki, Greece*
** e-mail: kldemertzi@ekby.gr*

Introduction

If the worst predictions of general circulation models (GCMs) about climate change become true, then lakes will hardly manage to maintain their current conditions (Zhang et al. 2016) especially in regions, which have been identified as climate change hot spots such as the countries of Mediterranean Basin (Loizidou et al. 2016) from which Greece is of special interest since it has 54 lakes/reservoirs of 0.5 km^2 minimum size.

The hydrological models are important tools for assessing the water balance components of lakes and for supporting the design of water management strategies. Depending on the modelling purposes and the specific attributes of a lake, different types of models and different levels of model complexities can be selected, starting from complex models such as MIKE SHE (Abbott et al. 1986), WATLAC (Zhang 2011) or using simpler methods (Yang et al. 2018). The MIKE model is among the most integrated models and has been used in the past for similar cases (Singh et al. 2010), while in combination with the future climate projections of general circulation models (GCMs), can be used to investigate lake conditions under future climate scenarios. The aim of this study is to present an application for analyzing the vulnerability of a lake to climate change using the MIKE SHE/11 model using as a case study the Lake Zazari in Greece.

Materials and methods

The study area is the sub-basin of Lake Zazari, which is located in the north-western Greece. The maximum allowed lake surface elevation (LSE) is at 602 m above sea level (a.s.l.) and the maximum lake depth is at 6 m regulated by a sluice gate. MIKE SHE coupled with MIKE 11 model for better delineation of channels and lake hydraulic attributes was calibrated based on the current conditions (1/1/2012-31/4/2017). The observed data used for calibration were the variation of lake surface elevation (LSE) and the daily temperature and precipitation data from the Amyntaion and Limnochori meteorological stations for the aforementioned period. The digital elevation model was obtained by the EU-DEM v1.1 database with a spatial resolution of 25 m in which lake bathymetry was incorporated. The land uses were obtained from Corine Land Cover 2012 database and the general soil properties from the ESDB-ESDAC soil database (Hiederer 2013). Soil hydraulic properties were estimated using the pedotransfer functions of Saxton and Rawls (2006). Potential evapotranspiration was calculated based on the Hargreaves and Samani (1982) equation considering the local revised coefficients provided by Aschonitis et al. (2017) for achieving equivalent estimations of FAO-56/ASCE reference crop evapotranspiration ET_o for short grass (Allen et al. 1998). The calibrated model was applied for analyzing the hydroclimatic conditions of the lake under climate change considering the predictions of 4 GCMs (GFDL-CM3, MIROC-ESM-CHEM, MIROC-ESM, IPSL-CM5A-LR) for the worst scenario of highest greenhouse gas emissions RCP8.5 (mean conditions of 2061-2080). These 4 GCMs were selected among 19 GCMs provided by the WorldClim database (Fick and Hijmans 2017) because they represented the worst conditions in terms of rainfall reduction and temperature increase compared to the current conditions at the position of the lake.

Results and concluding remarks

The mean annual lake surface elevation (LSE), basin precipitation (PCP), basin reference evapotranspiration (ET_o) and surface discharge outside the basin (Q_d) for the current conditions (2012-2017) and for the future conditions according to the 4 GCMs (GFDL-CM3, MIROC-ESM-CHEM, MIROC-ESM,

IPSL-CM5A-LR) for the RCP8.5 scenario are given in Table 1.

Table 1. Mean annual values of LSE, PCP, ETo, Qd for the current conditions and for the future conditions according to the four GCMs of the RCP8.5

Parameter (mean annual values)	2012-2017	Future scenarios according to RCP8.5 for 2061-2080			
	Current	GFDL-CM3	MIROC-ESM-CHEM	MIROC-ESM	IPSL-CM5A-LR
LSE (m.a.s.l.)	599.27	598.84	599.09	599.03	599.06
PCP (mm)	731	405	475	544	520
ET_o (mm)	970	1152	1067	1110	1133
Q_d (m^3)	9.51E+06	0.46E+06	2.89E+06	1.93E+06	2.20E+06

Taking into account Table 1, it is observed that the four climate projections will lead to significant changes in the hydrologic features of the lake. The most important changes are the extreme reduction of Q_d (70 up to 95%) and the LSE reduction (18 up to 43 cm lower water level). This indicates a severe disturbance in the downstream system that consists of another three interconnected lakes (Chimaditida, Petron, Vegoritida). The downstream lakes will face more severe problems not only due to the reduction of upstream flows but also due to the same climatic change within their sub-basins.

Acknowledgments: This study was implemented in the framework of the National Water Monitoring Network for lakes of Greece, according to the Joint Ministerial Decision 140384/2011, implemented by The Goulandris Natural History Museum, Greek Biotope/Wetland Centre.

References

Abbott MB, Bathurst JC, Cunge JA, O'Connell PE, Rasmussen J (1986) An introduction to the European Hydrological System - Systeme Hydrologique Europeen, "SHE", 1: History and philosophy of a physically-based, distributed modelling system. Journal of Hydrology 87(1-2):45-59. https://doi.org/10.1016/0022-1694(86)90114-9

Allen RG, Pereira LS, Raes D, Smith M (1998) Crop Evapotranspiration: Guidelines for computing crop water requirements. Irrigation and Drainage Paper 56, Food and Agriculture Organization of the United Nations, Rome.

Aschonitis VG, Papamichail D, Demertzi K, Colombani N, Mastrocicco M, Ghirardini A, Castaldelli G, Fano E (2017) High-resolution global grids of revised Priestley-Taylor and Hargreaves-Samani coefficients for assessing ASCE-standardized reference crop evapotranspiration and solar radiation. Earth System Science Data 9(2):615-638. https://doi.org/10.5194/essd-9-615-2017

Fick SE, Hijmans RJ (2017) WorldClim 2: new 1-km spatial resolution climate surfaces for global land areas. International Journal of Climatology 37(12):4302-4315. https://doi.org/10.1002/joc.5086

Hargreaves GH, Samani ZA (1982) Estimating potential evapotranspiration. Journal of Irrigation and Drainage Engineering - ASCE 108:225-230

Hiederer R (2013) Mapping Soil Properties for Europe - Spatial Representation of Soil Database Attributes. Publications Office of the European Union, EUR26082EN Scientific and Technical Research series, Luxembourg, 47 p. https://doi.org/10.2788/94128

Loizidou M, Giannakopoulos C, Bindi M, Moustakas K (2016). Climate change impacts and adaptation options in the Mediterranean basin. Regional Environmental Change 16(7):1859-1861. https://doi.org/10.1007/s10113-016-1037-9

Saxton KE, Rawls WJ (2006) Soil water estimates by texture and organic matter for hydrologic solutions. Soil Science Society of America 70:1569-1578. https://doi.org/10.2136/sssaj2005.0117

Singh CR, Thompson JR, French JR, Kingston DG, MacKay AW (2010) Modelling the impact of prescribed global warming on runoff from headwater catchments of the Irrawaddy River and their implications for the water level regime of Loktak Lake, northeast India. Hydrology and Earth System Sciences 14(9):1745-1765. https://doi.org/10.5194/hess-14-1745-2010

Yang K, Lu H, Yue S, Zhang G, Lei Y, La Z, Wang W (2018) Quantifying recent precipitation change and predicting lake expansion in the Inner Tibetan Plateau. Climatic Change 147(1-2):149-163. https://doi.org/10.1007/s10584-017-2127-5

Zhang Q (2011) Development and application of an integrated hydrological model for lake watersheds. Procedia Environmental Sciences 10:1630-1636. https://doi.org/10.1016/j.proenv.2011.09.257

Zhang C, Lai S, Gao X, Liu H (2016) A review of the potential impacts of climate change on water environment in lakes and reservoirs. Journal of Lake Sciences 28(4):691-700. https://doi.org/10.18307/2016.0401

11th World Congress on Water Resources and Environment (EWRA 2019)
"Managing Water Resources for a Sustainable Future", 25-29 June 2019, Madrid, Spain

Sustainability index assessment in the Flumendosa-Campidano water system management (Sardinia, Italy)

A. Sulis[1*], A. Ruiu[2], R. Zucca[2], G.M. Sechi[1,2]
[1] Center of Environmental Sciences (CINSA), University of Cagliari, 09123 Cagliari, Italy
[2] Dept. of Civil and Environmental Engineering (DICAAR), University of Cagliari, 09123 Cagliari, Italy
* e-mail: asulis@unica.it

Introduction

A sustainable planning and management of complex water resource systems requires that all the components in the system must be in balance (Sandoval-Solis et al. 2013). This concept of sustainability is a challenge to develop new methods and use better existing methods particularly when considering trade-off in resource use and consumption among different water users over different time horizons. While the issue of intergenerational equity is central to this concept (Loucks 1997), this paper focuses more on the evaluation of sustainability for different groups of water users when their properties change in terms of allocation priority and annual demand, and definition and application of an index to quantify sustainability in planning and management based on risk and uncertainty. The Sustainable Index (SI) developed by Loucks (1997) is an aggregate measure of a combination of probability-based performance measures, specifically reliability, resilience and vulnerability (Hashimoto et al. 1982). SI has been largely used in the past to evaluate and compare different water management policies, even if its practical application presents some hindrances (Hopkins 1991). An improvement of Loucks' SI has been recently proposed by Sandoval-Solis et al. (2013) to give more flexibility and be more practical to communicate. In this improved version, the SI is defined as a geometric average of M performance criteria. To compare groups of water users, the sustainability by groups (SG) was defined as a weighted average of different SI values. This paper presents an extensive application of the improved SI to the Flumendosa-Campidano water system located in South Sardinia (Italy) where severe droughts have occurred in the last 3 decades.

Materials and methods

Sandoval-Solis et al. (2013) have proposed SI as a function of *M* performance criteria for the i^{th} water user:

$$SI^i = \left[\prod_{m=1}^{M} C_m^i\right]^{1/M} \quad (1)$$

The SG was used to calculate the sustainability for a group *k* with i^{th} to j^{th} water users belonging to this group:

$$SG^k = \sum_{i=1\in k}^{i=j\in k} W^i \cdot SI^i \quad (2)$$

where W^i is the relative weight for the i^{th} water user, ranging from 0–1 and summing to one. Many weighting methods have been proposed. The SI of each water users is weighted by its annual demand. To compare different water system management options, in this paper we proposed the sustainability by system (SS) as a weighted average of SG. When considering *n* groups, SS is defined as:

$$SS = \sum_{k=1}^{n} C^k SG^k \quad (3)$$

When assessing the sustainability of the of the entire water system management, C^k in SS reflect the demand priorities that the user has assigned in the simulation model of the water system. Specifically, the generic simulation model WARGI-SIM (Sechi and Sulis 2009) has been applied to reproduce the management of the Flumendosa-Campidano water system. Resource to demand flows in the simulation module are activated by a combination of ordered instruction based on user-defined priority criteria.

The Flumendosa–Campidano water system extends over South Eastern Sardinia and up to Central

Sardinia. The system is the most extended and interconnected multireservoir and multiuse system in the region. Since the 1990s, droughts have been occurring with increased frequency and severity. The reader is referred to Sechi and Sulis (2009) for a deeper presentation of the system. Here we focus on the different water groups that compose the total water demand in the system. Specifically, water groups are of urban, industrial and agricultural demands, and environmental flow (e-flow). The latter is the water regime provided within a river as a rate of the reservoir release, to maintain ecosystems and their benefits where there are competing water uses. In this sense, e-flow is considered as a consumptive and competitive demand. The monthly demand of each demand is subdivided into few volumes with different priorities. Then, a configuration of water volumes and priorities is a key step in the definition of the allocation policies in the system. Three different configurations have been considered to assess how the SS change for different priority levels of the e-flow. Specifically, the base configuration requires the e-flow is supplied only when all water groups are satisfied, in the second configuration e-flow is competitive with the entire agricultural demand while in the third configuration e-flow is competitive with the entire industrial demand. It is to be noticed that only e-flow priority is changed between those management configurations while other system parameters (e.g., target releases or buffer volumes from and in the reservoir) were the same.

Results and concluding remarks

Table 1 summarized the main results when three different management configurations were simulated. Specifically, only the probability-based performance measures (vulnerability as maximum annual deficit and resilience as number of years with deficit) of the e-flows are shown.

Table 1. Probability-based performance measures of e-flow group and SG (Sustainability by Groups) and SS (Sustainability by System).

	Vuln	**Res**	**SG Ur**	**SG Ind**	**SG Agr**	**SS**
Configuration 1	7.3	22	0.8	0.6	0.4	0.8
Configuration 2	4.2	18	0.8	0.6	0.32	0.78
Configuration 3	2.1	14	08	0.51	0.21	0.72

Results in Table 1 show that performance measures of the e-flows increase as the e-flow priority increases. This is done at the cost of a decrease of the sustainability of the system, showing that a high priority of e-flow (same priority of agriculture and industry) produces a worse system management in term of sustainability.

Acknowledgments: This study was developed in the framework of the revision of the Sardinian Water Plan (Piano Stralcio per l'Utilizzo delle Risorse Idriche) with the financial support of the Agenzia Distretto Idrografico della Sardegna.

References

Hashimoto T, Stedinger JR, Loucks DP (1982) Reliability, resiliency and vulnerability criteria for water resource system performance evaluation. Water Resour. Res. 18(1):14–20

Hopkins M (1991) Human development revisited: A new UNDP report. World Dev. 19(10):1469–1473

Loucks DP (1997) Quantifying trends in system sustainability. Hydrol. Sci. J. 42(4):513–530

Sandoval-Solis S, McKinney DC, Loucks DP (2011) Sustainability Index for Water Resources Planning and Management. Journal of Water Resources Planning and Management 137(5):381–390

Sechi GM, Sulis A (2009) Water system management through a mixed optimization-simulation approach. Journal of Water Resources Planning and Management 135(3):160 – 170

11th World Congress on Water Resources and Environment (EWRA 2019)
"Managing Water Resources for a Sustainable Future", 25-29 June 2019, Madrid, Spain

Flow risk assessment under climate change effect in Yesilirmak basin, Turkey

U. Serencam[1], I. Dabanli[2,3*]
[1] Bayburt University, Engineering Faculty, Civil Engineering Department, 69000, Bayburt, Turkey
[2] Istanbul Medipol University, School of Engineering and Natural Sciences, Civil Engineering Department, Kavacık, 34181, Istanbul, Turkey
[3] Istanbul Medipol University, Climate Change Researches Application and Research Center, (IKLIMER) Kavacık, 34181, Istanbul, Turkey
* e-mail: idabanli@medipol.edu.tr

Introduction

In general, expectation for climate change impacts on flow regimes is not well-known in Turkey, but it is expected that impacts of climate changes have been changing from south to north. In north latitudes, extreme precipitations are expected be more frequent. Therefore, flow regimes in rivers may affect these sudden changes (flooding) directly. Flooding is singled out, because worldwide, it is the most common natural hazard and third most damaging effect (after storms and earthquakes) (World Bank 2010). Flooding is already described as the costliest natural hazard (Dankers and Feyen 2008; Kundzewicz et al. 2010). For example, in the Black Sea Region the flood disasters are very frequent due to sudden rainfall especially in recent years. These disasters have damaged agricultural areas, infrastructure and superstructure facilities. Not only physically damages, but also, human and animal life losses are observed in hazard areas. This situation has not been resolved by local authorities from both financial and technical ability shortage in Turkey. It is necessary to analyse the historical data in the context of trend and climate change clearly to reduce the damage of flooding due to the climate change. From this fact, the aim of this study is determined to examine how climate change affects the classical risk levels for flow regimes based on probabilistic approach in Yesilirmak basin, Turkey.

Materials and methods

In this paper, general procedure of risk assessment is implemented under climate change perspective. Theoretically, several convenient formulations have been generated for design level including discharge values. However, climate change effects are ignored in most of the evaluations. In classical approach, risk level is defined by considering to equal probability of the event occurrences. Mathematical definition of classical risk (r) is suggested by Benjamin and Cornell (1970) as follows:

$$r=1/R \quad (1)$$

where R is only once observed event during the whole planned life of any structure. This simple risk approach was modified by Şen et al. (2017) as:

$$C_r=(1+\alpha)/R \quad (2)$$

where C_r is the risk under the climate change effect and α is a factor of climate change. When α = 0, implies that there is no contribution of climate change neither positive nor negative. In this method, α is calculated as the slope of the trend behavior within the flow time series data after normalization.

Results and concluding remarks

This method is implemented by using 6 flow stations in Yesilirmak river. Sutluce station is selected for sample trend slope detection and risk assessment calculation based on several risk levels as seen in Figure 1. Cumulative distribution function (CDF) for reversal exceedance probability is calculated from 0.2% to 50% risk levels. In this Station data are perfectly fitted to Pearson-III PDF. Regarding, flow regime trend

analysis, trend slope is detected as -1.56% on Yesilirmak river. The risk ranges between lowest to highest levels as 170.12 m^3/s for Sutluce flow stations.

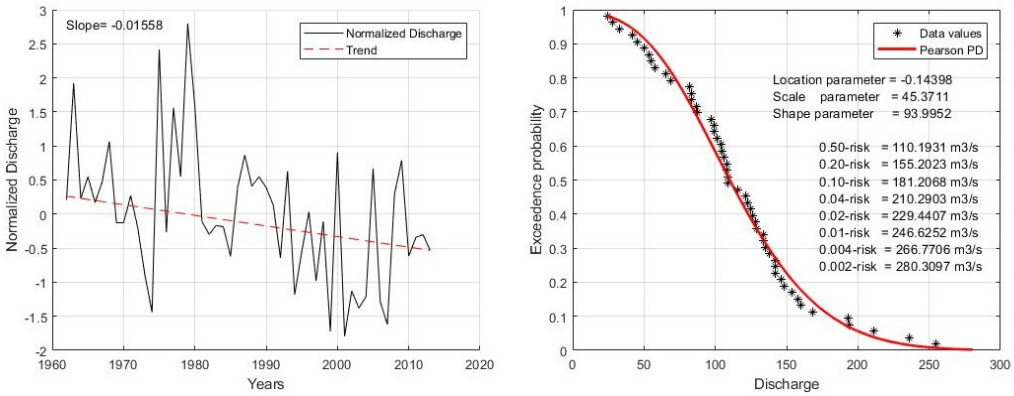

Figure 1. Precipitation trend slope and risk levels in Almus (above) and discharge trend slope and risk levels in Fatli stations (below).

In the classical approaches, return period can be easily calculated by using risk level (Eq. 1). As an example, 0.2% risk level corresponds to 500-year return period. Therefore, return period and risk levels are presented for climate change effects on flow regime jointly as seen in Table 1. Results show that there is no significant difference between classical and climate change risk levels. Trend slopes appear in quite low interval because of standardization. Therefore, climate change effects cannot be seen significantly on precipitation time series. Standardization procedure will be discussed and analysed for more significant results. Further studies are going to focus on trend slope detection to illustrate climate change impact on flow regimes.

Table 1. Climate change-based risk calculations for flow regimes in Yesilirmak basin.

	Return Period (year)	E14A001 (Fatli)	E14A002 (Kale)	E14A012 (Seyhoglu)	E14A013 (Durucasu)	E14A014 (Sutluce)	E14A022 (Cicekbuku)
Trend Slope (α)		-0,0371	-0,0346	-0,0382	-0,0119	-0,0156	-0,0262
Classical Risk Level (*r*)	2	378,33	616,78	45,97	301,53	110,19	77,14
	5	550,53	837,85	83,55	441,03	155,20	115,76
	10	669,78	971,60	109,32	518,42	181,21	143,11
	25	825,55	1128,60	141,77	603,05	210,29	179,44
	50	944,94	1238,12	165,55	658,54	229,44	207,68
	100	1067,01	1342,16	188,90	708,86	246,63	236,86
	250	1233,72	1473,45	219,25	769,37	266,77	277,14
	500	1364,51	1569,12	241,92	811,56	280,31	309,06
Climate Change Effected Risk Level (C_r)	2	370,56	606,59	44,27	299,18	109,23	75,93
	5	544,13	830,79	82,12	439,56	154,57	114,73
	10	663,58	965,41	107,96	517,21	180,67	142,10
	25	819,32	1123,06	140,47	602,04	209,84	178,41
	50	938,60	1232,89	164,28	657,64	229,04	206,61
	100	1060,51	1337,16	187,65	708,04	246,26	235,75
	250	1226,95	1468,69	218,02	768,63	266,45	275,97
	500	1357,52	1564,49	240,70	810,86	280,02	307,85

References

Benjamin JR, Cornell CA (1970) Probability, statistics and decisions for civil engineers. McGraw-Hill, New York

Dankers R and Feyen L (2008) Climate change impact on flood hazard in Europe: An assessment based on high resolution climate simulations. Journal of Geophysical Research 113:D19105

Kundzewicz ZW, Lugeri N, Dankers R et al. (2010) Assessing river flood risk and adaptation – review of projections for the future. Mitigation and Adaptation Strategies for Global Change 15:641–656

Şen, Z., Mohorji, A.M. & Almazroui, M. (2017), Engineering risk assessment on water structures under climate change effects, Arab J Geosci 10:517. https://doi.org/10.1007/s12517-017-3275-7

World Bank (2010) Natural Hazards, Unnatural Disasters. The Economics of Effective Prevention. Washington, DC

11th World Congress on Water Resources and Environment (EWRA 2019)
"Managing Water Resources for a Sustainable Future", 25-29 June 2019, Madrid, Spain

Trade-off between environmental flow and water availability: A mesoscale analysis for Europe

A. Sordo-Ward[1*], M.D. Bejarano[2], I. Granados[1], L. Garrote[1]
[1] Department of Civil Engineering: Hydraulics, Energy and Environment, Universidad Politécnica de Madrid, Spain
[2] Department of Natural Resources, Universidad Politécnica de Madrid, Spain
* e-mail: l.garrote@upm.es

Introduction

Environmental flow allocation is one of the key aspects of environmental policy regarding water management. Traditionally, water allocation decisions were mainly based on water productivity, accounting for the benefits obtained from using water for urban supply, agriculture, hydropower and other economic activities. In some basins, this approach caused excessive water abstraction and environmental degradation. Increasing social awareness of environmental problems led to a new paradigm for water resources management where the central objective is good ecological status of water bodies (Pahl-Wostl 2007). Water allocation is now subject to the pre-requisite of meeting environmental flow requirements (EFRs). However, the practical application of this principle is controversial due to the competing interests of affected stakeholders. A wide range of methods has been proposed to determine EFRs: hydrologic, hydraulic, habitat simulation and holistic methodologies provide an array of usually divergent values that challenge water allocation decisions (Arthington et al. 2018). The choice of a single method or value for EFR may lead to sub-optimal or inequitable allocation decisions, which would produce direct economic impacts on affected stakeholders.

The main objective of this work is to conduct a regional assessment in Europe of the trade-off between water allocation to environmental flow and to other productive uses. In this assessment we account for local conditions that determine the influence of environmental flow allocation on water availability as a function of hydrologic regime and available regulation storage.

Material and methods

We estimated water availability in the river network of Europe using the WAAPA model. WAAPA is a simple model that simulates the operation of a water resources system accounting for river network topology, streamflow, reservoir storage, evaporation and environmental flow (Garrote et al. 2015). One of the outputs of WAPA is the estimation of maximum potential water availability (MPWA) in every point of the river network. MPWA is defined as the maximum demand that can be supplied at a certain location with a given reliability criterion. It is estimated through an iterative algorithm by jointly managing the upstream reservoirs to minimize uncontrolled spills. Model topology was derived from the digital elevation model (DEM) of the HYDRO1K dataset. Reservoir data were obtained from the ICOLD World Register of Dams. A total of 2301 dams with storage larger than 5 hm^3 were georeferenced to the drainage network derived from the HYDRO1K DEM. Additional model nodes were defined at the outlet of HYDRO1K sub-basins. Model topology is composed of 3839 sub-basins, which belong 620 large basins covering 6M km^2.

Streamflow data were obtained from the application of the PCRGLOB-WB model in the ISIMIP-Inter-Sectoral Impact Model Intercomparison Project. The model was forced with the output of five climate models (GFDL-ESM2NM, HadGEM2-ES, IPSL-CM5A-LR, MIROC-ESM-CHEM and NorESM1-M) and produced results for the entire world at 0.5^o resolution. We selected the time slice from 1960 to 1999 to characterize current conditions. To explore the sensitivity of water availability to environmental flows, we chose a hydrological environmental flow method that can be parameterized. Environmental flow is computed as a given percentile of the marginal monthly flow distribution. Spanish legislation establishes for this method a range between 5% and 15% percentile. We covered a wider range, from 0% to 20% percentile, with values of 0 (no environmental flow allocation) and 3.3%, 6.3%, 10%, 13.3%, 16.6% and 20% percentile.

Results and discussion

We focus on the trade-off between water allocation to environmental flow and water availability. To estimate this effect, we compute the non-dimensional ratio between the reduction of water availability and the increase of water allocation to environmental flow as we move from one value of percentile to the next. Figure 1 presents the spatial distribution of this ratio for the step between 10% and 13.3% percentile.

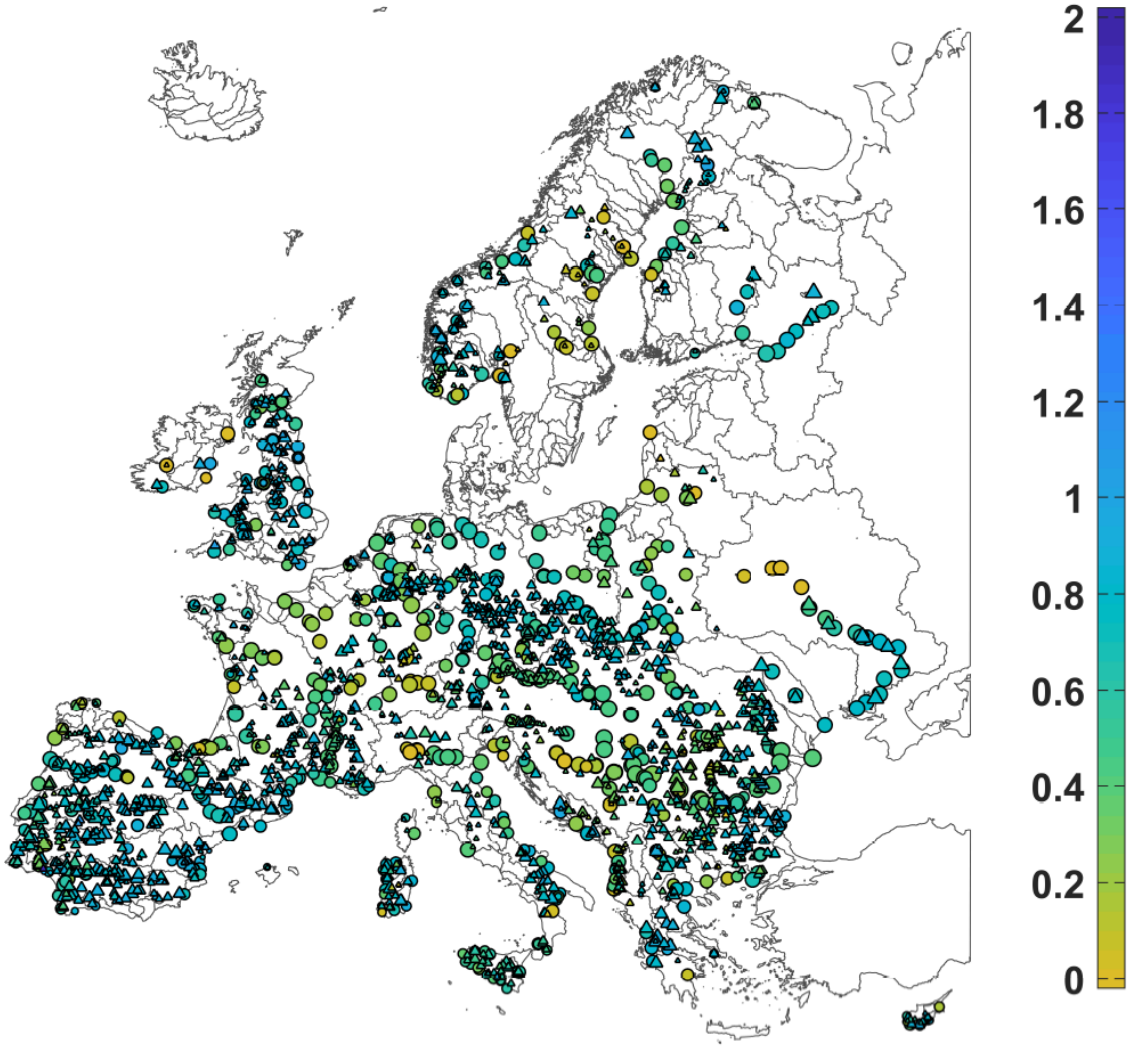

Figure 1. Ratio between reduction of water availability and increase of environmental flow for the transition between 10% and 13.3% percentile, represented by the colour code on the right. Reservoir locations are shown as triangles of size correlative to reservoir storage. River locations are shown as circles of size correlative to mean annual flow.

This ratio is unevenly distributed over Europe, suggesting that the implications of increasing water allocation to environmental flow may vary, depending on hydrologic regime and available storage. The ratio is larger for smaller percentiles of environmental flow.

Acknowledgments: We acknowledge support from the Spanish MINECO through the Juan de la Cierva actions (Ref. JC2016MDBC) and from UPM through ADAPTA project and his program for young researchers.

References

Arthington AH, Kennen G, Stein E, Webb JA (2018) Recent advances in environmental flows science and water management – Innovation in the Anthropocene. Fresh. Biol. 63(8):1022-1034. doi: 10.1111/fwb.13108

Garrote L, Iglesias A, Granados A et al. (2015) Quantitative Assessment of Climate Change Vulnerability of Irrigation Demands in Mediterranean Europe. Water Resour Manage 29(2):325-338

Pahl-Wostl C (2007) Transitions towards adaptive management of water facing climate and global change. Water Resour Manage 21(1):49-62

11th World Congress on Water Resources and Environment (EWRA 2019)
"Managing Water Resources for a Sustainable Future", 25-29 June 2019, Madrid, Spain

Evaluation of climate change impact on Arachthos river discharge using the SWAT model

G.D. Gikas[1*], G. Lampros[1], V.A. Tsihrintzis[2]
[1] Department of Environmental Engineering, School of Engineering, Democritus University of Thrace, 67100 Xanthi, Greece
[2] Centre for the Assessment of Natural Hazards and Proactive Planning & Laboratory of Reclamation Works and Water Resources Management, School of Rural and Surveying Engineering, National Technical University of Athens, Greece
* e-mail: ggkikas@env.duth.gr

Introduction

According to the Intergovernmental Panel on Climate Change (IPCC 2014), events such as droughts and floods will become more frequent and widespread in the future due to climate change. These events will have an impact on streamflow, ecosystems health, groundwater availability, reservoir storage, crop yield etc. Generally, climate change will influence the global hydrological cycle by increasing water holding capacity of the atmosphere due to increasing global temperature (Dahal et al. 2016). Some of climate change impacts could be reduced with foreknowledge of magnitude of future events. Hydrological models, for example, can estimate with adequate precision the differentiation in climate and hydrological attributes in a river basin and make some accurate predictions for the future situation.

The aim of the present study is to evaluate the impact of climate change on Arachthos river watershed located in western Greece. For this purpose, the Soil and Water Assessment Tool (SWAT) model (Arnold et al. 1998; Neitsch et al. 2005) was used. The focus was on river discharge under climate change scenario for years 2050-2051 and 2090-2091.

Materials and methods

The total length of Arachthos river is about 110 km. The river traverses a watershed of about 2005 km^2 which includes mountains, agricultural plains, forests and urban areas, and discharges to Amvrakikos gulf. The mean annual rainfall in the watershed is about 2000 mm and the mean annual flow of the river is about 66 m^3/s. Amvrakikos gulf is known for aquaculture which has been developed over the last 25 years. It is a semi-enclosed embayment, 35 km long, 6-15 km wide and of maximum depth of 65 m, connected to the Ionian Sea through a narrow natural channel.

SWAT is a continuous, distributed hydrological model, which simulates in detail various physical processes taking place in a watershed, including the rainfall-runoff process, and the transport of sediments and nutrients. The basic input data used in the model are topography, land use and soils, and, at a daily step, rainfall depth, and maximum and minimum temperature. SWAT subdivides the watershed into multiple sub-basins and further into hydrologic response units (HRUs), which are homogenous units that possess unique land use and soil attributes. This subdivision allows the model to identify differences in evapotranspiration and other hydrological processes for different areas, crops and soils, providing a very satisfactory physical description of the water balance.

The topography of the study area is described in the model by the Digital Elevation Model (DEM), which is used by SWAT as the basis for delineating rivers and streams. The DEM was created using satellite images from the ASTER satellite of the US Geological Survey (USGS). Map data of land use have been obtained from the Corine Land Cover database of the European Environment Agency (EEA). The watershed soil map was based on data obtained from the International Food and Agriculture Organization (FAO, http://faostat.fao.org). Meteorological data, daily rainfall and daily maximum and minimum temperature values were obtained from the Public Power Corporation (PPC) and the Hellenic National Meteorological Service (HNMS) for the period 01/01/2006 to 31/12/2011. The data used for the climate change scenario were obtained by the 2w2e Institute (wwee; water weather energy and ecosystem technology and data,

http://www.2w2e.com). The data refer to daily rainfall and temperature values in SWAT format derived using the ISI-MIP toolbox (Vaghefi et al. 2017) and the IPCC greenhouse gas emission scenario A2 (IPCC 2014).

Results and concluding remarks

The model was run successfully for the period 01/01/2006 to 31/12/2011, with the first two years used as warm-up period. The calibration and validation of SWAT model was conducted for total water volume and discharge using data from three gauging stations (ST1, ST2, ST3). Agreement between observed and predicted values of flow for both calibration and validation of the model is considered good, as all the calibration criteria used (Boskidis et al. 2010) were within permissible limits (Table 1).

Table 1. Best-fit criteria used for calibration and validation of SWAT model.

CALIBRATION CRITERIA	CALIBRATION			VALIDATION		
	ST1	ST2	ST3	ST1	ST2	ST3
γ (The slope of linear regression line)	0.94	1.12	0.94	0.93	1.06	1.04
R^2 (Correlation coefficient)	0.98	0.95	0.93	0.94	0.93	0.93
RMSE (Root mean square error, m^3/s)	3.65	2.09	10.23	4.76	1.24	9.30
NOF (Normalized objective function)	0.19	0.39	0.21	0.14	0.24	0.21
NSE (Nash-Sutcliffe coefficient of efficiency)	0.97	0.90	0.93	0.98	0.90	0.92

Two climate change scenarios were tested, referring to streamflow simulation for years 2050-51 (1st scenario) and 2090-91 (2nd scenario) using the climate model's weather prediction data. The mean annual water volume at the outlet of Arachthos watershed of each scenario was compared to the mean annual water volume of the period 2008-2011. Results showed significant reduction of water volume for both scenarios which were 60.1 % and 63.5 % for the 1st and 2nd scenario, respectively. This result is partly explained by the low rainfall values predicted for the area for future years and also the estimation of high temperatures in the future, resulting in an increase of evapotranspiration, which leads to a decrease in water availability.

The significant reduction in water availability makes a necessity the rational management of the water resources in the future. Adaptation to these new future conditions will directly affect the local community, as there are intense agriculture activities in the area and significant amounts of water are used for irrigation. In addition, the predicted significant reduction of water runoff into Amvrakikos bay will exacerbate the already existing serious problem of water renewal, as the gulf is already eutrophic. It is considered necessary to take measures and decisions to restore the ecosystem's hydrological balance and reduce the systematic pollution of its waters. The parameterization of the physical processes of the Arachthos drainage basin using SWAT hydrological model is a reliable step towards this direction.

References

Dahal V, Shakya NM, BhattaraiR (2016) Estimating the impact of climate change on water availability in Bagmati Basin, Nepal. Environmental Processes 3(1):1-17. doi: 10.1007/s40710-016-0127-5

Arnold JG, Srinivasan R, Muttiah RS, Williams JR (1998) Large area hydrologic modeling and assessment - part I: Model development. Journal of the American Water Resources Association 34(1):73-89

Neitsch SL, Arnold JG, Kiniry J, Srinivasan R, Williams JR (2002) Soil and Water Assessment Tool – user's manual. Texas Water Resources Institute, College Station, TWRI Report TR-192

Vaghefi SA, Abbaspour N, Kamali B, Abbaspour KC (2017) A toolkit for climate change analysis and pattern recognition for extreme weather conditions – Case study: California-Baja California Peninsula. Environmental Modelling and Software 96:181-198

Intergovernmental Panel on Climate Change (2014) Climate Change 2014: Synthesis Report. Contribution of Working Groups I, II and III to the Fifth Assessment Report of the Intergovernmental Panel on Climate Change [Core Writing Team, Pachauri R.K. and Meyer L.A. (eds.)], IPCC, Geneva, Switzerland, 151 p

Boskidis I, Gikas GD, Pisinaras V, Tsihrintzis VA (2010) Spatial and temporal changes of water quality, and SWAT modeling of Vosvozis river basin, North Greece. Journal of Environment Science and Health Part A 45(11):1421-1440. doi: 10.1080/10934529.2010.500936

11th World Congress on Water Resources and Environment (EWRA 2019)
"Managing Water Resources for a Sustainable Future", 25-29 June 2019, Madrid, Spain

A Drought Alert system based on seasonal forecasts

E. Arnone[1*], Marco Cucchi[1], Sara Dal Gesso[1], Marcello Petitta[1,2,3]
[1] Amigo s.r.l., Rome, Italy
[2] ENEA, SSPT-MET-CLIM, Rome, Italy
[3] EURAC, Institute for applied remote sensing, Bolzano, Italy
* e-mail: elisa.arnone@amigoclimate.com

Introduction

Water resources are under stress in many areas of the world, because of a combination of climatic and anthropogenic factors. The Mediterranean area is one of the regions mostly vulnerable to climate alterations (Forestieri et al. 2018). These alterations have direct impacts on the surface water balance and groundwater recharge (Arnone et al. 2018), and thus changes in the reservoir inputs and the management of water utilities (WUs) are severe challenges for water resources in the future. However, WUs management routines scarcely consider climate information and are based on the stationarity assumption, working on weekly or daily time scale.

The use of seasonal forecasts for guiding a strategic planning of the resources has been increasing across several climate-sensitive sectors, including water management and energy (e.g. De Felice et al. 2015, Viel et al. 2016). This is due to the fact that it is generally preferred to focus on the upcoming season rather than taking decisions on the basis of a 100-year climate projection. The project EUPORIAS promoted the use of climate information for decision support by involving both providers and potential users of seasonal data (Buontempo et al. 2017). It was demonstrated that seasonal forecasts may give important contributions in the fields of drought-risk assessment and mid-term reservoir management (Viel et al. 2016; Crochemore et al. 2017).

This study aims at providing some insights in using seasonal forecasts to derive supporting information for water management decision-makers based on drought assessment. Indeed, the exploitation of climate information as precipitation in a mid-term scale, as the seasonal scale, allows for understanding the possible shifts in water resource availability. We describe some results obtained for a case study in Greece.

Materials and methods

We used the System 5 (SEAS5) Seasonal Forecasts (SF) data released by ECMWF (European Centre for Medium-Range Weather Forecasts), and made available by the data access system Copernicus Climate Change Service (C3S). The SF the ensemble contains 51 members. To estimate the reliability of SEAS5, hindcasts are available from 1981 to 2016, and have 25 ensemble members. For the sake of data understanding, Figure 1 shows a graphical representation of forecast time series for a selected grid point.

The methodology developed in this study exploits the predictions on precipitation for the next few months to evaluate the climate state of the upcoming months compared to the climatology. The proposed procedure aims at targeting the following questions: (i) Are the upcoming months going to be dry? (ii) How confident are we that the upcoming months are going to be either dry or not dry?

At a given month, the climate state which characterizes the upcoming months is evaluated based on the prediction of cumulative precipitation computed over a cumulating period (CP) of given length, i.e. the number of months over which precipitation is cumulated. CP may vary from 1 to 6. Once CP is selected, precipitation is cumulated over a rolling window of CP length that determines the PERIOD of forecast (e.g., CP3 leads to a three-months rolling window of periods JJA, JAS, …).

Predictions for each period are compared with the climatology characterizing the same period, assessed over the hindcast data. The terciles of the distribution identify three classes: 1st 'dry', 2nd 'normal' and 3rd 'wet'. The comparison between predictions and climatology will reveal whether the forecasts will belong to the dry class or not, based on a discriminate threshold frequency.

The procedure evaluates a different monthly responses based on the lead time (LT), which is the

temporal distance, in months, between the release of the seasonal forecast and the first month of the CP. LT may vary from 0 to 5. Technically, the procedure applies for all the possible combinations between CP and LT. In this study, based on the specific needs of a water utility, we analyzed the combinations LT0-CP3, LT0-CP5, LT3-CP3, which are representative of a short-term prediction (for the next 3 months), a long-term prediction (for the next 5 months) and of outlook evaluation (for 3 months from next 2 months).

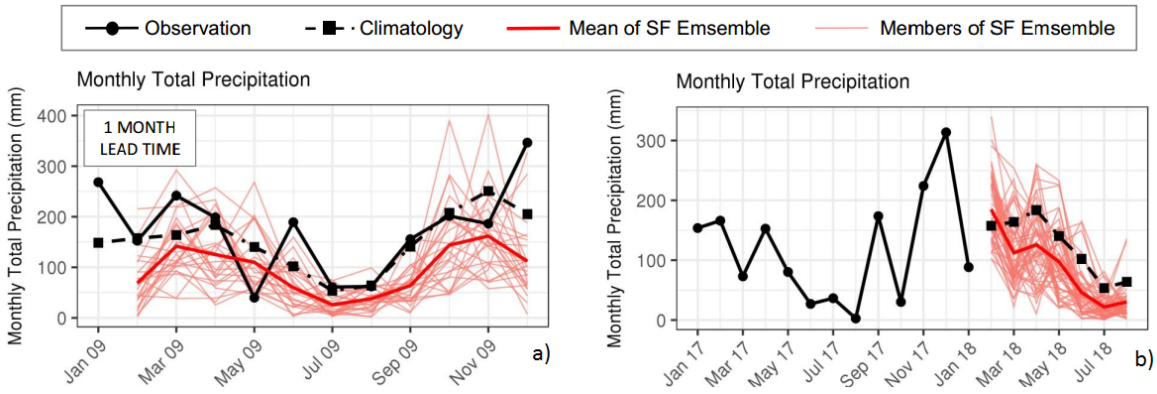

Figure 1. (a) Forecast time series for a selected grid point: comparison with hindcasts for 2009 of monthly total precipitation; (b) observed time series (2017) and future SF time series (2018) of monthly total precipitation.

Results and concluding remarks

Table 1 shows the results of the release obtained in November 2018 for the island of Zakynthos, Greece. None of the cases in a 'dry' climate state, based on the statistical comparison between the cumulated rainfall derived from seasonal forecasts and climatic reference. The state of Drought Alert is triggered when predictions fall within the 'dry' class. Conversely, a state of no-alert will be released, i.e. neither normal or wet conditions are contemplated by the procedure. Given the significant uncertainty that can be associated with the prediction, a reliability of the alert/no-alert information will be assessed through the evaluation of the false rate (0-100%) of the current prediction, which derives from the combination of the skill of the prediction system and the grade of predictability of the state of the upcoming months.

Table 1. Drought Alert: climate state of the upcoming months based on the SF of precipitation.

Current month: November 2018				
Lead Time/Timing		**0/short-term**	**0/long-term**	**3/outlook**
Period		***Nov-Dec-Jan***	***Nov-Dec-Jan-Feb-Mar***	***Feb-Mar-Apr***
Class	Dry			
	Not dry	X	X	X

References

Arnone E, Pumo D, Francipane A, La Loggia G, Noto LV (2018) The role of urban growth, climate change and their interplay in altering runoff extremes. Hydrological Processes 32(12):1755-1770

Buontempo C et al. (2017) What have we learnt from EUPORIAS climate service prototypes? Climate Services 9:21-23. http://dx.doi.org/10.1016/j.cliser.2017.06.003

Crochemore L, Ramos MH, Pappenberger F, Perrin C (2017) Seasonal streamflow forecasting by conditioning climatology with precipitation indices. HESS 21:1573–1591

De Felice M, Alessandri A, Catalano F (2015) Seasonal climate forecasts for medium-term electricity demand forecasting. Appl. Energ. 137:435–444

Forestieri A, Arnone E, Blenkinsop S, Candela A, Fowler HJ, Noto LV (2018) The impact of climate change on extreme precipitation in Sicily, Italy. Hydrological Processes 32(3):332-348. http://doi.org/10.1002/hyp.11421

Viel C, Beaulant A-L, Soubeyroux J-M, Céron J-P (2016) How seasonal forecast could help a decision maker: an example of climate service for water resource management. Adv. Sci. Res. 13:51–55

11th World Congress on Water Resources and Environment (EWRA 2019)
"Managing Water Resources for a Sustainable Future", 25-29 June 2019, Madrid, Spain

Coupling CFSv2 with ArcSWAT for seasonal hydrological forecasting in a Mediterranean basin

K. Kaffas[1*], M. Righetti[1], D. Avesani[1], M. Spiliotis[2], V. Hrissanthou[2]
[1] Faculty of Science and Technology, Free university of Bozen-Bolzano, Bolzano, Italy
[2] Civil Engineering Department, Democritus University of Thrace, Xanthi, Greece
* e-mail: konstantinos.kaffas@unibz.it

Introduction

In the context of a rapidly changing world climate, where matters such as water availability and scarcity, energy demand, and adequacy of crop production grow into first-line priorities for private and government entities, the need for knowledge -in advance- and future planning with regard to water budget availability and distribution becomes more and more essential. Seasonal hydrological forecasting constitutes the key solution that informs actions regarding drinking water needs, irrigation planning, as well as management optimization of hydroelectric power schemes. The efficiency of hydrological forecasting vastly relies on the accuracy of meteorological forecasting (Sehgal et al. 2018; Ye et al. 2017). In fact, it could be stated that in relative studies the efficacy of the hydrological forecasting is determined more on the basis of the accuracy of the meteorological forecasting rather than the competence of the hydrological model -used- itself.

In this study, the version 2 of the Climate Forecast System (CFSv2) is combined with the GIS version of the Soil and Water Assessment Tool (ArcSWAT) to provide mid-term hydrological predictions. More specifically, the CFSv2 is employed to forecast precipitation and temperature, two decisive meteorological parameters for hydrologic simulations. The forecasted variables are bias-corrected prior to their forcing to SWAT. The chain of the aforementioned processes is tested for a two-month period in Nestos River basin in northeastern Greece. It is a relatively large mountainous basin covering an area of approximately 840 km^2. A detailed description of Nestos River basin can be found in Kaffas et al. (2018). The results were validated with sparse discrete discharge measurements, at the outlet of the basin, and were deemed satisfactory.

Materials and methods

The CFSv2 (Saha et al. 2014) is the second generation of NOAA's National Centers for Environmental Prediction (NCEP) coupled ocean-atmosphere-land model with advanced model components, compared to its prior version CFS (retroactively referred to as CFSv1), to improve the skill of seasonal climate forecasting. The CFSv2 runs at a 0.937° spatial resolution and provides, for both the past and future, a four-member ensemble at a six-hourly time step and nine months ahead. CFSv2 is used for obtaining the necessary meteorological data, namely the retrospective forecasts (reforecasts) (period of record: 1982-2011), as well as the operational forecasts (period of record: 2011-present) for surface air temperature and precipitation rates. The retrospective forecasts and the operational forecasts are provided for four different initial conditions, namely 0000, 0600, 1200, 1800 UTC cycles, and every five days, and every day, accordingly.

Despite the increasing use of climate models and forecasting system simulations in hydrological climate-change impact studies, their application is challenging due to the risk of sizable biases (Teutschbein and Seibert 2012). To address this issue, several bias correction methods have been developed in the past years. The linear scaling method (Lenderink et al. 2007) is used for the correction of the mean monthly values of both retrospective and operational forecasts. The bias correction results in perfect agreement between the mean monthly values of the corrected CFSv2 simulations and the observations. The retrospective forecasts were corrected against observations from four meteorological stations, in the study area. The resulting calibrated parameters were employed for the correction of the forecasted data. At this point, it has to be mentioned that the bias correction of the meteorological data was carried out at a daily time step by aggregating or averaging six-hourly precipitation and temperature, accordingly. The outcome of this procedure is four different forecasts -one for each ensemble member- as well as an additional

forecast which was computed as the average of the four, for a two-month period (April-May, 2011). These five different forecasts are incorporated separately in a time series of observed precipitation and temperature covering a period from January 2003 to December 2011, constructing, thus, five time series of observed precipitation and temperature, each containing a two-month ensemble member forecast which are consequently inserted to SWAT to provide a five-member ensemble hydrological forecast.

SWAT (Neitsch et al. 2011) was calibrated as to various hydrological parameters (CN, available water capacity, baseflow recession constant, etc.) against observed discharges at different locations upstream of the outlet of the basin. The calibration was carried out so that the calibrated parameters maintain their physical meaning. The model was run at a daily time step for the period 2003-2011, with a two-year warm-up. The basin was divided into 25 sub-basins and calculations were carried out at an HRU level (991 HRUs).

Results and concluding remarks

In Figure 1, the mean monthly values of precipitation are shown for one of the meteorological stations, while in Figure 2 the five-member ensemble hydrological forecast is displayed as it results from SWAT.

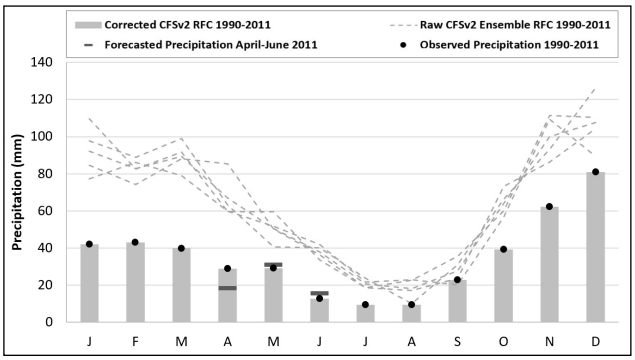

Figure 1. Mean monthly precipitation

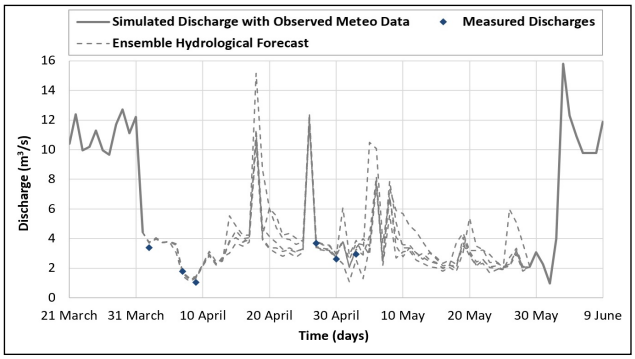

Figure 2. Ensemble hydrological forecast April-May 2011

From Figure 1, it is obvious that CFSv2 overestimates the intensity of precipitation. It is worth noting, however, that the raw ensemble reforecasted precipitation displays a quite similar pattern as the one of the observations. The integrated methodology, described above, is tested in the present study for a two-month period and is validated with only six discrete discharges which, as seen from the graph, were measured under low flow conditions. However, a Nash-Sutcliffe Efficiency (NSE) of 0.92, between measured and simulated discharges, indicates that the CFSv2 can be coupled with SWAT to successfully forecast the hydroclimatic processes in a Mediterranean basin.

References

Kaffas K, Hrissanthou V, Sevastas S (2018) Modeling hydromorphological processes in a mountainous basin using a composite mathematical model and ArcSWAT. Catena 162:108-129. https://doi.org/10.1016/j.catena.2017.11.017

Lenderink G, Buishand A, Van Deursen W (2007) Estimates of future discharges of the river Rhine using two scenario methodologies: direct versus delta approach. Hydrology and Earth System Sciences 11(3):1145-1159. https://doi.org/10.5194/hess-11-1145-2007

Neitsch SL, Arnold JG, Kiniry JR, Williams JR (2011) Soil and Water Assessment Tool Theoretical Documentation Version 2009. Texas Water Resources Institute, Texas A&M University, College Station, TX, USA.

Saha S, Moorthi S, Wu X, Wang J, Nadiga S, Tripp P, Behringer D, Hou YT, Chuang HY, Iredell M, Ek M (2014) The NCEP climate forecast system version 2. Journal of Climate 27(6):2185-2208. https://doi.org/10.1175/JCLI-D-12-00823.1

Sehgal V, Sridhar V, Juran L, Ogejo J (2018) Integrating Climate Forecasts with the Soil and Water Assessment Tool (SWAT) for High-Resolution Hydrologic Simulations and Forecasts in the Southeastern US. Sustainability 10(9):3079. https://doi.org/10.3390/su10093079

Teutschbein C, Seibert J (2012) Bias correction of regional climate model simulations for hydrological climate-change impact studies: Review and evaluation of different methods. Journal of Hydrology 456:12-29. http://dx.doi.org/10.1016/j.jhydrol.2012.05.052

Ye A, Deng X, Ma F, Duan Q, Zhou Z, Du C (2017) Integrating weather and climate predictions for seamless hydrologic ensemble forecasting: A case study in the Yalong River basin. Journal of Hydrology 547:196-207. https://doi.org/10.1016/j.jhydrol.2017.01.053

11th World Congress on Water Resources and Environment (EWRA 2019)
"Managing Water Resources for a Sustainable Future", 25-29 June 2019, Madrid, Spain

Preliminary long term changes in inter-annual precipitation variability in a Mediterranean region

A. Longobardi*, O. Boulariah
Department of Civil Engineering, University of Salerno, Fisciano, Italy
** e-mail: alongobardi@unisa.it*

Introduction

Precipitation trend analysis, on different spatial and temporal scales, has been of great concern during the past century because of the attention paid from the scientific community to global climate change. The IPCC reports confirm the increase of the surface temperature in the twentieth century and show a further increase for the twenty-first century. Studies involving Italian long record databases show a strong reduction in rainfall, rather significantly over the last 50 years (Brunetti et al. 2006). More detailed analyses indicate negative trends at regional level in the Italian Mediterranean regions (Piccarreta et al. 2004; Longobardi and Villani 2010; Caloiero et al. 2011a). To date a moderate interest has been given by the scientific community to the inter-annual precipitation variability issue which seems however to lead to an overall increase (Giorgi and Lionello 2008; He and Gautam 2016).

Materials and methods

Available data consist of annual and monthly precipitation time series for over 200 sites located across the Campania region and the Lazio region, Southern Italy, covering an area of about 25000 Kmq (Figure 1, left panel). For the period 1918-1999 the source of data is the Servizio Idrografico e Mareografico Nazionale SIMN. After this, regional Civil Protection Agencies were charged for raingauge network management since 2003. A change in the consistency, spatial location and typology of raingauge station occurred then which undermine the long term time series homogeneity. Homogeneity analyses aimed at comparing the two temporal dataset (1918-199 and 2013-current date) are still ongoing. For this reason, only the database referring to the longest period, 1918-1999, have been considered for this study. After a data quality control only 164 of total station were effectively tested for changes in precipitation variance on a long term scale. For the purpose 30 years moving average annual precipitation coefficient of variation time series where computed and tested for a significant tendency by using a modified Mann-Kendall trend test for autocorrelated data.

Results and concluding remarks

The same database was analysed in previous papers with regard to the changes in the precipitation mean values and seasonal distribution (Longobardi and Villani 2010; Longobardi et al. 2016). Changes in the mean values were overall moderate and oriented toward a negative tendency, with rates ranging between 1-10 mm/year. Also the seasonal precipitation distribution during the year was detected to change, overall oriented toward a more uniform distribution, untypically for this particular region. The statistical significance of changes was however very moderate.

The current study highlights additional interesting results about changes in the climatology of the region. The annual precipitation is indeed characterized by an important variability which changes over time. Typical patterns for the coefficient of variation are represented in Figure 1 (right panel). In some cases the cv appears featured by a continuous decreasing or increasing trend in time, which for some rain gauge stations approaches high slope values. In some other cases an increase in the variability, which overall occurs around the seventies, is preceded by either a stationary period or a period characterized by a reduction in the variability. The modified Mann-Kendall test revealed that for about the 79% of the total database the trend was significant and oriented, on the long term scale, on an increased variability.

Although the knowledge of the quantitative values of rainfall and its relevant changes is necessary and

unavoidable for a correct and sustainable water resources management, the same cannot ignore the inclusion of the study of the characteristics of inter-annual variability, in particular if we observe that the related changes, at least in the region under study, appear statistically more significant than changes in the average values.

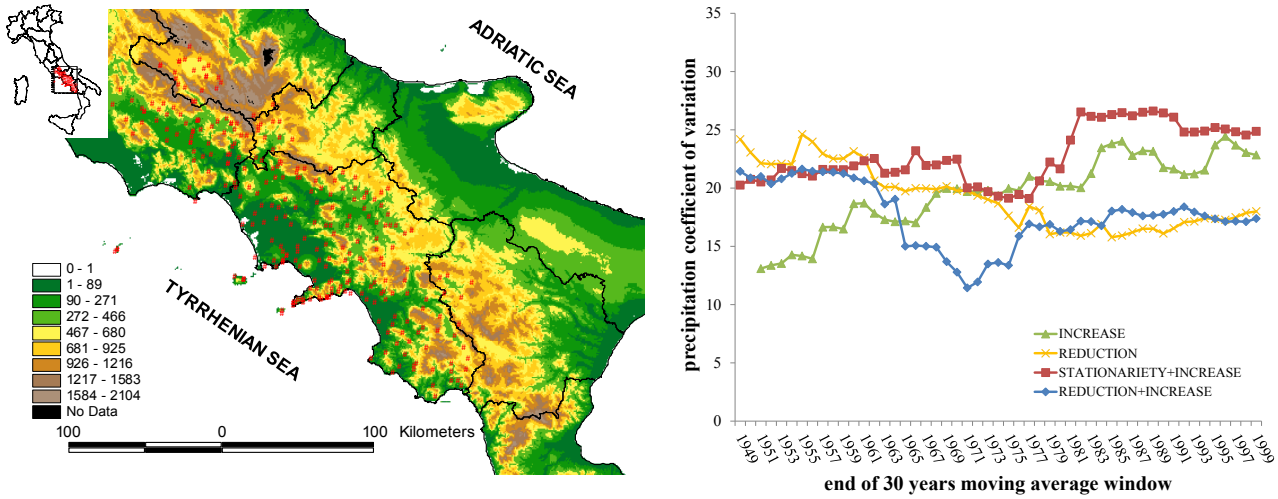

Figure 1. Study region (left panel) and precipitation cv patterns type (right panel).

References

Brunetti M, Maugeri M, Monti F, Nanni T (2006) Temperature and precipitation variability in Italy in the last two centuries from homogenised instrumental time series. International Journal of Climatology 26:345–381. doi: 10.1002/joc.1251

Caloiero T, Coscarelli R, Ferrari E, Mancini M (2011) Trend detection of annual and seasonal rainfall in Calabria (Southern Italy). International Journal of Climatology 31:44–56. doi: 10.1002/joc.2055

Giorgi F, Lionello P (2008) Climate change projections for the Mediterranean region. Global and Planetary Change 63(2-3):90-104. doi: 10.1016/j.gloplacha.2007.09.005

He M, Gautam M (2016) Variability and trends in precipitation, temperature and drought indices in the state of California. Hydrology 3(2):14. doi: 10.3390/hydrology3020014

Longobardi A, Villani P (2010) Trend analysis of annual and seasonal rainfall time series in a Mediterranean area. International Journal of Climatology 30(10):1538-1546. doi: 10.1002/joc.2001

Longobardi A, Buttafuoco G, Caloiero T, Coscarelli R (2016) Spatial and temporal distribution of precipitation in a Mediterranean area (southern Italy). Environmental Earth Sciences 75(3):189. doi: 10.1007/s12665-015-5045-8

Piccarreta M, Capolongo D, Boenzi F (2004) Trend analysis of precipitation and drought in Basilicata from 1923 to 2000 within a Southern Italy context. International Journal of Climatology 24:907–922. doi: 10.1002/joc.1038

11th World Congress on Water Resources and Environment (EWRA 2019)
"Managing Water Resources for a Sustainable Future", 25-29 June 2019, Madrid, Spain

Non stationary duration-frequency modelling of hydro-climatic extremes

T.B.M.J. Ouarda[1*], L. Youssef[2], C. Charron[1]
[1] National Institute for Scienfidic Resarch, INRS-ETE, 490 de la Couronne, Quebec, Qc, G1K9A9
[2] National Center of Meteorology, P.O. Box 4815, Abu Dhabi, UAE
* e-mail: taha.ouarda@ete.inrs.ca

Introduction

Rainfall Intensity-Duration-Frequency (IDF) curves are frequently used for the design and management of water resources infrastructure. IDF information is generally represented on plots of the intensity as a function of the duration, and for a family of curves representing a number of return periods. The use of IDF curves started gaining popularity worldwide since the 1930's (Bernard 1932; Hershfield 1961). It is now commonly accepted that climate change is affecting rainfall and hydrologic variable characteristics (Ouarda and El Adlouni 2011; Ouarda et al. 2014). Recently a few nonstationary IDF models have been proposed in the literature (Youssef and Ouarda 2015). In this work we propose a general methodology to integrate climate variability and change in IDF curves, by conditioning the parameters of the curves on the covariates of time and climate indices.

Extended periods of extreme temperature can have damaging impacts on the ecosystems, agriculture, infrastructure, water resources availability, and public health. Mean temperatures have been increasing worldwide leading to a significant increase in the frequency, magnitude and duration of severe heat waves with considerable consequences. It is also important to understand the impacts of global-scale modes of climate variability on temperature extremes. In the present work we propose nonstationary Temperature-Duration-Frequency (TDF) curves relating temperature intensities corresponding to different durations to a number of return periods. The proposed curves account for climate external forcings through the introduction of covariates that account for temporal trend and teleconnections. These TDF curves can find applications in such fields as agriculture, public health, global security, water resources management, and energy generation. For instance, nonstationary TDF curves would allow integrating information concerning the evolution of temperature extremes in the design and operation (cooling management) of nuclear power plants.

Materials and methods

The proposed approach is based on maximizing the composite likelihood of temperature extremes. This approach allows taking into consideration the fact that different points of the series correspond to different values of the covariates and hence it is not possible to use the maximum likelihood method to fit the data and estimate the values of the model parameters. The composite likelihood Akaike Information Criterion (CL-AIC) is used as performance criterion to compare the performance of stationary and non stationary models. Note that the CL-AIC is a criterion that penalizes models with a higher number of parameters. An application to rainfall and temperature data from North America is used to demonstrate the proposed approach and illustrate the importance of integrating information concerning climate change and variability in the modelling of future extreme rainfalls and heat waves. An additional complexity associated to non-stationary IDF and TDF modelling is related to the high dimensionality of the models, given that they depend on a number of covariates and that response surfaces need to be developed for different values of the covariates. It is hence not possible to present all results associated to all curves in a single plot. Different families of response surfaces need to be presented for different return periods, or durations if more than one covariate are used. An example illustrating the new nature of curves is presented (Figure 1).

Results and concluding remarks

The results of the fitting of stationary and non-stationary models to rainfall and temperature data show

that non stationary models provide a better fit than stationary ones. For instance for the Beausoleil station, a CL-AIC value of 1.53 is obtained for the stationary model while a value of 1.42 is obtained for the non stationary model using time and the AMO index as covariates. This indicates that, even if we take parsimony into consideration, non-stationary models can represent a viable alternative to stationary models.

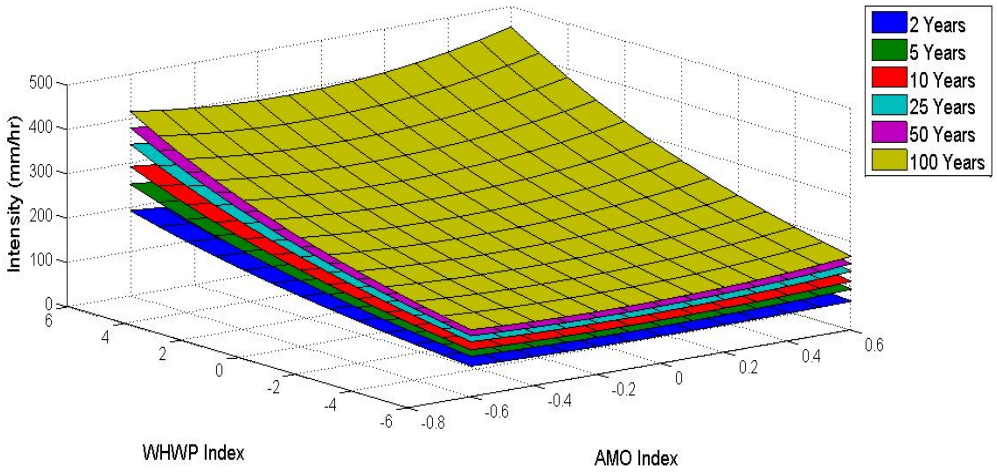

Figure 1. Non-stationary IDF curves with AMO and WHWP as the covariates for Beausoleil station with a fixed duration of 5 minutes.

However, extreme care needs to be taken to select models whose complexity is adapted to the amount of data that is available. Ideally both stationary and non-stationary models need to be used and their results combined through parametric Bayesian combination models (Seidou et al. 2006) and used in decision making. This helps leads to more robust estimates that integrate information concerning climate change and variability but also consider commonly accepted models. Future work needs to focus on the uncertainty associated to non-stationary IDF and TDF models. Future efforts should also focus on the development of duration-frequency models that are based on the Generalized Pareto Distribution (Ashkar and Ouarda 1996) in the Peaks-Over-Threshold (POT) approach.

References

Ashkar F, Ouarda TBMJ (1996) On some methods of fitting the generalized Pareto distribution. Journal of Hydrology 177:117-141

Bernard MM (1932) Formulas for rainfall intensities of long duration. Transactions of the American Society of Civil Engineers 96:592-606

Hershfield DM (1961) Rainfall frequency atlas of the United States: For durations from 30 minutes to 24 hours and return periods from 1 to 100 years. Department of Commerce. Weather Bureau, Washington, DC

Ouarda TBMJ, Charron C, Niranjan Kumar K, Marpu PR, Ghedira H, Molini A, Khayal I (2014) Evolution of the rainfall regime in the United Arab Emirates. Journal of Hydrology 514:258-270

Ouarda TBMJ, El-Adlouni S (2011) Bayesian Nonstationary Frequency Analysis of Hydrological Variables. JAWRA Journal of the American Water Resources Association 47(3):496-505. doi: 10.1111/j.1752-1688.2011.00544.x

Seidou O, Ouarda TBMJ, Barbet M, Bruneau P, Bobée B (2006) A parametric Bayesian combination of local and regional information in flood frequency analysis. Water Resources Research 42:W11408

Yousef LA, Taha B (2015) Adaptation of Water Resources Management to Changing Climate: The Role of Intensity-Duration-Frequency Curves. International Journal of Environmental Science and Development 6(6):478

11th World Congress on Water Resources and Environment (EWRA 2019)
"Managing Water Resources for a Sustainable Future", 25-29 June 2019, Madrid, Spain

Blue house: Attitudes toward sustainable water use

D. Kaposztasovar*, Z. Vranayova
Departmentof Building Services, Faculty of Civil Engineering, Technical University of Kosice, Kosice, Slovakia
** e-mail: daniela.kaposzatasova@tuke.sk*

Introduction

The topic of water covers a lot of interesting issues that can reveal the health of the environment and to preserve the water for future generations. We need to change the thinking of society to be in balance with nature. Small steps such as changing a family house to a "blue" family house can lead to greater changes in our lifestyle and our attitude towards water use. In Kaposztasova et al. (2019) we presented a wide range of options in the world of water conservation, collection and use. Common households consume a lot of water. There is a need to manage its end use as sustainable as conditions allow us (Silva-Afonso et al. 2011; Słyś et al. 2012). In the EU it is common to use well and rainwater source for the purposes of irrigation, toilet flushing, etc. Grey water reuse within Slovakia is still rare.

Materials and methods

The designers should complete the building and the site as one system – where water is conserved, energy saved and therefore reduced costs. New technologies and a better understanding of the in building water cycle allow us to reduce our water footprint. The public expects to have safe water and sanitation; therefore, when recycling water, it is essential to protect public health and the environment. The main aim of this work is to introduce water management strategies at the building level. Following the hypothesis that a small change in thinking of the society – by changing a house to a blue house could lead to a blue world.

Supported by mathematical methods, the comprehensive evaluation on water use was established to find the pattern of water consumers in Slovakia. The classic pattern consists of potable use for all purposes and when it is possible to have a well, the water is used for irrigation. It is essential to inform the public about the possibilities of saving water, but not limited to the building of a new house.

Figure 1. Water management options and evaluation scheme

Figure 1 describes the water management options that are considered at the building level. The intent of the integrated water management is to consider water management options that were identified by an expert group that might be useful in enhancing the water sustainability and reliability. Most of the water management options would reduce the demand on the potable water system. These reduced demands could result in cost savings for the potable water system in terms of smaller infrastructure needs and lower operating costs.

The ability of supply to meet demand will always need to be evaluated on a case-by-case basis. A balance evaluates how water is used in a building and can help identify opportunities for saving water. To

put it simply, four main water types were used in this evaluation. The evaluation was made by a sophisticated decision analysis based upon on the Saaty methodology - Analytical hierarchy process (AHP). They include various technical and management abilities, quality factors, end use purpose, local conditions and the water end use. The suitability and availability of the water dictates the behaviour of the system. Water management portfolios were prepared in two alternatives (Figure 2). According to the study eight portfolios were prepared for the house owner when connected to the main water supply and four without the connection. The evaluation of the two main criteria's as Economic and Environmental could be used as the tool to change the water habits or to help investors to make the right decision regarding water management portfolios (Figure 1).

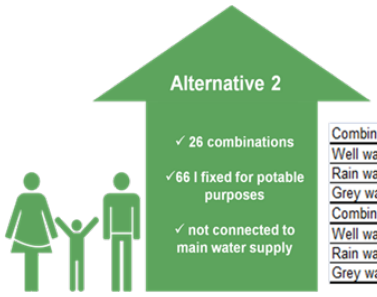

Combination	1	2	3	4	5	6	7	8	9	10	11	12	13
Well water	66	66	66	88	88	88	102	102	145	66	88	131	131
Rain water	22	36	79	0	14	57	0	43	0	65	43	0	14
Grey water	57	43	0	57	43	0	43	0	0	14	14	14	0
Combination	14	15	16	17	18	19	20	21	22	23	24	25	26
Well water	66	80	80	80	66	80	123	123	66	109	109	109	109
Rain water	14	0	22	65	57	43	0	22	43	0	22	36	14
Grey water	65	65	43	0	22	22	22	0	36	36	14	0	22

Figure 2. Water management portfolios – example of Alternative 2

Results and concluding remarks

The results were also supported by the questionnaire and can be used as a tool for water audits. Proposed eleven portfolios offer a plan of how to deal with the scarcity of water. It can guide the investor to see all possibilities of water management strategies directly aimed at his case. Each case should be evaluated independently set within the boundary conditions. The economic and environmental evaluation approach was presented to support investor's decisions and interests. The main aim was to give as much information as possible to the investor to change his thinking to that of a sustainable solution, even when they are not as cost effective.

The change from a classic family house to a BLUE house by implementing the portfolio led to a reduction of water bills. The reduced water costs for 2018 will be around 180 €.

Acknowledgments: Thanks to VEGA 1/0217/19 Research of Hybrid Blue and Green Infrastructure as Active Elements of a 'Sponge City' and VEGA 1/0697/17 Hygienic water audit platform as a transition tool to Legionella free water and HVAC systems in hospitals.

References

Káposztásová D, Vranayová Z (2018) Decision Analysis Tool for Appropriate Water Source in Buildings. In: Negm A., Zeleňáková M. (eds) Water Resources in Slovakia: Part II. The Handbook of Environmental Chemistry, vol 70, Springer, Cham

Kinkade-Levario H (2007) Design for Water. Gabriola Island: New Society Publisher, 240 p

Silva -Afonso S et al. (2011) Grey water in buildings. The Portuguese approach. In: Proceedings of 37th International Symposium CIB W062 on Water Supply and Drainage for Buildings. Aveiro

Słyś D, Stec A, Zeleňáková M (2012) A LCC analysis of rainwater management variants. Ecological Chemistry and Engineering 19(3):359-372

Water cycle safety plan framework (2010) Proposal

Yager RR, Kelman A (1999) An extension of the analytical hierarchy process using OWA operators. Journal of Intelligent and Fuzzy Systems 7(4):401–417

11th World Congress on Water Resources and Environment (EWRA 2019)
"Managing Water Resources for a Sustainable Future", 25-29 June 2019, Madrid, Spain

Assessment of climate change impacts on water supply systems: application to the Pozzillo reservoir, Sicily

D.J. Peres*, A. Cancelliere
Department of Civil Engineering and Architecture, University of Catania, Catania, Italy
** e-mail: djperes@dica.unict.it*

Introduction

Management of water resources has a strategic socio-economic role in facing the new challenges posed by climate change (Olmstead 2014; Garrote 2017).

Climate change impacts on water supply systems can be assessed by modelling approaches, which combine the climate projections and supply system simulation models (Garrote et al. 2015). In particular, several regional climate model (RCM) simulations are available from different research bodies in the world, which use dynamic downscaling techniques to increase the resolution of Global circulation models (GCMs). These simulations allow to assess, at a spatial resolution of few kilometres, the change in climate associated to several greenhouse gasses emission scenarios, better known as Representative Concentration Pathways (RCPs), which are related to socio-economic and political choices at the planetary scale.

In this work we use such a combined modelling approach to assess the future impacts of climate change for the Pozzillo reservoir, which represents the main reservoir of the most important water supply system in Sicily, a region that suffers water scarcity and drought problems. In particular, the work aims at assessing: a) the potential future changes in precipitation, temperature, and streamflow, and b) the impacts of such changes on future water supply reliability.

Materials and methods

RCM simulations provide data for an historical period (hindcast mode) and for future periods according to four possible RCP scenarios. In comparing the climate characteristics of historical simulations with observed, significant differences emerge, and, based on this comparison and on related indices of agreement, concurring RCMs can be ranked (Mascaro et al. 2018). In a previous study by the authors (Peres et al. 2017) 14 RCM of the Euro-CORDEX initiative were ranked based on such concepts. In this work, we use the RCM that showed the best performance, the dataset originated from downscaling the CNRM-CM5 (GCM) with the SMHI-RCA4 (RCM), which was developed by the Swedish Meteorological and Hydrological Institute. Though this model provides high quality data, correction techniques have been applied following a two-step procedure better described later in this section. The most common scenarios are analysed here: the RCP 4.5 (intermediate emissions) and the RCP 8.5 (high emissions). We assess the impacts of climate change for three future temporal horizons: 2011-2040, 2041-2070 and 2071-2100. The analysis is conducted using monthly data, referring to the Pozzillo reservoir. The reservoir has a capacity of 120 × 106 m^3 and the level of demand in the baseline historical period (1971-2000) is 88 × 106 m^3.

The proposed methodology in articulated in the following steps:

1. Estimation of mean areal temperature and precipitation (observed and RCM)
2. Calibration and validation of a regression-based streamflow model, using observed data
3. Correction of RCM monthly temperature and rainfall data (first step correction), using correction factors based on the comparison of observed and in the baseline period 1971-2000
4. Use of the adjusted temperature and precipitation data as input for the calibrated streamflow model developed at step 2
5. Adjustment of streamflow modelled data (second step correction), based on comparison of mean monthly observed and RCM hindcast data
6. Simulation of the reservoir by a water balance equation, using the generated streamflow data. A Standard operating policy (SOP) is assumed, in order to isolate the effects of climate change from

operational aspects. The three future periods and the historical one are simulated

7. Derivation of demand-performance curves for the three future periods and comparison to the historical curves. The following performances indices have been computed: temporal and volumetric reliability, sum of squared deficits, and Beard index.

Results and concluding remarks

Analysis of climate projection highlights a prevalent increase of monthly temperature and precipitation, which in turn induce a decrease of streamflow. This is reflected in the results relative to the water supply performance curves, shown in Figure 1.

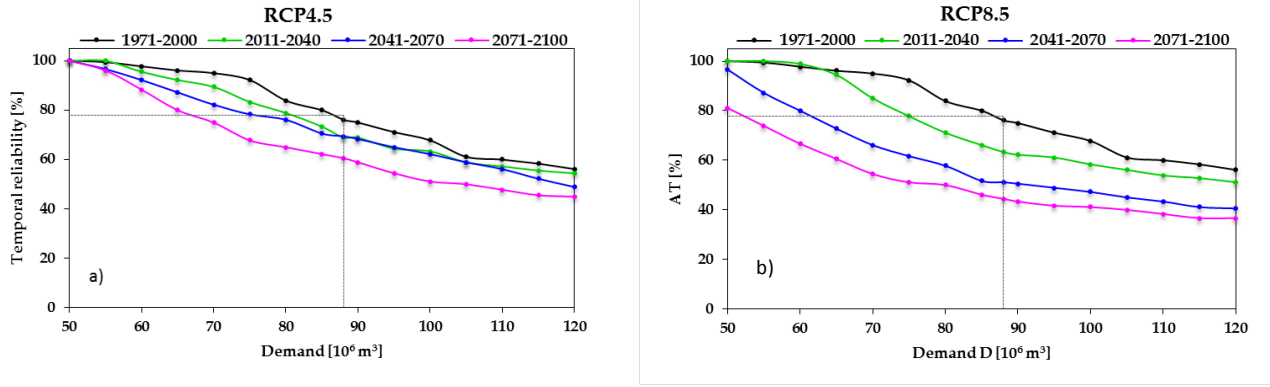

Figure 1. Curves showing temporal reliability as a function of demand, for the baseline historical period (1971-2000), and three future periods. Impacts of two emission scenarios are shown a) RCP 4.5, and b) RCP 8.5.

As can be seen reliability generally decreases progressively moving towards the end of the current century. Significant differences are present between the reliability curves in the historical baseline and the in the future periods. Impacts in the RCP 8.5 scenario are higher than those in RCP 4.5. The figure shows a dotted line indicating the current level of demand (irrigation purposes only) equal to 88 × 10^6 m^3, from which one could derive the corresponding future expected reliability. In particular, the current reliability of 76.11 % reduces to 68.89 % (2011-2040), 69.44 % (2041-2070), and 60.56 (2071-2100) in the RCP 4.5, and to 63.33 % (2011-2040), 51.11 (2041-2070) and 44.44 % (2070-2100). These changes are likely to produce sensible impacts on the supply system in question, inviting to take adaptation actions, for instance by programs oriented to increase irrigation efficiency.

The results of this study are a first step towards for an extended application to the whole water supply system including several reservoirs and water uses.

References

Garrote L, Iglesias A, Granados A, Mediero L, Martin-Carrasco F (2015) Quantitative assessment of climate change vulnerability of irrigation demands in Mediterranean Europe. Water Resources Management 29(2):325-338

Garrote L (2017) Managing water resources to adapt to climate change: facing uncertainty and scarcity in a changing context. Water Resources Management 31(10):2951-2963. https://doi.org/10.1007/s11269-017-1714-6

Mascaro G, Viola F, Deidda R (2018) Evaluation of Precipitation From EURO-CORDEX Regional Climate Simulations in a Small-Scale Mediterranean Site. Journal of Geophysical Research: Atmospheres 123(3):1604-1625

Olmstead SM (2014) Climate change adaptation and water resource management: A review of the literature. Energy Economics 46:500-509. https://doi.org/10.1016/j.eneco.2013.09.005.

Peres DJ, Caruso MF, Cancelliere A (2017) Assessment of climate-change impacts on precipitation based on selected RCM projections. European Water 59:9-15. https://www.ewra.net/ew/pdf/EW_2017_59_02.pdf

11th World Congress on Water Resources and Environment (EWRA 2019)
"Managing Water Resources for a Sustainable Future", 25-29 June 2019, Madrid, Spain

Investigations on the impacts of future climate change on the hydrology of a river basin in India using a macroscale hydrological model

P. Raghav, T.I. Eldho*
Department of Civil Engineering, Indian Institute of Technology Bombay, Mumbai, India
** e-mail: eldho@civil.iitb.ac.in*

Introduction

Different regions around the world are experiencing a different rate of warming due to anthropogenic activities and hence it becomes essential to find out the impacts of climate change on the water availability at river basin scale (Watson et al. 1998). In India, very few studies have been conducted for the assessment of impacts of climate change on basin scale hydrology by using a hydrological model that was well-calibrated with observed data in the basin. This study aims to investigate the impact of future climate change on the overall hydrology of upper Godavari river basin (UGRB) in India using a macroscale hydrological model H08 at a relatively fine scale (~10 km) grid size.

The main objectives of this study include (1) Model setting for the UGRB and calibration and validation of the model with the long-term observed streamflow data, and (2) to investigate the impact of future climate change on the basin-scale hydrology considering a high-emission climate scenario; RCP8.5. This study attempts to provide a quantitative assessment of various hydrological fluxes that are useful in water resources planning and management to implement adaptive means to deal with the possible climate change scenarios at the watershed scale.

Materials and methods

A macroscale hydrological model H08 (Hanasaki et al. 2008) is applied over the UGRB by integrating the fine-resolution (~30 m) DEM (digital elevation model) data for the accurate stream networks delineation. Meteorological inputs for the H08 model are albedo, precipitation, air temperature, specific humidity, surface pressure, wind speed, longwave downward radiation, and shortwave downward radiation. For historical simulations, the climate data was taken from the WATCH Forcing Dataset (WFD) (Weedon et al. 2011). For the future simulations, the H08 model was forced with climate data obtained from the Inter-Sectoral Impact Model Intercomparison Fast Track (ISIMIP-FT) project where bias-corrected climate data from five CMIP5 GCMs is available (Hempel et al. 2013). The albedo data was taken from the Second Global Soil Wetness Project (GSWP2).

The land surface module of H08 model that calculates the water and energy budgets above and beneath the land surface and river routing module that routes the runoff from upstream to downstream, have six most sensitive parameters; 1) The root-zone depth (d), 2) the bulk transfer coefficient (C_D) that controls potential evapotranspiration, 3) a time constant (τ) that determines the daily maximum subsurface runoff, 4) a shape parameter (λ) that controls the relationship between subsurface flow and soil moisture, 5) flow velocity and 6) meandering ratio. The model parameters were optimized using the Suffled complex evolution approach by NSE by comparing observed and simulated monthly streamflow. This optimized model was then used to simulate hydrological fluxes (runoff, evapotranspiration, and soil moisture) in three time-windows; the present day (1981-2000), the mid-future (2040-2059) and far-future (2080-2099) using the bias-corrected data from five CMIP5 GCMs; MIROC-ESM-CHEM, HadGEM2-ES, GFDL-ESM2M, IPSL-CM5A-LR, and NorESM1-M. The climate data have been interpolated to 5' × 5' (~10 km grid) from their original climate model resolution (ranging from 0.5° × 0.5° to 3.75° × 2.77°) using nearest four points linear interpolation method.

Results and concluding remarks

Table 1 shows the model performance in the river basin. All the model performance statistical indices are within their satisfactory ranges. Table 2 shows the annual mean and percentage changes of various hydrological and meteorological variables. The results are based on multi-GCMs ensembles to reduce the uncertainty in the projection. Change in temperature was more during the dry period (Oct-May) than the wet period (June-Sep) however reverse trend was observed for other hydro-meteorological variables. The results showed that by the end of the 21st century, a lower increase in ET (12.53%), a large increase in rainfall (33.3 %) and therefore significantly increase in runoff (63%) may result to an increased possibility of floods in low lying areas of the Upper Godavari River Basin.

Table 1. Model performance statistical indices during both calibration and validation periods.

	Time Period	NSE	d_r	PBIAS (%)	RMSE (m^3/s)	R^2
Calibration	1984-1994	0.84	0.87	-5.2	16.7	0.84
Validation	1995-2001	0.75	0.82	-14.1	17	0.79

Table 2. The annual mean and percentage changes in hydro-meteorological variables.

			% change (°C in case of temperature)		
Variable	**Time Period**	**Annual Mean (Monsoon, Non-monsoon)**	**Monsoon (June-Sep)**	**Non-monsoon (Oct-May)**	**Annual**
1. Meteorological Variables					
Rainfall (mm/year)	Historical (1981-2000)	862 (2172, 207)	-	-	-
	Mid-future (2040-2059)	986 (2495, 232)	14.9	12.1	14.4
	Far-future (2080-2099)	1149 (2957, 245)	36.2	18.4	33.3
Temperature (°C)	Historical (1981-2000)	26.31 (27.26, 25.83)	-	-	-
	Mid-future (2040-2059)	28.5 (29, 28.22)	1.74	2.36	2.19
	Far-future (2080-2099)	30.96 (31.15, 30.87)	3.89	5.04	4.65
Net Radiation (W/m^2)	Historical (1981-2000)	75 (86, 70)	-	-	-
	Mid-future (2040-2059)	77 (88, 70)	2.32	1.43	2.7
	Far-future (2080-2099)	81 (93, 75)	8.2	7.14	8.0
2. Hydrological Variables					
Soil Moisture (mm)	Historical (1981-2000)	62 (129, 28)	-	-	-
	Mid-future (2040-2059)	65 (135, 30)	4.65	7.1	4.8
	Far-future (2080-2099)	64 (135, 28)	4.65	0	3.2
Runoff (mm/year)	Historical (1981-2000)	353 (930, 64)	-	-	-
	Mid-future (2040-2059)	456 (1217, 75)	31	17.2	29.2
	Far-future (2080-2099)	575 (1561, 82)	68	28.1	63
Evapotranspiration (mm/year)	Historical (1981-2000)	511 (876, 328)	-	-	-
	Mid-future (2040-2059)	530 (896, 348)	2.3	6.1	3.72
	Far-future (2080-2099)	575 (987, 369)	12.7	12.5	12.53

Acknowledgments: The authors sincerely thank Dr Naota Hanasaki for providing us with the source code of the H08 model. The climate data was downloaded from the data distribution center (http://h08.nies.go.jp) that is developed and maintained by the H08 development team and the S-8 project team.

References

Hanasaki N, Kanae S, Oki T, Masuda K, Motoya K, Shirakawa N, Shen Y, Tanaka K (2008) An Integrated model for the assessment of global water resources-Part 1: Model description and input meteorological forcing. Hydrol. Earth Syst. Sci. 12:1007-1025. https://doi.org/10.5194/hess-12-1007-2008

Hempel S, Frieler K, Warszawski L, Schewe J, Piontek F (2013) A trend-preserving bias correction – the ISI-MIP approach. Earth Syst. Dynam. 4:219-236. https://doi.org/10.5194/esd-4-219-2013

IPCC (2014) Contribution of Working Groups I, II, and III to the Fifth Assessment Report of the intergovernmental panel on Climate Change. IPCC, Geneva, Switzerland

Watson RT, Zinyowera MC, Moss RH, Dokken DJ (1998) The regional impacts of climate change. An assessment of vulnerability: A Special Report of IPCC Working Group II, 517 p

Weedon GP, Gomes S, Viterbo P et al. (2011) Creation of the WATCH Forcing Data and its use to assess global and regional reference crop evaporation over land during the twentieth century. J. Hydrometeorol. 12:823-848. https://doi.org/10.1175/2011JHM1369.1

11th World Congress on Water Resources and Environment (EWRA 2019)
"Managing Water Resources for a Sustainable Future", 25-29 June 2019, Madrid, Spain

Impacts of climate change on the Tagus Segura interbasin water transfer

J. Senent-Aparicio[1*], A. López-Ballesteros[1], F. Cabezas[2], J. Pérez-Sánchez[1]
[1] Department of Civil Engineering, Catholic University of Murcia (UCAM), Murcia, Spain
[2] Euro-Mediterranean Water Institute, Murcia, Spain
* e-mail: jsenent@ucam.edu

Introduction

According to different previous studies, water resources availability in semi-arid regions will be highly affected by climate change very likely. The Segura river basin, located in the southeast of Spain, is one of the most water-stressed basins in Mediterranean Europe (EEA 2009). One of the major source of water in this basin is the Tagus-Segura interbasin water transfer (TSWT), whereby about 400 Mm^3/year of water is transported from the headwaters of the Tagus river basin, in central Spain, to the southeast along a 300 km channel. TSWT has enabled the socio-economic development of the south-east of Spain and supports important economic activities in this area (urban-industrial water consumption and irrigated fruits and vegetables production), although it involves political decisions at a national level, and has been the focus of territorial conflicts (Melgarejo-Moreno et al. 2019).

Recent studies (Lobanova et al. 2017; Pellicer-Martínez and Martínez-Paz 2018) reveal that climate change would imply reductions in the flows that could be transferred to the Segura basin. In this study, we have gone one step further, improving the modelization of the basin using the Soil & Water Assessment Tool (SWAT) model and SWAT2lake tool (Molina-Navarro et al. 2018). This tool let the modeller delineate the entire watershed flowing into a reservoir including not only the major streams but also those areas in-between river's subbasins that flow directly into the reservoir. Besides, the TSWT operating rules were simulated taking into account the effect of projected temperatures on the reservoirs evaporation. The overall objective of this study was to evaluate the hypothetical effects that both components of climate change -flows and evaporation from reservoirs- may have on the water transferred to the Segura river basin.

Materials and methods

In order to assess the impact of climate change in the water transferred to the Segura river basin, first of all, the headwaters of the Tagus river basin were modelled using SWAT model. The SWAT model (Arnold et al. 1998) is a public domain physically based, semi-distributed, and long-term continuous watershed scale model that runs on a daily time step to predict the impact of climate or land use management on hydrology, sediment and nutrients in large basins. The watershed is divided into a number of subbasins, each of which has a number of hydrologic response units (HRUs) with uniform land use and soil types. The responses at HRU level are aggregated at the sub-basin level and routed to the sub-basin outlet through the channel network.

Secondly, the predicted future climate change by two climate change scenarios (RCP 4.5 and RCP 8.5) and five general circulation models (GFDL-ESM2M, HadGEM2-ES, IPSL-CM5A-LR, MIROC and NoerESM1-M) were obtained using the Climate Change Toolkit (Vaghefi et al. 2017) and were used as an input data in the validated model, obtaining the future amount of water flowing to the Entrepeñas and Buendía reservoirs, in the Tagus headwater origin of the transfer.

Finally, these flows were used in the simulation of the TSWT operating rules on a monthly basis, which includes several constraints according to hydrological status, and provided a prediction of the volumes that could be transferred every month to the Segura river basin. The expected increase of the evaporation rate in Entrepeñas and Buendía reservoirs as a result of the temperature increase was taken into account in the application of the rules of operation of the TSWT. So, higher temperatures will directly influence not only runoff generation via increased ETP in the basin, but also evaporation processes from the reservoirs water bodies. The inclusion of variation in evaporation rate is could significantly affect the final results of the

water balance. Projection of evaporation rate in this study was estimated based on climatic average monthly temperature and using Malmstrom equation (Malmström 1969).

Results and concluding remarks

The SWAT simulation generated good results, both in calibration and validation periods, reproducing the observed discharge and their tendency in time. For the validation period, NSE and R^2 values were 0.74 and 0.86 in Entrepeñas reservoir, and 0.58 and 0.94 in Buendía reservoir. Comparing the long-term (2070-2099) to baseline periods (1970–1999), precipitation showed a decreasing trend of between 11% and 26%, whereas projected annual mean temperatures demonstrated a forecasted increase of 3.2–5.4°C (Table 1). As a result of rising surface temperature, results show that the averaged evaporation in 2040-2069 and 2070-2099 will increase about 18% and 39% of that order relative to the baseline period. The results of this study show that the inflow discharges to Entrepeñas and Buendía reservoirs are decreasing under both RCPs in both future periods. In RCP 8.5 and by the end of the century, water resources were predicted to experience a decrease of 59%. Despite its high uncertainty, these findings provide useful information for water management authorities in both the Tagus and Segura river basins, and alert about possible negative impacts for the involved water resources system in the face of climate change.

Table 1. Projected changes relative to the baseline period (1970-1999).

	Period	ΔRainfall	ΔTemperature	ΔEvaporation	ΔDischarge	ΔWater transfer
RCP 4.5	Medium (2040-2069)	-9%	+2.5°C	+18%	-27%	-25%
	Long (2070-2069)	-12%	+3.0°C	+23%	-34%	-73%
RCP 8.5	Medium (2040-2069)	-11%	+3.2°C	+24%	-30%	-34%
	Long (2070-2069)	-26%	+5.4°C	+41%	-59%	-74%

Acknowledgments: This research was supported by the Segura Hydrographic Confederation within the framework of the Research Project "Scientific Support Activities for the Hydrological Planning and European Cooperation Process". The second author was supported by the Ministry of Education of Spain (FPU 17/00923).

References

Arnold JG, Srinivasan R, Muttiah RS, Williams JR (1998) Large area hydrologic modeling and assessment part I: model development. Journal of of the American Water Resources Association 34(1):73-89. http://doi.org/10.1111/j.1752-1688.1998.tb05961.x

European Environment Agency (2009) Water resources across Europe - confronting water scarcity and drought. European Environment Agency, Copenhagen, Denmark

Lobanova A, Liersch S, Tábara JD, Koch H, Hattermann FF, Krysanova V (2017) Harmonizing human-hydrological system under climate change: A scenario-based approach for the case of the headwaters of the Tagus River. Journal of Hydrology 548:436-447. http://doi.org/10.1016/j.jhydrol.2017.03.015

Malmstrom VH (1969) A new approach to the classification of climate. Journal of Geography 68(6):351-357. http://doi.org/10.1080/00221346908981131

Melgarejo-Moreno J, López-Ortíz MI, Fernández-Aracil P (2019) Water distribution management in South-East Spain: A guaranteed system in a context of scarce resources. Science of the Total Environment 648:1384-1393. http://doi.org/10.1016/j.scitotenv.2018.08.263

Molina-Navarro E, Nielsen A, Trolle D (2018) A QGIS plugin to tailor SWAT watershed delineations to lake and reservoir waterbodies. Environmental Modelling & Software 108:67-71. http://doi.org/10.1016/j.envsoft.2018.07.003

Pellicer-Martínez F, Martínez-Paz JM (2018) Climate change effects on the hydrology of the headwaters of the Tagus River: implications for the management of the Tagus-Segura transfer. Hydrology & Earth System Sciences 22:6473-6491. http://doi.org/10.5194/hess-22-6473-2018

Vaghefi SA, Abbaspour N, Kamali B, Abbaspour K (2017) A toolkit for climate change analysis and pattern recognition for extreme weather conditions - Case study: California-Baja California Peninsula. Environmental Modelling & Software 96:181-198. http://doi.org/10.1016/j.envsoft.2017.06.033

11th World Congress on Water Resources and Environment (EWRA 2019)
"Managing Water Resources for a Sustainable Future", 25-29 June 2019, Madrid, Spain

Non-stationary behaviour of extreme events in Portugal: Droughts and rainfall trends

F.A. Albuquerque[1], M.M. Portela[2*]
[1] Instituto Superior Tecnico (IST), University of Lisbon (UL), Portugal
[2] Civil Engineering Research and Innovation for Sustainability (CERIS), Instituto Superior Tecnico (IST), University of Lisbon (UL), Portugal
* e-mail: maria.manuela.portela@tecnico.ulisboa.pt

Introduction

This study refers to an analysis about droughts and rainfall trends in Portugal mainland based on 105 hydrological years of monthly rainfall records, from Oct. 1912 to Sept. 2017 (1912/13 to 2016/2017) at 39 rain gauges fairly distributed over the country. In Portugal, the hydrological year starts in October.

Materials and methods

The drought analysis utilized the standardized precipitation index, SPI, applied to different time scales. The SPI is one of the most popular and common drought indexes. Originally developed by McKee et al. (1993), it remaps the rainfall records into a standardized probability distribution function so that an index of zero indicates the median rainfall amount, while a negative index stands for drought conditions and a positive one, for wet conditions.

The frequency of the droughts was also assed, aiming at ascertaining if, regardless the changes in the other characteristics, the droughts became more frequent. For that purpose the Kernel occurrence rate estimation (KORE) non-parametric method was used to quantify the yearly occurrence rates of the periods under droughts conditions. To account for the uncertainty of the KORE estimates, a pointwise 90% confidence band was constructed around the frequency estimates, by means of bootstrap simulations, according to the methodology described in Silva et al. (2012).

The trend analysis utilized the Mann-Kendall test to identify the significant trends, whose magnitude was then evaluated by applying the Sen slope estimator.

Results and concluding remarks

Based on the SPI the number of droughts, as well as their duration and magnitude were analysed for the whole time span but also for the initial period of 90 years (from Oct. 1912 to Sep. 2002), and for the last 15 years (from Oct. 2002 to Sept. 2017). The results thus achieved for the complete set of 39 rain gages are exemplified in Figure 1 based on a time scale of 3 months and moderate droughts ($-1.65 \leq SPI3 \leq -0.84$).

Figure 2 exemplifies the application of the KORE method to ascertain the frequency of the periods under drought conditions. Although it refers to a specific rain gage (n^{o} 3, code 03L/02UG), time step (SPI6), and category of drought (moderate), the general shape of the yearly frequency curve of the periods under drought conditions and of the confidence bands are almost the same regardless of the application conditions.

Although the trend analysis was applied to the monthly rainfall and to the cumulative rainfall in different periods of the year, only the results at the annual level are exemplified in Table 1.

Figure 1 clearly suggests a notorious increase of the magnitude and duration of the droughts towards the present. The comparison among drought characteristics for the entire period of 105 years, for the initial 90 years and for the final 15 years shows an astounding worsening in the drought conditions in the more recent period, with remarkable increase in the averages of the numbers of droughts per year, their magnitude and duration.

In what concerns the frequency of the periods under drought conditions, all the rain gages denote an increase towards the present similar to the one exemplified in Figure 2.

Regarding the trend analysis (Table 1), and except for the rainfall in July and August in a very few rain gages, all the remaining significant trends indicate a decrease in the rainfall. For the year such decrease can be greater than 10 mm/year.

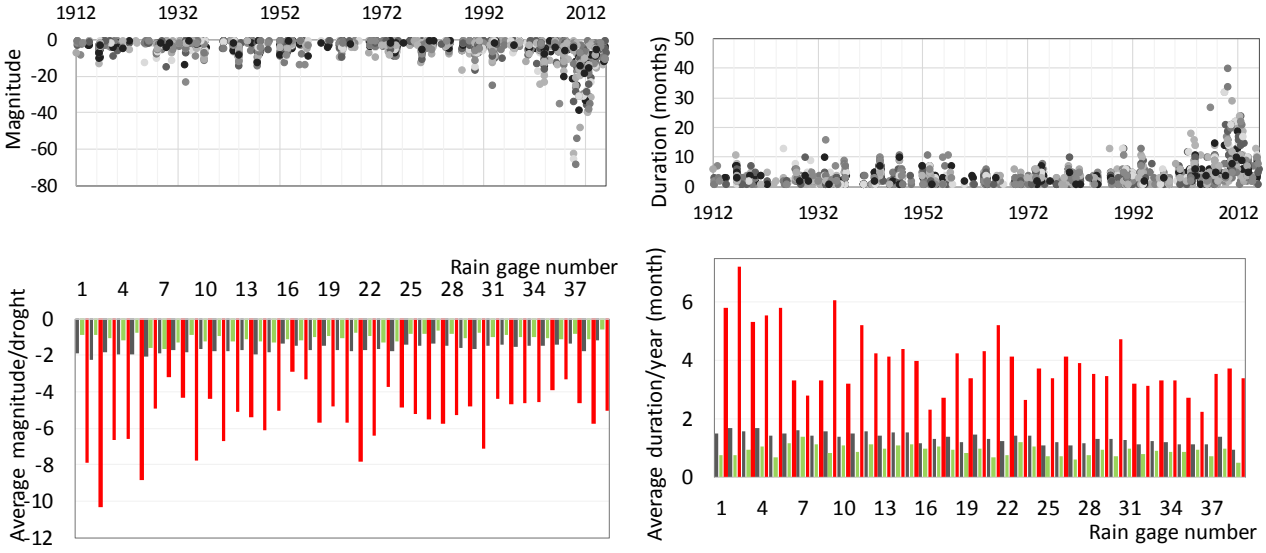

Figure 1. Characteristics of the moderate drought for the time scale of 3 months (-1.65 ≤ SPI3 ≤ -0.84).

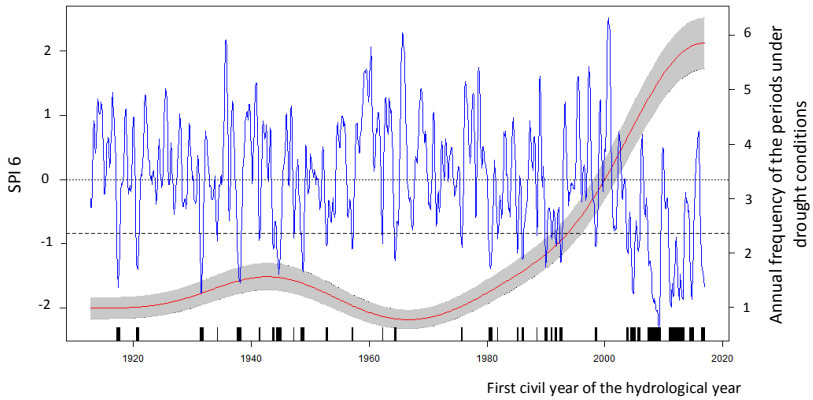

Figure 2. Rain gage n^{o} 3 (03L/02UG). Yearly frequency of the periods under drought conditions for -1.65 ≤ SPI6 ≤ -0.84.

Table 1. Significant trends in the annual rainfall.

Rain gage (n.º)	Variation (mm/year)	Rain gage (n^{o})	Variation (mm/year)	Rain gage (n^{o})	Variation (mm/year)	Rain gage (n^{o})	Variation (mm/year)	Rain gage (n^{o})	Variation (mm/year)	Rain gage (n^{o})	Variation (mm/year)	Rain gage (n^{o})	Variation (mm/year)
1	-5.440	7	--	13	-2.833	19	-1.531	25	--	31	--	37	--
2	-10.657	8	-1.416	14	-2.862	20	-3.466	26	--	32	--	38	--
3	-2.904	9	-3.111	15	-3.816	21	-1.670	27	-2.803	33	--	39	--
4	-2.078	10	--	16	-1.741	22	-2.764	28	-1.568	34	--		
5	-4.94	11	-5.661	17	-1.537	23	--	29	--	35	--		
6	--	12	-2.322	18	-4.660	24	--	30	-1.954	36	--		

References

McKee TB, Doesken NJ, Kleist J (1993) The relationship of drought frequency and duration to time scales. In: Proceedings of the 8th Conference on Applied Climatology. American Meteorological Society, Boston, pp 179–184

Silva AT, Portela MM, Naghettini M (2012) Nonstationarities in the occurrence rates of food events in Portuguese watersheds. Hydrology and Earth System Sciences 16:241-254. doi: 10.5194/hess-16-241-2012

11th World Congress on Water Resources and Environment (EWRA 2019)
"Managing Water Resources for a Sustainable Future", 25-29 June 2019, Madrid, Spain

The effect of climate change on fluvial ecosystems in the Sierra de Guadarrama National Park: Past, present and future

J.M. Santiago*, D. García de Jalón, C. Alonso, J. Solana-Gutiérrez
Laboratorio de Hidrobiología, ETSI Montes, Forestal y Medio Natural, Universidad Politécnica de Madrid, Madrid 28040, Spain
** e-mail: jmsant@picos.com*

Introduction

Climate change is one of the most important global processes that the Biosphere is experiencing, and mountain ecosystems are very sensitive to climate warming (Nogues-Bravo et al. 2007; Santiago et al. 2016). Mountain streams are directly affected by climate change, and populations of cold water organisms are expected to reduce in numbers in southern latitudes due to warming. Knowing how and how much they can be affected is key to plan conservation strategies.

This research aims to disentangle how climate change has affected the stream biology of the Sierra de Guadarrama National Park and to predict its evolution for implementing an adaptation strategy.

Materials and methods

The evolution of the air temperature (AT) since 1946, 1961 and 1986 was studied at three meteorological stations: Puerto de Navacerrada (AT1), Rascafría (AT2) and Soto de El Real (AT3), respectively. Stream temperature (ST) was recorded in several locations in the Cega (ST1, n=2), Lozoya (ST2, n=4) and Manzanares (ST3, n=2) streams as part of a monitoring program which is still active, and models were performed to rebuild streams historical temperature from air temperature (Santiago et al. 2017). Significance of air and stream temperature changes during last decades was analysed using Sen-slope (R Trend package (Pohlert 2016), p-value ≤ 0,05), and predicted changes due to climate change throughout the XXIth century were modelled (Ribalaygua et al. 2013) using IPCC scenarios RCP4.5 and RCP8.5 of the 5th Assessment Report (IPCC 2013). Studied variables were annual average of daily means, annual average of daily maxima, annual average of daily minima, and annual absolute maxima and minima.

To assess the effect of temperature changes on cold water biota we used brown trout (*Salmo trutta* Linnaeus, 1758) as indicator species, applying the thermal thresholds described in Santiago et al. (2016). Number of days, events of 7-consecutive days and maximum length of the events per year in which threshold was overpassed were studied for this purpose.

Results and concluding remarks

As a result, maximum air temperatures increased in the two highest meteorological stations during the second half of the past century, while annual average of daily minimum temperatures decreased in AT2 and increased in AT1. Changes in AT3 station were not significant except of absolute annual minimum which decreased. In contrast, models only showed significant stream temperature changes in the ST1 stream in the past.

Although the thermal changes are little conspicuous in the past, according to different climate change scenarios (RCP4.5 and RCP8.5), models predict significant increases in water temperature throughout the current century in the three streams. As it could be expected, these changes are highest in the RCP8.5 scenario. The temperature increase pathways are very similar for both scenarios until middle of the century; at this point, the increase in the RCP8.5 scenario is higher. From the middle of the century on, the brown trout thermal threshold violations will become more frequent, thus compromising the viability of resident trout populations in the lowest reaches.

We conclude that although stream thermal changes were not significant in the past in the study area, they are expected to be quantitatively important in a near future involving dramatic changes in the river

ecosystems. These findings might be useful for planning actions to prevent and mitigate the negative effects of climate change on streams in the range of the Sierra de Guadarrama National Park.

Acknowledgments: We are grateful to the Consejería de Medio Ambiente y O.T. of the Government of Castilla y León, especially to Patricia Riquelme, Mariano Anchuelo, Fabián Mateo and the forest ranger team of Navafría. Also, we are indebted to the Sierra of Guadarrama National Park staff, and especially with Juan Bielva and Ángel Rubio for the temperature data of Lozoya stream. The World Climate Research Programme's Working Group on Coupled Modelling is responsible for the 5th Coupled Model Intercomparison Project, and we thank the climate modelling groups for producing and making available their model output. Climate change study was partially funded by the Ministerio de Agricultura, Alimentación y Medio Ambiente of Spain through the Fundación para la Investigación del Clima (http://www.ficlima.org/); by the European Union, DG for Environment (DURERO project. C1.3913442).

References

IPCC (2013) Climate change 2013: The physical science basis. Working Group I Contribution to the Fifth Assessment Report of the Intergovernmental Panel on Climate Change. Stocker TF, Qin D, Plattner G-K, Tignor M, Allen SK, Boschung J, Nauels A, Xia Y, Bex V, Midgley PM (eds). Cambridge University Press, Cambridge, UK, and New York

Nogues-Bravo D, Araujo MB, Errea MP, Martinez-Rica JP (2007) Exposure of global mountain systems to climate warming during the 21st century. Global Environmental Change 17:420–428. https://doi.org/10.1016/j.gloenvcha.2006.11.007

Pohlert T (2016) Non-parametric trend tests and change-point detection. R package, version 0.1.0

Ribalaygua J, Torres L, Pórtoles J, Monjo R, Gaitán E, Pino MR (2013) Description and validation of a two-step analogue/regression downscaling method. Theoretical and Applied Climatology 114(1–2):253–269. https://doi.org/10.1007/s00704-013-0836-x

Santiago JM, García de Jalón D, Alonso C, Solana J, Ribalaygua J, Pórtoles J, Monjo R (2016) Brown trout thermal niche and climate change: expected changes in the distribution of cold-water fish in central Spain. Ecohydrology 9(3):514–528. https://doi.org/10.1002/eco.1653

Santiago JM, Muñoz-Mas R, Solana J, García de Jalón D, Alonso C, Martínez-Capel F, Pórtoles J, Monjo R, Ribabalaygua J (2017) Waning habitats due to climate change: the effects of streamflow and temperature changes at the rear edge of the distribution of a cold-water fish. Hydrology and Earth Systems Sciences 21:4073-4101. https://doi.org/10.5194/hess-21-4073-2017

11th World Congress on Water Resources and Environment (EWRA 2019)
"Managing Water Resources for a Sustainable Future", 25-29 June 2019, Madrid, Spain

Analyzing temperature attributes for the last half century in Heraklion – Crete, Greece

N. Proutsos[1*], E. Korakaki[1], A. Bourletsikas[1], K. Kaoukis[1], C. Georgiadis[2]
[1] Institute of Mediterranean Forest Ecosystems, Hellenic Agricultural Organization DEMETER, Athens, Greece
[2] Hellenic Society for the Protection of Nature, Athens, Greece
* e-mail: np@fria.gr

Introduction

Mediterranean has been identified as a climate change (Diffenbaugh and Giorgi 2012) and biodiversity hotspot (Myers et al. 2000). Heraklion-Crete is located in East Mediterranean and is the southernmost prefecture of Europe. In Heraklion, the impacts of climate change are already evident. During the last decades, raises in temperature have been identified in several places in Greece, even in mountainous forest areas (Proutsos et al. 2009, 2010). The aim of this study is to investigate the temperature trends in Heraklion, during the last 63 years. Temperature attributes such as average minimum (T_{min}), maximum (T_{max}) and mean (T_{mean}) play an important role in natural vegetation succession and conservation, drought tolerance, as well as in human health. Therefore any changes in these attributes can affect the species dynamics in plant communities, i.e. vegetation composition, spatial and temporal distribution, and also the quality of life of citizens. To evaluate the impacts of rising temperatures on natural vegetation, it is of critical importance to monitor climate conditions continuously in order to implement, in time, adaptation and mitigation actions for the preservation of local flora and fauna.

Materials and methods

Monthly values of T_{mean}, T_{max} and T_{min} were used in this study. Data were obtained, from the meteorological station of Heraklion South Greece (35.34° N, 25.18° E, 39 m asl), covering the time period 1955-2017. The data were analysed on a monthly, seasonal and annual basis. The climate trends were identified by employing the Mann-Kendall non parametric test for different confidence levels (α=0.001, 0.01, 0.05 and 0.1). Mann-Kendall method is widely used for climatic and environmental time series trends evaluation, since it is a reliable method to identify monotonic linear and non-linear trends in non-normal data sets (Helsel and Hirsch 1992). The slope of each trend evaluated from the climatic data, was identified by the method of Sen (Q Sen slope), as a median of all possible slopes.

Results and concluding remarks

The annual pattern of average temperature (Table 1) appears to increase from 1955, with average rate +0.008 °C/y. The annual trend, however, is statistically significant only at α=0.1 (Z=1.91). The seasonal T_{mean} values were increasing, during the last 63 years, in all seasons except winter. The trends were positive and statistically significant in summer and autumn with rates +0.012, +0.014 °C/y, respectively. In spring the rate was also positive (+0.007 °C/y) but not significant (Z=1.19). Similarly, the negative trend in winter was not significant (Z=-0.38). The monthly analysis indicated, statistically significant T_{mean} changes in July (Z=2.28, α=0.05), August (Z=2.86, α=0.01), September (Z=4.44, a=0.001) and October (Z=1.92, α=0.1) with increasing rates +0.014, +0.019, +0.025 and +0.020 °C/y, respectively.

T_{max} also increased with a rate of +0.009 °C/y on an annual basis, significant at α=0.1 (Z=1.90). The seasonal trend is significant in summer with increasing rate +0.012 °C/y (Z=2.11, α=0.1). During the rest seasons the changes were not significant, however appear to increase in spring and autumn and decrease in winter. The monthly values of T_{max} significantly increased in July (Z=2.03, α=0.05), August (Z=1.90, α=0.1) and September (Z=3.4, α=0.001). Especially in September, T_{max} increased with a rate of +0.026 °C/y.

Table 1. Mann-Kendall test Z statistics and Sen's slope estimates of the monthly, seasonal and annual mean (T_{mean}), maximum (T_{max}) and minimum (T_{min}) temperatures at different levels of significance.

Month	T_{mean}		T_{max}		T_{min}	
	Z	**Q** (^{o}C/y)	**Z**	**Q** (^{o}C/y)	**Z**	**Q** (^{o}C/y)
January	0.27	0.002	-0.06	0.000	1.12	0.008
February	-0.17	-0.002	-0.05	-0.001	0.46	0.004
March	0.79	0.006	1.03	0.008	0.91	0.007
April	1.32	0.008	0.97	0.010	2.84	0.016
May	0.89	0.007	1.09	0.008	2.69	0.018
June	1.12	0.005	0.81	0.005	**3.70**	0.018
July	**2.28**	0.014	**2.03**	0.017	**5.58**	0.032
August	2.86	0.019	1.90	0.016	**4.61**	0.028
September	**4.44**	0.025	**3.40**	0.026	**5.12**	0.032
October	1.92	0.020	1.25	0.017	3.02	0.025
November	0.20	0.001	0.00	0.000	1.32	0.010
December	-0.93	-0.008	-0.82	-0.008	0.29	0.002
Season						
Winter	-0.38	-0.002	-0.21	-0.002	0.95	0.005
Spring	1.19	0.007	1.35	0.009	3.13	0.014
Summer	2.73	0.012	**2.11**	0.012	**6.06**	0.024
Autumn	**2.22**	0.014	1.59	0.012	**3.72**	0.020
Annual	1.91	0.008	1.90	0.009	**4.66**	0.016
			α=0.001	α=0.01	**α=0.05**	α=0.1

The trend analysis indicated that T_{min} has significantly (Z=4.66, α=0.001) increased the last 63 years with a rate of +0.016 ^{o}C/y. The seasonal trends were also positive for summer, autumn and spring with rates +0.024 ^{o}C/y (Z=6.06, α=0.001), +0.020 ^{o}C/y (Z=3.72, α=0.001) and +0.014 ^{o}C/y (Z=3.13, α=0.01), respectively. All months from April to September show significantly increased T_{min} values compared to 1955, with greater changing rates in July, September (+0.032 ^{o}C/y) and August (+0.028 ^{o}C/y).

Our results present that the air temperature in Heraklion-Crete has significantly increased the last 63 years. The climate became hotter, especially during summer and autumn, while in spring and winter remained rather unchanged. The increased average temperature values attributed to the significant increase in minimum temperatures especially during summer and autumn, while their increase in spring did not affect the seasonal mean temperature trends. All trends however, appear decreasing from 1955 to 1980's and thereafter increasing rapidly, resulting to even more magnified trends during the last 40 years compared to the total 63-year study period.

Acknowledgments: The climate data used in this work were kindly provided by the Hellenic National Meteorological Service. This work was financially supported by the LIFE17 GIC/GR/000029 GrIn project "Promoting Urban Integration of GReen INfrastructure to improve climate governance in cities", which is co-funded by the European Commission under the Climate Change Action-Climate Change Governance and Information component of the LIFE Programme.

References

Helsel DR, Hirsch RM (1992) Statistical methods in water resources. Elsevier, New York

Diffenbaugh NS, Giorgi F (2012) Climate change hotspots in the CMIP5 global climate model ensemble. Climatic Change, 114:813–822. doi: 10.1007/s10584-012-0570-x

Myers N, Mittermeier RA, Mittermeier CG, da Fonseca GAB, Kent J (2000) Biodiversity hotspots for conservation priorities. Nature 403:853-858. doi: 10.1038/35002501

Proutsos N, Tsagari K, Karetsos G, Liakatas A, Kritikos T (2009) High altitude temperature variations over the last 50 years in Greece. In: Proceedings of EWRA 7th International Conference 'Water Resources Conservation and Risk Reduction under Climatic Instability', 25-27 June 2009, Limassol, Cyprus, pp 1009-1016

Proutsos N, Tsagari K, Karetsos G, Liakatas A, Kritikos T (2010) Recent temperature trends over mountainous Greece. European Water 32:15-23. http://www.ewra.net/ew/pdf/EW_2010_32_02.pdf

11th World Congress on Water Resources and Environment (EWRA 2019)
"Managing Water Resources for a Sustainable Future", 25-29 June 2019, Madrid, Spain

The challenges facing groundwater development companies in adopting new technologies and procedures in arid areas of the world

R.A. Sahi
Consultancy services, STTS Limited, Toronto, Canada
e-mail: riazasahi@gmail.com

Introduction

In the last decade, water exploration companies in arid regions of the world, and particularly in the Kingdom of Saudi Arabia; have experienced business uncertainty resulting from the impact of climate change on their operations. The combination of depleting groundwater resources and increasing water demands presents a significant challenge to business sustainability. In response to this changing environment, water exploration companies have sought solutions through the adoption of new technologies to improve productivity and efficiency (Stoneman 2001b). The adoption of new technologies is expected to provide salient opportunities to tackle water scarcity and improve productivity (Sahi 2018). The objective of this research was to assist water exploration companies in their management of adopting new technologies. This research drew from the academic literature concerning management of new procedures and technology adoption to support an action research design, conducted with the engagement of six water development companies in the Arabian Peninsula.

Materials and methods

The research design was organized in two stages. In the first stage, the important themes from the literature of technology adoption informed engagement with the water development companies. Qualitative interviews were conducted with management with a range of functions, to identify their present performance and functionality in adopting new water exploration technology and procedures (Sahi 1997). A thematic analysis of interview data was used to build an actionable framework. In the second stage of the research design, the actionable model was used by one of the companies to generate and implement a plan and evaluate the results. This research reports the success of the plan and the evaluation of its implementation.

Results and concluding remarks

The findings indicate that embracing new technologies within an organization can have a significant impact on efficiency gains and overall performance. In addition to overall productivity improvement, the technology adoption process considerably exceeded expectations. Four core benefits were identified, based on data collected at the post-implementation evaluation stages: return on investment, market image, competitive advantage and customer satisfaction. At the time of evaluation, the first benefit had come close to realization and would be achieved in a short time. The second benefit had been continuously improving. The third benefit, competitiveness, had made remarkable improvement. The fourth benefit, customer satisfaction, had conspicuously increased from 38% to 78%. This 40% increase strengthened the customer base and improved sales.

The information provided here consists of only a small part of the overall picture derived within the framework of this research. This study indicates that post-implementation assessment of new technologies adoption could serve as a valuable source of experience for other organizations in the water exploration sector and encourage further, smarter investments into new technologies. This approach could be significant in achieving water security solutions in the arid areas of the world.

Table 1. New technology adoption benefits

	Expected %	Observed %
1. Return on Investment	100	63
2. Market Image	36	55
3. Competiveness	42	58
4. Customer Satisfaction	38	78

References

Sahi RA (1997) Water Resource Development. In: Water Technology Conference, March 24, Doha, Qatar

Sahi RA (2018) How water security and sustainability challenges are emerging in Pakistan. In: International Conference on Water Security, March 22, Toronto, Canada

Stoneman P (2001) Technological Diffusion and the Financial Environment. EIFC Working Paper No. 2001-03, University of Warwick

11th World Congress on Water Resources and Environment (EWRA 2019)
"Managing Water Resources for a Sustainable Future", 25-29 June 2019, Madrid, Spain

Impacts of climate change in European agriculture: The interplay between irrigation and agrifood markets

M. Blanco[1*], P. Martínez[1], P. Witzke[2], J. Hristov[3], G. Salputra[3], J. Barreiro-Hurle[3]
[1] Department of Agricultural Economics & CEIGRAM, Universidad Politécnica de Madrid, Spain
[2] EuroCARE, Bonn, Germany
[3] European Commission, Joint Research Centre (JRC), Seville, Spain
* e-mail: maria.blanco@upm.es

Introduction and methodology

Water is vital for agriculture and thus food security. While irrigation has helped boost agricultural production in many areas, uncertainties linked to the effects of climate change on water supply and demand are expected to add new pressures on water resources and agricultural sustainability. Ensuring agricultural and water sustainability today and in the future requires more effort to analyse the challenges faced by agriculture. Nevertheless, despite the important role of water as a driver for agricultural production, the interplay between irrigation water and food production is lacking in most previous studies (Sulser et al. 2010).

The extension of the CAPRI (Common Agricultural Policy Regional Impact Analysis) model with a water module tries to address this gap (Blanco et al. 2018). A specificity of the CAPRI model is its capability for analysing impacts of climate change on agriculture both at the global level and at the regional level within the EU. In Europe, irrigation water use by agriculture has been identified as one of the major sustainable water management issues in the implementation of the WFD. Agriculture accounts for an estimated 24% of total water abstraction in Europe, although in parts of southern Europe this figure can reach up to 80% (EEA 2009). Moreover, unlike other sectors like energy production, the majority of the water abstracted for agriculture is consumed (evaporation, transpiration, loses) and is hence not returned to the water bodies (70% according to the EEA).

In this study, we show the capability of CAPRI-Water to integrate water issues in climate change impact assessments. To this end, we investigate the biophysical and socioeconomic impacts of climate change on European agriculture considering irrigation. In the presence of climate change, the regional allocation of agricultural production in the future might change due to the heterogeneous situation in the EU regarding (a) water availability (i.e. higher in the North), (b) agricultural production potential (i.e. higher in Western and Central regions), (c) climatic conditions (i.e. cold in the North and temperate in the Central and South regions), and (d) potential climate change effects (i.e. more visible in dry regions of the South). For instance, since 1985, the area of irrigated land in southern Europe has gone up by 20%, contributing to the fact that the balance between water supply and demand has reached a critical level in many irrigated areas of Europe. However, concerns about water scarcity and droughts are no longer limited to the Mediterranean basin. In fact, more and more regions are expected to be adversely affected by changes in the hydrological cycle in the future, with more frequent and severe droughts expected across Europe and the neighbouring countries (Ciscar et al. 2018; Donnelly et al. 2017).

There is an extensive literature on the impacts of climate change on agriculture using the scenario framework decided by the scientific community (Van Vuuren et al. 2012). In most cases, climate change scenarios are translated into crop productivity effect. Still, climate change is expected to also affect irrigation water requirements and availability. To account for these effects, we simulate a climate change scenario in 2030 implying a reduction in precipitation and thus water availability. The results of this climate change scenario are compared against a baseline scenario assuming no climate effects. Our modelling approach accounts for the role of adaptation in offsetting some of the negative consequences of climate change. Endogenous adaptation strategies include changes in cropland allocation, production intensity, irrigation decisions and agrifood trade adjustments.

Results and concluding remarks

The CAPRI model simulates cropping areas in 2030, distinguishing rainfed and irrigated crops. Compared to a baseline situation, the total irrigated area increases in most European regions in the climate change scenario. Simulation results show that, since rainfed crops are more negatively affected by climate change than irrigated crops, irrigation expansion is one of the endogenous adaptation strategies to climate change. However, since climate change also affects water availability, not all regions have the same potential for expanding irrigation. Water availability is already a limiting factor for agricultural production in many EU regions.

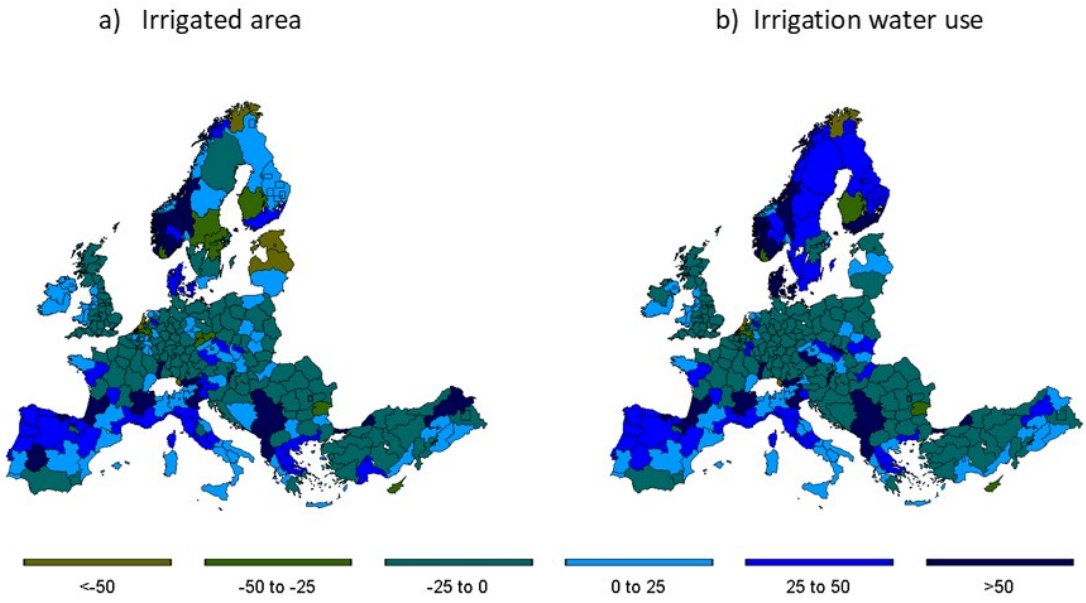

Figure 1. Effects of climate change on irrigated area and irrigation water use in 2030 (% change relative to the baseline). Source: CAPRI simulations

In brief, we find that irrigation plays a role as adaptation strategy, partially offsetting the negative effects on crop productivity. However, in areas where water availability is already a limiting factor for agricultural production, the pressures on water are increasing and climate change may add additional risks and jeopardize the sustainable use of this vital resource. It is, therefore, necessary to include water stress on impact assessments.

Acknowledgments: This research has been partially conducted in the framework of the project SYNERCAP (2013–2016 R&D National Plan, ECO2015-64438-R, funded by MINECO/ERDF).

References

Blanco M, Witzke P, Barreiro-Hurle J, Martinez P, Salputra G, Hristov J (2018) CAPRI Water 2.0: an upgraded and updated CAPRI water module. EUR 29498 EN, Publications Office of the European Union, Luxembourg, doi: 10.2760/83691

Ciscar JC, Ibarreta D, Soria A, Dosio A et al. (2018) Climate impacts in Europe: Final report of the JRC PESETA III project. EUR 29427 EN, Publications Office of the European Union, Luxembourg, doi: 10.2760/93257.

Donnelly C, Greuell W, Andersson J, Gerten D, Pisacane G, Roudier P, Ludwig F (2017) Impacts of climate change on European hydrology at 1.5, 2 and 3 degrees mean global warming above preindustrial level. Climatic Change 143(1-2):13-26

EEA (2009) Water resources across Europe – confronting water scarcity and drought. European Environment Agency

Sulser TB, Ringler C, Zhu T, Msangi S, Bryan E, Rosegrant MW (2010) Green and blue water accounting in the Ganges and Nile basins: Implications for food and agricultural policy. Journal of Hydrology 384(3-4):276-291

Van Vuuren DP, Riahi K, Moss R, Edmonds J, Thomson A, Nakicenovic N, Arnell N (2012) A proposal for a new scenario framework to support research and assessment in different climate research communities. Global Environmental Change 22:21-35

11th World Congress on Water Resources and Environment (EWRA 2019)
"Managing Water Resources for a Sustainable Future", 25-29 June 2019, Madrid, Spain

Adaptation of irrigated agriculture to climate change: A review focused on qualifying agriculture and forest stakeholders to cope with a changing climate

D.S. Martins[1*], T.A. do Paço[1], G.C. Rodrigures[1,2], L.M. da Silva[1], T. Pinto[3], A. Diogo[4], C. Santos Silva[5]
[1] LEAF, Research Center for Landscape, Environment, Agriculture and Food, Instituto Superior de Agronomia, University of Lisbon, 1349-017 Lisbon, Portugal
[2] COTR-Centro Operativo e de Tecnologia do Regadio, Beja, Portugal
[3] ANPROMIS – Associação Nacional dos Produtores de Milho e Sorgo, Lisbon, Portugal
[4] FNOP – Federação Nacional das Organizações de Produtores de Frutas e Hortícolas, Lisbon, Portugal
[5] UNAC – União da Floresta Mediterrânica, Lisbon, Portugal
* e-mail: dsmartins@isa.ulisboa.pt

Introduction

Climate Change (CC) is one of the most challenging problems of the 21st century. These changes will undoubtedly affect ecosystems and human activities, being the Mediterranean region particularly endangered. Possible impacts of CC on agriculture include the increase in irrigation requirements, changes in crop cycles, an increase in pests and an aggravated susceptibility to diseases. Irrigated agriculture is still the largest user of freshwater, accounting for 46% of total water use in Europe (European Environment Agency 2018). Thus, this reality, combined with the predicted water use due to population increase, exacerbates the need to make irrigated agriculture more efficient, regarding water use.

This study, under the scope of the project RIAAC-AGRI that aims identifying good practices and knowledge to promote the adaptation of relevant sectors (maize and sorghum, irrigation, industrial tomato and forestry) to a changing climate, is focused on the irrigation sector. For that, a thorough search of scientific studies and projects was performed, a methodology to identify the relevant studies on the subject was defined, and the best practices and innovation for the irrigation sector analysis were retrieved.

Materials and methods

A methodology to identify and select the relevant projects and scientific studies addressing CC in the Agriculture and Forestry sectors was defined for all sectors considered for the project, but allowing it to be generic enough to be implemented in any other sector of interest. Then, based on the projects and scientific papers identified, all the information was collected and homogenized in two unified databases focusing on identifying the best practices for each sector to cope with CC. Two databases were created, one relative to the projects and another for the scientific papers and are available in the "Rede Rural Nacional" website at https://inovacao.rederural.gov.pt/projetos/.

The process of identification and selection of relevant projects and scientific studies of interest to be included in the project databases had as guidelines the objectives of the project and the resulting restrictions. Therefore, the research focused on national (Portuguese) or international projects, with pertinent results for the Mediterranean region and more specifically for the Portuguese climatic and cultural characteristics. Moreover, taking into account the project's objectives, only projects and scientific papers approved from 2007 onwards were considered and the research was directed to four economic sectors, namely: corn and sorghum, irrigation, industry tomato and forests. Thus, this process was the following: (1) the main sources of financing for projects in the four sectors selected were identified; (2) for each source of project financing, different groups of keywords were tested to identify relevant projects; (3) data and information collected for each financing program and sector were retrieved and combined on a database. The process used for the scientific papers is analogous to the one described for the search of projects.

Results and concluding remarks

The ongoing project has identified, so far, 176 projects with relevant information and 300 scientific papers. More specifically, 28 projects and 39 scientific papers were identified for irrigated agriculture.

The large majority of the projects identified were financed by international programs such as the FP7 (40 projects) and H2020 programs (38), Life Programs (17) and by Interreg programs (6 projects). At a national level the Foundation for Science and Technology was the main financing source for projects in this area, with 20 relevant projects. Most international projects are still ongoing or are starting, which may indicate an increased interest in the subject. Moreover, the number of scientific papers published since 2007, increased from 2007 to 2011 when it reached its maximum value with 38 papers published.

Focusing on the data retrieved from scientific papers and projects relative to irrigation, results showed that the majority (14) of those studies and projects pursue the understanding of how the new climatic conditions will affect irrigation requirements in the Mediterranean region, estimating those in the future (e.g. El Chami and Daccache 2015; Rolim et al. 2017) with the concern that this may increase water scarcity in many vulnerable regions of the Mediterranean Basin. Another common research interest for the irrigation sector is the adoption of precision irrigation (8 projects or papers), to improve irrigation efficiency, and to help traditional rainfed crops of the region to thrive under CC scenarios, but with an increase in water consumption and CO_2 emissions. Moreover, 4 scientific studies focused on Regulated Deficit Irrigation systems as viable alternatives that allow for a reduction of water and energy consumptions, for example in Portugal, applied to maize, olive and pasture crops (Maia et al. 2016) for the all the Mediterranean for selected crops of sunflower, cotton and wheat (Daccache et al. 2014).

Many other possibilities are proposed, such as (1) alternative sources of water for irrigation, e.g., reclaimed water reuse in agriculture and use of desalination water; (2) testing new crop species and hybrids, better adapted to new climate conditions and pests or varieties with longer cycles to maintain current yields (e.g: de Sousa Fragoso and de Almeida Noéme 2018); (3) studies considering different water pricing policies to improve water management (e.g. García-Tejero et al. 2014) and (4) using seasonal forecasts to predict crop yields or sowing dates (Ben-Ari et al. 2016).

This review showed that there is a growing concern regarding the impacts of CC on agricultural systems in the Mediterranean region and that there is an effort to analyze those impacts and propose alternatives that can help to cope with the effects of CC on agriculture. Thus, the development of databases that contains this type of information, with an easy to use unified platform may be a useful tool for farmers and stakeholders.

Acknowledgments: This study was supported by the PDR2020 program through the project RIAAC AGRI - (PDR 2020 – 20.2.4-FEADER/032789).

References

Ben-Ari T, Adrian J, Klein T, Calanca P, Van der Velde M, Makowski D (2016) Identifying indicators for extreme wheat and maize yield losses. Agric For Meteorol 220:130–140. doi: 10.1016/J.AGRFORMET.2016.01.009

Daccache A, Ciurana JS, Rodriguez Diaz JA, Knox JW (2014) Water and energy footprint of irrigated agriculture in the Mediterranean region. Environ Res Lett 9:124014. doi: 10.1088/1748-9326/9/12/124014

de Sousa Fragoso RM, de Almeida Noéme CJ (2018) Economic effects of climate change on the Mediterranean's irrigated agriculture. Sustain Accounting, Manag Policy J 9:118–138. doi: 10.1108/SAMPJ-07-2017-0078

El Chami D, Daccache A (2015) Assessing sustainability of winter wheat production under climate change scenarios in a humid climate — An integrated modelling framework. Agric Syst 140:19–25. doi: 10.1016/J.AGSY.2015.08.008

European Environment Agency (2018) Use of freshwater resources. https://www.eea.europa.eu/data-and-maps/indicators/use-of-freshwater-resources-2/assessment-3

García-Tejero IF, Durán-Zuazo VH, Muriel-Fernández JL (2014) Towards sustainable irrigated Mediterranean agriculture: implications for water conservation in semi-arid environments. Water Int 39:635–648. doi: 10.1080/02508060.2014.931753

Maia R, Silva C, Costa E (2016) Eco-efficiency assessment in the agricultural sector: the Monte Novo irrigation perimeter, Portugal. J Clean Prod 138:217–228. doi: 10.1016/j.jclepro.2016.04.019

Rolim J, Teixeira JL, Catalão J, Shahidian S (2017) The Impacts of Climate Change on Irrigated Agriculture in Southern Portugal. Irrig Drain 66:3–18. doi: 10.1002/ird.1996

XI. Water Policy and Socioeconomic Issues

11th World Congress on Water Resources and Environment (EWRA 2019)
"Managing Water Resources for a Sustainable Future", 25-29 June 2019, Madrid, Spain

Pro-poor policy intervention in urban water management in Kenya: Towards universal access to affordable and safe water coverage

A. Sarkar
Department of Geography, Miranda House, University of Delhi, Delhi, India
e-mail: aninditasarkar28@gmail.com

Introduction

Water infrastructure in most parts of the world is characterised by different forms of technologies that shape service provision leading to inclusion of 'some' and exclusion of 'others' failing to meet the needs of the world's poorest urban residents by denying them their most basic rights (Bell 2015). Besides financial inadequacy of local utilities to extend service network, factors such as unplanned, illegal status of settlements, rapid population growth and the difficulty of obtaining finance to build or extend infrastructure to less profitable areas are cited as reasons for low coverage of safe water provisions for poor living in urban areas (Keener et al. 2010). Thus pro-poor policy interventions become mandatory in order to meet the Sustainable Development Goal (SDG) of achieving universal and equitable access to safe and affordable drinking water by 2030,

It is estimated that 60% of residents in Nairobi, the capital of Kenya, live in informal settlements (ISs) and low-income settlements (LISs) who do not have adequate access to affordable safe drinking water (Gerlach 2008). According to the National Water Services Strategy (2007-2015), only 20% of the populations in LISs have access to safe water with less than 5% having piped water connections at home. The Government declared access to "clean and safe water in adequate quantities" as a constitutional right and has made a mandatory condition for 'implementation of pro-poor strategies through promoting low cost technologies such as water kiosks and yard taps to ensure access to safe water at regulated prices' for granting licenses to water providers. Under this framework, Kenya introduced a new form of card operated water vending machine, popularly known as water ATMs first time in the Mathare slums of Nairobi in 2015 through a public private partnership programme. This study attempts to analyses the impact of this pro-poor policy intervention aimed at providing safe and affordable water along with cost recouping.

Materials and methods

The analysis of this study is built on field observations and structured interviews conducted during the month of November 2016 to December 2017 in 258 households of Mathare slum chosen randomly. Besides the exhaustive household schedule, participant observation, focus group discussions and key informant interviews with the slum residents, water industry experts in public and commercial enterprises forms the basis of my arguments.

Results and concluding remarks

With a tariff of half a Kenyan shilling (half a US cent) per 20 litres, there is no denying fact that the water ATMs are proving "affordable water" to the poor. It is the cheapest source of water available in the slum now with a fixed price unlike other available sources of water which vary according to demand in spite of price regulations. However its coverage remains low because of its small number of kiosks and a suboptimal location as compared to the shared standpipes. Even the quality of water sold by the water ATMs is doubted by the users as water is stored in the ATM tanks and carried by tankers which are never cleaned. This has implications on equity as well as wellbeing of its customers who use more time and energy in collecting water which may be also of poor quality. So the water ATMs can be more beneficial to the poor if they are more in number and are linked to the utility network.

Since one of the prime focuses the public utility is cost recovery, there is no doubt that the water ATMs are successful in generating some revenue. With pre-paid delivery, there is no need for costly metering and

billing process. Moreover, the system is more transparent as there is no cash handling between utility officers and kiosks managers (like in case of standpipes). The ATM management self-help groups (SHGs) get 40% water credit as profit. For example if the group buys water credit of Ksh. 100 (USD 1), then they get water worth Ksh. 140 (USD 1.4). However, the utility is bearing running cost on the production, distribution and collection of ATM cards, electricity uses to run the card swiping machines and also on fuel and manpower to run tankers to fill water in the ATM tanks. So, the ATMs may not be generating sufficient revenue as estimated and claimed by the government and in effect are not running at its optimum. If the ATMs are able to generate sufficient revenue as claimed, then they should be running in full capacity.

Certainly, the water ATMs have proven to be extremely beneficial to the managers who are benefiting by selling water as well as running parallel business in the ATM housed rooms. With empty water tanks, the ATM rooms are now vibrant commercial spaces running salons, tailoring shops, grocery and electronic goods shops. From my interviews and observations I could sense widespread nepotism in selection of the SHGs to manage the ATMs and there were also a lot of disputes even among the group members which hampered the day to day ATM functions.

It was envisaged that if this programme is successful, it will eradicate illegal tap connections and illegal water vendors. However, in reality, it is the other way round. The water ATMs were not working in profit because officials could not curb illegal connections and cartels were selling water at the illegal water connection points. They charged Ksh. 20 (USD 0.20) per day flat rate and customers preferred to buy this water as they could store as much water as they wanted and it was available near their premises at their convenience. Since at present the water ATMs are fewer in number with suboptimal location, the water vendors bought cheaper water from the ATMs and sold it to the slum residents making profit ranging from 99% to 75%. The utility officers and slum residents even alleged that the water vendors stole water from the ATM tanks to create a crisis to keep up their market demand and also make profit from this water. It is markedly unclear why the utility was not willing or was not in a position to stop such illegal siphoning of water even if they knew and reported about it in the interviews. For a successful impact of the water ATMs on the lives of the urban poor, the utility needs to protect the ATMs from getting misused by the cartels with regular supervisions and stringent punishment for law evaders.

The major findings of this research show that in this 'pro-poor intervention' in urban water management sector the donors did not think carefully about how a water ATMs would work in the socio-political context of this slum, and thus their installation though smart in its approach of providing "affordable water" has not been completely successful. The water source for the water ATM tanks has not been properly planned and since the tanks had to be filled by the utility's tanker trucks it cannot cope up with high demand and sometimes even provided poor quality water leading to its failure to provide "safe water". The location of the ATMs were also suboptimal because they were not sufficiently close to their customers and lugging water for long distances deterred its complete use even when it was the cheapest source. Most importantly, they were vulnerable to sabotage from the cartels of vendors. From the narratives of the slum residents it seems that water ATMs in Mathare slums is another example of a donor with a "technological" solution without an understanding of the socio-political context within which the new technology would be introduced. It seems that water ATMs have been encouraged by the government with the singular emphasis on economic viability without going deeper into the socio-economic set up of the slum.

Acknowledgments: This paper has been prepared from the project "Water insecurity among urban poor" funded by the University Grants Commission, India, under the Research award Programme 2016 -19.

References

Bell S (2015) Renegotiating Urban Water. Progress in Planning 96:1-28

Keener S Luengo M, Banerjee S (2010) Provision of Water to the Poor in Africa Experience with Water Standposts and the Informal Water Sector. Policy Research Working Paper 5387, World Bank, Washington DC

Gerlach E (2008) Regulating Water Services for Nairobi's Informal Settlements. Water Policy 10(5):531-548

11th World Congress on Water Resources and Environment (EWRA 2019)
"Managing Water Resources for a Sustainable Future", 25-29 June 2019, Madrid, Spain

Water poverty in large cities in Spain

S. López Ruiz[1*], C. Tortajada[2], F. González-Gómez[3]
[1] Faculty of Political Sciences and Sociology,University of Granada
[2] Institute of Water Policy, Lee Kuan Yew School of Public Policy, Singapore
[3] Water Research Institute, University of Granada, Spain
* e-mail: samaralopez.24@gmail.com

Introduction

The United Nations recognizes access to water as a human right. This implies access to sufficient, safe, acceptable, physically accessible and affordable water for personal and domestic use (United Nations 2010). The main problems of access to water occur in developing countries. Consequently, most research on water poverty focuses on developing countries (Biswas and Tortajada 2018). However, research is also needed in developed countries, where water may be too expensive for some households.

This research analyses access to water from the perspective of affordability. The problem of affordability is exacerbated when families are excluded from the service for not paying their bill. This paper examines the case of Spain. We study both national and local systems of regulation and governance. The objective is to determine whether low-income families face a genuine threat of exclusion from water supply. We ask whether the combination of the legal and institutional frameworks and pricing policies can lead to families at risk of poverty being denied access to domestic water. To this end, we analysed whether the Spanish legal framework allows that water supply is cut off for non-payment of the bill.

Materials and methods

The study is carried out on a sample of large Spanish cities. We studied 16 Spanish cities, which were selected for having more than 100,000 inhabitants, and a local regulation which explicitly states that the water supply may be cut off in case of non-payment of the water bill. The empirical strategy consists of estimating the proportion of the family budget spent on the water bill, on average, and under different assumptions. The analysis takes into account discounts on the water tariff and assistance programmes for low-income families.

To measure affordability, we estimate the financial effort a typical family has to make to pay the water bill for essential levels of consumption. To that end, we estimate the billing amount under the assumption of a three-person household (the household size was chosen because the average household in Spain has 2.5 people), with consumption of 100 litres of water per day per person, for a month. The water consumption per person was based on the finding that people need between 50 and 100 litres of water per person per day to guarantee that their basic needs are met (United Nations 2010).

Results and concluding remarks

It is important to note that, even at levels of consumption where water is considered an essential good, access to water differs by area. Comparing the extremes, water is most affordable in Zaragoza, where the price of the minimum essential level of water (100 L/c/d) is €11.19, while the equivalent price in Murcia is €30.17. This research allows us to show that there are also differences in the affordability of access to water at minimum consumption levels.

There are also differences in the proportion of the family budget allocated to the water bill in the three household income scenarios. For an average household, the water bill barely exceeds 1% of the family income in only three cities: Huelva, Murcia and Alicante. The price of water in Spain is low in relative terms (OECD 2015). On average, access to water to meet basic needs represents a relatively small budgetary effort for a typical family in Spain (AEAS 2016). However, in households with below-average incomes, the water bill may exceed the affordability threshold of 3%. For households with a single income equivalent to the national minimum wage, the water bill would represent more than 4% of that income in three cities of

the sample: Barcelona, Murcia and Huelva. In three other cities—Palma de Mallorca, Valencia and Alicante—it is close to the 3% threshold. The situation is more complicated for families that have had to fall back on the assistance offered by *Plan Prepara.*

Table 1. Monthly billing amount for consumption of 9 m^3 of water (2017)
Source: Compiled by the authors based on information collected from the utilities, municipalities, official gazettes of the provinces and autonomous communities, and the Ministry of Labour and Social Security.

	Bill (Euros)	As a percentage of income		
		Average salary	National minimum wage	Plan Prepara
Madrid	19.6762	0.63	2.38	4.93
Barcelona	28.6502	0.96	3.47	7.17
Valencia	22.3609	0.92	2.71	5.60
Seville	20.9903	0.91	2.54	5.26
Zaragoza	11.1870	0.44	1.35	2.80
Málaga	12.2705	0.61	1.49	3.07
Murcia	30.1716	1.29	3.65	7.55
Palma de Mallorca	23.0433	0.90	2.79	5.77
Las Palmas de Gran Canaria	13.9488	0.63	1.69	3.49
Bilbao	19.0598	0.68	2.31	4.77
Alicante	22.7936	1.10	2.76	5.71
Cádiz	20.2395	0.85	2.45	5.07
Huelva	24.8589	1.44	3.01	6.22
Tarragona	13.1194	0.53	1.59	3.28
Lleida	15.3650	0.65	1.86	3.85
Granada	16.0766	0.72	1.95	4.03

We find that the legal and institutional frameworks governing access to a minimum essential level of water in Spain depend on location. Similarly, there is not equal protection for the right of access to water in situations where people are at risk of social exclusion; it depends on the city where they live.

Although water services in Spain mostly comply with the principle of affordability, not all families are protected. On average, the water bill represents less than 3% of the family budget. In addition, tariff reductions and payment assistance schemes are generally available to help families in financial difficulty to pay their water bill. Even so, the water supply may be cut off in situations of severe poverty

With respect to these situations of extreme poverty, the Spanish legal framework is not in line with Resolution 64/292, of the General Assembly of the United Nations (2010). Families in extreme poverty face a real threat of having their water supply cut off.

Acknowledgments: This research was partially supported by the Ministry of Economy, Industry and Competitiveness, the State Research Agency, and the European Regional Development Fund (project reference ECO2017-86822-R).

References

Asociación Española de Abastecimientos de Agua y Saneamiento (AEAS) (2016) XIV Estudio Nacional de Suministro de Agua Potable y Saneamiento en España 2016. Madrid

Biswas AK, Tortajada C (2018) Safe water for the Developing World: Rethoric and Reality. In: Univer-cities: Strategic Dilemmas Of Medical Origins And Selected Modalities: Water, Quantum Leap & New Models, pp 129-149

Organisation for Economic Co-operation and Development (OECD) (2015) Environment at a Glance 2015. OECD Indicators. Paris

United Nations (2010) Resolution A/RES/64/292. July 2010, United Nations General Assembly

11th World Congress on Water Resources and Environment (EWRA 2019)
"Managing Water Resources for a Sustainable Future", 25-29 June 2019, Madrid, Spain

Cost-benefit analysis of river restoration in Switzerland

I. Logar[1*], R. Brouwer[1,2], A. Paillex[1]
[1] *Eawag: Swiss Federal Institute of Aquatic Science and Technology, Dübendorf, Switzerland*
[2] *The Water Institute and Department of Economics, University of Waterloo, Canada*
** e-mail: ivana.logar@eawag.ch*

Introduction

Over the last two centuries, rivers around the world have been heavily modified, causing the degradation of riverine ecosystems and the loss of biodiversity (MEA 2005). The adverse impacts of past river developments have received increasing attention in recent years (Malmqvist and Rundle 2002). A trend to return rivers to their near-natural state through river restoration can be observed (e.g. the special issue on river restoration in *Water Resources and Economics*; Brouwer and Sheremet 2017). River restoration is expected to improve the ecological state of rivers, prevent further biodiversity loss, and restore lost ecosystem services (Palmer et al. 2005; Bernhardt et al. 2005). Switzerland plans to restore 4000 kilometres of rivers by 2090. For this purpose, the government has allocated 60 million Swiss Francs (CHF) per year, which is equal to 4.8 billion CHF over the entire period of 80 years or 1,200 CHF/m.

However, the costs of restoration are often high (Bergstrom and Loomis 2017). The question is, therefore, whether the environmental, social and economic benefits outweigh the costs of river restoration. The main objective of this study is to answer this question using Switzerland as a case study. This study aims to: (1) translate the ecological benefits of river restoration into economic values expressed in monetary terms; (2) elicit public preferences and willingness to pay (WTP) for river restoration; and (3) conduct a cost-benefit analysis (CBA) of two typical river restoration projects in Switzerland, in order to inform the national policy on river restoration about the economic justification of the planned investment.

Our approach to estimating the economic benefits of restoring degraded river sections differs from the existing literature in that it explicitly integrates, into a stated preference (SP) survey, the results from an environmental impact assessment previously carried out by natural scientists for the same two river sites (rivers Thur and Töss). An additional novelty of this study is that it uses two SP valuation methods to elicit public preferences and WTP for river restoration: namely, the discrete choice experiment (DCE) and the contingent valuation (CV) method. This allowed us to compare the economic benefits derived from the two methods and check the robustness of the results. There are relatively few studies that conduct and report the results of a CBA of river restoration. This paper therefore contributes to this limited literature by providing further empirical evidence about the economic efficiency of river restoration projects.

Materials and methods

The results of environmental impact assessment are reported in Paillex et al. (2017). SP methods are most appropriate for estimating the total economic value of non-market commodities, such as ecosystem goods and services, whose value is not captured in existing markets or pricing mechanisms. We apply both SP methods, DCE and CV, in a large-scale representative survey, to derive WTP of the local population for further restoration measures on the rivers Thur and Töss. The WTP values are then aggregated over the local population in order to estimate the total benefits of river restoration. The survey was pretested and administered in-person in March 2015 by a professional marketing agency. Respondents were recruited by means of random sampling procedure at public places in towns and villages located within a distance of 35 km from the two river sites. Each river site sample consisted of 250 respondents, resulting in a total sample size of 500 individuals. The two samples were set up to be representative of the total population in the study area (the Cantons of Zurich and Thurgau) in terms of gender, age, and their spatial distribution.

In the CBA, the benefits of further river restoration are compared with the costs of past river restoration projects. The benefit and cost estimates are normalized for the river length and expressed per kilometre of river restoration. The recurring (maintenance) costs, as well as the benefits, are assumed to start in the

second year of the project, after the river restoration measures have been completed. The time period of 35 years was selected for the CBA after consulting the competent authorities about the expected duration of the restoration measures that have already been carried out along the rivers Thur and Töss. We apply a discount rate of 2% because this is the recommended discount rate for CBAs related to public infrastructure projects in Switzerland (Abay 2016).

Results and concluding remarks

The restoration costs are substantially higher for the Thur (4167 CHF/m) than for the Töss (2850 CHF/m). This can be explained by the fact that the river Thur is of a higher stream order and therefore wider than the river Töss, which is likely to increase the costs of restoration per stretch of river. The costs of river restoration per square meter of water surface are, however, higher for the river Töss than for the river Thur. A possible explanation is that past restoration at the river Töss included both active and passive restoration measures, while at the river Thur only passive restoration measures were implemented. The actual costs of restoration at both sites largely exceed the national benchmark, i.e. the available budget for river restoration of 1200 CHF/m.

The resulting mean WTP estimates derived from the DCE equal 144 CHF/person/year for the river Thur and 196 CHF/person/year for the river Töss. The average WTP estimates from the open-ended CV question are significantly lower than those derived from the DCE. For the sample as a whole, they amount to 52 CHF/person/year for the river Thur and 59 CHF/person/year for the river Töss. We opt to use the more conservative benefit estimates derived from the CV method in the CBA. The benefit estimates based on the CV method equal CHF 30 million and CHF 37 million per year for the rivers Thur and Töss, respectively.

The CBA results indicate that the discounted benefits of restoration are considerably higher than the discounted costs at both river sites. As a result, the net present values are positive and amount to CHF 706 million for the restoration of the river Thur and CHF 885 million for the river Töss. The benefit-cost ratios equal 173 and 318 for the rivers Thur and Töss, respectively. These results indicate that investments in further restoration measures are economically justified at both river sites, and that the Swiss tax payer is willing to pay substantially more for restoration projects at the local level than is legally required by the existing national policy on river restoration. A sensitivity analysis shows that the main results and conclusions are very robust to the key assumptions underlying the CBA.

Acknowledgments: This research was funded by Eawag, the Swiss Federal Institute of Aquatic Science and Technology. The study has benefited from the EU project REFORM.

References

Abay G (2006) Discount rate in cost-benefit analyses in traffic (in German). Swiss Association of Road and Transportation Experts (VSS). Swiss Federal Department of Environment, Transport, Energy and Communication, Vol. 1137. www.webcitation.org/6P4ihnika

Bergstrom J, Loomis JB (2017) Economic valuation of river restoration: An analysis of the valuation literature and its uses in decision-making. Water Resources and Economics 17:9-19

Bernhardt ES, Palmer MA, Allan JD, Alexander G, Barnas K, Brooks S, Carr J, Clayton S, Dahm C, Follstad-Shah J, Galat D, Gloss S, Goodwin P, Hart D, Hassett B, Jenkinson R, Katz S, Kondolf GM, Lake PS, Lave R, Meyer JL, O'Donnell TK, Pagano L, Powell B, Sudduth E (2005) Synthesizing US river restoration efforts. Science 308(5722):636-637

Brouwer R, Sheremet O (2017) The economic value of river restoration. Water Resources and Economics 17:1-8

Malmqvist B, Rundle S (2002) Threats to running water ecosystems of the world. Environmental Conservation 29(2):134-153

MEA Millenium Ecosystem Assessment (2005) Ecosystems and human well-being: Biodiversity synthesis. World Resources Institute, Washington DC

Paillex A, Schuwirth N, Lorenz AW, Januschke K, Peter A, Reichert (2017) Integrating and extending ecological river assessment: Concept and test with two restoration projects. Ecological Indicators 72:131-141

Palmer MA, Bernhardt ES, Allan JD, Lake PS, Alexander G, Brooks S, Carr J, Clayton S, Dahm CN, Follstad Shah J, Galat DL, Loss SG, Goodwin P, Hart DD, Hassett B, Jenkinson R, Kondolf GM, Lave R, Meyer JL, O'Donnell TK, Pagano L, Sudduth E (2005) Standards for ecologically successful river restoration. Journal of Applied Ecology 42(2):208-217

11th World Congress on Water Resources and Environment (EWRA 2019)
"Managing Water Resources for a Sustainable Future", 25-29 June 2019, Madrid, Spain

Effects of water pricing at river basin scale: The case of Guadalquivir (Southern Spain)

M.M. Borrego-Marín[1], A. Expósito[1,2], J. Berbel[1*]
[1] Department Agricultural Economics, WEARE Group, Universidad de Córdoba, Spain
[2] Universidad de Sevilla, Spain
* e-mail: berbel@uco.es

Introduction

This study describes a model of economic sectors in Guadalquivir river including inter sectoral and hydrological effects of changes in water use as a response to water pricing policy. The main economic variables include: water use, gross regional product, returns flows in the river and employment at sectoral and basin level. The response of the different sectors to water pricing and the sectoral productivity is derived from official data. The background of the model is based on previous research for the implementation of the UN System of Environmental-Economic Accounts and the application of this framework to Guadalquivir (Borrego-Marín et al. 2016).

Materials and methods

Different sources have been used either for the observed original data or the estimation of non-observed variables when necessary. Baseline situation has been defined using the Statistical National Institute (gross added value and employment by sector) and sectoral water use from the Hydrological Plan by the Water Agency (CHG 2015).

Once the current situation is defined, the response of the different sectors is simulated by using published elasticities of demand for the non-agricultural economic sectors. Table 1 summarizes the equation for isoelastic demand and the estimation of parameter 'K' that is found by solving the equation (1) for current water abstraction and price for each sector.

$$Q = K\, p^{\epsilon} \quad (1)$$

Elasticities (ε) for the different sectors can be found in Table 1 and has been taken according to Reynaud (2015) and Berbel et al. (2018).

Table 1. Estimated parameters for sectoral water demand, Guadalquivir 2012

$Q = K\, p^{\epsilon}$			Current (Baseline)	
	Elasticity (ε)	K (estimated)	Price (EUR/m^3)	Water used (m^3)
Livestock	-0,29	9,11	0,085	18,63
Households	-0,22	300,58	1,900	261,00
Industry (rest)	-0,29	70,12	1,112	68,00
Services	-0,38	80,40	1,900	63,00
Recreation	-0,29	0,34	0,025	1,00
Energy (cooling)	-0,894	0,37	0,025	10,00

Regarding irrigation sector, it has been modelized by dividing the basin in two main areas (upper and lower basin) and simulating present situation by crop area with the crop economic and agronomic estimated by our team based upon available data. The baseline price for irrigation is 0.06 €/m^3 although the variable part is around 30% of this figure (0.02 €/m^3) with the rest as a flat fixed component of water cost. The response of agricultural sector to water pricing has been simulated by abandoning irrigation and converting area in rainfed crops when water price makes unprofitable a specific crop. This is a simplification as some intra-sector water trade can be possible but out of the scope of this pilot analysis.

Price increase has been done by simulating the following scenarios: a) Current situation; b) Full financial

cost recovery (FCR), c) Financial cost recovery + environmental cost (FCR+EC), d) FCR + EC+ 150%, e) FRC + EC + 300% and f) FRC + EC + 500%. The values for the first two scenarios can found in (Borrego-Marín et al. 2015) and the estimation of the environmental cost is defined by the Ministry of environment and the values for Guadaquivir basin found in the mentioned hydrological plan (CHG 2015)

The impact of changes in water use by irrigation that accounts for 85% of water use is not only concentrated in agriculture but it also has a multiplier effect in the rest of the economy that has been simulated by using the value found for California agriculture (similar to Guadalquivir) in 1.4 according (Medellín-Azuara et al. 2016).

Results and concluding remarks

Table 2 illustrates the response of water demand in all sectors as the water price increases as response to the cost recovery implementation.

Table 2. Estimated water withdrawal vs. scenarios of water pricing Guadalquivir 2012.

	Gross water abstraction (hm^3)				GDP (10^6 EUR)				
	Irrigat.	**Non-Irrig**	**Total**	**% Water**	**Agr**	**Non-Agr**	**Regulatory Services**	**Total GDP**	**% GDP**
Baseline	3183	431	3614	*100*	3992	60742	47	64781	*100*
FCR	3183	399	3582	*99*	3992	60742	47	64781	*100*
FCR+EC	3183	383	3566	*99*	3992	60789	47	64828	*100*
FCR+ EC + 150%	2420	293	2713	*75*	3988	60656	71	64715	*100*
FCR + EC + 300%	1266	256	1522	*42*	3665	60488	71	64225	*99*
FCR + EC + 500%	1140	228	1368	*38*	3618	60469	71	64158	*99*

Observation of Table 2 shows that impact of extreme measures of water pricing reduces water abstraction to 38% vs baseline with the economic impact in regional GDP of 1% reduction as the agriculture (including livestock and rainfed) is only 6% of GDP. The bad news is that all the impact is supported by irrigated areas that are main activities in rural areas. The value of regulatory services estimated as the capacity of self-depuration of surface water for N and P pollution is very small compared to the water provision services in the economic sectors.

Acknowledgments: The authors have received financial support from MINECO-Grant: AGL-2014-53417-R.

References

Berbel J, Expósito A, Borrego-Marín M, Montilla-López N, Schellekens J (2018) Working document Blue2: Review of allocation regimes and water pricing."Universidad de Córdoba, WEARE

Borrego-Marín M, Gutiérrez-Martín C, Berbel J (2016) Water Productivity under Drought Conditions Estimated Using SEEA-Water. Water 8:138. https://doi.org/10.3390/w8040138

Borrego-Marín MM, Gutiérrez-Martín C, Berbel J (2015) Estimation of cost recovery ratio for water services based on the System of Enrivonmental-Economic Accounting for Water. Water Resources Management 30(2):767-783. https://doi.org/10.1007/s11269-015-1189-2

CHG (2015) Plan Hidrológico de la Demarcación Hidrográfica del Guadalquivir (2015-2021). Sevilla

Medellín-Azuara J, MacEwan D, Howitt RE, Sumner DA, Lund JR, Scheer J, Gailey R, Hart Q, Alexander ND, Arnold B (2016) Economic analysis of the 2016 California drought on agriculture. Calif. Dept. Food and Ag. UC Davis Cent. for Watershed Sci.

Reynaud A (2015) Modelling Household Water Demand in Europe—Insights from a Cross-Country Econometric Analysis of EU-28 Countries. In "JRC Technical Report EUR 27310 EN, 2015"

11th World Congress on Water Resources and Environment (EWRA 2019)
"Managing Water Resources for a Sustainable Future", 25-29 June 2019, Madrid, Spain

Structural analysis as a supporting tool in Strategic Prospective

R. Frota[1*], F.A. Souza Filho[2], R.V. Rocha[1], G.A Reis[1], V. C. Porto[1]
[1] Pursuing a doctorate´s degree in Water Resources, DEHA, UFC, Fortaleza, Brazil
[2] Professor of the Department of Hydraulic and Environmental Engineering at Federal University of Ceará
* e-mail: renata.locarno@hotmail.com

Introduction

To analyse a water resources system means to understand a double complexity: the environment and the system itself. This article proposes a method of analysis of water resources systems using strategic prospective as the main approach. The method is applied to the Jaguaribe-Metropolitan water system, located in the state of Ceará, Brazil. This system encompasses two connected basins with a large network of water transfer and faces various conflicts.

To execute the procedure, we used the Micmac (Matrix Multiplication applied to a classification) method, developed by Michel Godet in 1973. The approach allows us to identify the socioeconomic and the natural variables, and also the interrelationships existing between them. Thus, being able to identify the structure and interrelations of the socio-natural system. This representation allows the recognition of key variables and the construction of consistent scenarios for the water planning.

Prospective strategy was recently used by Abdoli et al. (2017) and Surahman et al. (2018). Both applied the approach for the construction of scenarios in different fields: development of the oil industry in Iran and sustainably agricultural in Indonesia, respectively.

Materials and methods

For the development of the study, a bibliographic survey was initially carried out to collect variables that characterize the water resources system of the state of Ceará. To describe the relationship between these variables, a square matrix was applied and called the structural analysis matrix in which the variables were related by multiple crosses. We identified 47 variables. Subsequently, the matrix was filled by actors (technicians, scientists and water users) involved in the management of water resources in Ceará. For each pair of variables, we attributed the existence or not of direct relation using the following indexes: (0) no influence; (1) weak influence; (2) average influence; (3) strong influence; (4) potential. From the 47 variables and the structural analysis matrices, a potential median matrix was created. This was evaluated by means of the MICMAC method that was developed using the software R.

The matrix can also be analysed considering the direct and indirect influences. Direct influence occurs when one variable directly affects another and vice versa. The indirect influence exists when one variable affects another and this affects a third one, therefore the first and third variable have an indirect influence. So, there is a hidden variable that in some cases can highly affect the result, being necessary to raise the matrix to a power. In this study we focused to use uniquely the direct matrix (Godet 1994).

Potential classification means that one variable has little influence over another directly, but will have a strong influence in the future (Godet 1994). Therefore, when the classification is non-potential, what has been classified as 4 (potential) becomes zero (no influence) and when it is potential, 4 (potential) becomes 3 (strong influence). For this study, we used potential classification.

The most influential and dependent variable was evaluated. The influence was given by the sum of the indices of the same row of the square matrix, while the dependency was represented by the sum of the indices of the same column. Using R, we built the influence x dependence diagram and identified the key system variables. This diagram is represented by the X-axis, the dependence, by the Y-axis, the influence, and the four quadrants. Each quadrant represents a variable profile:

- Quadrant 1 - Contains the input variables. They govern future events and are at the same time very influential and poorly dependent;
- Quadrant 2 - Contains the relay variables. These exert a high influence on the system, but it is also

very dependent, generating instability;

- Quadrant 3 - Contains the result variables. Their performance depends on the input variables;
- Quadrant 4 - Contains the excluded variables. They influence little or nothing in the system and can be eliminated.

Results and concluding remarks

The analysis performed in this study through the application of the Micmac method is a way to reflect on the behavior of the water system and to identify structural variables evaluating its influence and dependence. Assisting in the assembly of future scenarios.

We noted that 60% of the variables are relay and cause instability for the system due to its high dependence and influence on the other variables. In addition, 8.5% of variables influence little or nothing to the system and can be overlooked. 23% are strongly determined by the input and relay variables, meaning they are outcome variables. Lastly, 8.5% are high motor and low dependency and are responsible for future events.

The key variables of the system were identified: Critical hydrological events (Drought), Critical hydrological events (Flood), Climate change and Institutional Implementation of SINGERH. Droughts have historically marked Ceará and climate change has been the subject of several discussions at the global level. Managing river basins is a difficult and not trivial task. These four variables are critical uncertainties, so they outline the future and should be the basis of prospecting studies.

Acknowledgments: The authors thank National Council for the Improvement of Higher Education (CAPES), National Council for Scientific and Technological Development (CNPq) and Cearense Foundation for Scientific and Technological Development Support (FUNCAP) for the financial support.

References

Abdoli S, Habib F, Babazadeh M (2018) Making spatial development scenario for south of Bushehr province, Iran, based on strategic foresight. Environment, Development and Sustainability 20(3):1293-1309. doi: 10.1007/s10668-017-9940-x

Godet M (1994) From anticipation to action. Tradução de Clare Degenhardt. UNESCO Publishing, Paris

Grumbach RJDS, Marcial E (2008) Cenários prospectivos: como construir um futuro melhor. FGV, Rio de Janeiro

Kich JIDF, Pereira MF, Almeida MIRD, Moritz GDO (2010) Planejamento Estratégico: uma abordagem sistêmica. Revista Reuna 15(2):27-40

do Nascimento EP, Neves MJM, Christofidis D (2010) Prospecção no universo das águas: a experiência da construção de cenários no plano nacional de recursos hídricos no Brasil, 2005-2006. Geosul 25(49):27-62

Surahman A, Soni P, Shivakoti GP (2018) Improving strategies for sustainability of short-term agricultural utilization on degraded peatlands in Central Kalimantan. Environment, Development and Sustainability 21(3):1369–1389. doi: 10.1007/s10668-018-0090-6

11th World Congress on Water Resources and Environment (EWRA 2019)
"Managing Water Resources for a Sustainable Future", 25-29 June 2019, Madrid, Spain

Quantifying sensitivity to drought: Study case in São Paulo and Ceará, Brazil

G.A. Reis*, F.A. Souza Filho, R.L. Frota, L.Z.R. Rolim, T.M.N. Carvalho
Departament of Hydraulic and Environmental Eng., Federal University of Ceará, Fortaleza, Brazil
** e-mail: gabrielareisazevedo@gmail.com*

Introduction

The uncertainty in the capacity of water supply due to changes in nature and gaps in observations leads to the need for greater efficiency within the water resources management. An examination of the vulnerability of a water system is an essential step in the development of a strategy in the scope of management of drought and water safety.

IPCC (2001) divided vulnerability into three main factors: sensitivity, exposure and adaptive capacity. This paper proposes a method to quantify sensitivity to drought through the analysis of social, economic, environmental and hydric aspects. Sensitivity represents the degree of preparedness the system is in, reflecting its ability to respond to changes in the climate, whether beneficial or harmful. It also represents the system's ability to absorb impacts without suffering long-term damage or any significant changes of state (Thomas et al. 2016; Fontaine 2007; Abraham 2006).

The study was applied to the states of São Paulo and Ceará, located in southeast and northeast of Brazil, respectively. The states were chosen because they faced during this decade severe water crisis even though they present different climate characteristics and different social dynamic and economic activity.

Materials and methods

A multicriteria analysis was developed in order to calculate the sensitivity, using normalization and weighting of several indicators divided among four different sectors (social, economic, environmental and hydric conditions) composed by various indicators. The sectors present different weights and the indicators have specific weights within each sector.

The environmental sector is represented by the sanitary conditions, with weight 1, and considers the level of untreated sewage, which ends up being dumped into water bodies. With the increase of the organic load, the water bodies become unfit for use in the human supply and, consequently, in periods of drought, the number of alternatives of water sources is reduced. Drought has diverse impacts on the economic and social development of affected communities, since water is a natural resource used in the means of production and in the daily habits of the population. The precarious development of a society entails a poor preparation to deal with crises and emergencies (Veyret 2007). In this context, the social and economic aspects appear with weight 2 in the calculation of the sensitivity. Finally, the supply and demand scenarios of the population located in the study area were combined to represent the hydric conditions, which were attributed triple the importance in the sensitivity analysis considering that the study is focused on the susceptibility to a scenario of water scarcity.

The sensitivity index is then calculated by weighted average of all indicators and sectors considered. Finally, the indices were classified using the Jenks optimization (natural breaks) method and mapped for each hydrographic region of the states of São Paulo and Ceará.

Results and concluding remarks

The main results are presented by Figure 1, representing the spatial distribution of the sensitivity in Ceará and São Paulo. In both cases, the hydrographic region classified as Extreme encompasses the main metropolitan region of the state: Fortaleza Metropolitan Region (Ceará) and São Paulo Metropolitan Region. The population, GDP, and populational density are the main causes of the extremely aspect of

these regions. For the state of São Paulo, almost 30 million people are living in this extreme sensitivity to drought condition.

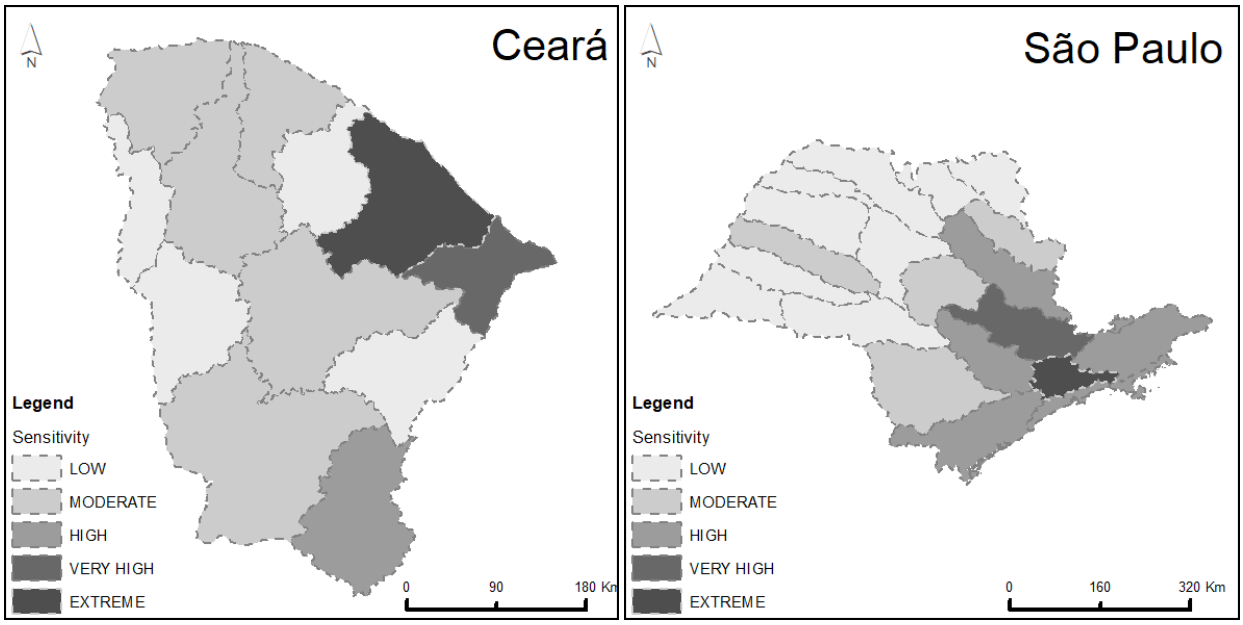

Figure 1. Spatial distribution of sensitivity to drought in Ceará and São Paulo, respectively.

It is also important to consider the vety high regions. In the state of Ceará, the Baixo Jaguaribe region was classified as very high due to the intense irrigation and shrimp farming activity, demanding high amount of water and presenting its sensitivity to water scarcity. In São Paulo, the Metropolitan Region of Campinas is also very high sensitive to drought. Its social dynamics is similar to the Metropolitan Region of Fortaleza and it has 3.2 million people.

Acknowledgments: The authors thank National Council for the Improvement of Higher Education (CAPES) and National Council for Scientific and Technological Development (CNPq) for the financial support.

References

Abraham JS (2006) Assessing drought vulnerability. University of Arizona, Arizona

Fontaine MM (2007) Assessing vulnerability to natural hazards: an impact-based method and application to drought in Washington State. University of Washington, Seattle

IPCC – Intergovernmental Panel on Climate Change (2001) Climate change 2001: Impacts, Adaptation, and Vulnerability. Contribution of Working Group II to the Third Assessment Report of the Intergovernmental Panel on Climate Change. Cambridge University Press, Cambridge and New York

Thomas T, Jaiswal RK, Galkate R, Nayak PC, Ghosh NC (2016) Drought indicators-based integrated assessment of drought vulnerability: a case study of Bundelkhand droughts in central India. Natural Hazards 81(3):1627–1652

11th World Congress on Water Resources and Environment (EWRA 2019)
"Managing Water Resources for a Sustainable Future", 25-29 June 2019, Madrid, Spain

Irrigation technology and water conservation: From panaceas to actual solutions

C. Dionisio Pérez-Blanco[1*], A. Hrast-Essenfelder[2], C. Perry[3]
[1] Department of Economics, Universidad de Salamanca, Spain
[2] Euro-Mediterranean Centre on Climate Change and Ca' Foscari University, Italy
[2] Independent Researcher
* e-mail: dionisio.perez@usal.es

Introduction

Efficiency improvements in agricultural water management that aim to increase water availability and reliability to other users (i.e. conservation) are typically formulated in two ways: i) by enhancing the *allocative efficiency* through Water Conservation Policies (WCPs) that redistribute the resource across uses (Hicks 1939); and ii) by increasing *physical irrigation efficiency* through the use of Water Conservation Technologies (WCTs) (Jensen 2007). Enhancing the *allocative efficiency* through WCPs such as charges or quotas implies a redistribution of water resources among competing uses, changing costs and benefits to users. Following the second fundamental theorem of welfare economics, these asymmetries are preferable to the *statu quo* if those who benefit from the changed policy could hypothetically compensate those who are made worse off and still be better off themselves. In practice, though, resistance to reform, institutional barriers and transaction costs (McCann 2013) have historically constrained the ability of institutional agents to solve complex water reallocation problems and achieve societal goals through WCPs. On the other hand, a growing number of water scarce regions worldwide are promoting higher *physical irrigation efficiency* through WCTs (see e.g. Perry and Steduto 2017). WCTs mostly include conversion to sprinkler or micro-irrigation systems, laser leveling of fields, piped delivery systems, canal lining, physical rehabilitation of irrigation and delivery systems, and (complementary) best management practices. The traditional assumption is that higher physical irrigation efficiency will reduce consumption of water, induce lower demand for scarce water resources *and* enhance both agricultural productivity and income *on site*. These outcomes facilitate, but do not in themselves achieve reallocation of water towards higher returns elsewhere. Nevertheless, a Pareto efficient outcome is projected, where no one is left worse off and at least one user is left better off.

The economic rationale underpinning WCTs is of course conditional on an effective contribution to water conservation targets. However, available evidence does not offer compelling arguments on the water conservation potential of WCTs. Analysts typically base their projections on field measures and estimates, which can be verified and replicated in a relatively straightforward way (Perry and Steduto 2017). In a recent literature review on the water conservation potential of drip irrigation, van der Kooij et al. (2013) noted that 44 out of 49 studies in the sample described experiments conducted at a field level in research institutes, while only one showed results from a water distribution model and only 3 articles modeled behavioral responses. Yet, water conserved at field levels cannot be generalized for other scales due to the capacity of water users to adapt e.g. by expanding irrigated land and changing the crop portfolio or management practices. On the other hand, evidence from modeling- or questionnaire-based studies that assess adaptive responses from a decision unit beyond the field scale (e.g. at farm or project scale) appears scattered and is case-specific. Validation and standardization from these studies is only possible where a critical evidence and knowledge base is reached. As a result, the scientific literature cites the paucity of quantitative data from accurately conducted WCTs research as a significant barrier in the development of sensibly designed interventions towards effective water conservation (van der Kooij et al. 2013): if WCTs contribute to increasing agricultural income and the evidence on their impacts on water conservation beyond the field scale is insufficient, an analyst looking at their performance may follow the traditional assumption that large quantities of water can be conserved by WCTs and resolve that the intervention is worthwhile, while arguing for more empirical work to better inform policy design the next time.

Materials and methods

In this paper, we investigate whether and how behavioral responses to WCTs can lead to actual water conservation and how this outcome can be supported or hampered by WCPs. After conducting a theoretical and empirical literature review on WCTs of more than 240 studies, the most extensive review to date to the best of our knowledge, this paper concludes that higher irrigation efficiency typically contributes to intensification of water scarcity through increased water consumption in the agricultural process.

Results and concluding remarks

In contrast to assumptions underpinning investment programs on WCTs, results from our review confirm that increased physical irrigation efficiency is unlikely to conserve water under commonly encountered conditions. WCTs interventions will typically lead to increased water consumption by farms and reduced return flows, which under prevalent recoverable return flow regimes will reduce water availability for other uses. This dichotomy between local irrigation efficiency and basin-wide economic efficiency occurs when WCTs increase local irrigation efficiency at the expense of reducing water availability in downstream areas –a negative externality leading to a potential decline in Pareto efficiency and equity issues. Where relinquished uses have a higher economic value than new uses, gains will be insufficient to offset losses, leading to a net welfare loss (allocatively inefficient). Only where the value of the social benefits (i.e. private benefit plus positive externalities) generated by a given WCT over its lifespan equals or exceeds the social costs (i.e. private cost plus negative externalities) will the intervention be allocatively efficient at a basin scale. However, without sensible policy guidance and *ad-hoc* WCPs this outcome is unlikely.

Acknowledgments: The research leading to these results has been funded by the Program for the Attraction of Scientific Talent under the SWAN Project.

References

Hicks JR (1939) The Foundations of Welfare Economics. Econ. J. 49:696–712. https://doi.org/10.2307/2225023

Jensen ME (2007) Beyond irrigation efficiency. Irrig. Sci. 25:233–245. https://doi.org/10.1007/s00271-007-0060-5

McCann L (2013) Transaction costs and environmental policy design. Ecol. Econ. 88:253–262

Perry C, Steduto P (2017) Does improved irrigation technology save water? A review of the evidence (Discussion paper on irrigation and sustainable water resources management in the Near East and North Africa), Regional Initiative on Water Scarcity for the Near East and North Africa. FAO, Cairo

van der Kooij S, Zwarteveen M, Boesveld H, Kuper M (2013) The efficiency of drip irrigation unpacked. Agric. Water Manag. 123:103–110. https://doi.org/10.1016/j.agwat.2013.03.014

11th World Congress on Water Resources and Environment (EWRA 2019)
"Managing Water Resources for a Sustainable Future", 25-29 June 2019, Madrid, Spain

Transitioning to sustainable groundwater use: An economic analysis of supply and demand management options in California's central valley

A. Escriva-Bou[1*], J. Medellín-Azuara[2], E. Hanak[1], J.R. Lund[3]
[1] Water Policy Center, Public Policy Institute of California, San Francisco, United States of America
[2] University of California, Merced, United States of America
[3] Center for Watershed Sciences, University of California, Davis, United States of America
* e-mail: escriva@ppic.org

Introduction

The San Joaquin Valley is home to more than four million people, half of California's agricultural output, and most of its critically overdrafted groundwater basins, where pumping exceeds replenishment. The Sustainable Groundwater Management Act of 2014 (SGMA) requires to bring groundwater basins into balance by 2040. Since agriculture is a leading economic driver in the Valley, a number of projects looking for supply augmentation and demand management are under scrutiny to avoid major economic impacts from SGMA (Hanak et al. 2017).

Materials and methods

Agriculture encompasses most water use in the Valley. To assess the economic cost of demand management solutions, we employ an agricultural economic production model (SWAP) (Howitt et al. 2012), which examines potential changes in cropping patters as result of limited access to groundwater to comply with SGMA. We connect crop production to downstream sectors including dairies, beef and processing to estimate total direct impacts of reduced water availability. Demand management alternatives include reductions in irrigated areas and deficit irrigation.

On the supply augmentation side, we study all major proposals using a marginal economic analysis. Every proposal is evaluated assessing the potential "new water" or "savings" that would provide on an annual basis, and the equivalent annual costs. To account for uncertainty, we include the likely ranges of water provided/saved and the costs of the projects.

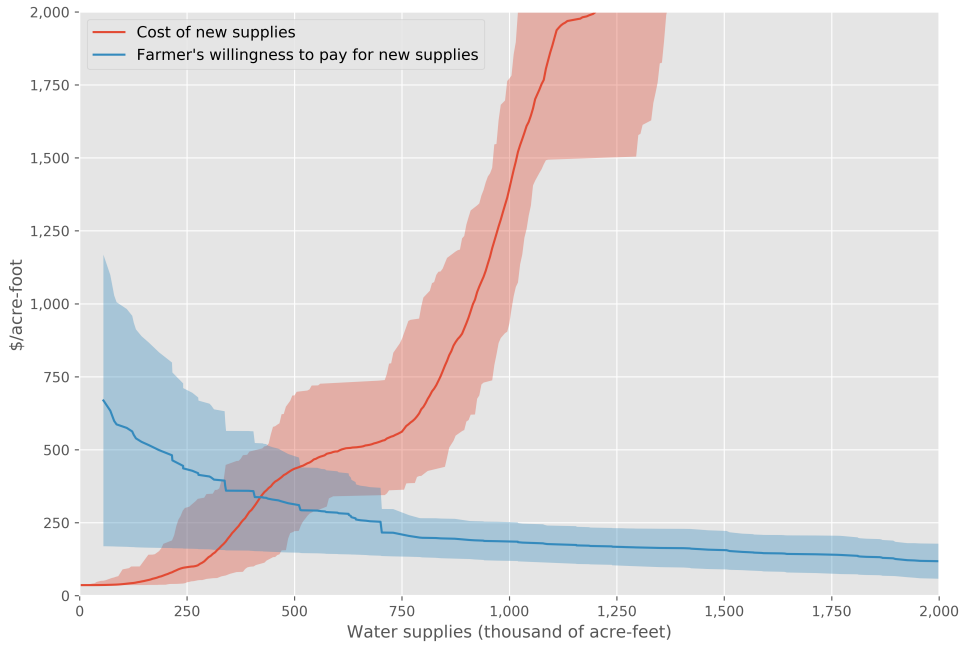

Figure 1. Cost of new supplies and farmer's willingness to pay to avoid groundwater cuts, under uncertainty.

Various demand and supply management strategies are bundled considering their uncertainties. For any future realization, we derive supply and demand curves representing marginal costs and benefits for each supply and demand management action (Figure 1). Actions selected for most realizations are considered "no-regret policy decisions". These actions are ranked to inform decision makers about promising economic pathways.

Results and concluding remarks

The analysis obtains the most promising options, and highlights the need to overcome the challenges to achieve economically desirable solutions. Groundwater recharge actions are one of the biggest hopes (Figure 2), but there is a need for cooperative agreements across groundwater basins. Water markets can also reduce the reduction of agricultural output significantly, but more flexible trading mechanisms will be essential.

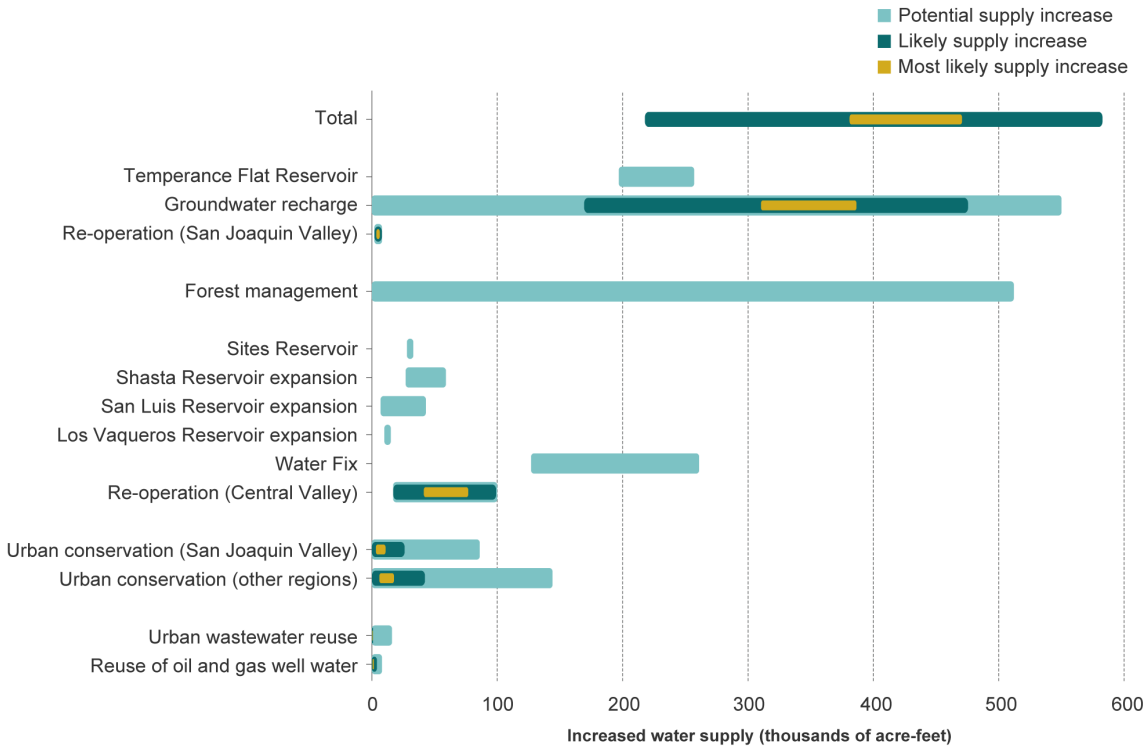

Figure 2. Likelihood of supply expansion options.

From these results, we will also discuss next stages of the project, that will focus on enhancing the ecosystem benefits of smart land fallowing—with respect to a laissez faire scenario—, and the role of the food-energy-water nexus in sustainable groundwater management. This analysis can be applied to similar irrigated areas in the world who might benefit from controlling long-term groundwater overdraft and improve future water supply reliability.

Acknowledgments: Supported with funding from the S. D. Bechtel, Jr. Foundation, the TomKat Foundation, the US Environmental Protection Agency, the US Department of Agriculture, and the Water Foundation.

References

Hanak E, Lund J, Arnold B, Escriva-Bou A, Gray B, Green S, Harter T, Howitt R, MacEwan D, Medellín-Azuara J, Moyle P, Seavy N (2017) Water stress and a changing San Joaquin Valley. Public Policy Institute of California

Howitt RE, Medellín-Azuara J, MacEwan D, Lund JR (2012) Calibrating disaggregate economic models of agricultural production and water management. Environmental Modelling and Software 38:244-258

11th World Congress on Water Resources and Environment (EWRA 2019)
"Managing Water Resources for a Sustainable Future", 25-29 June 2019, Madrid, Spain

Water values: Participatory water ecosystem services assessment in the Arno River basin

T. Pacetti[1*], G. Castelli[2], L. Cecconi[3], L. Tilli[4], E. Caporali[1], E. Bresci[2]
[1] Department of Civil and Environmental Engineering (DICEA), Università degli Studi di Firenze, Firenze, Italy
[2] Department of Agricultural, Food and Forestry Systems (GESAAF), Università degli Studi di Firenze, Firenze, Italy
[3] Rete Sviluppo – Social Research, Italy
[4] Figline-Incisa Municipality, Environment Division
* email: tommaso.pacetti@unifi.it

Introduction

Water-related Ecosystem Services (WES), namely the multiple benefits produced by water moving through the landscape (Duku et al. 2015), constitute an overlap of the biosphere and the anthroposphere (Spangenberg et al. 2014). On one hand, society acts as a driver of landscapes transformation, influencing the ecohydrological processes that underpin a large set of potential WES. On the other hand, society can be interpreted as a recipient of the WES provided by the ecosystems.

Taking advantage of hydrological modelling and social mapping techniques, the presented research focuses on the citizen-ecosystem nexus providing a sound basis to facilitate a shared watershed planning process within the EU Water Framework Directive (WFD 2000/60/EC).

Aiming at developing a transdisciplinary analysis framework to support the watershed management through the participatory evaluation of WES, the study takes into account the specific case of Figline-Incisa municipality (Tuscany Region, Italy). The territory, part of the Arno river watershed, is situated in an area where water has a strong socio-cultural and economic relevance for the citizens.

The objectives of the study are (1) to realize an assessment of the ecosystem services provided by water and land use setting in the territory of Figline-Incisa Municipality, within the Arno River basin in central Italy; (2) to carry out an analysis of the society perception regarding the value of water resources in the territory by utilizing a WES framework; (3) to develop a framework for the valuation of WES, by integrating the results of objectives (1) and (2).

The approach provides a sound basis to facilitate a shared watershed planning process within the WFD where the instances of population are combined with the experts' analysis. The conceptualization of the link between humans and environment can support the WFD in promoting wider policy objective of sustainability, moving from the achievement of a good ecological status as a target itself to the recognition of the fundamental role of the ecosystem in supporting societal goals.

Materials and methods

This study focused on the Figline-Incisa Municipality, Tuscany Region, Italy. The Municipality is located in the Arno River basin, with a territory of 98 km^2 that include the hilly territory between Valdarno and Chianti areas and the Arno River valley where the main settlements are located.

The territory is situated in an area that is deeply connected with water. The Arno River flowing in the administrative center of the Figline-Incisa Municipality and its tributaries, coming from the hilly surroundings, have a strong socio-cultural relevance for the citizens (e.g. fishing, gardening, recreation). Moreover, water represents a fundamental component of the economy of the area: besides the domestic consumption of the 23,000 inhabitants, water is used for industrial and agriculture. The river, together with its riparian areas, contributes to the landscape of the area and its touristic vocation.

At the same time, water can be a threat for the territory, especially due to hydrological extreme events. Recent drought events have jeopardized the agricultural sector and caused water rationing during summer in Incisa and Figline. On the other hand, the case study area is characterized by high flood risk as testified by several past flood events (e.g. the flood event of November 1966) that led to the realization of two

retention areas realized upstream of Figline (Galloway et al. 2017).

The proposed methodology took into account the following steps: (i) biophysical assessment of the ecosystem capacity to provide WES; (ii) preliminary evaluation of WES demand; (iii) participatory valuation of WES; (iv) scenarios analysis where the tradeoffs between different management options are highlighted.

The first step is carried out by means of simplified hydrological modeling that can provide a quantitative basis for the evaluation of the green and blue water provision as well as sediment and flow regulation. The second step focuses on water use to map WES in the area. The first two steps are developed to prepare the information that are necessary to define a common language among the participants and to support the following participatory process.

The third step is based on the use of Open Space Technology (OST) participatory methodology (Owen 1997) to involve the citizens of Figline and Incisa into the identification and valuation of the WES in their territory. The last step consists of a recap of the different perspective emerged during the participatory process to derive potential strategies that can serve as guidelines for the future territory development.

Results and concluding remarks

This study provides an overlap between social, biophysical and ecological analysis that give insights on the multiple roles that water resources have within a system (both as benefits and risks) suggesting that WES concept can facilitate an active dialogue with management institutions and all the other stakeholders.

Results allows the identification of the main WES provided by the Arno river basin to the Municipality of Figline-Incisa, their participatory valuation, and the identification of future policies to use their valuation to define different management scenarios. The inclusive approach adopted in the definition of the values of water, make clear the relationships between the citizens and the resources of the territory, highlighting their limits and potential. Water can be interpreted according to multiple scales of value: only by understanding and seeking an ideal convergence between different perspectives can lead to an effective watershed management. The work served as a pilot implementation of the Regional Law for Participation 46/2013 of Tuscany Region, as a support tool to the watershed development strategy of Arno River in integrating citizenship participation and ecosystem valuation in the management framework, as prescribed by EU Water Framework Directive as well as the more specific EU Floods Directive 2007/60/EC.

Acknowledgments: The present work is realized within the “WaterValues” Project, financed by the Tuscany Region (Italy) in the framework of the Regional Law for Participation 46/2013.

References

Duku C, Rathjens H, Zwart SJ, Hein L (2015) Towards ecosystem accounting. Hydrology and Earth System Sciences 19(10):4377-4396

Galloway G, Seminara G, Blöschl G, Garcia M, Montanari A, Solari L (2017) Saving a World Treasure: Protecting Florence from Flooding. Firenze University Press, Florence

Owen H (1997) Open Space Technology - A User's Guide. Benett-Koechler Publications, San Francisco, US

Spangenberg JH, von Haaren C, Settele J (2014) The ecosystem service cascade: Further developing the metaphor. Integrating societal processes to accommodate social processes and planning, and the case of bioenergy. Ecological Economics 104:22-32

11th World Congress on Water Resources and Environment (EWRA 2019)
"Managing Water Resources for a Sustainable Future", 25-29 June 2019, Madrid, Spain

Critical analysis of cross-subsidies between water users in the cost-recovery calculations: The Guadalquivir river basin case in Spain

C. Hervás-Gámez[1*], F. Delgado-Ramos[2]
[1] Department of Structural Mechanics and Hydraulic Engineering, University of Granada, Spain
[2] Institute of Water Research, University of Granada, Spain
* e-mail: karmina@correo.ugr.es

Introduction

Article 9 of the Water Framework Directive (WFD) establishes the application of the cost-recovery principle, including environmental and resource cost, through incentive water pricing instruments and in accordance with the polluter-pays principle. However, the forth European Commission report on the implementation of the WFD River Basin Management Plans (RBMPs) for Spain, highlighted the "lack of adequate incentives for efficient use of the resource and the adequate contribution to the recovery from different users" and recommended to present subsides and cross-subsidies transparently in the subsequent hydrological planning cycle (EC 2018).

In Spain, the cost recovery instruments are set out in the Recast Text of the Water Act (Royal Legislative Decree 1/2001, of 20 July) and the Regulation of the Hydraulic Public Domain (Royal Decree 849/1986, of 11 April). According to these, the beneficiaries of the publicly built infrastructure (dams, canals, etc) that are totally or partially funded by the State, will pay a fee (known as "Canon de Regulación") to contribute towards the investment, capital, operation and maintenance costs supported by the State.

In the upper Genil River Basin (Guadalquivir River Basin), the Canales and Quéntar reservoirs form the key infrastructures that provide surface water, primarily for urban water supply and irrigation purposes. This system is supplemented by a network of underground water wells, which were built after the serious 1992-1995 drought period by the Guadalquivir River Basin Authority (GRBA), to serve mainly Granada and its metropolitan area. This work assesses the contribution of the main competing water users to the recovery of water service cost and, in particular, whether there is a cross-subsidy among the different water users. This is, if any of the water users pay part of the cost attributable to other water users, justifying it as a theoretical greater guarantee of water supply during drought periods and water scarcity.

Materials and methods

Two alternative hypotheses have been evaluated: i) the urban water supply is assigned priority of use over agricultural demand and therefore, a 3 to 1 increase in the contribution costs is applied to the urban water supply (in line with the current GRBA methodology); ii) urban water supply and agriculture demand have the same priority of use and therefore, both contribute proportionally to the cost-recovery process. For each hypothesis, the following methodology has been carried out:

- *Modelling the water allocated to each water user based the historical monthly streamflow data series (1988-2018):* AquaSpread modelling software (own elaboration) has been used. This performs a volumetric balance on a monthly basis based on headwater inflows and water storage volume in reservoirs, environmental restrictions (ecological flows), water demands and groundwater pumping. In order to allocate the available water resources among the water users, the model takes into account the priority order assigned to each water user and water source, operating rules defined by the user (for example, the timing at which the wells will be put into operation) and other simulation settings such as the minimum, optimum and maximum storage volume in reservoirs. As a result, we obtain the volume of water consumed by each water user (urban water supply and irrigation) from each source (reservoirs and aquifer), as well as the water deficits (when the demand has not been met) for each month of the historical data series.

- *Calculation of surface water costs:* The annual surface water contribution costs by each user are calculated (known as "Canon de Regulación"), based on the monthly surface water volume consumed by each water user and for each year of the historical data series. The 2017 real costs (last year with known real data) published by the GRBA were used. The distribution coefficients of the costs among the water users were calculated based on their priority of use and in line with the current Spanish legislation and technical guidance.
- *Calculation of groundwater costs:* The annual groundwater contribution costs by each user are calculated, based on the monthly groundwater water volume consumed by each water user and for each year of the historical data series. In this case, the cost curves provided by the operating water company were used. It is important to note that the wells, even without being used, incur in a fixed monthly cost (contracted power, maintenance) which has also been considered.

Results and concluding remarks

The results show that the urban water supply pays an additional average annual cost of approximately 6,836 euros per cubic hectometre, for having a theoretical priority of water use over the agricultural demand.

However, the model simulation outputs demonstrate that if urban water supply and agriculture demand would have the same priority of use and with the optimal use of the supplementary underground wells, the current demands of the system would be met in practically all of the simulated series, with only a slight deficit in the driest year of 1995. This is, the priority of use will be only patent when all the resources of the system have been completely exhausted and are insufficient to satisfy the demands.

In fact, having priority of use does not have a significant effect on the availability of water resources during drought periods and water scarcity. This is because the drought management strategy in this river basin consists of mobilising the underground water resources in a relatively early drought phase to serve the water demand, thus avoiding or minimizing water deficits.

It is concluded that the existence of cross subsidies between water users of the same water system is one of the most important obstacles for the achievement of a rational water pricing policy consistent with the requirements of the WFD. Furthermore, it does not appear that sufficient attention has been paid to the critical role of water pricing as an effective and direct tool to communicate the real cost to the water user, which would contribute towards the achievement of a responsible, cost-efficient and sustainable consumption of water resources.

References

European Parliament and Council of the European Union (WFD) (2000) Directive 2000/60/EEC of the European Union and of the Council of 23 October 2000 establishing a framework for community action in the field of water policy. Official Journal of the European Communities, 2000, L327/1

European Commission (EC) (2018) Report on the implementation of the Water Framework Directive River Basin Management Plans Member State: Spain Accompanying the document Communication From The European Commission To The European Parliament And The Council The Water Framework Directive and the Floods Directive: Actions towards the 'good status' of EU water and to reduce flood risks SWD(2015) 56 final/2 17.7.2018

11th World Congress on Water Resources and Environment (EWRA 2019)
"Managing Water Resources for a Sustainable Future", 25-29 June 2019, Madrid, Spain

Monitoring WASH services at household and community level – Do variations exist?

J.A. Ríos-Hernández[1*], R. Giné-Garriga[2], A. Pérez-Foguet[1]
[1] Engineering Sciences and Global Development (EScGD), Civil and Environmental Enginnering Deparment, Polytechnic University of Catalonia, Barcelona, Spain
[2] Water Governance Department, Stockholm International Water Institute (SIWI), Stockholm, Sweden
* e-mail: julio.alejandro.rios@upc.edu

Introduction

In the era of the SDG's, where one of its main objectives is to guarantee universal access to water, sanitation and hygiene services (SDG 6.1 & SDG 6.2) global monitoring carry out by the Joint Monitoring Program (JMP) plays a key role tracking the progress and the progressive fulfillment of these objectives. JMP database incorporate WASH data obtained mainly from national censuses and representative household (HH) surveys (UN-Water 2018). In parallel, the sector has experienced the development of a variety of information systems (I.S.) to monitor WASH services at national or subnational level (e.g. SIASAR in Latin America, CSWA in Africa). The use of these I.S. has proven to be a useful tool to support decision-making processes and sector planning. In addition to the selection of indicators, data collection process is an important component for an effective monitoring (Bartram et al. 2014). However, since data collection through HH surveys are expensive and time-consuming activities, the described initiatives considers the community as the basic analysis unit to assess WASH services, shifting from user-based to provider-based evaluations (Requejo-Castro et al. 2017). Therefore, verifying the reliability of the data collected through this perspective is quite necessary. The aim of this study is to determine whether variations exist in the WASH status reported through different analysis units (household and community). To achieve it, WASH services were assessed using two distinct approaches: SIASAR methodology and HH surveys. In order to validate the research hypothesis, twenty rural communities in Mexico have been selected as case studies.

Materials and methods

First, two different tools were employed for data collection: structured interviews and surveys. Structured interviews were conducted with managers and technical staff of the organizations in charge of WASH services management (e.g. local water committees) which focused on determine WASH status from service provider perspective. In parallel, information related to WASH service level was captured through HH surveys, administered to household heads. For this study, the definition of adequate sample sizes followed the method proposed by (Pérez-Foguet and Giné-Garriga 2018) where those are computed from exact confidence limits for proportions (p) in terms of a given precision (e), confidence level (α) and population sizes (N). The selection of HH´s to be surveyed was completed by consulting with local leaders to identify a central point in the communities under study, and then data was collected from randomly chosen HH´s spread around the settlements. Subsequently, the proportion of HH´s (pi) that met the proposed indicators (xi) was estimated as xi/n, being xi the number of HH´s meeting the required indicator and n the total number of surveyed HH´s. To assess the precision of those estimates, confidence intervals for pi were calculated using the Clopper-Person interval corrected for finite populations. Finally, to determine if statistically significant variations exist between HH´s estimates and data reported by local water committees, a hypothesis test was conducted. For this paper, only the results for infrastructure-access indicators are discussed: Q1) access to piped water in the dwelling, Q2) access to improved sanitation, as defined by the JMP (UN-Water 2018) and Q3) availability of basic handwashing facility (with soap and water).

Table 1. Estimated proportions and confidence intervals for Q1, Q2 and Q3 indicators assessed at HH's and community level in the analysed communities.

Community	Access to piped water in the dwelling (Q1)			Access to improved sanitation (Q2)			Availability of basic handwashing facility (Q3)		
	P'	α = 0.1 Pl - Pu	Po	P'	α = 0.1 Pl - Pu	Po	P'	α = 0.1 Pl - Pu	Po
Community A (N = 122, n = 17)	0.235	0.093 - 0.446	0.492	0.941	0.761 - 0.997	0.902	0.941	0.761 - 0.997	0.492
Community B (N = 160, n = 15)	0.867	0.645 - 0.973	0.869	0.80	0.570 - 0.939	0.9	1	0.826 - 1	0.4
Community C (N = 190, n = 15)	0.667	0.431 - 0.853	0.632	0.933	0.727 - 0.997	0.947	0.933	0.727 - 0.997	0.5
Community D (N = 100, n = 14)	0.857	0.629 - 0.970	0.640	1	0.818 - 1	0.95	1	0.818 - 1	0.6

Notes: N = Community size (HH), n = Polled HH's, P' = Estimated proportion of HH's that verify the selected indicator (user-based), α = confidence level, Pl = Estimated lower confidence limit, Pu = Estimated upper confidence limit, Po = Proportion of HH's that verify the selected indicator (provider-based).

Results and concluding remarks

Table 1 presents the estimated proportions of HH's that verify the assessed indicators (p'), the confidence intervals for those estimates (Pl – Pu) and the reported proportions of HH's that met the proposed indicators (Po) by local water committees. A divergence degree can be observed in the results obtained through the different analysis units. Therefore, to determine if these variations are statistically significant a hypothesis test was conducted. Where H0: $P'=Po$ and H1: $P'\neq Po$ and a significance level (α) of 0.10 was employed. Subsequently, *Po* values were compared against the corresponding estimated confidence intervals of *P'.* Results for Q1 and Q2 show that not enough evidence exist to determine that the proportions of HH's with access to piped water and with access to improved sanitation obtained at the household and community level differ from each other. However, for Q3 statistically significant difference can be observed in the estimations of HH´s with handwashing facilities reported by local water committees and the calculated through HH´s analysis. In summary, the achieved results demonstrate that management information systems as SIASAR are capable to provide reliable information related to water and sanitation status to support sector decision-making. Nevertheless, to efficiently monitor the hygiene component and avoid undervalued or over-reporting values, assessments at household level are quite necessary.

Acknowledgments: The authors are grateful to G. Martínez (World Bank) and the State Water Commission of Oaxaca (CEA) for their support during all the stages of the study. Financial support from the National Council of Science and Technology of Mexico (CONACyT, grant ref: 541354) and the Centre for Development Cooperation of the Polytechnic University of Catalonia, Spain (CCD, project ref: 2018-O002) is gratefully acknowledged.

References

Bartram J, Brocklehurst C, Fisher MB, Luyendijk R, Hossain R (2014) Global Monitoring of Water Supply and Sanitation: History, Methods and Future Challenges. International Journal of Environmental Research and Public Health 11:8137–8165

Pérez-Foguet A, Giné-Garriga R (2018) Sampling in surveys with reduced populations: a simplified method for the water, sanitation, and hygiene sector. Waterlines 37(3):177–189

Requejo-Castro D, Giné-Garriga R, Flores-Baquero Martínez G, Rodríguez A, de Palencia Jiménez A., Pérez-Foguet A (2017) SIASAR: A country-led indicator framework for monitoring the rural water and sanitation sector in Latin America and the Caribbean. Water Practice and Technology 12(2):372–385

UN-Water (2018) Sustainable Development Goal 6: Synthesis Report on Water and Sanitation 2018. United Nations, New York

11th World Congress on Water Resources and Environment (EWRA 2019)
"Managing Water Resources for a Sustainable Future", 25-29 June 2019, Madrid, Spain

Water transfers from agriculture: The impact of land fallowing on aquifer conditions and agricultural production in northern California

E. Houk[1*], S. Mehl[2], K. Anderson[3]
[1] College of Agriculture, California State University, Chico. California, USA
[2] Department of Civil Engineering, California State University, Chico. California, USA
[3] Geosciences, California State University, Chico. California, USA
* e-mail: ehouk@csuchico.edu

Introduction

California has one of the largest, most productive, and most controversially managed water systems in the world (Hundley 2001). While the majority of California's fresh water supplies are located in the northern part of the state, the majority of the water demand occurs in the south. As such, large federal and state projects have been developed in order to transfer northern water supplies to southern water users. This ability to transfer water has placed more pressure upon northern California farmers to transfer their water and fallow their land and/or increase groundwater pumping to offset these transfers. However, some regions of California have local measures that prohibit increasing groundwater pumping and farmers must fallow their land and reduce production if they transfer their surface water. This is especially true for California rice farmers, who produced over US$750 ,000,000 worth of rice on approximately 500,000 acres (approximately 200,000 hectares) in 2017 (CDFA 2017). Although water is already being transferred from northern California rice farms and land is regularly being fallowed, the impact of these land fallowing decisions are often not well understood.

This study examines the impact of short and long-term water transfer induced rice land fallowing by identifying the impact on agricultural production (including regional impacts) and estimating the impact on regional aquifer levels.

Materials and methods

Although fallowing agricultural land will reduce total water consumption in the region, it can also reduce a source of local groundwater recharge. This is because rice farmers in northern California primarily apply surface water that has been diverted out of the river and the rice crop does not consume all of the water applied to the filed. The remaining water either evaporates, returns to surface water channels, or infiltrates into the ground. Because of the latter, water applied for agriculture can be a source of recharge to local aquifers. Consequentially, fallowing a field that has typically been irrigated can remove a source of potential groundwater recharge. This project models those impacts to demonstrate how fallowing rice fields in northern California could negatively affect the regional economy and aquifer conditions. This is done by first developing a set of potential land fallowing scenarios. The scenarios were identified by randomly selecting rice fields within the study area in five percent increments and changing the modeled land use to represent increased rice field fallowing (from 5% to 50% total rice field fallowing). To understand the difference between short-term and long-term changes, one set of scenarios reflect single year land fallowing while a second set represented ten consecutive years of land fallowing. The scenarios were first evaluated using the United States Geological Survey's (USGS) Central Valley Hydrologic Model (CVHM). The CVHM is built with MODFLOW, a three- dimensional finite-difference groundwater model that has become the international standard for simulating and predicting groundwater conditions (Faunt 2009). The CVHM allows us to predict the spatial and temporal effects of each scenario on the regional water table elevation. To view the distribution of these impacts across the region and over time, the results are presented graphically using ArcGIS. In addition to the impacts on aquifer conditions, the value of foregone rice production is estimated and the impact on the regional economy was modeled using IMPLAN (IMpact analysis for PLANning) Pro (IMPLAN 2017).

Results and concluding remarks

All modeled rice field fallowing scenarios showed decreased aquifer recharge and a reduced volume of groundwater storage within the study area. The magnitude of maximum storage loss increased as the proportion of single year fallow rice fields increased. Each five-percent increase in single year fallowing corresponds to a mean of about 67,000 acre-feet (82,643,160 m^3) of additional aquifer storage loss, but the aquifer would begin to recover in the following years as cropping patterns returned to normal. The ten-year continuous fallow scenarios showed a compounded effect with even larger losses in aquifer storage and no recovery as expected (Anderson et al. 2017). In addition, this study found that the lost value of rice production could have a negative impact on the regional economy through various multiplier (indirect and induced) effects.

Acknowledgments: Partial funding for this project has been provided by the California State University Agricultural Research Institute (ARI).

References

Anderson K, Houk E, Mehl S, Brown D (2017) The Modeled Effects of Rice Field Idling on Groundwater Storage in California's Sacramento Valley. Journal of Water Resource and Protection 9:786-798. doi: 10.4236/jwarp.2017.97052

California Department of Food and Agriculture (2017) California County Agricultural Commissioners' Reports, 2017. https://www.cdfa.ca.gov/statistics/

Faunt C (2009) Groundwater Availability of the Central Valley Aquifer, California. U.S. Geological Survey Professional Paper 1766

Hundley N (2001) The great thirst: Californians and water. University of California Press, Berkeley, California

IMPLAN (2017) IMPLAN Group LLC, IMPLAN Pro System. http://www.implan.com

11th World Congress on Water Resources and Environment (EWRA 2019)
"Managing Water Resources for a Sustainable Future", 25-29 June 2019, Madrid, Spain

Water rights valuation at Atacama Desert, Chile: Transactions characteristics and price dispersion

L. Mateo-Peinado[1*], L. Roco[1,2], M. Prieto[3]
[1] *Departamento de Economía, Universidad Católica del Norte, Antofagasta, Chile*
[2] *IDEAR, Universidad Católica del Norte, Antofagasta, Chile*
[3] *Instituto de Investigaciones Arqueológicas y Museo R.P.G. Le Paige, Universidad Católica del Norte, San Pedro de Atacama, Chile*
** e-mail: lmateo@ucn.cl*

Introduction

World water demand raises because of economic development together with population growth and its supply declines due to climate change (Vörösmartyet al. 2000; Endo et al. 2018). Chile is a world reference managing this scarce resource through water rights markets (Bauer 2004, 2008; World Bank 2011; Prieto 2016). On one side, certain authors (Rosgrant and Gazmuri 1995; Hearne and Easter 1995; Briscoe 1996; Quentin et al. 2012; Donoso et al. 2014; Donoso 2018) have found evidence favoring water rights markets as an assigning mechanism for the Chilean case. They point out the institutional design is efficient, since it contributes to assign the scarce resource towards its most productive ends. These researches consider small basins within Chile, where the agricultural production is the main activity, spatially restricted to the country's central regions in which water the hydric balances are positive or at least balanced (Valdés-Pineda et al. 2016). On the other side, some authors point out that the Chilean design is not efficient, and also has contributed to generate social tensions, among other problems (Bauer 2004, 2008; Prieto 2016). Both sides agree that more empirical research is necessary to assess the Chilean institutional design and the water market performance as a scarce resource assigning mechanism.

This research aims to assess how the Chilean institutional water right market design has assigned the scarce resource on conditions of extreme scarcity at Antofagasta region, in the hyper-arid Atacama Desert. The water availability represents 0,03% of the international threshold considered by the World Bank (2011) for sustainable economic development. There is a wide variety of agents using water towards multiple productive uses: mining industry, individual farmers, indigenous communities, farmers associations, among others. This case study is relevant for evidencing how the Chilean institutional design performs assigning the scarce resource on extreme scarcity conditions and in the presence of a variety of actors concurring at the market.

Materials and methods

The data source accounts for water rights official transactions transcription from to the year 1983 (market started operating) to the year 2017, extracted from the Conservador de Bienes Raícesat Calama (the legal body entitled for the water rights record). From 2897 transactions registered, the sample selected considers 962 buying and selling transactions performed over continuous water rights.

Price statistics for transactions evidence wide price dispersion: this might be an imperfect competition sign or a lack of market maturity (Colby et al. 1993; Lee and Jouravlev 1998; Brookshire et al. 2004; Brooks and Harris 2008). Therefore, we suppose that water rights are a non-homogeneous production factor. Then, we use hedonic price regression methodology to better understand in which measure each water right attribute considered contributes to conform marginally buying and selling transaction prices.

Results and concluding remarks

Results point out that the mining industry will pay on the average a price 300% higher for water rights compared to transactions produced among farmers. Agricultural associations and indigenous communities will pay over 100% than transaction produced among farmers. On the supply side, certain agents are not

selling their rights in the market, such as indigenous communities or farmers associations, rather an accumulation process occurs. These results point out that the water rights at Atacama Desert behave as a non-homogeneous production factor evidencing a sign of imperfect competition. This could explain why this market is far from reaching an equilibrium price, even if some water rights are being assigned to its most productive ends (i.e. mining industry). Also, we find intermediaries between farmers and the mining industry which could evidence transaction costs.

This evidence towards imperfect competition calls for additional research to assess the Chilean institutional design concerning the water right market functioning on conditions of extreme scarcity.

Acknowledgments: This work was funded by the CONICYT PFCHA/DOCTORADO NACIONAL BECAS CHILE/2018 – 21181753. Data source is a project research outcome from Fondecyt de Iniciación en Investigación 2015 nº 11150130.

References

Bauer CJ (2004) Siren song: Chilean water law as a model for international reform. Routledge

Bauer CJ (2008) The experience of Chilean water markets. Management 3:146-165

Briscoe J (1996) Water as an economic good: The idea and what it means in practice. Paper presented at the World Congress of International Commission on Irrigation and Drainage, Cairo, Egypt

Brooks R, Harris E (2008) Efficiency gains from water markets: empirical analysis of Watermove in Australia. Agricultural Water Management 95(4):391-399

Brookshire DS, Colby B, Ewers M, Ganderton PT (2004) Market prices for water in the semiarid West of the United States. Water Resources Research 40(9):W09S04

Colby BG, Crandall K, Bush DB (1993) Water right transactions: market values and price dispersion. Water Resources Research 29(6):1565-1572

Hearne R, Easter KW (1995) Water allocation and water markets an analysis of gains-from-trade in Chile. World Bank, Washington, DC

Donoso G, Melo O, Jordán C (2014) Estimating water rights demand and supply: Are non-market factors important? Water Resources Management 28(12):4201-4218

Donoso G (2018) Overall Assessment of Chile's Water Policy and Its Challenges. Water Policy in Chile, pp 209-219

Endo T, Kakinuma K, Yoshikawa S, Kanae S (2018) Are water markets globally applicable? Environmental Research Letters 13(3):034032

Lee TR, Jouravlev A (1998) Los precios, la propiedad y los mercados en la asignación del agua.

Prieto M (2016) Bringing water markets down to Chile's Atacama Desert. Water International 41(2):191-212

Quentin Grafton R, Libecap G, McGlennon S, Landryj C, O'Brien B (2012) An integrated assessment of water markets: a cross-country comparison. Rev Environ Econ Policy 5(2):219–239

Rosegrant WM, Gazmuri R (1994) Reforming water allocation policy through markets in tradable water rights: lessons from Chile, Mexico and California. EPTD discussion paper Nı 6, IFPRI

Valdés-Pineda R, Pizarro R, García-Chevesich P, Valdés JB, Olivares C, Vera M. et al. (2014) Water governance in Chile: Availability, management and climate change. Journal of Hydrology 519:2538-2567

Vörösmarty CJ, Green P, Salisbury J, Lammers RB (2000) Global water resources: vulnerability from climate change and population growth. Science 289(5477):284-288

World Bank (2011) Chile: Diagnóstico de la gestión de los recursos hídricos. No. 63392

11th World Congress on Water Resources and Environment (EWRA 2019)
"Managing Water Resources for a Sustainable Future", 25-29 June 2019, Madrid, Spain

Identification of correlation between residential demand and average income using pool regression model

G.A. Reis*, F.A. Souza Filho, T.A. Oliveira, L.Z.R. Rolim, T.M.N. Carvalho
Department of Hydraulic and Environmental Eng., Federal University of Ceará, Fortaleza, Brazil
** e-mail: gabrielareisazevedo@gmail.com*

Introduction

In the face of increasingly frequent water crises, human supply becomes an even more complex challenge. In large urban centers, due to changes in consumption patterns, the values of residential water demand are high. The need for an offer that meets this growing demand pushes decision makers to an analysis of increasingly critical scenarios in order to achieve a balance in supply and demand (Fielding et al. 2013). The decision-making process, when done from a robust, technical and scientific base, promotes benefits and efficiencies that result in positive impacts at all levels: social, economic and environmental. In order to provide subsidies for the decision-making process, this paper proposes to analyze the variation of demand in urban centers through the application of a pool regression model, seeking to identify the existence of some statistical correlation between the water consumption variation pattern and mean income. The area of application is the city of Fortaleza, in the northeast of Brazil.

Materials and methods

We have used monthly water demand data on a local scale, from 2009 to 2017, where each scale unit is called "census sector". In the first stage, we have grouped the monthly data into annual data and the acquired *per capita* values. Census sectors with no population were removed. These are unpopulated green areas. In order to avoid tabular error, demands with a zero value and greater than 1000 L/hab.day were also removed.

The first regression analysis was implemented using annual demand data and time values, through the software of statistical analysis R. The demand data were represented by $D_{i,t}$ so that i was the index indicating the census sector and t was the corresponding year. To simplify the data, the years were represented with integers beginning at 0 (2009) until 8 (2017). A second degree linear regression was developed, aiming to obtain a regression equation between the demand and the year of each sector (Equation 1).

$$D_{i,t} = \beta_i^1 + \beta_i^2 t + \beta_i^3 t^2 \quad (1)$$

We obtained three coefficients for each sector, in order to analyze the correlation of each of them with the average income data of the sectors. Thus, three equations were elaborated (Equations 2, 3, and 4) which by linear regression related each coefficient to average income.

$$\beta_i^1 = \alpha R_i + \alpha_0 \quad (2) \qquad \beta_i^2 = \gamma R_i + \gamma_0 \quad (3) \qquad \beta_i^3 = \delta R_i + \delta_0 \quad (4)$$

Results and concluding remarks

The demand data were grouped in order to organize a large matrix with 2993 sectors and their respective *per capita* demands. Due to pre-processing, this table was reduced to 2952 sectors considered with adequate data. After this processing, the linear regression of the second degree was performed, in order to obtain the three coefficients of each sector. Then, the linear regression equation was established between each coefficient and the income, in order to obtain the following relations:

$$\beta^1 = 86{,}102 R_i + 0{,}011 \quad (5) \qquad \beta^2 = 5{,}587 R_i + 0{,}0007 \quad (6) \qquad \beta^3 = -0{,}8217 R_i - 0{,}0001 \quad (7)$$

It is worth mentioning that the coefficient β^1 is the interceptor of the second degree equation, which means the demand value when the time (t) was 0 (initial year of 2009). To illustrate the above linear regressions, the graphs in Figures 1 and 2 were generated.

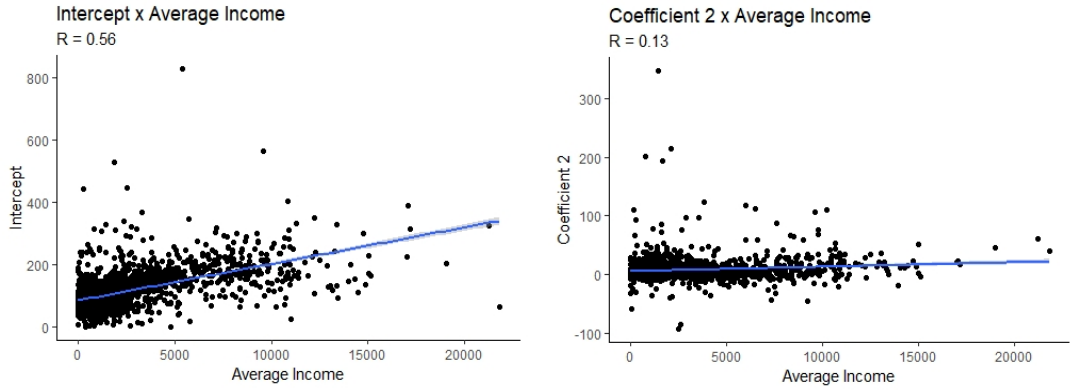

Figure 1. Regression graphs of intercepts with average income and with coefficients 1 and average income, respectively.

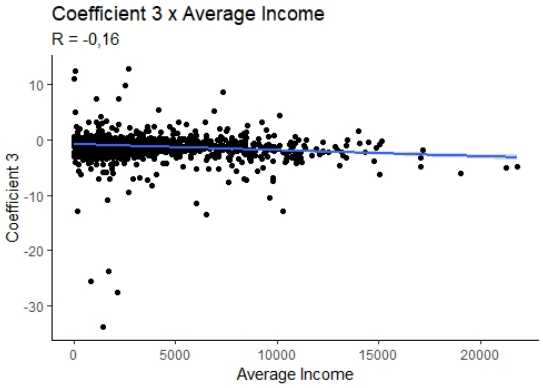

Figure 2. Regression graph between coefficients 3 with average income.

Considering the correlation coefficient (R) of each regression it is possible to analyze that the relation presented a slightly significant correlation (R = 0.56) in relation to the intercepts with the average incomes, however, the correlations of coefficients 2 and 3 were low (0.13 and -0.16, respectively). In view of this situation, we can infer that the average income of the sector has a stronger directly proportional relation with the intercept of demand, that is, with the initial value of demand. Another point to be evaluated is that in the regressions of coefficients 2 and 3 the regression lines presented a low slope, showing that when varying the income the coefficients presented a reduced variation. We can deduce that, in general, the Fortaleza sectors presented a similar variation between 2009 and 2017 since the coefficients present similar values. Thus, it is not possible to estimate a relation between the demand and the time of each sector from the knowledge of the sector's average income, because it does not explain the coefficients of variation (2 and 3).

Finally, it's recommended for a more complex analysis that the series of demand data be more extensive as well as the average income considered in each sector being estimated from a time series, not only of a specific year, as was done in this study which considered only the average income of 2010.

Acknowledgments: The authors thank National Council for the Improvement of Higher Education (CAPES) and National Council for Scientific and Technological Development (CNPq) for the financial support.

References

Gelman A, Hill J (2006) Data analysis using regression and multilevel/hierarchical models. Cambridge University Press, Cambridge

Fielding KS, Spinks A, Russell S, McCrea R, Stewart R, Gardners J (2013) An experimental test of voluntary strategies to promote urban water demand management. Journal of Environmental Management 114:343-351

11th World Congress on Water Resources and Environment (EWRA 2019)
"Managing Water Resources for a Sustainable Future", 25-29 June 2019, Madrid, Spain

Mapping water scarcity in India using Water Poverty Index

A. Chopra*, P. Ramachandaran
Department of Management Studies, Indian Institute of Science, Bangalore, India
** e-mail: ashishc@iisc.ac.in*

Introduction

For a country like India, it's a matter of concern as nearly 600 million people face high to extreme stress (Addams et al. 2009). India ranks 120th among 122 countries in water quality index (Aayog 2018). As water scarcity is not only concerned about the physical non-availability of water resources but also arises due to lack of proper access to clean water and improved sanitation, low water use efficiency, water pollution and mismanagement. It's important to quantify water scarcity from multidimensional perspective. Also, it is interesting to see how different states in India are managing their water resources as they all are having their own geo-political challenges.

It is evident from the literature that research lack in the multidimensional approach that is required to mitigate the problem in water resource management (Sullivan 2006). Water Poverty Index (WPI) is one such multidimensional index which have been used worldwide to capture the multidimensional aspect of water scarcity. Moreover, WPI has not been applied to analyse the water scarcity situation at state level in India. Hence, the main objective of this paper is to map water scarcity in different states of India and to compare their performance using WPI.

Materials and methods

Water Poverty Index (WPI) was developed by researchers from UK back in 2002 for integrated assessment of water stress and scarcity (Sullivan 2002). It's a multidimension index, which not only consider the physical availability of water but also consider socioeconomic factors while evaluating water scarcity. It is having five dimensions namely Resources (R), Access (A), Capacity (C), Use (U) and Environment (E). These different dimensions are trying to capture different aspects of water scarcity that are important for overall water sector performance and its management.

All these five components are ranging from 0 to 1. The WPI is an aggregated score calculated using a weighted average of its five components and equal weights have been given to all the components. Final WPI score is in the range of 0 to 100, which can be obtained by multiplying the weighted average score by 100.

Literature review of WPI shows that a number of WPI have been developed all around the world to quantify water scarcity at different scales for e.g. International (Jemmali 2016), National (Heidecke 2006), Basin and Sub-basin (Manandhar 2012) and Community (Wilk 2013). Number of combinations of different variables divided among the basic five dimensions is used to compute the WPI as per the requirement of scale and data availability (Garriga 2010).

For our analysis, we have used total 20 different variables in order to quantify the different aspect of water scarcity in India. These 20 variables are used to calculate the aggregate value of the main five components of WPI. In this study we choose 11 different major states of India to see and compare the effect of these different variables on the water sector and its performance. Andhra Pradesh, Bihar, Gujrat, Haryana, Karnataka, Kerala, Maharashtra, Madhya Pradesh, Punjab, Tamil Nadu and Uttar Pradesh are the states used for this study.

Data regarding these 20 variables for these 11 states was collected from different sources i.e. state and central government published reports and websites, planning commission reports, central ground water board and RBI etc. The normalization of the data was done using min-max approach and value of all these variables ranges from 0 to 1.

Results and concluding remarks

The normalized score of these 20 variables, was then used to calculate the final WPI score. The aggregated score of different dimensions and WPI for these 11 states is given in table 1.

Table 1. Water Poverty Index(WPI) for 11 states of India

State	R_agg	A_agg	C_agg	U_agg	E_agg	WPI
Punjab	0.7	0.94	0.57	0.57	0.27	59.8
Haryana	0.54	0.89	0.61	0.70	0.13	57.64
Kerala	0.53	0.56	0.59	0.29	0.81	55.71
Maharashtra	0.62	0.43	0.67	0.19	0.65	51.25
Tamil Nadu	0.56	0.60	0.63	0.15	0.56	50.16
Andhra Pradesh	0.69	0.52	0.47	0.30	0.47	49
Gujrat	0.59	0.44	0.51	0.31	0.54	48.01
Madhya Pradesh	0.69	0.18	0.47	0.40	0.62	47.45
Karnataka	0.39	0.42	0.62	0.31	0.5	44.7
Bihar	0.45	0.41	0.29	0.24	0.58	39.41
Uttar Pradesh	0.53	0.6	0.34	0.12	0.34	38.51

Results shows that if we give equal importance to all the five dimensions then the top performing state is Punjab followed by Haryana and Kerala while Bihar and Uttar Pradesh are the least performing states. It is difficult to tell about the importance of one dimension or variables as for this analysis equal weights have been used.

Although WPI have been used at different scales but it has its own shortcomings. Major concern is about the subjectivity of weights being used for calculating the final Index (Molle 2003). In order to improve this methodology, number of methods has been used by researchers to overcome these limitations.

This is one of its kind study, in Indian context, which have used WPI to analyse water scarcity at state level. In India, water is a state subject and hence this analysis can be useful for the policymakers to prioritise and make future water policies by taking the multidimensional aspect of water scarcity.

References

Aayog NA (2018) Composite water management index: a tool for water management. NITI Aayog, Government of India, Delhi

Addams L, Boccaletti G, Kerlin M, Stuchtey M (2009) Charting our water future: Economic frameworks to inform decision-making. McKinsey & Company, New York

Garriga RG (2010) Improved method to calculate a water poverty index at local scale. Journal of Environmental Engineering 136(11):1287-1298

Heidecke C (2006) Development and evaluation of a regional water poverty index for Benin. Intl Food Policy Res Inst

Jemmali HA-G (2016) Multidimensional analysis of the water-poverty nexus using a modified Water Poverty Index: a case study from Jordan. Water Policy 18(4):826-843

Manandhar SA (2012) Application of water poverty index (WPI) in Nepalese context: a case study of Kali Gandaki River Basin (KGRB). Water Resources Management 26(1):89-107

Molle FA (2003) Water poverty indicators: conceptual problems and policy issues. Water Policy 5:529-544

Sullivan C (2002) Calculating a water poverty index. World Development 30(7):1195-1210

Sullivan CA (2006) Application of the Water Poverty Index at Different Scales: A Cautionary Tale. Water International 31(3):412-426

Wilk JA (2013) From water poverty to water prosperity—a more participatory approach to studying local water resources management. Water Resources Management 27(3):695-713

11th World Congress on Water Resources and Environment (EWRA 2019)
"Managing Water Resources for a Sustainable Future", 25-29 June 2019, Madrid, Spain

A protocol-based integrated microeconomic Positive Multi-Attribute Utility Programming and HEC-HMS modeling framework to assess economic efficiency-water conservation tradeoffs in water reallocation policies

H. González López[1], C.D. Pérez-Blanco[1], A. Hrast-Essenfelder[2]
[1] Department of Economics and Economic History, Universidad de Salamanca, Spain
[2] Centro Euro-Mediterraneo sui Cambiamenti Climatici and Università Ca' Foscari di Venezia, Italy
* e-mail: hector.gonzalez.lopez@usal.es

Introduction

Water demand is increasing due to population growth and changing distributions of wealth (OECD 2015), and climate change is reducing water availability in arid and semi-arid basins (Bates et al. 2008). The combined effects of growing demand and diminishing supply will cause relevant impacts on the environment and the economy, particularly the agricultural sector, the largest water user and that concentrating the marginal uses (i.e. least valuable) of the resource. Policies that reallocate available water among users are necessary to mitigate economic losses and ensure sufficient resources are conserved for the environment. To this end, Spanish river basin authorities have developed Drought Management Plans (DMPs) aiming at minimizing the environmental, economic and social impacts of drought episodes. DMPs define drought indices and apply temporary water restrictions, which are now under revision to adapt to most recent socioeconomic and climatic changes and forecasts (CHT 2017). In defining drought indices and restrictions, hydrologic and economic information plays a critical role: it informs policy makers on the economic and environmental outcomes of projected policies and the relevant tradeoffs between them, and thus prevents maladaptation. This study presents a methodological framework to couple a microeconomic Positive Multi-Attribute Utility Programming (PMAUP) model that represents the behavior of economic agents and simulates their policy responses with a Hydrologic Modeling System (HEC-HMS) designed to simulate the precipitation-runoff processes of dendritic basins. While the HEC-HMS model is a popular tool for the development of hydrologic applications this is, to the best of our knowledge, the first study that uses the HEC-HMS model in concert with an agricultural economics module. The coupling between the PMAUP and HEC-HMS models occurs in a sequential, modular fashion through common spatial (land use and land use changes) and water availability variables (water yield and availability). The resulting coupled PMAUP - HEC-HMS model seeks to represent the feedback between the behavior of socio-economic agents and their impact on land use and water availability. The integrated model is illustrated by simulating the impacts of alternative drought episodes and the corresponding irrigation restrictions foreseen under the new Tagus River Basin DMP in the Upper Tagus Sub-basin in the center of the Iberian Peninsula.

Materials and methods

Under the current Drought Management Plans, irrigation restrictions are based on the water stock available in reservoirs and streamflow. These indicators are used to obtain a state index that assesses the scarcity situation in accordance to four levels: normality, pre-alert, alert and emergency. When the indicator goes below a predetermined threshold, a predefined amount of water is relinquished from users, which can cause changes in the crop portfolio and related land use and management. This response is assessed through a Positive Multi-Attribute Utility Programming (PMAUP) that simulates the behaviour of socioeconomic agents and their impacts on land uses (and related impacts on employment, gross margin, etc.) according to water availability in each drought scenario.

On the other hand, the hydrologic semidistributed model HEC-HMS is used to assess the climatic, physical and ecological variables (e.g. precipitation, ground surface and vegetation) at a basin scale. The basin is divided into sub-basins, and streamflows are estimated at the outlet of each sub-basin. Sub-basins are divided into smaller units that share a common land use. This subdivision allows the HEC-HMS model to

reproduce land use changes emerging from the simulation of water policies as predicted by the PMAUP model.

The proposed integrated hydroeconomic modeling framework operates through an iterative modular approach that runs the microeconomic and hydrologic modules independently; modules, in turn, are connected and exchange information through protocols, i.e. rules designed to manage relationships and processes between modules, which enable the simulation of the interconnected dynamics and feedback responses between human-water and human-human systems.

Results and concluding remarks

The success of adaptive actions and policy design in social-ecological systems is determined by our understanding of the dynamics of human-water systems (Essenfelder et al. 2018). This paper presents a coupling exercise that offers insights into the socioeconomic and hydrologic repercussions of water conservation policies, and the two-way feedbacks at the human-water interface. Thus far, the study has developed the coupling methodology and calibrated both models, and authors are now working on preliminary simulations. The next step is to fine-tune the coupling and feedback protocols between the HEC-HMS and PMAUP models, and obtain the final results.

Acknowledgments: The research leading to these results has been funded by the Program for the Attraction of Scientific Talent under the SWAN Project.

References

Bates et al. (2008) Climate Change and Water. Intergovernmental Panel on Climate Change. http://hdl.handle.net/123456789/552

CHT (2017) Plan Especial de Sequía. Ministerio de Agricultura y Pesca, Alimentación Y Medio Ambiente. http://www.chtajo.es/LaCuenca/Planes/Documents/20171222%20Borrador%20PES%20para%20consulta%20p%C3%BAblica.pdf

Essenfelder AH, Pérez-Blanco CD, Mayer AS (2018) Rationalizing Systems Analysis for the Evaluation of Adaptation Strategies in Complex Human-Water Systems. Earth's Future 6. https://doi.org/10.1029/2018EF000826

OECD (2015) Water Resources Allocation.Sharing risks and opportunities. OECD Studies on Water. https://read.oecd-ilibrary.org/environment/water-resources-allocation_9789264229631-en#page1

11th World Congress on Water Resources and Environment (EWRA 2019)
"Managing Water Resources for a Sustainable Future", 25-29 June 2019, Madrid, Spain

Monitoring the access to water, sanitation and hygiene in the MENA region: Survey errors and compositional nature

F. Ezbakhe*, A. Pérez-Foguet
Research Group on Engineering Sciences and Global Development, Department of Civil and Environmental Engineering, School of Civil Engineering, Universitat Politècnica de Catalunya BarcelonaTech, Barcelona, Spain
** e-mail: fatine.ezbakhe@upc.edu*

Introduction

In the Middle East and North African (MENA) region, access to safe drinking water, sanitation and hygiene (WASH) has increased significantly over the last decades. According to WHO/UNICEF Joint Monitoring Programme (JMP) estimates, coverage of improved drinking water rose from 89% in 2000 to 93% in 2015, and from 84% to 90% for improved sanitation. While these trends in WASH service levels are encouraging, there is a substantial heterogeneity between countries (Fullet et al. 2016). For instance, while countries like Morocco, Tunisia and Egypt have made substantial progress (with a coverage above 80% for both water and sanitation in 2015), others like Mauritania have stagnated.

Furthermore, in estimating these trends in WASH coverage, two key issues are overlooked: (i) *the survey errors* in data sources and (ii) the *compositional nature* of the data. While the problem of compositional data (i.e. populations in the JMP dataset are not independent of each other, but rather related by being expressed as percentage of the total) has been recently addressed by Pérez-Foguet et al. (2017), the issue of the statistical uncertainty underlying data estimates remains untackled. However, these errors must be considered when interpreting and using coverage estimates derived from household surveys (Ezbakhe and Pérez-Foguet 2018).

In this work, we examine the importance of including survey errors when developing coverage trends. We study the case of Morocco, a country with a relatively high access to improved drinking water and sanitation, but with a significant component of sampling error in its JMP estimates. By doing so, we aim to illustrate the importance of taking into account the error of estimates when assessing trends over time or comparing coverage between countries.

Materials and methods

We select Morocco as an initial case study. The JMP estimates for water coverage in urban areas are shown in Figure 1 (blue: improved water; red: unimproved water).

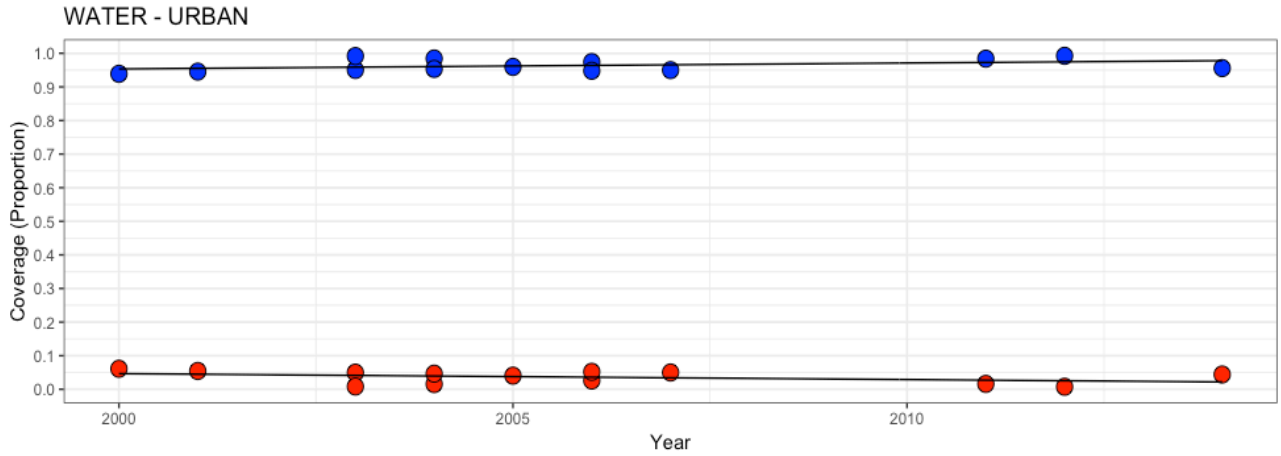

Figure 1. Coverage of water in urban Morocco (improved in blue and unimproved in red). Source: JMP estimates

However, these estimates have a component of uncertainty due to survey errors, as well as a compositional nature. Therefore, we develop a methodology that includes both components, which can be summarized in the next steps:

- Obtaining the sampling errors of JMP estimates from household surveys.
- Translating these errors to the space of compositional data through the use of extended Beta distribution and Monte Carlo simulations.
- Employing isometric log-ratio transformation (ilr) for maintaining the compositional nature of the data in statistical analysis.

Results and concluding remarks

Preliminary results show the importance of including survey errors when developing coverage trends. For instance, in the case of coverage of improved access to water in urban Morocco (Figure 2), the statistical uncertainty underlying the estimates leads to wide confidence bands. Also, our methodology of reinterpreting survey errors with the use of extended Beta distributions and Monte Carlo simulations allows for a simple way of including the survey errors of the data, and its compositional nature, when performing statistical analysis of JMP data.

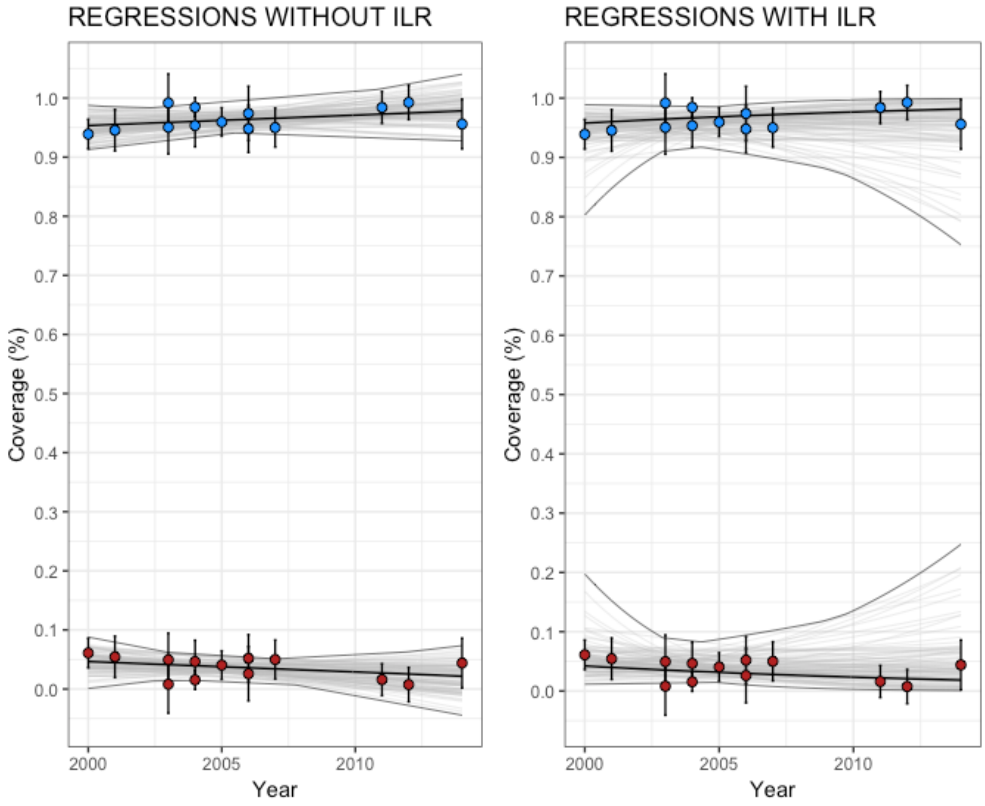

Figure 2. Regression analysis (ordinary least squares) of water coverage in urban Morocco, without (left) and with ilr (right). (Legend - Blue dots: JMP estimates for improved water; Red dots: JMP estimates for unimproved water).

References

Ezbakhe F, Pérez-Foguet A (2018) Multi-criteria decision analysis under uncertainty: two approaches to incorporating data uncertainty into water, sanitation and hygiene planning. Water Resources Management 32(15):5169-5182. http://doi.org/10.1007/s11269-018-2152-9

Fuller JA, Goldstick J, Bartram J, Eisenberg JNS (2016) Tracking progress towards global drinking water and sanitation targets: A within and among country analysis. Science of the Total Environment 541:857-864. https://doi.org/10.1016/j.scitotenv.2015.09.130

Pérez-Foguet A, Giné-Garriga R, Ortego MI (2017) Compositional data for global monitoring: The case of drinking water and sanitation. Science of the Total Environment 590-591:554-565. https://doi.org/10.1016/j.scitotenv.2017.02.220

11th World Congress on Water Resources and Environment (EWRA 2019)
"Managing Water Resources for a Sustainable Future", 25-29 June 2019, Madrid, Spain

Managing uncertainties in the decision-making process within water users association

Z. Srđević*, B. Srđević
Faculty of Agriculture, Department of Water Management, University of Novi Sad, Novi Sad, Serbia
** e-mail: srdjevicz@polj.uns.ac.rs*

Introduction

There are important issues related to the decision-making processes within water users associations (WUAs). Internal structure of the WUA means that: (1) there are required normative documents; (2) administrative personnel are in place; and (3) mechanisms will be provided to the water users (primarily farmers) to participate in making decisions they are interested for. Decisions are most often made in presence of other interests and impacts such as political influence, NGOs' initiatives, pressure of in-situ municipalities, inspection services, or consultancy provided from independent (mainly academic) experts. Essential questions are how to assure fair process and reduce uncertainty in decision making process, and motivate water users or their interest sub-groups to participate in deriving final decision(s).

Continuing our earlier research (Srdjevic et al. 2011), in this paper we present case study implementation of hesitant analytic hierarchy process (H-AHP) for performing group decision-making process in the WUA, i.e. in its Water Committee (WA) composed of delegates from different sub-groups. By assumption, there are several sub-groups of stakeholders, where farmers can be grouped into one or more sub-groups depending on the size and/or potential of their properties. Each sub-group can be represented by 'virtual individual', after members of the sub-group reach internal consensus or expose their judgments in some other (but unified) way. The H-AHP is proven to be useful in cases when sub-groups have different positions and intents during elicitation of their judgments and in the presence of uncertainty.

Materials and methods

To demonstrate how the trustful decision can be derived in hesitancy framework, we assumed that there are five sub-groups within the WA. They have to decide which of four feasible technical solutions should be accepted to enable use of existing drainage canal network for irrigation. Namely, experts' has already advised Public Water Management Company Vode Vojvodine in Serbia to divert waters from open drainage canals into small and medium sized irrigation systems for supplying water to properties ranging from 20 to 100 hectares. Uncertainties related to each alternative include estimation of quantity and quality of supplied water, as well as expected costs and profits of produced agricultural products. In addition, alternatives could be characterized by required (re)investments, rules and procedures for collecting taxes and fees from the users, opportunities of getting loans for irrigation equipment, and agricultural inputs such as seeds, fertilizers and pesticides. Operation of lockers and pumps along canals can be defined for each alternative, as well as additional financing instruments anticipated for changing existing drainage function of canals into an (additional) irrigation function during vegetation season from April through September.

If alternatives will be evaluated and ranked within WUA, the decision-making problem can be structured as a hierarchy, and multi-criteria method AHP can be applied. AHP is commonly used in a way that the decision-maker(s) provide crisp values for judgments over paired comparisons of decision elements at a given level with respect to adjacent elements in the upper level of a hierarchy. Usually, in such cases the Saaty's scale (Saaty 1980) enables to formalize the translation of any judgment linguistic terms into a corresponding numeric value and in each step to construct a comparison matrix. Once all matrices are constructed, AHP uses the so-called prioritization method, computes the weights for each compared element in each matrix, all weights summing to 1. After all the local weights of the criteria (vs goal) and alternatives (vs criteria) are derived, a synthesis provides the set of weights of the alternatives with respect to the stated goal.

Zhu et al. (2016) argue that increasing complexity of modern society requires new options for judgment representations, especially in regard to raising the uncertainty experienced by decision-makers. Hesitancy is thus a common phenomenon in human reasoning with different meanings such as 'uncertain', 'unsure', 'doubtful', 'sceptical' or 'reluctant'. Therefore the hesitant AHP method is proposed as the new decision-making tool for individual and group decision-making (Zhu et al. 2016; Zhu and Xu 2014).

We used H-AHP to simulate the decision making process in WUA and rank four alternatives of exploiting drainage canals for irrigation. To allow more freedom to sub-groups, criteria set is defined within each sub-group (SG) separately according to SG's own interests. Reasonable assumption was that given SG would anticipate that forthcoming 'negotiation' process with the other SBs requires awareness about not only own but also broader interests of community and possibly quite different priorities of other SGs.

Results and concluding remarks

If the WC of WUA'a works in plenary, Srdjevic and Srdjevic (2008) suggest that the decision-making process should be conducted in the decentralized manner, i.e. to start as parallel SGs' sessions and then SGs' decisions to delegate the final voting and identification of the best alternative to the WC. In this illustrative example, each of five SGs used the H-AHP to evaluate the set of four alternatives with respect to each predefined criterion agreed upon by this SG, independently from other SGs. The results of their H-AHP applications are presented in Table 1. The final voting by Borda count identified the final ranking of alternatives, Table 2. When presented to the delegates in WC, the final result (ranking: #4 $\succ$ #3 $\succ$ #1 $\succ$ # 2) was anonymously 'accepted' as the best compromise solution. Standard aggregation of SGs' rankings confirmed obtained result derived by H-AHP.

Table 1. Alternatives' weights derived by interest sub-groups

	Interest sub-groups	Weights of alternatives			
		#1	#2	#3	#4
SG1	Existing users	0.18	0.28	0.21	0.33
SG2	Municipality	0.22	0.37	0.09	0.32
SG3	Public Water Management Co. Vode Vojvodine	0.14	0.20	0.41	0.25
SG4	Inspection	0.34	0.13	0.17	0.26
SG5	Province Secr. for Agriculture, Forestry and Water Management	0.13	0.16	0.47	0.24

Table 2. Borda count ranking of alternatives by interest sub-groups (based on weights in Table 1)

	Interest sub-groups	Ranks of alternatives			
		#1	#2	#3	#4
SG1	Existing users	4	2	3	1
SG2	Municipality	3	1	4	2
SG3	Public Water Management Co. Vode Vojvodine	4	3	1	2
SG4	Inspection	1	4	3	2
SG5	Province Secr. for Agriculture, Forestry and Water Management	4	3	1	2
	TOTAL (* is the best)	16	13	12	9*

Acknowledgments: This work was supported by the Ministry of Education, Science and Technological Development of Serbia under the grant 174003 (2011–2018).

References

Saaty TL (1980) The analytic hierarchy process. McGraw-Hill, NewYork

Srdjevic Z, Srdjevic B (2008) Two purpose systems (irrigation and drainage) and associations of water users in Vojvodina. J of Water Resources 40:69-80

Srdjevic B, Srdjevic Z, Pantelic-Miralem S, Blagojevic B, Suvocarev K (2011) Legal, Financial and Organizational Framework for Establishing Water Users Associations and Related Decision Making Issues, Global Conference on Business and Finance proceedings, Las Vegas, Nevada

Zhu B, Xu Z, Zhang R, Hong M (2016) Hesitant analytic hierarchy process. European Journal of Operational Research 250(2):602-614

Zhu B, Xu Z (2014) Analytic hierarchy process-hesitant group decision making. European Journal of Operational Research 239(3):794–801

11th World Congress on Water Resources and Environment (EWRA 2019)
"Managing Water Resources for a Sustainable Future", 25-29 June 2019, Madrid, Spain

A market mechanism for sharing a polluted river

A. Abraham*, P. Ramachandran
Department of Management Studies, Indian Insititute of Science Bengaluru, Bengaluru, India
** e-mail: anandj@iisc.ac.in*

Introduction

There has been a sufficient number of studies which use game theoretic models to allocate river water among riparian states. Such studies adopt cooperative game theoretic methods (Ambec and Spurmont 2002; Ambec and Ehlers 2008) and market based approaches (Giannias and Lekakis 1998; Wang 2011) but largely seem to focus on prescribing solutions in a static setting. Ni and Wang (2007) and Gengenbach et al. (2010) extended the set up to study the allocation of pollution damages along riparian states. However, the models for allocation of water assume the river to be devoid of pollution damages. Therefore, these water allocation models do not capture the effects of pollution on water allocation which are often interlinked (Giordano 2003).

In this work, we attempt to address this gap in literature and propose a two-agent game theoretic model of a river with a pollution externality. We study the behaviour of states under non-cooperation using the solution concept of subgame perfect equilibrium. Further, we study conditions for cooperation between the riparian states, when a market mechanism is put in place. Finally, we show that this mechanism can encourage the upstream riparian state to abate pollution, when the share of surplus derived by upstream agent through trade is sufficiently high enough.

Game theoretic model

Consider a transboundary river shared by two agents *i* (upstream state) and *k* (downstream state) each having annual endowments of s_i and s_k, respectively (see Figure 1). Let $b_j(x_j)$ denote the value of benefit derived by an agent $j \in \{i,k\}$ upon consumption of x_j amount of water. In this work, the benefit function of both agents are single peaked concave functions with maxima at x_j'. Due to pollutant effluents from the upstream state, a pollutant concentration of $q(x_i)$ is observed in the downstream state. Concentration $q(x_i) = \kappa x_i + q_0$ where κ is a positive constant which describes the variation of concentration with flow. The positive constant q_0 depends only on the amount of pollutant stock in the river. When the downstream state consumes x_k quantum of water, the state encounters a cost at the rate of d_p per unit of pollutant consumed by the state. The total pollutant cost is thus $d_p q(x_i) x_k$. To make the problem non-trivial we assume that there is a positive flow from state *i* towards state *k*. Additionally, we assume that the downstream state faces a scarcity of water. The water flow, pollutant concentration, and benefit functions are common knowledge and the states are assumed to be rational and intelligent. Under these assumptions, the agents act as utility maximizers subject to water availability constraints. The utility functions are given by:

$$u_i(x_i) = b_i(x_i) \text{ for agent } I \tag{1}$$

$$u_k(x_k) = b_k(x_k) - d_p\, q(x_i)\, x_k \tag{2}$$

Cooperation is induced between the states by using a market mechanism which allows for bilateral trade between the states. Using this formalism, it is possible to derive the conditions under which water is transferred along the river in exchange for side payments. We are also able to derive the total amount of water thus traded using the condition of market equilibrium.

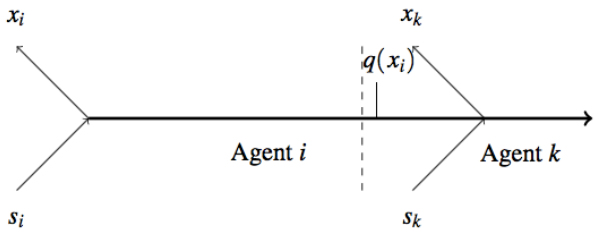

Figure 1. Stylized model of polluted river shared by two riparian states

Results and concluding remarks

We obtain the following results through this analysis.

- The analysis of non-cooperative consumption behaviour suggests the following Subgame Perfect Equilibrium (SGPE) consumption profile.

$$x_i^{NC}=\min(x'_j,s_i) \quad x_k^{NC}=\min(db^{-1}/dx_k\,(d_p\kappa x_i+d_p\,q_0),s_k+s_i-x_i^{NC}) \tag{3}$$

- If $q_0-\kappa(s_i+s_k-2x_i')<0$ then the agents would participate voluntarily in bilateral trade when

$$d_p \geq b_k'(s_k+s_i-x_i')/(q_0-\kappa(s_i+s_k-2x_i')) \tag{4}$$

This inequality reverses if $q_0-\kappa(s_i+s_k-2x_i')>0$. This denotes the condition for cooperation in the basin.

- The maximum amount of transfer which one can expect to see through the bilateral trade mechanism is given by x^*. Where x^* solves the differential equation given below

$$b_i'(x_i^{NC}-x^*) = b_k'(x_k^{NC}+x^*)-d_p\,[\kappa(x_i^{NC}-x_k^{NC}-2\,x^*)+q_0] \tag{5}$$

- Let γ denote the share of social surplus received by the upstream state and γ^* be the value of this social surplus share at market equilibrium. Then the upstream state would abate the pollutant stock at a marginal cost of c_A only if the following inequality holds true

$$\gamma^*-d\gamma/dq_0 \geq c_A/(d_p\,x^*) \tag{6}$$

References

Ambec S, Ehlers L (2008) Sharing a river among satiable agents. Games and Economic Behavior 64(1):35–50

Ambec S, Sprumont Y (2002) Sharing a river. Journal of Economic Theory 107(2):453–462

Gengenbach MF, Weikard HP, Ansink E (2010) Cleaning a river: An analysis of voluntary joint action. Natural Resource Modeling 23(4):565–590

Giannias DA, Lekakis JN (1996). Fresh surface water resource allocation between Bulgaria and Greece. Environmental and Resource Economics 8(4):473–483

Giordano MA (2003) Managing the quality of international rivers: Global principles and basin practice. Natural Resources Journal 43(1):111–136

Ni D, Wang Y (2007) Sharing a polluted river. Games and Economic Behavior 60(1):176–186

Wang Y (2011). Trading water along a river. Mathematical Social Sciences 61(2):124–130

11th World Congress on Water Resources and Environment (EWRA 2019)
"Managing Water Resources for a Sustainable Future", 25-29 June 2019, Madrid, Spain

Modeling of flows from some springs in the Bouzizi - Seraidi sector, N-E Algeria

H. Majour[1], A. Hani[2]
[1] Laboratory of Geology, Université Badji Mokhtar Annaba, Algeria
[2] Water Resource and Sustainability Laboratory, Université Badji Mokhtar Annaba, Algeria
* e-mail: yah_majour@yahoo.fr

Introduction

In this work, artificial neural networks have been used to simulate flows and mineralization of springs water. Consequently, we have shown the effect of physico-chemical and climatic factors, and more particularly, the geological characteristics on the hydrological behaviour of the springs. On the basis of a statistical treatment, the main processes ruling the observed chemical evolution within the aquifer were defined. The infiltration of meteoric water governs the dilution of the chemical elements and the increase of potassium contents. The wastewater increases the mineralization of groundwater. The rock matrix is submitted to dissolution according to the carbon dioxide contribution, which explains mineralization.

During the last decade, Artificial Neural Networks modelling has been applied with success to various hydrological processes, such as rainfall–runoff modelling (Minns et al. 1996), rainfall forecasting (Lallahem et al. 2003a, b), water demand modelling (Liu et al. 2003), water quality modelling, ground water problems and reservoir operation problems, among others. In this study, the ANN model is presented with the same input time-series parameters in order to find a relationship between them to simulate spring flows.

The Edough massif contains in its subsoil a rather valuable hydraulic capacity. It consists of spring system mainly used for feed water and irrigation. However, the enlargement of Seraidi city and the increase in water needs may induce the degradation of the water quality. Moreover, this water constitutes a great supply for the gravel aquifer.

Materials and methods

The study of the physico-chemical characteristics of the aquifer was based on the analytical results carried from sampling water from seven springs, in order to study the mechanisms that governs the spatial and temporal evolution of the water quality from the Edough crystalline reservoir.

Results and concluding remarks

Concerning the simulation of spring flows, the results of the investigation show a perfect superposition of the curves of the measured and calculated flow curves during the training, validation and testing steps (Figure 1). They also show minimum deviations with very low RMSE values, ranging from 0.67% to 5%. The coefficients of correlation of training, validation and test were higher than 0.92. The introduction of the climatic parameters allows a good reconstitution of the flows from the two studied springs. Therefore, this method can be used to decompose the flow hydrographs or to validate the hypothesis. In addition, Figure 1 shows that the survey period starts by a very short infiltration corresponding to the last rainstorms of June which passes from rising (November to February), falling limb (June-July) flow periods to base flow recession period (August to October) that mobilize the water supply. The sampling period corresponds to the curve data samples collected during the high water stages of the winter flood.

The use of the ANNs has permitted to demonstrate the influence of the climatic factors (rainfall, temperature and evaporation) on the variation of spring flow, and the simulation of spring flow to reconstruct missing flow data for the analysis of the physico-chemical elements.

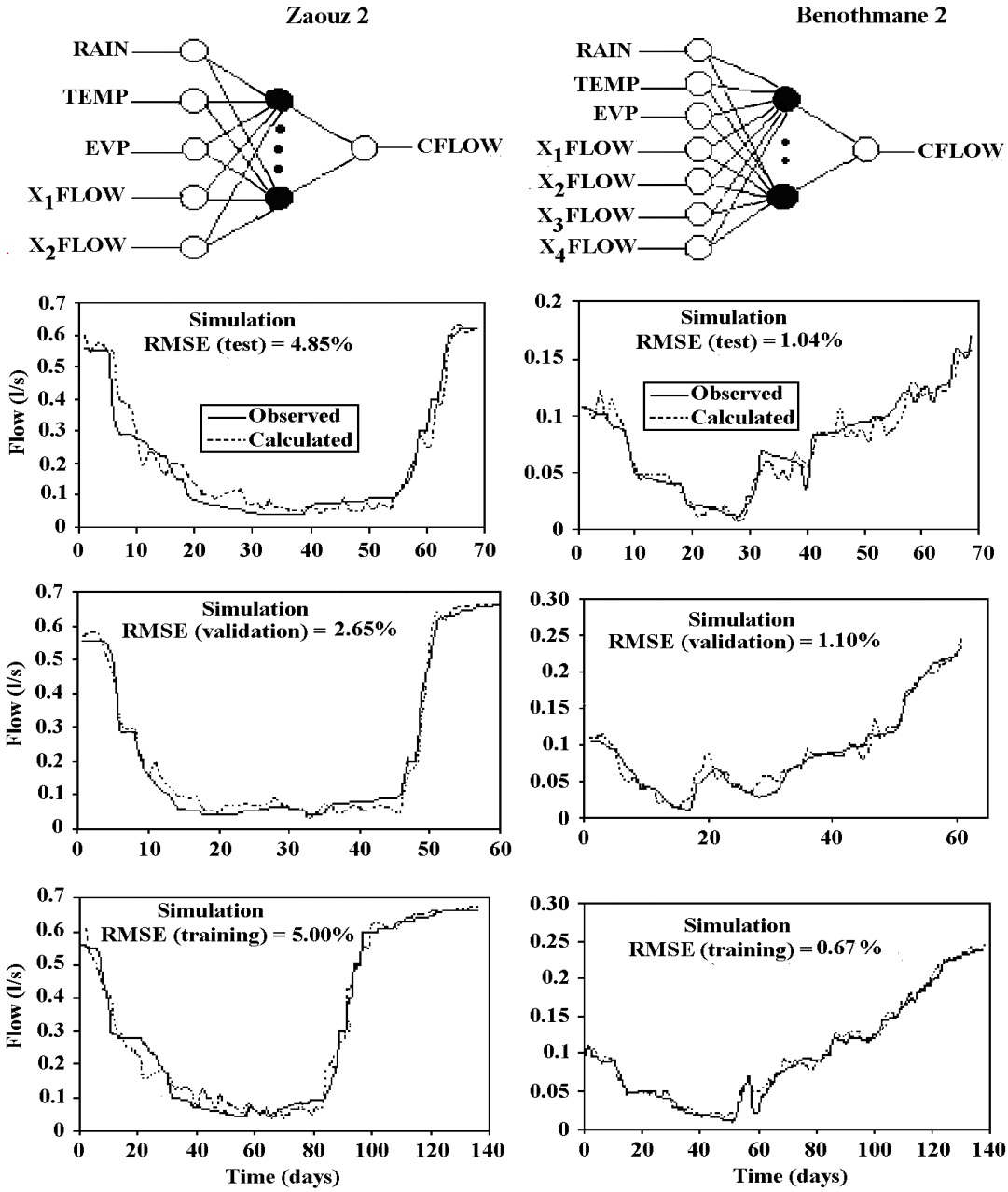

Figure 1. Flow curves measured and calculated

References

Lallahem S, Mania J (2003a) A nonlinear Rainfall-Runoff Model using Neural Network Technique: Example in Fractured Porous Media Math. and Comp. Model. 37:1047-1061

Lallahem S, Mania J (2003b) Evaluation and forecasting of daily groundwater outflow in a small chalky watershed. Hydrol. Process. 17:1561-1577

Liu H, Savernake HG, Xu J (2003) Forecast of water demand in Weinan City in China using WDF-ANN model. Phys. and Chemist. of the Earth 28:219-224

Minns AW, Hall MJ (1996) Artificial Neural Networks as rainfall-runoff models. Hydrol. Sci. 41(3):399-417

11th World Congress on Water Resources and Environment (EWRA 2019)
"Managing Water Resources for a Sustainable Future", 25-29 June 2019, Madrid, Spain

DEM-resolution control on rainfall-triggered landslide modeling within a triangulated network-based model

E. Arnone[1*], Y.G. Dialynas[2], A. Francipane[3], L.V. Noto[3]
[1] Amigo s.r.l., Rome, Italy
[2] Department of Civil and Environmental Engineering, University of Cyprus, Nicosia, Cyprus
[3] Department of Engineering, Università degli Studi di Palermo, Palermo, Italy
* e-mail: elisa.arnone@amigoclimate.com

Introduction

Catchment slope distribution significantly controls rainfall-triggered landslide modeling, in both direct and indirect ways. Slope directly determines the soil volume associated with instability. Indirectly, it affects the subsurface lateral redistribution of soil moisture across the basin, which in turn determines the water pore pressure conditions that impact slope stability. It is thus clear that the accuracy in reproducing slope distribution may be crucial in slope stability analysis.

The resolution of Digital Elevation Model (DEM) regulates the description of topography. The correlation between raster resolution and landslide model outputs has been investigated in literature, both in terms of landslide susceptibility (Arnone et al. 2016) and landslide dynamics (Tran de Viet et al. 2017; Keijsers et al. 2011; Tarolli and Tarboton 2006). Results demonstrate that the optimal DEM resolution may not necessarily exclude the use of coarser DEMs.

This study evaluates the influence of DEM resolution on the slope stability analysis by using a distributed eco-hydrological-landslide model, which implements a Triangulated Irregular Network (TIN) to describe the topography; as well, the model is capable of evaluating vegetation dynamics and predicting shallow landslides triggered by rainfall.

Materials and methods

We used the distributed eco-hydrological and landslide model, the tRIBS-VEGGIE-Landslide (Triangulated Irregular Network (TIN)-based Real-time Integrated Basin Simulator - VEGetation Generator for Interactive Evolution) (Lepore et al. 2013). The study area is the Mameyes Basin, which is located in the Luquillo Experimental Forest (Puerto Rico), where numerous landslide analyses have been carried out (Lepore et al. 2013).

Grid-DEMs at 20, 30, 50, and 70 m resolution were resampled from the available 10 m Grid-DEM, and were used to derive the corresponding hydrologically-significant TINs (Vivoni et al. 2004) (Table1), for a total of 5 configurations. As the Grid-DEM resolution increases, the DEM-to-TIN ratio required to preserve topographic attributes increases (Table 1). The corresponding voronoi meshes are then derived by tRIBS-VEGGIE. The model inputs (meteorological forcing, soil properties, model parameters) come from Lepore et al. (2013).

Table 2. Number of DEM cells, TIN nodes, and Voronoi cells for each Grid-DEM resolution. Because some nodes are used as catchment boundaries, the final number of Voronoi cells is lower than the TIN nodes

GRID-DEM Resolution [m]	DEM Cells	TIN Nodes	DEM to TIN Ratio	Voronoi Cells
10	169,615	6,974	4%	6,276
20	42,400	3,605	9%	3,131
30	18,837	2,603	14%	2,190
50	6,782	2,274	34%	1,908
70	3,462	2,416	70%	2,177

Results and concluding remarks

Application of a TIN-based hydrological-landslide model to different DEM-derived resolutions showed that: irregular mesh reduces the loss of accuracy in the derived slope distribution when coarser resolutions are used; at 'steady' state (either at dry or saturated conditions), soil moisture dynamics through the resolutions are almost invariant; in the transient, the different topography leads to slightly different soil moisture patterns; predicted failure area decreases with resolution, but statistics of slope at failure are almost invariant (Figure 1). In fact, the finer the resolution, the larger the area affected by landslide (Figure 1a); whereas only the 70 m case shows lower median and smaller range in the statistics (Figure 1b).

Overall, the use of the irregular mesh reduced the loss of accuracy in the derived slope distribution when coarser resolutions were used. The impact on soil moisture patterns was significant only when the lateral redistribution was considerable, depending on hydrological properties and rainfall forcing. In some cases, the use of different DEM resolutions did not significantly affect the model output, in terms of landslide locations and values of slope and soil moisture at failure (Arnone et al. 2013; Dialynas 2017).

In conclusion, as many other studies in literature, our results suggest that the optimal DEM resolution may not necessarily lead to the best landslide modeling.

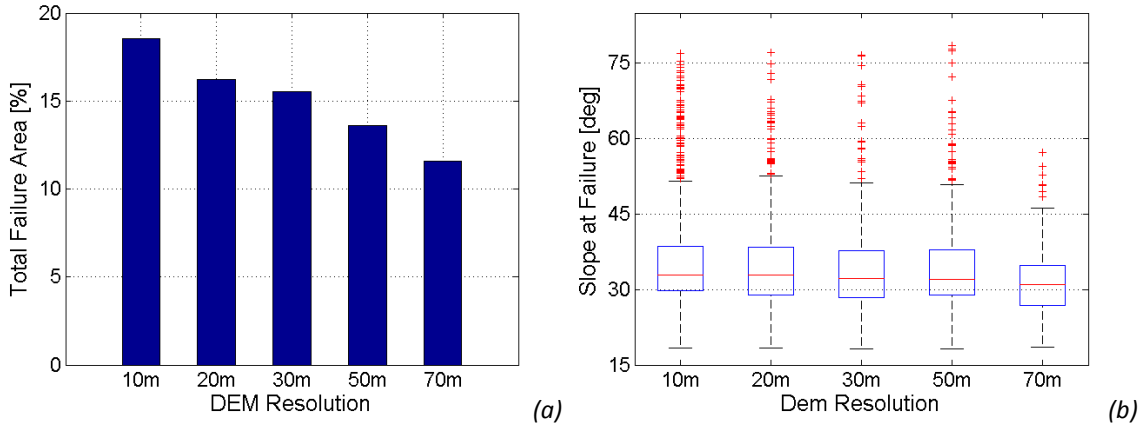

Figure 1. (a) Total failing area at different resolutions; (b) Box plots of slope values at slope for the five resolutions.

References

Arnone E, Dialynas YG, Noto LV, Bras RL (2013) Effect of DEM resolution on rainfall-triggered landslide modeling within a triangulated network-based model. A case study in the Luquillo Forest, Puerto Rico. American Geophysical Union

Arnone E, Francipane A, Scarbaci A, Puglisi C, Noto LV (2016) Effect of raster resolution and polygon-conversion algorithm on landslide susceptibility mapping. Environ. Modeling & Software 84C:467-481

Dialynas YG (2017) Influence of Linked Hydrologic and Geomorphic Processes on the Terrestrial Carbon Cycle. Doctorate thesis, School of Civil and Environmental Engineering, Georgia Institute of Technology, 234 p

Keijsers JGS, Schoorl JM, Chang KT, Chiang SH, Claessens L, Veldkamp A (2011) Calibration and resolution effects on model performance for predicting shallow landslide locations in Taiwan. Geomorphology 133:168-177

Lepore C, Arnone E, Noto LV, Sivandran G, Bras RL (2013) Physically based modeling of rainfall-triggered landslides: a case study in the Luquillo forest, Puerto Rico. HESS 17:3371-3387

Tarolli P, Tarboton DG (2006) A new method for determination of most likely landslide initiation points and the evaluation of digital terrain model scale in terrain stability mapping. HESS 10:663-677

Viet TT, Lee G, Thu TM, An HU (2017) Effect of digital elevation model resolution on shallow landslide modeling using TRIGRS. Natural Hazards Review 18(2)

Vivoni ER, Ivanov VY, Bras RL, Entekhabi D (2004) Generation of triangulated irregular networks based on hydrological similarity. Jour. of Hydr. Eng. 9:288-302

ISBN 978-618-84419-0-3